



Resource Report
For the Costa Fuego Copper Project
Located in Atacama, Chile

TECHNICAL REPORT NI 43-101

Prepared by: Haren Consulting and ABGM

Report by: Anton von Wielligh, FAusIMM (325251)
Elizabeth Haren, MAIG (6646) MAusIMM (CP) (208050)

Report Date: 13 May 2022

Mineral Resource Effective Date: 31 March 2022

DATE AND SIGNATURE PAGE

This report is effective as of the 31st day of March 2022.

DIGITAL DIGITAL DIGITAL DIGITAL
DIGITAL DIGITAL DIGITAL DIGITAL
DIGITAL DIGITAL DIGITAL DIGITAL
DIGITAL DIGITAL DIGITAL DIGITAL
DIGITAL DIGITAL DIGITAL DIGITAL
DIGITAL DIGITAL DIGITAL DIGITAL
DIGITAL DIGITAL DIGITAL DIGITAL

Elizabeth Haren

13 May 2022

Date



Anton von Wielligh

13 May 2022

Date

Table of Contents

1	Summary	32
1.1	Introduction	32
1.2	Property Description and Location	33
1.2.1	Productora	34
1.2.2	Cortadera	36
1.2.3	San Antonio	38
1.3	Accessibility, Climate, Local Resources, Infrastructure and Physiography	39
1.4	History	39
1.4.1	Productora	39
1.4.2	Cortadera	40
1.4.3	San Antonio	41
1.4.4	Production History	45
1.5	Geological Setting and Mineralization	45
1.5.1	Productora	45
1.5.2	Cortadera	47
1.5.3	San Antonio	48
1.6	Exploration	48
1.6.1	Productora	48
1.6.2	Cortadera	49
1.6.3	San Antonio	49
1.7	Drilling	49
1.7.1	Productora	49
1.7.2	Cortadera	51
1.7.3	San Antonio	51
1.8	Sampling, Analysis and Security	52
1.8.1	Productora	52
1.8.2	Cortadera	53
1.8.3	San Antonio	54
1.9	Data Verification	55
1.10	Metallurgy	56
1.10.1	Testwork	56
1.10.2	Copper Oxide Recoveries	57
1.10.3	Sulphide Mineralogy	59
1.10.4	Sulphide Comminution	59
1.10.5	Sulphide Flotation	59
1.10.6	Sulphide Flotation Copper Performance	60
1.10.7	Sulphide Flotation Gold Performance	61
1.10.8	Molybdenum Metallurgical Testwork	62

1.10.9	Cortadera	63
1.11	Mineral Resource Estimates	63
1.12	Mineral Reserve Estimate	67
1.13	Environmental and Social	67
1.14	Recommendations	68
1.14.1	Prefeasibility Study	68
1.14.2	Costa Fuego Environmental Works	68
1.14.3	Regional Targeting	68
1.14.4	Mineral Resource Development Drilling and Estimation	68
1.14.5	Cortadera Geotechnical and Metallurgical Drilling and Development Studies	69
1.15	Summary	70
2	Introduction	70
2.1	Terms of Reference	70
2.2	Purpose of Report	71
2.3	Cautionary Notes	71
2.4	Sources of Information	71
2.5	Site Visits	72
2.6	Definitions	72
3	Reliance on Other Experts	75
4	Property Description and Location	76
4.1	Property Location, Access, and Site Layout	76
4.2	Mineral Tenure	77
4.2.1	Productora	77
4.2.2	Cortadera	81
4.2.3	San Antonio and Valentina	85
4.3	Specific Tax of Mining, Water Regulation and Encumbrances	85
4.3.1	Specific Tax on Mining	85
4.3.2	Water Rights Legislation in Chile and HCH Strategy for Water Usage	86
4.3.3	Encumbrances	86
4.4	Environmental	86
4.5	Legal Review	87
4.5.1	Productora	87
4.5.2	Cortadera	88
5	Accessibility, Climate, Local Resources, Infrastructure and Physiography	89
5.1	Accessibility	89
5.2	Site Facilities	89
5.3	Climate	90
5.4	Vegetation	90
5.5	Physiography	90

6	History	92
6.1	Productora	92
6.1.1	Ownership History	92
6.1.2	Historical Exploration and Development Work	92
6.1.3	CCHEN Exploration	92
6.1.4	GMC Exploration	93
6.1.5	Thesis – Colorado School of Mines (USA)	93
6.1.6	Historical Exploration Data Collection	96
6.2	Productora Previous Mineral Resource and Reserve Estimates	96
6.2.1	Introduction	96
6.3	Productora Production History	99
6.3.1	2006-2011	99
6.3.2	2020 to present	99
6.4	Cortadera Historical Exploration and Development Work	100
6.4.1	Empresa Nacional de Minería	100
6.4.2	Minera Mt Isa, Chile	100
6.4.3	Minera Fuego Limited	101
6.4.4	Previous Mineral Resource and Reserve Estimates	104
6.4.5	Historical Production	105
6.5	San Antonio Historical Exploration and Development Work	105
6.5.1	Historical Mineral Resource and Mineral Reserve Estimates	105
6.5.2	Historical Production	105
7	Geological Setting and Mineralization	106
7.1	Productora-Alice Regional Setting	106
7.2	Cortadera-San Antonio Regional Setting	107
7.3	Local Geology	109
7.3.1	Productora-Alice Local Geology	109
7.3.2	Cortadera Local Geology	113
7.3.3	San Antonio Local Geology	113
7.4	Property Geology	114
7.4.1	Productora Property Geology	114
7.4.2	Alice Property Geology	115
7.4.3	Cortadera Property Geology	116
7.4.4	San Antonio Property Geology	120
7.5	Property Mineralisation	121
7.5.1	Productora Mineralisation	121
7.5.2	Productora Supergene Mineralisation	123
7.5.3	Alice Mineralisation	124
7.5.4	Cortadera Mineralisation	126

7.5.4.1	Cortadera Calculated Mineralogy	128
7.5.5	Cortadera oxide mineralisation	129
7.5.6	San Antonio Mineralisation	129
8	Deposit Types	129
8.1	Productora	129
8.2	Alice	130
8.3	Cortadera	130
8.4	San Antonio	133
8.5	Deposit Mineralisation	136
8.5.1	IOCG Style Deposits	136
8.5.2	Porphyry Cu-(Mo-Au) Style Deposits	136
8.5.3	Manto-type copper deposits	137
9	Exploration	140
9.1	Productora	140
9.1.1	Introduction	140
9.1.2	Airborne Magnetic and Radiometric survey	140
9.1.3	Induced Polarisation and Magnetotelluric (IP/MT) survey	141
9.1.4	Surface Mapping and Structural Review	142
9.1.5	Petrography	144
9.1.6	Fathom 3D geochemical modelling	144
9.2	Cortadera	145
9.2.1	Petrological and Mineragraphic Studies	145
9.2.2	Surface Mapping and Structural Review	147
9.2.3	Cuerpo 1, Cuerpo 2 and Cuerpo 3 Mapping	147
9.2.4	Cuerpo 3 Norte Mapping	150
9.2.5	Surveying	154
9.3	San Antonio	154
9.3.1	Introduction	154
9.3.2	Geological Mapping	154
9.3.3	Surface Geochemistry	156
9.3.4	Surveying	156
10	Drilling	159
10.1	Productora	159
10.1.1	Introduction	159
10.1.2	Drilling Methods	159
10.1.3	Drilling execution and data flow	160
10.1.4	Hole Planning and Set-up	161
10.1.5	Validation	162
10.1.6	Collar Validation	162

10.1.7	Downhole Survey Validation	162
10.1.8	Drilling Orientation	163
10.1.9	Geological Logging	164
10.1.10	Bulk Density	164
10.1.11	Bulk Density Method Comparison for Productora	165
10.1.12	Bulk Density Method Comparison for Alice	169
10.1.13	Drilling Results	171
10.2	Cortadera	171
10.2.1	Hot Chili (2019 to Present)	171
10.2.2	Phase 1 Minera Fuego Confirmation Program	171
10.2.3	Phase 2 Cuerpo 2 and Cuerpo 3 Mineralisation Extension Program	172
10.2.4	Phase 3 Cuerpo 3 Norte Exploration Program & Cuerpo 3 Mineralisation Confirmation Program	173
10.2.5	Phase 4 Cortadera Delineation and Extension Program	174
10.2.6	Significant Drillhole Intercepts	176
10.2.7	Drilling Procedures	179
10.2.8	RC drilling tools	180
10.2.9	Diamond drilling tools	180
10.2.10	Hole Planning and Set-up	180
10.2.11	Naming Convention and Meta Data Management	180
10.2.12	Internal database audit - 2020	181
10.2.13	External database audit – 2022	182
10.2.14	Surveying and Orientations	183
10.2.15	Collar Surveying	183
10.2.16	Collar Validation	183
10.2.17	Downhole Surveying	184
10.2.18	Survey Validation	184
10.2.19	Hole Logging Procedures	184
10.2.20	Reverse Circulation Logging	186
10.2.21	Diamond Drill Logging	186
10.2.22	Structural Logging	187
10.2.23	Geotechnical Logging	188
10.2.24	Dry Bulk Density	190
10.2.25	Historical Dry Bulk Density Testwork	191
10.3	San Antonio	191
10.3.1	Hot Chili (2018 to Present)	191
10.3.2	San Antonio Resource Definition Drilling	192
10.3.3	Significant Drillhole Intercepts	193
10.4	Drilling Procedures	194

10.4.1	RC drilling tools	194
10.4.2	Hole Planning and Set-up	194
10.4.3	Naming Convention and Meta Data Management	195
10.4.4	Geological Database	195
10.5	Surveying and Orientations	195
10.5.1	Collar Surveying	195
10.5.2	Collar Validation	195
10.5.3	Downhole Surveying	195
10.5.4	Survey Validation	196
10.5.5	Hole Logging Procedures	196
10.5.6	Reverse Circulation Logging	196
10.5.7	Diamond Drilling Logging	196
10.6	Dry Bulk Density	196
11	Sample Preparation, Analyses and Security	197
11.1	Introduction	197
11.2	RC Sampling Methods	197
11.3	DD Sampling Methods	198
11.4	Relationship between sample length and thickness	198
11.5	Impact of significantly higher-grade intervals	199
11.6	Historical Work	199
11.7	Chain of Custody and Transport	199
11.8	Assay Sample Preparation	200
11.9	Minera Fuego	201
11.10	QAQC Program	202
11.11	Conclusions	204
12	Data Verification	205
12.1	Productora	205
12.1.1	Independent Qualified Person Review and Verification	205
12.1.2	Assay Standards	205
12.1.3	Certified Reference Material – Mineralised	206
12.1.4	Certified Reference Material – Non-mineralised (“Blank”)	209
12.1.5	Coarse “Blank” Material	211
12.1.6	Field Duplicates	212
12.1.7	Umpire Laboratory Checks	213
12.1.8	Twin Hole Analysis	214
12.1.9	Sample Condition and Recovery	217
12.1.10	Wet vs. Dry Samples	219
12.1.11	Independent Samples and Assay Verification	221
12.2	Cortadera	222

12.2.1	Independent Qualified Person Review and Verification	222
12.2.2	Internal Verification Programs	222
12.2.3	QA/QC Program	222
12.2.4	Blanks	242
12.3	San Antonio	254
12.3.1	Independent Qualified Person Review and Verification	254
12.3.2	Internal Verification Programs	254
12.3.3	QA/QC Program	254
12.3.4	Twin Holes	264
12.3.5	Umpire Checks	264
12.4	Conclusion	266
13	Mineral Processing and Metallurgical Testing	267
13.1	Introduction	267
13.2	Copper Oxide	267
13.2.1	Background	267
13.2.2	Results of Testwork Program	273
13.2.3	Conclusions	306
13.2.4	Further Testwork	307
13.3	Copper Sulphide and Molybdenum	307
13.3.1	History of Testwork	307
13.3.2	Results of Testwork Program	310
13.3.3	Mineralogical Analysis	363
13.3.4	Conclusions	372
13.4	Cortadera	380
13.5	Background to the Metallurgical Sample Collection	380
13.6	Sulphide Flotation testwork	381
13.7	Key outcomes from Comminution testwork	383
13.8	Conclusions and Recommendations	384
13.8.1	Cortadera	384
13.8.2	Productora	384
14	Mineral Resource Estimates	387
14.1	Productora	387
14.1.1	Model Area	387
14.1.2	Database	388
14.1.3	Data Manipulation	392
14.1.4	Geological and Mineralisation Interpretation	392
14.1.5	2013 Predictive Modelling	393
14.1.6	2013 Predictive Modelling Files	400
14.1.7	Weathering Domain Modelling	400

14.1.8	Data Flagging	401
14.1.9	Block Modelling	404
14.1.10	Dynamic Anisotropy Modelling	404
14.1.11	Categorical Domaining	405
14.1.12	Compositing	421
14.1.13	Statistical Analysis	422
14.1.14	Variography	444
14.1.15	Estimation	451
14.1.16	Model Validation	458
14.1.17	Resource Classification	462
14.1.18	Alice	462
14.1.19	Reasonable Prospects for Eventual Economic Extraction (RPEEE)	473
14.1.20	Previous Mineral Resource Estimates	473
14.2	Cortadera	474
14.2.1	Introduction	474
14.2.2	Summary of Data Used in Estimate	476
14.2.3	Data Manipulation	477
14.2.4	Geological and Mineralisation Interpretation	481
14.2.5	Mineralisation Model	484
14.2.6	Weathering Domains	492
14.2.7	Data Flagging and Compositing	493
14.2.8	Mining and Tenement Flagging In The Model	494
14.2.9	Compositing	495
14.2.10	Statistical Analysis	496
14.2.11	Top Cuts	499
14.2.12	Variography	500
14.2.13	Block Modelling	510
14.2.14	Grade Estimation	512
14.2.15	Bulk Density	544
14.2.16	Estimate Validation	545
14.2.17	Resource Classification	550
14.2.18	Reasonable Prospects for Eventual Economic Extraction	551
14.3	San Antonio	557
14.3.1	Introduction	557
14.3.2	Summary of Data Used in Estimate	560
14.3.3	Interpretation and Modelling	561
14.3.4	Data Flagging and Compositing	565
14.3.5	Mining and Tenement Flagging In The Model	565
14.3.6	Compositing	567

14.3.7	Statistical Analysis	568
14.3.8	Top Cuts	569
14.3.9	Block modelling	570
14.3.10	Grade Estimation	572
14.3.11	Bulk Density	576
14.3.12	Estimate Validation	577
14.3.13	Resource Classification	579
14.4	Calculation of Copper Equivalent	581
14.5	Costa Fuego Resource Reporting	581
14.6	Relevant Factors Affecting Resource Estimates	586
15	Mineral Reserve Estimates	587
16	Mining Methods	588
17	Recovery Methods	589
18	Project Infrastructure	590
19	Market Studies and Contracts	591
20	Environmental Studies, Permitting and Social or Community Impact	592
20.1	Summary	592
20.2	Permit Requirements, Status of Permit Applications and Bond Requirements	593
20.2.1	Legislation	593
20.3	EIA Content	594
20.4	Environmental Protection Act Approvals	595
20.5	Main Environmental Considerations	595
20.6	Social and Community Related Requirements	596
20.6.1	Stakeholder Engagement Plan	596
20.7	Closure and Rehabilitation	596
21	Capital and Operating Costs	598
22	Economic Analysis	599
23	Adjacent Properties	600
24	Other Relevant Data and Information	601
25	Interpretation and Conclusions	602
25.1	Geology and Resources	602
25.1.1	Productora and Alice	602
25.1.2	Cortadera	602
25.1.3	San Antonio	603
25.2	Relevant Risks and Opportunities	603
26	Recommendations	604
26.1	Prefeasibility Study	604
26.2	Costa Fuego Environmental Works	604
26.3	Regional Targeting	604

26.4	Mineral Resource Development Drilling and Estimation	604
26.5	Cortadera Geotechnical and Metallurgical Drilling and Development Studies	604
26.6	Summary	605
27	References	606

Figures

Figure 1.1	Costa Fuego Project location in Chile. (HCH, 2022).....	33
Figure 1.2	Location of Costa Fuego Project and Infrastructure relative to Vallenar, Chile. (HCH, 2022)	34
Figure 1.3	Productora Mining Rights under WGS84. (HCH, 2021).....	35
Figure 1.4	Location of HCH's Mining Rights under WGS84. (HCH, 2021)	37
Figure 1.5	Metallurgical drillhole locations and metallurgical domains (HCH, 2016).....	57
Figure 1.6	Heap leach recovery vs. Head grade.....	58
Figure 1.7	Copper head grade vs. Cu recovery	61
Figure 1.8	Gold head grade vs. Recovery.....	62
Figure 1.9	Molybdenum head grade vs. Recovery	63
Figure 4.1	Costa Fuego Project location in relation to Vallenar and the surrounding infrastructure, Chile. (HCH, 2021)	76
Figure 4.2	Productora Mining Rights under WGS84. (HCH, 2021).....	80
Figure 4.3	Productora surface area (approximately 4,111 hectares) (HCH, 2016)	81
Figure 4.4	Image of HCH tenements. (HCH, 2021)	83
Figure 5.1	Infrastructure proximal to the Costa Fuego Project. (HCH, 2016)	89
Figure 6.1	Stratigraphic column for Productora.....	94
Figure 7.1	Regional geological setting (Escolme, 2016, modified from Marschik and Fontboté 2001)	106
Figure 7.2	Broad 2D structural framework. Left; compared to ground mapping, centre; compared to previous IP data, right; compared to rock chip sampling. (HCH, 2016).....	110
Figure 7.3.	Stylised regional type section across the Productora project area. Image looking north (Escolme, 2016)	111
Figure 7.4	2D structural framework compared to radiometric data. (HCH, 2016)	112
Figure 7.5	Example outcrop of Serrano fault in a drill pad (fault dipping steeply to NE). Note altered footwall. Hanging wall to the fault is off picture as this fault appears to be moderately thick.	113
Figure 7.6	Alice hanging wall fault out cropping on Docherty Rd. Fault is steeply dipping to the west (image looking south). Porphyry in footwall, altered volcanic rocks in the hanging wall.	113
Figure 7.7	Cross section of San Antonio regional geology.....	114
Figure 7.8	A) Ductile shearing in tourmaline breccia in PRD0011, B) hydraulic fracturing (PRD0011), C) Tourmaline vein network in rhyolite C) Tourmaline vein cutting NNE fault zone, earlier veining and breccia in rhyolitic rock.....	116
Figure 7.9	Cortadera Vein Paragenesis model (HCH geologists and Steve Garwin, 2021). Veins have been classified on vein morphology, composition and texture. They have then been grouped by interpreted relative age based on cross-cutting textural relationships.....	117

Figure 7.10 (Above) Stereo net indicating primary orientation of quartz veins. (Below) cross-section through Cuerpo 3 facing northwest, showing the primary vein orientation relative to the 0.17% Cpy, 1.2% Cpy and 1.65% Cpy mineralisation models.	118
Figure 7.11 Long section facing north-east (+/-50m clipping) showing the interpreted lithogeochemical stratigraphy relative to downhole copper grades and intrusive models from geological logging.	120
Figure 7.12 Plan view and cross section schematic showing interpretation of structural controls inferred from surface mapping campaigns Beeson et al (2018)	121
Figure 7.13. Example cross section at Productora. Selected significant intersections (previously published) highlight drilling from the Habanero zone. 6822215mN. Section looking north. (HCH, 2016)	122
Figure 7.14. Example of manto-style mineralisation at Productora South. As is typical, manto horizons (black outline) are hosted within volcanic breccia zones (cyan on drill string). Cross-section view at 6,819,800mN.....	123
Figure 7.15 Alice holes PXP0001D. A). Interval with typical porphyry veining. Late albite fluids propagating up fracture network and removing sulphides, B) close up of box in A with albitic fluids move up, and then outward, C) complete albitisation.....	125
Figure 7.16 Alice type section on 6822600mN. Section looking north. (HCH, 2016)	126
Figure 7.17 Location plan displaying tenement outlines, drilling completed and +0.7% CuEq (yellow) and +0.3% copper (orange), +0.4% copper (light pink) and +0.6 copper (magenta) mineralisation envelopes at Cortadera. North. (HCH, 2022).....	127
Figure 8.1 Example cross section of Porphyry Systems in an Arc Settings, showing geological variations (Sillitoe, 2010).....	131
Figure 8.2 Example cross section of Porphyry Systems in an Arc Settings, showing alteration variations (Sillitoe, 2010)	132
Figure 8.3 A cross section through the Ann-Mason Porphyry deposit at Yerington, showing the trace element distribution (Cohen, 2011 and Halley et al., 2015) with elemental ratio annotations based on Garwin (2019).	132
Figure 8.4 First Skarnification event with mineralisation of pyrite and lesser chalcopyrite. For reference, Cpy – chalcopyrite, Grt-Epi – Garnet-Epidote, Py – pyrite, Esp – specularite.....	133
Figure 8.5 Intrusion of Qtz-Dioritic and Dacitic Porphyry	134
Figure 8.6 Mineralisation event with infill of veinlets and fractures. For reference, Cpy – chalcopyrite, Esp – specularite, Qz – quartz, Grt – garnet, Py – pyrite, Mgt – magnetite.	135
Figure 8.7 Schematic evolution for San Antonio Skarn Deposit	135
Figure 8.8 Pacific porphyry Cu belt with Productora for reference (Escolme, 2016, modified from Maksaev et al. (2007))	137
Figure 8.9 Mesozoic Manto-type Cu and skarn deposits with Productora for reference. Modified from Maksaev et al. (2002).....	139
Figure 9.1 Flight lines and example magnetic data from the 2010 Productora airborne geophysical survey (plan view with drilling traces shown)	141
Figure 9.2 Example radiometric data from the 2010 Productora airborne geophysical survey (plan view). (HCH, 2016).....	141
Figure 9.3 Example section of the IP/MT 2015 Productora ground geophysical survey. Chargeability shown on Alice type section (6822600mN). Image looking north. (HCH, 2016)	142
Figure 9.4 Extent of 2014 Productora soil sampling programme. Example elements shown. (HCH, 2016)	143
Figure 9.5 Example thin section image M-92. Sample take from Productora deposit drilling, PRP0420D at 356.18m depth. A and B are in transmitted light, C and D are reflected light. Image A) provides an overview, principally composed of interstitial feldspar (Fk) with development of biotite (Bt). B) An aplitic,	

albitised plagioclase (Plag) texture being altered to K-feldspar (Fk) and clays (Ar). C) A micro veinlet filled with chalcopyrite (Cpy). D) Pyrite (Py) being replaced by Chalcopyrite (Cpy) in texture decay.	144
Figure 9.6 Geological map of Cuerpo 1 to Cuerpo 3 from Tapia (2019) showing major intrusions (refer to legend for details) and quartz-vein abundance as a percentage Hot Chili-only mapping (HCH, 2021).	150
Figure 9.7 Geological interpretation of Cuerpo 3 Norte as mapped by Beeson (2019)	151
Figure 9.8 Oblique view of the Cortadera lithology showing the IP chargeability and MT conductivity anomalies located at Cuerpo 3 Norte as modelled by Garwin (2020a)	151
Figure 9.9 Geological map of Cortadera Norte interpreted by Beeson (2019)	153
Figure 9.10 Left: Reduced-to-pole (RTP) image of ground magnetic data showing a broad magnetic low (magnetite destruction) with a cusped magnetic high to the north associated with elevated Mo in soil samples. Right: IP chargeability image covering the Cortadera to Cortadera Norte area showing the IP chargeability anomaly closely associated with Cu-Au-Mo mineralisation at Cortadera as well as a similar, NE-SW trending IP chargeability anomaly slightly offset from the Mo-in-soil anomaly at Cortadera Norte. Note that the Mo-in-soil anomaly at Cortadera is also laterally displaced from the IP chargeability anomaly (HCH, 2021)	153
Figure 9.11 San Antonio Geology Map from Satellite Imagery.....	155
Figure 9.12 Lithology fact mapping of San Antonio (Feb. 2018)	155
Figure 9.13 Surface Geochemistry Sampling over San Antonio	156
Figure 9.14 Cross section 6819000mN showing the topography model used in estimation with the drone survey derived topography model.....	157
Figure 10.1 Drill Data flow showing drill planning, drill execution, logging, sampling and data entry and capture	161
Figure 10.2 Plot showing the downhole difference between the original downhole survey and its resurvey (image from 2014 resource report). Overall the minor differences were deemed to have negligible impact on the resource model.	163
Figure 10.3 Example of comparison of Fe values across Productora (data outside the orange box was outside model extents but is included in this image to show larger regional trends). Note: The relatively sedate “background” values compared to the observe	166
Figure 10.4 Example density data for samples within the 0.2% Cu domain with core differentiated to pulp data.	167
Figure 10.5 Example density data for samples within the 0.3% Cu domain with core differentiated to pulp data. Top: location depth by northing. Middle: density by northing. Bottom: density by elevation	168
Figure 10.6 Left: QQ plot of core vs. pulp for samples within the 0.2% Cu domain. Right: experimental regressions to “correct” pulp pycnometer density values	168
Figure 10.7 Validation of applied regressions on pulp pycnometer density data for key domains	169
Figure 10.8 Comparison between Alice bulk density and pycnometer data populations.....	171
Figure 10.9 Plan view of Cortadera 0.1% Cu shape showing Hot Chili’s Phase 1 drilling in red, and all other previous drilling in black. (HCH, 2022).....	172
Figure 10.10 Plan view of Cortadera 0.1% Cu shape showing Hot Chili’s Phase 2 drilling in red, and all other previous drilling in black. (HCH, 2022)	173
Figure 10.11 Plan view of Cortadera 0.1% Cu shape showing Hot Chili’s Phase 3 drilling in red, and all other previous drilling in black. (HCH, 2022)	174
Figure 10.12 Plan view of Cortadera 0.1% Cu shape showing Hot Chili’s Phase 4 drilling in red, and all other previous drilling in black. (HCH, 2022)	175

Figure 10.13 Drill Data flow showing drill planning, drill execution, logging, sampling and data entry and capture	182
Figure 10.14 San Antonio RC Drill program hole locations relative to existing underground mine development.....	192
Figure 11.1 Idealised diagrammatic illustration of a cone splitter	197
Figure 11.2 Flow chart of sample preparation.....	201
Figure 11.3 Pulp bag containing certified reference material (image from sampling procedure) ..	204
Figure 12.1 CRM performance from 2014/2015 – Cu%. Note: Upper and lower lines represent three standard deviations	207
Figure 12.2 CRM performance from 2014/2015 – Mo ppm. Note: Upper and lower lines represent three standard deviations.....	208
Figure 12.3 CRM performance from 2014/ 2015 – Au g/t. Note: Upper and lower lines represent three standard deviations	208
Figure 12.4 Review of certified “blank” material for copper during the 2014/2015 program	210
Figure 12.5 Review of certified “blank” material for molybdenum during the 2014/2015 program	210
Figure 12.6 Certified “blank” pulp material – copper	211
Figure 12.7 Coarse blank material performance during 2014/2015 drilling campaign.....	212
Figure 12.8 Duplicate sample comparison with original for major elements during the 2014/2015 drilling campaign	213
Figure 12.9 Umpire laboratory results for the 2014/2015 drilling campaign (known swapped sample pair highlighted in red).....	214
Figure 12.10 Example graphical analysis of twin holes at Productora	215
Figure 12.11 Visual comparison between core and RC twins within the 0.3% mineralisation envelope. The two holes compared in the previous figure are shown in the middle of this image. Sample and histogram are coloured by copper. Image is viewed looking north and width of image is approximately 80m. (HCH, 2016)	216
Figure 12.12 Example graphical analysis of twin holes at Alice (note: absent metallurgical samples in MET024).....	217
Figure 12.13 Alice and Productora sample condition and sample recovery	218
Figure 12.14 QQ comparison of (left) “dry” and “moist” RC samples within the 0.3% Cu mineralised domain for Cu. Right is a comparison of “wet” and “dry” for Productora	220
Figure 12.15 QQ comparison of (left) “wet” and “dry” RC samples within the 0.3% Cu mineralised domain for Au. Right is a Mo comparison	220
Figure 12.16 Graphical samples comparison with twin holes. Sample condition (wet/dry/moist) is flagged by RC sample logging	221
Figure 12.17 Location of RC and DD drilling added during the reporting period undertaken by HCH	223
Figure 12.18 OREAS-501b results for Cu ppm.....	225
Figure 12.19 OREAS-501b results for Au ppm.....	225
Figure 12.20 OREAS-501b results for Ag ppm.....	226
Figure 12.21 OREAS-501b results for Mo ppm	226
Figure 12.22 OREAS-502 results for Cu ppm.....	228
Figure 12.23 OREAS-502 results for Au ppm.....	228
Figure 12.24 OREAS-502 results for Ag ppm.....	228

Figure 12.25 OREAS-502 results for Mo ppm	229
Figure 12.26 OREAS-502c results for Cu ppm	230
Figure 12.27 OREAS-502c results for Au ppm	230
Figure 12.28 OREAS-502c results for Ag ppm	231
Figure 12.29 OREAS-502c results for Mo ppm	231
Figure 12.30 OREAS-503b results for Cu ppm.....	232
Figure 12.31 OREAS-503b CRM results for Au ppm	233
Figure 12.32 OREAS-503b CRM results for Ag ppm	233
Figure 12.33 OREAS-503b CRM results for Mo ppm.....	234
Figure 12.34 OREAS-504 CRM results for Cu ppm	235
Figure 12.35 OREAS-504 CRM results for Au ppm	236
Figure 12.36 OREAS-504 CRM results for Ag ppm	236
Figure 12.37 OREAS-504 CRM results for Mo ppm.....	237
Figure 12.38 OREAS-505 CRM results for Cu ppm	238
Figure 12.39 OREAS-505 CRM results for Au ppm	238
Figure 12.40 OREAS-505 CRM results for Ag ppm	239
Figure 12.41 OREAS-505 CRM results for Mo ppm.....	239
Figure 12.42 OREAS-902 CRM results for Cu ppm	241
Figure 12.43 OREAS-902 CRM results for Ag ppm	241
Figure 12.44 OREAS-902 CRM results for Mo ppm.....	241
Figure 12.45. IN-BMF-172 CRM results for Cu.....	243
Figure 12.46. IN-BMF-172 CRM results for Cu.....	243
Figure 12.47. IN-BMF-172 CRM results for Mo	243
Figure 12.48. IN-BMF-172 CRM results for Ag.....	244
Figure 12.49. IN-BMF-333 CRM results for Cu.....	245
Figure 12.50. IN-BMF-333 CRM results for Au.....	245
Figure 12.51. IN-BMF-333 CRM results for Ag.....	245
Figure 12.52 Coarse Blank / Qtz Blank results for Cu ppm	247
Figure 12.53. Quartz Blank fails by sample collection method	247
Figure 12.54 HCH duplicate samples displaying Cu ppm analysed by ME-ICP61 technique.....	248
Figure 12.55 Distribution of Normal (within +/- 10%), Warning (between +/- 10 and +/- 20%), and Error (above +/- 20%) results for field duplicates.....	248
Figure 12.56 Distribution of results by Hole Type	249
Figure 12.57 Frequency distribution of Error results by Cu Grade and Hole Type.....	249
Figure 12.58 HCH duplicate samples displaying Au ppm analysed by AA23 technique, excluding the outlier pair (CX05891 - 4.22ppm vs 2.17ppm)	250
Figure 12.59 HCH duplicate samples displaying Mo ppm analysed by ME-ICP61 technique	250
Figure 12.60 HCH duplicate samples displaying Ag ppm analysed by ME-ICP61 technique.....	251
Figure 12.61 Scatter plot of Cu% by Laboratory and Original Sample Type	252
Figure 12.62 Scatter plot of Mo ppm by Laboratory and Original Sample Type.....	252

Figure 12.63 Scatter plot of Au ppm by Laboratory and Original Sample Type	253
Figure 12.64 Scatter plot of Ag ppm by Laboratory and Original Sample Type	253
Figure 12.65 OREAS-501b results for Cu ppm.....	256
Figure 12.66 OREAS-501b results for Au ppm.....	257
Figure 12.67 OREAS-501b results for Ag ppm.....	257
Figure 12.68 OREAS-501b results for Mo ppm	257
Figure 12.69 OREAS-22c CRM results for Cu ppm	259
Figure 12.70 OREAS-22c CRM results for Au ppm.....	259
Figure 12.71 OREAS-22c CRM results for Mo ppm	259
Figure 12.72 Coarse Blank / Qtz Blank results for Cu ppm	261
Figure 12.73 HCH duplicate samples displaying Cu ppm analysed by ME-ICP61 technique.....	262
Figure 12.74 HCH duplicate samples displaying Au ppm analysed by ICP21 technique	263
Figure 12.75 HCH duplicate samples displaying Mo ppm analysed by ME-ICP61 technique	263
Figure 12.76 HCH duplicate samples displaying Ag ppm analysed by ME-ICP61 technique.....	264
Figure 12.77 Scatter plot of Cu% by Laboratory	265
Figure 12.78 Scatter plot of Au ppm by Laboratory	265
Figure 12.79 Scatter plot of Ag ppm by Laboratory	266
Figure 13.1 Sample location (HCH, 2016)	268
Figure 13.2 Preliminary heap leach characterisation testwork flowsheet	269
Figure 13.3 Crushing testwork flowsheet.....	270
Figure 13.4 Crushing testwork flowsheet.....	271
Figure 13.5 Heap agglomeration and stacking testwork flowsheet	272
Figure 13.6 1m column testwork flowsheet.....	273
Figure 13.7 Copper head assay vs. insoluble copper tail	275
Figure 13.8 Bottle roll test results (pH=1)	277
Figure 13.9 Southern Mantos pH=1 bottle roll leach kinetics	279
Figure 13.10 Main Pit pH=1 bottle roll leach kinetics.....	281
Figure 13.11 Main Pit pH=1 bottle roll leach kinetics.....	282
Figure 13.12 Santa Innes pH=1 bottle roll leach kinetics.....	283
Figure 13.13 Alice pH=1 bottle roll leach kinetics	284
Figure 13.14 Eastern Oxide pH=1 bottle roll leach kinetics	285
Figure 13.15 Acid consumption and Cu extraction characteristics	286
Figure 13.16 Acid consumption and Cu extraction characteristics	286
Figure 13.17 PSD for crushed Southern Mantos (Sm3)	289
Figure 13.18 PSD for crushed Northern Oxide (No4).....	289
Figure 13.19 PSD for crushed Main Pit 9 (Cc9).....	290
Figure 13.20 Density vs. potential heap height profiles	292
Figure 13.21 Hydraulic conductivity vs. potential heap height profiles	293
Figure 13.22 Hydraulic conductivity vs. potential heap height profiles	293

Figure 13.23 Hydraulic conductivity vs. potential heap height profiles	294
Figure 13.24 Porosity partitioning	295
Figure 13.25 Liquid saturation at variable application rates	296
Figure 13.26 Gas conductivity.....	297
Figure 13.27 Northern Oxide 3 – 1m column results	299
Figure 13.28 Northern Oxide 3 – 1m column results	300
Figure 13.29 Southern Mantos 2 – 1m column results	301
Figure 13.30 Southern Mantos 2 – 1m column results	301
Figure 13.31 Main Pit 7 (Cc7) 1 m column results.....	302
Figure 13.32 Main Pit 7 (Cc7) 1m column results.....	303
Figure 13.33 Main Pit 8 (Cc8) 1m column results.....	303
Figure 13.34 Main Pit 8 (Cc8) 1m column results.....	304
Figure 13.35 Santa Innes 4 – 1m column results	305
Figure 13.36 Santa Innes 4 – 1m column results	305
Figure 13.37 Grind optimisation analysis results	313
Figure 13.38 Productora – Central – Primary grind size copper results.....	316
Figure 13.39 Productora – Central – Primary grind size molybdenum results	316
Figure 13.40 Productora – Central – head grade vs. copper rougher recovery	318
Figure 13.41 Productora – Central – FD2 RTD2086 vs. A3894/SMBS copper grade recovery.....	321
Figure 13.42 Productora – Central – FD-6 copper grade recovery curve	323
Figure 13.43 Productora – Central – FD-13 copper grade recovery curve	324
Figure 13.44 Productora – Central – FD-13 molybdenum grade recovery curve.....	324
Figure 13.45 Productora – Central (In Pit Fresh) copper head grade vs. recovery	328
Figure 13.46 Productora – Central (In Pit Fresh) gold head grade vs. recovery	329
Figure 13.47 Productora – FD-3 and FD-4 copper grade recovery	330
Figure 13.48 Productora – FD-5 copper grade recovery – diesel comparison.....	331
Figure 13.49 >10% acid soluble copper/transitional sulphide – copper head grade vs. recovery.....	334
Figure 13.50 Productora – Habanero – RTD2086 vs. C4403 rougher results	337
Figure 13.51 Productora – Habanero – V-12 - RTD2086 vs. C4403 cleaner results	338
Figure 13.52 Productora – Habanero – V-12 - RTD2086 vs. C4403 cleaner results	338
Figure 13.53 Productora – Habanero – gold head grade vs. recovery (125µm)	339
Figure 13.54 Alice – primary grind size copper results.....	340
Figure 13.55 Alice – primary grind size molybdenum results	341
Figure 13.56 Alice – head grade vs. copper rougher recovery (180µm)	342
Figure 13.57 Alice – copper head grade vs. recovery	344
Figure 13.58 Alice – gold head grade vs. recovery	345
Figure 13.59 Cayenne – primary grind size copper results	346
Figure 13.60 Cayenne – primary grind size molybdenum results.....	346
Figure 13.61 Cayenne – head grade vs. copper rougher recovery (125µm).....	347

Figure 13.62 Alice – copper head grade vs. recovery	349
Figure 13.63 Copper head grade vs. recovery	352
Figure 13.64 Gold head grade vs. recovery.....	353
Figure 13.65 Molybdenum head grade vs. recovery	354
Figure 13.66 Molybdenum head grade vs. recovery	360
Figure 13.67 Molybdenum cleaner flotation – seawater vs. tap water	362
Figure 13.68 Molybdenum cleaner – tap water test.....	363
Figure 13.69 Copper head grade vs. Cu recovery.....	374
Figure 13.70 Gold head grade vs. recovery.....	378
Figure 13.71 Molybdenum head grade vs. recovery	379
Figure 13.72 Flowsheet of Flotation Testwork.....	382
Figure 14.1 Productora model areas, drillhole traces and fault blocks coloured	387
Figure 14.2 Ca:K:Na ternary plot showing bimodal alteration assemblage diverging from precursor rhyodacitic whole rock compositions (~160,000 down hole multi-element geochemistry data points). 394	
Figure 14.3 Al:K:Fe ternary plot demonstrating alteration index classification of ~200,000 data points relating to every drillhole sample interval within the Productora Project drillhole database.	395
Figure 14.4 Probability plots showing the correlation of Cu & Mo grade with each of the alteration domains. Note: K-spar and Sericite domains are equally likely to host mineralisation.	395
Figure 14.5 750m RL Level Slice through the 3D Alteration Model	396
Figure 14.6 Left: 750mRL level slice through the 3D Tourmaline Breccia Model with Leapfrog 3D Cu isosurface contours. Right: 3D view of Breccia model.....	397
Figure 14.7 750m RL slices through 3D model of acid intrusives and associated acid alteration carapace (left), 3D isosurface of >3wt% Pyrite domain (right).	398
Figure 14.8 S:Na Ratio - 750mRL slice through S:N ratio model. Warm colours depict high S:Na ratios which shown a moderate correlation with proximal alteration assemblages and Cu mineralisation. 399	
Figure 14.9 Example of use of loGAS and Cu:S ratios for copper species flagging at Productora. 401	
Figure 14.10 Comparison of conceptual interpretation, top, to coded model, bottom on EW section 6822215mN.....	415
Figure 14.11 Productora sample lengths.....	422
Figure 14.12 Comparison of distributions using box and whisker plots for Cu, top, and Au, bottom	423
Figure 14.13 Scatterplots between Cu and Au for highest grade domains	424
Figure 14.14 Comparison of distributions using box and whisker plots for Fe, top, and S, bottom...	425
Figure 14.15 Scatterplots between Fe and S for Breccia and Stage 2 domains	426
Figure 14.16 Comparison of distributions using box and whisker plots for Fe, top, and S, bottom...	427
Figure 14.17 Comparison of distributions using box and whisker plots for Al, top, and K, bottom....	428
Figure 14.18 Potassium and aluminium by domain.....	429
Figure 14.19 Iron and sulphur by domain	429
Figure 14.20 Normal score variogram model for mid area Cu high grade and low grade combined	450
Figure 14.21 Cross section at 6822215mN displaying a georeferenced interpreted distribution of breccia facies from Escolme (2016).....	453

Figure 14.22	Northing trend validation for Cu in domain 50022	460
Figure 14.23	Visual validation of Cu for EW section 6822215 mN	461
Figure 14.24	Visual validation of Cu for section 6821915 mN	461
Figure 14.25	Graphical results of alteration mineral sample flagging at Alice	465
Figure 14.26	Statistical review of copper assay results from Alice drilling. Note: Population breaks	465
Figure 14.27	Statistical review of the "chalcopyrite dominant" flagged samples	466
Figure 14.28	Lithology and select assays shown from the channel sampling along Docherty Road. (HCH, 2016)	466
Figure 14.29	Section example of mineralisation domain creation, looking north (HCH, 2016)	467
Figure 14.30	Example of copper oxide mineral flagging of Alice drilling	467
Figure 14.31	Alice sample lengths	468
Figure 14.32	Plan view of Classified Resource in the Alice deposit (Indicated Resources shown in red, Inferred in yellow)	472
Figure 14.33	Oblique view looking northeast displaying Indicated and Inferred resource blocks +0.2% CuEq, coloured by CuEq% grade. (HCH, 2022)	476
Figure 14.34	Long section looking NE showing lithological domains comprising Cuerpo 1, 2 and 3. (HCH, 2022)	481
Figure 14.35	Cross sections looking NW showing lithological domains comprising Cuerpo 1, 2 and 3. (HCH, 2022)	482
Figure 14.36	Combined geological model of Cortadera in plan-view illustrating the key lithological units (excluding host rocks). (HCH, 2022)	482
Figure 14.37	Plan view showing the Cortadera dyke model used for March 2022 Mineral Resource Estimate (HCH, 2022)	483
Figure 14.38	Cross section showing the final Cu% estimation domain (grey) for Cuerpo 3 compared to the original 1.2% cpy interpolant (red). Calcium-rich alteration front (blue) and 2% A- + B- vein interpolant (green) shown for reference.	487
Figure 14.39	Final Cu% estimation domains (grey) compared to the original cpy interpolants (red). Calcium-rich alteration front (blue) and 2% A- + B- vein interpolants (green) shown for reference. ..	488
Figure 14.40	Comparison between Cu% and Au interpolants at 500 mRL. Drillholes displaying Cu% grades on left image and Au grades on right image.	489
Figure 14.41	A cross section through the Ann-Mason Porphyry deposit at Yerington, showing the trace element distribution (Cohen, 2011 and Halley et al., 2015).	490
Figure 14.42	Plan section comparison between Cu% and Mo interpolants at 500 mRL. Drillholes displaying Cu% grades on left image and Mo grades on right image.	490
Figure 14.43	Plan view showing the 0.1% CuEq interpolant (blue) with 1% A- + B-vein interpolant (grey) and HG Cu% estimation domains (red) for reference	491
Figure 14.44	Cross section (looking SE) showing final weathering model (fresh is green, transitional is blue, oxide is red) compared to drillholes displaying sulphide percentage and the location of intrusive porphyries	492
Figure 14.45	Cross section (looking SE) showing final weathering model compared to logged regolith (fresh is green, transitional is blue, oxide is red)	493
Figure 14.46	Plan view of the area of Cuerpo 1 which lies outside the current HCH tenement boundary.	494
Figure 14.47	Histogram of Cortadera sample lengths	495
Figure 14.48	Histogram of Cortadera composite lengths	496

Figure 14.49 Oblique cross section of Cuerpo 3 showing Cu% estimation domains used for mineral resource	498
Figure 14.50 Variogram for IND field – Cuerpo 3	506
Figure 14.51 Normal Scores Variogram for Cu% HG_CIK domain – Cuerpo 3	507
Figure 14.52 Normal Scores Variogram for AG – Cuerpo 3	508
Figure 14.53 Box-whisker plots showing Cu% grade distributions for each initial estimation domain	513
Figure 14.54 Log-probability plot for Cuerpo 3 Cu%, showing interpreted ‘breaks’ in the grade population to be used as cut-offs for the binary indicator coding.....	514
Figure 14.55 Indicator estimate on binary fields BIND and BINDH showing the probability of a block being above 0.2% (left) and 0.5% (right). Plan view section at 500 mRL.....	515
Figure 14.56 Iterative CIK sub-domain selection, showing two different probability threshold selections (from v1 (left) and v7 (right) estimates). Plan view section at 300 mRL.	516
Figure 14.57 Distribution of binary coded samples within each of the CIK sub-domains and log-probability plot showing grade distributions within each sub-domain.	517
Figure 14.58 Boundary analysis (completed using Snowden Supervisor) comparing HG and MG Cu% CIK sub-domains for Cuerpo 3 justifying the use of a one-way soft boundary. Schematic shown to the right shows the typical trend displayed by one-way soft boundaries.	518
Figure 14.59 Scatter plot between Cu% (y-axis) and AU (x-axis) showing strong correlation between two elements.	521
Figure 14.60 Composites selected in CIK sub-domains for Cuerpo 3 HG Au estimate	522
Figure 14.61 Boundary analysis (completed using Snowden Supervisor) comparing MG and LG CIK Au sub-domains for Cuerpo 3 justifying the use of a one-way soft boundary. Schematic shown to the right shows the typical trend displayed by one-way soft boundaries (HCH, 2022).....	523
Figure 14.62 Various cross-section views showing Ag estimates for each Cuerpo. (Cuerpo 1 – top left, Cuerpo 2 – top right, Cuerpo 3 – bottom left)	528
Figure 14.63 Various cross-section views showing Mo estimates for each Cuerpo. (Cuerpo 1 – top left, Cuerpo 2 – top right, Cuerpo 3 – bottom left)	532
Figure 14.64 Plan view of the Cuerpo 2 iron oxide horizon interpretation, showing geology model compared to drillhole Cu% grades.....	533
Figure 14.65 Example of mixed grade distribution in Cuerpo 1 iron oxide horizon	534
Figure 14.66 Log-probability plot for Cuerpo 2 Cu%, showing interpreted ‘break’ in the grade population to be used as cut-offs for the binary indicator coding.	535
Figure 14.67 Cross-section showing indicator estimate on binary field BIND showing the probability of a block being above 0.30%. Long-section view at 6,813,935 mN.	537
Figure 14.68 CIK sub-domain selection for iron oxide horizon above Cuerpo 2. Long-section view at 6,813,935 mN.....	537
Figure 14.69 Plan-view section at 950 mRL showing Cuerpo 2 Cu% estimate within iron oxide horizon compared to the 10 and 20 series porphyries.....	540
Figure 14.70 Plan-view section at 950 mRL showing Cuerpo 2 Au estimate within iron oxide horizon compared to the 10 and 20 series porphyries.....	540
Figure 14.71 Log-histogram (left) and log-probability plot (right) showing near log-normal distribution of Mo grades for Cuerpo 3 within iron oxide horizon.	541
Figure 14.72 Plan-view section at 950 mRL showing Cuerpo 2 Mo estimate within iron oxide horizon compared to the 10 and 20 series porphyries.....	542
Figure 14.73 Plan-view section at 950 mRL showing Cuerpo 2 Ag estimate within iron oxide horizon	543

Figure 14.74 Cross section (at 6,813,840 mN) looking north through Cuerpo 2 showing the bulk density assignment to the block model.....	545
Figure 14.75 Creation of validation data set for Cuerpo 3 Cu% LG domain	546
Figure 14.76 Validation trend plot – Cu% – Cuerpo 1 - HG domain. Red = composite grades, blue = declustered composite grades, black = estimated block grades.	548
Figure 14.77 Visual validation of drillholes versus modelled Cu% grade. Plan view (top) showing location of sections A-A' and B-B'; cross sections shown on bottom.	549
Figure 14.78 Long-section view looking north showing Indicated and Inferred blocks where Cu% \geq 0.2	550
Figure 14.79 Long-section looking north showing mining shapes used to define Reasonable Prospects of Eventual Economic Extraction by Block Cave Mining. (HCH, 2022)	553
Figure 14.80 Long-section view looking north showing pit shell surfaces used to define Reasonable Prospects of Eventual Economic Extraction by Open Pit Mining. (HCH, 2022)	556
Figure 14.81 Long-section view looking north showing pit shell surfaces and block cave mining shapes used to define Reasonable Prospects of Eventual Economic Extraction by Open Pit Mining. (HCH, 2022)	556
Figure 14.82 Plan view showing pit shell surfaces and block cave mining shapes used to define Reasonable Prospects of Eventual Economic Extraction by Open Pit Mining. (HCH, 2022)	557
Figure 14.83 Oblique view looking northwest displaying Inferred resource blocks +0.2% CuEq, coloured by copper equivalent grade. (HCH, 2022)	560
Figure 14.84 Surface Expressions of Main and Parallel lodes at San Antonio	562
Figure 14.85 Typical cross section of the San Antonio lodes (looking north at 6,818,965mN).	563
Figure 14.86 Cross Section on San Antonio showing chronology of different interpretations.....	564
Figure 14.87 Long section looking east showing mined voids as informed by historic pickups and drone survey (HCH, 2022)	566
Figure 14.88 Long section looking east showing San Antonio depleted blocks (HCH, 2022).....	567
Figure 14.89 Histograms of San Antonio sample lengths by lode	568
Figure 14.90 Domain Analysis by lode for Au, Ag and Cu% elements.....	569
Figure 14.91 Cu/S scatter plot showing presence of non-chalcopryrite species	569
Figure 14.92 Variograms for Main lode Cu% variable	573
Figure 14.93 KNA for Main lode Cu% variable	574
Figure 14.94 Comparison of different estimation methodologies for the San Antonio Main lode Cu% estimate (plan view section at 1,190 mRL)	575
Figure 14.95 Comparison of OK and ID ³ methodologies for the San Antonio HW1 lode Cu% estimate (long section view looking east)	576
Figure 14.96 Validation trend plot – Cu% – Main Lode search pass 1	578
Figure 14.97 Visual validation of drillholes versus model Cu% grade – Main Lode, Cross Section 6818775mN.....	578
Figure 14.98 Plan view on 1190mRL showing Main domain and Cu% in the drillholes and mineralised block model.	579
Figure 14.99 Oblique view looking west Blocks CuEq% \geq 0.2 , and insitu =0. Inferred only.	580
Figure 14.100 Longsection looking West, showing Inferred and Unclassified block extents across San Antonio	581
Figure 14.101 Costa Fuego grade-tonnage curves – (Open pit – above and Underground – below)	585

Figure 20.1 Environmental Assessment Process	594
Figure 20.2 Stakeholder Engagement Plan	596

Tables

Table 1.1 Report Qualified Persons	32
Table 1.2 Frontera JV option and 100% owned leases at San Antonio	38
Table 1.3 Ownership History	40
Table 1.4 Productora Maiden Resource (Central) declared under the JORC 2004 edition and were rounded to a single decimal place for reporting purposes	42
Table 1.5 Along-strike extensions (added to the Central resource) was declared under the JORC 2004 edition and rounded to a single decimal place for reporting purposes. This resource was reported at a cut-off of greater than or equal to 0.3% Cu.	42
Table 1.6 Resource Revision 2 Resource table. This Resource was declared under the JORC 2012 edition and was reported at a cut-off of greater than or equal to 0.25% Cu.	43
Table 1.7 Productora JORC 2012 Ore Reserve, March 2016*	43
Table 1.8 Productora Mineral Resource Summary (using +0.25% CuEq cut-off grade), 29 October 2021*	43
Table 1.9 Cortadera Mineral Resource Summary – reported by classification (29th October 2021) and by open pit (top), underground (middle) and total (bottom)*	44
Table 1.10 Comminution testwork results – all samples	59
Table 1.11 Costa Fuego Project Mineral Resource Summary – reported by classification (31st March 2022) *	64
Table 1.12 Cortadera Mineral Resource Summary – reported by classification (31st March 2022) and by open pit (top), underground (middle) and total (bottom) *	65
Table 1.13 Productora Mineral Resource Summary – reported by classification (31st March 2022) *	65
Table 1.14 San Antonio Mineral Resource Summary – reported by classification (31st March 2022) *	66
Table 1.15 Future Work Programme	70
Table 2.1 Definitions	73
Table 4.1 SMEA SpA mining tenement holding for Productora	78
Table 4.2 Cortadera Ownership History	84
Table 4.3. Summary of Cortadera mining rights	84
Table 4.4 Purísima mining rights	84
Table 6.1 Ownership History	92
Table 6.2 Productora Maiden Resource (Central) declared under the JORC 2004 edition and were rounded to a single decimal place for reporting purposes	96
Table 6.3 Along-strike extensions (added to the Central resource) was declared under the JORC 2004 edition and were rounded to a single decimal place for reporting purposes. This resource was reported at a cut-off of greater than or equal to 0.3% Cu.	97
Table 6.4 Resource Revision 2 Resource table. This Resource was declared under the JORC 2012 edition and was reported at a cut-off of greater than or equal to 0.25% Cu.	98
Table 6.5 Productora JORC 2012 Ore Reserve, March 2016	98
Table 6.6 Productora Mineral Resource Summary (using +0.25% CuEq cut-off grade), 29 October 2021*	98
Table 6.7 Production history from the Productora underground mine	99

Table 6.8 CortADERA Mineral Resource Summary – reported by classification (29th October 2021) and by open pit (top), underground (middle) and total (bottom)*	104
Table 9.1 Results from Geochronological and Mineragraphic Studies at CortADERA.....	146
Table 9.2 Comparison between logging codes (as defined by Tobey, 2012) and intrusion series at CortADERA	148
Table 10.1 Final applied regression ranges and formulas for the conversion of pulp pycnometer density data	169
Table 10.2 Analysis of Alice density data.....	170
Table 10.3 Breakdown of the drilling completed by Hot Chili Limited from 2019 – 2021.....	171
Table 10.4 Significant drillhole intercepts for Phase 1 - 4 drilling at CortADERA	176
Table 10.5 Nominal drill bit size changes in RC drilling	180
Table 10.6 Updated Alteration logging template following 2021 review	186
Table 10.7 Updated Vein logging template following 2021 review	186
Table 10.8 Updated Vein logging template following 2021 review	191
Table 10.9 Significant drillhole intercepts for HCH drilling at San Antonio	193
Table 10.10 Nominal drill bit size changes in RC drilling	194
Table 12.1 Comparison of samples recovery and sample weights for Alice and Productora	219
Table 12.2 CortADERA Drilling Program QAQC Insertion Rates	223
Table 12.3 HCH QAQC CRM details	224
Table 12.4 OREAS-501b Reference Material Statistics as recorded in HCH database.....	224
Table 12.5 Performance statistics for OREAS-501b CRM results.....	225
Table 12.6 OREAS-502 Reference Material Statistics as recorded in HCH database.....	227
Table 12.7 Performance statistics for OREAS-502 CRM results.....	227
Table 12.8 OREAS-502c Reference Material Statistics as recorded in HCH database.....	229
Table 12.9 Performance statistics for OREAS-502c CRM results.....	229
Table 12.10 OREAS-503b Reference Material Statistics as recorded in HCH database	232
Table 12.11 Performance statistics for OREAS-503b CRM results.....	232
Table 12.12 OREAS-504 Reference Material Statistics as recorded in HCH database.....	234
Table 12.13 Performance statistics for OREAS-504 CRM results.....	235
Table 12.14 OREAS-505 Reference Material Statistics as recorded in HCH database.....	237
Table 12.15 Performance statistics for OREAS-505 CRM results.....	237
Table 12.16 OREAS-902 Reference Material Statistics as recorded in HCH database.....	240
Table 12.17 Performance statistics for OREAS-902 CRM results.....	240
Table 12.18 IN-BMF-172 Reference Material Summary Statistics as included in the HCH database	242
Table 12.19 Statistics from IN-BMF-172 CRM results for all elements as exported from HCH database	242
Table 12.20 IN-BMF-333 Reference Material Summary Statistics as included in the HCH database	244
Table 12.21 Statistics from IN-BMF-333 CRM results for all elements as exported from HCH database	244
Table 12.22 Performance statistics for uncertified coarse blanks	246

Table 12.23 San Antonio Drilling Program QAQC Insertion Rates.....	254
Table 12.24 HCH CRM Details	255
Table 12.25 OREAS-501b Reference Material Statistics as recorded in HCH database	256
Table 12.26 Performance statistics for OREAS-501b CRM results.....	256
Table 12.27 Performance statistics for OREAS-501b CRM results OREAS-22c Reference material summary statistics as recorded in the HCH database	258
Table 12.28 Performance statistics for OREAS-22c CRM results	258
Table 12.29 Performance statistics for uncertified coarse blanks	260
Table 12.30 Investigation results for Qtz Blanks >30ppm Cu.....	261
Table 13.1 Size-by-size analysis of oxide samples	274
Table 13.2 Summary of size-by-size sequential analysis	274
Table 13.3 Bottle roll test results.....	275
Table 13.4 Northern Oxide sequential Cu and QEMScan analysis	276
Table 13.5 Bottle roll test results (pH=1)	277
Table 13.6 Southern Mantos sequential Cu and QEMScan analysis	278
Table 13.7 Southern Mantos pH=1 bottle roll test results.....	278
Table 13.8 Main Pit sequential Cu and QEMScan analysis	280
Table 13.9 Main Pit pH=1 bottle roll test results	280
Table 13.10 Santa Innes sequential Cu and QEMScan analysis	282
Table 13.11 Santa Innes pH=1 bottle roll test results	283
Table 13.12 Alice and Central Eastern Oxide Sequential Cu analysis	284
Table 13.13 Bottle roll test results (pH=1)	284
Table 13.14 Summary of optimal Cu extraction vs. acid consumption	287
Table 13.15 Crushing and UCS test results.....	288
Table 13.16 PSD summarised results	290
Table 13.17 Agglomeration and leach conditions	291
Table 13.18 Agglomeration level and moisture content.....	291
Table 13.19 Hydrodynamic columns testing conditions.....	295
Table 13.20 Salts concentration used to prepare synthetic raffinate.....	296
Table 13.21 Mineralized material agglomeration acid and column leach solution acid.....	298
Table 13.22 Bottle rolls vs. column leach results.....	298
Table 13.23 Comminution tests – summarised results.....	309
Table 13.24 Bond Abrasion Index – summarised results	310
Table 13.25 Bond Abrasion Index – Productora deposit samples.....	311
Table 13.26 Bond Abrasion Index – Alice deposit samples.....	311
Table 13.27 Comminution testwork results – all samples.....	311
Table 13.28 Productora standardised flotation scheme	314
Table 13.29 Productora – Central – Primary grind size copper rougher results.....	317
Table 13.30 Productora – Central – FD-6 flotation scheme	322

Table 13.31 Productora – Central – rougher, cleaner and locked cycle copper results	326
Table 13.32 Productora – Central – rougher, cleaner and locked cycle molybdenum results	326
Table 13.33 Productora – Central – rougher, cleaner and locked cycle gold results	327
Table 13.34 Productora – >10% acid soluble copper (transitional containing) samples – copper mineral distribution	330
Table 13.35 Productora – >10% acid soluble copper (transitional containing) samples – flotation conditions	332
Table 13.36 >10% acid soluble copper samples – rougher, cleaner and locked cycle copper results	333
Table 13.37 >10% acid soluble copper samples – rougher, cleaner and locked cycle molybdenum results	333
Table 13.38 >10% acid soluble copper samples – rougher, cleaner and locked cycle gold results ..	333
Table 13.39 >10% acid soluble copper samples – rougher, cleaner and locked cycle gold results ..	336
Table 13.40 Alice – primary grind size copper rougher results.....	341
Table 13.41 Alice – rougher, cleaner and locked cycle copper results	343
Table 13.42 Alice – rougher, cleaner and locked cycle molybdenum results	343
Table 13.43 Alice – rougher, cleaner and locked cycle gold results.....	343
Table 13.44 Cayenne – primary grind size copper rougher results	347
Table 13.45 Alice – rougher, cleaner, and locked cycle copper results	349
Table 13.46 Comprehensive concentrate analysis	350
Table 13.47 Tailings sample make up	356
Table 13.48 Copper concentrate and tailings thickening results	357
Table 13.49 Flotation tailings rheology results.....	359
Table 13.50 Molybdenum – rougher, cleaner and locked cycle copper results.....	361
Table 13.51 XRD results – Productora – Central (In Pit Fresh samples)	364
Table 13.52 XRD results – Productora – Habanero (In Pit samples)	365
Table 13.53 XRD results – Alice samples.....	365
Table 13.54 XRD results – Productora - >10% acid soluble copper (transitional containing) samples	366
Table 13.55 XRD results – Productora – Cayenne (Out of Pit samples).....	366
Table 13.56 QEMScan Mineral Mass Distribution – Productora – Central (In Pit Fresh samples)	367
Table 13.57 QEMScan mineral mass distribution – Productora – Habanero Lode samples	369
Table 13.58 QEMScan mineral mass distribution – Alice samples	370
Table 13.59 QEMScan mineral mass distribution – >10% acid soluble copper samples.....	371
Table 13.60 QEMScan mineral mass distribution – Cayenne samples.....	372
Table 13.61 Productora – Central – rougher, cleaner and locked cycle copper results	375
Table 13.62 Alice – rougher, cleaner and locked cycle copper results	375
Table 13.63 >10% Acid Soluble Copper composites – rougher, cleaner and locked cycle copper results	376
Table 13.64 Cayenne – rougher, cleaner and locked cycle copper results	377
Table 13.65 Molybdenum – rougher, cleaner and locked cycle results	380

Table 13.66 Metallurgical Sample Details.....	381
Table 13.67 Recleaner Concentrate Assays for Sulphide Testwork	382
Table 13.68 Flotation testwork results – Sample CRP0013D – P80 Grind Size of 106 µm	382
Table 13.69. Flotation testwork results – Sample CRP0013D – P80 Grind Size of 150 µm	383
Table 13.70 Flotation testwork results - Sample CRP0011D – P80 Grind Size of 106 µm.....	383
Table 13.71. Flotation testwork results – Sample CRP0011D – P80 Grind Size of 150 µm	383
Table 13.72 Summary of Comminution Testwork Results.....	384
Table 14.1 Drillhole data edits to lithology table.....	389
Table 14.2 Drillhole data edits to alteration table	389
Table 14.3 Drillhole data edits to weathering table	390
Table 14.4 Drillhole data edits to faults table	390
Table 14.5 Drillhole data edits to Mineralisation table	390
Table 14.6 Drillhole data edits to Veining table.....	390
Table 14.7 Drillholes excluded from the database	391
Table 14.8 Productora drillhole database	391
Table 14.9 Wireframes used for flagging drillholes and models	402
Table 14.10 Drillholes and models coding	403
Table 14.11 Block model dimensions	404
Table 14.12 Dynamic anisotropy trend wireframes	405
Table 14.13 Categorical indicator coding of drillholes	406
Table 14.14 Ratio calculation for drillholes	407
Table 14.15 Categorical variogram models – Mid Area.....	408
Table 14.16 Categorical variogram models – South Area	409
Table 14.17 Categorical variogram models – North Area.....	410
Table 14.18 Search strategy for categorical estimation for mid area	411
Table 14.19 Search strategy for categorical estimation for south area	411
Table 14.20 Search strategy for categorical estimation for north area	411
Table 14.21 Combination of variogram and search for categorical estimation mid area	412
Table 14.22 Combination of variogram and search for categorical estimation south area	412
Table 14.23 Combination of variogram and search for categorical estimation north area	413
Table 14.24 Model coding for copper domaining.....	414
Table 14.25 Model coding for molybdenum domaining	417
Table 14.26 Model coding for iron and sulphur domaining.....	419
Table 14.27 Model coding for potassium and aluminium domaining.....	419
Table 14.28 Copper statistics.....	430
Table 14.29 Gold statistics.....	431
Table 14.30 Molybdenum statistics.....	432
Table 14.31 Cobalt statistics	434
Table 14.32 Calcium statistics	435

Table 14.33 Iron statistics	435
Table 14.34 Sulphur statistics	436
Table 14.35 Potassium statistics	438
Table 14.36 Aluminium statistics	439
Table 14.37 Correlation matrix – Mid Area – F3B (1,2) LG Cu – 50011	442
Table 14.38 Correlation matrix – Mid Area – F3B(1,2) HG Cu- 50012.....	443
Table 14.39 Correlation matrix – Mid Area – Stage 2 LG Cu – 50021	443
Table 14.40 Correlation matrix – Mid Area – Stage 2 HG Cu – 50022	444
Table 14.41 Grade variogram models – Mid Area.....	445
Table 14.42 Grade variogram models – South Area	447
Table 14.43 Grade variogram models – North Area.....	449
Table 14.44 Search strategy for grade estimation.....	452
Table 14.45 Combination of variogram and search for grade estimation mid area.....	454
Table 14.46 Combination of variogram and search for grade estimation south area.....	456
Table 14.47 Combination of variogram and search for grade estimation south area.....	458
Table 14.48 Global comparison of Cu composites and estimates	459
Table 14.49 List of mineralisation wireframes used for the Alice deposit model.....	468
Table 14.50 Validation of compositing samples to 2m for Alice	469
Table 14.51 Application and validation of top-cuts on 2m composites at Alice	469
Table 14.52 List of applied variograms and search ellipse directions	470
Table 14.53 Variables in the Alice Resource model	470
Table 14.54 Estimation sample selection and search distances – Alice	471
Table 14.55 List of wireframes used in classification for Alice.....	472
Table 14.56 Productora Mineral Resource Summary (using +0.25% CuEq cut-off grade), 29 October 2021.....	473
Table 14.57 Drillhole data edits to lithology table	478
Table 14.58 Drillhole data edits to Copper Soluble Assay table.....	479
Table 14.59 Rules applied to Assay table.....	480
Table 14.60 Examples of Query Filters used to assist in dyke modelling at El Fuego	484
Table 14.61 Grade cut-offs used for mineralised domain interpretations.....	485
Table 14.62 List of final wireframes used for estimation coding	493
Table 14.63 Grade estimation domains	497
Table 14.64 Cortadera mineralised domains top-cut analysis.....	499
Table 14.65 Variogram models for Limonites	502
Table 14.66 Variogram models for Cu%.....	504
Table 14.67 Variogram models for Ag	507
Table 14.68 Variogram models for MO.....	509
Table 14.69 Block model dimensions	510
Table 14.70 Cortadera volume model coding.....	511

Table 14.71 Cortadera Mineralisation model coding	511
Table 14.72 Cortadera Final Block Model Coding	512
Table 14.73 Cu% estimate cut-off grades used for probability estimate	515
Table 14.74 Cu% probability threshold selection.....	517
Table 14.75 Soft boundary usage for Cu% estimates	519
Table 14.76 Cu% search parameters	520
Table 14.77 Au estimation methodologies used by domain	521
Table 14.78 Soft boundary usage for Au estimates.....	524
Table 14.79 Au search parameters.....	525
Table 14.80 Ag estimation methodologies used by domain	526
Table 14.81 Soft boundary usage for Ag estimates.....	526
Table 14.82 Ag search parameters.....	527
Table 14.83 Mo estimation methodologies used by domain.....	529
Table 14.84 Soft boundary usage for Mo estimates	530
Table 14.85 Mo search parameters	531
Table 14.86 Comparison between lithology and Cu% grade for Cuerpo 2 iron oxide horizon	536
Table 14.87 Iron Oxide estimate types and cut-off grades/conditions used.....	536
Table 14.88 Cu%/Au probability threshold selection	538
Table 14.89 Cu%/Au search parameters.....	539
Table 14.90 Ag/Mo search parameters.....	542
Table 14.91 Bulk density value assignment.....	544
Table 14.92 Estimation validation – comparison of top-cut, declustered composites to output block model.....	547
Table 14.93 Key revenue and cost parameters for estimating the breakeven grade for Reasonable Prospects of Eventual Economic Extraction by Block Cave Mining	551
Table 14.94 The calculation of the breakeven caving grade to define Reasonable Prospects of Eventual Economic Extraction	552
Table 14.95 Key open pit optimisation parameters applied to generate a pit shell defining Reasonable Prospects of Eventual Economic Extraction	554
Table 14.96 Number of Drillhole Samples used in estimation	561
Table 14.97 List of final wireframes used for estimation coding	565
Table 14.98 San Antonio mineralised domains top-cut analysis	570
Table 14.99 Block model dimensions	571
Table 14.100 San Antonio volume model coding	572
Table 14.101 Block Model fields	572
Table 14.102 Estimation parameters	574
Table 14.103 Bulk Density Values by Lithology.....	577
Table 14.104 Estimation global validation – Cu%	577
Table 14.105 Costa Fuego Project Mineral Resource Summary – reported by classification (31st March 2022)	582

Table 14.106 Cortadera Mineral Resource Summary – reported by classification (31st March 2022)	583
Table 14.107 Productora Mineral Resource Summary – reported by classification (31st March 2022)	583
Table 14.108 San Antonio Mineral Resource Summary – reported by classification (31st March 2022)	583
Table 14.109 Costa Fuego Grade Tonnage CuEq cut-offs by classification (Open pit – top and Underground – bottom)	584
Table 26.1 Future Work Programme	605

1 SUMMARY

1.1 Introduction

At the request of Hot Chili Limited (HCH or the Company), Haren Consulting and ABGM have prepared the Mineral Resources for the Productora, Cortadera and San Antonio deposits contained within the Costa Fuego Copper Project (the Costa Fuego Project or the Project).

This Technical Report has been prepared for the Project to the standard of the Canadian National Instrument 43-101 – *Standards of Disclosure for Mineral Projects* (NI 43-101).

HCH is a mineral exploration company focused on the acquisition, exploration, and development of mineral properties in Chile.

Haren Consulting is an independent geological consulting firm based in Perth, Australia

ABGM is an independent mining consulting firm based in Perth, Australia.

The Qualified Persons for this assignment are as follows:

Table 1.1 Report Qualified Persons

Qualified Person Name	Title, Company	Items of QP Responsibility
Anton von Wielligh FAusIMM (325251)	Principal Mining Engineer and Director, ABGM	4, 5, 6, 13, 15, 16, 17, 18, 19, 20, 21, 22, 23, 24, 27
Elizabeth Haren MAIG (6646) MAusIMM (CP) (208050)	Director, Haren Consulting	1, 2, 3, 7, 8, 9, 10, 11, 12, 14, 25, 26

1.2 Property Description and Location

The Costa Fuego Project is located 17 kilometres (km) south of the regional township of Vallenar, in the Atacama region of Chile, in the low altitude coastal range belt (at ~800 m elevation).

The Costa Fuego Project contains three deposits with current Mineral Resources (Productora, Cortadera and San Antonio). The Project will leverage existing surface rights and the proposed central processing facilities at Productora, and existing infrastructure access for powerline and sea water pipeline easements.

The Project has a unique location, see Figure 1.1 and Figure 1.2, surrounded by existing infrastructure with the Project centre at Productora located just 15 minutes by car from Vallenar on the Pan-American Highway.

An aerodrome is located approximately 14km from Productora, and the Las Losas Port facility and Maintencillo power substation are located 55 km and 20 km away, respectively.



Figure 1.1 Costa Fuego Project location in Chile. (HCH, 2022)

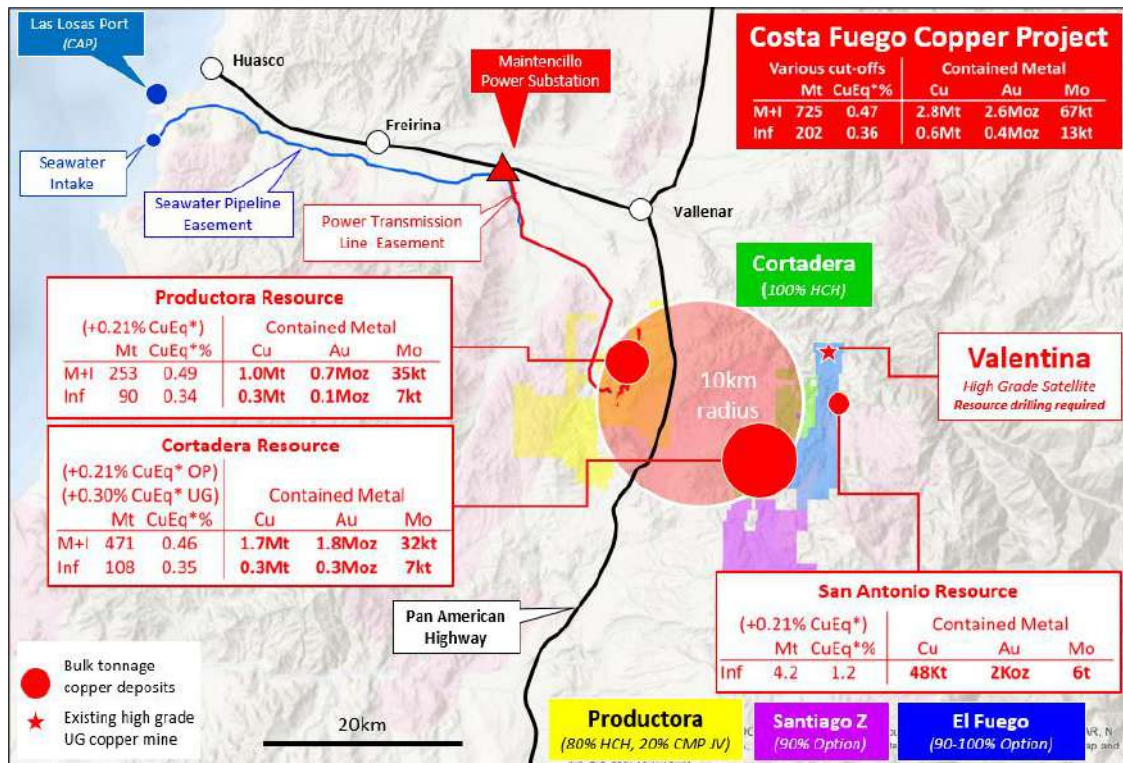


Figure 1.2 Location of Costa Fuego Project and Infrastructure relative to Vallenar, Chile. (HCH, 2022)

1.2.1 Productora

Productora is 100% owned by the Chilean incorporated company Sociedad Minera El Aguila SpA (SMEA). SMEA is a joint venture company – 80% owned by Sociedad Minera El Corazón Limitada (a 100% subsidiary of Hot Chili Limited (HCH) – ASX: HCH), and 20% owned by Compañía Minera del Pacífico S.A (CMP), a major Chilean iron ore producer.

In August 2015, a joint venture (JV) agreement and merger was established between SMEA and one of CMP’s wholly owned vehicles that resulted in the JV company, SMEA. This partnership has enabled security of the majority of surface rights required for developing key infrastructure for the project, as well as the majority of easements required for water and power transmission lines.

In addition, the JV agreement has consolidated the mining rights required for the development of Productora.

The only economic commitment to keep the project in good standing are mining patents, which can be summarized as a mining tax paid to the government on a yearly basis (March each year). Total mining patent costs for the year 2022 were around US\$75,000.

A 30-year lease agreement exists for the mining right Uranio 1-70 between the Chilean Commission of Nuclear Energy (CCHEN) and SMEA, dated 22nd August 2012. This agreement incurs an annual lease payment of US\$250,000 per year (paid no later than 31 August) and expires on 22 August 2042.

Productora has the following annual royalties:

- On the CCHEN mining right "Uranio 1 al 70": NSR for Non-gold = 2%; Gold = 4% and Non-metallic = 5%
- On the mining right "Montosa 1 al 4": NSR = 3% all products
- On the mining right "Zapa 1 al 6": Gross Royalty = 1% all products

1.2.2 Cortadera

HCH, through its 100% subsidiary company Sociedad Minera Frontera SpA (Frontera), controls an area measuring approximately 17,000 ha at Cortadera through various 100% purchase option agreements with private mining title holders and 100% owned tenure.

All mining tenements are in good standing and all mining requirements have been met for the exploration phase. At this stage, there are no legal requirements for any kind of bonds to be issued.

The Cortadera Mineral Resource Estimate is contained within two Mining Rights:

- 'CORTADERA 1/40' (374 hectares). Mining tax (or cost per year to keep the mining right) USD 2,673. Such mining right 1/40 is owned 100% by Frontera (wholly owned by Hot Chili).
- 'Purísima 1/8 (1/2-5/6)'. (20 hectares). Mining tax (or cost per year to keep the mining right) USD 142. Such mining right is owned 100% by Frontera (wholly owned by Hot Chili) with a 1.5% NSR attached.

The current exploration activities for Cortadera have been approved under the Environmental Approval number 48, dated March 24, 2021, granted by the Environmental Assessment Service.

Surface land access for exploration activities (and for the future mining operations) have also been reached with the owner, Mr. Pedro Prokurika Morales by agreement acknowledged and approved by the local Court of Vallenar on March 30th, 2022.

A map of HCH mining rights under WGS84 is shown below (Figure 1.4).

1.2.3 San Antonio

Hot Chili Limited, through Frontera, executed an option agreement with a private party to earn a 90% interest in the San Antonio copper-gold project over a four-year period. The proposed JV involves an option agreement over 27 mining rights (~4,727ha), whereby full ownership of 90% of the mining rights of the project will be transferred upon satisfaction of a payment of US\$300,000 by November 2022 and then a final payment of US\$6,700,000 a year after.

Exploration by Frontera at San Antonio shall be at its discretion and the owner will have the right to lease to any third party the exploitation of the mining rights with an annual cap of 50,000 tonnes of ore until exercise of the option.

Frontera also has other 100% owned leases around the project.

The leases in the JV option are shown below (Table 1.2).

Table 1.2 Frontera JV option and 100% owned leases at San Antonio

Licence ID	Holder	% Interest	Licence Type	Area (ha)
Santiago 21 al 36	Frontera	90%	Exploitation concession	76
Santiago 37 al 43	Frontera	90%	Exploitation concession	26
Santiago A, 1 al 26	Frontera	90%	Exploitation concession	236
Santiago B, 1 al 20	Frontera	90%	Exploitation concession	200
Santiago C, 1 al 30	Frontera	90%	Exploitation concession	300
Santiago D, 1 al 30	Frontera	90%	Exploitation concession	300
Santiago E, 1 al 30	Frontera	90%	Exploitation concession	300
Prima Uno	Frontera	90%	Exploitation concession	1
Prima Dos	Frontera	90%	Exploitation concession	2
Santiago 15 al 19	Frontera	90%	Exploitation concession	25
San Antonio 1 al 5	Frontera	90%	Exploitation concession	25
Santiago 1 AL 14 Y 20	Frontera	90%	Exploitation concession	75
Mercedes 1 al 3	Frontera	90%	Exploitation concession	50
Romero 1/31	Frontera	90%	Exploitation concession	31
Porfiada A	Frontera	90%	Exploration concession	200
Porfiada B	Frontera	90%	Exploration concession	300
Porfiada C	Frontera	90%	Exploration concession	300
Porfiada D	Frontera	90%	Exploration concession	300
Porfiada E	Frontera	90%	Exploration concession	300

Licence ID	Holder	% Interest	Licence Type	Area (ha)
Porfiada F	Frontera	90%	Exploration concession	300
Porfiada G	Frontera	90%	Exploration concession	200
Porfiada VII	Frontera	90%	Exploration concession	300
Porfiada VIII	Frontera	90%	Exploration concession	300
Porfiada IX	Frontera	90%	Exploration concession	300
Porfiada X	Frontera	90%	Exploration concession	200
Kreta 1 al 4	Frontera	90%	Exploitation concession	16
Mari 1 al 12	Frontera	90%	Exploitation concession	64

1.3 Accessibility, Climate, Local Resources, Infrastructure and Physiography

The Project can be accessed by following the main sealed Pan-American Highway connecting Vallenar to Coquimbo in the south.

The Project has a favourable location surrounded by infrastructure which can be utilised for developing a greenfield copper project, and benefits from the following infrastructure items:

- Regional township of Vallenar
- Pan-American Highway
- Airport located approximately 3km south of Vallenar
- Las Losas Port
- Power substations located approximately 20km northwest at Maintencillo, connected to the Chilean electrical grid.

1.4 History

1.4.1 Productora

The Productora camp has a long mining history for iron, copper and gold extending back to pre-Hispanic times. Historical iron mining has occurred at the La Chulula, La Bandera, Mariposa, Carmen, and La Negra mines. Copper mining in the past century has occurred regionally and locally at the Productora and Santa Innes mines (operated by Playa Brava and ENAMI), Remolina, and Montserrat mines. In addition, there are more than 80 smaller pits, workings, or mineralised outcrops in the area containing iron, copper, or gold mineralisation.

In the 1980s, the Chilean Commission for Nuclear Energy (CCHEN) explored the area near and to the south of the Productora mine for uranium. At least ten shallow (35 to 101m) Reverse Circulation (RC) holes were completed and while minor uranium oxide was intersected, no significant deposits were found.

CCHEN completed mapping, surface geochemical sampling, ground spectrometry and magnetometry, trenching, drilling (28 shallow percussion holes) and resource estimation, focusing almost entirely on the near-surface, secondary uranium potential at Productora.

General Minerals Corporation (GMC) acquired the Productora area in 1995 to search for a Candelaria type iron-oxide-copper-gold (IOCG) deposit. In 1997, eight reverse circulation drillholes (PR-1 to PR-8) were completed. Additional work also involved compilation of earlier mapping, surface geochemical sampling, ground geophysics surveys (IP) and percussion drilling.

In 1999, GMC entered into a joint venture with Teck Corporation and completed an additional eleven reverse circulation holes (PR-9 to PR-19). The holes targeted secondary copper enrichment zones in the southern portions of the central lease at Productora.

HCH completed acquisition of the main tenement package in 2012.

Table 1.3 Ownership History

Year	Company
1980's	Chilean Commission for Nuclear Energy (CCHEN) and several private tenement owners
1995 - 1999	General Minerals Corporation (GMC) explored the area
1999 - 2005	GMC (in joint venture with Teck Corp) explored the area
2008 - 2015	HCH Limited through its wholly owned Chilean subsidiary Sociedad Minera El Águila options and consolidates the area
2015 - present	Joint venture agreement between HCH (80%) and CMP (20%) owners of Sociedad Minera El Águila SpA.

1.4.2 Cortadera

The Cortadera deposit underwent substantial drilling between 2010 - 2013 while the deposit was under the control of Minera Fuego Limited (Minera Fuego), during an option agreement they had entered into with Sociedad Contractual Minera Carola (SCM Carola).

Drilling completed prior to HCH securing the deposit comprised 39 diamond drillholes for 23,231m, with this drilling successful in defining three mineralised porphyries (Cuerpo 1, 2 and 3).

Following execution of the Cortadera option agreement in February 2019, HCH undertook a resource drill out focussed on extending and infilling previously defined mineralisation. HCH drilling was successful in improving geological understanding, growing the deposit size, and discovering a bulk-tonnage high grade zone at Cortadera.

Drilling completed by HCH between February 2019 and December 2021 comprised 137 RC holes, and 38 RCDD holes and 12 DD holes for a total of 31,388m of RC, 33,301m of RCDD and 8,538m of DD.

1.4.3 San Antonio

In November 2017, HCH's subsidiary company Frontera executed a joint venture (JV) option agreement with the private owner to earn a 90% interest in the San Antonio copper-gold project over a four-year period.

As part of the JV arrangement, the San Antonio owner has the right to lease exploitation of the mining rights to any third party with an annual cap of 50,000t of ore until exercise of the option. While lease mining activities are only small-scale, the information produced is invaluable in providing further insight into the potential for direct mine extensions of high-grade copper mineralisation. The mine has been exploited over a 200m strike length to a vertical depth of 130m.

Historical production records indicate sulphide copper grades of approximately 3% to 3.5% (associated with chalcopyrite and bornite) were exploited in the upper levels of the underground, gradually decreasing to 1.5 to 2% at the base of development.

Since executing the option agreement, HCH has initiated multiple work streams including reconnaissance mapping and geochemical sampling over priority areas, with legacy data compilation completed.

Drilling completed by HCH in 2018 comprised 41 RC holes for a total of 4,922m.

1.4.3.1 Previous Resources and Previous Reserve Estimates

1.4.3.1.1 Productora (including Alice)

There have been previous Resources and Reserves for the Productora and/or Alice deposits reported by HCH under:

- a) the Joint Ore Reserves Committee of the Australasian Institute of Mining and Metallurgy, Australian Institute of Geosciences and Minerals Council of Australia (JORC Code 2012 Edition) code
- b) the standard of the Canadian NI 43-101.

These previous estimates have been provided for historical context only and the Issuer is not treating these estimates as current.

1.4.3.1.2 JORC 2004 Resource, HCH, July 2011

Following the completion of initial project assessment, HCH commenced an extensive Resource definition drilling programme in August 2010 which was completed in early July 2011. A total of 141 RC holes for 28,308m and 22 DD holes for 5,012m were drilled by HCH and were used to define the maiden Resource (Table 1.4).

Table 1.4 Productora Maiden Resource (Central) declared under the JORC 2004 edition and were rounded to a single decimal place for reporting purposes

Productora Maiden Resource - 2011							
Classification	Tonnes (millions)	Grade			Contained Metal		
		Cu %	Au g/t	Mo ppm	Copper (tonnes)	Gold (ounces)	Molybdenum (tonnes)
Indicated	31.1	0.6	0.1	159	184,612	109,711	4,942
Inferred	54.0	0.6	0.1	138	298,062	179,895	7,476
Total	85.1	0.6	0.1	146	482,673	289,606	12,418

1.4.3.1.3 JORC 2004 Resource Revision 1, HCH, February 2013

Following on from the estimation of the maiden Resource, HCH commenced an extensive exploration and resource definition drilling programme in October 2011 to test for mineralisation along strike. This programme was completed in December 2012.

This revision was modelled exclusively outside the extents of the maiden (Central) Resource. The final public reporting of Resource Revision 1 was from the combined figures of the maiden (Central) Resource and the subsequent revision (Table 1.5).

Table 1.5 Along-strike extensions (added to the Central resource) was declared under the JORC 2004 edition and rounded to a single decimal place for reporting purposes. This resource was reported at a cut-off of greater than or equal to 0.3% Cu.

Productora Resource Revision 1 - February 2013								
Classification	Resource Series	Tonnes (millions)	Grade			Contained Metal		
			Cu %	Au g/t	Mo ppm	Copper (tonnes)	Gold (ounces)	Molybdenum (tonnes)
Indicated	Res Upgrade 1	39.4	0.6	0.1	124	230,000	150,000	5,000
	Central	31.1	0.6	0.1	159	185,000	110,000	5,000
	Total	70.6	0.6	0.1	139	420,000	260,000	10,000
Inferred	Res Upgrade 1	40.6	0.5	0.1	110	200,000	130,000	4,000
	Central	54.0	0.6	0.1	138	298,000	180,000	8,000
	Total	94.6	0.5	0.1	126	500,000	310,000	12,000
Total	Res Upgrade 1	80.0	0.5	0.1	117	440,000	290,000	9,000
	Central	85.2	0.6	0.1	146	480,000	290,000	13,000
	Total	165.2	0.6	0.1	132	920,000	580,000	22,000

1.4.3.1.4 JORC 2012 Resource Revision 2, HCH, March 2014

Following on from Resource Revision 1, HCH commenced an extensive resource definition drilling programme from December 2012 to December 2013 to infill and test near-resource mineralisation.

A total of 905 holes for a cumulative 238,185m (211,708.5m of RC, 26,476.5m of DD) was available for use in resource estimation. This provided a nominal 40m x 80m drillhole coverage across the majority of the Productora and Alice Resource.

The Resource Revision 2 is shown in Table 1.6.

Table 1.6 Resource Revision 2 Resource table. This Resource was declared under the JORC 2012 edition and was reported at a cut-off of greater than or equal to 0.25% Cu.

Resource Classification by Weathering								
Weathering	Classification	Mt	Grade			Contained Metal		
			Cu %	Au g/t	Mo ppm	Copper (tonnes)	Gold (ounces)	Molybdenum (tonnes)
Oxide	Indicated	20.5	0.52	0.10	57	106,000	64,000	1,000
	Inferred	5.1	0.51	0.08	88	26,000	12,000	500
	Sub-total	25.6	0.52	0.09	63	132,000	76,000	2,000
Transitional	Indicated	17.6	0.53	0.10	102	93,000	54,000	2,000
	Inferred	7.5	0.35	0.07	47	26,000	16,000	500
	Sub-total	25.1	0.48	0.09	85	119,000	70,000	2,000
Fresh	Indicated	120.6	0.50	0.11	175	601,000	423,000	21,000
	Inferred	43.1	0.41	0.08	107	177,000	105,000	5,000
	Sub-total	163.6	0.48	0.10	157	777,000	531,000	26,000
Total		214.3	0.48	0.10	138	1,029,000	675,000	29,000

1.4.3.1.5 JORC 2012 Ore Reserve, March 2016

Following completion of a Prefeasibility Study in March 2016, an ore reserve for the Productora and Alice deposits was declared under JORC 2012 as shown in Table 1.7.

Table 1.7 Productora JORC 2012 Ore Reserve, March 2016*

Ore type	Reserve category	Mt	Cu (%)	Au (g/t)	Mo (ppm)	Contained metal			Payable metal		
						Cu (kt)	Au (koz)	Mo (kt)	Cu (kt)	Au (koz)	Mo (kt)
Oxide	Probable	24.1	0.43	0.08	49	103.0	59.6	1.2	55.6		
Transitional		20.5	0.45	0.08	92	91.3	54.7	1.9	61.5	24.4	0.8
Sulphide		122.4	0.43	0.09	163	522.5	356.4	20.0	445.8	167.5	10.4
Total	Probable	166.9	0.43	0.09	138	716.8	470.7	23.1	562.9	191.9	11.2

*Cu price - US\$3.00/lb; Au price US\$1,200/oz; Mo price US\$14.00/lb

Weighted average metallurgical recoveries for sulphide and transitional are 86.1% for Cu; 51.9% for Au; 52.2% for Mo. Heap leach average recoveries are 54.0% for Cu and nil for Au and Mo. Payability factors for metal contained in concentrate are 96% for Cu; 90% for Au; and 98% for Mo. Payability factor for Cu contained in Cu cathode is 100%

1.4.3.1.6 NI 43-101 2021 Resource Revision 3, HCH, October 2021

The Productora and Alice estimation was reviewed and released as Resource Revision 3 to comply with NI 43-101 as shown in Table 1.8. This was released with the Cortadera resource as part of a combined Costa Fuego Resource with an effective date of 29th October 2021.

Table 1.8 Productora Mineral Resource Summary (using +0.25% CuEq cut-off grade), 29 October 2021*

Productora Resource		Grade				Contained Metal			
Classification	Tonnes (millions)	CuEq	Cu %	Au g/t	Mo ppm	Copper Eq	Copper	Gold	Molybdenum
(+0.25% CuEq*)	(Mt)	(%)	(%)	(g/t)	(ppm)	(tonnes)	(tonnes)	(ounces)	(tonnes)
Measured	0	0	0	0	0	0	0	0	0
Indicated	208	0.54	0.46	0.10	140.0	1,122,000	960,000	643,000	29,200
Total	208	0.54	0.46	0.10	140.0	1,122,000	960,000	643,000	29,200
Inferred	67	0.44	0.38	0.08	109	295,000	255,000	167,000	7,200

Reported at or above 0.25% CuEq. Figures in the above table are rounded, reported to appropriate significant figures, and reported in accordance with CIM and NI-101. Metal rounded to nearest thousand, or if less, to the nearest hundred.

Copper Equivalent (CuEq) reported for the resource were calculated using the following formula: $CuEq\% = ((Cu\% \times Cu \text{ price } 1\% \text{ per tonne} \times Cu_recovery) + (Mo \text{ ppm} \times Mo \text{ price per g/t} \times Mo_recovery) + (Au \text{ ppm} \times Au \text{ price per g/t} \times Au_recovery) + (Ag \text{ ppm} \times Ag \text{ price per g/t} \times Ag_recovery)) / (Cu \text{ price } 1\% \text{ per tonne})$. The Metal Prices applied in the calculation were: Cu=3.00 USD/lb, Au=1,550 USD/oz, Mo=12 USD/lb, and Ag=18 USD/oz. For Productora (Inferred + Indicated), the average Metallurgical Recoveries were Cu=83%, Au=43% and Mo=42%

1.4.3.2 Cortadera

1.4.3.2.1 NI 43-101 2021 Maiden Resource, HCH, October 2021

Following execution of the Cortadera option agreement in February 2019, HCH undertook a Resource drill-out focussed on extending and infilling previously defined mineralisation. The maiden resource was released in compliance with NI 43-101 and is shown in Table 1.9. This was released with the Productora resource as part of a combined Costa Fuego Resource with an effective date of 29th October 2021.

Table 1.9 Cortadera Mineral Resource Summary – reported by classification (29th October 2021) and by open pit (top), underground (middle) and total (bottom)*

Cortadera OP Resource		Grade					Contained Metal				
Classification	Tonnes	CuEq	Cu	Au	Ag	Mo	Copper Eq	Copper	Gold	Silver	Molybdenum
(+0.25% CuEq*)	(Mt)	(%)	(%)	(g/t)	(ppm)	(ppm)	(tonnes)	(tonnes)	(ounces)	(ounces)	(tonnes)
Measured	0	0	0	0	0	0	0	0	0	0	0
Indicated	135	0.47	0.38	0.15	0.66	32	634,500	513,000	650,000	2,865,000	4,300
M+I Total	135	0.47	0.38	0.15	0.66	32	634,500	513,000	650,000	2,865,000	4,300
Inferred	100	0.44	0.35	0.14	0.65	45	440,000	350,000	450,000	2,090,000	4,500

Cortadera UG Resource		Grade					Contained Metal				
Classification	Tonnes	CuEq	Cu	Au	Ag	Mo	Copper Eq	Copper	Gold	Silver	Molybdenum
(+0.25% CuEq*)	(Mt)	(%)	(%)	(g/t)	(ppm)	(ppm)	(tonnes)	(tonnes)	(ounces)	(ounces)	(tonnes)
Measured	0	0	0	0	0	0	0	0	0	0	0
Indicated	48	0.55	0.44	0.15	0.87	73	264,000	211,000	232,000	1,343,000	3,500
M+I Total	48	0.55	0.44	0.15	0.87	73	264,000	211,000	232,000	1,343,000	3,500
Inferred	167	0.44	0.35	0.11	0.68	90	735,000	585,000	591,000	3,651,000	15,000

Cortadera Total Resource		Grade					Contained Metal				
Classification	Tonnes	CuEq	Cu	Au	Ag	Mo	Copper Eq	Copper	Gold	Silver	Molybdenum
(+0.25% CuEq*)	(Mt)	(%)	(%)	(g/t)	(ppm)	(ppm)	(tonnes)	(tonnes)	(ounces)	(ounces)	(tonnes)
Measured	0	0	0	0	0	0	0	0	0	0	0
Indicated	183	0.49	0.4	0.15	0.7	43	905,000	728,000	889,000	4,227,000	7,900
M+I Total	183	0.49	0.4	0.15	0.7	43	905,000	728,000	889,000	4,227,000	7,900
Inferred	267	0.44	0.35	0.12	0.7	73	1,181,000	935,000	1,022,000	5,633,000	19,400

*Reported at or above 0.25% CuEq. Figures in the above table are rounded, reported to appropriate significant figures, and reported in accordance with CIM and NI 43-101. Metal rounded to nearest thousand, or if less, to the nearest hundred.

Copper Equivalent (CuEq) reported for the drillholes were calculated using the following formula: $CuEq\% = ((Cu\% \times Cu \text{ price } 1\% \text{ per tonne} \times Cu_recovery) + (Mo \text{ ppm} \times Mo \text{ price per g/t} \times Mo_recovery) + (Au \text{ ppm} \times Au \text{ price per g/t} \times Au_recovery) + (Ag \text{ ppm} \times Ag \text{ price per g/t} \times Ag_recovery)) / (Cu \text{ price } 1\% \text{ per tonne})$. The Metal Prices applied in the calculation were: Cu=3.00 USD/lb, Au=1,550 USD/oz, Mo=12 USD/lb, and Ag=18 USD/oz. Average Metallurgical Recoveries used were Cu=83%, Au=56%, Mo=82%, and Ag=37%

1.4.3.3 San Antonio

No previous Mineral Resource or Reserve has been reported for the San Antonio deposit.

1.4.4 Production History

1.4.4.1 Productora

Copper mining at Productora commenced in 2006 and was operational until 2012 and again briefly in 2021.

Mining was completed by a modern 4.5m x 4.5m decline access exploiting 15m sub-level room and pillar development. The mine extends to ~120m below surface and produced cupriferous mineralized materials at a head grade of 0.8 to 1.2% Cu over a strike length of 300m and a width of 50m.

The mineralized material was stockpiled then trucked off-site for toll-treatment at ENAMI's Vallenar processing facility. Drilling by the mine operators and by Hot Chili demonstrates that the mineralisation exploited in the underground mine is contiguous with the larger Mineral Resource.

1.4.4.2 Cortadera

At Cortadera, previous mining has taken place upon mining leases Purísima 1/8 and Cortadera 1/40, where several small workings (pirquineros) have been developed in the oxide zone as trenches, surface excavations and short tunnels.

The largest of these previous workings is the Purísima Mine (Cuerpo1) where in 1990, previous miners R.G Grego and J.R Alday developed a tunnel approximately 70m long in the oxide zone.

Further mining at Purísima took place during 2003-2004 when a small open pit was developed to extract copper oxides at a grade of approximately 0.9% copper.

1.4.4.3 San Antonio

The San Antonio project has been privately owned since 1953 and has been mined by several operators over this time via lease from the owners. Limited historic documents provided the following production data:

- 1965-1972: produced 100,000t at ~2.5% soluble-copper (3% Cu total).
- 1980: 30,000t of 3.0% oxide and 25,000t at 2.0% copper sulphide mineralisation
- 1988-1995: ~399,000t at 1.6% copper.

The current owner has indicated that total historic production is approximately 2Mt of material grading approximately 2% copper and 0.3 g/t gold. There is current small-scale mining activity at the project.

1.5 Geological Setting and Mineralization

1.5.1 Productora

The region lies at the boundary between the Coastal Cordillera and the Atacama fault system. During the Cretaceous, a thick sequence of andesite and minor sediments (Bandurrias Group) developed in an extensional regime within volcanic island-arc

settings. A variety of porphyritic formations have intruded this sequence, some of which are probably contemporaneous with the host volcanic rocks. These porphyritic intrusions appear to be responsible for most of the alteration and mineralisation observed in the area. Jurassic to Late Cretaceous granodioritic and monzodioritic batholiths are exposed over large areas throughout the Coastal Cordillera.

The project area encompasses a small part of the Chilean Iron Belt. The Iron Belt extends for more than 600km along a 20 to 30km wide, north-northeast trending zone at the east side of the Coastal Cordillera.

The project is hosted in the (lower Cretaceous) Bandurrias Group, a thick volcano-sedimentary sequence comprising intermediate to felsic volcanic rocks and intercalated sedimentary rocks. Dioritic dykes intrude the volcano-sedimentary sequence at Productora, typically along west- to northwest-trending late faults, and probably represent sub-volcanic feeders to an overlying andesitic sequence not represented in the project area.

The host volcanic and sedimentary sequence dips gently (15 to 30°) west to west-northwest and is transected by several major north to northeast-trending faults zones, including the Productora fault zone, which coincides with the main mineralised trend. These faults are likely sympathetic to the nominally parallel but distal Atacama fault system. In the Productora deposit, these major fault zones are commonly associated with extensive tectonic breccia (damage zones) that host copper-gold-molybdenum mineralisation. Later faults crosscut and offset the volcano-sedimentary sequence together with the Productora (and sub-parallel) major faults. Late faults generally show a west to north-westerly strike and while generally narrow, are locally up to 20m wide.

The volcano-sedimentary sequence at Productora is extensively altered, particularly along major faults and associated damage zones, and a distinctive alteration zonation is evident. The distribution of alteration mineral assemblages and spatial zonation suggest a gentle northerly plunge for the Productora mineral system, disrupted locally via vertical and strike-slip movements across late faults. These late faults appear to be trans-tensional and nominally normal to the distal Atacama fault system.

Mineralisation at the Productora deposit is structurally controlled, hosted within a hydrothermal tourmaline breccia unit, with predominantly sub-vertical mineralisation.

At depth, the Productora mineralisation is hosted in narrow (~2 to 5m), north to northeast trending, sub-vertical lodes, blowing out into wider high-grade mineralised zones near the upper surface of the tourmaline breccia. The wider brecciated zones vary in orientation but tend to be sub-vertical with an upper flex in wider mineralised zones to dip approximately 70° west. There are also some locally steeply east dipping high grade zones (e.g., Habanero lode).

Secondary and relatively lower-grade mineralized material controls are evident as manto (or manto-like) horizons in the southern, far northern and far eastern flanks of

Productora. Lodes within the manto horizons are typically shallow dipping at -20° to -30° to the east or west and enclosed by lower grade mineralisation.

The Alice porphyry is located immediately beneath an extensive, pyrophyllite-rich advanced argillic lithocap, with a porphyry stock of quartz diorite to granodiorite composition, characterised by biotite and hornblende phenocrysts. The mineralisation at Alice is hosted in a northeast trending dyke-like porphyry with sheeted and stockwork A- and B-type quartz veinlets, within additional locally disseminated background mineralisation. Highest grade mineralisation is associated with alteration overprinting, with replacement of the biotite-altered porphyry by quartz, actinolite, chlorite and magnetite.

The margins and deeper parts of the stock, have been overprinted by albite ± epidote ± sericite alteration, causing destruction of biotite, removal of chalcopyrite and a reduction in pyrite.

1.5.2 Cortadera

Cortadera is a copper-gold-molybdenum porphyry hosted deposit, comprising a series of mineralised centres (Cuerpo 1, 2 and 3) within a NW striking structural corridor.

The Cortadera deposit is characterised by early- and intra-mineralisation, porphyritic tonalitic to quartz dioritic intrusions and adjacent volcano-sedimentary wall-rocks that have been recrystallised to hornfels and skarn. Hydrothermal alteration consists of moderate to strong phyllic (+chloritic) alteration, characterised by quartz/silica, sericite, and lesser amounts of chlorite.

Chalcopyrite occurs as disseminations of variable intensity within the porphyritic host rocks, particularly in association with stockwork A- and B-type veins. There is a clear correlation between increased percentage of quartz-bearing stockwork veining and sulphide content with elevated copper-gold grades.

Vein systems at Cortadera are typical of those found within porphyry-style mineralised systems. Early quartz-rich veins observed at Cuerpo 1 and Cuerpo 2 exhibit unidirectional solidification textures (UST) that are commonly associated with high-temperatures during vein emplacement. Veins formed subsequent to UST veins comprise quartz rich A-veins (chalcopyrite- pyrite± magnetite), banded MAB veins (quartz-magnetite-chalcopyrite-pyrite) and B-veins (molybdenite), cut by sericitic/chlorite C-veins (pyrite-chalcopyrite), D-veins (quartz-pyrite-sericite) and late calcite-bearing fractures. Anhydrite is locally present within some of the B and C veins.

Chalcopyrite also occurs as disseminations of variable intensity within the porphyritic host rocks, particularly in association with stockwork A-type veins. There is a very clear correlation between increased percentage of quartz-bearing stockwork veining and sulphide content with elevated copper-gold grades.

1.5.3 San Antonio

San Antonio is a Skarn style occurring in the periphery of the Cortadera copper-gold-molybdenum porphyry system.

Chalcopyrite occurs as disseminations of variable intensity within the dioritic host rocks and appears to have some structural control based upon field and underground mapping. Late-stage cross cutting faults appear to increase the width and contained metal of the mineralised zones.

The mineralised system is enriched in copper, silver, and cobalt, and depleted in gold and molybdenum when compared to the Cortadera deposit.

1.6 Exploration

1.6.1 Productora

An extensive data compilation and validation exercise was performed by Hot Chili Limited (HCH) in 2010. Historical data was collected from several sources including hard copy reports, public disclosure, and both hard copy and digital maps. Ground reconnaissance was also completed.

Several detailed litho-structural mapping campaigns by HCH allowed compilation and validation of geological information along the Productora main mineralised zone. This work showed that the mineralisation at Productora is hosted within relatively permeable units of a felsic-intermediate volcanic sequence. The mineralisation was evident in a series of permeable units and fault-controlled disseminations and breccia that trend N-S, E-W and NW-SE. Jogs and intersections between fault-sets as well as between faults and permeable volcanic units appeared to have assisted the mineralisation process.

Geochemical sampling demonstrated that significantly elevated copper-gold-molybdenum grades, together with other elevated pathfinder elements, were evident within soils. Molybdenum in soils appeared to define an anomaly immediately above the Productora mineralisation. Where uranium assays were elevated, uranium showed an association with copper, silver, molybdenum, gold, and cobalt. Zones dominated by albite versus K-feldspar-sericite alteration were defined, with copper-gold being associated with the K-feldspar-sericite alteration and magnetite being associated with the albitic alteration zones. These results were consistent with earlier petrographic work completed by Fox (2000).

Multi element ME-MS61 (48 element) analysis has been collected on surface soil samples, rock chips and selected downhole samples over several exploration and drilling campaigns. This data was used for 3D geochemical modelling completed independently by Fathom Geophysics in 2021 following the geochemical element zoning models for the Yerington porphyry copper deposit in Nevada (Cohen, 2011]; and Halley et al., 2015).

1.6.2 Cortadera

Following execution of the Cortadera option agreement in February 2019, HCH undertook a Resource drill-out focussed on extending and in-filling previously defined mineralisation. Drilling was successful in improving geological understanding, growing the deposit size, and discovering a bulk-tonnage high grade zone at Cortadera.

1.6.3 San Antonio

Since executing the San Antonio option agreement in November 2017, HCH has undertaken a range of exploration activities including field mapping, soil and rock sampling, underground mapping, underground chip sampling, a reverse circulation drill program, and a survey of accessible mined excavations to verify depletion and void models.

1.7 Drilling

1.7.1 Productora

All drilling and assay results used for the Productora, and Alice Mineral Resource estimates were generated by HCH exploration and Resource development drilling programmes conducted between 2010 and 2015.

Drilling completed at Productora used a nominal drill pattern of 80m spaced east-west sections, with drilling approximately 40m apart along section. This allowed optimal drill orientation for intersection of the north-northeast trending mineralisation. The majority of drilling plunged -60 to -80° toward 090° azimuth, but there were numerous scissor drillholes oriented at -60 to -80° degrees towards an azimuth of 270° to ensure geological representivity and to also preferentially target east dipping mineralisation.

Drilling in or out of sections (“off section”) was required on an ad-hoc basis due to limitations on drill platform availability or were designed to preferentially test specific structural orientations.

The drill pattern as described above is consistent to a depth of approximately 300m vertical from surface.

Drilling at Alice also used a similar pattern, but due to limited pad availability had an increased number of “off section” drillholes.

Downhole surveying at Productora has been completed by contracting companies Wellfield and North Tracer. Wellfield undertook downhole surveys from the beginning of HCH drilling until May 2013. North Tracer undertook downhole surveys from May 2013 onwards. There was some overlap of surveying companies during the transition period.

Down-hole survey validation checks were completed by subsequent umpire survey checks as well as within-company resurveys. Results from resurveys and cross-company checks provided a good correlation between the two companies as well as within-company resurveys and provides confidence in the survey data for the drillholes used for resource estimation.

Geological logging was recorded in a systematic and consistent manner such that the data was able to be interrogated accurately using modern mapping and geological modelling software programs. Field logging templates were used to record details related to each drillhole. All geological logging was completed by qualified and experienced company geologists. Collar, survey, sample register and sample condition, sample recovery data or comments (and commonly magnetic susceptibility) were recorded by a competent field technician.

All reverse circulation (RC) holes were logged using the standard company logging codes, and washed chip samples were stored in chip trays retained at the company's operational storage facility in Vallenar. All diamond drill core was subjected to detailed lithological and structural logging.

Geological attributes logged in RC chips includes colour, weathering/oxidation, regolith, lithology, veining, alteration assemblages and their intensities, texture, mineralogy and sulphides and their percentages.

Core reconstruction and orientation was attempted in every drilling run and completed where possible before marking up or logging core.

Geological attributes logged in diamond core includes the same attributes as RC drilling, and additionally the following structural attributes:

- Linear structures (e.g., lineations)
- Planar structures (e.g., shears, veins, dykes, faults, cleavage, joints/fractures, schistosity)
- Preliminary geotechnical features such as RQD and FPM.

A total of 2,164 bulk densities were available for the Productora Resource estimate, and 74 for the Alice deposit.

One in every five samples of diamond drill core was submitted for bulk density analysis as performed by ALS (ALS Code OA-GRA09). Every sample that ends in a "5" or a "0" is labelled with the words "Density test".

The test work was undertaken on an approximate 10cm piece of core taken from the designated sample bag and is used to determine the bulk density for the 1m interval. The bulk density test consists of using the Archimedean water submersion method of analysis.

Pycnometer density data was generated due to the predominance of RC drilling over diamond drilling at Productora. Pycnometer tests were completed at a rate of one in 20 samples for most of the HCH drilling.

A total of 4,966 sample pulp pycnometer densities were available for the Productora deposit Resource estimation.

1.7.2 Cortadera

Drilling completed prior to HCH securing the deposit comprises 39 DD holes for 23,230.85m, with this drilling successful in defining three mineralised porphyries (Cuerpo 1, 2 and 3).

Between February 2019 and September 2020 HCH drilled 32 RC holes and 11 DD holes for a total of 10,126m of RC and 7,064.4m of DD.

Drilling completed by HCH between September 2020 and December 2021 comprises 105 RC holes, 38 RCDD holes, 4 RCDD hole extensions and 1 DD hole for a total of 21,262m of RC, 33,301m RCDD and 1,474m DD.

Drill spacing is nominally 80m across strike by 80m along strike. The current drilling density provides sufficient information to support a robust geological and mineralisation interpretation as the basis for Indicated and Inferred Classified Mineral Resources for the majority of the deposit.

The Cortadera mineral resource estimate (MRE) used a total drill inventory of 228 holes for a cumulative 96,847.7m (37,725.5m of RC and 59,142.2m of DD), with drill data collected during the period from November 2011 to February 2022, using industry standard techniques for drilling and sampling collection.

1,248 bulk densities were available for the Cortadera Resource estimate. Samples collected by MF comprised of 10cm piece of whole core was selected every 40m, wax coated, then immersed in water to determine bulk density from water displacement. MF density samples were validated by HCH using the current procedure. Density samples are taken by HCH every 30m downhole over each lithology. Determination of Bulk density is done by paraffin coated specimens using the water displacement method (OA-GRA09A). A programme to collect densities in the weathered material has commenced and results will be included in the next mineral resource update.

1.7.3 San Antonio

Drilling completed by HCH in 2018 comprises 41 RC holes for a total of 4,922m.

Drilling completed prior to HCH securing San Antonio, comprises 11 RC holes for 3,887m. HCH undertook a further 823m of underground chip sampling across a mixture of face sampling and sludge hole wall sampling across 3 mined levels.

Drill spacing is variable across the deposit from less than 5m in the underground mining levels and up to an approximate 120m across strike by 120m along strike.

The current drilling density provides sufficient information to support a robust geological and mineralisation interpretation as the basis for an Inferred Classified Mineral Resources for San Antonio.

The San Antonio MRE used a total drill inventory of 109 holes for a cumulative 9,632m. HCH directed the collection of 98 holes (RC or underground channel/chip samples) between 2017 - 2022 with drill data collected using industry standard techniques for drilling and sampling collection.

1.8 Sampling, Analysis and Security

1.8.1 Productora

A fixed cone splitter was used to create two nominal 12.5% samples (Sample “A” and “B”), along with the large bulk reject sample. The “A” sample is always taken from the same sampling chute, and comprises the primary sample submitted to the laboratory. The “B” samples were retained for use as the field duplicate sample. The coarse residues were collected into large plastic bags and were retained on the ground near the drillhole collar, generally in rows of 50 bags.

All RC drillhole sampling was executed at one metre intervals. Within logged mineralisation zones, the 1m sample (“A” sample) was submitted. Outside the main mineralised zones (as determined by the logging geologist), 4m composite were created from scoops of 1m sample residues over this interval. The composited 4m samples were analysed first and if required, the individual and original 1m “A” samples comprising this 4m interval were sent for analysis. This ensured that no mineralisation was missed while minimising analytical costs.

At Productora, the majority of diamond core has had systematic whole core sampled at 1m intervals. Whole core was chosen as the preferred sampling method to ensure a larger and more representative sample for analysis. This was based upon the nature of the porous and brecciated mineralisation. Some core has been half cored or completely retained for geological reference.

At Alice, all diamond core was systematically half core sampled at 1m intervals. The decision to retain half core was based upon a generally more homogenous style of mineralisation and, typically, more coherent core samples. The retained half core is available for future reviews, QA/QC sampling and geological reference.

Once assigned a sample number, individual samples to be sent to ALS laboratories were sealed using a staple gun and accompanied by three identical sample tickets (one stapled to plastic bag to identify any tampering/breakage of seal prior to opening at the laboratory in preparation and another placed in the bag). Any broken staple seals on samples were to be notified by ALS to HCH. No sealed bags were reported as being opened or broken by ALS.

For both RC and diamond samples, sample bags were placed inside larger plastic bags and delivered by a dedicated truck to the ALS analytical laboratory in Coquimbo (Chile) for sample preparation and routine analysis.

Following analysis at ALS, the RC and diamond drilling coarse rejects were returned to site and stored in sequence in plastic bags under shade cloth next to the Productora site camp. The laboratory pulps were returned and stored at the HCH site camp and stored in organised, dry, and safe storage containers.

HCH has strict chain of custody security procedures for all samples sent to and from the analytical laboratories.

The ALS analytical laboratory in Coquimbo (Chile) and Lima (Peru), completed all analytical assays and specific gravity test work for the Productora samples used in this Resource estimate.

Periodic inspections of the laboratory facilities and meetings with ALS staff have been conducted since drilling commenced at Productora. Inspections of the laboratory facilities have found them to be of a suitable standard. Any concerns HCH may have had regarding laboratory practices or equipment, or unexpected results, has been openly discussed with ALS and rectified at the earliest opportunity.

1.8.2 Cortadera

A fixed cone splitter was used to create two nominal 12.5% samples (Sample “A” and “B”), along with the large bulk reject sample. The “A” sample is always taken from the same sampling chute, and comprises the primary sample submitted to the laboratory. The “B” samples were retained for use as the field duplicate sample. The coarse residues were collected into large plastic bags and were retained on the ground near the drillhole collar, generally in rows of 50 bags.

All RC drillhole sampling was executed at 2m intervals. Within logged mineralisation zones, the 2m sample (“A” sample) was submitted. Outside the main mineralised zones (as determined by the logging geologist), 4m composites were created from scoops of 2m sample residues over this interval. The composited 4m samples were analysed first and, if required, the individual and original 2m “A” samples comprising this 4m interval were sent for analysis. This ensured that no mineralisation was missed while minimising analytical costs.

At Cortadera, the majority of diamond core has had systematic half-core sampled at 2m intervals. Half-core was chosen as the preferred sampling method to ensure a representative sample was submitted for analysis, while also retaining half-core for review of lithology and mineralisation and for further test work as required.

Prior to the cutting and sample process, two additional samples are also taken for Cortadera, being Density and Geotechnical samples.

- Density samples are selected every 30m if the geological conditions allow it and are provided to the laboratory for testwork.
- Geotechnical samples are taken for tests including triaxial (one sample per 250m) and uniaxial tests (one sample per 50m).

Once assigned a sample number, individual samples to be sent to ALS laboratories were sealed using a staple gun and accompanied by three identical sample tickets (one stapled to plastic bag to identify any tampering/breakage of seal prior to opening at the laboratory in preparation and another placed in the bag). Any broken staple seals on samples were to be notified by ALS to HCH. No sealed bags were reported as being opened or broken by ALS.

For both RC and diamond samples, sample bags were placed inside larger plastic bags and delivered by a dedicated truck to the ALS analytical laboratory in Coquimbo (Chile) for sample preparation and routine analysis.

Following analysis at ALS, the RC and diamond drilling coarse rejects were returned to site and stored in sequence in plastic bags under shade cloth at HCH's nearby Productora core farm. The laboratory pulps were returned and stored at the Productora core farm where they are stored in organised, dry, and safe storage containers.

HCH has strict chain of custody security procedures for all samples sent to and from the analytical laboratories.

The ALS analytical laboratory in Coquimbo (Chile) completed all sample preparation and specific gravity test work, while ALS Santiago (Chile) completed all gold analysis, and ALS Lima (Peru) completed all other multielement analysis for the Cortadera assays used in the resource estimate. HCH has implemented rigorous sample preparation and analytical procedures for both RC and diamond core samples, following consultation with ALS in Chile, to ensure that mineralised assays were reported with a high degree of confidence and a wide range of appropriate commodities were assessed.

Samples have been analysed by certified laboratories in Chile and Lima, Peru by standard analytical techniques including:

- Copper, silver, and molybdenum were analysed by 4-acid digestion (Hydrochloric-Nitric- Perchloric-Hydrofluoric) followed by evaluation using Inductively Coupled Plasma - Optical Emission Spectrometry (ICP-OES) or Atomic Absorption Spectrometry (AAS)
- Copper results > 10,000 ppm were analysed by "ore grade" method Cu-AA62 (upper limit 40% Cu)
- Samples within the oxide and transitional weathering domains (as determined by geologists' logging) were analysed for "soluble copper" (upper limit 10% Cu) to detect the leachability of copper oxide minerals within these domains
- Gold was analysed by 30 or 50 g lead-collection Fire Assay, followed by ICP-OES or AAS.

1.8.3 San Antonio

A fixed cone splitter was used to create two nominal 12.5% samples (Sample "A" and "B"), along with the large bulk reject sample. The "A" sample is always taken from the same sampling chute, and comprises the primary sample submitted to the laboratory. The "B" samples were retained for use as the field duplicate sample. The coarse residues were collected into large plastic bags and were retained on the ground near the drillhole collar, generally in rows of 50 bags.

All RC drillhole sampling was executed at one-metre intervals. Within logged mineralisation zones, the 1m sample ("A" sample) was submitted. Outside the main mineralised zones (as determined by the logging geologist), 4m composites were created from scoops of 1m sample residues over this interval. The composited 4m samples were analysed first and, if required, the individual and original 1m "A" samples comprising this 4m interval were sent for analysis. This ensured that no mineralisation was missed while minimising analytical costs.

Once assigned a sample number, individual samples to be sent to ALS laboratories were sealed using a staple gun and accompanied by three identical sample tickets (one

stapled to plastic bag to identify any tampering/breakage of seal prior to opening at the laboratory in preparation and another placed in the bag). Any broken staple seals on samples were to be notified by ALS to HCH. No sealed bags were reported as being opened or broken by ALS.

Sample bags were placed inside larger plastic bags and delivered by a dedicated truck to the ALS analytical laboratory in Coquimbo (Chile) for sample preparation and routine analysis.

Following analysis at ALS, the coarse rejects were returned to site and stored in sequence in plastic bags under shade cloth at HCH's nearby Productora core farm. The laboratory pulps were returned and stored at the Productora core farm where they are stored in organised, dry, and safe storage containers.

HCH has strict chain of custody security procedures for all samples sent to and from the analytical laboratories.

The ALS analytical laboratory in Coquimbo (Chile) completed all sample preparation, while ALS Santiago (Chile) completed all gold analysis, and ALS Lima (Peru) completed all other multielement analysis for the HCH initiated assays used in the resource estimate. HCH has implemented rigorous sample preparation and analytical procedures for both RC and diamond core samples, following consultation with ALS in Chile, to ensure that mineralised assays were reported with a high degree of confidence and a wide range of appropriate commodities were assessed.

Samples have been analysed by certified laboratories in Chile and Lima, Peru by standard analytical techniques including:

- Copper, silver, and molybdenum were analysed by 4-acid digestion (Hydrochloric-Nitric- Perchloric-Hydrofluoric) followed by evaluation using Inductively Coupled Plasma - Optical Emission Spectrometry (ICP-OES) or Atomic Absorption Spectrometry (AAS)
- Copper results > 10,000 ppm were analysed by "ore grade" method Cu-AA62 (upper limit 40% Cu)
- Samples within the oxide and transitional weathering domains (as determined by geologists' logging) were analysed for "soluble copper" (upper limit 10% Cu) to detect the leachability of copper oxide minerals within these domains
- Gold was analysed by 30 or 50 g lead-collection Fire Assay, followed by ICP-OES or AAS.

1.9 Data Verification

HCH has implemented rigorous sample preparation and analytical procedures for both Reverse Circulation (RC) and Diamond Drilling (DD) samples, following consultation with ALS in Chile, to ensure high-grade assays were reported with a high degree of confidence and a wide range of appropriate commodities were assessed.

The results from HCH's QA/QC analysis as well as RC vs DD twinned analysis provides a high level of confidence in the precision and accuracy of the assays used for the Resource estimations.

The sample lengths, preparation and assay techniques are considered suitable for the styles of mineralisation and deposit types.

The verification of input data included the use of company QA/QC blanks and reference material, field and laboratory duplicates, umpire laboratory checks and independent sample and assay verification.

The Qualified Person has assessed the drillhole database validation work and QA/QC undertaken by HCH and was satisfied the input data could be relied upon for the estimation of the Mineral Resources.

1.10 Metallurgy

1.10.1 Testwork

Metallurgical testwork was conducted on the copper-gold-molybdenum sulphide mineralized material as well as copper oxide mineralized material, with the aim of providing design criteria for the sulphide and oxide process plants and to provide metallurgical recoveries.

The testwork was conducted at ALS Laboratories; ALS Perth, Australia (flotation and comminution testwork) and ALS Santiago, Chile (leaching and comminution testwork), Outotec in Perth, Australia (sulphide concentrate thickening and filtration), and HydroGeoSense (oxide testwork) in the USA.

Figure 1.5 depicts the location of metallurgical drilling in relation to deposit areas and metallurgical domains.

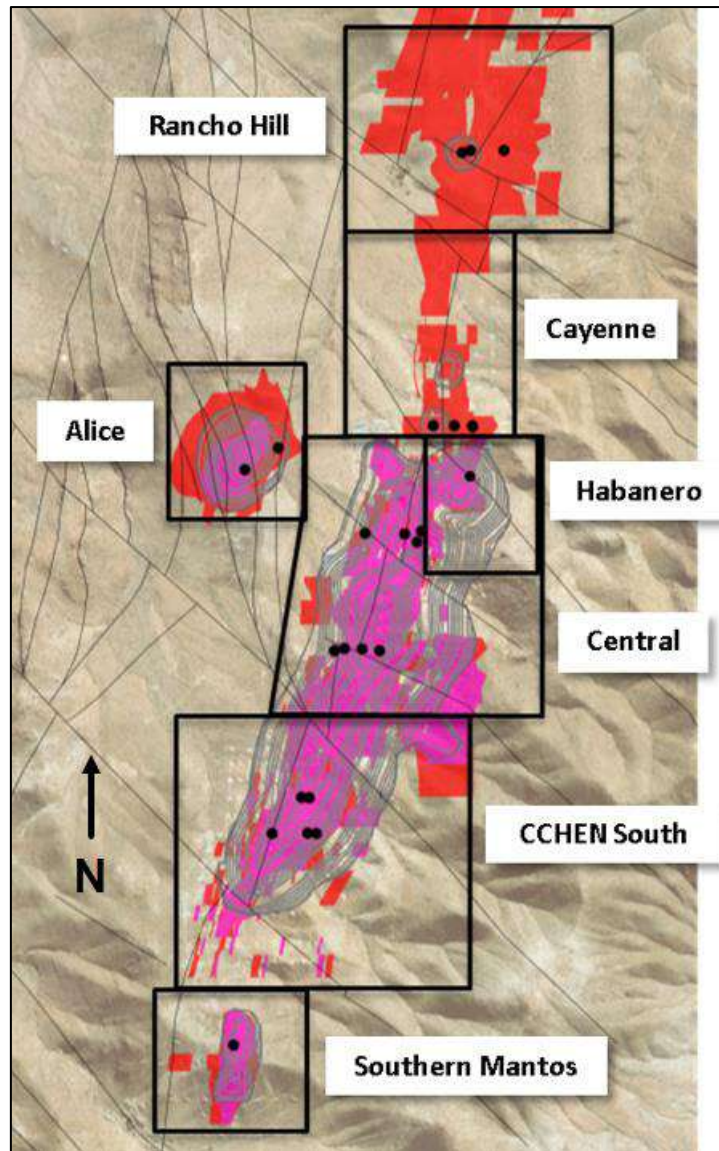


Figure 1.5 Metallurgical drillhole locations and metallurgical domains (HCH, 2016)

1.10.2 Copper Oxide Recoveries

The overall design copper recovery for mineralized material greater than 0.2% Cu is 56%, based on interpretation of bottle roll and 1m column tests on various mineralized material zones (ranging from 46% to 71% Cu recoveries). The head grade/recovery relationship for oxide mineralized materials in Productora, Alice and Southern Mantos deposits is shown in Figure 1.6.

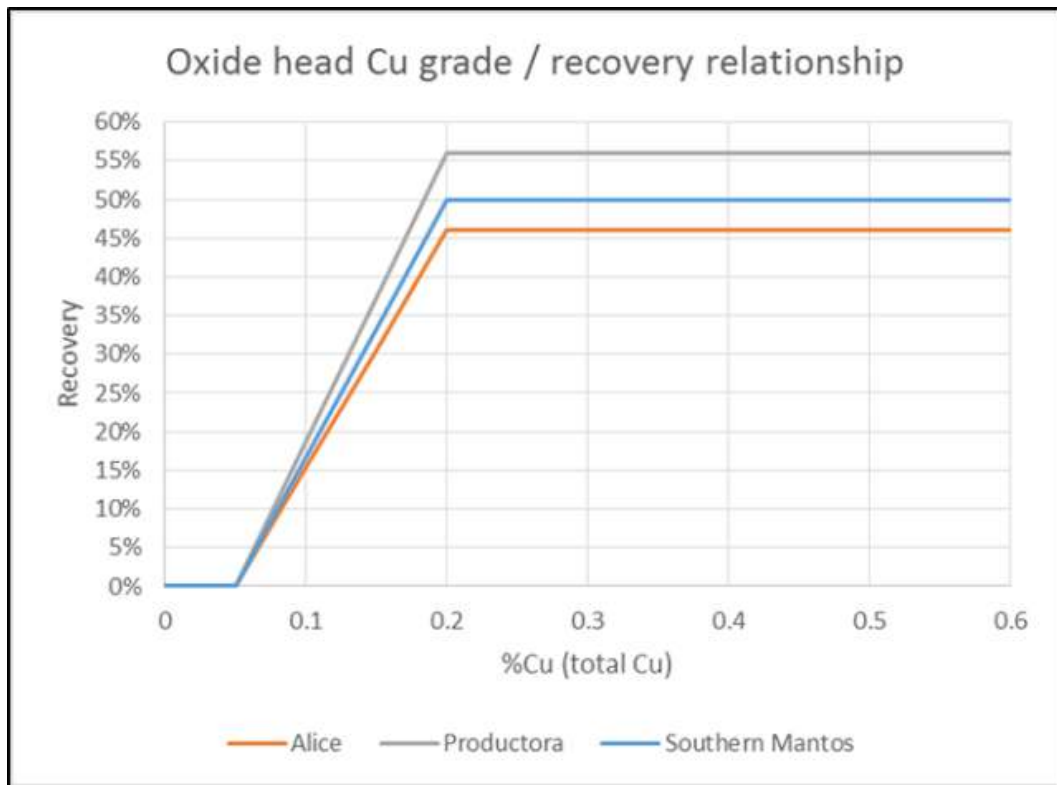


Figure 1.6 Heap leach recovery vs. Head grade

Major conclusions from the copper oxide testwork include:

- The major oxide minerals present in the majority of samples are slow leaching copper bearing silicates and chrysocolla.
- There is significant benefit in utilising seawater as, when acidified, it has the potential to allow for the leaching of secondary sulphides such as chalcocite and digenite, which are the main secondary sulphides present in the oxide/transition mineralized material types. However, the leaching kinetics of these secondary sulphides is slow and due to competing acid consumption, the leaching of these minerals is incomplete.
- Generally, the host rock presents an environment of reasonably high acid consumption and a number of test samples required leaching to be terminated due to excessive acid consumption.
- The bottle roll tests have provided (in most cases) good guidance for conditions for column leaching and an indication of likely copper recovery and acid consumption characteristics.
- The 1m column tests provided good guidance with regards to data required for the PDC and subsequent “scale-up”.
- The stacking and hydrodynamic column testwork confirmed that the agglomerated mineralized materials tested will support percolation heap leaching at the stack heights and application rates provided in the PDC.

1.10.3 Sulphide Mineralogy

QEMScan results for the Productora deposit Central and Habanero zone samples (in-pit and fresh) showed chalcopyrite as the main copper sulphide bearing mineral and pyrite as the other main sulphide mineral. The main non-sulphide minerals are K-feldspar, quartz and mica, with chlorite, kaolinite and tourmaline present in some samples.

For the Alice deposit, chalcopyrite is the only dominant Cu-bearing mineral, with only traces of other Cu minerals detected (a couple of grains of Cu-(Zn) oxide, covellite and chalcocite/digenite). Pyrite is the dominant sulphide gangue. The main non-sulphides are quartz, albite, plagioclase feldspar, micas, chlorite and epidote.

1.10.4 Sulphide Comminution

Comminution testwork was performed at the ALS Metallurgy Santiago and Perth laboratories.

The comminution testwork results, which are summarised in Table 1.10, showed that the samples tested displayed medium to medium high competency and require moderate to high grinding energies. The Abrasion index (Ai) results indicated average abrasiveness, which would result in relatively moderate ball and liner consumptions. Alice mineral material seems to be harder and tougher than material from the main pit.

Table 1.10 Comminution testwork results – all samples

Comminution parameter	Average	Minimum value	Maximum value
CWi (kWh/t)	7.4	2.1	12.4
BWi (kWh/t)	18.1	14.8	23.1
RWi (kWh/t)	22.6	19.6	26.7
Ai	0.27	0.11	0.43
Axb	48.0	31.3	78.0
DWi (kWh/m ³)	7.4	4.6	9.6
UCS	51.6	14.5	111.8
SG (kg/m ³)	2.65	2.07	3.01

Following a trade-off study, the comminution circuit selected for the sulphide concentrator is Primary Crushing followed by SAG and ball milling with recycle crushing – Primary SABC.

Comminution circuit modelling for the project was undertaken by DMCC Pty Ltd. (four grind sizes of 106 µm, 125 µm, 150 µm and 180 µm were modelled). A 150 µm design grind was selected as the optimum grind for the Productora mineralized material and 180 µm for the Alice mineralized material.

1.10.5 Sulphide Flotation

A large program of flotation testwork was conducted on the Productora and Alice deposits. Testwork was based on a standardised flowsheet and reagent scheme. The

scheme used RTD2086 (Xanthate Ester supplied by Tall Bennett) at a natural pH (~pH 8) with two stages of cleaning and a 25 µm regrind. Seawater (as received) was used.

A target copper grade for the final concentrate was 25% Cu and optimisation testwork included the following:

- Primary grind size
- Reagent dosage
- Flotation time
- Alternate reagents
- Diesel addition for increased molybdenum flotation
- Seawater vs. tap water.

1.10.6 Sulphide Flotation Copper Performance

Copper head grade vs. copper recoveries achieved from the optimisation testwork, are depicted in Figure 1.7.

- For the Central in Pit samples, the correlation for head grade vs. recovery was very good and had an R2 of 0.89.
- For the Alice samples, recoveries are potentially higher, however, with only three samples, there is not enough data to state this with confidence.
- For the transitional sulphides (>20% Acid Soluble Copper), a separate grade recovery curve was determined. The grade recovery curve gave on average 18% lower recoveries compared to the Central Fresh in Pit curve.
- Cayenne sample results were similar to Productora, with a potentially slightly lower overall copper recovery.
- The Habanero zone may have a potentially higher recovery than the Central zone, although with only three samples, there is insufficient data to produce a separate head grade vs. recovery formula.

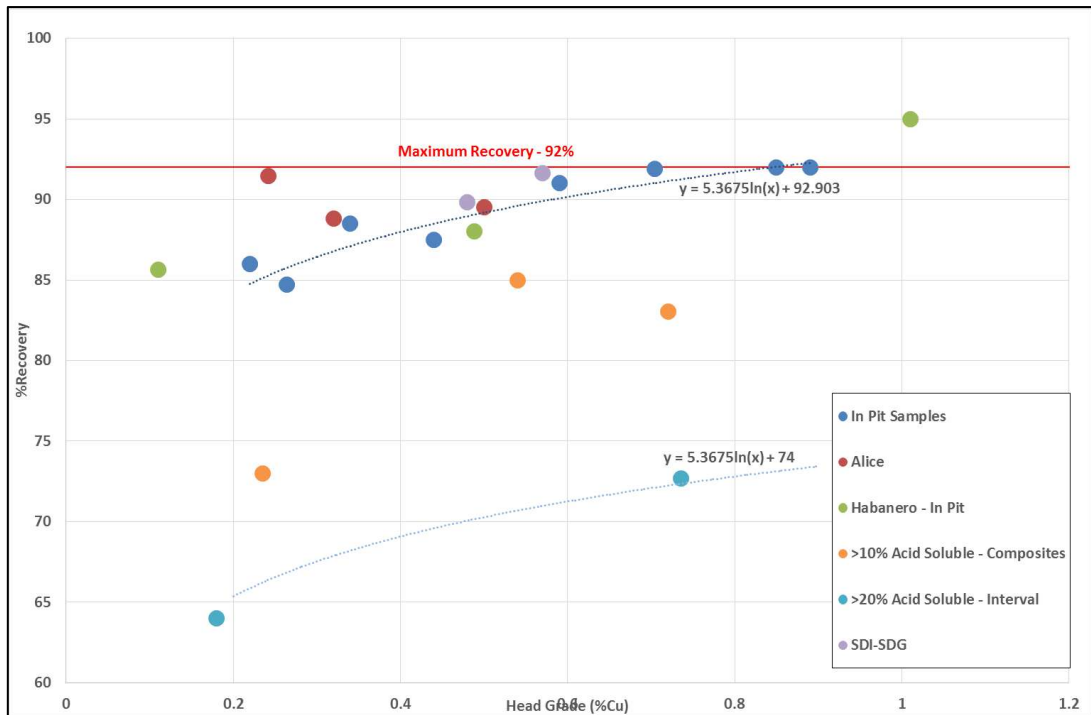


Figure 1.7 Copper head grade vs. Cu recovery

1.10.7 Sulphide Flotation Gold Performance

Gold head grade vs. gold recoveries can be seen in Figure 1.8.

- As for the copper, a line of best fit was determined for the Central in Pit Fresh zone. The formula derived for this line is shown on the figure above.
- This formula was also applied to the >10% Acid Soluble samples and for all samples a maximum recovery was set at 85%.
- For Alice, gold recoveries were higher than for Productora. The grade/recovery formula derived for Alice is shown on the figure above.

As can be seen in Figure 1.8, Habanero composites gave a very low gold recovery compared to other Productora samples. More samples need to be tested from Habanero to confirm both copper and gold performance.

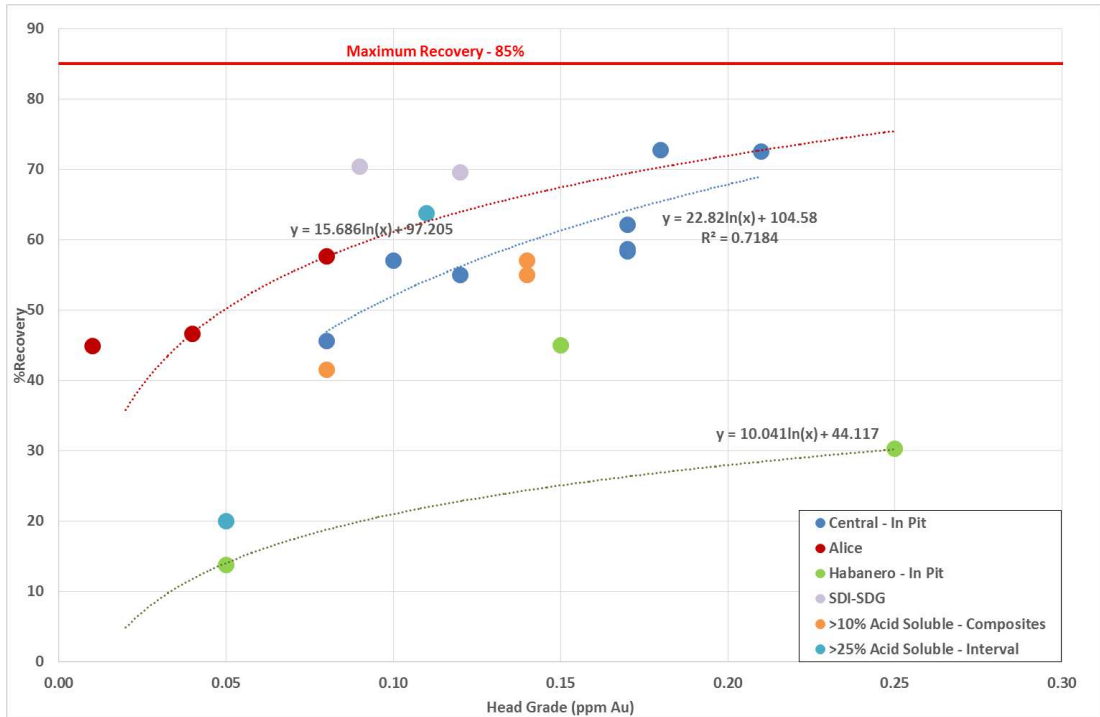


Figure 1.8 Gold head grade vs. Recovery

1.10.8 Molybdenum Metallurgical Testwork

A specific molybdenum testwork program was conducted to determine if a molybdenum concentrate greater than 50% Mo could be produced. Molybdenum recoveries for each flotation sample were also determined and a relationship established. Molybdenum flotation was not fully optimised in either the copper circuit or the molybdenum circuit.

From the batch flotation open cleaners and locked cycles, molybdenum recoveries were determined for each composite for a 25% copper concentrate. Recovery data was tabulated and graphed, and a formula was derived (best fit) namely “ $16.886\ln(x) - 29.974$ ” for the Central zone. The graph of molybdenum grade versus molybdenum recovery to copper concentrate is depicted in Figure 1.9. A constant factor of 90% has then been applied to the recovery to copper concentrate to represent the extraction efficiency in the Mo recovery plant.

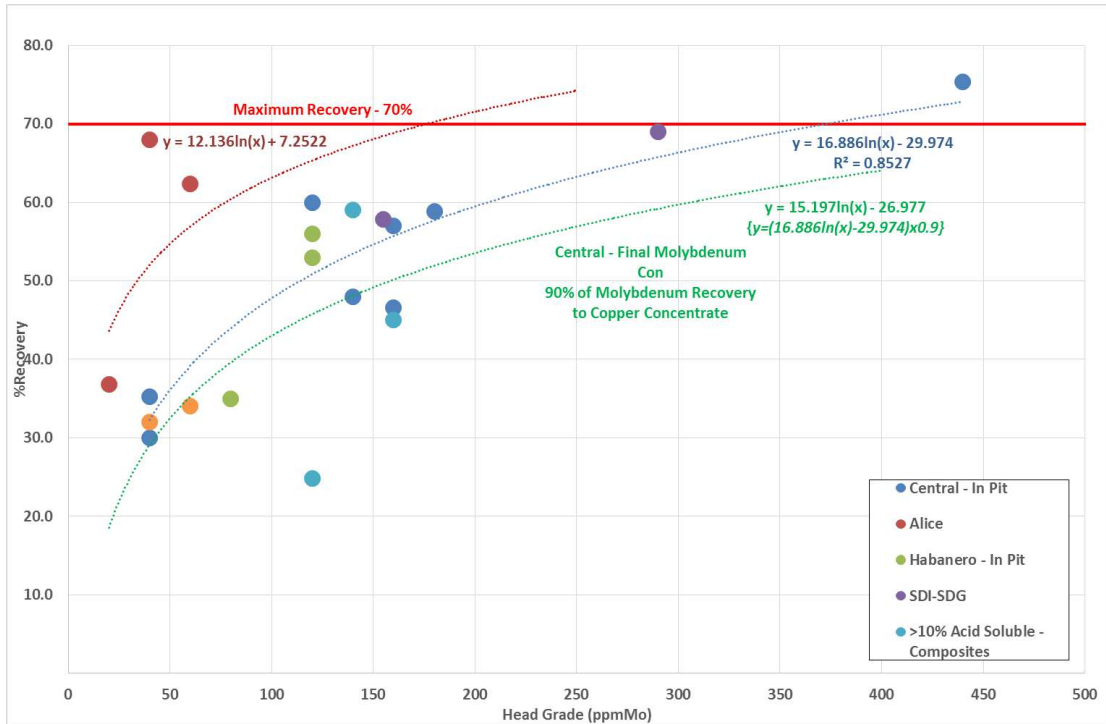


Figure 1.9 Molybdenum head grade vs. Recovery

More testwork is required during the DFS stage to better define the molybdenum recoveries to the copper concentrate and the extraction efficiencies in the molybdenum recovery plant.

1.10.9 Cortadera

The metallurgical test work undertaken supports processing of the Cortadera sulphide mineralized material using the conventional concentrator at Productora.

Rougher sulphide flotation results indicate high copper recoveries and similar crushing/grinding characteristics to that used for Productora. This confirms the strategy that Cortadera and Productora be fed into a single conventional processing facility.

Following these initial positive results, the next phase of test work will be directed towards grind size optimisation, cleaner flotation and locked-cycle test work in advance of assessing the commercial grade of copper concentrates that may be produced from the Cortadera mineralized material.

1.11 Mineral Resource Estimates

The information in this report that relates to Mineral Resources for Cortadera, Productora and San Antonio which constitute the combined Costa Fuego Project is based on information compiled by Ms. Elizabeth Haren, a Qualified Person who is a Member and Chartered Professional of The Australasian Institute of Mining and Metallurgy and a Member of the Australian Institute of Geoscientists.

Estimation of the main grade variables (copper, gold, silver, and molybdenum) was completed using categorical indicator kriging, ordinary block kriging and inverse distance

interpolation within either manually interpreted mineralisation domains or software-guided grade interpolants.

Extensive validation was completed on the Resource estimations, including internal company peer review.

Classification took into consideration data spacing and quality, geological understanding, grade continuity and output information from the grade estimation.

The combined Mineral Resource summary for the Costa Fuego Project is presented in Table 1.11. Tables for the individual deposits are included in Table 1.12 to Table 1.14.

Table 1.11 Costa Fuego Project Mineral Resource Summary – reported by classification (31st March 2022) *

Costa Fuego OP Resource		Grade					Contained Metal				
Classification (+0.21% CuEq*)	Tonnes (Mt)	CuEq (%)	Cu (%)	Au (g/t)	Ag (g/t)	Mo (ppm)	Copper Eq (tonnes)	Copper (tonnes)	Gold (ounces)	Silver (ounces)	Molybdenum (tonnes)
Indicated	576	0.46	0.37	0.10	0.37	91	2,658,000	2,145,000	1,929,000	6,808,000	52,200
M+I Total	576	0.46	0.37	0.10	0.37	91	2,658,000	2,145,000	1,929,000	6,808,000	52,200
Inferred	147	0.35	0.30	0.05	0.23	68	520,000	436,000	220,000	1,062,000	10,000

Costa Fuego UG Resource		Grade					Contained Metal				
Classification (+0.30% CuEq*)	Tonnes (Mt)	CuEq (%)	Cu (%)	Au (g/t)	Ag (g/t)	Mo (ppm)	Copper Eq (tonnes)	Copper (tonnes)	Gold (ounces)	Silver (ounces)	Molybdenum (tonnes)
Indicated	148	0.51	0.39	0.12	0.78	102	750,000	578,000	559,000	3,702,000	15,000
M+I Total	148	0.51	0.39	0.12	0.78	102	750,000	578,000	559,000	3,702,000	15,000
Inferred	56	0.38	0.30	0.08	0.54	61	211,000	170,000	139,000	971,000	3,400

Costa Fuego Total Resource		Grade					Contained Metal				
Classification	Tonnes (Mt)	CuEq (%)	Cu (%)	Au (g/t)	Ag (g/t)	Mo (ppm)	Copper Eq (tonnes)	Copper (tonnes)	Gold (ounces)	Silver (ounces)	Molybdenum (tonnes)
Indicated	725	0.47	0.38	0.11	0.45	93	3,408,000	2,755,000	2,564,000	10,489,000	67,400
M+I Total	725	0.47	0.38	0.11	0.45	93	3,408,000	2,755,000	2,564,000	10,489,000	67,400
Inferred	202	0.36	0.30	0.06	0.31	66	731,000	605,000	359,000	2,032,000	13,400

* Reported on a 100% Basis - combining Mineral Resource estimates for the Cortadera, Productora and San Antonio deposits. Figures are rounded, reported to appropriate significant figures, and reported in accordance with CIM and NI 43-101. Metal rounded to nearest thousand, or if less, to the nearest hundred. Total Resource reported at +0.21% CuEq for open pit and +0.30% CuEq for underground

Copper Equivalent (CuEq) reported for the resource were calculated using the following formula: $CuEq\% = ((Cu\% \times Cu\ price\ 1\% \text{ per tonne} \times Cu_recovery) + (Mo\ ppm \times Mo\ price\ per\ g/t \times Mo_recovery) + (Au\ ppm \times Au\ price\ per\ g/t \times Au_recovery) + (Ag\ ppm \times Ag\ price\ per\ g/t \times Ag_recovery)) / (Cu\ price\ 1\% \text{ per tonne})$.

The Metal Prices applied in the calculation were Cu=3.00 USD/lb, Au=1,700 USD/oz, Mo=14 USD/lb, Ag=20 USD/oz. For Cortadera and San Antonio, the average Metallurgical Recoveries were Cu=83%, Au=56%, Mo=82%, Ag=37%. For Productora, the average Metallurgical Recoveries were Cu=83%, Au=43%, Mo=42%.

Table 1.12 Cortadera Mineral Resource Summary – reported by classification (31st March 2022) and by open pit (top), underground (middle) and total (bottom) *

Cortadera OP Resource		Grade					Contained Metal				
Classification (+0.21% CuEq*)	Tonnes (Mt)	CuEq (%)	Cu (%)	Au (g/t)	Ag (g/t)	Mo (ppm)	Copper Eq (tonnes)	Copper (tonnes)	Gold (ounces)	Silver (ounces)	Molybdenum (tonnes)
Indicated	323	0.44	0.34	0.12	0.66	53	1,411,000	1,102,000	1,284,000	6,808,000	17,100
M+I Total	323	0.44	0.34	0.12	0.66	53	1,411,000	1,102,000	1,284,000	6,808,000	17,100
Inferred	53	0.32	0.25	0.08	0.46	62	168,000	132,000	135,000	778,000	3,300

Cortadera UG Resource		Grade					Contained Metal				
Classification (+0.30% CuEq*)	Tonnes (Mt)	CuEq (%)	Cu (%)	Au (g/t)	Ag (g/t)	Mo (ppm)	Copper Eq (tonnes)	Copper (tonnes)	Gold (ounces)	Silver (ounces)	Molybdenum (tonnes)
Indicated	148	0.51	0.39	0.12	0.78	102	750,000	578,000	559,000	3,702,000	15,000
M+I Total	148	0.51	0.39	0.12	0.78	102	750,000	578,000	559,000	3,702,000	15,000
Inferred	56	0.38	0.30	0.08	0.54	61	211,000	170,000	139,000	971,000	3,400

Cortadera Total Resource		Grade					Contained Metal				
Classification (+0.21% CuEq*)	Tonnes (Mt)	CuEq (%)	Cu (%)	Au (g/t)	Ag (g/t)	Mo (ppm)	Copper Eq (tonnes)	Copper (tonnes)	Gold (ounces)	Silver (ounces)	Molybdenum (tonnes)
Indicated	471	0.46	0.36	0.12	0.69	68	2,161,000	1,680,000	1,843,000	10,509,000	32,200
M+I Total	471	0.46	0.36	0.12	0.69	68	2,161,000	1,680,000	1,843,000	10,509,000	32,200
Inferred	108	0.35	0.28	0.08	0.50	62	379,000	301,000	274,000	1,749,000	6,700

*Reported on a 100% Basis. Figures are rounded, reported to appropriate significant figures, and reported in accordance with CIM and NI 43-101. Metal rounded to nearest thousand, or if less, to the nearest hundred. Total Resource reported at +0.21% CuEq for open pit and +0.30% CuEq for underground

Copper Equivalent (CuEq) reported for the resource were calculated using the following formula: $CuEq\% = ((Cu\% \times Cu \text{ price } 1\% \text{ per tonne} \times Cu_recovery) + (Mo \text{ ppm} \times Mo \text{ price per g/t} \times Mo_recovery) + (Au \text{ ppm} \times Au \text{ price per g/t} \times Au_recovery) + (Ag \text{ ppm} \times Ag \text{ price per g/t} \times Ag_recovery)) / (Cu \text{ price } 1\% \text{ per tonne})$.

The Metal Prices applied in the calculation were Cu=3.00 USD/lb, Au=1,700 USD/oz, Mo=14 USD/lb, Ag=20 USD/oz. For Cortadera and San Antonio, the average Metallurgical Recoveries were Cu=83%, Au=56%, Mo=82%, Ag=37%. For Productora, the average Metallurgical Recoveries were Cu=83%, Au=43%, Mo=42%

Table 1.13 Productora Mineral Resource Summary – reported by classification (31st March 2022) *

Productora Total Resource		Grade					Contained Metal				
Classification (+0.21% CuEq*)	Tonnes (Mt)	CuEq (%)	Cu (%)	Au (g/t)	Ag (g/t)	Mo (ppm)	Copper Eq (tonnes)	Copper (tonnes)	Gold (ounces)	Silver (ounces)	Molybdenum (tonnes)
Indicated	253	0.49	0.41	0.08		139	1,247,000	1,043,000	646,000		35,100
M+I Total	253	0.49	0.41	0.08		139	1,247,000	1,043,000	646,000		35,100
Inferred	90	0.34	0.29	0.03		75	305,000	259,000	91,000		6,800

*Reported on a 100% Basis. Figures are rounded, reported to appropriate significant figures, and reported in accordance with CIM and NI 43-101. Metal rounded to nearest thousand, or if less, to the nearest hundred. Total Resource reported at +0.21% CuEq for open pit.

Copper Equivalent (CuEq) reported for the resource were calculated using the following formula: $CuEq\% = ((Cu\% \times Cu \text{ price } 1\% \text{ per tonne} \times Cu_recovery) + (Mo \text{ ppm} \times Mo \text{ price per g/t} \times Mo_recovery) + (Au \text{ ppm} \times Au \text{ price per g/t} \times Au_recovery) + (Ag \text{ ppm} \times Ag \text{ price per g/t} \times Ag_recovery)) / (Cu \text{ price } 1\% \text{ per tonne})$.

The Metal Prices applied in the calculation were Cu=3.00 USD/lb, Au=1,700 USD/oz, Mo=14 USD/lb, Ag=20 USD/oz. For Cortadera and San Antonio, the average Metallurgical Recoveries were Cu=83%, Au=56%, Mo=82%, Ag=37%. For Productora, the average Metallurgical Recoveries were Cu=83%, Au=43%, Mo=42%

Table 1.14 San Antonio Mineral Resource Summary – reported by classification (31st March 2022) *

San Antonio Total Resource		Grade					Contained Metal				
Classification (+0.21% CuEq*)	Tonnes (Mt)	CuEq (%)	Cu (%)	Au (g/t)	Ag (g/t)	Mo (ppm)	Copper Eq (tonnes)	Copper (tonnes)	Gold (ounces)	Silver (ounces)	Molybdenum (tonnes)
Inferred	4.2	1.2	1.1	0.01	2.1	1.5	48,100	47,400	2,000	287,400	6

*Reported on a 100% Basis. Figures are rounded, reported to appropriate significant figures, and reported in accordance with CIM and NI 43-101. Metal rounded to nearest thousand, or if less, to the nearest hundred. Total Resource reported at +0.21% CuEq for open pit

Copper Equivalent (CuEq) reported for the resource were calculated using the following formula: $CuEq\% = ((Cu\% \times Cu \text{ price } 1\% \text{ per tonne} \times Cu_recovery) + (Mo \text{ ppm} \times Mo \text{ price per g/t} \times Mo_recovery) + (Au \text{ ppm} \times Au \text{ price per g/t} \times Au_recovery) + (Ag \text{ ppm} \times Ag \text{ price per g/t} \times Ag_recovery)) / (Cu \text{ price } 1\% \text{ per tonne})$.

The Metal Prices applied in the calculation were Cu=3.00 USD/lb, Au=1,700 USD/oz, Mo=14 USD/lb, Ag=20 USD/oz. For Cortadera and San Antonio, the average Metallurgical Recoveries were Cu=83%, Au=56%, Mo=82%, Ag=37%. For Productora, the average Metallurgical Recoveries were Cu=83%, Au=43%, Mo=42%

HCH was responsible for all data verification, geological and mineralisation interpretation, and three-dimensional surface creation. Work completed by HCH was peer reviewed prior to block model Resource estimation and classification by Elizabeth Haren of Haren Consulting. Ms Haren was responsible for all aspects of geostatistical analysis, variography modelling, and determination of parameters for block model and resource estimation.

The Mineral Resource Estimation (MRE) process included:

- Statistical analysis of the composites, within appropriate mineralisation domains
- Compositing of the drilling results to an appropriate length
- Top-cut and variographic analysis within mineralisation and weathering domains, as appropriate
- Volume modelling within mineralisation domains, taking into consideration drill spacing, mineralisation continuity and potential mining methods
- Estimation of a grade model via categorical indicator kriging, ordinary block kriging or inverse distance interpolation within resultant estimation domains, using both soft and hard boundaries to reflect geological understanding
- Assignment of density using fresh density data, within lithological domains. Fresh density data was discounted by 10% for transitional and 20% for oxide (owing to the lack of density data for the oxide and transitional material)
- Validation of the estimated grades using visual and statistical analysis, swath and QQ plots and analysis of estimation produced variables such as Kriging Efficiency and Slope of Regression
- Depletion of the MRE using the mined void model, comprising surveyed and openings implied by mine level plans.

A range of criteria were considered in determining the Resource Classification, including:

- Geological and grade continuity between drillholes
- Drillhole spacing
- Proposed high-tonnage mining method
- 3D surfaces to define an open pit and underground mining shapes (under optimistic long-term copper prices).

Where significant extrapolation occurred, or the material was located outside the open pit shell or underground stope shapes (as defined by an RPEEE optimisation), the mineralisation was categorised as Unclassified.

There are currently no known environmental, permitting, legal, title, taxation, socio-economic, marketing, political or other relevant factors which could affect the MRE.

1.12 Mineral Reserve Estimate

As no current feasibility or pre-feasibility studies have been completed to the standard of NI 43-101, no Mineral Reserves have been estimated for the Costa Fuego Project on or before the submission date.

1.13 Environmental and Social

The Environmental Impact Assessment (EIA) of the Project will be submitted for approval using the Environmental Impact Assessment System (EIA System) that is currently being applied in Chile.

The environmental baselines describe the condition of relevant environmental components that may be affected by the Project. Baselines for the Project included the following activities:

- Multiple baseline campaigns covering the Project area and all associated infrastructure areas have been covered since 2012. For seasonal baselines like flora and fauna, four campaigns have been organised to cover passive and active season's changes.
- The list of non-seasonal baselines comprises 19 components such as archaeology, landscape, palaeontology, human environment, geomorphology, natural risks, etc.
- Main findings in the Project area refer to flora and fauna species under conservation status, archaeology findings with high value and the presence of some families living at the Project.

HCH interacts with many regional and local stakeholders who have an interest in the Project. The stakeholder engagement plan is divided in two sections to cover firstly the consultation of key stakeholders and secondly the community development issues. Key stakeholders have been identified in the three concerned districts: Vallenar, Freirina,

and Huasco. The outcomes of this exercise will be used as the basis to create a stakeholder engagement plan.

The process to assess the environmental impacts of the Project utilised a methodology comprising three stages:

1. Identification of impacts in relation to the activities and project works
2. Impacts evaluation
3. Impacts ranking.

The outcome of the assessment process identified four significant impacts that require special attention for future work:

- Alteration and/or loss of terrestrial flora and vegetation
- Alteration and/or loss of habitat for fauna
- Significant changes in the livelihood of human groups
- Alteration of archaeological sites with high value.

1.14 Recommendations

1.14.1 Prefeasibility Study

Based on the results of the 2022 Costa Fuego MRE, it is recommended that the Costa Fuego Project be advanced to the Pre-feasibility stage. Following positive results to the outcome of this work, a Feasibility study would then be recommended.

1.14.2 Costa Fuego Environmental Works

Ongoing environmental works at Costa Fuego will include drill permitting with associated palaeontology and archaeology surveys and coincident fauna and flora relocation during track and drill pad construction.

1.14.3 Regional Targeting

Drilling to test regional targets within the range of the Costa Fuego development will determine if these targets can be incorporated into the Project. This includes both drilling (Reverse Circulation and Diamond Drilling) and assaying as required.

1.14.4 Mineral Resource Development Drilling and Estimation

Resource development drilling at Cortadera paused in December 2021 for the Costa Fuego Mineral Resource. The result has provided a number of prospective targets around the Cortadera mineralised porphyry system which have the potential to grow both the underground and open pit mineral resource.

The Productora Resource and mineralisation is currently open at depth in several places as well as laterally. Additional drilling may add additional mineralisation volume and has the potential to upgrade resource classification of currently Inferred resource.

Additional exploration drilling around the Alice area is still very prospective and should be considered. An updated Alice resource estimate should incorporate learnings from the recently completed Cortadera resource as both are centred on porphyry intrusions.

The San Antonio deposit requires the drilling of twinned diamond holes to validate the location of the mineralisation and improve confidence in a data set derived mostly of pre-HCH data.

1.14.5 Cortadera Geotechnical and Metallurgical Drilling and Development Studies

A specific metallurgical and geotechnical drilling program of approximately 2,600m is required for a better definition of geotechnical domains and the drill core will also supply further variability and composite samples to the metallurgical test work program. This metallurgy program is predominantly assessing comminution, flotation, filtration and thickening at Cortadera. A smaller program at Productora will add to the substantial work already completed for this resource.

The development studies for Costa Fuego are ongoing, having commenced in June 2021. A mining study will be required, comprising the entire open cut mining studies involving pit optimisation, mine designs, mining schedule/sequence, waste dump designs, mine fleet analysis and operating cost and capital cost estimates

The mining study will cover open pit and underground mining, geotechnical and groundwater and surface water studies.

Geotechnical drilling will allow better definition of geotechnical domains and additional engineering will be undertaken to prepare detailed pit slope stability analysis for the first mining phase and the final pit as a minimum. It will also include detailed stability analysis for waste dumps.

Groundwater and surface water studies shall include hydrogeological assessment and complementary field works to improve the information quality for a robust PFS.

1.15 Summary

The estimated work programme budget for the 12 months beginning January 2022 within the Project area is summarised below (Table 1.15).

Table 1.15 Future Work Programme

Work Programme	Cost (USD)
Environmental Costs – Costa Fuego	340,000
Cortadera Resource Development Drilling	600,000
Regional Targets Drilling and Assaying	6,675,000
Cortadera Geotechnical and Metallurgical Drilling and Assaying	1,850,000
Development Studies – Mining, Metallurgy, Geotechnical and Environmental	3,590,000
Total	13,055,000

The Qualified Persons (QPs) have reviewed the proposed program of work and budget and finds them to be reasonable and justified considering the observations made in this report. The recommended work program and proposed expenditures are appropriate and well thought out. The proposed budget reasonably reflects the type and scope of the contemplated activities.

The QPs recommend that HCH conduct the planned activities subject to availability of funding and any other matters which may cause the objectives to be altered in the normal course of business activities.

2 INTRODUCTION

2.1 Terms of Reference

At the request of Hot Chili Limited (HCH or the Company), Haren Consulting and ABGM have prepared the Mineral Resources for the Productora, Cortadera and San Antonio deposits that comprise the Costa Fuego Copper Project (the Costa Fuego Project or the Project).

This Technical Report has been prepared for the Project to the standard of the Canadian National Instrument 43-101 – *Standards of Disclosure for Mineral Projects* (NI 43-101).

There has been no material change to the Costa Fuego Project between the effective date of this Technical Report and the signature date.

HCH is a mineral exploration company focused on the acquisition, exploration, and development of mineral properties in Chile.

The Productora deposit is 100% owned by a Chilean incorporated company named Sociedad Minera El Aguila SpA (SMEA). SMEA is a joint venture company – 80% owned

by Sociedad Minera El Corazón Limitada (a 100% subsidiary of HCH), and 20% owned by CMP Productora (a 100% subsidiary of Compañía Minera del Pacífico S.A (CMP), a major Chilean iron ore producer).

In August 2015, a joint venture (JV) agreement was established between HCH and CMP. This resulted in the formation of a JV company named SMEA. This partnership has enabled securement of the majority of surface rights required for developing key infrastructure for the Productora project, as well as the majority of easements required for water and power transmission lines.

The Cortadera and San Antonio deposits are controlled by a Chilean incorporated company named Sociedad Minera Frontera SpA (Frontera). Frontera is a subsidiary company – 100% owned by Sociedad Minera El Corazón Limitada, which is a 100% subsidiary of HCH.

Frontera owns the Cortadera deposit and controls an area approximately 12.5 km N-S by 7 km E-W through various option earn in agreements with private landholders, and through 100% ownership of certain leases.

Haren Consulting is an independent geological consulting firm based in Perth, Australia.

ABGM is an independent mining consulting firm based in Perth, Australia.

2.2 Purpose of Report

This report details the results from resource drilling and estimation of the Costa Fuego Project Mineral Resources.

This technical report is intended to comply with disclosure obligations under NI 43-101 and conforms to the standards prescribed by NI 43-101 and pursuant to Form 43-101F1 – *Technical Report*.

2.3 Cautionary Notes

This report has been compiled based on information available up to and including the date of this report.

The status of agreements, royalties or tenement standing pertaining to the assets, have not been investigated by contributing consultants and were not required to be. All matters relating to ownership are to be directed to HCH for clarification if required.

2.4 Sources of Information

This report relies on historic and recent data generated by HCH, including:

- Information provided by qualified geologists employed by HCH regarding the geology, drilling, sampling and other exploration procedures and processes adopted by HCH
- Information provided by HCH pertaining to the past history of the Project
- Information provided by HCH in relation to the property location, property title and ownership and mineral tenure.

HCH has engaged specialist consultants and information from these reports, prepared by independent consultants, has been utilised in the compilation of this report.

Section 27 provides a list of references relied upon in preparation of this report.

2.5 Site Visits

The COVID-19 global pandemic has prohibited the Costa Fuego Mineral Resource Qualified Person (QP) Elizabeth Haren from visiting site.

The COVID-19 global pandemic has prohibited the Costa Fuego Mineral Resource Qualified Person (QP) Anton von Wielligh from visiting site.

2.6 Definitions

In this Technical Report, all currency amounts are stated in US Dollars (USD or US\$) unless otherwise stated. Commodity prices are typically expressed in USD and will be noted where so appropriated. Quantities are generally stated in Systeme International d' Unites (SI) metric units.

Grid coordinates for maps are given in world grid latitude and longitude.

Certain abbreviations and terminology used in this Technical Report are summarised in Table 2.1 below.

Table 2.1 Definitions

Abbreviations	Meaning
\$	Dollars
°	Degree
°C	Degrees Celsius
asl	Above sea level
\$M	Dollars, million
ASX	Australian Stock Exchange
Au	Gold
Company	Hot Chili Limited
cm	Centimetre
CMP	Compañía Minera del Pacífico S.A
COG	Cut off grade
Conc.	concentrate
CWi	Crusher Work Index
Cu	Copper
dmt	Dry Metric Tonne
DD	Diamond Drill
HCH	Hot Chili Limited
lb	Pound
oz	Ounce
tr. oz	Troy Ounce
g	Gram
kg	Kilogram
m	Metre
mm	Millimetre
Mo	Molybdenum
MRE	Mineral Resource Estimate
OPEX	Operating Cost Estimate
N	North
S	South
E	East
W	West
mtpa	Million tonnes per annum

Abbreviations	Meaning
PEA	Preliminary Economic Assessment
PSD	Particle Size Distribution
ppm	Parts per million
QA/QC or QC	Quality Assurance/Quality Control
QP	Qualified Person
RC	Reverse Circulation
ROM	Run of Mine
SMU	Selective Mining Units
SX-EW	Solvent Extraction Electro Winning
RC	Reverse Circulation
Project	Costa Fuego Copper Project
SMEA	Sociedad Minera El Aguila SpA (
t	Tonne
WGS84	World Geodetic System
TSF	Tailings Storage Facility
kWh	Kilowatt-hours
kV	Kilovolts
kL	Kilolitre
l/s	Litres per second
HV	High Voltage
m ³ /h	Cubic Metres per Hour
STP	Sewage Treatment Plant
SBR	Sequence Batch Reactor
WRD	Waster Rock Dump
Wood	Wood Australia Pty Ltd
wmt	Wet Metric Tonne

3 RELIANCE ON OTHER EXPERTS

This report is based, in part, on the review, analysis, interpretation and conclusions derived from information which has been provided by HCH staff and its consultants and have opined upon it.

The QPs used their experience to review such information and determine if the information was suitable for inclusion in this Technical Report. The QPs do not disclaim any responsibility for this information.

This report includes technical information which required subsequent calculations to derive subtotals, totals, and weighted averages. Such calculations inherently involve a degree of rounding and consequently introduce a margin of error. Where these occur, the QPs do not consider them to be material.

The QPs have relied upon the following various independent consulting companies that contributed to the development of this report:

- Dr Steve Garwin – Chief Technical Advisor regarding the understanding and development of porphyry, epithermal and Carlin-style mineralisation.
- Dr John Beeson – Lead Structural Geologist who completed mapping and soil sampling at San Antonio.
- Grasty, Quintana, Majlis - Legal opinion in connection to the current status of the Cortadera deposit mining rights.

4 PROPERTY DESCRIPTION AND LOCATION

4.1 Property Location, Access, and Site Layout

The Costa Fuego Project, which includes the Productora, Cortadera and San Antonio project areas, is centred 17km south of Vallenar in the Region III of Chile (Región de Atacama). The Project is located approximately 155km south of Copiapó, the capital of Region III, and 140km north of the city of La Serena.

Productora lies 5km off the main sealed Pan-American Highway which connects Vallenar to La Serena in the south and can be accessed via the Quebrada Arenas gravel road 2.2km towards the west. From that point, the Project can be accessed by continuing along the Quebrada Verde track for 5km.

Cortadera and San Antonio lie approximately 15km to the east of the Pan-Highway and are accessed through gravel roads and trails.

The Project lies within the low altitude coastal range belt and has an average altitude of 740m above sea level. Costa Fuego has good access to infrastructure and facilities in the regional mining town of Vallenar.

Figure 4.1 outlines the location of the Project relative to Vallenar and the surrounding infrastructure.

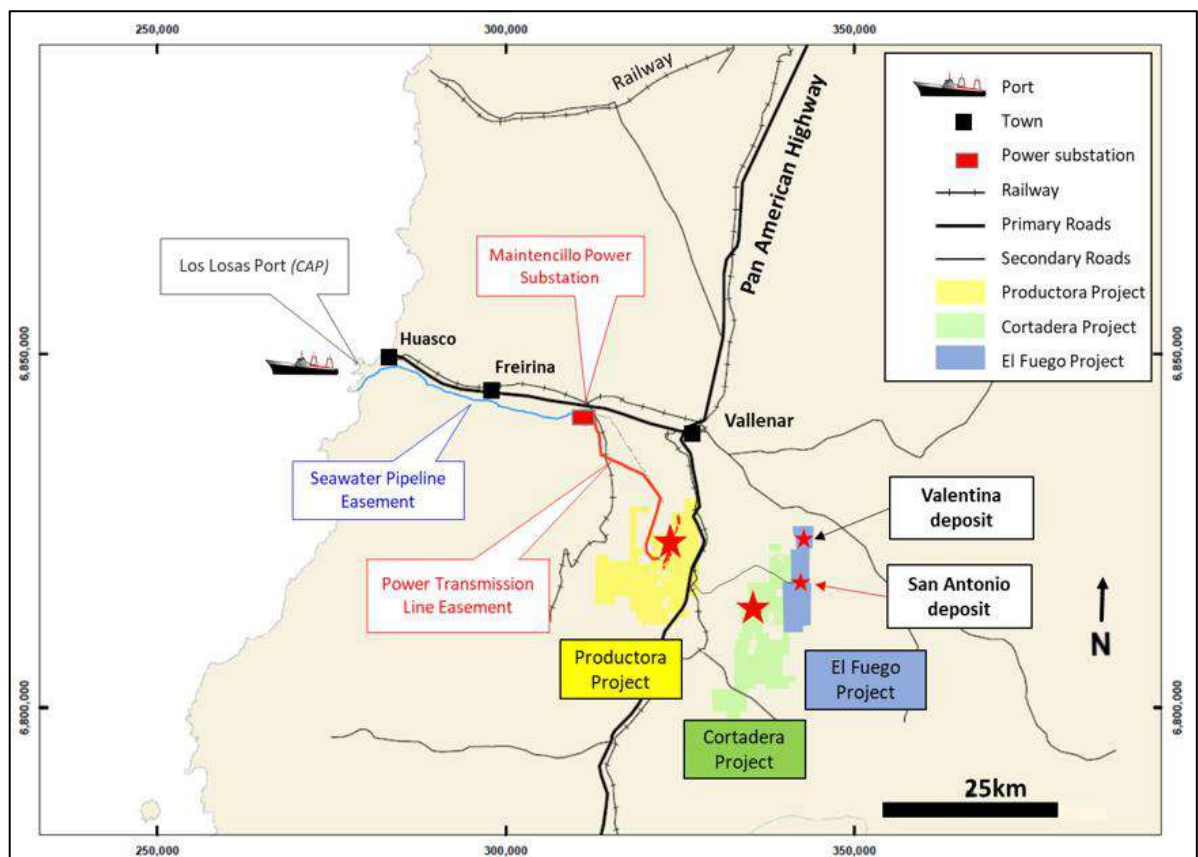


Figure 4.1 Costa Fuego Project location in relation to Vallenar and the surrounding infrastructure, Chile. (HCH, 2021)

4.2 Mineral Tenure

4.2.1 Productora

The Productora project is owned by a Chilean incorporated company named Sociedad Minera El Aguila SpA (SMEA) which is a subsidiary of Sociedad Minera El Corazón Limitada, which in turn is also a subsidiary of the HCH.

SMEA owns 80% of Productora; the other 20% is owned by Compañía Minera del Pacífico S.A (CMP), a major Chilean iron ore producer.

The project is approximately 18 km long by 14 km wide, with a total landholding of 13,605 hectares.

SMEA controls Productora primarily through direct ownership, except for one exploitation concession (Uranio 1/70), in which a 30-year lease agreement has been executed with The Chilean Nuclear Energy Commission (CCHEN) which commenced in 2012.

Two underground copper mines were in operation within the central mining lease of Productora from late 2006 until mid-2013. SMEA executed a purchase option agreement with owners of the Productora 1/16 concession where the underground mines were located. In February 2013, following exercise of the purchase option, mining activities ceased, and all equipment was removed from the project area.

Mining concessions (or mining rights, as they are also known in Chile) are granted by a judicial award issued by a court of justice in the context of a non-litigious proceeding. Mining rights are protected by the Chilean Constitution as well as many different legal bodies, of which the Mining Code is the most important legislation. The territorial extension of a mining concession takes on the shape of a solid, the surface of which is a horizontal parallelogram of right angles, and the depth of which is indefinite within the vertical planes that establish its boundaries.

In general, the Political Constitution of the Republic and the provisions of Chilean law make no distinction among Chileans and non-Chileans regarding the enjoyment of basic rights, the acquisition of property, and the development of economic activities.

According to Article 2 of the Constitutional Law on Mining Concessions (Law 18,097), a mining concession is: “an in-rem property right, different and independent from ownership of the surface land, even if it belongs to one and the same owner; enforceable against the State and any other person; transferable and transmissible; subject to mortgage and other in rem rights and, in general, to any act or contract”.

Under Chilean law, there are two types of mining concessions:

- Exploration concessions which are for the purpose of exploring and expire after a period of two years; and
- Exploitation concessions which are for the exploitation of minerals and have no expiry date, some annual rent payments are required.

Table 4.1 details the SMEA tenement holding at Productora, tenement ownership, and mining concession type.

Table 4.1 SMEA SpA mining tenement holding for Productora

Licence ID	Holder	% Interest	Licence Type	Area (ha)
FRAN 1, 1-60	SMEA	100%	Exploitation concession	220
FRAN 2, 1-20	SMEA	100%	Exploitation concession	100
FRAN 3, 1-20	SMEA	100%	Exploitation concession	100
FRAN 4, 1-20	SMEA	100%	Exploitation concession	100
FRAN 5, 1-20	SMEA	100%	Exploitation concession	100
FRAN 6, 1-26	SMEA	100%	Exploitation concession	130
FRAN 7, 1-37	SMEA	100%	Exploitation concession	176
FRAN 8, 1-30	SMEA	100%	Exploitation concession	120
FRAN 12, 1-40	SMEA	100%	Exploitation concession	200
FRAN 13, 1-40	SMEA	100%	Exploitation concession	200
FRAN 14, 1-40	SMEA	100%	Exploitation concession	200
FRAN 15, 1-60	SMEA	100%	Exploitation concession	300
FRAN 18, 1-60	SMEA	100%	Exploitation concession	273
FRAN 21, 1-46	SMEA	100%	Exploitation concession	226
ALGA 7A, 1-32	SMEA	100%	Exploitation concession	89
ALGA VI, 5-24	SMEA	100%	Exploitation concession	66
MONTOSA 1-4	SMEA	100%	Exploitation concession	35
CHICA	SMEA	100%	Exploitation concession	1
ESPERANZA 1-5	SMEA	100%	Exploitation concession	11
LEONA 2A 1-4	SMEA	100%	Exploitation concession	10
CARMEN I, 1-50	SMEA	100%	Exploitation concession	222
CARMEN II, 1-60	SMEA	100%	Exploitation concession	274
ZAPA 1, 1-10	SMEA	100%	Exploitation concession	100
ZAPA 3, 1-23	SMEA	100%	Exploitation concession	92
ZAPA 5A, 1-16	SMEA	100%	Exploitation concession	80
ZAPA 7, 1-24	SMEA	100%	Exploitation concession	120
CABRITO, CABRITO 1-9	SMEA	100%	Exploitation concession	50
CUENCA A, 1-51	SMEA	100%	Exploitation concession	255
CUENCA B, 1-28	SMEA	100%	Exploitation concession	139
CUENCA C, 1-51	SMEA	100%	Exploitation concession	255
CUENCA D	SMEA	100%	Exploitation concession	3
CUENCA E	SMEA	100%	Exploitation concession	1
CHOAPA 1-10	SMEA	100%	Exploitation concession	50
ELQUI 1-14	SMEA	100%	Exploitation concession	61
LIMARÍ 1-15	SMEA	100%	Exploitation concession	66
LOA 1-6	SMEA	100%	Exploitation concession	30
MAIPO 1-10	SMEA	100%	Exploitation concession	50
TOLTÉN 1-14	SMEA	100%	Exploitation concession	70
CACHIYUYITO 1, 1-20	SMEA	100%	Exploitation concession	300
CACHIYUYITO 2, 1-60	SMEA	100%	Exploitation concession	300
CACHIYUYITO 3, 1-60	SMEA	100%	Exploitation concession	300
LA PRODUCTORA 1-16	SMEA	100%	Exploitation concession	75
ORO INDIO 1A, 1-20	SMEA	100%	Exploitation concession	82
AURO HUASCO I, 1-8	SMEA	100%	Exploitation concession	35
URANIO, 1-70	CCHEN	100%	Exploitation concession	350
JULI 9 1/60	SMEA	100%	Exploitation concession	300
JULI 10 1/60	SMEA	100%	Exploitation concession	300
JULI 11 1/60	SMEA	100%	Exploitation concession	300
JULI 12 1/42	SMEA	100%	Exploitation concession	210
JULI 13 1/20	SMEA	100%	Exploitation concession	100
JULI 14 1/50	SMEA	100%	Exploitation concession	250
JULI 15 1/55	SMEA	100%	Exploitation concession	275

Licence ID	Holder	% Interest	Licence Type	Area (ha)
JULI 16 1/60	SMEA	100%	Exploitation concession	300
JULI 17 1/20	SMEA	100%	Exploitation concession	100
JULI 19	SMEA	100%	Exploration concession	300
JULI 20	SMEA	100%	Exploration concession	300
JULI 21 1/60	SMEA	100%	Exploitation concession	300
JULI 22	SMEA	100%	Exploration concession	300
JULI 23 1/60	SMEA	100%	Exploitation concession	300
JULI 24 1/60	SMEA	100%	Exploitation concession	300
JULI 25	SMEA	100%	Exploration concession	300
JULI 27 1/30	SMEA	100%	Exploitation concession	146
JULI 27 B 1/10	SMEA	100%	Exploitation concession	48
JULIETA 5	SMEA	100%	Exploration concession	200
JULIETA 6	SMEA	100%	Exploration concession	200
JULIETA 7	SMEA	100%	Exploration concession	100
JULIETA 8	SMEA	100%	Exploration concession	100
JULIETA 9	SMEA	100%	Exploration concession	100
JULIETA 10 1/60	SMEA	100%	Exploitation concession	300
JULIETA 11	SMEA	100%	Exploration concession	300
JULIETA 12	SMEA	100%	Exploration concession	300
JULIETA 13 1/60	SMEA	100%	Exploitation concession	300
JULIETA 14 1/60	SMEA	100%	Exploitation concession	300
JULIETA 15 1/40	SMEA	100%	Exploitation concession	200
JULIETA 16	SMEA	100%	Exploration concession	200
JULIETA 17	SMEA	100%	Exploration concession	200
JULIETA 18 1/40	SMEA	100%	Exploitation concession	200
ARENA 1 1/6	SMEA	100%	Exploitation concession	40
ARENA 2 1/17	SMEA	100%	Exploitation concession	113
ZAPA 1 - 6	SMEA	100%	Exploitation concession	6

All mining rights at Productora are exploitation concessions with no risk of expiring if the mining taxes are duly paid annually.

Surface rights are 100% owned by SMEA, as are the maritime concession to extract sea water from the coast and the corridor of easements to construct a pipeline and electrical transmission line to Productora.

A map of HCH's mining rights under WGS84 is shown below (Figure 4.2).

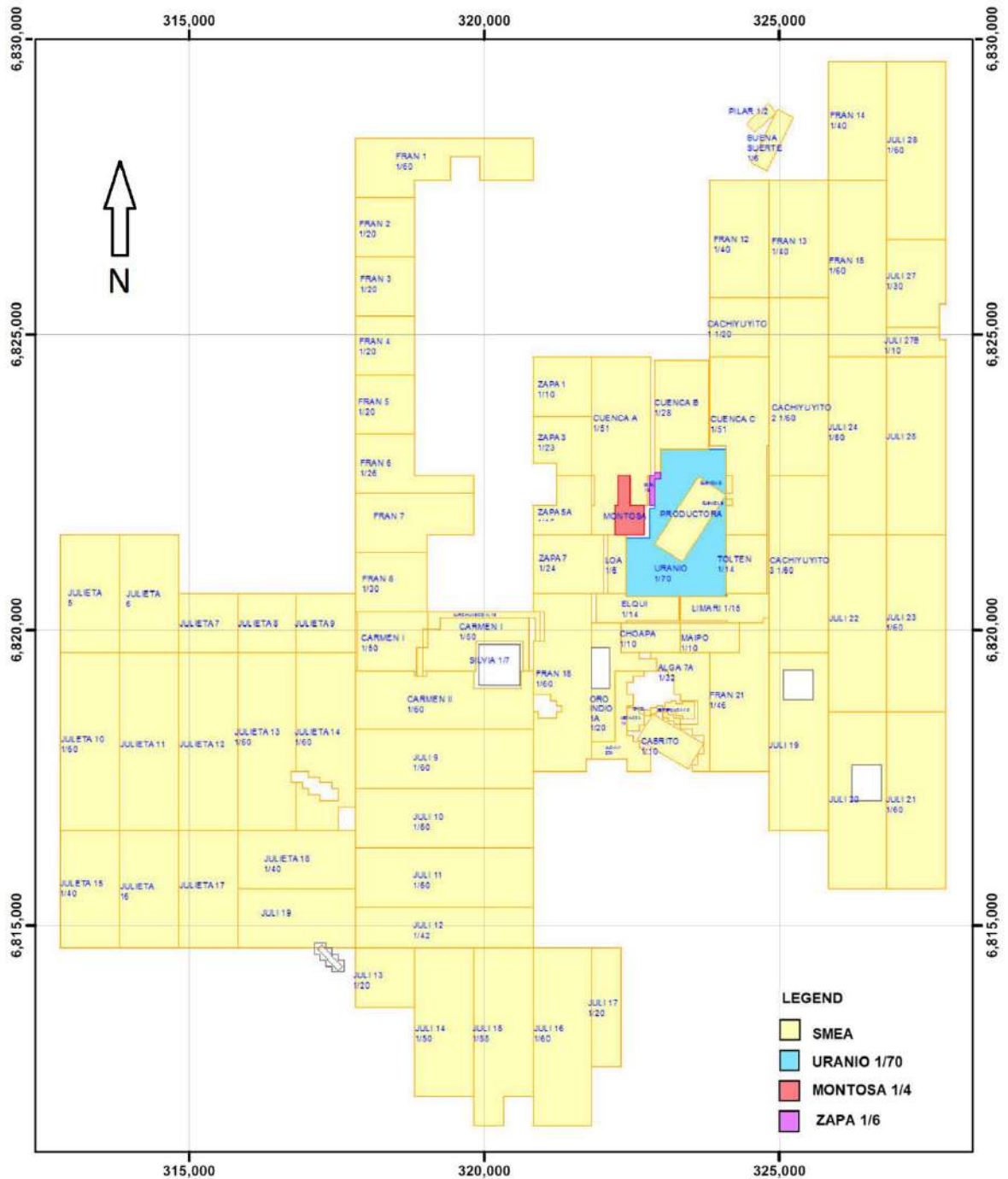


Figure 4.2 Productora Mining Rights under WGS84. (HCH, 2021)

SMEA is the owner of the majority of the surface rights required for the infrastructure of Productora (an area of approximately 4,111 ha), including the surface rights for the mining area, sulphide processing plant, TSF area, access roads and associated supporting facilities.

SMEA has all the required easements for both the seawater pipeline and power line corridors.

A map showing the surface area owned by SMEA for developing Productora is shown in Figure 4.3.

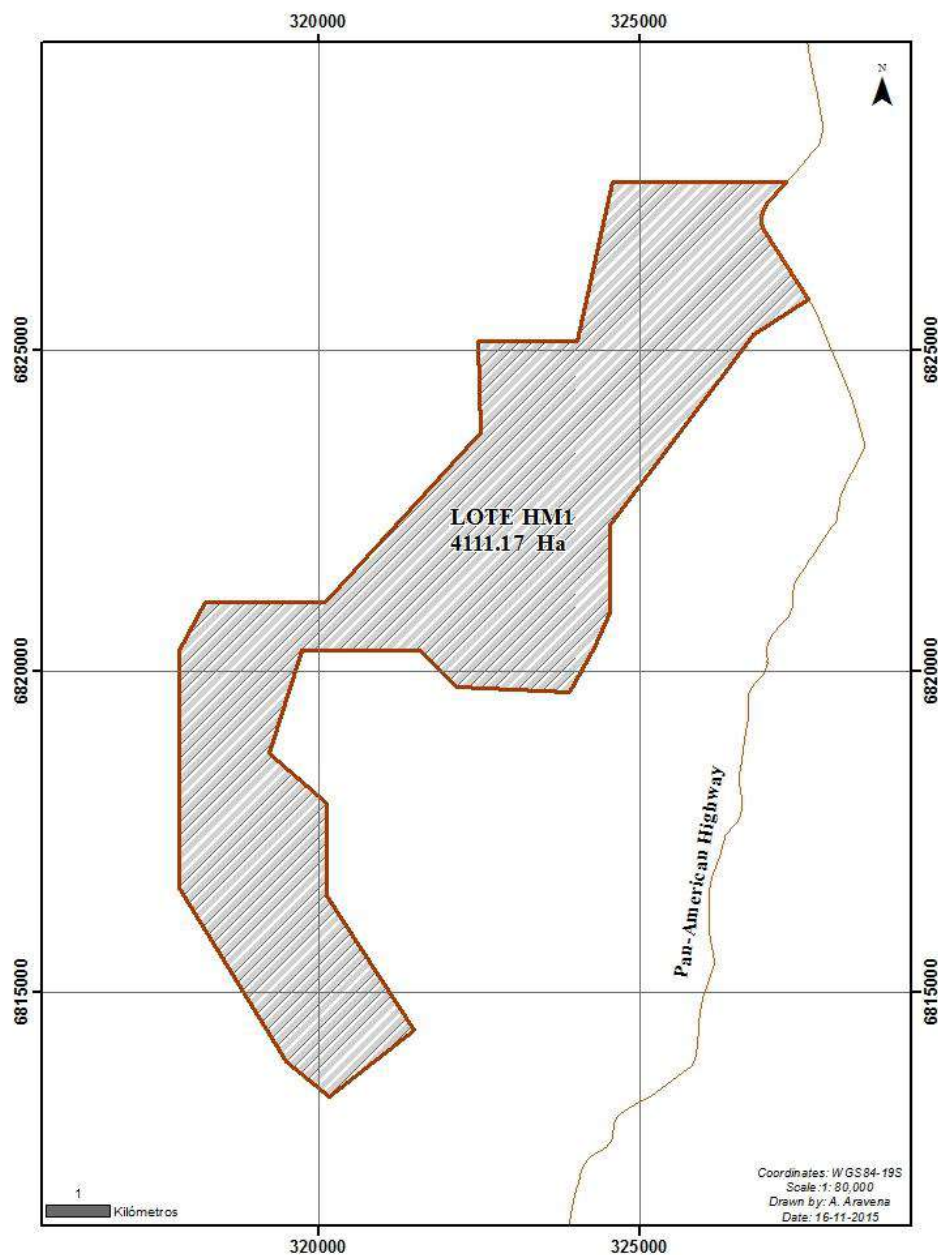


Figure 4.3 Productora surface area (approximately 4,111 hectares) (HCH, 2016)

4.2.2 Cortadera

Hot Chili Limited owns the Cortadera project through Frontera and controls an area measuring approximately 17,000 hectares at the project through various 100% purchase option agreements with private mining title holders and 100% owned tenure.

Figure 4.4 shows Frontera consolidated position over the mining rights at the Cortadera and El Fuego projects.

As a summary:

- Frontera has full ownership over the mining rights coloured in pink and in red.
- Frontera has a six-year Option Agreement over the mining rights coloured in light blue (San Antonio Option Agreement).
- Frontera has a six-year Option Agreement over the mining rights coloured in magenta (Valentina Option Agreement).
- Frontera has a five-year Option Agreement over the mining rights coloured in gray (Santiago Z Option Agreement).

All mining tenements are in good standing and all mining requirements have been met for the exploration phase. At this stage, there are no legal requirements for any kind of bonds to be issued.

The current exploration activities for the project have been approved under the Environmental Approval number 48, dated March 24, 2021, granted by the Environmental Assessment Service.

Surface land access for exploration activities have also been granted by the owner, Mr. Pedro Prokurika Morales by agreement acknowledged and approved by the local Court of Vallenar on March 30th, 2022. by virtue of private document, dated October 14, 2019.

The area covered by the surface rights are sufficient for any potential open pit and underground mining operation together with the potential area for waste disposal and potential dump leach pads.

All power, water and personnel will be sourced from Productora, and any mineralized material will be transported to the Productora site for processing and subsequent tailings disposal.

Cortadera has no current social and/or community requirements.

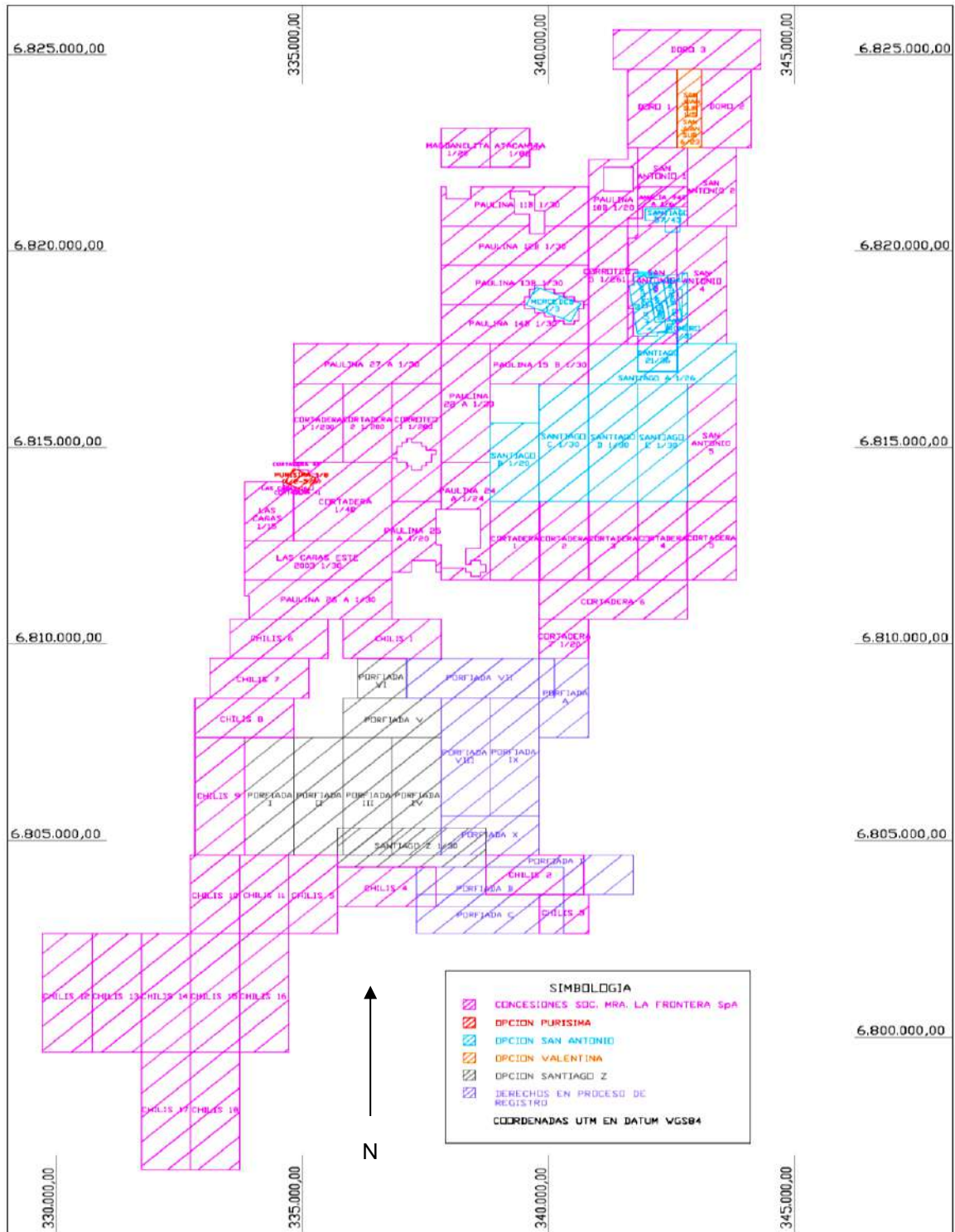


Figure 4.4 Image of HCH tenements. (HCH, 2021)

From the 1990's, beginning with initial small-scale mining, several companies explored and mined copper oxides in the Cortadera area. Some small open pit mining was completed in the 2000's but it wasn't until Minera Fuego took ownership in 2009 that significant exploration using modern exploration techniques occurred (Table 4.2).

Since securing the deposit in 2019, HCH has continued advancing Cortadera with modern exploration techniques, such as Diamond drilling (DD), Reverse Circulation drilling (DD), surface geochemical sampling and litho-structural mapping.

Table 4.2 Cortadera Ownership History

Year	Owner
1990	R.G Grego and J.R Alday
1993	Empresa Nacional de Minería (Enami)
1994 - 2009	Sociedad Contractual Minera Carola (SCM Carola)
2009 - 2013	Mineral Fuego Limitada (Minera Fuego or MFL) under an option agreement with Sociedad Contractual Minera Carola (SCM Carola). This option was not exercised, and ownership reverted back to SCM.
2010	Minera Fuego purchased Purísima from a small local miner
2015	Minera Fuego awarded Purísima to R. Jammás (a geologist who worked for them during the period 2010-2015)
February 2019 - Current	Hot Chili Limited - Cortadera and Purísima through Option agreements

4.2.2.1 Cortadera (mining rights in blue)

Table 4.3 shows Frontera 100% full ownership of the mining rights acquired by execution of the former Option Agreement between Sociedad Contractual Minera Carola (SCM Carola) and Frontera.

Table 4.3. Summary of Cortadera mining rights

Name	Area (ha)	Name	Area (ha)
MAGDALENITA 1/20	100	PAULINA 26 A 1/30	294
ATACAMITA 1/82	82	PAULINA 27A 1/30	300
AMALIA 942 A 1/6	53	CORTADERA 1 1/200	200
PAULINA 10 B 1/16	136	CORTADERA 2 1/200	200
PAULINA 11 B 1/30	249	CORTADERA 41	1
PAULINA 12 B 1/30	294	CORTADERA 42	1
PAULINA 13 B 1/30	264	LAS CANAS 16	1
PAULINA 14 B 1/30	265	LAS CANAS 1/15	146
PAULINA 15 B 1/30	200	CORTADERA 1/40	374
PAULINA 22 A 1/30	300	LAS CANAS ESTE 2003 1/30	300
PAULINA 24 1/24	183	CORROTEO 1 1/260	260
PAULINA 25 A 1/19	156	CORROTEO 5 1/261	261

4.2.2.2 Purísima (mining rights in red)

Table 4.4 shows Frontera 100% full ownership of the mining right (with an annual 1.5% NSR) acquired by execution of the former Option Agreement between Sociedad Legal Minera Purísima Una Sierra La Cortadera and Frontera.

Table 4.4 Purísima mining rights

Name	Area (ha)
PURISIMA	20

4.2.3 San Antonio and Valentina

Hot Chili Limited (HCH), through Frontera, executed an Option Agreement with a private party to earn a 90% interest in the San Antonio copper-gold project over a six-year period. The proposed JV involves an option agreement over 27 exploitation leases (~4,727ha), whereby full ownership of 90% of the mining rights of the project will be transferred upon satisfaction of a payment of US\$300,000 in October 2022 and then a final payment of US\$6,700,000 a year later.

HCH, through Frontera, executed an option agreement with a private party to earn a 90% interest in the Valentina copper-gold project over a six-year period. The proposed JV involves an option agreement over two exploitation leases (100ha), whereby full ownership of 90% of the mining rights of the project will be transferred upon satisfaction of a payment of US\$150,000 by June 2023 and then a final payment of US\$4,000,000 a year after. Contract committed drilling is currently underway at Valentina.

Exploration by Frontera at San Antonio and Valentina shall be at its discretion and the owner will have the right to lease to any third party the exploitation of the mining rights with an annual cap of 50,000 tonnes of ore until exercise of the option.

Frontera also has other 100% owned leases around the project.

4.3 Specific Tax of Mining, Water Regulation and Encumbrances

4.3.1 Specific Tax on Mining

Chilean legislation establishes a tax on mining activities (Specific Tax on Mining), which is levied over the operational income of the metal mining activity obtained by a mining exploiter (individuals or legal entities that extract and sell mineral substances).

The tax rate will be defined according to the annual sales of the mining exploiter:

- Annual sales less than 12,000 metric tonnes of fine copper are exempt of this tax.
- Annual sales between 12,000 and 50,000 metric tonnes of fine copper are taxed with a progressive tax rate that varies from 0.5% to 4.5%.
- Annual sales in excess of the value of 50,000 metric tonnes of fine copper are taxed according to the “mining operational margin” of the mining exploiter (a ratio between the taxable mining income and the gross mining income multiplied by 100), as follows:
 - When the mining operational margin of the mining exploiter does not exceed 85%, the tax rate applies progressively between each tax bracket, with a tax rate from 5% to 34.5%.
 - With a 14% flat rate when the mining operational margin exceeds 85%.

The Specific Tax on Mining regulation includes a special anti-avoidance rule to avoid the artificial segregation of the operational income from mining activity (taxable income) to obtain a reduction in the tax rate (e.g., creating different companies for one operation in order to reduce operational income). Accordingly, for purposes of calculating the

specific tax, the mining exploiter must include in the amount of its annual sales, the amount of the annual sales obtained by their related parties.

The value of a metric tonne of fine copper is calculated according to the average value on the London Metal Exchange and the operational income of the mining activity is calculated over the rules of the corporate income tax, with minor amendments.

4.3.2 Water Rights Legislation in Chile and HCH Strategy for Water Usage

A mining concession grants its holder the right to use the water resources found while developing exploration and/ or exploitation works, whichever the case may be, but only for the purposes of such exploration and/or exploitation works.

Water can be bought from certified suppliers (as HCH does for the exploration phase works).

As per the community engagement strategy, the exploitation of the Project contemplates operating with sea water. SMEA currently holds a valid Maritime Concession Licence for the extraction of saltwater from a location south of the Huasco area.

4.3.3 Encumbrances

The only third-party encumbrance in Productora is an electric transmission line on the extreme north of the Project, but there are no major impediments to developing the Project because this power line sits well outside of the area where most of the Project infrastructure is located.

4.4 Environmental

Productora and Cortadera have robust environmental baseline studies, completed over a 10-year period, commencing in 2011 (in the case of Productora).

Environmental baseline studies developed at Productora and Cortadera cover areas where mining infrastructure is proposed. This includes stockpiles, waste dumps, and tailings storage facility.

Studies comprise archaeological baselines, Flora and Fauna baselines, and groundwater monitoring and landscape analysis. A surrounding community's study has been carried out to identify the potential impacts on dwellings within proximal to the project (majadas).

A thorough baseline campaign was carried out at Puerto Las Losas to measure marine wildlife and flora. Also, a one-year atmospheric conditions measurement was carried out at Productora.

Full environmental studies are going underway for Cortadera and Productora.

4.5 Legal Review

4.5.1 Productora

Correa Squella Legal, Chile, was requested to render a legal opinion in connection to the status of the HCH mining rights constituted or acquired by the Company in the Productora project, including its superficial rights, such as easements, and its maritime concession.

- SMEA was duly incorporated and transformed into a company by shares, in both cases under the laws of Chile. Therefore, it legally exists and is in good standing.
- HCH's investment in Chile is fully protected under national foreign investment protection legislation.
- To this point, SMEA holds all licenses, certificates, and permits from public entities necessary for conducting its business at the project.
- Regarding the legal status of the mining concessions:
 - the mining exploitation concessions constituted by SMEA in the project have been duly constituted and are currently in force
 - the mining claims currently being processed by SMEA have followed, to date, all the legal steps outlined in the Mining Code. Therefore, there has not been any error in their constitutive proceedings
 - both exploitation concessions and mining claims are duly registered on behalf of SMEA. Therefore, such mining rights are the exclusive property of SMEA
 - mining patents and fees of these mining rights have been fully and timely paid.
- As of July 2021, the previously referred rights are not subject to liens, prohibitions, embargoes, encumbrances, or lawsuits of any kind.
- The CCHEN Agreement constitutes a valid and binding agreement, and all obligations stipulated therein are enforceable against the parties bound thereby.
 - Therefore, the Uranium Property:
 - has been duly constituted and is currently in force
 - is duly registered under the name of CCHEN. Consequently, it has the sole and exclusive ownership over the Uranium Property
 - from 1990 onward, all mining patents have been paid
 - is not subject to liens, prohibitions, embargoes or lawsuits of any kind, except for the prohibition registered in favour of SMEA under the Uranio Lease Agreement
 - does not grant to its holder the right to explore or exploit other minerals than uranium

- The maritime concession has been lawfully granted.
 - To this date, SMEA has followed all the legal steps outlined in the maritime concessions regulation to enter in possession.
- All superficial rights are valid, binding, and enforceable against third parties.

4.5.2 Cortadera

Grasty, Quintana, Majlis, Chile, were requested by HCH to issue a legal opinion based on Chilean law in regard to mining titles that the Company currently holds in Chile by means of its subsidiary, Frontera, a company duly incorporated under Chilean law.

Frontera is the holder of rights in five mining projects called “Cortadera”, “San Antonio”, “Santiago Z”, “Valentina” and “Purísima”.

- Frontera was duly incorporated in accordance with the laws of Chile, it legally exists and is in good standing.
- The Option Agreements constitute valid and binding agreements and all obligations stipulated therein are enforceable against the parties respectively bound thereby.
- All payments accrued with regards to the Option Agreements have been timely and fully paid.
- Regarding to the mining rights:
 - All mining rights included in Option Agreements were established in accordance with the requirements of the Mining Code. There were no third parties’ concessions overlapping the mining rights.
 - Currently, the mining exploitation concession “Cortadera 7 1/20” (Cortadera project) and the mining exploration concessions “Porfiada I” to “Porfiada IV” and “Chilis 1” to “Chilis 18” (Santiago Z project) are in process of being constituted and they are not affected by lapse causes.
- Based on the review, there are no agreements regarding the mining concessions that could affect Frontera's tenure or Frontera's right to acquire the mining rights.
- The Cortadera project and the Purísima project have sufficient provisional surface rights for exploration. The exploration stage was approved by the Environmental Approval number 48 dated March 24 2021 granted by Environmental Assessment Service; there is an agreement for the surfaces rights to execute the exploitation project, to obtain the required surface easements or other similar title that allows the operator of the project to occupy the superficial terrain so as to cover and protect all manner of installations such as offices, mineral deposits, clearings, dumps, tailings, mineral extraction plants, communication systems, channels, dams, pipes, housing, transportation routes, aqueducts, electrical lines, among others.

5 ACCESSIBILITY, CLIMATE, LOCAL RESOURCES, INFRASTRUCTURE AND PHYSIOGRAPHY

5.1 Accessibility

The Project is in a favourable location surrounded by infrastructure which can be utilised for developing a greenfield copper project. Figure 5.1 displays the location of the following infrastructure items:

- Regional township of Vallenar
- Pan-American Highway
- Airport located approximately 3km south of Vallenar
- Access to the Huasco Port
- Power substations located approximately 20km northwest at Maintencillo, connected to the Chilean electrical grid.



Figure 5.1 Infrastructure proximal to the Costa Fuego Project. (HCH, 2016)

The Project centre is 17km south of Vallenar, a city and commune in Atacama Region, Chile. It is the capital of the Huasco Province and is located in the valley of the Huasco River. Vallenar has a population of approximately 52,000 people and its main activities are farming and mining.

The Project centre can be accessed by following the main sealed Pan-American Highway connecting Vallenar to Coquimbo in the south.

5.2 Site Facilities

The Project already has temporary facilities available to service approximately 50 people on site. These facilities may be used for initiating the Project development activities, with the site infrastructure items already in place being:

- Access road
- Temporary offices
- Power diesel generator
- Toilets and sanitation facility (water treatment plant)
- Small, fenced storage area
- Diamond drill core storage facility
- RC drill pulp storage facility
- Drill core logging area.

5.3 Climate

The Project is located in two Koeppen climates: BWn desert with abundant clouds, and BWk normal desert with characteristics of low marginal desert. The biggest difference between both climates is the maritime influence of the first one, that generates high episodes of high humidity throughout the year, creating abundant cloudiness that penetrates from the coastal sector through the Huasco river valley.

For Huasco, Freirina and Vallenar, the annual mean temperatures respectively correspond to 14.9°C, 15.7°C, and 15.6°C, observing an annual mean amplitude of 4°C, 3.4° and 4.5°C, respectively. Also, the highest amounts of accumulated annual average rainfall reach 50.4mm/year, the wettest months being between May and August. Associated with warm ENSO events, strong rainfall events are concentrated over a few hours, and can bring climate hazards related to river floods, mudflows etc.

5.4 Vegetation

The Project area is located within the “Highland Flowering Desert” plant formation. Characterized by high floristic diversity, this plant formation is predominated by scrub formations and bushes. Herbs are also abundant during years of high rain.

Nearly all vegetation present at Productora have xerophytic species listed in Chilean Act N°68, therefore, are protected and subject to a revegetation plan.

5.5 Physiography

The Project is located in a transition zone between the desert plains and pre-altiplanic mountain ranges and coastal plains. The geomorphological units directly involved in the Project are characterized by a rocky and mountainy desert landscape with elevations ranging from sea level to altitudes above 1,500m above sea level, which causes a medium to gentle relief.

The landscape is dominated by a system of mountain ranges with little vegetation consisting of bushes and cacti, typical of the coastal desert. Overall, the Project is entirely within a desert area under the influence of tropical bio-climate, which despite having strong water restrictions, due to its wide geographical spread and range of thermal conditions, it benefits from a large variety of vegetation floors. In addition, because of the latitude and the proximity of the ocean, it receives favourable conditions for the growth of vegetation, such as some xerophytic plants communities. However,

different vegetation communities (shrubs, cacti, amongst others) have been strongly intervened by human activity as a result of the charcoal production, heavy grazing of goats and mining developments. As for the water network in the study area, no permanent or seasonal courses of water are observed – however sporadic water courses superficially flow after heavy rains.

The coastal zone is represented by coastal plains and a coastal mountain range with hills up to 1,500 m high. Huasco river, at its mouth in the town of Huasco, has geofoms associated with river erosion, such as fluvial terraces and meanders. The interior zone is represented by moderately sloping alluvial desert plains.

6 HISTORY

6.1 Productora

6.1.1 Ownership History

The Productora camp has a long mining history for iron, copper and gold extending back to pre-Hispanic times. Historical iron mining has occurred at the La Chulula, La Bandera, Mariposa, Carmen, and La Negra mines. Copper mining in the past century has occurred regionally and locally at the Productora and Santa Innes mines (operated by Playa Brava and ENAMI), Remolina, and Montserrat mines. In addition, there are more than 80 smaller pits, workings, or mineralised outcrops in the Project area containing iron, copper, or gold mineralisation.

Exploration activities at Productora prior to 2010 are summarised in Table 6.1. HCH completed acquisition of the main tenement package in 2012.

6.1.2 Historical Exploration and Development Work

This section describes the work carried out by different owners over time. Table 6.1 presents a summary of the different owners and their work at Productora since the 1980's.

Table 6.1 Ownership History

Year	Company
1980's	Chilean Commission for Nuclear Energy (CCHEN) and several private tenement owners
1995 - 1999	General Minerals Corporation (GMC) explored the area
1999 - 2005	GMC (in joint venture with Teck Corp) explored the area
2008 - 2015	HCH Limited through its wholly owned Chilean subsidiary Sociedad Minera El Aguila options and consolidates the area
2015 - present	Joint venture (JV) agreement between HCH (80%) and CMP (20%) owners of Sociedad Minera El Aguila SpA.

6.1.3 CCHEN Exploration

In the 1980s, the Chilean Commission for Nuclear Energy (CCHEN) explored the area near and to the south of the Productora mine for uranium. At least ten shallow (35 to 101m) RC holes were completed and while minor uranium oxide was intersected, no significant deposits were found.

CCHEN then completed mapping, surface geochemical sampling, ground spectrometry and magnetometry, trenching, drilling (28 shallow percussion holes) and resource estimation, focusing almost entirely on the near-surface, secondary uranium potential at Productora.

Soil sampling defined eight copper-molybdenum-uranium anomalies interpreted as being largely in-situ. The arid environment was invoked to explain an apparent lack of large-scale chemical dispersion during weathering. Trenching across some of the anomalies returned a peak uranium assay of 7m at 1,820ppm. Drilling by CCHEN focused on testing the near-surface uranium potential. The CCHEN exploration model

was based on a secondary mineralisation control exerted by andesitic dykes that cut across the host sequence.

This work defined an area of near-surface uranium mineralisation at Productora over 2km within a zone of hydrothermal alteration 3km long by 500m to 800m wide, trending 010°.

6.1.4 GMC Exploration

General Minerals Corporation (GMC) acquired the Productora area in 1995 to search for a Candelaria- type iron-oxide-copper-gold (IOCG) deposit. In 1997, eight reverse circulation drillholes (PR-1 to PR-8) were completed. Additional work also involved compilation of earlier mapping, surface geochemical sampling, ground geophysics surveys (IP) and percussion drilling.

In 1999, GMC entered into a joint venture with Teck Corporation and completed an additional eleven reverse circulation holes (PR-9 to PR-19). The holes targeted secondary copper enrichment zones in the southern portions of the central lease at Productora.

The work defined a 2km long copper-gold-molybdenum-uranium trend that was compared to Candelaria in terms of mineralisation style, interpreted as IOCG mineralisation. Mineralisation was interpreted to be controlled by a large NNE-trending structure and a system of cross-cutting, NW trending faults. Copper-gold-molybdenum-uranium mineralisation was found to be associated with iron oxides and strong potassic (K-feldspar) alteration. IP surveys delineated a 6.1km long by 2km wide linear anomaly thought to represent continuations of the mineralised zone. In addition, a 2km long IP anomaly was detected to the west. Drill testing of the main Productora IP anomaly returned encouraging results. However, drill testing of the western IP anomaly returned disappointing results for copper-molybdenum-gold. Despite encouraging results on the main Productora trend, funding issues caused termination of exploration work.

6.1.5 Thesis – Colorado School of Mines (USA)

During 1998-1999, a MSc. thesis was completed by Ms. Kari-Ann Fox under the supervision of Professor Murray Hitzman (Colorado School of Mines). This work involved field mapping (down to 1:5,000 scale) and laboratory studies, including petrology, whole-rock geochemistry, geochronology (Ar39-Ar40, U-Pb zircon), X-ray diffraction and sulphur isotope analysis. To date, the thesis completed by Fox (2000) represents by far the most detailed description of the geology of Productora.

The following sections summarise the work described in Fox (2000).

The Bandurias Formation comprises a thick sequence of volcanic flows and ash flow tuffs intruded by the Cachiyuyito intrusion (129.8±0.1 Ma) and the Ruta 5 Batholith (border phase dated as 96.1±0.2 Ma). These age determinations were made using a U-Pb zircon technique. Broadly, the stratigraphically oldest to youngest rocks comprise andesitic ash-flow tuff, then lower dacitic ash flow tuff, dacitic welded ash flow tuff, upper

dacitic ash flow tuff, volcanoclastic sedimentary rocks and basalt and basaltic andesite flows which overlie the volcanoclastic/ tuffaceous sequence.

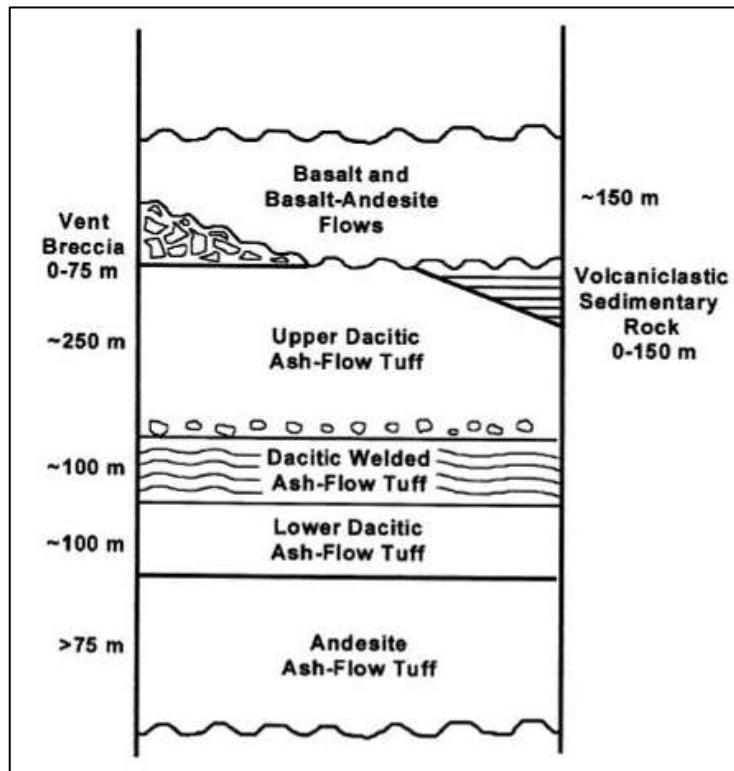


Figure 6.1 Stratigraphic column for Productora

The Cachiyuyito and Ruta 5 intrusive rocks intrude the volcanic sequence. The older Cachiyuyito intrusion is an NNE elongated, elliptical and concentrically zoned body with a tonalitic core and a dioritic border phase. The Ruta 5 intrusion represents a portion of a composite batholith with at least two phases. The Ruta 5 intrusion at Productora is zoned outwards from a granodiorite core (with biotite > hornblende) outwards to a slightly magnetic quartz monzodiorite border phase (with hornblende > biotite).

Fox (2000) identifies a suite of later andesitic dykes that cut most of the above rock types. This late dyke suite cuts all lithological units except the Ruta 5 batholith and trends generally NW-NNW, with other trends evident locally. The andesitic dykes vary from phaneritic to porphyritic and locally contain minor chalcopyrite or pyrite. Magnetite of both primary and hydrothermal origin is present locally in these dykes.

Three hydrothermal systems associated with NW and N trending structures have been recognised comprising the following:

- Cachiyuyito system – magnetite-apatite system hosted in andesitic tuff adjacent to the sodic altered Cachiyuyito intrusion, similar to iron deposits in the Cretaceous iron belt of Chile. Associated alteration and veining comprise albite-chlorite-actinolite-magnetite-calcite-epidote-apatite.
- The Cachiyuyito intrusion is slightly depleted in FeO and P₂O₅ despite the presence of apatite veins. Fe, Ca, P and Mg have been mobilised and

reconcentrated into magnetite-epidote-apatite veins. Na₂O and K₂O show an inverse relationship, with most samples being enriched in Na₂O and some enriched in K₂O (sericitisation of albite during the subsequent Productora alteration event). Highest uranium and REE assays appear to be related to this system.

- Productora system – multi-stage potassium-iron alteration involving silica (albite)-sericite alteration along north-trending fault zones. The early pyrite alteration is associated with elevated cobalt (but not significant copper-gold enrichment) and was followed by copper-gold-uranium-REE-(molybdenum) mineralisation, with associated chlorite-Kfeldspar-tourmaline-epidote-magnetite-hematite alteration and hypogene sulphides comprising chalcopyrite (molybdenite). This later alteration stage shows Au in strong positive correlation with chalcopyrite and pyrite (Au may be intergrown with these sulphides). REE's are also elevated in the chalcopyrite-pyrite zone (REE's with apatite or allanite?). K-feldspar-chalcopyrite veining and alteration has been dated at 91.4±0.2Ma (slightly discordant Ar³⁹-Ar⁴⁰ age determination). This potassic alteration system is distributed around and perhaps genetically linked the Ruta 5 intrusion. Potassium-iron alteration mineralogy appears to reflect primary lithology and progresses from early biotite-pyrite-(K-feldspar) to chlorite-magnetite-(K-feldspar)-chalcopyrite-gold to late epidote-chlorite-specularite-tourmaline-magnetite with chalcopyrite developed in tourmaline veins and epidote-chlorite-specularite-(tourmaline) veins.
- Ruta 5 system – propylitic alteration (chlorite-actinolite-epidote-magnetite) affecting andesite dykes and the upper andesite-basalt flow unit, associated with emplacement of late-stage quartz-hematite-Au veins. Chalcopyrite and pyrite are present locally in epidote-quartz veins.
- Supergene alteration – magnetite, sulphides and hematite altered to goethite, copper oxides and carbonates and silicates, chalcocite, covellite and digenite.

Hydrothermal alteration is pervasive at the scale of the project with virtually all rocks being altered.

At a broader scale, mineralisation and alteration is broadly north trending, while at a finer scale mineralised veins trend NW and are locally disrupted by later faulting.

Sulphur isotope work on pyrite, chalcopyrite and chalcocite mineralisation indicate a lack of isotopically heavy sulphur values appearing to rule out evaporates as a sulphur source. Pyrite and chalcopyrite pairs used to estimate formation temperature are wildly variable indicating that the pyrite and chalcopyrite were not precipitated in isotopic equilibrium (i.e., were precipitated during different stages of the Productora alteration system). Fox (2000) makes comparisons between the Productora copper-gold (Cu-Au) system and other Cu-Au deposits in Chilean Cretaceous Iron Belt. Fox's conclusion is that Productora is most similar to a Candelaria type Cu-Au (magnetite-sulphide) system,

which at Productora overprints an earlier magnetite-apatite system associated with the Cachiyuyito intrusion.

6.1.6 Historical Exploration Data Collection

An extensive data compilation and validation exercise was performed by Hot Chili Limited in 2010. Historical data was collected from several sources including hard copy reports, public disclosure, and both hard copy and digital maps. Ground truthing via project reconnaissance was also completed. This data compilation resulted in an Access geological database and an ArcGIS database being created.

While both the historical geological drill database and ArcGIS database was useful for planning exploration drilling, neither of these historical data sources have been used for Resource estimation.

6.2 Productora Previous Mineral Resource and Reserve Estimates

6.2.1 Introduction

Previous Resource and Reserve estimates have been undertaken by HCH and reported either under the Joint Ore Reserves Committee of the Australasian Institute of Mining and Metallurgy, Australian Institute of Geosciences and Minerals Council of Australia (JORC Code 2012 Edition) code or to the standards of NI 43-101.

These previous estimates are provided for historical context only and the Issuer is not treating these estimates as current.

6.2.1.1 JORC 2004 Maiden Resource (Central), HCH, September 2011

Following the completion of initial project assessment, HCH commenced an extensive Resource definition drilling programme in August 2010 which was completed in early July 2011. This programme recorded several significant intercepts in extensional areas along strike from existing underground development. A total of 141 RC holes for 28,308m and 22 DD holes for 5,012m was drilled by HCH and were used to define the maiden Resource (Table 6.2).

Table 6.2 Productora Maiden Resource (Central) declared under the JORC 2004 edition and were rounded to a single decimal place for reporting purposes

Productora Maiden Resource - 2011							
Classification	Tonnes (millions)	Grade			Contained Metal		
		Cu %	Au g/t	Mo ppm	Copper (tonnes)	Gold (ounces)	Molybdenum (tonnes)
Indicated	31.1	0.6	0.1	159	184,612	109,711	4,942
Inferred	54.0	0.6	0.1	138	298,062	179,895	7,476
Total	85.1	0.6	0.1	146	482,673	289,606	12,418

6.2.1.2 JORC 2004 Resource Revision 1, HCH, February 2013

Following on from the estimation of the maiden Resource, HCH commenced an extensive exploration and Resource definition drilling programme in October 2011 to test for mineralisation along strike. This programme was completed in December 2012. Several significant intercepts were recorded in areas along strike (both south and north) from the existing Central Resource area. A total of 398 RC holes for 97,756m and 27 RCDD for 11,538m were drilled by HCH and used to define the further extents to mineralisation.

This revision was modelled exclusively outside the extents of the maiden (Central) Resource. The final public reporting of Resource Revision 1 was from the combined figures of the maiden (Central) Resource and the subsequent revision (Table 6.3).

Table 6.3 *Along-strike extensions (added to the Central resource) was declared under the JORC 2004 edition and were rounded to a single decimal place for reporting purposes. This resource was reported at a cut-off of greater than or equal to 0.3% Cu.*

Productora Resource Revision 1 - February 2013								
Classification	Resource Series	Tonnes (millions)	Grade			Contained Metal		
			Cu %	Au g/t	Mo ppm	Copper (tonnes)	Gold (ounces)	Molybdenum (tonnes)
Indicated	Res Upgrade 1	39.4	0.6	0.1	124	230,000	150,000	5,000
	Central	31.1	0.6	0.1	159	185,000	110,000	5,000
	Total	70.6	0.6	0.1	139	420,000	260,000	10,000
Inferred	Res Upgrade 1	40.6	0.5	0.1	110	200,000	130,000	4,000
	Central	54.0	0.6	0.1	138	298,000	180,000	8,000
	Total	94.6	0.5	0.1	126	500,000	310,000	12,000
Total	Res Upgrade 1	80.0	0.5	0.1	117	440,000	290,000	9,000
	Central	85.2	0.6	0.1	146	480,000	290,000	13,000
	Total	165.2	0.6	0.1	132	920,000	580,000	22,000

6.2.1.3 JORC 2012 Resource Revision 2, HCH, March 2014

Following on from Resource Revision 1, HCH commenced an extensive Resource definition drilling programme from December 2012 to December 2013 to infill and test near-resource mineralisation. A total of 351 RC holes for 85,645m and 41 RCDD for 9,926m were drilled by HCH and used to define the further extents to mineralisation.

A total of 905 holes for a cumulative 238,185m (211,708.5m of RC, 26,476.5m of DD) was available for use in Resource estimation. This provided a nominal 40m x 80m drillhole coverage across the majority of the Productora Resource.

The Resource Revision 2 is shown in Table 6.4.

Table 6.4 Resource Revision 2 Resource table. This Resource was declared under the JORC 2012 edition and was reported at a cut-off of greater than or equal to 0.25% Cu.

Resource Classification by Weathering								
Weathering	Classification	Mt	Grade			Contained Metal		
			Cu %	Au g/t	Mo ppm	Copper (tonnes)	Gold (ounces)	Molybdenum (tonnes)
Oxide	Indicated	20.5	0.52	0.10	57	106,000	64,000	1,000
	Inferred	5.1	0.51	0.08	88	26,000	12,000	500
	Sub-total	25.6	0.52	0.09	63	132,000	76,000	2,000
Transitional	Indicated	17.6	0.53	0.10	102	93,000	54,000	2,000
	Inferred	7.5	0.35	0.07	47	26,000	16,000	500
	Sub-total	25.1	0.48	0.09	85	119,000	70,000	2,000
Fresh	Indicated	120.6	0.50	0.11	175	601,000	423,000	21,000
	Inferred	43.1	0.41	0.08	107	177,000	105,000	5,000
	Sub-total	163.6	0.48	0.10	157	777,000	531,000	26,000
Total		214.3	0.48	0.10	138	1,029,000	675,000	29,000

6.2.1.4 JORC 2012 Ore Reserve, March 2016

Following completion of a Prefeasibility Study in March 2016, an ore reserve for the Productora and Alice deposits was declared according to JORC 2012 as shown in Table 6.5.

Table 6.5 Productora JORC 2012 Ore Reserve, March 2016

Ore type	Reserve category	Mt	Cu (%)	Au (g/t)	Mo (ppm)	Contained metal			Payable metal		
						Cu (kt)	Au (koz)	Mo (kt)	Cu (kt)	Au (koz)	Mo (kt)
Oxide	Probable	24.1	0.43	0.08	49	103.0	59.6	1.2	55.6		
Transitional		20.5	0.45	0.08	92	91.3	54.7	1.9	61.5	24.4	0.8
Sulphide		122.4	0.43	0.09	163	522.5	356.4	20.0	445.8	167.5	10.4
Total	Probable	166.9	0.43	0.09	138	716.8	470.7	23.1	562.9	191.9	11.2

Cu price - US\$3.00/lb; Au price US\$1,200/oz; Mo price US\$14.00/lb

Weighted average metallurgical recoveries for sulphide and transitional are 86.1% for Cu; 51.9% for Au; 52.2% for Mo. Heap leach average recoveries are 54.0% for Cu and nil for Au and Mo. Payability factors for metal contained in concentrate are 96% for Cu; 90% for Au; and 98% for Mo. Payability factor for Cu contained in Cu cathode is 100%

6.2.1.5 NI 43-101 2021 Resource Revision 3, HCH, October 2021

The Productora and Alice estimation was reviewed and released as Resource Revision 3 to comply with NI 43-101 as shown in Table 6.6. Note this was released as part of a combined Costa Fuego Resource with the Cortadera deposit.

Table 6.6 Productora Mineral Resource Summary (using +0.25% CuEq cut-off grade), 29 October 2021*

Productora Resource		Grade				Contained Metal			
Classification	Tonnes (millions)	CuEQ	Cu %	Au g/t	Mo ppm	Copper Eq	Copper	Gold	Molybdenum
(+0.25% CuEq*)	(Mt)	(%)	(%)	(g/t)	(ppm)	(tonnes)	(tonnes)	(ounces)	(tonnes)
Measured	0	0	0	0	0	0	0	0	0
Indicated	208	0.54	0.46	0.10	140.0	1,122,000	960,000	643,000	29,200
Total	208	0.54	0.46	0.10	140.0	1,122,000	960,000	643,000	29,200
Inferred	67	0.44	0.38	0.08	109	295,000	255,000	167,000	7,200

Reported at or above 0.25% CuEq. Figures in the above table are rounded, reported to appropriate significant figures, and reported in accordance with CIM and NI-101. Metal rounded to nearest thousand, or if less, to the nearest hundred.

Copper Equivalent (CuEq) reported for the resource were calculated using the following formula: $CuEq\% = ((Cu\% \times Cu \text{ price } 1\% \text{ per tonne} \times Cu_recovery) + (Mo \text{ ppm} \times Mo \text{ price per g/t} \times Mo_recovery) + (Au \text{ ppm} \times Au \text{ price per g/t} \times Au_recovery) + (Ag \text{ ppm} \times Ag \text{ price per g/t} \times Ag_recovery)) / (Cu \text{ price } 1\% \text{ per tonne})$. The Metal Prices applied in the calculation were: Cu=3.00 USD/lb, Au=1,550 USD/oz, Mo=12 USD/lb, and Ag=18 USD/oz. For Productora (Inferred + Indicated), the average Metallurgical Recoveries were Cu=83%, Au=43% and Mo=42%

6.3 Productora Production History

6.3.1 2006-2011

Copper mining at Productora commenced in 2006 and was operational until 2012.

Mining was completed by a modern 4.5m x 4.5m decline access exploiting 15m sub-level room and pillar development. The mine extends to ~120m below surface and produced cupriferous mineralized material at a head grade of 0.8 to 1.2% Cu over a strike length of 300m and a width of 50m.

The mineralized material was stockpiled then trucked off-site for toll-treatment at ENAMI's Vallenar processing facility. Drilling by the mine operators and by HCH demonstrates that the mineralisation exploited in the underground mine is contiguous with the larger Mineral Resource. Refer to Table 6.7 for the summarised underground mine production history from 2006 to 2011.

Table 6.7 Production history from the Productora underground mine

Year	Weight (kg)	Weight (tonnes)	GRADE Cu%	Cumulative Weight (kg)	Cumulative Weight (tonnes)
2006	5,738,160	5,738	1.23	5,738,160	5,738
2007	123,572,990	12,3573	1.07	129,311,150	129,311
2008	168,610,080	168,610	1.11	297,921,230	297,921
2009	151,218,070	151,218	1.02	449,139,300	449,139
2010	77,717,750	77,718	0.8	526,857,050	526,857
2011	33,735,050	33,735	0.79	560,592,100	560,592

6.3.2 2020 to present

HCH, through its Chilean subsidiary company SMEA, entered into a lease mining and processing agreement with Chilean government agency ENAMI, with underground mining recommencing at Productora in July 2020. As part of the agreement, mineralized material will be processed at ENAMI's Vallenar processing facility, located 15km north of Productora.

The agreement provides a low-risk pathway to bring forward first production from Productora whilst also providing certainty of mineralized material supply and employment at ENAMI's nearby processing facility in the township of Vallenar.

The Productora joint venture company SMEA (80% HCH) will be paid US\$2 per tonne for mineralized material purchased by ENAMI and a 10% royalty on the sale value of extracted minerals subject to ENAMI toll treatment conditions.

Under the agreement, ENAMI has a two-year concession for lease mining and processing approximately 180,000tpa of mineralized material through ENAMI's Vallenar

plant (located 15km north of Productora) over a two-year period with an option to extend the agreement by a further year.

6.4 Cortadera Historical Exploration and Development Work

6.4.1 Empresa Nacional de Minería

Empresa Nacional de Minería (Enami) is reported by Brionnes (2013) as having completed a small percussion drilling program comprising four holes drilled some time before 1994. These drillholes were supposedly completed prior to open pit mining and presumably were shallow holes aimed at defining near-surface oxide Resources for open pit extraction. Only two of the collars can now be located according to Brionnes (2013).

6.4.2 Minera Mt Isa, Chile

Minera Mt Isa, Chile (MMIC) explored the Johanna project between late 1993 and 1995 under a purchase option agreement with two Chilean owners: Minera Carola and Raul Flores (as summarised below from Alegria 1995). MMIC detected porphyry-style mineralisation and propylitic alteration within overlying volcano-sedimentary rocks defining an approximately 2km long by 1km wide NW-SE trending mineralised corridor, now known as the Cortadera prospect. MMIC also identified two small areas of potassic alteration at Cuerpo 1 and Cuerpo 2 (Szakács & Pop 2001). Work completed under the option agreement included the following:

- 1:5,000 scale geological mapping (lithology, alteration, structure, lithocap and regolith)
- Excavation of six trenches through recent cover to expose and sample the alteration zone
- Roadside sampling and assaying for gold, silver, arsenic, molybdenum, lead, zinc and copper (total and soluble)
- IP-Resistivity surveying (50 m spaced dipoles on thirteen 200m spaced lines)
- Terrestrial magnetometry on 5m spacing collected along the IP-Resistivity lines
- Drilling of 10 diamond holes (HQ in oxide zone and NQ in fresh rock) targeting anomalous geological, geochemical and geophysical features.

The MMIC work programs confirmed the presence of porphyry-style copper-gold-molybdenum mineralisation which extended into fresh rock, proposing localisation of mineralisation in a potassic-altered porphyritic stock, with host volcano-sedimentary rocks showing propylitic alteration and more distal sodic-calcic alteration.

Potassic alteration zones recognised at surface and in drill core are described as containing intense stockwork quartz veins (A-type veins) with accessory magnetite, chalcopyrite, pyrite, actinolite, bornite and molybdenite. These were observed by MMIC geologists to be cut by quartz-pyrite-molybdenite B-type veins, anhydrite veins and pyritic D-type veins. In relatively intense zones of potassic alteration, the mapping and logging identified sulphide volume percentages close to 5%, a chalcopyrite-pyrite ratio up to 1.5:1, and an association between biotite and magnetite alteration.

Phyllic alteration was recognised towards the periphery of the porphyritic stock, as well as overprinting potassic alteration, with associated quartz veins containing sericite, pyrite, chalcopyrite and/or molybdenite. The phyllic alteration zone was described as having up to 10% pyrite, with pyrite-chalcopyrite ratio of 10:1 and containing a few stockwork quartz A veins and chalcopyrite-mineralised B veins, with weak disseminated chalcopyrite also recognised in the host rock.

Propylitic alteration comprising chlorite-epidote-pyrite and minor iron-sphalerite was recognised as an extensive halo peripheral to the phyllic alteration zone, and locally overlapping the potassic alteration zone. Argillic alteration was also recognised exhibiting an irregular distribution along the periphery of Quebrada Cortadera, possibly representing remnant pendants of a much larger but now eroded argillic halo. Leached areas mapped at surface are described as corresponding to areas containing relatively high pyrite concentrations as well as supergene copper minerals and iron oxy-hydroxides.

Szakács & Pop (2001) identified structural trends in previous oxide mines defined by mineralisation that predominantly trend NNE-SSW and NW-SE, with a subordinate ENE-WSW trend. Late mineral and post mineral dykes were also identified as defining structural trends that are predominantly oriented N-S to NNE-SSW. Szakács & Pop (2001) postulated that such structural trends may have facilitated supergene upgrading in the oxide zone and may also have been important controls on bedrock mineralisation.

6.4.3 Minera Fuego Limited

Exploration in and around the Cortadera prospect was conducted at both prospect and regional scale by Mineral Fuego Limitada (Minera Fuego).

6.4.3.1 Cortadera Prospect Exploration

Much of the information collected by Minera Fuego at Cortadera was obtained by diamond drilling aimed at evaluating resources identified in three porphyry-style mineralised bodies located within an extensive alteration colour anomaly along Quebrada Cortadera. The colour anomaly represents a zone of alteration and mineralised tonalitic porphyry outcrops which trend NW-SE along the quebrada for at least 1500 m. The Purísima mine (Cuerpo 1) is located within the NW sector of the colour anomaly, lying above one of the three known zones of porphyry-style mineralisation, and Cu oxides have been exploited via shallow open pit mining (the open pit is generally <15m deep). The other two known porphyry-style mineralised occurrences are known as Stockwork Hill (Cuerpo 2) and Breccia Hill (Cuerpo 3), located in the centre and southeast of the colour anomaly respectively. Other work programs completed by Minera Fuego at Cortadera include detailed mapping, soil sampling, rock chip sampling, collection of geophysical data, metallurgical test work and Resource calculation.

A total of 39 diamond holes (23,230.85m) were drilled by Minera Fuego at Productora. The diamond drilling was completed in two campaigns during 2011 (drillholes FJOD-01 to FJOD-09, 4,279.1m) and 2012 (drillholes FJOD-10 to FJOD-39, 18,951.75m). After initial logging, a standardised Rapid Logging technique was introduced by Eugene Tobey (see Tobey 2011a, 2011b, 2012a, 2012b, 1021c, 2013a), enabling capture of standardised and appropriate data from selected drillholes, including lithology, alteration

mineralogy, structures, oxide ratios, vein mineralogy and percentages, and sulphide mineralogy and percentages for comparison against visual estimates and assay determinations of copper, gold and molybdenum grades. Tobey's method also included preparation of 1:100 scale graphic logs. Based upon the rapid logging results and detailed mapping results, lithological sections and a preliminary geological model of the Breccia Hill (Cuerpo 3) mineralisation was developed. During logging of the diamond drillholes geotechnical data, bulk density data and magnetic susceptibility data was collected from selected drillholes. Brionnes (2013) notes that SGS Lakefield Research Chile S.A. was commissioned by Minera Fuego to complete some metallurgical test-work on selected drill core consisting of a rougher flotation test, the objective being to obtain preliminary information concerning recovery percentages and copper grade of the concentrates from the porphyry-style mineralisation.

Geological mapping studies in and around Cortadera were completed during four mapping campaigns, with the mapping undertaken at scales ranging from 1:2,000 to 1:500, and by different mapping teams. These mapping studies targeted bedrock exposures in the Purísima mine workings and areas surrounding Quebrada Cortadera and Quebrada Las Cañas. The four lithological maps were created using different background images, and this together with differences in observation criteria, lack of control points and inaccuracies of Global Positioning System (GPS) units, led to geological inconsistency and spatial displacement between the maps. Work towards merging the maps and removing geological and spatial inconsistencies was planned by Minera Fuego but not completed prior to cessation of work on-site, although a series of systematic geological cross-sections were interpreted at 1:5,000 scale along the axis of the Cortadera colour anomaly. These cross sections differentiated between early, intermediate and late-stage dacitic porphyry intrusions based upon mapping and quick log results.

Based upon the drilling and mapping described above, Eugene Tobey prepared a series of activity reports within which are established criteria for the recognition of lithological types, alteration types and vein types. Tobey also established relationships between mineralization, quartz vein density and sulfide ratios, relationships between alteration patterns and lithology, and discussed the observed relationships on copper-gold-molybdenum metal distribution. During 2012, Tobey also commenced work on construction of a geological model of the Breccia Hill (Cuerpo 3) mineralisation based upon vein mineralogy and percentage, and copper-gold assay results. During late 2012, statistical models of the Purísima mine (Cuerpo 1), Stockwork Hill (Cuerpo 2) and Breccia Hill (Cuerpo 3) were prepared by Core Mining Studies, resulting in estimation of Mineral Resources for the three mineralised bodies at Cortadera. Brionnes (2013) states that the estimation method consisted of generating 3D mineralisation envelopes and grade continuity analysis.

Rock chip sampling was carried out in old MMIC trenches and at points of interest along roads and surface outcrops where bedrock exposures show traces of hydrothermal alteration. Assaying was completed using an ICP method through ALS Laboratories (ALS). Soil sampling was also completed along and adjacent to the mineralised corridor at nominal 200m x 100m and 100m x 100m sample spacings, and extended to the north, south, southeast and east at completion of drilling. All soil samples were analysed using a hand-held Niton Portable X-Ray Fluorescence (pXRF) unit.

Geophysical data collection included terrestrial and airborne magnetometry. Terrestrial magnetometry was collected by Argali Geophysics E.I.R.L (Jordan, 2009) on nominally 100m-spaced lines, with 1.0 second data intervals (equating to survey stations spaced approximately 0.3 to 1.3m apart). An airborne magnetometry survey was completed by Fugro on a nominal 400m line spacing, with lines oriented 165°-345°.

Seven N-S oriented Induced Polarisation (IP) chargeability and resistivity profiles were collected along Quebrada Cortadera in two stages. In a first stage (May 2011), four profiles each 4.5km long were measured, passing through the mineralised bodies of the Purísima mine (Cuerpo 1), Stockwork Hill (Cuerpo 2) and Breccia Hill (Cuerpo 3). During August 2012 a further three profiles were measured, each 4 km long and located to the east of the 2011 lines. The IP profiles were collected using a pole-dipole arrangement with a spacing of 150m, with the data presented as pseudosections of apparent resistivity and chargeability.

In addition, two MIMDAS profiles (Battig, 2011) were measured on lines oriented 070°-250° E, with lines located approximately 500m apart. The northern line is 3.8km long and passes through the Purísima mine (Cuerpo 1) and the southern line is 4km long and passes through Stockwork Hill (Cuerpo 2). The method used was pole-dipole IP / Resistivity and EMAP Magnetotellurics.

6.4.3.2 Regional Exploration

Regional-scale exploration of Minera Fuego's Johanna project, which contains the Cortadera prospect, included surface sampling, regional mapping, interpretation of remote sensing data and regional target generation. These work programs are summarised below:

Surficial sampling utilised a variety of techniques including soil sampling, bulk-leach extractible gold (BLEG) sampling and rock chip sampling, as follows:

- A regional (BLEG) sampling program was completed over the Johanna project area, sampling drainage confluences (Alegria, 2011).
- Niton pXRF analyses were obtained from a regional soil sampling grid targeting a 59 km long corridor enclosing the Agua de los Burros and Johanna Faults on nominal 500m x 200m centres.
- Infill soil sampling was completed on selected prospect areas with samples analysed using a Niton pXRF. The infill grids varied between 200m x 200m, 200m x 100m, 200m x 50m, 100m x 100m and 100m x 50m.

Rock chip sampling and assaying was completed on an ad hoc basis covering various regional prospect areas and targeting other areas of interest.

Advanced Spaceborne Thermal Emission and Reflection Radiometer (ASTER) data interpretation attempted to map the distribution of seventeen clay and silicate minerals related to hydrothermal alteration. Spectral processing of the colour bands enabled production of various false-colour images to map mineral distribution and zonation, and alteration centres that may be associated with polymetallic occurrences; structural interpretation was also completed. Images used included False-colour 321, Iron Oxide Alteration and Thermal Infrared False- colour.

Regional reconnaissance mapping was completed at 1:50,000 scale by Dietrich (2012). This work leveraged regional mapping by Sernageomin and other regional datasets to compile a regional geological map that focused upon defining litho-stratigraphic units, intrusive centres, alteration domains, and key structural corridors and mineralised centres at regional scale. The aim of the compilation was to define and characterise prospective corridors and identify areas for possible follow-up exploration. More detailed mapping studies in the southern part of the Johanna project area were also completed by Minera Fuego staff and contractors at Vizcacha, Las Tunas, Barranconcito and Corroteo (see Brionnes, 2013).

The above work assisted in defining a number of areas of interest and supported the generation of several regional target areas. Brionnes (2013) states that work by Juan Carlos Castelli advanced the regional targeting by considering controls on porphyry mineralisation at Cortadera and adding geological context to the areas of interest, together with some more detailed mapping (1:25,000 scale), emphasising enhanced prospectivity proximal to the deep-tapping Johanna and Agua de los Burros fault zones.

6.4.4 Previous Mineral Resource and Reserve Estimates

6.4.4.1 NI 43-101 2021 Maiden Resource, HCH, October 2021

Following execution of the Cortadera option agreement in February 2019, HCH undertook a Resource drill-out focussed on extending and infilling previously defined mineralisation. The maiden resource was released in compliance with NI 43-101 and is shown in Table 6.8. This was released with the Productora resource as part of a combined Costa Fuego Resource with an effective date of 29th October 2021.

Table 6.8 Cortadera Mineral Resource Summary – reported by classification (29th October 2021) and by open pit (top), underground (middle) and total (bottom)*

Cortadera OP Resource		Grade					Contained Metal				
Classification	Tonnes	CuEQ	Cu	Au	Ag	Mo	Copper Eq	Copper	Gold	Silver	Molybdenum
(+0.25% CuEQ*)	(Mt)	(%)	(%)	(g/t)	(ppm)	(ppm)	(tonnes)	(tonnes)	(ounces)	(ounces)	(tonnes)
Measured	0	0	0	0	0	0	0	0	0	0	0
Indicated	135	0.47	0.38	0.15	0.66	32	634,500	513,000	650,000	2,865,000	4,300
M+I Total	135	0.47	0.38	0.15	0.66	32	634,500	513,000	650,000	2,865,000	4,300
Inferred	100	0.44	0.35	0.14	0.65	45	440,000	350,000	450,000	2,090,000	4,500

Cortadera UG Resource		Grade					Contained Metal				
Classification	Tonnes	CuEQ	Cu	Au	Ag	Mo	Copper Eq	Copper	Gold	Silver	Molybdenum
(+0.25% CuEQ*)	(Mt)	(%)	(%)	(g/t)	(ppm)	(ppm)	(tonnes)	(tonnes)	(ounces)	(ounces)	(tonnes)
Measured	0	0	0	0	0	0	0	0	0	0	0
Indicated	48	0.55	0.44	0.15	0.87	73	264,000	211,000	232,000	1,343,000	3,500
M+I Total	48	0.55	0.44	0.15	0.87	73	264,000	211,000	232,000	1,343,000	3,500
Inferred	167	0.44	0.35	0.11	0.68	90	735,000	585,000	591,000	3,651,000	15,000

Cortadera Total Resource		Grade					Contained Metal				
Classification	Tonnes	CuEQ	Cu	Au	Ag	Mo	Copper Eq	Copper	Gold	Silver	Molybdenum
(+0.25% CuEQ*)	(Mt)	(%)	(%)	(g/t)	(ppm)	(ppm)	(tonnes)	(tonnes)	(ounces)	(ounces)	(tonnes)
Measured	0	0	0	0	0	0	0	0	0	0	0
Indicated	183	0.49	0.4	0.15	0.7	43	905,000	728,000	889,000	4,227,000	7,900
M+I Total	183	0.49	0.4	0.15	0.7	43	905,000	728,000	889,000	4,227,000	7,900
Inferred	267	0.44	0.35	0.12	0.7	73	1,181,000	935,000	1,022,000	5,633,000	19,400

*Reported at or above 0.25% CuEq. Figures in the above table are rounded, reported to appropriate significant figures, and reported in accordance with CIM and NI 43-101. Metal rounded to nearest thousand, or if less, to the nearest hundred.

Copper Equivalent (CuEq) reported for the drillholes were calculated using the following formula: $CuEq\% = ((Cu\% \times Cu \text{ price } 1\% \text{ per tonne} \times Cu_recovery) + (Mo \text{ ppm} \times Mo \text{ price per g/t} \times Mo_recovery) + (Au \text{ ppm} \times Au \text{ price per g/t} \times Au_recovery) + (Ag \text{ ppm} \times Ag \text{ price per g/t} \times Ag_recovery)) / (Cu \text{ price } 1\% \text{ per tonne})$. The Metal Prices applied in the

calculation were: Cu=3.00 USD/lb, Au=1,550 USD/oz, Mo=12 USD/lb, and Ag=18 USD/oz. Average Metallurgical Recoveries used were: Cu=83%, Au=56%, Mo=82%, and Ag=37%

6.4.5 Historical Production

The Cortadera project is located in the Agua Amarga Mining District, Region III, Chile. This district has seen previous mining of silver, lead, zinc and copper mineralized material since 1811, as summarised below from Szakács & Pop (2001). Historical copper mining in the Agua Armaga district took place at Marqueza Elena, Abundancia, San Antonio and La Pepa. Silver has been mined historically at Magdalena, Borkoski, Caldera, Colorada, Aris, las Vizcahitas and las Tunas, while lead has been mined historically at Cañas Norte, Las Cañas and Fortuna. The majority of these mines are now closed, with the notable exceptions of Abundancia mine (open pit copper-oxide mining) and San Antonio mine (copper oxides and sulphides mined by open pit and underground methods) where systematic, small-scale mining is ongoing.

At Cortadera, previous mining has taken place upon mining leases Purísima 1/8 and Cortadera 1/40, where several small workings (pirquineros) have been developed in the oxide zone as trenches, surface excavations and short tunnels. The largest of these previous workings is the Purísima Mine (Cuerpo1) where in 1990, previous miners R.G Grego and J.R Alday developed a tunnel approximately 70 m long in the oxide zone. Further mining at Purísima took place during 2003-2004 when a small open pit was developed to extract copper oxides at a grade of approximately 0.9% Cu.

6.5 San Antonio Historical Exploration and Development Work

There has been very limited exploration activity in areas beyond the San Antonio mine. Historic drilling was undertaken in two periods; initially Chilean government company ENAMI (Empresa Nacional de Minería) completed 4 drillholes in 1993, and then a later drilling programme by company Minera Tauro (between 1998 and 2002) completed 4 further holes.

6.5.1 Historical Mineral Resource and Mineral Reserve Estimates

There are no previous Mineral Resources or Reserves published regarding the San Antonio deposit.

6.5.2 Historical Production

The San Antonio project has been privately owned since 1953 and has been mined by several operators over this time via lease from the owners. Limited historic documents provided the following production data:

- 1965-1972: produced 100,000t at ~2.5% Cu soluble (3%Cu total).
- 1980: 30,000t of 3.0% Oxide and 25,000t at 2.0% Cu sulphide mineralisation
- 1988-1995: ~399,000t at 1.6% Cu.

The current owner has indicated that total historic production is approximately 2Mt of material grading approximately 2% copper and 0.3g/t gold, however no documentation has been provided that verifies this.

7 GEOLOGICAL SETTING AND MINERALIZATION

7.1 Productora-Alice Regional Setting

The Productora-Alice region lies at the boundary between the Coastal Cordillera and the Atacama fault system (Figure 7.1). During the Cretaceous, a thick sequence of andesite and minor sediments (Bandurrias Group) developed in an extensional regime within volcanic island-arc settings. A variety of porphyritic intrusions have been emplaced in this sequence, some of which are probably contemporaneous with the host volcanic rocks. These porphyritic intrusions appear to be responsible for most of the alteration and mineralisation observed in the area. Jurassic to Late Cretaceous granodioritic and monzodioritic batholiths are exposed over large areas throughout the Coastal Cordillera.

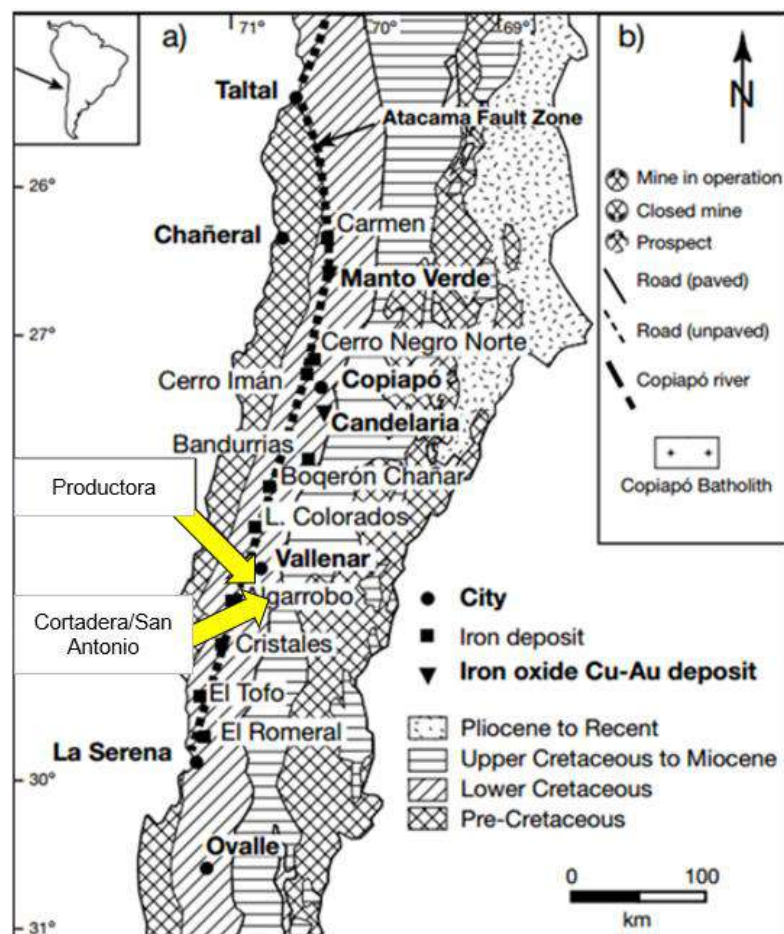


Figure 7.1 Regional geological setting (Escolme, 2016, modified from Marschik and Fontboté 2001)

The Project area encompasses a small part of the Chilean Iron Belt. The Iron Belt extends for more than 600 km along a 20 to 30 km wide, north-northeast trending zone at the east side of the Coastal Cordillera.

Several large copper deposits within this belt are currently in production including the Candelaria, Manto Verde, and Punta del Cobre. It is interesting to note that all three have significant iron contents. Many of the iron deposits within and near the Productora are known to carry low copper content, and a few very small deposits were mined for

copper oxide. There has been very little exploration in this area for large bulk tonnage copper mineralisation.

Beeson (2011) provides the most recent summary of the regional setting of the Productora deposit. The Project lies within the Chilean Coastal Cordillera which represents a broadly longitudinal calc-alkaline magmatic arc marking the start of eastward-migrating magmatic activity during the Andean tectonic cycle (Coira et al 1982). This early-Andean magmatic arc comprises Jurassic-Cretaceous volcanic and minor sedimentary rocks of predominantly intermediate-felsic composition intruded by intermediate granitoids of the Coastal Batholith (Cretaceous age – from 130+1 Ma to 87+3 Ma – Reyes 1991). An ensialic back-arc basin, within which thousands of metres of shallow marine calcareous and siliciclastic sediments were deposited, is located east of the magmatic arc. Fox (2000) describes the main components of this magmatic arc in the Productora region as:

- the Bandurias volcanic arc,
- the Chañarcillo back-arc basin,
- the Cretaceous coastal batholith, and
- the syn-arc, strike-slip Atacama Fault Zone.

7.2 Cortadera-San Antonio Regional Setting

The Cortadera and San Antonio prospects are located within a late Mesozoic volcano-sedimentary host-rock sequence that ranges in age from uppermost Jurassic to the middle of the early-Cretaceous. The regional stratigraphy comprises the following lithostratigraphic units of the Chañarcillo Group (Szakács & Pop, 2001), presented in order from youngest to oldest (after Dietrich, 2012); Cainozoic gravels, colluvial and alluvial deposits overly the now dissected Mesozoic sequence described below:

- Cerrillos Formation: well stratified basal sequence of volcano-sedimentary sequence comprising andesitic lava, volcanoclastics and tuff; overlying siliciclastic and calcareous rocks.
- Pabellón Formation: lower sequence of calcareous mudstone, wackestone, marl and tuff and an upper sequence of calcarenite and fossiliferous limestone, capped by volcanoclastic rocks.
- Totorolillo Formation: alternating and well stratified sequence of calcarenites, volcarenites and breccia with bioclastic lenses; similar to the Nantoco Formation in the project tenements. The uppermost portion of this sequence comprises interbedded andesite and bioclastic rocks.
- Nantoco Formation: well stratified chalky sequences of fine to medium grained of limestone to marl, calcarenites and calcilutites.
- Punta del Cobre Formation: variable sequence of lava, tuffs and epiclastic rocks of dacitic to andesitic composition, interspersed by siliciclastic rocks and locally limestone banks.

Much of the stratigraphic succession exposed in the project tenements has been variably affected by deformation. The most significant structural elements include the N-S to NNE-trending Agua de los Burros fault system and sub-parallel, linked (presumably) fault systems, collectively forming a deformation corridor up to 10 km wide. These generally steeply east-dipping and deep-tapping fault zones show both reverse and strike-slip offsets and are likely to have been reutilised during multiple episodes of deformation.

A series of NW-trending and subordinate NE- to NNE-trending faults cross-cut and locally offset the larger longitudinal fault zones, forming important corridors for mineralisation, particularly at or near fault intersections. Individual fault zones comprise domains of strong brecciation that may be >10 m wide. Dietrich (2012) suggests that some of the mapped faults may have been active during basin formation and may thus have influenced the primary distribution of the volcano-sedimentary sequences. For example, Dietrich (2012) proposes that the Agua de los Burros fault zone forms a boundary between marine sequences of the Chañarcillo Group and continental rocks located to the east.

Some of the cross-cutting faults might also be inherited structures that may have acted as transfer faults during basin formation. These fault systems are also likely to have had a significant influence on the distribution of subsequent intrusive rocks, hydrothermal alteration and mineralisation. Dietrich (2012) proposes that the Agua de los Burros fault significantly influences the distribution of upper Cretaceous plutonic complexes that intrude the Mesozoic volcano-sedimentary sequences. These plutonic complexes form lobate, kilometre-scale bodies that vary in composition between granite, granodiorite, tonalite and monzodiorite.

Regional mapping by Sernageomin shows a series of gentle to open folds that trend NE to NNE, defining an en échelon geometry and suggestive of bulk sinistral transpressional movement along the longitudinal regional fault systems. In addition, regional mapping by Dietrich (2012) and Sernageomin shows a prominent right-stepping kilometre-scale flexure in the Agua de los Burros fault zone.

Dietrich (2012) interprets this step-over as being consistent with dextral reactivation of the Agua de los Burros fault zone, proposing that extensional zones in local right-stepping jogs formed preferential sites for granitoid emplacement, citing a date of 74-71Ma for intrusive rocks in the flexure-zone as evidence for the age of dextral reactivation. The cross-cutting NW-trending faults may also be implicated in Cretaceous volcanism and sedimentation, and late Cretaceous plutonism (Dietrich, 2012), based upon the distribution of stratigraphic units around the larger-scale NW-trending faults (e.g., the Huasco Valley fault zone).

The Cortadera region shows regionally extensive sodic-calcic alteration related to the thermal aureoles of large intrusive bodies and major fault corridors. The sodic-calcic alteration observed regionally typically comprises albite- actinolite- epidote- chlorite ± magnetite/ haematite ± garnet (Dietrich, 2012). At smaller scales, hydrothermal alteration, dominated by various assemblages that typically include silica-quartz, sericite, chlorite, biotite, potassic feldspar, clay, Fe oxy-hydroxides and/or sulphides are commonly associated with vein systems developed around porphyry-style mineralised

centres and mineralised fault zones. These porphyry-style and fault-related alteration zones overprint the regional scale sodic-calcic alteration.

These observations emphasise the importance of structural intersections and structural corridors in controlling the distribution of mineralisation and related hydrothermal alteration.

7.3 Local Geology

7.3.1 Productora-Alice Local Geology

The host volcanic and sedimentary sequence dips gently (15 to 30°) west to west-northwest and is transected by several major north- to northeast-trending faults zones, including the Productora fault zone, which coincides with the main mineralised trend. These faults are likely sympathetic to the nominally parallel but distal Atacama fault system. In the Productora deposit, these major fault zones are commonly associated with extensive tectonic breccia (damage zones) that host copper-gold-molybdenum mineralisation. Later faults cross-cut and offset the volcano-sedimentary sequence together with the Productora (and sub-parallel) major faults. Late faults generally show a west to north-westerly strike and while generally narrow, are locally up to 20 m wide.

The volcano-sedimentary sequence at Productora is extensively altered, particularly along major faults and associated damage zones, and a distinctive hydrothermal alteration zonation is evident. The distribution of alteration mineral assemblages and spatial zonation suggest a gentle northerly plunge for the Productora mineral system, disrupted locally by vertical and strike-slip movements across late faults. These late faults appear to be trans-tensional and oriented at a high-angle to the distal Atacama fault system (Figure 7.2).

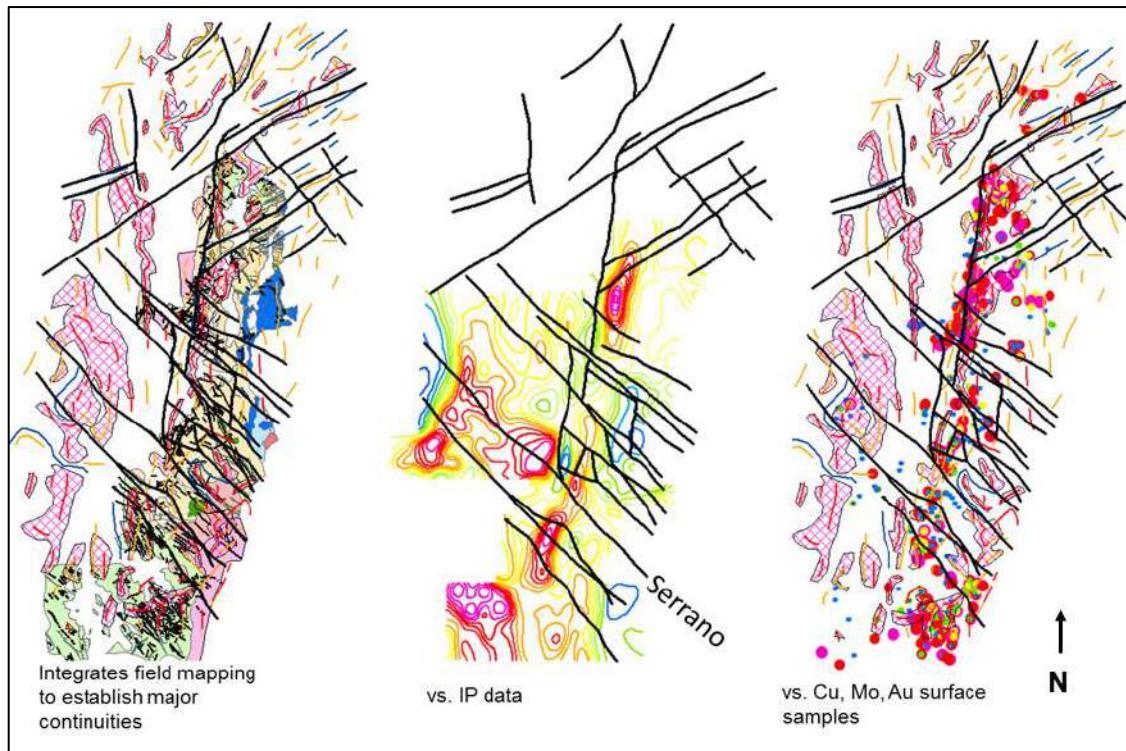


Figure 7.2 Broad 2D structural framework. Left; compared to ground mapping, centre; compared to previous IP data, right; compared to rock chip sampling. (HCH, 2016)

The following sections summarise the work described by Fox (2000), Beeson et al. (2012) and HCH geologists.

The Bandurrias Formation comprises a thick sequence of volcanic flows and ash flow tuffs intruded by the Cachiyuyito intrusion (129.8±0.1 Ma) and the Ruta 5 Batholith (border phase dated as 96.1±0.2 Ma). These age determinations were made using the U-Pb zircon method. The stratigraphically oldest to youngest rocks comprise andesitic ash-flow tuff, lower dacitic ash-flow tuff, dacitic welded ash flow tuff, upper dacitic ash-flow tuff, volcanoclastic sedimentary rocks and basalt and basaltic andesite flows that overlie the volcanoclastic / tuffaceous sequence. The Cachiyuyito and Ruta 5 intrusive rocks intrude the volcanic sequence. The older Cachiyuyito intrusion is a NNE-elongated, elliptical and concentrically zoned body with a tonalitic core and a dioritic border phase. The Florida Granite is located to the southwest of the project and is thought to be equivalent or coeval to the Cachiyuyito intrusion. The Ruta 5 intrusion represents a portion of a composite batholith with at least two phases and at Productora is zoned outwards from a granodiorite core (with biotite>hornblende) to a slightly magnetic quartz monzodiorite border phase (with hornblende >biotite). Fox (2000) identified a suite of later andesitic dykes that cut most of the above rock types. This late dyke suite cuts all lithological units except the Ruta 5 batholith and trends generally NW-NNW, with other trends evident locally. The andesitic dykes vary from phaneritic to porphyritic and locally contain minor chalcopyrite and pyrite. Magnetite of both primary and hydrothermal origin is present locally in these dykes.

The Productora copper-gold-molybdenum deposit is hosted by the Neocomian (lower Cretaceous) Bandurrias Group, a thick volcano-sedimentary sequence comprising intermediate to felsic volcanic rocks and intercalated sedimentary rocks. The Bandurrias Group consists of variably plagioclase-porphyritic and amygdaloidal andesitic rocks overlain by a felsic volcanic sequence composed of weakly porphyritic rhyolitic to rhyodacitic lavas, tuffs and volcanic breccias. Intercalated sedimentary rocks are volumetrically minor and comprise well-bedded volcanic sandstones. Surface exposures in the project area are highly silicified reflecting significant surficial leaching. Dioritic dykes intrude the volcano-sedimentary sequence at Productora, typically along west- to northwest-trending late faults, and probably represent sub-volcanic feeders to an overlying andesitic sequence not represented in the resource area. Regionally, the Bandurrias Group is preserved as a series of linear to radiating belts and remnant blocks intruded by middle-upper Cretaceous granitoids varying from granodioritic to dioritic in composition. A large dioritic-granodioritic intrusion lies just to the east of Productora (Figure 7.3).

The volcano-sedimentary sequence at Productora is extensively altered, particularly along major faults and associated damage zones, and a distinctive hydrothermal alteration zonation is evident. Common alteration assemblages include K-feldspar-tourmaline-magnetite-silica-(hematite), typically associated with higher-grade polymetallic mineralisation along the trace of the Productora fault zone, with flanking distal zones of relatively lower-temperature alteration comprising chlorite-magnetite-epidote-albite-silica-carbonate-(hematite).

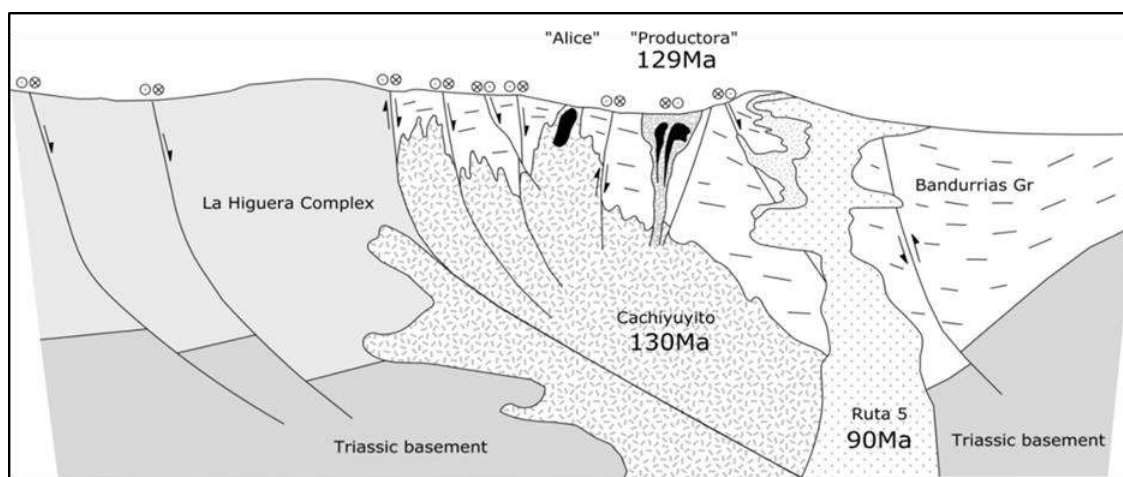


Figure 7.3. Stylised regional type section across the Productora project area. Image looking north (Escolme, 2016)

A project-scale interpretation of the airborne geophysical datasets was undertaken in mid-2013, which provided a broad 2D structural framework (Figure 7.4).

An exercise integrating field observations, magnetic interpretation and a review of previous work allowed for the construction of a schematic structural model, which is aimed at illustrating the structural architecture of the Productora mineralised system. The structural model showed the interplay of preferred host rocks (volcanic units with relatively high primary permeability) with fault zones. Preferred sites for mineralisation

are interpreted to be associated with fault jogs, fault intersections, fault bifurcations, damage zones adjacent to faults and permeable volcanic units located adjacent to any of these fault-related features. It is suspected that Cu-Au-Mo mineralisation may migrate along permeable stratigraphic units as well as fault zones, giving the impression that mineralisation is developed both along the fault zone and adjacent gently-dipping stratigraphic units.

Field checks of key faults support their modelling orientation and profile. In particular, the Serrano fault ("Fault 27" wireframe) was included in the Productora deposit resource model as a major definition feature. This fault (Figure 7.5) has variously acted as a mineralisation conduit and as a mineralisation limiter. There are other interpreted faults not included in this Resource model but these faults will be considered in future resource and structural modelling projects.

The Alice Resource is constrained on the west by the "Alice Fault". This fault dips steeply towards the west and strikes north to north-northeast through the Resource area (Figure 7.6).

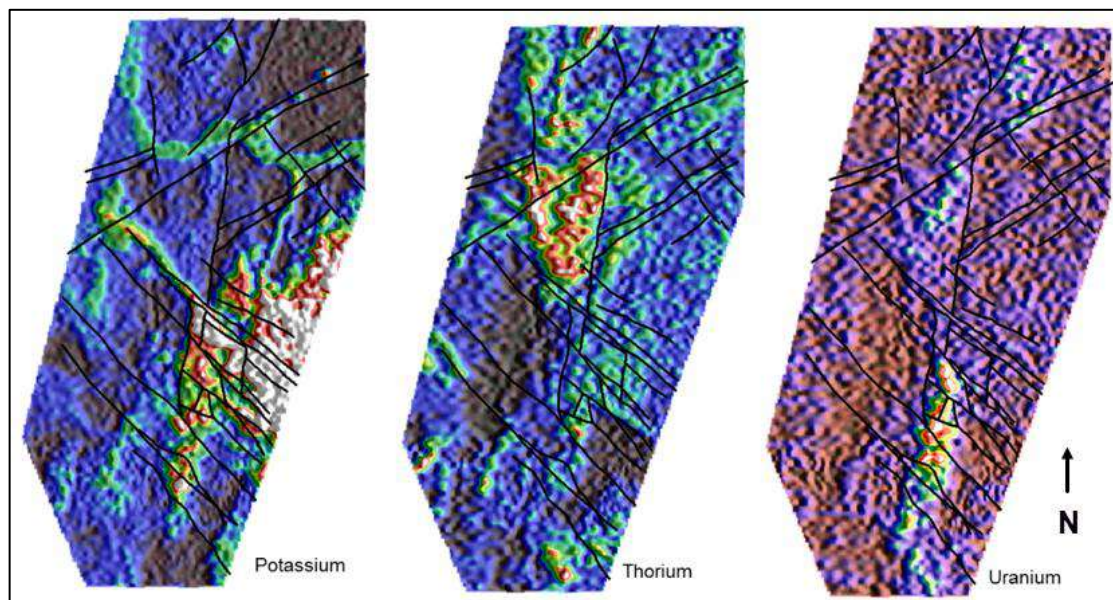


Figure 7.4 2D structural framework compared to radiometric data. (HCH, 2016)



Figure 7.5 Example outcrop of Serrano fault in a drill pad (fault dipping steeply to NE). Note altered footwall. Hanging wall to the fault is off picture as this fault appears to be moderately thick.

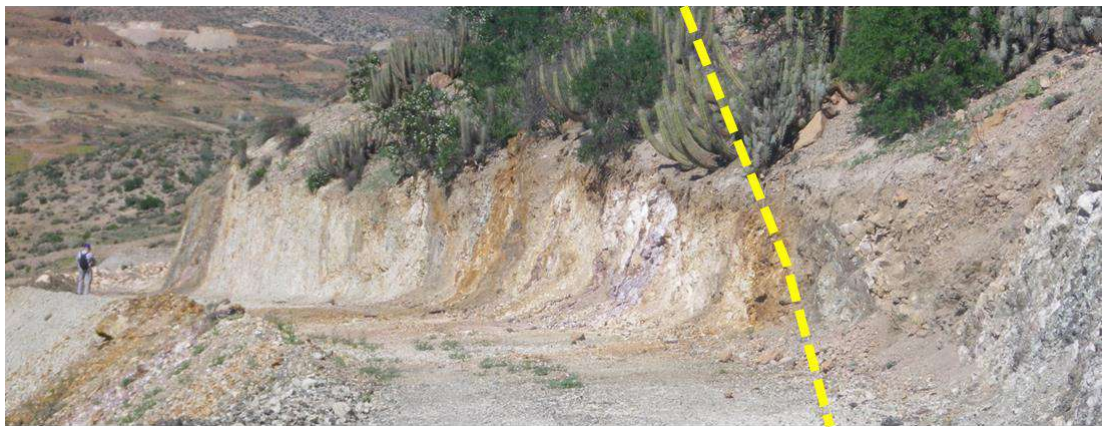


Figure 7.6 Alice hanging wall fault out cropping on Docherty Rd. Fault is steeply dipping to the west (image looking south). Porphyry in footwall, altered volcanic rocks in the hanging wall.

7.3.2 Cortadera Local Geology

Given the scale of the Cortadera Property, the local geology is considered satisfactorily covered in section 7.4.3 Cortadera Property Geology.

7.3.3 San Antonio Local Geology

The San Antonio area is dominated by an extensive early Cretaceous volcano-sedimentary sequence and a range of felsic to intermediate intrusions.

The San Antonio copper deposit is largely hosted within a 20-150m wide microdiorite body. The microdiorite comprises a plagioclase-hornblende +/- quartz rock that is strongly altered. The microdiorite contains equant sub-millimetre hornblendes hosted in a plagioclase-rich matrix. The San Antonio microdiorite may represent a syn-volcanic sill or the basal sequence of a thick (>150m) andesitic lava flow. Contact relationships are obscured by hydrothermal alteration and deformation.

To the east of the microdiorite is an andesitic volcano-sedimentary sequence that consists of massive to porphyritic, vesicular/amygdaloidal lava flows and tuffs. Underlying this andesitic – dioritic sequence is an extensive sedimentary sequence.

These predominantly siliciclastic rocks comprise fine- to medium-grained arenitic sandstone and plagioclase-rich volcanic-derived wacke interbedded with siltstone and shale that is may be weakly graphitic. The siliciclastic rocks are locally calcareous and include fine grained limestone sequences south of the San Antonio mine. These rocks typically show planar and graded bedding at millimetre- to centimetre-scale and local cross-bedding. Sedimentary structures suggest that the sequence is broadly upright and shows eastwards younging. Figure 7.7 shows the interpretation of the regional geology to the south of San Antonio, as determined by HCH.

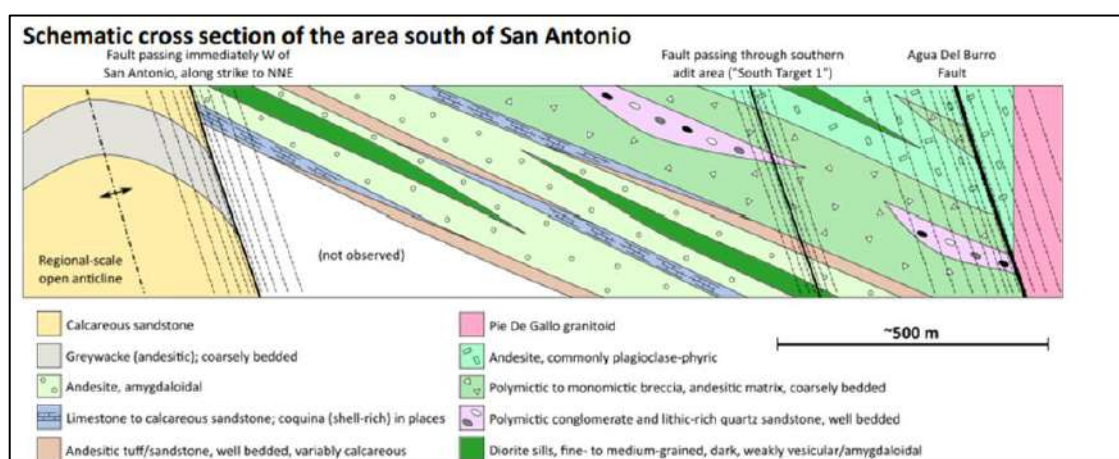


Figure 7.7 Cross section of San Antonio regional geology

The microdiorite is intruded by a 5-100m thick felsic body that also hosts copper mineralisation. The felsic intrusion shows ghosted feldspar phenocrysts and is strongly altered. Intrusive contacts are typically faulted.

Felsic and andesitic dykes intrude the andesitic and siliciclastic sequences. Andesitic dykes are typically steeply dipping and orientated NW-NNW and NE, while felsic dykes show a wide range of orientations.

7.4 Property Geology

7.4.1 Productora Property Geology

The Productora system is a late, ductile to brittle release event, with multi-stage potassium-iron alteration involving silica-(albite)-sericite alteration along north-trending fault zones. The early pyrite alteration is associated with elevated Co (but not significant Cu-Au enrichment) and was followed by Cu-Au-U-REE-(Mo) mineralisation, with associated chlorite-K-feldspar-tourmaline-epidote-magnetite-hematite alteration and hypogene sulphides comprising chalcopyrite-(molybdenite) (Figure 7.8). This later alteration stage shows Au in strong positive correlation with chalcopyrite and pyrite (Au may be intergrown with these sulphides). Rare Earth Elements (REE's) are also elevated in the chalcopyrite-pyrite zone (REE's with apatite or allanite). K-feldspar-chalcopyrite veining and alteration has been dated by Fox at 91.4 +/- 0.2 Ma (slightly discordant Ar39-Ar40 age determination) and more recently, molybdenite veining at Productora was dated at 128.9 +/- 0.6 Ma (Marquardt et al 2015). Potassium-iron

alteration mineralogy appears to reflect primary lithology and progresses from early biotite-pyrite-(K-feldspar) to chlorite-magnetite-(K-feldspar)-chalcopyrite-gold to late epidote-chlorite-specularite-tourmaline-magnetite with chalcopyrite developed in tourmaline veins and epidote-chlorite-specularite-(tourmaline) veins. Locally, the Productora deposit is flanked on the east by section of (alunite absent) advanced argillic alteration (in particular, Habanero).

7.4.2 Alice Property Geology

The Alice porphyry is located immediately beneath an extensive, pyrophyllite-rich advanced argillic lithocap, with a porphyry stock of quartz diorite to granodiorite composition. Mineralisation at Alice comprises predominantly copper, with silver and molybdenum also present. Unlike at the Cortadera porphyry system, little gold is present. Mineralisation is hosted in a porphyry with sheeted and stock work quartz veinlets, within additional locally disseminated background mineralisation. Post-mineralisation albitisation can decrease mineralisation grades locally.

Currently, the Alice mineralisation is thought to be spatially and temporally linked to the Cachiyuyito/Florida system. The Alice porphyry is dated as having been intruded in the late Cretaceous.

The Cachiyuyito/Florida system is a magnetite-apatite system hosted in andesitic tuff adjacent to the sodic altered Cachiyuyito intrusion, similar to iron deposits in the Cretaceous iron belt of Chile. Associated alteration and veining comprises albite-chlorite-actinolite-magnetite-calcite-epidote-apatite. The Cachiyuyito intrusion is slightly depleted in FeO and P₂O₅ despite the presence of apatite veins. Fe, Ca, P and Mg have been mobilised and reconcentrated into magnetite-epidote-apatite veins. Na₂O and K₂O show an inverse relationship, with most samples being enriched in NaO and some enriched in K₂O (sericitisation of albite during the subsequent Productora alteration event).

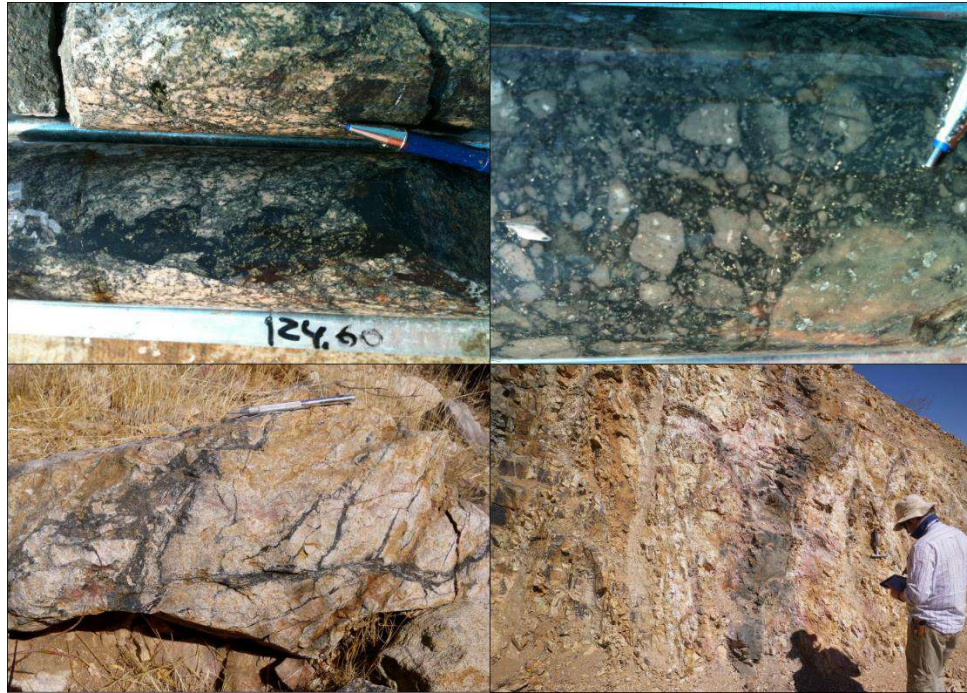


Figure 7.8 A) Ductile shearing in tourmaline breccia in PRD0011, B) hydraulic fracturing (PRD0011), C) Tourmaline vein network in rhyolite C) Tourmaline vein cutting NNE fault zone, earlier veining and breccia in rhyolitic rock.

7.4.3 Cortadera Property Geology

A WNW-trending fault corridor is inferred to host the three, known porphyry-style mineralised centres at Cortadera. An associated colour anomaly and domain of hydrothermal alteration also extends along this trend for at least 2,300 m. It is possible, the structural corridor may also extend further along strike to the WNW and ESE, influencing the location of additional porphyry-style intrusive centres and related alteration cells with associated mineralisation.

Tobey (2011a, 2011b, 2012a, 2012b, 2012c, 2013a, 2013b) provides a comprehensive discussion regarding mineralised porphyry-style vein systems at Cortadera, as summarised below. At Cortadera, the porphyry-style vein systems are associated with a multi-phase tonalitic intrusive system showing hydrothermal alteration zonation typical of such mineralised systems. Propylitic (chlorite \pm epidote) alteration has been mapped at the kilometre-scale surrounding more discrete potassic (biotite and secondary feldspar) alteration zones. The extensive WNW-trending colour anomaly, mappable in Quebrada Cortadera and well exposed along the base of Breccia Hill (Cuerpo 3), is most likely associated with a late-stage phyllic (quartz-sericite-pyrite) alteration.

The vein systems at Cortadera appear typical of those found within porphyry-style mineralised systems elsewhere. Tobey describes some of the early quartz-rich veins observed at Purísima (Cuerpo 1) and Stockwork Hill (Cuerpo 2) as showing unidirectional solidification textures (UST). Tobey notes that such textures are commonly associated with relatively high temperatures during vein emplacement and indicates the crystallising magma became saturated with respect to vapour before complete solidification. Tobey notes that veins formed after the UST veins comprise quartz rich A-veins (chalcopyrite-pyrite \pm magnetite bearing), banded MAB-veins (quartz-

magnetite-chalcopyrite-pyrite) and B-veins (molybdenite-bearing quartz veins) cut by sericitic/chloritic C-veins (pyrite-chalcopyrite bearing), pyritic D-veins with sericitic selvages and late calcite-bearing fractures. The A-, B- and D-vein nomenclature follows that of Gustafson and Hunt (1975). Anhydrite is locally present within some of the B- and C-veins.

Chalcopyrite also occurs as disseminations of variable intensity within the porphyritic host rocks, particularly in association with stockwork A- & throughgoing B-veins. Tobey also demonstrates a very clear correlation between increased volume percentage of quartz-bearing stockwork veining and sulphide content with elevated copper-gold grades. Tobey also noted that many of the veins may have formed as true stockworks, but other veins show a preferred orientation sub-parallel to nearby fault zones.

Tobey's extensive vein studies have been further developed by HCH geologists to create a paragenetic model (Figure 7.9). Cross-cutting relationships have been used to define and interpret the relative ages of each vein group. Veins groups are classified by vein morphology, composition, and texture. The early discontinuous A-veins (quartz-chalcopyrite-pyrite±magnetite) represent the beginning of the main mineralisation event at Cortadera. The main mineralisation stages are associated with through going B-veins (quartz-chalcopyrite-pyrite±molybdenite) and the later chalcopyrite-pyrite-bearing C-veins. A- & B-type quartz veins are most abundant in the centre of the porphyry system, where the copper metal tonnage is largest. Sulfide mineral-bearing C-veins are associated with mineralisation but are volumetrically less significant within the deposit than the A- & B-type quartz veins.

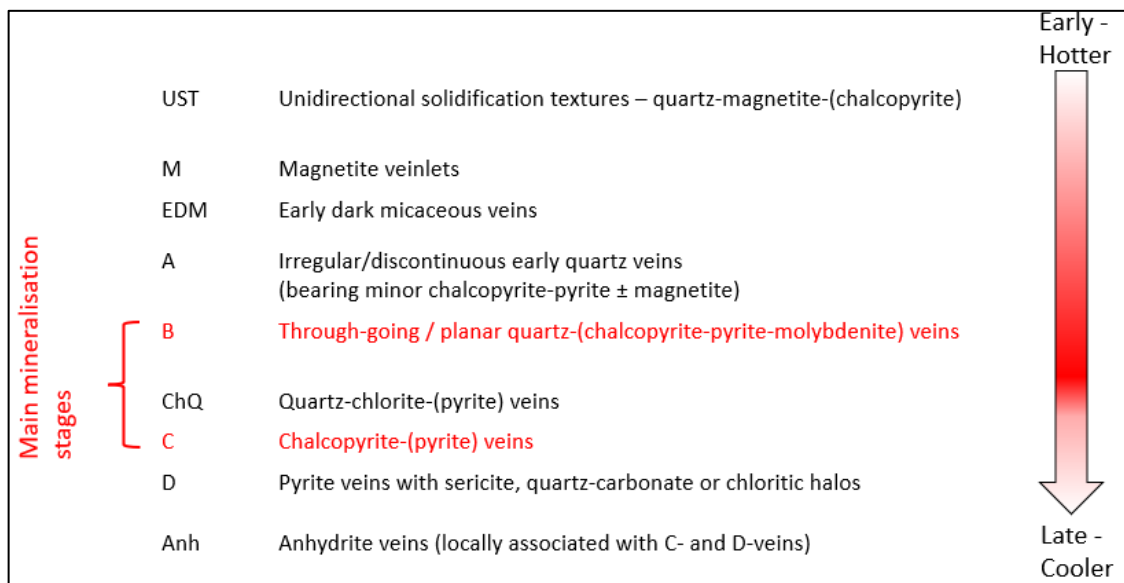


Figure 7.9 Cortadera Vein Paragenesis model (HCH geologists and Steve Garwin, 2021). Veins have been classified on vein morphology, composition and texture. They have then been grouped by interpreted relative age based on cross-cutting textural relationships.

A review of the orientation of quartz veins within the Cortadera high-grade copper zones was completed by Beeson (2021) with the understanding that changes in vein geometry may influence metal distribution, potentially amplifying other structural controls (e.g. quartz vein density). Alpha-beta measurements of quartz rich (A- & B-) veins were converted to dip – dip direction from HCH diamond drill holes.

Data was subset into intervals of approximately 100 m downhole width and plotted to assess changes in gross quartz-rich vein geometry with depth. Vein orientations dominantly strike NW-SE, N-S and NE-SW. The dip of primary quartz veins varies significantly; at Cuerpo 3 a distinct dominance of flat veins is apparent between 400 – 0 m elevation; these veins coincide with the base of high-grade Cu mineralisation (Figure 7.10).

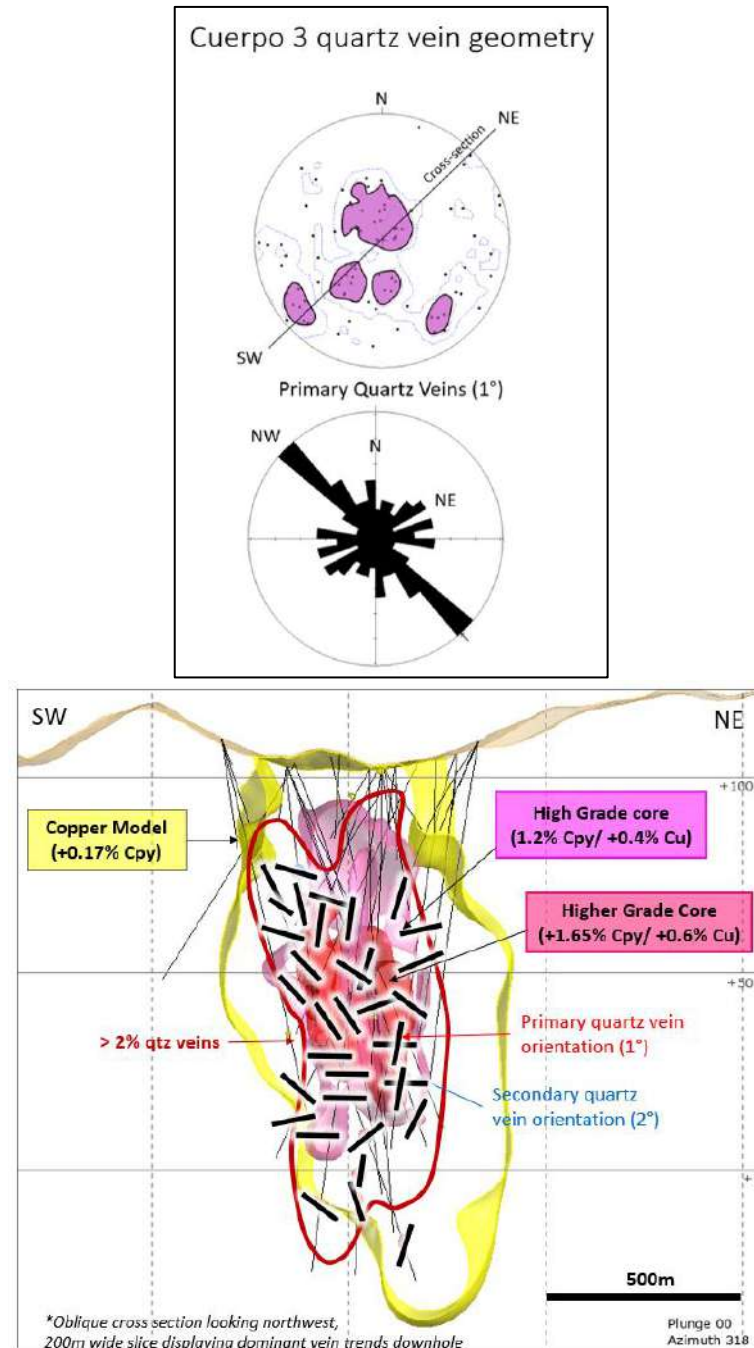


Figure 7.10 (Above) Stereo net indicating primary orientation of quartz veins. (Below) cross-section through Cuerpo 3 facing northwest, showing the primary vein orientation relative to the 0.17% Cpy, 1.2% Cpy and 1.65% Cpy mineralisation models.

Tobey (2012) states that the proportion (percentage) and type(s) of veining present in the porphyry intrusions can be used as tools to separate the various stages of tonalitic intrusion. Early stage tonalites contain >5% A- + B- quartz veins and will henceforth be referred to as '10-series'. Intramineralisation tonalites contain 1 to 5% A- + B- quartz veins and are referred to as '20-series'. Much of the copper-gold-molybdenum mineralisation is hosted in these two intrusions.

Late-stage tonalite dykes post-date the mineralisation, with the cross-cutting relationship clearly evidenced in diamond drill core. These contain very <1% A- + B- quartz veins and host extremely low copper-gold-molybdenum grades unless xenoliths of 10- and 20-series porphyry are present. These are referred to as 30-series intrusions.

Late-stage andesite dykes also post-date the mineralisation and are easily identified by their darker colour compared to the tonalitic intrusions, and their lack of A- and B- quartz veins. As with the 30-series intrusions described above, they host extremely low-grades. These are referred to as 40-series intrusions.

The presence of a calcium-rich alteration front is considered to exert a significant geological control on mineralisation and appears to correlate well with zones of higher A- and B-type quartz vein abundances and copper grades that extend outward from the mineralised porphyry intrusions. This geometrical relationship is consistent with the addition of potassium and sodium to the porphyry core (along with Cu, Au, Mo, Ag and other metals), where calcium has been depleted. The calcium has been remobilised and driven outwards along permeable pathways that developed in zones of higher fracture- and vein-abundance and within adjacent competent hornfels and permissive stratigraphic units.

A lithogeochemical approach was used on ICP-MS data at Cortadera to identify stratigraphic horizons that could preferentially act as pathway for fluids being driven out of the porphyry intrusions (Halley, HCH geologists 2022). A series of distinct stratigraphic horizons (Figure 7.11) were interpreted and modelled using Leapfrog, further work is required to validate against logging and drill core.

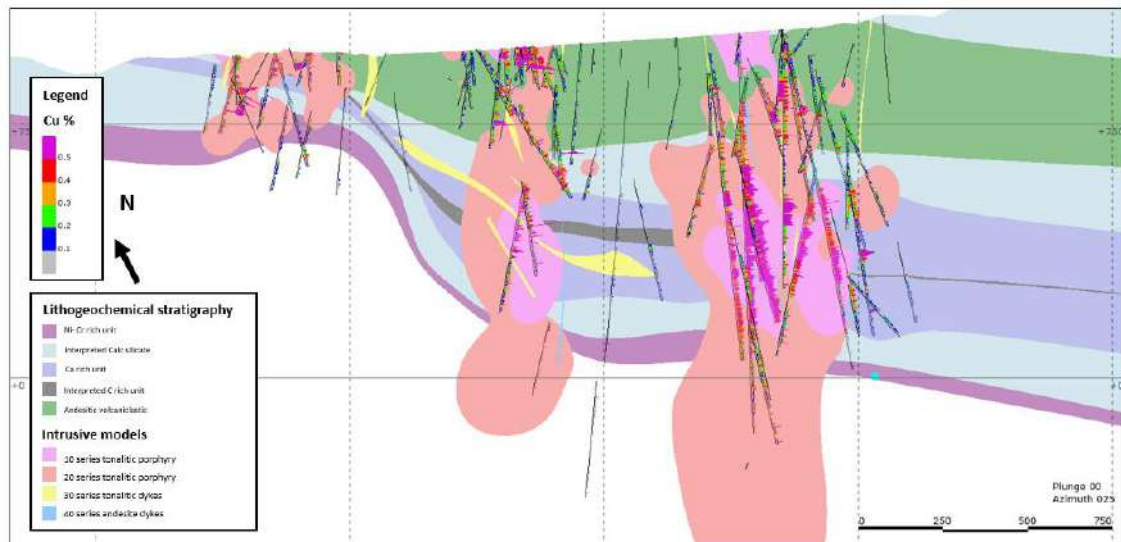


Figure 7.11 Long section facing north-east (+/-50m clipping) showing the interpreted lithochemical stratigraphy relative to downhole copper grades and intrusive models from geological logging.

7.4.4 San Antonio Property Geology

San Antonio is a volcanic hosted, lode style base metal deposit of the type that often occur on the peripheries of porphyry systems, potentially in this case the Cortadera system which is located 8km to the SW.

The geology of San Antonio has been interpreted from field and underground mapping, underground channel and sludge sampling, and surface and underground drill holes.

Copper mineralisation at San Antonio appears related to a structural control of narrow fault zones that strike NE to N and are typically dipping steeply NW or SE to E or W, (Figure 7.12), respectively and carry visible copper outside and in the central microdiorite unit preferentially. Copper mineralisation is mostly in the form of disseminated chalcopyrite associated with pyrite, magnetite, quartz and minor specular hematite.

Chrysocolla and Malachite is observed as oxide copper mineralisation near surface, however a continuous oxide defined blanket is not observed across the deposit. Epidote alteration is dominant and closely related with copper oxide mineralisation.

Highest copper grades (up to 2% Cu) are usually hosted within a microdiorite unit displaying intense chlorite-epidote, sericite, calcite and especularite alteration with minor pyrite (~5%) and magnetite (5 to 10%). A pyrite-dominant halo (up to 25%) with magnetite (up to 10%) is observed into the microdiorite unit with intense epidote-chlorite-calcite alteration.

Copper mineralisation is also observed in the faulted contacts and within the adjacent lithological units (felsic porphyry and sedimentary-clastic units). These zones are generally intensely epidote altered with albite and chlorite also present. Copper grades are normally lower (0.3 to 0.5% Cu).

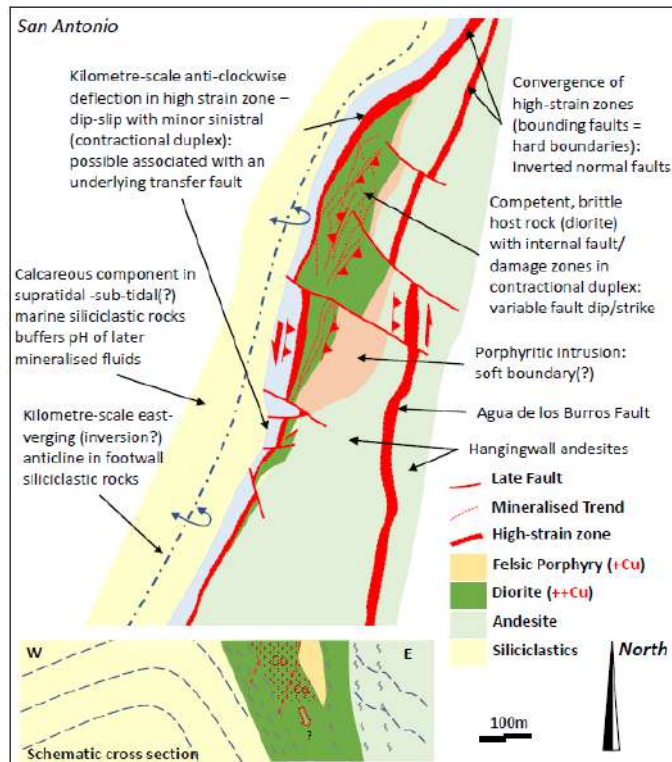


Figure 7.12 Plan view and cross section schematic showing interpretation of structural controls inferred from surface mapping campaigns Beeson et al (2018)

7.5 Property Mineralisation

7.5.1 Productora Mineralisation

The Productora copper-gold-molybdenum deposit is an enigmatic breccia complex that presents characteristics consistent with both the porphyry and IOCG models (Escolme, 2016).

Mineralisation in the Productora deposit comprises two contrasting styles. The predominant style is characterised by narrow, north to north-east trending tourmaline-cemented breccia bodies. Sub-vertical feeder stocks, of 2 to 5m width at depth, increase with elevation, to wider high-grade mineralisation zones. These wider brecciated zones vary in orientation with central lodes tending to be sub-vertical with an upper flex in wider mineralised zones to dip approximately 70° towards the west, also flanking shallower eastern and western lodes dip moderately west and east respectively. There are also some locally steeply east dipping lodes e.g., Habanero (Figure 7.13). In structurally conducive dilation zones, these discrete breccia zones hydraulically propagate outward and can commonly coalesce to become larger zones of hydrothermal damage. These larger damage zones are most probably defined by a combination of structural and intra-lithological controls. Drilling at deeper levels at Productora has demonstrated thinning breccia lodes, with some ductile features, that continue to a greater depth.

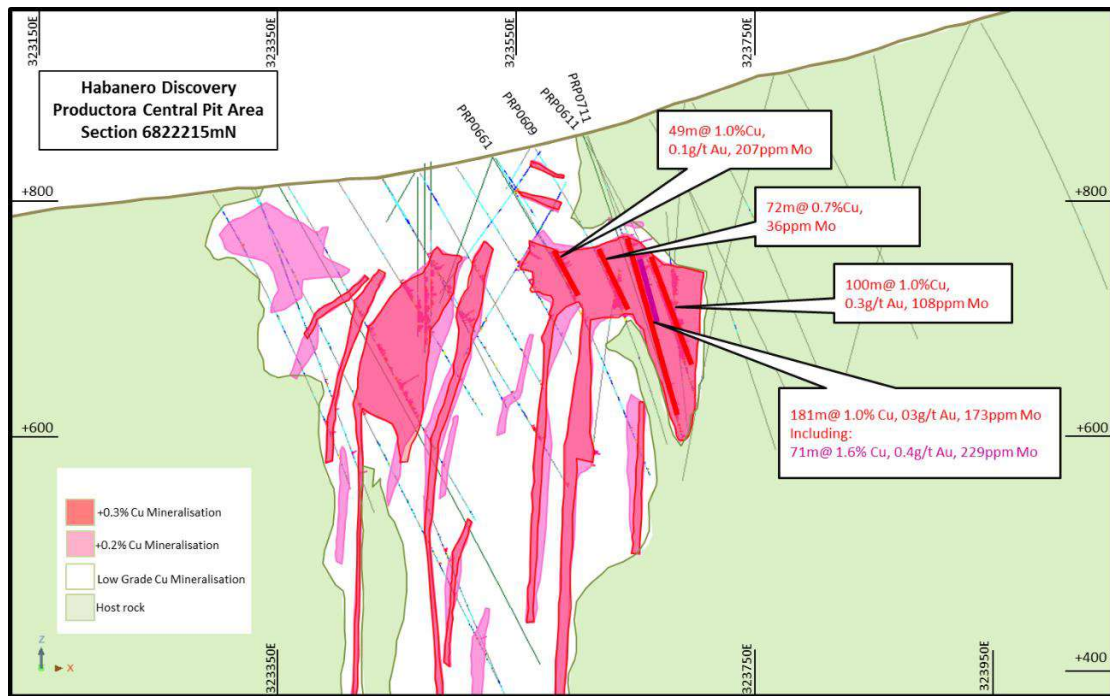


Figure 7.13. Example cross section at Productora. Selected significant intersections (previously published) highlight drilling from the Habanero zone. 6822215mN. Section looking north. (HCH, 2016)

The copper, gold and molybdenum mineralisation is also strongly coincident with the potassic alteration. Determining the detailed primary host lithology, within and proximal to mineralisation, is problematic due to the extent of brecciation and hydrothermal alteration.

Secondary and relatively lower-grade mineralized material controls are evident as manto or manto-like horizons in the southern, far northern, and far eastern flanks of Productora. Manto mineralisation appears to be locally focused along the upper part of the volcanic breccia and intercalated, weakly-foliated volcanic and sedimentary rocks (Figure 7.13). Lodes within the manto horizons are typically gently-dipping at -20° to -30° to the east or west and enclosed by lower grade mineralisation. Also, relative to the Productora breccia mineralisation, manto mineralisation typically exhibits elevated levels of iron (in hematite or magnetite) and calcium (in calcite).

7.5.3 Alice Mineralisation

The Alice copper-molybdenum porphyry mineralisation is likely deeper than the Productora mineralisation, in terms of genetic emplacement, and has a single porphyry body near a remnant lithocap.

The lithocap is physically disconnected with (the assumed) coeval porphyry. The lithocap overprints the regional volcanic stratigraphy and can be seen as a silica ridge and is comprised a number of advanced argillic alteration types, including quartz-alunite, quartz-pyrophyllite, alunite-dominant and pyrophyllite-dominant zones.

Within the zones of mineralisation, there appears to be a distinct domain difference between chalcopyrite-dominant and pyrite-dominant areas. Chalcopyrite-dominant zones (i.e., low pyrite: chalcopyrite ratio) correlate with intense A-veins and B-veins and higher copper grades. Copper mineralisation appears both within veining and within the groundmass proximal to veining. Early biotite (EB) veins are present at Alice.

Late albite (+/- epidote +/- sericite) appears to have removed chalcopyrite (copper, sulfur) and biotite. Albitic alteration also appears to locally reduce the amount of pyrite in the quartz vein network (e.g., Figure 7.15). This can also be seen in the sodium and sulphur chemistry in the Alice drilling; both correlate with domains of much lower copper grades.

Molybdenum mineralisation appears discretely associated with vein networks and appears to be less impacted by the late albite alteration compared to the chalcopyrite (most impacted) and pyrite (moderately impacted). This may be primarily driven by the majority of molybdenite being contained within discrete quartz veins which may offer some protection to late fluids.

There is evidence that anhydrite was present, but cavities evident in the diamond core suggest anhydrite has been chemically removed.

Late supergene weathering has impacted some of the Alice mineralisation (Figure 7.16). Overall, the higher-grade domain appears to be effectively in situ, but perhaps with some minor down-fault upgrading via fluid movement. The low-grade mineralisation appears slightly more impacted with minor lateral spread within the oxide domain. The contact between 'oxide' and 'fresh' mineralisation appears to be very discrete, with effective 'transitional' material evident. This likely due to low porosity nature of the Alice porphyry and mineralisation, which is in stark contrast to the (relatively) highly porous Productora deposit.

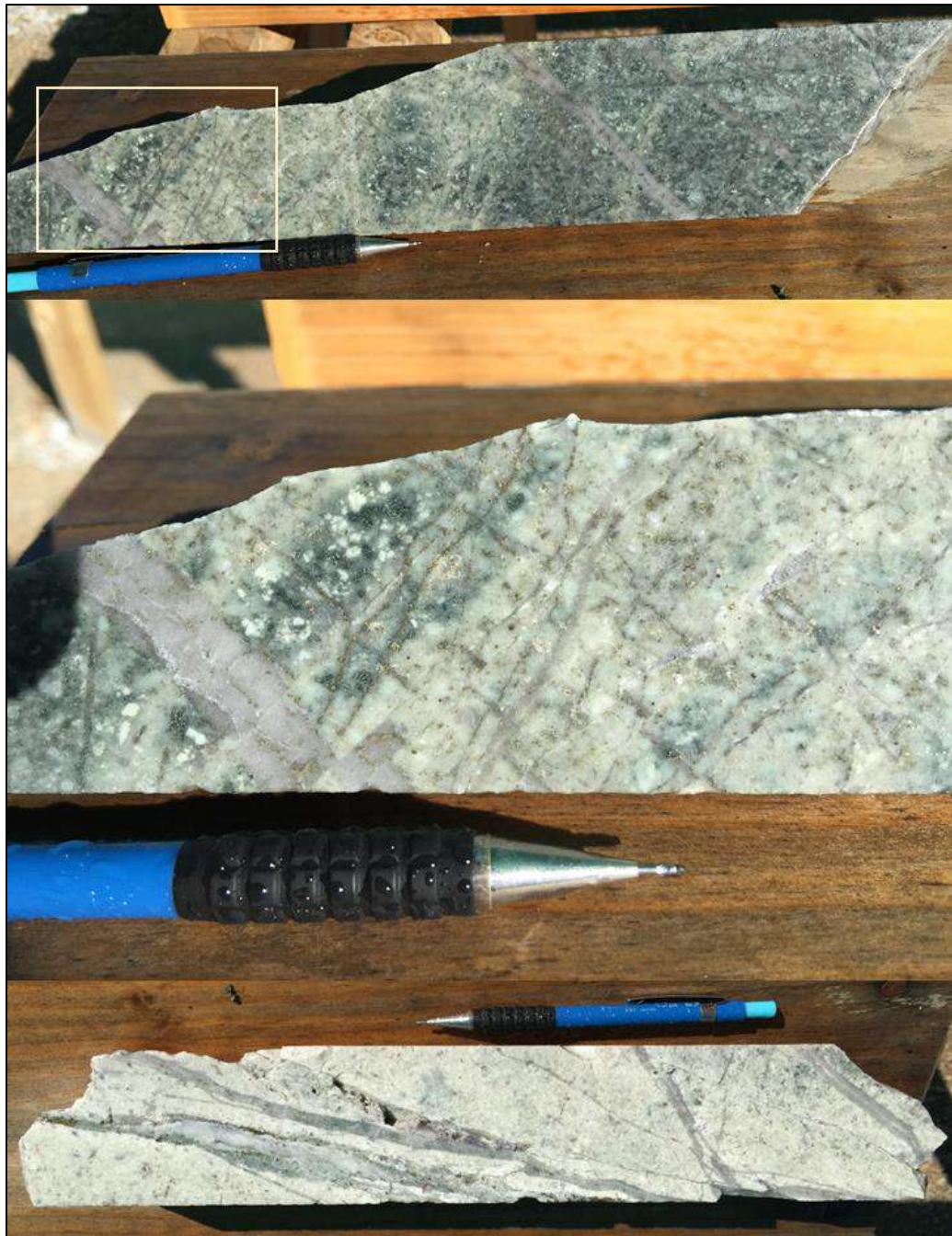


Figure 7.15 Alice holes PXP0001D. A). Interval with typical porphyry veining. Late albite fluids propagating up fracture network and removing sulphides, B) close up of box in A with albitic fluids move up, and then outward, C) complete albitisation

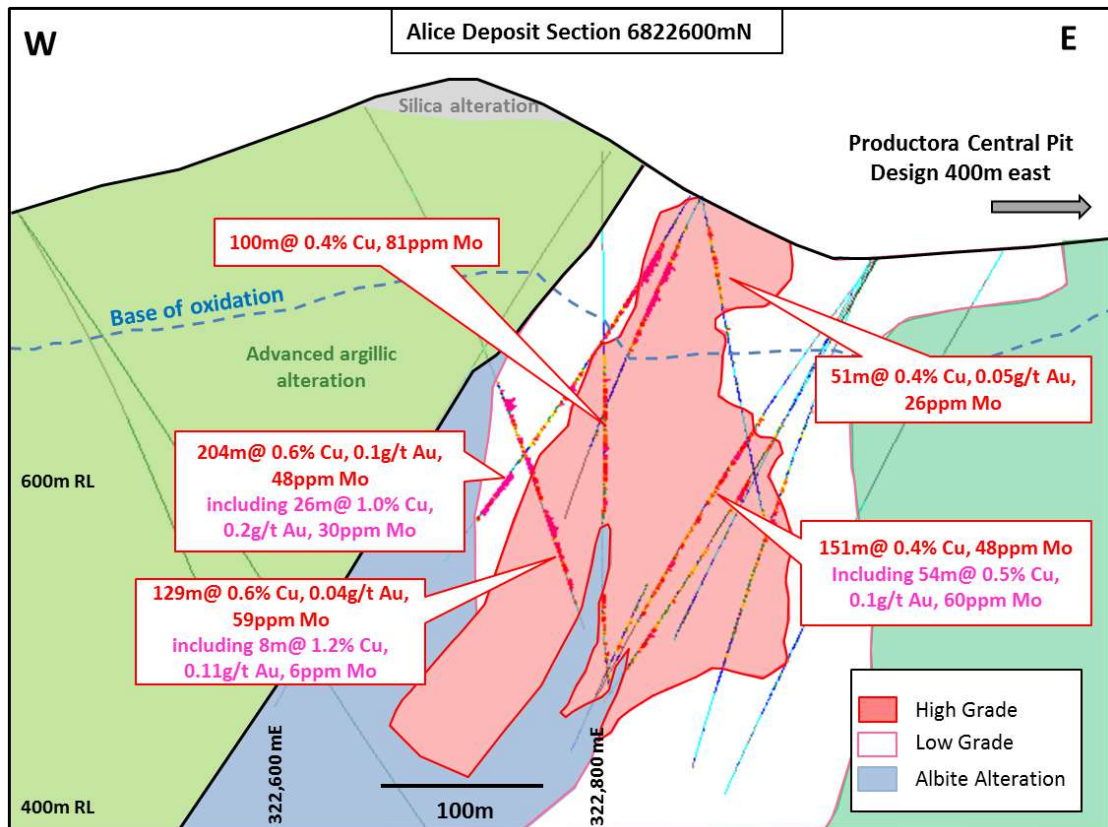


Figure 7.16 Alice type section on 6822600mN. Section looking north. (HCH, 2016)

7.5.4 Cortadera Mineralisation

An interpreted west-northwesterly-trending fault corridor hosts the three defined porphyry-style mineralised centres at Cortadera (Cuerpo 1, 2, and 3) (Figure 7.17). The colour anomaly and associated feldspar-destructive, phyllic alteration extends along this trend for at least 1.5 km, with the structural corridor extending along strike, and potentially controlling additional porphyry-style intrusive centres and related alteration cells with associated mineralisation. The depth of the current known mineralisation is at least 1 km, open in all directions.

Based on the genetic understanding of the deposit and geological logging undertaken by HCH, a 3D model of the multi-phase intrusions was developed using Leapfrog software. Wireframes for +0.1% Cu, +0.4% Cu and lithology were constructed based on the observations of Cu assays, geometry, trends, and vein percentages logged in drill-core as well as surface mapping.

Weathering wireframes were constructed using copper solubility thresholds, logged information and geochemistry ratios (Cu:S).

The earlier, higher grade mineralisation phases were modelled as they would have formed originally, allowing for a high confidence to be gained in the original geometry and continuity of these well-mineralised bodies before their continuity was interrupted by subsequent intrusive phases. Mineralisation tenor and distribution is consistent with that seen in similar Porphyry Cu-Au-Mo deposits; a strong correlation with A+ B quartz veining and associated chalcopyrite.

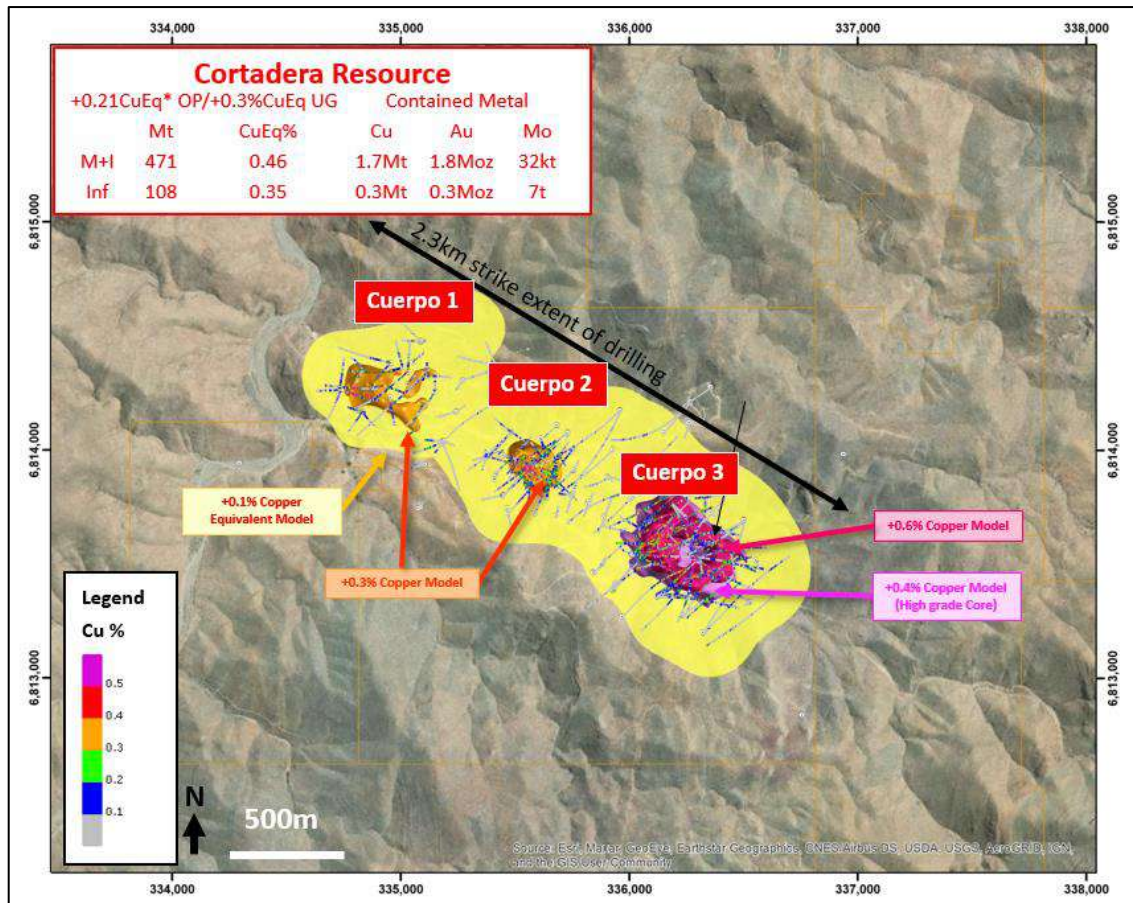


Figure 7.17 Location plan displaying tenement outlines, drilling completed and +0.7% CuEq (yellow) and +0.3% copper (orange), +0.4% copper (light pink) and +0.6 copper (magenta) mineralisation envelopes at Cortadera North. (HCH, 2022)

The Cortadera deposit is characterised by early- and intra-mineralisation, porphyritic tonalitic to quartz dioritic intrusions and adjacent volcano-sedimentary wall-rocks that have been recrystallised to hornfels and skarn. The hydrothermal alteration consists of moderate- to strong-phyllitic (+ chloritic) alteration, characterised by quartz/ silica, sericite and lesser amounts of chlorite.

Vein systems at Cortadera are typical of those found within porphyry-style mineralised systems. Early quartz-rich veins observed at Cuerpo 1 and Cuerpo 2 exhibit unidirectional solidification textures (UST) that are commonly associated with relatively high-temperatures during vein emplacement. Veins formed subsequent to UST veins comprise of A-veins (quartz-chalcopryrite-pyrite±magnetite), B-veins (quartz-chalcopryrite-pyrite±molybdenite) and the later C-veins (chalcopryrite-pyrite). A- & B-veins are most abundant in the centre of the porphyry system, where the copper is highest. C-veins are associated with mineralisation but are volumetrically less significant within the deposit than the A- & B- veins. D-veins (quartz-pyrite-sericite) with feldspar-destructive selvages and late calcite-bearing fractures formed subsequent to C veins. Anhydrite is locally present within some of the B and C veins and disseminated within the wall-rock.

Chalcopryrite also occurs as disseminations of variable intensity within the porphyritic host rocks, particularly in association with stockwork A & B veins. There is a very clear

correlation between increased percentage of quartz-bearing stockwork veining and sulphide content with elevated copper-gold grades.

The Cortadera deposit underwent considerable drilling between 2010 and 2013 while the project was under the control of Minera Fuego Limited (Minera Fuego), during an option agreement the company had entered with Sociedad Contractual Minera Carola (SCM Carola).

A second large campaign of drilling was undertaken in 2019 and 2020 following execution of a 100% purchase option agreement by HCH. Drilling undertaken by HCH consisted of verification, infill, and extensional drilling, which resulted in the Cortadera Maiden Mineral Resource Estimate (October 2020).

From 2020 to Late 2021, extensive in-fill and extensional drilling was undertaken at Cortadera for the Cortadera MRE March 2022 update.

7.5.4.1 Cortadera Calculated Mineralogy

During August 2020, Scott Halley (Mineral Mapping Pty Ltd) was commissioned to provide Quantitative Mineralogical Estimates or calculated mineralogy using a calculation method developed by Associate Professor Ron Berry at the University of Tasmania (CODES). This method involves linear programming calculations using the Simplex method, which utilises the Solver add-in within Excel spreadsheet software to solve the mineralogical calculations. The calculated mineralogy is influenced by far more variables than constraints and thus many combinations of minerals can give exact matches to a whole rock geochemical analysis. As such, the resultant calculated mineralogy must be considered to provide a non-unique solution and should be treated with an appropriate level of caution. One means of addressing the non-uniqueness of the solution is to apply training data to identify the most likely solution, but this is limited by the nature and extent of training data as well as the rigour with which it is applied. Thus, these calculations tend to be completed on an iterative basis, with multiple feedback loops between mineralogical calculations and drill core observations. Further updates to the mineralogical calculations were made over the course of 2021, the mineralogy results were used in constructing multiple mineralisation wireframes at Cortadera.

The data used was 4-acid digest ICP data collected from routine assaying of drill core and drill chip samples. Multiple calculation iterations have been made at this stage, with the intention to best represent the mineralogy of the Cortadera system. The calculated mineralogy has been modeled in 3D and compared to visual logging results. The alteration model provides some geological insights around alteration zonation, mineralisation style, metal distribution and rock properties in relation to alteration mineralogy, which feed into mineralisation controls and targeting.

Chalcopyrite mineralisation wireframes (0.17% Cpy, 1.0% Cpy 1.2% Cpy, 1.65% Cpy) were constructed using visually logged chalcopyrite estimates, but where mineralisation logging was unavailable in the historic data, calculated mineralogy chalcopyrite estimates were used to inform these areas. These shapes were then validated using copper assays and calculated chalcopyrite abundance. Calculated abundances of chlorite and sericite have been used to better determine the phyllic (quartz-sericite),

intermediate argillic (sericite-chlorite), and propylitic (chlorite) alteration zones. These alteration zones were then validated with the alteration logging by geologists.

7.5.5 Cortadera oxide mineralisation

Following the Maiden MRE, further drilling at each of the Cuerpo's indicated the presence of near surface limonites with varying copper content, as well as minor chalcocite, tenorite and clays with copper oxides. This shallow oxide copper domain was modelled in Leapfrog software using a combination of logging (copper oxide mineralisation and extent of iron-oxide mineral development) and copper grade cut-offs. These domains are wholly contained within the Oxide and Transition surfaces and are considered a Supergene enrichment zone, particularly at Cuerpo 2. Further mineralogical analysis is recommended to confirm the presence of logged limonites.

7.5.6 San Antonio Mineralisation

The San Antonio deposit has been interpreted as a lode- or vein-style copper skarn deposit that shows fault- and lithological-controls. The styles of mineralisation is consistent with those formed on the peripheries of porphyry systems.

At San Antonio, mineralisation presents as a main lode, and stacked hanging wall lenses. The main lode represents the largest lens along strike and in width; along with the highest concentrations of contained metal. Hanging wall lenses generally run sub-parallel to this lode and are less continuous in all orientations.

Chalcopyrite is the primary mineral material. The mineral resource estimate identified that, relative to the Cortadera porphyry, San Antonio was depleted in Au and Mo, yet enriched in Ag and Co.

The deposit has been largely drilled using reverse circulation methods, and therefore structural evidence on the type and local controls on mineralisation are not yet known.

8 DEPOSIT TYPES

8.1 Productora

Geology and mineralisation at the Productora deposit were first documented in an MSc study by Fox (2000) titled 'Fe-oxide (Cu-U-Au-REE) mineralisation and alteration at the Productora prospect'. This provided the most comprehensive documentation of the geology of the Productora deposit prior to the current study. Key outcomes included geological map and cross section interpretations, alteration paragenesis and geochronology (39Ar-40ArK-feldspar and U-Pb zircon), alteration map and cross section, interpretations, volcanic stratigraphy interpretation, description and dating of the Cachiyuyito and Ruta Cinco intrusions, sulphur isotope analyses, mass balance evaluations, comparison to other regional deposit styles and interpretations of the geological history and genetic model. Fox (2000) concluded that Productora was similar to the Candelaria deposit — a magnetite-dominant IOCG with significant sulphide mineralisation associated with potassic alteration. Magnetite-apatite mineralisation at

Productora was interpreted to be part of the Cachiyuyito hydrothermal system, emplaced at 129.8 ± 0.1 Ma (U-Pb zircon). The Ruta Cinco border phase was dated by Fox (2000) at 96.1 ± 0.2 Ma (U-Pb zircon) and hydrothermal K-feldspar associated with copper mineralisation was dated at 91.4 ± 0.2 Ma (39Ar-40ArK-feldspar). Fox (2000) speculated that regional evaporite deposits may be a source of boron for abundant tourmaline and dumortierite but that magmatic fluids were the likely sulphur source.

8.2 Alice

The Alice copper-molybdenum porphyry deposit is situated 400m to the west of Productora. Mineralisation occurs as disseminated chalcopyrite and quartz–pyrite–chalcopyrite \pm molybdenite vein stockwork hosted by a granodiorite porphyry stock (121.1 ± 2.1 Ma). Potassic alteration (biotite \pm actinolite replacing hornblende) is associated with quartz–sulphide veins. Mineralisation was dated by Re-Os on molybdenite at 124.1 ± 0.6 Ma (within section of the porphyry stock). The margins and deeper parts of the system are overprinted by albite \pm epidote \pm sericite alteration, which locally caused destruction of biotite and chalcopyrite.

The Alice porphyry is spatially associated with the Silica Ridge lithocap, which is characterised by massive quartz-altered rock above domains of alunite, pyrophyllite and dickite (Escolme, 2016).

8.3 Cortadera

Cortadera is a copper-gold-molybdenum porphyry hosted mineral deposit type, comprising a series of mineralised centres (Cuerpo 1, 2 and 3) within a structural corridor.

Porphyry systems are typically characterised by:

- Deposits occurring in clusters
- Small diameter (0.5 to 2km) causative intrusions of intermediate to felsic composition
- Shallow depth of emplacement (1 to 4km)
- Porphyritic texture, being mm scale phenocrysts in a sub-mm scale groundmass
- Multiple phases of intrusion, including pre-, early-, syn-, late- and post ore.
- Extensive hydrothermal alteration associated with each mineralising intrusion
- Fracture and vein-controlled alteration and mineralisation
- Metal zoning, comprising a central zonation of iron-copper-gold, with proximal molybdenum and distal gold-silver-lead-zinc
- Sulphide and oxide minerals which vary from early magnetite-(bornite) through transitional chalcopyrite-pyrite-(hematite) to late pyrite, pyrite-bornite or pyrite-enargite-(covellite)

- Temporal fluid evolution, with early higher temperatures with high salinity to later lower temperatures of lower salinity (Garwin, 2019).

An example of the geometry of a Porphyry System in Arc Settings is shown in Figure 8.1, and the hydrothermal alteration of the same system in Figure 8.2. An example of the trace element distribution at the Ann-Mason Porphyry deposit at Yerington can be seen in Figure 8.3.

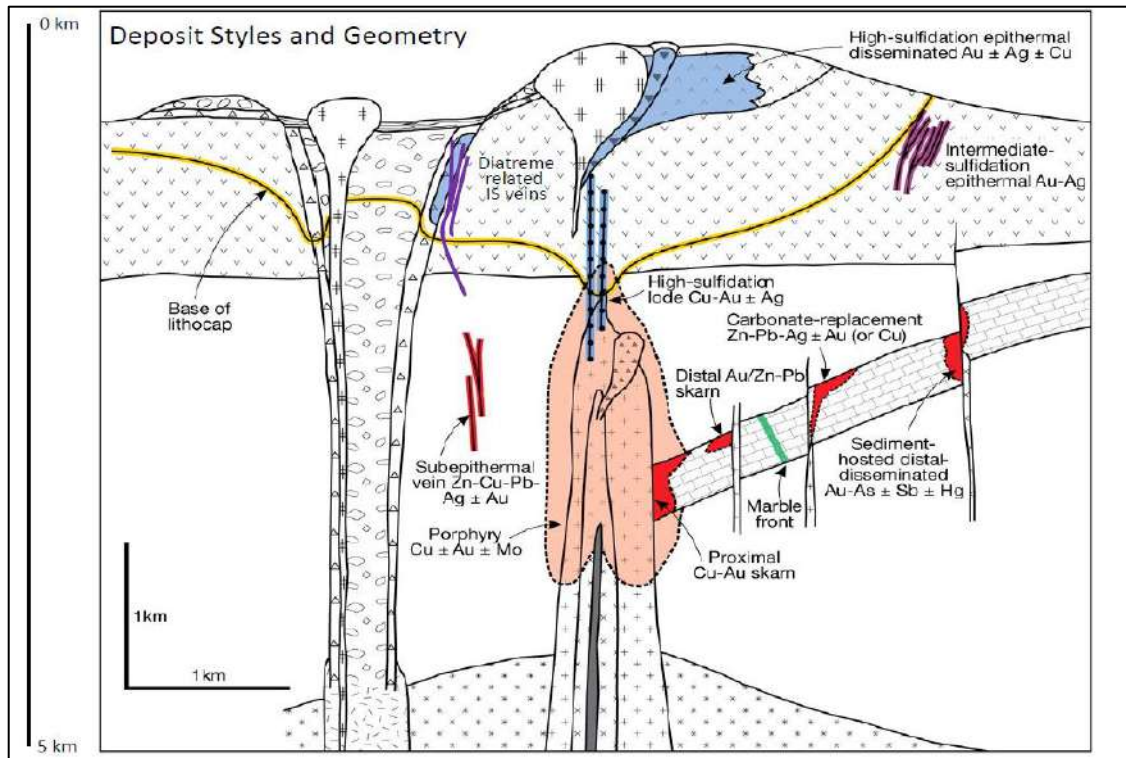


Figure 8.1 Example cross section of Porphyry Systems in an Arc Settings, showing geological variations (Sillitoe, 2010)

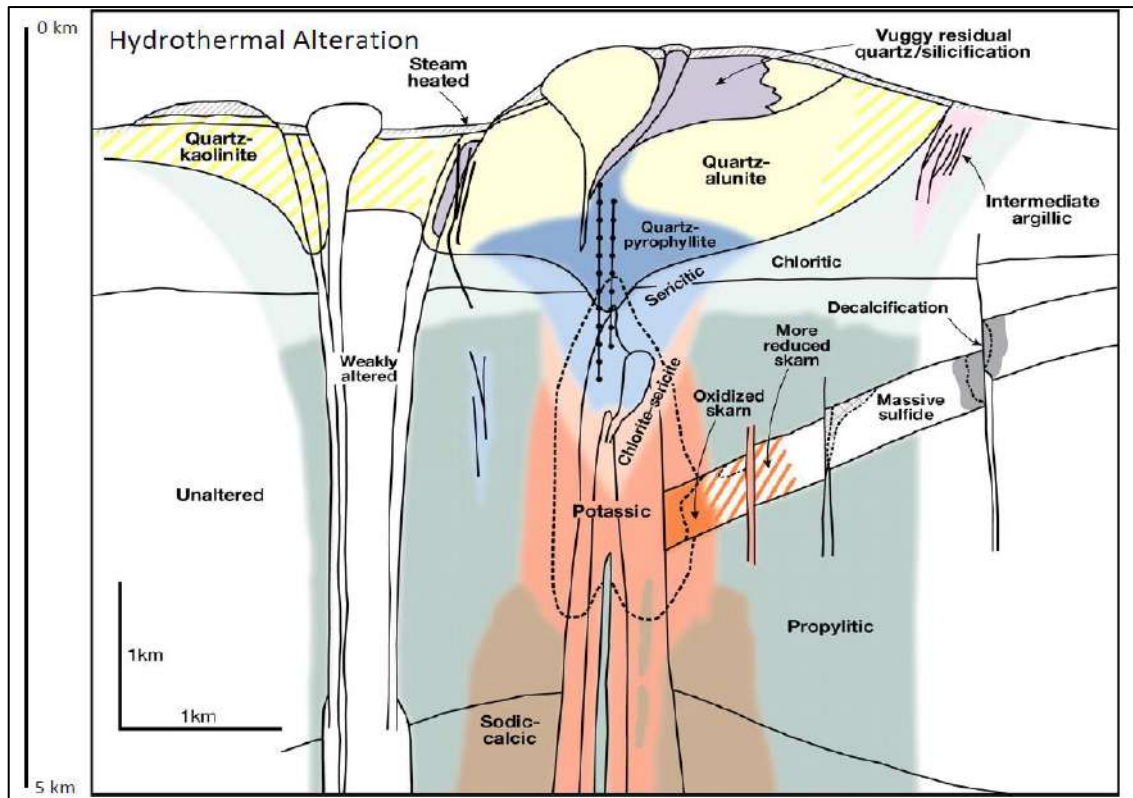


Figure 8.2 Example cross section of Porphyry Systems in an Arc Settings, showing alteration variations (Sillitoe, 2010)

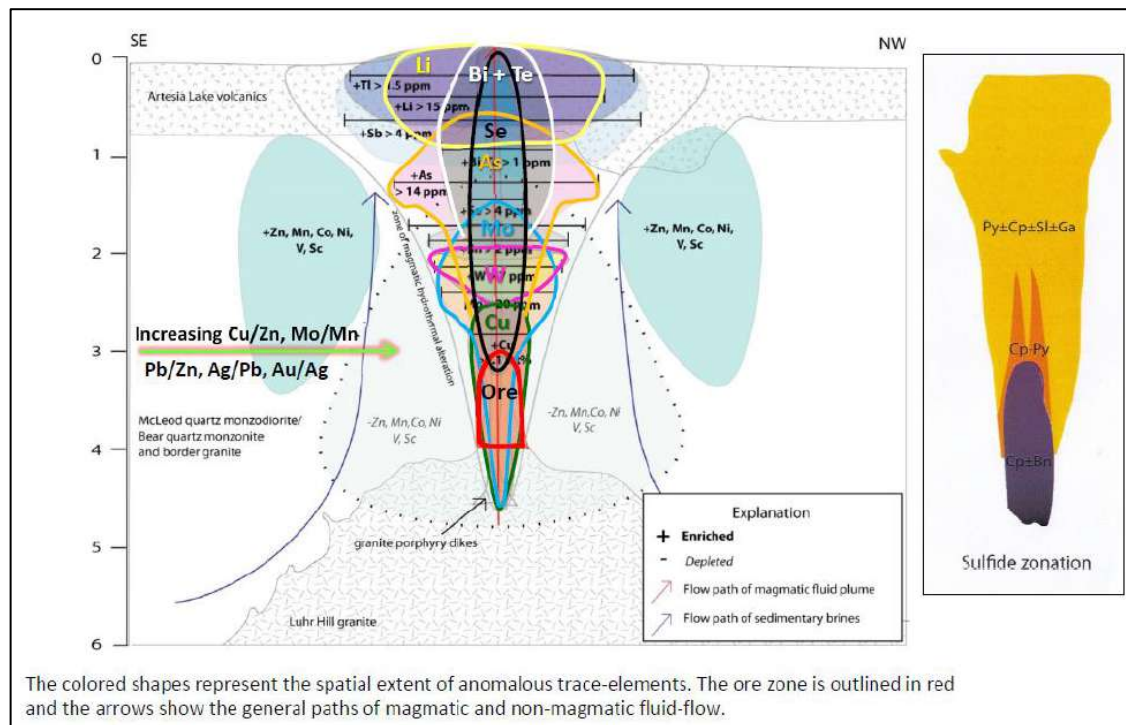


Figure 8.3 A cross section through the Ann-Mason Porphyry deposit at Yerington, showing the trace element distribution (Cohen, 2011 and Halley et al., 2015) with elemental ratio annotations based on Garwin (2019).

8.4 San Antonio

San Antonio appears as a skarn-like deposit, with mineralisation presenting in faults and strata, linked to the nearby porphyry environment. At this early stage of definition, HCH has not conclusively established the deposit type, controls and mechanisms for mineralisation for San Antonio.

HCH has investigated the mineralisation at San Antonio using surface and underground mapping and petrographic studies.

The first event, related to the intrusion of the Quartzodiorite Unit, generates stratabound bodies related the metasomatic replacement of the Calcareous and Volcanosedimentary units, with silica-epidote-garnet, silica-epidote, garnet-silica. Microscopic studies indicate that this first skarnification event is related to mineralization mainly of pyrite (Py) with lesser chalcopyrite (Cpy) (Py-Cpy ratio 9:1) (Figure 8.4).

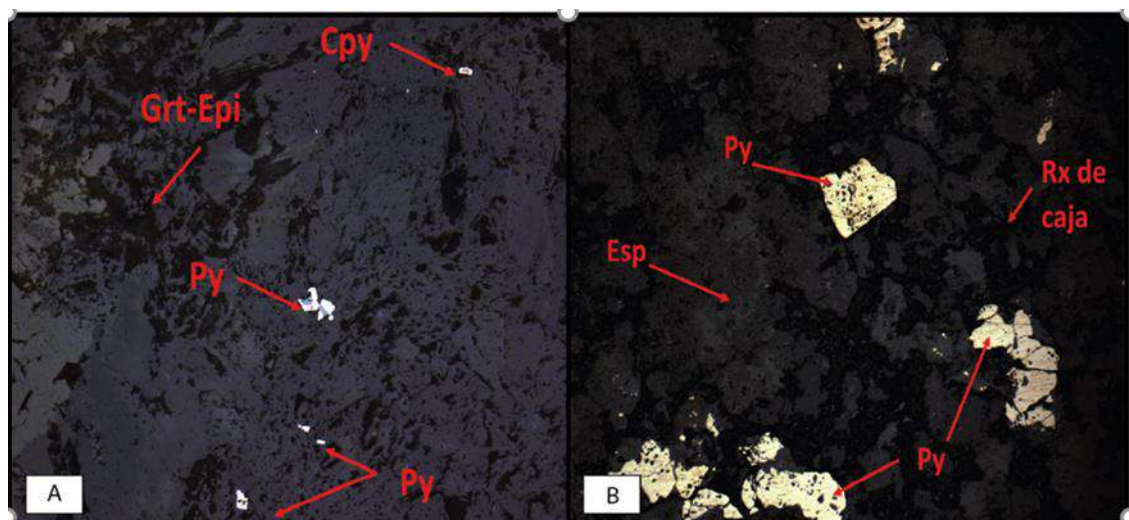


Figure 8.4 First Skarnification event with mineralisation of pyrite and lesser chalcopyrite. For reference, Cpy – chalcopyrite, Grt-Epi – Garnet-Epidote, Py – pyrite, Esp – specularite.

The second event, related to the presence of quartz-dioritic and dacitic porphyries, which cut through the skarnified areas and outcrop in the vicinity of the San Antonio and Santiago mines. Figure 8.5 This second mineralization event is spatially related to an epidote, chlorite, and sericite alteration, in addition to few quartz and calcite veinlets. The degree of alteration is moderate in the periphery of the mining district to intense in the vicinity of the main mineralized zones.

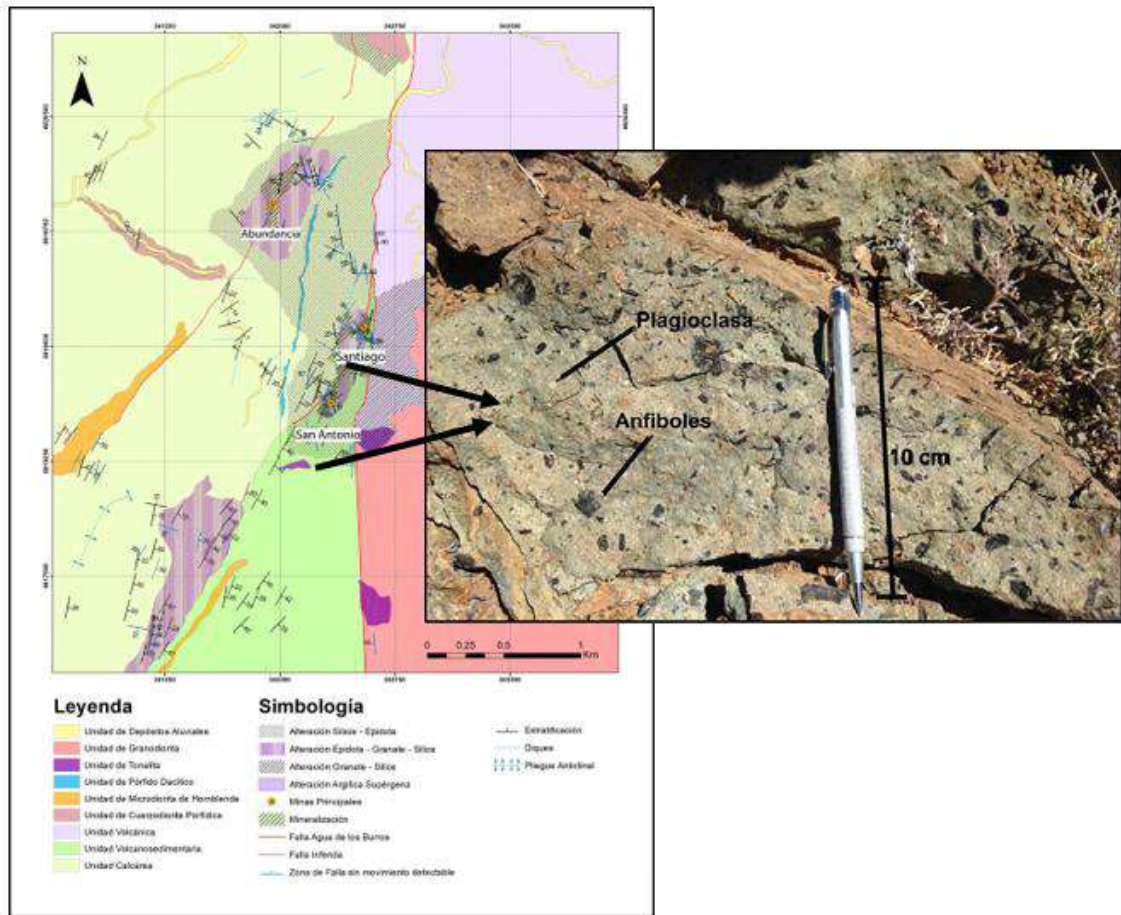


Figure 8.5 *Intrusion of Qtz-Dioritic and Dacitic Porphyry*

The third event, and the most important from the economic point view, is associated with the filling of veinlets and fractures by chalcopyrite-specular hematite-magnetite-quartz-calcite within fault zones. Microscopic studies indicate that in this mineralization event is associated with the replacement of chalcopyrite by specular hematite and the replacement of pyrite by chalcopyrite. These replacements are spatially related with quartz-dioritic porphyry, but the genetic relationship is not clear (Figure 8.6). A summary of the evolution is provided in Figure 8.7.

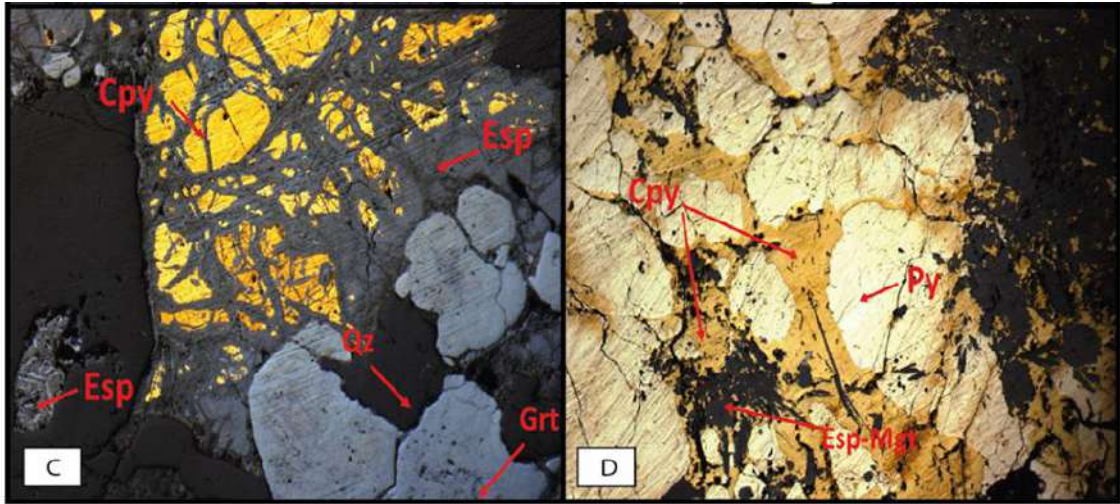


Figure 8.6 Mineralisation event with infill of veinlets and fractures. For reference, Cpy – chalcopyrite, Esp – specularite, Qz – quartz, Grt – garnet, Py – pyrite, Mgt – magnetite.

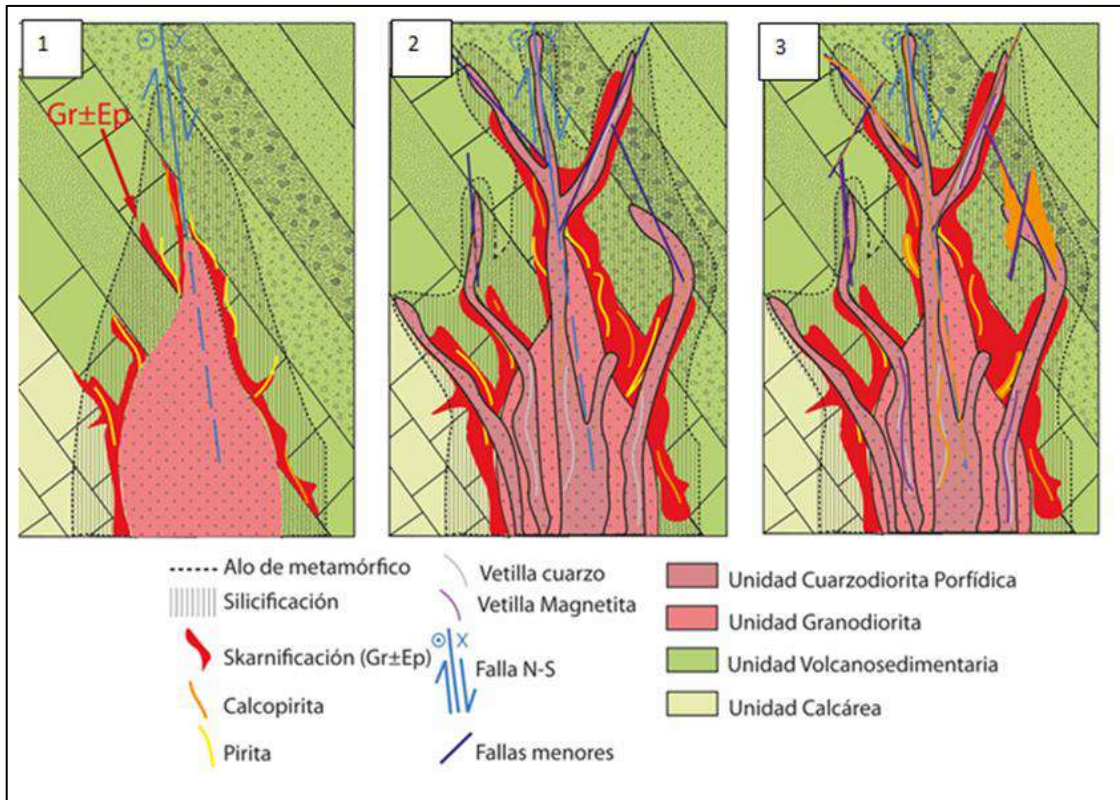


Figure 8.7 Schematic evolution for San Antonio Skarn Deposit

8.5 Deposit Mineralisation

8.5.1 IOCG Style Deposits

A variety of IOCG mineralisation styles have been documented including veins and stockworks (hosted by intrusive rocks, particularly equigranular gabbrodiorite and diorite), hydrothermal breccias, calcic skarns, replacement horizon (mantos) and 'composite' styles, which generally include veins and a combination of other styles (Sillitoe, 2003). Composite deposits hosted within volcano-sedimentary sequences, such as Candelaria, tend to be the largest and have the most complicated alteration assemblages and overprinting relationships (Sillitoe, 2003).

The Chilean IOCG deposits are characterised by low titanium hydrothermal magnetite, and/or specular hematite, which occur together with chalcopyrite as the dominant hypogene copper phase, plus gold and anomalous concentrations of cobalt, uranium, rare-earth-elements, molybdenum, zinc, silver and other elements (Hitzman et al., 1992; Barton and Johnson, 1996). The iron oxides are typically post-dated by pyrite and copper-bearing sulphides (Ruiz et al. 1965). Candelaria is an example of a magnetite-dominated deposit where magnetite-rich veins also contain significant actinolite, biotite and quartz with local apatite, clinopyroxene, garnet, hematite, and K-feldspar. Hematite-rich veins typically contain sericite and/or chlorite ± K-feldspar or albite. In many cases, these shallow hematite veins transition downwards to magnetite (e.g., Ruiz et al., 1965) suggesting that although distinction of the two deposit styles is reasonable, separation into different geological systems is debatable.

Alteration in IOCG deposits is typically complex and varied. A generalised upward and outward zonation is typically observed in deposits that have sodic, calcic and/or potassic alteration, deep magnetite-actinolite-apatite transitions to shallow specular hematite-chlorite-sericite (Escolme, 2016). In general, tourmaline is common and quartz is sparse, although not totally absent (Sillitoe, 2003).

8.5.2 Porphyry Cu-(Mo-Au) Style Deposits

The 'Pacific Porphyry Cu Belt' defined by Llaumett et al. (1975) encompasses of a number of Early Cretaceous (132-97 Ma) porphyry deposits in the Coastal Cordillera, including Andacollo (the only deposit currently being exploited), Galenosa, Puntillas, Antucoya-Buey Muerto, Dos Amigos at Domeyko, Pajonales and Colliguay (Maksaev et al. 2007) (Figure 8.4). The deposits are generally small, <300 Mt, and low grade (up to 0.4 % Cu) making most of them uneconomic (Sillitoe, 2003). Copper mineralisation is related to small porphyry stocks of quartz diorite to granodiorite emplaced in the contemporaneous volcano-plutonic arc with associated potassic (biotite, K-feldspar) alteration and intermediate argillic overprints of chlorite, sericite, illite and/or smectite assemblages (Sillitoe and Perrelló, 2005). The porphyry prospects contain Mo but are relatively poor in Au, with the exception of Andacollo (Sillitoe and Perrelló, 2005).

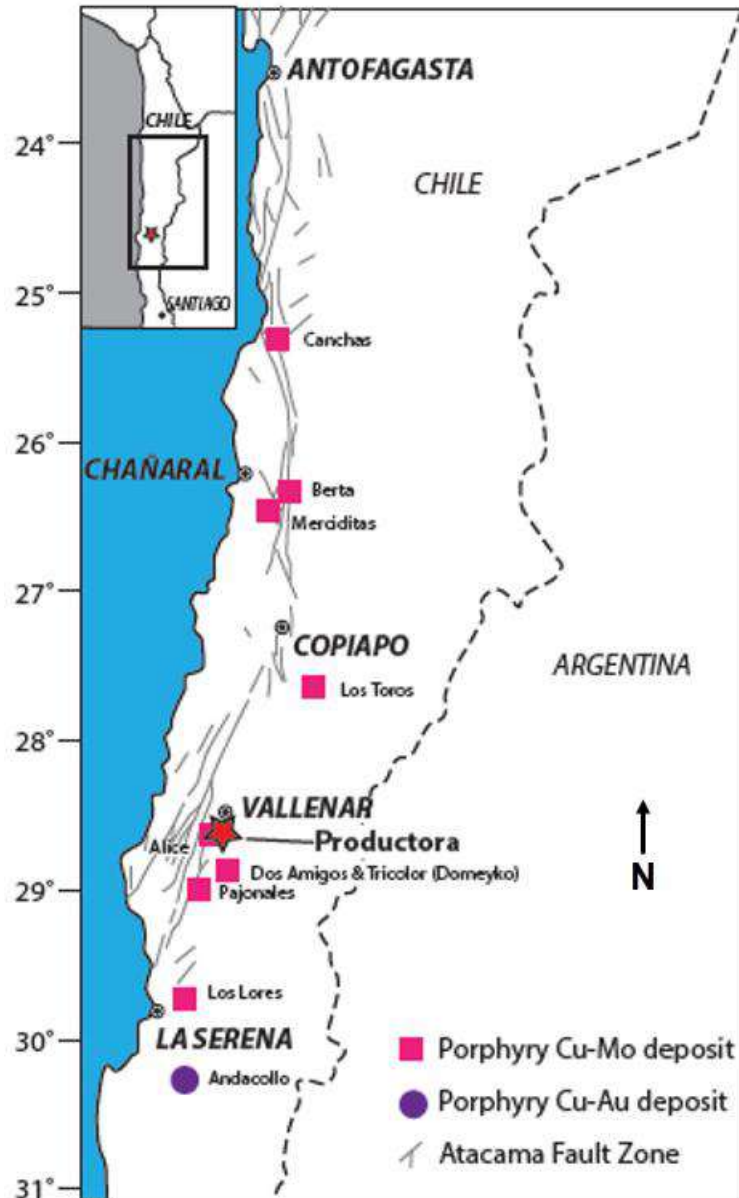


Figure 8.8 Pacific porphyry Cu belt with Productora for reference (Escolme, 2016, modified from Makshev et al. (2007))

8.5.3 Manto-type copper deposits

The Chilean manto-type copper deposits, also known as stratabound, are currently the third largest source of copper production in Chile (Figure 8.4). They can be divided into two groups based on their age and location:

1. Jurassic volcanic-hosted deposits, including Mantos Blancos and the Michilla District which occur in northern Chile between 21°30'S and 26°S
2. Lower Cretaceous volcanic hosted deposits, including El Soldado and Lo Aguirre which occur in the intra-arc basin of central Chile from 30°S and 34°S (Makshev et al., 2007; Figure 8.5). The manto-type deposits are considered a distinctive

class which is relatively uncommon outside of the Coastal Cordillera of northern and central Chile (Sillitoe, 2003).

Manto deposits are generally hosted in Mesozoic basaltic and andesitic, volcanic and volcano-sedimentary rocks in distal, peripheral locations to coeval dioritic to granodioritic plutons (Maksaev and Zentilli, 2002; Sillitoe and Perrelló, 2005). Mineralisation occurs in stratabound disseminated bodies and steeply dipping hydrothermal breccias surrounding barren diorite intrusions with associated veins (Sillitoe and Perrelló, 2005). The highest grades are typically found in zones of high permeability, such as permeable faults, hydrothermal breccia, dike contacts, vesicular flow tops and flow breccia. The dominant hypogene sulphide phases are bornite, chalcopyrite, chalcocite and pyrite plus occasional covellite and digenite, with additional minor sphalerite and galena identified in the Early Cretaceous deposits (Maksaev and Zentilli, 2002).

Hypogene gangue minerals include quartz, hematite, pyrite, chlorite, albite, calcite and local magnetite as well as zeolites, epidote and bitumen in the Early Cretaceous deposits (Maksaev and Zentilli, 2002). Hypogene mineral zonation has been observed at a number of deposits, including Mantos Blancos, Santo Domingo, Lo Aquirre and El Soldado, with high grade cores centred on redox fronts in the host stratigraphy (Sillitoe, 1992; Sillitoe and Perrelló, 2005). The deposits are characterised by a core of Cu-rich minerals (chalcocite – bornite ± digenite), surrounded by successive zones of chalcopyrite ± bornite, chalcopyrite - pyrite and pyrite (Maksaev and Zentilli, 2002; Sillitoe and Perrelló, 2005). Mineralisation is commonly rich in silver, and lacks gold (Sillitoe and Perrelló, 2005).

Most of the manto-type deposits are weathered and have an upper oxidized zone. However, supergene enrichment has only occurred at some of the larger deposits. This is probably due to low pyrite abundance, which limited acid production, and abundant calcite gangue which neutralised acid fluids (Maksaev et al., 2007). Cu-oxide minerals include atacamite, minor chrysocolla, malachite, Cu-sulphate and rare cuprite and native Cu (Maksaev et al., 2007).

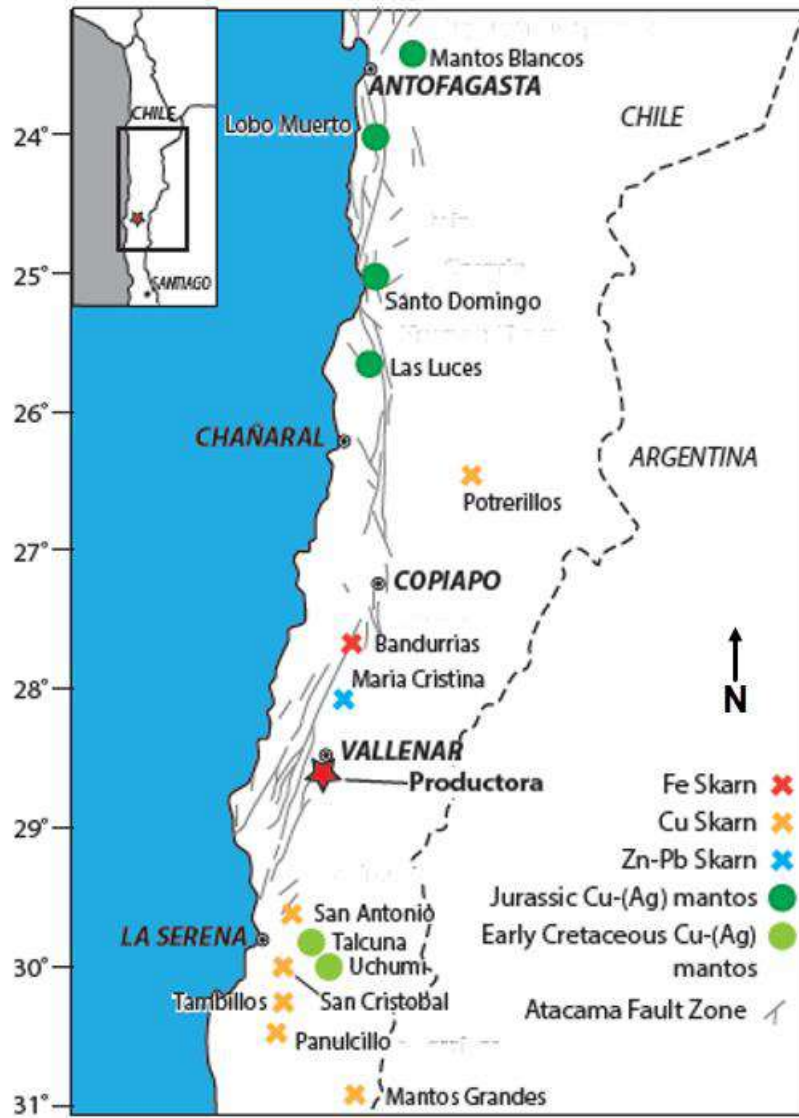


Figure 8.9 Mesozoic Manto-type Cu and skarn deposits with Productora for reference. Modified from Makshev et al. (2002).

9 EXPLORATION

9.1 Productora

9.1.1 Introduction

An extensive data compilation and validation exercise was performed by HCH in 2010. Historical data was collected from several sources including hard copy reports, public disclosure, and both hard copy and digital maps. Ground reconnaissance was also completed.

Several detailed litho-structural mapping campaigns by HCH allowed compilation and validation of geological information along the Productora main mineralised zone. This work showed that the mineralisation at Productora is hosted within relatively permeable units of a felsic-intermediate volcanic sequence. The mineralisation was evident in a series of permeable units and fault-controlled disseminations and breccia that trend N-S, E-W and NW-SE. Jogs and intersections between fault sets as well as between faults and permeable volcanic units appeared to have assisted the mineralisation process.

Geochemical sampling demonstrated that significantly elevated copper-gold-molybdenum grades, together with other elevated pathfinder elements, were evident within soils. In particular, molybdenum in soils appeared to define an anomaly immediately above the Productora mineralisation. Where uranium assays were elevated, uranium showed an association with copper, silver, molybdenum, gold and cobalt. Zones dominated by albite versus K-feldspar-sericite alteration were defined, with copper-gold being associated with the K-feldspar-sericite alteration and magnetite being associated with the albitic alteration zones. These results were consistent with earlier petrographic work completed by Fox (2000).

9.1.2 Airborne Magnetic and Radiometric survey

HCH undertook an airborne geophysical survey in 2010. The survey was conducted by contractor Geodatos and flown by helicopter with an average sensor height of about 145m, on 100m spaced east-west flight lines, and 1,000m spaced north-south tie lines. Data collected included standard flight height, magnetic and radiometric data.

This geophysical survey data was processed by geophysical consultants Southern Geoscience, with several magnetic and radiometric products provided which have enabled structural, lithological and alteration mapping which has assisted greatly with drill targeting.

A subsequent 3D magnetic inversion model was produced in August 2015, which provides an additional dataset for construction of a 3D litho-structural model (Figure 9.1 and 9.2).

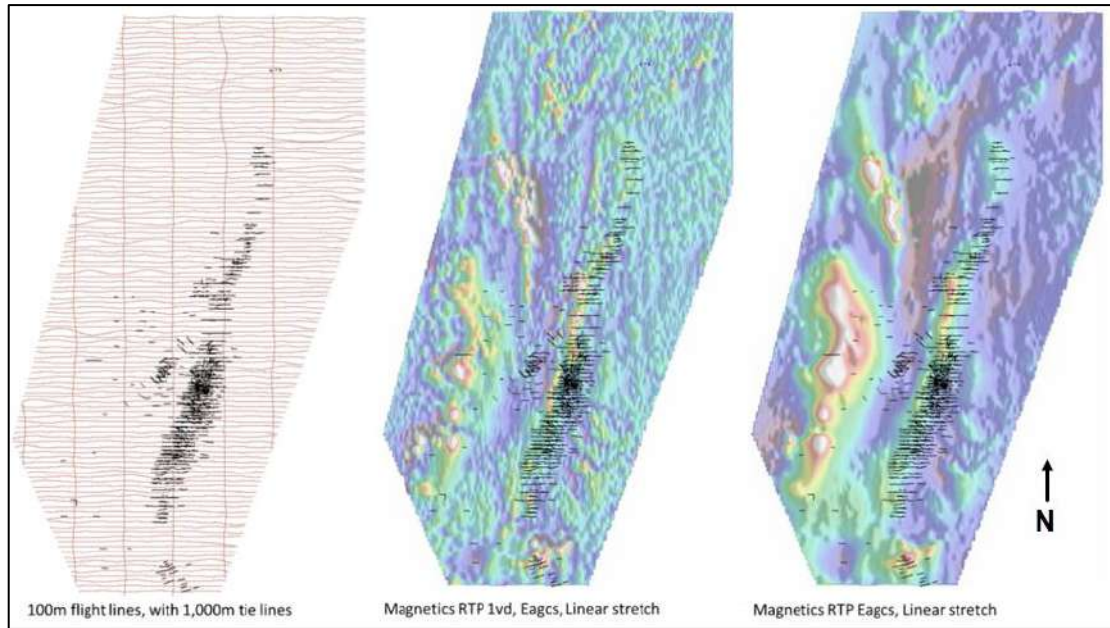


Figure 9.1 Flight lines and example magnetic data from the 2010 Productora airborne geophysical survey (plan view with drilling traces shown)

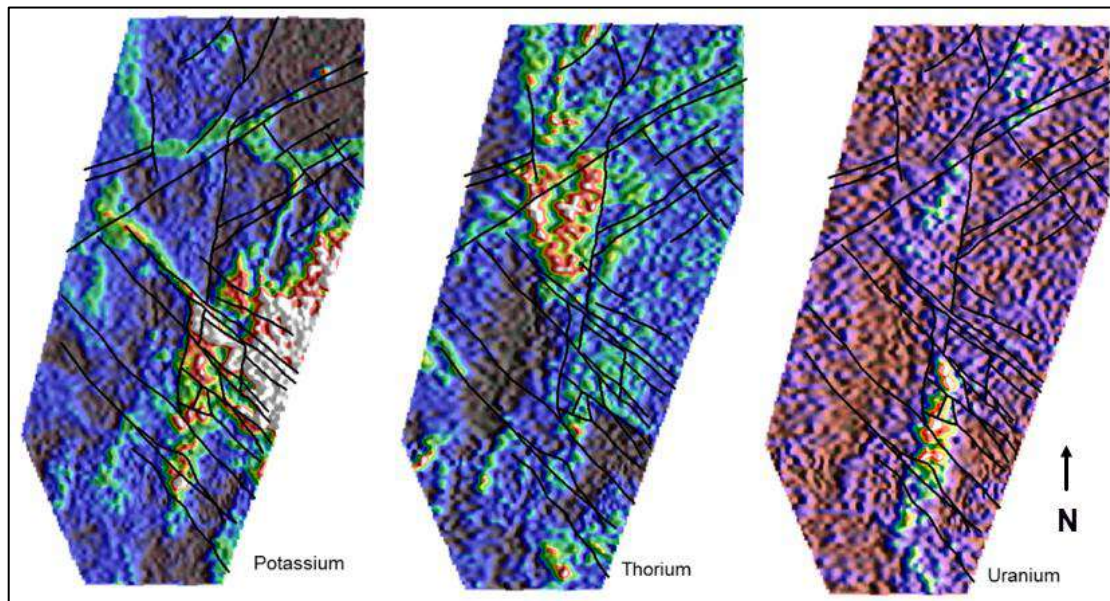


Figure 9.2 Example radiometric data from the 2010 Productora airborne geophysical survey (plan view). (HCH, 2016)

9.1.3 Induced Polarisation and Magnetotelluric (IP/MT) survey

An Induced Polarisation and Magnetotelluric (IP/MT) survey was completed in late August 2015 (Figure 9.3). SouthernRock Geophysics was contracted to complete a 26.7 line-km, 150m Pole-Dipole Induced Polarization / Resistivity and Magnetotelluric (IP/MT) survey at the project. The survey was focused over the western part of the project known as the Alice porphyry corridor. This survey provided a detailed 2D and pseudo 3D mapping of the resistivity and chargeability of the 6.5km-long porphyry-style target area

at the project. An example type section displaying the IP 2D chargeability response can be seen in Figure 9.3.

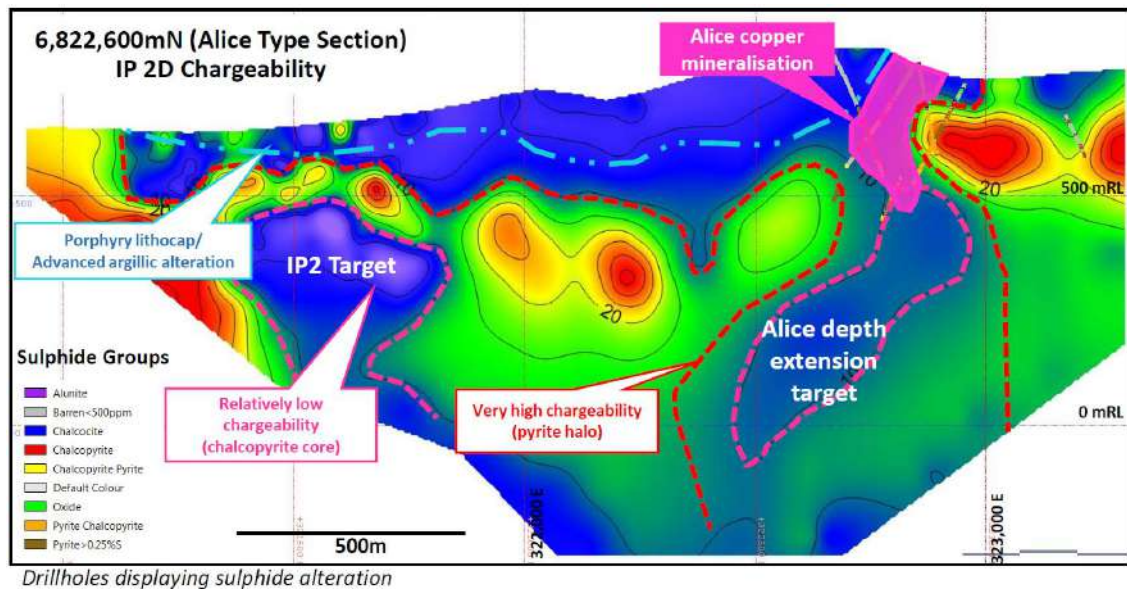


Figure 9.3 Example section of the IP/MT 2015 Productora ground geophysical survey. Chargeability shown on Alice type section (6822600mN). Image looking north. (HCH, 2016)

9.1.4 Surface Mapping and Structural Review

Pre-2014, soil sampling and rock chip sampling had been undertaken by HCH in localised areas, but mainly within the central corridor “main zone”.

In 2014, as part of a comprehensive targeting exercise, HCH invested in a large systematic soil sampling programme across the entire project area (Figure 9.4). Samples were collected on a 400m x 400m staggered grid across the tenement package, with infill sampling completed in high priority areas on a 400m x 200m spacing. Samples were nominally taken in an area of 30cm x 30cm, at a depth of 15cm to 20cm. A 500 - 800g sample was put through a 2mm sieve with all passing material collected for assay. The samples were assayed at ALS laboratories by four acid digestion and ICP-MS which provided a 48-element analysis of all samples.

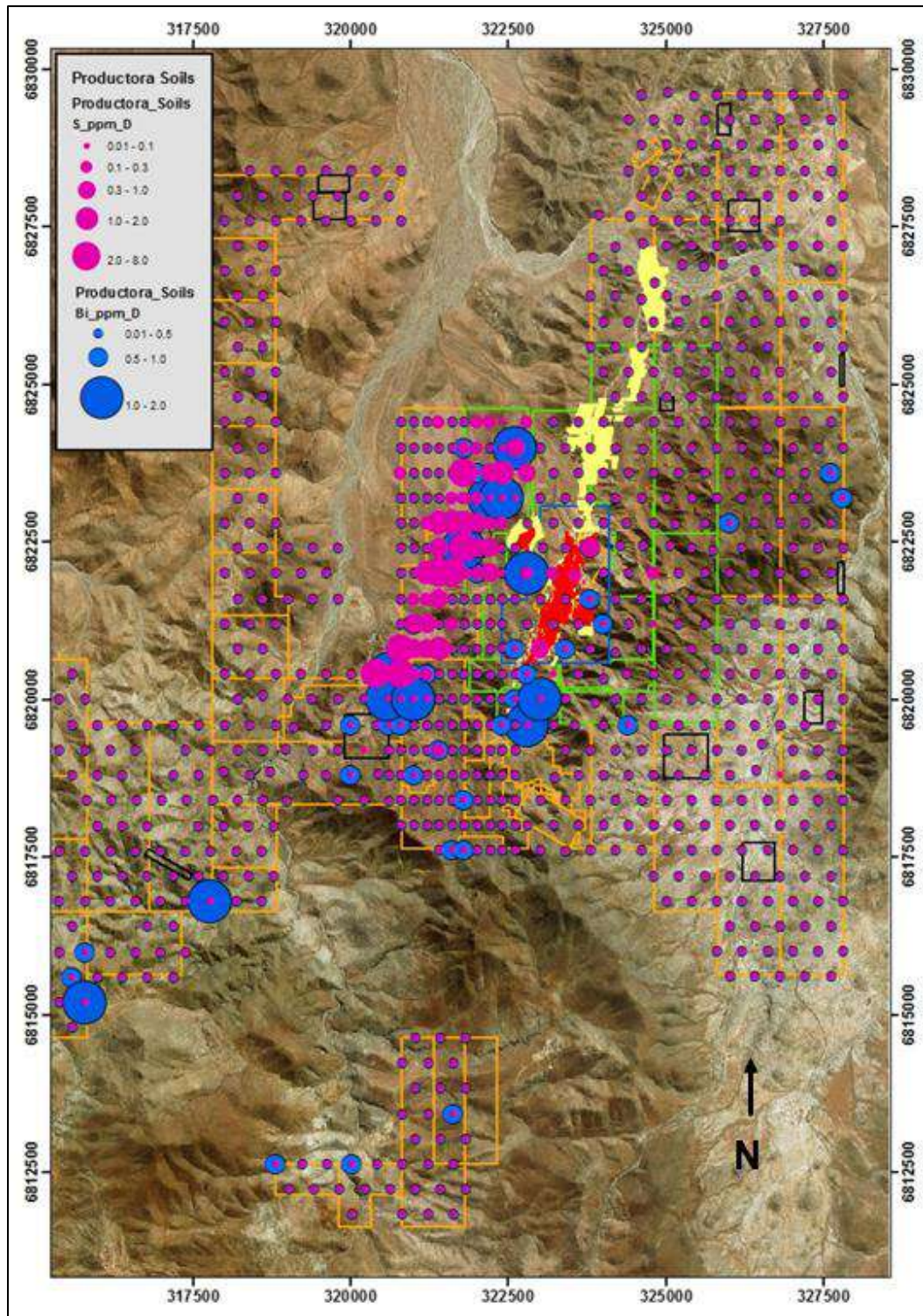


Figure 9.4 Extent of 2014 Productora soil sampling programme. Example elements shown. (HCH, 2016)

9.1.5 Petrography

HCH has an extensive collection of thin sections taken from diamond core by HCH which have accompanying imagery and thin section descriptions. These images and descriptions are available for future studies and data interrogation. Thin sections and analysis were completed by Ron Berry at CODES University, Tasmania.

An example is shown in Figure 9.5. This sample is taken from PRP0420D (356.18 m) which was drilled into the Productora deposit.

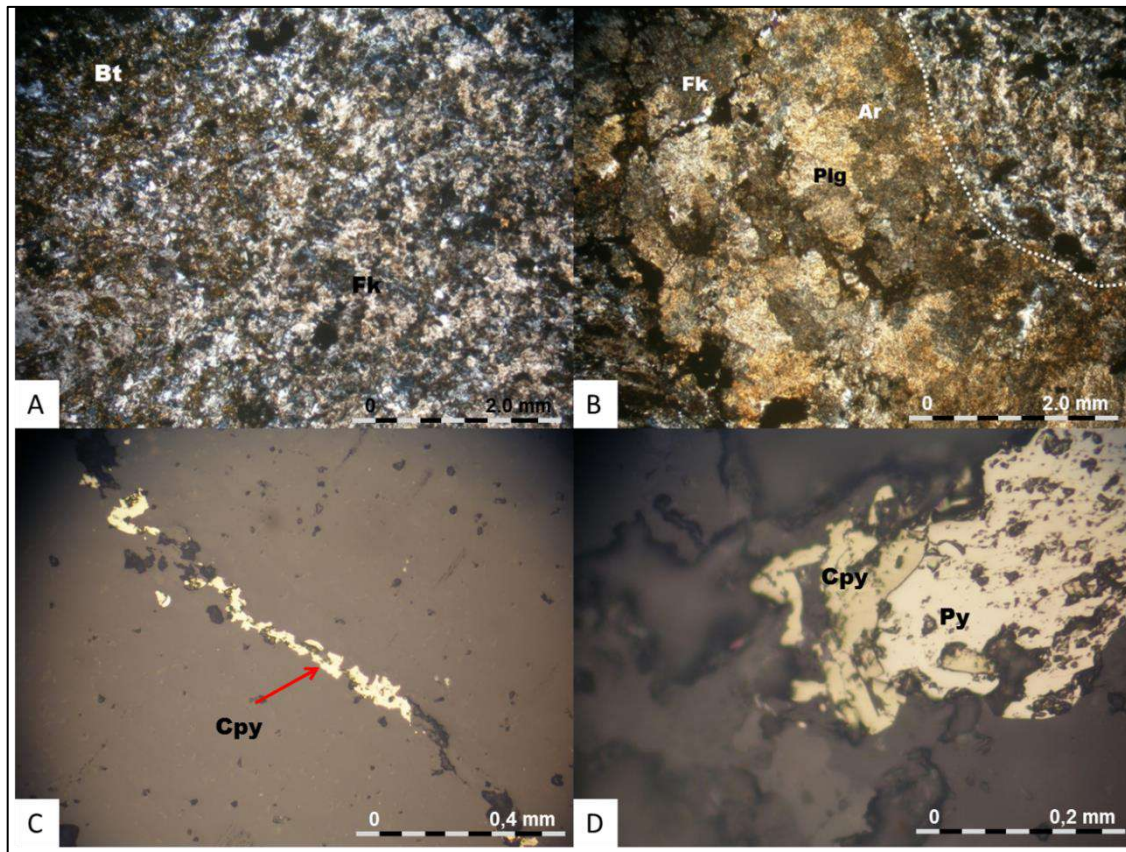


Figure 9.5 Example thin section image M-92. Sample take from Productora deposit drilling, PRP0420D at 356.18m depth. A and B are in transmitted light, C and D are reflected light. Image A) provides an overview, principally composed of interstitial feldspar (Fk) with development of biotite (Bt). B) An aplitic, albitised plagioclase (Plg) texture being altered to K-feldspar (Fk) and clays (Ar). C) A micro veinlet filled with chalcocopyrite (Cpy). D) Pyrite (Py) being replaced by Chalcocopyrite (Cpy) in texture decay.

9.1.6 Fathom 3D geochemical modelling

Probability models of potential mineralisation were generated by Fathom Geophysics, using advanced algorithms developed from an extensive study of the spatial distribution of pathfinder element associations across the Yerrington copper-gold porphyry deposit in Nevada, USA (928Mt grading 0.51% Cu, 0.05g/t Au and 1.85g/t Ag – source USGS) and several other Cordilleran porphyry systems (Cohen, 2011; Halley et al, 2015).

The highest scoring parts of the porphyry algorithm target at Productora and Cortadera are located within the high copper areas delineated by drilling, giving confirmation that

this technique is sufficient in identifying the main mineralized systems. Drilling of these 3D geochemical targets was underway at the time of reporting.

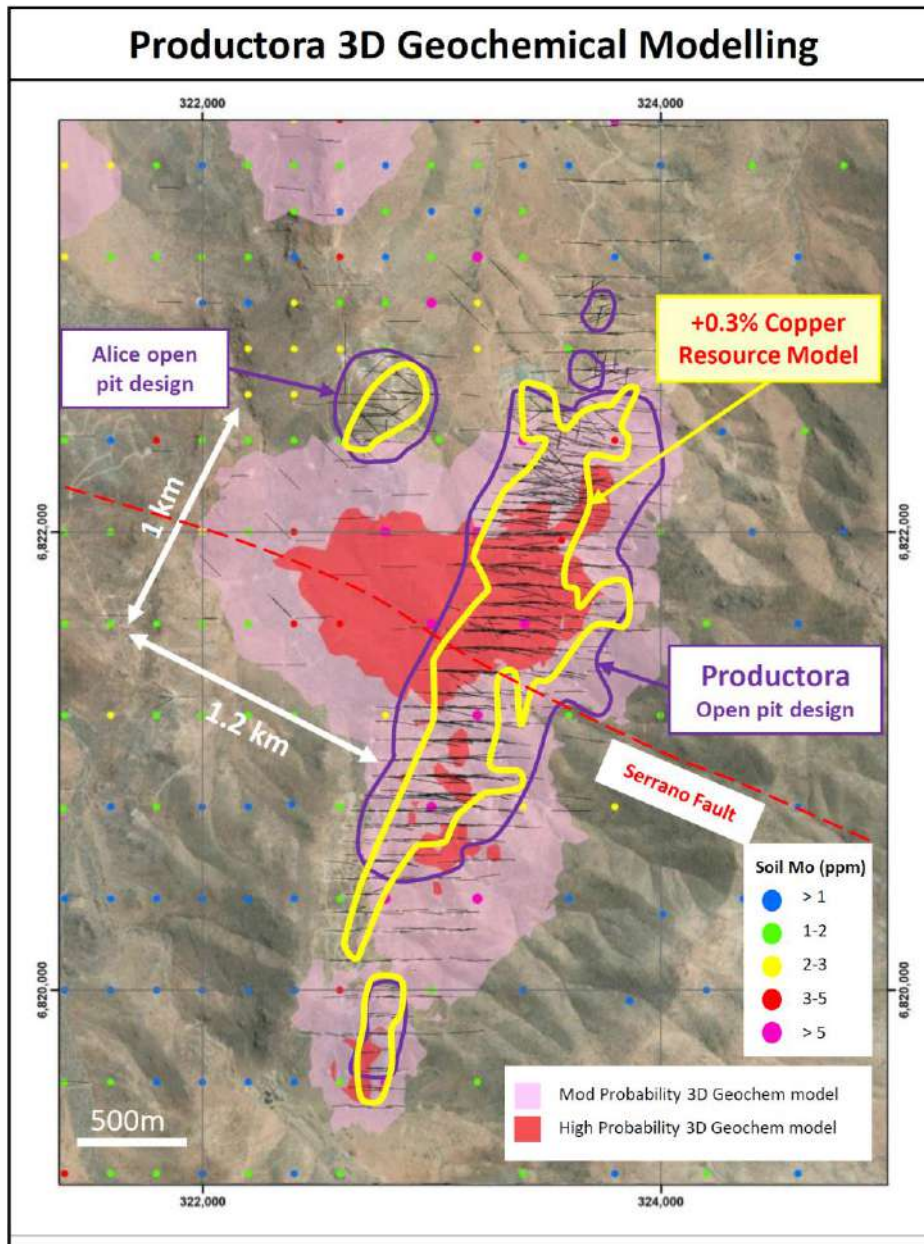


Figure 9.6 Plan view across the Productora central resource area displaying 2021 3D Geochemical Modelling of surface geochemistry. A large very high probability target has been modelled along the northwest-trending Serrano fault and flanking the western margin of the central resource drilling coverage.

9.2 Cortadera

9.2.1 Petrological and Mineragraphic Studies

Exploration work by HCH has included RC and DD, along with petrological and mineragraphic studies on samples. This work was conducted using petrographic analysis, scanning electron microscopy (SEM), back-scattered electron (BSE) imaging and energy dispersive X-ray spectroscopy (EDS).

During October 2019, six drill-core specimens were selected from Cuerpo 3, comprising examples of PD1, PD3, PD4, PT1 and AN lithologies, for sensitive high-resolution ion microprobe (SHRIMP) U-Pb geochronological studies and petrological-mineragraphic analysis. U-Pb SHRIMP dating (Armstrong 2020) established dates on zircons extracted from the six Cuerpo 3 porphyry samples, all of which yielded zircons of exceptional quality, with mainly negligible common Pb, few inclusions and moderate U and Th contents. The well-preserved zircons had not suffered any significant Pb-loss, which combined with evidence from cathodoluminescence (CL) imaging, gave confidence that the $^{206}\text{Pb}^*/^{238}\text{U}$ ages provide reliable magmatic crystallisation age estimates.

The striking similarity in the morphologies, structures and growth histories (from CL) of the zircons from all six samples suggests they have a very similar source and probable age. This is reinforced by the closeness of the ages measured for all samples, although one sample of PT1 (CX006) has a slightly older apparent age. A statistical assessment of the data, both by age and by equivalent $^{206}\text{Pb}^*/^{238}\text{U}$ indicated that the results are identical, with no significant scatter, and yield a weighted mean age of 92.05 ± 0.59 Ma (95% confidence limits, including the error in the standard calibration). Table 9.1 summarises the geochronological samples and results, together with mineragraphic results.

Table 9.1 Results from Geochronological and Mineragraphic Studies at Cortadera

Sample ID	Drill-Hole	Sample Interval	Mineragraphy	Chronology	Age (95%)	Lithology	Lithology Summary
CX0003	CRP0013D	773-774 m	yes - electrum	10	92.6 ± 0.7	PD4	early-mineralization porphyry
CX0002	CRP0019D	587-589 m	yes - electrum	20	92.2 ± 1.0	PD3	early- to intra-mineralization porphyry
CX0005	CRP0019D	571-572.92 m	no	20	91.60 ± 0.7	PD1	early- to intra-mineralization porphyry
CX0004	CRP0019D	348-349 m	no - electrum	30	91.62 ± 0.85	PT1	late-mineralization porphyry
CX0006	CRP0018D	370-372 m	no	30	93.14 ± 0.83	PT1	late-mineralization porphyry
CX0001	CRP0017D	426-426.26 m	no	40	91.3 ± 1.3	AN	Post-mineral andesite

age range: $93.14 \pm 0.83 = 93.97$ to $91.62 - 0.85 = 90.77$
90.8 to 94.0 Ma
FINAL accepted age for all ages, which are not statistically different, is 92.05 ± 0.59 Ma.

Petrological and mineragraphic studies (Muhling 2020) were completed on the six samples selected for geochronological analysis described above. This work was completed to identify metallic minerals containing Au, Ag, Cu and Mo in thin sections and polished sections, with emphasis on grain sizes, textures and compositions, as well as complete partial chemical analyses of these minerals in selected samples (CX002 – PD3 and CX003 – PD4). This work was conducted using petrographic analysis, scanning electron microscopy (SEM), back-scattered electron (BSE) imaging and energy dispersive X-ray spectroscopy (EDS).

Petrographic analysis by Muhling (2020), supported by previous work described in Szakács & Pop (2001) and Tobey (2011a, 2012b), classifies the 10-, 20- and 30-series porphyritic intrusions at Cortadera as ranging in composition from tonalite to quartz diorite, and confirmed the andesitic composition of the 40-series dykes; this recent work by Muhling (2020) is summarised below.

Variably albitised plagioclase phenocrysts within the 10-, 20- and 30-series porphyritic intrusions show sericite, calcite, patchy K-feldspar and minor, localised clinozoisite alteration, while ferromagnesian minerals are completely altered to chlorite, calcite, anhydrite, epidote, rutile, quartz, titanite and pyrite. Red-brown biotite phenocrysts and aggregates are present in some samples (CX003 – PD4), and possibly pseudomorph

mafic phenocrysts, and while the biotites appear largely fresh, they show chlorite, epidote and titanite alteration locally.

The predominantly fine-grained equigranular groundmass of the 10-, 20- and 30-series intrusions comprises quartz (~20%), albite (~30%) and K-feldspar (~10%), with minor sericite, chlorite, anhydrite, calcite, epidote, rutile, pyrite, chalcopyrite, and locally biotite and magnetite (CX003 – PD4), with accessory apatite, zircon, monazite and thorite. Veinlets dominated by quartz, anhydrite, chlorite or calcite cross-cut the host rocks and locally contain pyrite, chalcopyrite and/or molybdenite. Where magnetite is present it is commonly associated with pyrite and chalcopyrite; furthermore, magnetite developed along the margins of quartz veinlets commonly contains inclusions of chalcopyrite and vice versa (CX003 – PD4), while magnetite elsewhere locally contains both pyrite and chalcopyrite inclusions (CX005 – PD1).

Quantitative EDS analyses targeted pyrite, chalcopyrite, molybdenite, pyrrhotite, galena and electrum grains in samples CX002, CX003 and CX004. Most of these metallic mineral phases were determined to have compositions close to ideal end-members, with the exception that some molybdenite grains contained oxygen and some galena grains contained minor selenium. Electrum grains were measured to range in composition from ~75 to 76.5 wt% Au, 20 to 24 wt% Ag, and 1 to 1.5 wt% Fe.

9.2.2 Surface Mapping and Structural Review

Detailed mapping and rock chip sampling studies were completed by Dr John Beeson and other HCH employees along the Cuerpo 1, 2 and 3 trend, as well as immediately north of Cuerpo 3 and at Cortadera Norte, to increase geological understanding and assist in targeting extensions to mineralisation. Mapping was completed at either 1:1000 or 1:2000 scales using the Anaconda method (lithology, structure, alteration) and included compilation of a geological map as well as compilation of a table of mapping points detailing lithology, alteration, structural features, strain intensity and rock chip sampling details.

Surface mapping procedures were developed by HCH's chief technical advisor, Dr Steve Garwin.

9.2.3 Cuerpo 1, Cuerpo 2 and Cuerpo 3 Mapping

Following the work done as outlined above, detailed geological mapping of the Cuerpo 1 to Cuerpo 3 area was conducted at 1:1000 scale focusing upon surface outcrops and exposures along tracks and creeks (Figure 9.6). Elements of at least three regional stratigraphic units were recognised, Punta del Cobre, Nantoco, and Totoralillo Formations, composed of marine calcareous sandstone and andesitic volcanic flows and volcanic breccia, with interbedded limestone. These rocks have been variably overprinted by hydrothermal alteration, forming extensive skarn and hornfels zones around the porphyry systems.

Various dykes of the pre-mineral, mineral, and post-mineral porphyry stages were recognised, including PD, PD1, PD3, PD4, PT1, PT2 and AN, following criteria defined by Tobey (2012b), refer Figure 9.6 for details.

Logging codes for Cortadera are based off those described above. For the purposes of building the mineralisation model, these have been simplified into four different intrusion stages (named 10-series, 20-series, 30-series and 40-series). The comparison between the two nomenclatures is described in Table 9.2 below.

Table 9.2 Comparison between logging codes (as defined by Tobey, 2012) and intrusion series at Cortadera

Logging Code	Intrusion coding for mineralisation model
PD4	10-series (>5% A- + B- quartz veins)
PD, PD1, PD3	20-series (1% to 5% A- + B- quartz veins)
PT1, PT2	30-series (post-mineralisation tonalite dykes)
AN	40-series (post-mineralisation andesite dykes)

Major overall observations from this detailed mapping included the following:

- Geological units recognised in drillholes can also be recognised in surface exposures, allowing for the correlation and projection of geological features between surface and subsurface.
- Surface mapping shows that the early- and intra-mineralisation intrusions (10- and 20-series, respectively) are structurally controlled by N-, WNW-, NW- and NE-striking faults. This structural control is also observed in the distribution of the A-, B- and D-veins. This variation exhibits more than one pattern, and these patterns are either related to structural features with a hard boundary or appear to be more gradual with no definitive relationship to a structural feature with a hard boundary.
- 30-series intrusions are quartz-bearing porphyritic tonalite, locally hosting igneous-hydrothermal breccia with silica-pyrite ± tourmaline alteration, that vary in trend between N, NE, WNW and NE. These late intrusions are commonly associated with red to orange colour anomalies due to supergene weathering (jarositic±hematitic±goethitic) of sulfide-bearing clay-mica alteration (e.g., argillic- and phyllic-alteration).
- Minor copper oxides exposed at surface typically comprise chrysocolla, copper wad intergrown with goethite and clay, with minor native copper, atacamite and brochantite, and are mainly present at Cuerpo 2 and 3. In general, this oxide zone is associated with 20-series porphyry intrusions showing chlorite-sericite and/or relict biotite alteration.

Cuerpo 1: Four main intrusive units are mappable at Cuerpo 1 which all fall into either 10-series or 20-series, based upon early quartz-vein content, sulphide mineralogy and hydrothermal alteration, together with petrographic observations. Quartz veining observed in outcrop is stockwork style with a dominance of NE, NNW and WNW trends, and post-mineral NW to NE trending normal faults, commonly dipping - 60 to 80 E, are also mappable. Drilling at Cuerpo 1 intersected several porphyry phases together with sparse A-B veining, consistent with strong local variations in vein density observed in outcrop. To the northeast, at Cuerpo 4, a domain of strong to intense vein density with a NW trend

was mapped (i.e., sub- parallel to the Cortadera valley). 30-series dykes observed at Cuerpo 1 and Cuerpo 4 are pyritic, lack quartz veining and show an intense supergene argillic alteration overprint.

Cuerpo 2: Two dominant mineralised porphyry phases are distinguishable in outcrop at Cuerpo 2 (which could both be considered 20-series) based upon mineralogical and textural characteristics, as well as variations in early quartz vein content. WNW-trending quartz veins are predominant, although NE-trending quartz veins are also present. 30-series dykes with a general NNE trend, and 40-series with NNW trend, cross-cut mineralisation. Copper oxide bearing zones exposed at surface are dominated by chrysocolla, copper wad, with minor atacamite and brochantite, and are interpreted to be related to the lixiviation of copper from A-B vein stockworks in the proximal 10-series intrusion.

Cuerpo 3: Six intrusive phases are mappable at Cuerpo 3, which cover the entire range from early 10-series to late 40-series. Observations are based upon variations in early quartz vein abundance, sulphide mineralogy, hydrothermal alteration, as well as textural and mineralogical characteristics. Quartz veining is of stockwork style, with quartz veins predominantly oriented NNW and NE, although some quartz veins trend WNW. Surface mapping revealed a high density of A-B veins in 10-series exposures. Copper mineralised porphyries exposed at surface show intense supergene argillic alteration overprinting sericitic alteration. Late 30- and 40-series dykes observed in outcrop are pyritic, lack quartz veining and are commonly barren. 30-series dykes typically trend NNE and are locally associated with sericitic hydrothermal breccia. 40-series dykes mapped at surface typically trend NNE. These track towards a Cu soil anomaly (> 1000 ppm) associated with a discrete magnetic high located immediately south of Cuerpo 3 and extend north into the Cuerpo 3 Norte area where copper oxides are exposed in surficial workings.

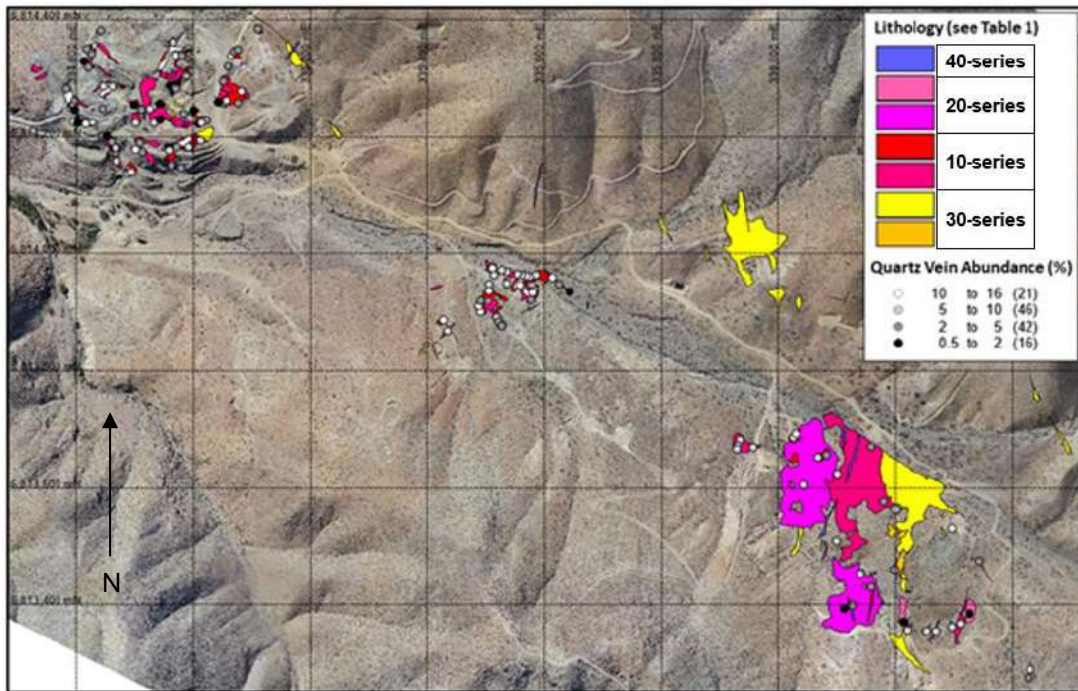


Figure 9.6 Geological map of Cuerpo 1 to Cuerpo 3 from Tapia (2019) showing major intrusions (refer to legend for details) and quartz-vein abundance as a percentage Hot Chili-only mapping (HCH, 2021).

9.2.4 Cuerpo 3 Norte Mapping

Reconnaissance geological mapping of Cuerpo 3 Norte (Beeson, 2019) targeted a geophysical anomaly semi-coincident with the N-S dyke corridor trending immediately north of Cuerpo 3 (Figure 9.7). Mapping showed that the Cuerpo 3 Norte area is dominated by chlorite skarn with variable intensity epidote-garnet alteration, as well as silica-sericite-chlorite hornfels, with overlying limestone exposed to the west. Several porphyritic tonalitic to granodioritic dykes can be traced northwards into the mapped area and some of these host sugary and porphyry-style quartz-rich veining (vein% shown as magenta text) which is locally associated with copper oxides; post-mineral andesitic dykes also intrude the host sequence. A hectometre-scale intrusive tonalitic stock in the SW corner of the Cuerpo 3 Norte area hosts mineralised porphyritic intrusive rocks that contain significant quartz veining. This exposure may represent part of the Cuerpo 3 mineralisation exposed at surface, or a separate mineralised stock located immediately north of Cuerpo 3. Both the narrow dykes and broader domains of 10 and 20 series intrusive rocks host quartz vein arrays at up to 7% vein abundance.

Geological mapping thus indicates that the Cuerpo 3 mineralisation remains open to the north of the current drilling coverage at Cuerpo 3, as is also suggested by inversion modelling of IP and MT data related to two MIMDAS (a multichannel data acquisition system) lines located in the Cuerpo 3 Norte area, supporting this as a high priority target area. The inversion modelling involved producing a resistivity model by inversion of MT data, which was used as a reference for the inversion of the DC resistivity data using UBC software. Using the MT inversion allowed for better definition of the resistivity variation at depth. University of British Columbia (UBC) software was also used to produce the chargeability model. The red in the chargeability images shown in Figure 9.8 is >40 ms. As can be seen on Figure 9.8, there are some significant coincident MT

conductivity and IP chargeability anomalies at depth that may not have been obvious in conventional IP. These anomalies are located along the N-S-oriented dyke corridor that passes through Cuerpo 3 and underlie surficial exposures where quartz vein abundances of >3% and copper oxides have been identified during outcrop mapping.

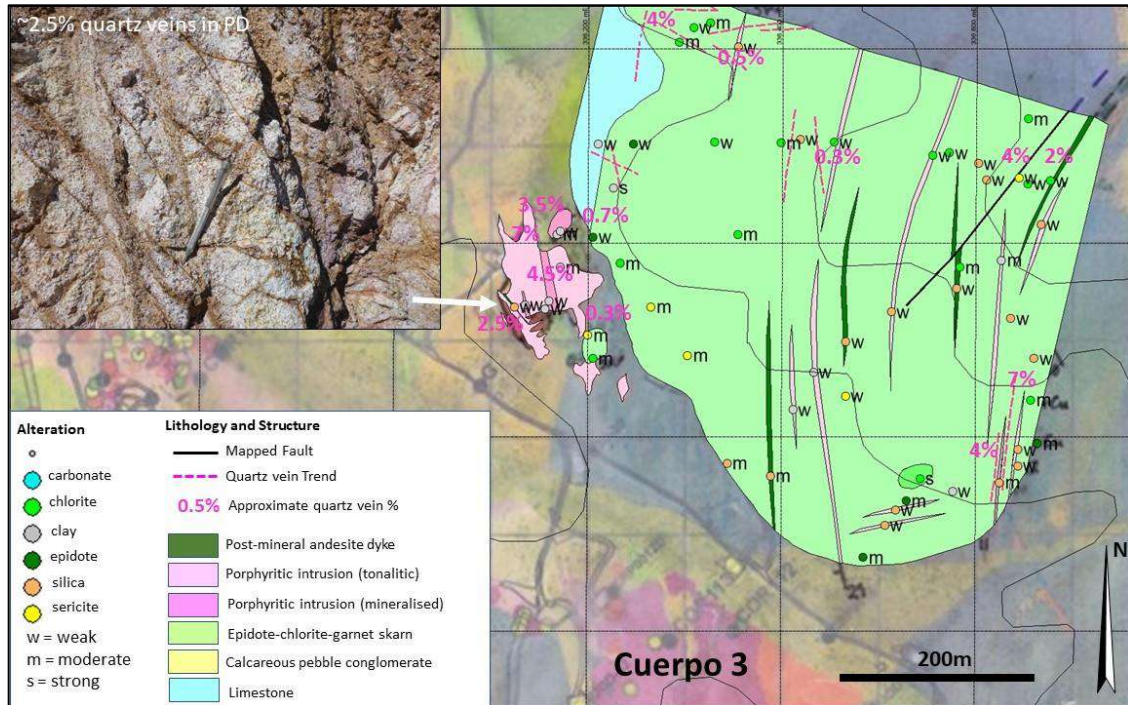


Figure 9.7 Geological interpretation of Cuerpo 3 Norte as mapped by Beeson (2019)

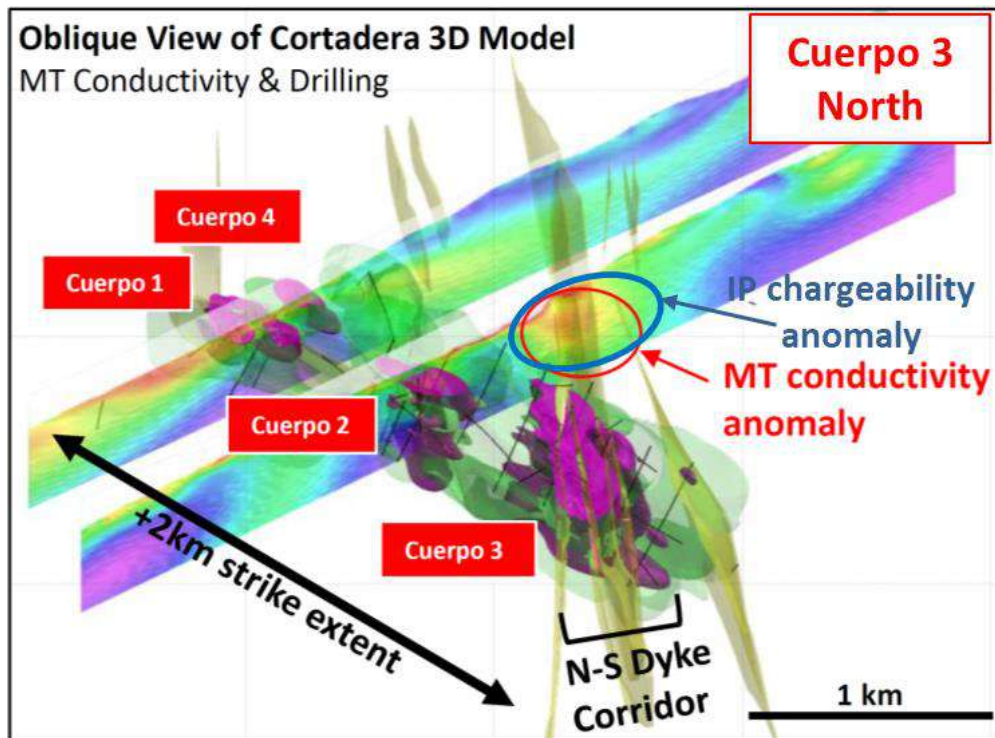


Figure 9.8 Oblique view of the Cortadera lithology showing the IP chargeability and MT conductivity anomalies located at Cuerpo 3 Norte as modelled by Garwin (2020a)

Geological mapping of the Cortadera Norte target area (Beeson 2019) targeted a coincident geophysical and geochemical anomaly, identifying a steeply-incised limestone sequence showing weak to moderate epidote-chlorite-garnet skarn alteration in exposures along creek beds, grading upwards into weakly marbelised limestone towards hill tops. A calcareous sequence of polymictic pebble conglomerate occurs within the limestones and also shows skarn alteration locally. In the northeast corner of the mapped area a tonalitic stock, similar to late porphyritic tonalite (PT1) observed at Cortadera, forms a cupola that penetrates the calcareous sequences. Several north-south, east-west, northwest and northeast trending faults and lineaments were mapped or interpreted across the target area, and many of these structures host variably-mineralised porphyritic tonalitic dykes, pebble dykes and post-mineral andesitic dykes. Arrays of quartz-rich veins that vary in texture from sugary to massive (A veins) and laminated (B veins) are present locally within mineralised porphyry dykes, with some of these occurrences associated with nearby supergene copper mineralisation. Where quartz-rich veins were mapped vein % was estimated and varies up to 8%. Late-stage carbonate veins are more common across the target area but do not appear to be mineralised.

A preliminary geological interpretation based upon the traverse mapping is included as Figure 9.9. The Cortadera Norte target area is outlined by the red dashed line, based upon results from soil geochemical sampling integrated with electrical geophysics data (Figure 9.10). Overlain are dots showing dominant alteration mineral with intensity indicated (w = weak; m = moderate). The vein% of quartz-rich veins is shown at each mapping location in magenta text. A domain outlined by the green dashed line on Figure 9.9 represents the strongest domain of skarn alteration exposed in the valley that dissects the target area.

Chlorite alteration and smaller domains of sericite-silica alteration form a halo around the skarn. This pattern is compelling, but the domain outlined could at least partially represent a topographic effect and thus may be more extensive than is apparent from mapping. The mapping supports the Cortadera Norte geochemical-geophysical anomaly (Figure 9.10) as a high-priority target.

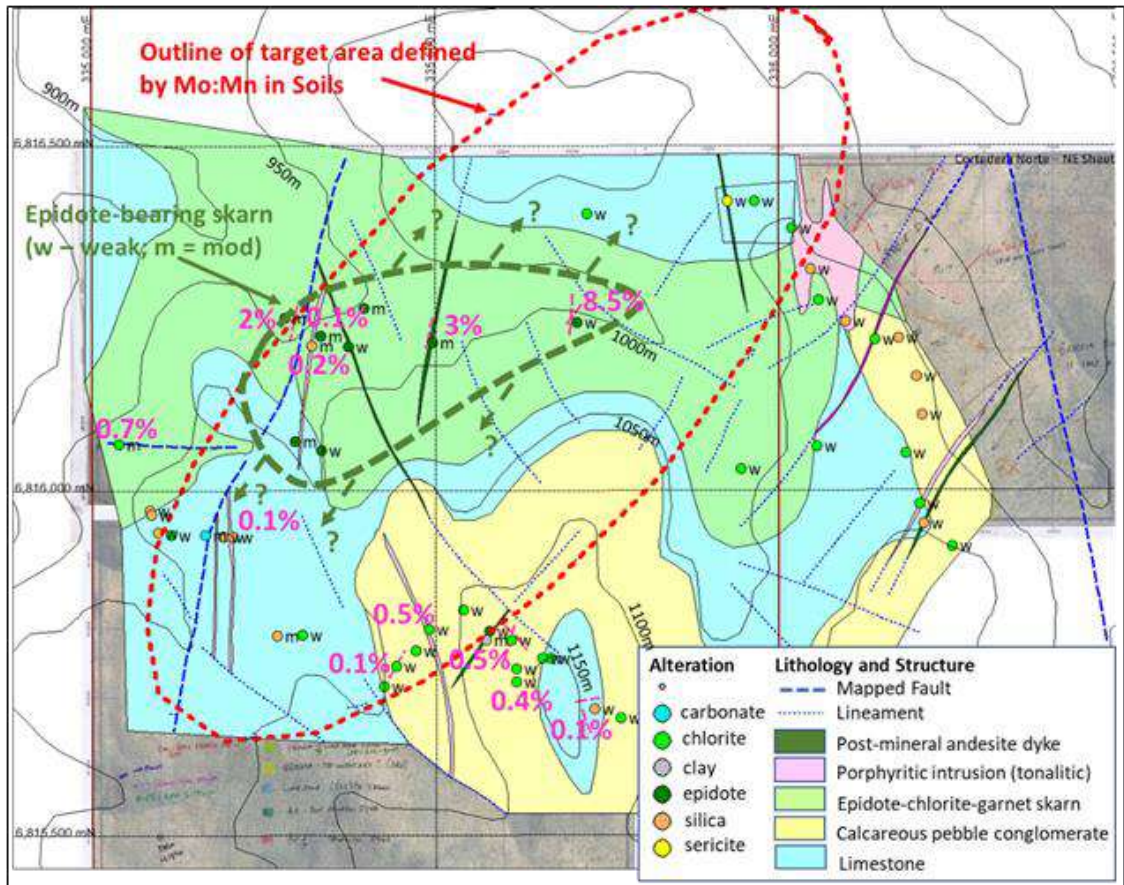


Figure 9.9 Geological map of Cortadera Norte interpreted by Beeson (2019)

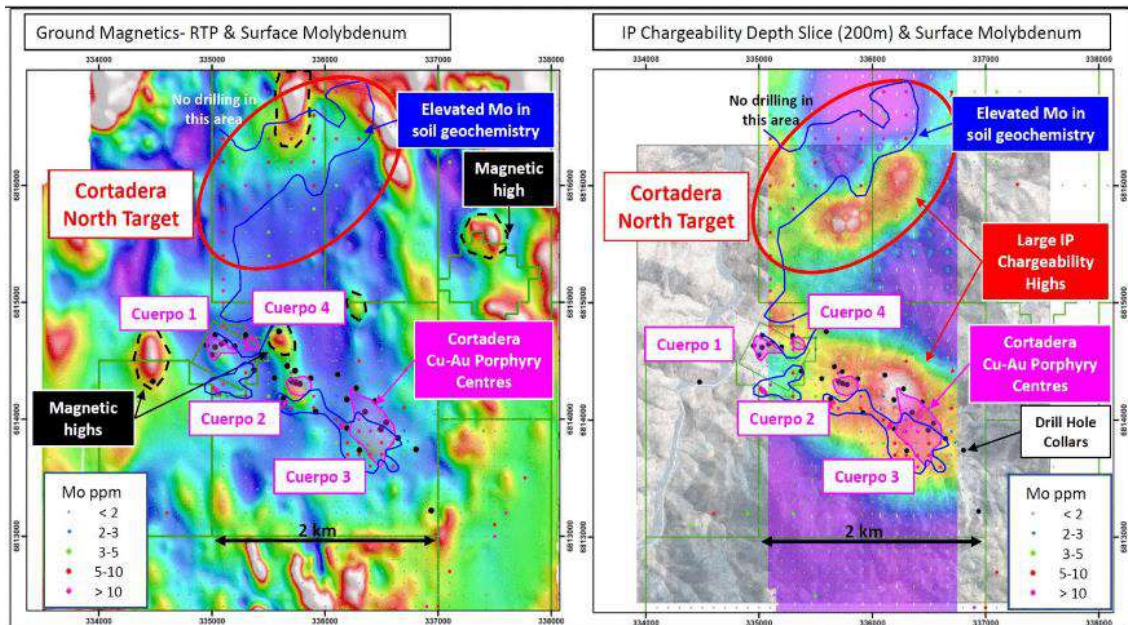


Figure 9.10 Left: Reduced-to-pole (RTP) image of ground magnetic data showing a broad magnetic low (magnetite destruction) with a cusped magnetic high to the north associated with elevated Mo in soil samples. Right: IP chargeability image covering the Cortadera to Cortadera Norte area showing the IP chargeability anomaly closely associated with Cu-Au-Mo mineralisation at Cortadera as well as a similar, NE-SW trending IP chargeability anomaly slightly offset from the Mo-in-soil anomaly at Cortadera Norte. Note that the Mo-in-soil anomaly at Cortadera is also laterally displaced from the IP chargeability anomaly (HCH, 2021)

9.2.5 Surveying

Cortadera topographical data was supplied by Minera Fuego upon exercise of the purchase option agreement for the project. Topographical surveys were undertaken by contract survey company Geodesia Topografía Exploraciones in 2011 and 2012 with the following methodology utilised for the survey.

Base Station “SIRGAS VALLENAR at HM Cortadera 1 to 40” was selected as the control point and the survey was undertaken within a polygon area, followed by:

- Measurement with Dual Frequency GPS Ashtech Brand Model Z-Xtreme and Allegro CX Electronic Notebook
- HM Cortadera Base Station 1 to 40 Z-Xtreme GPS Equipment
- Rover or Mobile Equipment, Z-Xtreme with Allegro System Notebook (RTK) Real Time Kinematic

The topographical data points were then used to create a digital elevation model (DEM). The software used to create the DEM is unknown.

9.3 San Antonio

9.3.1 Introduction

The San Antonio deposit has been privately owned and mined for more than 50 years. Exploration work that has been conducted by HCH includes prospecting, geological mapping, geochemistry, and reverse circulation testing of interpreted geological targets.

9.3.2 Geological Mapping

Geological mapping was conducted by HCH geologists and contracted geologists to HCH in February and May 2018.

The February campaign covered the San Antonio area and was conducted using 1:2500 scale orthorectified satellite imagery. A focused program of 1:500 scale geological mapping was also conducted on selected areas of the San Antonio Copper Mine.

The aim of this work was to:

- Construct detailed lithological maps of the areas (Figure 9.11, Figure 9.12)
- Improve understanding of the mineralisation controls
- Develop inputs to exploration target ranking for the area.

The program also delivered a database of photography, geological observations, rock chip and soil samples. Samples were assessed for infield XRF, magnetic susceptibility and scintillometer results, and geochemically assessed under the HCH sample protocol.

The May 2018 campaign built upon the findings of the previous campaign and included a greater focus on the area south of the San Antonio copper Mine, including prospecting and inspection of five exploration targets.

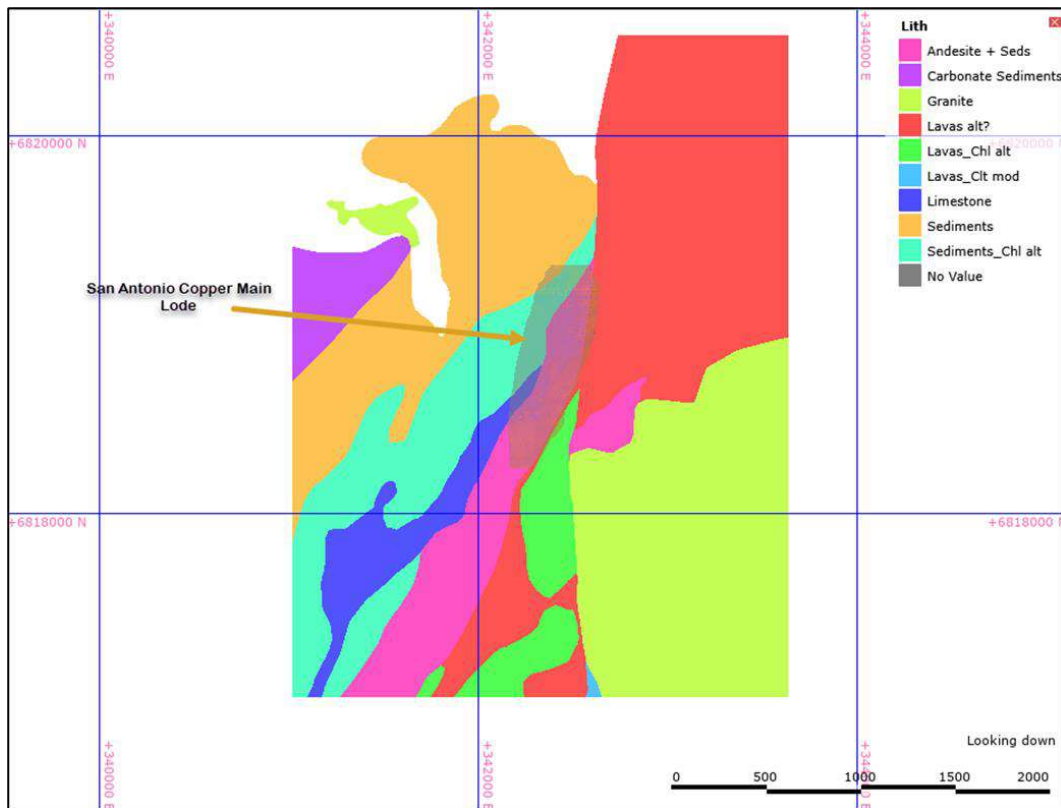


Figure 9.11 San Antonio Geology Map from Satellite Imagery

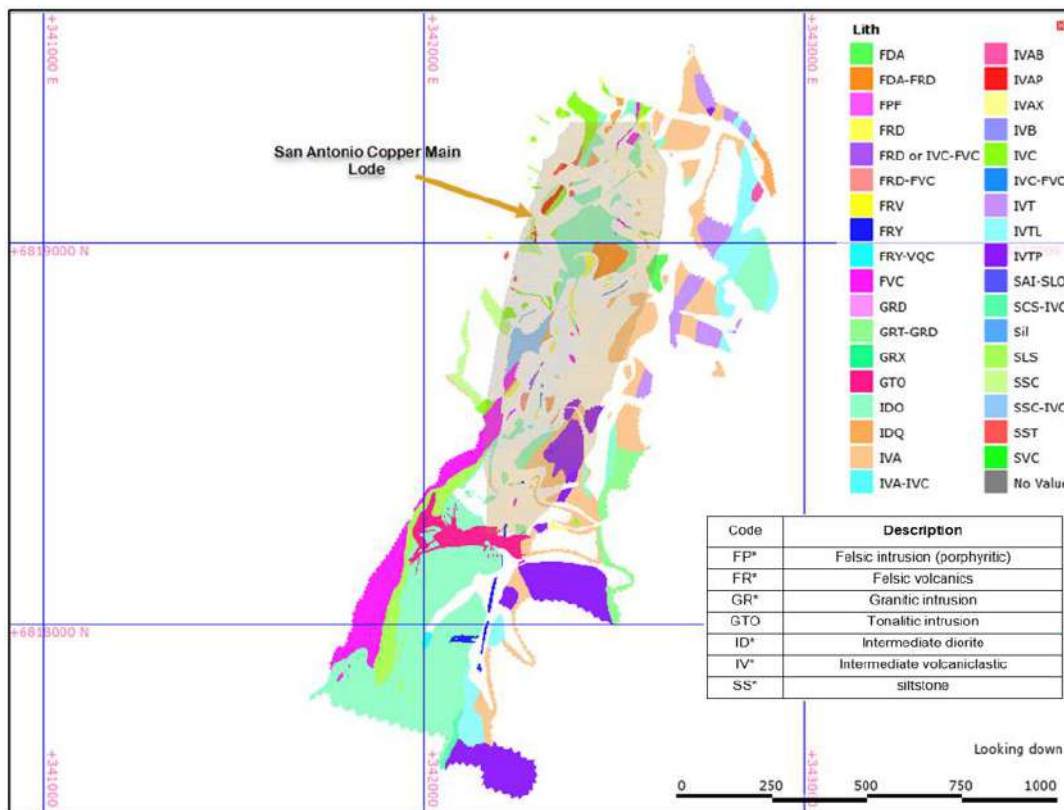


Figure 9.12 Lithology fact mapping of San Antonio (Feb. 2018)

9.3.3 Surface Geochemistry

HCH has undertaken surface rock chip and soil sampling Figure 9.13. Samples were taken by geologists from existing workings, or from surface outcrop. These samples were crushed and split at the laboratory, with ~1kg pulverised, with ~150g used for ICP-AES assay determination (for multi-elements including Cu). A 50g charge taken for fire assay fusion (for gold).

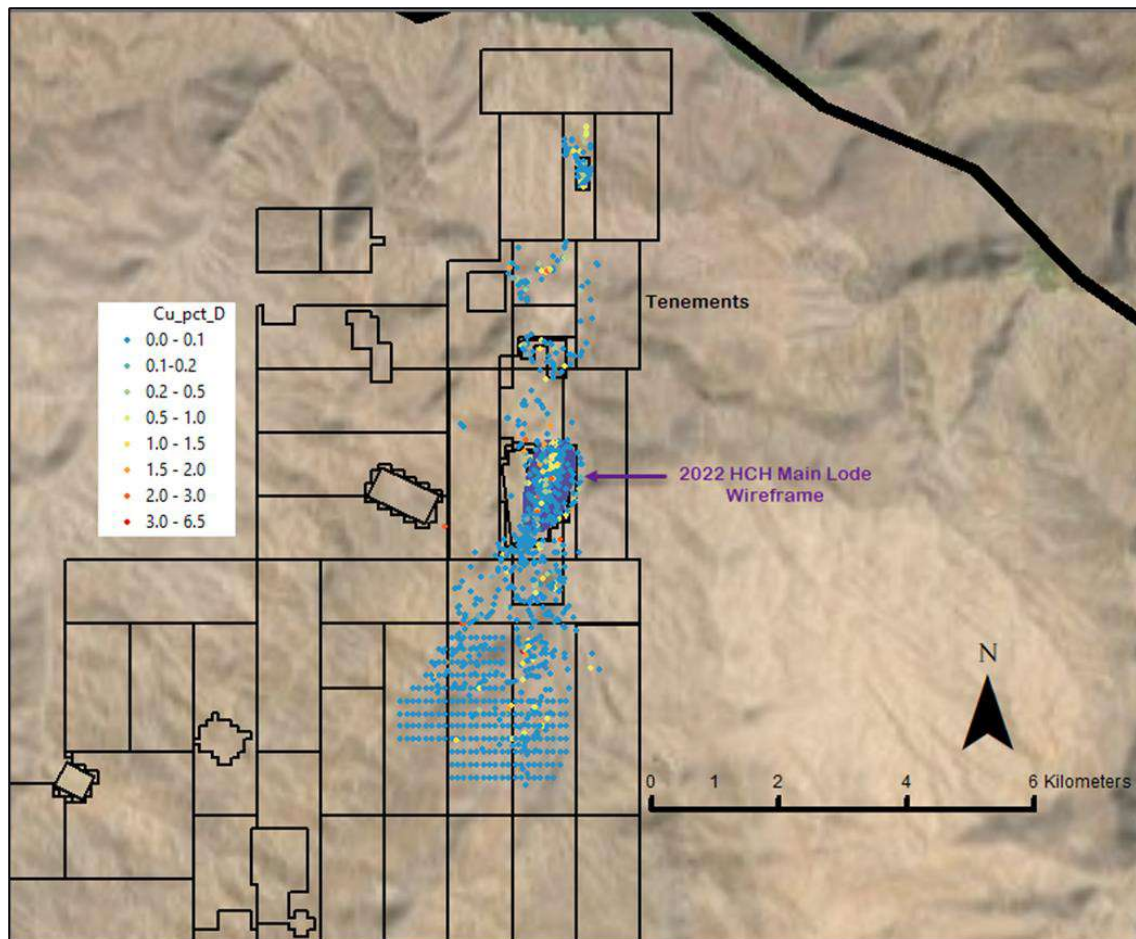


Figure 9.13 Surface Geochemistry Sampling over San Antonio

9.3.4 Surveying

It is currently unclear how the topographic surface for San Antonio has been created. It is inferred that a digital terrain model (DTM) was created from elevation contours from historic maps and verified with collar surveys.

Where a discrepancy exists the collar surveys are taken as priority. The topography model was also verified with a drone survey and found to be suitable for mineral resource estimation Figure 9.14.

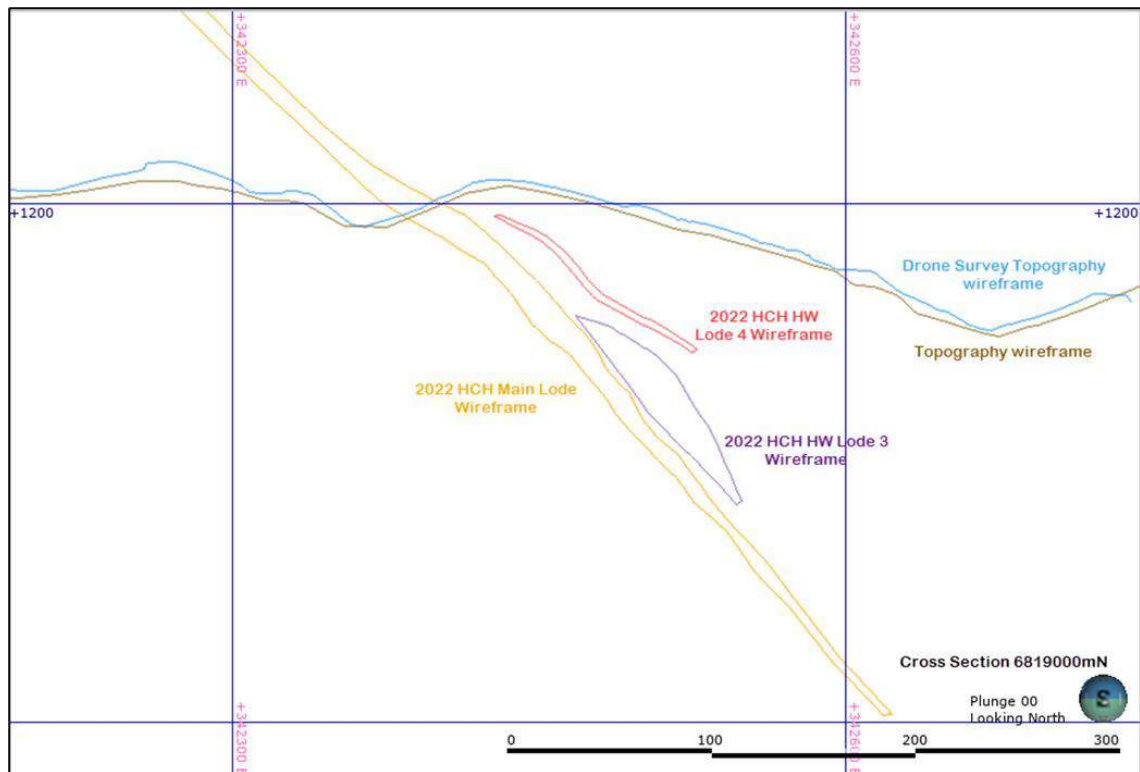


Figure 9.14 Cross section 6819000mN showing the topography model used in estimation with the drone survey derived topography model.

A handheld GPS is used for mapping and surface geochemistry sampling.

In 2021 HCH commissioned a drone laser scanning survey of accessible mine areas. The survey was conducted by Aerodyne Chile. The project included:

- 6 scans covering drill hole collars, to be used for post-processing georeferencing
- 8 scans on the terrain
- 23 scans on the underground environment

The processing method was:

1. Point Cloud Registration to achieve accurate relative position accuracy between the scans data in Trimble Realworks
2. Point Cloud Georeference to achieve accurate absolute position accuracy between the scans data in Trimble Realworks
3. Point Cloud Segmentation into smaller sector in Trimble Realworks for resource efficient deliverable output creation.
4. Small Segmented Sector scans data export into georeferenced .las format.
5. Exported .las scan data is converted into Mesh in Leica Cyclone 3DR
6. Scan data Points Cloud is resampled and reduced in Leica Cyclone 3DR
7. Points Cloud is converted into Mesh in Leica Cyclone 3DR
8. Mesh is exported into georeferenced .dxf format drawing file

9. DXF drawing files are grouped into their own drawing cluster in Trimble Business Center
10. Colours are assigned to different drawing cluster in Trimble Business Center
11. The drawing cluster is exported into 2018 .dxf format in Trimble Business Center.

HCH received DXF outputs of the drone survey and used these to update the mined void (depletion) model for San Antonio, as well as to contribute to the data set for geological interpretation as a proxy for mineralisation location.

10 DRILLING

10.1 Productora

10.1.1 Introduction

Drilling completed at Productora used a nominal drill pattern of 80m spaced east-west sections, with drilling approximately 40m apart along section. This allowed optimal drill orientation for intersection of the north-northeast trending mineralisation. The majority of drilling plunged -60 to -80° toward 090° azimuth, but there were numerous scissor drillholes oriented at -60 to -80° degrees towards an azimuth of 270° to ensure geological representivity and to also preferentially target east dipping mineralisation. Drilling in or out of sections (“off section”) was required on an ad-hoc basis due to limitations on drill platform availability or were designed to preferentially test specific structural orientations.

The nominal spaced drill pattern is consistent to a depth of approximately 300m vertical from surface.

The Alice drilling also used a similar pattern, but due to limited pad availability had an increased number of “off section” drilling.

10.1.2 Drilling Methods

The majority of drilling commissioned by HCH for the Productora and Alice Resource estimates was conducted by Blue Spec Sondajes (Bluespec). All drill rigs are EDM type and configuration is as follows:

Exploration Drill Masters (EDM) custom built EDM2000 and 1200 High Capacity Multi-purpose RC and diamond drill rigs. The rigs were supported by an Atlas Copco Hurricane B4-41/750 Booster, and a Sullair Air Compressor Model 1150/900.

The drilling rigs were manned by Australian drillers and well-trained local drilling offsideers. All custom-built drill rigs used during the program were convertible to either reverse circulation or diamond core drilling.

The drilling was undertaken on pads established that provided adequate space for drilling and sampling equipment. Booster pressure during RC drilling was high (700-800 psi) which allowed fair sample return and penetration rates. As a standard, on-drill sampling equipment consisted of a cyclone unit for pressure release and sample collection, and a static cone splitter to sub-sample the collected sample. The cyclone and cone splitter’s vertical position was monitored using a spirit level for multi-level checks to minimise any potential sample bias. Drillholes were routinely downhole surveyed during the drilling, or else shortly after drilling completion.

RC drilling utilised a face sampling downhole hammer with cyclone sample recovery. Drill hammers used were 542/543, PR 54 (Sandvik) and MR 120 (Mincon).

Adjustments to drill bit size were made as drillholes reached certain intervals so to ensure successful end of hole depth. Changes to bit sizes were recorded in drill logs. The general practice for bit size changes followed by Bluespec at Productora was to collar the hole with a 140mm bit, and step down progressively to the smallest size of 130mm (generally any drilling beyond 450m in depth).

Diamond drilling was conducted using HQ diameter core (96mm outside diameter and 63.5mm inside diameter). Orientation of diamond core was controlled by the Reflex ACT III core orientation tool.

Downhole surveys were completed in rod and at end of hole.

10.1.3 Drilling execution and data flow

All holes drilled at Productora were prefixed with 'PRP' for RC holes, 'PRD' for diamond holes cored from surface or diamond tails. Holes suffixed with 'A' denote abandoned holes, and 'PRP' holes with a 'D' suffix denote an RC pre-collar with a diamond tail.

An internally managed and audited acQuire geological database was used to capture and manage geological drill data. A detailed internal review of data management was undertaken in 2014 and was deemed satisfactory.

Strict data flow procedures were followed during drilling. This ensured that all drill data was collected in a systematic, repeatable, and accurate manner allowing consistent and validated data for resource estimation. The steps taken in drilling data capture completed by HCH are summarised in Figure 10.1.

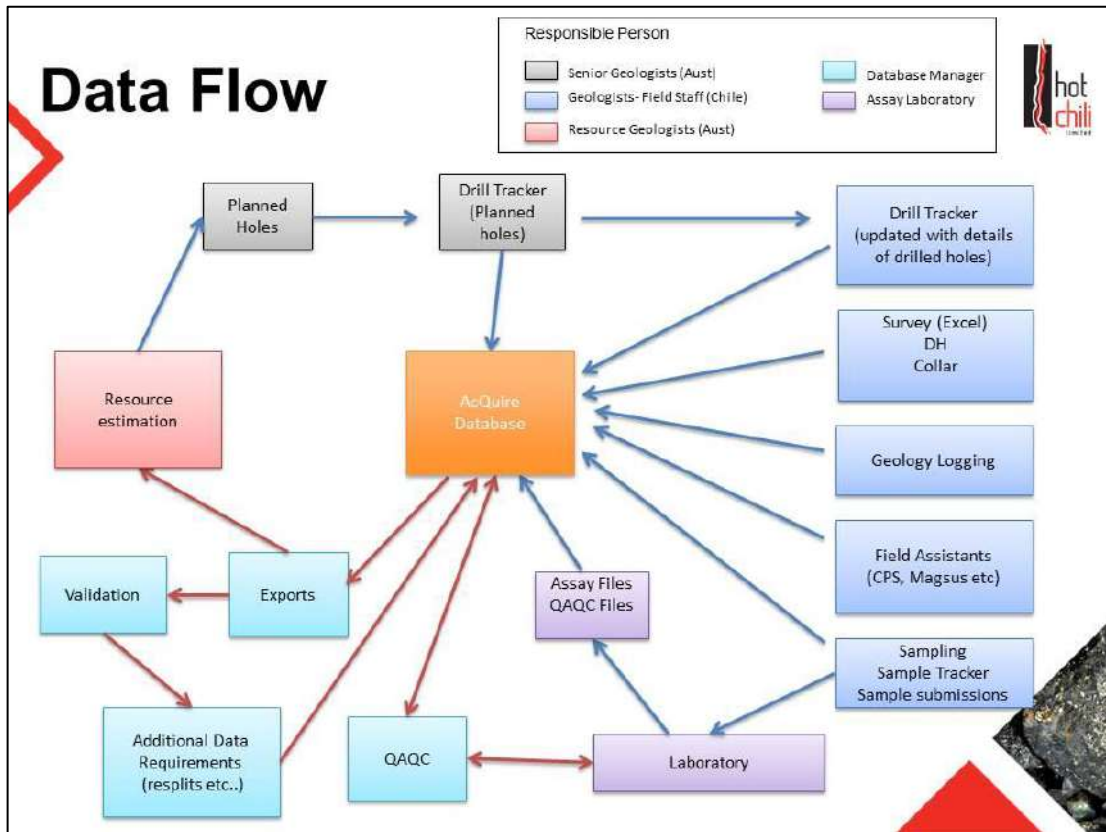


Figure 10.1 Drill Data flow showing drill planning, drill execution, logging, sampling and data entry and capture

10.1.4 Hole Planning and Set-up

10.1.4.1 Collar Surveying

Drill collars were routinely surveyed on a fortnightly basis by contract surveying company Geotopo Exploraciones Limited. Topographical equipment used was a Topcon HiPer GPS, dual frequency, Real Time with 0.1cm accuracy (mN, mE and mRL). Topographical collar surveys were supplied in WGS84 Zone 19S coordinate system.

10.1.4.2 Downhole Surveying

The downhole surveying at Productora has been completed by contracting companies Wellfield and North Tracer. Wellfield undertook downhole surveys from the beginning of HCH drilling until May 2013. North Tracer undertook downhole surveys from May 2013 onwards. There was some overlap of surveying companies during the transition period.

Wellfield downhole surveyors used a mechanical Gyroscope instrument (non-north-seeking). Gyroscopic surveys provide accurate directional data (azimuth and dip) relative to an initial starting orientation at any interval. The instrument's accuracy is not affected by magnetic interference and can be used inside all types of drill rods or in magnetic rock types.

Because the gyroscope instrument measures relative shifts in orientation, the survey operator was provided with an accurate dip and azimuth of the drillhole collar prior to surveying. This dip and azimuth were provided to the Wellfield survey operator by the supervising geologist. The gyroscope tool-face was referenced to this known drill azimuth orientation.

10.1.4.3 North Tracer

North Tracer used a north-seeking, high speed continuous gyroscopic camera which is unaffected by magnetic interference. Unlike other continuous gyroscope systems, the GyroTracer Directional does not require any surface alignment or surface calibration prior to survey.

10.1.5 Validation

HCH has employed a variety of QA/QC measures to assess and ensure the quality of the drill data used for resource estimation.

The methods and results (by exception) from these QA/QC measures are detailed in the following sections.

10.1.6 Collar Validation

Validation of collar survey locations was completed by:

- Comparing planned coordinates with subsequent picked up coordinates to detect any material differences in location
- Visual checking of collar points against the topographical surface model
- Random GPS field checks of collar coordinates by HCH employees
- Random GPS field check of collar coordinates by independent auditors during documented site visits.

10.1.7 Downhole Survey Validation

Down-hole survey validation checks were completed by subsequent umpire survey checks as well as within-company resurveys (e.g., Figure 10.2). Results from resurveys and cross-company checks provided a good correlation between the two companies as well as within-company resurveys and provides confidence in the survey data for the drillholes used for resource estimation.

Routine 3D review of the drilling database was also performed as part of drillhole survey validation, to detect any spurious survey measurements.

During the 2014 programme, one hole (PRP0867) had an unexpected drilling deviation “lift”. Check surveys were immediately requested and run to check for survey error. In addition, the drilling company (Bluespec) also undertook several downhole dip measurements with their own equipment. These supported the North Tracer survey results. The mineralisation intercept location was in line with previous modelling predictions. The deviation in this hole was attributed to in-ground structure.

Overall, the surveys at Productora continued to show that RC drilling dip (usually) dropped slightly at depth but that there was limited azimuth deviation. Drillhole deviations and corresponding down-hole sample locations are adequately measured; deviations are not considered to have any adverse impact on this resource estimate.

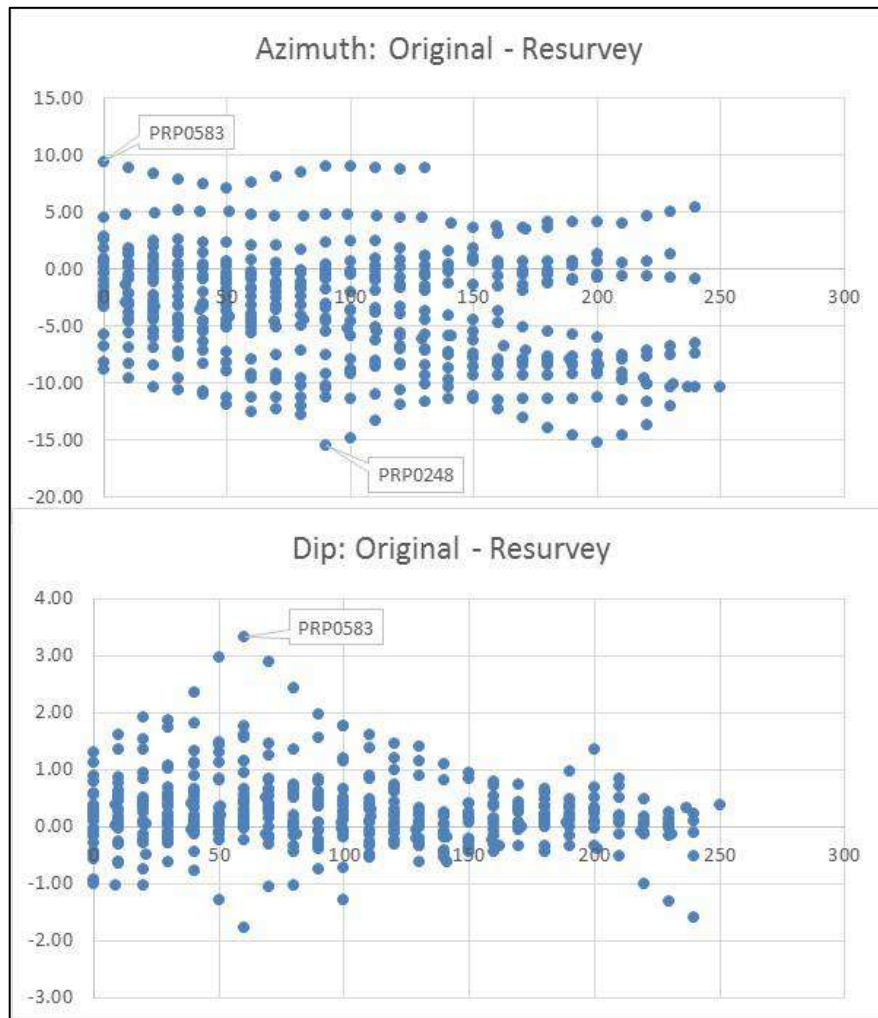


Figure 10.2 Plot showing the downhole difference between the original downhole survey and its resurvey (image from 2014 resource report). Overall the minor differences were deemed to have negligible impact on the resource model.

10.1.8 Drilling Orientation

The Productora drilling nominally used drill collar pattern as typically 80m spaced east-west sections to allow optimal drill orientation to intersect the mineralisation. Drilling was nominally spaced at 40m apart along sections. Drilling was predominantly oriented at -60 to -80° toward 090° azimuth, but numerous scissor drillholes were oriented at -60 to -80° degrees towards an azimuth of 270° to ensure geological representivity and to also target east dipping mineralisation preferentially. This ensured perpendicular intersection of the predominantly steeply west dipping mineralized material lodes and flatter east dipping mineralized material lodes at Productora. Drilling off section was required on an ad hoc basis due to limitations on drill position availability or to preferentially test specific structural orientations.

The Alice drilling also used a similar pattern but, due to limited pad availability, had an increased number of “off section” drilling. This resulted in a nominal 80m by 50m grid spacing. The style of mineralisation at Alice, being a vertical porphyry deposit, means it is challenging to ensure perpendicular intersection of the mineralisation for every drillhole, but every attempt was made by HCH.

The nominal spaced drill patterns are consistent to a depth of approximately 300m vertical from surface.

10.1.9 Geological Logging

Geological logging was recorded in a systematic and consistent manner such that the data was able to be interrogated accurately using modern mapping and geological modelling software programs. Field logging templates were used to record details related to each drillhole. All geological logging was completed by qualified and experienced company geologists. Collar, survey, sample register and sample condition, sample recovery data or comments (and commonly magnetic susceptibility) were recorded by a competent field technician.

All reverse circulation (RC) holes were logged using the standard company logging codes, and washed chip samples were stored in chip trays retained at the company’s operational storage facility in Vallenar. All diamond drill core was subjected to detailed lithological and structural logging.

Geological attributes logged in RC chips includes colour, weathering/oxidation, regolith, lithology, veining, alteration assemblages and their intensities, texture, mineralogy and sulphides and their percentages.

Core reconstruction and orientation was attempted in every drilling run and completed where possible before marking up or logging core.

Geological attributes logged in diamond core includes the same attributes as RC drilling, and additionally the following structural attributes:

- Linear structures (e.g., lineations)
- Planar structures (e.g., shears, veins, dykes, faults, cleavage, joints/fractures, schistosity)
- Preliminary geotechnical features such as RQD and FPM.

All diamond drill core was captured with digital photography, and all core photos are retained on HCH servers.

10.1.10 Bulk Density

A total of 2,164 bulk densities were available for the Productora Resource estimate, and 74 for the Alice deposit.

One in every five samples of diamond drill core was submitted for bulk density analysis as performed by ALS (ALS Code OA-GRA09). Every sample that ends in a “5” or a “0” is labelled with the words “Density test”.

The test work was undertaken on an approximate 10 cm piece of core taken from the designated sample bag and is used to determine the bulk density for the 1 m interval. The bulk density test consists of using the Archimedean water submersion method of analysis; a description of the ALS technique is outlined below.

- Bulk density analysis on solid objects is carried out by weighing the object, then slowly placing it into a bulk density apparatus which is filled with water. The displaced water is collected into a graduated cylinder and measured. The bulk density calculation considers the weight of the sample and the volume of water displaced; the result is expressed as g/cm³.
- Once the bulk density measurement is complete, the 10 cm length of core is returned to the sample bag ensuring the 1 m interval is complete and intact prior to analysis for ME-ICP61.

These were performed as pycnometer tests by ALS (ALS Code OA-GRA08b). A description of the ALS technique is outlined below.

- Specific gravity (SG) analysis on pulps was carried out by placing 3 g of pulp into a pycnometer, which is then filled with a solvent.
- The SG calculation was made comparing the weight of the sample and the weight of the displaced solvent.

10.1.11 Bulk Density Method Comparison for Productora

In practice, there is an expectation that the pycnometer method will return elevated density results due to the fact it is measuring mineral density without accounting for natural rock porosity. The pulverisation process essentially removes that porosity. The expected “error” in the pycnometer results is proportional to the porosity.

For the 2014 Resource estimate, a full review of the available core and pulp data was performed. This involved a comparison of core and pulp density values, as well as comparisons by spatial parameters and between mineralisation and weathering domains.

The following are highlighted observations from the review of the density data:

- Broadly, the density decreases with increased mineralisation across the deposit (e.g., the 0.3% Cu mineralised domain is globally less dense than the 0.2% Cu mineralised domain and so forth)
- There is an apparent correlation between sample density and iron content
- The southern mineralised “manto” lodes are significantly denser than the majority of Productora mineralisation due to elevated iron content
- The background host formations’ density appears uniform (Figure 10.3)
- The spatial spread of density data across Productora allows for estimation to be undertaken rather than an application of default density values (e.g., Figure 10.4 to Figure 10.6)

- The northern areas of Productora have the least density data, but also a wider spread of values. The spread of values is largely defined by changing iron content in mineralisation.

The correlation between core density (bulk) density and the pulp (pycnometer) density for the major mineralisation domains was not a fixed factor/discount but changed with increasing density. The population differences were best determined via core bulk density versus pulp pycnometer density QQ plots (Figure 10.6 left image). This enabled the fitting an experimental (approximated) correlation slopes appropriate at key ranges from zero density to the maximum density values (Figure 10.6 right image). These formulas were then applied to the pulp density values and then validated back against the original QQ plots (Figure 10.6 and

Table 10.1).

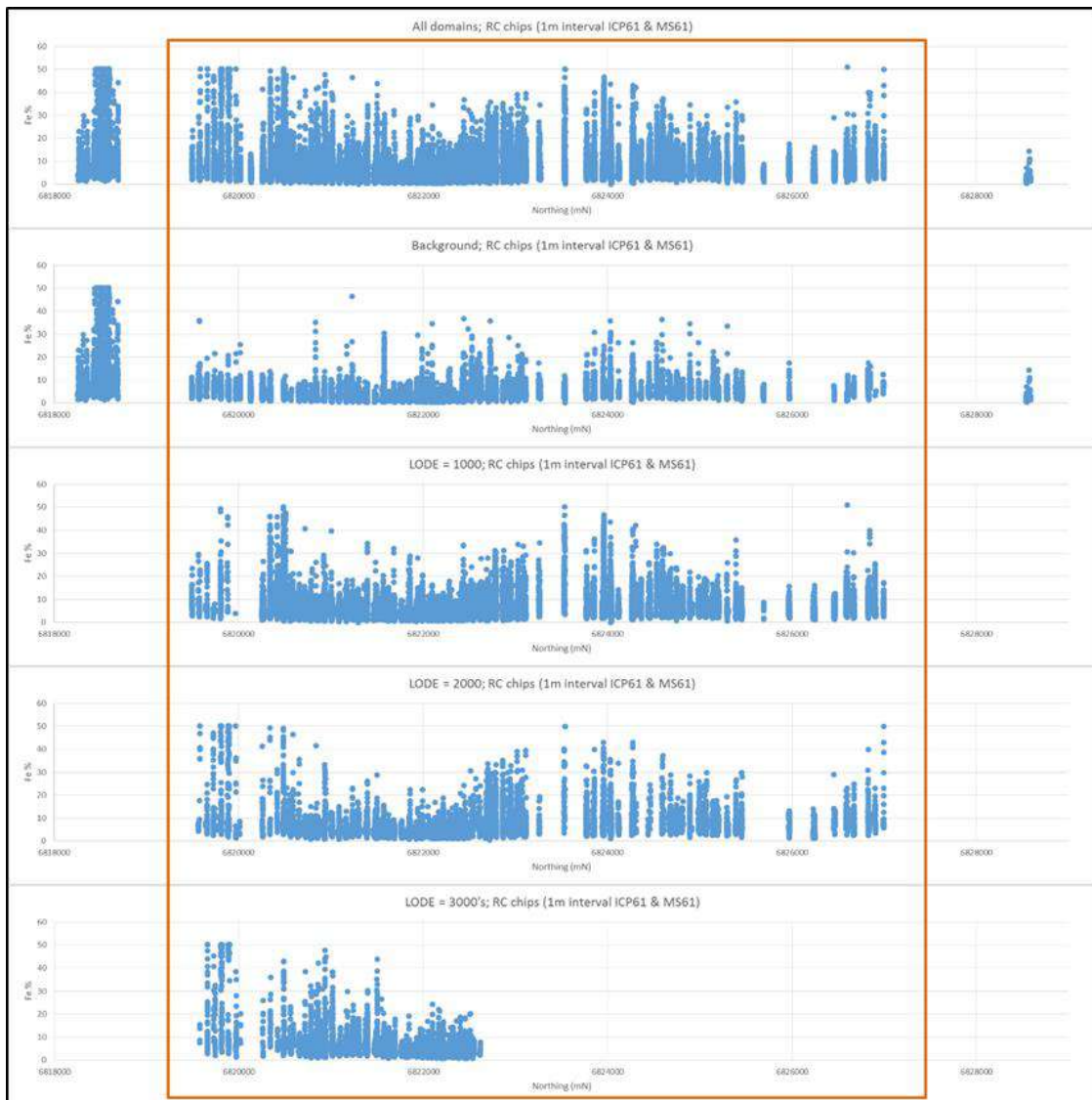


Figure 10.3 Example of comparison of Fe values across Productora (data outside the orange box was outside model extents but is included in this image to show larger regional trends). Note: The relatively sedate “background” values compared to the observe

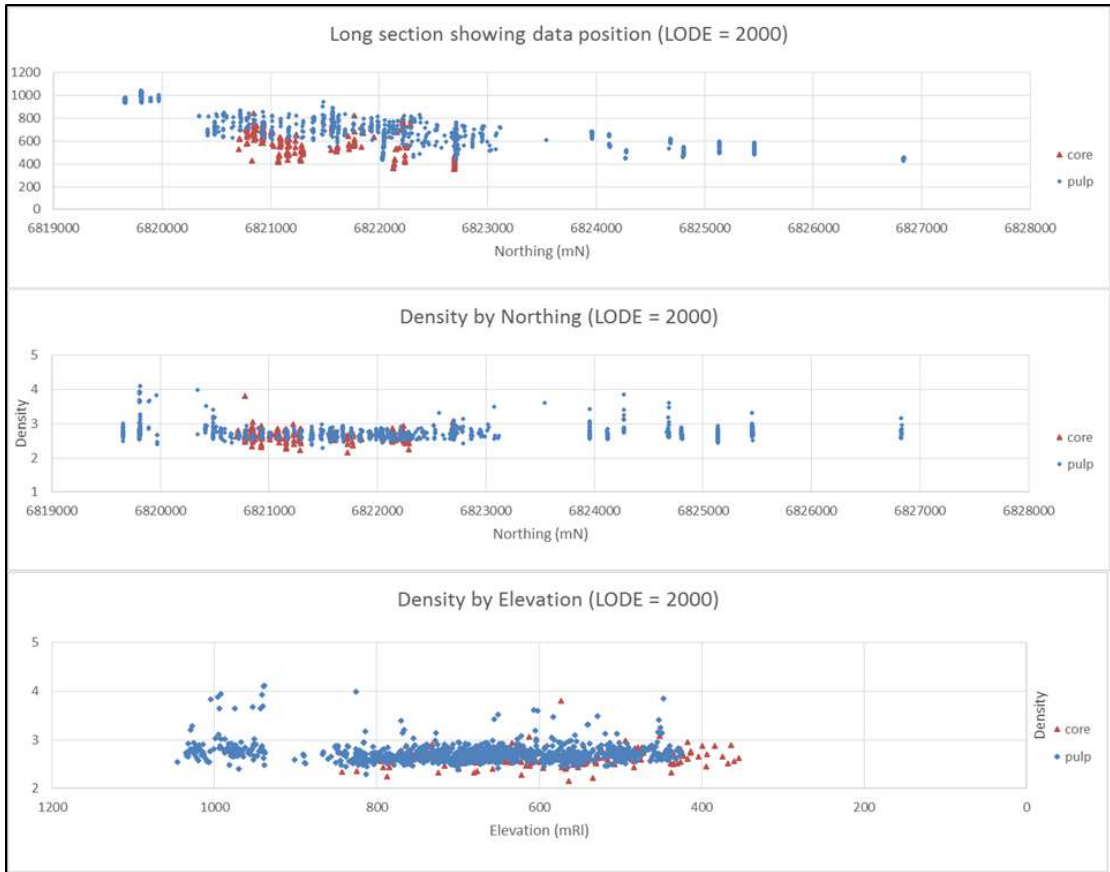


Figure 10.4 Example density data for samples within the 0.2% Cu domain with core differentiated to pulp data.

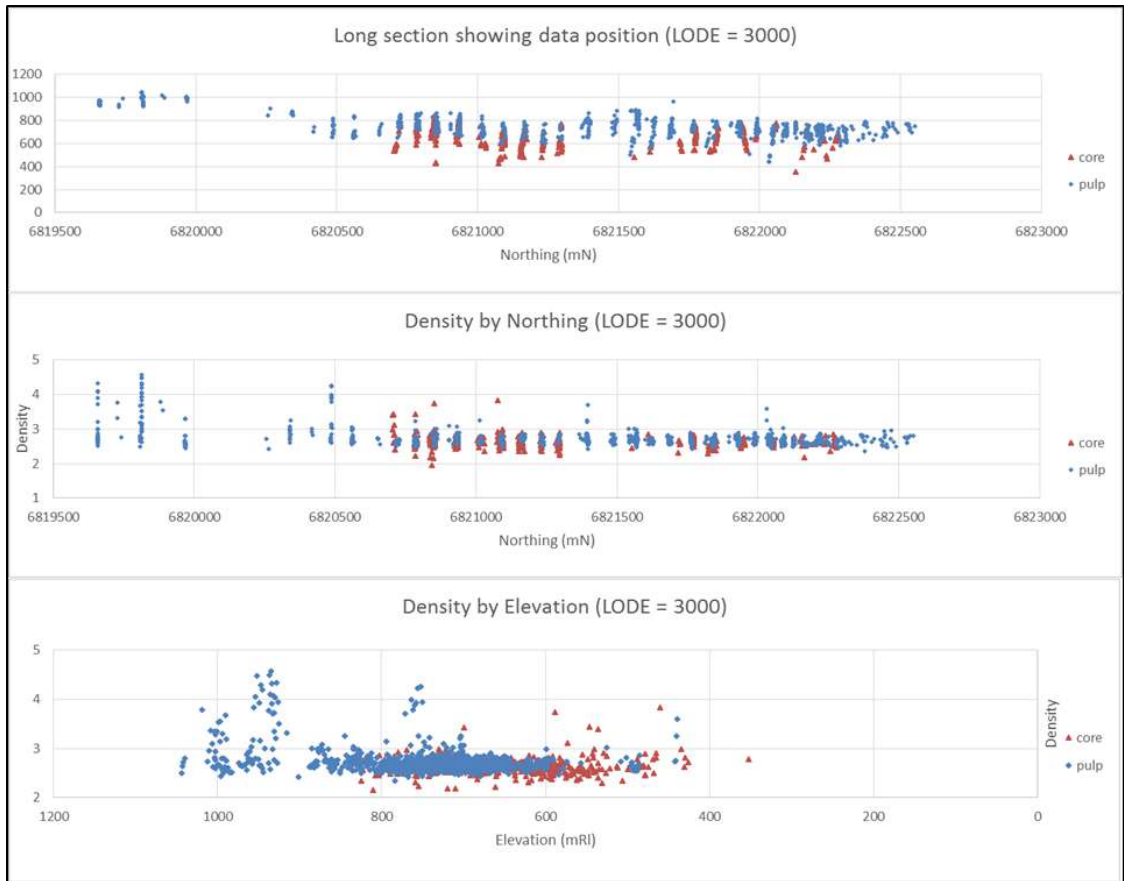


Figure 10.5 Example density data for samples within the 0.3% Cu domain with core differentiated to pulp data. Top: location depth by northing. Middle: density by northing. Bottom: density by elevation

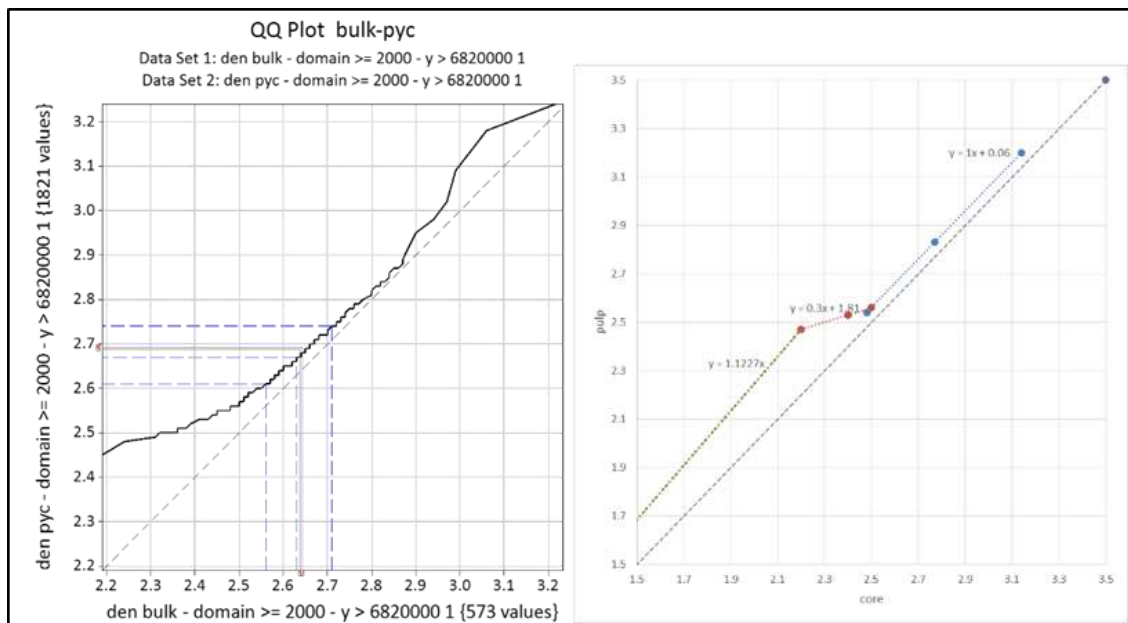


Figure 10.6 Left: QQ plot of core vs. pulp for samples within the 0.2% Cu domain. Right: experimental regressions to “correct” pulp pycnometer density values

Table 10.1 Final applied regression ranges and formulas for the conversion of pulp pycnometer density data

Applied to all LODE, and 'pyc' only	pycnometer range	Formula to convert to bulk density
y >=6820000 and weath=1(trans+fresh)	0 to <=2.47	calcBD = pyc/1.1223
	>2.7 to <= 2.56	calcBD = (pyc-1.81)/0.3
	>2.56 to 999	calcBD = pyc-0.06
y >=6820000 and weath=0 (oxide)	0 to <=2.5	calcBD = pyc/1.1521
	>2.5 to <= 2.74	calcBD = (pyc-1.5356)/0.4444
	>2.74 to 999	calcBD = pyc-0.03
y <6820000	all	calcBD = pyc-0.06

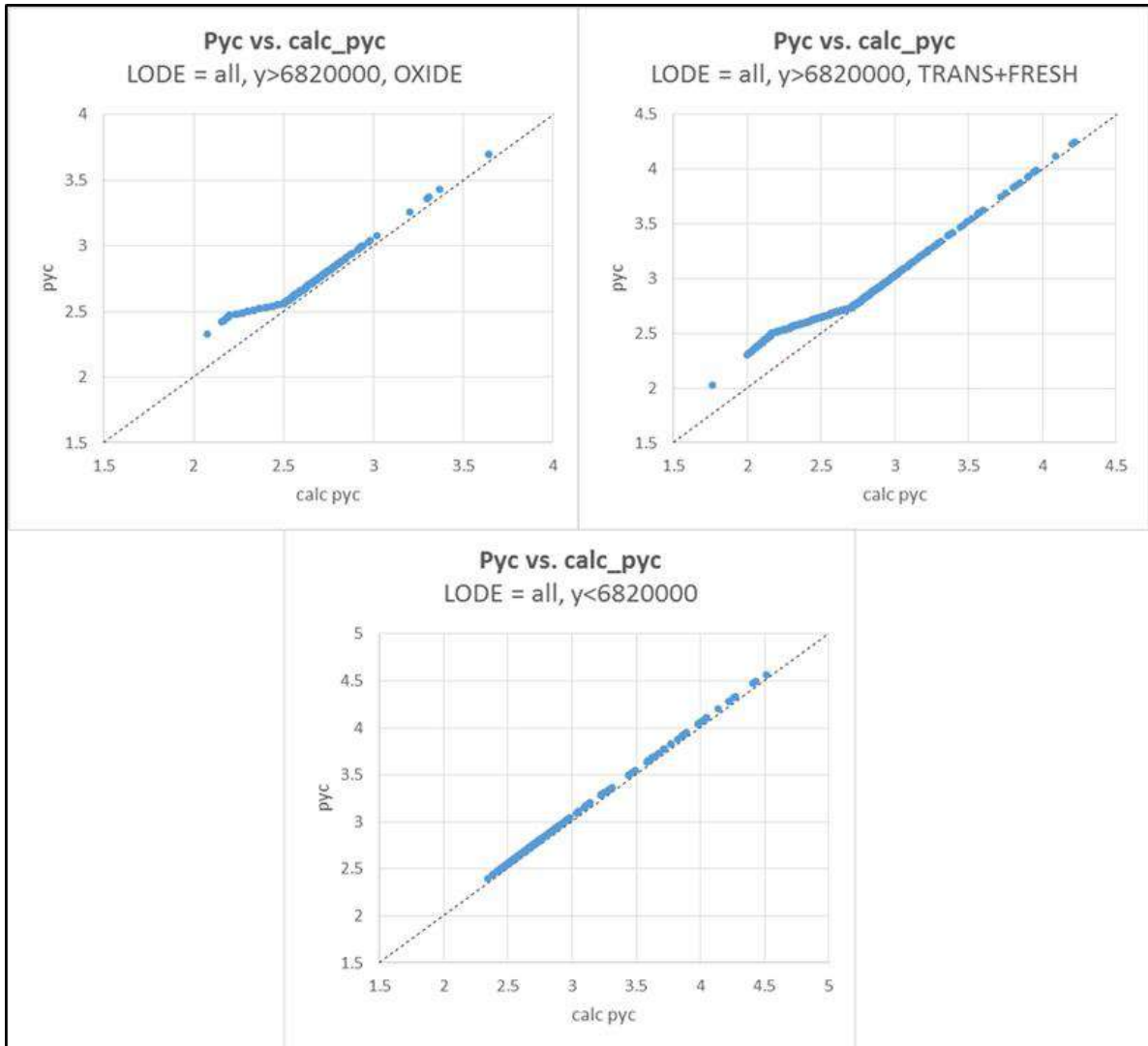


Figure 10.7 Validation of applied regressions on pulp pycnometer density data for key domains

10.1.12 Bulk Density Method Comparison for Alice

There were 71 bulk density (core) samples of fresh Alice mineralisation, and three for oxide. These were compared to the pycnometers (pulp) density results. For the fresh mineralised material, the average values for the bulk and pycnometer results appeared similar, but with the exception of outliers, the core results were within a much tighter

range compared to the “noisier” pycnometer results (Figure 10.8). This is different when compared to the Productora deposit comparisons. In practice there is an expectation that the pycnometer method may return elevated density results reflecting a density value of a theoretical sample with no porosity (due to being completely crushed). The correlation between pulp and core density values for Alice is supported by site observations of outcrop and core, that Alice is a generally low-porosity deposit. A similar observation and rationale has previously been established at the HCH Frontera porphyry deposit.

It was decided to use the average domain fresh bulk density results for application of density to the equivalent blocks.

There were only three bulk density measurements for the mineralised oxide material. Reviewing the core images in respect to sample locations, and being mindful of the reviewed available outcrop, there is a strong likely hood that these three samples are not likely to be representative of the Alice oxide mineralisation. A correlation between these samples and the pycnometer data was not achievable. In the absence of further data for correlation, it was deemed more preferable to use an average achieved after the application of the Productora deposit density formula to the 91 mineralised, oxide pycnometer results (of 2.53), rather than using the unmodified pycnometer average (of 2.66). No differentiation was made between mineralised domains in the oxide.

- The fresh “chalcopyrite-dominant” domain density = 2.66 (g/cm³)
- The fresh “pyrite-dominant” domain specific density = 2.68 (g/cm³)
- The density applied to Alice mineralised oxide material = 2.53 (g/cm³).

Table 10.2 Analysis of Alice density data

Summary of density test results at the Alice deposit							
Lode	Total	Oxide			Fresh		
		all	core	pulp	all	core	pulp
All	Samples	94	3	91	314	71	243
	Mean	2.65	2.25	2.66	2.64	2.67	2.64
	Minimum	2.12	2.12	2.55	2.42	2.43	2.42
	Maximum	2.82	2.32	2.82	3.23	2.95	3.23
Chalcopyrite dominant (high grade)	Samples	43	3	40	147	40	107
	Mean	2.63	2.25	2.66	2.63	2.66	2.62
	Minimum	2.12	2.12	2.57	2.42	2.46	2.42
	Maximum	2.76	2.32	2.76	3.21	2.82	3.21
Pyrite dominant (low grade)	Samples	51	-	51	167	31	136
	Mean	2.66	-	2.66	2.65	2.68	2.65
	Minimum	2.55	-	2.55	2.43	2.43	2.43
	Maximum	2.82	-	2.82	3.23	2.95	3.23

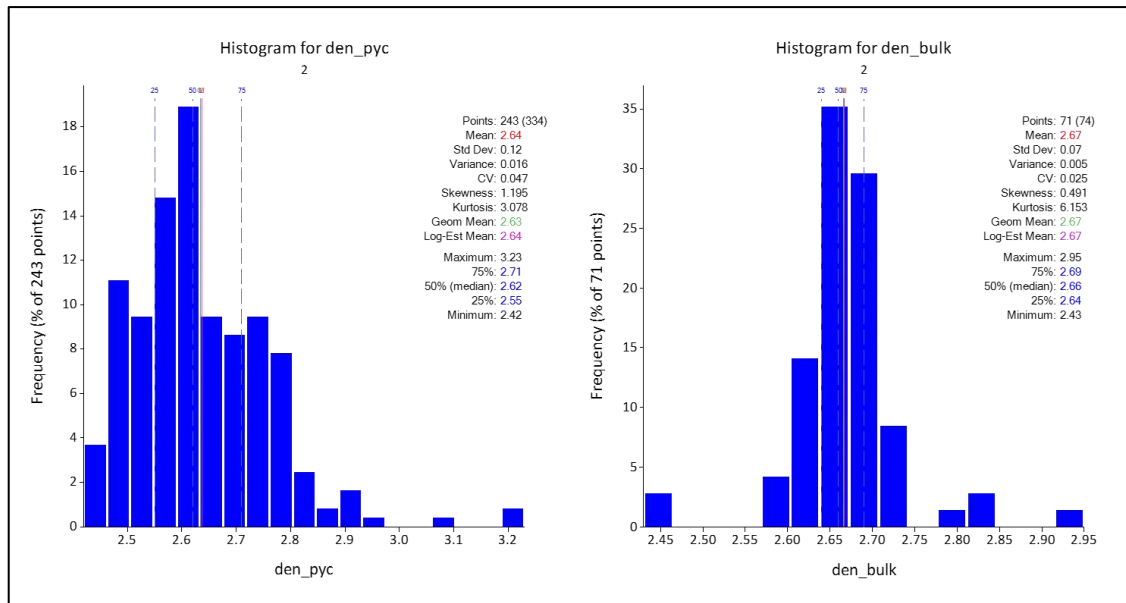


Figure 10.8 Comparison between Alice bulk density and pycnometer data populations

10.1.13 Drilling Results

All drilling and assay results used for the Productora, and Alice Mineral Resource estimates were generated by HCH exploration and Resource development drilling programmes conducted between 2010 and 2015.

10.2 Cortadera

10.2.1 Hot Chili (2019 to Present)

In April 2019, HCH began exploring and drilling activities at Cortadera. Further to drilling completed by Minera Fuego, Resource development and exploration drilling has been completed by HCH over four phases, as shown in Table 10.3. A list of significant intersections for each phase of drilling is listed in Table 10.4.

Table 10.3 Breakdown of the drilling completed by Hot Chili Limited from 2019 – 2021

Phase	Year	Meters (DD)	Meters (RC)
1	2019	1,851.7	3,922.7
2	2019	3,828.5	4,442
3	2020	1,413.8	1,761
4	2021	22,767.6	29,622.2

10.2.2 Phase 1 Minera Fuego Confirmation Program

Phase 1 drilling comprised of a RC and DD campaign carried out in April 2019, aimed to confirm and validate mineralisation intersected by Minera Fuego drilling within the three tonalitic porphyry-style mineralised bodies identified previously at Cortadera (Cuerpo 1, Cuerpo 2 and Cuerpo 3) (Figure 10.9). Drilling during Phase 1 was carried out using existing Minera Fuego access tracks and platforms and comprised 16 drillholes (CRP0001 to CRP0016) totalling 5,774.4m, including four twinned drillholes

across of the three porphyry centres at Cuerpo 1 (Purísima Mine), Cuerpo 2 and Cuerpo 3 for quality control and data verification purposes.

Phase 1 included RC drilling, approximately 250m average hole depth, at Cuerpo 1 and Cuerpo 2, and deep RC collar with DD tail (RC-DD) drilling averaging 900m hole depth at Cuerpo 3. RC-DD drilling at Cuerpo 3 drill-tested from surface to ~1km depth and intersected wide sulphide zones containing high-grade copper and gold confirming previous diamond drilling results by Minera Fuego. These intersections remained open vertically and laterally and the upper 200m (from surface) of the main porphyry remained undrilled. High-grade sulphide copper-gold mineralisation at Cuerpo 3 is associated with relatively high vein abundance, relatively high sulphide content and elevated magnetite, with copper sulphide mineralogy dominantly chalcopyrite.

Phase 1 RC drilling at Cuerpo 2 confirmed near-surface copper oxide mineralisation (mainly chrysocolla, copper wad and copper clays) and chalcocite enrichment within the wide copper and gold mineralised intercepts identified by Minera Fuego diamond drilling. Phase 1 RC drilling at Cuerpo 1 also confirmed copper oxide mineralisation to approximately 100 m depth associated with malachite and chalcocite. Phase 1 drilling included first-pass RC drilling immediately northeast to Purísima mine, recognising a fourth porphyry centre (Cuerpo 4) hosting near-surface copper mineralisation.

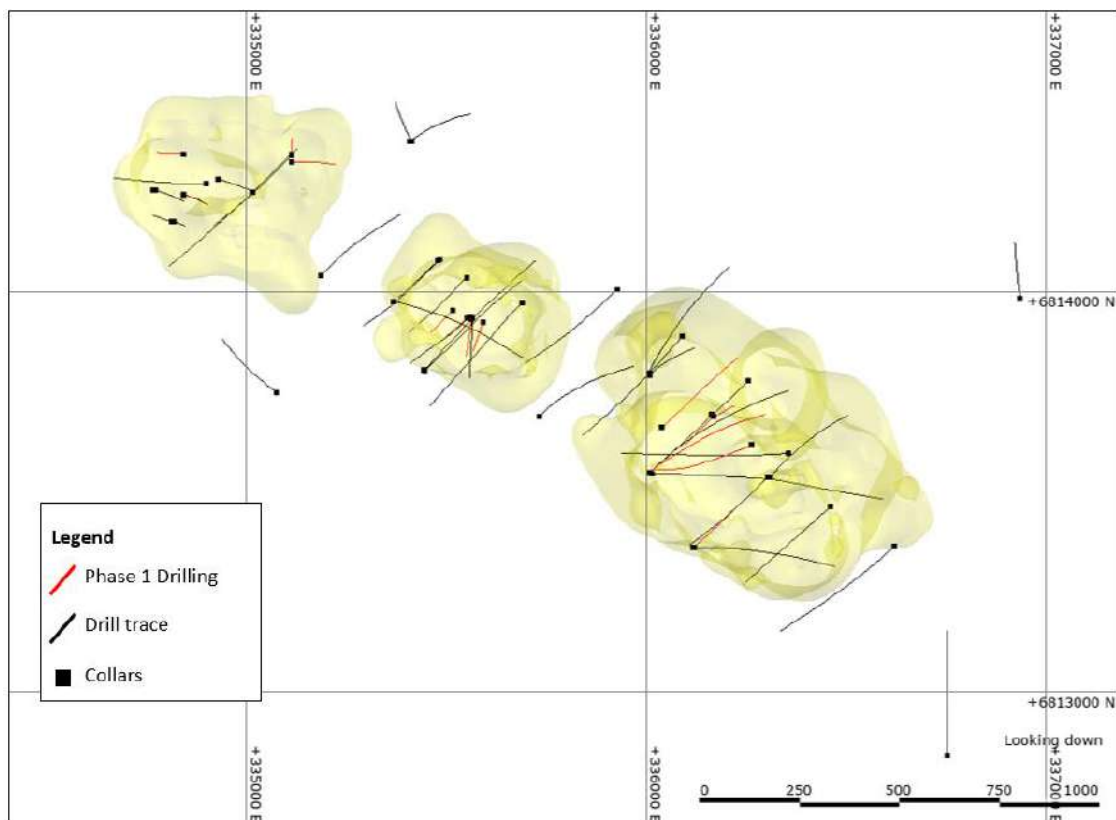


Figure 10.9 Plan view of Cortadera 0.1% Cu shape showing Hot Chili's Phase 1 drilling in red, and all other previous drilling in black. (HCH, 2022)

10.2.3 Phase 2 Cuerpo 2 and Cuerpo 3 Mineralisation Extension Program

During August 2019, Phase 2 RC-DD drilling commenced with the aims of testing for extensions of the mineralised zones at Cuerpo 2 and 3, in particular gaining better

definition of both the high-grade zone at Cuerpo 3 and near-surface chalcocite mineralisation at Cuerpo 2. Phase 2 drilling comprised 20 RC and RC-DD drillholes (CRP0017D to CRP0036) totalling 8,270.5m (Figure 10.10).

The Phase 1 and Phase 2 drilling campaigns completed during 2019 confirmed, extended and further defined the large-scale domain of copper and gold mineralisation at Cuerpo 3 and showed that the high-grade zone remained open with potential to extend across the entirety of Cuerpo 3. In addition, Phase 1 and Phase 2 drilling has confirmed and extended previously defined domains of surface copper enrichment at both Cuerpo 1 and Cuerpo 2.

The average grade of drill intersections recorded by HCH during 2019 within the high-grade zone of Cuerpo 3 (at approximately 500m depth from surface) ranges between 0.7% - 0.9% Cu and 0.3 - 0.4g/t Au. High-grade zones related to near-surface chalcocite enrichment at Cuerpo's 1, 2 and 4 during 2019 have been confirmed by drilling, with assayed copper grades ranging between 0.7% -1.6% Cu and gold grades ranging between 0.3 - 0.7 g/t Au.

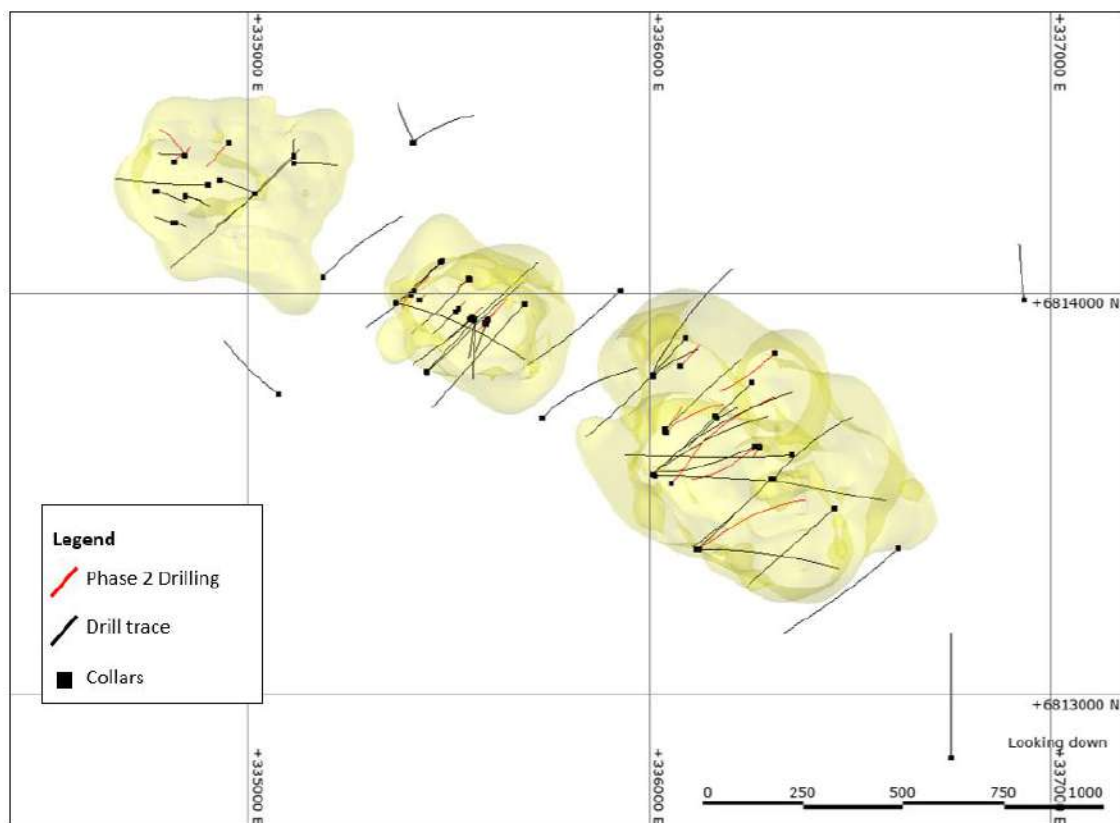


Figure 10.10 Plan view of Cortadera 0.1% Cu shape showing Hot Chili's Phase 2 drilling in red, and all other previous drilling in black. (HCH, 2022)

10.2.4 Phase 3 Cuerpo 3 Norte Exploration Program & Cuerpo 3 Mineralisation Confirmation Program

The Phase 3 drilling campaign commenced in January 2020, with the aim of further evaluating copper-gold mineralisation identified in earlier drilling phases and to test the Cuerpo 3 Norte target located immediately north of Cuerpo 3 (Figure 10.11). The Cuerpo 3 Norte target was identified as a strong coincident IP/ Magnetotellurics (MT)

geophysical anomaly located at depth within the same N-S corridor of dykes which transect Cuerpo 3 porphyry. Six Phase 3 RC-DD holes (CRP0038 to CRP0043) were completed at Cuerpo 3 up to March 2020 totalling 3,174.8m. Assay results from Phase 3 diamond drilling at Cuerpo 3 have confirmed the high-grade zone over 500m strike length, 200m width and 200m vertical extent.

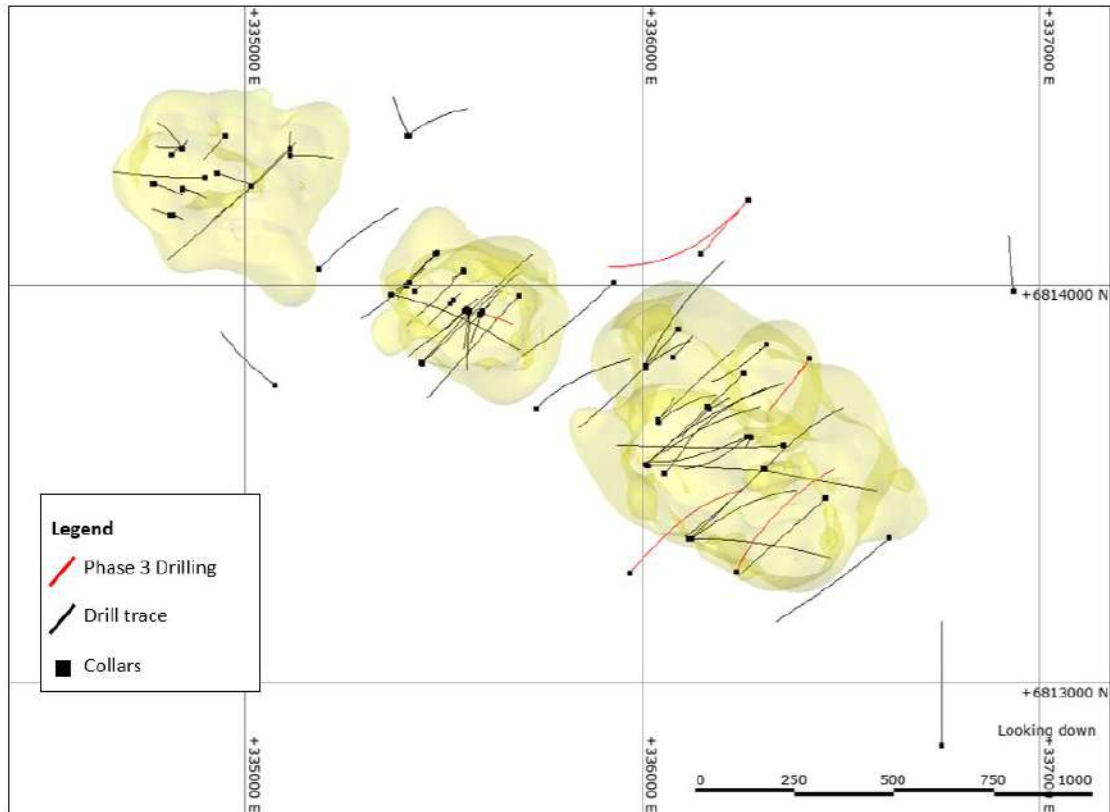


Figure 10.11 Plan view of Cortadera 0.1% Cu shape showing Hot Chili's Phase 3 drilling in red, and all other previous drilling in black. (HCH, 2022)

10.2.5 Phase 4 Cortadera Delineation and Extension Program

Phase 4 drilling comprised 133 RC and RC-DD drillholes (CRP0044 to CRP0189) totalling 52,389.8m (Figure 10.12). This phase of drilling commenced Jan 2021 with the aim of testing the mineralization at Cuerpo's 1, 2 and 3 both along strike and at depth. A particular effort was given to testing the Cuerpo 1-2 gap zone, and Cuerpo 2-3 gap zone. A continuation of Cuerpo 1's mineralized porphyry was identified towards the southeast of Cuerpo 1. In the Cuerpo 2-3 gap zone, the porphyry was confirmed to connect at depth but without significant mineralization.

Infill drilling at each of the Cuerpo porphyry bodies increased definition of both near surface oxide material at Cuerpo's 1 and 2 and gave increased understanding and confidence of the high-grade core at Cuerpo 3.

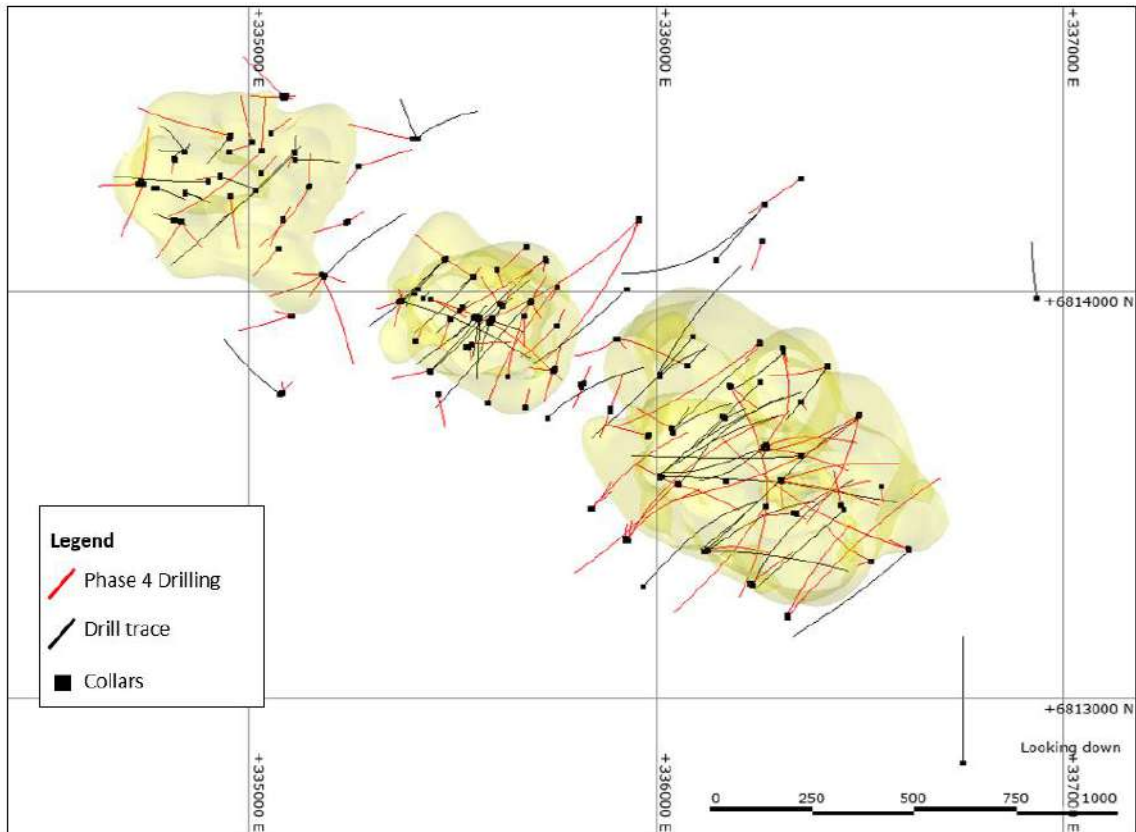


Figure 10.12 Plan view of Cortadera 0.1% Cu shape showing Hot Chili's Phase 4 drilling in red, and all other previous drilling in black. (HCH, 2022)

10.2.6 Significant Drillhole Intercepts

Significant drillhole intercepts for Drill phases 1 - 4 at Cortadera are provided in Table 10.4.

Table 10.4 Significant drillhole intercepts for Phase 1 - 4 drilling at Cortadera

Hole_ID	Coordinates			Azim	Dip	Hole Depth	Intersection		Interval (m)	Copper (% Cu)	Gold (g/t Au)	Silver (ppm Ag)	Molybdenum (ppm Mo)	Phase		
	North	East	RL				From	To								
CRP0001	6813928	335566	980	185	-60	200	0	118	118	0.5	0.3	1.0	4	1		
							including		26	48	22	0.7	0.4		1.2	4
							100	104	4	1.2	0.9	2.6	4			
CRP0002	6813931	335552	982	225	-70	200	0	72	72	0.5	0.3	1.0	4	1		
CRP0003	6813918	335603	990	200	-60	150	0	122	122	0.6	0.3	1.3	4			
							including		40	60	20	1.2	0.5		2.4	2
CRP0004	6813947	335520	982	224	-59	150	106	114	8	1.0	0.6	2.7	2			
							2	76	74	0.5	0.2	0.9	3			
CRP0005	6814245	334853	976	106	-75	180	52	58	6	1.1	0.4	2.2	2	1		
							including		0	144	144	0.5	0.1		1.1	4
CRP0006	6814257	334773	977	360	-90	294	58	126	68	0.7	0.1	1.5	3	1		
							including		0	24	24	0.3	0.1		0.9	16
CRP0007	6814345	334840	975	270	-70	240	108	128	20	0.3	0.0	0.7	88	1		
							including		206	236	30	0.3	0.0		0.4	41
							12	20	8	0.3	0.1	0.9	27			
CRP0008	6814322	335111	966	90	-60	240	58	122	64	0.3	0.1	0.7	18	1		
							including		162	170	8	1.0	0.0		4.4	95
							194	234	40	0.3	0.0	0.6	21			
CRP0009	6814341	335114	966	360	-90	222	22	80	58	0.2	0.0	0.4	21	1		
CRP0010	6814341	335114	966	360	-75	180	22	40	18	0.3	0.1	0.9	19			
CRP0011D	6813547	336008	1027	45	-65	960	112	960	848	0.4	0.2	0.8	50			
							including		720	904	184	0.7	0.3	1.4	74	
CRP0012D	6814039	336224.38	1016.647	44	-60	667	378	578	200	0.4	0.2	0.7	116	1		
							including		494	570	76	0.5	0.2		0.9	205
CRP0013D	6813692	336163	1020	360	-90	1186	98	118	20	0.4	0.2	0.5	12	1		
							including		204	954	750	0.6	0.2		1.1	79
							516	704	188	0.9	0.4	1.7	94			
CRP0014	6813695	336162.7	1010	225	-60	204	530	630	100	1.0	0.5	2.4	96	1		
							or including		140	204	64	0.5	0.2		0.8	29
CRP0015	6813362	336124	1070	45	-60	348	230	348	118	0.3	0.1	0.3	10	1		
CRP0016D	6813616.511	336264	1027.623	247	-60	652	106	240	134	0.4	0.2	0.8	19			
							including		178	220.0	42	0.6	0.3		1.0	28
CRP0017D	6813739	336307	1066	75	-75	1134	360	610	250	0.5	0.2	0.7	61	1		
							including		392	582	190	0.6	0.2		0.9	58
							484	634	150	0.6	0.3	1.0	54			
CRP0018D	6813995	336448.9	1035	360	-90	763	496	578	82	0.8	0.4	1.5	50	1		
							including		430	614	184	0.7	0.3		1.3	6
CRP0019D	6813620	336260	1035	244	-81	1306	56	320	264	0.4	0.2	0.5	18	2		
							including		484	634	150	0.6	0.3		1.0	54
							including		496	578	82	0.8	0.4		1.5	50
CRP0020D	6813855	336256	989	45	-65	1037	44	212	168	0.4	0.1	0.4	37	2		
							including		138	212	74	0.6	0.3		0.9	58
							including		654	988	334	0.5	0.2		0.9	191
CRP0020D	6813855	336256	989	45	-65	1037	758	822	64	0.6	0.2	1.3	146	2		
							including		934	988	54.1	0.7	0.2		1.3	256
							including		0	972	972	0.5	0.2		0.9	49
including		436	848	412	0.7	0.3	1.5	59								

Hole_ID	Coordinates			Azim	Dip	Hole Depth	Intersection		Interval (m)	Copper (% Cu)	Gold (g/t Au)	Silver (ppm Ag)	Molybdenum (ppm Mo)	Phase
	North	East	RL				From	To						
CRP0021	6814266	335790	989	220	-70	120	0	80	80	0.8	0.3	3.8	1	2
					including		54	80	26	1.7	0.7	2.6	3	
CRP0029D	6814031	336225	1017	47	-73	979	330	979.2	649	0.4	0.1	0.8	101	
					including		472	912	440	0.5	0.2	0.9	115	
CRP0030	6813962	335525	1007	44	-79	150	4	28.0	24	0.4	0.1	0.4	3	
CRP0032D	6813851	336312	1057	224	-70	1021	532	576	44	0.5	0.2	1.0	204	
							648	1,021	373	0.4	0.1	0.7	116	
					including		676	806	130	0.5	0.2	0.9	165	
CRP0034	6814328	334814	985	44	-69	220	0	24	24	0.3	0.1	0.9	6	
							82	128	46	0.6	0.1	1.4	5	
					including		102	122	20	1.0	0.2	2.3	3	
CRP0037	6813929	335595	1012	109	-59	200	0	76.0	76	0.4	0.2	0.7	7	
CRP0040D	6813278	336235	1082	25	-60	1027	294	364.0	70	0.4	0.2	0.4	4	
							422	964	542	0.5	0.2	0.9	103	
					including		616	834	218	0.7	0.2	1.2	119	
CRP0041D	6814214	336267	1079	221	-60	890	574	602	28	0.2	0.1	1.1	5	
CRP0042D	6813273	335968	1106	40	-62	943	616	930.0	314	0.4	0.1	0.3	213	
CRP0046D	6813763	336183	1026	147	-60	1101	248	362	114	0.5	0.2	0.7	17	
							568	753	185	0.5	0.2	0.9	41	
CRP0047D	6813692	336497	1050	227	-60	1149	282	326	44	0.3	0.1	0.4	40	
							414	426	12	0.3	0.1	0.3	29	
							470	492	22	0.3	0.1	0.4	20	
							576	588	12	0.3	0.2	0.6	23	
							632	646	14	0.4	0.2	0.7	10	
							720	938	218	0.5	0.1	0.8	147	
					including		720	744	24	0.7	0.2	1.2	74	
					and including		756	890	134	0.6	0.2	1.0	177	
CRP0052D	6813690	336496	1051	195	-70	1036	524	906	382	0.4	0.1	1.1	229	
					including		646	790	144	0.5	0.2	2.3	229	
					or including		654	734	80	0.6	0.2	0.9	246	
CRP0053D	6814075	335726	997	240	-70	844	230	844	614	0.3	0.1	0.6	41	
					including		446	694	248	0.4	0.1	0.8	15	
					including		502	534	32	0.6	0.3	1.5	10	
					and including		634	658	24	0.6	0.2	1.7	3	
CRP0058D	6814177	335957	1032	223	-66	1163	70	84	14	0.3	0.2	0.8	7	
							570	576	6	0.5	0.0	4.4	5	
							784	810	26	0.4	0.1	0.8	32	
CRP0061D	6813542	336010	1027	109	-77	867	54	867	813.1	0.4	0.1	0.7	72	
					including		440	758	318	0.6	0.2	1.0	89	
CRP0063	6814476	335088	969	272	-61	132	58	70	12	0.5	0.0	2.9	30	
CRP0064	6814470	335080	968	271	-60	171	60	74	14	0.4	0.0	2.3	38	
CRP0068D	6814344	335030	955	225	-61	679	0	22	22	0.5	0.1	0.9	26	
CRP0069	6814338	335031	960	0	-60	296	0	62	62	0.3	0.1	31.4	1	
CRP0074	6814337	334950	950	71	-58	120	0	104	104	0.2	0.0	30.2	1	
CRP0075	6814295	335031	955	41	-59	120	0	36	36	0.4	0.1	0.9	27	
					including		24	34	10	0.7	0.2	1.8	46	
CRP0079	6815374	335273	1062	39	-59	468	92	216	124	0.0	0.0	1.3	4	
CRD0080	6813391	335926	1093	35	-70	1474	536	1372	836	0.4	0.1	0.8	109	
					including		536	972	436	0.5	0.2	0.9	154	
CRP0088D	6813365	336621	1060	286	-63	1434	426	912	486	0.5	0.2	0.8	77	
					Including		682	850	168	0.8	0.3	1.4	109	
					or including		714	830	116	0.9	0.3	1.5	130	

Hole_ID	Coordinates			Azim	Dip	Hole Depth	Intersection		Interval (m)	Copper (% Cu)	Gold (g/t Au)	Silver (ppm Ag)	Molybdenum (ppm Mo)	Phase
	North	East	RL				From	To						
CRP090D	6813872	336253	1060	231	-64.6	999	310	648	338	0.3	0.1	1.0	128	
CRP0091	6814199	335058	962	27	-69	106	0	14	14	0.4	0.1	0.8	6	
							76	106	30	0.3	0.1	0.3	83	
CRP0092D	6814256	335147	972	209	-74.2	635	4	8	4	0.3	0.1	0.3	10	
							68	136	68	0.2	0.0	0.5	59	
					Including		68	84	16	0.3	0.1	0.5	79	
							112	122	10	0.3	0.0	0.5	36	
							500	506	6	0.4	0.0	0.8	5	
CRP0094	6814200	335059	962	209	-60	150	2	12	10	0.5	0.1	0.9	4	
CRP0098	6814226	334956	975	174	-60	282	40	96	56	0.4	0.1	1.0	17	
							56	76	20	0.7	0.2	1.6	7	
CRP0099	6814342	335109	960	201	-61.1	84	26	85	59	0.4	0.1	1.0	15	
CRP100D	6814041	335183	965	239	-69.8	439	184	236	52	0.3	0.1	1.0	76	
CRP106	6814366	335009	954	343	-60.3	271	0	58	58	0.3	0.0	1.0	39	
					Including		0	12	12	0.5	0.1	1.0	13	
CRP108D	6814105	335074	946	227	-69.9	288	28	80	52	0.3	0.1	0.8	60	
CRP111D	6813884	335905	999	105	-80	1039	412	456	44	0.2	0.1	0.4	27	
							536	574	38	0.2	0.1	0.9	49	
							612	670	58	0.2	0.0	0.6	42	
							774	992	218	0.2	0.0	0.4	36	
CRP116D	6814035	335552	980	302	-80	717	254	280	26	0.2	0.0	0.6	36	
							336	394	58	0.2	0.0	0.5	77	
CRP122	6813663	336037	1016	300	-70	270	72	106	34	0.2	0.1	0.3	53	
CRP126	6813622	336269	1028	32	-59	192	14	30	16	0.2	1.2	0.3	16	
					Including		14	22	8	0.3	2.4	0.4	16	
CRP127D	6813534	336306	1035	98	-67	637	232	290	58	0.3	0.1	0.4	67	
							298	332	34	0.3	0.1	0.3	139	
CRP124D	6813694	336500	1049	239	-75	1020	480	842	362	0.5	0.2	0.9	123	
					Including		628	776	148	0.6	0.3	1.3	150	
					Or including		628	730	102	0.7	0.3	1.3	195	
CRP132D	6813861	336310	958	170	-76	766	300	766	466	0.2	0.1	0.4	89	
					Including		540	576	36	0.4	0.1	0.6	169	
							714	764	50	0.3	0.1	0.7	92	
CRP133	6813977	335692	985	150.16	-60	108	12	108	96	0.2	0.1	0.4	34	
					Including		12	54	42	0.3	0.1	0.5	15	
CRP134D	6813615	336269	1027	96	-76	1025	216	826	610	0.4	0.1	0.7	206	
					including		502	568	66	0.6	0.2	0.9	159	
					and including		634	772	138	0.6	0.1	1.4	486	
CRP136D	6813389	335926	1097	41	-74	982	360	428	68	0.3	0.1	0.5	10	
							548	674	126	0.4	0.1	0.7	126	
CRP138D	6813204	336322	1092	26	-64	685	352	542	190	0.2	0.1	0.4	63	
					including		368	462	94	0.3	0.1	0.5	70	
							608	685	77	0.3	0.1	0.4	103	
CRP139	335446	6813981	969	115	-61	222	0	222	222	0.2	0.1	0.5	7	
					including		180	222	42	0.4	0.3	0.8	4	
CRP140	335695	6813975	985	25	70	92	10	62	52	0.2	0.1	0.4	23	
CRP144D	6813453	336344	1043	51	-73	941	14	941.2	927	0.2	0.1	0.6	65	
					including		382	590	208	0.3	0.1	0.5	142	
					and including		682	714	32	0.8	0.2	1.5	287	
					or including		682	728	46	0.6	0.1	1.1	224	
					and including		854	872	18	0.6	0.1	1.9	48	
CRP146D	6813367	336126	1066	80.63	-79	1051	378	614	236	0.3	0.1	0.6	90	
					including		532	596	64	0.4	0.1	0.8	148	
CRP148	6813870	335545	993	84	-61	252	0	252	252	0.3	0.1	0.6	4	
					including		0	156	156	0.4	0.2	0.8	5	
CRP149D	6813791	335636	1009	10	-58	637	102	192	90	0.3	0.1	0.4	3	
							294	522	228	0.3	0.1	0.6	34	

4

Hole_ID	Coordinates			Azim	Dip	Hole Depth	Intersection		Interval (m)	Copper (% Cu)	Gold (g/t Au)	Silver (ppm Ag)	Molybdenum (ppm Mo)	Phase		
	North	East	RL				From	To								
CRP0150D	6813982	335427	968	109	-54	699	34	96	62	0.2	0.1	0.3	23			
							136	184	48	0.4	0.1	0.6	5			
							including		144	158	14	0.6	0.3	0.9	4	
							including		248	632	384	0.3	0.1	0.6	21	
							including		318	338	20	0.5	0.3	0.7	0	
							and including		430	476	46	0.5	0.1	0.9	15	
CRP0151	6813865	335540	992	168.81	-75	162	0	30	30	0.3	0.1	0.6	13			
							48	118	70	0.3	0.1	0.5	19			
CRP0152	6813938	335679	982	180	-60	162	10	158	148	0.2	0.1	0.5	10			
CRP0153	6813959	335619	977	31	-60	102	36	86	50	0.3	0.1	0.5	18			
CRP0154	6813959	335619	977	321	-60	168	8	114	106	0.2	0.1	0.4	17			
CRP0155D	6813620	336273	1028	65.29	-76	1140	248	316	68	0.4	0.1	0.5	69			
							492	694	202	0.4	0.1	0.8	108			
							including		596	638	42	0.6	0.2	1.2	86	
							and including		664	692	28	0.5	0.1	1.1	126	
CRP0158	6813926	335491	977	200	-60	150	4	66	62	0.4	0.1	0.6	11			
							including		26	44	18	0.6	0.2	1.0	3	
CRP0161D	335586	6813726	1006	21	-59	708	380	620	240	0.3	0.1	0.6	46			
							including		390	406	16	0.6	0.2	1.5	11	
							and including		434	480	46	0.4	0.1	0.7	11	
CRP0162	6813453	336343	1043	115	-80	115	18	163	145	0.2	0.0	0.5	20			
CRP0163	6813455	336337	1043	262	-74	262	150	324	174	0.3	0.1	0.6	7			
CRP0164D	6813535	336309	1035	70	-72	934	338	398	60	0.3	0.1	0.4	127			
							504	642	138	0.3	0.1	0.4	143			
							including		540	592	52	0.4	0.1	0.4	259	
CRP0167D	6813336	336528	1081	297	-78	906	540	906	366	0.2	0.0	0.5	99			
							including		540	640	100	0.3	0.1	0.5	143	
							or including		562	604	42	0.4	0.1	0.5	181	
CRP0170D	335837	6813464	1085	21	-59	840	366	840	473.7	0.3	0.1	0.6	176			
							including		524	732	208	0.4	0.1	0.6	188	
							and including		732	792	60	0.3	0.1	0.8	477	
							and including		814	832	18	0.5	0.1	0.8	174	
CRP0176	334831	6814172	953	143	-71	252	0	114	114	0.3	0.1	0.6	46.8			
							including		0	24	24	0.6	0.1	1.2	7.7	
CRP0177	334735	6814270	976	10	-60	294	14	34	20	0.3	0.1	0.5	34			
CRP0178	334834	6814171	953	210	-70	312	0	72	72	0.4	0.1	0.8	46			
							including		0	28	28	0.7	0.1	1.5	17	
							including		192	214	22	0.3	0.0	0.7	28	
CRP0180D	6813470	336268	1059	-58	215	727	130	370	240	0.2	0.1	0.3	44			
							including		194	210	28	0.3	0.1	0.3	51	
							and including		246	260	14	0.4	0.1	0.6	38	
CRP0183	334935	6814283	960	257	-74	234	10	90	80	0.4	0.1	0.8	8			
							including		44	56	12	0.6	0.1	1.1	12	
							192	214	22	0.3	0.0	0.7	28			
CRP0184	334814	6814328	957	199	-75	150	0	80	80	0.2	0.1	0.3	3			
							124	150	26	0.4	0.1	1.2	2			
CRP0186	6814053	335610	991	-61	169	100	26	100	74	0.2	0.0	0.3	27			
CRP0188	6813475	336454	1044	-65	347	204	14	62	48	0.2	0.1	0.4	5			

4

10.2.7 Drilling Procedures

All drilling commissioned by HCH for the Cortadera Resource estimates was conducted by Blue Spec Sondajes (Bluespec). All drill rigs are Exploration Drill Masters-type (EDM) and configuration is as follows:

- Custom built EDM2000 and 1200 High-Capacity Multi-purpose RC and DD rigs
- These rigs were supported by an Atlas Copco Hurricane B4-41/ 750 Booster compressor and a Sullair Air Compressor Model 1150/900
- The drilling rigs were manned by Australian or Australian-trained Chilean drillers and well-trained local drilling offsidars. All the custom-built drill rigs used during the programme were convertible to either RC or diamond core drilling.

The drilling was undertaken on established platforms that provided adequate space for drilling and sampling equipment. Booster pressure during RC drilling was high (700-800 psi) which allowed fair sample return and penetration rates. As a standard, on-drill

sampling equipment consisted of a cyclone unit for pressure release and sample collection, and a static cone splitter to sub-sample the collected sample. The cyclone and cone splitter's vertical position was monitored using a spirit level to minimise any potential sample bias. Drillholes were routinely down-hole surveyed during drilling, or else immediately following drilling completion.

10.2.8 RC drilling tools

RC drilling utilised a face sampling down-hole hammer with cyclone sample recovery. Drill hammers used were 542/543, PR 54 (Sandvik) and MR 120 (Mincon).

Adjustments to drill bit size were made as drillholes reached certain intervals, to ensure successful end of hole depths. Changes to bit sizes were recorded in drill plods (Table 10.5).

Table 10.5 Nominal drill bit size changes in RC drilling

Bluespec bit size changes	
Depth	RC Bit Size
0m - 200m	140mm
200m - 320m	137mm
320m - 450m	133mm
> 450m	130mm

10.2.9 Diamond drilling tools

Diamond drilling was conducted using HQ3 diameter core (96mm outside diameter and 63.5mm inside diameter) and NQ3 diameter core (75.7mm outside diameter and 45mm inside diameter).

Orientation of diamond core was controlled by the Reflex ACT III core orientation tool.

Down hole surveys were completed in-rod by Bluespec using an Axis Champ Navigator north-seeking gyroscope.

10.2.10 Hole Planning and Set-up

The spacing and location of much of the drilling at Cortadera is variable and averages approximately 80m along strike and 150m across strike, allowing for optimal drill orientation to intersect perpendicular to mineralisation. The majority of drilling plunged -60 to -80° toward northeast, with some scissor holes drilled to the southwest, although additional orientations were used to ensure geological representivity and to increase the use of available drill platforms.

10.2.11 Naming Convention and Meta Data Management

Holes drilled at Cortadera used the following labelling system:

- HCH holes drilled by RC were prefixed with 'CRP', followed by the hole number
- HCH holes drilled using an RC pre-collar with a DD tail were prefixed with 'CRP', followed by the hole number, finishing with the suffix 'D'.

- Minera Fuego holes are prefixed 'FJOD', then the hole number for diamond holes cored from surface.

10.2.12 Internal database audit - 2020

An internally managed and audited acQuire drilling database was used to capture and manage geological drill data. A detailed internal review of data management processes was undertaken in 2020 with the results deemed satisfactory and no errors identified. The outcomes of this audit are summarised below:

This report outlines an internal company review of the HCH geological logging data as supplied the site geologists and the assay information received from ALS Laboratories.

While there were minor issues noted, none degrade the confidence in the ability to use the HCH database in Resource estimation. These inconsistencies were largely caused during data transfer from the Company's FTP hosted in Chile to HCH's Perth based server.

The methodology taken for the internal audit is outlined below:

HCH has drilled 43 drillholes at Cortadera, with 39 holes being drilled by previous owner Minera Fuego. The HCH drillholes have the prefix CRP, and Minera Fuego prefix FJOD.

A random list of five drillholes from the 82 available was created to represent approximately 6% of the Cortadera database for the review:

- CRP0013D
- CRP0020D
- CRP0037
- FJOD-023
- FJOD-032

Each hole was subjected to the following queries:

- Are the ALS assay certificates (pdf format) accessible on HCH server?
- Are the assay results available in HCH's database?
- Are the geology logs of this hole accessible on the HCH server?
- Are the geology logs of this hole available in HCH's database?

Each hole was subjected to the following validations:

- Do the HCH database values reflect those on the certificate and datafile?
- Do the logged excel geology files match the data displayed in the database?
- Do the additional datafiles (CPS, Magsus etc.) from site match the data displayed from the database?

Strict data flow procedures were followed during drilling campaigns, ensuring that all drill data was collected in a systematic, repeatable, and accurate manner allowing consistent

and valid data for resource estimation. The steps taken in drilling data capture completed by HCH are summarised in Figure 10.13.

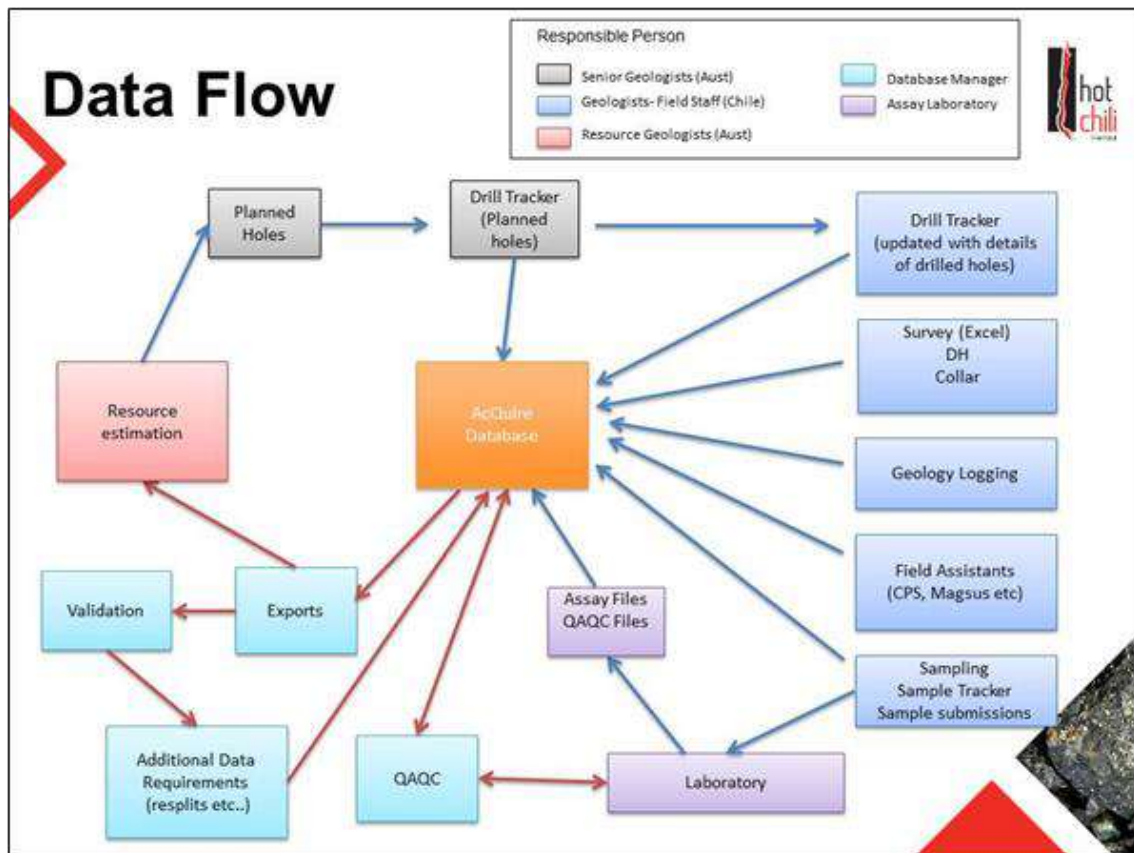


Figure 10.13 Drill Data flow showing drill planning, drill execution, logging, sampling and data entry and capture

10.2.13 External database audit – 2022

In November of 2021 Expedio Services were commissioned to undertake an audit of the HCH database. A high-level review of the data was completed to ensure accuracy and repeatability in data extraction procedures.

Expedio was granted access to the acquire cloud environment under HCH user accounts and licenses in order to complete the database audit work. The audit work consisted of checking the integrity of the database schema and running health checks on the data contained within. This entailed schema checks on relationships, triggers and constraints with a focus on library table and downhole depth referential integrity. Invalid data was flagged for further analysis and checks for case sensitivity carried out. Data auditing within the schema, duplication checks and export query designs and execution protocols were also reviewed.

There were no major issues identified with the quality of the data and no material bias apparent from the check work. The data as reviewed is suitable for resource estimation and other project development work.

10.2.14 Surveying and Orientations

Cortadera topographical data was supplied by Minera Fuego upon exercise of the purchase option agreement for the project. Topographical surveys were undertaken by contract survey company Geodesia Topografía Exploraciones in 2011 and 2012 with the following methodology utilised for the survey.

Base Station “SIRGAS VALLENAR at HM Cortadera 1 to 40” was selected as the control point and the survey was undertaken within a polygon area, followed by:

- Measurement with Dual Frequency GPS Ashtech Brand Model Z-Xtreme and Allegro CX Electronic Notebook
- HM Cortadera Base Station 1 to 40 Z-Xtreme GPS Equipment
- Rover or Mobile Equipment, Z-Xtreme with Allegro System Notebook (RTK) Real Time Kinematic
- The topographical data points were then used to create a digital elevation model (DEM). The software used to create the DEM is unknown.
- The validation of the final topography model used for the resource model was via:
 - Visual validation against drilling (two surveys undertaken by independent survey contractors)
 - Visual validation against known infrastructure (roads, tenement pegs etc.)
 - Visual validation against drone orthophotography completed in 2019.

HCH also commissioned TOPGEO E INGENIERÍA LTDA to undertake a topographical survey of drill collar locations in May 2019 to validate the coordinates of Minera Fuego drilling. This survey was able to locate 36 of the 39 drillholes completed by Minera Fuego, with survey results being within centimetres of those co-ordinates provided by Minera Fuego.

This resolution of the topographical model is considered suitable for resource estimation purposes.

10.2.15 Collar Surveying

Drill collars were routinely surveyed following completion of drilling campaigns up until June 2021, from this time onwards the frequency of surveying increased to monthly. HCH drill collars were surveyed by contract surveying company Topgeo Chile SpA. Topographical equipment used was a CHCNAV model i80 Geodetic GPS, dual frequency, Real Time with 0.1cm accuracy (mN, mE and mRL). Topographical collar surveys were supplied in both WGS84 Zone 19S and PSAD Zone 19S coordinate systems.

10.2.16 Collar Validation

Validation of collar survey locations was completed by:

- Comparing planned coordinates with subsequent picked up coordinates to detect any material differences in location
- Visual checking of collar points against the topographical elevation model
- Random GPS field checks of collar coordinates
- Surveying of FJOD collar points by Geotopo for comparison against original files supplied by Minera Fuego.

10.2.17 Downhole Surveying

The downhole surveying at Cortadera for HCH's drilling was completed by Bluespec drilling contractor using the Axis Champ Navigator north seeking gyroscope tool and Reflex GYRO north seeking gyroscope tool. In 2021 HCH geologists reviewed the gyroscope tool's downhole survey types (continuous, multi-shot and over-shot) to ensure that the highest quality data was being ranked as priority 1 in the database.

Where possible the over-shot survey is used at 30m intervals downhole.

Minera Fuego downhole surveys were completed using a north-seeking gyro, although the details of the instrument type are not known.

10.2.18 Survey Validation

Routine 3D review of the drilling database was performed as part of drillhole survey validation, to detect any spurious survey measurements.

During the 2019/2020 programme, two holes (CRP0014 and CRP0038) did not have downhole surveys reported. CRP0014 experienced issues with the hole collapsing and needed steel casing downhole, preventing accurate surveys. CRP0038 surveys were not uploaded to the database but have been added subsequent to the resource estimation.

Overall, the surveys at Cortadera show that in general the dip dropped slightly with depth (i.e., steepened), and the azimuth swung to the right (i.e., increased). Drillhole deviations and corresponding down-hole sample locations are adequately measured; deviations are not considered to have any adverse impact on this resource estimate.

10.2.19 Hole Logging Procedures

Geological logging was recorded in a systematic and consistent manner such that the data was able to be interrogated accurately using modern mapping and geological modelling software programs. Field logging templates were used to record details related to each drillhole. All geological logging was completed by qualified and experienced company geologists. Collar, survey, sample register and sample condition, sample recovery data or comments (and commonly magnetic susceptibility) were recorded by a competent field technician.

All relevant procedures were taken from the Productora project and adjusted where necessary.

In 2021 an extensive review of the geological logging procedures was undertaken by HCH geologists under the supervision of Dr Steve Garwin to ensure all relevant data was being captured. Updates were made to the Alteration (Table 10.6) and Vein (Table 10.7) logging templates in order to best represent timing and overprinting relationships within the Cortadera porphyry system. All historic logs have been updated to be consistent with new logging classifications.

Table 10.6 Updated Alteration logging template following 2021 review

Timing	Type	Dominant mineral
Early	Potassic	Biotite present
Early	Clt-Propylitic	Chlorite (with little to no sericite)
Early	Ep-Propylitic	Epidote -Chlorite (with little to no sericite)
Early	Hornfels (bedding/texture preserved)	<i>Include mineralogy in alt min 1/2</i>
Early	Hornfels (bedding/texture destroyed)	<i>Include mineralogy in alt min 1/2</i>
Transitional	Anhydrite	Anhydrite dominant
Transitional	Intermediate Argillic	Sericite with chlorite
Late	Phyllic	Sericite no chlorite
Late	Argillic	Clays present
	Unknown	Unknown
	Unaltered	Unaltered

Table 10.7 Updated Vein logging template following 2021 review

Vein type	Vein compositions						Log type
M	Vmt						Present or Absent
EDM	Vbt	Vbtcp					Present or Absent
A	Vqz						Abundance (%)
B1 +B2	Vqcp	Vqpcp	Vqp	Vqm	Vqpm		Abundance (%)
C1	Vchp	Vch	Vchpyqz	Vqc			Present or Absent
C2	Vcppy	Vcp	Vpy				Abundance (%)
D + E	Vpy	Vqb	Vcbp	Vepchs	Vqpsr	Vcb	Present or Absent
Ep	Vep						Present or Absent
Ahn	Vanh						Present or Absent
Gyp	Vgy						Present or Absent

10.2.20 Reverse Circulation Logging

All RC holes were logged using the standard company logging codes, and washed chip samples stored in chip trays retained at the company's operational storage facility in Vallendar.

All diamond drill core was subjected to detailed lithological and structural logging prior to cutting (halving) and sampling.

Geological attributes logged in RC chips includes Colour, Weathering / Oxidation, Regolith, Lithology, Veining, Alteration assemblages and their intensities, Texture, Mineralogy and sulphides and their percentages.

10.2.21 Diamond Drill Logging

Core reconstruction and orientation was attempted in every drilling run and completed where possible before marking up or logging core.

Geological attributes logged in diamond core includes the same attributes as RC drilling, and additionally the following structural attributes:

- Linear structures e.g., Lineations
- Planar structures e.g., Shears, veins, dykes, faults, cleavage, joints/ fractures, schistosity

- Preliminary geotechnical features such as RQD and FRM
- All diamond drill core was captured with digital photography, and all core photos are retained on HCH's data servers.

10.2.22 Structural Logging

Core reconstruction and orientation was attempted in every drilling run and completed where possible before marking up or logging core. The following industry standard procedure was used and relates to bottom of hole (BOH) orientation marks:

- Rotate the mark to the top of the cradle (a 7m length of angle iron is used to cradle the core as orientation of core is completed) and reconstruct the core as far as it can be extended with confidence.
- Draw a line (omnichrome pencil is best) along from the mark. This line represents the lowermost line of the hole and is termed a bottom of hole (BOH) orientation line.
- Once core is orientated it is possible to collect orientated structural measurements. Generally, it is necessary to complete two measurements (α and β) to define each structural surface. The gamma angle can also be measured.
- “ α ” angle is the angle between the structural surface and the long core axis and is hence always between 0° and 90° . It is best measured using a clear protractor.
- “ β ” angle is the angle measured clockwise (looking down-hole) from the orientation line to the structural surface down-hole apex (i.e., the down-hole pointing toe position) and will range between 0° and 360° . Flexible, clear, plastic, 360° graduated strips are best for measuring angles.
- “Gamma” angle is the angle of line within the plane of the structure. Different conventions are in use for measurement.
- These measurements were recorded on the structural template for direct data entry and validation. The depth, and reliability of each orientation mark, as well as the depth of each structural measurement and the quality of orientation line extrapolation to that depth, was also recorded.

Downhole structural measurements are considered during the interpretation of stratigraphy, understanding vein paragenesis and are incorporated into the geological modelling process. As discussed in section 7.4.4 a review of the orientation of quartz veins within the Cortadera high grade copper zones was completed by Beeson (2021) with the understanding that changes in vein geometry may influence metal distribution, potentially amplifying other structural controls (e.g. quartz vein density). Alpha-beta measurements of quartz rich (A- & B-) veins were converted to dip – dip direction from HCH diamond drillholes.

Data was subset into intervals of approximately 100m downhole width and plotted to assess changes in gross quartz-rich vein geometry with depth. An example of this

analysis is shown in Figure 10.14, where the vein orientations of CRP0011D are shown downhole.

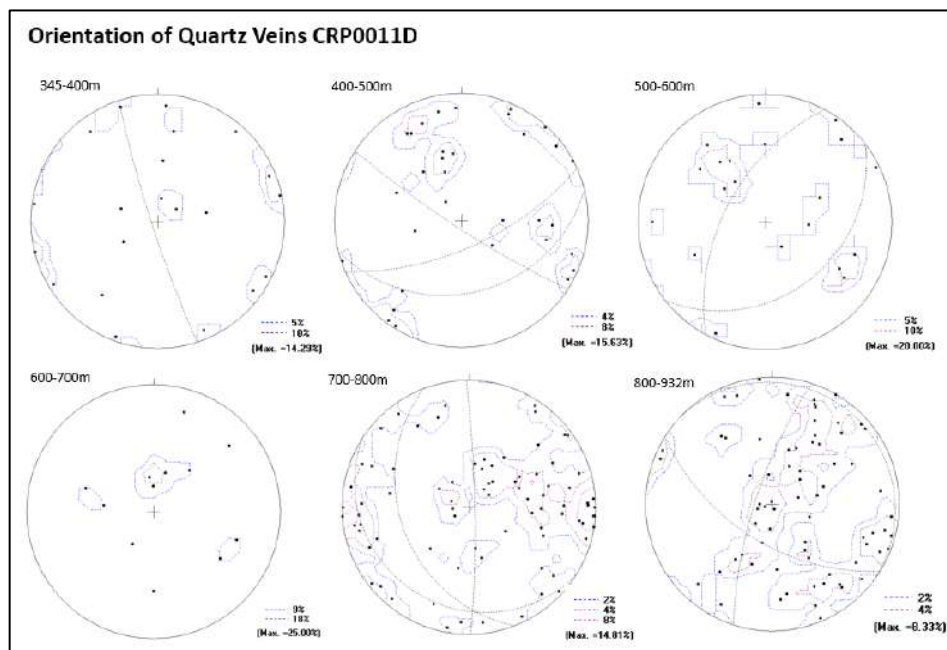


Figure 10.14 Orientation of quartz veins in diamond drillhole CRP0011D. Structural measurements are subset into intervals of approximately 100m downhole width (Beeson, November 2021)

10.2.23 Geotechnical Logging

Both RQD and Recovery measurements were taken using the orientation &/or cutting line from the mark up of the core. The following industry standard procedure was used on HCH drillholes at Cortadera:

- Measurements were recorded mainly on a 1m basis.
- Recovery was a measurement of the total amount of core between each metre. This will be 100% unless the core-block indicates otherwise. For example, if a core block shows 0.13 m core-loss (CL) then the percent recovered is 87%. Note that if core loss occurs in an interval of less than, or greater than one-metre it will have to be calculated using the formula's listed below.
- RQD %: Was calculated as all the pieces of core that were individually longer than 10cm are added up to give a percentage. For example, if there are three pieces of core in a one-metre interval that are over 10cm - 19cm, 17cm & 16cm - then the total RQD is 52%. If the interval is not equal to 1m then the RQD will have to be calculated using the formula below.

Core Recovery Calculations

For a one-metre core interval:

$$\begin{aligned}\text{Core Recovery} &= 100\text{cm} - \text{Core Loss (cm)} \\ &= 100 - 13 \\ &= 87 \%\end{aligned}$$

When the interval is less than or greater than one-metre core (130cm of core with 15cm of core loss):

$$\begin{aligned}\text{Core Recovery} &= \left(\frac{\text{Length of Interval} - \text{CL}}{\text{Entire Core Interval}} \right) \times 100 \\ &= \left(\frac{130 - 15}{130} \right) \times 100 \\ &= \left(\frac{115}{130} \right) \times 100 \\ &= 88.46 \%\end{aligned}$$

RQD Calculations:

$$\begin{aligned}\text{RQD}(\%) &= \left(\frac{\text{Total length of core pieces} \\ &\quad \text{independently greater than 10cm}}{\text{Entire Core Interval}} \right) \times 100 \\ &= \left(\frac{19+17+16}{100} \right) \times 100 \\ &= 52 \%\end{aligned}$$

A review of the HCH geotechnical logging procedures was completed in 2021 by Ingeroc. The review found the data to be adequate for identifying different geotechnical units. Recommendations from Ingeroc were to drill six additional diamond drillholes for geotechnical logging by geotechnical engineers in order to validate logging procedures further. Drilling of these holes is currently underway, and the results not yet compiled for this report.

No RQD and Fracture frequency data was captured by Minera Fuego on the historic dataset of 39 holes. In 2021 core imagery of the Minera Fuego drilling was supplied to Datarock Pty Ltd to extract the following information using their machine learning application:

- Cropped and depth registered imagery
- Fracture analysis (classification, spacing, joint set number, joint set roughness coefficient)
- RQD.

4 HCH drillholes (CRP0088D, CRP0047D, CRP0046D and CRD0080) were selected for a trial to compare the manually collected geotechnical data with the predicted data. The comparison found the Datarock method to collect a compatible dataset that can be used to effectively discern the downhole fracture frequency and RQD (Figure 10.4). The minor variance between the two datasets is attributed to:

- Depth registration discrepancies
- False positives in coherent mask predictions
- Human error in manual RQD collection.

Following this comparative exercise the algorithm was applied to all available Minera Fuego core photos. Some core trays were unable to be processed due to poor image quality (1 tray from FJOD-19, FJOD-32, FJOD-34, 10 trays from FJOD-35).

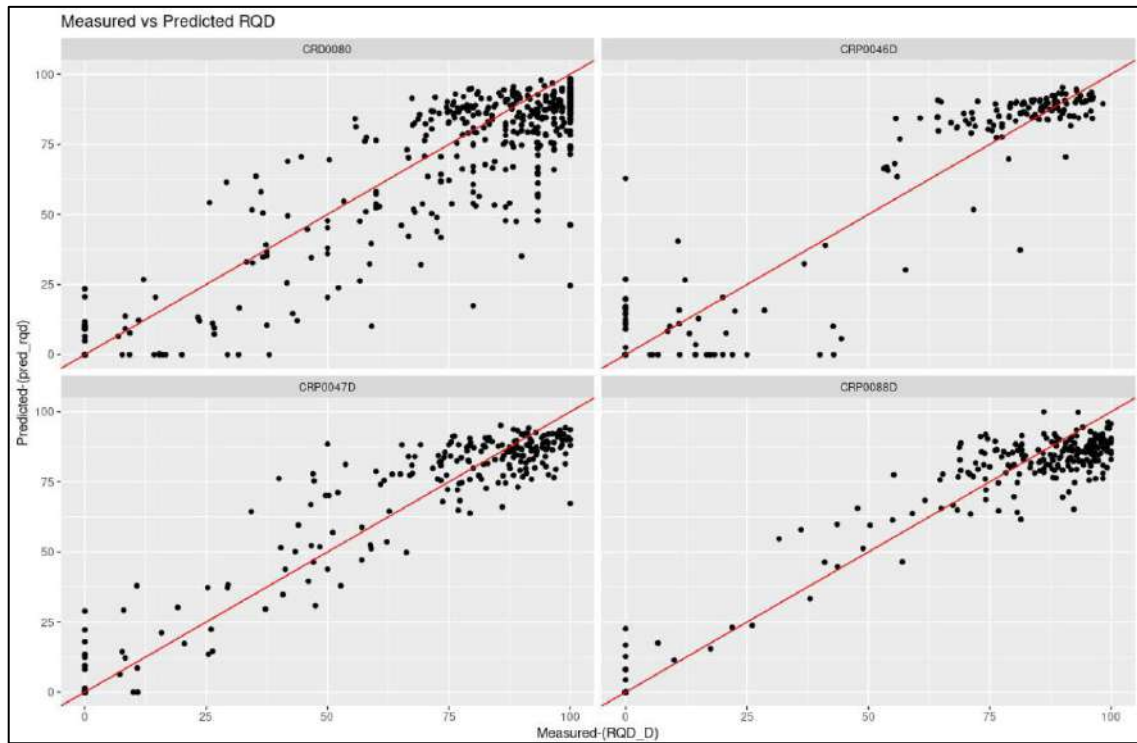


Figure 10.15 Comparison of Measured RQD vs Predicted RQD for CRD0080, CRP0046D, CRP0047D, CRP0088D (Datarock, 2021)

10.2.24 Dry Bulk Density

Cortadera has density data derived from diamond core. Minera Fuego and HCH conducted specific gravity testwork, with the techniques outlined in the section below.

A total of 762 bulk densities were available for the Cortadera Resource estimate.

One sample in every 15 samples of diamond core was submitted for bulk density analysis as performed by ALS (ALS Code OA-GRA09). Those samples are then labelled with the words 'Density test'. A total of 241 bulk density results were returned on the HCH core.

The test work was undertaken on an approximate 10cm piece of core taken from the designated sample bag and is used to determine the bulk density for the 1m interval. The bulk density test consists of using the Archimedean water submersion method of analysis; a description of the ALS technique is outlined below:

'Bulk density analysis on solid objects is carried out by weighing the object, then slowly placing it into a bulk density apparatus which is filled with water. The displaced water is collected into a graduated cylinder and measured. The bulk density calculation takes

into account the weight of the sample and the volume of water displaced; the result is expressed as g/cm³.

Once the bulk density measurement is complete, the 10cm length of core is returned to the sample bag ensuring the 1m interval is complete and intact prior to analysis for ME-ICP61'

10.2.25 Historical Dry Bulk Density Testwork

For Minera Fuego core, selected samples were submitted to Vigalabs for density test work. Although the Vigalabs company no longer exists to confirm the methods, the certificates provided confirms that the method used is a bulk density with paraffin coating.

The sample is initially weighed, then wax coated and then weighed again. It is then placed in water and the water displacement is measured.

The calculation used to measure bulk density is Weight of Sample (g) / Volume of sample (ml).

As part of the validation process, HCH sent additional FJOD series samples to ALS for OA-GRA09 analysis. These bulk density results were found to be comparable with previous result and are in line with density values typically associated with copper-gold porphyry deposits.

10.3 San Antonio

10.3.1 Hot Chili (2018 to Present)

In 2018, HCH drilled and sampled 41 reverse circulation drillholes at the project using reverse circulation methods (Table 10.8).

Table 10.8 Updated Vein logging template following 2021 review

Prospect	Number of holes	Metres (percussion)
San Antonio	41	4,922

10.3.2 San Antonio Resource Definition Drilling

San Antonio drilling completed in 2018 comprised 4,922m over 41 RC holes. The target was primarily the San Antonio Main Lode, with parallel hanging wall lodes also intersected, and San Antonio East and San Antonio South Targets. (Figure 10.14)

The drilling was mainly focused in the San Antonio main lode mineralisation, in the microdiorite target, to confirm the continuity of the lode below, and along strike of, the current underground mining operation. The majority of the holes were drilled beneath the existing small scale, privately-owned San Antonio copper mine.

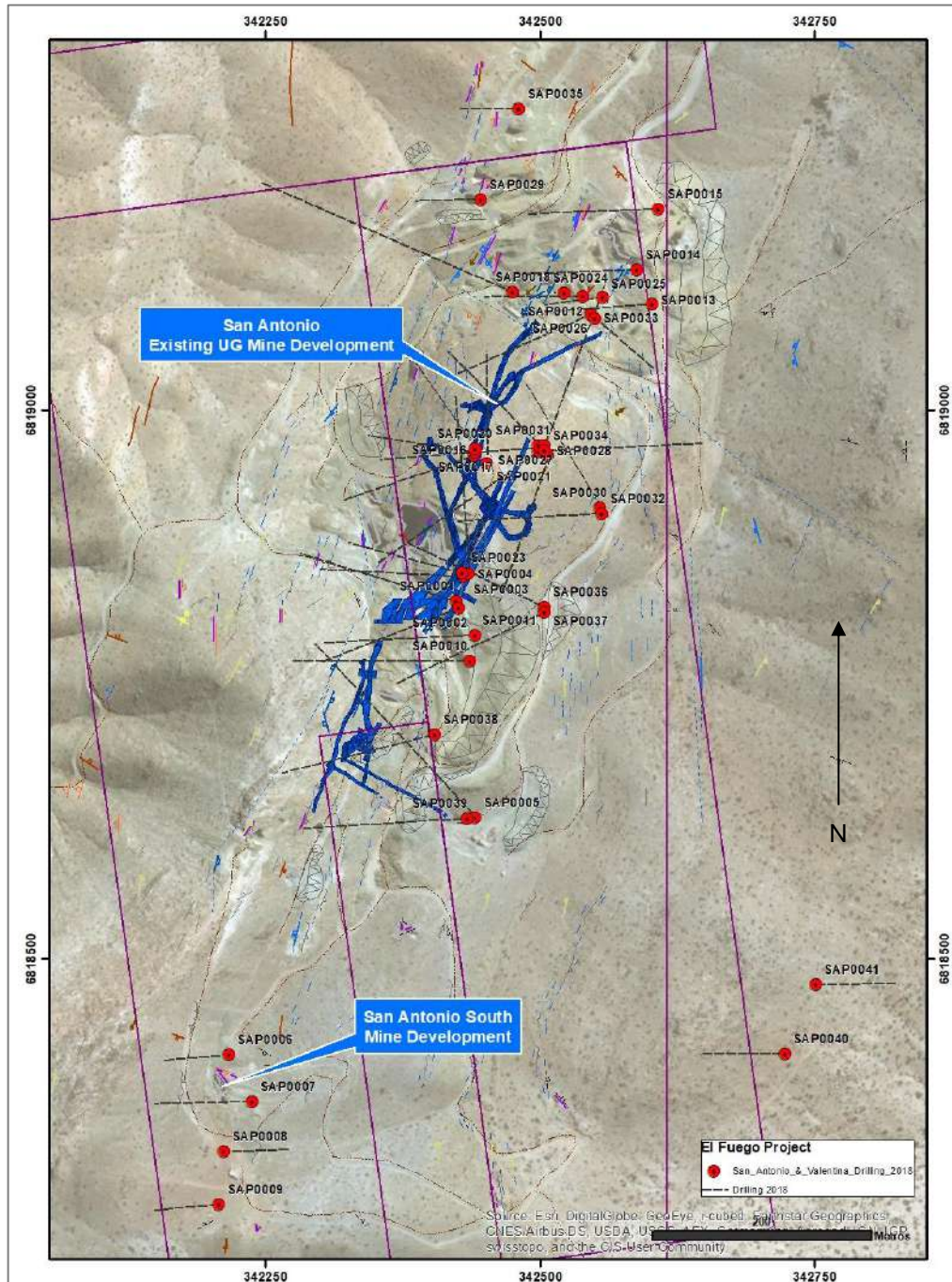


Figure 10.14 San Antonio RC Drill program hole locations relative to existing underground mine development.

Two drillholes were drilled to test the Parallel lode target, located west of the Main Lode diorite-hosted mineralization, which is exposed in a shallow pit as a ~3m wide copper-bearing fault zone. This mineralisation is associated with a suite of felsic dykes within the host structure and shallow dipping copper oxide manto hosted mineralisation is also exposed at surface.

In addition, two holes were completed in the San Antonio East Target, to test the potential of porphyry copper mineralisation and a flanking K-feldspar-tourmaline breccia zone in an area east of the Main Lode of San Antonio mine. Typical porphyry copper vein hosted mineralisation is observed at surface, outcropping in two small prospecting pits and nearby road cuttings. It is also defined in both regional and detailed soil sampling as a zone of elevated copper in XRF analyses.

10.3.3 Significant Drillhole Intercepts

Significant drillhole intercepts for HCH drilling at San Antonio are provided in Table 10.9.

Table 10.9 Significant drillhole intercepts for HCH drilling at San Antonio

HoleID	Prospect	Easting	Northing	RL	Drilling End		From	To	Interval (m)	Cu %	Au ppm	Ag ppm	Mo ppm	
					Date									
SAP0001	San Antonio	342422.35	6818828.073	1210.665	2-Jun-18		0	6	6	0.4	0.0	0.8	1	
							and	65	80	15	1.6	0.0	3.4	1
SAP0002	San Antonio	342424.25	6818824.332	1210.605	3-Jun-18		0	11	11	0.2	0.0	0.6	2	
							and	60	84	24	0.2	0.0	0.7	7
							and	85	90	5	2.0	0.0	4.2	2
							and	92	96	4	1.4	0.0	3.0	3
SAP0003	San Antonio	342428.41	6818852.732	1211.79	5-Jun-18		76	82	6	1.2	0.0	3.0	3	
SAP0004	San Antonio	342433.38	6818854.214	1211.65	6-Jun-18		77	88	11	0.3	0.0	1.3	1	
SAP0005	San Antonio	342435.11	6818626.765	1191.875	8-Jun-18		139	143	4	2.0	0.0	2.9	2	
SAP0010	San Antonio	342436.21	6818770.911	1209.07	13-Jun-18		0	12	12	0.2	0.0	0.3	2	
							and	20	24	4	0.3	0.0	0.3	3
SAP0012	San Antonio	342531.91	6819104.306	1151.07	15-Jun-18		0	8	8	0.3	0.0	0.4	1	
							and	12	30	18	1.0	0.0	2.9	1
							including	18	30	12	1.4	0.0	3.8	1
SAP0017	San Antonio	342437.14	6818963.992	1218.414	21-Jun-18		27	46	19	0.2	0.0	0.5	1	
SAP0018	San Antonio	342473.46	6819110.758	1165.116	22-Jun-18		12	17	5	0.9	0.0	2.0	2	
SAP0019	San Antonio	342496.07	6818967.2	1201.124	2-Jul-18		58	68	10	1.6	0.0	3.2	1	
SAP0020	San Antonio	342439.04	6818967.634	1218.43	2-Jul-18		28	55	27	0.3	0.0	0.6	1	
SAP0021	San Antonio	342448.34	6818956.881	1218.783	3-Jul-18		31	70	39	1.0	0.0	2.6	2	
							including	31	36	5	2.5	0.0	9.3	2
							and including	56	70	14	1.6	0.0	3.4	2
SAP0022	San Antonio	342496.42	6818965.053	1201.123	4-Jul-18		83	94	11	1.6	0.0	11.1	1	
SAP0023	San Antonio	342428.8	6818854.786	1211.876	5-Jul-18		65	72	7	1.8	0.0	2.8	2	
SAP0026	San Antonio	342540.53	6819086.832	1149.281	6-Jul-18		51	56	5	1.3	0.0	5.1	-	
SAP0028	San Antonio	342499.72	6818961.21	1201.301	7-Jul-18		48	109	61	0.3	0.0	0.9	1	
							including	93	109	16	1.1	0.0	2.7	1
SAP0029	San Antonio	342446.3	6819194.959	1195.277	8-Aug-18		0	5	5	1.1	0.0	2.6	1	
SAP0030	San Antonio	342554.78	6818913.068	1177.762	9-Jul-18		63	72	9	0.2	0.0	0.7	3	
SAP0031	San Antonio	342502.06	6818970.892	1201.179	9-Jul-18		59	151	92	0.6	0.0	1.9	1	
							including	60	99	39	1.0	0.0	3.1	1
							and including	119	128	9	1.2	0.0	3.0	1
SAP0032	San Antonio	342552.8	6818907.942	1178.079	10-Jul-18		93	115	22	1.0	0.0	1.7	2	
SAP0037	San Antonio	342501.25	6818817.883	1183.65	13-Jul-18		110	117	7	0.2	0.0	1.0	2	
SAP0038	San Antonio	342403.89	6818704.517	1212.53	13-Jul-18		93	127	34	0.4	0.0	1.0	1	
							including	93	97	4	2.7	0.0	5.8	1
SAP0040	San Antonio	342722.06	6818414.866	1214.754	16-Jul-18		42	49	7	0.2	0.0	0.9	8	

10.4 Drilling Procedures

All drilling commissioned by HCH for the San Antonio Resource estimates was conducted by Blue Spec Sondajes (Bluespec).

All drill rigs are Exploration Drill Masters-type (EDM) and configuration is as follows:

- Custom built EDM2000 and 1200 High-Capacity Multi-purpose RC and DD rigs
- These rigs were supported by an Atlas Copco Hurricane B4-41/ 750 Booster compressor and a Sullair Air Compressor Model 1150/900
- The drilling rigs were manned by Australian or Australian-trained Chilean drillers and well-trained local drilling offsideers. All the custom-built drill rigs used during the programme were convertible to either RC or diamond core drilling.

The drilling was undertaken on established platforms that provided adequate space for drilling and sampling equipment. Booster pressure during RC drilling was high (700-800 psi) which allowed fair sample return and penetration rates. As a standard, on-drill sampling equipment consisted of a cyclone unit for pressure release and sample collection, and a static cone splitter to sub-sample the collected sample. The cyclone and cone splitter's vertical position was monitored using a spirit level to minimise any potential sample bias. Drillholes were down-hole surveyed immediately following drilling completion.

10.4.1 RC drilling tools

RC drilling utilised a face sampling down-hole hammer with cyclone sample recovery. Drill hammers used were 542/543, PR 54 (Sandvik) and MR 120 (Mincon).

Adjustments to drill bit size were made as drillholes reached certain intervals, to ensure successful end of hole depths. Changes to bit sizes were recorded in drill plods (Table 10.10).

Table 10.10 Nominal drill bit size changes in RC drilling

Bluespec bit size changes	
Depth	RC Bit Size
0m - 200m	140mm
200m - 320m	137mm
320m - 450m	133mm
> 450m	130mm

10.4.2 Hole Planning and Set-up

The HCH RC drill program resulted in approximately 40m x 40m spacing along strike and between 40m x 40m and 80m x 80m spacing up and down dip of the mineralised diorite unit. Historic drilling includes underground channel and sludge drilling, providing localised drill spacing down to 20m spacing. Drill spacing has the highest density around the old underground workings. Broader spacing of approximately 300m x 300m covers the modelled extensions of the diorite unit.

Topography plays a major role in hole planning at San Antonio, with steep slopes limiting access to much of the near-surface resource.

10.4.3 Naming Convention and Meta Data Management

Holes drilled used the following labelling system:

- HCH holes drilled by RC at San Antonio were prefixed with 'SAP', followed by the hole number
- Holes not drilled by HCH have various naming conventions, however the hole meta data is captured in HCH's geological database.

10.4.4 Geological Database

As per the Productora section. A single Acquire database captures all HCH data.

10.5 Surveying and Orientations

10.5.1 Collar Surveying

Collar surveys were undertaken by contract survey company TopGeo Ingenieria Limitada in 2019 with the following methodology utilised for the survey.

- For San Antonio, the base station was "HM NITE 1 AL 40. Base stations were located in the PSAD 56 coordinate reference system. These co-ordinates were later transferred to the Datum WGS84, and the was undertaken within a polygon area, followed by measurement of drillhole collars
- Measurement with Geodesic GPS of High Precision brand CHCNAV model i80 and Landstar 7
- Each collar was measured using average consecutive measurements per drillhole in Static Real Time system (not kinetic).

Collar surveys were reported in a table to HCH and imported to the Acquire database.

Historic drill collars and surface sample locations were provided to the Company as part of a data compilation and appear to have been provided in the PSAD56 UTM coordinate system. These were transformed by the company to WGS84 UTM zone 19S via the following method (PSAD easting minus 184.13m, PSAD northing minus 375.38m). This shift is considered appropriate for the project location.

10.5.2 Collar Validation

Validation of collar survey locations was completed by:

- Visual checking of collar points against the topographical elevation model
- Some collars were validated in the 2021 drone survey project

10.5.3 Downhole Surveying

Downhole surveying at San Antonio for HCH's 2018 RC drilling was completed by Bluespec drilling contractor using the Axis Champ Navigator north seeing gyroscope tool post hole completion.

10.5.4 Survey Validation

Routine 3D review of the drilling database was performed as part of drillhole survey validation, to detect any spurious survey measurements.

10.5.5 Hole Logging Procedures

Geological logging was recorded in a systematic and consistent manner such that the data was able to be interrogated accurately using modern mapping and geological modelling software programs. Field logging templates were used to record details related to each drillhole. All geological logging was completed by qualified and experienced company geologists. Collar, survey, sample register and sample condition, sample recovery data or comments (and commonly magnetic susceptibility) were recorded by a competent field technician.

All relevant procedures were taken from HCH's Productora project and adjusted for the specifics of the San Antonio deposit style where necessary.

10.5.6 Reverse Circulation Logging

All RC holes were logged using the standard company logging codes, and washed chip samples stored in chip trays retained at the company's operational storage facility in Vallenar.

Geological attributes logged in RC chips includes Colour, Weathering / Oxidation, Regolith, Lithology, Veining, Alteration assemblages and their intensities, Texture, Mineralogy and sulphides and their percentages.

10.5.7 Diamond Drilling Logging

At the time of this report, no diamond drilling has been completed at San Antonio.

Diamond drill programs are planned in future phases of mineral resource definition, to deliver greater information on structure within the geology and mineralisation, geotechnical logging and material testing, density testing, and metallurgical testwork.

10.6 Dry Bulk Density

At the time of this report, no bulk density samples have been collected for San Antonio.

11 SAMPLE PREPARATION, ANALYSES AND SECURITY

11.1 Introduction

The following provides a summary of HCH's reverse circulation (RC) and diamond sampling, splitting, sample security, geological logging and laboratory analytical techniques. The processes and resulting sample analysis are deemed adequate by the Qualified Person for the Mineral Resource for inclusion in the Mineral Resource Estimate.

It is relevant for all deposits included in the Costa Fuego Mineral Resource.

11.2 RC Sampling Methods

All RC samples were collected from the drilling rig by Blue Spec (drilling contractor) employees. A fixed cone splitter was used to create two nominal 12.5% samples (Sample "A" and "B"), along with the large bulk reject sample. The "A" sample is always taken from the same sampling chute, and comprises the primary sample submitted to the laboratory. The "B" samples were retained for use as the field duplicate sample. The coarse residues were collected into large plastic bags and were retained on the ground near the drillhole collar, generally in rows of 50 bags.

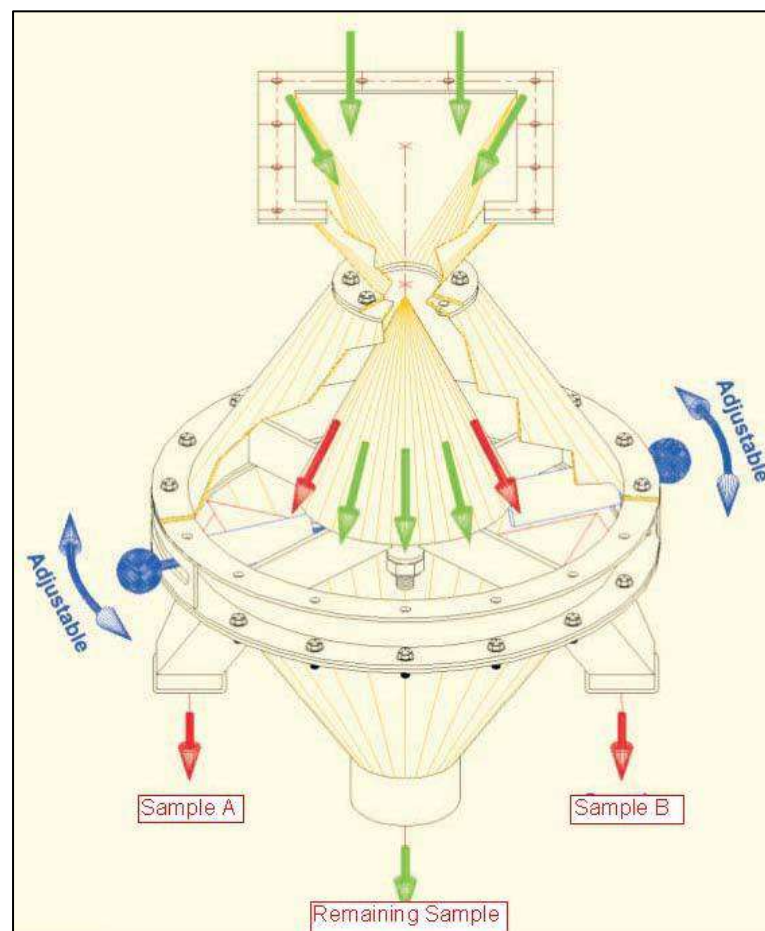


Figure 11.1 Idealised diagrammatic illustration of a cone splitter

All RC drillhole sampling was executed at one metre intervals by HCH employees. Within logged mineralisation zones, the 1m sample (“A” sample) was submitted. Outside the main mineralised zones (as determined by the logging geologist), 4m composite were created from scoops of 1m sample residues over this interval. The composited 4m samples were analysed first and if required, the individual and original 1m “A” samples comprising this 4m interval were sent for analysis. This ensured that no mineralisation was missed while minimising analytical costs.

11.3 DD Sampling Methods

All DD samples were collected from the drilling rig by Blue Spec (drilling contractor) employees. At Productora, the majority of diamond core has had systematic whole core sampled at one metre intervals by HCH employees. Whole core was chosen as the preferred sampling method to ensure a larger and more representative sample for analysis. This was based upon the nature of the porous and brecciated mineralisation. Some core has been half cored or completely retained for geological reference.

At Alice, all diamond core was systematically half core sampled at one metre intervals. The decision to retain half core was based upon a generally more homogenous style of mineralisation and, typically, more coherent core samples. The retained half core is available for future reviews, QA/QC sampling and geological reference.

At Cortadera, the majority of diamond core has had systematic half-core sampled at two-metre intervals by HCH employees. Half-core was chosen as the preferred sampling method to ensure a representative sample was submitted for analysis, while also retaining half-core for review of lithology and mineralisation, and for further test work as required.

Prior to the cutting and sample process, two additional samples are also taken for Cortadera being Density and Geotechnical samples.

- Density samples are selected every 30m if the geological conditions allow it and are provided to the laboratory for testwork.
- Geotechnical samples are taken for tests including triaxial (one sample per 250m) and uniaxial tests (one sample per 50m).

No diamond drilling has been completed at San Antonio.

11.4 Relationship between sample length and thickness

No relationship between sample length and true thickness of the mineralisation is known for Productora; due to the complex mineralisation observed, the true thickness of individual higher-grade lodes at Productora varied considerably across the deposit.

No relationship between sample length and true thickness of the mineralisation is known for Alice.

No relationship between sample length and true thickness of the mineralisation is known for Cortadera. Mineralisation tenor and distribution is consistent with that seen in similar

porphyry copper-gold-molybdenum deposits, a strong correlation with quartz veining and associated chalcopyrite.

The thickness of the San Antonio deposit varies from the minimum sample length of 1m to over 30m wide. Mining activities have concentrated in areas of increased thickness, and as no diamond drilling has been completed at San Antonio, it is not possible to determine the minimum width of the lodes in areas where they may be less than 1m thick.

11.5 Impact of significantly higher-grade intervals

Given the nature of the mineralisation at Cortadera, Productora, and Alice, this is not a factor when considering drilling or sample preparation.

At San Antonio, HCH have lessened the impact of significantly higher-grade intervals in the sampling program through the selection of a 1m sample interval. Any outlier grades will be top cut during the estimation of the resource.

11.6 Historical Work

There is no record of procedures employed by Minera Fuego for their drilling, sampling, and logging at Cortadera. The remaining half-core has been obtained by HCH and validation work completed suggests reasonable correlation exists.

To the Company's best knowledge, the historic drilling results for San Antonio provided in this report were drilled by ENAMI circa 1968/69, by a small percussion machine, with pulverised material collected for each 1m sample length. Method or quality of sampling or splitting in the field or at the laboratory is unknown.

11.7 Chain of Custody and Transport

Once assigned a sample number, individual samples to be sent to ALS laboratories were sealed using a staple gun and accompanied by three identical sample tickets (one stapled to plastic bag to identify any tampering/breakage of seal prior to opening at the laboratory in preparation and another placed in the bag). Any broken staple seals on samples were to be notified by ALS to HCH. No sealed bags were reported as being opened or broken by ALS.

For both RC and diamond samples, sample bags were placed inside larger plastic bags and delivered by a dedicated truck to the ALS analytical laboratory in Coquimbo (Chile) for sample preparation and routine analysis.

Following analysis at ALS, the RC and diamond drilling coarse rejects were returned to site and stored in sequence in plastic bags under shade cloth next to the La Productora site camp. The laboratory pulps were returned and stored at the HCH site camp and stored in organised, dry and safe storage containers.

HCH has strict chain of custody security procedures for all samples sent to and from the analytical laboratories.

11.8 Assay Sample Preparation

The ALS analytical laboratory in Coquimbo (Chile) and Lima (Peru), completed all analytical assays and specific gravity test work for the Productora samples used in this Resource estimate.

Periodic inspections of the laboratory facilities and meetings with ALS staff have been conducted since drilling commenced at Productora. Inspections of the laboratory facilities have found them to be of a suitable standard. Any concerns HCH may have had regarding laboratory practices or equipment, or unexpected results, has been openly discussed with ALS and rectified at the earliest opportunity.

The ALS analytical laboratory in Coquimbo (Chile) completed all sample preparation and specific gravity test work, while ALS Santiago (Chile) completed all gold analysis, and ALS Lima (Peru) completed all other multielement analysis for the Cortadera assays used in the Resource estimate.

Periodic meetings with ALS staff have been conducted prior to drilling commencing at Cortadera.

HCH has implemented rigorous sample preparation and analytical procedures for both RC and diamond core samples, following consultation with ALS in Chile, to ensure high-grade assays were reported with a high degree of confidence and a wide range of appropriate commodities were assessed.

A summary of the sample preparation (ALS Code Prep 31b) procedures is provided below:

- Crushing of RC and whole-core samples such that a minimum of 70% is less than 2 mm:
 - to obtain whole diamond core sample duplicates, selected crushed core samples were split into two halves, with one half flagged as the original sample and the other half flagged as the duplicate sample.
 - empty numbered bags were inserted at the standard duplicate interval by HCH's geologists to indicate the requirement for a duplicate. (Note: RC duplicates were collected at a rate of approximately 1 in 50m.)
- Splitting out via a riffle splitter/rotary splitter of approximately 1 kg of the crushed product for pulverising such that a minimum of 85% passes 75 um and the remainder was retained as coarse reject material.
- The analytical pulp was extracted from the finely pulverised and homogenised product.
- Initial analysis was by ALS Method ME-ICP61, with additional analytical stages triggered when results met certain criterion. These criteria are:
 - Samples with results of >1,000 ppm Cu were analysed for Au by ALS Method Au-ICP61 (upper limit 10 ppm Au)
 - Samples with results >10,000 ppm Cu were analysed by "ore grade" method Cu-AA62 (upper limit 40% Cu).

- ALS Method ME-ICP61 involves four-acid digestion (Hydrochloric, Nitric, Perchloric, Hydrofluoric) followed by ICP-OES determination.
- ALS Method ME-MS61 involves the same or a similar digestion, with the analytical step by ICP-MS. Mass Spectrometry achieving lower detection limits for some of the elements.
- Method Au-ICP21 is a 30 g lead-collection fire assay, followed by ICP-OES to a detection limit of 0.001 ppm Au.
- Method Cu-AA62 is four-acid digestion, followed by AAS measurement to 0.001% Cu.

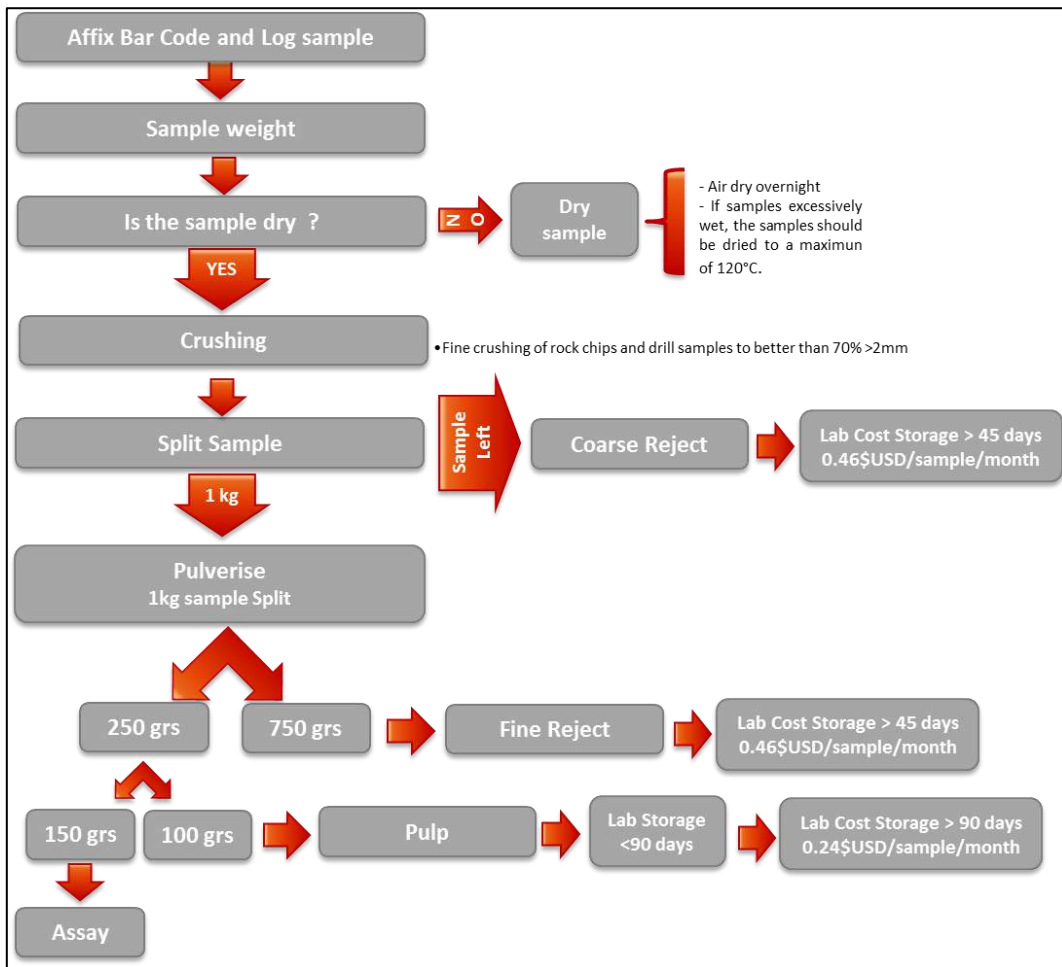


Figure 11.2 Flow chart of sample preparation.

11.9 Minera Fuego

Analytical work by Minera Fuego was conducted over three laboratories: Activation Labs (ACTLAB), ALS and Andes Analytical Assay (AAA) between 2011 and 2013.

- FJOD-01 to FJOD-09 were analysed by ACTLAB
- FJOD-10 to FJOD-24 were analysed by ALS
- FJOD-25 to FJOD-39 were analysed by AAA.

Minera Fuego supplied a full assay spreadsheet outlining the sample details including QAQC standards, blanks and duplicates with analytical result and laboratory batch details. Of the 10,949 primary assays received 7,727 (70.6%) have original lab datafiles to verify the source spreadsheet.

No assessment of laboratory standards and practises have been undertaken by HCH for the Minera Fuego drill results.

- Lab preparation methods employed by the three laboratories used by Minera Fuego has not been documented
- ACTLAB method ARMS is a 3-acid digestion followed by a Mass Spectrometry (MS) finish to a detection limit of 0.01 ppm Cu
- ACTLAB method 3ACID-AAS is a 3-acid digestion followed by Atomic Absorption Spectroscopy (AAS) to a detection of 0.001 % Cu
- ACTLAB method FA-AAS is a 30-gram lead-collection Fire Assay, followed by Atomic Absorption to a detection of 0.01 ppm Au
- Samples sent to ALS were routinely analysed by AA61 and with additional Cu AA62 analysis undertaken on samples > 10,000 ppm Cu
- ALS method AA61 is a 4-acid digestion (HF-HNO₃ -HClO₄ digestion, HCl leach) with Atomic Absorption Spectroscopy (AAS) finish to a detection limit of 1 ppm Cu
- ALS method AA62 is four-acid digestion (HF-HNO₃ -HClO₄ digestion with HCl leach), followed by AAS measurement to 0.001% Cu
- ALS method AA23 is a Fire Assay followed by AAS to a detection of 0.005 ppm Au
- AAA method 4AHF is a 4-acid near total digestion, followed by atomic absorption to a detection of 0.01% Cu
- AAA method ICP-AES is an Inductively coupled plasma atomic emission spectroscopy analysis to a detection of 1 ppm Cu
- AA method AEF

Where analysis returned results below detection limit, these have been set in the database to show the value as half the detection limit of that method. Results that are returned as over range are set as the upper detection limit.

These database rules apply to both HCH or Minera Fuego samples.

11.10 QAQC Program

HCH utilised several multielement mineralised “standards” (certified reference material or CRM) and two certified “blank” samples supplied by Ore Research & Exploration Pty Ltd. The standards used by HCH for QAQC are packaged as 60 g pulp bags (Figure 11.3).

One mineralised standard was chosen at random and inserted every 50th metre into each batch of samples submitted for analysis. The reference material type and grade ranges for the CRM standards used for QAQC correspond to the rock type and mineralisation grades (copper, gold and molybdenum) routinely encountered within the Project. These standards enable checks on analytical accuracy.

One unmineralised “blank” was inserted every 100th sample submitted for analysis. These blanks enable checks on any potential analytical contamination.

As company practise, the lab is to be notified of any instance when a certified reference standard or blank returns a value outside three standard deviations. If this occurs, typically the 10 preceding and 10 following samples from the CRM are requested to be re-assayed by the laboratory. This is undertaken to check for any potential smearing or sample contamination.

HCH submits its own coarse blanks (as distinct from the HCH-submitted ‘blank’ pulp), as pulp CRMs bypass and as such do not check most of the initial sample preparation process in the laboratory. The submission of coarse blank material allows investigation of any potential crushing and milling bias. The coarse blank samples were inserted at the geologist’s discretion with an emphasis on placement visual high-grade zones as well as being inserted at the start and end of a batch.

In addition to the above HCH steps, ALS process their own quartz blank at the start and end of sample batches for their own internal QA/QC purposes.

To date, there have not been any instances of complete batch rejections.

Minera Fuego supplied their QAQC data, and where possible, certificates for CRM (standards) have been found and parameters applied in the database. The origins of the blank used throughout the FJOD drilling was not specified as a certified/pulp or unmineralised coarse material. Minera Fuego also analysed field duplicates and undertook umpire laboratory checks.



Figure 11.3 Pulp bag containing certified reference material (image from sampling procedure)

11.11 Conclusions

The results from HCH's QAQC analysis, as well as RC vs Diamond drillhole twinned analysis, provides a high level of confidence in the precision and accuracy of the assays used for the Costa Fuego Mineral Resource estimation.

Sample lengths, preparation and assay techniques are considered suitable for the styles of mineralisation and deposit types present at Costa Fuego.

12 DATA VERIFICATION

12.1 Productora

12.1.1 Independent Qualified Person Review and Verification

AMC Consultants were engaged on a fee basis to conduct a peer review and external audit of the Productora Resource estimate.

A representative of AMC Consultants visited the Productora area in late September/early October 2014 as part of an independent site review, as well as completing an audit of the ALS preparation laboratory facilities in La Serena, Chile. AMC Consultants had access to the data, models and reports referred to in this report, and were involved in reviewing the Resource estimation process and inputs. As no significant additional drilling has been completed since the AMC audit, their findings remain current.

Subsequent verification of the Productora database was completed by the QP in 2021, during review of the Productora Mineral Resource Estimate.

12.1.2 Assay Standards

HCH utilised several main multi-element mineralised “standards” (certified reference material (CRM)) and one certified “blank” supplied by Ore Research & Exploration Pty Ltd. The standards used by HCH are packaged as small 60g pulp bags.

One mineralised standard was chosen at random and inserted every 50th sample into each batch of samples submitted for analysis. The reference material type and grade ranges for the CRM standards correspond to the rock type and mineralisation grades routinely encountered within the HCH projects. These standards enable checks on analytical accuracy.

One unmineralised certified “blank” was inserted every 100th sample submitted for analysis. These blanks enable checks on analytical contamination.

The lab was notified in any instance of a CRM standard or blank returning a value outside three standard deviations, and typically the 10 preceding and 10 following samples from the CRM were re-assayed. This was undertaken as a check on any potential smearing or other such sample contamination.

To date, there have not been any instances of complete batch rejections.

QA/QC samples and their insertion rates (IR), as a percentage of the 174,476 samples from all HCH Project drilling to date are:

- 3,081 certified mineralised pulp standards “CRM”, IR = 1.8%
- 830 certified “blanks” pulp standards, IR = 0.5% (note; use of these began at the beginning of 2013)
- 954 coarse blanks, IR = 0.5% (note; use of these ceased at the beginning of 2013 and restarted during the 2014 drilling campaign)

- 4,860 coarse (RC and diamond drilling) duplicates, IR = 2.8%.

12.1.3 Certified Reference Material – Mineralised

There have been 3,081 mineralised CRMs inserted in the 174,476 samples taken at the project, at an insertion rate of 1.8% of sampling.

The assay results from submitted CRMs show acceptable correlation with their expected value without any fatal analytical drift over time (Figure 12.1 to Figure 12.3).

There were no returned values outside three standard deviations for copper, molybdenum, or gold.

QAQC reviews conducted by HCH indicated improvement in the overall insertion rates (and placement) of QA/QC standards was required. The insertion of “blanks” targeting specific intervals of mineralisation is desirable to test preparation smearing, and the submission of additional standards in any umpire laboratory check. In 2014, this was partly addressed by the addition of coarse blank material inserted into visual high-grade intervals.

Another recommendation of the QAQC review is to formalise company procedures, with routine data reviews into the use of standards and blanks, and subsequent actions formalised the instance of any standard or blank analytical result “failures”. In 2014, monthly QA/QC reports created to track lab performance. This improved tracking of any laboratory issues.

The following graphs are from the 2014/2015 drilling campaigns.

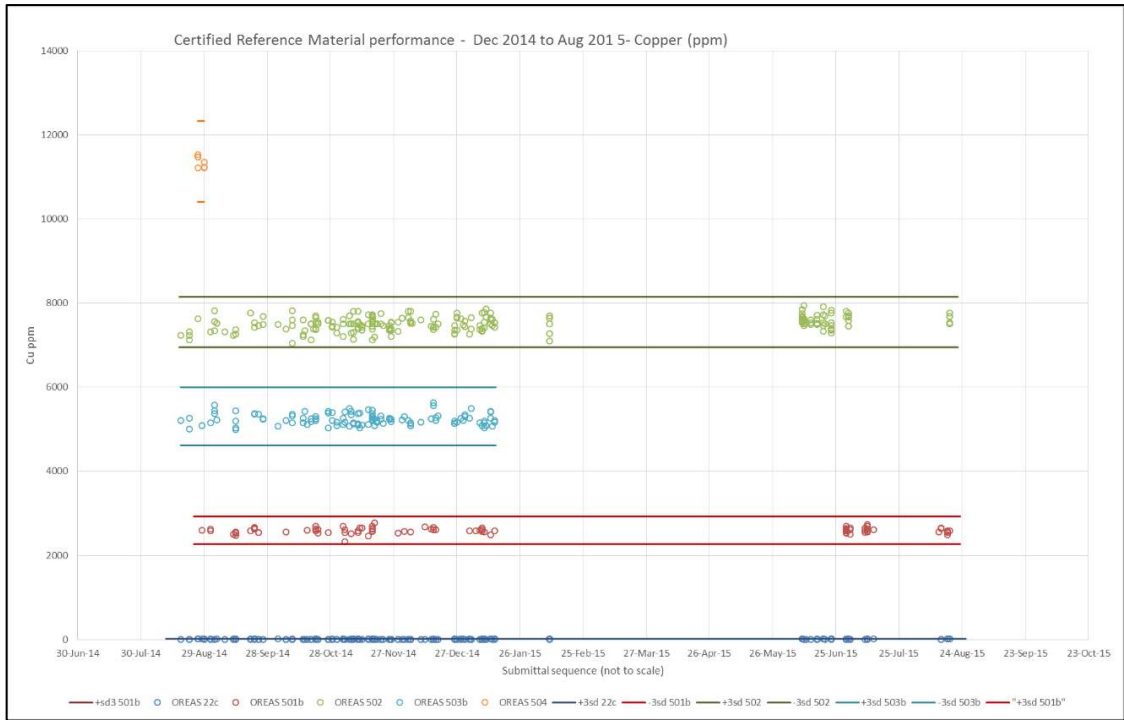


Figure 12.1 CRM performance from 2014/2015 – Cu%. Note: Upper and lower lines represent three standard deviations

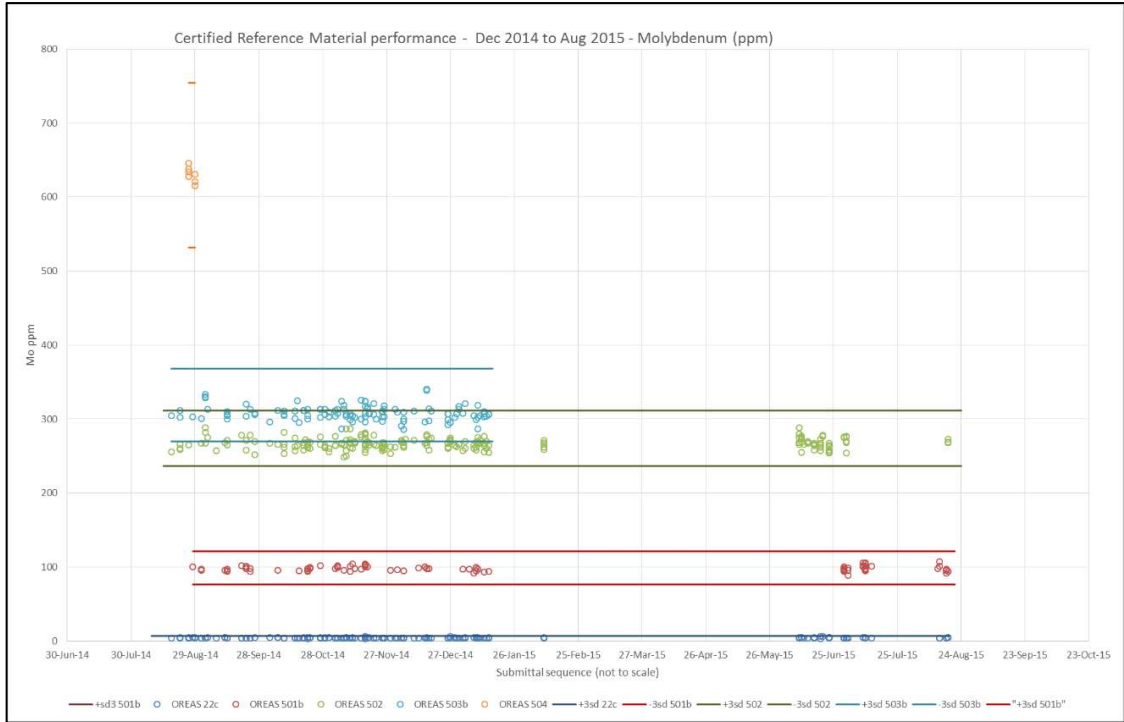


Figure 12.2 CRM performance from 2014/2015 – Mo ppm. Note: Upper and lower lines represent three standard deviations



Figure 12.3 CRM performance from 2014/2015 – Au g/t. Note: Upper and lower lines represent three standard deviations

12.1.4 Certified Reference Material – Non-mineralised (“Blank”)

There are 830 “blank” CRMs inserted in the 174,476m of samples taken at the project, at an insertion rate of 0.5% of sampling. Insertion of blanks only began in 2013, which has resulted in the low insertion rate.

During the 2014/2015 drilling program, HCH regularly reviewed the monthly QA/QC performance. The October QA/QC update highlighted that the thresholds for the “blank” CRM (22c) needed to be reviewed and was also recommended by the ALS laboratory manager. The previous HCH threshold was based on the three standard deviations based on OREAS certified tolerance values. The OREAS certified tolerance values are based on seven laboratories with six samples tested at each (42 samples in total).

A review was undertaken by HCH and was based on 720 samples submitted to ALS between 27 May 2013 to 29 November 2014. The following observations and decisions were taken.

Molybdenum:

- The previous OREAS certified three standard deviation upper threshold is given as 5.2ppm.
- The reviewed HCH data gave a three standard deviation upper limit of 6.59ppm.
- For practical implementation, this was rounded to 7ppm to be used as the revised upper threshold limit. This limit appeared to be robust.

Copper:

- The previous OREAS certified three standard deviation upper threshold is given as 13ppm.
- The reviewed HCH data gave a three standard deviation upper limit of 17.82ppm.
- Again, for practical implementation, this was rounded to 18ppm as the revised upper threshold limit. While there were some outliers still presenting in the dataset, this value appeared robust.

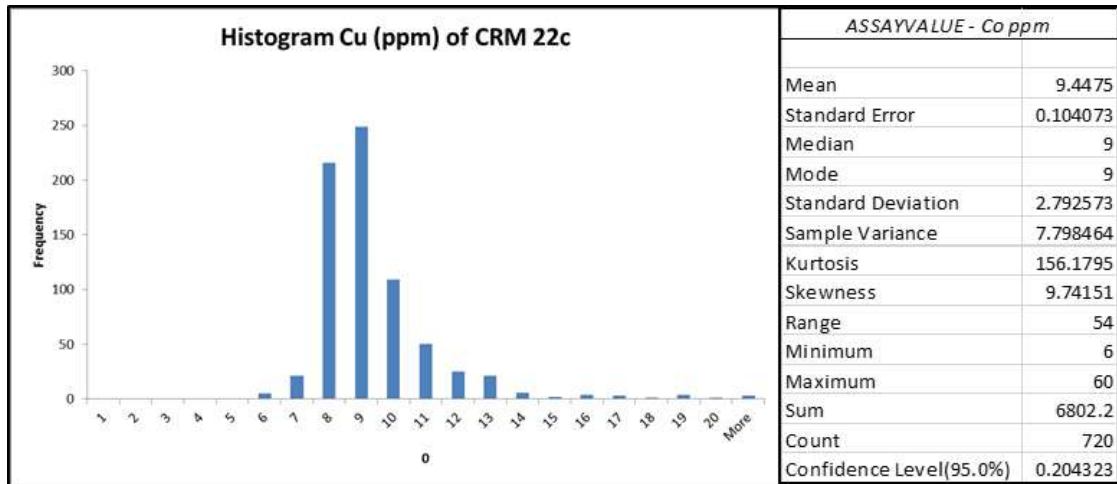


Figure 12.4 Review of certified “blank” material for copper during the 2014/2015 program

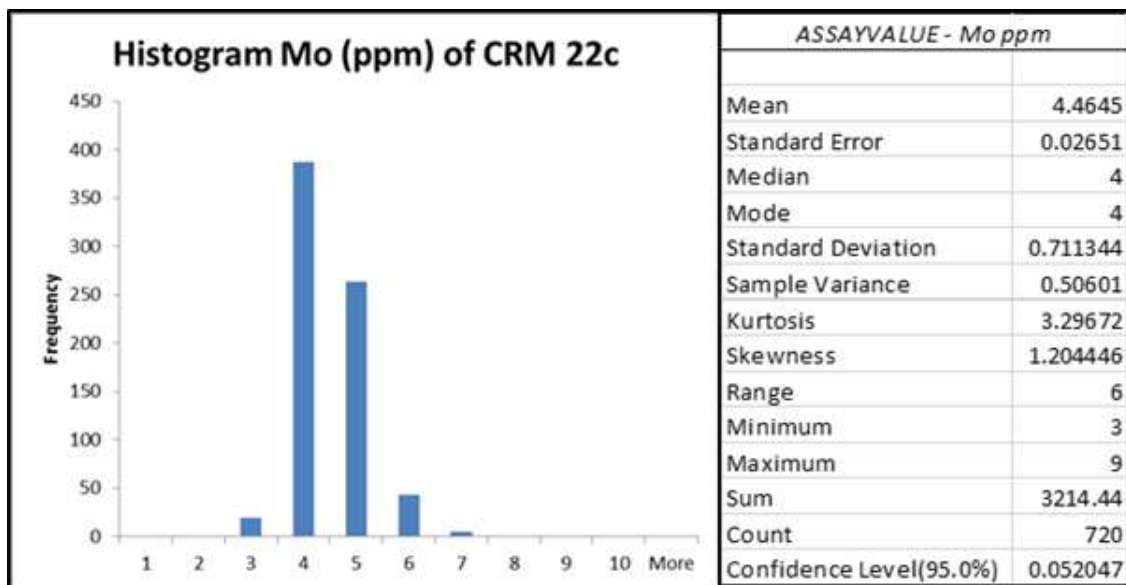


Figure 12.5 Review of certified “blank” material for molybdenum during the 2014/2015 program

Within the dataset, there are some instances where returned assay values lie outside the expected threshold. The largest copper outlier returned was of less than 20ppm Cu (Figure 12.6). While these were above the define threshold, they were of sufficiently low grade and imply negligible analytical contamination. These outliers (and their respective batches) were considered to have no adverse impact on batch results.

Results returned from the blank reference material were generally well within an acceptable tolerance supporting confidence in the laboratories cleanliness, sample preparation procedures and subsequent assay results determined. Blank sample results highlight there is little evidence of sample contamination/smearing at the analytical stage.

There were no outliers for Molybdenum for the 2014/2015 drilling program.

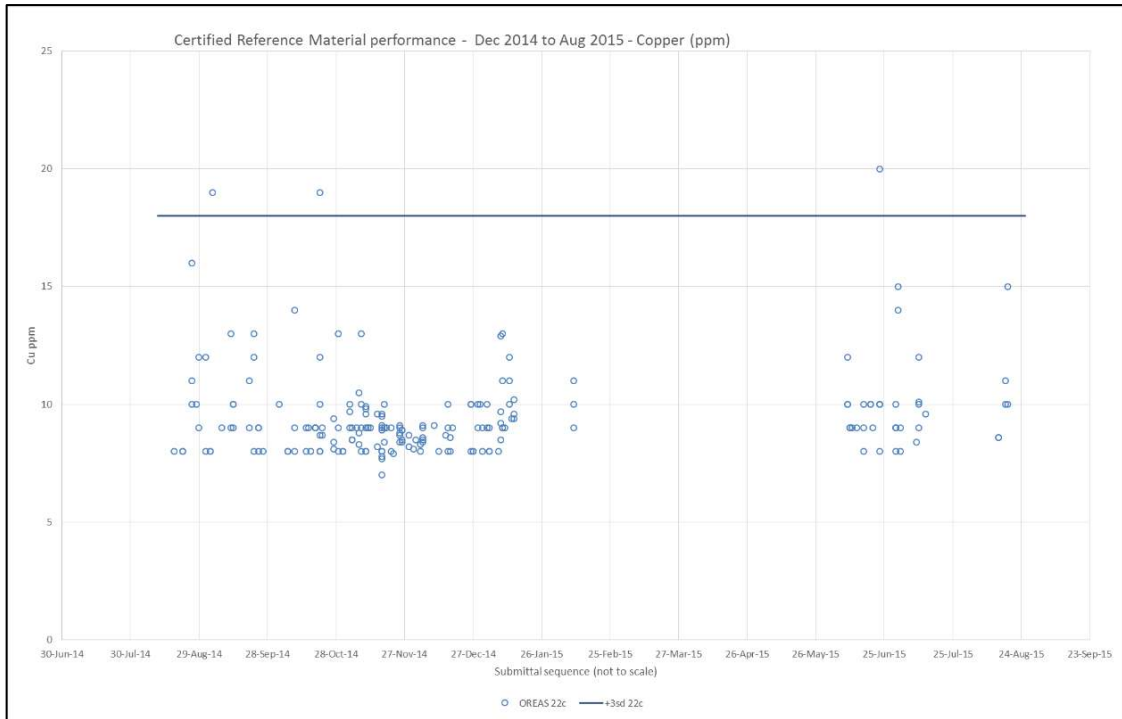


Figure 12.6 Certified “blank” pulp material – copper

12.1.5 Coarse “Blank” Material

In 2014, HCH began resubmitting its own coarse blank after the practice was halted in early 2013. These were reintroduced as the HCH-submitted “blank” pulp CRMs bypass much of the initial sample preparation process in the laboratory. The coarse blank material (quartz) allowed for the investigation of any crushing and milling bias in this initial sample preparation process. The coarse blank samples were inserted at the geologist’s discretion with an emphasis on placement in visually high-grade zones.

There are 954 coarse “blanks” inserted in the 174,476m of samples taken at the project, with an insertion rate of 0.5% of sampling.

Any samples that returned with values about threshold were investigated and discussions held with the respective laboratory managers. In all cases, investigation and checks determined that over threshold values were preceded by several high-grade samples, suggesting limited and extremely rare smearing. In all cases all other reference material in the batches were checked and at no stage was there a requirement to request full reanalysis.

In the case of molybdenum over-limits, these were preceded by single samples of extreme molybdenum values (>10,000ppm Mo) and the result of the coarse blank was within the 0.5% carry over allowance designated by ALS Global laboratories. The impact of any copper and molybdenum smearing is considered non-material to the current Productora and Alice estimations.

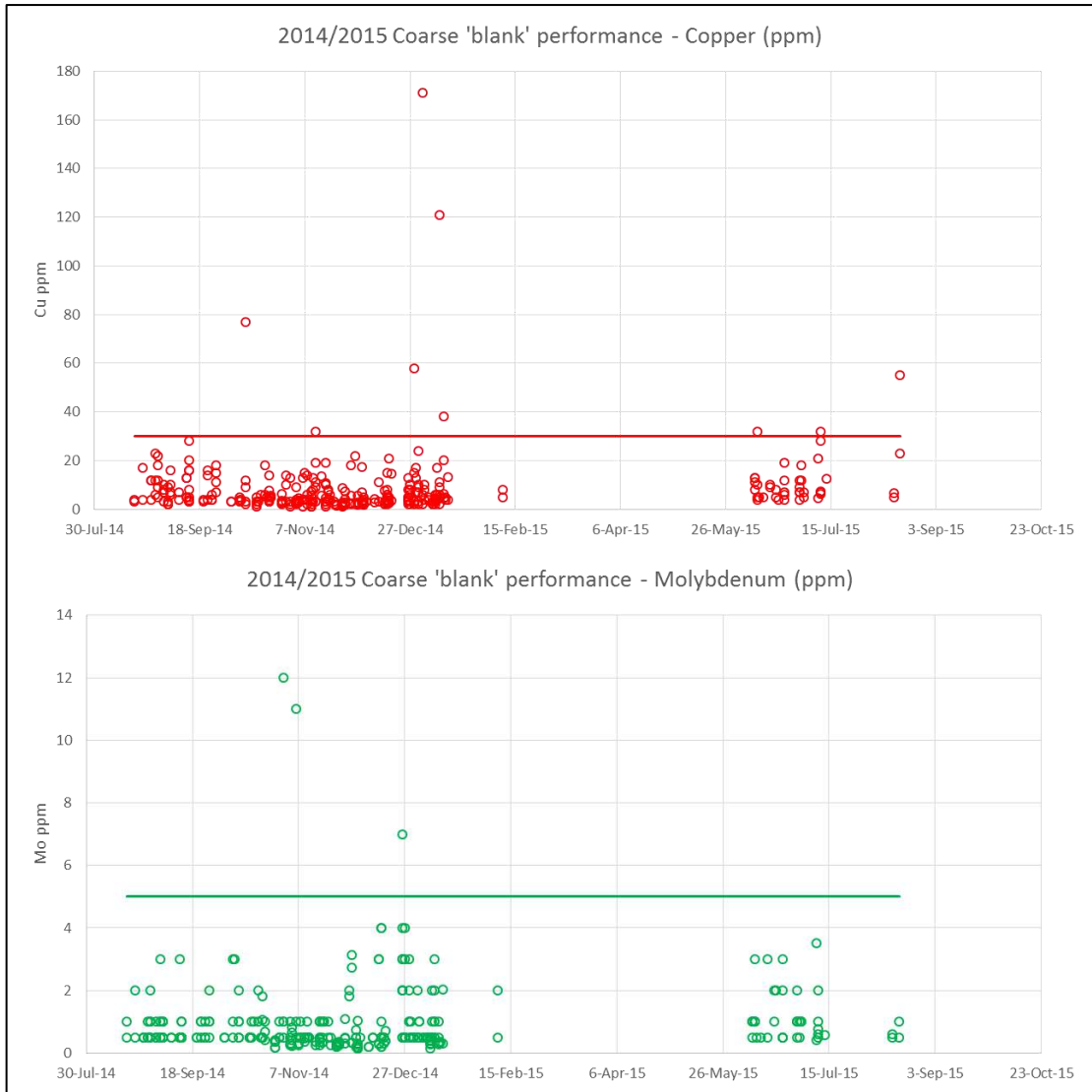


Figure 12.7 Coarse blank material performance during 2014/2015 drilling campaign

12.1.6 Field Duplicates

The field duplicates were collected on RC samples during the drilling process, at a targeted rate of one in 50m drilled. The procedure involves placing a second sample bag on the cone splitter to collect the duplicate sample. The duplicate sample is first collected at the 25m-26m interval and every 50th drill metre thereafter until the end of hole.

Diamond core field duplicates are collected on diamond drill core samples during the sample preparation process at the laboratory. Although whole core was sampled, the lab (instructed by HCH) collected a second coarse duplicate sample after the initial crushing process of the original sample. Crushed samples were split into two halves, with one half flagged as the original sample and the other half flagged as the duplicate sample. Duplicates from core were collected at a rate of approximately one in 50 samples.

There are 4,860 field duplicates from the 174,476m of samples taken at the project, with an insertion rate of 2.8% of sampling.

Field duplicate assays were compared against the original assay values. These comparisons showed no evidence of bias, with a robust correlation achieved between the datasets for copper, gold, and molybdenum (Figure 12.8). Correlation coefficients were well within acceptable tolerance limits for field duplicates and support confidence the relative accuracy and repeatability of rig sample collection through to assay.

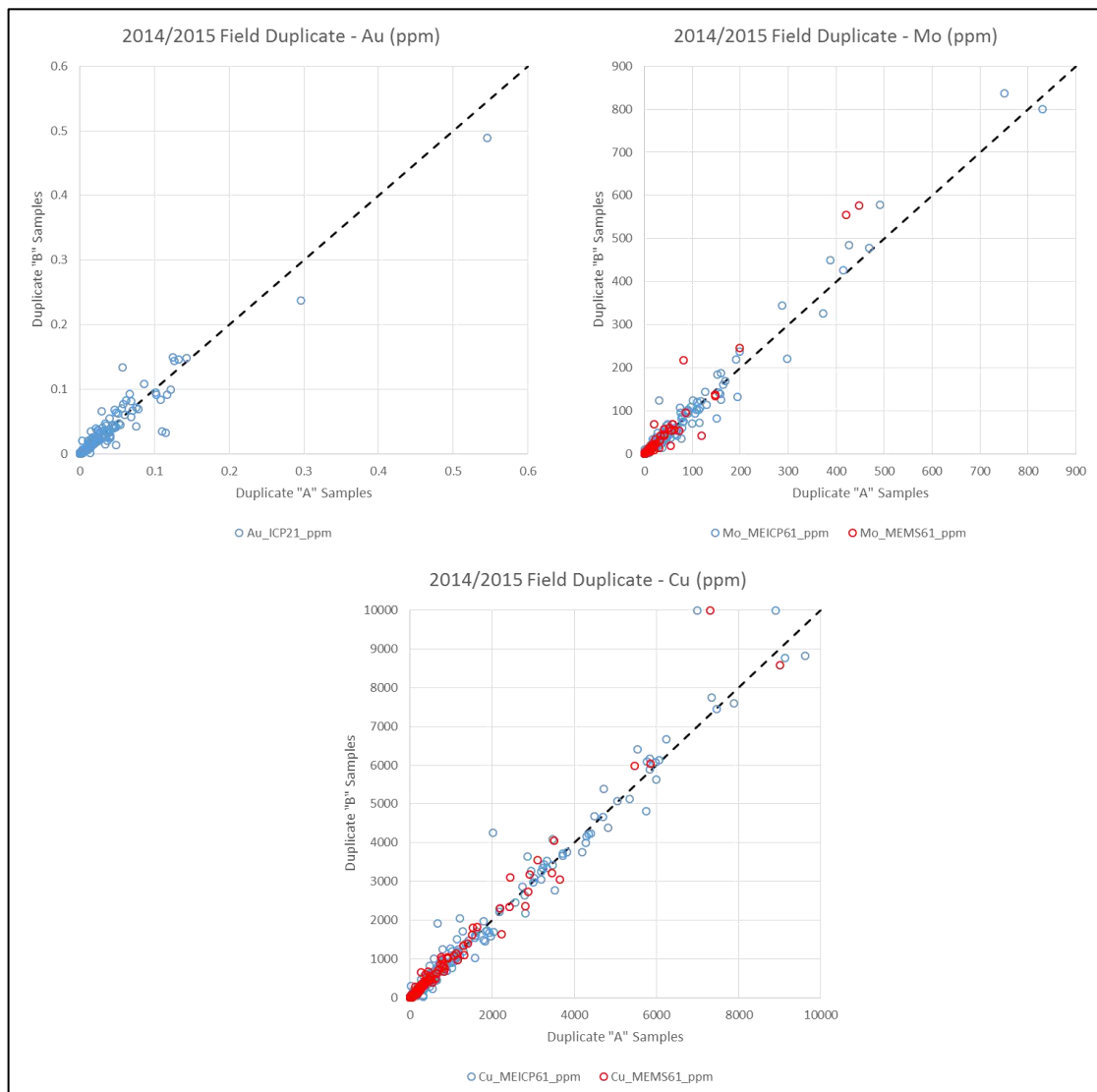


Figure 12.8 Duplicate sample comparison with original for major elements during the 2014/2015 drilling campaign

12.1.7 Umpire Laboratory Checks

During the 2014/2015 drilling campaign, pulp and coarse rejects were chosen from those submitted to ALS Global for umpire testing. These were submitted to Bureau Veritas in Santiago for assay as umpire checks on ALS's analysis. The analytical method is similar to that used by ALS (four-acid digestion, followed by ICP-AES determination).

Umpire results for copper and molybdenum showed a fair correlation. Gold showed a noisier but overall fair correlation with no quantifiable bias relative to the original samples. This gives sufficient confidence in the relative accuracy and repeatability of ALS's analytical assay technique.

In Figure 12.9 below, the red highlighted outlier was investigated and confirmed as a swapped sample pair.

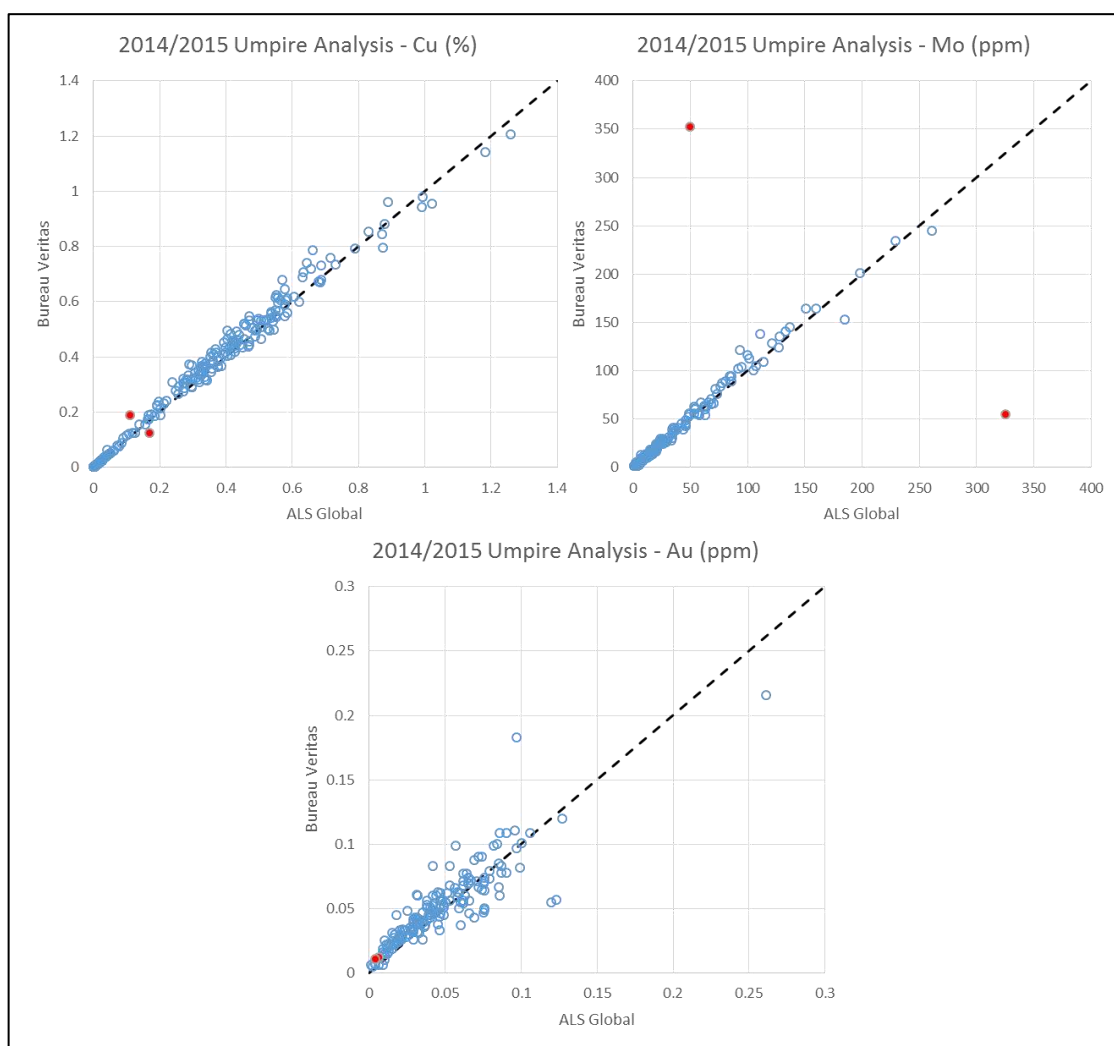


Figure 12.9 Umpire laboratory results for the 2014/2015 drilling campaign (known swapped sample pair highlighted in red)

12.1.8 Twin Hole Analysis

12.1.8.1 Productora

At Productora, there are quite a number of twinned holes with different drill methodologies (RC and DD). A direct comparison between nominally equivalent intervals shows there is some short-scale structural and mineralisation noise in all elements (Figure 12.10). QQ plots for matched twins was attempted but were not informative. This does make quantitative correlation troublesome, but visual validation

of mineralisation domains (Figure 12.11) suggest that there is acceptable correlation, and no apparent bias in the twinned mineralisation intervals and assay ranges.

Future studies will continue to address twinning analysis in further detail.

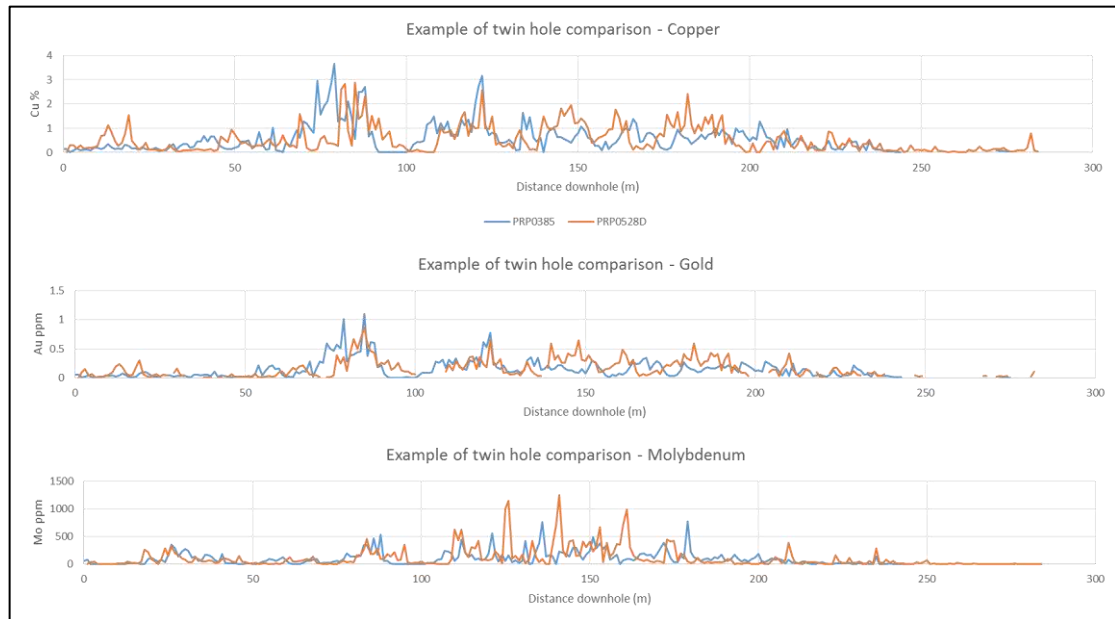


Figure 12.10 Example graphical analysis of twin holes at Productora

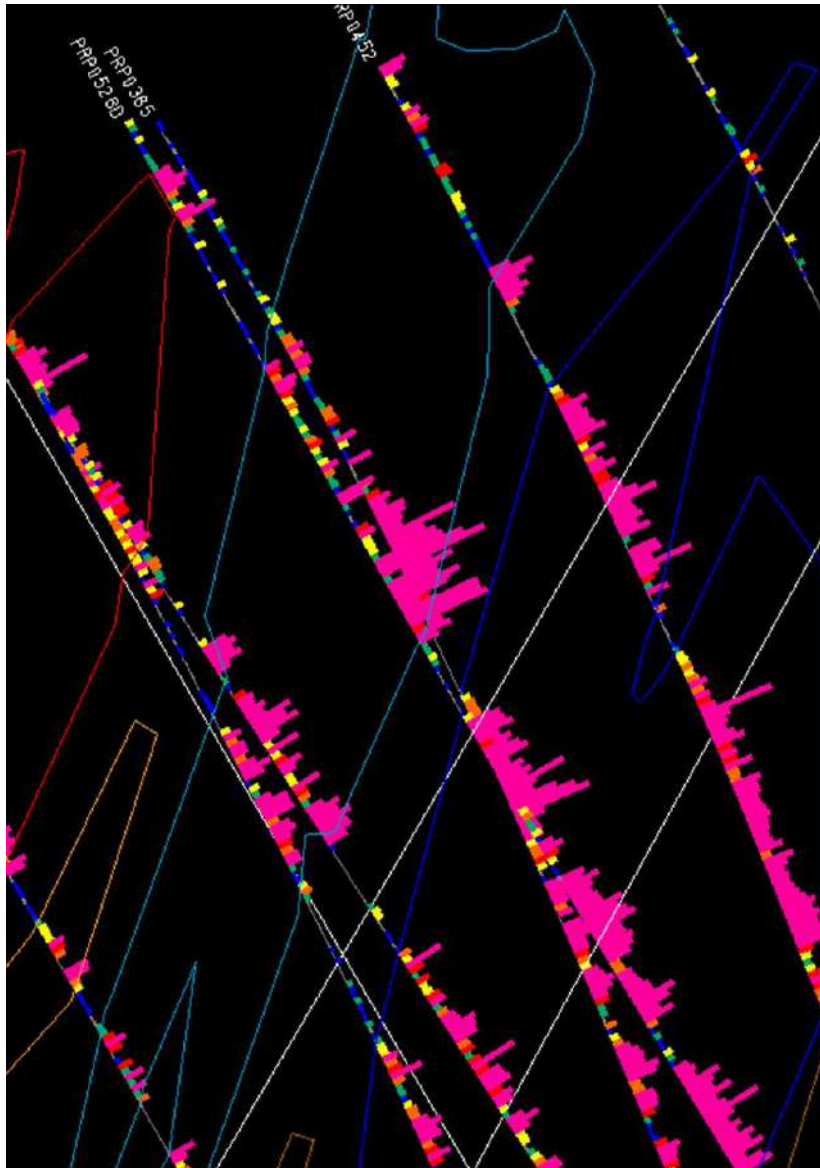


Figure 12.11 Visual comparison between core and RC twins within the 0.3% mineralisation envelope. The two holes compared in the previous figure are shown in the middle of this image. Sample and histogram are coloured by copper. Image is viewed looking north and width of image is approximately 80m. (HCH, 2016)

12.1.8.2 Alice

At Alice, there are two dedicated twin holes. These are: PXP0001D (twinning PRP0851) and MET024 (twinning PRP0923). A graphical analysis suggested no noticeable bias and that differences were due to increased hole separation with depth and changing geological conditions (Figure 12.12). Statistical comparison was inconclusive; overall the visual and graphical correlation was considered acceptable.

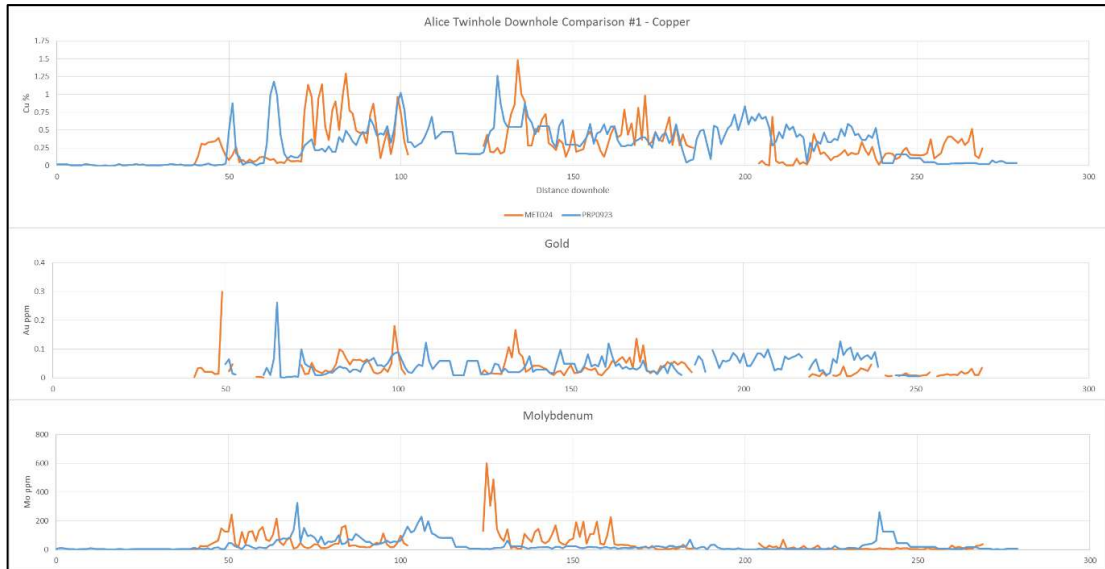


Figure 12.12 Example graphical analysis of twin holes at Alice (note: absent metallurgical samples in MET024)

12.1.9 Sample Condition and Recovery

The condition and recovery of each sample were qualitatively recorded during drilling by field technicians. The condition of the sample was recorded as either “dry”, “moist”, or “wet”, and the recovery (subjectively against other drilling and expectations) as “good”, “moderate” or “poor”. Figure 12.13 provides a summary of these qualitative sample descriptors, and Table 12.1 provides a comparison between the qualitative recovery and quantitative sample weights.

Much of the drilling at Productora and Alice had acceptable documented recovery and expectations on the ratio of wet and dry drilling were met.

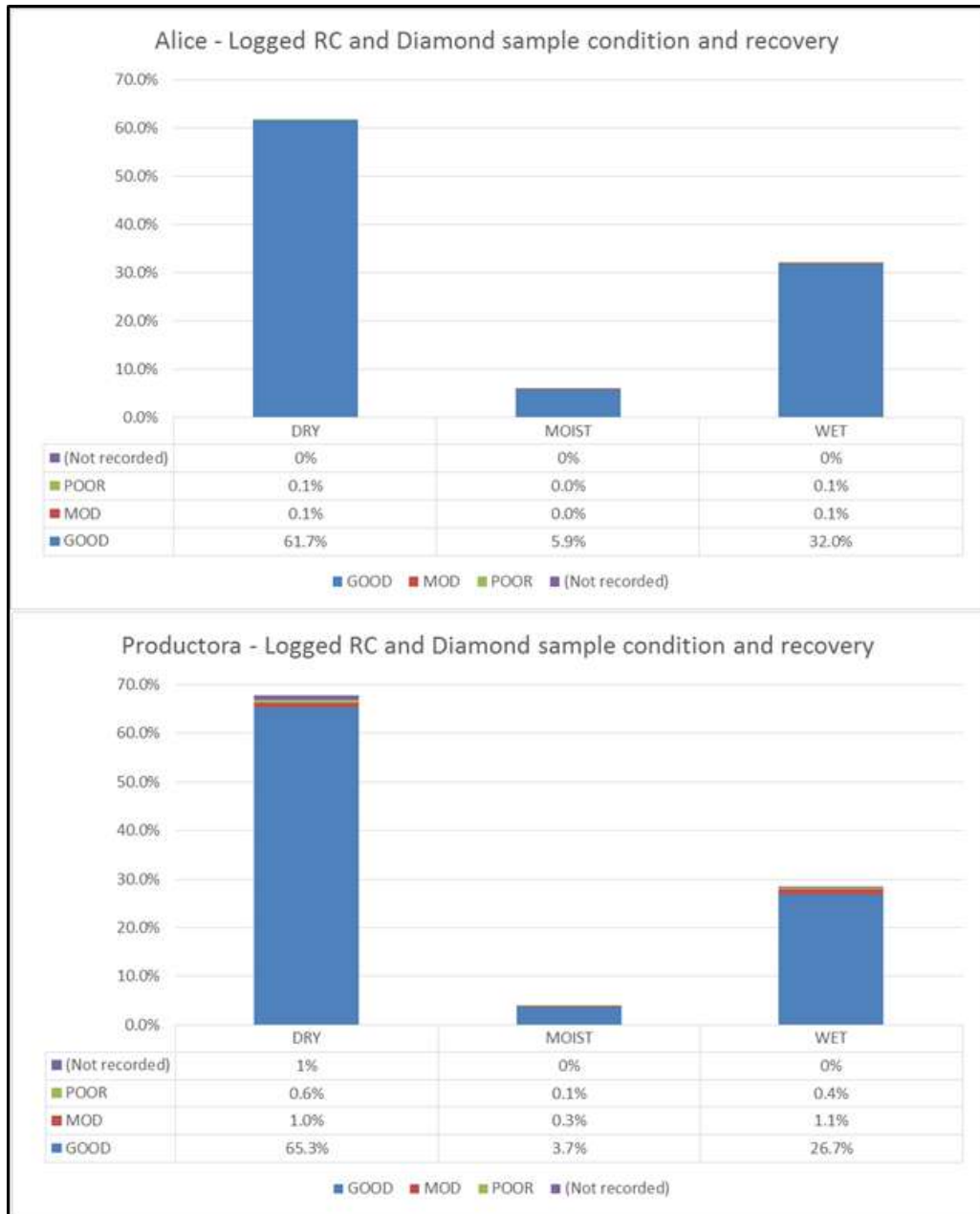


Figure 12.13 Alice and Productora sample condition and sample recovery

Table 12.1 Comparison of samples recovery and sample weights for Alice and Productora

Productora 1m sample logged recovery vs. sample weight				
Logged Recovery	RC samples		CORE samples	
	Av. kg	Count	Av. kg	Count
GOOD	3.6	76,873	6.8	21,504
MOD	2.5	2,238	4.3	384
POOR	1.5	869	2.6	341
(Not recorded)	2.8	812	2.8	870
Alice 1m sample logged recovery vs. sample weight				
Logged Recovery	RC samples		CORE samples	
	Av. kg	Count	Av. kg	Count
GOOD	3.4	3,370	3.6	412
MOD	1.2	6	1.7	2
POOR	0.9	5	1.6	5
(Not recorded)			3.6	96

12.1.10 Wet vs. Dry Samples

A non-spatial comparison between wet and dry samples was undertaken on the Productora data to define confidence in wet sample quality and to assist potential domain decisions. The comparison of sample condition within all mineralisation domains suggested that there was some difference between wet and dry samples (Figure 12.14 and Figure 12.15).

The current explanation for the “wet” and “dry” Cu and Au differences as analysed below currently relates to observed volume and grade decreases with increasing depth at Productora, where mineralisation nature is zoned due to differentiation in mineralisation fluid movement within the shatter complex with elevation. Alternatively, (and less likely) this could relate to a wet RC sample drilling bias.

Regarding the differences in the Mo, an additional factor is the nature of the creation of the mineralised domains which are primarily designed for Cu and Au and not for Mo mineralisation; this QQ comparison may not be comparing appropriate populations.

Comparisons between “dry” and “moist” suggest that there may either be sampling bias or there is some discrete mineralogical change at the water table interface. The volume of “moist” samples is minor compared to “wet” or “dry” samples.

A recommendation of this report is for undertake additional studies to refine, define or refute these observations and statements.

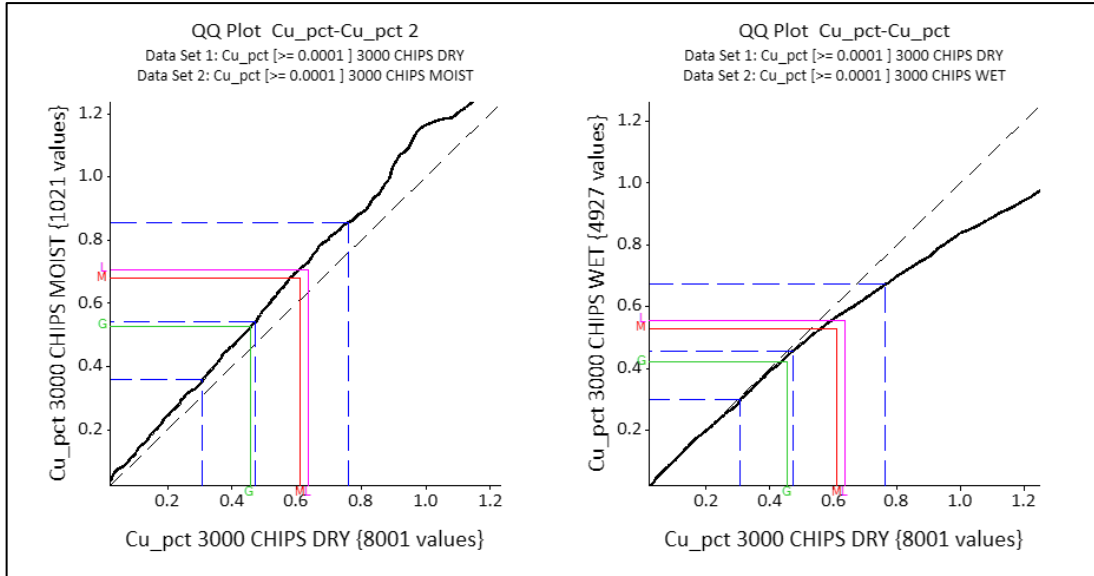


Figure 12.14 QQ comparison of (left) “dry” and “moist” RC samples within the 0.3% Cu mineralised domain for Cu. Right is a comparison of “wet” and “dry” for Productora

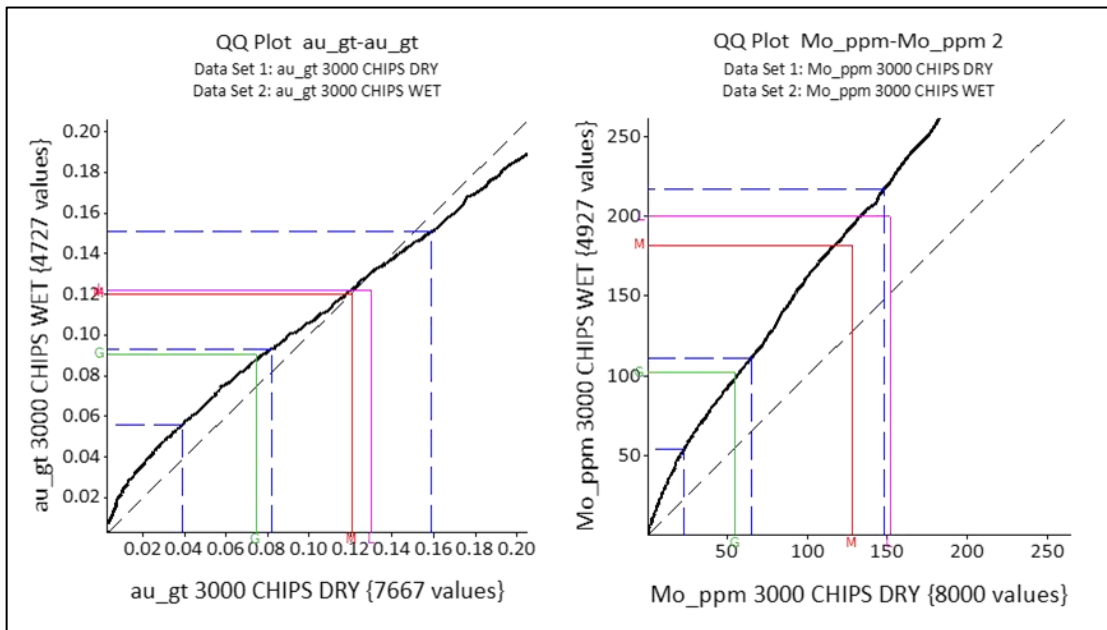


Figure 12.15 QQ comparison of (left) “wet” and “dry” RC samples within the 0.3% Cu mineralised domain for Au. Right is a Mo comparison

A non-spatial comparison between wet and dry samples was undertaken on the Alice twin hole data (Figure 12.16). Statistical QQ plots were generated but were considered inconclusive due to the limited data set available for comparison.

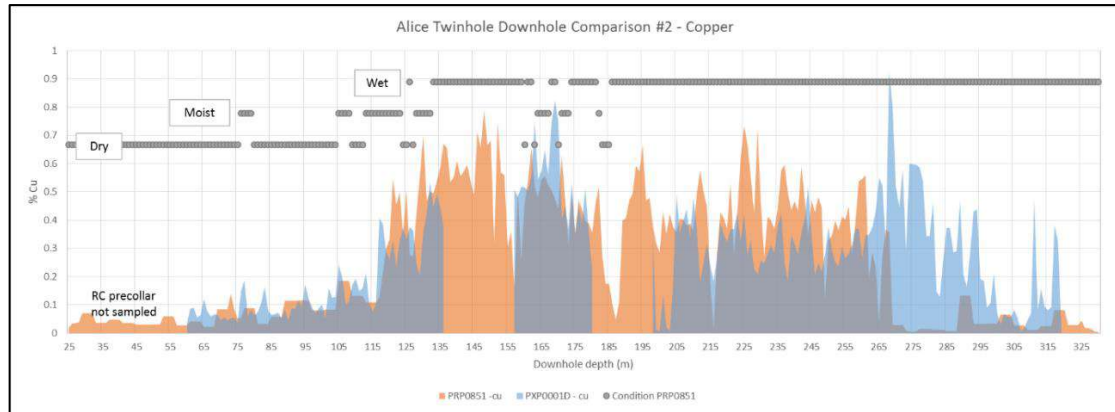


Figure 12.16 Graphical samples comparison with twin holes. Sample condition (wet/dry/moist) is flagged by RC sample logging

12.1.11 Independent Samples and Assay Verification

12.1.11.1 Pre-2013 Independent Sample and Assay Verification

A limited number of verification samples were taken by Coffey Mining during a site visit in November 2012. A total of 17 samples from four drillholes were selected at random. Samples were taken by Coffey and delivered in person to the ALS analytical laboratory in Coquimbo, Chile. The results were directly sent to Coffey in Perth (Australia) and supported the original assays.

12.1.11.2 2014 Independent Sample and Assay Verification

AMC Consultants was engaged on a fee for service basis to undertake an independent review of site procedures and sampling.

Part of the review's scope of work was to collect independent check samples of the Productora mineralisation. These samples included:

- "B" field duplicates on current drillholes
- Five consecutive field duplicates were collected from PRP0864
- Laboratory coarse rejects or "C" bulk sample rejects

In total, 60 samples were collected from approximately 18 drillholes for various locations, styles of mineralisation, levels of mineralisation, levels of weathering/oxidation.

The samples were taken by a representative of AMC Consultants and delivered in person to the ALS analytical laboratory in Coquimbo, Chile. The results were sent directly from ALS to AMC, which determined that they supported the original assays.

12.2 Cortadera

12.2.1 Independent Qualified Person Review and Verification

No third-party audits were conducted on the Mineral Resource Estimate as the internal data verification and quality assurance programs were deemed adequate by the Qualified Person for the Mineral Resource Estimation. The Qualified Person is a third party to HCH and completed extensive independent data verification prior to estimation being completed.

12.2.2 Internal Verification Programs

HCH employed a variety of QA/QC measures to assess and ensure the quality of the drill data used for resource estimation. QA/QC for sampling and assay data has included the use of certified reference material (CRM) “standards” and “blanks”, field duplicates, umpire laboratory checks, and audits.

Conclusions from this review found an overall performance of QAQC samples that gave a good level of confidence in the dataset from HCH. Points below were recommended for future work:

- Review the suitability of the current suite of CRMs for Ag, and analysis methods, to ensure adequate quality reference points for future sampling
- Investigate the materiality of the higher incidence of low-grade duplicate errors using RC collection methods, and improvements to mitigate the risk if required
- Review individual batch QAQC procedure to ensure prompt re-assaying of QAQC samples when required
- Review the approach for uncertified blanks and tolerance limits, specifically to consider the tolerance for contamination as a percentage of the assay value, over the current discrete cut off.

12.2.3 QA/QC Program

HCH has compiled a QAQC report for data generated by the drilling campaign undertaken between June 2020 and December 2021, and the Minera Fuego Limited (MFL) campaigns undertaken between October 2011 and December 2012 at the Cortadera project in Chile.

The HCH drilling campaign totalled 54,588 metres: 27,519m RC (50.5%), 10,655m HQ diamond (19.6%), 16,200m NQ diamond (29.7%), 112m PQ diamond (0.2%), and 102m no recovery (0.2%) which corresponds to 146 new drillholes and 22,585 assay samples (Figure 12.17).

QAQC reports are separated into two parts - one for the HCH drilling campaign, and the other for the MFL drilling campaign. QAQC data reported includes field duplicates, mineralised standards (certified reference material), certified blanks, coarse (uncertified) blanks, umpire laboratory checks and twin hole (RC - DD) analysis.

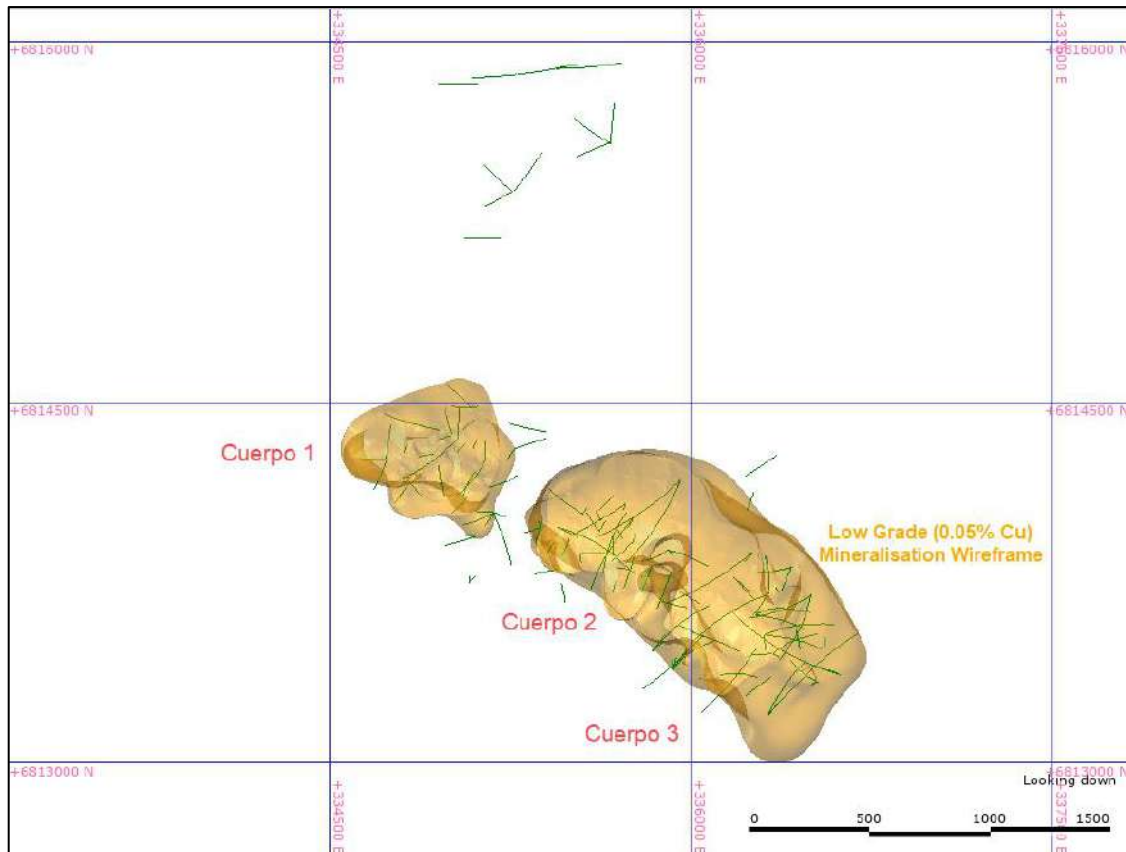


Figure 12.17 Location of RC and DD drilling added during the reporting period undertaken by HCH

QA/QC samples and their insertion rates (IR), as a percentage of the 22,585 samples from all HCH drilling to date at the project are provided in Table 12.2.

Table 12.2 Cortadera Drilling Program QAQC Insertion Rates

QC Type	Number of Samples	IR
Mineralised Standard	540	2.4%
Certified Blank	251	1.1%
Coarse Blank	1,184	5.2%
Coarse Duplicate	1,110	4.9%
Assay Samples	22,585	-

12.2.3.1 Standards

There were 540 mineralised CRMs inserted in the 54,588m of drilling completed by HCH at Cortadera at an insertion rate of 2.4% of samples. Eight distinct CRMs were used in the program (Table 12.3).

Table 12.3 HCH QAQC CRM details

CRM Ref Name	Number of Samples	Expected Cu pct	Expected Au ppm	Expected Mo ppm	Expected Ag ppm
IN-BMF-172	16	0	0	1	0
OREAS-501b	26	0.260	0.248	99	0.778
OREAS-502	17	0.755	0.491	274	2.14
OREAS-502c	68	0.783	0.488	226	0.779
OREAS-503b	178	0.531	0.695	319	1.54
OREAS-504	112	1.137	1.48	643	3.13
OREAS-505	81	0.321	0.555	65	1.53
OREAS-902	42	0.301	0.046	12.2	0.343

The assay results from submitted CRMs show acceptable correlation with their expected value without any appreciable analytical drift over time.

12.2.3.1.1 IN-BMF-172

IN-BMF-172 is a certified blank material that was inserted as a CRM on 16 occasions. Results are included in the Blanks section of this report.

12.2.3.1.2 OREAS-501b

Table 12.4 OREAS-501b Reference Material Statistics as recorded in HCH database

Element	Expected Value	Standard Deviation	Accepted Min	Accepted Max
Cu pct	0.260	0.011	0.227	0.293
Au ppm	0.248	0.010	0.218	0.278
Ag ppm	0.778	0.128	0.394	1.162
Mo ppm	99	7.5	76.5	121.5

Table 12.5 Performance statistics for OREAS-501b CRM results

Statistics - OREAS-501b				
	Cu ppm	Au ppm	Ag ppm	Mo ppm
# Outside Error Limit	0	1	2	0
# of Analyses below Threshold	0	0	0	0
% Outside Error Limit	0	3.8462	7.6923	0
Mean	2670.3846	0.2502	0.6038	97.4231
Median	2665	0.249	0.6	98
Min	2580	0.238	0.25	90
Max	2810	0.291	0.9	109
Standard Deviation	44.3153	0.0095	0.163	4.2443
% Rel. Std. Dev.	1.6595	3.8036	27.0016	4.3565
Coeff. of Var.	0.0166	0.038	0.27	0.0436
Standard Error	8.6909	0.0019	0.032	0.8324
% Rel. Std. Err.	0.3255	0.746	5.2954	0.8544
Total Bias	0.0271	0.0088	-0.2238	-0.0159
% Mean Bias	2.7071	0.884	-22.3848	-1.5929

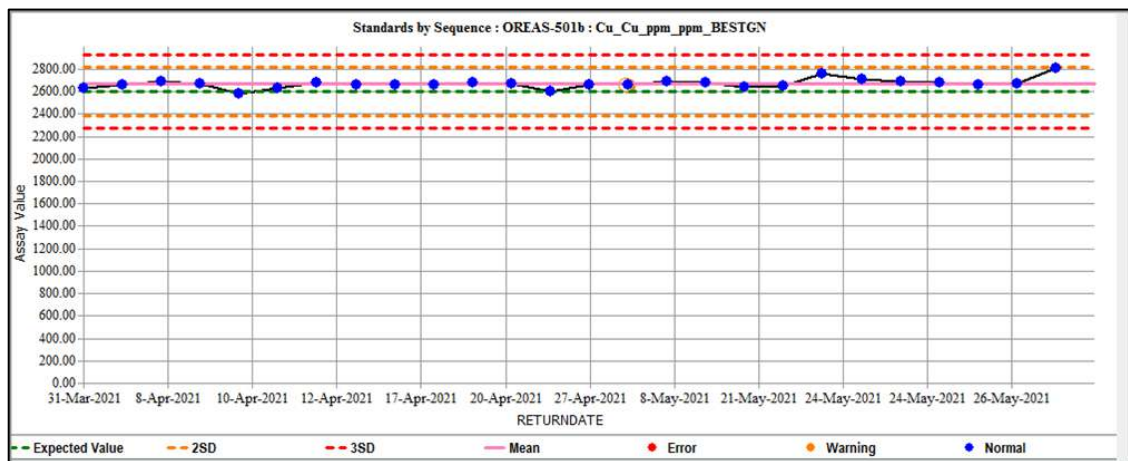


Figure 12.18 OREAS-501b results for Cu ppm

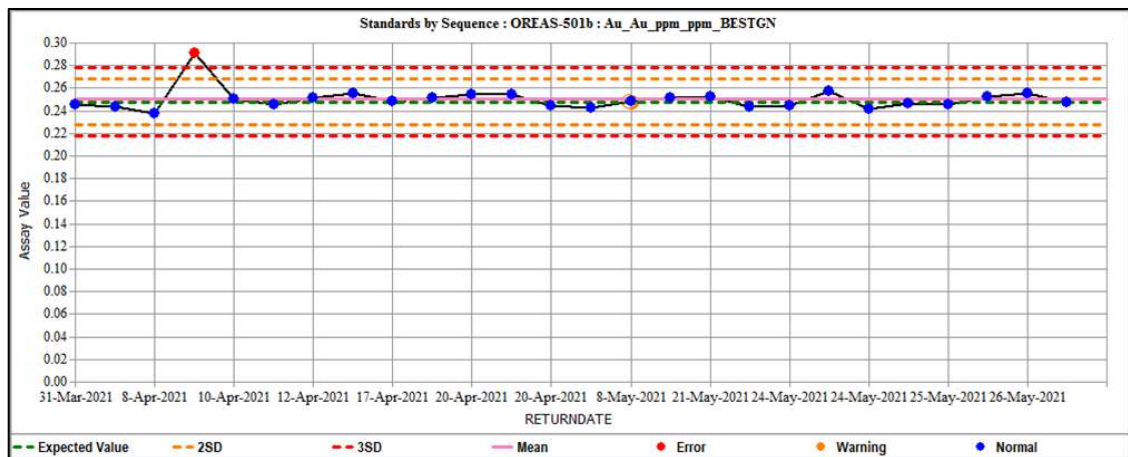


Figure 12.19 OREAS-501b results for Au ppm

While one sample failed, the job was accepted on the balance of the other elements passing. Outside of this sample Au performed tightly to the expected value with no apparent bias.

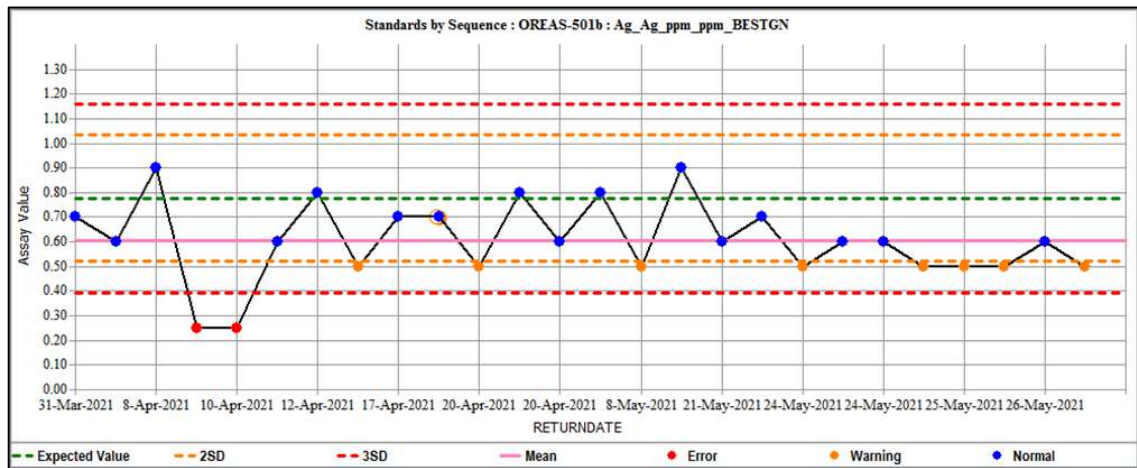


Figure 12.20 OREAS-501b results for Ag ppm

The two failing samples have returned at detection limit (0.25ppm). The apparent bias shown in the mean to the expected value is also influenced by the accuracy possible within close proximity to the detection limit.

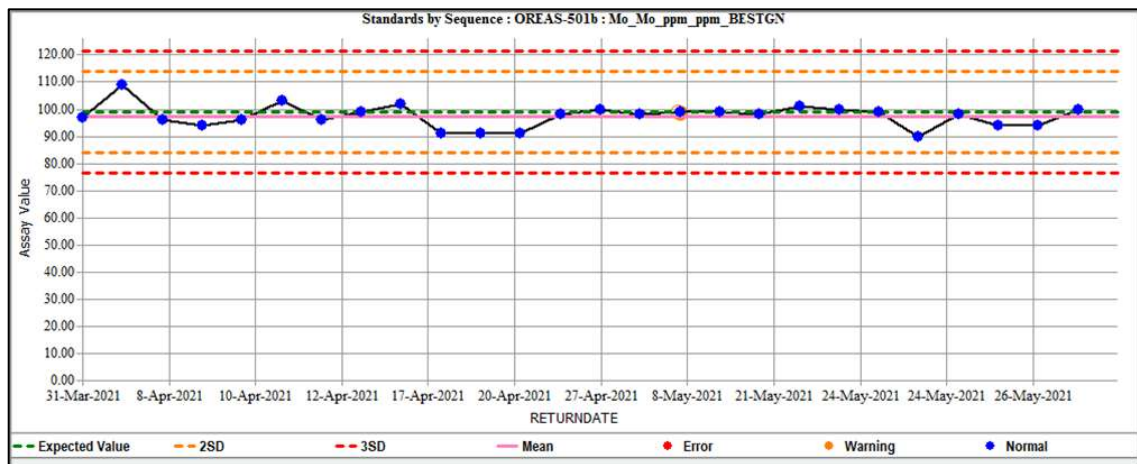


Figure 12.21 OREAS-501b results for Mo ppm

12.2.3.1.3 OREAS-502

Table 12.6 OREAS-502 Reference Material Statistics as recorded in HCH database

Element	Expected Value	Standard Deviation	Accepted Min	Accepted Max
Cu ppm	7550	200	6950	8150
Au ppm	0.491	0.02	0.431	0.551
Ag ppm	2.14	0.195	1.555	2.725
Mo ppm	274	12.5	236.5	311.5

Table 12.7 Performance statistics for OREAS-502 CRM results

Statistics - OREAS-502				
	Cu ppm	Au ppm	Ag ppm	Mo ppm
# of Analyses above Threshold	17	17	17	17
# Outside Warning Limit	1	0	0	0
# Outside Error Limit	0	0	0	0
# of Analyses below Threshold	0	0	0	0
% Outside Error Limit	0	0	0	0
Mean	7546.4706	0.4909	2.0647	270.8824
Median	7570	0.492	2.1	272
Min	7090	0.472	1.8	253
Max	7820	0.508	2.4	290
Standard Deviation	176.0661	0.008	0.173	11.0673
% Rel. Std. Dev.	2.3331	1.6334	8.3786	4.0857
Coeff. of Var.	0.0233	0.0163	0.0838	0.0409
Standard Error	42.7023	0.0019	0.042	2.6842
% Rel. Std. Err.	0.5659	0.3962	2.0321	0.9909
Total Bias	-0.0005	-0.0001	-0.0352	-0.0114
% Mean Bias	-0.0467	-0.012	-3.5184	-1.1378

One sample (CX03425) was identified as a standard swap error and was reassigned from OREAS-502 to OREAS-502c.

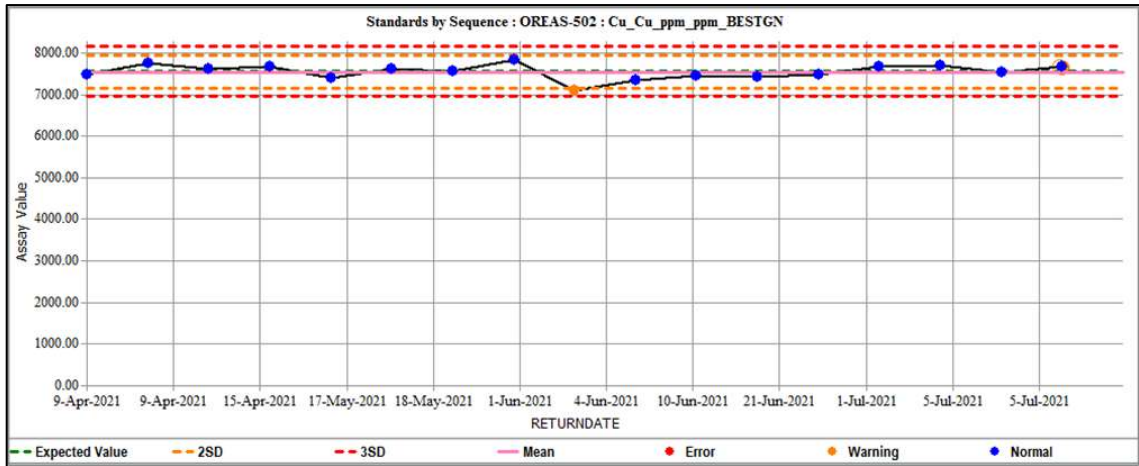


Figure 12.22 OREAS-502 results for Cu ppm

Cu values largely performed close to the expected values without bias, a potential calibration event is seen on the 4th June 2021 with sample CX02125 which triggered the 95% confidence warning and subsequently drifted back to expected values.

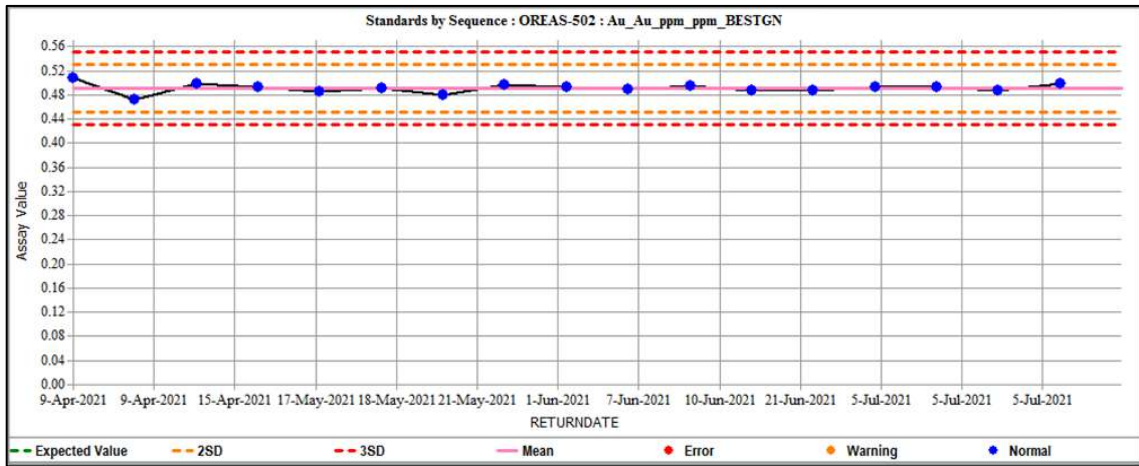


Figure 12.23 OREAS-502 results for Au ppm

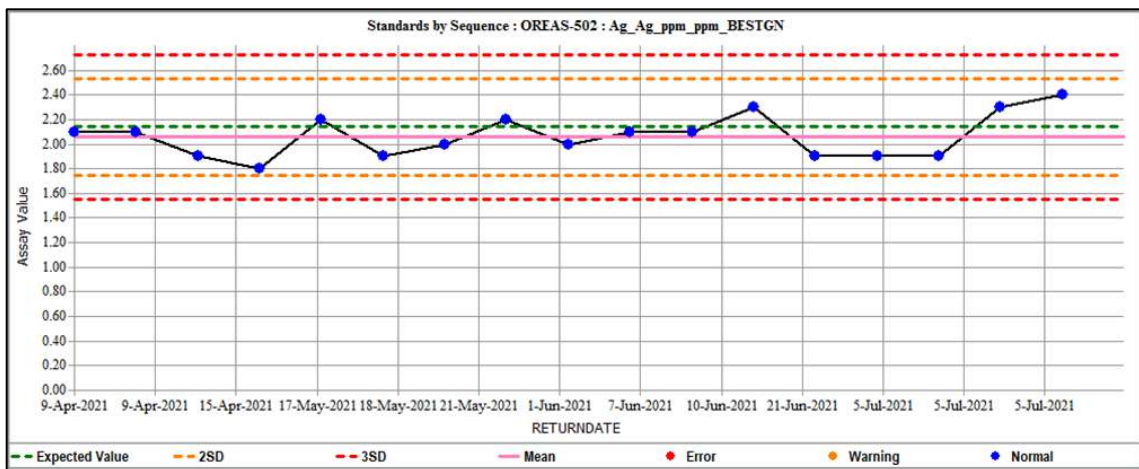


Figure 12.24 OREAS-502 results for Ag ppm

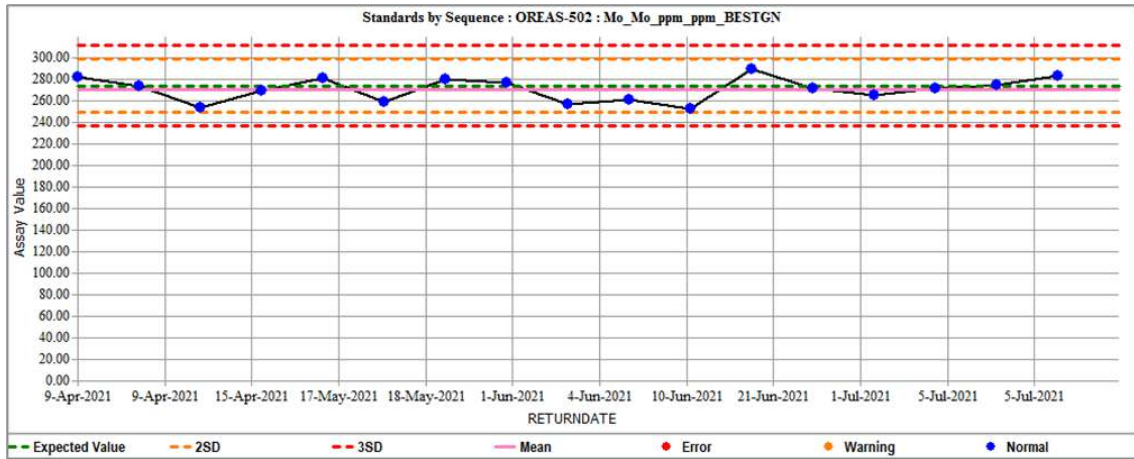


Figure 12.25 OREAS-502 results for Mo ppm

12.2.3.1.4 OREAS-502c

Table 12.8 OREAS-502c Reference Material Statistics as recorded in HCH database

Element	Expected Value	Standard Deviation	Accepted Min	Accepted Max
Cu ppm	7830	220	7170	8790
Au ppm	0.488	0.015	0.443	0.533
Ag ppm	0.779	0.076	0.551	1.007
Mo ppm	226	12	190	262

Table 12.9 Performance statistics for OREAS-502c CRM results

Statistics - OREAS-502c				
	Cu ppm	Au ppm	Ag ppm	Mo ppm
# of Analyses above Threshold	68	68	68	68
# Outside Warning Limit	2	4	35	1
# Outside Error Limit	1	1	15	0
# of Analyses below Threshold	0	0	0	0
% Outside Error Limit	1.4706	1.4706	22.0588	0
Mean	7757.7941	0.4785	0.7066	224.1176
Median	7745	0.48	0.7	225
Min	7100	0.422	0.25	201
Max	8170	0.498	1.2	242
Standard Deviation	206.2664	0.0124	0.1918	8.4598
% Rel. Std. Dev.	2.6588	2.5963	27.1422	3.7747
Coeff. of Var.	0.0266	0.026	0.2714	0.0377
Standard Error	25.0135	0.0015	0.0233	1.0259
% Rel. Std. Err.	0.3224	0.3148	3.2915	0.4578
Total Bias	-0.0092	-0.0196	-0.0929	-0.0083
% Mean Bias	-0.9222	-1.9558	-9.2917	-0.8329

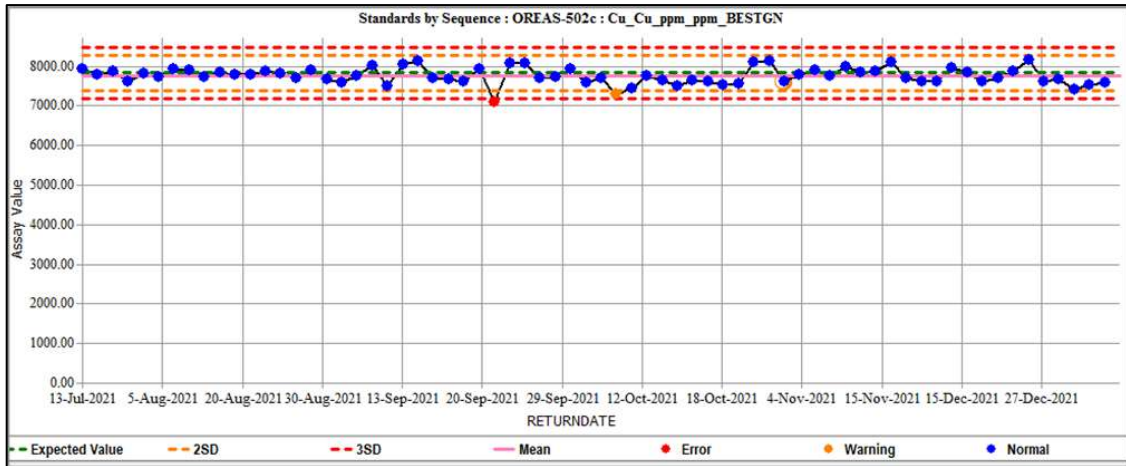


Figure 12.26 OREAS-502c results for Cu ppm

Cu values generally performed close to the expected value, with a slight negative bias developing from September 2021. One erroneous value (CX09275 22nd September 2021) was accepted, with warning values on Mo and Au analytes, and an expected Ag value.

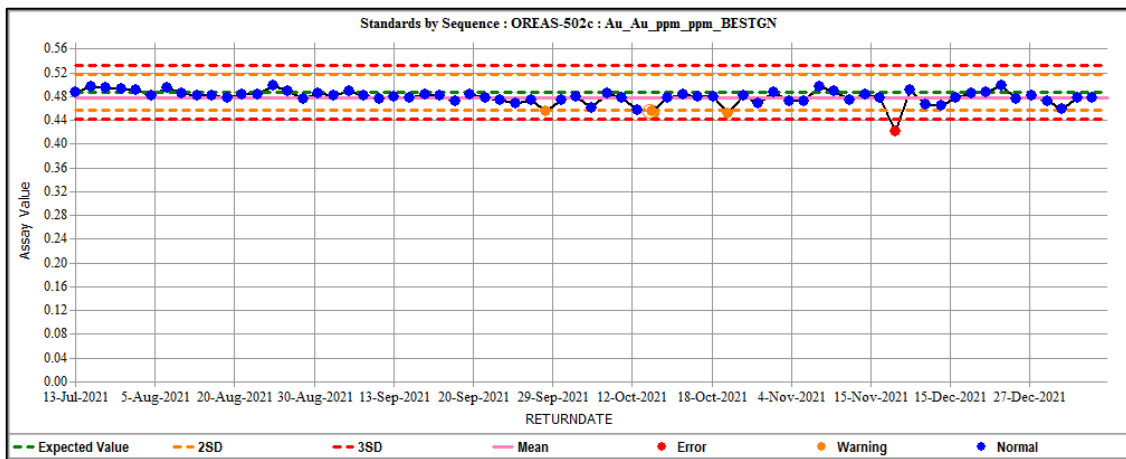


Figure 12.27 OREAS-502c results for Au ppm

Au results performed close to the expected value with a slight negative bias driven mostly through the period September – November 2021 which included 3 warning triggers outside the 95% confidence bands. One erroneous value on 22nd November 2021 (CX015175) was accepted with expected values for all other elements.

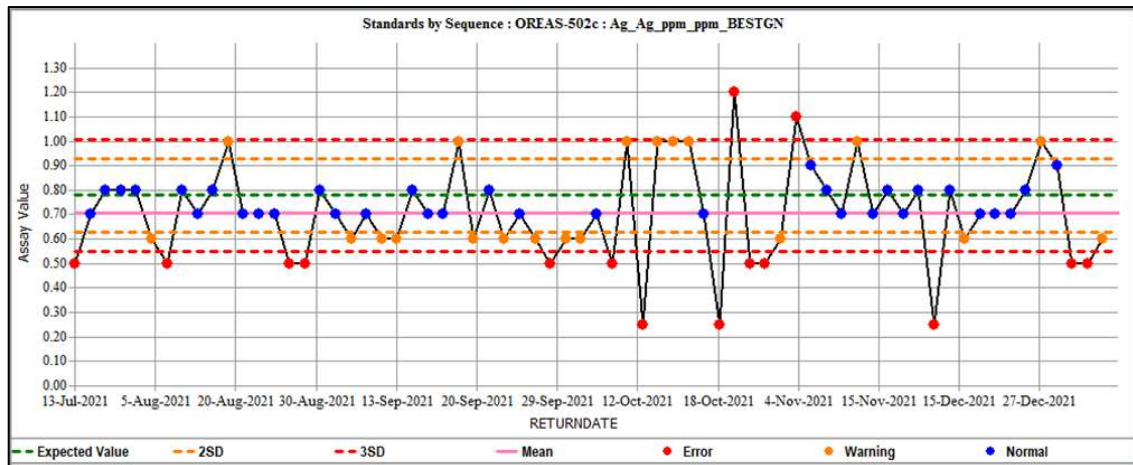


Figure 12.28 OREAS-502c results for Ag ppm

Ag results were variable with this standard, showing a wide distribution of warning and erroneous values along with a negative bias, likely influenced by proximity to the detection limit (0.25ppm). This result is restricted to Ag within the standard, and a recommendation is to review the continued use of OREAS-502c as it may not be suitable for validation of the Ag assay at these ranges.

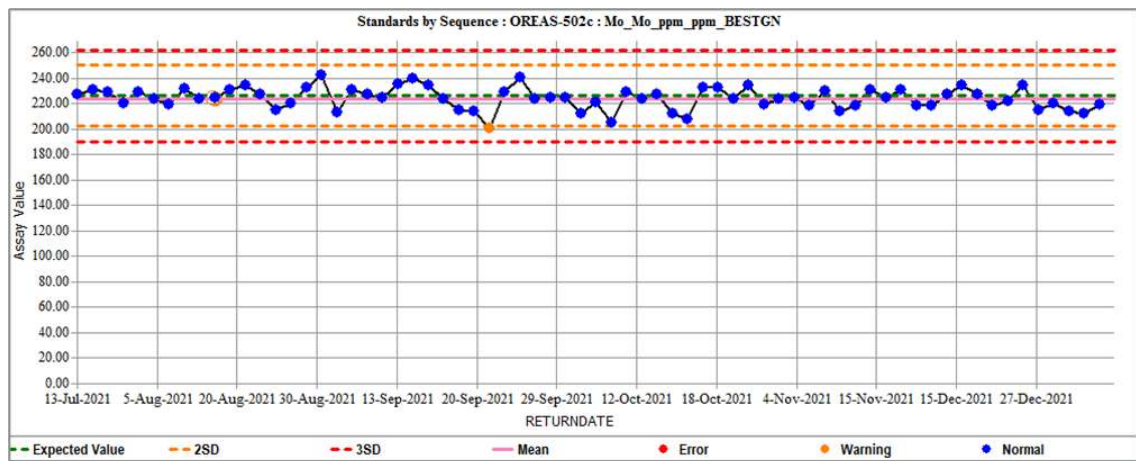


Figure 12.29 OREAS-502c results for Mo ppm

Mo generally performed very closely to the expected value with a period of increased negative bias in September – October 2021 as noted in other elements, suggesting a possible calibration event by the laboratory in mid-October 2021.

12.2.3.1.5 OREAS-503b

Table 12.10 OREAS-503b Reference Material Statistics as recorded in HCH database

Element	Expected Value	Standard Deviation	Accepted Min	Accepted Max
Cu pct	0.531	0.023	0.462	0.600
Au ppm	0.695	0.021	0.632	0.758
Ag ppm	1.54	0.19	0.218	2.11
Mo ppm	319	16	271	367

Table 12.11 Performance statistics for OREAS-503b CRM results

Statistics - OREAS-503b				
Element	Cu ppm	Au ppm	Ag ppm	Mo ppm
# of Analyses above Threshold	178	178	178	178
# Outside Warning Limit	3	6	6	3
# Outside Error Limit	1	4	0	1
# of Analyses below Threshold	0	0	0	0
% Outside Error Limit	0.5618	2.2472	0	0.5618
Mean	5247.0506	0.686	1.4747	306.7921
Median	5270	0.691	1.5	307
Min	1985	0.022	1	8
Max	5640	0.753	2	344
Standard Deviation	286.3157	0.0541	0.1625	25.0274
% Rel. Std. Dev.	5.4567	7.8884	11.0218	8.1578
Coeff. of Var.	0.0546	0.0789	0.1102	0.0816
Standard Error	21.4603	0.0041	0.0122	1.8759
% Rel. Std. Err.	0.409	0.5913	0.8261	0.6114
Total Bias	-0.0119	-0.013	-0.0424	-0.0383
% Mean Bias	-1.1855	-1.2998	-4.239	-3.8269

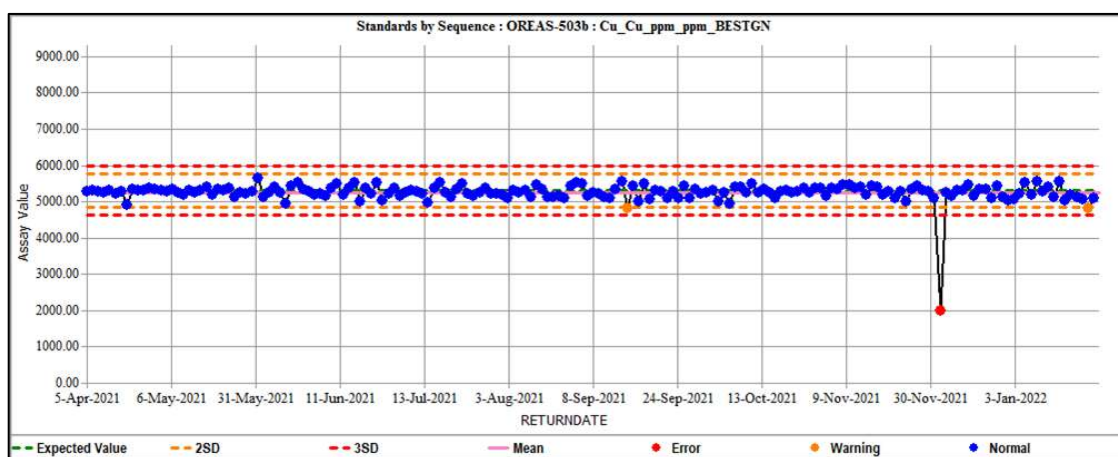


Figure 12.30 OREAS-503b results for Cu ppm

Generally, Cu values returned within the two standard deviation warning limits, with no apparent bias. One erroneous result on 30th November 2021 (CX015775) remains in the database. This sample was also an erroneous result for Mo, a warning flag for Ag,

yet an expected result for Au. This combination of assays does not fit the profile of any standard for a standard swap, and therefore has been retained as indicated following investigation.

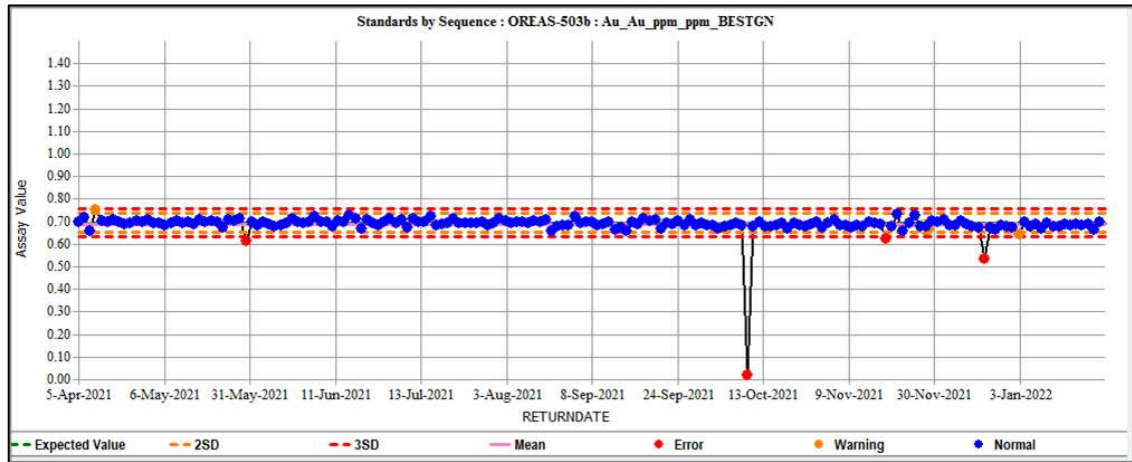


Figure 12.31 OREAS-503b CRM results for Au ppm

Four samples returned values for Au outside of error limits. Other elements (Cu, Mo, and Ag) for each of these samples came back within range and thus the samples were accepted.

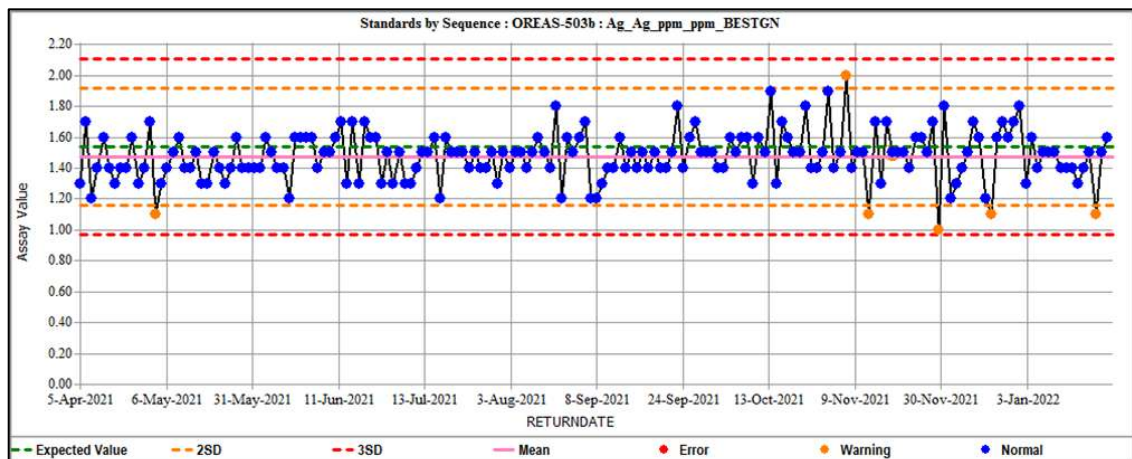


Figure 12.32 OREAS-503b CRM results for Ag ppm

All Ag values returned within the 2x standard deviation warning limits, however a greater variation in the spread of values was observed from November 2021 to the end of the reporting period. A small negative bias is noted.

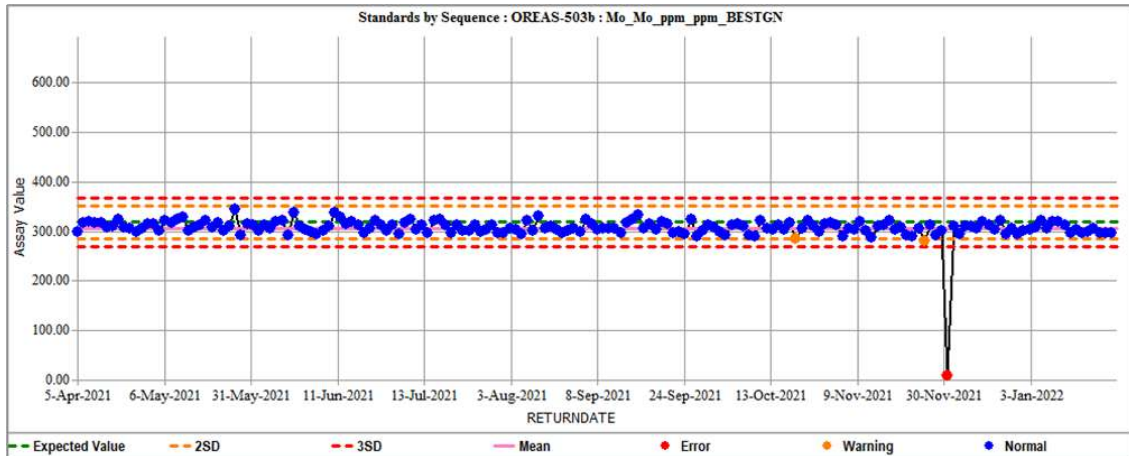


Figure 12.33 OREAS-503b CRM results for Mo ppm

All Mo values returned within the 2x standard deviation warning limits, except for one erroneous result on 30th November 2021 CX015775 as discussed in the Cu section above. A consistent negative bias is noted.

12.2.3.1.6 OREAS-504

Table 12.12 OREAS-504 Reference Material Statistics as recorded in HCH database

Element	Expected Value	Standard Deviation	Accepted Min	Accepted Max
Cu pct	1.137	0.032	1.041	1.233
Au ppm	1.48	0.04	1.36	1.6
Ag ppm	3.13	0.21	3.5	3.76
Mo ppm	643	37.1	531.7	754.3

Table 12.13 Performance statistics for OREAS-504 CRM results

Statistics - OREAS-504				
Element	Cu pct	Au ppm	Ag ppm	Mo ppm
# of Analyses above Threshold	77*	116	116	116
# Outside Warning Limit	0	6	7	0
# Outside Error Limit	0	1	2	0
# of Analyses below Threshold	0	0	0	0
% Outside Error Limit	0	0.8621	1.7241	0
Mean	1.1246	3.2276	1.4879	633.5431
Median	1.123	3.2	1.495	633
Min	1.082	2.7	1.3	589
Max	1.166	3.8	1.585	690
Standard Deviation	0.0182	0.1801	0.0392	19.3316
% Rel. Std. Dev.	1.62	5.5812	2.6375	3.0513
Coeff. of Var.	0.0162	0.0558	0.0264	0.0305
Standard Error	0.0021	0.0167	0.0036	1.7949
% Rel. Std. Err.	0.1846	0.5182	0.2449	0.2833
Total Bias	-0.0109	0.0312	0.0053	-0.0147
% Mean Bias	-1.0897	3.1178	0.533	-1.4707

*77 samples reported in Cu pct, balance reported in Cu ppm and converted to Cu Pct in the graphing.

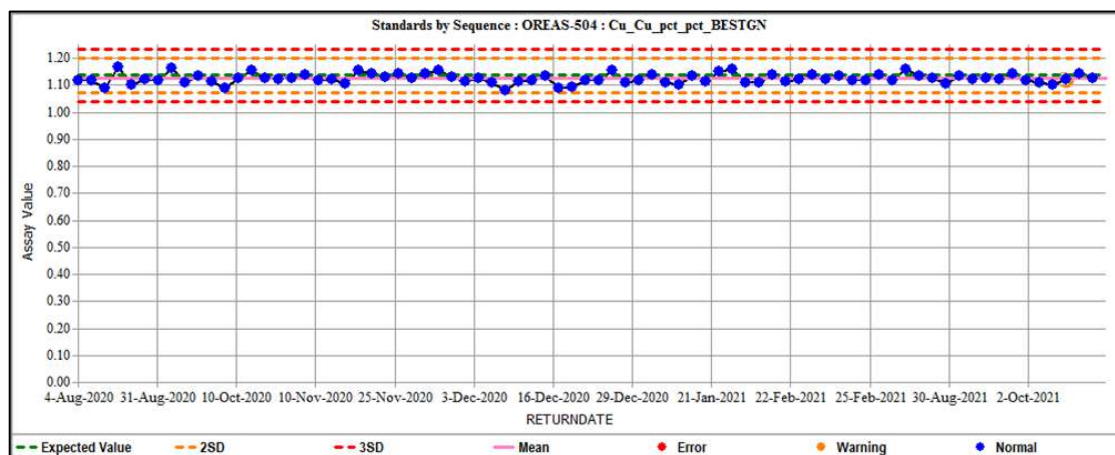


Figure 12.34 OREAS-504 CRM results for Cu ppm

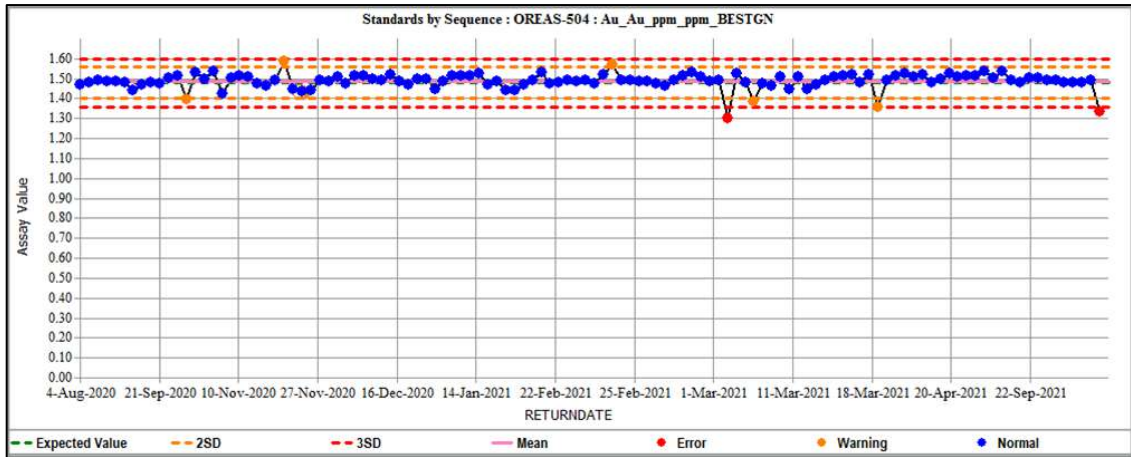


Figure 12.35 OREAS-504 CRM results for Au ppm

Two samples returned values for Au outside of error limits: 2nd March 2021 (MX06725) and 1st December 2021 (CX015525). All other elements in both samples returned expected values. Generally, samples returned values close to the expected value without significant bias.

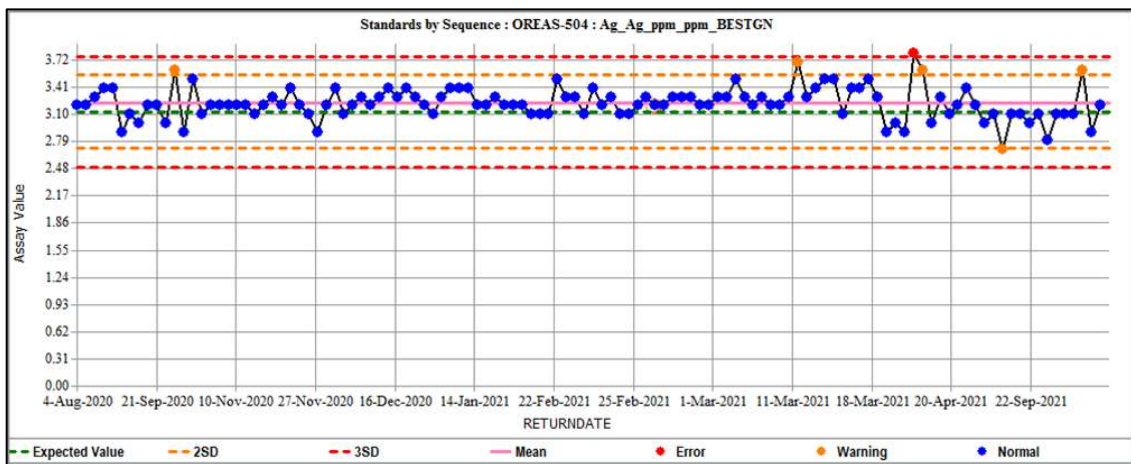


Figure 12.36 OREAS-504 CRM results for Ag ppm

One erroneous Ag sample is noted on 25th March 2021 (MX07525), this is accepted with other elements (Cu, Mo, Au) returning expected results. A small positive bias is noted, along with a possible calibration event in mid-March 2021.

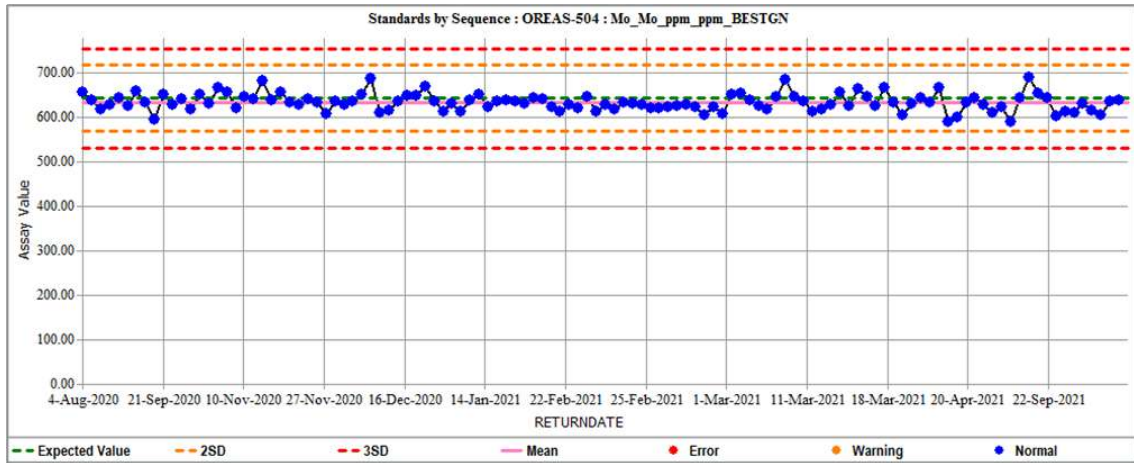


Figure 12.37 OREAS-504 CRM results for Mo ppm

12.2.3.1.7 OREAS-505

Table 12.14 OREAS-505 Reference Material Statistics as recorded in HCH database

Element	Expected Value	Standard Deviation	Accepted Min	Accepted Max
Cu ppm	3210	80	2970	3450
Au ppm	0.555	0.014	0.513	0.597
Ag ppm	1.53	0.072	1.314	1.746
Mo ppm	65	1.8	59.6	70.4

Table 12.15 Performance statistics for OREAS-505 CRM results

Statistics - OREAS-505				
Element	Cu ppm	Au ppm	Ag ppm	Mo ppm
# of Analyses above Threshold	81	81	81	81
# Outside Warning Limit	10	6	29	6
# Outside Error Limit	2	3	25	2
# of Analyses below Threshold	0	0	0	0
% Outside Error Limit	2.4691	3.7037	30.8642	2.4691
Mean	3178.7654	0.5394	1.4728	65.5802
Median	3160	0.548	1.5	65
Min	2980	0.005	1.2	62
Max	3630	0.581	1.9	76
Standard Deviation	113.7144	0.0618	0.1658	2.5143
% Rel. Std. Dev.	3.5773	11.4594	11.2599	3.8339
Coeff. of Var.	0.0358	0.1146	0.1126	0.0383
Standard Error	12.6349	0.0069	0.0184	0.2794
% Rel. Std. Err.	0.3975	1.2733	1.2511	0.426
Total Bias	-0.0097	-0.0282	-0.0374	0.0089
% Mean Bias	-0.973	-2.8184	-3.736	0.8927

One sample, CX03425, was identified as a standard swap error and was reassigned from OREAS-502 to OREAS-502c.

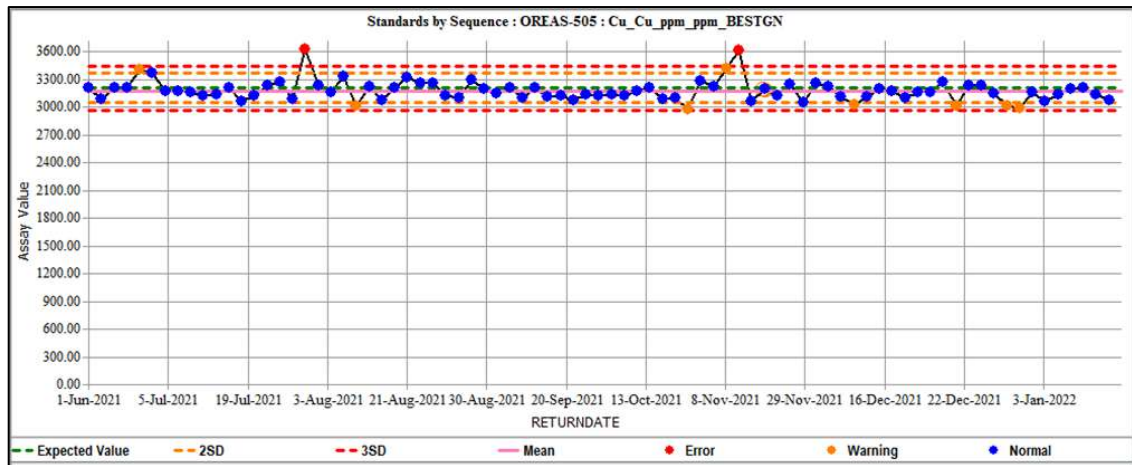


Figure 12.38 OREAS-505 CRM results for Cu ppm

Generally, Cu values returned close to the expected value, with no apparent bias, however an increase in warning flags (95% confidence) is noted from November 2021-Jan 2022. One erroneous result on 3rd August 2021 (CX05175) is noted, which returned expected values for the other elements (Mo, Au, and Ag). A second erroneous result on 10th November 2021 (CX013775) has been identified as a standard swap (originally OREAS-902) and has been included as best fit to this standard.

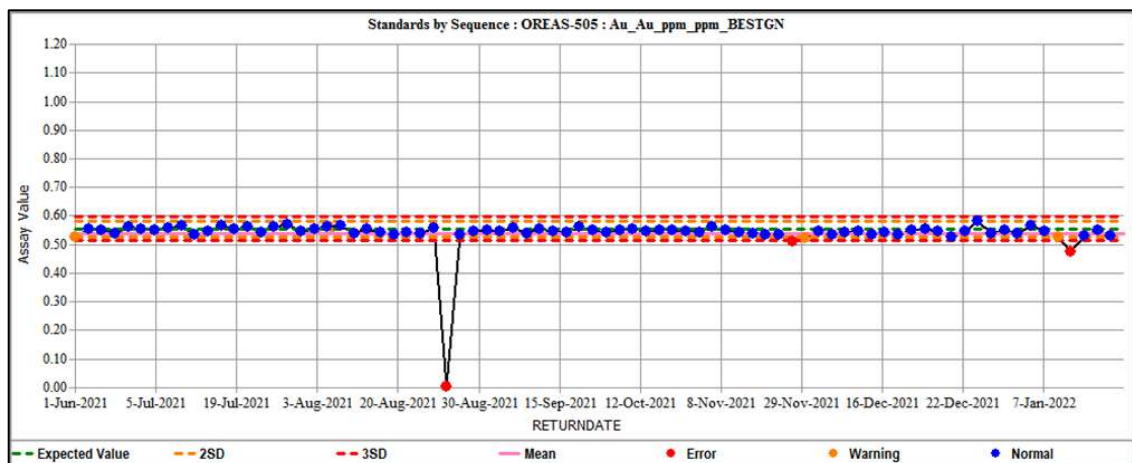


Figure 12.39 OREAS-505 CRM results for Au ppm

Three samples returned values for Au outside of error limits. Other elements (Cu, Mo, and Ag) for each of these samples came back within range and thus the samples were accepted. A small negative bias is present in the graph however this is likely biased by the erroneous sample with 0 assay value (CX07525).

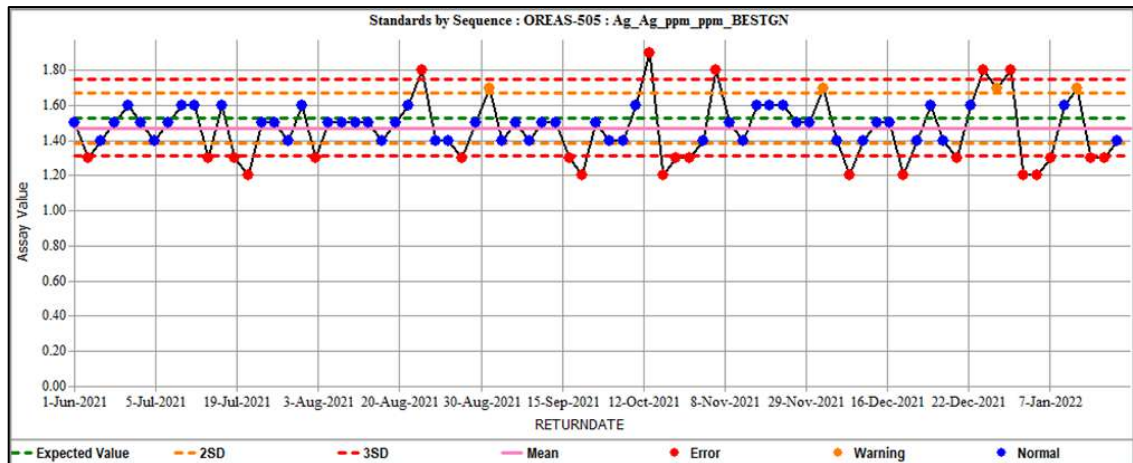


Figure 12.40 OREAS-505 CRM results for Ag ppm

Ag results were variable with this standard, showing a wide distribution of warning and erroneous values along with a negative bias, likely influenced by proximity to the detection limit (0.25ppm). This result is restricted to Ag within the standard, and a recommendation is to review the continued use of OREAS-505 as it may not be suitable for validation of the Ag assay at these ranges.

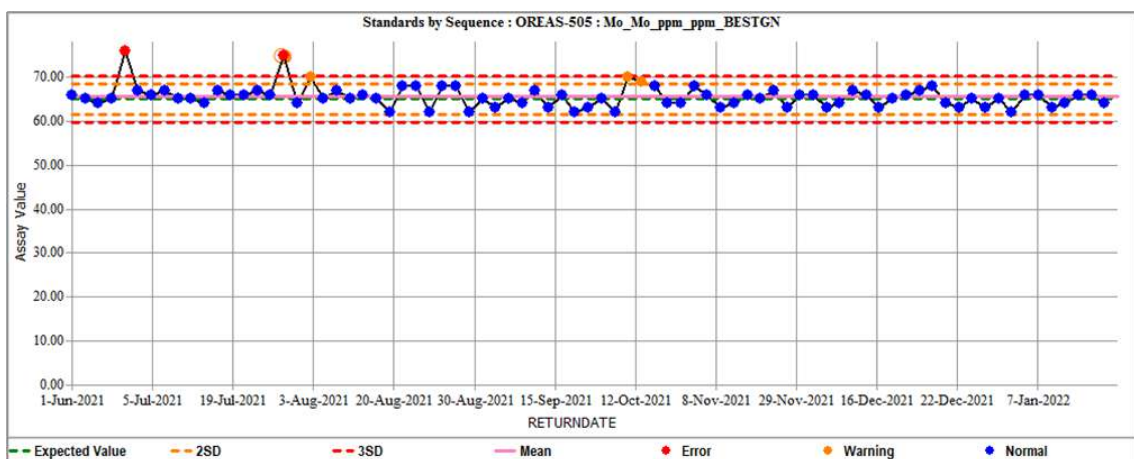


Figure 12.41 OREAS-505 CRM results for Mo ppm

Two samples returned erroneous results on 21st June 2021 (CX02475) and 3rd August 2021 (CX05175). Both samples returned expected values in the other elements (Cu, Au, and Ag).

12.2.3.1.8 OREAS-902

Table 12.16 OREAS-902 Reference Material Statistics as recorded in HCH database

Element	Expected Value	Standard Deviation	Accepted Min	Accepted Max
Cu ppm	3010	80	2770	3250
Ag ppm	0.343	0.043	0.214	0.472
Mo ppm	12.2	0.65	10.25	14.15

Table 12.17 Performance statistics for OREAS-902 CRM results

Element	Cu ppm	Ag ppm	Mo ppm
# of Analyses above Threshold	42	42	42
# Outside Warning Limit	5	42	1
# Outside Error Limit	0	3	1
# of Analyses below Threshold	0	0	0
% Outside Error Limit	0	7.1429	2.381
Mean	3063.8095	0.2679	11.5476
Median	3060	0.25	12
Min	2890	0.25	10
Max	3230	0.5	12
Standard Deviation	89.4414	0.0652	0.5501
% Rel. Std. Dev.	2.9193	24.3284	4.7633
Coeff. of Var.	0.0292	0.2433	0.0476
Standard Error	13.8011	0.0101	0.0849
% Rel. Std. Err.	0.4505	3.754	0.735
Total Bias	0.0179	-0.2191	-0.0535
% Mean Bias	1.7877	-21.9075	-5.3474

Two samples were identified as standard swaps with OREAS-505 and have been updated in the database to reflect this. These are 19th October 2021 (CX012625) and 10th November 2021 (CX013775).

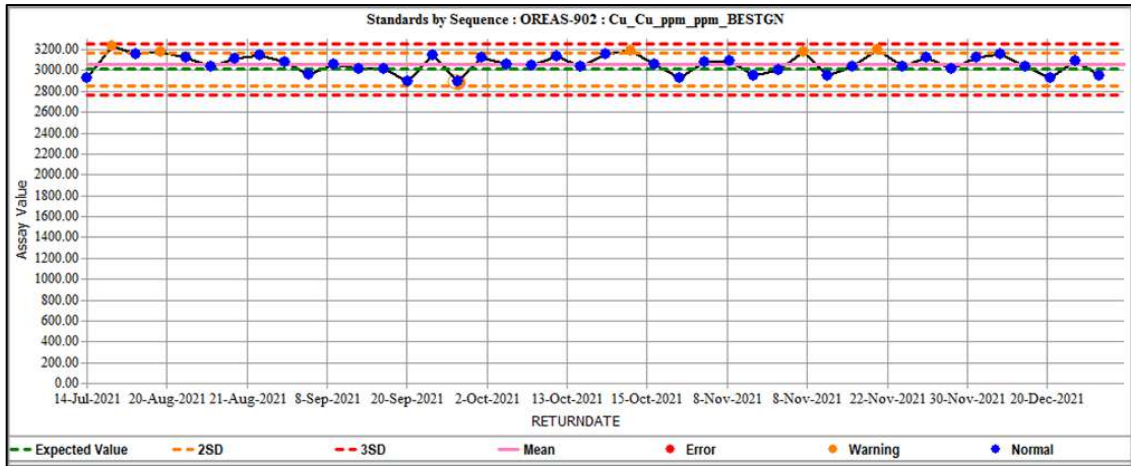


Figure 12.42 OREAS-902 CRM results for Cu ppm

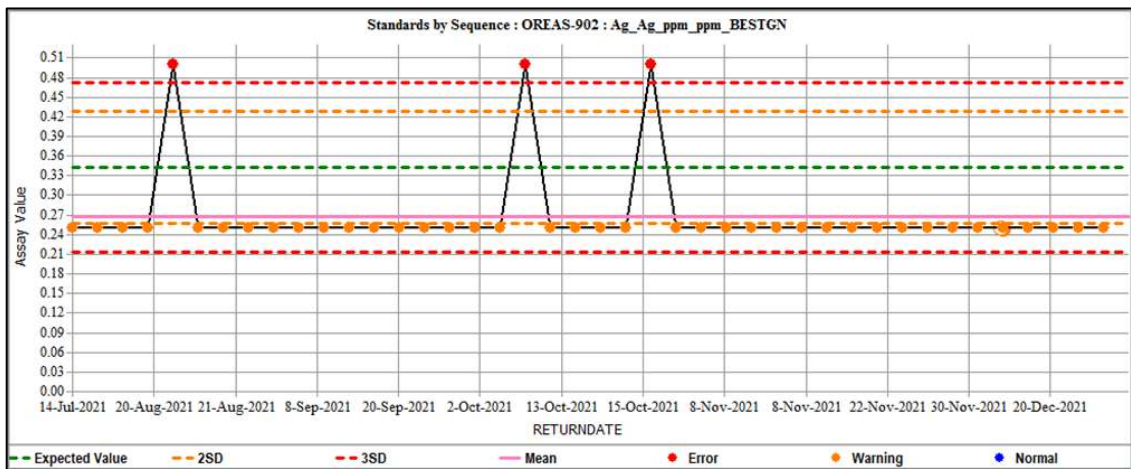


Figure 12.43 OREAS-902 CRM results for Ag ppm

Ag cannot be accurately reflected by OREAS-902 as the expected value is the same as the detection limit for this methodology.

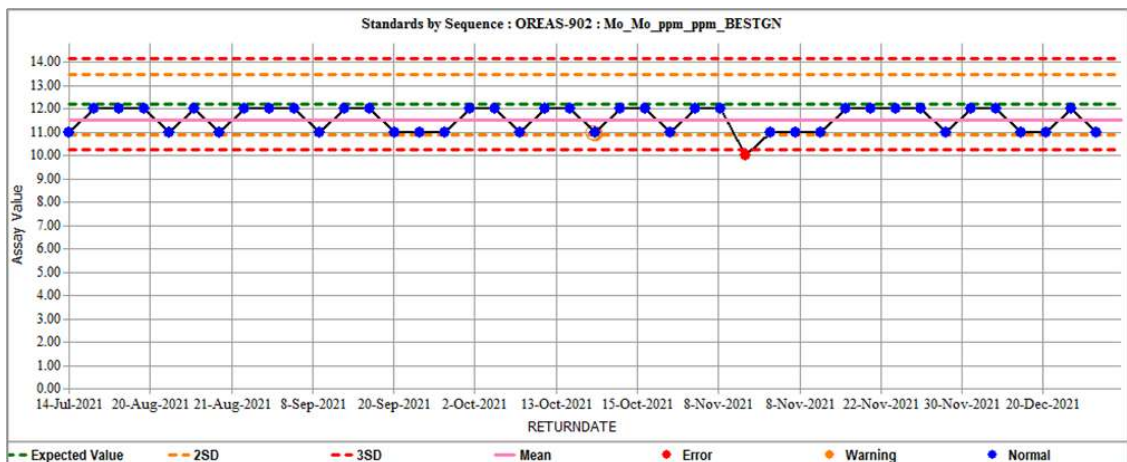


Figure 12.44 OREAS-902 CRM results for Mo ppm

One erroneous value on 8th November 2021 (CX013325), which passed on Cu. A consistent negative bias is noted.

12.2.4 Blanks

12.2.4.1 Certified Blanks

12.2.4.1.1 IN-BMF-17

Table 12.18 IN-BMF-172 Reference Material Summary Statistics as included in the HCH database

Element	Expected Value	Standard Deviation	Accepted Min	Accepted Max
Cu ppm	1	20	0.5	60
Au ppm	0	0.1	-0.3	0.3
Ag ppm	0	0.5	-1.5	1.5
Mo ppm	1	20	0.5	20

Table 12.19 Statistics from IN-BMF-172 CRM results for all elements as exported from HCH database

Statistics- IN-BMF-172				
Element	Cu ppm	Au ppm	Mo ppm	Ag ppm
# of Analyses above Threshold	141	14	165	167
# Outside Warning Limit	0	14	0	0
# Outside Error Limit	0	0	0	0
# of Analyses below Threshold	0	0	0	0
% Outside Error Limit	0	0	0	0
Mean	5.8865	0.0067	2.0485	0.253
Median	5	0.006	2	0.25
Min	3	0.005	1	0.25
Max	20	0.011	5	0.5
Standard Deviation	2.7648	0.0019	0.6325	0.0273
% Rel. Std. Dev.	46.9685	27.6659	30.8772	10.7814
Coeff. of Var.	0.4697	0.2767	0.3088	0.1078
Standard Error	0.2328	0.0005	0.0492	0.0021
% Rel. Std. Err.	3.9555	7.394	2.4038	0.8343
Total Bias	4.8865	n/a	1.0485	n/a
% Mean Bias	488.6525	n/a	104.8485	n/a

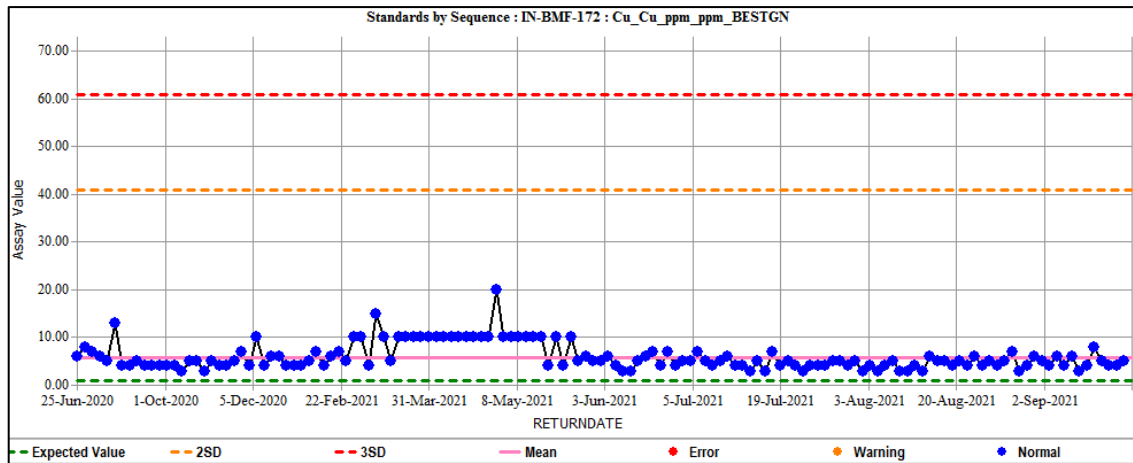


Figure 12.45. IN-BMF-172 CRM results for Cu

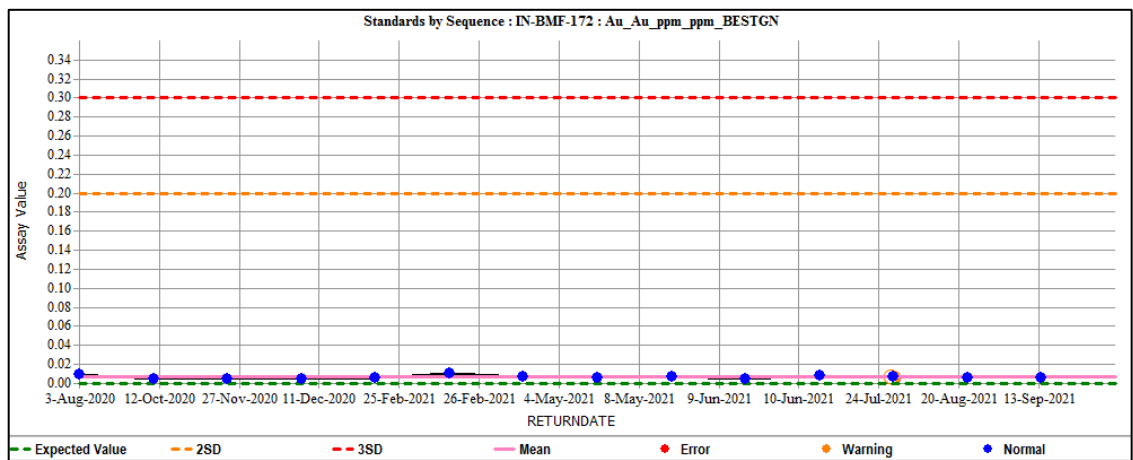


Figure 12.46. IN-BMF-172 CRM results for Au

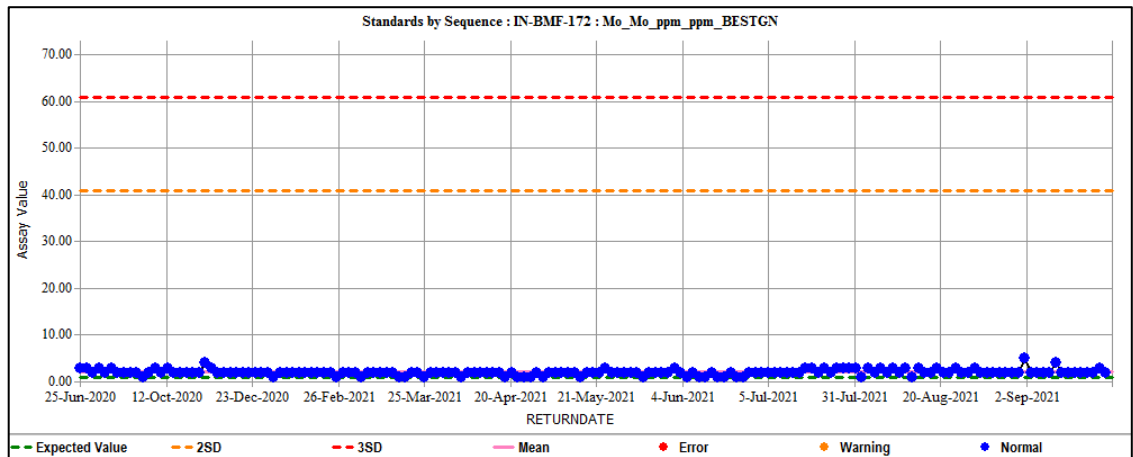


Figure 12.47. IN-BMF-172 CRM results for Mo

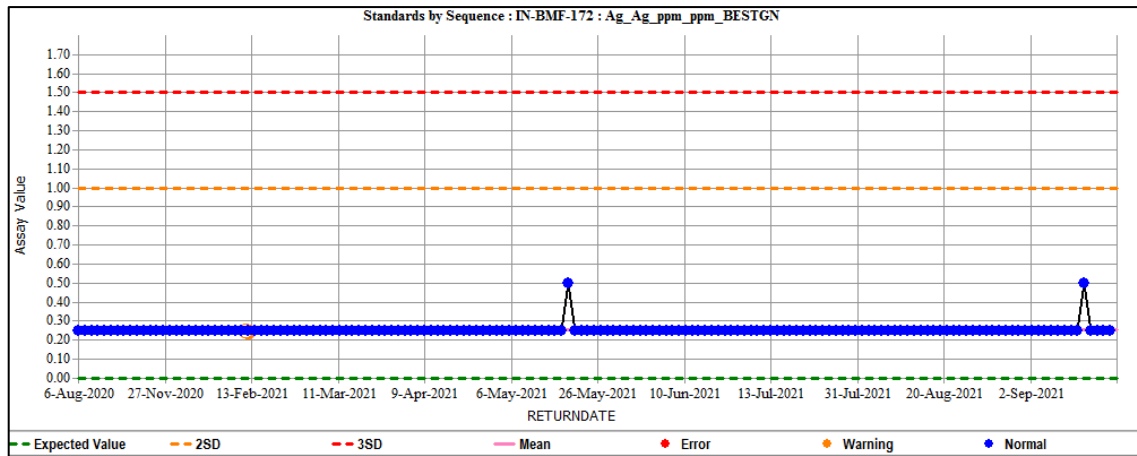


Figure 12.48. IN-BMF-172 CRM results for Ag

12.2.4.1.2 IN-BMF-333

Table 12.20 IN-BMF-333 Reference Material Summary Statistics as included in the HCH database

Element	Expected Value	Standard Deviation	Accepted Min	Accepted Max
Cu ppm	10	13.333	0	40
Au ppm	0	0.033	0	0.1
Ag ppm	0	0.333	0	1

Table 12.21 Statistics from IN-BMF-333 CRM results for all elements as exported from HCH database

Element	Cu ppm	Au_ppm	Ag ppm
# of Analyses above Threshold	101	15	101
# Outside Warning Limit	0	0	0
# Outside Error Limit	0	0	0
# of Analyses below Threshold	0	0	0
% Outside Error Limit	0	0	0
Mean	9.703	0.0089	0.25
Median	9	0.005	0.25
Min	6	0.005	0.25
Max	31	0.047	0.25
Standard Deviation	3.1322	0.0107	0
% Rel. Std. Dev.	32.2812	120.7096	0
Coeff. of Var.	0.3228	1.2071	0
Standard Error	0.3117	0.0028	0
% Rel. Std. Err.	3.2121	31.1671	0
Total Bias	-0.0297	n/a	n/a
% Mean Bias	-2.9703	n/a	n/a

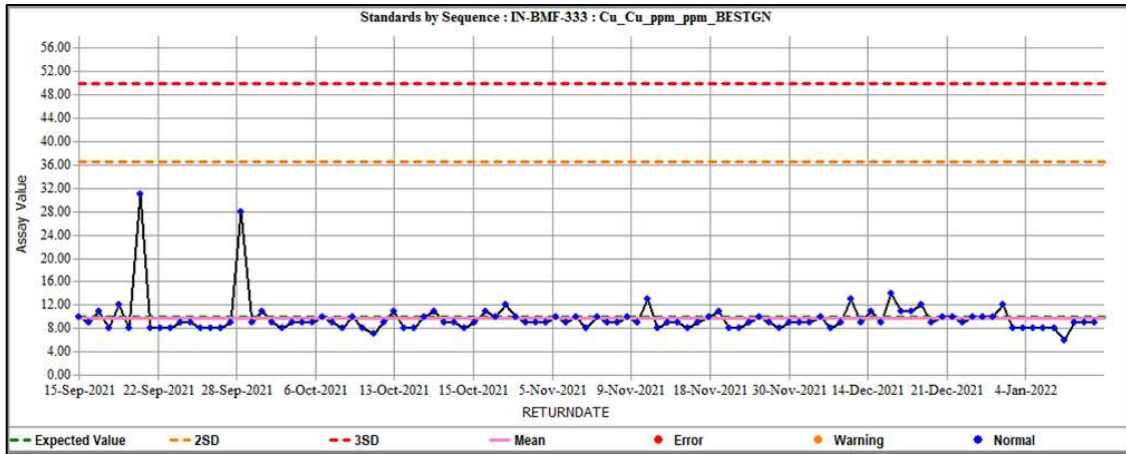


Figure 12.49. IN-BMF-333 CRM results for Cu

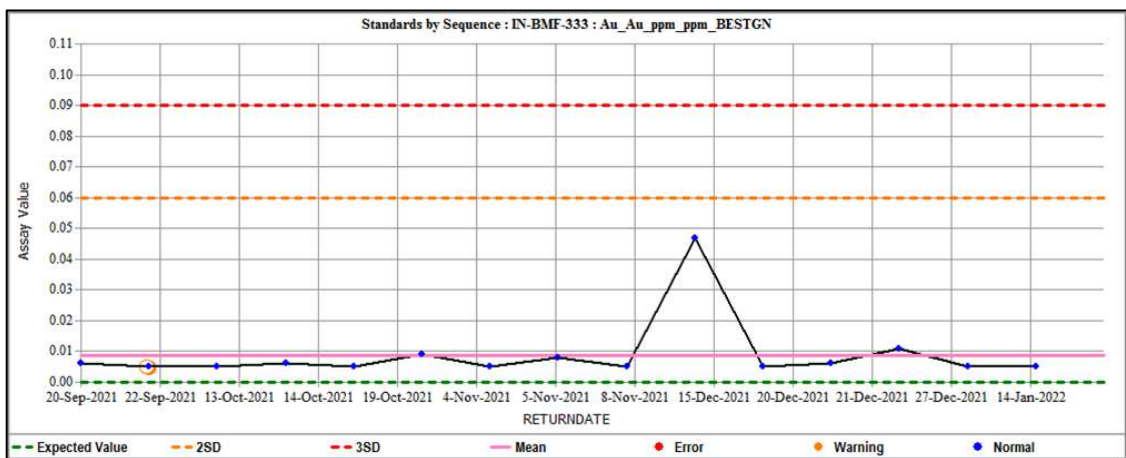


Figure 12.50. IN-BMF-333 CRM results for Au

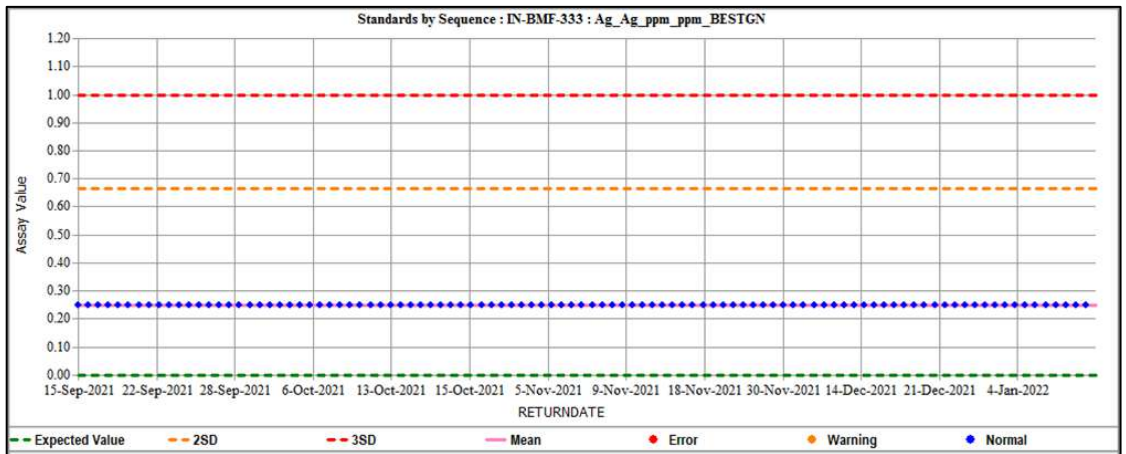


Figure 12.51. IN-BMF-333 CRM results for Ag

12.2.4.2 Uncertified Blanks

One unmineralised “blank” was inserted every 100th sample submitted for analysis. These blanks enable checks on any potential analytical contamination.

HCH submits its own coarse blanks (as distinction from the HCH - submitted ‘blank’ pulp. The submission of coarse blank material allows investigation of any potential crushing and milling bias). The coarse blank samples were inserted at the geologist’s discretion with an emphasis on placement in visual high-grade zones as well as being inserted at the start and end of a batch.

Table 12.22 Performance statistics for uncertified coarse blanks

Statistics- QtzBLK				
	Cu ppm	Au ppm	Mo ppm	Ag ppm
# of Analyses above Threshold	1123	118	274	1244
# Outside Warning Limit	37	10	25	0
# Outside Error Limit	16	7	13	0
# of Analyses below Threshold	0	0	0	0
% Outside Error Limit	1.4248	5.9322	4.7445	0
Mean	7.6776	0.0106	1.5073	0.2502
Median	5	0.006	1	0.25
Min	1	0.005	1	0.25
Max	1045	0.296	19	0.5
Standard Deviation	31.7154	0.0274	1.5341	0.0071
% Rel. Std. Dev.	413.0868	259.4246	101.7773	2.833
Coeff. of Var.	4.1309	2.5942	1.0178	0.0283
Standard Error	0.9464	0.0025	0.0927	0.0002
% Rel. Std. Err.	12.3268	23.882	6.1486	0.0803
Total Bias	6.6776	1.1119	0.5073	n/a
% Mean Bias	667.7649	111.1864	50.7299	n/a

All graphs are filtered to exclude sample CX015880 which returned an extreme value of 1045 ppm Cu and 0.3 ppm Au, for clarity of plotting. This sample was investigated and determined to be contamination at the RC sampling likely from mistakenly loading the next mineralised sample, as it immediately followed a passing blank. The result is retained in the statistical analysis.

A recommendation of this review is to determine a more appropriate criteria for error flagging, likely as a percentage carry over from the previous sample.

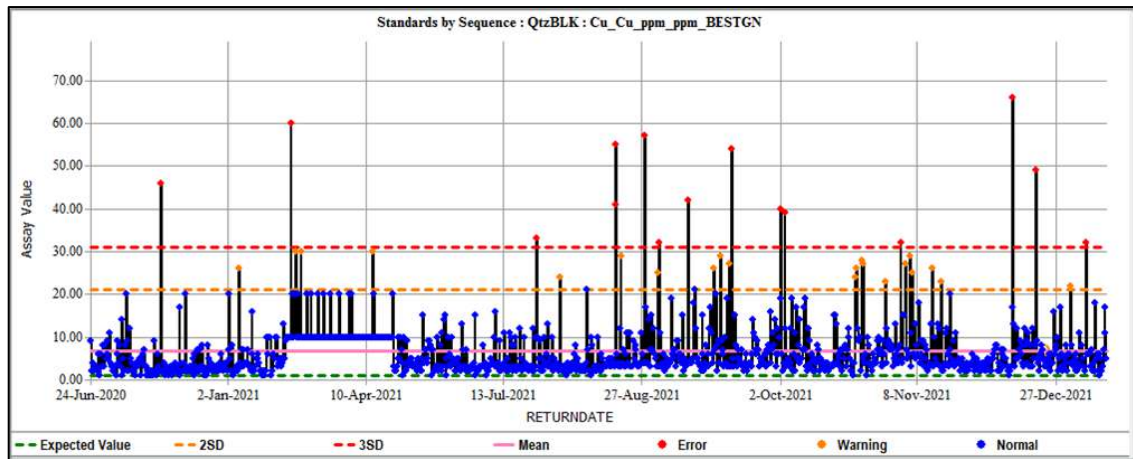


Figure 12.52 Coarse Blank / Qtz Blank results for Cu ppm

Values returned above 30ppm Cu were investigated, and they were found to follow elevated grade samples (>7000 ppm) and have the potential to be caused by smear contamination in the crushing/processing phase. Values returned within limits (<15ppm Cu) have not been reviewed. The sample collection method was investigated and found not to be a contributing factor, with RC vs DD roughly equivalent, and Scoop vs Cone methods within RC also equivalent. Figure 12.53 shows sample collection method, with number of failed samples and as a percentage of the total number of failed samples.

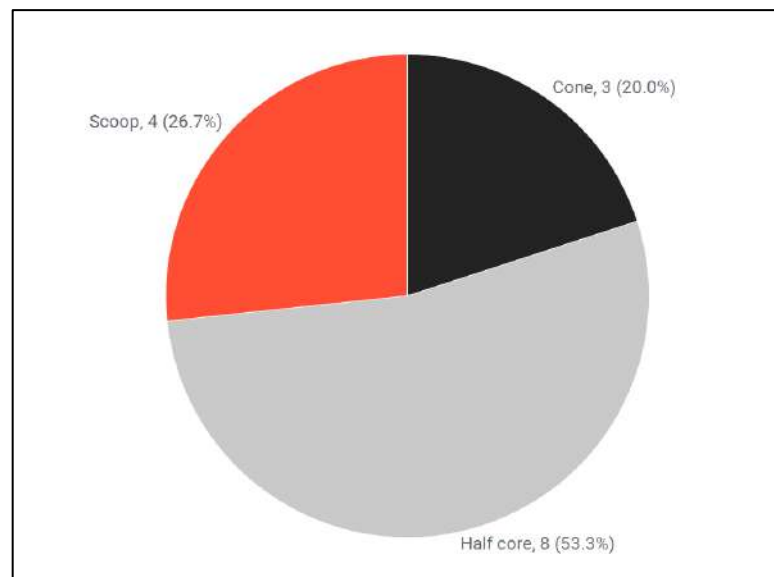


Figure 12.53. Quartz Blank fails by sample collection method

12.2.4.3 Field Duplicates

Most duplicates were returned within an acceptable range. Although some outliers were found, they are generally not across multiple elements per sample. The regression line shows strong correlation across the dataset, with only Au being skewed and largely due to one high value pair.

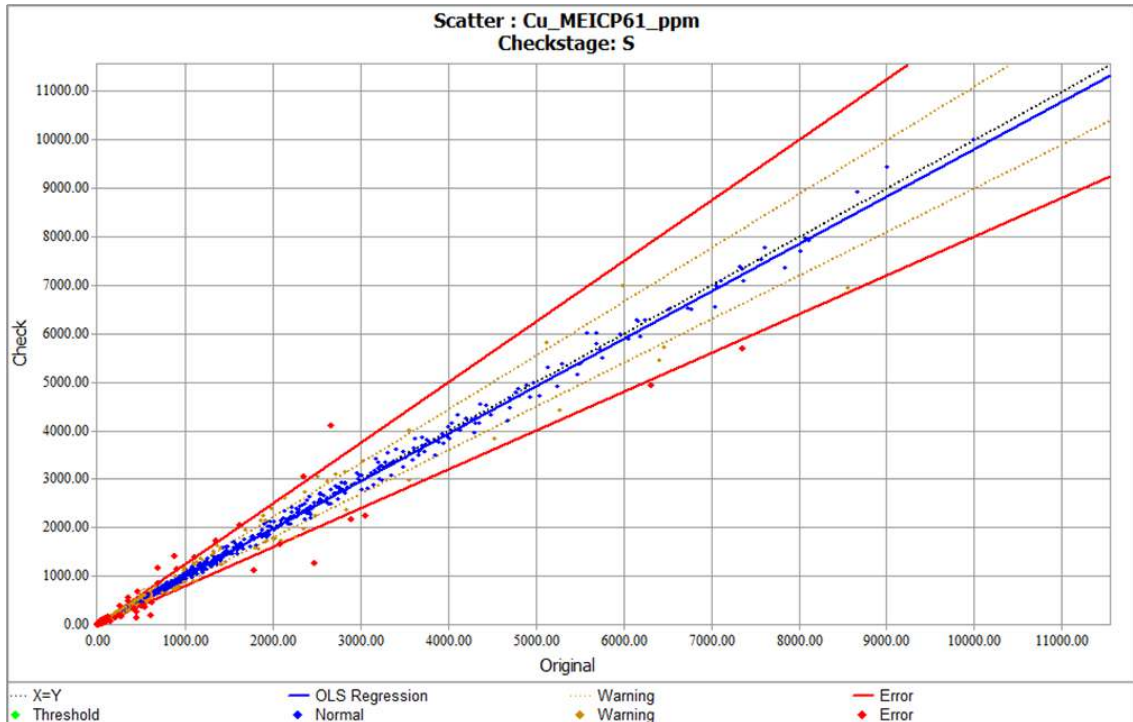


Figure 12.54 HCH duplicate samples displaying Cu ppm analysed by ME-ICP61 technique

For Cu, ~75% of pairs returned with a high level of precision ($\pm 10\%$). 10.8% returned outside $\pm 20\%$. The RC drilling methodology has a higher percentage of low-precision results compared to DD, however reviewing the frequency distribution over Cu grade shows that most of these errors are at very low ($<0.05\%$ Cu) grade.

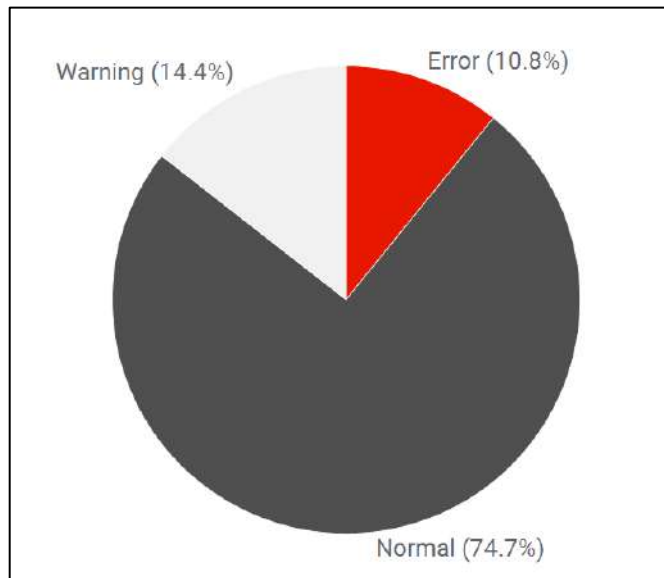


Figure 12.55 Distribution of Normal (within $\pm 10\%$), Warning (between ± 10 and $\pm 20\%$), and Error (above $\pm 20\%$) results for field duplicates

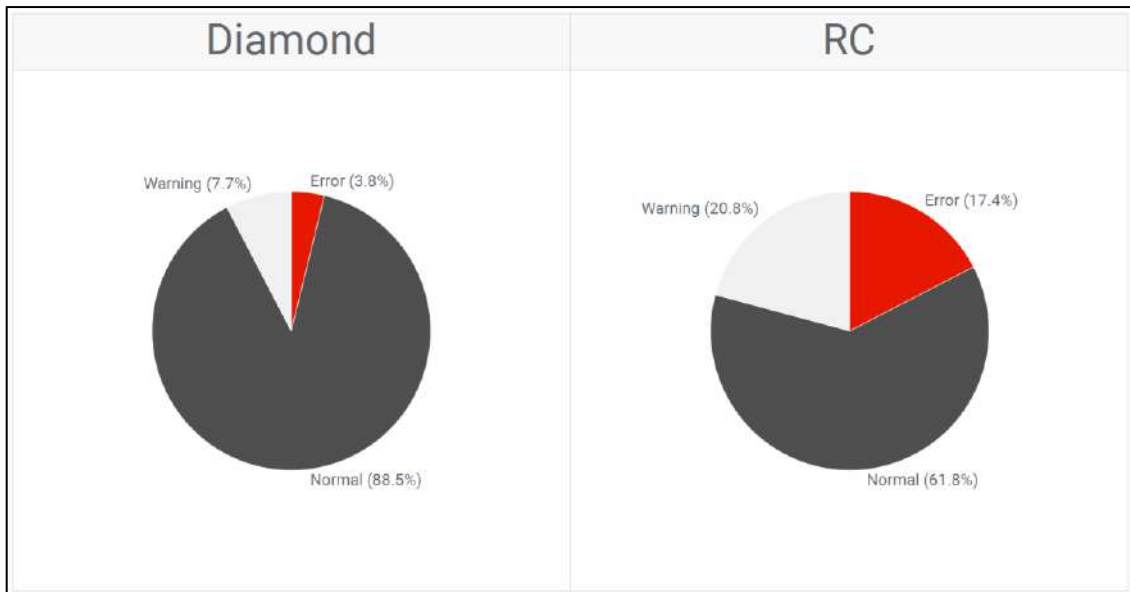


Figure 12.56 Distribution of results by Hole Type

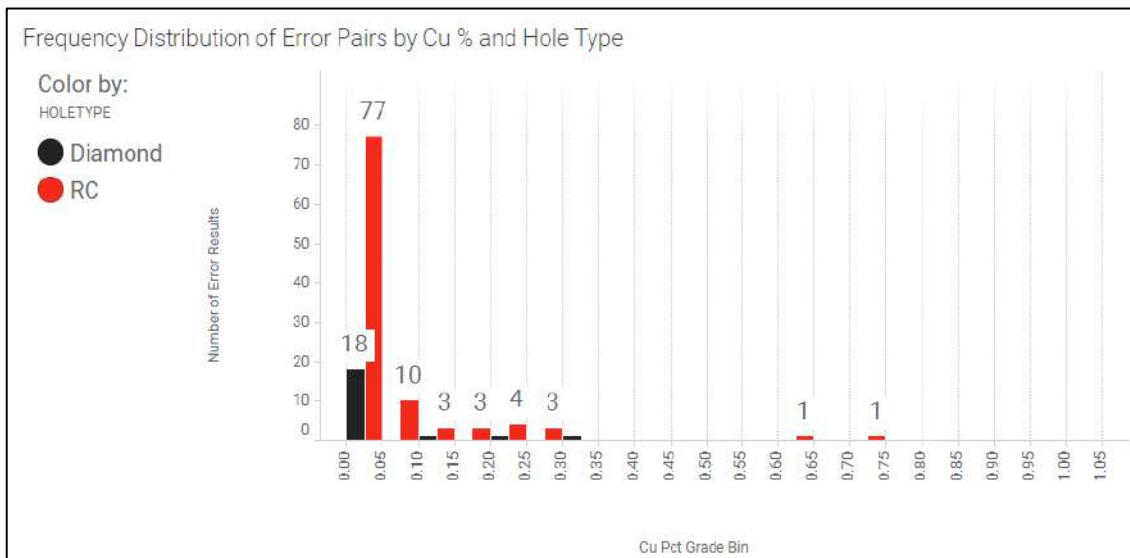


Figure 12.57 Frequency distribution of Error results by Cu Grade and Hole Type

Field duplicates for Au are generally low grade, with the method detection limit being 0.001 and most results within 10x of this number. Considering this, precision is reasonable, with most sample pairs returning a high-level of precision (+/- 10%).

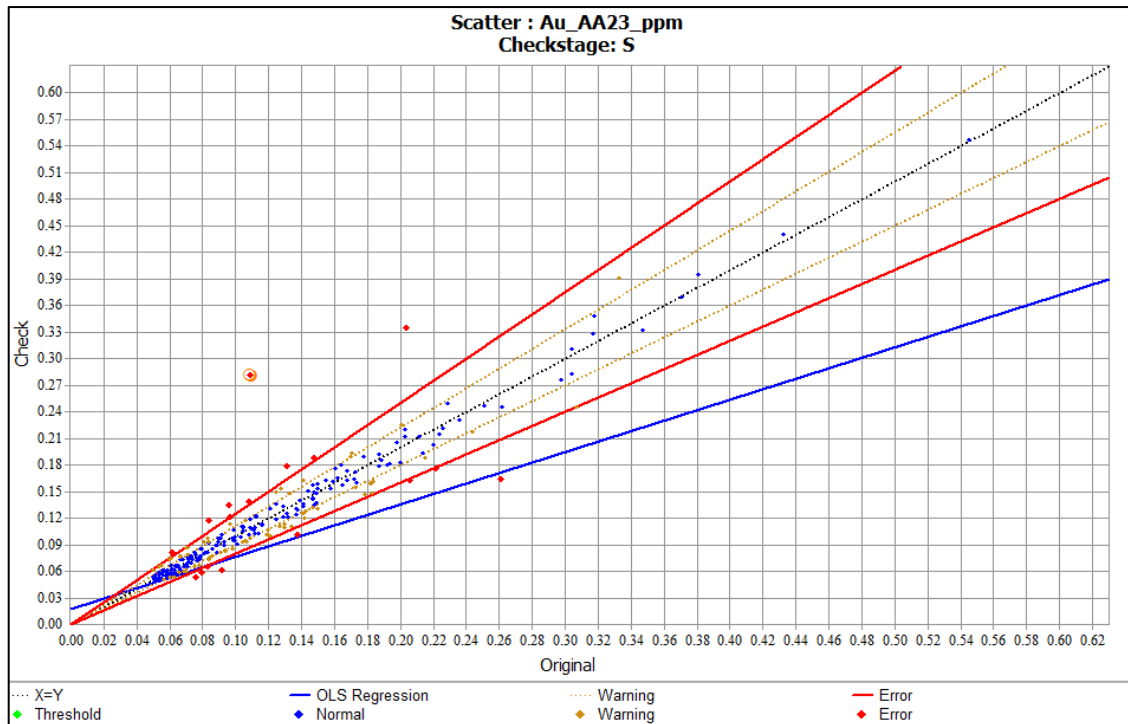


Figure 12.58 HCH duplicate samples displaying Au ppm analysed by AA23 technique, excluding the outlier pair (CX05891 - 4.22ppm vs 2.17ppm)

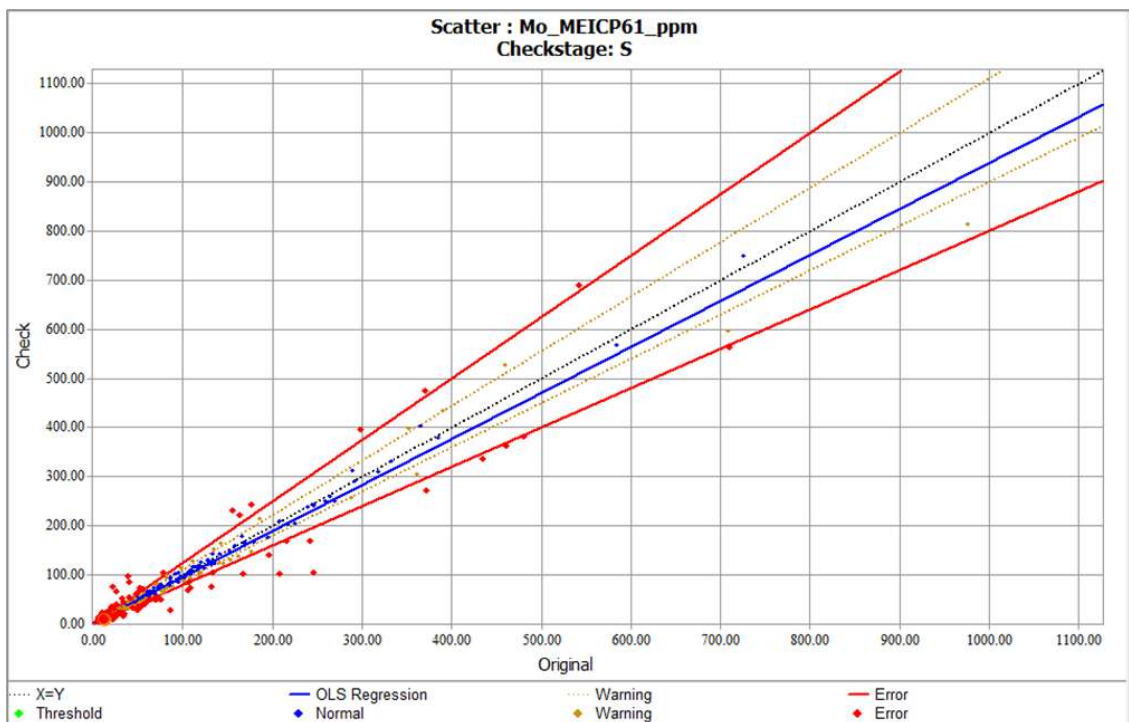


Figure 12.59 HCH duplicate samples displaying Mo ppm analysed by ME-ICP61 technique

Of all elements, Mo shows the poorest precision over a range of grade levels. No bias is noted, and it is possible that the higher rate of variance within the pairs reflects the spotty nature of Mo mineralisation, rather than sample collection or preparation factors.

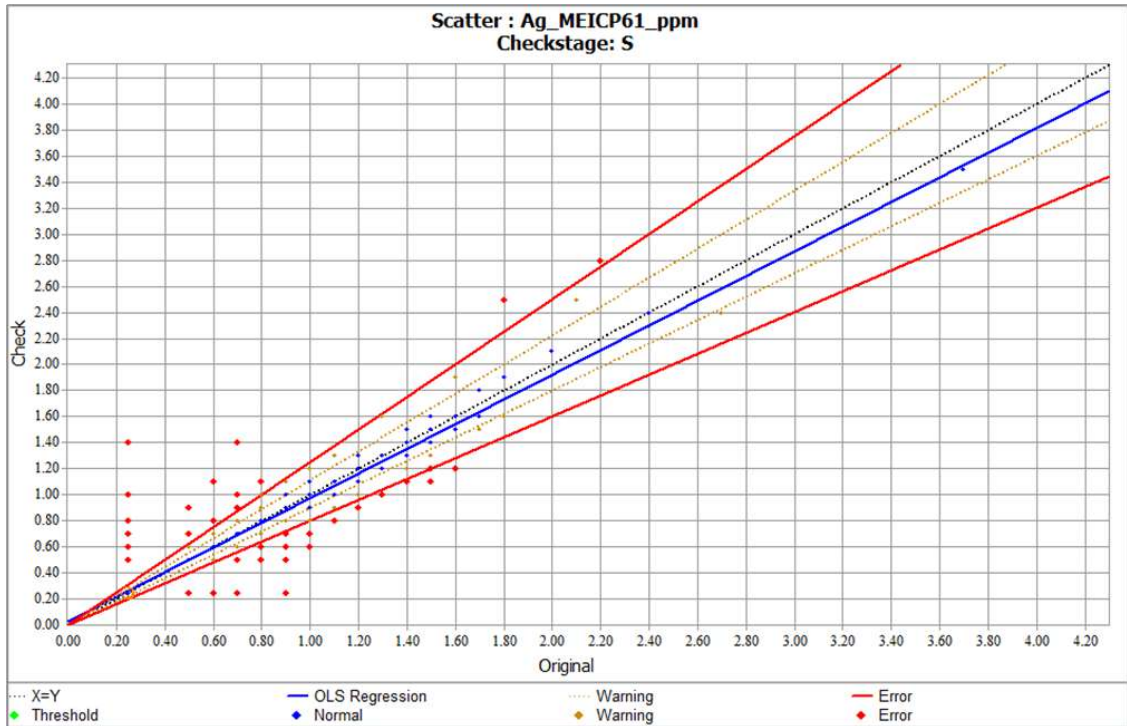


Figure 12.60 HCH duplicate samples displaying Ag ppm analysed by ME-ICP61 technique

Ag samples results are influenced by proximity to the detection limit (0.25ppm) and no meaningful information can be gained from comparing data pairs in this range.

12.2.4.4 Umpire Checks

In May 2021 108 samples, including 9 QAQC samples (7 certified reference material, and 2 Blanks), were collected for the program. Sample types included RC rock chips, and NQ and HQ half core DD samples. Samples were sent to Bureau Veritas Laboratory and results analysed in September 2021.

The Analysis found no consistent or material bias between the ALS and Bureau Veritas Laboratory across the analytes of Cu, Mo, Au, and Ag.

Scatter plots showing correlations between the primary assay and the umpire assay for each element and sample type are shown in Figure 12.61 to Figure 12.64.

No further recommendations are made in relation to this program.

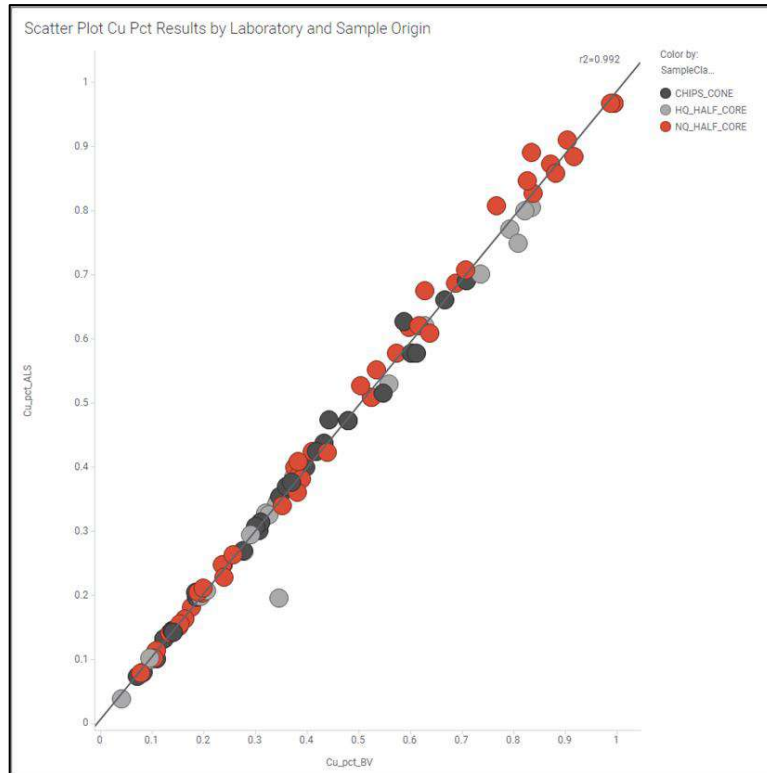


Figure 12.61 Scatter plot of Cu% by Laboratory and Original Sample Type

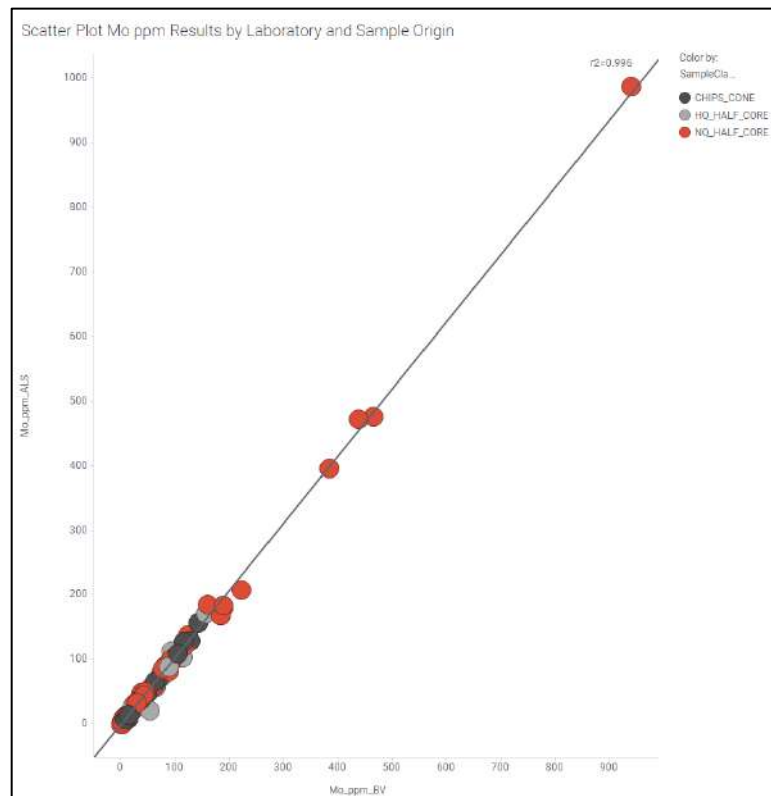


Figure 12.62 Scatter plot of Mo ppm by Laboratory and Original Sample Type

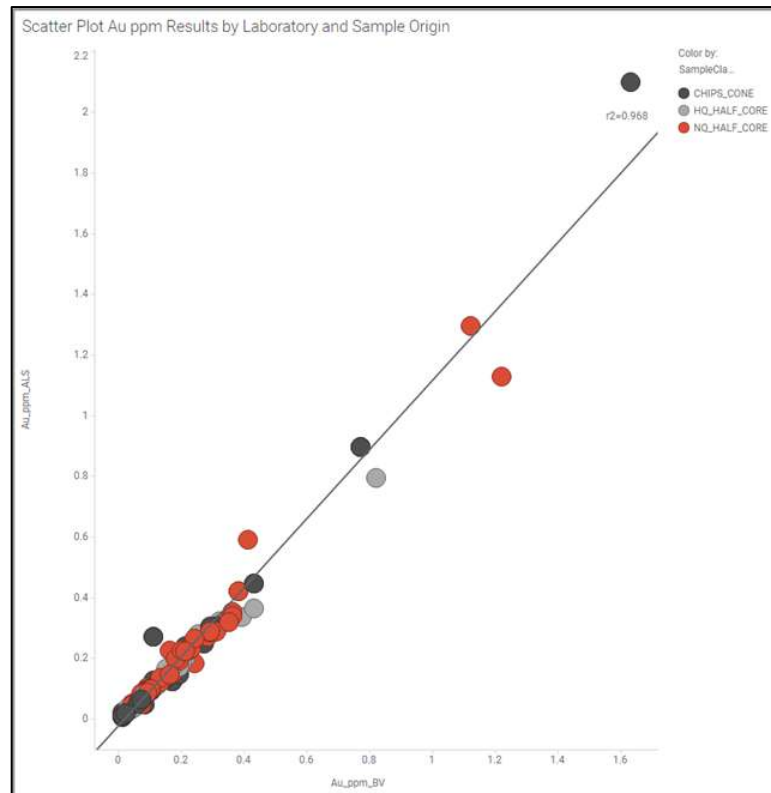


Figure 12.63 Scatter plot of Au ppm by Laboratory and Original Sample Type

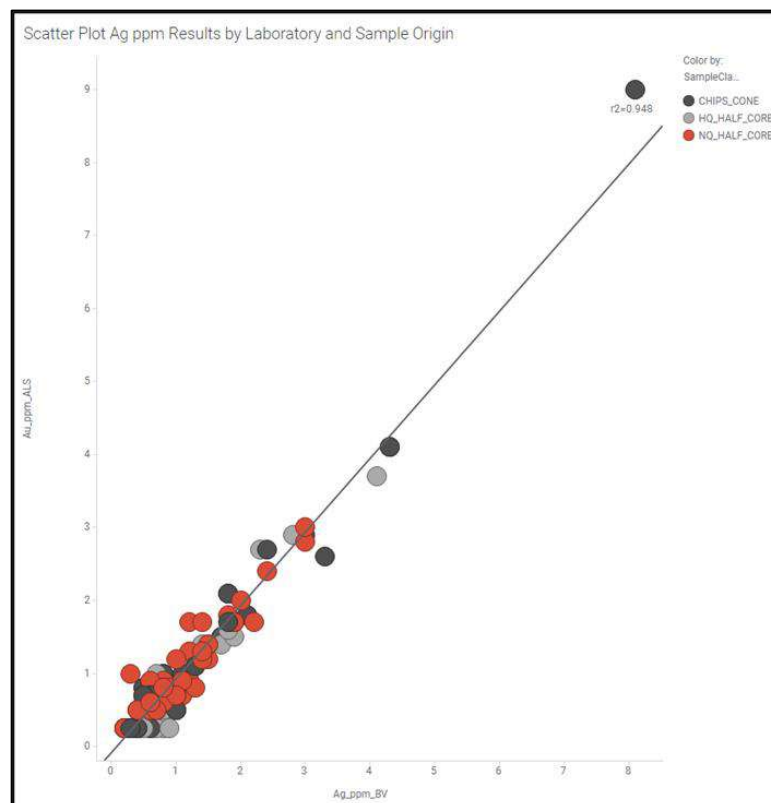


Figure 12.64 Scatter plot of Ag ppm by Laboratory and Original Sample Type

12.3 San Antonio

12.3.1 Independent Qualified Person Review and Verification

No third-party audits were conducted on the Maiden Mineral Resource Estimate as the internal data verification and quality assurance programs were deemed adequate by the Qualified Person for the Mineral Resource Estimation. The Qualified Person is a third party to HCH and completed independent data verification prior to estimation being completed.

12.3.2 Internal Verification Programs

HCH employed a variety of QA/QC measures to assess and ensure the quality of the drill data used for resource estimation. QA/QC for sampling and assay data has included the use of certified reference material (CRM) “standards” and “blanks”, field duplicates, umpire laboratory checks, and audits.

Conclusions from this review can be found below:

- Overall performance of QAQC samples gives a good level of confidence in the datasets from HCH. Points below were noted for future work:
- Ensure that QAQC sample selection and insertion rates are to the HCH standard
- Review the approach for uncertified blanks and tolerance limits, specifically to consider the tolerance for contamination as a percentage of the assay value, over the current discrete cut off.
- Review individual batch QAQC assessment procedure to ensure prompt re-assaying of QAQC samples when required.
- Select umpire laboratories with closer alignment of detection limits.
- Twin hole data for historic drilling should be conducted to ascertain confidence in historic work.

12.3.3 QA/QC Program

QA/QC samples and their insertion rates (IR), as a percentage of the 1,720 samples from all HCH drilling to date at the project are provided in Table 12.23.

Table 12.23 San Antonio Drilling Program QAQC Insertion Rates

QC Type	Number of Samples	Insertion Rate
Mineralised Standard	39	2.3%
Certified Blank	16	0.9%
Coarse Blank	56	3.3%
Coarse Duplicate	16	0.9%
Assay Samples	1,720	-

12.3.3.1 Standards

There were 39 mineralised CRMs inserted in the 1,720m of drilling completed at San Antonio at an insertion rate of 2.3% of samples. Two distinct CRMs were used in the program (Table 12.24), OREAS-22c and OREAS-501b. OREAS-22c was also used as a certified blank.

Table 12.24 HCH CRM Details

CRM Ref Name	Number of Samples	Expected Cu pct	Expected Au ppm	Expected Mo ppm	Expected Ag ppm
OREAS-22c	18	0.001	-	4.3	-
OREAS-501b	37	0.260	0.248	99	0.778

The assay results from submitted CRMs show acceptable correlation with their expected value without any appreciable analytical drift over time (Figure 12.65 to Figure 12.71).

There were no returned values outside three standard deviations for copper, gold, or molybdenum. Several silver results charted below the 3 standard deviations for OREAS-501b, but this was found to be due to the lower detection limit and is of no concern.

12.3.3.1.1 OREAS-501b

Table 12.25 OREAS-501b Reference Material Statistics as recorded in HCH database

Element	Expected Value	Standard Deviation	Accepted Min	Accepted Max
Cu pct	0.260	0.011	0.227	0.293
Au ppm	0.248	0.010	0.218	0.278
Ag ppm	0.778	0.128	0.394	1.162
Mo ppm	99	7.5	76.5	121.5

Table 12.26 Performance statistics for OREAS-501b CRM results

Statistics - OREAS-501b				
	Cu ppm	Au ppm	Ag ppm	Mo ppm
# of Analyses above Threshold	37	37	37	37
# Outside Warning Limit	0	0	10	0
# Outside Error Limit	0	0	4	0
# of Analyses below Threshold	0	0	0	0
% Outside Error Limit	0	0	10.8108	0
Mean	2600	0.2439	0.6541	99.1351
Median	2610	0.242	0.7	100
Min	2490	0.237	0.25	93
Max	2740	0.255	1	106
Standard Deviation	55.4276	0.0046	0.1945	3.3678
% Rel. Std. Dev.	2.1318	1.8671	29.7376	3.3972
Coeff. of Var.	0.0213	0.0187	0.2974	0.034
Standard Error	9.1122	0.0007	0.032	0.5537
% Rel. Std. Err.	0.3505	0.3069	4.8888	0.5585
Total Bias	0	-0.0167	-0.1593	0.0014
% Mean Bias	0	-1.6674	-15.9314	0.1365

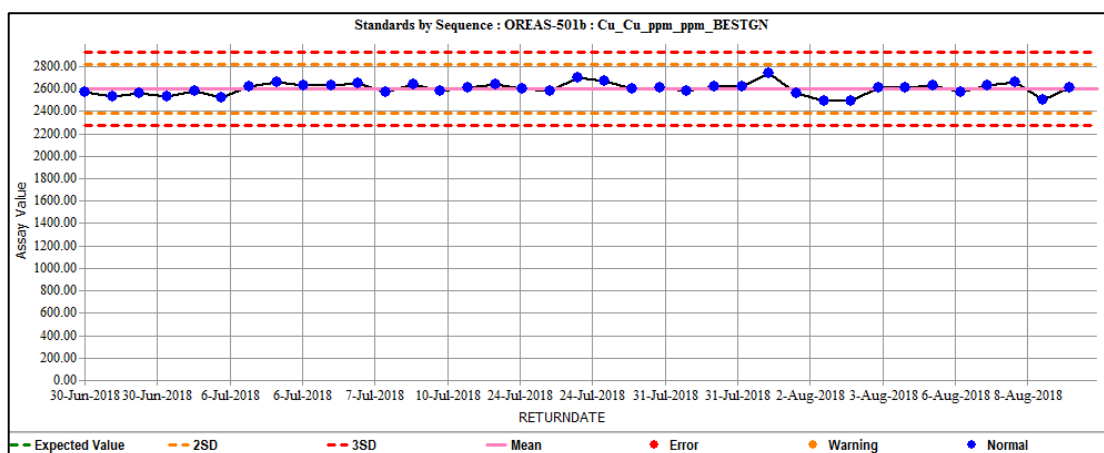


Figure 12.65 OREAS-501b results for Cu ppm

12.3.3.1.2 OREAS-22c

Table 12.27 Performance statistics for OREAS-501b CRM results OREAS-22c Reference material summary statistics as recorded in the HCH database

Element	Expected Value	Standard Deviation	Accepted Min	Accepted Max
Cu ppm	10	2.7	7	18
Au ppm	0	0.01	-0.01	0.03
Ag ppm	0	0.5	-1.5	1.5
Mo ppm	4.3	0.9	3.4	7

Table 12.28 Performance statistics for OREAS-22c CRM results

Statistics - OREAS-22c				
	Cu ppm	Au ppm	Ag ppm	Mo ppm
# of Analyses above Threshold	17	3	17	17
# Outside Warning Limit	1	0	0	0
# Outside Error Limit	1	0	0	1
# of Analyses below Threshold	0	0	0	0
% Outside Error Limit	5.8824	0	0	5.8824
Mean	9.9412	0.0017	0.25	4.2353
Median	9	0.001	0.25	4
Min	7	0.001	0.25	3
Max	26	0.003	0.25	5
Standard Deviation	4.3225	0.0012	0	0.5623
% Rel. Std. Dev.	43.4806	69.282	0	13.2764
Coeff. of Var.	0.4348	0.6928	0	0.1328
Standard Error	1.0484	0.0007	0	0.1364
% Rel. Std. Err.	10.5456	40	0	3.22
Total Bias	-0.0059	Na	Na	-0.015
% Mean Bias	-0.5882	Na	Na	-1.5048

One sample (AX195201, SAP0031) failed at high range. Otherwise, the standard performed as expected. No CRM in use at the time of analysis has an expected value in the range of 26ppm, permitting a swap. Investigation of the batch indicates that it is a possible case of instrument contamination, with the CRM in the middle of a high-grade zone. The zone includes 10m (10 samples) averaging ~11,000ppm.

As the QAQC report was compiled three years post-drilling, to coincide with the maiden resource estimate, the QP notes that this batch should have been re-analysed to check for contamination throughout the batch.

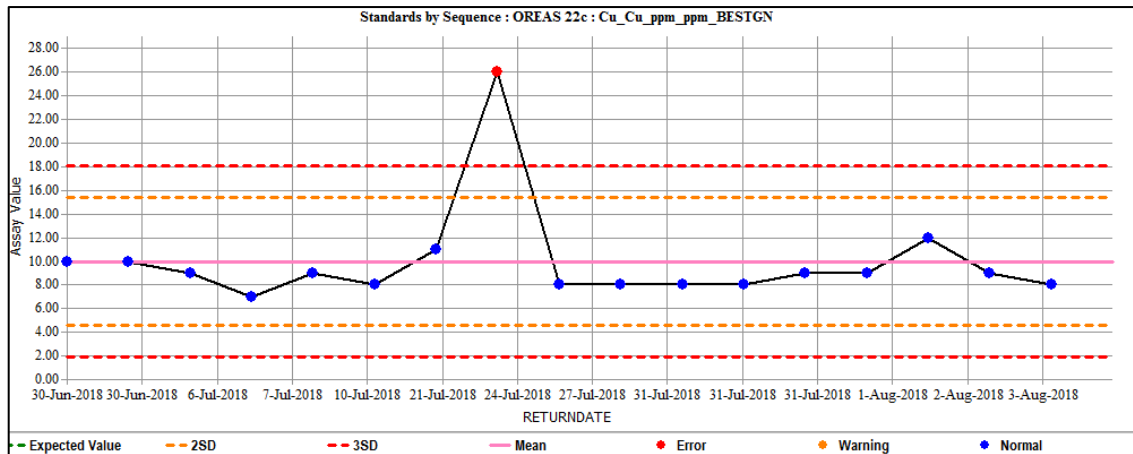


Figure 12.69 OREAS-22c CRM results for Cu ppm

OREAS22c was not certified for an Au value (certified below detection limit). Of the 17 analysis events, 3 occurred above detection limit and at a maximum of 3x detection limit.

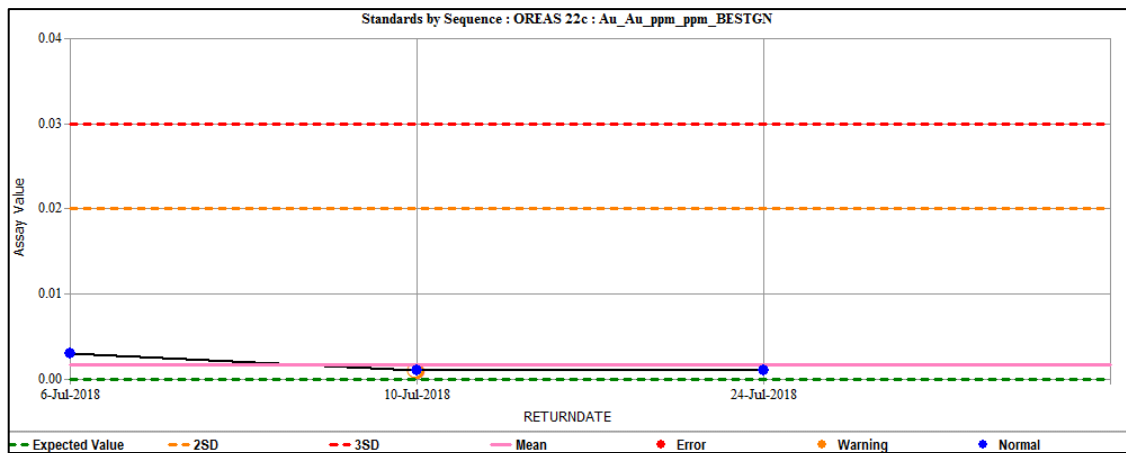


Figure 12.70 OREAS-22c CRM results for Au ppm

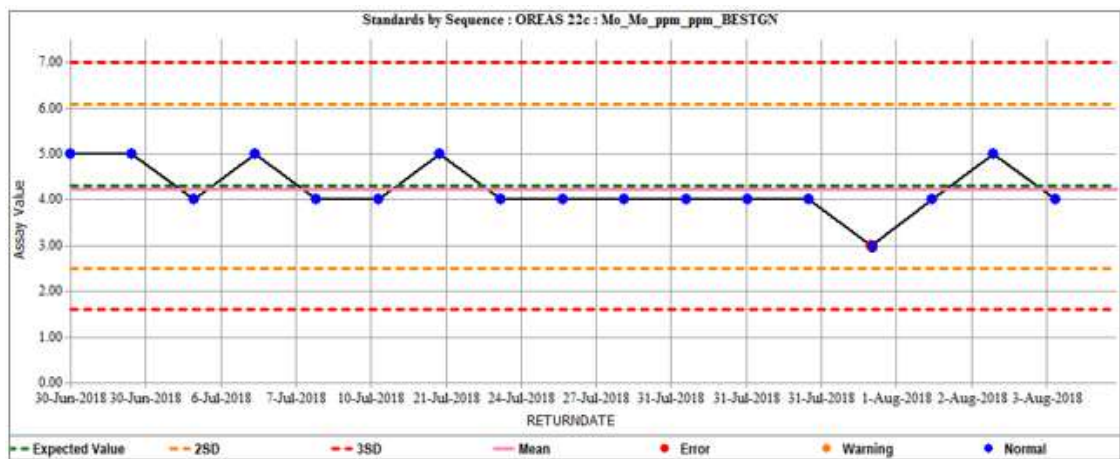


Figure 12.71 OREAS-22c CRM results for Mo ppm

12.3.3.2 Blanks

CRMs selected as certified blanks are included in the CRM analysis above.

Uncertified, coarse blanks were inserted at a rate of 3.3%, or 56 samples throughout the program. The coarse blank samples were inserted at the geologist's discretion with an emphasis on placement in visual high-grade zones as well as being inserted at the start and end of a batch.

Table 12.29 Performance statistics for uncertified coarse blanks

Statistics- QtzBLK				
	Cu ppm	Au ppm	Mo ppm	Ag ppm
# of Analyses above Threshold	56	4	49	56
# Outside Warning Limit	15	0	1	0
# Outside Error Limit	10	0	0	0
# of Analyses below Threshold	0	0	0	0
% Outside Error Limit	17.8571	0	0	0
Mean	34.1071	0.001	1.2449	0.25
Median	7	0.001	1	0.25
Min	2	0.001	1	0.25
Max	415	0.001	3	0.25
Standard Deviation	76.6695	0	0.48	0
% Rel. Std. Dev.	224.79	0	38.5609	0
Coeff. of Var.	2.2479	0	0.3856	0
Standard Error	10.2454	0	0.0686	0
% Rel. Std. Err.	30.0388	0	5.5087	0
Total Bias	33.1071	-0.08	0.2449	Na
% Mean Bias	3310.7143	-80	24.4898	Na

Values returned above 30ppm Cu were investigated, and they were found to follow elevated grade samples (>7000ppm) and have the potential to be caused by smear contamination in the crushing/processing phase. Values returned within limits (<15ppm Cu) have not been reviewed.

A recommendation of this review is to determine a more appropriate criteria for error flagging, likely as a percentage carry over from the previous sample.

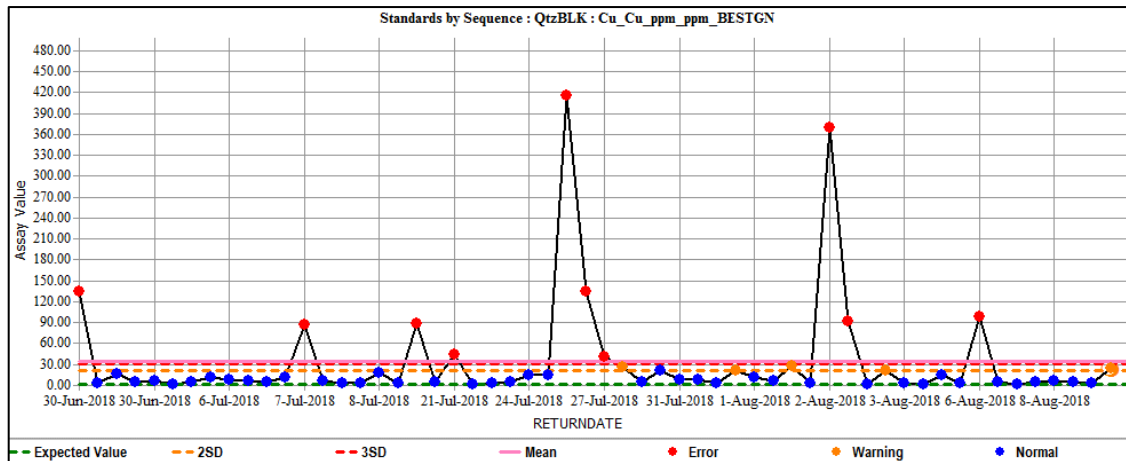


Figure 12.72 Coarse Blank / Qtz Blank results for Cu ppm

Table 12.30 Investigation results for Qtz Blanks >30ppm Cu

Qtz Blank Sample ID (>30ppm Cu)	Source Drill Hole	Value Returned (Cu ppm)	Investigation Finding
AX190040	SAP0001	134	Contamination – follows a 15m intercept of 1%-2% Cu
AX190285	SAP0005	87	Contamination – follows a 3m intercept of 1.6%- 4.2% Cu.
AX190691	SAP0017	45	Low grade fail. Follows 1m at 0.5% Cu
AX190709	SAP0017	89	Contamination / Recovery issues – follows 10m zone at 1.3% Cu (no recovery in part of this zone)
AX190930	SAP0021	415	Contamination – follows 5m intercept of 0.01%- 4.6% Cu..
AX190952	SAP0021	135	Contamination – follows large intercept of 20m of 1.2% - 2.9% Cu.
AX190888	SAP0020	41	Low grade fail. Follows zone of 0.1-0.2% Cu.
AX194886	SAP0023	98	Contamination – follows 6m intercept of 1.4-5% Cu.
AX194920	SAP0026	92	Contamination / Recovery issues– 2m of 0.5% Cu and 2m of no recovery.
AX194938	SAP0026	370	Contamination- follows a 4m interval of 1.1-2.1% Cu.

12.3.3.3 Field Duplicates

A small population of field duplicates were inserted at a rate of 0.9% of the total sample population. Current HCH QAQC procedure produces an insertion rate targeting 5%. The

results below generally have a high fail-rate; however, these samples are also noted as being at low-grade and close to the tolerance limits.

Refinement of the HCH QAQC procedure following this drill campaign has included the increasing of the field duplicate insertion rate, and selective insertion at higher grades or critical grade boundaries.

For copper the highest-grade samples showed a good degree of precision. Many errors are at very low (<0.05% Cu) grade. One result (AX195365, SAP0035) of mid-range grade returned the result of 3190ppm vs 5690ppm, which is of note within the resource modelling range of values.

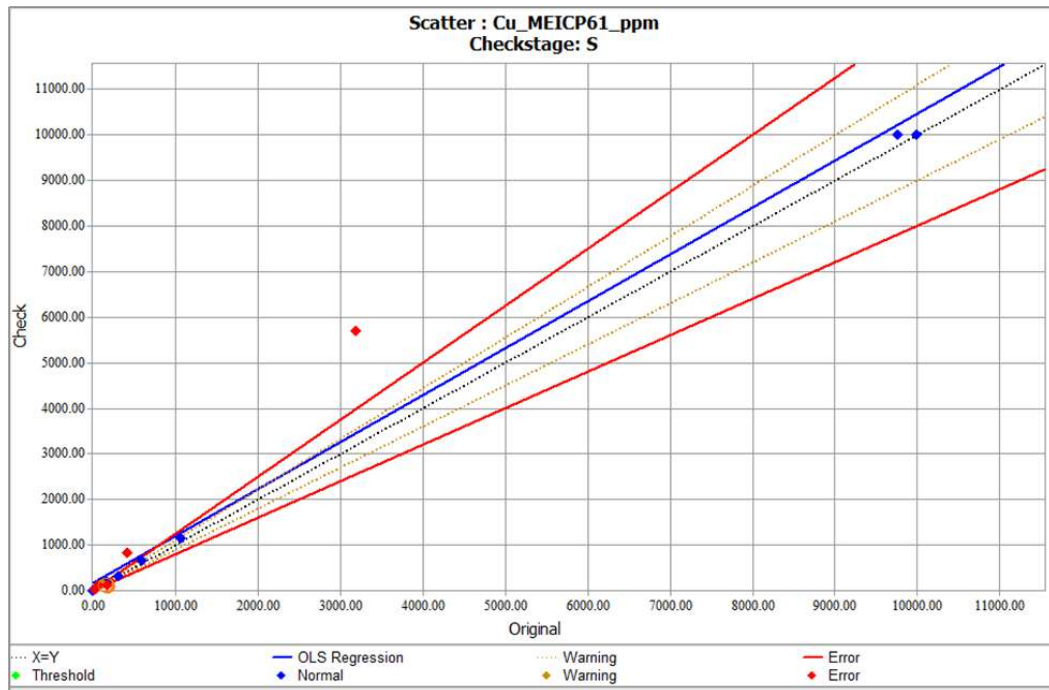


Figure 12.73 HCH duplicate samples displaying Cu ppm analysed by ME-ICP61 technique

Gold values are low, with the method detection limit being 0.001 and most results within a factor of 10 of this number. The highest returned error value (AX195203, SAP0031) returned a pair result of 0.043 vs 0.058ppm Au although did have another passing pair in the batch.

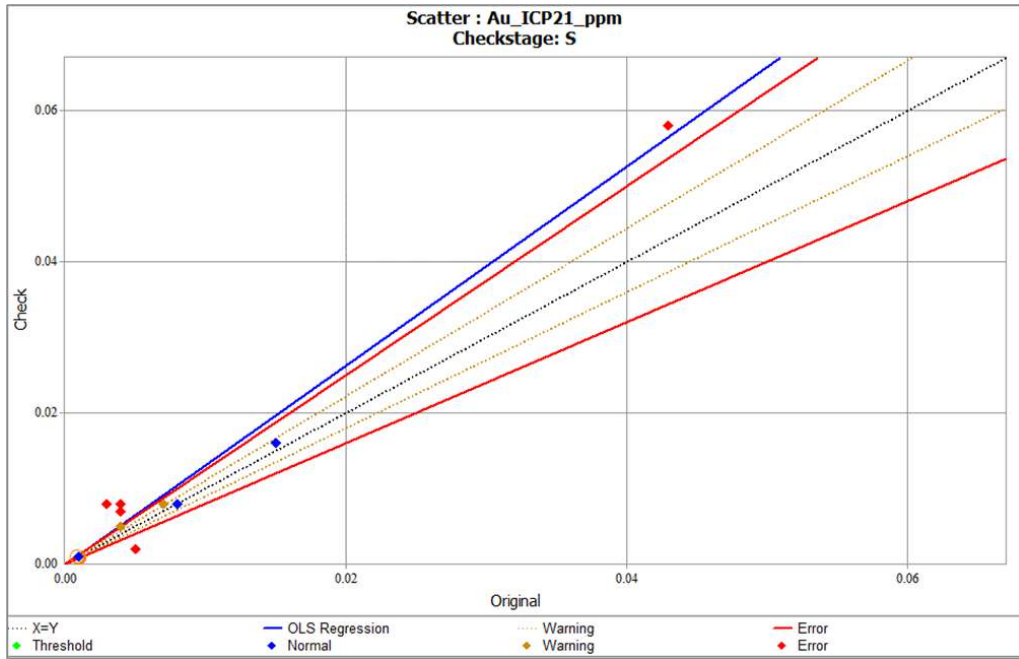


Figure 12.74 HCH duplicate samples displaying Au ppm analysed by ICP21 technique

A single molybdenum field duplicate result returned above the threshold. This result returned within tolerance.

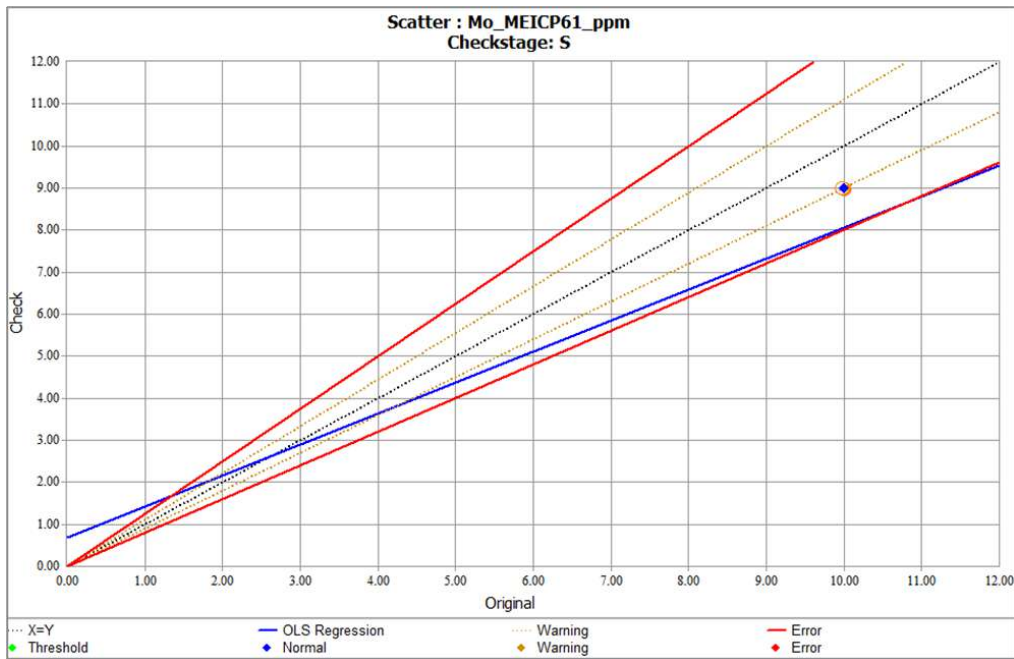


Figure 12.75 HCH duplicate samples displaying Mo ppm analysed by ME-ICP61 technique

Ag samples generally returned within the tolerance limits. The two error results were at moderate grade and included AX195365 (SAP0035) and AX195203 (SAP0031) and correspond to precision failures in copper and gold respectively.

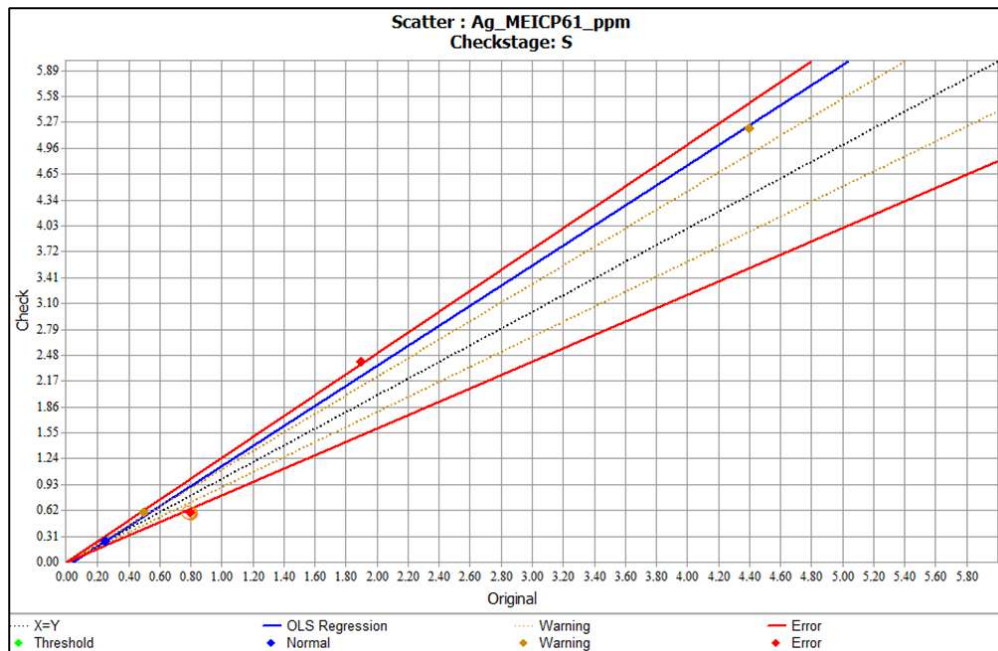


Figure 12.76 HCH duplicate samples displaying Ag ppm analysed by ME-ICP61 technique

12.3.4 Twin Holes

No twin holes have been drilled at this time.

12.3.5 Umpire Checks

In September 2018, 37 samples were collected for the umpire program. Source drillholes were SAP0031 and SAP0032 and samples were sent to ACME Analytical Laboratories (Chile).

The analysis found no consistent or material bias between the ALS and ACME Laboratory across the analytes of copper, gold, and silver. Analysis for molybdenum was not possible, with ALS returning assay values with a mean of 0.26ppm (generally at or below the detection limit) while ACME detection limit was 5ppm and all samples returned either at this value or below detection. Molybdenum is only present in very low concentrations, so this is not considered material to the Mineral Resource.

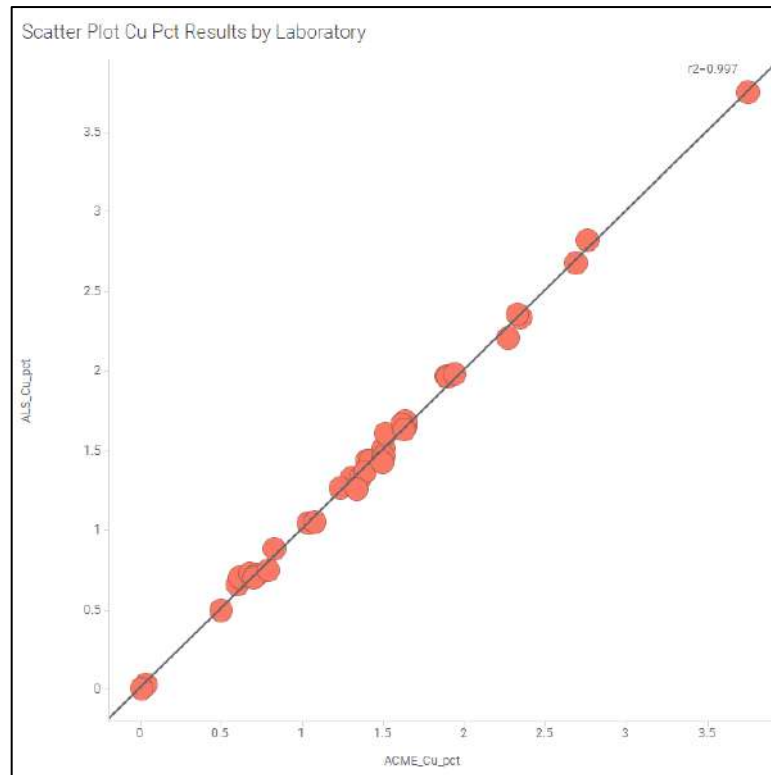


Figure 12.77 Scatter plot of Cu% by Laboratory

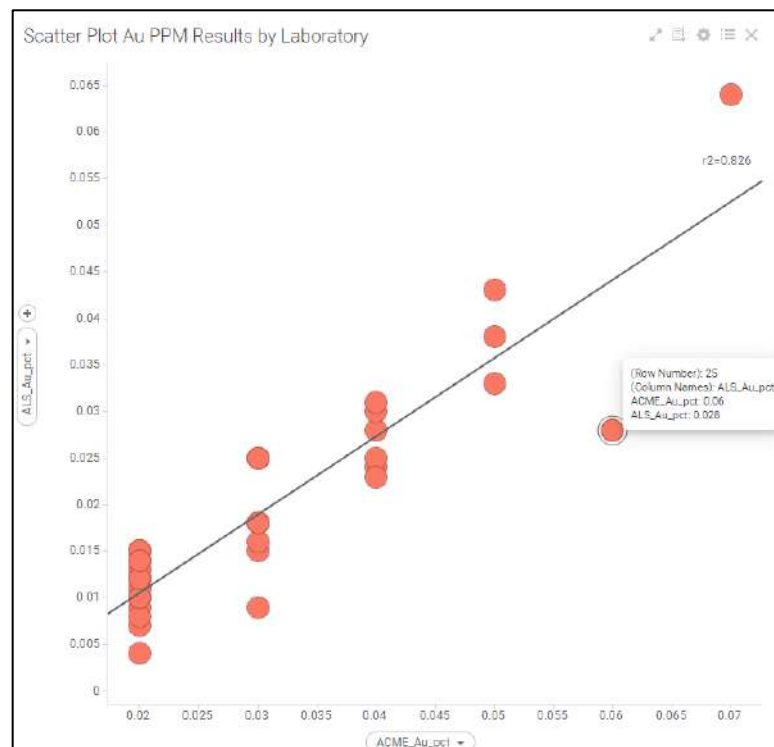


Figure 12.78 Scatter plot of Au ppm by Laboratory

A bias to the ACME laboratory is observed in the Au ppm results, however this is greatly influenced by a single sample. Excluding this sample, the data set returns a R² value of 0.9.

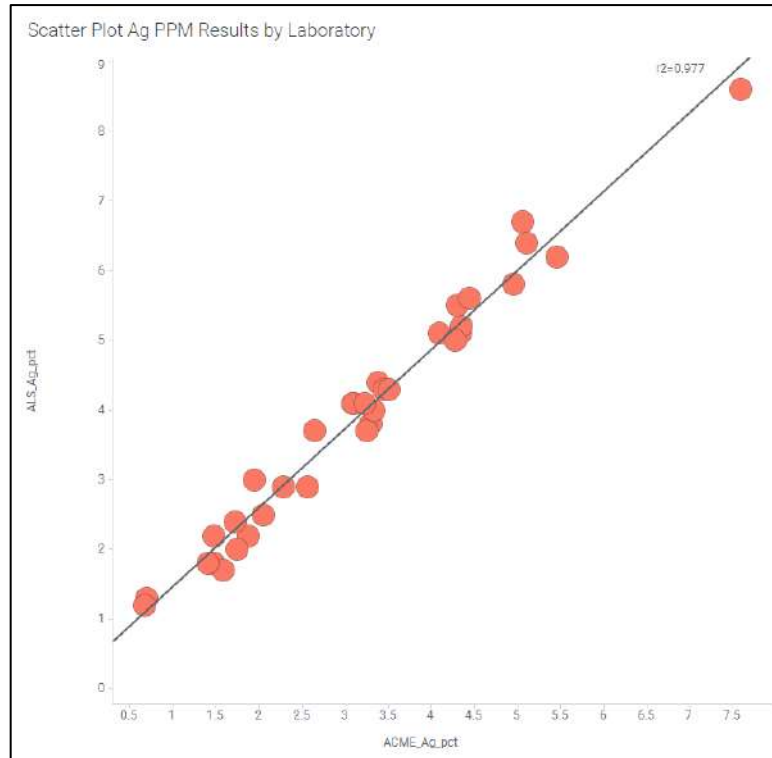


Figure 12.79 Scatter plot of Ag ppm by Laboratory

12.4 Conclusion

The QP is satisfied with the exploration, sampling, security, and QA/QC procedures employed by HCH for Costa Fuego and that their results are sufficient to produce data suitable for the purposes described in this technical report.

13 MINERAL PROCESSING AND METALLURGICAL TESTING

13.1 Introduction

This section is a summary of the metallurgical testwork conducted on the copper/molybdenum sulphide mineralized material as well as copper oxide mineralized material with the aim of providing process plant design criteria for the sulphide and oxide process plants and to provide metallurgical recoveries.

The testwork was conducted at ALS Laboratories, i.e., ALS Perth in Australia (all the flotation testwork and comminution testwork), ALS Santiago in Chile (oxide testwork and comminution testwork), Outotec in Perth (sulphide concentrate thickening and filtration) as well as HydroGeoSense (oxide testwork) in the United States of America.

This section describes the metallurgical testwork programs for copper oxide, copper sulphide and molybdenum process plants by discussing sample selection, mineralogy, process design and variability testwork.

13.2 Copper Oxide

13.2.1 Background

Testing of the Productora oxide mineralized material has been undertaken to establish their amenability to heap leaching.

The composite samples were selected to provide information regarding variability across the known oxide and transitional mineralised zones and copper grade ranges typical of those expected for both the heap and dump leach operations.

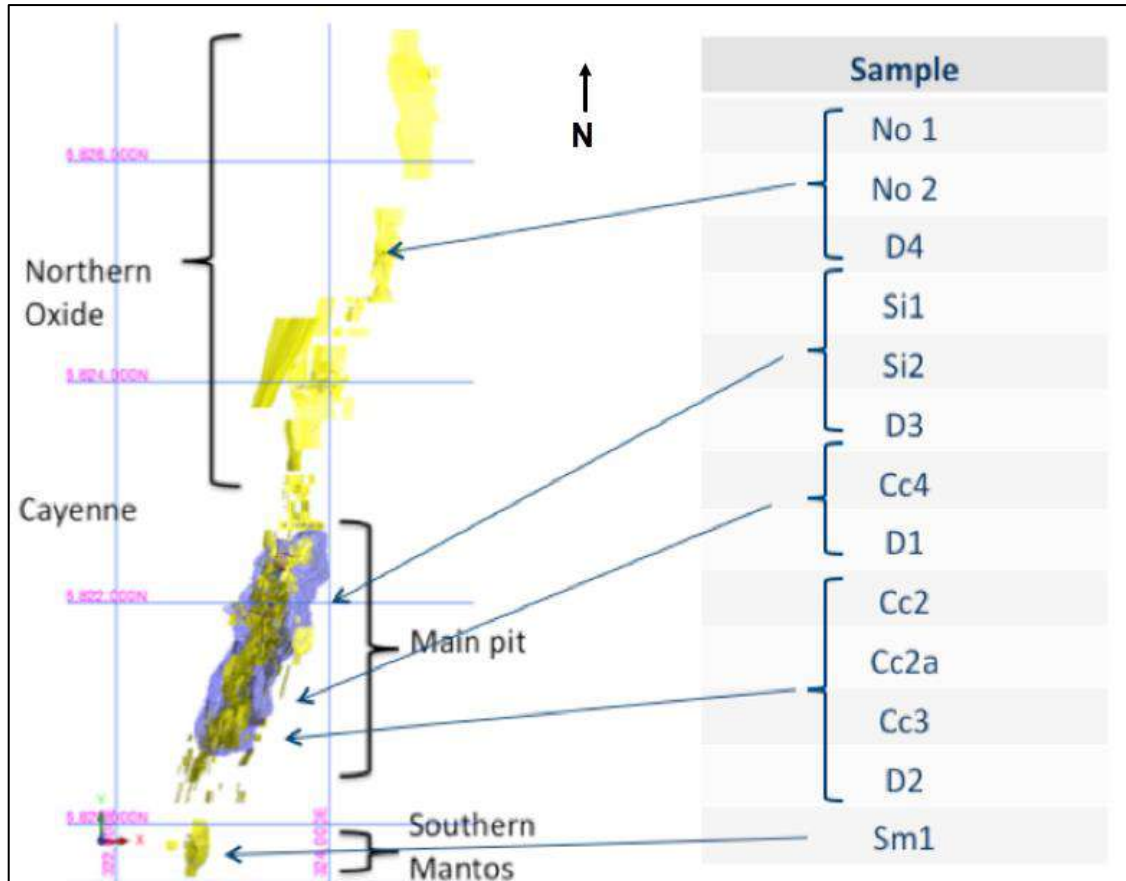


Figure 13.1 Sample location (HCH, 2016)

13.2.1.1 Preliminary Heap Leach Characterisation

The aim of this stage of the testwork was to determine the chemical and mineralogical assembly of both the host rock and copper minerals (via QEMScan and Sequential Cu Analysis) and, by using a simple bottle rolls technique, to then establish the copper leaching and acid consumption characteristics of each mineralized material type.

As the Project considered the use of seawater, duplicate tests were performed with both tap water and seawater (at one pH) to establish any variance in behaviour. Two acid regimes (pH=1 and pH=2) were also tested. This was then used to calculate expected copper recoveries and acid consumptions for subsequent 1 m and 6 m column tests. This testwork program was conducted at ALS Santiago in Chile.

Due to a lack of core sample available for testing, it was necessary to use half core rejects (crushed to -10# equivalent to -2 mm) for this phase of the testwork and retain the half core samples for subsequent testing.

The testwork flowsheet is presented in Figure 13.2.

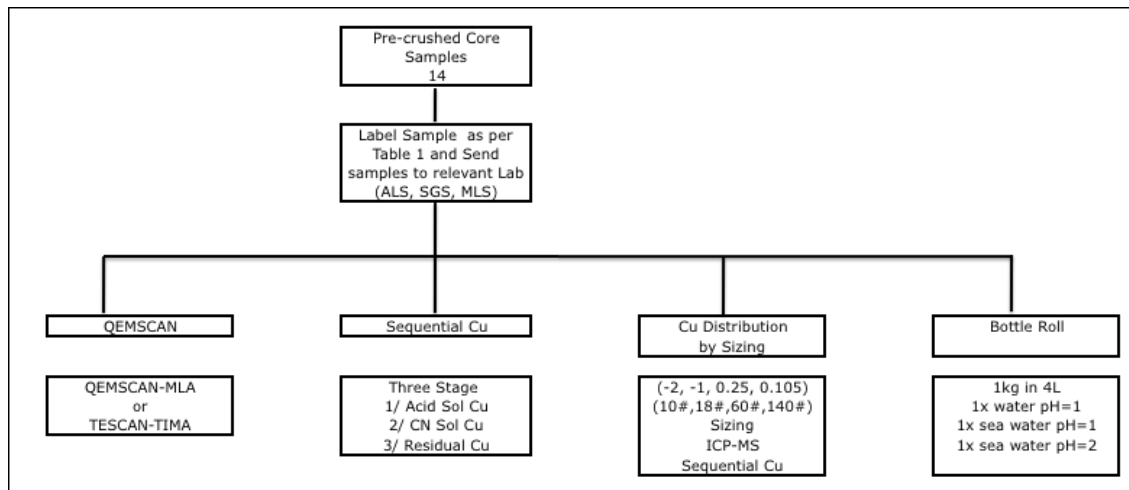


Figure 13.2 Preliminary heap leach characterisation testwork flowsheet

13.2.1.2 Crushing Testwork and Dump Leach Stacking and Hydrodynamic Testing

The crushing testwork consisted of the determination of the following variables:

- Bond Abrasion Index (half core 75 mm particles) – Ai
- Bond Impact Crushing Work Index (5 kg ¾" material) – CWi
- UCS (half core).

This testwork allowed for initial inputs required for the PDC for crushing the mineralized materials. Sampling and testwork flowsheet details for the abovementioned tests are shown in Figure 13.3. This testwork program was conducted at ALS Santiago in Chile.

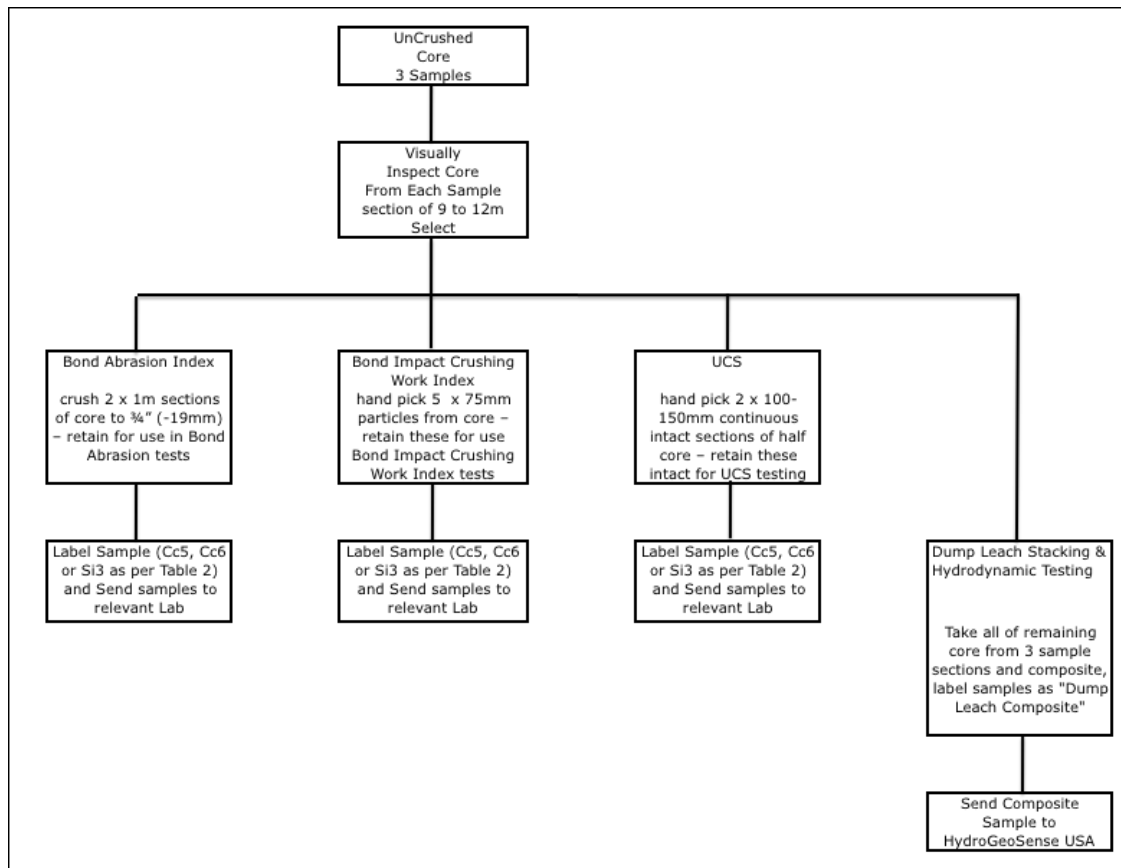


Figure 13.3 Crushing testwork flowsheet

13.2.1.3 Heap Agglomeration, Stacking and Hydrodynamic Testwork

The aim of this testwork was to establish an optimal crush size and agglomeration regime suited to the specific mineralized material types to optimise heap leaching performance. The agglomeration conditions consider the acid consumption characteristics of the mineralized material to assist maximising the utilisation of acid and minimising its overall consumption. Once agglomeration is optimised, the stacking test then establishes the stacking bulk density and hydraulic conductivity profiles with heap height. This will allow the crush size, agglomeration, stack density, stacking height and heap leach inputs for the design criteria to be established.

The hydrodynamic testing phase is utilised to establish solution hydraulic and gas conductivity as a function of moisture content and pore pressure. It also provides hydraulic and geotechnical parameters as well as critical parameters regarding heap porosity and heap height and density determination. This testwork program was conducted at HydroGeoSense Laboratories in Tuscon, Arizona in the United States of America.

The agglomeration conditions and conditions used in the hydrodynamic testing are established based on results from the bottle roll testing and preliminary heap characterisation data.

Figure 13.4 and Figure 13.5 shows the flowsheet for the sampling and agglomeration and stacking characterisation testwork, respectively.

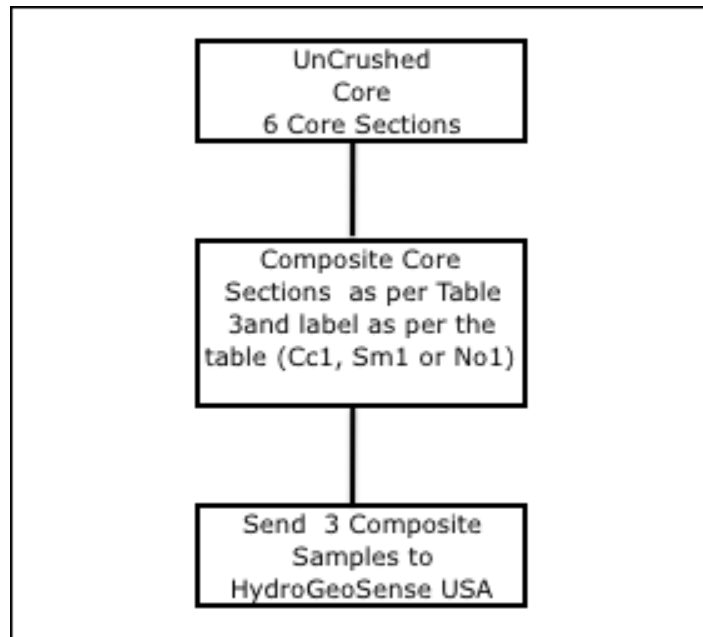


Figure 13.4 Crushing testwork flowsheet

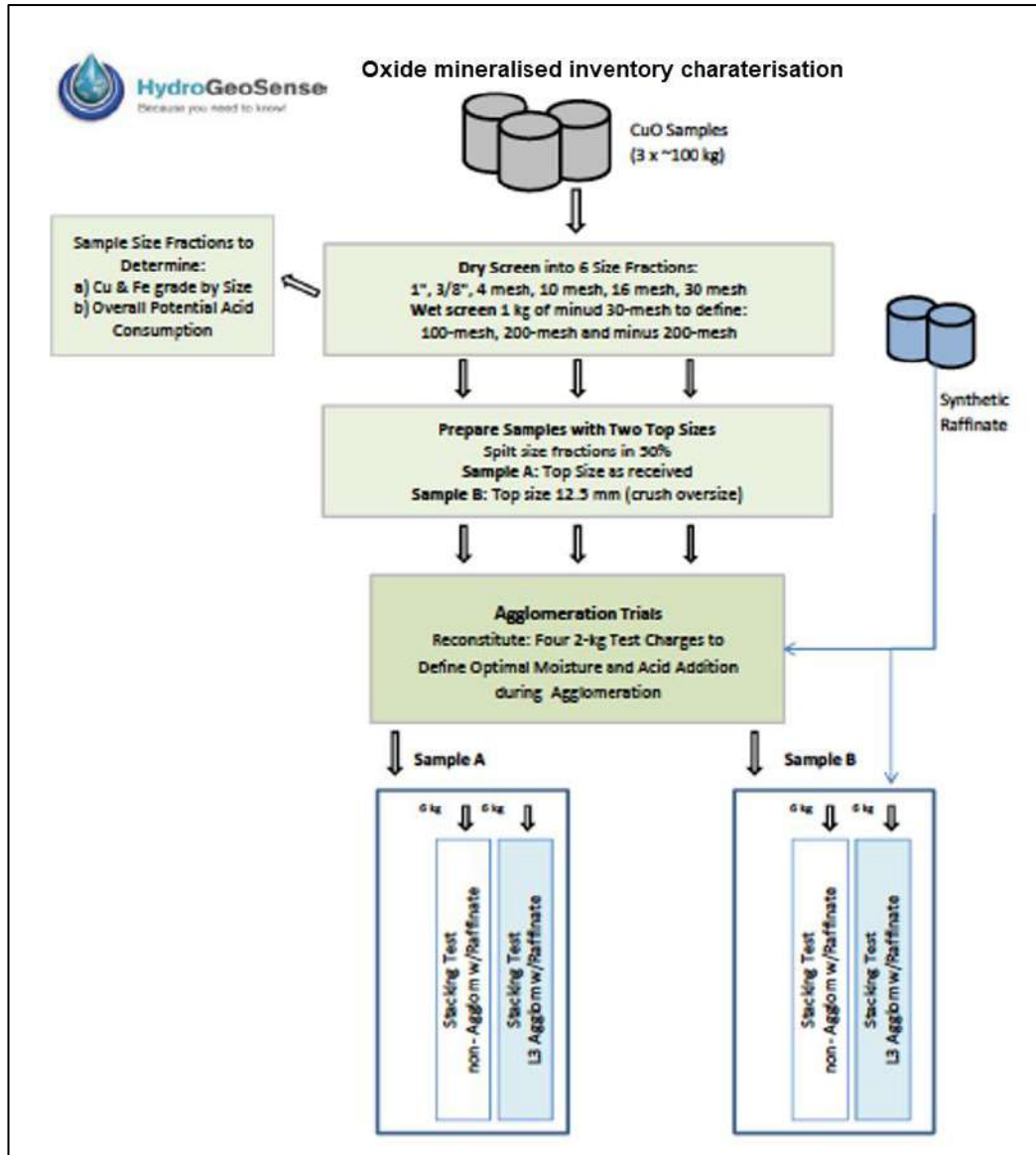


Figure 13.5 Heap agglomeration and stacking testwork flowsheet

13.2.1.4 Column Testwork (1m)

The 1m column testwork program flowsheet is depicted in Figure 13.6. This program assists in establishing the rate and extent of copper recovery with leach solution application as expected from heap leaching, as well as rate and extent of acid consumption. The results from this testwork program can then be scaled-up to provide inputs for the oxide heap leach PDC.

Included in this program were also components of the preliminary leach characterisation test program. This was included so that the leaching characteristics of the entire suite of samples available could be compared to assist in determining variability in metallurgical response of the oxide material.

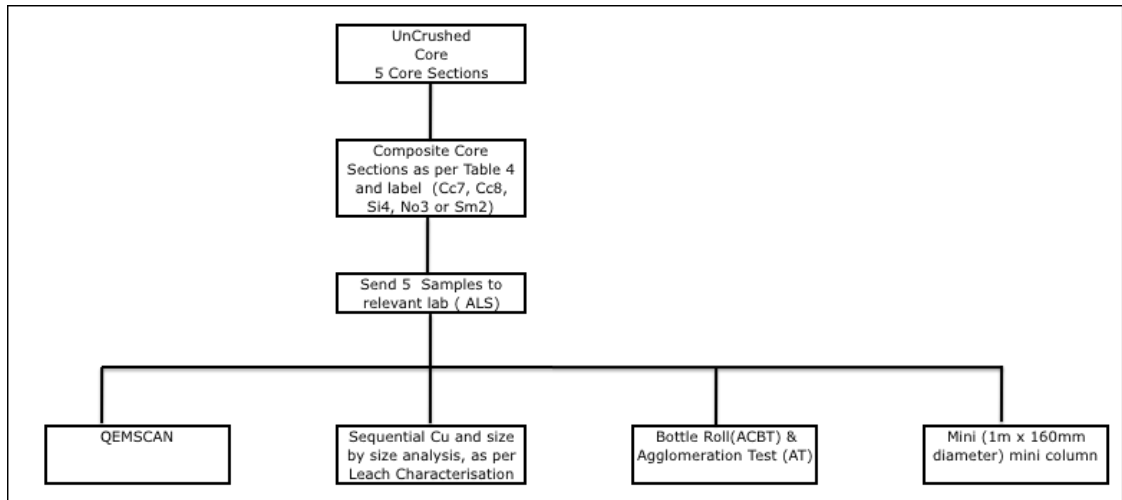


Figure 13.6 1m column testwork flowsheet

13.2.1.5 Column Testwork (6m)

This component of the testwork provides additional data to that of the 1m columns regarding scale-up for rate and extent of both copper and acid consumption. The results from this testwork program were to be used to validate the PDC.

13.2.2 Results of Testwork Program

13.2.2.1 Preliminary Heap Leach Characterisation

13.2.2.1.1 Size-by-Size Analysis and Sequential Copper Analysis

Table 13.1 shows that the majority of samples selected as oxide exhibit strong oxide tendencies as the majority of the copper (40% to 80%) is typically associated with copper oxides. There was a reasonable correlation with head assays; however, there were some variations with the previously determined acid soluble copper content which is considered acceptable as the analytical procedure/analysis differed (citric acid vs. sulphuric acid determination).

Table 13.1 Size-by-size analysis of oxide samples

Sample	Domain	Previous Data Available from Core Sample				PreFeasibility Study Testwork Results				
		Head Grade Total Cu (%)	Head Grade Acid Sol Cu (%), determined by citric method	Acid Sol Cu (% of Total Cu)	weath model	Head Grade Total Cu (%)	Head Grade Acid Soluble Cu (%), sequential analysis	Head Grade Cyanide Soluble Cu (%), sequential analysis	Head Grade Insoluble Cu (%), sequential analysis	Classification
No1	North Ox	0.47	0.31	66%	0	0.51	0.40	0.01	0.10	Oxide
No2	North Ox	0.54	0.36	67%	0/t	0.55	0.43	0.04	0.09	Oxide
No3	North Ox	0.54	0.36	67%	0/t	0.51	0.36	0.02	0.10	Oxide
Sm1	Sth Mantos	0.84	0.17	20%	t	0.95	0.30	0.46	0.19	Oxide/Transition
Sm2	Sth Mantos	0.45	0.13	29%	0	0.43	0.15	0.14	0.11	Oxide/Transition
Cc1	CCHEN Sth	0.49	0.25	51%	0	0.58	0.37	0.04	0.17	Oxide
Cc2	CCHEN Sth	0.57	0.11	19%	0	0.57	0.25	0.22	0.11	Oxide/Transition
CC2a	CCHEN Sth	0.75	0.35	47%	0	0.76	0.60	0.03	0.13	Oxide
Cc3	CCHEN Sth	0.45	0.13	29%	0	0.48	0.24	0.07	0.17	Oxide
Cc4	CCHEN Sth	0.61	0.26	43%	t	0.64	0.31	0.16	0.16	Oxide/Transition
Cc7	CCHEN Sth	0.82	0.17	21%	0	0.79	0.18	0.37	0.22	Oxide/Transition
Cc8	CCHEN Sth	0.57	0.11	20%	0	0.56	0.20	0.22	0.13	Oxide/Transition
Si1	Santa In	0.39	0.21	54%	0	0.43	0.24	0.03	0.15	Oxide
Si2	Santa In	0.57	0.16	28%	0/t	0.59	0.26	0.17	0.16	Oxide/Transition
Si4	Santa Innes	0.39	0.21	54%	0	0.35	0.18	0.03	0.11	Oxide
D1	CCHEN Sth	0.24	0.02	8%	0/t	0.21	0.02	0.08	0.11	Transition
D3	Sant In	0.25	0.13	52%	o/t	0.16	0.10	0.03	0.03	Oxide
D4	North Ox	0.40			0	0.41	0.35	0.01	0.05	Oxide

The two Main Pit samples (Cc7 and Cc8) selected for the column tests fall into the category of mixed oxide/transition.

Size-by-size sequential analysis was undertaken, and comments on the distribution of oxide copper in the samples tested are shown in Table 13.2.

Table 13.2 Summary of size-by-size sequential analysis

Sample	Domain	Comments
No1	North Ox	ratio of oxide Cu relatively constant over particle size range
No2	North Ox	ratio of oxide Cu relatively constant over particle size range
No3	North Ox	ratio of oxide Cu increases with decreasing particle size range
Sm1	Sth Mantos	ratio of oxide Cu slightly decreases with decreasing particle size
Sm2	Sth Mantos	ratio of oxide Cu relatively constant over particle size range
Cc1	CCHEN Sth	ratio of oxide Cu slightly decreases with decreasing particle size
Cc2	CCHEN Sth	ratio of oxide Cu slightly decreases with decreasing particle size
CC2a	CCHEN Sth	ratio of oxide Cu relatively constant over particle size range
Cc3	CCHEN Sth	ratio of oxide Cu slightly decreases with decreasing particle size
Cc4	CCHEN Sth	ratio of oxide Cu slightly decreases with decreasing particle size
Cc7	CCHEN Sth	ratio of oxide Cu relatively constant over particle size range
Cc8	CCHEN Sth	ratio of oxide Cu increases with decreasing particle size range
Si1	Santa In	ratio of oxide Cu slightly decreases with decreasing particle size
Si2	Santa In	ratio of oxide Cu relatively constant over particle size range
Si4	Santa In	ratio of oxide Cu relatively constant over particle size range
D1	CCHEN Sth	ratio of oxide Cu relatively constant over particle size range
D3	Sant In	ratio of oxide Cu slightly decreases with decreasing particle size
D4	North Ox	ratio of oxide Cu relatively constant over particle size range

Generally, it would be expected that those samples that have the copper oxide biased to the finer fractions should exhibit more rapid and higher extent of copper dissolution during leaching. This was the case for the lower acidity bottle roll leaches (higher pH) but was not reflected in results at the higher acidity.

This data tends to indicate a variable insoluble tail (residual insoluble copper) that increases with increasing grade (see Figure 13.7).

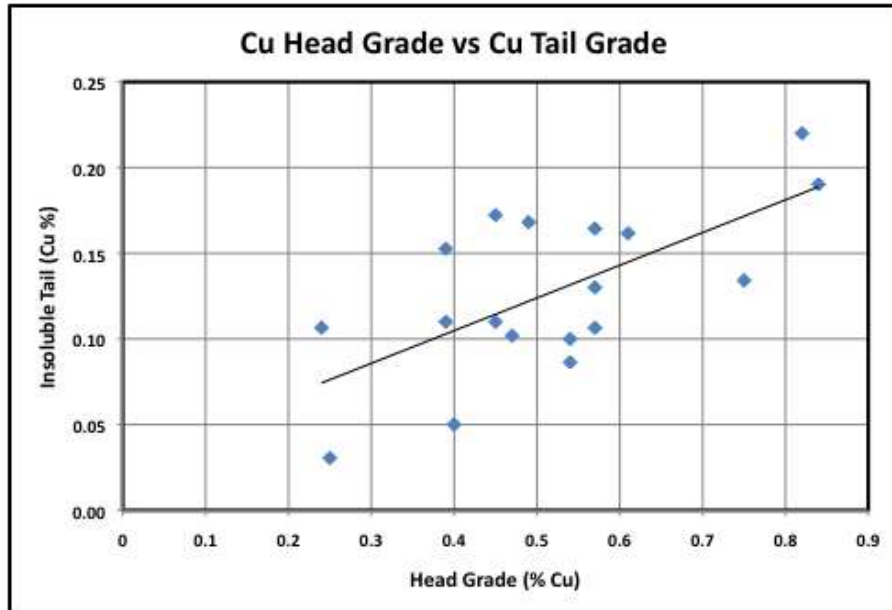


Figure 13.7 Copper head assay vs. insoluble copper tail

13.2.2.1.2 Bottle Roll Tests

The complete results of the bottle roll tests are summarised in Table 13.3. Bottle roll tests were also completed on samples selected for the 1m columns to establish leaching parameters for the column tests, so these have been included for completeness.

Table 13.3 Bottle roll test results

Sample	Domain	Head Grade Total Cu (%)	Head Grade Acid Soluble Cu (%)	pH=2 Tap Water			pH=2 Sea Water			pH=1 Sea Water		
				Total Cu Recovery (%)	Acid Soluble Cu Recovery (%)	Acid Cons (kg/t)	Total Cu Recovery (%)	Acid Soluble Cu Recovery (%)	Acid Cons (kg/t)	Total Cu Recovery (%)	Acid Soluble Cu Recovery (%)	Acid Cons (kg/t)
No1	North Ox	0.46	0.40	52	60	53	14	16	42	82	95	192
No2	North Ox	0.52	0.43	67	82	43	30	37	31	84	103	108
No3	North Ox	0.49	0.33	83	125	58	28	43	35	89	134	99
D4	North Ox	0.37	0.35	55	59	33	33	36	28	84	90	73
Sm1	Sth Mantos	0.65	0.30	5	10	11	47	101	4	61	131	43
Sm2	Sth Mantos	0.44	0.17	52	132	43	51	132	14	64	165	187
Cc1	CCHEN Sth	0.56	0.37	57	85	15	41	61	6	67	100	60
Cc2	CCHEN Sth	0.65	0.25	44	114	7	47	120	3	59	152	46
CC2a	CCHEN Sth	0.74	0.60	69	85	7	39	49	4	80	99	45
Cc3	CCHEN Sth	0.47	0.24	47	90	18	37	72	8	66	127	70
Cc4	CCHEN Sth	0.60	0.31	48	93	28	42	81	19	66	127	67
Cc7	CCHEN Sth	0.80	0.18	47	210	29	51	228	12	70	313	114
Cc8	CCHEN Sth	0.58	0.22	61	160	14	61	160	4	73	191	66
D1	CCHEN Sth	0.25	0.02	14	156	16	18	206	8	21	235	49
Sl1	Santa In	0.40	0.24	53	88	7	47	78	4	64	106	40
Sl2	Santa In	0.59	0.26	43	97	8	42	97	4	56	128	42
Sl4	Santa Innes	0.44	0.26	69	116	17	64	108	4	76	127	59
D3	Sant In	0.17	0.10	54	97	7	53	95	4	64	115	50
D1	CCHEN Sth	0.25	0.02	14	156	16	18	206	8	21	235	49
D3	Sant In	0.17	0.10	54	97	7	53	95	4	64	115	50
D4	North Ox	0.37	0.35	55	59	33	33	36	28	84	90	73
AL1	Alice 1	1.12	0.93				38	46	4	88	106	70
AL2	Alice 2	0.48	0.16				39	118	4	57	173	44
ADD_BR_1	East Oxide	1.22	0.98				39	49	5	76	95	25
ADD_BR_2	East Oxide	0.44	0.26				56	94	4	70	118	25

The results show a significant range of copper recoveries and acid consumption; however, this is to be expected as the samples represent a number of different mineralized material bodies and also range from oxide to transitional mineralized material, as well as there being significant copper head grade variation. All samples show a strong relationship between available acid, copper recovery and acid

consumption. All samples show significantly increased copper recoveries at pH=1 compared to pH=2 with subsequent increased acid consumptions. The acid consumption characteristics of all samples show an increasing cumulative acid consumption with time.

To provide a more detailed analysis of the results, the sequential copper analysis and the QEMScan mineralogy have been incorporated into the analysis. The performance of each of the mineralized materials and additionally the performance for oxide and oxide/transition mineralized materials within each mineralized material type are described in the following sections.

Northern Oxide:

These samples are all classified as oxide and show very similar head grades, sequential copper analysis characteristics and QEMScan based copper mineralogy. The copper mineralogy for No1 and No2 samples was determined to be dominated (80% of the Cu) by copper bearing/rich silicates, as discrete from the common copper silicate mineral chrysocolla which 17% of the copper was associated. The QEMScan report suggests these silicates are “*Combined chlorite, biotite, clays and similar silicates containing variable amounts of Cu (Cu above QEMSCAN detection limit). May include intergrowths of other copper minerals with silicates*”. The No3 sample (1m column sample) differed in that it contained 22% Cu as copper metal/cuprite with 54% of copper as combined copper rich silicates. The interpretation of the QEMScan mineralogy is compared to the sequential copper analysis for each sample in Table 13.4.

Table 13.4 Northern Oxide sequential Cu and QEMScan analysis

Sample	Domain	Head Grade Total Cu (%) (ICP Head Assay)	Sequential Cu Analysis				Ore Classification	QEMScan Cu Mineralogy Analysis		
			Head Grade Total Cu (%) (Calculated from Sequential Assay)	Head Grade Acid Soluble Cu (%), sequential analysis	Head Grade Cyanide Soluble Cu (%), sequential analysis	Head Grade Insoluble Cu (%), sequential analysis		Head Grade Acid Soluble Cu (%), QEMScan	Head Grade Cyanide Soluble Cu (%), QEMScan	Head Grade Insoluble Cu (%), QEMScan
No1	North Ox	0.46	0.51	0.40	0.01	0.10	Oxide	0.49	0.00	0.02
No2	North Ox	0.52	0.55	0.43	0.04	0.09	Oxide	0.51	0.02	0.02
No3	North Ox	0.49	0.49	0.33	0.02	0.18	Oxide	0.41	0.06	0.02
D4	North Ox	0.37	0.41	0.35	0.01	0.05	Oxide	0.39	0.00	0.02

The bottle roll leaching characteristics in terms of total copper and acid soluble copper of the samples are shown in Table 13.5 and Figure 13.8. In terms of copper recovery and rate of copper recovery (both total and acid soluble), all of the samples behave similarly and as expected with regards to the oxide mineral assemblage which consists predominantly of copper rich silicates. Sample No3 varies due to the presence of copper metal/cuprite. The acid consumption results were reasonably consistent. The acid soluble copper analysis (from sequential analysis) appears at times to understate the recoverable copper.

Table 13.5 Bottle roll test results (pH=1)

Sample	Domain	pH=1 Bottle Roll Results					Acid Consumption (kg/t)
		Total Cu Recovery (%)	Acid Soluble Cu Recovery (%) sequential analysis	Acid Sol +CN Sol Cu Recovery (%) sequential analysis	Acid Soluble Cu Recovery (%) QEMScan Analysis	Acid Sol +CN Sol Cu Recovery (%) QEMScan analysis	
No1	North Ox	82	95	103	86	86	192
No2	North Ox	84	103	100	91	87	108
No3	North Ox	89	134	119	104	92	99
D4	North Ox	84	90	96	89	89	73

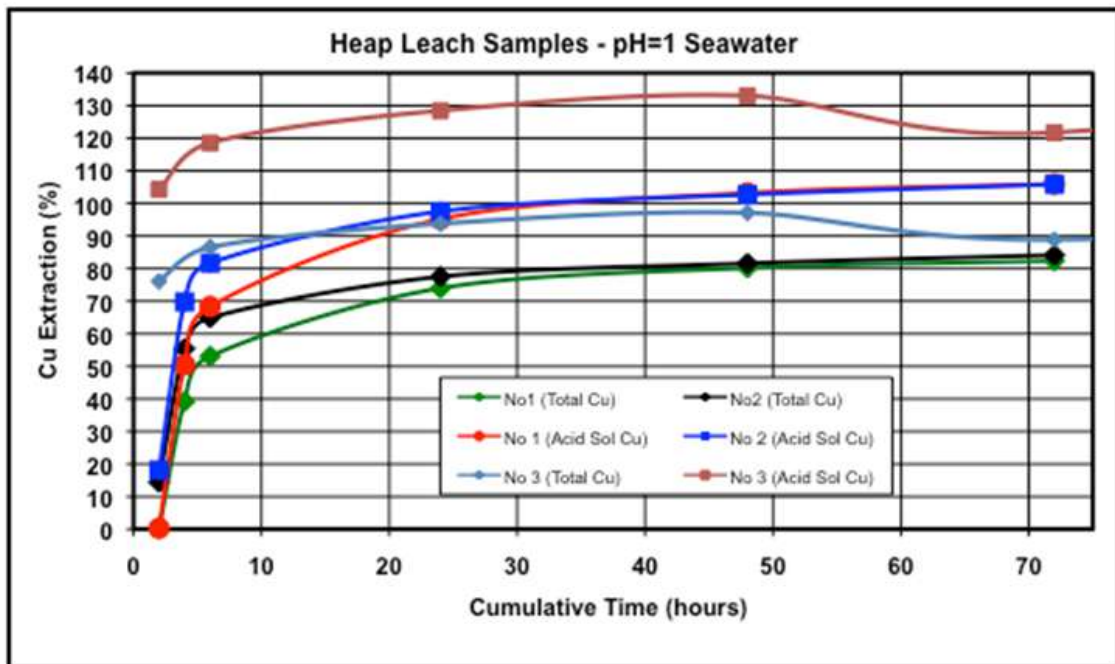


Figure 13.8 Bottle roll test results (pH=1)

It appears that the copper bearing silicates probably have similarly slow leaching characteristics as chrysocolla typically exhibits. The slow leaching is typically a function of the copper being leached from the stable silica matrix. As leaching progresses, the silica matrix remains intact and the acid must penetrate much deeper into the matrix to leach the remaining copper.

The QEMScan mineralogy of the host rock indicates a high proportion of acid consuming minerals with ~45% feldspars, 8-17% amphibole, 8% chlorite and 1-2% calcite. The calcite will tend to react rapidly whilst the others tend to react slowly with time, hence the ongoing acid consumption trend that is noted in the bottle rolls.

It can be seen from the summary above that the No3 sample (Table 13.5), which was used for the column testwork, exhibited a lower soluble copper content (via sequential analysis and QEMScan) than the other samples due to the presence of copper metal/cuprite. However, a proportion of this copper metal/cuprite has leached, hence

the acid soluble and acid plus CN soluble copper recoveries are elevated. Sample No3 also exhibited a higher insoluble copper content.

Southern Mantos:

These samples are classified as oxide/transition. The two samples have quite a significant grade variation, however, despite this they show very similar sequential copper analysis characteristics and QEMScan based copper mineralogy (Table 13.6). The QEMScan copper mineralogy is quite variable indicating about 10 - 30% of the copper present as copper bearing/rich silicates, 10 - 20% as copper in goethite, 30 - 45% as chalcocite/digenite and 10 - 20% as chalcopyrite. The QEMScan mineralogy also shows the host rock being dominated by magnetite/hematite 20 - 60% and goethite/limonite 10 - 25%. Sample Sm2 also has 1.5% calcite.

Table 13.6 Southern Mantos sequential Cu and QEMScan analysis

Sample	Domain	Head Grade Total Cu (%) (ICP Head Assay)	Sequential Cu Analysis				Ore Classification	QEMScan Cu Mineralogy Analysis		
			Head Grade Total Cu (%) (Calculated from Sequential Assay)	Head Grade Acid Soluble Cu (%) sequential analysis	Head Grade Cyanide Soluble Cu (%) sequential analysis	Head Grade Insoluble Cu (%) sequential analysis		Head Grade Acid Soluble Cu (%) QEMScan	Head Grade Cyanide Soluble Cu (%) QEMScan	Head Grade Insoluble Cu (%) QEMScan
Sm1	Sth Mantos	0.86	0.95	0.30	0.46	0.19	Oxide/Transition	0.34	0.30	0.29
Sm2	Sth Mantos	0.44	0.44	0.17	0.15	0.12	Oxide/Transition	0.07	0.20	0.14

The bottle roll leaching characteristics in terms of copper recovery and rate of copper recovery (total, acid and CN soluble) were consistent between the two samples (Table 13.7). These results indicate that, in the presence of seawater at a pH=1, a significant amount of the secondary sulphides, namely chalcocite and digenite (CN soluble) are soluble with calculated acid soluble copper recoveries in the range of 165 to 191% and combined acid soluble plus CN soluble copper recoveries in the range of 76 to 89%. The QEMScan copper solubilities for sample Sm2 show significant variation to the sequential determinations due to the presence of significant chalcocite and goethite.

Table 13.7 Southern Mantos pH=1 bottle roll test results

Sample	Domain	pH=1 Bottle Roll Results					
		Total Cu Recovery (%)	Acid Soluble Cu Recovery (%) sequential analysis	Acid Sol +CN Sol Cu Recovery (%) sequential analysis	Acid Soluble Cu Recovery (%) QEMScan Analysis	Acid Sol +CN Sol Cu Recovery (%) QEMScan analysis	Acid Consumption (kg/t)
Sm1	Sth Mantos	61	191	76	168	89	43
Sm2	Sth Mantos	64	165	89	519	142	187

There was a significant variation in acid consumption from 40 to 190 kg/t (Table 13.7) which can be explained by the significant difference in host rock mineralogy. The QEMScan mineralogy of the host rock for sample Sm1 indicates moderate amounts of acid consuming minerals with ~14% feldspars, 1% amphibole, 7% chlorite and 0.1% calcite, and also the presence of 18% magnetite/hematite and 27% goethite/limonite. The QEMScan mineralogy for sample Sm2 is quite different with acid consuming

minerals 7% chlorite and 1.4% calcite, and also the presence of 60% magnetite/hematite and 7% goethite/limonite.

The rate of copper recovery is slow (Figure 13.9) and this reflects the slow leaching copper silicates (as discussed previously for the Northern Oxide samples) and the slow chemical leaching of the chalcocite and digenite. These secondary sulphides typically have leaching rates of two to three times that of typical acid soluble copper oxides such as malachite and azurite.

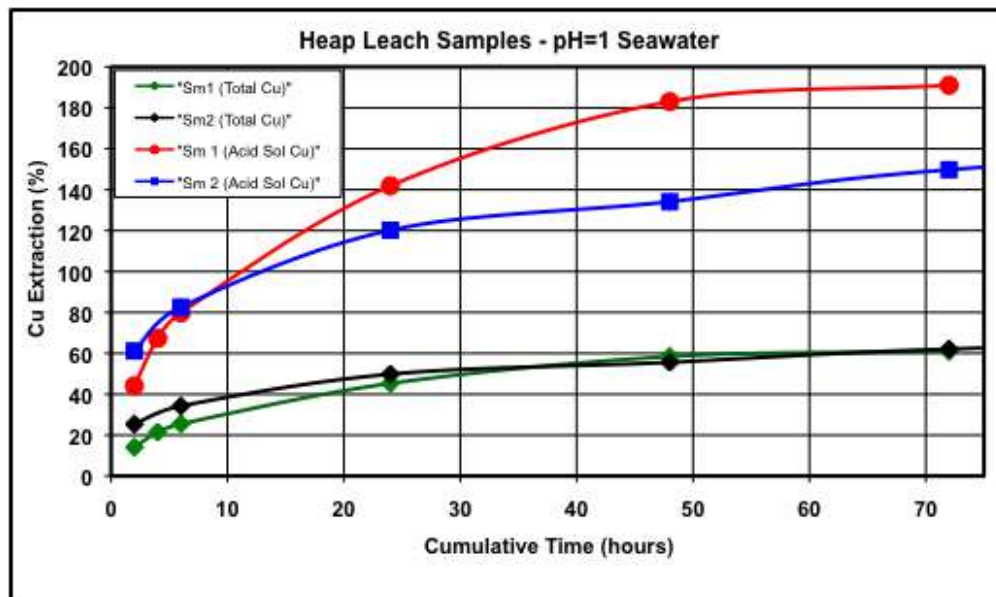


Figure 13.9 Southern Mantos pH=1 bottle roll leach kinetics

Sample Sm2 that was used for the column testwork exhibited a lower copper head grade and a significantly higher acid consumption than the other sample tested via bottle roll only.

Main Pit (CCHEN Sth):

These samples are all classified as oxide or oxide/transition and analyses are summarised in Table 13.8.

Table 13.8 Main Pit sequential Cu and QEMScan analysis

Sample	Domain	Head Grade Total Cu (%) (ICP Head Assay)	Sequential Cu Analysis				Ore Classification	QEMScan Cu Mineralogy Analysis		
			Head Grade Total Cu (%) (Calculated from Sequential Assay)	Head Grade Acid Soluble Cu (%), sequential analysis	Head Grade Cyanide Soluble Cu (%), sequential analysis	Head Grade Insoluble Cu (%), sequential analysis		Head Grade Acid Soluble Cu (%), QEMScan	Head Grade Cyanide Soluble Cu (%), QEMScan	Head Grade Insoluble Cu (%), QEMScan
Cc1	CCHEN Sth	0.56	0.58	0.37	0.04	0.17	Oxide	0.54	0.02	0.03
CC2a	CCHEN Sth	0.74	0.76	0.60	0.03	0.13	Oxide	0.69	0.01	0.06
Cc3	CCHEN Sth	0.47	0.48	0.24	0.07	0.17	Oxide	0.44	0.03	0.01
Cc2	CCHEN Sth	0.65	0.57	0.25	0.22	0.11	Oxide/Transition	0.21	0.18	0.17
Cc4	CCHEN Sth	0.60	0.64	0.31	0.16	0.16	Oxide/Transition	0.38	0.12	0.12
Cc7	CCHEN Sth	0.80	0.80	0.18	0.35	0.23	Oxide/Transition	0.56	0.16	0.08
Cc8	CCHEN Sth	0.58	0.58	0.22	0.23	0.13	Oxide/Transition	0.26	0.19	0.12
D1	CCHEN Sth	0.25	0.21	0.02	0.08	0.11	Oxide/Transition	0.07	0.06	0.08

For the oxide samples, the CN soluble and insoluble copper contents were consistent and independent of head grade. The acid soluble component of the copper varied with head grade. The QEMScan mineralogy indicated the majority of copper present as copper bearing silicates and chrysocolla. The sequential and QEMScan results were consistent but the sequential indicated a higher insoluble copper component of 0.17% Cu compared to 0.03% Cu.

For the oxide/transition samples, the acid and CN soluble and insoluble copper contents vary quite significantly with no apparent trend. The QEMScan mineralogy indicated about 30 - 40% of the copper present as copper rich silicates and chrysocolla, 25 - 40% as chalcocite/digenite and 5 - 10% as chalcopyrite and goethite. The sequential and QEMScan results were consistent.

The Bottle Roll leaching characteristics are summarised in Table 13.9. For the oxide samples, the total copper recovery was reflective of the quantity of acid soluble copper present. There was some variation in acid consumption from 40 to 70 kg/t where the QEMScan mineralogy indicates is due to higher chlorite content of 10% compared to the other samples having 2.5 - 3.5%.

Table 13.9 Main Pit pH=1 bottle roll test results

Sample	Domain	pH=1 Bottle Roll Results					Acid Consumption (kg/t)
		Total Cu Recovery (%)	Acid Soluble Cu Recovery (%) sequential analysis	Acid Sol +CN Sol Cu Recovery (%) sequential analysis	Acid Soluble Cu Recovery (%) QEMScan Analysis	Acid Sol +CN Sol Cu Recovery (%) QEMScan analysis	
Cc1	CCHEN Sth	67	100	94	73	70	60
CC2a	CCHEN Sth	80	99	98	89	88	45
Cc3	CCHEN Sth	66	127	102	71	67	70
Cc2	CCHEN Sth	59	152	72	101	71	46
Cc4	CCHEN Sth	66	127	88	110	84	67
Cc7	CCHEN Sth	70	313	101	122	94	114
Cc8	CCHEN Sth	73	191	97	189	109	66
D1	CCHEN Sth	21	235	42	58	33	49

For the oxide/transition samples the leaching characteristics in terms of copper recovery and rate of copper recovery (total, acid and CN soluble) were consistent. The copper

recovery in terms of total copper and acid soluble copper are shown in Table 13.9. These results indicate that in the presence of seawater at a pH=1 a significant amount of the secondary sulphides (CN soluble) are soluble with calculated combined acid soluble plus CN soluble copper recoveries in the range of 72 to 107%. There was a variation in acid consumption for the oxide/transition samples from 45 to 114 kg/t for which there is insufficient data to explain.

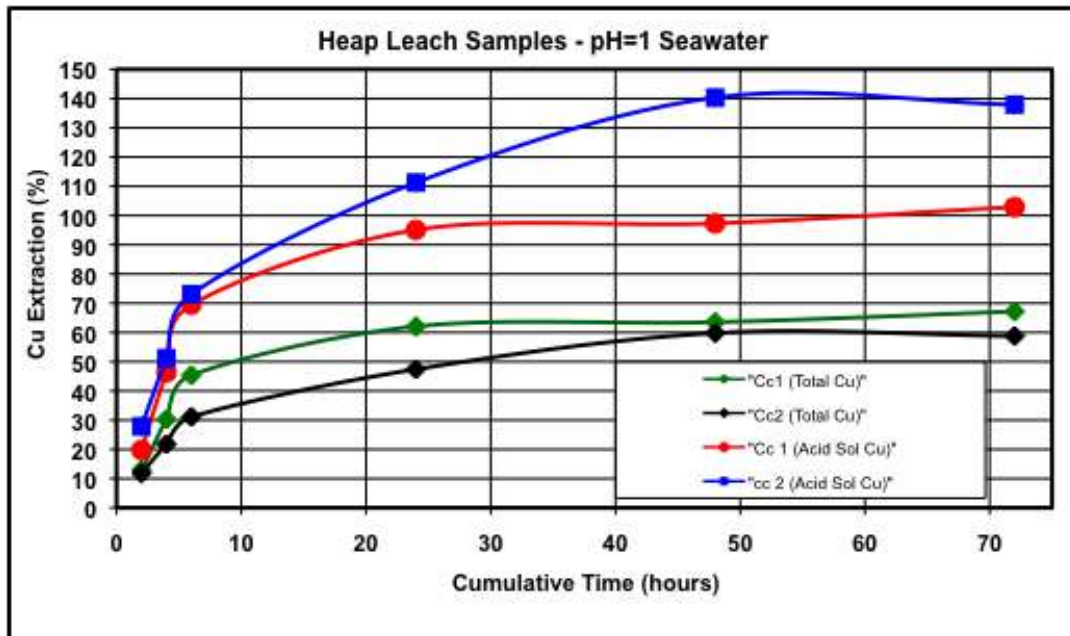


Figure 13.10 Main Pit pH=1 bottle roll leach kinetics

Figure 13.10 characterises the slow copper leach kinetics for both a typical oxide sample (Cc1) which contains slow leaching copper silicates and a typical oxide/transition sample (Cc2) which contains slow leaching silicates and slow leaching secondary sulphides, chalcocite and digenite.

The Cc7 and Cc8 samples were used in the column testing. Sample Cc7 has a higher grade than the rest of the samples with a lower acid soluble content and higher relative abundance of CN soluble copper. The Cc8 sample was similar to the other oxide/transition samples tested. The bottle roll performance in terms of total copper recovery was similar (Table 13.9 and Figure 13.11), however, due to the lower acid soluble copper and higher CN soluble copper the acid soluble copper recovery varies significantly, as expected.

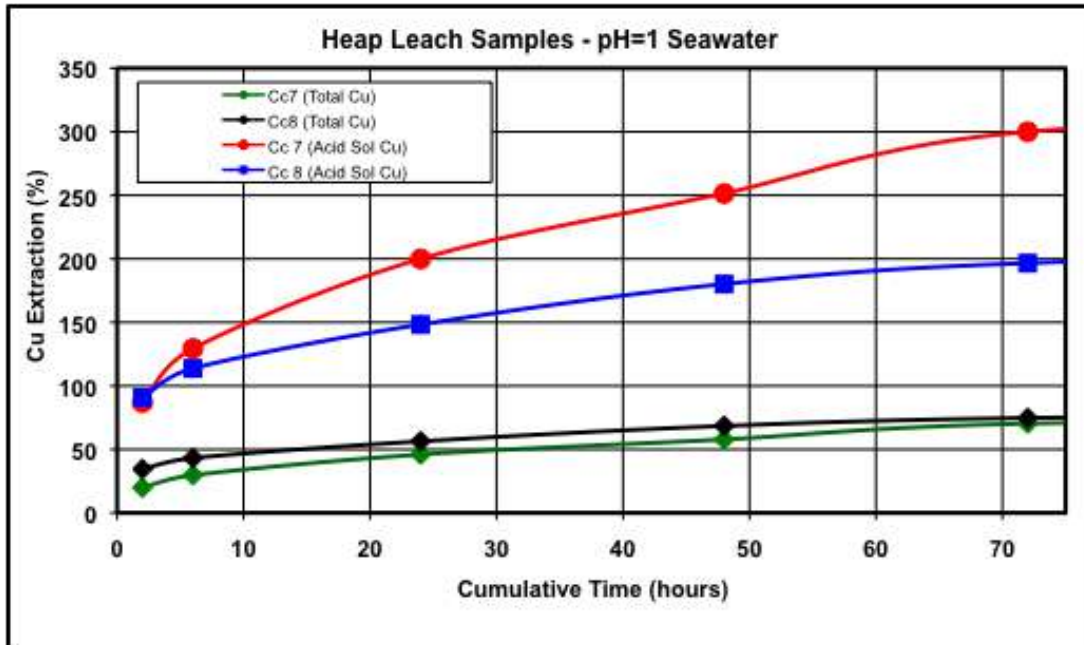


Figure 13.11 Main Pit pH=1 bottle roll leach kinetics

Santa Innes:

These samples are all classified as oxide and oxide/transition and analyses are summarised in Table 13.10.

Table 13.10 Santa Innes sequential Cu and QEMScan analysis

Sample	Domain	Head Grade Total Cu (%) (ICP Head Assay)	Sequential Cu Analysis				Ore Classification	QEMScan Cu Mineralogy Analysis		
			Head Grade Total Cu (%) (Calculated from Sequential Assay)	Head Grade Acid Soluble Cu (%), sequential analysis	Head Grade Cyanide Soluble Cu (%), sequential analysis	Head Grade Insoluble Cu (%), sequential analysis		Head Grade Acid Soluble Cu (%), QEMScan	Head Grade Cyanide Soluble Cu (%), QEMScan	Head Grade Insoluble Cu (%), QEMScan
Si1	Santa Innes	0.40	0.43	0.24	0.03	0.15	Oxide	0.39	0.00	0.04
Si4	Santa Innes	0.44	0.44	0.26	0.04	0.14	Oxide	0.37	0.01	0.05
D3	Santa Innes	0.17	0.16	0.10	0.03	0.03	Oxide	0.12	0.02	0.01
Si2	Santa Innes	0.59	0.59	0.26	0.17	0.16	Oxide/Transition	0.30	0.20	0.09

The two oxide samples at similar grades show very similar sequential analysis. The QEMScan mineralogy indicated the majority of the copper present as copper bearing silicates and chrysocolla. The sequential and QEMScan results vary with the QEMScan showing lower CN soluble and insoluble copper.

For the oxide/transition sample, copper is present as 40% copper bearing silicates, 30% as chalcocite/digenite and 10% as chalcopyrite and 10% as Cu/Mn WAD. The sequential and QEMScan results were reasonably consistent.

Leaching characteristics in terms of copper recovery and rate of copper recovery (total, acid and CN soluble) were consistent. There was a very significant variation in acid consumption from 40 to 150 kg/t for which there is insufficient data to explain. The copper recovery in terms of total copper and acid soluble copper are shown in Table

13.11. These results indicate that in the presence of seawater at a pH=1 a significant amount of the secondary sulphides (CN soluble) are soluble with calculated combined acid soluble plus CN soluble copper recoveries in the range of 76 to 89%.

Table 13.11 Santa Innes pH=1 bottle roll test results

Sample	Domain	pH=1 Bottle Roll Results					Acid Consumption (kg/t)
		Total Cu Recovery (%)	Acid Soluble Cu Recovery (%) sequential analysis	Acid Sol +CN Sol Cu Recovery (%) sequential analysis	Acid Soluble Cu Recovery (%) QEMScan Analysis	Acid Sol +CN Sol Cu Recovery (%) QEMScan analysis	
Si1	Santa In	64	106	99	71	71	40
Si4	Santa Innes	76	127	112	101	98	59
D3	Sant In	64	115	79	83	71	50
Si2	Santa In	56	128	78	112	67	42

The Santa Innes mineralized material types share common copper mineralogy with the Main Pit samples and also share the same characteristic slow leach kinetics (Figure 13.12). The Si4 sample that was used for the column testwork had similar characteristics to the other oxide samples tested.

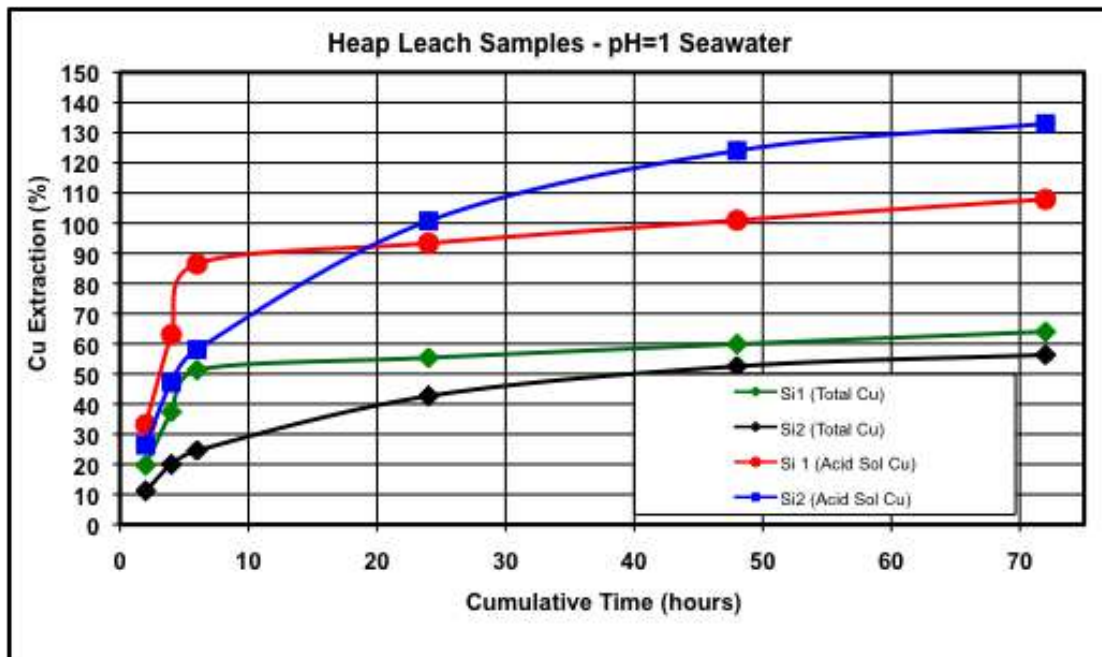


Figure 13.12 Santa Innes pH=1 bottle roll leach kinetics

Alice and Central Eastern Oxide

The Alice (AL1 and AL2) and Central Eastern Oxide samples (ADD_BR_1 and 2) are classified as oxide. No QEMScan data was available. The sequential analysis (Table 13.12) shows dominant acid soluble copper. Both sets of samples have a significant copper head grade variation. Both low grade samples have elevated insoluble copper contents of 35 and 43%, respectively.

Table 13.12 Alice and Central Eastern Oxide Sequential Cu analysis

Sample	Domain	Head Grade Total Cu (%) (ICP Head Assay)	Sequential Cu Analysis				Oxide mineralised inventory characterisation
			Head Grade Total Cu (%) (Calculated from Sequential Assay)	Head Grade Acid Soluble Cu (%), sequential analysis	Head Grade Cyanide Soluble Cu (%), sequential analysis	Head Grade Insoluble Cu (%), sequential analysis	
AL1	Alice	1.12	1.11	0.93	0.04	0.13	Oxide
AL2	Alice	0.48	0.48	0.16	0.08	0.21	Oxide
ADD_BR_1	Eastern Oxide	1.22	1.21	0.98	0.04	0.20	Oxide
ADD_BR_2	Eastern Oxide	0.44	0.48	0.26	0.02	0.17	Oxide

The bottle roll results (Table 13.13, Figure 13.13 and Figure 13.14) show high copper recoveries for both acid and CN soluble copper and tend to indicate the sequential analysis is understating total soluble copper. Acid consumptions are reasonable for the Central Eastern Oxide at 25 kg/t but higher for Alice.

Table 13.13 Bottle roll test results (pH=1)

Sample	Domain	pH=1 Bottle Roll Results					Acid Consumption (kg/t)
		Total Cu Recovery (%)	Acid Soluble Cu Recovery (%) sequential analysis	Acid Sol +CN Sol Cu Recovery (%) sequential analysis	Acid Soluble Cu Recovery (%) QEMScan Analysis	Acid Sol +CN Sol Cu Recovery (%) QEMScan analysis	
AL1	Alice	88	105	100			70
AL2	Alice	57	171	114			44
ADD_BR_1	Eastern Oxide	76	94	90			25
ADD_BR_2	Eastern Oxide	70	130	120			25

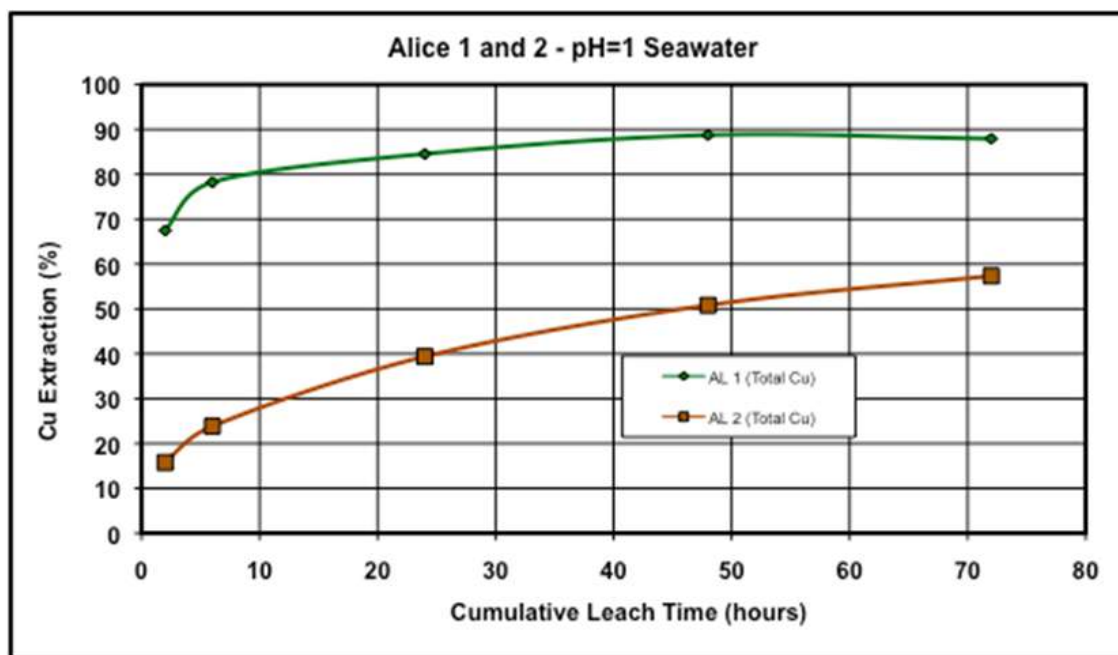


Figure 13.13 Alice pH=1 bottle roll leach kinetics

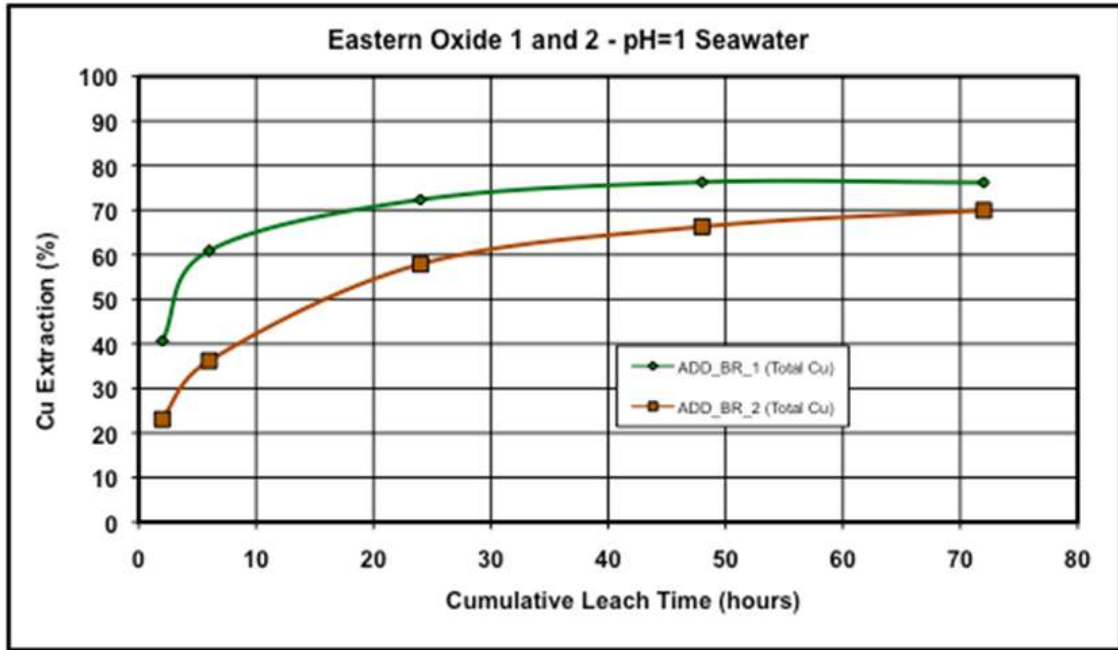


Figure 13.14 Eastern Oxide pH=1 bottle roll leach kinetics

13.2.2.1.3 Estimate of Economic Operating Point from Bottle Roll Results

Acid consumption can be characterised by the performance of the Main Pit (Cc2a as an example) depicted in Figure 13.15 and Figure 13.16. Acid consumption does increase with time. These characteristics should allow for heap leaching to target an economic copper recovery based on acid consumption. From this sample, it can be seen that acid consumption increases more than 100% (from 24 to 56 kg/t) whilst the copper recovery only increases from 73 to 80% (Figure 13.16).

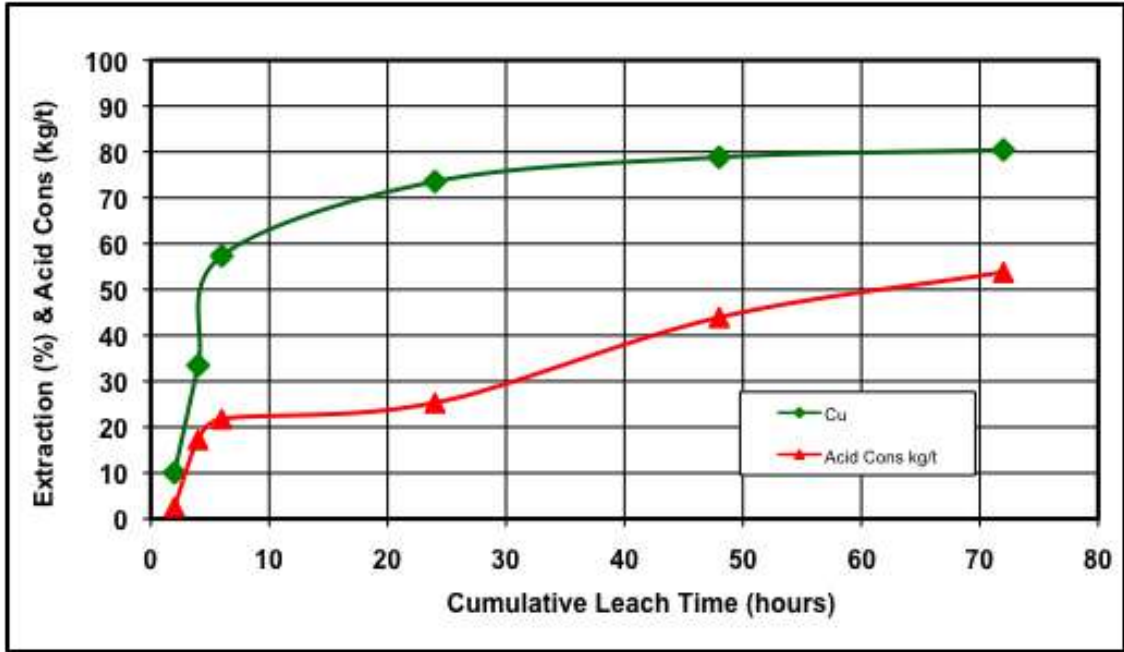


Figure 13.15 Acid consumption and Cu extraction characteristics

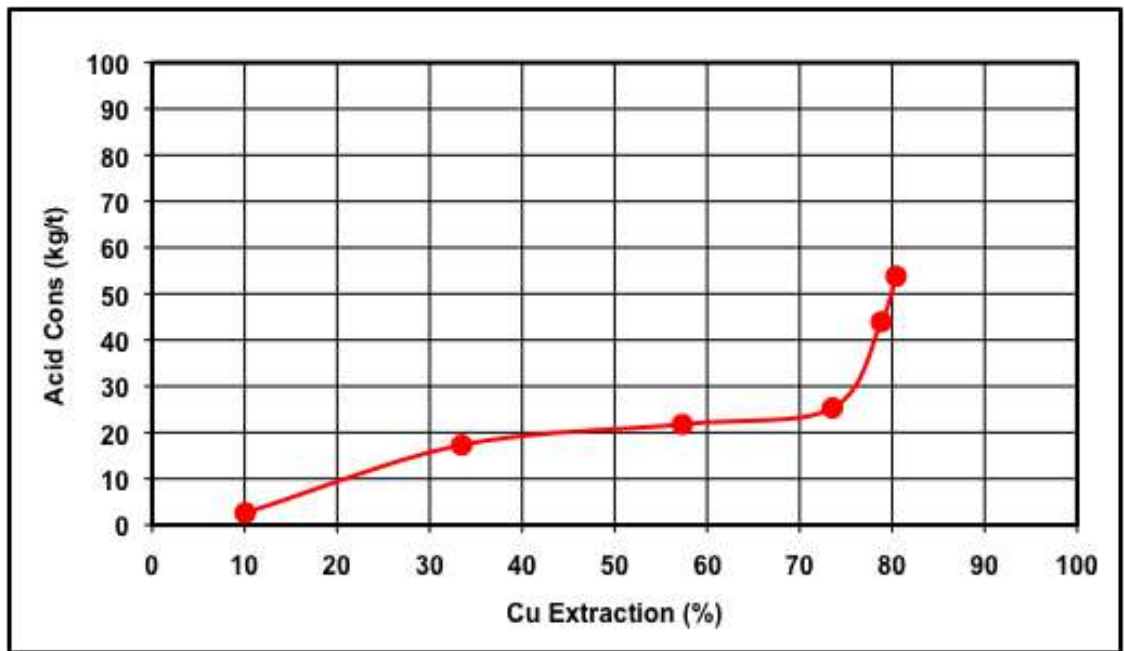


Figure 13.16 Acid consumption and Cu extraction characteristics

On the basis of the increased and variable acid consumption rate, it was decided to apply a limit to the economic acid consumption. Based on the Project acid cost of US\$100/t, it was assumed that the acid consumption became sub-economic in the range of 25 to 30 kg of acid per kg of copper extracted. This represents an operating cost for acid alone of US\$1.38/lb to US\$1.66/lb. Using this factor, the revised copper extraction at this acid consumption could be obtained. The copper extraction and acid consumption values obtained for the pH=1 leaches were then compared to the pH=2 leaches to

determine if there was a more economically attractive leach regime. This analysis resulted in Table 13.14 which summarises the results of the bottle roll tests in terms of copper extraction and acid consumption data that was then used to establish optimal conditions for the column tests and then to compare results obtained from the 1m columns with regard to copper recovery and acid consumption profiles.

Table 13.14 Summary of optimal Cu extraction vs. acid consumption

Sample	Domain	%Cu (head)	pH=1 Economic Point	
			%CuRec	Acid Con kg/t
No1	North Ox	0.47	39	47
No2	North Ox	0.54	55	40
No3	North Ox	0.54	76	50
D4	North Ox	0.4	57	36
Sm1	Sth Mantos	0.84	45	25
Sm2	Sth Mantos	0.45	34	49
Cc1	CCHEN Sth	0.49	62	28
Cc2	CCHEN Sth	0.57	47	21
CC2a	CCHEN Sth	0.75	73	25
Cc3	CCHEN Sth	0.45	45	31
Cc4	CCHEN Sth	0.61	58	41
Cc7	CCHEN Sth	0.82	46	56
Cc8	CCHEN Sth	0.57	56	37
D1	CCHEN Sth	0.24		
Si1	Santa In	0.39	55	22
Si2	Santa In	0.57	43	22
Si4	Santa Innes	0.39	70	32
D3	Sant In	0.25	39	18
AL1	Alice 1	1.12	84	40
AL2	Alice 2	0.48	51	36
ADD_BR_1	East Oxide	1.22	76	25
ADD_BR_2	East Oxide	0.44	70	25

13.2.2.2 Crushing Testwork and Dump Leach Stacking and Hydrodynamic Testing

A summary of the results of the crushing/comminution testing is shown in Table 13.15.

Table 13.15 Crushing and UCS test results

18 Samples for bond crushing tests and six samples for UCS tests	
Specific gravity	2.62
Bond CWi	
Minimum	1.3 kWh/t
Maximum	29.7 kWh/t
Average	7.9 kWh/t
Standard deviation	6.9 kWh/t
UCS	17.9 Mtpa (6.1 to 32.4)

These results indicate a moderately hard mineralized material that will require probably at least three stages of crushing to achieve a target crush size range of $P_{80} = -25$ mm to -12.5 mm.

13.2.2.3 Heap Agglomeration, Stacking and Hydrodynamic Testing

The samples for testing were crushed to minus 1 inch or 25.4 mm (Sample A) and minus 0.5 inch or 12.7 mm (Sample B). The crushed product was dry screened to -30 mesh (-0.6 mm) and then wet screened to determine the finer fractions (+100 mesh, +200 mesh and -200 mesh, thus 0.15 mm, +74 μ m and -74 μ m).

Figure 13.17 to Figure 13.19 summarise the particle size distribution (PSD) for samples A and B. Table 13.16 summarises the main size fractions (fines, sand and gravel) for each of these samples and shows that even the samples crushed to minus 12.7 mm have a minimum amount of fines (from 2.0% to 3.4%).

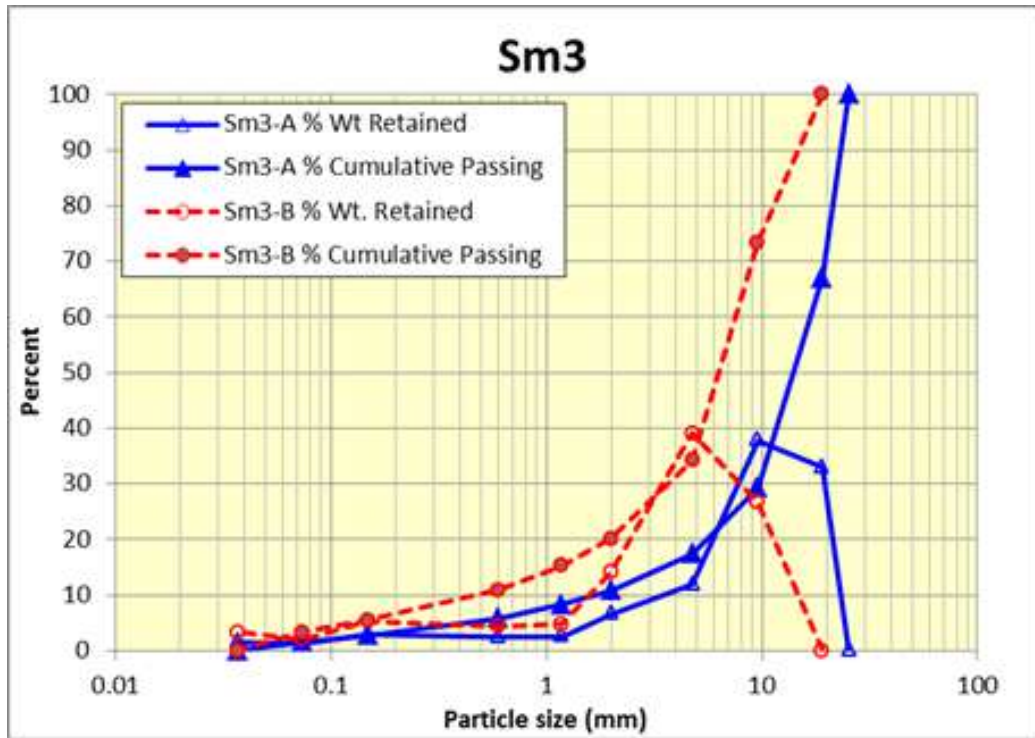


Figure 13.17 PSD for crushed Southern Mantos (Sm3)

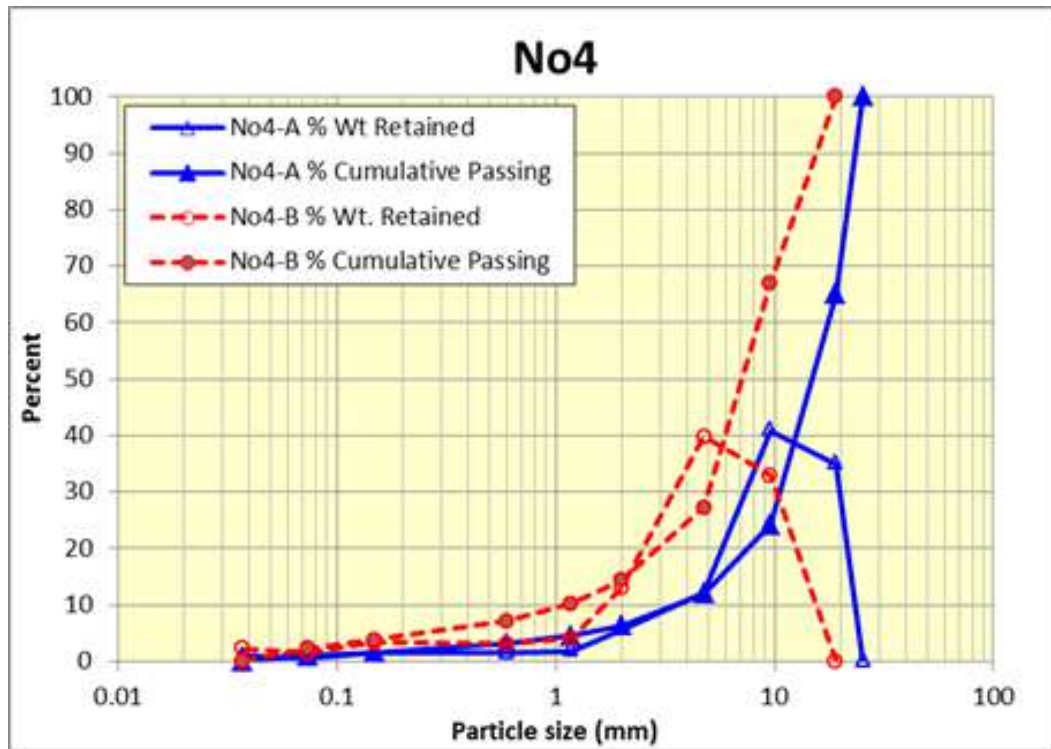


Figure 13.18 PSD for crushed Northern Oxide (No4)

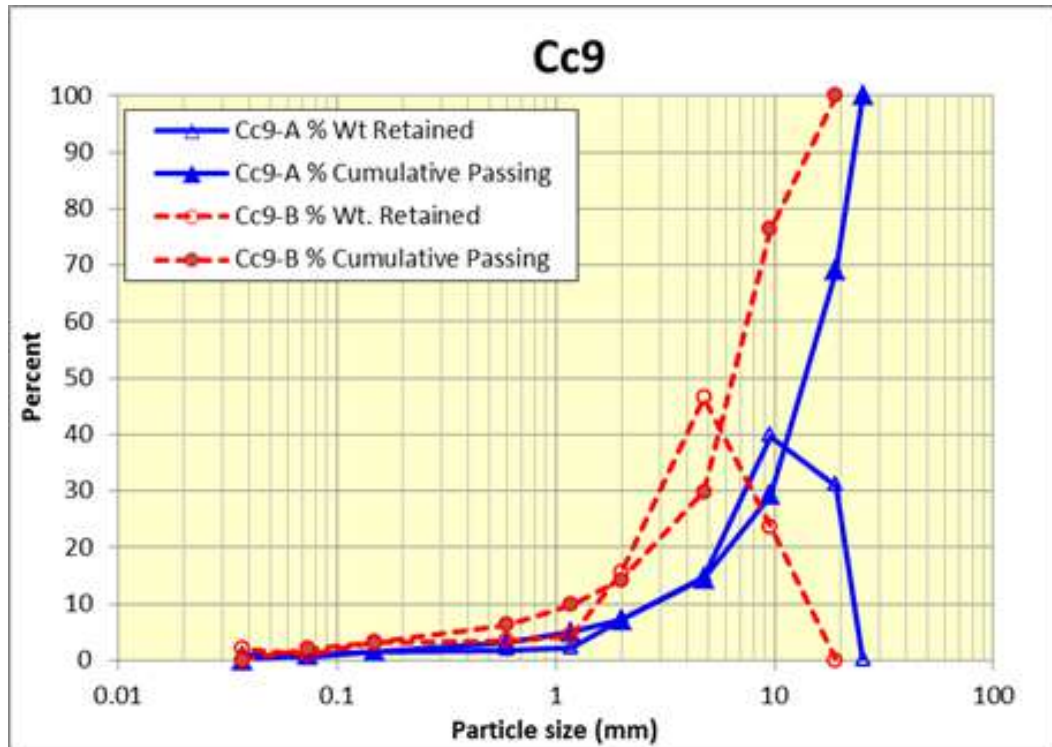


Figure 13.19 PSD for crushed Main Pit 9 (Cc9)

Table 13.16 PSD summarised results

Top size (mm)	Sample	Fines (%)	Sand (%)	Gravel (%)
25.4	Sm3-A	1.59	9.22	89.20
25.4	No4-A	1.02	5.36	93.62
25.4	Cc9-A	0.99	6.18	92.83
12.7	Sm3-B	3.42	16.75	79.83
12.7	No4-B	2.35	11.98	85.67
12.7	Cc9-B	2.03	12.25	85.72

When sufficient mineralized material was available, the samples were agglomerated to two different levels of agglomeration; incipient (L1) and intermediate (L3). Agglomeration of the samples followed the conditions established after analysis of the bottle roll test results and the effects of acid on rate and extent of copper recovery. These conditions are summarised in Table 13.17.

Table 13.17 Agglomeration and leach conditions

Sample	Agglomeration Acid (kg/t)	Leach Solution Acidity (g/L)	Leach Solution Ferric (g/L)
Cc9	10	5	0
Sm3	10	5	1.5
No4	25	10	0

An L1 agglomeration level is easily obtained via conveyor-belt agglomeration and an L3 is easily obtained via drum-agglomeration. It is noted that some of the samples (Cc9) could not reach a L3 agglomeration level given the nature and the low content of the fines. The level of agglomeration and moisture content required to achieve each level are shown in Table 13.18.

Table 13.18 Agglomeration level and moisture content

Test ID	Agglomeration level	Moisture content (%)
Cc9-A-L1	L1	2.4
Cc9-A-L2	L2	4.0
Cc9-B-L1	L1	3.9
Cc9-B-L2	L2	5.2
No4-A-L3	L3	3.5
No4-B-L3	L3	5.8
Sm3-A-L1	L1	4.8
Sm3-A-L2	L2	5.5
Sm3-B-L1	L1	5.8
Sm3-B-L2	L2	6.5

A positive outcome to a Stacking Test (ST) indicates that the sample is a candidate for percolation heap leaching and further testing can be pursued. Negative results, on the other hand, indicate categorically the mineralized material as prepared would not support percolation leaching. The results from the ST are summarised in terms of the following:

- The density profile
- The conductivity profile
- The partitioning between micro- and macro-porosity.

The following sections present these results for each of the composites.

Figure 13.20 shows the stacked mineralized material density variation with heap height. In general, as the heap height increases, the density of the stacked material increases. However, the level of agglomeration has a significant effect on the density profile. For example, for Cc9 by effective agglomeration (L3), it is possible to achieve a density of

0.06 t/m³ at an equivalent heap height compared to incipient (L1) agglomeration with decreased density providing improved porosity and permeability for heap leaching.

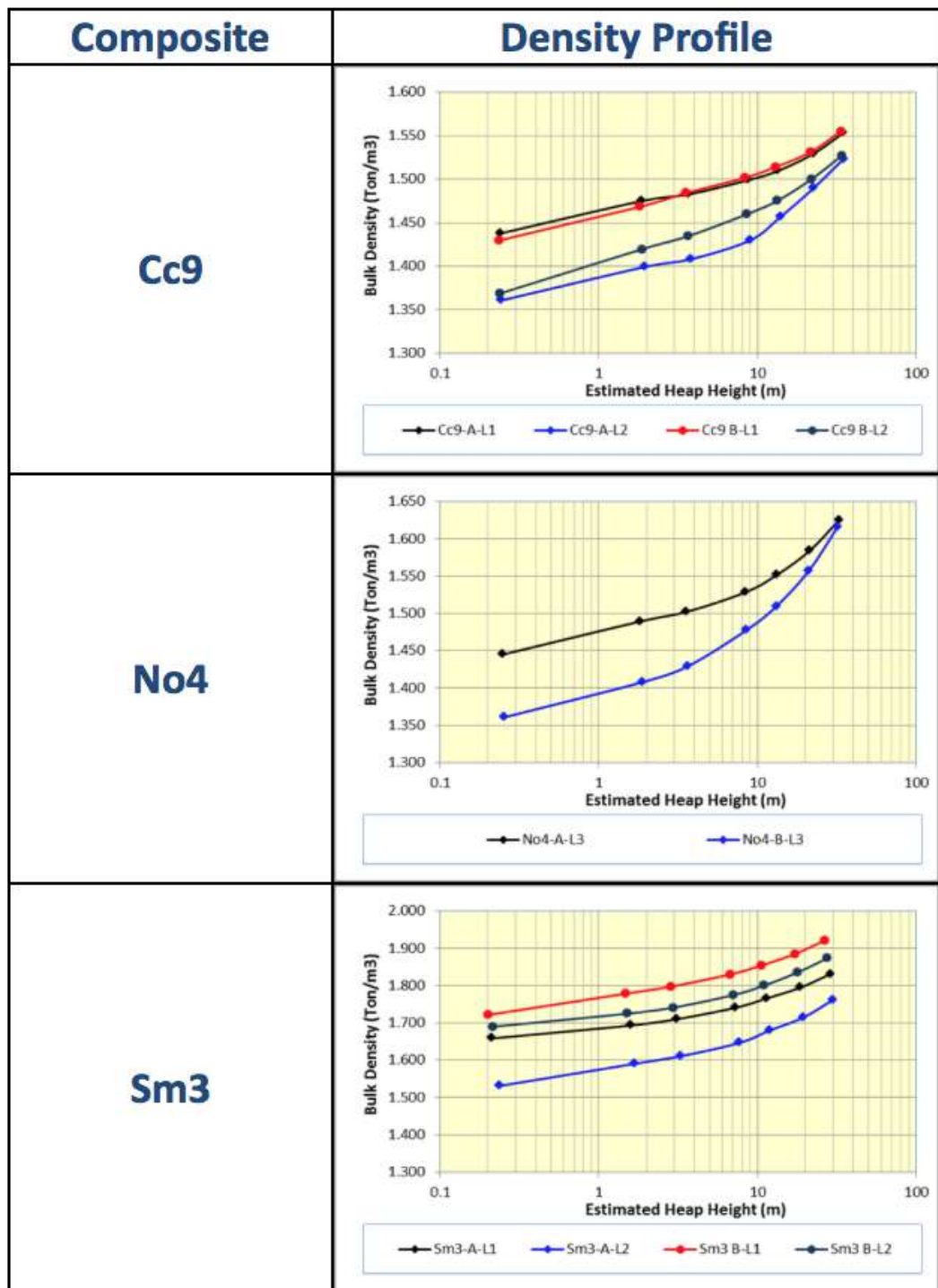


Figure 13.20 Density vs. potential heap height profiles

As depicted in the following figures (Figure 13.21 to Figure 13.23), the hydraulic conductivity of all the samples remains above the minimum value of 1.67×10^{-1} cm/s, which represents a leach solution application rate of 100 times the target mid-point

application rate of 6 l/h/m², even at the maximum heap height tested during this investigation (~36 m).

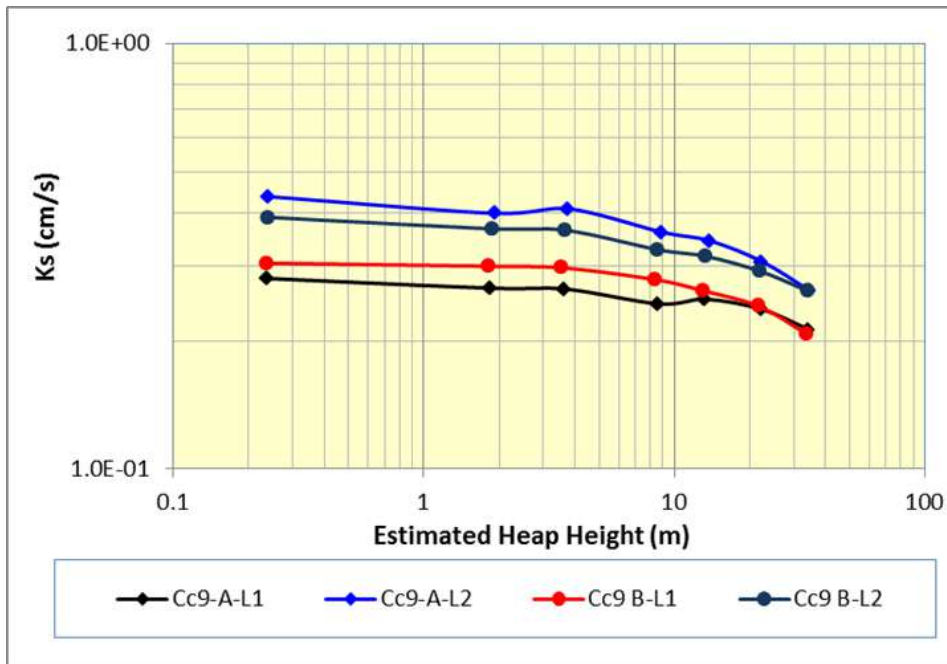


Figure 13.21 Hydraulic conductivity vs. potential heap height profiles

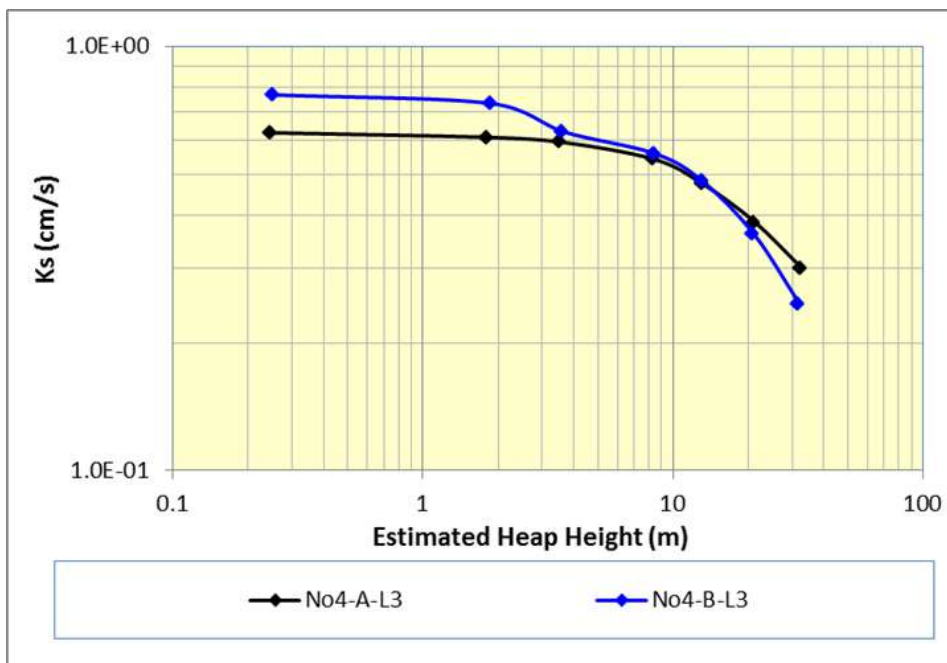


Figure 13.22 Hydraulic conductivity vs. potential heap height profiles

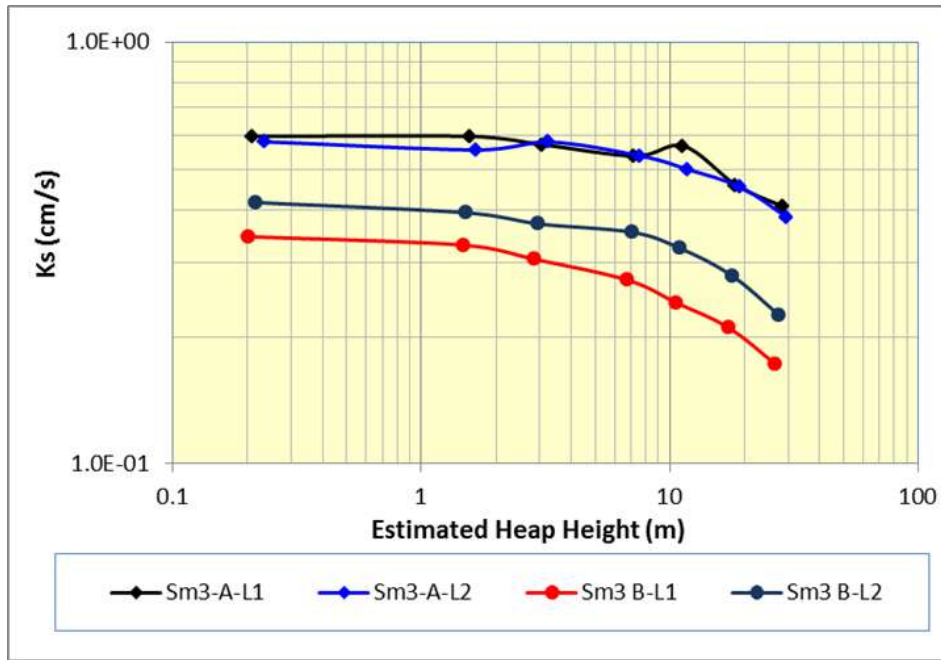


Figure 13.23 Hydraulic conductivity vs. potential heap height profiles

Partitioning of porosity into micro and macro categories has also been determined (Figure 13.24). The resulting porous structure produces a total porosity larger than 30% for all of these samples which is partitioned between macro- and micro-porosity of about 50:50. The work indicates that this ratio facilitates bulk solution movement and intimate contact between solution and mineralized material.

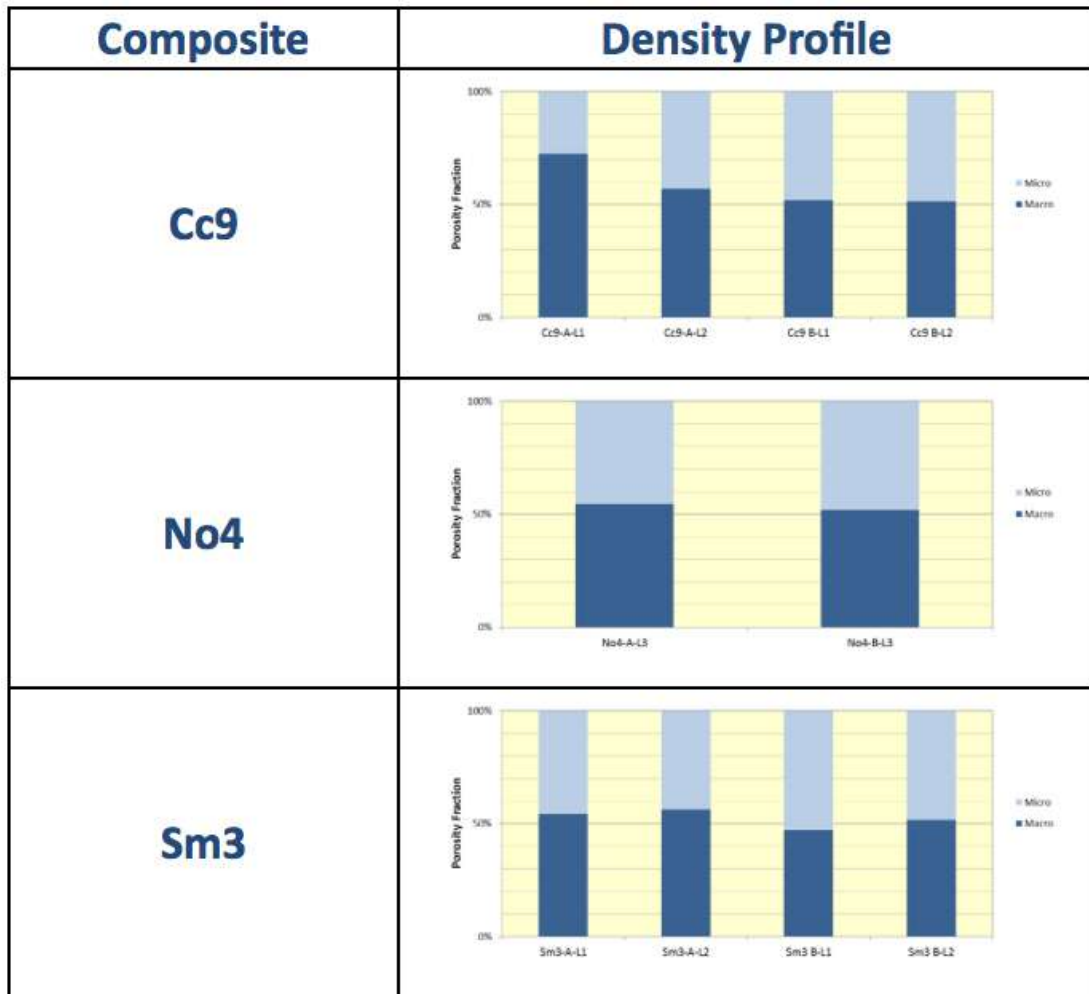


Figure 13.24 Porosity partitioning

One Hydrodynamic Column Test (HCT) was conducted for each of the samples crushed to -12.7 mm (Sample B) to determine the hydrodynamic response of the bottom portion of a 16 m lift. Table 13.19 summarises the conditions for each of the samples. Importantly, synthetic raffinate solution was prepared for each sample and used during the process of agglomeration. Table 13.20 summarises the concentrations of the salts used to prepare each of these synthetic solutions.

Table 13.19 Hydrodynamic columns testing conditions

Sample ID	SG (t/m ³)	Grav. moisture content (%)	Initial liquid saturation (%)	Dry bulk density (t/m ³)	Porosity partitioning macro (%)	Porosity partitioning micro (%)
Sm3-B 16m (L3)	3.644	7.4	26.2	1.824	47.6	52.4
No4-B 16m(L3)	3.186	6.3	17.9	1.527	55.9	44.1
Cc9-B 16m (L3)	2.734	5.3	16.8	1.485	55.3	44.7

Table 13.20 Salts concentration used to prepare synthetic raffinate

Sample ID	H ₂ SO ₄ (g/L)	Fe ₂ .(SO ₄) ₃ (g/L)	NaCl (g/L)	MgSO ₄ (g/L)
Sm3-B 16m (L3)	5.4	7.7	32	13.4
No4-B 16m (-L3)	10.75	0	32	13.4
Cc9-B 16m (L3)	5.4	0	32	13.4

As indicated by the porosity partitioning of these samples (Table 13.19), the mineralized material samples at agglomeration levels of L3 results in a nearly optimal macro:micro ratio (50:50) for the Sm3 sample and slightly higher macro porosity for samples No4 and Cc9 (~55%).

Figure 13.25 shows the degree of saturation associated to various solution application rates imposed during the HCTs and Figure 13.26 shows the gas conductivity as a function of liquid saturation for each of the samples.

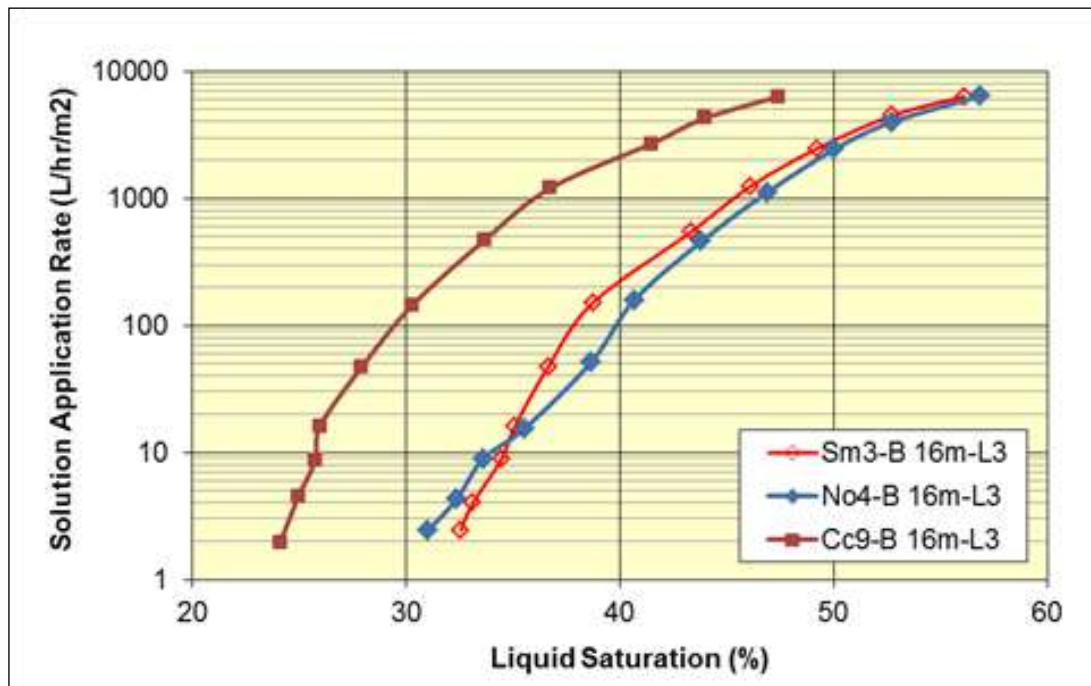


Figure 13.25 Liquid saturation at variable application rates

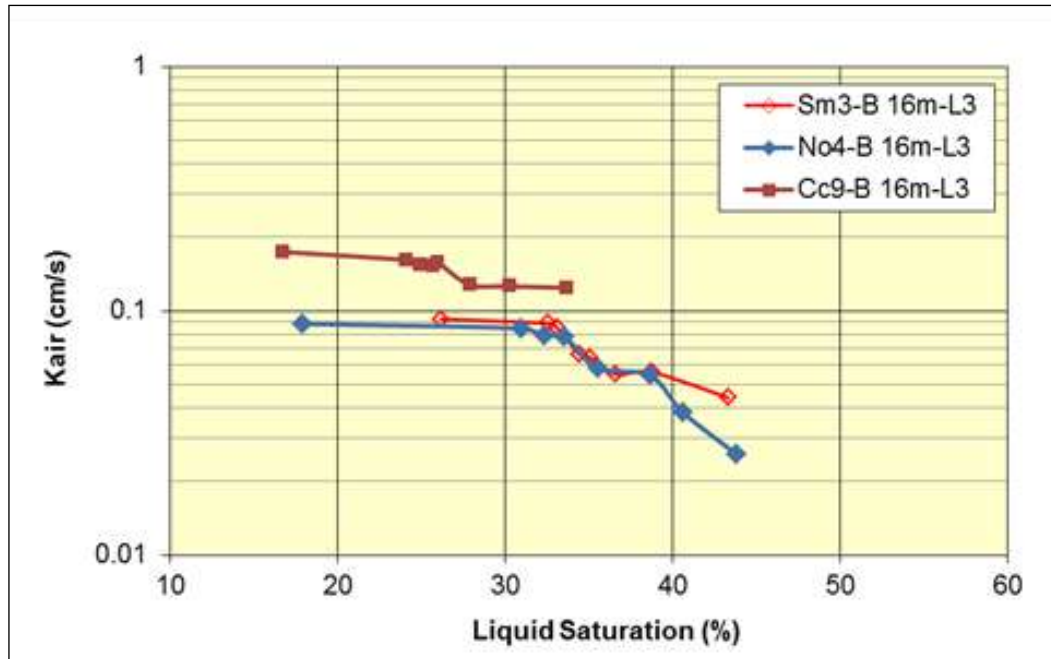


Figure 13.26 Gas conductivity

Although crushing the samples from a top size of 25.4mm to a -12.7mm has a noticeable effect on the physical and hydraulic properties of the Productora composite samples, the samples with a top size of 12.7mm are sufficiently robust to potentially support multi-lift percolation leaching. These data confirm that all of these samples agglomerated to a Level 3 (L3) would efficiently support percolation leaching.

If necessary, the maximum heap height supported by the samples crushed to a top size of -12.7mm is approximately 40m (which could translate to four 10m lifts or five 8m lifts).

Regarding the state K_s threshold, the stated value of 1.67×10^{-1} cm/s corresponds to 100 times the application rate, in this case assumed to be a nominal value of 6 l/h/m². Experience shows that for a multiple-lift heap this is the best starting condition to account for slumping, chemical degradation and variability in the mineralized material and conditions of stacking. All these samples satisfy this condition, have sufficient porosity (>30%) and good ratio between micro- and macro-porosity.

The excellent hydrodynamic performance of the minus 12.7 mm crushed samples is congruent with the minimum amount of fines present on these samples.

The operational degree of saturation under standard solution application rates ($4 \text{ l/h/m}^2 < q < 15 \text{ l/h/m}^2$) is below 40%. These operational saturation values indicate that all these samples would be able to support the percolation process for the heap up to 16 m without any difficulty.

Almost no slumping was noted during the duration of the HCTs, indicating a robust porous structure for all of these samples.

13.2.2.4 Column Testwork (1m) Results

Based on the bottle roll test results and preliminary agglomeration trials, agglomeration and leach solution acid concentrations were selected as shown in Table 13.21. All mineralized material types showed high acid consumption potential under highly acidic leach conditions. They also all showed some degree of reduced copper recovery under more moderate acidic conditions. The Northern Oxide samples show a very strong copper recovery dependence on acid and this is reflected in the conditions selected.

Table 13.21 Mineralized material agglomeration acid and column leach solution acid

Samples	Acid Addition to Agglom (kg/t)	Acid in Leach Solution (g/L)
Cc7	10	5
Cc8	5	5
Si4	5	5
No3	25	10
Sm2	10	5

Table 13.22 shows a comparison of results of the bottle roll results to the completed 1m column results. The high-level summarised results appear to be reasonably consistent with the bottle roll tests and indicate that the agglomeration and solution acidities used were adequate. For Cc7, Cc8 and No3 samples, the acid soluble copper recovery (as determined by sequential copper analysis of head samples) has exceeded 100%, as would be expected, as these are oxide/transition samples.

Table 13.22 Bottle rolls vs. column leach results

Sample	Domain	%Cu (head)	Economic Point from Bottle Roll Tests		1m Column Day 50 Results		
			Total Cu Recovery (%)	Acid Consumption (kg/t)	Total Cu Recovery (%)	Acid Sol Cu Recovery (%)	Acid Con kg/t
No3	North Ox	0.54	76	50	80	120	54
Sm2	Sth Mantos	0.45	34	49	48	124	24
Cc7	CCHEN Sth	0.82	46	56	49	220	16
Cc8	CCHEN Sth	0.57	56	37	60	157	7
Si4	Santa Innes	0.39	70	32	60	101	7

The following sections summarise the performance of each of the five individual column tests. For each test, two graphs are provided. The first graph for each sample shows copper recovery and the total acid consumption in kg of acid per tonne of mineralized material (kg/t) vs. leach time (days). The second graph shows copper recovery, net acid consumption (kg/t) and acid consumption based on kg of acid consumed per kg of copper extracted (kg/kg) vs. solution application (kL/t).

13.2.2.4.1 Northern Oxide (No3)

No3 (Northern Oxide 3) leach performance (Figure 13.27 and Figure 13.28) reflects the slow leaching characteristics that would be expected from a mineralogy that is dominated by copper silicates. Despite this sample exhibiting lower acid soluble copper content and an elevated insoluble copper content its performance was very similar to other samples based on bottle roll testing. Total copper recovery of 80% was achieved using a solution application of 5.5 kL/t. A 120% recovery of the acid soluble copper was achieved which would indicate that for this particular sample there were probably some secondary sulphides present that were leached.

The mineralized material shows steady but high acid consumption characteristics, and it is the acid consumption that will dictate the maximum economic extraction of copper achievable. Leaching was terminated at day 30 as acid consumption had exceeded the economic limit of 25 kg/kg copper produced.

From the bottle rolls, it was predicted that the economic copper recovery would be 76% at 50 kg/t of acid consumed. Interpretation of the column tests result indicated although the maximum copper recovery was 80%, the economic maximum recovery based on acid consumption was 76% total copper recovery at 50 kg/t of acid consumed and solution application of 4.5 kL/t.

The variability in acid consumption (kg/kg) is a function of fluctuations in leach solution feed rate and the effect of the residence time of the leach solution within the column. This variation is quite acceptable and usual.

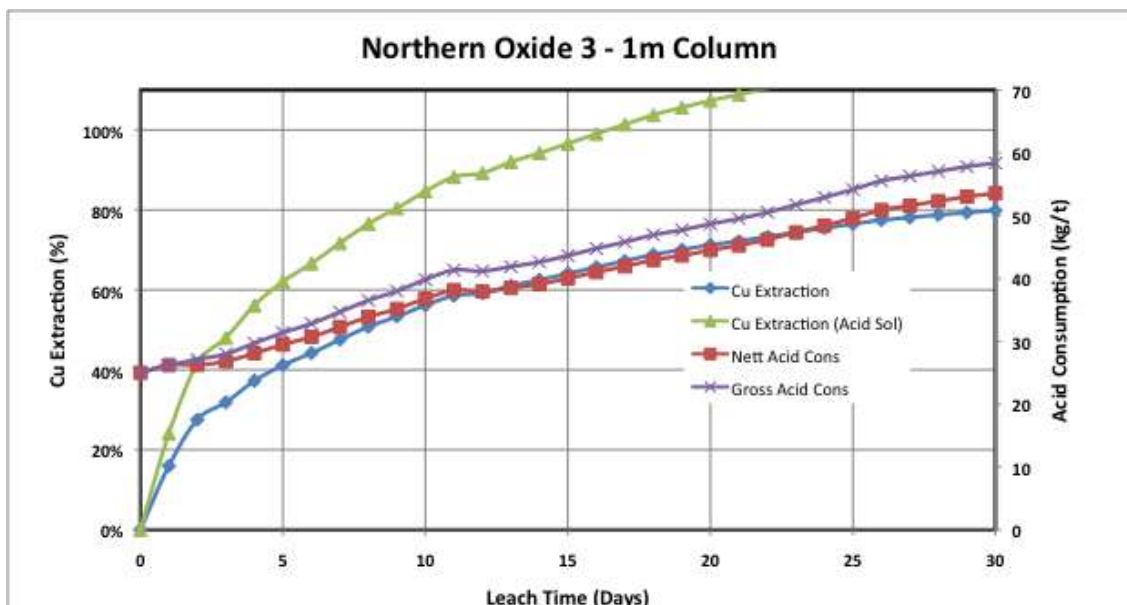


Figure 13.27 Northern Oxide 3 – 1m column results

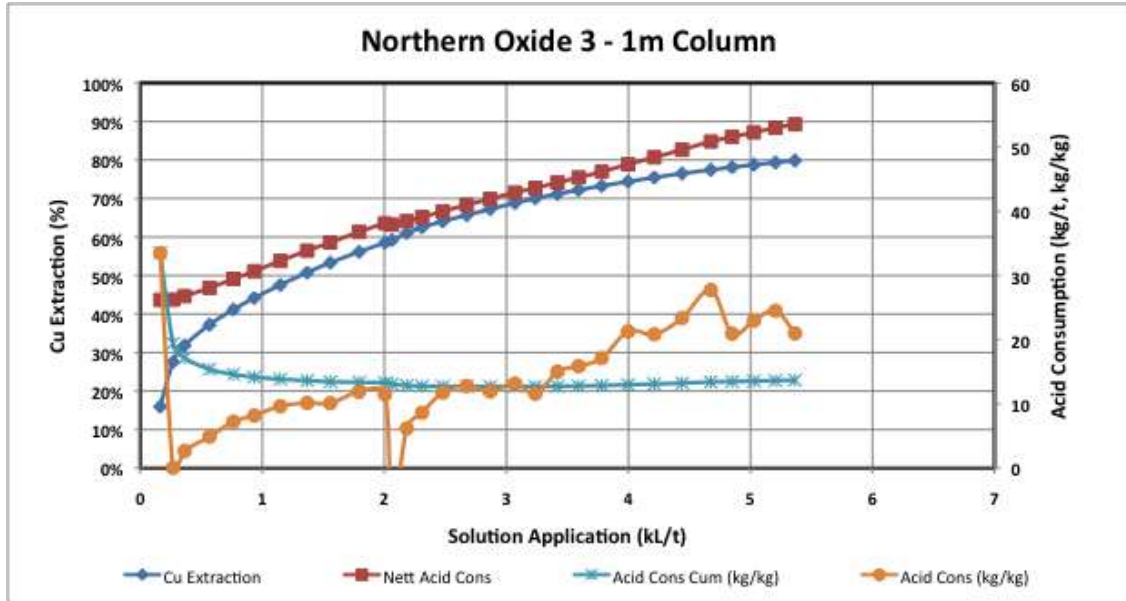


Figure 13.28 Northern Oxide 3 – 1m column results

13.2.2.4.2 Southern Mantos (Sm2)

Sm2 column test was terminated at Day 50 and a solution application of 6.5 kL/t mineralized material, as the acid consumption had exceeded the economic limit (Figure 13.29 and Figure 13.30). As would be expected from a combination of copper silicate minerals and secondary sulphides (chalcocite/digenite) the leaching kinetics are slow. Acid soluble copper recovery was 120% with an acid soluble plus CN soluble copper recovery of 67% indicating a significant proportion of the chalcocite and digenite are yet to leach.

From the bottle rolls, it was predicted that the economic copper recovery would be 51% at 14 kg/t of acid consumed. The column tests results were 49% total copper recovery at 25 kg/t of acid consumed. The acid consumption characteristics of the sample were higher than in the bottle roll testing and varied significantly from other Southern Mantos samples tested by the bottle roll test.

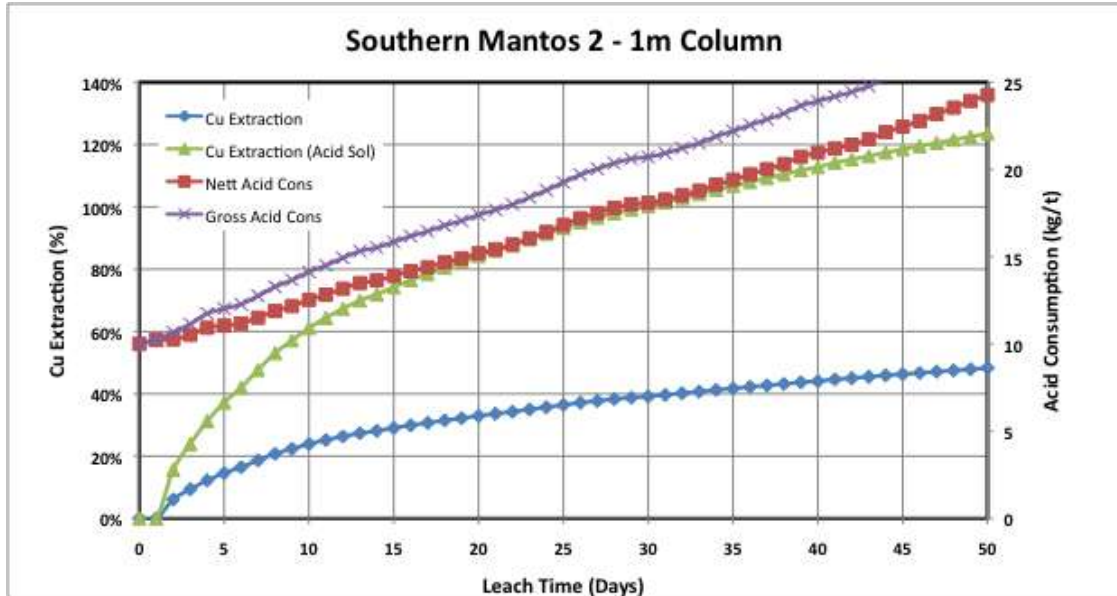


Figure 13.29 Southern Mantos 2 – 1m column results

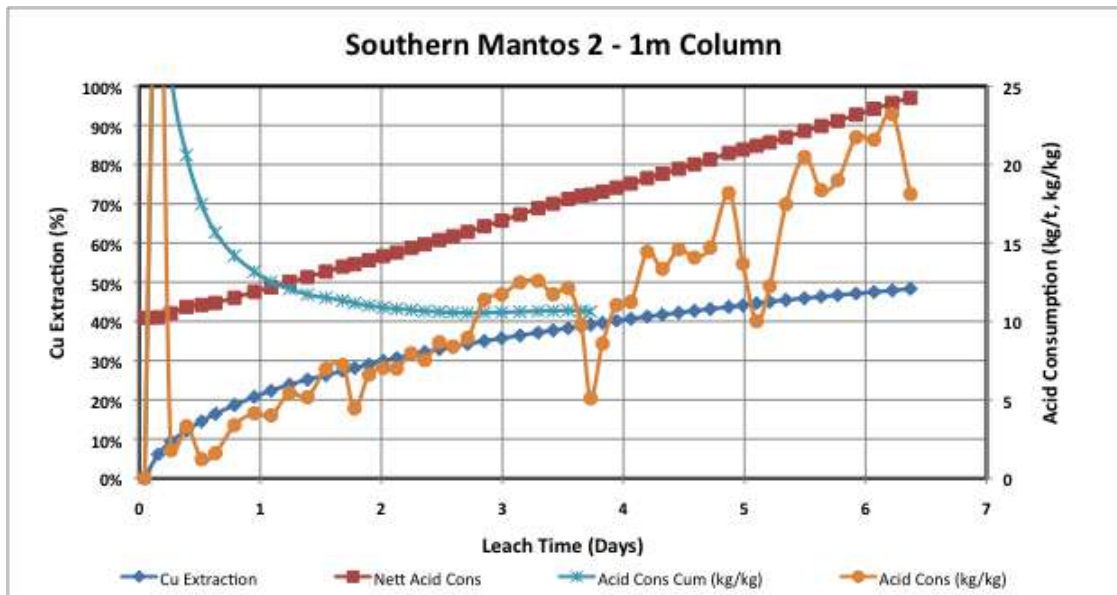


Figure 13.30 Southern Mantos 2 – 1m column results

13.2.2.4.3 Main Pit (Cc7 and Cc8)

Both samples Cc7 and Cc8 exhibit slow copper leaching kinetics (Figure 13.31 to Figure 13.34) symptomatic of the copper mineralogy present, slow leaching copper silicates and secondary sulphides (chalcocite and digenite). The total copper recovery is low for both (49% and 60%) but consistent with the low content of acid soluble copper (23% and 38% of total copper). Acid soluble copper extraction was 160 and 220%, reflecting the influence of leaching of the secondary copper sulphides. The acid soluble plus CN soluble copper recoveries were actually very similar at 76 and 77%. Both columns were terminated at 40 days and solution application of 7 kL/t of mineralized material due to

increasing acid consumption (in kg/kg copper leached which was approaching the economic limit) and the slow leaching rates that were indicating that ultimate copper recovery (based on bottle roll tests) was being approached.

From the bottle rolls, it was predicted that the economic total copper recovery would be 51% and 61% at an acid consumption of 12 and 4 kg/t for Cc7 and Cc8, respectively. The column tests results were 49% and 60% total copper recovery at 16 and 7 kg/t of acid consumed, respectively.

For both samples, acid consumption trends higher with time and solution application. This is consistent with bottle roll results and the host rock mineralogy.

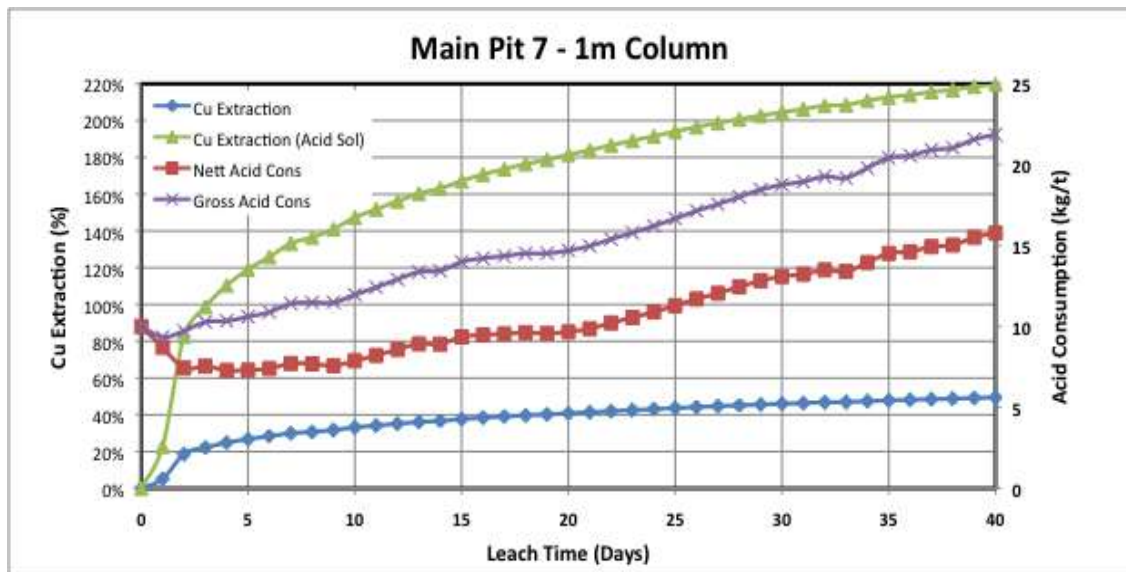


Figure 13.31 Main Pit 7 (Cc7) 1 m column results

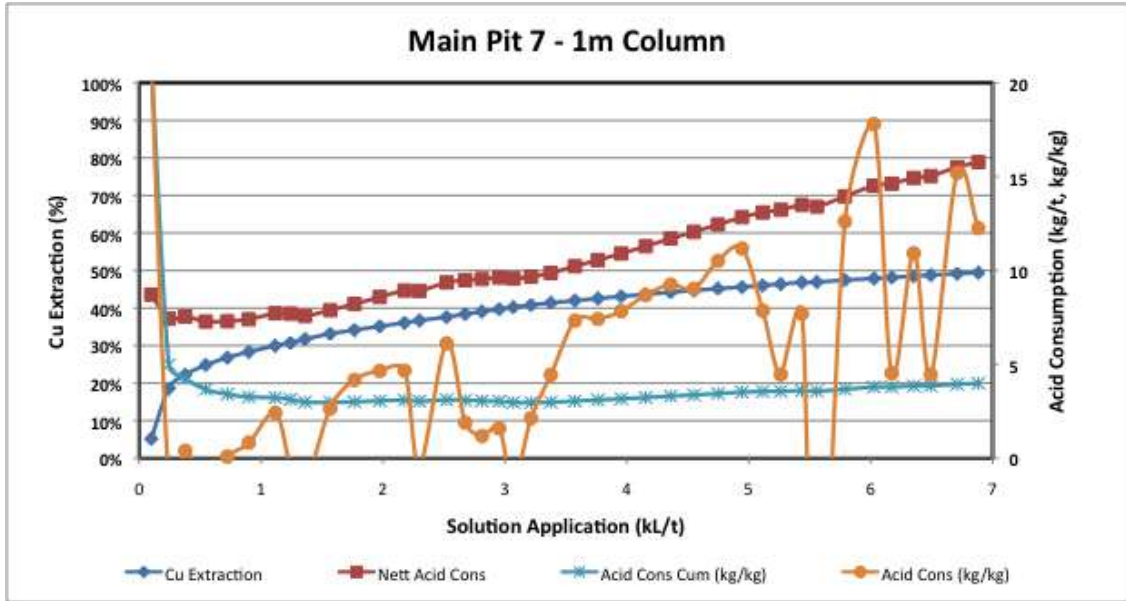


Figure 13.32 Main Pit 7 (Cc7) 1m column results

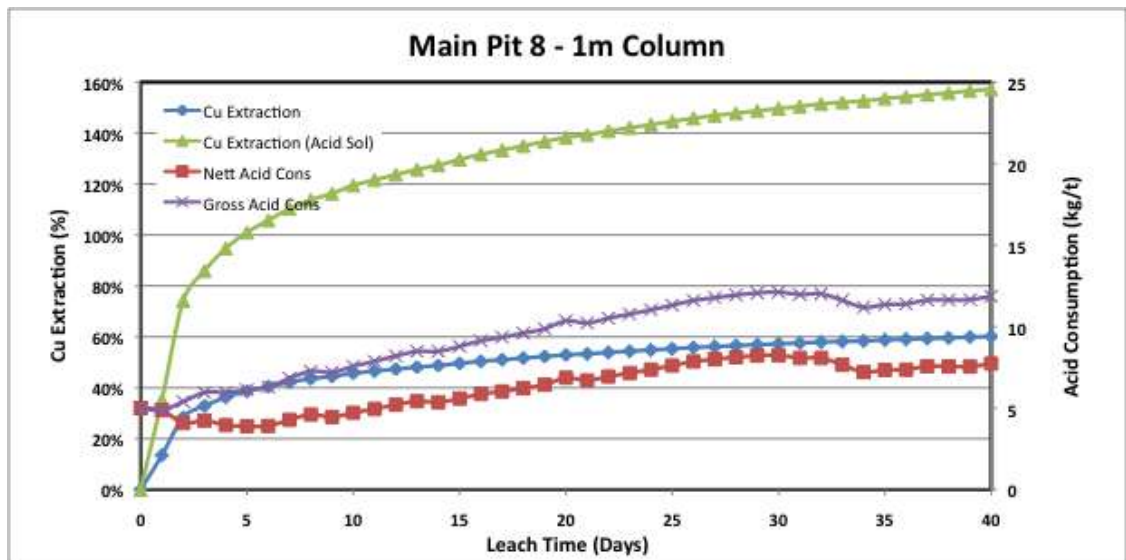


Figure 13.33 Main Pit 8 (Cc8) 1m column results

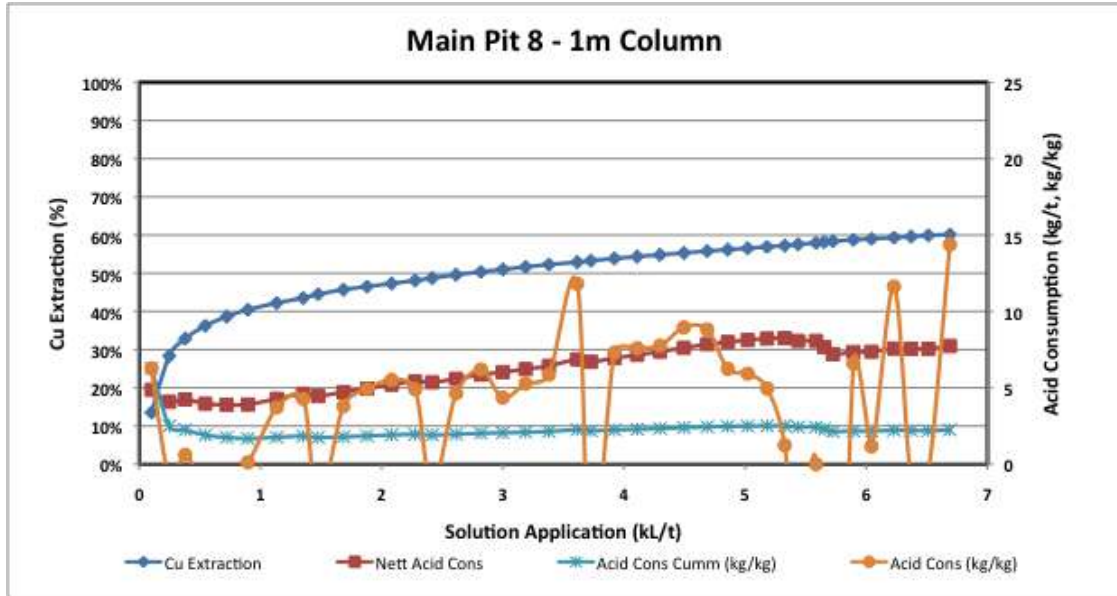


Figure 13.34 Main Pit 8 (Cc8) 1m column results

13.2.2.4.4 Santa Innes (Si4)

Santa Innes (Si4) column test was terminated at Day 30 and a solution application of 5.3 kL/t mineralized material, as the acid consumption had exceeded the economic limit (Figure 13.35 and Figure 13.36). As would be expected from a combination of copper silicate minerals and secondary sulphides (chalcocite/digenite) the leaching kinetics were very slow. Acid soluble copper recovery was 120% with an acid soluble plus CN soluble copper recovery of 67%, indicating a significant proportion of the chalcocite and digenite are yet to leach.

From the bottle rolls, it was predicted that the economic total copper recovery would be 64% at an acid consumption of 4 kg/t. The column tests results were 49% total copper recovery at 25 kg/t of acid consumed. The acid consumption characteristics of the sample were higher than in the bottle roll testing and varied significantly from other Southern Mantos sample tested by the bottle roll.

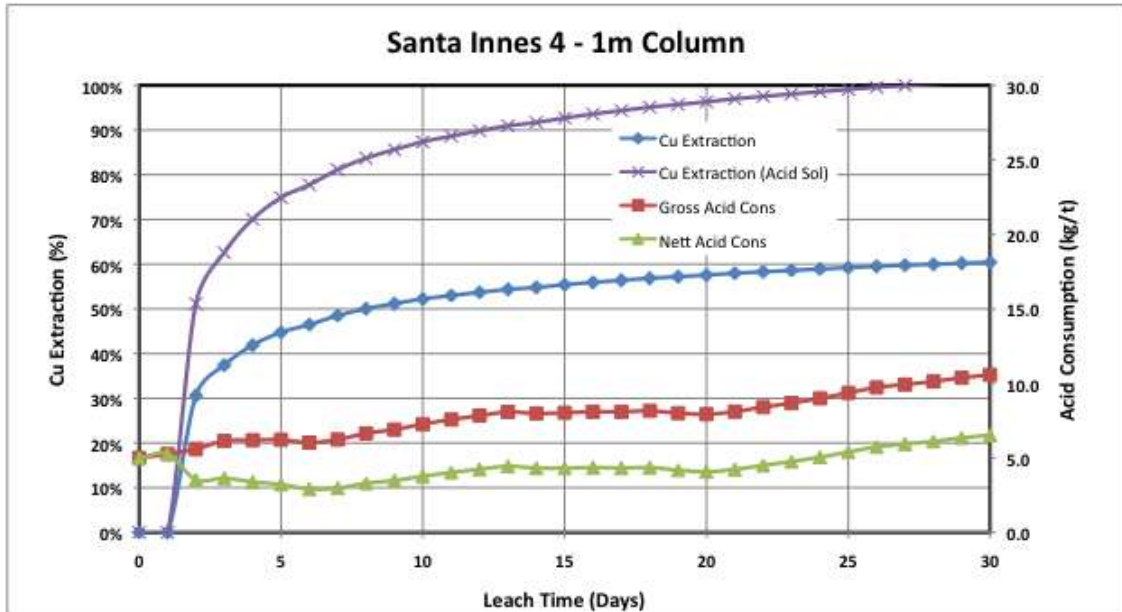


Figure 13.35 Santa Innes 4 – 1m column results

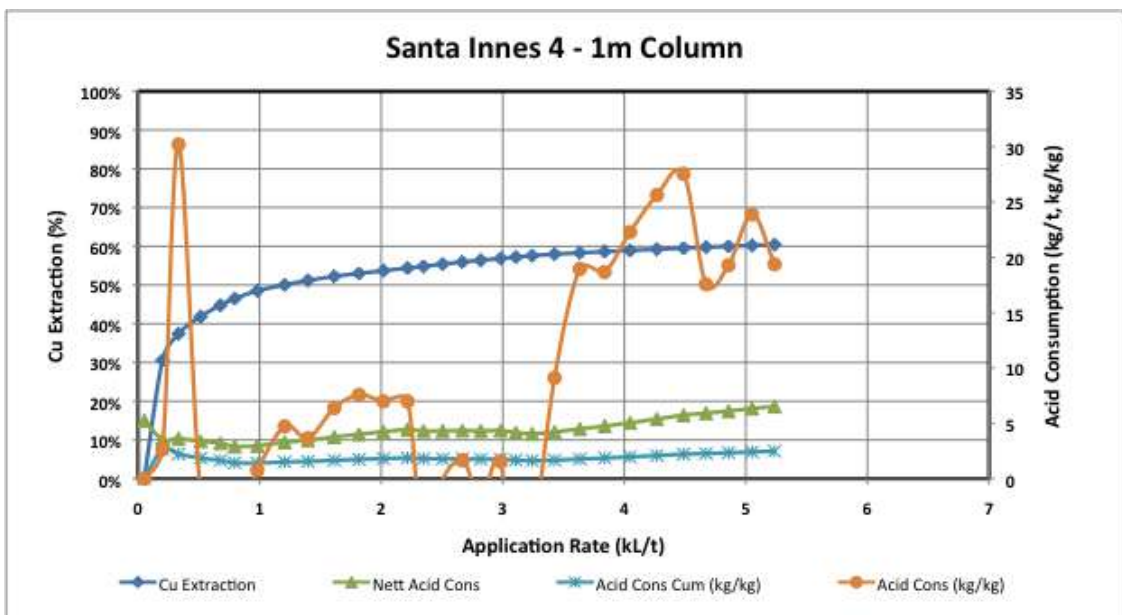


Figure 13.36 Santa Innes 4 – 1m column results

13.2.2.4.5 Summary of 1 m Column Testwork

All 1m column tests showed similar general characteristics with slow copper leach kinetics, symptomatic of the oxide and secondary sulphide minerals present. In addition, they show relatively high acid consumptions, again symptomatic of the host rock mineralogy. The acid consumption increases with time almost independent of copper recovery, and certainly as the copper recovery approached terminal extraction acid consumption continues at a reasonably constant rate.

These general characteristics mean that the copper extractions targeted are dictated by the resultant economic acid consumption. This feature results in a leaching strategy that dictates that the leach cycle time is kept to a minimum to minimise acid consumption. Consequently, it is necessary to consider commercial scale heaps with a limited heap height, as the higher the heap the more extended the leach time.

The stacking and hydrodynamic testing support heap heights from a geotechnical, hydrological and permeability perspective of up to 16 m with application rates in the order of 5 - 10 L/hr/m². They also show a potential to allow for over-stacking of up to five 8 m lifts.

For scaling up from a 1m column, a 6m heap height requiring 5.4 kL/t of solution and assuming a design application rate of 10 L/hr/m², the leaching will take 265 days as compared to the 1m column taking 45 days. For scaling up of a 1m column, an 8m heap requiring 5.4 kL/t of solution and assuming a design application rate of 10 L/hr/m², the leaching will take 353 days as compared to the 1m column taking 45 days. Therefore, an 8m heap will require an additional 90 days of leaching with the additional acid consumption.

Stacking mineralized material at less than 6m is not considered economically practical at this stage, however, there is precedence for operations in Chile with specific mineralized material types whereby leaching has been conducted with heaps as low as 3m to 4m.

For this study, without additional testwork on 6m or 8 m columns available, 6m heap heights have been considered to be acceptable.

13.2.3 Conclusions

Major conclusions of the copper oxide testwork include the following:

- The Productora mineralized material present a range of oxidation states and mineralogical compositions.
- The major oxide minerals present in the majority of samples are the slow leaching copper bearing silicates and chrysocolla.
- There is significant benefit in utilising seawater as when this is acidified it has the potential to allow for the leaching of secondary sulphides such as chalcocite and digenite, which are the main secondary sulphides present in the oxide/transition mineralized material types. However, the leaching kinetics of these secondary sulphides is slow and due to competing acid consumption, the leaching of these minerals is incomplete.
- Generally, the host rock presents an environment of reasonably high acid consumption, and a number of samples require leaching to be terminated due to excessive acid consumption.

- The techniques and analyses conducted are appropriate and the sequential analytical technique has provided a reasonable indication of mineralogy following confirmatory QEMScan analysis.
- The bottle roll tests have provided, in most cases, good guidance for conditions for column leaching and an indication of likely copper recovery and acid consumption characteristics.
- The 1m columns provide good guidance for data required for the “scale-up” and determination of the PDC.
- The stacking and hydrodynamic column testing confirm that the agglomerated mineralized material tested will support percolation heap leaching at the stack heights and application rates provided in the PDC. The tests also indicate that the mineralized material will have the necessary geotechnical stability to allow for multiple lift stacking of the heaps.

13.2.4 Further Testwork

Testwork recommended to be undertaken during the PFS includes the following:

- Additional metallurgical drilling/sampling of all areas, especially those deemed economically sensitive to mine scheduling.
- Additional copper solubility and acid consumption testwork (sequential analysis) at Productora to be able to directly estimate and inform the block model.
- Undertake additional bottle roll and 6/8 m column tests to add additional data for scale up, optimisation and to further understand spatial variability.

13.3 Copper Sulphide and Molybdenum

13.3.1 History of Testwork

13.3.1.1 Metallurgical Testwork Program (Ausenco, 2013)

During this programme, the following testwork was completed:

- Comminution calibration results: Four samples were sent to SGS for SMC and/or JK testing, as well as normal crushing and bond work index testwork.
- Initial flotation testwork: 14 samples were selected; four in a team selection between HCH and Ausenco, and the remaining 10 were chosen exclusively by HCH. Also, HCH and Ausenco agreed at that stage of the program on variability testwork which would be conducted in ALS Santiago and would cover comminution, first flotation stage and second flotation stage.
- No samples were selected or testwork performed on any oxide samples during this stage.

13.3.1.2 Sulphide Comminution Testwork (Mintrex, 2014-15)

Comminution testwork was performed on Productora flowsheet development (FD) and variability (V) samples at the ALS Metallurgy Santiago and Perth laboratories. Comminution testwork was conducted to determine the variability of comminution parameters throughout the mineralized material body and allow parameters for comminution circuit design to be derived. Tests conducted included the following:

- Unconfined compressive strength (UCS). UCS testing results indicate the strength of a rock in terms of resisting compressive forces prior to breakage
- Bond Crushing Work Index (CWi). CWi test results allow determination of crushing energy requirements
- Bond Rod Mill Work Index (RWi). RWi test results allow determination of power requirements for a rod milling grinding process
- Bond Ball Mill Work Index (BWi). BWi test results allow determination of power requirements for a ball milling grinding process
- Abrasion Index (Ai). This test is used to determine the abrasiveness of mineralized material
- JK Drop Weight tests (JKDWi). Determination of Drop Weight Index (DWi)
- SAG mill comminution (SMC) tests. JK analysis of SMC test results.

13.3.1.3 Copper Sulphide Flotation Testwork (Mintrex, 2014-2015)

A large program of flotation testwork was conducted on HCH's Productora and Alice deposits. Testwork was based on a standardised flowsheet and reagent scheme. The scheme used RTD2086 (Xanthate Ester supplied by Tall Bennett) at a natural pH (~pH 8) with two stages of cleaning and a 25 µm regrind. Seawater as received was preferred, as the use of lime in seawater can have negative effects on flotation performance.

A target copper grade for the final concentrate was 25% Cu. To achieve this, optimisation testwork was conducted on a number of samples to improve copper grade and recovery. Optimisation testwork included the following tests:

- Primary grind size
- Reagent dosage
- Flotation time
- Alternate reagents
- Diesel addition for increased molybdenum flotation
- Seawater vs. tap water.

When optimised conditions were tested, it was identified that samples from different zones of the deposit gave a different flotation response. Some samples were also later identified as containing transitional sulphide and oxide material (designated as

containing greater than 10% acid soluble copper). These samples gave reduced performance with the standardised reagent scheme.

13.3.1.4 Molybdenum Testwork (Mintrex, 2014-2015)

A specific molybdenum testwork program was conducted to determine if a molybdenum concentrate greater than 50% Mo could be produced. Molybdenum recoveries for each flotation sample were also determined and a relationship established. Molybdenum flotation was not fully optimised in either the copper circuit or the molybdenum circuit.

Flotation cleaner testwork was conducted to determine if molybdenum could be easily separated from the bulk copper/molybdenum concentrate and if a greater than 50% Mo concentrate could be obtained. The initial testwork was conducted on the FD1 composite and the larger bulk copper floats and multi-stage molybdenum cleaners were conducted on a specific sample (PRP0812) with a high molybdenum head grade (0.56%Mo). The PRP0812 was a reverse circulation (RC) chip sample which is not ideal for flotation process design testwork.

Table 13.23 summarises some of the laboratory comminution results for the Central Area samples and CCHEN South Area samples and compares these results with previous results. Table 13.24 summarises the Abrasion Index results of the Central Area samples, as the CCHEN South samples results for these parameters are not available. Some general comments include the following:

- It is evident that Axb values average around 40. These values are similar to the values used for the scoping study. However, there are one or two outliers such as the CCHEN HC material which is very hard, reporting an Axb value of 21
- Table 13.23 shows Bond Ball Mill Work Index (BWI) results. Values averaged about 22 to 23 kWh/t.

Table 13.23 Comminution tests – summarised results

Sample ID	Lab	SMC DWi (kWh/m ³)	A*b (JK test)	A*b (SMC test)	Bond Rod Mill Wi (kWh/t)	Bond Ball Mill Wi (kWh/t) Pi 150µm	Bond Ball Mill Wi (kWh/t) Pi 150µm	Bond Ball Mill Wi (kWh/t) Pi 150µm
Scoping Study (with sample) MS _{AU}	AMMTEC	6.43	41.4	--	26.4	23.4	23.4	--
Scoping Study (with sample) SDI	AMMTEC	6.57	40.6	--	25.4	21.4	--	--
Scoping Study (with sample) SDI	AMMTEC	4.51	57.6	--	24.1	21.4	--	--
Laboratory validation (with sample) MS _{CH}	AMINPRO	7.30	36.0	--	19.0	21.9	--	22.2

Sample ID	Lab	SMC DWi (kWh/m ³)	A*b (JK test)	A*b (SMC test)	Bond Rod Mill Wi (kWh/t)	Bond Ball Mill Wi (kWh/t) Pi 150µm	Bond Ball Mill Wi (kWh/t) Pi 150µm	Bond Ball Mill Wi (kWh/t) Pi 150µm
HC sample Central Area	SGS	6.86	40.9	38.9	19.3	20.2	--	--
LC sample Central Area	SGS	6.42	41.3	40.9	19.2	20.4	--	--
HC sample CCHEN South Area	SGS	12.09	21.0	21.0	21.0	25.8	--	--
LC sample CCHEN South Area	SGS	6.94	40.6	39.7	18.2	26.5	--	--

Table 13.24 Bond Abrasion Index – summarised results

Sample ID	Laboratory	Bond Abrasion Index, Ai
Scoping Study (with MS _{AU} sample)	AMMTEC	0.50
HC sample Central Area	SGS	0.79
LC sample Central Area	SGS	0.53
HC sample CCHEN South Area	SGS	0.60
LC sample CCHEN South Area	SGS	0.75

13.3.2 Results of Testwork Program

13.3.2.1 Copper Sulphide Comminution Testwork Program

13.3.2.1.1 Sulphide Comminution Testwork Results

Selection of the comminution testwork program was dependent on the samples available, especially for the comminution circuit development testwork program (FD-CH) and the variability (V-CH) program. For the 14 comminution circuit development samples (FD-CH) and 10 variability samples (V-1CH to 10CH), the quality, quantity and integrity of the core available was such that only SMC and Bond Work Index tests could be conducted on the core samples. For Habanero (V-10CH and V-11CH) and Alice (V-13CH, V-14CH and V-18CH), enough full core sample was available to also conduct some JKDWi (Drop Weight tests) in addition to SMC and Bond Work Index tests.

There were some full core sections available from the drillholes used to make up the FD-1 to FD-4 composite samples previously selected for the flotation testwork program. These full core sections were combined to make a “Crusher Composite 1” sample which was used to conduct an additional JKDWi test.

The planned testwork was designed to obtain the maximum information available from the specific core (diameter and volume). In almost all cases full or half core were available for use and only SMC and limited Bond Work index tests were possible on these. Where full core was available JK Drop Weight tests were also done. The aim of these tests was to obtain the maximum amount of information possible to model and

design any possible comminution circuit. The results for the testwork are depicted in Table 13.25 to Table 13.27.

Table 13.25 Bond Abrasion Index – Productora deposit samples

Comminution parameter	Average	Minimum value	Maximum value
CWi (kWh/t)	7.5	2.1	7.9
BWi (kWh/t)	18.5	14.8	23.4
RWi (kWh/t)	23.0	20.0	26.7
Ai	0.28	0.11	0.43
Axb	49.3	40.6	78.0
DWi (kWh/m ³)	7.5	4.6	9.6
UCS	51.6	14.5	111.8
SG (kg/m ³)	2.68	2.50	3.01

Table 13.26 Bond Abrasion Index – Alice deposit samples

Comminution parameter	Average	Minimum value	Maximum value
CWi (kWh/t)	6.6	2.4	12.4
BWi (kWh/t)	17.4	15.5	18.9
RWi (kWh/t)	20.0	19.6	20.6
Ai	0.27	0.20	0.33
Axb	36.0	31.3	41.1
DWi (kWh/m ³)	7.0	6.5	7.5
SG (kg/m ³)	2.69	2.66	2.70

Table 13.27 Comminution testwork results – all samples

Comminution parameter	Average	Minimum value	Maximum value
CWi (kWh/t)	7.4	2.1	12.4
BWi (kWh/t)	18.1	14.8	23.1
RWi (kWh/t)	22.6	19.6	26.7
Ai	0.27	0.11	0.43
Axb	48.0	31.3	78.0
DWi (kWh/m ³)	7.4	4.6	9.6
UCS	51.6	14.5	111.8
SG (kg/m ³)	2.65	2.07	3.01

The comminution testwork showed that the samples tested displayed medium to medium high competency and would require moderate to high grinding energies. The Abrasion index results indicated average abrasiveness, which will result in relatively moderate ball and liner consumptions. Alice material seems to be harder and tougher than the material from the main pit.

The comminution testwork results showed that there are probably three comminution circuit options viable namely:

- Primary crushing followed by SAG and ball milling with recycle crushing – Primary SABC (Option 1)

- Three-stage crushing followed by ball mill circuit – 3CBM (Option 2)
- Two-stage crushing, HPGR and ball mill circuit – 2C/HPGR/BM (Option 3).

13.3.2.2 Copper Sulphide Flotation Testwork Program

13.3.2.2.1 Introduction

Sulphide flotation on the Productora deposit has been conducted in previous testwork programs. These programs included optimisation of the reagent scheme and had identified the use of a Xanthate Ester (Tall Bennett RTD2086) as giving good copper recovery with selectivity against pyrite at natural pH when the floats are conducted in seawater. Xanthate (Sodium Ethyl Xanthate) and lime schemes had also been tested. This scheme performed well in tap water, however, when seawater was used the copper upgrade was not as good as with RTD2086. Due to availability and cost issues with using potable water, good performance in seawater was necessary.

One composite (FD-7) was identified as being of oxide mineralogy and was therefore not tested.

During the program of work, the pit model was updated and a number of composites from the Cayenne zone (FD-8 to FD-12 and V-3 to V-6) were forecast to be outside the proposed Productora pit. These composites were therefore not fully optimised with grade and recovery not modelled during the flotation testwork programme.

13.3.2.2.2 Grind size optimisation

Following completion of a series of rougher flotation grind recoveries on the FD and V samples in the testwork program, a preliminary economic analysis was completed to select the optimum grind size for the process plant. This then allowed the balance of the flotation testwork including locked cycles to be completed at the selected grind size. The procedure adopted for the analysis is outlined below.

- Rougher recoveries from testwork recorded over a range of grinds from 75µm to 180µm
- The rougher recoveries were selected at concentrate grades of 9-12% that had been shown could be upgraded by cleaning to the target concentrate grade of 25%
- A constant cleaner loss of 4% applied to all results
- All test results “equalised” to a constant grade of 0.51% Cu to match the assumed grade of the first 5 years of production. Equalisation was achieved by varying the recovery by +/-1% for every 0.1% Cu the tested head grade was higher or lower than the target 0.51%. (higher head grades had the recovery reduced and lower head grades vice versa)
- Baseline power operating costs were established using Bond Ball Mill Work index results from each sample and for each grind size using standard bond

formulae for ball mill power ($10 \cdot BW_i \cdot (P80_{\text{grind}})^{-0.5} \cdot 1000 \mu\text{m}^{-0.5}$) including pinion losses of 7.5%, using an input power cost of 10c/kWh

- Thickening costs varied for grind size estimated using power, labour, flocculants, maintenance materials etc.
- Ball mill liner consumption, factored off consumed kWh/t
- Grinding media consumption factored off consumed kWh/t
- Variable grinding capital based on the required MW installed and a constant \$0.7M/MW and an installation multiplier of 2.57 (estimated from previous projects)
- Variable thickening capital based on estimated thickener requirements.

Adopting 150µm as the base case, recoveries, capital costs and operating costs for each grind was then averaged across the 19 samples tested.

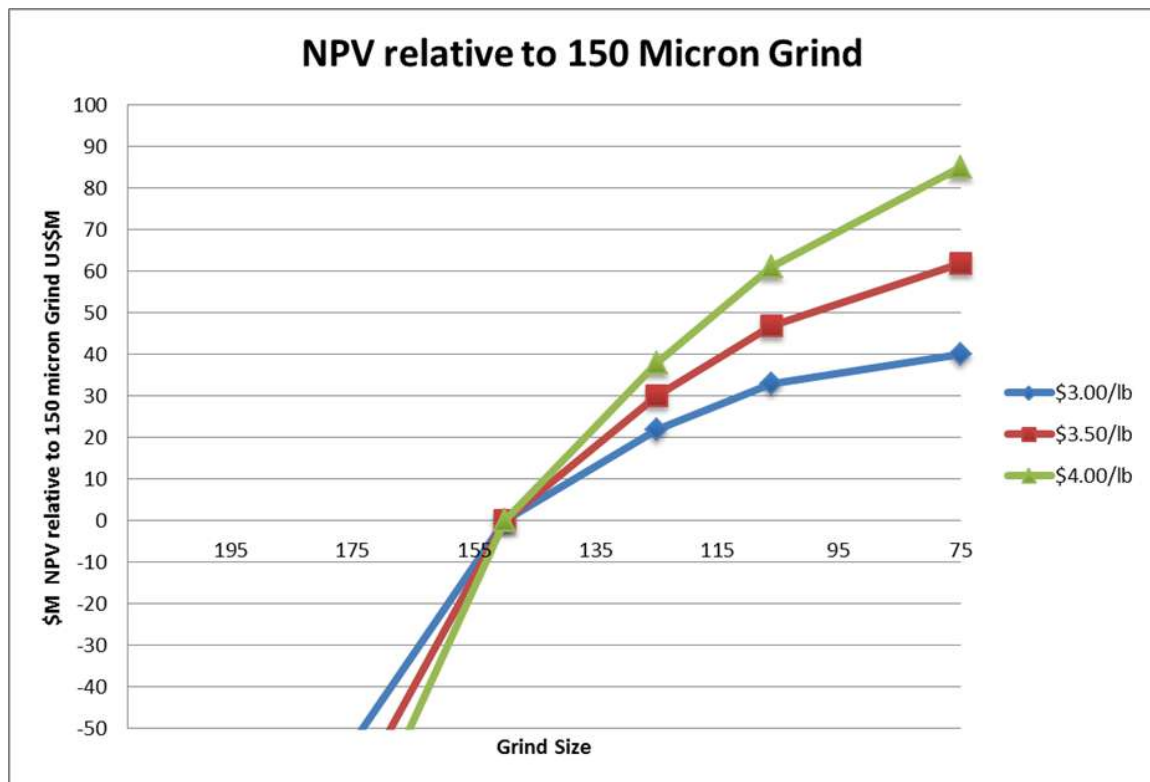


Figure 13.37 Grind optimisation analysis results

The grind size at 125 micron although not optimum was selected to provide a conservative result particularly at lower copper price environments, i.e. less than \$3.00/lb. The grind size optimisation should be updated prior to commencing any further testwork as part of a subsequent PFS. Copper price and power costs are a key driver of this variable.

Consideration has been given to the target primary grind size to be utilised for process and plant design purposes due to the manner in which laboratory data interpolate into

the practical plant operating situation. There is an inconsistency between laboratory and plant performance data in base metal (copper) operations due to the different effects that result from closed batch laboratory grinding mill and the open circuit configuration of a typical plant grinding circuit. This difference results in preferential grinding of the copper compared to the host rock. Therefore, a target metal recovery can be obtained at a coarser grind size in the plant than would have been anticipated from laboratory predictions.

13.3.2.2.3 Copper Sulphide Flotation Testwork

A standardised flowsheet and reagent scheme had been determined in previous programs and was used as the base for this testwork. The scheme used RTD2086 (Xanthate Ester supplied by Tall Bennett) at a natural pH (~pH 8) with two stages of cleaning and a 25µm regrind. The standardised scheme is presented in Table 13.28.

Table 13.28 Productora standardised flotation scheme

Operation	Conditioning time (minutes)	pH	RTD2086 (g/t)	MIBC (drops)	Float time (minutes)
Mill					
Cu Con 1	1	Nat pH	10	As required	1
Cu Con 2	1		5		2
Cu Con 3	1		5		3
Cu Con 4	1		5		7
Regrind - P80 25µm					
Cu Cleaner Con 1	1		5		1
Cu Cleaner Con 2					2
Cu Cleaner Con 3	1		5		3
Cu Cleaner Con 4					5
Cu Cleaner Scav Con	1		2		7
Cu Re-Cleaner Con 1	1		5		1
Cu Re-Cleaner Con 2					2
Cu Re-Cleaner Con 3					3
Cu Re-Cleaner Con 4					6

Optimisation testwork was conducted on a number of samples, though was mainly focused on the FD-1 composite sample. Primary grind size tests were conducted on all the Flotation Development, Habanero and Alice samples. For the majority of composites, initial optimisation and cleaner testwork was based on a primary grind size of $P_{80}=106\mu\text{m}$ (some composites were at $150\mu\text{m}$). Later in the testwork program, the plant target grind size was confirmed to be $P_{80}=150\mu\text{m}$. Based on historical industry analysis showing that typical plant milling and classifying circuits giving a finer sulphide P_{80} , to represent the plant sulphide grind size, the testwork primary grind size was set at $P_{80}=125\mu\text{m}$ for all Productora composites. All Productora pit composites had baseline rougher tests conducted at $P_{80}=125\mu\text{m}$ and all except FD1, FD14 and V2 had recleaners conducted at $P_{80}=125\mu\text{m}$. From these results and the six composites with locked cycles at $P_{80}=125\mu\text{m}$ (and one at $P_{80}=106\mu\text{m}$), head grade vs. final locked cycle recovery

results were able to be modelled and enable copper, molybdenum and gold recovery predictions (at $P_{80}=125\mu\text{m}$) at varying head grades.

Alice composites gave improved copper recoveries at coarser grind sizes and due to the intent to not blend, but campaign treat the Alice deposit, the grind size for Alice testwork was set at $P_{80}=180\mu\text{m}$.

Optimisation testwork included reagent dosage, alternate reagents, diesel addition for improved molybdenum recovery, water type (sea and tap) and flotation time. When optimised conditions were being tested on the remaining samples, it was identified that samples from different zones were giving different flotation performance. Some samples were also later identified as containing transitional sulphide and oxide material (designated as containing greater than 10% acid soluble copper). These samples gave reduced performance with the standardised scheme.

Due to performance and copper recovery variations, for modelling of the copper head grade vs. final copper recovery, samples were grouped based on location of samples, percentage acid soluble copper, flotation performance and alternate reagent schemes.

Grouping of the samples was as follows:

- Central (In Pit Fresh) – FD-1, FD-2, FD-6, FD-13, FD-14, V-2, V-7, V-8
- Habanero Lode (In Pit) – V-10, V-11, V-12
- >10% Acid Soluble Cu – FD-3, FD-4, FD-5, V-1, V-9
- Alice – V-13, V-14, V-18.

As noted, part-way through the program, composites from the Cayenne zone of the deposit (FD-8 to FD-12 and V-3 to V-6) were determined to be out of pit and were therefore not optimised and modelled. Results for these are included, though optimised recoveries at 25% Cu have not been determined.

13.3.2.2.4 Productora – Central (In Pit Fresh samples) Flotation Testwork Results

The Central part of Productora mineralized material represents the largest tonnage of copper mineralisation and along with Habanero and CCHEN South, forms the main pit. The Central zone represents approximately 55% of the main pit (~38% CCHEN South and ~7% Habanero) and was therefore the main focus for testwork optimisation. Samples from the Central zone include FD-1, FD-2, FD-5, FD-6, FD-13, FD-14, V-2, V-7 and V-8.

Sample V-10 borders Central and Habanero, but as it mainly extends into the Habanero zone and due to the flotation performance being similar to other Habanero composites, it has been grouped with the Habanero results.

Sample FD-5 contains a high percentage of transitional sulphides (approximately 55% by mass) and has been grouped with other composites that assayed greater than 10% acid soluble copper (samples containing transitional sulphides and oxides, aside from FD-5, these are all from the CCHEN South zone).

13.3.2.2.5 Primary Grind Series Testwork

For the Central zone, primary grind sizes were tested on each of the Flotation Development (FD) samples. Grind sizes tested ranged from $P_{80}=75\mu\text{m}$ to $212\mu\text{m}$. Grind size vs. overall copper and molybdenum rougher recovery are shown in Figure 13.38 and Figure 13.39.

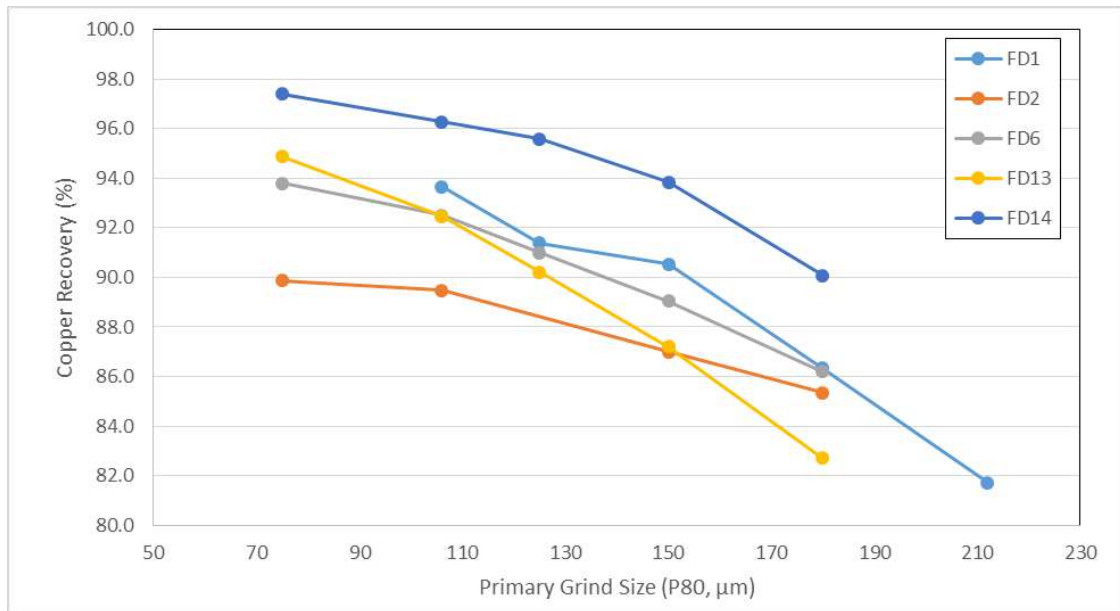


Figure 13.38 Productora – Central – Primary grind size copper results

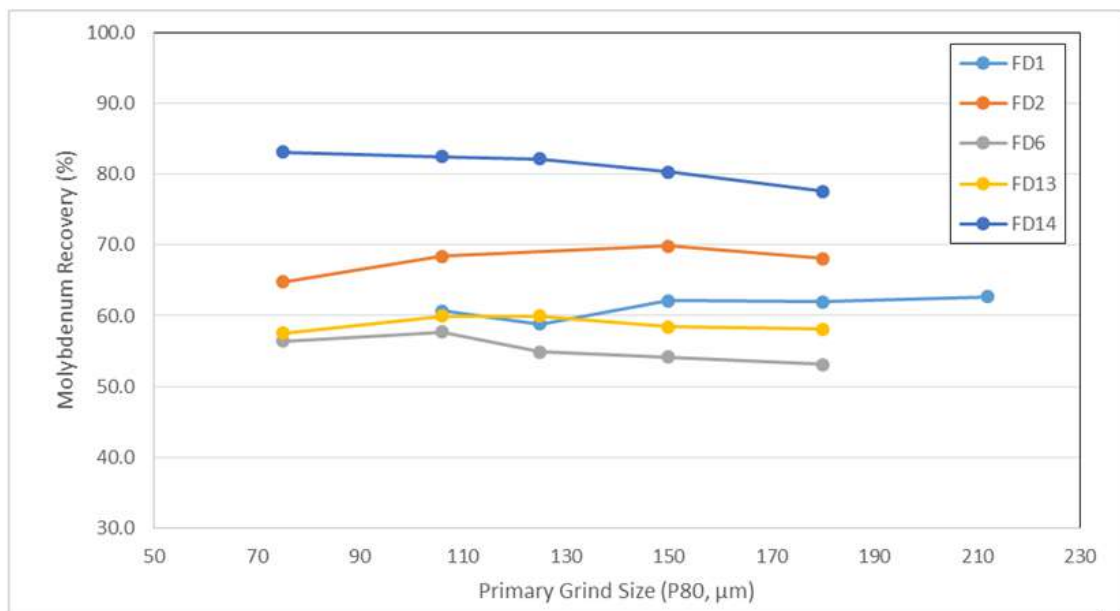


Figure 13.39 Productora – Central – Primary grind size molybdenum results

Overall copper rougher recoveries varied from 82.7% to 90.1% at $180\mu\text{m}$ (FD-13 and FD-14, respectively) and 89.5% to 96.3% at $106\mu\text{m}$ (FD-2 and FD-14, respectively). Overall copper rougher grade and recovery are shown in Table 13.29. Between $180\mu\text{m}$ and $106\mu\text{m}$, copper rougher recovery varied from 4.1% (FD-2) to 9.8% (FD-13).

However, for molybdenum the recovery did not increase significantly with reduced grind size. Based on the grind series results, subsequent cleaner testwork was conducted at $P_{80}=106\mu\text{m}$ for FD-1, FD-13 and FD-14. FD-2 and FD-6 cleaner tests were conducted at $150\mu\text{m}$.

Table 13.29 Productora – Central – Primary grind size copper rougher results

Sample	Overall copper rougher results – grind size (P_{80} , μm)												
	Head grade (%)	212		180		150		125		106		75	
		%	% dist.	%	% dist.	%	% dist.	%	% dist.	%	% dist.	%	% dist.
FD-1	0.44	9.90	81.7	11.0	86.3	10.6	90.5	9.29	91.4	11.2	93.7	-	-
FD-2	0.59	-	-	11.2	85.3	12.2	87.0	-	-	9.41	89.5	12.1	89.9
FD-6	0.22	-	-	6.23	86.2	6.24	89.0	6.26	91.0	7.28	92.5	7.39	93.8
FD-13	0.89	-	-	15.7	82.7	16.5	87.2	14.4	90.2	17.1	92.5	17.8	94.9
FD-14	0.85	-	-	9.89	90.1	10.5	93.8	10.5	95.6	11.2	96.3	10.6	97.4
V-2	0.26	-	-	-	-	-	-	-	-	8.90	89.8	8.26*	91.4*
V-7	0.34	-	-	-	-	-	-	8.00	91.9	-	-	-	-
V-8	0.70	-	-	-	-	-	-	12.1	96.4	-	-	-	-

* V-2 – $90\mu\text{m}$ grind

Later in the program, the primary grind size was revised to $P_{80}=125\mu\text{m}$ for all Productora composites. This was to represent a plant grind of $P_{80}=150\mu\text{m}$. Figure 13.40 shows copper rougher recovery at $P_{80}=125\mu\text{m}$ vs. the copper head grade for all the Central (In Pit Fresh) samples. Copper recoveries showed a good correlation between head grade and rougher recovery (note that data is based on optimised conditions for each sample). When recoveries at a rougher concentrate grade of 10% Cu are used, the R^2 improves to 0.86.

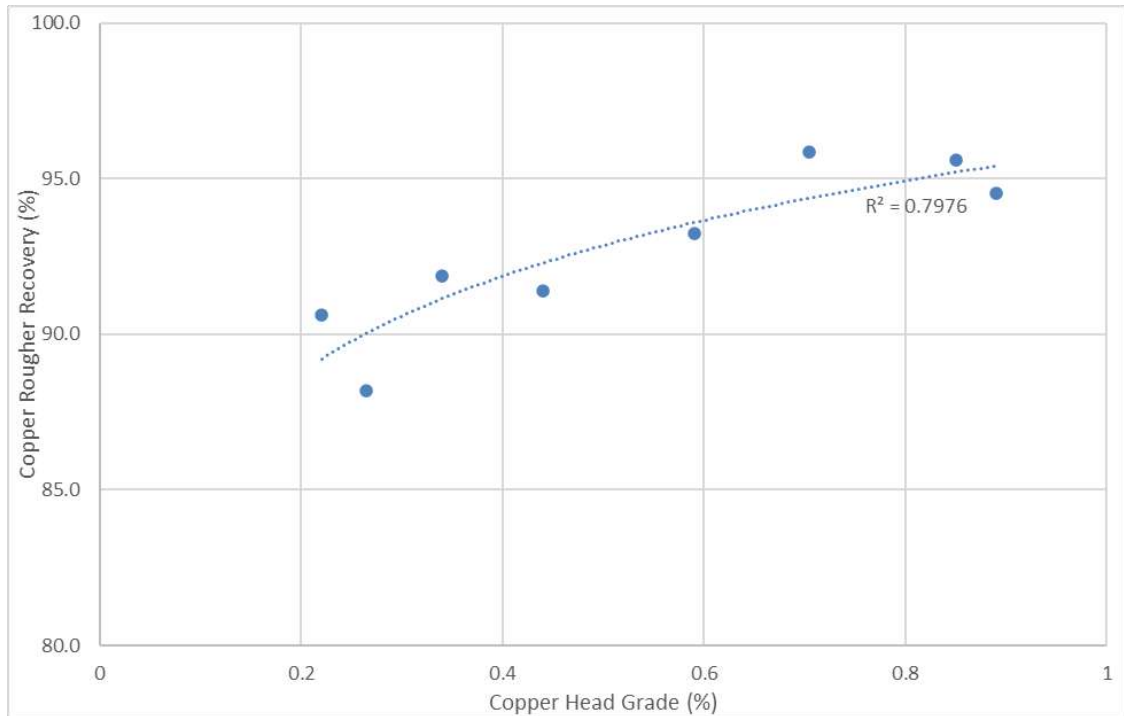


Figure 13.40 Productora – Central – head grade vs. copper rougher recovery

13.3.2.2.6 Optimisation Testwork – FD-1

Numerous tests were conducted to determine if the standardised RTD2086 scheme could be optimised. Tests included changes to collector dosage, alternate collectors, reduced flotation time and the use of diesel to improve molybdenum recovery.

The majority of optimisation testwork was conducted on the FD-1 composite sample. For FD-1, tests included increasing and decreasing the RTD2086 dosage, as well as changes to the stage dosing, changes in collector type, the addition of diesel to the primary grinding mill to improve molybdenum recovery and coarser and finer regrind sizes.

For changes in dosage of RTD2086, reducing the dosage from the 25 g/t in the rougher, tends to reduce the overall copper and molybdenum recovery. Increasing the dosage to up to 45 g/t gave a small increase in copper recovery and a significant increase in molybdenum recovery. However, the increased dosage also increased the pyrite recovery and subsequently reduced the copper grade in both the rougher and cleaner concentrates. Cleaner concentrate grades failed to achieve the desired 25% Cu. Altering the stage dosage to a single lower dose of two dosage points instead of the four used tended to show a decrease to the copper grade and recovery curve. The results were, however, not absolute and some decreases were seen with exactly the same dosage. Further testwork should be conducted to define if there is an optimal dosage and staging of reagent to achieve 25% Cu in the final concentrate which also maximises molybdenum recovery.

Collectors tested on the FD-1 composite sample included:

- SEX – Sodium Ethyl Xanthate
- A3894 – Cytec - Isopropyl Ethyl Thionocarbamate
- A3302 – Cytec - Xanthate Ester
- C4403 – SNF Flomin – Xanthate Ester/Hydrocarbon blend
- C4410 – SNF Flomin – Xanthate Ester
- RTD162 – Tall Bennett
- RTD2116 – Tall Bennett
- RTD2209 – Tall Bennett.

None of the alternate collectors gave improvement to the copper grade and recovery curve. SEX and A3894 increased copper rougher recovery, though these reagents require a depressant for pyrite (lime or SMBS), as sulphur recoveries increased by up to 70% (approximately 25% for RTD2086 up to 95%) in the roughers with no depressant. Both SEX and A3894 also gave a significant decrease in molybdenum recovery, though Au recoveries tend to increase. C4403 was the only collector that improved molybdenum recoveries, though it did show a small decrease in mass and sulphur recovery and a subsequent small reduction in copper recovery. The increase in molybdenum and reduced sulphur recovery is due to the hydrocarbon content (e.g., kerosene, diesel). Results though, were better than adding diesel into the mill in combination with RTD2086. Further work should be conducted with C4403 to determine if it can be beneficial for all fresh mineralized material within the Productora and Alice deposits.

To help improve molybdenum recovery, diesel was added to the primary grinding mill for some tests. When using SEX or A3894, the diesel showed significant improvements in molybdenum recovery without detriment to the copper recovery. When used with RTD2086, there did not appear to be great benefit and in some tests, gave large decreases in sulphur recovery and loss of copper recovery. Along with C4403, further work should be conducted to determine if diesel will be beneficial to the copper and molybdenum flotation.

The standardised regrind size prior to cleaner flotation had been set at $P_{80}=25\mu\text{m}$. Tests were conducted with coarser ($37\mu\text{m}$ to $45\mu\text{m}$) and finer ($15\mu\text{m}$) regrinds. Increasing regrind to approximately $P_{80}=40\mu\text{m}$ was still able to achieve the desired 25% Cu, though copper recoveries decreased by 1.5% (at 25% Cu). Molybdenum recoveries also decreased by approximately 5%, though gold recoveries improved marginally. Decreasing the regrind size to $P_{80}=15\mu\text{m}$ gave similar high copper grades to $25\mu\text{m}$, though copper and molybdenum kinetics decreased and reduced overall recoveries to the final concentrate.

Three stages of cleaning were also investigated on the FD-1 composite sample. The additional stage of cleaning gave little benefit, with grades only improving slightly. With no collector, copper kinetics in the third stage of cleaning of the batch open cleaner test was slow and there was a high copper recovery to the third cleaner tail. The locked

cycle did show this copper would be recovered to final concentrate with the recirculating products and water.

13.3.2.2.7 Optimisation Testwork – FD-2

For the FD-2 composite samples, optimisation tests included increasing the RTD2086 dosage and using the A3894/SMBS (Sodium Metabisulphite) reagent scheme.

Increasing RTD2086 dosage was conducted to increase copper rougher recovery and improve cleaner kinetics, as a number of the composites showed slow copper kinetics and high losses to the recleaner tailing (later testwork indicated that this was potentially due to overgrinding or inefficient grinding in the regrind). Like other composites, increasing the RTD2086 dosage gave a small increase in copper recovery and a large increase in molybdenum recovery. Though, the increased collector also increased pyrite recovery and in combination with higher collector in the cleaner, copper grade did not upgrade to the desired 25% Cu.

The use of A3894 on the FD-1 composite sample did not show any benefit. Though, on the FD-2 composite sample, the A3894/SMBS scheme gave a significant improvement in copper recovery while still maintaining greater than 25% Cu. In the rougher circuit, A3894 increased copper recovery by 3.5% and sulphur recoveries by over 50%. However, molybdenum recoveries decreased by 6.7%. Even though sulphur recoveries were significantly higher, copper grade was only reduced marginally (10% to 7%), as mass only increased from 5.4% to 7.8%. The biggest difference with the A3894/SMBS scheme was seen in the cleaner circuit. Copper recoveries increased by 10% (at 25% Cu) and in the locked cycle test, recovery was 6.7% higher at similar grade (A3894/SMBS test was also at a coarser grind size. 125µm vs. 106µm). The improvement in the batch cleaner test is shown in Figure 13.41. The A3894/SMBS scheme also showed greater rougher to cleaner upgrade (approximately three times) compared to RTD2086 (approximately 2.1 times) and allowed for a lower rougher copper grade and increased recovery.

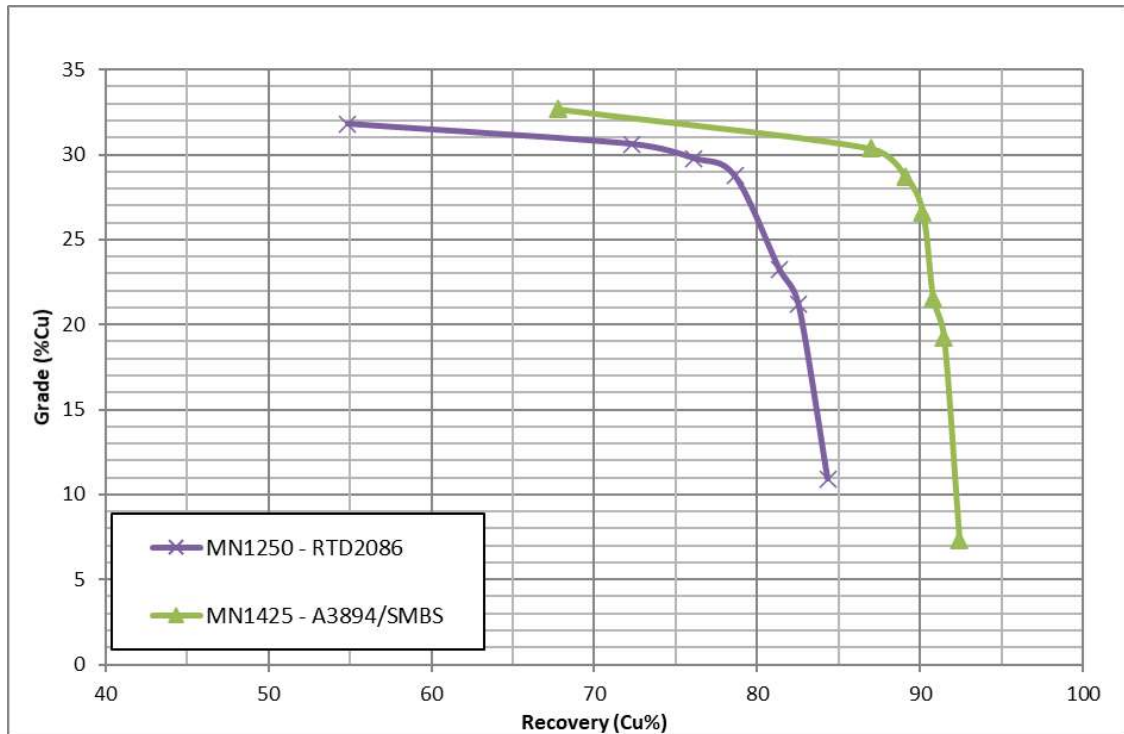


Figure 13.41 Productora – Central – FD2 RTD2086 vs. A3894/SMBS copper grade recovery

The FD-2 composite sample contains 37% transitional sulphides by weight. The improvement is due to the improved recovery of secondary copper minerals with a thionocarbamate (A3894). Xanthate esters (RTD2086) tend to be highly selective against pyrite and can also tend to have reduced selectivity when secondary copper minerals are present.

13.3.2.2.8 Optimisation Testwork – FD-6

The FD-6 sample had the lowest head grade (0.22% Cu) for all the Central samples and has the third highest sulphur to copper ratio (9.2:1) out of all the tested samples (V-12 has highest at 19.7:1 with a very low head grade of 0.12% Cu and V-1 at 11.8:1, also with a low head grade of 0.18% Cu. V-1 was also identified as transitional sulphide sample). As a result, copper selectivity was reduced with increased levels of both pyrite and non-sulphide gangue and made achieving greater than 25% copper with the standard scheme difficult.

To improve copper selectivity, tests were conducted with both a decrease in collector dosage and a decrease in float time. Flotation scrape rate was also reduced from six seconds to 10 seconds during the cleaner stages. This was to reduce water recovery and entrained non-sulphide gangue (especially mica, which represent 26.6% of the feed in FD-6 and as muscovite, can be easily entrained). Table 13.30 shows the FD-6 and standard flotation scheme. Reduction in both collector dosage and flotation time resulted in only a small decrease in copper recovery in the rougher (approximately 3%). Kinetics in the cleaner circuit was reduced and high levels of copper reported to the recleaner tail, though in the locked cycle test, essentially all copper that had reported to the cleaner

scavenger concentrate and recleaner tail reported to the final concentrate. The reduction in collector, flotation time and scrape rate resulted in a 28% Cu concentrate (85.1% at 28.1% Cu) with just two stages of cleaning from a 0.22% Cu head grade.

Table 13.30 Productora – Central – FD-6 flotation scheme

Operation cycle 4	Standard flotation scheme			FD-6 flotation scheme		
	RTD2086 (g/t)	Scrape rate (seconds)	Float time (minutes)	RTD2086 (g/t)	Scrape rate (seconds)	Float time (minutes)
Cu Con 1	10	6	1	10	6	1
Cu Con 2	5	6	2	1	6	2
Cu Con 3	5	6	3		6	5
Cu Con 4	5	6	7			
Regrind						
1st Cleaner Con 1	5	6	1	5	6	1
1st Cleaner Con 2		6	2		6	2
1st Cleaner Con 3	5	6	3		10	4
1st Cleaner Con 4		6	5			
1st Cleaner Scav Con	2	6	7	3	6	6
2nd Cleaner Con 1	5	6	1	2	10	1
2nd Cleaner Con 2		6	2		10	2
2nd Cleaner Con 3		6	3		10	5
2nd Cleaner Con 4		6	6			

Other optimisation tests were also conducted on the FD-6 sample. These included increased collector to improve copper kinetics and the use of alternate reagents. Increasing collector dosage improved copper and molybdenum rougher recovery, however, higher levels of pyrite floated through the cleaner and resulted in a low copper grade.

Alternate reagents used included replacing RTD2086 with C4403 and A3894 with SMBS in the cleaners. The use of C4403, gave similar copper results to RTD2086, though molybdenum recoveries increased by over 5%. The test conducted achieved over 25% Cu in recleaner Con 1, though the overall recleaner was only 21.7% Cu. Further optimisation with C4403 and reduction in time and scrape rate should be able to improve the copper grade without a high loss of copper recovery. C4403 should also be able to improve the molybdenum recovery over the low dose RTD2086.

A single test was conducted with the A3894/SMBS scheme as used in the composites containing transitional material. Copper rougher recoveries were increased by approximately 4%, though rougher grade was low (2.9% Cu). The low rougher copper grade made it difficult to upgrade the copper to achieve a greater than 25% Cu concentrate. Though, the copper grade recovery curve was better than for RTD2086 and with further optimisation, could give greater than 25% Cu at a high recovery. The additional cost of the SMBS, may make this scheme not a viable option, though further work (including with the addition of diesel to improve molybdenum) should be conducted

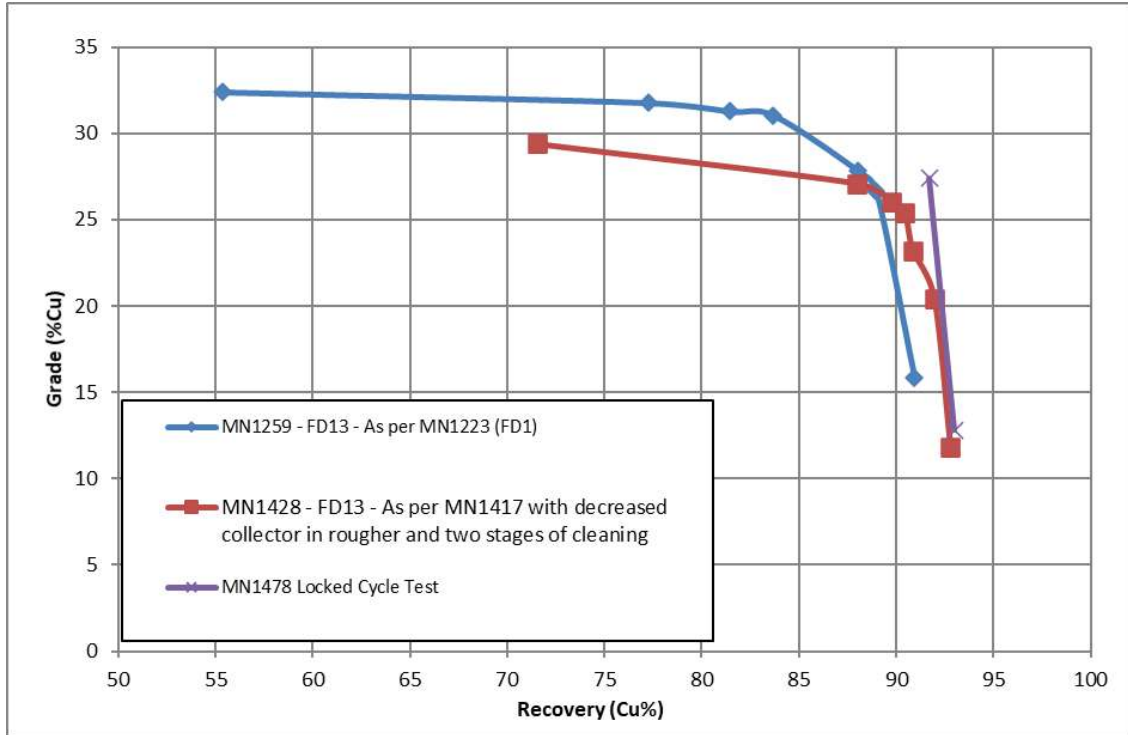


Figure 13.43 Productora – Central – FD-13 copper grade recovery curve

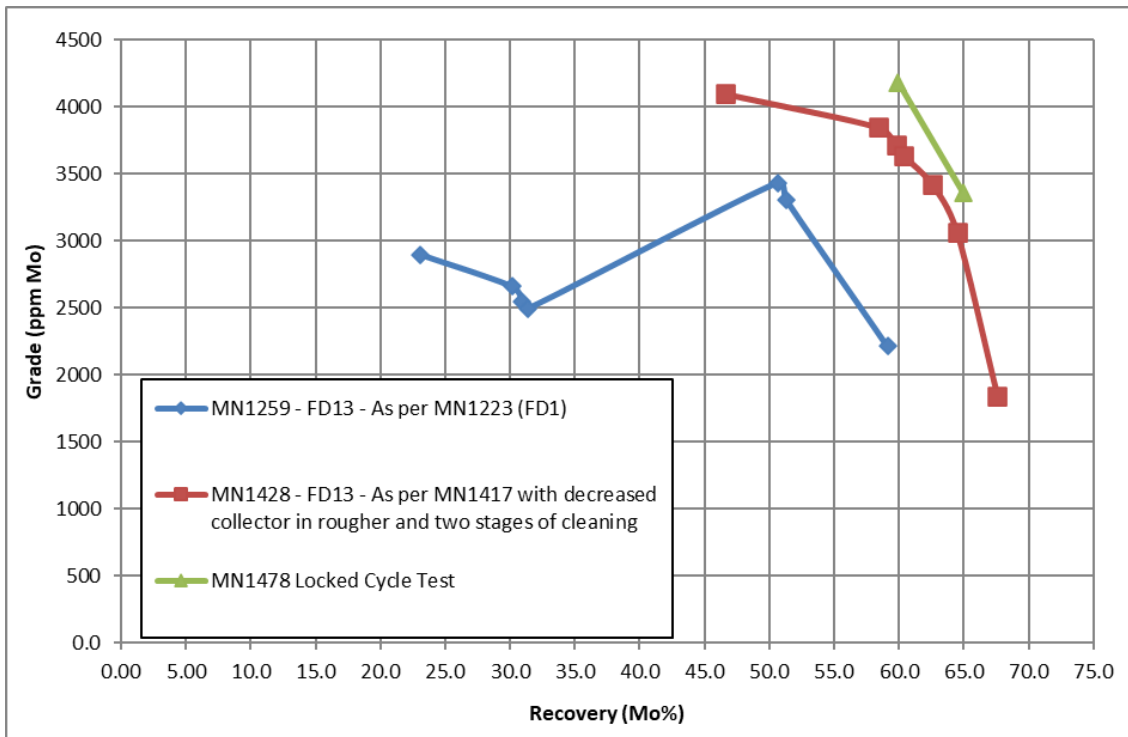


Figure 13.44 Productora – Central – FD-13 molybdenum grade recovery curve

13.3.2.2.10 Quality of Water Testwork

All the Productora flotation testwork was conducted using seawater. This is due to insufficient availability of potable water at the Productora site. Supply of potable water

would require producing large volumes of the water from a reverse osmosis (RO) plant. The cost to install and operate would be high and a significant increase in copper recovery would be needed to offset this cost.

Rougher testwork using Perth tap water was performed on FD-1 sample with both RTD2086 and Sodium Ethyl Xanthate (SEX) to compare with RTD2086 in seawater. For the RTD2086 scheme, tap water increased the copper grade and recovery slightly (91.6% at 8.2%Cu vs 90.8% at 7.5% Cu) and also the molybdenum and sulphur grade and recovery. Using SEX in tap water, mass pull increased from 4.8% to 6.6% and copper recovery increased by 1.2% to 92.8%, though copper grade decreased to 5.9% Cu. Molybdenum recovery decreased by 2%, however, sulphur recovery increased 62.6% to 94.7%.

Due to the small increase in copper rougher recovery with RTD2086, further cleaning tests were not performed. Cleaner tests were also not conducted with SEX, as a change in reagent scheme back to a xanthate (previous testwork went away from xanthate) was not desired. However, in the next phase of testwork, it is suggested to conduct further cleaner testwork with SEX to determine if lime will be more successful in potable water and give comparable or improved copper and molybdenum results to RTD2086. Xanthates though are less effective molybdenum collectors than the xanthate esters (RTD2086) and diesel may also be required if the SEX/Lime scheme is used.

13.3.2.2.11 Cleaner and Locked Cycle Testwork

As part of the testwork program, both single and two-stage cleaner floats were conducted on most of the composites and three stage cleaning was also conducted on the FD-1 composite sample. In general, the majority of the tests were conducted using the standard RTD2086 scheme at $P_{80}=125\mu\text{m}$ and optimisation for each composite was not conducted for the first stage of cleaning. As described in previous sections, some composites had optimisation on the rougher and recleaner tests.

For the final cleaner results for the Central (Fresh In Pit) samples, the standard RTD2086 scheme was used for FD-1, FD-14, V-2, V-7 and V-8 samples. Reduced RTD2086, float time and scrape rate was used for the FD-6 sample, increased RTD2086 was used for FD-13 and the A3894/SMBS scheme was used for the FD-2 composite sample. Locked cycle tests were conducted on all samples except FD-14, V2- and V-8, with conditions as indicated above.

For each of the samples, locked cycle copper recovery at 25% Cu was determined. Molybdenum and gold recoveries were also determined at a 25% Cu concentrate grade. Final results for copper, molybdenum and gold are shown in Table 13.31, Table 13.32 and Table 13.33.

Locked cycle results at 25% Cu were determined either from cleaner grade recovery curves or for tests without a locked cycle, estimated based on losses to cleaner scavenger tail in the open circuit cleaner tests and the expected recovery of copper reporting to the recleaner tail and cleaner scavenger concentrate.

Table 13.31 Productora – Central – rougher, cleaner and locked cycle copper results

Sample	Overall copper results (P80=125µm)										
	Head grade (%)	Rougher		Recleaner		Recleaner @ 25%Cu		Locked cycle*		Locked cycle @ 25%Cu	
		% Cu	% dist.	% Cu	% dist.	% Cu	% dist.	% Cu	% dist.	% Cu	% dist.
FD-1	0.44	9.3	91.4	28.0	78.0	25.0	82.0	28.2	88.8	25.0	87.5
FD-2	0.59	7.2	93.2	26.6	90.2	25.0	90.5	27.2	91.0	25.0	91.0
FD-6	0.22	10.2	90.6	29.7	71.5	25.0	77.0	28.1	85.1	25.0	86.0
FD-13	0.89	11.6	94.5	25.4	90.4	25.0	90.5	27.4	91.7	25.0	92.0
FD-14	0.85	10.5	95.6	25.6	89.3	25.0	89.5			25.0	92.0
V-2	0.26	9.0	88.2	26.9	78.7	25.0	80.5			25.0	84.7
V-7	0.34	8.0	91.9	25.1	90.0	25.0	90.0	29.7	87.5	25.0	88.5
V-8	0.70	10.1	95.9	26.5	92.3	25.0	93.0			25.0	93.5

* FD-1 locked cycle at 125µm primary grind

Table 13.32 Productora – Central – rougher, cleaner and locked cycle molybdenum results

Sample	Overall molybdenum results (P80=125µm)										
	Head grade (ppm)	Rougher		Recleaner		Recleaner @ 25%Cu		Locked cycle*		Locked cycle @ 25%Cu	
		% Mo	% dist.	% Mo	% dist.	% Mo	% dist.	% Mo	% dist.	% Mo	% dist.
FD-1	160	0.31	58.8	0.48	24.4	0.75	46.6	0.74	42.9	0.76	46.6
FD-2	180	0.23	61.2	0.79	55.5	0.73	56.0	0.89	58.8	0.83	58.8
FD-6	140	0.79	69.2	1.13	28.8	1.20	40.0	1.34	46.7	1.34	48.0
FD-13	120	0.18	67.6	0.36	60.4	0.36	60.4	0.42	59.9	0.42	59.9
FD-14	440	0.57	82.4	1.26	69.7	1.26	69.7			1.26	75.4
V-2	40	0.14	42.3	0.32	33.2	0.37	26.2			0.37	35.3
V-7	40	0.80	35.2	0.29	42.5	0.29	42.5	0.28	29.4	0.28	30.0
V-8	160	0.24	63.5	0.56	54.7	0.52	56.0			0.52	57.0

* FD-1 locked cycle at 125µm primary grind

Table 13.33 Productora – Central – rougher, cleaner and locked cycle gold results

Sample	Overall gold results (P80=125µm)										
	Head grade (ppm)	Rougher		Recleaner		Recleaner @ 25%Cu		Locked cycle*		Locked cycle @ 25%Cu	
		ppm Au	% dist.	ppm Au	% dist.	ppm Au	% dist.	ppm Au	% dist.	ppm Au	% dist.
FD-1	0.17	1.9	67.0	3.9	49.7	3.5	52.0	3.9	58.4	3.5	58.4
FD-2	0.17	1.3	71.7	4.3	62.6	4.3	62.6	5.3	62.2	5.3	62.2
FD-6	0.12	1.5	33.1	3.7	20.6	3.6	23.0	4.8	57.1	4.8	55.0
FD-13	0.18	2.0	77.3	4.0	69.6	4.0	69.6	5.2	72.7	5.2	72.7
FD-14	0.21	2.5	80.5	5.5	88.2	5.5	88.2			5.5	72.5
V-2	0.10	1.4	53.6	3.3	44.4	4.0	36.7			4.0	45.6
V-7	0.10	0.9	52.7	2.9	33.3			4.2	56.9	4.2	57.0
V-8	0.17	1.4	71.5	3.2	58.0	3.0	58.5			3.0	58.7

* FD-1 locked cycle at 125µm primary grind

From the locked cycle results, head grade vs. cleaner recovery was graphed and a relationship was determined for copper, molybdenum and gold. For copper, the head grade vs recovery is shown in Figure 13.45. The results at 25% Cu show a very good correlation ($R^2=0.89$) and from this, a line of best fit with a derived formula of “ $y=5.3675\ln(x)+92.903$ ” determined. Above 0.7% Cu head grade, the recovery looks to have reach a maximum of approximately 92%. This maximum is shown in Figure 13.45. Recovery for below 0.2% Cu is not calculated, as there is no data from the Central pit below 0.22% Cu. The only composites below 0.22% are from Habanero (V-12 – 0.12% Cu) and CCHEN South (V-1 – 0.18% Cu) and both of these do not follow the Central trend (V-1 is a transitional sulphide).

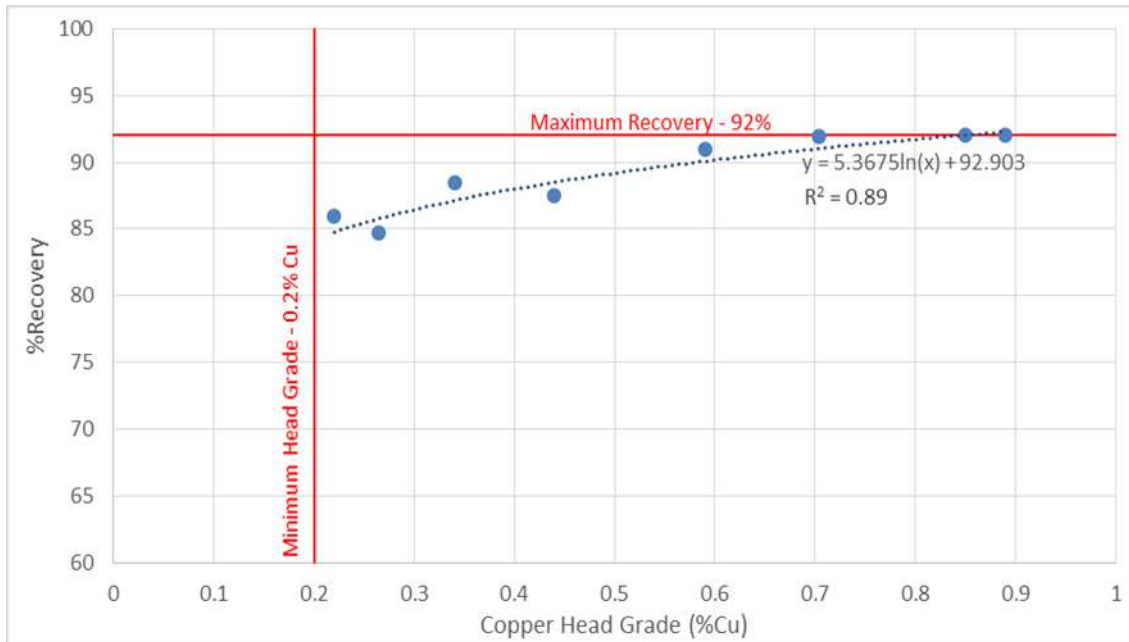


Figure 13.45 Productora – Central (In Pit Fresh) copper head grade vs. recovery

For gold, the gold head grade vs final concentrate recovery (for a 25%Cu concentrate) had a lower correlation than copper ($R^2 = 0.72$), though the trend was still good and can be seen in Figure 13.46. The formula derived for the line of best fit was “ $y = 22.82\ln(x) = 104.58$ ”. Gold head grades are low for all composites and the highest head grade was 0.21 ppm for FD-14. A maximum recovery has been set at 80% (based on formula this would be approximately a 0.35 ppm head grade), though further flotation tests would need to be conducted on samples with higher head grades to determine potential recoveries at the higher head grade levels.

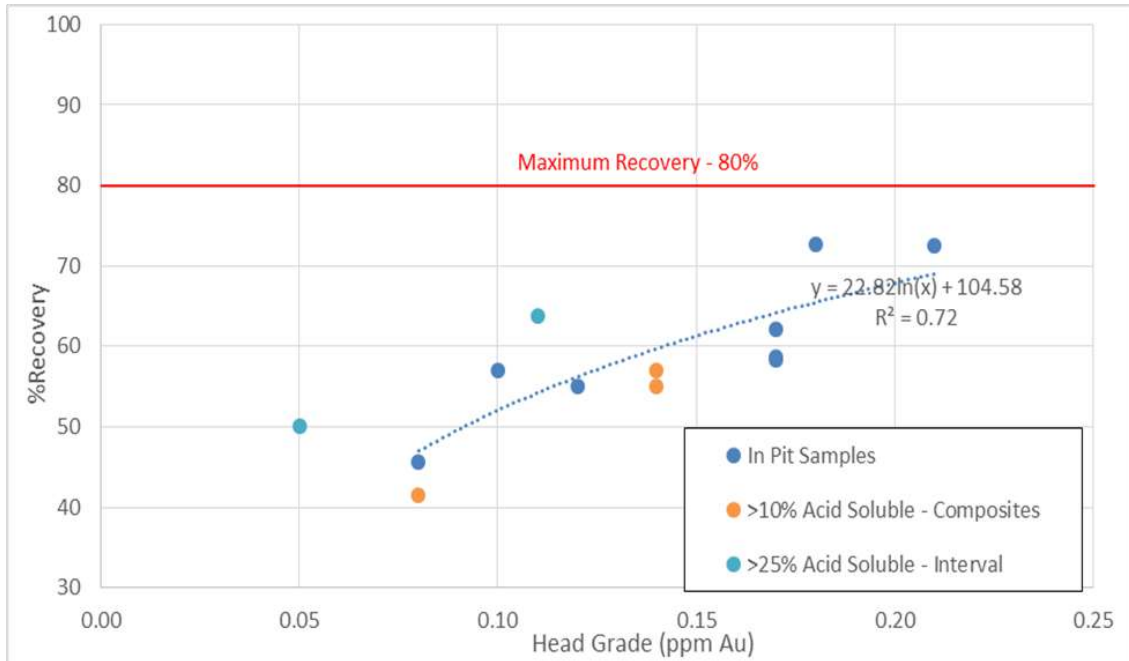


Figure 13.46 Productora – Central (In Pit Fresh) gold head grade vs. recovery

13.3.2.2.12 Productora - >10% Acid Soluble Copper – Flotation Testwork Results

During the testwork program, it was noted that a number of samples were giving a lower copper recovery performance. Initially, two of the samples were identified as containing high levels of transitional sulphides (FD-5 and V-1). With further testwork, additional geological and mineralogical data and review of acid soluble copper levels, other samples (FD-3, FD-4 and V-9) were determined to be containing transitional sulphides and some transitional oxides (in FD-4). These samples were also noted as having greater than 10% acid soluble copper in the feed. All of these samples, except FD-5, originated from the CCHEN South zone.

Acid soluble copper assays (5% H₂SO₄) generally indicate the presence of oxide copper minerals. Primary and secondary copper minerals normally have low solubility, though in the Productora mineralized material, secondary copper minerals have a higher level of acid solubility and these assays are not giving a good indication of the copper minerals present.

Mineralogical analysis shows that the higher acid soluble copper in these samples is mainly due to secondary copper minerals. Copper contained within secondary copper mineral and as intergrowth ranged from 14% in FD-3 (10% acid soluble Cu) to 50% for V-1 (25% acid soluble copper). Sample V-9 had a high acid soluble assay (32%) and visually, the flotation concentrate looked like chalcocite and would be predicted to have a high secondary copper content like V-1. The distribution of copper minerals can be seen in Table 13.34.

Table 13.34 Productora – >10% acid soluble copper (transitional containing) samples – copper mineral distribution

Mineral group	FD-3	FD-4	FD-5	V-1
Chalcopyrite	86%	81%	54%	50%
Chalcocite group	7%	9%	32%	34%
Bornite	4%	4%	4%	4%
Other Cu including intergrowths	3%	6%	9%	11%
Secondary and intergrowth Cu	14%	19%	46%	50%
Acid soluble copper	10%	16%	26%	25%

Due to the poor performance and the presence of secondary copper minerals, an alternate reagent scheme was determined for the high acid soluble/transitional sulphide samples. Xanthate esters are very selective for chalcopyrite against pyrite, though can also not always work well for secondary copper minerals. Based on this, an alternative reagent scheme with a thionocarbamate (A3894) collector and SMBS (sodium metabisulphite) for pyrite depression was used. As was seen for the FD-2 composite sample, this reagent scheme increased copper recoveries (over 10% at 25% Cu for some samples) and gave very good rougher to cleaner upgrades. For FD-5 and V-1, a significant reduction in collector and float time enabled these samples to achieve greater than 25% copper. Figure 13.47 shows the difference in performance for the standard scheme using RTD2086 and the revised scheme with A3894 and SMBS for FD-3 and FD-4.

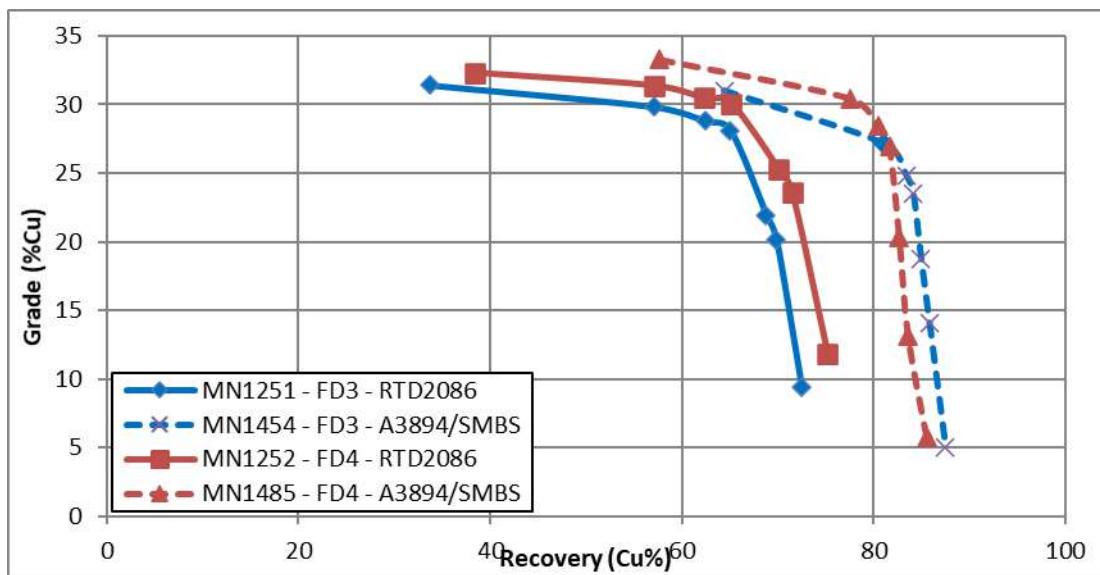


Figure 13.47 Productora – FD-3 and FD-4 copper grade recovery

Though the A3894/SMBS scheme gave improved copper results, the thionocarbamates (A3894) do not recover molybdenum as well as the xanthate esters (RDT2086). To improve molybdenum recovery, diesel was added to the primary mill. The addition of diesel gave variable results (due to decreasing sulphur/pyrite recovery), though in general gave significant improvements in molybdenum recovery when used with A3894,

with results comparable to RTD2086. Figure 13.48 shows the difference with diesel on the FD-5 sample with A3894/SMBS scheme.

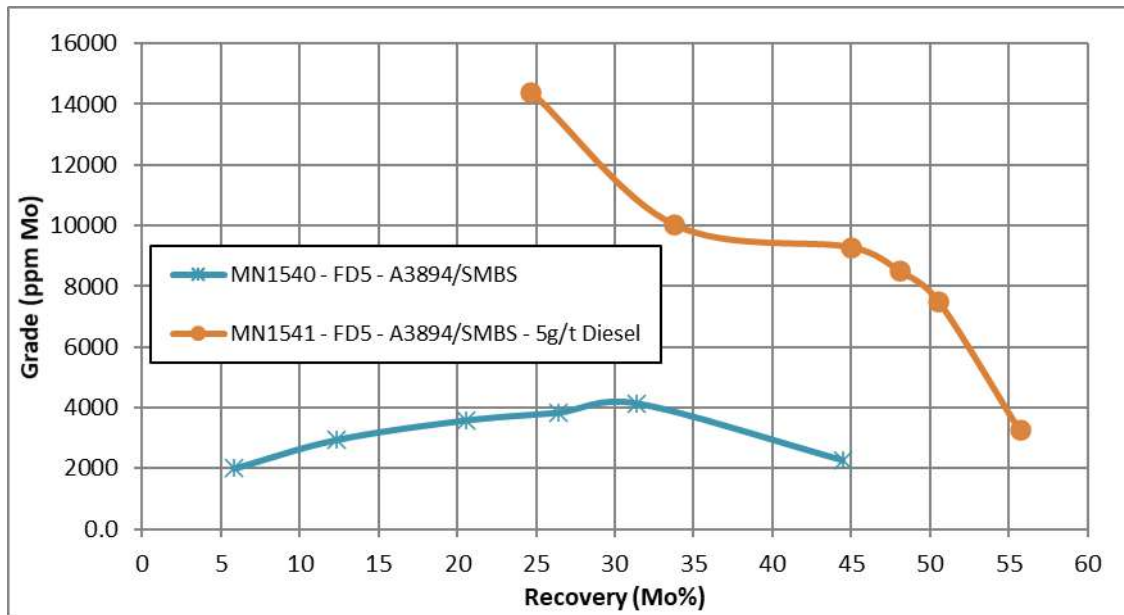


Figure 13.48 Productora – FD-5 copper grade recovery – diesel comparison

The reagent scheme and float times used for the >10% acid soluble/transitional sulphide samples is shown in Table 13.35.

Table 13.35 Productora – >10% acid soluble copper (transitional containing) samples – flotation conditions

Operation cycle 4	Standard flotation scheme		Reagents and flotation time FD-3 and FD-4			Reagents and flotation time FD-5/V-1			
	RTD20 86 (g/t)	Float time (mins)	SMB S (g/t)	A3894 (g/t)	Float time (mins)	Diesel (g/t)	SMB S (g/t)	A3894 (g/t)	Float time (mins)
Mill						5	300		
Cu Con 1	10	1		10	1			5/3	1
Cu Con 2	5	2			2				1
Cu Con 3	5	3		5	3				2
Cu Con 4	5	7			7				
Regrind						5	300		
1st Cleaner Con 1	5	1	300	5	1			3/2	1
1st Cleaner Con 2		2			2				1
1st Cleaner Con 3	5	3	100	2	3				2.5/2
1st Cleaner Con 4		5			5				
1st Cleaner Scav Con	2	7	100	5	7		300		4
2nd Cleaner Con 1	5	1	50	2	1			2/2	1
2nd Cleaner Con 2		2			2				1
2nd Cleaner Con 3		3			3				1
2nd Cleaner Con 4		6			6				2
<i>Note – FD-5 and V-1 also had reduce scrape rate to 10 seconds in the cleaners</i>									

Final cleaners for the >10% acid soluble copper samples were conducted $P_{80}=125\mu\text{m}$ using the above conditions. Locked cycle tests were conducted on all composites except FD-3 with the A3894/SMBS scheme and on FD-4 with the standard RTD2086 scheme.

For each of the samples, locked cycle copper recovery at 25% Cu was determined. Molybdenum and gold recoveries were also determined at a 25% Cu concentrate grade. Final results for copper, molybdenum and gold are shown in Table 13.36, Table 13.37 and Table 13.38. Aside from FD-3, locked cycle results at 25% Cu were determined from open cleaner test grade recovery curves and also based on losses to cleaner scavenger tail and the expected recovery of copper reporting to the recleaner tail and cleaner scavenger concentrate.

Table 13.36 >10% acid soluble copper samples – rougher, cleaner and locked cycle copper results

Sample	Overall copper results (P80=125µm)										
	Head grade (%)	Rougher		Recleaner		Recleaner @ 25% Cu		Locked cycle*		Locked cycle @ 25% Cu	
		% Cu	% dist.	% Cu	% dist.	% Cu	% dist.	% Cu	% dist.	% Cu	% dist.
FD-3	0.54	5.7	87.5	23.5	84.1	25.0	83.2	30.7	82.3	25.0	85.0
FD-4	0.72	5.8	85.5	26.9	81.6	25.0	82.0	28.8	69.3	25.0	83.0
FD-5	0.24	5.8	78.7	23.8	66.7	25.0	62.5			25.0	73.0
V-1	0.18	5.9	72.1	26.1	48.4	25.0	58.0			25.0	64.0
V-9	0.74	9.8	76.2	29.1	70.8	25.0	71.3			25.0	72.7

* FD-4 locked cycle at 106µm primary grind and RTD2086 scheme

Table 13.37 >10% acid soluble copper samples – rougher, cleaner and locked cycle molybdenum results

Sample	Overall molybdenum results (P80=125µm)										
	Head grade (ppm)	Rougher		Recleaner		Recleaner @ 25% Cu		Locked cycle*		Locked cycle @ 25% Cu	
		% Mo	% dist.	% Mo	% dist.	% Mo	% dist.	% Mo	% dist.	% Mo	% dist.
FD-3	120	0.12	58.5	0.47	41.8	0.48	39.9	0.35	24.8	0.35	24.8
FD-4	140	0.13	65.9	0.52	55.6	0.50	56.0	0.39	36.2	0.50	59.0
FD-5	160	0.30	55.3	0.83	30.7	0.78	26.4			0.80	45.0
V-1	40	0.13	43.2	0.48	20.8	0.43	23.2			0.43	32.0
V-9	60	0.09	36.4	0.24	34.1	0.24	34.1			0.24	34.1

* FD-4 locked cycle at 106µm primary grind and RTD2086 scheme

Table 13.38 >10% acid soluble copper samples – rougher, cleaner and locked cycle gold results

Sample	Overall gold results (P80=125µm)										
	Head grade (ppm)	Rougher		Recleaner		Recleaner @ 25% Cu		Locked cycle*		Locked cycle @ 25% Cu	
		ppm Au	% dist.	ppm Au	% dist.	ppm Au	% dist.	ppm Au	% dist.	ppm Au	% dist.
FD-3	0.08	1.1	72.7	5.3	52.6	5.6	51.9	4.6	41.5	4.6	41.5
FD-4	0.14	1.3	71.7	5.1	57.0	5.1	57.0	4.6	53.2	5.1	57.0
FD-5	0.14	1.6	67.5	3.2	47.6	3.4	44.9			3.5	55.0
V-1	0.05	0.8	75.5								50.0
V-9	0.11	2.1	69.6	5.0	63.7	4.8	60.2			4.8	63.7

* FD-4 locked cycle at 106µm primary grind and RTD2086 scheme

From the locked cycle and cleaner results, head grade vs. cleaner recovery was graphed to determine if there was a relationship for copper, molybdenum and gold. Samples V-1 and V-9 were designated as >20% acid soluble copper/transitional sulphide and a relationship was determined for these based on the Central Fresh In Pit curve (change

from 92.903 to 74 on the y axis). The line of best fit with a derived formula of “ $y=5.3675\ln(x)+74$ ” was determined and can be seen in Figure 13.49. As this is based on only two points, more transitional sulphide composites are required to confirm this relationship.

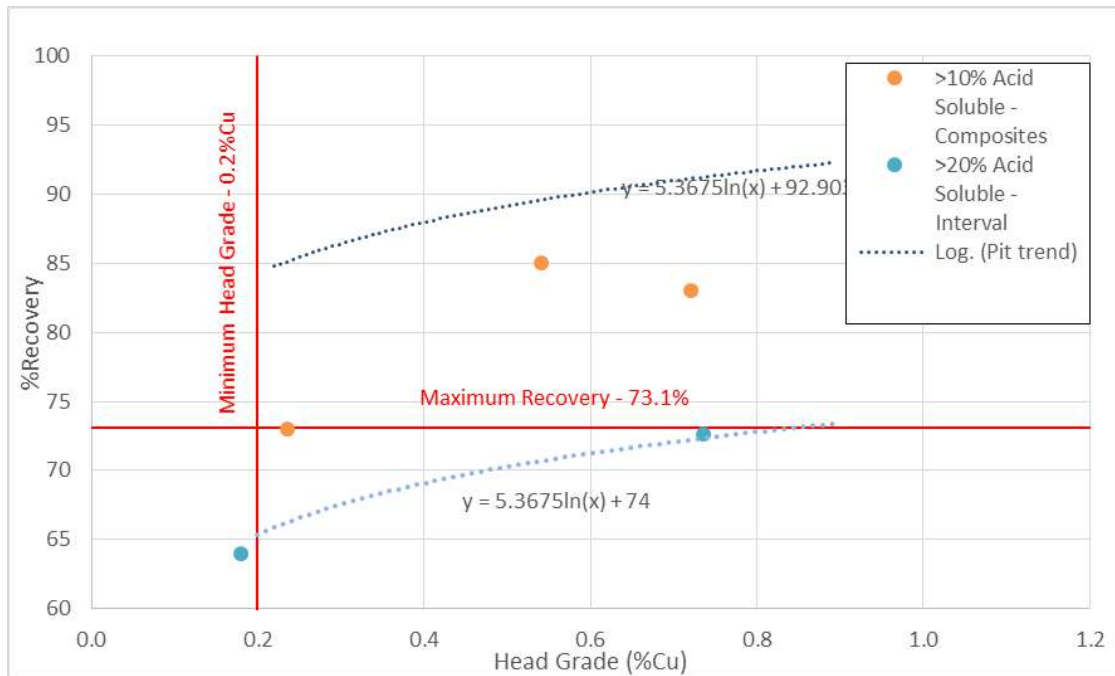


Figure 13.49 >10% acid soluble copper/transitional sulphide – copper head grade vs. recovery

For molybdenum and gold, head grade vs. recovery was similar to the Central Fresh samples and the same recovery curve and maximum recoveries were applied to the >10% acid soluble copper samples.

For FD-3, FD-4 and FD-5, the mass percentage of fresh and transitional material was calculated. When the Central curve formula is applied to the fresh portion of these samples and the Transition Sulphide formula applied to the transitional mass percentage, the combined recoveries were similar to the actual recoveries achieved (FD-4 was out the most as it contains Transition Oxide material).

Table 13.39 shows the weight percentages and the calculated recoveries. These calculations help back up the Transitional Sulphide head grade vs. copper recovery relationship, though further work is still required to confirm the relationship. For FD-4, a formula of $5.3675 \cdot \ln(x) + 40$ was derived and also applied to the transitional portion. With this formula, calculated recovery was closer to actual recovery.

Table 13.39 >10% acid soluble copper samples – rougher, cleaner and locked cycle gold results

Sample	Head grade (% Cu)	Transitional/Fresh	Calculated recovery (%)	Mass percentage (%)	Calculated recovery for mass (%)	Composite calculated recovery (%)	Actual recovery (%)
FD-3	0.54	Transitional	70.7	26%	18.7	84.6	85.0
		Fresh	89.6	74%	65.9		
FD-4	0.72	Transitional	72.2	14%	10.3	88.4	83.0
		Fresh	91.1	86%	78.1		
		Oxide	38.2	14%	5.5	83.6	
FD-5	0.235	Transitional	66.2	59%	38.8	74.1	73.0
		Fresh	85.1	41%	35.2		

13.3.2.3 Productora – Habanero Lode – Flotation Testwork Results

The Habanero part of Productora mineralized material represents 7% of the main pit (remaining ~55% Central and ~38% CCHEN South). Samples V-11 and V-12 from the MET023 drillhole were from the Habanero zone. Samples V-10 (MET008) was identified as Central, though, based on the depth of the sample and the performance of the flotation tests, V-10 has also been classified as Habanero. The MET023 samples have the highest and lowest copper head grade (V-11 – 1.01% Cu. V-12 – 0.11% Cu) out of all the composites tested.

Mineralogically, the Habanero zone is similar to the Central zone (Chalcopyrite with relatively free pyrite and little association between the two. Non-sulphides distribution is different though, with lower feldspars and higher levels of quartz and mica). However, with the standard flotation collector (RTD2086), high levels of pyrite continued to float into the final copper concentrate and even with the high head and rougher grade in V-11, 25% Cu could not be achieved. The V-11 standard recleaner test (at $P_{80}=125\mu\text{m}$) achieved 94.7% at 20.2% Cu and a sulphur grade of 39% S. With the very low head grade of V-12, only a small amount of pyrite would make 25% Cu difficult. The standard RTD2086 recleaner achieved 91.9% at 3.7% Cu with 44.7% S. The Habanero zone, therefore, looks to have some mineralogical difference, with pyrite being more active than in the Central zone.

Grind series rougher tests were conducted on V-11 and V-12, though all further rougher and cleaner tests were conducted at $P_{80}=125\mu\text{m}$. To improve selectivity against pyrite, optimisation tests were conducted with C4403 and reduced flotation and scrape times (for V-12).

A xanthate ester (RTD2086) was selected for the Productora deposit as it is highly selective against pyrite and works well at natural pH (remove issues with lime in sea water). Collector C4403 (also a xanthate ester, though includes a hydrocarbon) had been previously tested on FD-1 and had given similar copper results to RTD2086 with improved molybdenum recoveries (due to hydrocarbon). This was tested on V-11 and V-12 and was shown to give significantly greater selectivity against the active pyrite and resulted in improved copper grades with very little loss of recovery. Figure 13.50 shows

the rougher results for RTD2086 and C4403 with the same dosage for both V-11 and V-12.

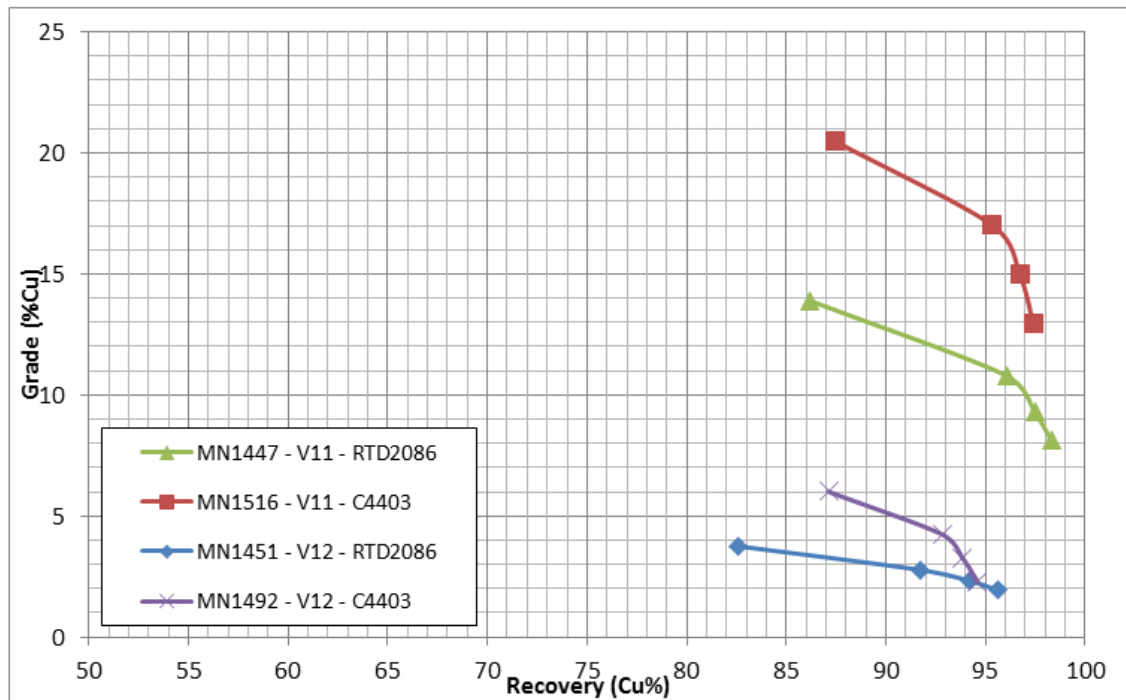


Figure 13.50 Productora – Habanero – RTD2086 vs. C4403 rougher results

Based on the improved rougher results, cleaner and recleaner tests were conducted with C4403. Figure 13.51 and Figure 13.52 show the upgrade with C4403 compared to RTD2086. For V-11, changing to C4403 with dosage and flotation time remaining as standard, copper results improved, though were still below desired grade. Reducing C4403 dosage and flotation time (approximately half of standard time), recleaner grades exceeded 30% Cu. Copper grade with just a single stage of cleaning exceeded 25% Cu. A locked cycle test was conducted as per MN1532, low dose C4403 and reduced time, and achieved 94.3% at 31.7% Cu.

For V-12, even though the head grade is very low (0.12% Cu), using C4403 still managed to achieve over 29% copper. The recovery of 78% was also very good for the low head grade and with 11% of the copper reporting to the recleaner tail, overall recovery in a locked cycle would be expected to be over 85% (well above Productora prediction for a 0.12% head grade). Upgrade ratio from rougher to cleaner was very good at 3.2 and loss to cleaner scavenger tail was only 1.8% of the copper.

For the V-10 sample, only a single recleaner test with C4403 was conducted. Collector dosage and flotation time was as per standard RTD2086 scheme and further optimisation may further improve results. Compared to the RTD2086, C4403 increased copper grade from 26% to 30% Cu with a 1.2% decrease in recovery and increased molybdenum recovery by 18% (31% vs. 49%).

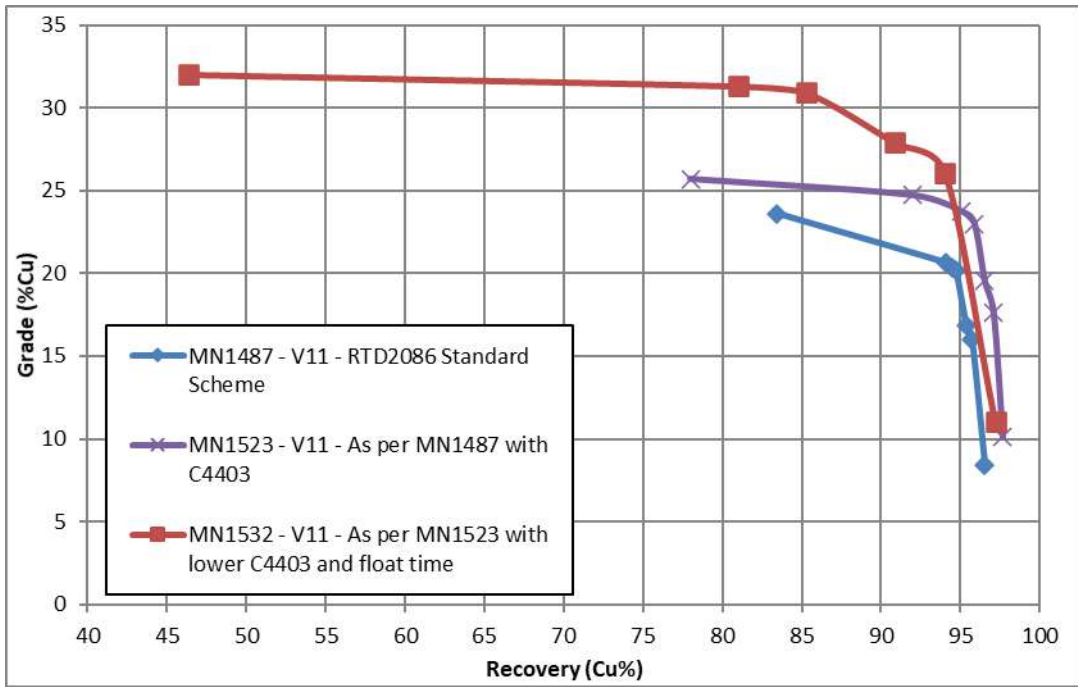


Figure 13.51 Productora – Habanero – V-11 - RTD2086 vs. C4403 cleaner results

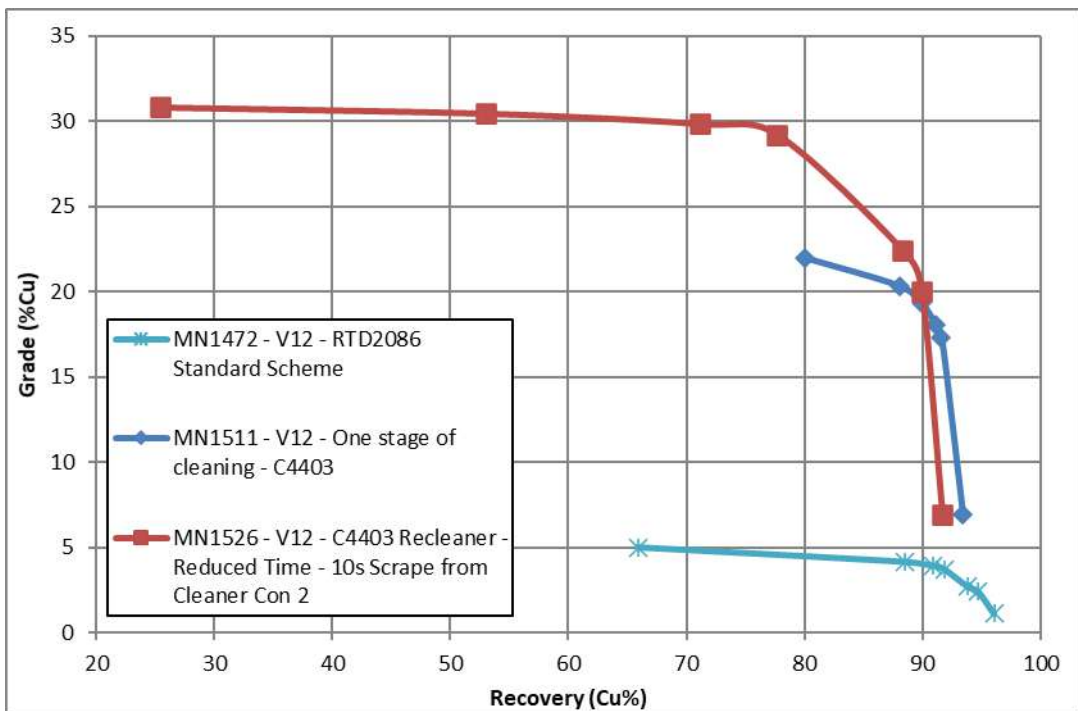


Figure 13.52 Productora – Habanero – V-12 - RTD2086 vs. C4403 cleaner results

For the Habanero zone, gold recoveries were significantly lower than the Central zone. Flotation results indicate that the gold has a higher association with pyrite and even though rougher recoveries are similar to Central, losses are high to the cleaner scavenger tail (V-11 decreases from 89% in rougher con to 30% in recleaner con). The V-10 sample gold recovery was not as low, though this sample borders the Central zone

and has flotation response in between other Central and Habanero samples. Figure 13.53 shows head grade vs. cleaner flotation recovery for gold (at 25% Cu).

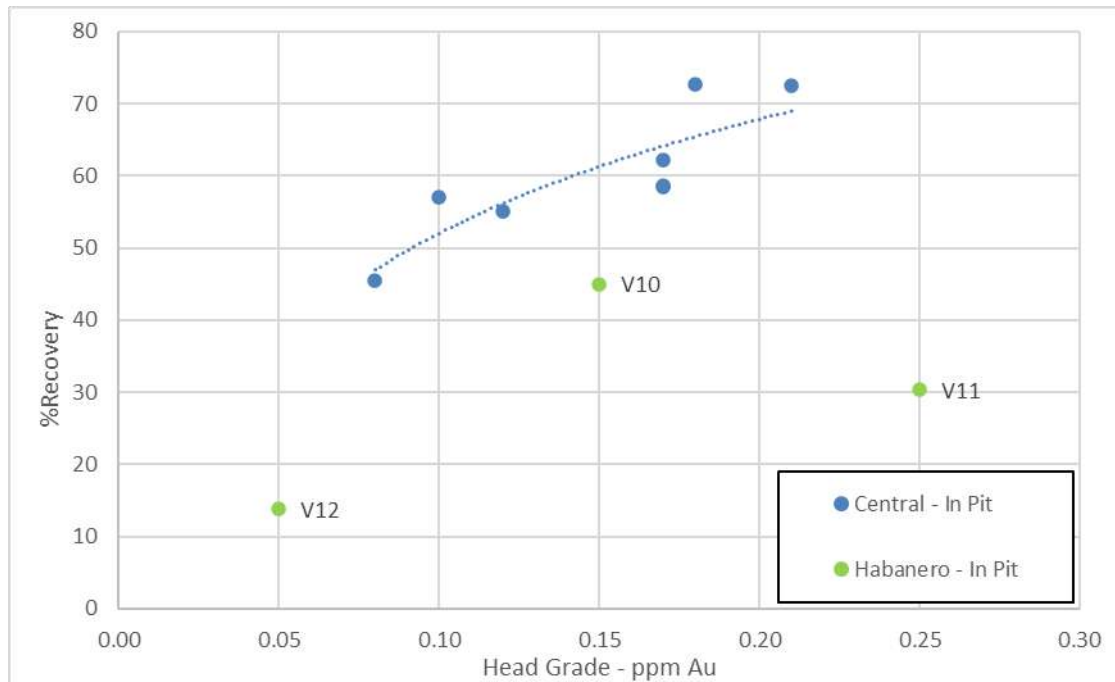


Figure 13.53 Productora – Habanero – gold head grade vs. recovery (125µm)

Further Habanero samples need to be tested to show there is a different response in this zone for both copper and gold. The C4403 dosage and flotation times would also need optimising for copper and pyrite and to see if there is a relationship with head grades. Further tests with RTD2086 at lower dosages and flotation times would also be recommended.

13.3.2.4 Productora – Alice - Flotation Testwork Results

Three samples were prepared from the Alice mineralized material body (V-13 and V14 from PXP0001 and V-18 from MET024) for comminution and flotation testwork. The set standard flotation tests were conducted on these samples including rougher grind series, two stage cleaners and locked cycles (V-13 and V-18 only). Due to time constraints, no single stage cleaners were conducted on the Alice samples.

Mineralogically, the Alice mineralized material is slightly different to Productora. Main sulphide minerals are still chalcopyrite and pyrite (with similar grain size, but slightly better liberation and lower locked copper in +125 µm fraction), though the non-sulphides have changed. In the Productora deposit, K-feldspars are generally the dominant mineral present, followed by quartz, chlorites and micas. In the Alice samples, there are very little K-feldspars. These have been replaced by albite (Na-feldspar) and other plagioclase feldspars and higher levels of Calcite. Quartz levels are slightly higher and mica and chlorite are similar to Productora Central mineralized material. Aside from V-

18 (due to low head grade), the sulphur to copper ratio was low compared to the Productora Central samples.

13.3.2.4.1 Primary Grind Series Testwork

For the Alice samples, primary grind sizes tested ranged from $P_{80}=106 \mu\text{m}$ to $180 \mu\text{m}$. Grind size vs. overall copper and molybdenum rougher recovery are shown in Figure 13.54 and Figure 13.55. Though V-18 copper head grade was low (0.24% Cu), copper recovery was very high.

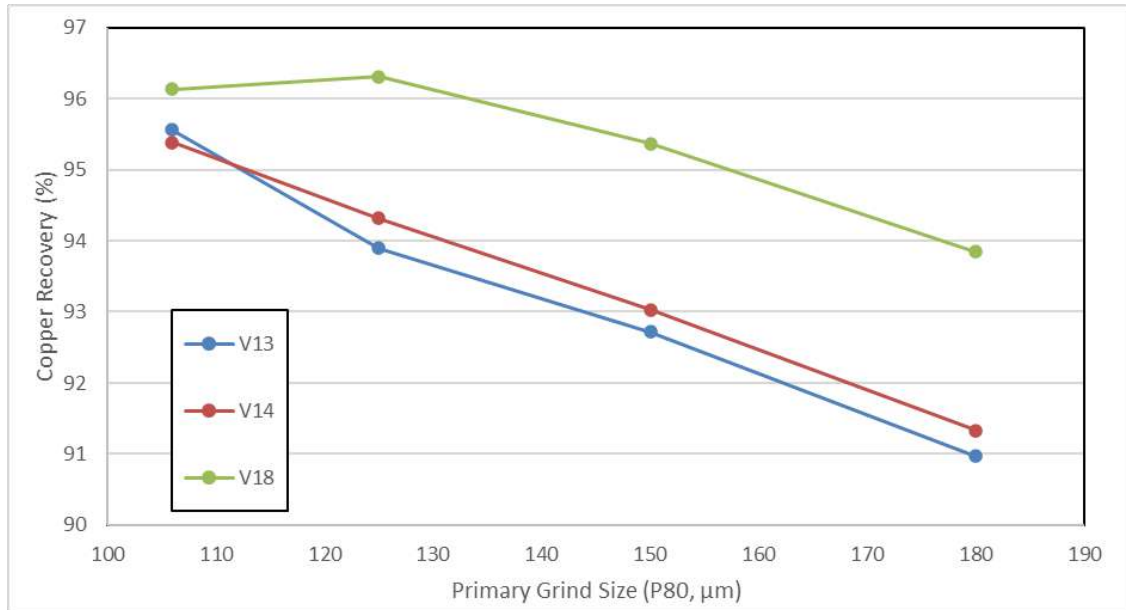


Figure 13.54 Alice – primary grind size copper results

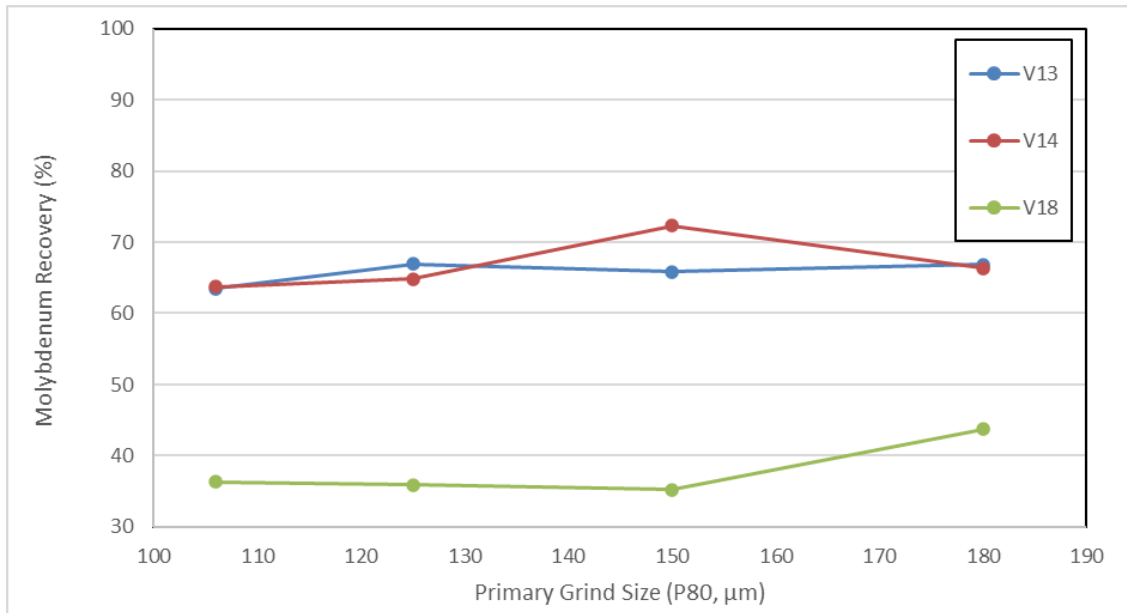


Figure 13.55 Alice – primary grind size molybdenum results

Overall copper rougher recoveries were high for all three composites, with 91% or greater recovery at 180 µm. The overall copper rougher grade and recovery are shown in Table 13.40. From 180 µm to the selected 125 µm grind size, copper rougher recovery increased by less than 3% and molybdenum recovery tended to be slightly better at the coarser grind size. Rougher concentrate copper grades for all three samples were around the desired 8 to 10% range and molybdenum and gold recoveries were higher than for Central samples at similar head grades. Though the grind size had been set at P₈₀=125 µm for the Productora deposit, as results were good at the coarser grind sizes and due to economic benefits and that the Alice mineralized material would be treated separately to Productora, the P₈₀=180 µm grind size was selected for modelling and cleaner testwork.

Table 13.40 Alice – primary grind size copper rougher results

Sample	Overall copper rougher results – grind size (P80, µm)								
	Head grade (%)	180		150		125		106	
		%	% dist.	%	% dist.	%	% dist.	%	% dist.
V-13	0.50	8.65	91.0	8.66	92.7	9.35	93.9	10.01	95.6
V-14	0.32	9.56	91.3	9.65	93.0	9.71	94.3	9.16	95.4
V-18	0.24	7.72	93.8	7.54	95.4	8.10	96.3	7.99	96.1

Figure 13.56 shows copper rougher recovery at P₈₀=180 µm vs. the copper head grade for the Alice samples. The Central (In-Pit Fresh) rougher trend line at P₈₀=125 µm is also shown. Copper rougher recoveries did not show good correlation. Even if V-18 grade increased to 10%, recovery would still be higher than V-13, V-14 as well as the

Productora trend. Discounting V-18, V-13 and V-14 follow Productora recoveries, though at a coarser grind size.

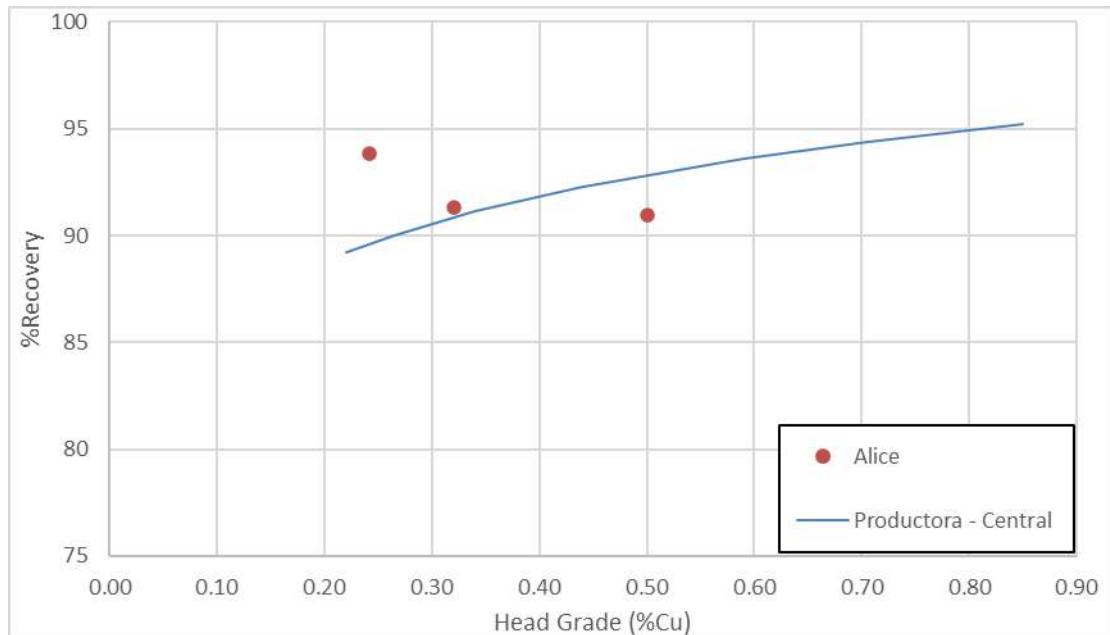


Figure 13.56 Alice – head grade vs. copper rougher recovery (180µm)

13.3.2.4.2 Cleaner and Locked Cycle Testwork

As part of the testwork program, both single and two stage cleaner floats were to be conducted each of the samples. Due to time constraints, only two stage cleaners were conducted on each of the Alice samples. For each sample, tests were conducted using the standard RTD2086 scheme at a primary grind of $P_{80}=180\ \mu\text{m}$ and regrind of $P_{80}=25\ \mu\text{m}$. No other optimisation was conducted.

Locked cycle tests were conducted on V-13 and V-18, with standard conditions (cleaner scavenger con recirculated to regrind of next cycle, recleaner tail recirculated to cleaner feed) at $P_{80}=180\ \mu\text{m}$. An additional test was conducted on V-13 at $P_{80}=125\ \mu\text{m}$.

From the results, locked cycle recoveries at 25% Cu were determined for modelling. For the V-14 sample, the recovery was based on the open cleaner results. As for Productora, molybdenum and gold recoveries were also determined at a 25% Cu concentrate grade. Final results for copper, molybdenum and gold are shown in Table 13.41, Table 13.42 and Table 13.43.

Table 13.41 Alice – rougher, cleaner and locked cycle copper results

Sample	Overall copper results (P80=180µm)										
	Head grade (%)	Rougher		Recleaner		Recleaner @ 25% Cu		Locked cycle		Locked cycle @ 25% Cu	
		% Cu	% dist.	% Cu	% dist.	% Cu	% dist.	% Cu	% dist.	% Cu	% dist.
V-13	0.50	8.7	91.0	25.4	83.2	25.0	83.5	29.8	88.3	25.0	89.5
V-13								28.7*	91.9*		
V-14	0.32	9.6	91.3	29.3	85.7	25.0	87.5			25.0	88.8
V-18	0.24	7.7	93.8	28.0	90.2	25.0	90.5	25.1	91.5	25.1	91.5

* V-13 locked cycle conducted at P₈₀=125µm

Table 13.42 Alice – rougher, cleaner and locked cycle molybdenum results

Sample	Overall molybdenum results (P80=180µm)										
	Head grade (ppm)	Rougher		Recleaner		Recleaner @ 25% Cu		Locked cycle		Locked cycle @ 25% Cu	
		% Mo	% dist.	% Mo	% dist.	% Mo	% dist.	% Mo	% dist.	% Mo	% dist.
V-13	60	0.09	66.8	0.26	52.3	0.26	52.3	0.32	62.3	0.32	62.3
V-13	60							0.33*	62.5*		
V-14	40	0.15	78.2	0.46	61.4	0.42	68.0			0.42	68.0
V-18	20	0.06	43.8	0.19	34.2	0.17	35.0	0.16	36.9	0.16	36.9

* V-13 locked cycle conducted at P₈₀=125µm

Table 13.43 Alice – rougher, cleaner and locked cycle gold results

Sample	Overall gold results (P80=180µm)										
	Head grade (ppm)	Rougher		Recleaner		Recleaner @ 25%Cu		Locked cycle		Locked cycle @ 25%Cu	
		ppm Au	% dist.	ppm Au	% dist.	ppm Au	% dist.	ppm Au	% dist.	ppm Au	% dist.
V-13	0.08	1.0	58.5	2.7	51.7	2.7	51.7	3.0	57.7	2.0	57.7
V-13	0.08							2.0*	53.8*		
V-14	0.04	0.8	55.1	2.0	35.0	2.1	33.0			2.1	46.6
V-18	<0.02	0.6	31.0	1.9	23.0	1.9	23.0	1.0	44.9	1.0	44.9

* V-13 locked cycle conducted at P₈₀=125µm

From the locked cycle results, head grade vs. cleaner recovery were graphed and compared to the Productora results (at 125 µm) to determine a relationship for head grade vs. copper, molybdenum and gold recoveries. For copper, the head grade vs recovery is shown in Figure 13.57. At P₈₀=180 µm and 25% Cu, samples V-13 and V-14 show similar recoveries to Productora. The Productora line of best fit at 125 µm, a derived formula of “ $y=5.3675\ln(x)+92.903$ ”, was therefore applied to the Alice deposit at 180 µm. The same maximum recovery of 92% was also applied. Results for V-18 were quite higher than other Alice and Productora samples. Results from this test were, therefore, not used to derive the formula for the curve.

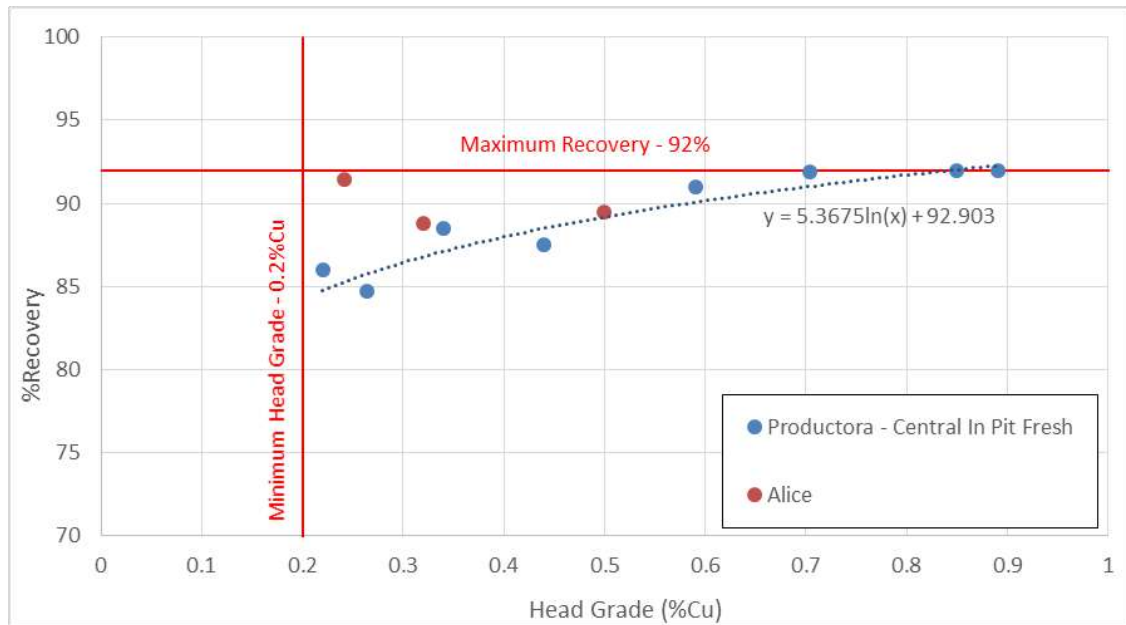


Figure 13.57 Alice – copper head grade vs. recovery

For gold, head grade vs. final concentrate recovery (for a 25% Cu concentrate) was plotted and, discounting V-18, a trend line was derived and expanded to estimate higher gold head grades. The formula derived for the line of best fit was “ $y=15.686\ln(x)+97.205$ ”. The trend line and data points can be seen in Figure 13.58. Gold head grades are very low for all three composites, with the highest head grade of 0.08 ppm for V-13. As for Productora, maximum recovery has been set at 80% (based on formula this would be approximately a 0.35 ppm head grade), though further flotation tests need to be conducted on samples with higher head grades to determine potential recoveries at the higher head grade levels.

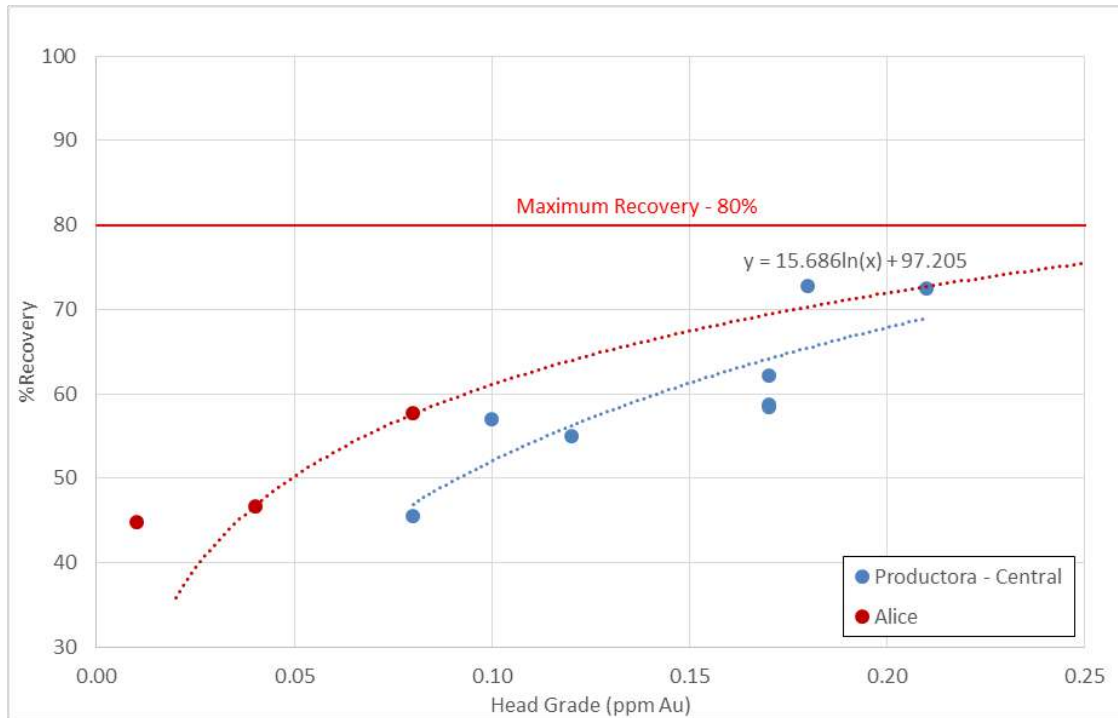


Figure 13.58 Alice – gold head grade vs. recovery

With only a small number of samples tested and one being an outlier, further testwork needs to be conducted on additional samples to confirm the Alice head grade vs. recovery relationships.

13.3.2.5 Productora – Cayenne – Flotation Testwork Results

For the Cayenne zone of the Productora deposit (composites FD-8, FD-9, FD-10, FD-11, FD-12, V-3, V-4, V-5, V-6), the set standard flotation tests were conducted on these composites. Tests included rougher grind series, single stage cleaners, two stage cleaners and locked cycles (FD-12 only). During the testwork program, the Cayenne zone was defined as out of the main pit. Therefore, optimisation and recovery modelling was not conducted.

Mineralogically, the Cayenne mineralized material is similar to the Central zone, though it does contain high levels of magnetite (5.6% to 25.6%) compared to 1.2% average in Central. Main sulphide minerals are still chalcopyrite and pyrite, with small amounts of secondary copper minerals in some composites. Liberation, locking and associations are also similar to the Central zone.

13.3.2.5.1 Primary Grind Series Testwork

For the Cayenne composites, primary grind size tests were conducted on the Flotation Development (FD) samples. Grind sizes tested ranged from $P_{80}=75 \mu\text{m}$ to $180 \mu\text{m}$. For the Variability samples (V-3 to V-6), two grind sizes were tested on each composite. Grind size vs. overall copper and molybdenum rougher recovery for the FD samples are shown in Figure 13.59 and Figure 13.60.

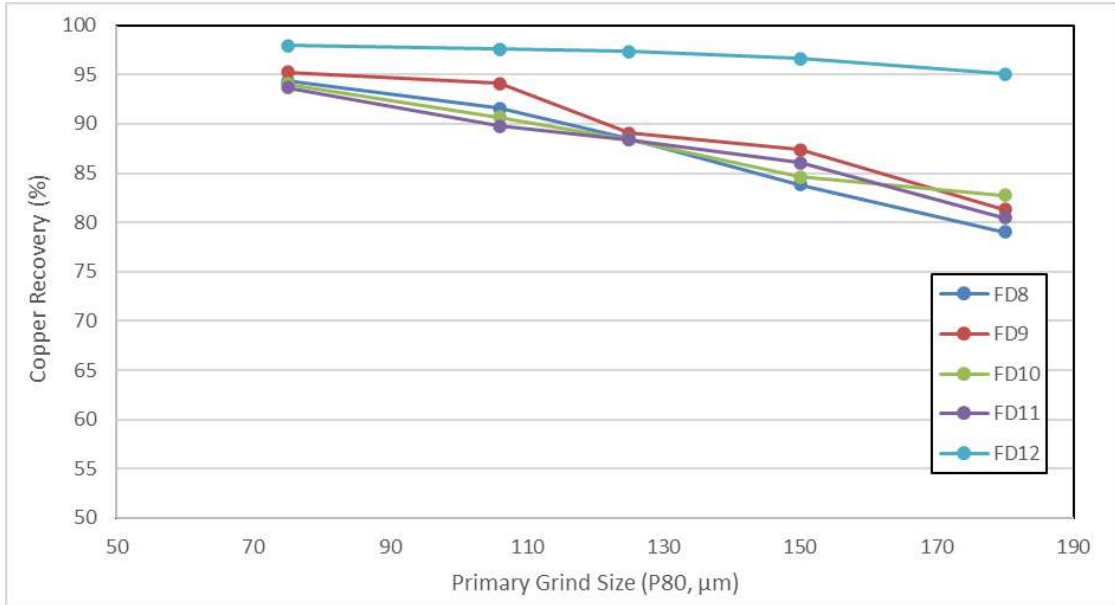


Figure 13.59 Cayenne – primary grind size copper results

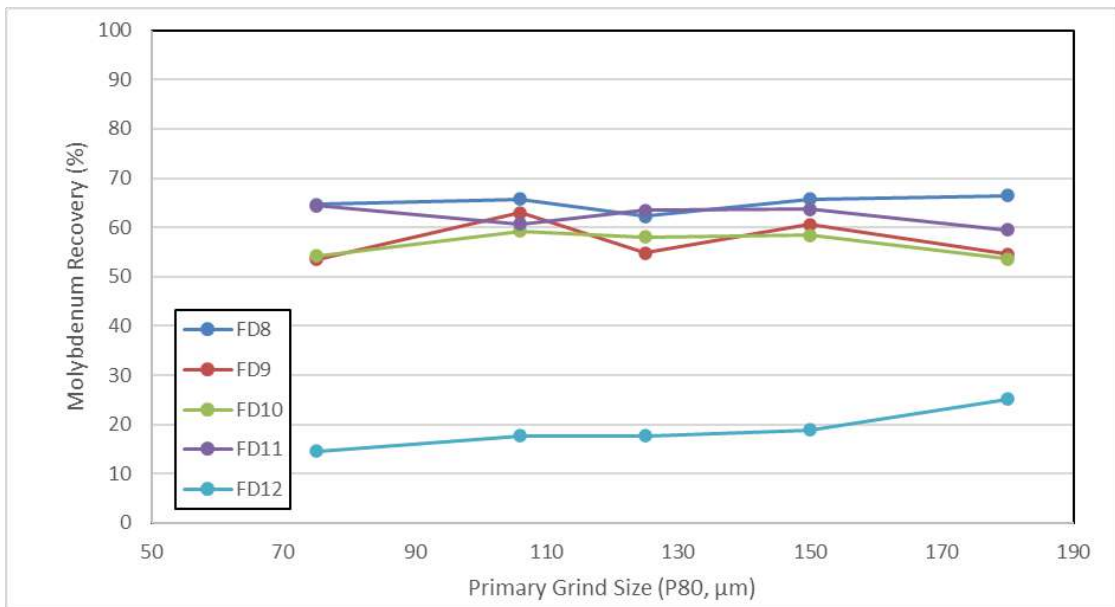


Figure 13.60 Cayenne – primary grind size molybdenum results

Overall copper rougher recoveries were similar for all composites except for FD-12, which had significantly higher recoveries of over 95% for all grind sizes. The overall copper rougher grade and recoveries are shown in Table 13.44. Aside from FD-12, copper rougher recovery from 180 μm to 75 μm grind size, increased by 11.3% to 15.3% (only 2.9% for FD-12). Rougher concentrate copper grades for all samples were over 10% Cu and molybdenum and gold recoveries tended to be slightly higher than for Central composites at similar head grades.

Table 13.44 Cayenne – primary grind size copper rougher results

Samples	Overall copper rougher results – grind size (P80, μm)										
	Head grade (%)	180		150		125		106		75	
		%	% dist.	%	% dist.	%	% dist.	%	% dist.	%	% dist.
FD-8	0.66	14.4	79.0	14.0	83.8	14.2	88.5	15.7	91.6	15.1	94.3
FD-9	0.32	12.7	81.3	12.0	87.4	12.2	89.1	10.8	94.1	12.6	95.2
FD-10	0.44	9.81	82.7	9.66	84.6	10.3	88.4	10.2	90.7	8.79	94.0
FD-11	0.58	12.0	80.5	12.4	86.1	12.2	88.4	13.6	89.8	11.6	93.7
FD-12	0.51	15.5	95.0	15.6	96.6	15.5	97.3	16.6	97.6	16.5	98.0
V-3	0.45	-	-	11.6	85.8	-	-	12.6	92.9	-	-
V-4	0.38	-	-	9.51	86.5	-	-	9.69	91.9	-	-
V-5	0.32	-	-	8.33	89.5	8.35	90.4	-	-	-	-
V-6	0.42	-	-	11.2	90.6	12.0	93.8	-	-	-	-

Figure 13.61 shows copper rougher recovery at $P_{80}=125 \mu\text{m}$ vs. the copper head grade for the Cayenne samples. The Central In-Pit Fresh rougher trend line at $P_{80}=125 \mu\text{m}$ is also included. In general, copper rougher recoveries did not show good correlation and also gave lower recoveries than the Central samples. Only the V-6 sample fit the Central line and FD-12 are well above (~4.5%) the line.

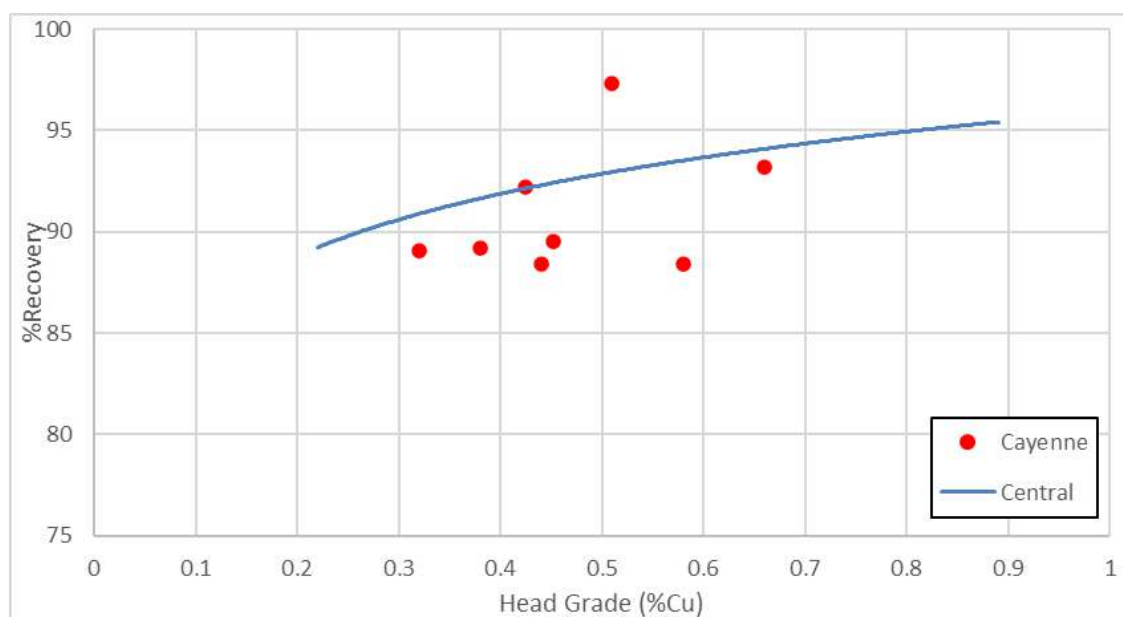


Figure 13.61 Cayenne – head grade vs. copper rougher recovery (125 μm)

13.3.2.5.2 Cleaner and Locked Cycle Testwork

As part of the testwork program, both single and two stage cleaner floats were to be conducted each of the composites with the standardised flowsheet. For each composite, tests were conducted using the standard RTD2086 scheme at a primary grind of

$P_{80}=106 \mu\text{m}$ ($P_{80}=150 \mu\text{m}$ for FD-12 and V-5) and a regrind of $P_{80}=25 \mu\text{m}$. No optimisation was conducted.

Two locked cycle tests were conducted on FD-12, a single stage cleaner and a two stage cleaner. The two stage cleaner used the standard conditions (cleaner scavenger con recirculated to regrind of next cycle, recleaner tail recirculated to cleaner feed) at $P_{80}=150 \mu\text{m}$, whilst the single stage cleaner locked cycle was conducted at a $P_{80}=125 \mu\text{m}$ and had an additional 5 g/t of collector in both the rougher and cleaner circuits and an extra 3 g/t in the cleaner scavenger.

From the results, locked cycle recoveries at 25% Cu were determined, though this data was not used to determine a specific head grade vs. recovery curve or used for modelling. Only FD-12 had a locked cycle, therefore all other results in Table 13.45 were based on the Productora average of rougher less 3.5%. Molybdenum and gold recoveries at a 25% Cu concentrate grade were not determined.

Head grade vs. estimated locked cycle recoveries is presented in Figure 13.62. It can be seen that the Cayenne samples are in general, lower than the Central samples, although they are following the same trend. Samples FD-11 and FD-12 are the main outliers. Sample FD-11 has a higher sulphur to copper ratio (7:1) compared to other samples and a very high concentration of magnetite (25.6%). Compared to other samples, FD-12 has a very high level of copper liberation (84%) for all size fractions and it is the reason for the above average recoveries.

If the Cayenne zone is to be mined at some stage, it is suggested that further optimisation testwork is conducted to improve on recoveries and to determine a head grade vs. recovery relationship.

Table 13.45 Alice – rougher, cleaner, and locked cycle copper results

Samples	Overall copper results										
	Head grade (%)	Rougher ¹		Recleaner ²		Recleaner @ 25% Cu		Locked cycle ⁴		Locked cycle ³ @ 25% Cu	
		% Cu	% dist.	% Cu	% dist.	% Cu	% dist.	% Cu	% dist.	% Cu	% dist.
FD-8	0.66	13.6	93.2	25.4	89.0	25.0	89.0			25.0	89.7
FD-9	0.32	12.2	89.1	29.6	76.4	25.0	84.5			25.0	85.6
FD-10	0.44	10.3	88.4	28.8	76.6	25.0	83.2			25.0	84.9
FD-11	0.58	12.2	88.4	28.9	78.6	25.0	85.0			25.0	84.9
FD-12	0.51	15.5	97.3	31.3	84.5	25.0	93.5	31.3	90.3	25.0	94.0
V-3	0.45	11.6	89.5	30.0	79.5	25.0	85.0			25.0	86.0
V-4	0.38	9.5	89.2	28.4	80.1	25.0	84.5			25.0	85.7
V-5	0.32	8.4	90.4	28.1	75.8	25.0	80.0			25.0	86.9
V-6	0.42	11.6	92.2	28.3	85.2	25.0	88.0			25.0	88.7

1. Rougher tests all at 125µm
 2. Recleaners all at 106µm except FD-12 and V-5 at 150µm
 3. Locked cycle based on 125µm grind
 4. FD-12 locked cycle result – two stage cleaner at 150µm

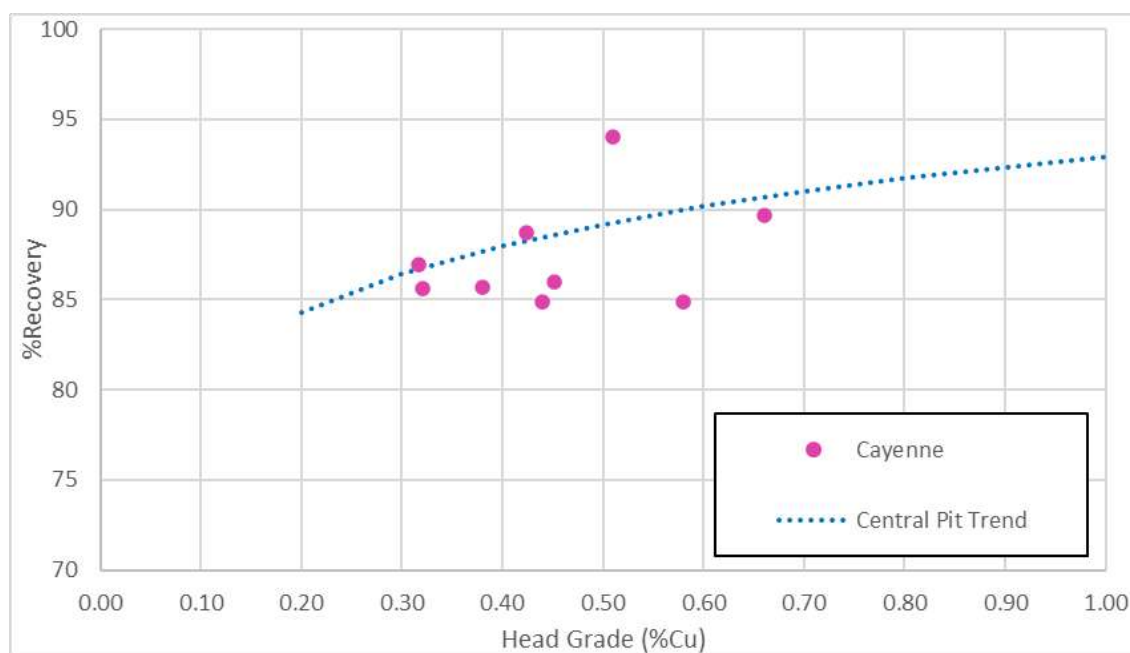


Figure 13.62 Alice – copper head grade vs. recovery

13.3.2.5.3 Copper Concentrate Comprehensive Analysis

Comprehensive concentrate assays were conducted on final concentrate from the FD-6, FD-13 and V13 locked cycle tests. Assays were conducted to determine diluent elements and potential level of penalty elements in the Productora mineralized material. Comprehensive assay results are shown in Table 13.46.

Table 13.46 Comprehensive concentrate analysis

Element	MN1537 FD-6 Final Con	MN1478 FD-13 Final Con	MN1536 V13 Final Con
Al ₂ O ₃ (%)	1.22	2.41	1.17
As (%)	0.02	<0.01	0.02
Au (ppm)	4.77	5.23	2.96
Ba (%)	<0.01	<0.01	<0.01
Be (ppm)	<20	<20	<20
Bi (%)	0.003	<0.002	0.005
CaO (%)	0.09	0.10	0.3
Cd (ppm)	<20	<20	<20
Cl (ppm)	360	350	160
Co (%)	0.2	0.063	0.009
Cr (%)	0.01	0.02	<0.01
Cu (%)	28.1	27.6	29.4
F (ppm)	80	140	90
Fe (%)	27.6	26.2	27.9
Hg (ppm)	2	0.7	1.1
K (%)	0.38	0.68	0.10
MgO (%)	0.06	0.39	0.20
Mn (%)	0.01	<0.01	<0.01
Ni (%)	0.02	0.02	<0.01
P (%)	<0.01	0.01	<0.01
Pb (%)	0.42	<0.01	<0.01
S (%)	33.5	30.1	32.2
Sb (%)	0.04	0.02	<0.01
Se (ppm)	80	75	160
SiO ₂ (%)	3.8	8.76	3.63
Sn (%)	<0.01	<0.01	<0.01
Sr (%)	<0.001	<0.001	<0.001
Te (ppm)	4.4	2.6	0.8
Th (ppm)	4	8	2
Ti (%)	0.05	0.1	0.22
U (ppm)	14	38	<2
V (%)	<0.001	<0.001	<0.001
Zn (%)	0.18	0.02	<0.01
Zr (%)	0.014	0.023	0.009

13.3.2.6 Copper Sulphide Flotation Testwork Summary

A large program of flotation testwork was conducted on the HCH Productora and Alice deposits. Testwork was based on a standardised flowsheet and reagent scheme which had been determined from previous testwork programs. The scheme used RTD2086 (Xanthate Ester supplied by Tall Bennett) at a natural pH of seawater with two stages of cleaning and a 25 µm regrind. Natural seawater pH was preferred as the use of lime in seawater can have negative effects on flotation performance.

A desired copper grade for the final concentrate was 25% Cu. To achieve this, optimisation testwork was conducted on a number of composites to improve copper grade and recovery. Optimisation testwork included the following:

- Primary grind size tests
- Reagent dosage
- Flotation time
- Alternate reagents
- Diesel addition for increased molybdenum flotation
- Seawater vs. tap water.

When optimised conditions were tested, it was identified that samples from different zones were reporting different flotation response. Some samples were also later identified as containing transitional sulphide and oxide material (designated as containing greater than 10% acid soluble copper). These samples gave sub-optimal results with the standardised scheme.

A primary grind size of $P_{80}=125\ \mu\text{m}$ was selected for all Productora samples to target a similar sulphide P_{80} compared to a plant grind of $P_{80}=150\ \mu\text{m}$. For the Alice deposit, a primary grind size of $P_{80}=180\ \mu\text{m}$ was chosen. Alice samples gave good copper recoveries at coarser grind sizes and as a result of the intent to not blend but campaign treat the Alice deposit, the coarser grind size was desirable.

Due to performance and copper recovery variations, for modelling of the copper head grade vs. final copper recovery, samples were grouped based on location, percentage acid soluble copper, flotation performance and alternate reagent schemes. Grouping the samples resulted in the following:

- Central In Pit Fresh – FD-1, FD-2, FD-6, FD-13, FD-14, V-2, V-7, V-8
- Habanero Lode In Pit – V-10, V-11, V-12
- >10% Acid Soluble Cu – FD-3, FD-4, FD-5, V-1, V-9
- Alice Deposit – V-13, V-14, V-18
- Cayenne – FD-8, FD-9, FD-10, FD-11, FD-12, V-3, V-4, V-5, V-6.

The Cayenne zone of the deposit was determined to be out of the current pit and was therefore not optimised and modelled at this stage.

From the optimisation testwork, copper head grade vs. recoveries achieved is presented in Figure 13.63.

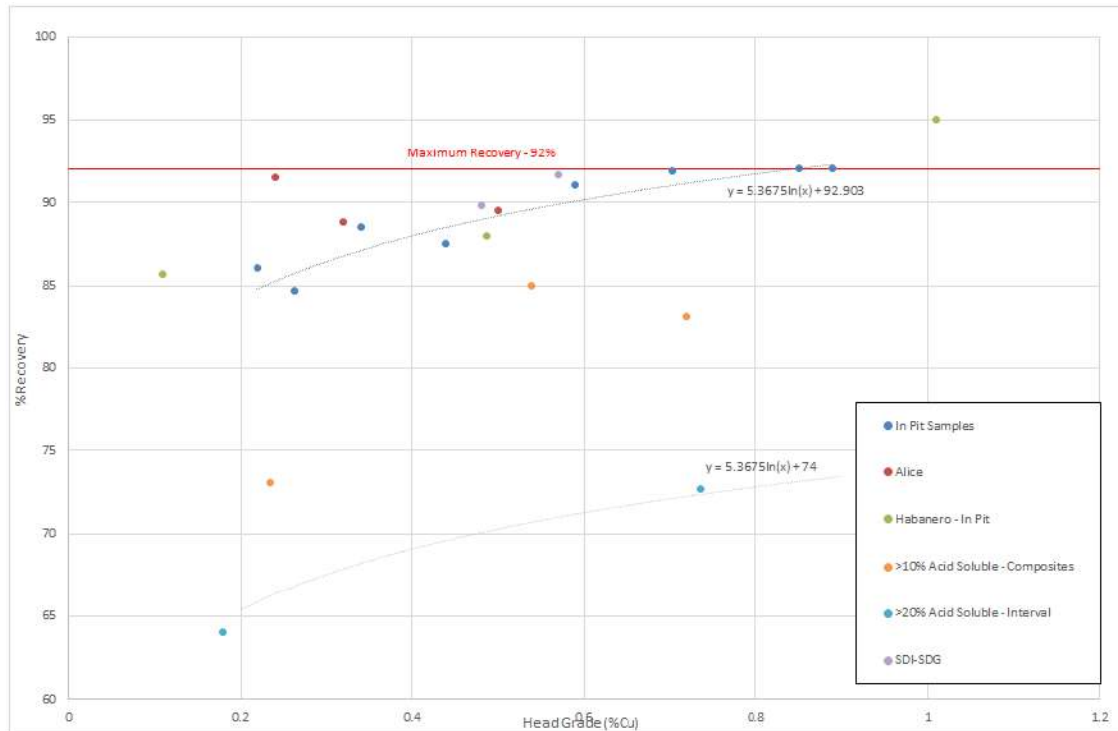


Figure 13.63 Copper head grade vs. recovery

For the Central In Pit samples, the correlation for head grade vs. recovery was very good and had an R^2 of 0.89. The derived curve for the line of best fit was “ $y=5.3675\ln(x)+92.903$ ” with a maximum set at 92% recovery. Aside from FD-2, the reagent regime and flowsheet were as per standard, with RTD2086 collector at natural seawater pH as received. For FD-2, the A3894/SMBS scheme was used.

For the Alice samples, recoveries are potentially higher, however, with only three samples, there is not enough data to state this with confidence. The Central In Pit curve was therefore, applied to the Alice mineralized material as well. The Alice flotation was done at $P_{80}=180\ \mu\text{m}$ instead of the $125\ \mu\text{m}$ as for Productora. The Alice samples also used the standard flowsheet (RTD2086), though at the coarser grind size.

As for Alice, the Habanero Lobe zone may have increased recovery over the Central zone, though, with only three samples (V-10 bordering Central and Habanero), there is insufficient data to produce a separate head grade vs. recovery formula for Habanero and the Central formula has been applied to the Habanero Lobe.

For Habanero, high levels of pyrite floated with the standard RTD2086 scheme. To achieve 25% Cu, collector C4403 was used (xanthate ester with a hydrocarbon). This collector gave greater pyrite selectivity without significant copper loss. It also improved molybdenum recovery.

For the transitional sulphides (>20% Acid Soluble Copper), a separate grade recovery curve was determined. This curve was based on results from V1 and V9 and also on the Central head grade vs. recovery curve. The grade recovery curve gave average 18% lower recoveries compared to the Central Fresh In Pit curve. The formula derived is

" $y=5.3675\ln(x)+74$ ". As this data is based on only two points, more work is required on the "Transitional Sulphides". The reagent scheme used for the >10% Acid Soluble sample (V-1 and V-9, as well as FD-3, FD-4, and FD-5) was A3894 and SMBS at pH of seawater as received. This scheme gave significant increases in copper recovery for some samples. This is due to xanthate esters (RTD2086) not always being suitable when secondary copper minerals are present.

Samples FD-3, FD-4 and FD-5 all have high levels of "transitional sulphides". FD-4 also contains "transitional oxide". When the Central curve formula is applied to the fresh portion of these composites and the Transitional curve is applied to the transitional portion, the calculated recoveries are similar to the actual recoveries achieved (FD4 not as good due to the copper oxides present). This further helps to confirm the use of the "Transitional Sulphide" formula.

Gold head grade vs. gold recoveries can be seen in Figure 13.64. As for the copper, a line of best fit was determined for the Central In-Pit Fresh zone. The formula derived for this line is " $y=22.82\ln(x)+104.58$ ". This formula was also applied to the >10% Acid Soluble samples. A maximum recovery was set at 80%.

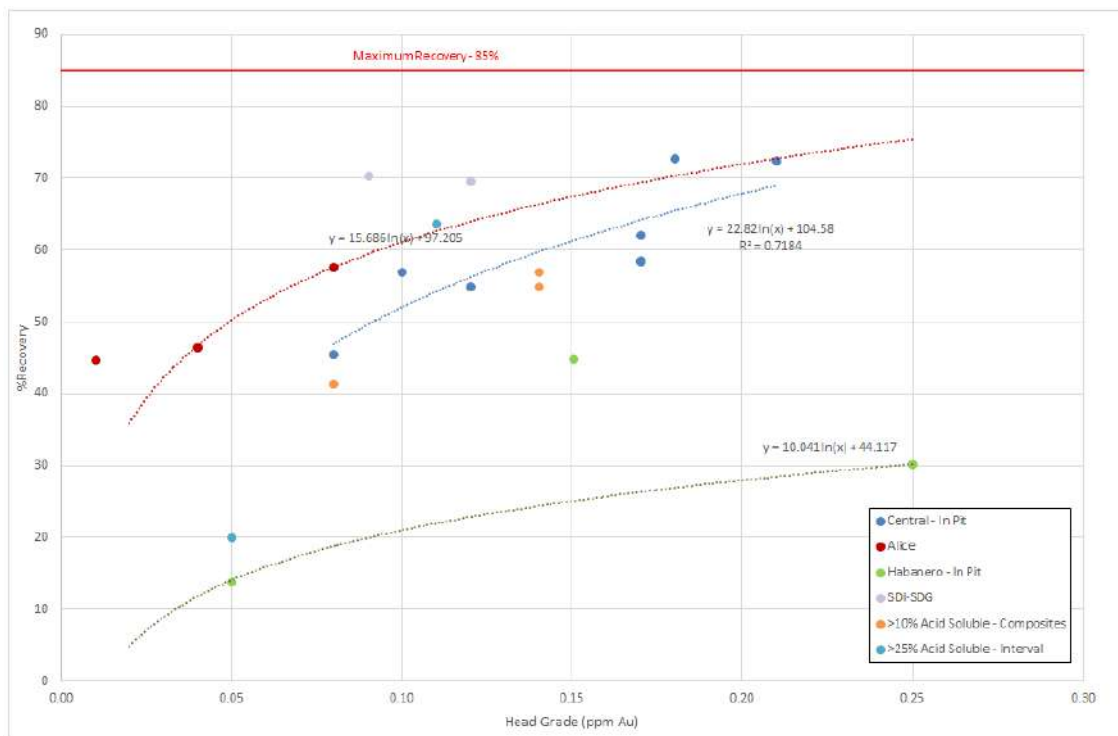


Figure 13.64 Gold head grade vs. recovery

For Alice, gold recoveries were higher than for Productora. Gold head grades for Alice were low and recoveries for greater than a 0.15 ppm Au need to be determined to give confidence in the data. The V18 results were high (for the head grade), therefore, this result was not used for the head grade vs. recovery curve. Based on the remaining two samples, the derived formula is " $y=15.686\ln(x)+97.205$ " for Alice.

As can be seen in Figure 13.64, Habanero composites gave a very low gold recovery compared to other Productora samples. Gold recoveries in the rougher were high, however, high losses of gold reported to the cleaner scavenger tail. This indicates that gold has a lower association with copper minerals in the Habanero Lode compared to other Productora and Alice samples. This also confirms the different copper and pyrite flotation performance and that alteration have occurred in the Habanero zone. If V-10 result is excluded (due to close proximity to Central zone) a derived curve of “ $y=10.041\ln(x)+44.117$ ” could be applied to the Habanero zone. More samples need to be tested from Habanero to confirm both copper and gold performance.

The molybdenum performance for all the Productora and Alice samples can be seen in Figure 13.65. Aside from Alice samples, all the Productora samples is in close proximity to the curve derived from the Central In Pit samples, “ $y=16.886\ln(x)-29.974$ ”. The same formula was therefore applied to the Habanero and >10% Acid Soluble samples. A maximum recovery of molybdenum was set at 70%.

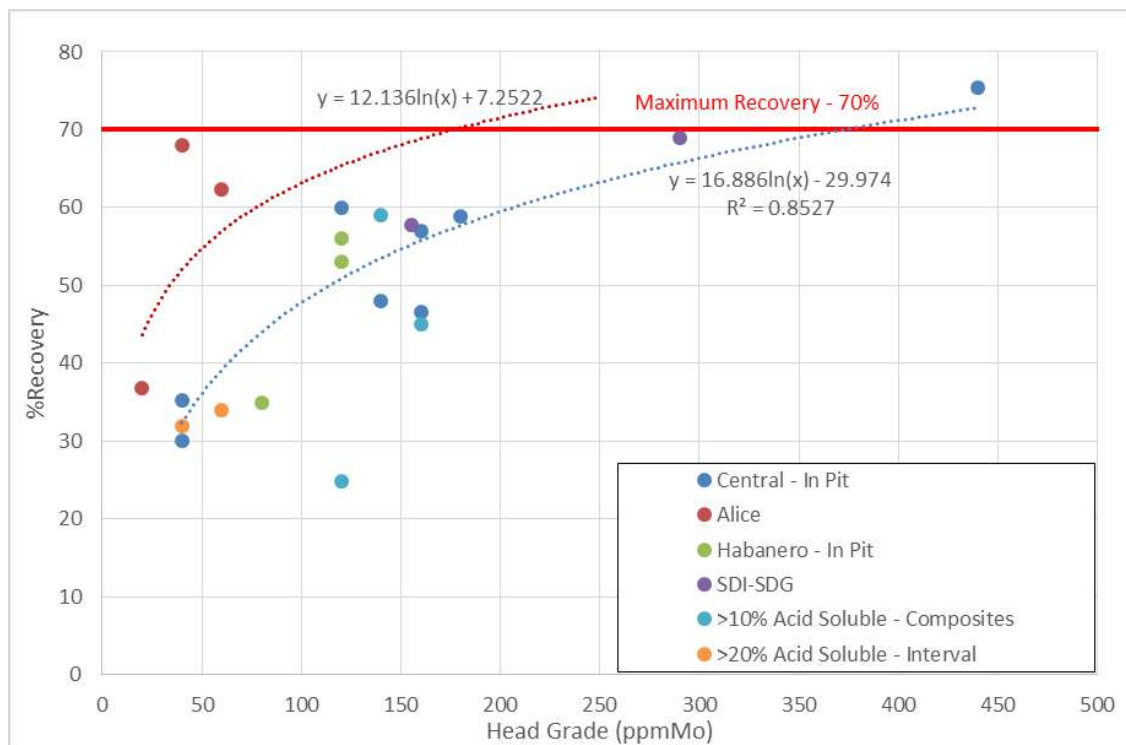


Figure 13.65 Molybdenum head grade vs. recovery

For Alice samples, molybdenum recoveries were a significantly higher than for Productora. As there were only three samples for curve fitting, it is difficult to set to the achieved results, a curve was derived which was similar to the Productora curve, though recovery was 10 to 20% higher. Though higher recoveries were achieved for Alice samples, a maximum molybdenum recovery was still set at 70%. The formula for Alice samples was derived as “ $y=12.136\ln(x)+7.2522$ ”.

13.3.2.7 Copper Sulphide Dewatering Testwork

13.3.2.7.1 Introduction

Tailing and concentrate samples from the sulphide flotation testwork underwent physical testing. The tests conducted included:

- Concentrate thickening and filtration
- Tailings rheology, thickening and filtration.

The tailings samples underwent rheology testwork at ALS Perth and Newpark, tailings evaluation at Knight Piesold and thickening and filtration testwork at Outotec.

The concentrate and tailings samples were prepared from various flotation tests. The concentrate was from bulk flotation conducted for molybdenum testwork. The sample used for the molybdenum testwork was PRP0812 and was supplied as RC Chip. The concentrate tested was at P80=29.9 μm , though it contained a high level of fines (due to being from RC Chip), and copper grade was 23% Cu. The concentrate had the copper/molybdenum separation conducted and was then dispatched to Outotec for thickening and filtration testwork. Due to low flotation mass pulls and high mass requirement for the thickening and filtration testwork, a high mass (300 to 500 kg) is required to produce sufficient concentrate mass. The molybdenum bulk flotation testwork were the only flotation tests to produce enough concentrate. This sample is not ideal (due to being RC Chip) and further testwork should be conducted on concentrate produced from drill core.

Samples for tailings testwork were composited from the rougher tailings from flowsheet development flotation tests. Two composites were made up, one at a P80 grind size of 106 μm and the other of 150 μm . Details of mass for each composite (showing a high proportion of FD-1) used in the tailings samples are shown in Table 13.47.

Dried rougher tailings from the 1kg batch flotation tests, using the RTD 2086 collector, were selected for compositing, to make up 15 kg of dry tailings for each composite. Due to sample limitations, a number of P80=180 μm samples were ground to 150 μm , and a number of P80=125 μm samples were ground to 106 μm . The dry tailings composites were slurried in seawater. Furthermore, to simulate cleaner tailings, approximately 4% of the dry sample mass was ground to $\approx 25 \mu\text{m}$, then added back to each composite.

Table 13.47 Tailings sample make up

FD composite	Tailings sample			
	106µm		150µm	
	Mass (g)	Dist'n (%)	Mass (g)	Dist'n (%)
1	5,170	30.0	6,155	35.7
2	836	4.9	1,547	9.0
6	1,752	10.2	1,744	10.1
8	844	4.9	889	5.2
9	851	4.9	850	4.9
10	855	5.0	887	5.1
11	1,675	9.7	1,739	10.1
12	1,806	10.5	904	5.2
13	1,679	9.8	1,662	9.6
14	1,738	10.1	867	5.0
Total	17,206	100.0	17,244	100.0

13.3.2.7.2 Copper Concentrate and Tailings Thickening Testwork Results

Concentrate from the molybdenum bulk flotation testwork (conducted on reverse circulation chip material) was dispatched to Outotec for thickening and filtration testwork. A bulk Cu/Mo concentrate was produced by the standard RTD2086 flotation scheme and this was then treated with NaHS (sodium hydrosulphide) to separate the copper and molybdenum. The copper concentrate produced was sent to Outotec.

Two tailing sample were prepared to P_{80} of 106µm and 150µm from batch flotation tailings. Both samples were dispatched to Knight Piesold for tailings evaluation. These samples were returned to ALS Perth and just the $P_{80}=150\mu\text{m}$ was forwarded to Outotec for thickening testwork.

Testing showed that the flotation tailings could achieve the desired underflow density of 70% solids (w/w) at 0.5 t/m²h and 10 g/t of flocculant. Under these conditions, the overflow solids content was less than 150 mg/l. For the concentrate, underflow density of 65% solids (w/w) was achievable at 0.25 t/m²h and 10 g/t of flocculant. Overflow solids under these conditions was less than 150 mg/l.

From the testwork, the thickeners recommended for the Project were the Outotec high-rate thickener with Outotec Vane feedwell. Other recommendations are given in Table 13.48.

Table 13.48 Copper concentrate and tailings thickening results

Process stream	Flotation tails	Copper concentrate
Solids feed rate (tph)	1,724	30
Solids loading (t/m ² h)	0.5	0.25
Feed slurry density (% w/w solids)	26	18.3
Slurry pH	7-8	7-8
Flocculant dosage (g/t)	10	10
Underflow density (% w/w solids)	69.6-72.6	66.9-69.9
Overflow clarity (ppm)	<150	<150
Required thickener diameter (m)	1 x 67 or 2 x 47	13

It should be noted that the concentrate used was not ideal, as reverse circulation (RC) chips were used to produce the sample and concentrate. The concentrate contained a high level of fines (from the RC Chip), and this may have influenced the concentrate thickening. More thickening testwork is recommended to be conducted on concentrate generated from diamond drill samples during the feasibility study.

13.3.2.7.3 Copper Concentrate Filtration Testwork Results

The same concentrate sample that was used for thickening testwork was also used for filtration testwork. The thickened product from the thickening testwork (set at 65% solids) was used as the starting product for the filtration testwork. Initially testwork focused on membrane filter press technology and pressure filtration technology was then tested as an alternative to possibly reduce wash times. A summary of the major outcomes from the Outotec report are as follows.

Membrane Filter Press (MFP):

- Pumping and pressing stages are relatively short with air drying achieving further dewatering. Introducing a wash stage significantly increases the total cycle time
- Using high pressure (10 bar) air for drying reduces cake moisture content. Introducing a wash stage increases cake moisture content. Target moisture of 8% was achieved in the 25 mm chamber using 10 bar air for drying
- There is a direct relationship between increasing filtration rate and increasing cake moisture content. Introducing a wash stage significantly decreases filtration rate by increasing total cycle time
- Using a wash volume of 0.34 m³/t, it is possible to achieve a test filtration rate of 56 kg D.S./m²h with a cake moisture content of 9.7%
- Using a wash volume of 0.34 m³/t achieved a total filter efficiency of 98.8%
- Results showed that using a wash volume of 0.34 m³/t results in 355 ppm Cl remaining in the cake (target of <500 ppm) and 625 ppm Cl in the entrained liquor (target 6000 ppm).

Pressure Filtration (PF):

- Cycle time with washing is significantly less for pressure filtration technology than it is for membrane filter press technology
- Target moisture of 8% was not achieved. During testing, the particle size distribution (PSD) was received and the grind size was deemed to be finer than anticipated (correspondence with ALS). With such a fine grind size, the transportable moisture level (TML) would be higher. Testing using MFP technology showed that higher pressure air (10 bar) would lower cake moisture content by approximately 1%
- There is a direct relationship between increasing filtration rate and increasing cake moisture content. Introducing a wash stage significantly decreases filtration rate by increasing cycle time
- Using a wash volume of 0.29 m³/t, it is possible to achieve a test filtration rate of 179 kg D.S./m²h with a cake moisture content of 9.9%
- Using a wash volume of 0.29 m³/t achieved a total filter efficiency of 98.6 %.
- Results shows that using a wash volume of 0.29 m³/t, results in 405 ppm Cl remaining in the cake (target of <500 ppm) and 628 ppm Cl in the entrained liquor (target 6000 ppm).

Filtration testwork was conducted in seawater. Testwork shows that the molybdenum flotation circuit may require a reduced TDS water and the copper concentrate going to filtration would therefore have a lower Cl level than tested.

For the molybdenum testwork, only tap water was tested and not any other reduced TDS levels from seawater. Further molybdenum flotation testwork is required to define a maximum water TDS. This level would then need to be used for further filtration testwork.

It was noted that the sample contained more than the usual level of fines and that this made filtration and the subsequent wash stage difficult. This high level of fines was due to the sample coming from RC Chip. It is therefore recommended that further filtration testwork should be conducted from concentrate produced from diamond drill samples.

13.3.2.7.4 Copper Tailings Rheology Testwork Results

The tailing sample produced for testwork at Knight Piesold (at $P_{80}=106$ and $150\mu\text{m}$) was also used for rheology testwork at ALS Perth and Newpark. Results from the Newpark testwork are shown in Table 13.49.

Table 13.49 Flotation tailings rheology results

FD tailings ($P_{80}=106\mu\text{m}$)		FD tailings ($P_{80}=150\mu\text{m}$)	
Solids (%)	Yield (Pa)	Solids (%)	Yield (Pa)
74	31.02	74	22.56
65	2.268	65	1.62
57	0.594	57	0.216
50	0	50	0
45	0	45	0

Significant comments from the Newpark report include:

- The rheograms show that the samples exhibit shear thinning behaviour
- No significant settling was observed during the testing period for each rheogram
- The percentage solids required to get yield stress readings of 10, 30 and 100 Pa is very high.

13.3.2.8 Molybdenum Flotation Testwork Program

13.3.2.8.1 Introduction

A specific molybdenum testwork program was conducted to determine if a molybdenum concentrate of greater than 50% Mo could be produced. Molybdenum recoveries for each flotation composite were also determined and a relationship determined. Molybdenum flotation was successful, but not fully optimised in either the copper circuit or the molybdenum circuit.

Mineralogically, generally in all the samples tested, molybdenite (MoS_2) had little to no association with other sulphides (copper or iron sulphides). Molybdenite tended to be well liberated in the $-125\mu\text{m}$ fractions, though in the $+125\mu\text{m}$ fraction, liberation was poor and some composites had 100% of the molybdenite as locked.

13.3.2.8.2 Molybdenum Flotation Testwork Results

In the previous section, the batch flotation tests conducted and discussed on the Productora and Alice samples was optimised mainly for the best copper recovery at a 25% copper grade. In the majority of tests, molybdenum was not optimised for recovery. However, the RTD2086 collector (xanthate ester) is generally good for molybdenite recovery.

For some tests, diesel was added to the primary mill to improve molybdenum recovery. For flotation using the A3894/SMBS scheme, the addition of diesel gave a significant increase in molybdenum recovery. With RTD2086, diesel gave improvements in some

floats and was detrimental to copper in other floats. Further testwork with diesel or kerosene is required to determine the benefits of usage and also to optimise dosage.

For the Habanero samples, collector C4403 (xanthate ester with hydrocarbon) was used. This reagent gave increased molybdenum recovery compared to RTD2086.

From the batch flotation open cleaners and locked cycles, molybdenum recoveries were determined for each composite for a 25% copper concentrate. This recovery data was plotted and a line of best fit was derived. For the Central zone, the results gave a good correlation ($R^2=0.85$) and from this data, a formula, “ $16.886\ln(x)-29.974$ ”, for the line of best fit was derived. The graph of molybdenum grade vs. recovery to copper concentrate is presented in Figure 13.66.

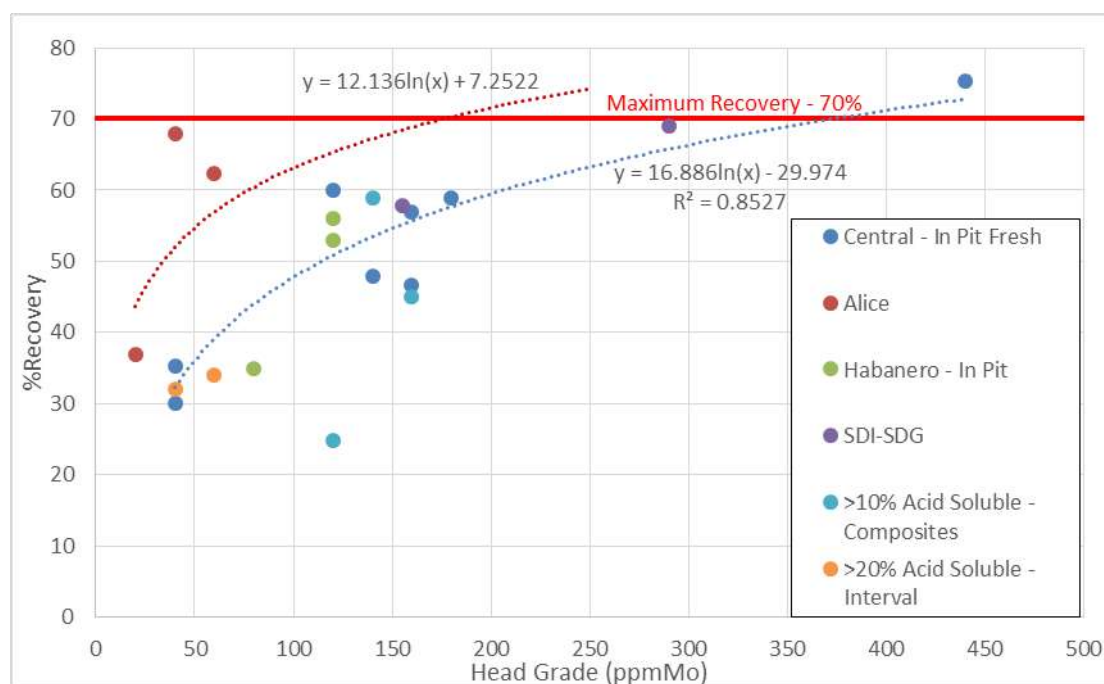


Figure 13.66 Molybdenum head grade vs. recovery

Unlike for copper, molybdenum recoveries for the samples with high acid soluble copper were similar to the Central Fresh In Pit samples. This is due to the molybdenite having little association with copper minerals or pyrite and that molybdenite still floats freely when other minerals have started to oxidise (transitional sulphides).

As can be seen in Figure 13.66, most of the molybdenum head grades are in two groups, with recoveries up to 10 to 15% either side of the line. As the Habanero and high acid soluble copper samples are generally following the Central curve, the same recovery model has been applied to these samples/zones. A maximum recovery of 70% has been set.

For the Alice samples, molybdenum recoveries were significantly higher (+20%) than for Productora samples. Though, as there were only three samples, the recovery curve was lowered to follow the Productora Central curve. A maximum recovery was also set at 70%.

More work is required to better define the molybdenum recoveries to the copper concentrate. More and higher head grade samples are required for the Alice mineralized material. More samples are also required in the transitional and Habanero zones and more in pit samples with head grades between 50 and 100 ppm and 200 to 300 ppm.

Molybdenum recoveries for the rougher and recleaner testwork for Central In-Pit and Alice samples are shown in Table 13.50. Molybdenum recoveries for the locked cycles at 25% Cu are also presented.

Table 13.50 Molybdenum – rougher, cleaner and locked cycle copper results

Sample	Overall molybdenum results (25% Cu concentrate)										
	Head grade (%)	Rougher		Recleaner		Recleaner @ 25% Cu		Locked cycle		Locked cycle @ 25% Cu	
		% Mo	% dist.	% Mo	% dist.	% Mo	% dist.	% Mo	% dist.	% Mo	% dist.
V-2	40	0.14	42.3	0.32	33.2	0.37	26.2			0.37	35.3
V-7	40	0.08	35.2	0.29	42.5	0.29	42.5	0.28	29.4	0.28	30.0
FD-13	120	0.18	67.6	0.36	60.4	0.36	60.4	0.42	59.9	0.42	59.9
FD-6	140	0.79	69.2	1.13	28.8	1.20	40.0	1.34	46.7	1.34	48.0
FD-1	160	0.31	58.8	0.48	24.4	0.75	46.6	0.74	42.9	0.75	46.6
V-8	160	0.24	63.5	0.56	54.7	0.52	56.0			0.52	57.0
FD-2	180	0.23	61.2	0.79	55.5	0.73	56.0	0.89	58.8	0.83	58.8
FD-14	440	0.57	82.4	1.26	69.7	1.26	69.7			1.26	75.4
V-13	60	0.09	66.8	0.26	52.3	0.26	52.3	0.32	62.3	0.32	62.3
V-14	40	0.15	78.2	0.46	61.4	0.42	68.0			0.42	68.0
V-18	20	0.06	43.8	0.19	34.2	0.17	35.0	0.16	36.9	0.16	36.9

13.3.2.8.3 Molybdenum Cleaner Testwork

Flotation testwork was conducted to determine whether molybdenum could be easily separated from the bulk copper/molybdenum concentrate and if a greater than 50% Mo concentrate could be achieved.

The testwork was conducted in two phases. The first phase used the FD-1 composite sample as mentioned before, with only a few tests being completed. These tests gave an initially positive response that a good molybdenum concentrate could be achieved (32% Mo after one stage of cleaning). However, with the low molybdenum head grade and limited sample, molybdenum testwork was not able to be further optimised.

For the second phase of the testwork, a composite was produced from PRP0812 (RC Chips as explained before) with a high molybdenum head grade (0.56% Mo) to produce higher mass pulls through the cleaners. RC Chip samples generally have a high content of fines and can also cause oxidation of the sulphides and subsequent reduction/change in flotation performance (so not an ideal sample, but the best available).

To produce sufficient copper concentrate for the molybdenum testwork, bulk copper cleaner floats (350kg total) were conducted. The concentrate produced was combined, blended and split into 1kg charges. These charges were then tested individually to achieve copper and molybdenum separation.

All tests conducted used NaHS for copper depression and kerosene added to aid molybdenum recovery. The NaHS was used to target a slurry potential. However, the slurry tended to buffer and excess NaHS was required. This resulted in depression of both copper and molybdenum.

The initial tests were all conducted in sea water. The froth during these floats was very poor and quite unstable. Final tests switched to using Perth tap water and a significant change was seen in the flotation performance. Froth was heavily loaded with molybdenite and additional cleaners were able to be performed without depression of the molybdenum.

With the use of tap water, a +50% molybdenum concentrate was easily achieved with little recovery loss. This can be further seen in Figure 13.67 and Figure 13.68. Tests showed that the use of sea water may not be possible in the molybdenum circuit and that a thickening/wash stage may be required prior to the copper/molybdenum separation. Further testwork is required to determine the TDS (total dissolved salts) level that will still give a good molybdenum separation and cleaning.

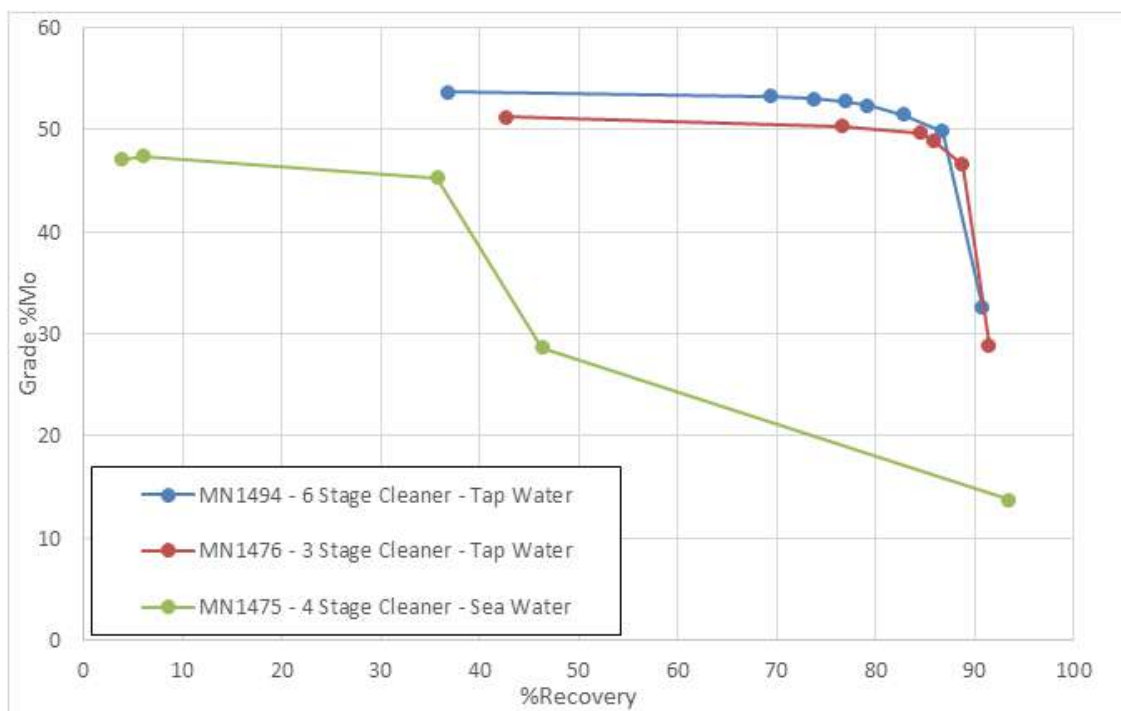


Figure 13.67 Molybdenum cleaner flotation – seawater vs. tap water

Further cleaner tests were conducted with up to six stages of cleaning (MN1494). Results achieved for this was over 53% Mo with 69% recovery (recovery based on molybdenum cleaner feed). The main gangue diluting the grade was mica (muscovite).

Mica can be an issue, as it can be easily entrained. The use of column cells on the final cleaners is recommended to help reduce gangue entrainment.



Figure 13.68 Molybdenum cleaner – tap water test

13.3.3 Mineralogical Analysis

13.3.3.1 Introduction

Mineralogical examination was conducted at ALS Metallurgy (Perth) on samples used for flotation testwork. Mineralogy included x-ray diffraction (XRD) and QEMScan (Quantitative Evaluation of Minerals by Scanning Electron Microscopy). Samples examined included FD-1 to FD-14 (excluding FD-7), V-1 to V-6, V-11 to V-14 and V-18. All samples were either composites from various metallurgical drillholes (FD-1 to FD-4) or composites from sections of a specific metallurgical drillhole (FD-5, V-1 and V-2) or specific sections of a specific metallurgical drillhole (FD-7 to FD-14 and V-3 to V-6 and V-11 to V-15 and V-18).

Mineralogical examination on FD-1, FD-2, FD-3 and FD-4 composite samples (previously referred to as Composite 1, 2, 3 and 4) was conducted as part of an earlier testwork program. However, a summary of results from these composites has been included here.

13.3.3.2 X-ray Diffraction

XRD examination was conducted on each of the Flotation Development samples (FD-1 to FD-14, excluding FD-7), the initial Variability samples (V-1 to V-6), the Habanero MET023 samples (V11 and V12) and the three Alice samples (V-13, V-14 and V-18).

A summary of the main minerals from the XRD results are presented in Table 13.51 to Table 13.55. Data in tables are grouped into mineralized material body zones as was identified during the flotation testwork.

Note: results in the tables preceded by an asterisk generally indicate a larger than usual uncertainty with regard to the quantity of the phase reported; for some of the minor and trace phases it might also indicate an uncertainty in regard of the phase itself, or both.

XRD results for the Productora Central samples (In Pit and Fresh) showed that copper was mainly present as chalcopyrite, with pyrite being the main other sulphide. The main non-sulphide gangue minerals were K-feldspar and alpha quartz. High level of mica (mainly muscovite as indicated in QEMScan) is present in most samples. Due to its platy nature, muscovite can cause issues in sulphide flotation through froth entrainment. The muscovite can carry over to the final concentrate and reduce the grade. This can be of greater issue in the molybdenite circuit and is normally reduced with froth washing.

Table 13.51 XRD results – Productora – Central (In Pit Fresh samples)

Mineral ID	Mass percentage (%)					
	FD-1	FD-2	FD-6	FD-13	FD-14	V-2
Pyrite	5	4	4	5	6	5
Chalcopyrite	-	-	*1	4	4	2
Calcite and/or Chalcopyrite	*2	*2	-	-	-	-
Magnetite/Maghemite	-4	-3	-	< 1	< 1	*1
Clinochlore	9	4	2	5	3	8
Mica	5	4	11	2	3	6
K-Feldspar	30	26	18	25	25	33
Sodic Plagioclase	3	3	3	6	1	3
Alpha Quartz	39	50	54	46	50	38
Clay Mineral	*1	*1	< 1	*1	< 1	*1
Amphibole	<1	*1	*1	< 1	< 1	*1
Serpentine	-	-	< 1	< 1	< 1	< 1
Tourmaline	-	-	4	6	6	-
Dolomite - ankerite	-	-	-	-	< 1	< 1

Table 13.52 gives XRD results for the Productora Habanero samples (In Pit and Fresh). As for the Central mineralized material, the XRD showed that copper was mainly present as chalcopyrite and pyrite being the main other sulphide. K-feldspar is lower than the central mineralized material and the main non-sulphide is alpha quartz. A high level of mica (muscovite) is also present. Sample V-11 also has a high level of kaolinite present.

Table 13.52 XRD results – Productora – Habanero (In Pit samples)

Mineral ID	Mass percentage (%)	
	V-11	V-12
Pyrite	7	5
Chalcopyrite	4	-
Calcite and/or Chalcopyrite	-	< 1
Kaolinite	7	2
Mica	8	7
K-Feldspar	11	12
Sodic Plagioclase	-	*1
Alpha Quartz	62	71
Clay Mineral	< 1	< 1
Tourmaline	*1	*1

Samples from the Alice deposit are shown in Table 13.53. These differ from the Productora Central mineralized material with no K-feldspar and a higher level of sodic plagioclase and clinochlore present. Chalcopyrite and pyrite are the main sulphides present and alpha quartz is the main non-sulphide present. Lower levels of mica (muscovite) are present, though this can still be sufficient to cause issues.

Table 13.53 XRD results – Alice samples

Mineral ID	Mass percentage (%)		
	V-13	V-14	V-18
Pyrite	2	*1	3
Chalcopyrite	*1	*1	*1
Clinochlore	12	7	4
Mica	4	2	3
Sodic Plagioclase	15	26	26
Alpha Quartz	59	56	59
Clay Mineral	*1	*1	< 1
Amphibole	-	*1	-
Calcite	6	5	4

Table 13.54 gives XRD results for the Productora samples that contained greater than 10% acid soluble copper. FD-3, FD-4 and V-1 are from the CCHEN South part of the Productora pit and FD-5 is from the Santa Innes zone. The XRD showed that copper was mainly present as chalcopyrite, though QEMScan mineralogy does show 30% and 40% of the copper as chalcocite for FD-5 and V-1, respectively. FD-3 and FD-4 have less than 10% chalcocite, though both these composites contain bornite and copper intergrowths. All these composites (along with V-9) were identified as having a portion of transitional sulphides (FD-4 has some transitional oxide) present in the composition.

As for the other samples, pyrite is the main other sulphide present, with K-feldspar and alpha quartz being the main non-sulphides. FD-3 and FD-4 had high levels of chlorite, which was not noted in any other composite, and the mica levels are also high.

Table 13.54 XRD results – Productora - >10% acid soluble copper (transitional containing) samples

Mineral ID	Mass percentage (%)			
	FD-3	FD-4	FD-5	V-1
Pyrite	6	6	5	6
Chalcopyrite	2	4	*1	-
Calcite and/or Chalcopyrite	-	-	-	< 1
Magnetite/Maghemite	3	5	< 1	< 1
Clinocllore	-	-	6	4
Mica	12	9	6	9
K-Feldspar	21	23	27	28
Sodic Plagioclase	6	5	8	4
Alpha Quartz	38	35	35	47
Clay Mineral	< 1	< 1	*2	*1
Amphibole	3	3	7	-
Chlorite	8	9	-	-
Serpentine	< 1	< 1	1	-

Samples from the Cayenne deposit, to the north of the pit, are shown in Table 13.55. These gave similar mineral distribution to the Productora in pit samples, however, all but FD-12 and V-3 gave high levels of magnetite being present.

Table 13.55 XRD results – Productora – Cayenne (Out of Pit samples)

Mineral ID	Mass percentage (%)								
	FD-8	FD-9	FD-10	FD-11	FD-12	V-3	V-4	V-5	V-6
Pyrite	1	*1	4	12	2	*1	2	2	2
Pyrrhotite	-	-	-	-	-	-	< 1	< 1	-
Chalcopyrite	*2	*1	*1	*2	1	2	1	2	1
Magnetite/Maghemite	19	13	11	15	4	*2	12	13	11
Clinocllore	13	11	19	13	54	18	25	12	18
Mica	3	2	5	3	1	2	4	2	4
K-Feldspar	27	20	19	16	15	22	24	33	29
Sodic Plagioclase	8	17	10	4	5	13	7	7	6
Alpha Quartz	20	31	21	25	18	38	12	23	27
Clay Mineral	*1	*2	*2	*2	< 1	< 1	*1	*1	*1
Amphibole	3	-	5	6	< 1	-2	11	3	-
Serpentine	*1	-	< 1	*1	-	-	< 1	*1	< 1

13.3.3.3 Particle Mineralogical Analysis (PMA) by QEMScan

A detailed mineralogical analysis was conducted at ALS Metallurgy (Perth) using QEMScan on the FD-1 to FD-14 (excluding FD-7), V-1 to V-6, V-11 to V-14 and V-18 samples.

QEMScan was conducted on samples ground to $P_{80}=150\mu\text{m}$ and sized into three size fractions (+125 μm , -125/+38 μm , -38 μm). Mineralogical analysis was conducted on FD-1, FD-2, FD-3 and FD-4 as part of a previous testwork program. However, a summary of the analysis is included for these composites in the following sections. As for the XRD,

the composite summaries are grouped into mineralized material body zones as determined in the flotation testwork program.

13.3.3.3.1 QEMScan – Productora Central (In Pit Fresh samples)

From the flotation testwork, six of the samples were identified as “In Pit” and also “Fresh”. These were Flotation Development samples FD-1, FD-2, FD-6, FD-13, FD-14, and Variability sample V-2.

Mineral distribution is very similar for each of these samples, with chalcopyrite being the main copper bearing mineral and pyrite the other main sulphide (67% to 85% of the sulphur is contained in pyrite). The main non-sulphide minerals are K-feldspar, quartz, mica and chlorite. These minerals represent between 85% and 91% of the total mass. The main difference in the samples with regards to the non-sulphides is the high mica content in FD-6 (replacing feldspar). Table 13.56 gives the mineral mass distribution for the In Pit Fresh samples.

Table 13.56 QEMScan Mineral Mass Distribution – Productora – Central (In Pit Fresh samples)

Mineral	Mass percentage (%)					
	FD-1	FD-2	FD-6	FD-13	FD-14	V-2
Chalcopyrite	1.69	2.21	0.92	3.71	3.22	1.01
Pyrite	4.20	4.94	3.99	7.33	4.83	4.12
Feldspar	50.8	43.5	25.1	42.8	41.5	59.3
Quartz	19.1	24.5	31.3	25.5	26.8	16.0
Mica	8.66	8.30	26.6	4.00	8.86	8.86
Chlorite	7.88	9.18	5.80	14.6	12.5	6.08

Results of the QEMScan analyses indicate that the bulk mineralogy of composites FD-1 and FD-2 is very similar. Feldspars and quartz together account for about 70% (by mass) of FD-1 and about 68% (by mass) of FD-2. When micas and chlorite are added the overall amount is about 85.5% (by mass) for both samples.

Chalcopyrite and pyrite contents are 1.7% and 4.2%, respectively, in FD-1 and 2.2% and 4.9%, respectively, in FD-2. Notably, in both samples the pyrite content is highest in the -125/+38 µm fraction while the chalcopyrite content increases towards the finest grained fraction.

Mineral abundance ranges from 3.3% to 3.9% of Cu minerals for samples FD-13 and FD-14, and ranges between 1.0% and 2.3% for the remaining samples. Cu mineral abundance increases towards finer fractions. Liberation of Cu minerals varies between about 70 % in samples FD-13 and FD-14, and about 90% in sample FD-6. Liberation improves significantly towards finer fractions in all samples. Liberation of Cu minerals varies between about 70% in samples FD-13 and FD-14, and about 90% in sample FD-6. Liberation improves significantly towards finer fractions in all samples.

The proportion of “free” chalcopyrite (i.e., occurring in particles having 100% chalcopyrite exposure) is estimated to be about 58% and 49% for FD-1 and FD-2, respectively. The chalcopyrite in the -38µm fractions shows the highest degree of

liberation (about 70% “free” chalcopyrite) but the degree of liberation in the two coarser fractions is significantly lower. Locking and association data shows that the unliberated chalcopyrite is strongly associated with silicates. Grain size distribution data indicates that the P_{80} of chalcopyrite reporting to the two coarser size fractions is between 60 μm and 80 μm .

The degree of pyrite liberation for FD-1 and FD-2 is generally better than that of the chalcopyrite, especially in the coarser-grained fractions. Unliberated pyrite is also strongly associated with silicates. Pyrite reporting to the coarse fractions is coarse-grained; the P_{80} is about 100 μm in the -125/+75 μm fractions and 150 to 200 μm in the +125 μm fractions. Although based on a small population of particles (about 0.05% in each sample), it appears that liberation trends for molybdenite are similar to that of the chalcopyrite and pyrite.

Other Cu-bearing minerals present are bornite, Cu silicate (chrysocolla), Cu-bearing silicates (Cu-chlorite, Cu-mica and Cu-clay), Cu-bearing limonite, Cu phosphate (turquoise) and Cu chloride (atacamite). All of these minerals are present in trace amounts and contribute negligible amounts of elemental Cu. All Cu-bearing minerals are grouped together as “Cu minerals”.

Generally, 70% to 90% of molybdenite is classified as “free” or “well liberated”. Molybdenite liberation improves significantly towards finer fractions. Unliberated molybdenite is mainly locked with silicates, and very rarely with apatite, magnetite and pyrite. Unliberated Cu minerals are mainly locked with silicates in binary “Cu minerals + silicates” and “liberated silicates” particles. Some unliberated Cu minerals especially in samples V-4, V-5 and V-6 are locked with magnetite, typically occurring as fine inclusions. Unliberated molybdenite is mainly locked with silicates and very rarely with magnetite. An exception is sample V-6, where the detected molybdenite grains are well liberated even in the +125 μm fraction.

13.3.3.3.2 QEMScan – Productora – Habanero (In Pit samples)

The two MET023 drillhole samples (V-11 and V-12) from the Habanero Lode zone were sized and the three size fractions underwent mineralogical examination by QEMScan.

A summary of some of the minerals present are shown in Table 13.57.

Table 13.57 QEMScan mineral mass distribution – Productora – Habanero Lode samples

Mineral	Mass percentage (%)	
	V-11	V-12
Chalcopyrite	3.20	0.40
Pyrite	7.50	6.80
K-Feldspar	13.9	21.2
Quartz	38.6	36.6
Mica	29.7	26.7
Chlorite	0.10	0.20

Chalcopyrite is the only dominant Cu-bearing mineral detected. Only a couple grains of Cu-(Zn) oxide, covellite and chalcocite/digenite were detected. Chalcopyrite makes up 3.2% by mass in sample V-11, and 0.4% in sample V-12. In both samples, chalcopyrite abundance is significantly higher in the two fine fractions than in the +125µm fraction.

About 65% of the chalcopyrite is classified as “free” or “well liberated”. The degree of chalcopyrite liberation increases significantly towards finer fractions. Unliberated chalcopyrite is mainly locked with silicates in binary “chalcopyrite + silicates” and “liberated silicates” particles. The P_{80} of chalcopyrite in both samples is about 80µm.

Not many molybdenite grains were detected in each fraction. Information regarding the mode of occurrence of molybdenite is only indicative due to the very low grain statistics. The size of some molybdenite grains is close to the detection limit of QEMScan (1 to 2µm), and the phase identification is of low confidence.

Molybdenite liberation is very poor in the +125µm fraction, but improves significantly in the two fine fractions. Unliberated molybdenite is mainly locked with silicates. One molybdenite grain detected is locked with rutile/titanite in sample V-12.

Pyrite is the only dominant sulphide gangue mineral detected, and it (P_{80} about 130µm) is coarser than chalcopyrite. Pyrite makes up about 7% by mass in both samples, and about 80% of it is classified as “free” or “well liberated”. Silicates dominate both samples, and make up about 90% by mass. The main silicates are quartz, micas, K-feldspar, kaolinite and tourmaline.

The Habanero samples have an increased level of pyrite floating into the copper concentrate under the standard RTD2086 scheme. However, aside from higher level of mica, mineralogy does not indicate much difference with the Central zone. There was no copper rimming detected on pyrite, and either it was not observed or pyrite is being active during milling or float.

13.3.3.3.3 QEMScan – Alice Samples

Three samples were prepared from the Alice deposit, namely two sections of drillhole PXP0001 – V-13 and V-14 as well as one section of drillhole MET024 – V-18. The composites were sized and the three size fractions underwent mineralogical

examination by QEMScan. A summary of some of the minerals present are shown in Table 13.58.

Table 13.58 QEMScan mineral mass distribution – Alice samples

Mineral	Mass percentage (%)		
	V-13	V-14	V-18
Chalcopyrite	1.84	1.19	1.03
Pyrite	1.27	0.83	2.18
K-Feldspar/Na-Feldspar	0.46/9.22	0.35/11.3	0.33/4.02
Alibite	25.49	31.87	31.25
Quartz	29.08	29.71	36.40
Mica	11.98	7.35	10.13
Chlorite	8.96	5.88	3.93
Calcite	6.57	5.29	7.54

Chalcopyrite is the only dominant Cu-bearing mineral, with only traces of other Cu minerals detected (a couple of grains of Cu-(Zn) oxide, covellite and chalcocite/digenite). Chalcopyrite makes up between 1.0% and 1.8% by mass, slightly variable between the three samples. Chalcopyrite abundance is significantly higher in the two finer fractions than in the +125µm fraction. About 65% of the chalcopyrite is classified as “free” or “well liberated” in sample V-13, and 75% in samples V-14 and V-18. Unliberated chalcopyrite is mainly locked with silicates. Chalcopyrite has a P₈₀ of 80µm for samples V-13 and V-18, and 98µm for sample V-14.

A very small number of molybdenite grains were detected in a single polished block of each fraction. Molybdenite mode of occurrence is only indicative due to the very low grain statistics. The size of some molybdenite grains is close to the detection limit of QEMScan (1 to 2µm), and the phase identification is of low confidence.

Molybdenite is typically fine-grained (typically less than 53µm). Molybdenite liberation is very poor in the +125µm fraction, but significantly improved in the two fine fractions. Unliberated molybdenite is mainly locked with silicates. Two of the molybdenite grains were locked with calcite.

Pyrite abundance in these three samples is between 0.8% and 2.2% by mass, being less abundant than in samples V-11 and V-12. Pyrite has a P₈₀ about 160µm and about 80% of it is classified as “free” or “well liberated”, in all three samples. Silicates (about 90% by mass) dominate the samples and some calcite (about 6%) is also present. The main silicates are quartz, albite, plagioclase feldspar, micas, chlorite and epidote.

13.3.3.3.4 QEMScan – Productora - >10% Acid Soluble Copper Samples

Four composite samples were prepared from the Productora samples that contained greater than 10% acid soluble copper. The composites were sized and the three size fractions underwent mineralogical examination by QEMScan. A summary of some of the minerals present are shown in Table 13.58.

Table 13.59 QEMScan mineral mass distribution – >10% acid soluble copper samples

Mineral	Mass percentage (%)			
	FD-3	FD-4	FD-5	V-1
Chalcopyrite	1.44	2.17	0.37	0.28
Pyrite	6.00	6.07	4.69	6.31
K-Feldspar	41.90	47.91	46.80	44.57
Quartz	19.57	17.71	19.13	24.35
Mica	14.86	10.04	11.43	16.59
Chlorite	6.54	6.12	8.39	3.65
Magnetite	4.22	3.97	1.80	1.74

Feldspars (dominated by K-feldspar with less albite), quartz and micas, together account for about 76.3% (FD-3) and 75.6% (FD-4) by mass. Chlorite, magnetite, epidote, amphibole, magnetite, apatite, calcite, rutile and titanite (sphene) make up most of the remainder of the non-sulphide gangue component of the samples.

Pyrite contents are close to 6% in both FD-3 and FD-4 with the relative abundance of pyrite highest in the -125/+38 µm fraction. Pyrite is the dominant sulphide gangue. Between 75% and 85% of pyrite are classified as “free” or “well liberated” in all samples. The degree of pyrite liberation varies only slightly across size fractions. Cu mineral rims on pyrite grains were detected in samples FD-5 and V-1, which may potentially result in pyrite dilution of the concentrate during flotation.

Although chalcopyrite is the dominant copper mineral, accounting for about 79.5% of the Cu in FD-3 and 75.3% of the Cu in FD-4, these samples also contain Cu-sulphides (i.e., chalcocite group minerals), bornite and various other copper minerals including Cu-bearing chlorite and mica, Cu-bearing limonite and chrysocolla which together host the remainder of the copper in the sample. In FD-5, chalcopyrite hosts about 40% of the elemental Cu and chalcocite group minerals (i.e. chalcocite/digenite) as well as covellite host most of the remaining Cu. For sample V-1, chalcopyrite hosts about 40% of the elemental Cu while chalcocite group minerals (as well as trace covellite) host most of the remainder.

The proportion of free “Cu minerals” (i.e., occurring in particles having 100% “Cu mineral” exposure) is estimated to be about 60.7% and 52.8% for FD-3 and FD-4, respectively. Locking and association data shows that the unliberated “Cu minerals” are strongly associated with silicates. Some unliberated Cu minerals in sample V-1 are locked with pyrite, typically occurring as rims on pyrite grains. The degree of pyrite liberation is generally better than that of the “Cu minerals”. Unliberated pyrite is also strongly associated with silicates.

13.3.3.3.5 QEMScan – Productora – Cayenne (Out of Pit) samples

Nine samples were prepared from the Cayenne zone. The samples were sized and the three size fractions underwent mineralogical examination by QEMScan. A summary of some of the minerals present are shown in Table 13.60.

Table 13.60 QEMScan mineral mass distribution – Cayenne samples

Mineral	Mass percentage (%)								
	FD-8	FD-9	FD-10	FD-11	FD-12	V-3	V-4	V-5	V-6
Chalcopyrite	1.84	1.71	2.60	8.71	4.06	1.41	4.09	2.50	2.96
Pyrite	2.19	1.17	1.58	1.95	1.68	1.79	1.47	1.33	1.79
K-Feldspar	37.22	44.07	35.14	23.75	54.44	46.20	35.56	41.63	38.92
Quartz	11.25	19.99	13.99	14.02	15.26	22.23	8.82	16.35	20.17
Mica	6.98	3.45	10.01	6.54	4.28	6.18	7.56	7.69	8.64
Chlorite	12.24	10.38	16.37	10.76	10.33	10.79	15.60	6.62	10.25
Magnetite	22.11	16.81	14.24	25.58	6.49	5.55	17.16	20.47	14.44

Mineralogy for the Cayenne zone is similar to the Central zone. The main difference is the high level of magnetite present in most of the Cayenne samples.

Liberation of Cu minerals varies between samples. About 60% of the Cu minerals are classified as “free” or “well liberated” in samples FD-10 and FD-11, about 70% in samples FD-8 and FD-9, and about 90% in sample FD-12. Liberation improves significantly towards finer fractions in all samples, except for FD-12. Silicates and magnetite are dominant non-sulphide gangue minerals accounting for 87% to 95% of sample mass across the sample set. Silicates are mainly feldspars, quartz, micas and chlorite. Some unliberated Cu minerals especially in samples V-4, V-5 and V-6 are locked with magnetite, typically occurring as fine inclusions.

13.3.4 Conclusions

13.3.4.1 Comminution

The comminution testwork showed that the samples tested displayed medium to medium-high competency and would require moderate to high grinding energies. Results indicated average abrasiveness, which will result in relatively moderate ball and liner consumptions. The Alice material seems to be harder and tougher than the material from the main pit.

The comminution testwork results showed that there are probably three comminution circuit options viable, namely:

- Primary crushing followed by SAG and ball milling with recycle crushing – Primary SABC (Option 1)
- Three-stage crushing followed by ball mill circuit – 3CBM (Option 2)
- Two-stage crushing, HPGR and ball mill circuit – 2C/HPGR/BM (Option 3).

13.3.4.2 Copper Sulphide Flotation

A large program of flotation testwork was conducted on the HCH Productora and Alice deposits. Testwork was based on a standardised flowsheet and reagent scheme which

had been determined from previous testwork programs. The scheme used RTD2086 (Xanthate Ester supplied by Tall Bennett) at a natural pH of seawater with two stages of cleaning and a 25µm regrind. Natural seawater pH was preferred as the use of lime in seawater can have negative effects on flotation performance.

A desired copper grade for the final concentrate was 25% Cu. To achieve this, optimisation testwork was conducted on a number of composites to improve copper grade and recovery. Optimisation testwork included the following:

- Primary grind size tests
- Reagent dosage
- Flotation time
- Alternate reagents
- Diesel addition for increased molybdenum flotation
- Seawater vs. tap water.

When optimised conditions were tested, it was identified that samples from different zones were reporting different flotation response. Some samples were also later identified as containing transitional sulphide and oxide material (designated as containing greater than 10% acid soluble copper). These samples gave sub-optimal results with the standardised scheme.

A primary grind size of $P_{80}=125\mu\text{m}$ was selected for all Productora samples to target a similar sulphide P_{80} compared to a plant grind of $P_{80}=150\mu\text{m}$. For the Alice deposit, a primary grind size of $P_{80}=180\mu\text{m}$ was chosen. Alice samples gave good copper recoveries at coarser grind sizes and as a result of the intent to not blend but campaign treat the Alice deposit, the coarser grind size was desirable.

Due to performance and copper recovery variations, for modelling of the copper head grade vs. final copper recovery, samples were grouped based on location, percentage acid soluble copper, flotation performance and alternate reagent schemes. Grouping the samples resulted in the following:

- Central In Pit Fresh – FD-1, FD-2, FD-6, FD-13, FD-14, V-2, V-7, V-8
- Habanero Lode In Pit – V-10, V-11, V-12
- >10% Acid Soluble Cu – FD-3, FD-4, FD-5, V-1, V-9
- Alice Deposit – V-13, V-14, V-18
- Cayenne – FD-8, FD-9, FD-10, FD-11, FD-12, V-3, V-4, V-5, V-6.

The Cayenne zone of the deposit was determined to be out of the current pit and was therefore not optimised and modelled at this stage.

From the optimisation testwork, copper head grade vs. copper recoveries achieved are depicted in Figure 13.69.

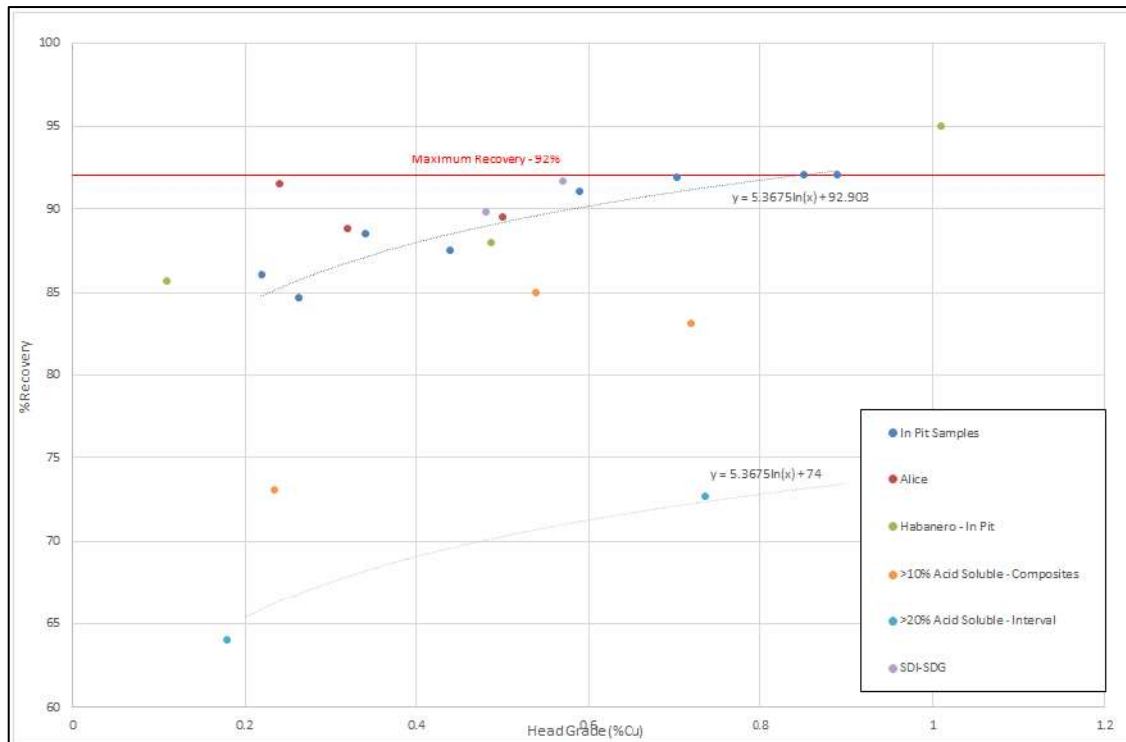


Figure 13.69 Copper head grade vs. Cu recovery

For the Central in-pit samples, the correlation for head grade vs. recovery was very good and had an R^2 of 0.89. The derived curve for the line of best fit was “ $y=5.3675 \ln(x)+92.903$ ” with a maximum set at 92% recovery. Aside from FD2, the reagent regime and flowsheet were as per standard, with RTD2086 collector at seawater pH as received. For FD-2, the A3894/SMBS scheme was used. The final results for the Central in-pit samples are presented in Table 13.61.

Table 13.61 Productora – Central – rougher, cleaner and locked cycle copper results

Sample	Overall copper results (P80=125µm)										
	Head grade (%)	Rougher		Recleaner		Recleaner @ 25% Cu		Locked cycle*		Locked cycle @ 25% Cu #	
		% Cu	% dist.	% Cu	% dist.	% Cu	% dist.	% Cu	% dist.	% Cu	% dist.
FD-1	0.44	9.3	91.4	28.0	78.0	25.0	82.0	28.2	88.8	25.0	87.5
FD-2	0.59	7.2	93.2	26.6	90.2	25.0	90.5	27.2	91.0	25.0	91.0
FD-6	0.22	10.2	90.6	29.7	71.5	25.0	77.0	28.1	85.1	25.0	86.0
FD-13	0.89	11.6	94.5	25.4	90.4	25.0	90.5	27.4	91.7	25.0	92.0
FD-14	0.85	10.5	95.6	25.6	89.3	25.0	89.5			25.0	92.0
V-2	0.26	9.0	88.2	26.9	78.7	25.0	80.5			25.0	84.7
V-7	0.34	8.0	91.9	25.1	90.0	25.0	90.0	29.7	87.5	25.0	88.5
V-8	0.70	10.1	95.9	26.5	92.3	25.0	93.0			25.0	93.5

Note 1: * FD1 Locked Cycle at 106µm primary grind; % dist (% distribution).

Note 2: # Locked Cycle at 25% Cu results were determined either from cleaner grade recovery curves or for tests without a locked cycle, estimated based on losses to cleaner scavenger tail in the open circuit cleaner tests and the expected recovery of copper reporting to the recleaner tail and cleaner scavenger concentrate.

For the Alice samples, recoveries are potentially higher; however, with only three samples, there is not enough data to state this with confidence. The Central in-pit curve was therefore, applied to the Alice mineralized material as well. As stated, flotation was carried out for Alice at P₈₀=180µm instead of the 125µm as for Productora. The Alice samples also used the standard flowsheet (RTD2086), though at the coarser grind size. Final copper results for the Alice samples are presented in Table 13.62.

Table 13.62 Alice – rougher, cleaner and locked cycle copper results

Sample	Overall copper results (P80=180µm)										
	Head grade (%)	Rougher		Recleaner		Recleaner @ 25% Cu		Locked cycle		Locked cycle @ 25% Cu	
		% Cu	% dist.	% Cu	% dist.	% Cu	% dist.	% Cu	% dist.	% Cu	% dist.
V-13	0.50	8.7	91.0	25.4	83.2	25.0	83.5	29.8	88.3	25.0	89.5
V-13								28.7*	91.9*		
V-14	0.32	9.6	91.3	29.3	85.7	25.0	87.5			25.0	88.8
V-18	0.24	7.7	93.8	28.0	90.2	25.0	90.5	25.1	91.5	25.1	91.5

* V13 locked cycle conducted at P₈₀=125µm

For the transitional sulphides, a separate grade recovery curve was determined. This curve was based on results from V-1 and V-9 and also on the Central head grade vs. recovery curve. The grade recovery curve gave on average 18% lower recoveries compared to the Central Fresh in-pit curve. The formula derived is “ $y=5.3675\ln(x)+74$ ”. As this data is based on only two points, more work is required on the “Transitional Sulphides”. The reagent scheme used for the >10% Acid Soluble sample (V-1 and V-9, as well as FD-3, FD-4 and FD-5) was A3894 and SMBS at pH of seawater as received.

This scheme gave significant increases in copper recovery for some composites. This is due to xanthate esters (RTD2086) not always being suitable when secondary copper minerals are present. Final copper results for the >10% Acid Soluble Copper samples are presented in Table 13.63.

As for Alice, the Habanero Lode zone may have increased recovery over the Central zone, though, with only three samples (V-10 bordering Central and Habanero), there is insufficient data to produce a separate head grade vs. recovery formula for Habanero and the Central formula has been applied to the Habanero Lode.

For Habanero, high levels of pyrite floated with the standard RTD2086 scheme. To achieve 25% Cu, collector C4403 was used (xanthate ester with a hydrocarbon). This collector gave greater pyrite selectivity without significant copper loss. It also improved molybdenum recovery.

Table 13.63 >10% Acid Soluble Copper composites – rougher, cleaner and locked cycle copper results

Sample	Overall copper results (P ₈₀ =125µm)										
	Head grade (%)	Rougher		Recleaner		Recleaner @ 25% Cu		Locked cycle*		Locked cycle @ 25% Cu	
		% Cu	% dist.	% Cu	% dist.	% Cu	% dist.	% Cu	% dist.	% Cu	% dist.
FD-3	0.54	5.7	87.5	23.5	84.1	25.0	83.2	30.7	82.3	25.0	85.0
FD-4	0.72	5.8	85.5	26.9	81.6	25.0	82.0	28.8	69.3	25.0	83.0
FD-5	0.24	5.8	78.7	23.8	66.7	25.0	62.5			25.0	73.0
V-1	0.18	5.9	72.1	26.1	48.4	25.0	58.0			25.0	64.0
V-9	0.74	9.8	76.2	29.1	70.8	25.0	71.3			25.0	72.7

* FD-4 locked cycle at 106µm primary grind and RTD2086 scheme

Samples FD-3, FD-4 and FD-5 all have high levels of “transitional sulphides”. FD-4 also contains “transitional oxide”. When the Central curve formula is applied to the fresh portion of these samples and the transitional curve is applied to the transitional portion (as determined by the individual metre samples), the calculated recoveries are similar to the actual recoveries achieved (FD-4 not as good due to the copper oxides present). This further helps to confirm the use of the “Transitional Sulphide” formula.

Although Cayenne samples were not optimised or modelled, locked cycle recovery at 25% Cu was still determined. Results for these are presented in Table 13.64. Results were similar to Productora, with a potentially slightly lower overall copper recovery. Further optimisation would improve data correlation and a head grade vs. recovery curve could be determined if required in the future.

Table 13.64 Cayenne – rougher, cleaner and locked cycle copper results

Sample	Overall Copper Results										
	Head grade (%)	Rougher ¹		Recleaner ²		Recleaner @ 25% Cu		Locked cycle ⁴		Locked cycle ³ @ 25% Cu	
		% Cu	% dist.	% Cu	% dist.	% Cu	% dist.	% Cu	% dist.	% Cu	% dist.
FD-8	0.66	13.6	93.2	25.4	89.0	25.0	89.0			25.0	89.7
FD-9	0.32	12.2	89.1	29.6	76.4	25.0	84.5			25.0	85.6
FD-10	0.44	10.3	88.4	28.8	76.6	25.0	83.2			25.0	84.9
FD-11	0.58	12.2	88.4	28.9	78.6	25.0	85.0			25.0	84.9
FD-12	0.51	15.5	97.3	31.3	84.5	25.0	93.5	31.3	90.3	25.0	94.0
V-3	0.45	11.6	89.5	30.0	79.5	25.0	85.0			25.0	86.0
V-4	0.38	9.5	89.2	28.4	80.1	25.0	84.5			25.0	85.7
V-5	0.32	8.4	90.4	28.1	75.8	25.0	80.0			25.0	86.9
V-6	0.42	11.6	92.2	28.3	85.2	25.0	88.0			25.0	88.7

1. Rougher tests all at 125µm
2. Recleaners all at 106µm except FD-12 and V-5 at 150µm
3. Locked cycle based on 125µm grind
4. FD-12 locked cycle result – Two stage cleaner at 150µm

Gold head grade vs. gold recoveries can be seen in Figure 13.70. As for the copper, a line of best fit was determined for the Central in-pit Fresh zone. The formula derived for this line is “ $y=22.82\ln(x)+104.58$ ”. This formula was also applied to the >10% Acid Soluble samples. A maximum recovery was set at 80%.

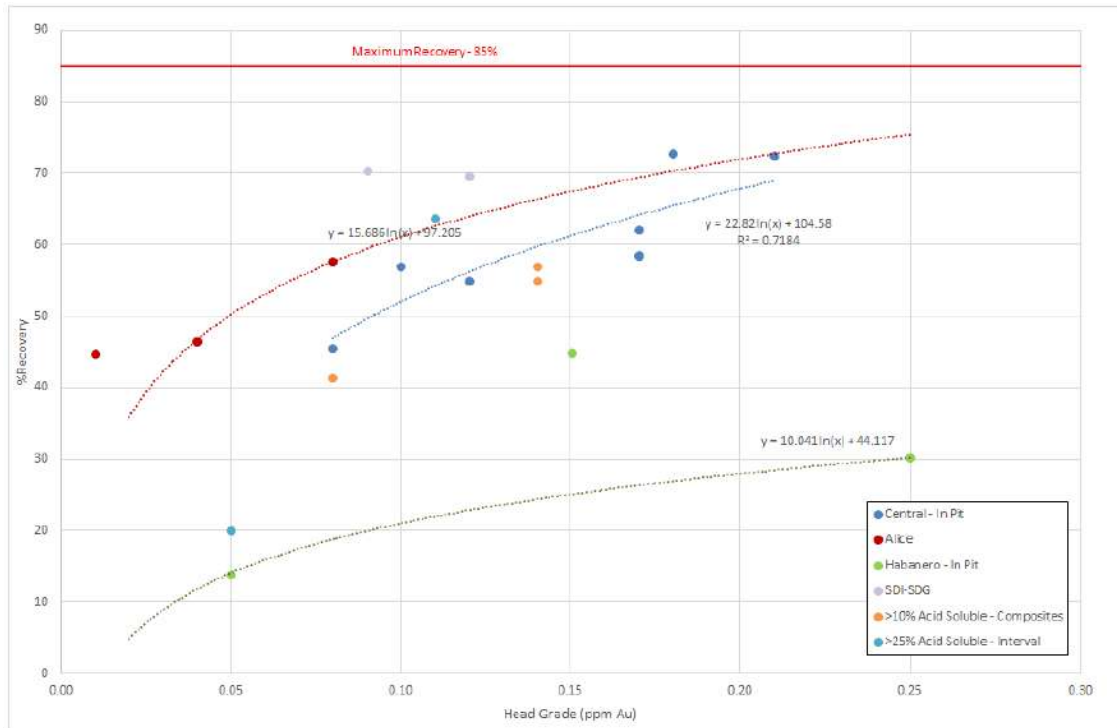


Figure 13.70 Gold head grade vs. recovery

For Alice, gold recoveries were higher than for Productora. Gold head grades for Alice were low and recoveries for greater than a 0.15 ppm Au need to be determined to give confidence in the data. The V18 results were high (for the head grade), therefore, this result was not used for the head grade vs. recovery curve. Based on the remaining two samples, the derived formula for Alice is “ $y=15.686\ln(x)+97.205$ ”.

As can be seen in Figure 13.70, Habanero composites gave a very low gold recovery compared to other Productora samples. Gold recoveries in the rougher were high, however, high losses of gold reported to the cleaner scavenger tail. This indicates that gold has a lower association with copper minerals in the Habanero Lode compared to other Productora and Alice samples. This also confirms the different copper and pyrite flotation performance, and that alteration has occurred in the Habanero zone. If the V10 result is excluded (due to proximity to Central zone) a derived curve of “ $y=10.041\ln(x)+44.117$ ” could be applied to the Habanero zone. More samples need to be tested from Habanero to confirm both copper and gold performance.

13.3.4.3 Molybdenum Flotation

From the mineralogy conducted, molybdenite (MoS_2) had little to no association with other sulphides (copper or iron sulphides). Molybdenite tended to be well liberated in the -125 μm fractions, though in the +125 μm fraction liberation was quite poor and some samples had as much as 100% of the molybdenite locked.

Copper batch flotation testwork conducted on the Productora and Alice samples was optimised mainly to obtain the best copper recovery at a 25% copper grade. In the

majority of tests, molybdenum was not optimised for recovery. However, the RTD2086 collector (xanthate ester) used in the testwork is generally good for molybdenite recovery.

For some tests, diesel was added to the primary mill to improve molybdenum recovery. For flotation using the A3894/SMBS scheme, the addition of diesel gave a significant increase in molybdenum recovery (A3894/thionocarbamate does not collect molybdenum as well as a xanthate ester). With RTD2086, diesel gave improvements in some float tests but was detrimental to copper recoveries in other float tests.

For the Habanero samples, collector C4403 (xanthate ester with hydrocarbon) was used. This reagent gave increased molybdenum recovery compared to RTD2086.

From the batch flotation open cleaners and locked cycles, molybdenum recoveries were determined for each composite for a 25% copper concentrate. Recovery data was tabulated and graphed and a formula was derived (best fit) namely “ $16.886\ln(x)-29.974$ ” for the Central zone. The graph of molybdenum grade vs. molybdenum recovery to copper concentrate is depicted in Figure 13.71.

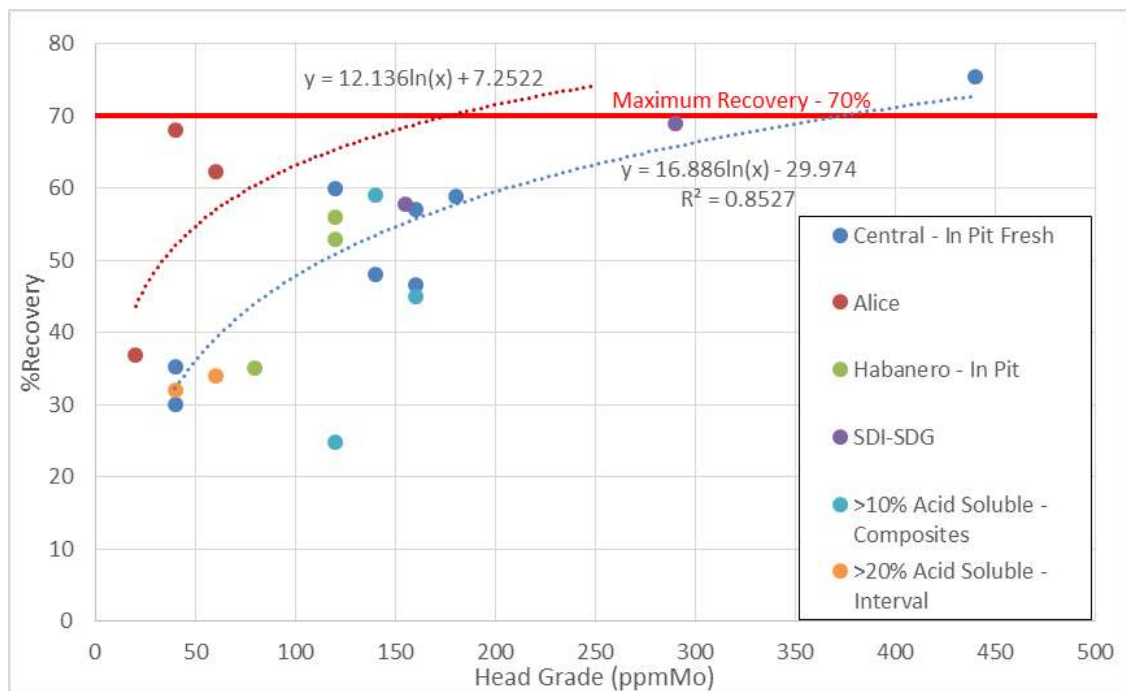


Figure 13.71 Molybdenum head grade vs. recovery

More testwork is required during the PFS stage to better define the molybdenum recoveries to the copper concentrate.

Molybdenum recoveries for the rougher and recleaner testwork as well as molybdenum recoveries for locked cycles at 25% Cu for Central in-pit and Alice composites are presented in Table 13.65.

Table 13.65 Molybdenum – rougher, cleaner and locked cycle results

Sample	Overall molybdenum results (25% Cu concentrate)										
	Head grade (%)	Rougher		Recleaner		Recleaner @ 25% Cu		Locked cycle		Locked cycle @ 25% Cu	
		% Mo	% dist.	% Mo	% dist.	% Mo	% dist.	% Mo	% dist.	% Mo	% dist.
V-2	40	0.14	42.3	0.32	33.2	0.37	26.2			0.37	35.3
V-7	40	0.08	35.2	0.29	42.5	0.29	42.5	0.28	29.4	0.28	30.0
FD-13	120	0.18	67.6	0.36	60.4	0.36	60.4	0.42	59.9	0.42	59.9
FD-6	140	0.79	69.2	1.13	28.8	1.20	40.0	1.34	46.7	1.34	48.0
FD-1	160	0.31	58.8	0.48	24.4	0.75	46.6	0.74	42.9	0.75	46.6
V-8	160	0.24	63.5	0.56	54.7	0.52	56.0			0.52	57.0
FD-2	180	0.23	61.2	0.79	55.5	0.73	56.0	0.89	58.8	0.83	58.8
FD-14	440	0.57	82.4	1.26	69.7	1.26	69.7			1.26	75.4
V-13	60	0.09	66.8	0.26	52.3	0.26	52.3	0.32	62.3	0.32	62.3
V-14	40	0.15	78.2	0.46	61.4	0.42	68.0			0.42	68.0
V-18	20	0.06	43.8	0.19	34.2	0.17	35.0	0.16	36.9	0.16	36.9

13.4 Cortadera

Test work from Cortadera has demonstrated consistent and compatible mineralized material metallurgy to HCH's other nearby deposits (Productora and San Antonio), with all mineralized material sources expected to be processed using sea water and conventional sulphide flotation.

Rougher sulphide flotation results indicate high copper recoveries and similar crushing/grinding characteristics to that used for Productora. This confirms the strategy that Cortadera and Productora be combined into one development, "Costa Fuego", utilising a single conventional processing facility.

Initial rougher recoveries suggest that final copper recovery levels into a commercial grade concentrate are likely to be high. Optimised commercial concentrate grade estimation will be determined following the completion of grind size optimisation, cleaner flotation and locked-cycle test work.

These first results provide a solid foundation from which to carry out further optimisation of the metallurgical flowsheet for life-of-mine mineralized material source supply from the Cortadera deposit.

13.5 Background to the Metallurgical Sample Collection

Two representative composite samples of sulphide mineralized material were selected from Cortadera for metallurgical testwork. The samples comprised quarter drill core sample intervals across the high grade and low-grade drilling intersections within the main porphyry (Cuerpo 3).

13.6 Sulphide Flotation testwork

Key outcomes from the sulphide flotation testwork are as follows (Table 13.66 - Table 13.71 and Figure 13.72):

- Rougher flotation test work over a range of relatively coarse primary grind sizes (106 µm, 150 µm and 212 µm) indicated that the copper recovery in all samples increased as the fineness of grind increased. All grind sizes performed on tests are in-line with results from Productora and indicate similar grind size is likely
- Flotation recovery of copper minerals, gold, and molybdenum at Cortadera is similar to results from Productora. Flotation of silver (absent at Productora) is similar to gold
- Cortadera test work included a high-grade and low-grade sample
- The 106 µm P80 float test on the Cortadera high-grade sample recovered >95% of the copper in the rougher float. Recleaning produced a concentrate grading 28% copper with minor recovery loss
- The corresponding float test on the Cortadera low-grade sample recovered 89% of copper in the rougher float. Recleaning produced a concentrate grading 22% copper with minor recovery loss
- Preliminary recovery estimates for other payable metals at Cortadera include gold (56-60%), molybdenum (83 to 90%) and silver (37 to 59%)
- Molybdenum recovery assays were contaminated by molybdenum contained within the stainless steel of the grinding media. Subsequently, recovery in-line with the copper recovery was assumed and this issue will be addressed in future flotation testwork
- Flotation was performed using salt water in alignment with Productora
- Samples were assayed for multiple elements and no significant levels of concentrate impurities were identified.

Table 13.66 Metallurgical Sample Details

Sample Type		Low Grade	High Grade
Hole ID		CRP0011D	CRP0013D
Cu Head Assay (%)		0.35	
Mass (kg)		35.8	37.6
Location		Collar	Collar
Coordinates (WGS84 Zone 19 South)	Easting (m)	336,008	336,164
	Northing (m)	6,813,547	6,813,692
	Elevation ASL (m)	1,027	1,020
Downhole Distance	From (m)	400	538
	To (m)	422	560

Table 13.67 Recleaner Concentrate Assays for Sulphide Testwork

Sample	Recleaner Concentrate Assays for P80=106µm												
	%			ppm									
	Cu	Fe	S	Mo	Au	Ag	As	Bi	Cd	Pb	Sb	U	Zn
CRP0013D High Grade	28.0	30.0	31.9	2275	7.6	47.9	35	5.1	2.6	158	11	3.8	598
CRP0011D Low Grade	22.1	30.8	33.8	2959	6.8	17.8	29	1.8	1.8	82	2	1.3	150

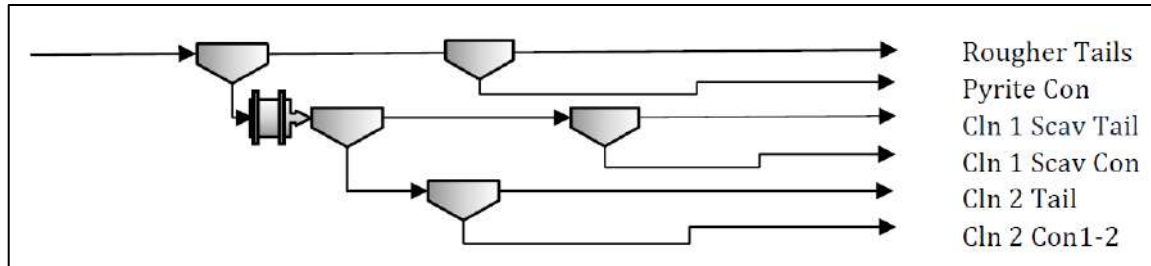


Figure 13.72 Flowsheet of Flotation Testwork

Table 13.68 Flotation testwork results – Sample CRP0013D – P80 Grind Size of 106 µm

PRODUCT	WEIGHT		COPPER		IRON		SULPHUR		MOLYBDENUM		GOLD		SILVER	
	Gram	%	%	% dist	%	% dist	%	% dist	ppm	% dist	ppm	% dist	ppm	% dist
Cln 2 Con 1	20.9	2.09	29.1	82.0	30.1	19.4	32.3	16.6	2456	43.9	7.38	49.5	46	60.1
Cln 2 Con 2	3.5	0.35	21.5	10.2	29.3	3.17	30.0	2.59	1197	3.60	9.04	10.2	59	12.9
Cln 2 Tail	2.3	0.23	3.37	1.04	24.7	1.75	25.4	1.43	314	0.62	5.00	3.67	22	3.15
Cln 1 ScavCon	1.8	0.18	3.20	0.76	29.1	1.59	32.6	1.42	320	0.48	3.00	1.70	26	2.88
Cln 1 Scav Tail	25.4	2.54	0.38	1.28	12.0	9.40	12.5	7.85	269	5.85	0.54	4.43	5	7.94
Pyrite Con	14.7	1.47	0.50	0.99	25.2	11.4	29.4	10.6	132	1.66	1.40	6.59	11	10.1
Tails	931.7	93.1	0.03	3.77	1.85	53.2	2.59	59.5	55	43.9	0.08	23.9	0.1	2.91
Calc'd Head	1000.3	100.0	0.74	100.0	3.24	100.0	4.06	100.0	117	100.0	0.31	100.0	2	100.0
Assay Head			0.78		3.21		4.44		69		0.37		2	
Cln 2 Con 1		2.09	29.1	82.0	30.1	19.4	32.3	16.6	2456	43.9	7.38	49.5	46	60.1
Cln 2 Con 1-2		2.44	28.0	92.2	30.0	22.6	31.9	19.2	2275	47.5	7.62	59.7	48	73.0
Cln 1 Con		2.67	25.9	93.2	29.5	24.4	31.4	20.6	2107	48.1	7.39	63.4	46	76.2
Cln 1 Con + ClnScavCon		2.85	24.5	94.0	29.5	26.0	31.4	22.1	1996	48.6	7.12	65.1	44	79.0
Ro Con		5.39	13.1	95.2	21.2	35.3	22.5	29.9	1182	54.5	4.02	69.5	26	87.0

Note: Cln 2 Tail and Cln 1 Scav Con Au assays estimated due to insufficient weight

Table 13.69. Flotation testwork results – Sample CRP0013D – P80 Grind Size of 150 µm

PRODUCT	WEIGHT		COPPER		IRON		SULPHUR		MOLYBDENUM		GOLD		SILVER	
	Gram	%	%	% dist	%	% dist	%	% dist	ppm	% dist	ppm	% dist	ppm	% dist
Cln 2 Con 1	19.5	1.95	28.9	72.7	30.5	17.8	28.4	13.7	2630	51.8	8.27	45.4	45	45.5
Cln 2 Con 2	5.3	0.53	22.5	15.4	30.6	4.86	32.1	4.22	1329	7.12	8.31	12.4	57	15.7
Cln 2 Tail	3.8	0.38	4.88	2.37	28.5	3.22	31.7	2.97	415	1.58	5.00	5.31	25	4.90
Cln 1 ScavCon	2.1	0.20	3.79	1.00	30.6	1.87	33.7	1.71	253	0.52	3.00	1.73	26	2.76
Cln 1 Scav Tail	25.7	2.57	0.55	1.81	12.2	9.34	11.9	7.55	254	6.59	0.57	4.13	5	6.66
Tails	944.3	94.4	0.06	6.69	2.23	63.0	2.99	69.8	34	32.4	0.12	31.1	0.5	24.5
Calc'd Head	1000.6	100.0	0.78	100.0	3.34	100.0	4.04	100.0	99	100.0	0.36	100.0	2	100.0
Assay Head			0.78		3.21		4.44		69		0.37		2	
Cln 2 Con 1		1.95	28.9	72.7	30.5	17.8	28.4	13.7	2630	51.8	8.27	45.4	45	45.5
Cln 2 Con 1-2		2.48	27.6	88.1	30.5	22.6	29.2	17.9	2352	58.9	8.28	57.8	48	61.2
Cln 1 Con		2.86	24.6	90.5	30.2	25.8	29.5	20.9	2096	60.5	7.85	63.1	45	66.1
Cln 1 Con + ClnScavCon		3.06	23.2	91.5	30.2	27.7	29.8	22.6	1972	61.0	7.52	64.8	43	68.9
Ro Con		5.63	12.9	93.3	22.0	37.0	21.6	30.2	1188	67.6	4.35	68.9	26	75.5

Note: Cln 2 Tail and Cln 1 Scav Con Au assays estimated due to insufficient weight

Table 13.70 Flotation testwork results - Sample CRP0011D – P80 Grind Size of 106 µm

PRODUCT	WEIGHT		COPPER		IRON		SULPHUR		MOLYBDENUM		GOLD		SILVER	
	Gram	%	%	% dist	%	% dist	%	% dist	ppm	% dist	ppm	% dist	ppm	% dist
Cln 2 Con 1	7.5	0.75	25.3	53.5	31.1	7.16	34.3	9.96	3685	32.6	7.41	31.9	17	14.8
Cln 2 Con 2	5.0	0.50	17.3	24.4	30.4	4.68	33.2	6.46	1874	11.1	5.88	17.0	19	11.1
Cln 2 Tail	6.3	0.63	3.40	6.09	30.2	5.89	33.9	8.36	359	2.70	2.10	7.68	8	5.90
Cln 1 ScavCon	3.5	0.35	1.76	1.73	27.6	2.96	30.4	4.11	205	0.84	1.14	2.29	6	2.43
Cln 1 Scav Tail	34.2	3.42	0.38	3.67	12.7	13.4	12.4	16.5	218	8.83	0.31	6.19	2	7.96
Pyrite Con	17.0	1.70	0.32	1.51	21.7	11.4	22.6	14.9	111	2.23	0.41	4.04	2	3.96
Tails	926.5	92.7	0.04	9.16	1.91	54.5	1.10	39.7	38	41.7	0.06	31.0	0.5	53.9
Calc'd Head	1000.0	100.0	0.35	100.0	3.25	100.0	2.57	100.0	84	100.0	0.17	100.0	1	100.0
Assay Head			0.35		3.17		2.99		45		0.17		<1	
Cln 2 Con 1		0.75	25.3	53.5	31.1	7.16	34.3	9.96	3685	32.6	7.41	31.9	17	14.8
Cln 2 Con 1-2		1.25	22.1	77.8	30.8	11.8	33.8	16.4	2959	43.7	6.80	48.8	18	25.8
Cln 1 Con		1.88	15.8	83.9	30.6	17.7	33.9	24.8	2083	46.4	5.21	56.5	14	31.7
Cln 1 Con + ClnScavCon		2.23	13.6	85.7	30.1	20.7	33.3	28.9	1789	47.2	4.58	58.8	13	34.2
Ro Con		5.65	5.60	89.3	19.6	34.1	20.7	45.4	838	56.1	2.00	65.0	6	42.1

Table 13.71. Flotation testwork results – Sample CRP0011D – P80 Grind Size of 150 µm

PRODUCT	WEIGHT		COPPER		IRON		SULPHUR		MOLYBDENUM		GOLD		SILVER	
	Gram	%	%	% dist	%	% dist	%	% dist	ppm	% dist	ppm	% dist	ppm	% dist
Cln 2 Con 1	7.7	0.77	24.2	55.2	30.2	7.51	34.4	10.7	3508	33.5	7.54	33.4	17	16.6
Cln 2 Con 2	4.1	0.41	18.2	21.8	29.9	3.91	33.4	5.46	1905	9.57	6.76	15.8	17	8.76
Cln 2 Tail	4.8	0.48	4.15	5.94	30.3	4.74	32.5	6.34	450	2.70	2.57	7.18	7	4.31
Cln 1 ScavCon	2.9	0.29	1.94	1.67	28.7	2.70	28.9	3.38	180	0.65	1.46	2.45	5	1.85
Cln 1 Scav Tail	31.9	3.19	0.45	4.20	13.6	14.0	13.3	17.2	224	8.87	0.28	5.13	2	8.12
Tails	948.6	94.9	0.04	11.2	2.19	67.1	1.49	57.0	38	44.7	0.07	36.1	0.5	60.3
Calc'd Head	1000.0	100.0	0.34	100.0	3.10	100.0	2.48	100.0	81	100.0	0.17	100.0	1	100.0
Assay Head			0.35		3.17		2.99		45		0.17		<1	
Cln 2 Con 1		0.77	24.2	55.2	30.2	7.51	34.4	10.7	3508	33.5	7.54	33.4	17	16.6
Cln 2 Con 1-2		1.17	22.2	77.0	30.1	11.4	34.1	16.1	2955	43.0	7.27	49.2	17	25.4
Cln 1 Con		1.66	16.9	82.9	30.2	16.2	33.6	22.5	2224	45.8	5.90	56.4	14	29.7
Cln 1 Con + ClnScavCon		1.95	14.7	84.6	29.9	18.9	32.9	25.9	1919	46.4	5.24	58.8	13	31.5
Ro Con		5.14	5.84	88.8	19.8	32.9	20.8	43.0	867	55.3	2.16	63.9	6	39.7

13.7 Key outcomes from Comminution testwork

Key outcomes from the comminution testwork are as follows (Table 13.72):

- Samples were sent for SAG Mill Comminution (SMC) Testing, which determines the so-called JK Drop-Weight Index (DWi), a measure of the strength of the rock when it is broken under impact conditions. The DWi is directly related to the JK rock breakage parameters A and B and can therefore be used to estimate the values of these parameters.
- The same tests were used to design the sulphide concentrator for Productora.

- The comminution results for the high grade and low grade at Cortadera are within the range of Productora values measured. It is reasonable to assume that the sulphide mineralized material from Cortadera will have a similar processing throughput and cost as mineralized material from Productora.

Table 13.72 Summary of Comminution Testwork Results

Comminution Test Result	Productora		Cortadera	
	Average	Range (24 Samples)	Low-grade	High grade
Axb	48	31.3 – 78.0	30.2	33.1
DWI	7.4	4.6 – 9.6	9.0	8.3
SG	2.65	2.07 – 3.01	2.73	2.74

13.8 Conclusions and Recommendations

13.8.1 Cortadera

The metallurgical test work undertaken on a high- and low-grade sample supports processing of the Cortadera sulphide mineralized material using the conventional concentrator at Productora.

Following these initial positive results, the next phase of test work will be directed towards grind size optimisation, cleaner flotation and locked-cycle test work in advance of assessing the commercial grade of copper concentrates that may be produced from the Cortadera mineralized material.

13.8.2 Productora

13.8.2.1 Copper Sulphides

Based on metallurgical issues and to better represent the current Productora and Alice pits, recommended further testwork includes:

- Increase samples from the transitional zones and a flotation program investigating transitional sulphide performance. Investigate alternate reagent schemes
- Testing of fresh primary copper samples and determining head grade vs. recovery for copper, gold, and molybdenum for the CCHEN South zone. All composites tested in this program contained transitional sulphides. Further testing on 100% transitional sulphides should also be conducted
- Single stage cleaner flotation kinetics. Determine kinetics, optimise regrind, reagent dosage, flotation time and flotation scrape rate. Use this data to create a grade recovery curve for a single stage of cleaning
- Further collector optimisation. Test RTD2086, C4403 and equivalent replacements to determine if a single collector can be used.

- Further test the A3894/SMBS scheme to optimise dosage of both A3894 and SMBS and optimise flotation time. Determine if the A3894/SMBS can be applied to other than transitional sulphide composites
- Test A3894/SMBS with the addition of diesel or kerosene to define improvements to molybdenum recoveries. Refine dosage of diesel/kerosene
- Test diesel/kerosene with other collectors and the effect it has on reducing sulphur recovery
- Further test xanthate (SEX) scheme with diesel/kerosene to aid pyrite rejection. Also test SEX/SMBS and other pyrite depressants
- Test collector dosage and flotation time and if it can be related to head grade (copper and sulphur). Most composites were tested with a set collector dosage and flotation time
- For the Habanero zone, test lower levels of RTD2086 and reduced flotation time and scrape rate
- Test more Habanero samples with C4403 and other collectors to determine an optimised head grade vs. recovery for copper gold and molybdenum
- Conduct mineralogy on Habanero concentrate and cleaner tailings to investigate reason for active pyrite and what the gold may be associated with (may be difficult with low head grades)
- Test more Habanero composites to determine gold head grade vs. recovery relationship and if possible, determine gold associations and if recovery can be improved
- Test more samples from the Alice deposit and investigate alternate reagent schemes. Further refine the head grade vs. recovery for copper, gold and molybdenum
- Re grind size. Conduct multiple re grind size tests for different parts of the mineralized material body. Determine optimal re grind size for each zone. For some areas, the re grind size may be able to be coarser, whereas other areas may need to be finer
- Relate re grind size to rougher mass pull and the effect it will have on re grind mill size. Conduct IsaMill (or similar) signature plots to determine re grind power requirements
- Investigate flotation scrape rate for improved copper grades by the rejection of entrained non-sulphide gangue (mainly mica)
- Water type. Test water with varying reduced levels of TDS on a number of reagent schemes (RTD2086, A3894/SMBS, SEX/Lime, etc.)
- Conduct BWi, RWi, Ai and JKDWi tests on additional diamond drillholes from some areas in the main pit (five samples) and the Alice deposit (another two samples)

13.8.2.2 Molybdenum

Aside from refining molybdenum recovery in the copper concentrate, further bulk testwork should be conducted from multiple zones within the Productora and Alice pits to optimise molybdenum grade and recoveries. Samples should be drill core and not reverse circulation chip. Further testwork could include the following:

- Bulk copper flotation on multiple pit zones (two or three, 500 to 1,000 kg each, dependent on head grades)
- Test the regrind size. Determine the optimum copper regrind size and does molybdenum grind size need to be reduced
- Conduct mineralogy on copper and molybdenum concentrates. Identify sulphide and non-sulphide gangue and their liberation and associations with molybdenite
- Water TDS tests. Conduct tests at TDS levels varying from potable to seawater levels. Determine whether molybdenum flotation will work successfully at a higher TDS than tap water
- If TDS levels increase, as concentrate washing will be affected, thickening and filtration testwork will need to be conducted at the determined TDS levels
- Test drill core only
- Test effect of diesel or kerosene on molybdenum recovery in copper and molybdenum circuits. Determine ideal dosage and whether it varies for different zones in the pit
- Conduct molybdenum testwork with a wider range of head grades from each distinct pit zone.

14 MINERAL RESOURCE ESTIMATES

14.1 Productora

14.1.1 Model Area

The area to be modelled is approximately 3km in easting and 8km in northing and has been split into three sub-areas defined by the Rancho and Serrano faults. The north area is further split by another four faults as illustrated in Figure 14.1.

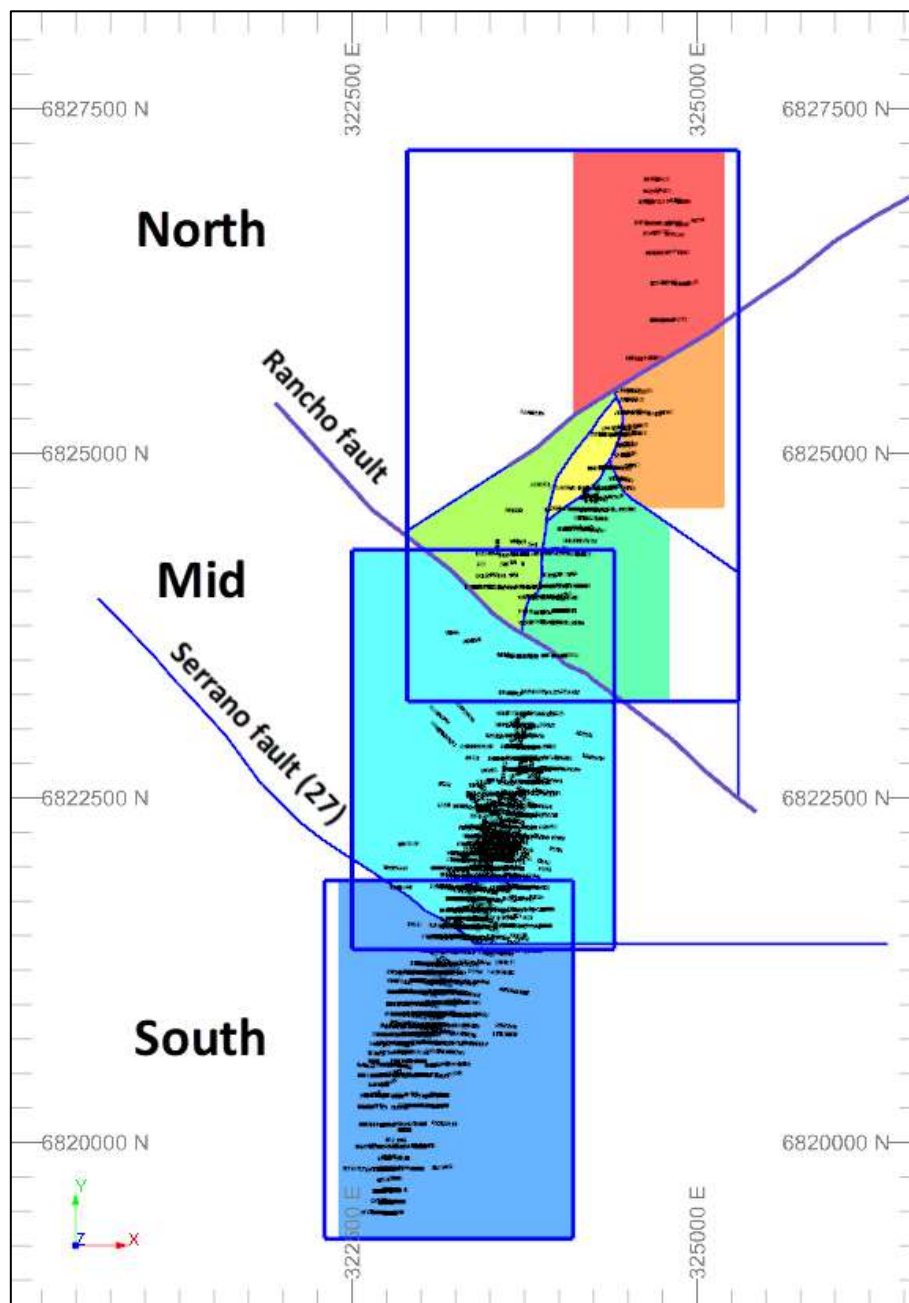


Figure 14.1 Productora model areas, drillhole traces and fault blocks coloured

14.1.2 Database

14.1.2.1 Database Validation

The Productora database was validated through multiple checks. Validation steps included, (but were not limited to) the following:

- Drill collars – a comparison of planned and actual survey pick up coordinates is completed to check for any discrepancies or potential mislabelling of holes or survey errors.
- Drill collars are checked by 3D visual validation of location against expected centre of drill pads (as corresponded with the digital terrain model).
- A drill program “tracker” spreadsheet was filled out by field geologists during the drilling program. This tracker stores details such as hole identification, date drilled, geologist responsible for logging, sample dispatch date etc. The tracker data was cross-referenced with the final database export.
- Downhole surveys were cross-referenced against planned survey orientation, and drill traces were checked visually in 3D for obvious errors.
- Mineralisation intensity logs were completed for each drillhole, and this was compared by field geologist with the returned assay results from the laboratory. This mineralisation intensity log also serves as a tool for calibration of geologist’s mineralisation logging, and as a check for any obvious deviations between mineralisation intensity and assays returned.
- A 3D visualisation of assays is completed to check for any possible downhole sample smearing/contamination.
- Data entry objects are reviewed and validated through data import validation rules when imported into the AcQuire database. This ensured that there were no overlapping intervals, no blanks (data gaps), and that geological coding (and similar logging field) are valid.
- Routine batch QA/QC analysis such as results for certified standards, blanks and field duplicates are checked before loading to the AcQuire database.
- AcQuire database exported csv files are loaded into the Datamine database and secondary validation was performed by Datamine software on import (i.e., checks for overlapping intervals, survey depths greater than hole depths etc.).

The above validation and audit steps have ensured that the database contains minimal errors, and thus the database is considered suitable for this resource estimate.

In addition to the above routine steps, a detailed internal review of data management was undertaken in 2014 which involved several randomly chosen holes, and a full comparison between of lab certificates, data transfer and steps, and a check against final results as stored in the database. This review deemed the data and processes were satisfactory.

14.1.2.2 Summary of Data Used in Estimate

All drilling data is stored in the Hot Chili Limited exploration acQuire™ drillhole database. The system is backed up daily to a server based in Perth.

Data table records consist of:

- Collars – Collars.csv
- Surveys – Survey.csv
- Assays – PROD_assayPREF_20150622.csv
- Assays – Assays_missing.csv
- Geology – Lithology_edit.csv
- Geology – Alteration_edit.csv
- Geology – Weathering.csv
- Geology – Veining_edit.csv
- Geology – Mineralisation_edit.csv
- EH_Fault1.csv
- EH_Fault2.csv
- EH_Fault3.csv
- Colours_modifiedEH.csv

Minor errors and overlaps were adjusted with a full list of actions in Table 14.1 to Table 14.6.

Table 14.1 Drillhole data edits to lithology table

ACTION	HOLEID	FROM	TO
Delete	PRP0765	2	2
Delete	PRP0783	232	232
Delete	PRP0807	155	155
Delete	PRP0626D	575.4	583.3
Delete	PRP0756	133	250
Delete	PRP0783	232	243

Table 14.2 Drillhole data edits to alteration table

ACTION	HOLEID	FROM	TO
Delete	PRD0006	440.6	446.56
Delete	PRP0032D	186.63	189.1
Delete	PRP0057D	447.2	447.7
Delete	PRP0063D	173.7	179.6
Delete	PRP0080D	291.55	292.9
Delete	PRP0424D	169	174
Delete	PRP0760	313	313
Delete	PRP0772	346	346
Delete	PRP0868	45	45
Change 'TO' to 223.4	PRP0874D	222	222
Delete	PRP0878	213	213
Delete	PRP0879	282	282

ACTION	HOLEID	FROM	TO
Delete	PRP0893	209	209

Table 14.3 Drillhole data edits to weathering table

ACTION	HOLEID	FROM	TO
Change 'FROM' to 1	NS4D	2	2
Delete	PRP0541D	441	441
Delete	PRP0795	84	84

Table 14.4 Drillhole data edits to faults table

ACTION	HOLEID	FROM	TO
Change 'TO' to 494.1	PRP0457D	494	494

Table 14.5 Drillhole data edits to Mineralisation table

ACTION	HOLEID	FROM	TO
Delete	PRP0854	337	337

Table 14.6 Drillhole data edits to Veining table

ACTION	HOLEID	FROM	TO
Delete no values	PRP0086	10.98	10.98
Delete no values	PRP0086	14.5	14.5
Delete no values	PRP0086	27.94	27.94
Delete no values	PRP0086	132.66	132.66
Delete no values	PRP0086	157.23	157.23
Delete no values	PRP0086	159.16	159.16
Delete no values	PRP0086	164.93	164.93
Delete no values	PRP0086	165.63	165.63
Delete no values	PRP0089D	237.58	237.58
Delete no values	PRP0089D	297.17	297.17
Delete no values	PRP0089D	314.63	314.63
Delete no values	PRP0089D	324.16	324.16
Delete no values	PRP0112D	224.67	224.67
Delete no values	PRP0112D	226.27	226.27
Delete no values	PRP0112D	240.47	240.47
Delete no values	PRP0244D	241.73	241.73
Delete no values	PRP0244D	249.29	249.29
Delete no values	PRP0244D	277.9	277.9
Delete no values	PRP0244D	282.98	282.98
Delete no values	PRP0244D	285.36	285.36
Delete no values	PRP0244D	300.28	300.28
Delete no values	PRP0244D	302.33	302.33
Delete no values	PRP0244D	336.54	336.54
Delete no values	PRP0244D	363.91	363.91
Delete no values	PRP0244D	384.6	384.6

ACTION	HOLEID	FROM	TO
Delete no values	PRP0244D	387.7	387.7
Delete no values	PRP0244D	389.79	389.79
Delete no values	PRP0244D	393.3	393.3
Delete no values	PRP0300D	88.91	88.91
Delete no values	PRP0300D	94.73	94.73
Delete no values	PRP0300D	96.26	96.26
Delete no values	PRP0300D	115.65	115.65
Delete no values	PRP0300D	130.17	130.17
Delete	PRP0620	219	219
Delete	PRP0626D	150	150
Delete	PRP0735	144	144

All instances of commas were replaced with semi-colons in Lithology table 'Comments' field.

Geological and assay information for the deposit has been obtained by reverse circulation (RC) and diamond drilling (DD). A selection of holes drilled for metallurgical sampling was excluded from the database for estimation along with some holes which had no sampling information. The excluded hole list is in Table 14.7

Table 14.7 Drillholes excluded from the database

MET001	MET011	MET023	PR-12
MET002	MET012	MW12	PR-13
MET003	MET014	NS7AD	PR-14
MET004	MET015	PR-1	PR-15
MET005	MET016	PR-4	PR-16
MET006	MET017	PR-6	PR-17
MET007	MET018	PR-7	PR-18
MET008	MET020	PR-8	PR-19
MET008B	MET021	PR-10	PR-24
MET009	MET022	PR-11	

A summary of the drilling data used to compile the estimate is listed in Table 14.8.

Table 14.8 Productora drillhole database

Drilling Method	Holes	Metres
RC	532	233,672.00
DD	16	7,795.05
RC with DD tail	58	42,257.57

The average drillhole spacing across the deposit is nominally 40mE by 80mN with substantial infill drilling at 20mE by 20mN and areas where the coverage is sparser.

14.1.3 Data Manipulation

Specific negative grade values are used in the assay database to indicate a number of events or conditions. To successfully use these assays for grade estimation, edits were made to remove non-numeric, zero and negative values.

For Copper, Gold, and Molybdenum:

- If the assay value was less than zero, the assay was set to missing.
- If the assay value was equal to zero and there was a recorded weight of sample the assay was set to 0.001.
- If the assay value was equal to zero and there was no recorded weight of sample the assay was set to missing.

14.1.4 Geological and Mineralisation Interpretation

Multi-element mineralisation at Productora is developed mostly within a large intrusive hydrothermal breccia-dominated domain that trends in a north-north easterly direction.

The host-breccia has been modelled from drillhole data over the following dimensions:

- Strike length: 7,900m
- Depth from surface: 700m
- Width: 850m

The breccia does not outcrop within the lease area. However, the distinctive nature of the host and controlling structural mechanisms have been observed in the extensive core collection produced by HCH, together with underground inspection of the mineralized material controls in the Productora Mine.

The predominant style of the breccia is narrow, north to northeast trending tourmaline-cemented bodies. Sub-vertical feeder stocks, of 2m to 5m width at depth, increase with elevation, to wider high-grade mineralisation zones. These wider brecciated zones vary in orientation with central lodes tending to be sub-vertical with an upper flex in wider mineralised zones to dip approximately 70° towards the west, also flanking shallower eastern and western lodes dip moderately west and east respectively. There are also some locally steeply east dipping lodes (e.g., Habanero).

Drilling at deeper levels at Productora has demonstrated thinning breccia lodes, with some ductile features, that continue to a greater depth.

The copper, gold and molybdenum mineralisation are also strongly coincident with the potassic alteration. Determining the detailed primary host lithology, within and proximal to mineralisation, is problematic due to structural and hydraulic damage, and also extensive fluid-alteration overprinting.

Secondary and relatively lower-grade mineralized material controls are evident as manto or manto-like horizons in the southern, far northern and far eastern flanks of Productora. Lodes within the manto horizons are typically shallow dipping at -20° to -30° to the east or west and enclosed by lower grade mineralisation.

14.1.5 2013 Predictive Modelling

Hot Chili Limited in 2013 delivered the 3D predictive Productora mineral system alteration model. The predictive targeting model comprises five components derived from a combination of alteration geochemical indices, lithogeochemical indices, geological and geotechnical logging. Components of this model are detailed under the headers below.

14.1.5.1 3D alteration model

A comprehensive set of alteration indices have been derived from ~160,000 drillhole sample database (comprising: 33 element, 4 acid digest, ICP-OES data, plus Au by FA) through the application of multi-variant X-Y & Ternary analysis of all available geochemistry data (Figure 14.2, Figure 14.3 and Figure 14.4). An alteration classification has been applied to every drillhole sample interval, and interpolated utilising Leapfrog to create a comprehensive 3D model of the alteration domains within the Productora Mineral System (Figure 14.5).

The Productora hydrothermal alteration model comprises seven distinct alteration assemblages/domains:

1. K-Feldspar Domain: highly potassic proximal alteration spatially associated with tourmaline (+/- magnetite) breccias hosting the bulk of Productora copper sulphide mineralisation. (magmatic-hydrothermal fluid source, most probably related to the polyphase Ruta 5 intrusion).
2. Sericite Domain: proximal-intermediate moderately potassic alteration, usually just outboard of the K-spar/tourmaline breccia domain. The sericite alteration domain also hosts significant Cu mineralisation both as tourmaline breccia lodes and finely disseminated Habanero-style mineralisation (Magmatic-hydrothermal fluid source).
3. Sericite-Albite Domain: intermediate alteration, locally mineralised on discrete structures. The Sericite-Albite domain represents an important indicator of proximity to the mineralised potassic alteration domains, forming a large alteration halo up to 300m radius around the outer extents of the ore grade mineralisation (Magmatic-hydrothermal fluid source).
4. Albite Domain: distal alteration signal for the Productora mineralising event (Magmatic-hydrothermal fluid source).
5. Sodic-Calcic Domain: regional sodic-calcic alteration assemblages, most likely associated with circulation/convection of non-magmatic resident formation fluids, with possible evaporitic brine component. The sodic-calcic alteration appears to have been overprinted by the magmatic-hydrothermal alteration associated with copper mineralisation, and thus likely either predates the main copper mineralising event or represents a second “resident” fluid mixing with the magmatic hydrothermal fluids.
6. Magnetite-Amphibole Domain: magnetite-amphibole alteration seems to be a hotter more focussed/localised component of the basinal/resident hydrothermal fluid system. It is closely associated with strata-bound “manto-style replacement” magnetite/pyrite/chalcopyrite mineralisation as well as locally semi-massive structurally-controlled magnetite deposits to the West of the main Productora

mineral system. Copper mineralisation observed within the magnetite-amphibole alteration domain exhibits much closer morphological and mineralogical affinities with Candelaria-style IOCG mineralisation, with chalcopyrite in magnetite-rich breccias.

7. “Kaolinite” Domain: The “Kaolinite” alteration domain samples have been so-named because they plot close to the Kaolinite composition on a K:Al:Fe ternary plot. These samples are not simply kaolinite altered. Rather, they reflect a Si/Al rich assemblage that seems to have been stripped of almost all mobile elements (Na/K/Cu/Fe, etc.). This sample group is completely stripped of all chalcophile elements (with copper at <<average crustal abundance). The Kaolinite classified samples exhibit significant overlap with the acid alteration and intrusive complex described below.

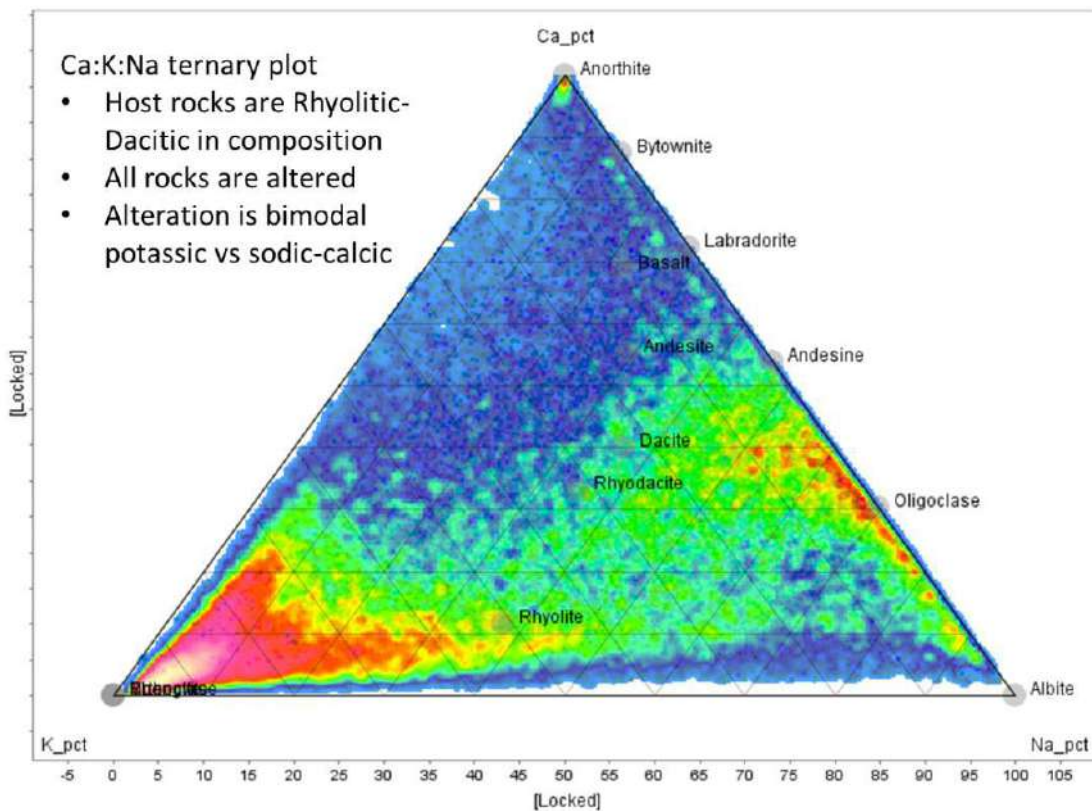


Figure 14.2 Ca:K:Na ternary plot showing bimodal alteration assemblage diverging from precursor rhyodacitic whole rock compositions (~160,000 down hole multi-element geochemistry data points).

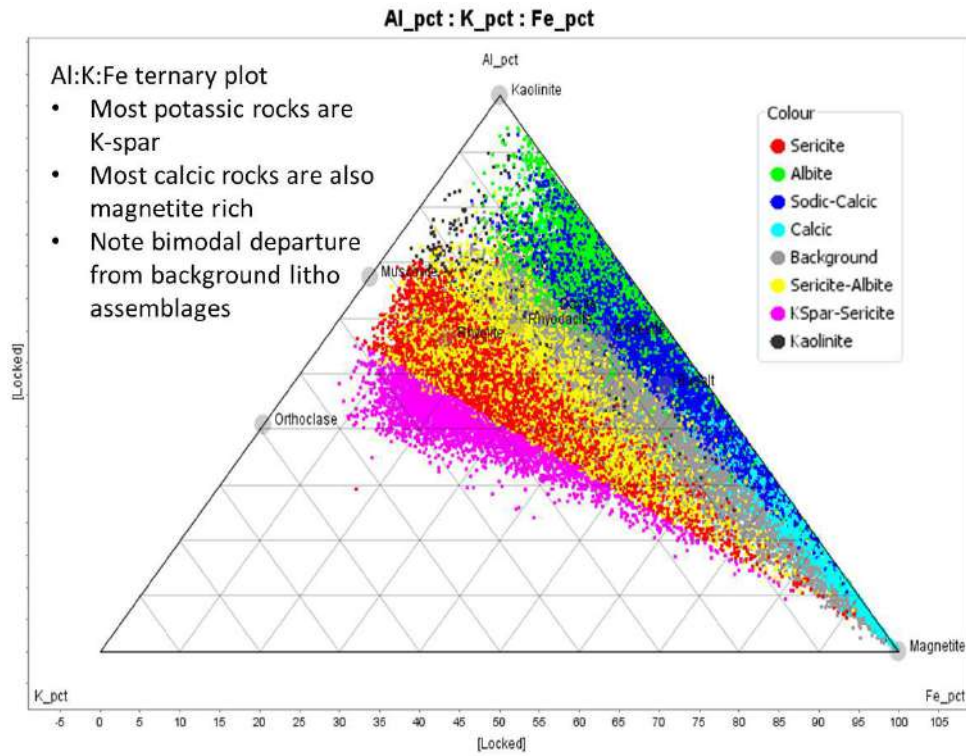


Figure 14.3 Al:K:Fe ternary plot demonstrating alteration index classification of ~200,000 data points relating to every drillhole sample interval within the Productora Project drillhole database.

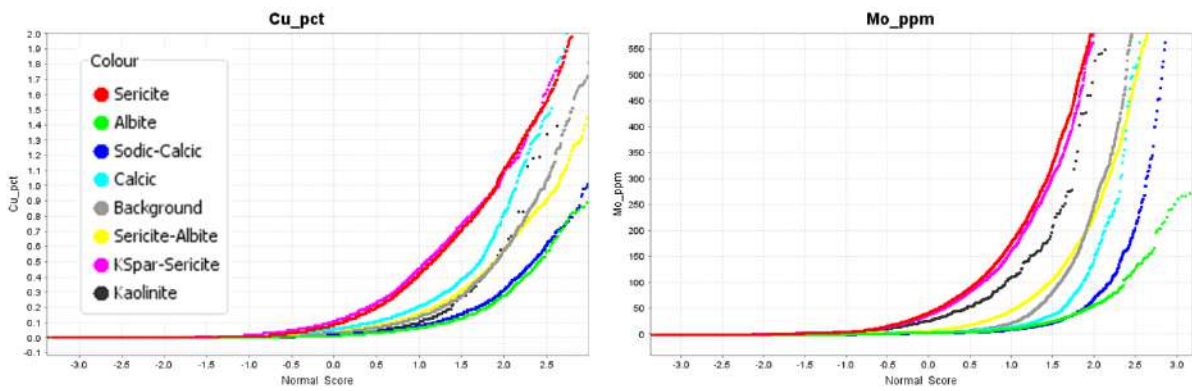
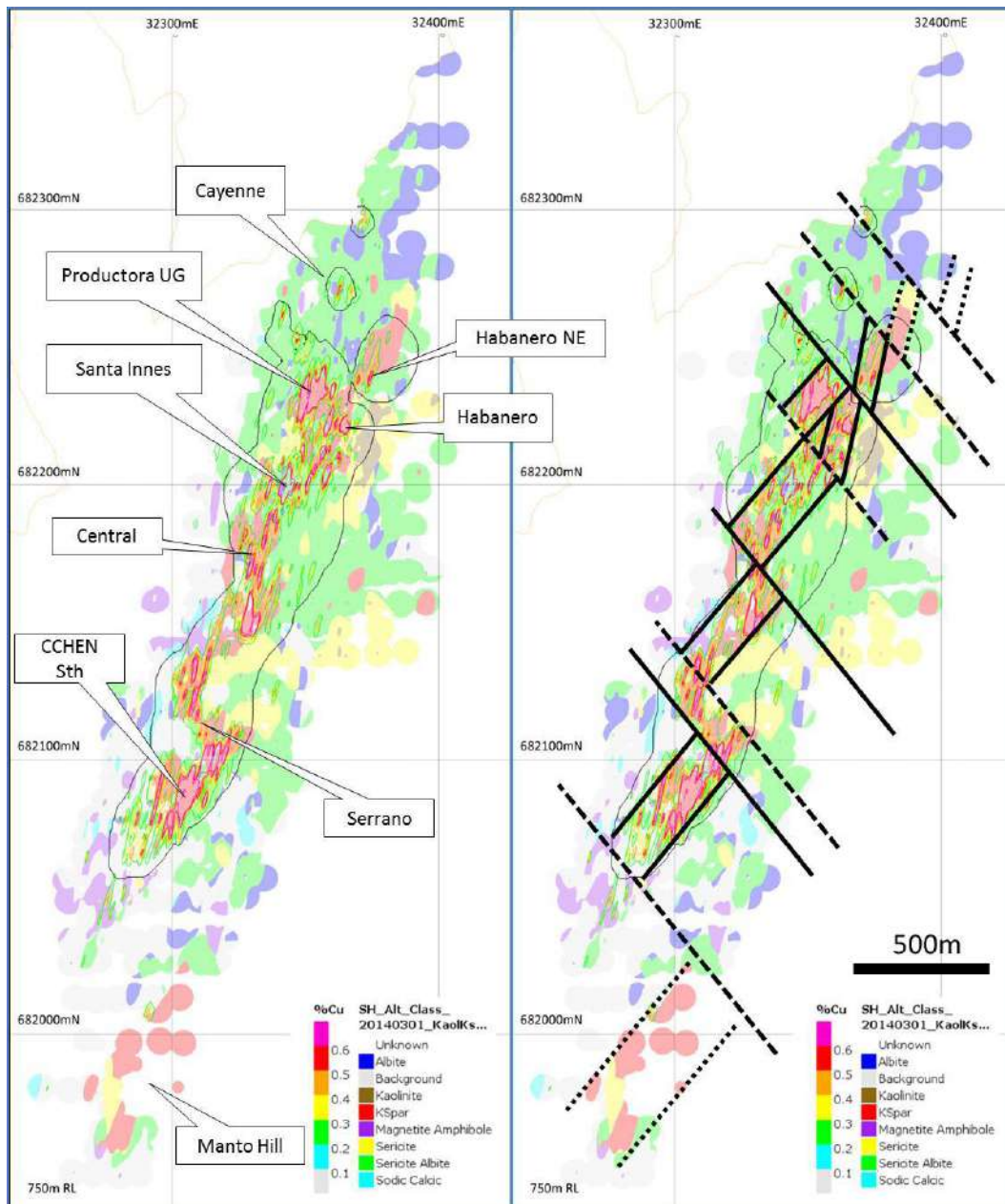


Figure 14.4 Probability plots showing the correlation of Cu & Mo grade with each of the alteration domains. Note: K-spar and Sericite domains are equally likely to host mineralisation.



Alteration domains shown as partially transparent colour fill and Leapfrog 3D Cu% isosurfaces as coloured contours. RH image (duplicate of LH image) is annotated with NW cross faults and mineralisation domain trends at the 750m RL.

Figure 14.5 750m RL Level Slice through the 3D Alteration Model

14.1.5.2 3D tourmaline breccia model

A preliminary three-dimensional (3D) interpolation of the tourmaline breccia carapace has been created in Leapfrog utilising a combination of geological and alteration logging, presence/absence of tourmaline and fracture frequency data (Figure 14.6).

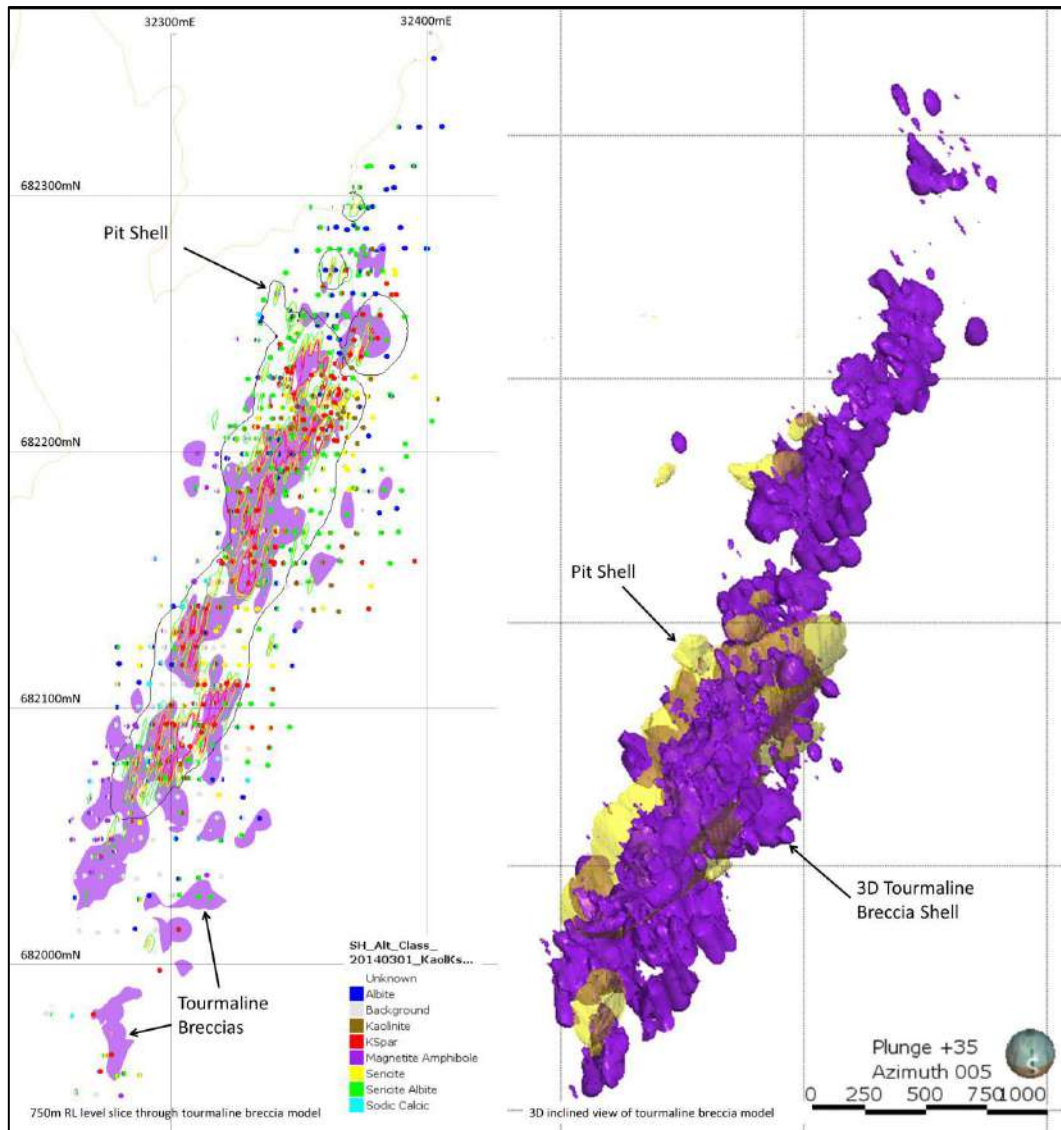


Figure 14.6 Left: 750mRL level slice through the 3D Tourmaline Breccia Model with Leapfrog 3D Cu isosurface contours. Right: 3D view of Breccia model.

14.1.5.3 Acid intrusives & associated Cu depleted alteration halo model

Field investigation of the highly bleached, silica enriched, Cu/K/Na depleted domain immediately east of the Habanero high grade lodes has revealed that this domain is associated with a series of small acid intrusives (granitic dykes & sills) that crop out along the eastern side of the main tourmaline breccia trend. There appears to be a genetic correlation between these intrusives and the high grade Habanero mineralisation, which has led to an emphasis being placed on understanding the spatial distribution and geochemical signature of these intrusive phases in an attempt to identify additional Habanero-type lodes on the eastern side of the deposit. The resultant 3D model of the intrusives and their alteration carapace (the two cannot be confidently separated geochemically) now forms an important component of the integrated 3D geological model and targeting process (Figure 14.7).

14.1.5.4 Pyrite enrichment model

Weight percent Pyrite has been calculated for each sample interval from the multi-element geochemistry. The >3wt% 3D isosurface has been presented in Figure 14.7 to demonstrate the relationship between pyrite enrichment, copper grades and the acid alteration domain. It is evident that in the Northern part of the deposit there is not a 1:1 relationship between pyrite abundance and copper grades, however the greatest pyrite enrichment does appear to have a close (but inverse) spatial correlation with the acid assemblages.

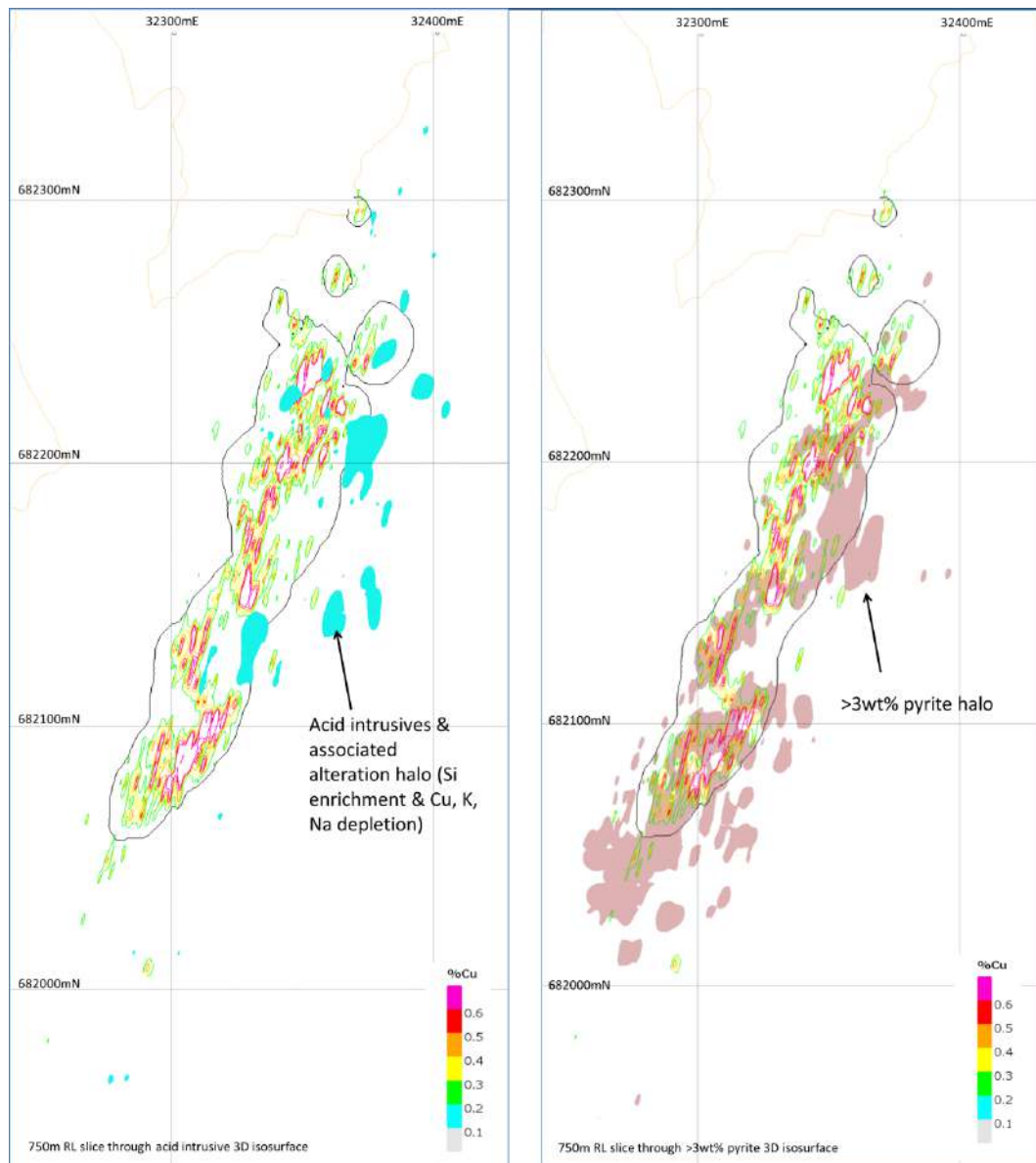


Figure 14.7 750m RL slices through 3D model of acid intrusives and associated acid alteration carapace (left), 3D isosurface of >3wt% Pyrite domain (right).

14.1.5.5 S:Na alteration intensity index

Sulfur:Sodium (S:Na) ratios (Figure 14.8) provide a workable proxy for a magmatic hydrothermal alteration intensity index demonstrating a broad correlation between elevated S:Na ratios (>2:1) and elevated copper grades. Importantly, this indicator

seems to highlight proximity to Habanero-type mineralisation on the margins of the acid intrusives.

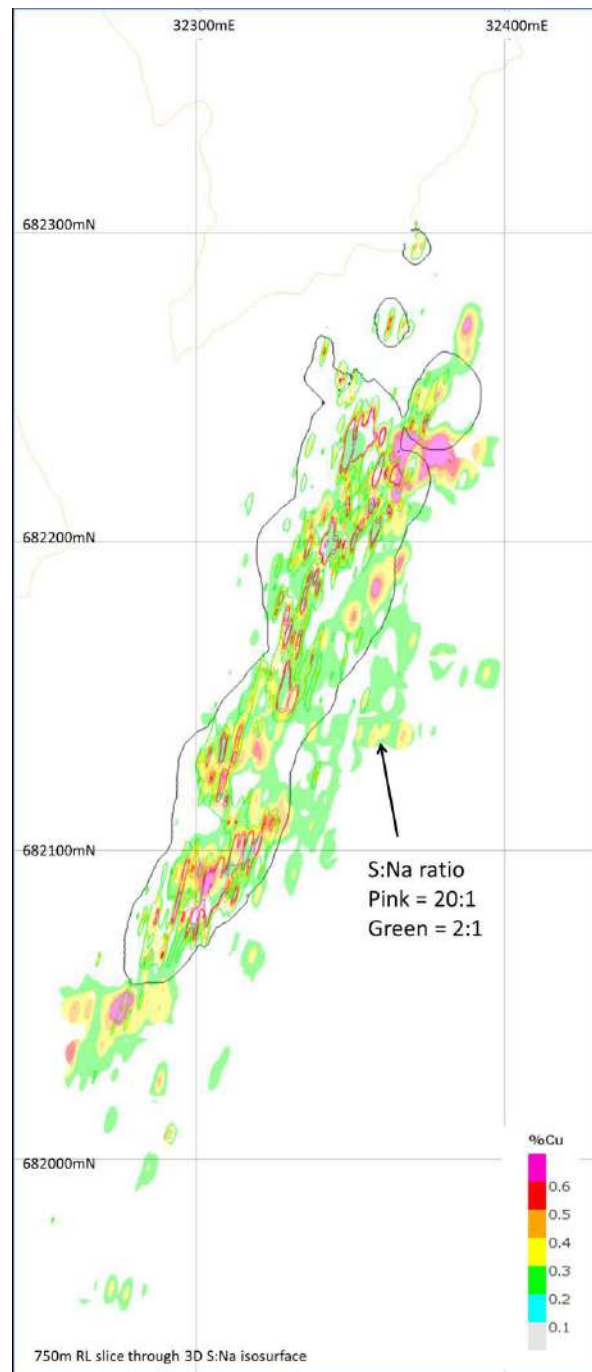


Figure 14.8 S:Na Ratio - 750mRL slice through S:N ratio model. Warm colours depict high S:Na ratios which shown a moderate correlation with proximal alteration assemblages and Cu mineralisation.

14.1.6 2013 Predictive Modelling Files

14.1.6.1 Generation 1 Files

The 2013 alteration files in .dxf, .dtm, .str format are as follows:

- Albite_20131213
- Background_20131213
- Kaolinite_20131213
- KSpar_20131213
- Magnetite Amphibole_20131213
- Sericite Albite_20131213
- Sericite_20131213
- Sodic Calcic_20131213
- Unknown_20131213

The 2013 files in Datamine wireframe format are as follows:

- Sulphide sub-domain – sulph_10_smooth1.{tr/pt}
- Quartz sub-domain – qtz_5_smooth1.{tr/pt}
- Tourmaline sub-domain – tourm_15_smooth1.{tr/pt}
- Epidote sub-domain – epidote_10_smooth1.{tr/pt}

14.1.6.2 Generation 2 Files

Generation 2 2014 calculated mineralogy wireframes:

- pyrite_wt_pct3.0.{tr/pt}
- s_na2.0.{tr/pt}
- tourmaline-breccia_60.{tr/pt }

14.1.7 Weathering Domain Modelling

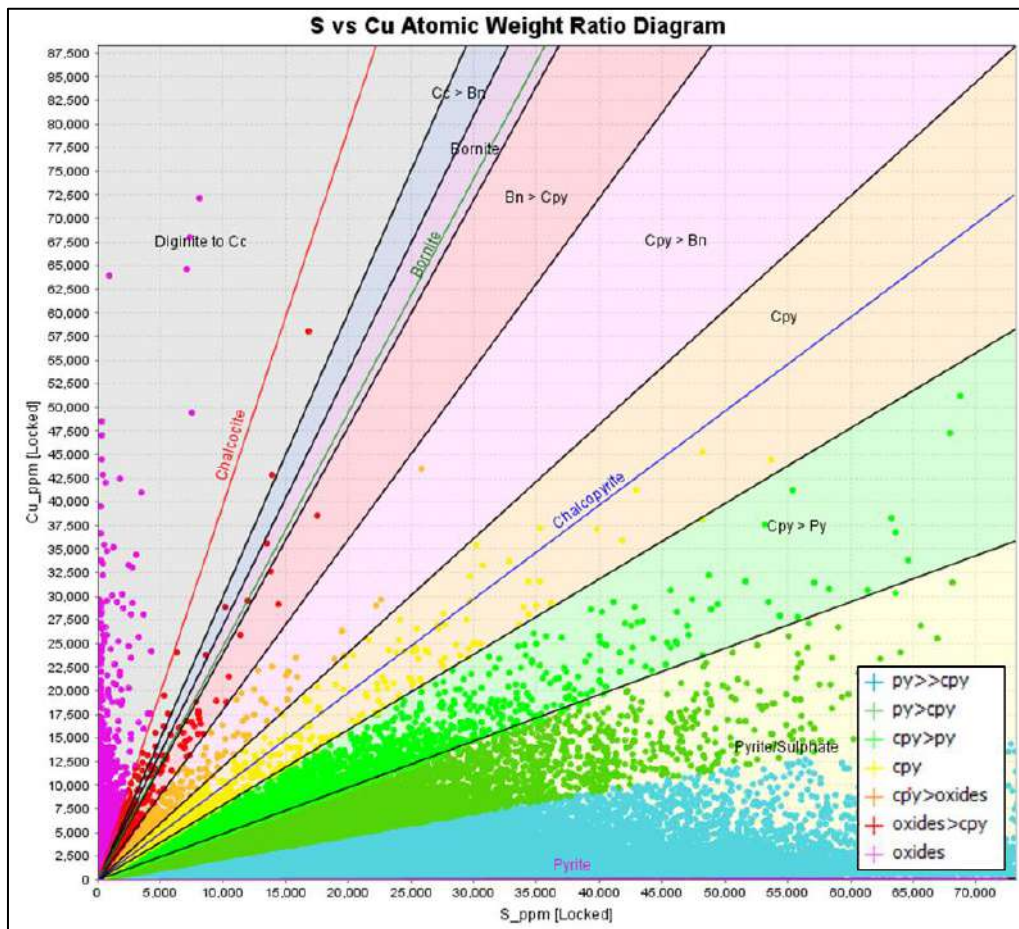
Mineralisation domains were interrogated for potential sub-domaining by weathering surfaces. Domain samples were flagged by modelled surfaces as either oxide, transitional or fresh. Their statistics were compared, either as absolute values, relative to transitional + fresh or relative to “background” (un-mineralised) formation.

The differentiation supported the flagging of weathering zones within the block model due to differences in mineralogy and multi-element geochemistry and assumed differences in potential mining and processing scenarios.

The weathering surfaces were constrained by a combination of qualitative measures such as visual geological logging of drilling for weathering, as well as quantitative analysis such as limited sequential acid test work and extensive multi-element geochemistry. These surfaces were then further refined by the copper species flagging using copper:sulfur (Cu:S) ratio illustrated in Figure 14.9, as well as a dataset generated by PhD student Angela Escolme. The wireframes were validated against the metallurgical drilling and various flotation and leaching results generated by Mintrex.

Copper was estimated across weathering domains. This was based on the current assumption that the majority of mineralisation within the oxide material is relatively in situ and comparable to primary mineralisation. In some areas, there may be some supergene mineralisation and subsequent lateral movement, but this is not currently observed to be a predominant feature and is therefore not well understood. Variography and estimation sample selection therefore did not differentiate between weathering domains, i.e., the weathering domains were used as an estimation soft domain boundary primarily to flag material types.

During the modelling of the oxide profile, there appeared to be some moderate lateral mineralisation mobility in the oxide, but only within the “low grade” copper domain. This was considered during variography and estimation sample selection and orientation for low grade mineralisation.



(Note: As Productora has no bornite, all samples flagged red in diagram are considered as mixed oxide/sulphides.)

Figure 14.9 Example of use of loGAS and Cu:S ratios for copper species flagging at Productora.

14.1.8 Data Flagging

The drillhole data and block model were flagged using wireframes to define various features. The wireframes used are shown in Table 14.9 with an explanation of the fields and their coding in Table 14.10.

Table 14.9 Wireframes used for flagging drillholes and models

Wireframe	Zone Field	Type	Model Area
2021_f27_limited	FAULTBLOCK	Surface	South, Mid, North
2021_faultblock_10	FAULTBLOCK	Solid	North
2021_faultblock_6	FAULTBLOCK	Solid	North
2021_faultblock_7	FAULTBLOCK	Solid	North
2021_faultblock_8	FAULTBLOCK	Solid	North
2021_faultblock_9	FAULTBLOCK	Solid	North
2021_mod_lim	MOD_LIM	Surface	South, Mid, North
2021_oxide_prod_all	WEATH	Surface	South, Mid, North
2021_trans_prod_all	WEATH	Surface	South, Mid, North
interp_1_central_split	CENDOM	Solid	Mid
pit_ox_05	PIT	Surface	Mid
pit_ox_06	PIT	Surface	Mid
pit_ox_07	PIT	Surface	South
pit_ox_08	PIT	Surface	North
pit_ox_09	PIT	Surface	North
pr_04_clip_	PIT	Surface	Mid, South
v2015_a_py_cleaned	PYR	Solid	South, Mid, North
v2015_a_s_na_clean	SUL	Solid	South, Mid, North
v2015_a_tou_brec_clean	TOU	Solid	South, Mid, North
v2015_fault_rancho	FAULTBLOCK	Surface	Mid
v2015_topo_clean	TOPO	Surface	South, Mid, North
weath_zone_nth	WEATHZONE	Solid	Mid
weath_zone_sth	WEATHZONE	Solid	South
tenements_for_model	TENEMENT	Solid	South, Mid, North

Table 14.10 Drillholes and models coding

Field	Code	Model Area	Description
FAULTBLOCK	40000	South	South of Serrano fault
FAULTBLOCK	50000	Mid	Between Serrano and Rancho faults
FAULTBLOCK	60000	North	North of Rancho fault sub-domain
FAULTBLOCK	70000	North	North of Rancho fault sub-domain
FAULTBLOCK	80000	North	North of Rancho fault sub-domain
FAULTBLOCK	90000	North	North of Rancho fault sub-domain
PIT	1	South, Mid	Main pit design circa 2015
PIT	5	Mid	Minor oxide pit circa 2015
PIT	6	Mid	Minor oxide pit circa 2015
PIT	7	South	Minor oxide pit circa 2015
PIT	8	North	Minor oxide pit circa 2015
PIT	9	North	Minor oxide pit circa 2015
PYR	0	South, Mid, North	2015 calculated mineralogy < 3% pyrite
PYR	1	South, Mid, North	2015 calculated mineralogy >= 3% pyrite
SUL	0	South, Mid, North	2015 calculated S:Na ratio < 2:1
SUL	10	South, Mid, North	2015 calculated S:Na ratio >= 2:1
TOU	0	South, Mid, North	2015 outside tourmaline breccia
TOU	100	South, Mid, North	2015 tourmaline breccia
CENDOM	1	South, Mid, North	Eastern orientation domain in Mid area
CENDOM	2	South, Mid, North	Not eastern orientation domain
WEATH	1000	South, Mid, North	Oxide
WEATH	2000	South, Mid, North	Transition
WEATH	3000	South, Mid, North	Fresh
WEATHZONE	0	South, Mid, North	Outside horizontal eastern Cu sub-domain
WEATHZONE	10	South, Mid, North	Horizontal eastern Cu sub-domain
WEATHZONE	20	South, Mid, North	Horizontal eastern Cu sub-domain
TENEMENT	1	South, Mid, North	Tenement number
TENEMENT	3	South, Mid, North	Tenement number
TENEMENT	4	South, Mid, North	Tenement number
TENEMENT	7	South, Mid, North	Tenement number

Elements were converted and combined to create a calculated total assay field. This was used to generate a calculated silica percentage field, CALC_SI, to investigate whether this would be useful in domain generation.

14.1.9 Block Modelling

Block models were created to encompass each areas mineralisation. The parent block size was selected to ensure a realistic grade estimate was achieved in each block considering the average drillhole spacing and mineralisation orientation. The block models and drillholes were flagged with weathering and various features as described in section 14.1.8 Data Flagging in Table 14.10. Sub-celling was set at a level to provide sufficient resolution of the blocks compared to the wireframes and mineralisation characteristics. The block model dimensions are shown in Table 14.11.

Table 14.11 Block model dimensions

Area	Dimension	Minimum	Maximum	Extent (m)	Block Size (m)	
					Parent	Minimum
South	Easting	322400	324100	1,700	5.0	5.0
	Northing	6819300	6821900	2,600	20.0	5.0
	Elevation	200	1200	1,000	5.0	5.0
Mid	Easting	322500	324400	1,900	5.0	5.0
	Northing	6821400	6824300	2,900	20.0	5.0
	Elevation	200	1200	1,000	5.0	5.0
North	Easting	322900	325200	2,300	5.0	5.0
	Northing	6823200	6827200	4,000	20.0	5.0
	Elevation	200	1200	1,000	5.0	5.0
Combined	Easting	322400	325200	2,800	5.0	5.0
	Northing	6819300	6827300	8,000	20.0	5.0
	Elevation	200	1200	1,000	5.0	5.0

Density was estimated into the model using the inverse distance to the power of two technique. A minimum of 12 and maximum of 24 composites were chosen in a search of 200m by 200m by 50m which was oriented 0° → 000°.

14.1.10 Dynamic Anisotropy Modelling

Due to the variable strike, dip and plunge over the Productora area, dynamic anisotropy was used to locally adjust the orientation of the search ellipse and variogram model. Trend wireframes were used to create a point file where each point relates to a triangle centroid and contains the true dip and true dip direction of the wireframe triangle. This point file was then used to estimate the local true dip and dip direction into the block model for each block. The estimates of true dip (TRDIP) and dip direction (TRDIPDIR)

were subsequently used to locally adjust the variogram and search orientations during the categorical indicator estimation and some of the grade estimations.

The trend models used were restricted to the specific fault blocks as described in Table 14.12.

Table 14.12 Dynamic anisotropy trend wireframes

Wireframe	Zone Field	Code	Model Area
da_trend_v3_02_sthof27_a	FAULTBLOCK	40000	South
da_trend_v4_01_nthof27_a	FAULTBLOCK	50000	Mid
da_trend_v2_nth_fb678_b	FAULTBLOCK	60000	North
da_trend_v2_nth_fb678_b	FAULTBLOCK	70000	North
da_trend_v2_nth_fb678_b	FAULTBLOCK	80000	North
da_trend_v2_nth_fb910_b	FAULTBLOCK	90000	North
da_trend_v2_nth_fb910_b	FAULTBLOCK	100000	North

14.1.11 Categorical Domaining

14.1.11.1 Strategy

This update to the Productora model was aimed at understanding and using chemistry associations to help define domains for estimation.

Through the process the following observations were made regarding the wireframe interpretations from the 2014 and 2015 interpretation work:

- Generation 1 alteration wireframes (2014) were difficult to understand spatially, though kspar was correlated broadly to highest copper
- Generation 2 alteration wireframes (generated from 2015 calculated mineralogy) have good relationships with iron and sulfur
- Alteration coding to drillholes via chemistry was also difficult to interpret – lacked easily identifiable cohesive zones.

The wireframes were unsuitable to be used directly for grade estimation therefore a strategy to investigate a number of key elements and ratios of elements was pursued.

Previous attempts to discretely model individual domains of mineralisation have been difficult due to the lack of large coherent and consistent mineralisation between and along sections. This has resulted in significant small, mineralised zones to be excluded from estimation. The approach taken to acknowledge the individual zones of mineralisation within the deposit is to use a categorical kriging approach alongside estimates of ratios of elements to initially domain common geological zones through chemistry and then subsequently separate mineralised and un-mineralised material within these geological zones.

14.1.11.2 Categorical Domaining Data

The drillhole data was coded with indicator fields of one by being above the grade/value specified or zero for below as described in Table 14.13. Various ratios were also calculated and applied as shown in Table 14.13.

A total of 17 indicators and 16 ratios of elements were tested along with the calculated silica. Additionally, for the north area, a combined variable was created and used to create a combined indicator using the formula $COMBASS = Cu*10 + Au*10 + Mo/100$. If $COMBASS > 0.4$ then $IND_COMB = 1$ else $IND_COMB = 0$.

Table 14.13 Categorical indicator coding of drillholes

Indicator Field	Test for Indicator to be 1, else 0
SIND	S_PCT_D >= 0.4
COIND1	CO_PPM_D >= 50
COIND2	CO_PPM_D >= 300
MOIND	MO_PPM_D >= 50
CUIND05	CU_PCT_D >= 0.05
CUIND1	CU_PCT_D >= 0.1
CUIND2	CU_PCT_D >= 0.2
CUIND3	CU_PCT_D >= 0.3
CUIND4	CU_PCT_D >= 0.4
CUIND5	CU_PCT_D >= 0.5
VEINPCTIND1	VEIN1PCT >= 1 OR VEIN2PCT >= 1
CAPIND	CA_PCT_D >= 0.8 or CA_PCT_D >= 0.3 AND R_P_CA < 800
CUSIND	R_CU_S >= 1.0
CUSIND2	R_CU_S >= 0.6 exclude Oxide
KALIND	R_K_AL >= 0.47
KSIND	R_K_S >= 10
ALSIND	R_AL_S >= 20
FESIND	R_FE_S >= 5

Table 14.14 Ratio calculation for drillholes

Ratio Field	Calculation of ratio
R_CU_S	CU_PCT_D / S_PCT_D
R_CU_AU	CU_PCT_D / AU_PPM_D
R_CU_MO	CU_PCT_D / MO_PPM_D
R_K_S	K_PCT_D / S_PCT_D
R_K_NA	K_PCT_D / NA_PCT_D
R_NA_AL	NA_PCT_D / AL_PCT_D
R_AL_K	AL_PCT_D / K_PCT_D
R_K_AL	K_PCT_D / AL_PCT_D
R_FE_AL	FE_PCT_D / AL_PCT_D
R_K_FE	K_PCT_D / FE_PCT_D
R_AL_S	AL_PCT_D / S_PCT_D
R_CA_NA	CA_PCT_D / NA_PCT_D
R_CA_MG	CA_PCT_D / MG_PCT_D
R_P_CA	P_PPM_D / CA_PCT_D
R_FE_S	FE_PCT_D / S_PCT_D
R_S_NA	S_PCT_D / NA_PCT_D
R_V_SC	V_PPM_D / SC_PPM_D

Compositing is the process of equalising the length of samples used for statistical and geostatistical analysis. This is required to ensure that samples of equal support are considered, and it is essential from a statistical viewpoint. Most estimation algorithms do not take into account the sample size, e.g., there is no difference between a 10m sample and a 1m sample. A 1m composite length was chosen as this represented the dominant sample length.

Datamine software (process COMPDH) was used to extract variable length 1m down-hole composites. This adjusts the sample intervals where required to ensure all samples were included in the composite file (i.e., no residuals) while keeping the sample interval as close to the desired sample interval as possible. The compositing was run within domains which honour the coded indicators described in Table 14.13 as well as weathering to ensure that no composite intervals crossed any potential boundaries.

14.1.11.3 Categorical Domaining Variography

The indicator and ratio data were used to generate variogram models reflecting the continuity of each of the indicators and ratios where possible. The mid area had the largest amount of data and was the area which produced the most robust variogram models. The resulting variogram models used for estimation of the indicators and ratios

presented in Table 14.15 for the mid area, Table 14.16 for the south area and Table 14.17 for the north area. The directions modelled represents the various orientations along the Productora corridor.

Table 14.15 Categorical variogram models – Mid Area

VREF	Variable	Rotation*			Nugget	Structure 1		Structure 2		Structure 3	
					C ₀	C ₁	R ₁	C ₁	R ₁	C ₁	R ₁
1	CUIND05	110	115	0	0.12	0.38	60	0.23	110	0.27	700
							20		100		260
							15		130		200
2	CUIND15	110	115	0	0.12	0.17	20	0.44	25	0.27	135
							15		75		85
							15		20		40
3	MOIND	110	110	0	0.15	0.26	20	0.30	25	0.29	100
							20		70		100
							10		20		60
4	COIND1	100	110	0	0.1	0.46	50	0.14	120	0.30	600
							35		135		280
							20		105		230
5	COIND2	100	110	0	0.1	0.36	20	0.20	30	0.34	200
							30		90		95
							20		60		90
6	SIND	115	160	0	0.06	0.28	50	0.23	180	0.43	1100
							50		80		380
							20		180		180
7	CALC_SI	110	100	0	0.15	0.30	60	0.30	70	0.25	800
							25		80		250
							15		55		250
8	R_P_CA	120	50	0	0.11	0.33	40	0.22	200	0.34	1050
							40		350		560
							40		200		300
9	R_P_CA	120	90	0	0.11	0.31	40	0.24	200	0.34	1050
							70		300		300
							30		140		380
10	R_K_AL	105	110	0	0.09	0.47	40	0.17	105	0.27	460
							40		150		260
							20		65		200
11	R_CU_S Ox/Tr	110	170	0	0.03	0.41	50	0.27	170	0.29	800
							15		200		200
							15		100		130
12	R_CU_S	110	110	0	0.11	0.21	50	0.34	60	0.34	800
							15		80		320
							15		40		280

Table 14.16 Categorical variogram models – South Area

VREF	Variable	Rotation*			Nugget	Structure 1		Structure 2		Structure 3	
					C ₀	C ₁	R ₁	C ₁	R ₁	C ₁	R ₁
1	CUIND05	110	115	0	0.12	0.46	70	0.17	160	0.25	600
							70		200		260
							60		100		100
2	CUIND15	110	115	0	0.12	0.40	20	0.29	35	0.19	120
							50		60		80
							15		20		20
3	MOIND	110	110	0	0.15	0.26	20	0.30	25	0.29	100
							20		45		110
							10		20		30
4	COIND1	100	110	0	0.1	0.46	50	0.14	120	0.30	600
							35		15		280
							20		105		230
5	COIND2	100	110	0	0.1	0.36	30	0.34	50	0.20	200
							30		60		110
							20		30		40
6	SIND	115	160	0	0.06	0.30	80	0.37	1200	0.27	1200
							80		900		900
							40		150		150
7	CALC_SI	110	100	0	0.12	0.30	60	0.29	75	0.29	800
							25		40		150
							15		60		325
8	R_P_CA	120	50	0	0.11	0.26	40	0.36	100	0.27	670
							15		135		230
							15		65		180
9	R_P_CA	120	90	0	0.11	0.47	40	0.15	100	0.27	670
							15		230		230
							25		100		420
10	R_K_AL	105	110	0	0.09	0.47	40	0.14	140	0.30	600
							70		250		250
							20		190		200
11	R_CU_S Ox/Tr	110	170	0	0.03	0.20	50	0.27	80	0.50	200
							40		50		150
							10		20		30
12	R_CU_S	110	110	0	0.03	0.35	90	0.22	180	0.40	900
							30		140		240
							30		140		240

Table 14.17 Categorical variogram models – North Area

VREF	Variable	Rotation*			Nugget	Structure 1		Structure 2		Structure 3	
					C ₀	C ₁	R ₁	C ₁	R ₁	C ₁	R ₁
41	CU_PCT_D	115	15	0	0.17	0.21	40	0.21	130	0.41	150
							40		60		90
							10		40		60
43	R_CU_S	115	15	0	0.11	0.27	40	0.21	130	0.41	240
							40		60		150
							10		40		40
44	R_K_AL	115	40	0	0.07	0.29	40	0.36	80	0.28	270
							40		60		150
							10		30		40
45	R_CA_NA	125	100	0	0.11	0.27	40	0.36	100	0.26	550
							25		55		300
							10		40		60
46	R_P_CA	115	90	0	0.11	0.36	40	0.31	90	0.22	380
							15		60		260
							10		40		100
47	FE_PCT_D	115	15	0	0.14	0.30	20	0.23	60	0.33	180
							20		60		90
							10		20		40

14.1.11.4 Categorical Domaining Estimation

To perform the categorical kriging block models were created using very small blocks of 5 mE by 5 mN by 5 mRL size. The estimation was split into the three fault block areas.

The search strategy for estimation either used the established dynamic anisotropy to locally tune the search orientations or used the search orientations derived from the continuity analysis. The search strategy for each area and variable estimated is contained in Table 14.18, Table 14.19 and Table 14.20 with the combination of search and variogram parameters listed in Table 14.21, Table 14.22 and Table 14.23.

Table 14.18 Search strategy for categorical estimation for mid area

SREF	Orientation			Search			2 nd search factor	Number of Composites				
	Rot1	Rot2	Rot3	D1	D2	D3		First Search		Second Search		Max Per Drillhole
								Min	Max	Min	Max	
1	Dynamic			50	50	20	4	6	12	6	12	3
6	115	160	0	50	50	20	4	6	12	6	12	3
8	120	50	0	50	50	20	4	6	12	6	12	3
9	120	90	0	50	50	20	4	6	12	6	12	3
11	110	170	0	50	50	20	4	6	12	6	12	3

Table 14.19 Search strategy for categorical estimation for south area

SREF	Orientation			Search			2 nd search factor	Number of Composites				
	Rot1	Rot2	Rot3	D1	D2	D3		First Search		Second Search		Max Per Drillhole
								Min	Max	Min	Max	
21	Dynamic			50	50	20	4	6	12	6	12	3
26	130	170	0	50	50	20	4	6	12	6	12	3
28	110	50	0	50	50	20	4	6	12	6	12	3
29	110	90	0	50	50	20	4	6	12	6	12	3
31	110	170	0	50	50	20	4	6	12	6	12	3

Table 14.20 Search strategy for categorical estimation for north area

SREF	Orientation			Search			2 nd search factor	Number of Composites				
	Rot1	Rot2	Rot3	D1	D2	D3		First Search		Second Search		Max Per Drillhole
								Min	Max	Min	Max	
41	Dynamic			150	150	60	-	6	12	-	-	3
42	110	150	150	150	150	60	-	6	12	-	-	3
43	90	150	150	150	150	60	-	6	12	-	-	3

Table 14.21 Combination of variogram and search for categorical estimation mid area

Variable	Model Variable	SREF	VREF	Description
CUIND05	CUIND05	1	1	Using dynamic search
CUIND3	CUIND3	1	2	Using dynamic search
MOIND	MOIND	1	3	Using dynamic search
COIND1	COIND1	1	4	Using dynamic search
COIND2	COIND2	1	5	Using dynamic search
SIND	SIND	6	6	Using static search
CALC_SI	CALC_SI	1	7	Using dynamic search
CAPIND	CAPIND	8	8	Using static search
CAPIND	CAPIND2	9	9	Using static search
KALIND	KALIND	1	10	Using dynamic search
CUSIND	CUSIND	11	11	Using static search
CUSIND2	CUSIND2	1	12	Using dynamic search

Table 14.22 Combination of variogram and search for categorical estimation south area

Variable	Model Variable	SREF	VREF	Description
CUIND05	CUIND05	21	21	Using dynamic search
CUIND3	CUIND3	21	22	Using dynamic search
MOIND	MOIND	21	23	Using dynamic search
COIND1	COIND1	21	24	Using dynamic search
COIND2	COIND2	21	25	Using dynamic search
SIND	SIND	26	26	Using static search
CALC_SI	CALC_SI	21	27	Using dynamic search
CAPIND	CAPIND	28	28	Using static search
CAPIND	CAPIND2	29	29	Using static search
KALIND	KALIND	21	30	Using dynamic search
CUSIND	CUSIND	31	31	Using static search
CUSIND2	CUSIND2	21	32	Using dynamic search

Table 14.23 Combination of variogram and search for categorical estimation north area

Variable	Model Variable	SREF	VREF	Description
CUIND05	CUIND05	41	41	Using dynamic search
CUIND1	CUIND1	41	41	Using dynamic search
CUIND3	CUIND3	41	41	Using dynamic search
MOIND	MOIND	41	41	Using dynamic search
COIND1	COIND1	41	47	Using dynamic search
COIND2	COIND2	41	47	Using dynamic search
SIND	SIND	41	47	Using dynamic search
CALC_SI	CALC_SI	41	47	Using dynamic search
R_P_CA	R_P_CA	41	46	Using dynamic search
KALIND	KALIND	41	44	Using dynamic search
CUSIND	CUSIND	42	43	Using static search
CUSIND2	CUSIND2	41	41	Using dynamic search
R_CA_NA	R_CA_NA	41	45	Using dynamic search
CUIND05	CUIND05A	43	41	Using static search
IND_COMB	IND_COMB	41	41	Using dynamic search

The estimate was compared in detail to the drillhole data visually to fine tune the estimation parameters to reflect the spatial distribution of the conceptual mineralisation model described previously.

14.1.11.5 Categorical Domaining Interpretation

Escolme (2016) interpreted the distribution of breccia facies as shown in Figure 14.10, top, based on graphic core logging, core photo library, drillhole data base (provided by Hot Chili Limited), detailed hand specimen and thin section observations and WLSQ-QXRD data. Breccia cross-cutting relationships are indicated by the inclusion of clasts of earlier breccia stages. Stage 2 breccias are cross-cut by stage 3 and overprint stage 3 due to later fault reactivation. Variable breccia morphology (clast supported vs. cement supported) in stage 3 breccias are shown by fill pattern. Highest copper is associated with Facies 3B-1, 3B-2 and Stage 2 breccias.

Using the Escolme interpretation as a guide, various combinations of the indicators and ratios were used to define geological/chemical material types. The results show that:

- Indicators for sulphur and molybdenum together could broadly outline the facies 3B-1 and facies 3B-2 – “Breccias”
- Within the breccias the potassium: aluminium ratios or cobalt indicators broadly outline the Stage 2 material

- Calcium and phosphorus broadly outline a wedge of high calcium material between Productora and Alice which is generally very poorly mineralised
- Copper: Sulphur ratios outline oxidised sub horizontal features and faults where deep weathering occurs – pyrite higher in south
- Copper indicators at 0.05% Cu and 3.00% Cu were used to defined high- and low-grade copper sub-domains.

14.1.11.6 Copper domains

The model was coded with a combination of indicators and ratios for copper domains as shown in Table 14.13 and compared to the interpretation on east-west section 6822215mN in Figure 14.10.

Table 14.24 Model coding for copper domaining

Description	Condition	TYPE6
Facies 3B(1,2) LG	SIND \geq 0.30 and MOIND \geq 0.10 and CUIND05 \geq 0.60	11
Facies 3B(1,2) HG	SIND \geq 0.30 and MOIND \geq 0.10 and CUIND3 \geq 0.35	12
Facies 3B(1,2) VLG	SIND \geq 0.30 and MOIND \geq 0.10 and CUIND05 $<$ 0.60	19
Stage 2 LG	SIND \geq 0.30 and MOIND \geq 0.10 and CUIND05 \geq 0.60 and (KALIND \geq 0.50 OR COIND2 \geq 0.1)	21
Stage 2 HG	SIND \geq 0.30 and MOIND \geq 0.10 and CUIND3 \geq 0.35 and (KALIND \geq 0.50 OR COIND2 \geq 0.1)	22
Stage 2 VLG	SIND \geq 0.30 and MOIND \geq 0.10 and CUIND05 $<$ 0.60 and (KALIND \geq 0.50 OR COIND2 \geq 0.1)	29
Rhyolite/Rhyodacite lapilli tuff LG	CAPIND \geq 0.20 and CAPIND2 \geq 0.20 and CUIND05 \geq 0.60	51
Rhyolite/Rhyodacite lapilli tuff HG	CAPIND \geq 0.20 and CAPIND2 \geq 0.20 and CUIND3 \geq 0.35	52
Rhyolite/Rhyodacite lapilli tuff VLG	CAPIND \geq 0.20 and CAPIND2 \geq 0.20 and CUIND05 $<$ 0.60	59
East oxide LG	WEATHZONE == 10 OR WEATHZONE == 20	61
East oxide HG	WEATHZONE == 10 OR WEATHZONE == 20	62
East oxide VLG	WEATHZONE == 10 OR WEATHZONE == 20	69
Background LG	Not previously coded and CUIND05 \geq 0.60	31
Background HG	Not previously coded and CUIND3 \geq 0.35	32
Background VLG	Not previously coded and CUIND05 $<$ 0.60	39

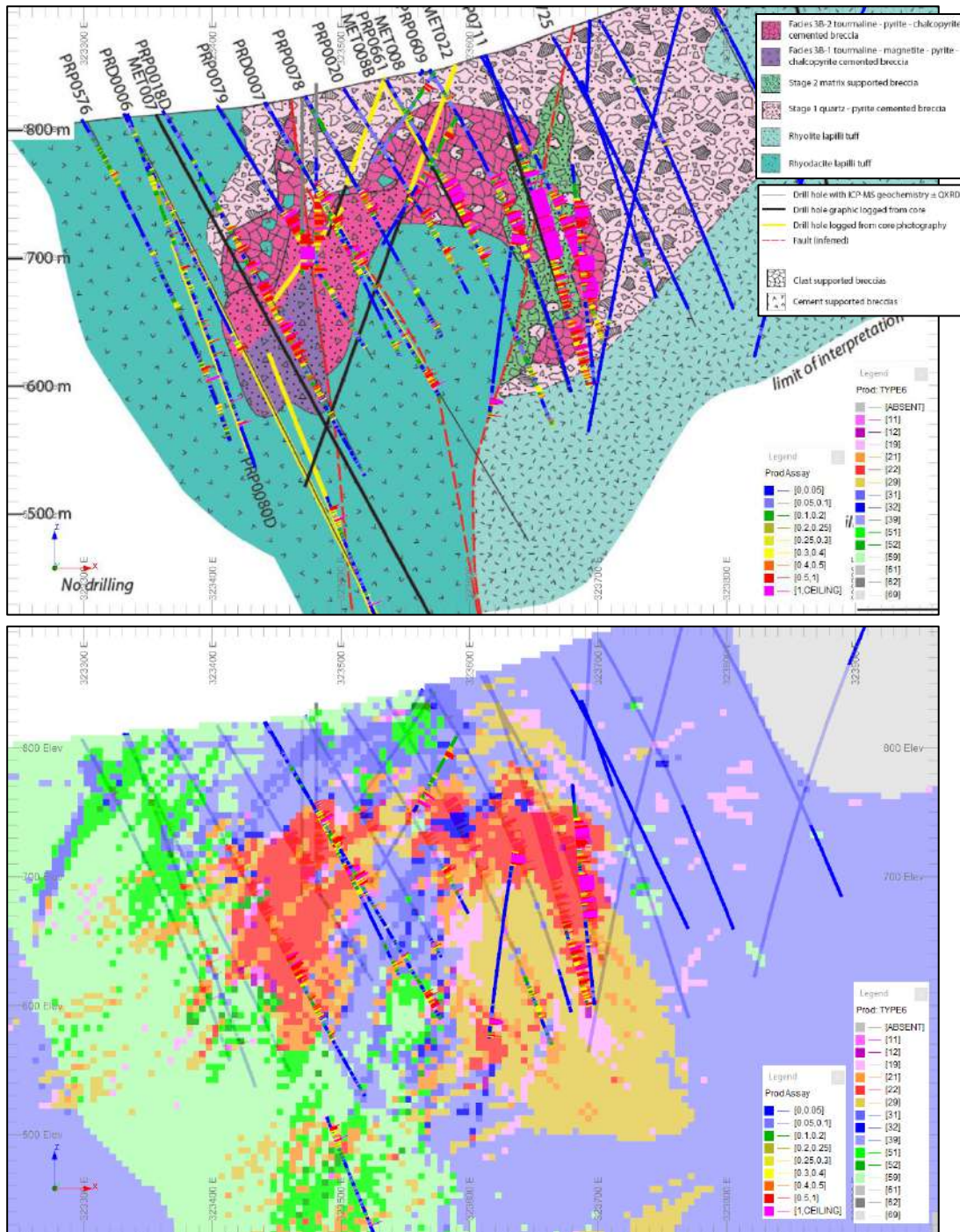


Figure 14.10 Comparison of conceptual interpretation, top, to coded model, bottom on EW section 6822215mN

14.1.11.7 Soluble copper domains

The model was coded with a combination of indicators for soluble copper domains as:

- CUSOL = 100 Soluble copper near surface where material is coded as oxide or transitional and CUSIND ≥ 0.5
- CUSOL = 200 Soluble copper in faults where material is coded as fresh and CUSIND2 ≥ 0.5 .

14.1.11.8 Cobalt domains

It is understood the early pyrite alteration is associated with elevated cobalt. The model was coded with a combination of the pyrite wireframe and indicators for cobalt domains as:

- CODOM = 1 Within pyrite wireframe and COIND1 ≥ 0.5
- CODOM = 2 Within pyrite wireframe and COIND1 < 0.5 or absent
- CODOM = 3 Outside pyrite wireframe and COIND1 ≥ 0.5
- CODOM = 4 Outside pyrite wireframe and COIND1 < 0.5 or absent

14.1.11.9 Calcium domains

Calcium and phosphorus broadly outline a wedge of high calcium material between Productora and Alice which is generally very poorly mineralised. The model was coded with a combination of the two Ca/P ratio indicators as:

- CADOM = 5 where CAPIND ≥ 0.2 AND CAPIND2 ≥ 0.2
- CADOM = 9 remainder of material

14.1.11.10 Molybdenum domains

The model was coded with a combination indicators and ratios for molybdenum domains as shown in Table 14.25.

14.1.11.11 Iron and sulphur domains

The lithology divisions were combined with the pyrite and sulphur wireframes to generate iron and sulphur domains as shown in Table 14.26.

14.1.11.12 Potassium and aluminium domains

The lithology divisions were combined with the indicators to generate potassium and aluminium domains as shown in Table 14.27.

Table 14.25 Model coding for molybdenum domaining

Description	Condition	MODOM1
High Mo Facies 3B(1,2) LG	SIND>=0.30 and MOIND>=0.30 and CUIND05>=0.60	111
High Mo Facies 3B(1,2) HG	SIND>=0.30 and MOIND>=0.30 and CUIND3>=0.35	112
High Mo Facies 3B(1,2) VLG	SIND>=0.30 and MOIND>=0.30 and CUIND05<0.60	119
High Mo Stage 2 LG	SIND>=0.30 and MOIND>=0.30 and CUIND05>=0.60 and (KALIND>=0.50 OR COIND2>=0.1)	121
High Mo Stage 2 HG	SIND>=0.30 and MOIND>=0.30 and CUIND3>=0.35 and (KALIND>=0.50 OR COIND2>=0.1)	122
High Mo Stage 2 VLG	SIND>=0.30 and MOIND>=0.10 and CUIND05<0.60 and (KALIND>=0.50 OR COIND2>=0.1)	129
High Mo Rhyolite/Rhyodacite lapilli tuff LG	CAPIND>=0.20 and CAPIND2>=0.20 and CUIND05>=0.60 and MOIND>=0.3	151
High Mo Rhyolite/Rhyodacite lapilli tuff HG	CAPIND>=0.20 and CAPIND2>=0.20 and CUIND3>=0.35 and MOIND>=0.3	152
High Mo Rhyolite/Rhyodacite lapilli tuff VLG	CAPIND>=0.20 and CAPIND2>=0.20 and CUIND05<0.60 and MOIND>=0.3	159
High Mo Background LG	Not previously coded and CUIND05>=0.60 and MOIND>=0.3	131
High Mo Background HG	Not previously coded and CUIND3>=0.35 and MOIND>=0.3	132
High Mo Background VLG	Not previously coded and CUIND05<0.60 and MOIND>=0.3	139
Facies 3B(1,2) LG	SIND>=0.30 and MOIND<0.30 and CUIND05>=0.60	911
Facies 3B(1,2) HG	SIND>=0.30 and MOIND<0.30 and CUIND3>=0.35	912
Facies 3B(1,2) VLG	SIND>=0.30 and MOIND<0.30 and CUIND05<0.60	919
Stage 2 LG	SIND>=0.30 and MOIND<0.30 and CUIND05>=0.60 and (KALIND>=0.50 OR COIND2>=0.1)	921
Stage 2 HG	SIND>=0.30 and MOIND<0.30 and CUIND3>=0.35 and (KALIND>=0.50 OR COIND2>=0.1)	922
Stage 2 VLG	SIND>=0.30 and MOIND<0.30 and CUIND05<0.60 and (KALIND>=0.50 OR COIND2>=0.1)	929
Rhyolite/Rhyodacite lapilli tuff LG	CAPIND>=0.20 and CAPIND2>=0.20 and CUIND05>=0.60 and MOIND<0.30	951
Rhyolite/Rhyodacite lapilli tuff HG	CAPIND>=0.20 and CAPIND2>=0.20 and CUIND3>=0.35 and MOIND<0.30	952
Rhyolite/Rhyodacite lapilli tuff VLG	CAPIND>=0.20 and CAPIND2>=0.20 and CUIND05<0.60 and MOIND<0.30	959
Background LG	Not previously coded and CUIND05>=0.60 and MOIND<0.30	931
Background HG	Not previously coded and CUIND3>=0.35 and MOIND<0.30	932

Description	Condition	MODOM1
Background VLG	Not previously coded and CUIND05<0.60 and MOIND<0.30	939

Table 14.26 Model coding for iron and sulphur domaining

Description	Condition	FESDOM
Facies 3B(1,2), Stage 2	Outside pyrite and outside sulphur wireframes and SIND \geq 0.30 and MOIND \geq 0.10	1500000
Facies 3B(1,2), Stage 2	Within pyrite and outside sulphur wireframes and SIND \geq 0.30 and MOIND \geq 0.10	1500001
Facies 3B(1,2), Stage 2	Outside pyrite and within sulphur wireframes and SIND \geq 0.30 and MOIND \geq 0.10	1500010
Facies 3B(1,2), Stage 2	Within pyrite and within sulphur wireframes and SIND \geq 0.30 and MOIND \geq 0.10	1500011
Rhyolite/Rhyodacite lapilli tuff	Outside pyrite and outside sulphur wireframes and CAPIND \geq 0.20 and CAPIND2 \geq 0.20	5000000
Rhyolite/Rhyodacite lapilli tuff LG	Within pyrite and outside sulphur wireframes and CAPIND \geq 0.20 and CAPIND2 \geq 0.20	5000001
Rhyolite/Rhyodacite lapilli tuff LG	Outside pyrite and within sulphur wireframes and CAPIND \geq 0.20 and CAPIND2 \geq 0.20	5000010
Rhyolite/Rhyodacite lapilli tuff LG	Within pyrite and within sulphur wireframes and CAPIND \geq 0.20 and CAPIND2 \geq 0.20	5000011
Background	Outside pyrite and outside sulphur wireframes and (CAPIND < 0.20 or CAPIND2 < 0.20)	9900000
Background	Outside pyrite and outside sulphur wireframes and (SIND < 0.30 or MOIND < 0.10)	9900000
Background	Within pyrite and outside sulphur wireframes and (CAPIND < 0.20 or CAPIND2 < 0.20)	9900001
Background	Within pyrite and outside sulphur wireframes and (SIND < 0.30 or MOIND < 0.10)	9900001
Background	Outside pyrite and within sulphur wireframes and (CAPIND < 0.20 or CAPIND2 < 0.20)	9900010
Background	Outside pyrite and within sulphur wireframes and (SIND < 0.30 or MOIND < 0.10)	9900010
Background	Within pyrite and within sulphur wireframes and (CAPIND < 0.20 or CAPIND2 < 0.20)	9900011
Background	Within pyrite and within sulphur wireframes and (SIND < 0.30 or MOIND < 0.10)	9900011

Table 14.27 Model coding for potassium and aluminium domaining

Description	Condition	KALDOM
Facies 3B(1,2) LG	KALIND \geq 0.1 and KALIND < 0.5 and SIND \geq 0.30 and MOIND \geq 0.10 and CUIND05 \geq 0.60	111
Facies 3B(1,2) HG	KALIND \geq 0.1 and KALIND < 0.5 and SIND \geq 0.30 and MOIND \geq 0.10 and CUIND3 \geq 0.35	112

Description	Condition	KALDOM
Facies 3B(1,2) VLG	KALIND >= 0.1 and KALIND < 0.5 and SIND >= 0.30 and MOIND >= 0.10 and CUIND05 < 0.60	119
Stage 2 LG	KALIND >= 0.1 and KALIND < 0.5 and SIND >= 0.30 and MOIND >= 0.10 and CUIND05 >= 0.60 and COIND2 >= 0.1	121
Stage 2 HG	KALIND >= 0.1 and KALIND < 0.5 and SIND >= 0.30 and MOIND >= 0.10 and CUIND3 >= 0.35 and COIND2 >= 0.1	122
Stage 2 VLG	KALIND >= 0.1 and KALIND < 0.5 and SIND >= 0.30 and MOIND >= 0.10 and CUIND05 < 0.60 and COIND2 >= 0.1	129
Rhyolite/Rhyodacite lapilli tuff LG	KALIND >= 0.1 and KALIND < 0.5 and CAPIND >= 0.20 and CAPIND2 >= 0.20 and CUIND05 >= 0.60	131
Rhyolite/Rhyodacite lapilli tuff HG	KALIND >= 0.1 and KALIND < 0.5 and CAPIND >= 0.20 and CAPIND2 >= 0.20 and CUIND3 >= 0.35	132
Rhyolite/Rhyodacite lapilli tuff VLG	KALIND >= 0.1 and KALIND < 0.5 and CAPIND >= 0.20 and CAPIND2 >= 0.20 and CUIND05 < 0.60	139
Background LG	KALIND >= 0.1 and KALIND < 0.5 and Not previously coded and CUIND05 >= 0.60	151
Background VLG	KALIND >= 0.1 and KALIND < 0.5 and Not previously coded and CUIND05 < 0.60	159
Stage 2 LG	KALIND >= 0.5 and SIND >= 0.30 and MOIND >= 0.10 and CUIND05 >= 0.60 and COIND2 >= 0.1	221
Stage 2 HG	KALIND >= 0.5 and SIND >= 0.30 and MOIND >= 0.10 and CUIND3 >= 0.35 and COIND2 >= 0.1	222
Stage 2 VLG	KALIND >= 0.5 and SIND >= 0.30 and MOIND >= 0.10 and CUIND05 < 0.60 and COIND2 >= 0.1	229
Rhyolite/Rhyodacite lapilli tuff LG	KALIND >= 0.5 and CAPIND >= 0.20 and CAPIND2 >= 0.20 and CUIND05 >= 0.60	231
Rhyolite/Rhyodacite lapilli tuff HG	KALIND >= 0.5 and CAPIND >= 0.20 and CAPIND2 >= 0.20 and CUIND3 >= 0.35	232
Rhyolite/Rhyodacite lapilli tuff VLG	KALIND >= 0.5 and CAPIND >= 0.20 and CAPIND2 >= 0.20 and CUIND05 < 0.60	239
Background LG	KALIND >= 0.5 and Not previously coded and CUIND05 >= 0.60	251
Background VLG	KALIND >= 0.5 and Not previously coded and CUIND05 < 0.60	259
Facies 3B(1,2) LG	KALIND < 0.1 and SIND >= 0.30 and MOIND >= 0.10 and CUIND05 >= 0.60	911
Facies 3B(1,2) HG	KALIND < 0.1 and SIND >= 0.30 and MOIND >= 0.10 and CUIND3 >= 0.35	912
Facies 3B(1,2) VLG	KALIND < 0.1 and SIND >= 0.30 and MOIND >= 0.10 and CUIND05 < 0.60	919
Stage 2 LG	KALIND < 0.1 and SIND >= 0.30 and MOIND >= 0.10 and CUIND05 >= 0.60 and COIND2 >= 0.1	921
Stage 2 HG	KALIND < 0.1 and SIND >= 0.30 and MOIND >= 0.10 and CUIND3 >= 0.35 and COIND2 >= 0.1	922
Stage 2 VLG	KALIND < 0.1 and SIND >= 0.30 and MOIND >= 0.10 and CUIND05 < 0.60 and COIND2 >= 0.1	929

Description	Condition	KALDOM
Rhyolite/Rhyodacite lapilli tuff LG	KALIND < 0.1 and CAPIND >= 0.20 and CAPIND2 >= 0.20 and CUIND05 >= 0.60	931
Rhyolite/Rhyodacite lapilli tuff HG	KALIND < 0.1 and CAPIND >= 0.20 and CAPIND2 >= 0.20 and CUIND3 >= 0.35	932
Rhyolite/Rhyodacite lapilli tuff VLG	KALIND < 0.1 and CAPIND >= 0.20 and CAPIND2 >= 0.20 and CUIND05 < 0.60	939
Background LG	KALIND < 0.1 and Not previously coded and CUIND05 >= 0.60	951
Background HG	KALIND < 0.1 and Not previously coded and CUIND3 >= 0.35	952
Background VLG	KALIND < 0.1 and Not previously coded and CUIND05 < 0.60	959

14.1.11.13 Drillhole coding

The various domains were back-flagged onto the drillholes to ensure consistency between the model and the data used for grade estimation.

14.1.12 Compositing

Most (82%) of the drill sampling at Productora was on 1m lengths (Figure 14.11). This proportion increased to 97% in likely economic mineralised domains where Cu was greater than 0.1%. The decision to composite data to 1m was based on the length of the sample interval, the short-range mineral and structural control and relatively narrow mineralised zones in some areas.

The compositing process used the relevant domain and weathering as a boundary to ensure no composites were created across domains.

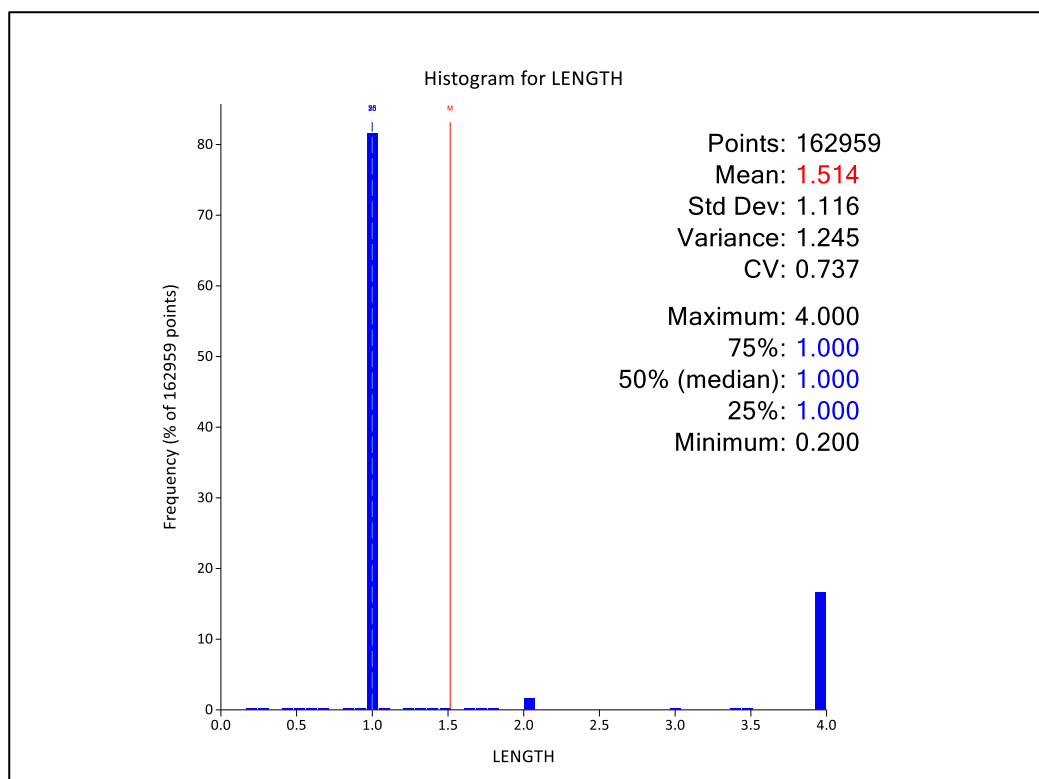


Figure 14.11 Productora sample lengths

14.1.13 Statistical Analysis

Statistical analysis of copper (Cu), gold (Au), molybdenum (Mo), cobalt (Co), calcium (Ca), potassium (K) and aluminium Al) were undertaken using Snowden Supervisor Version 8.14.3.0 software and Microsoft Excel.

The analysis was completed to understand the global representative distribution of each element and account for any bias introduced by clustering of data or by extreme outliers.

Cell declustering was performed using an 80mX by 80mY by 80mZ cell size.

Top-cutting is the process where the values greater than the top-cut value are reduced to the top-cut value. When computing statistics, we make the assumption that there is only one population and that all samples belong to that population. Outliers or extreme values are often observed. Their impact can be a serious overestimation of the average grade and metal and their variability. The mean, variance, variogram and block model estimates are also affected by extreme values. The selection of an appropriate top cut involves some subjectivity but takes into account the characteristics of the population distribution.

Each element in each domain were examined using log histograms, log probability plots, grade disintegration and the general statistics of each lode. The top-cuts have been chosen to reduce the potential smearing of extremely high grades.

The chosen top-cuts with the number of composites affected for the mineralised composites are shown in Table 14.28 for Cu, Table 14.29 for Au, Table 14.30 for Mo, Table 14.31 for Co, Table 14.32 for Ca, Table 14.33 for Fe, Table 14.34 for S, Table 14.35 for K and Table 14.36 for Al.

A comparison of the Cu and Au grades is presented in Figure 14.12 as two box and whisker plots with scatterplots in Figure 14.13 for the highest Cu grade domains in the Breccia 11, 12 and Stage 2, 21 and 22 demonstrating the good correlations.

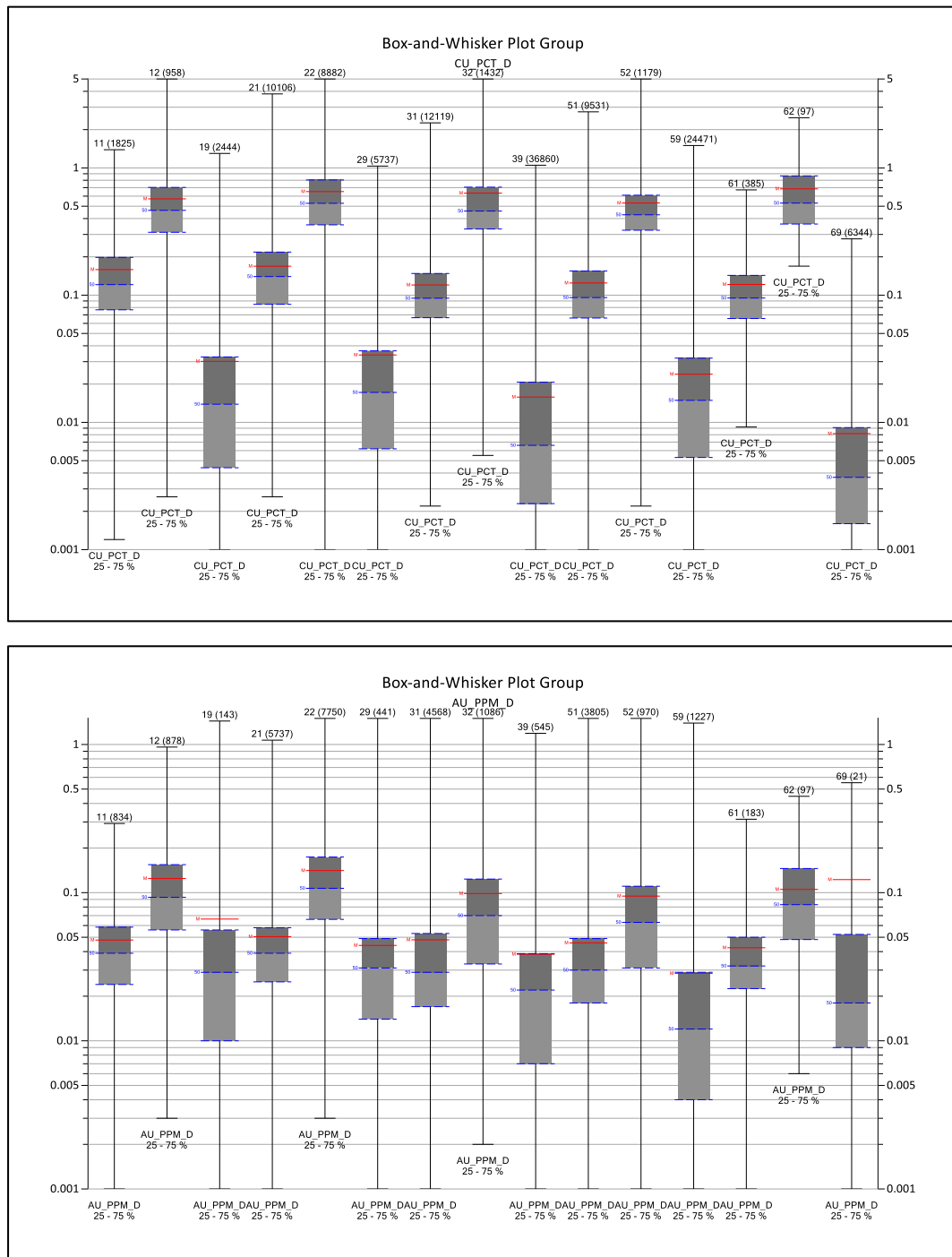


Figure 14.12 Comparison of distributions using box and whisker plots for Cu, top, and Au, bottom

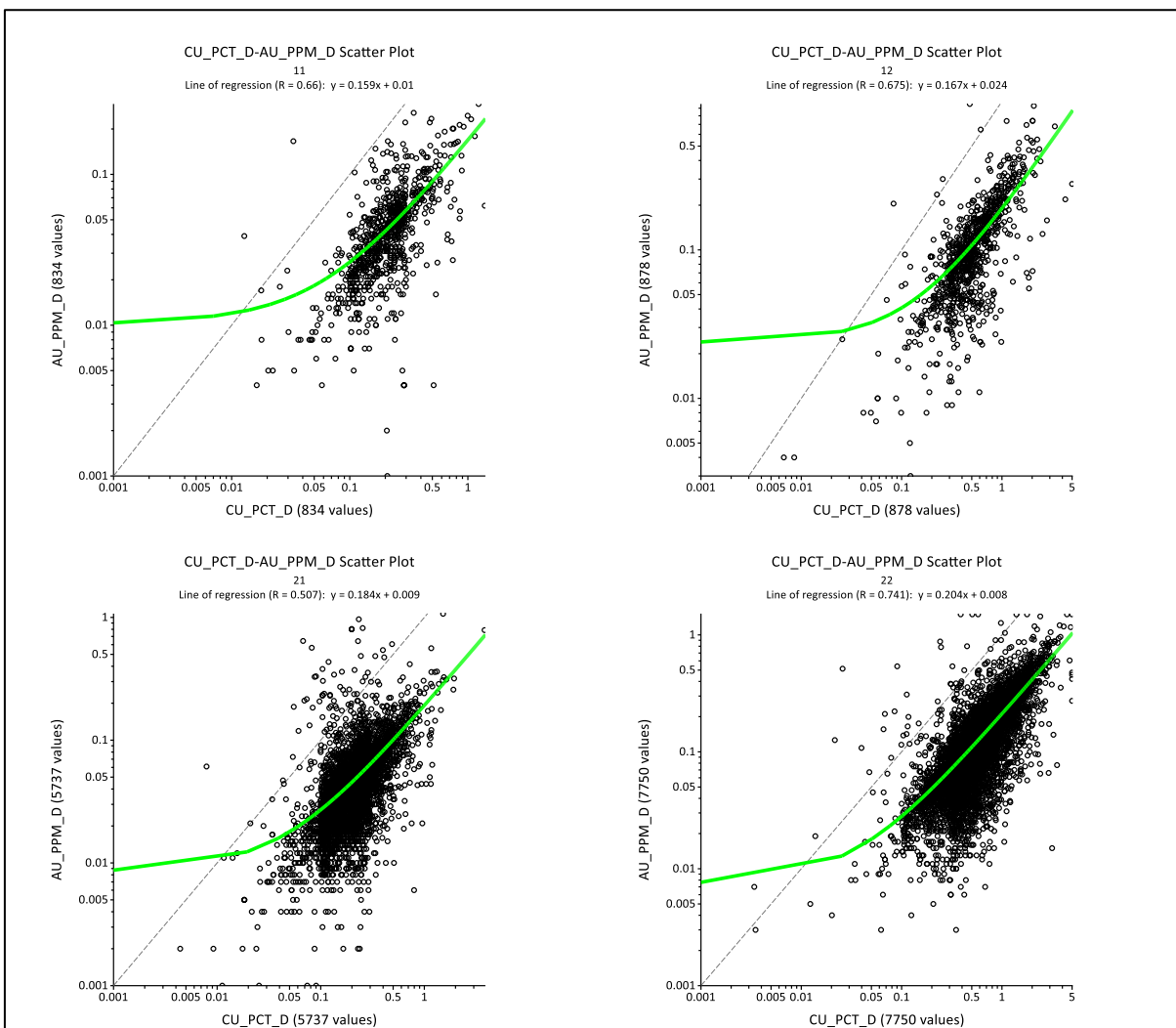
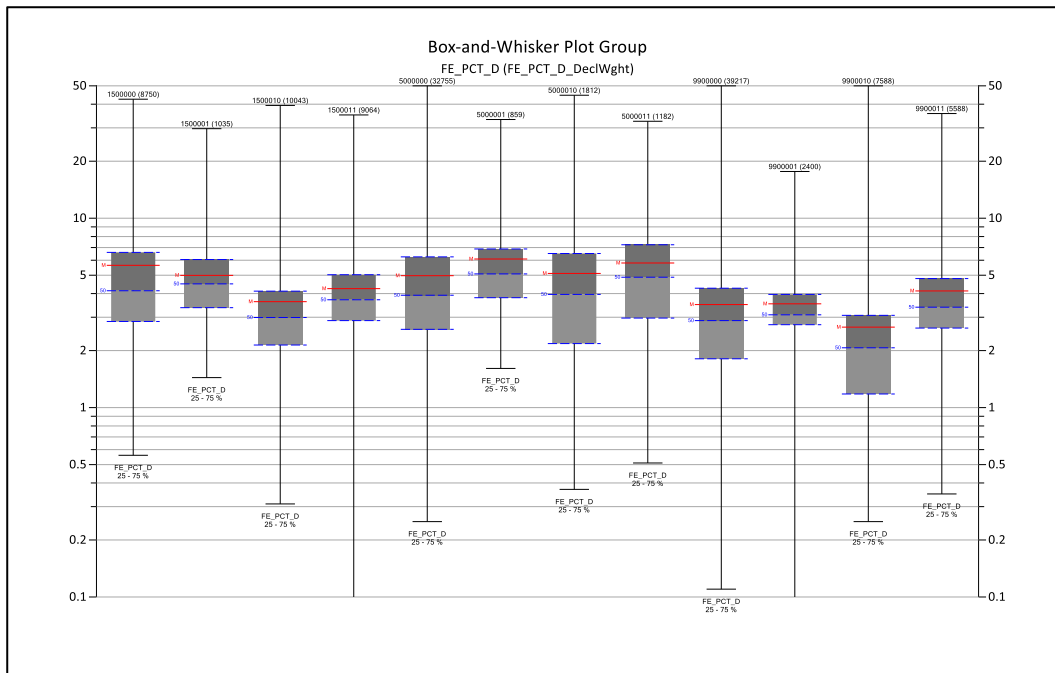


Figure 14.13 Scatterplots between Cu and Au for highest grade domains



F3B(1,2) Stg2				RRLT LG Cu				Background			
-	Py	S	Py+S	-	Py	S	Py+S	-	Py	S	Py+S

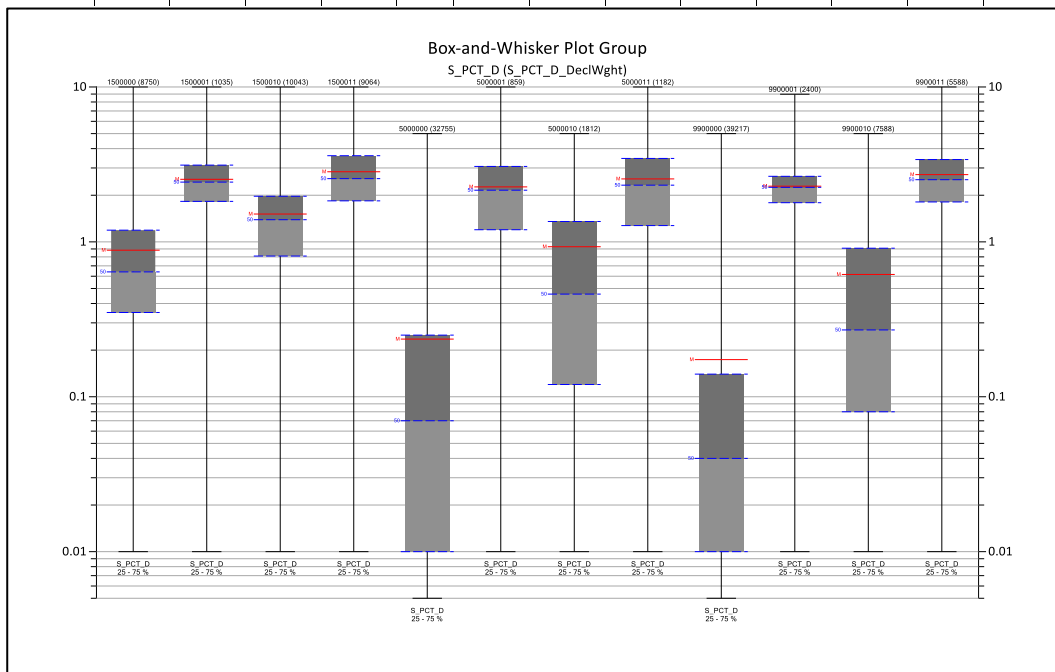


Figure 14.14 Comparison of distributions using box and whisker plots for Fe, top, and S, bottom

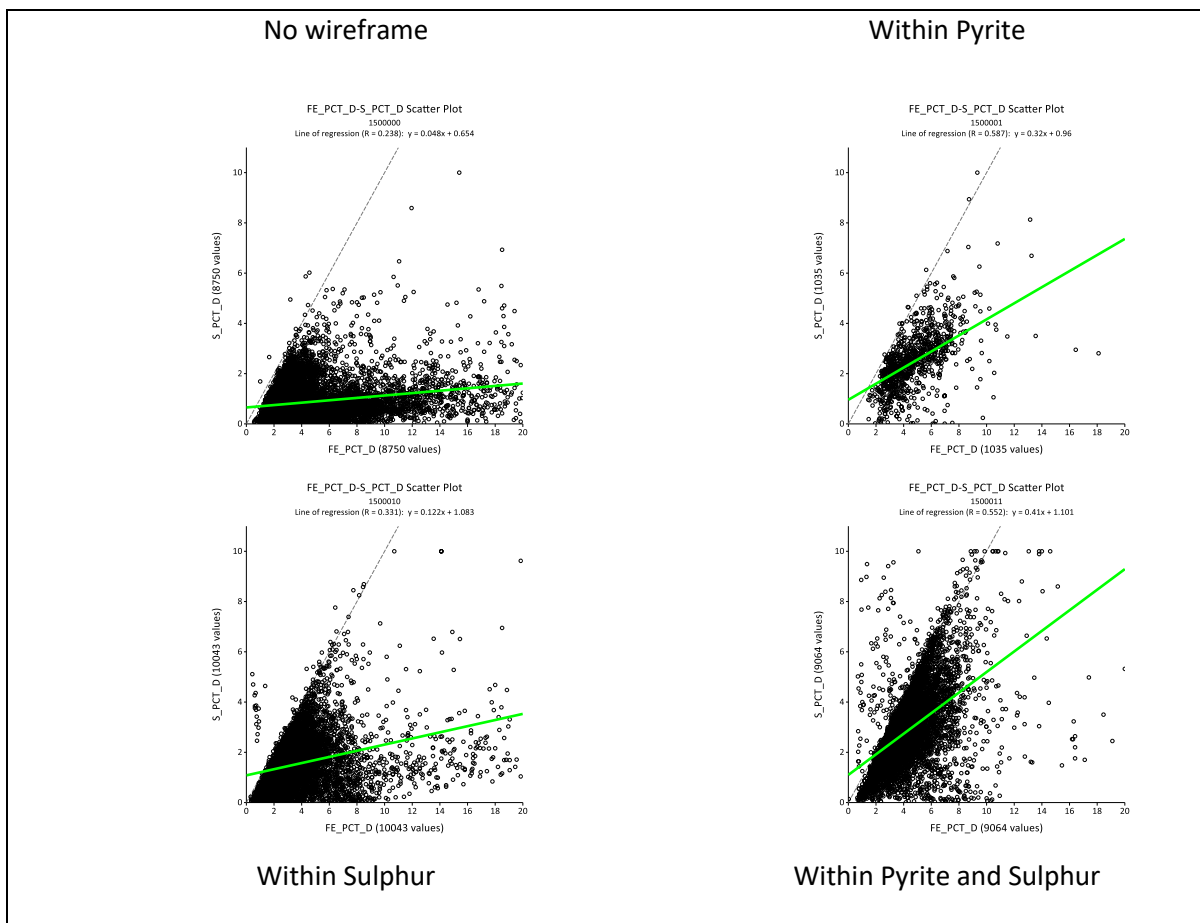


Figure 14.15 Scatterplots between Fe and S for Breccia and Stage 2 domains

Iron and sulphur show the highest correlation in the wireframed pyrite domain which is the top right and within the wireframed pyrite domain and sulphur-sodium domain, bottom right.

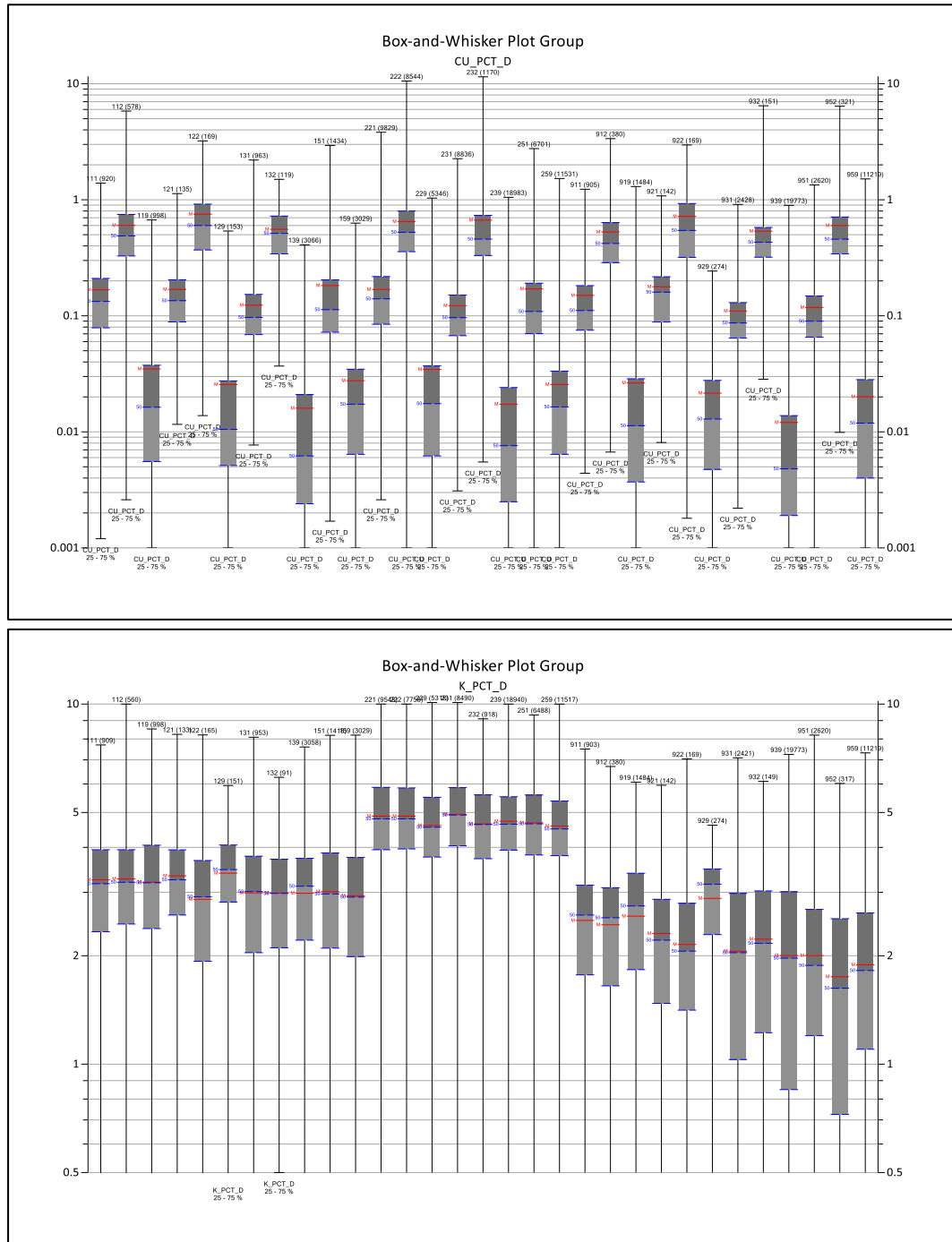


Figure 14.16 Comparison of distributions using box and whisker plots for Fe, top, and S, bottom

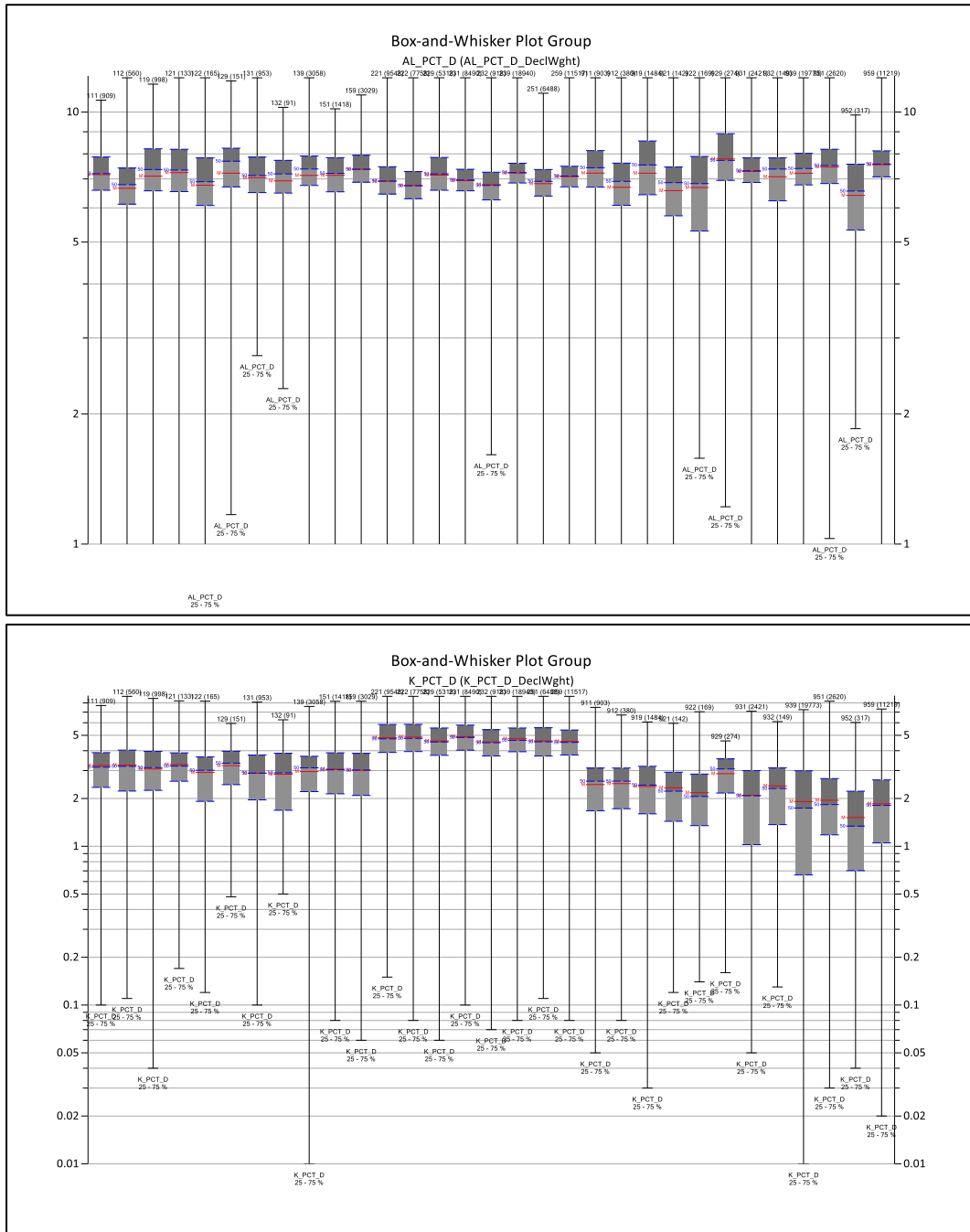


Figure 14.17 Comparison of distributions using box and whisker plots for Al, top, and K, bottom

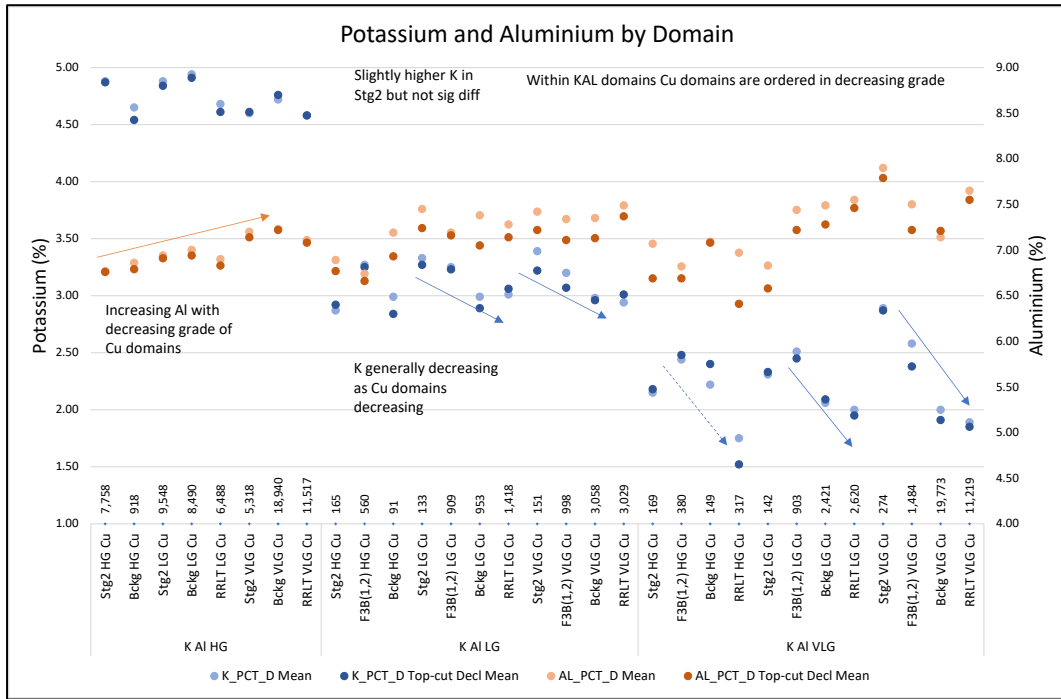


Figure 14.18 Potassium and aluminium by domain

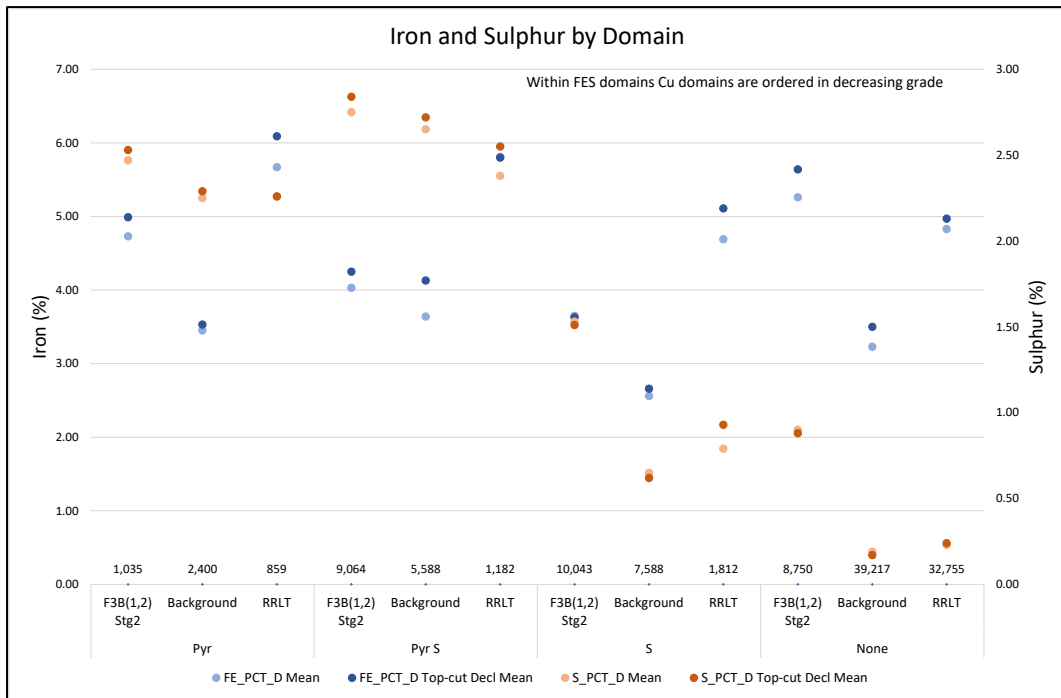


Figure 14.19 Iron and sulphur by domain

Table 14.28 Copper statistics

Domain				Raw					Top-cut			%Diff Raw to Top-cut	Top-cut Decl	%Diff Top-cut to Top-cut Decl	Domain			
Code	Lith	Min	Number	Min	Max	Mean	CV	Value	Num cut	Max	Mean	CV	Mean	CV	Mean	CV	Mean	CV
12	F3B(1,2)	HG Cu	958	0.001	5.81	0.57	0.81	5.00	1	5.00	0.57	0.80	0.0%	-1.2%	0.54	0.81	-5.3%	1.3%
22	Stg2	HG Cu	8,882	0.001	10.55	0.65	0.77	5.00	6	5.00	0.65	0.75	0.0%	-2.6%	0.61	0.73	-6.2%	-2.7%
32	Bckg	HG Cu	1,432	0.010	11.47	0.64	1.05	5.00	4	5.00	0.63	0.94	-1.6%	-10.5%	0.55	0.90	-12.7%	-4.3%
52	RRLT	HG Cu	1,179	0.001	6.40	0.53	0.82	5.00	1	5.00	0.53	0.79	0.0%	-3.7%	0.50	0.78	-5.7%	-1.3%
62	EastOx	HG Cu	97	0.170	2.48	0.68	0.66	5.00	-	2.48	0.68	0.66	0.0%	0.0%	0.65	0.56	-4.4%	-15.2%
11	F3B(1,2)	LG Cu	1,825	0.001	1.39	0.16	0.84	5.00	-	1.39	0.16	0.84	0.0%	0.0%	0.16	0.84	0.0%	0.0%
21	Stg2	LG Cu	10,106	0.001	3.82	0.17	0.80	5.00	-	3.82	0.17	0.80	0.0%	0.0%	0.17	0.82	0.0%	2.5%
31	Bckg	LG Cu	12,119	0.001	2.26	0.12	0.78	5.00	-	2.26	0.12	0.78	0.0%	0.0%	0.12	0.77	0.0%	-1.3%
51	RRLT	LG Cu	9,531	0.001	2.76	0.12	0.80	5.00	-	2.76	0.12	0.80	0.0%	0.0%	0.12	0.89	0.0%	11.3%
61	EastOx	LG Cu	385	0.010	0.67	0.12	0.74	5.00	-	0.67	0.12	0.74	0.0%	0.0%	0.12	0.68	0.0%	-8.1%
19	F3B(1,2)	VLG Cu	2,444	0.001	1.30	0.03	2.04	1.50	-	1.30	0.03	2.04	0.0%	0.0%	0.03	1.94	0.0%	-4.9%
29	Stg2	VLG Cu	5,737	0.001	1.03	0.03	1.76	1.50	-	1.03	0.03	1.76	0.0%	0.0%	0.04	1.64	33.3%	-6.8%
39	Bckg	VLG Cu	36,860	0.001	1.05	0.02	1.73	1.50	-	1.05	0.02	1.73	0.0%	0.0%	0.02	1.89	0.0%	9.2%
59	RRLT	VLG Cu	24,471	0.001	1.53	0.02	1.48	1.50	2	1.50	0.02	1.48	0.0%	0.0%	0.02	1.48	0.0%	0.0%
69	EastOx	VLG Cu	6,344	0.001	0.28	0.01	1.59	1.50	-	0.28	0.01	1.59	0.0%	0.0%	0.01	1.56	0.0%	-1.9%

Table 14.29 Gold statistics

Domain				Raw					Top-cut			%Diff Raw to Top-cut	Top-cut Decl	%Diff Top-cut to Top-cut Decl	Domain			
Code	Lith	Min	Number	Min	Max	Mean	CV	Value	Num cut	Max	Mean	CV	Mean	CV	Mean	CV	Mean	CV
12	F3B(1,2)	HG Cu	878	0.00	0.96	0.12	0.89	1.50	-	0.96	0.12	0.89	0.0%	0.0%	0.12	0.85	0.0%	-4.5%
22	Stg2	HG Cu	7,750	0.00	3.11	0.14	0.96	1.50	7	1.50	0.14	0.89	0.0%	-7.3%	0.13	0.88	-7.1%	-1.1%
32	Bckg	HG Cu	1,086	0.00	2.21	0.10	1.25	1.50	2	1.50	0.10	1.15	0.0%	-8.0%	0.10	1.23	0.0%	7.0%
52	RRLT	HG Cu	970	0.00	3.07	0.10	1.72	1.50	3	1.50	0.09	1.38	-10.0%	-19.8%	0.09	1.31	0.0%	-5.1%
62	EastOx	HG Cu	97	0.01	0.45	0.11	0.75	1.50	-	0.45	0.11	0.75	0.0%	0.0%	0.10	0.74	-9.1%	-1.3%
11	F3B(1,2)	LG Cu	834	0.00	0.29	0.05	0.80	1.50	-	0.29	0.05	0.80	0.0%	0.0%	0.05	0.80	0.0%	0.0%
21	Stg2	LG Cu	5,737	0.00	1.07	0.05	1.07	1.50	-	1.07	0.05	1.07	0.0%	0.0%	0.05	1.01	0.0%	-5.6%
31	Bckg	LG Cu	4,568	0.00	14.15	0.05	4.35	1.50	2	1.50	0.05	1.57	0.0%	-63.9%	0.04	1.40	-20.0%	-10.8%
51	RRLT	LG Cu	3,805	0.00	3.76	0.05	2.69	1.50	9	1.50	0.05	2.05	0.0%	-23.8%	0.05	2.33	0.0%	13.7%
61	EastOx	LG Cu	183	0.00	0.31	0.04	0.90	1.50	-	0.31	0.04	0.90	0.0%	0.0%	0.04	0.90	0.0%	0.0%
19	F3B(1,2)	VLG Cu	143	0.00	1.44	0.07	2.57	1.50	-	1.44	0.07	2.57	0.0%	0.0%	0.04	2.54	-42.9%	-1.2%
29	Stg2	VLG Cu	441	0.00	1.57	0.04	1.95	1.50	1	1.50	0.04	1.90	0.0%	-2.6%	0.04	2.36	0.0%	24.2%
39	Bckg	VLG Cu	545	0.00	1.19	0.04	2.36	1.50	-	1.19	0.04	2.36	0.0%	0.0%	0.03	2.25	-25.0%	-4.7%
59	RRLT	VLG Cu	1,227	0.00	1.40	0.03	2.58	1.50	-	1.40	0.03	2.58	0.0%	0.0%	0.02	2.35	-33.3%	-8.9%
69	EastOx	VLG Cu	21	0.00	0.55	0.12	1.71	1.50	-	0.55	0.12	1.71	0.0%	0.0%	0.10	1.93	-16.7%	12.9%

Table 14.30 Molybdenum statistics

Domain				Raw					Top-cut			%Diff Raw to Top-cut	Top-cut Decl	%Diff Top-cut to Top-cut Decl	Domain			
Code	Lith	Min	Number	Min	Max	Mean	CV	Value	Num cut	Max	Mean	CV	Mean	CV	Mean	CV	Mean	CV
111	F3B(1,2) LG Cu	HG Mo	1,595	0.50	2680.0	125.21	1.64	2700.0	-	2680.0	125.21	1.64	0.0%	0.0%	125.10	1.64	-0.1%	0.0%
112	F3B(1,2) HG Cu	HG Mo	910	0.50	8450.0	269.19	2.13	7000.0	1	7000.0	267.60	2.07	-0.6%	-2.8%	297.38	2.09	11.1%	1.0%
119	F3B(1,2) VLG Cu	HG Mo	1,962	0.50	4330.0	103.19	2.02	2000.0	5	2000.0	100.78	1.73	-2.3%	-14.4%	96.43	1.71	-4.3%	-1.2%
121	Stg2 LG Cu	HG Mo	8,784	0.50	6190.0	136.10	1.64	4000.0	2	4000.0	135.85	1.60	-0.2%	-2.4%	149.27	1.56	9.9%	-2.5%
122	Stg2 HG Cu	HG Mo	7,748	0.50	10000.0	213.16	1.49	5000.0	5	5000.0	211.93	1.37	-0.6%	-8.1%	219.86	1.31	3.7%	-4.4%
129	Stg2 VLG Cu	HG Mo	4,813	0.50	3850.0	120.98	1.58	2000.0	6	2000.0	119.81	1.46	-1.0%	-7.6%	119.05	1.44	-0.6%	-1.4%
131	Bckg LG Cu	HG Mo	2,999	0.50	2190.0	105.75	1.30	2700.0	-	2190.0	105.75	1.30	0.0%	0.0%	99.82	1.20	-5.6%	-7.7%
132	Bckg HG Cu	HG Mo	390	3.00	2120.0	124.76	1.29	1000.0	1	1000.0	121.89	1.09	-2.3%	-15.5%	129.43	1.07	6.2%	-1.8%
139	Bckg VLG Cu	HG Mo	2,907	0.50	1700.0	93.81	1.13	1000.0	4	1000.0	93.17	1.05	-0.7%	-7.1%	90.38	1.04	-3.0%	-1.0%
151	RRLT LG Cu	HG Mo	1,466	0.50	4360.0	94.32	1.79	1000.0	6	1000.0	91.29	1.34	-3.2%	-25.1%	87.74	1.36	-3.9%	1.5%
152	RRLT HG Cu	HG Mo	191	1.00	1070.0	112.72	1.38	600.0	5	600.0	106.70	1.20	-5.3%	-13.0%	111.56	1.19	4.6%	-0.8%
159	RRLT VLG Cu	HG Mo	1,406	0.50	2120.0	72.71	1.66	700.0	7	700.0	69.99	1.35	-3.7%	-18.7%	71.90	1.34	2.7%	-0.7%

Domain				Raw					Top-cut			%Diff Raw to Top-cut	Top-cut Decl	%Diff Top-cut to Top-cut Decl	Domain			
Code	Lith	Min	Number	Min	Max	Mean	CV	Value	Num cut	Max	Mean	CV	Mean	CV	Mean	CV	Mean	CV
911	F3B(1,2) LG Cu	LG Mo	217	0.50	982.0	56.18	2.22	350.0	5	350.0	47.02	1.49	-16.3%	-32.9%	48.28	1.54	2.7%	3.4%
912	F3B(1,2) HG Cu	LG Mo	30	1.00	557.0	111.73	1.29	400.0	2	400.0	104.43	1.20	-6.5%	-7.0%	78.76	1.38	-24.6%	15.0%
919	F3B(1,2) VLG Cu	LG Mo	520	0.50	1960.0	42.24	2.80	400.0	5	400.0	36.62	1.58	-13.3%	-43.6%	36.43	1.67	-0.5%	5.7%
921	Stg2 LG Cu	LG Mo	1,039	0.50	863.0	45.12	1.30	350.0	6	350.0	44.26	1.15	-1.9%	-11.5%	44.23	1.16	-0.1%	0.9%
922	Stg2 HG Cu	LG Mo	344	1.00	725.0	65.50	1.27	400.0	5	400.0	64.12	1.17	-2.1%	-7.9%	59.02	1.21	-8.0%	3.4%
929	Stg2 VLG Cu	LG Mo	930	0.50	409.0	35.43	1.29	450.0	-	409.0	35.43	1.29	0.0%	0.0%	34.32	1.38	-3.1%	7.0%
931	Bckg LG Cu	LG Mo	8,865	0.50	672.0	21.83	1.42	600.0	2	600.0	21.82	1.41	0.0%	-0.7%	19.98	1.60	-8.4%	13.5%
932	Bckg HG Cu	LG Mo	768	0.50	2960.0	39.79	2.97	400.0	3	400.0	36.18	1.46	-9.1%	-50.8%	32.65	1.63	-9.8%	11.6%
939	Bckg VLG Cu	LG Mo	38,864	0.39	2695.7	10.45	2.38	350.0	13	350.0	10.24	1.54	-2.0%	-35.3%	8.43	4.30	-17.7%	179.2%
951	RRLT LG Cu	LG Mo	8,252	0.50	1160.0	19.55	2.22	1000.0	1	1000.0	19.53	2.20	-0.1%	-0.9%	17.71	2.45	-9.3%	11.4%
952	RRLT HG Cu	LG Mo	934	0.50	2300.0	35.22	2.89	600.0	4	600.0	32.73	1.95	-7.1%	-32.5%	25.51	2.10	-22.1%	7.7%
959	RRLT VLG Cu	LG Mo	24,359	0.50	939.0	8.30	2.89	600.0	12	600.0	8.21	2.61	-1.1%	-9.7%	6.65	2.63	-19.0%	0.8%

Table 14.31 Cobalt statistics

Domain				Raw					Top-cut			%Diff Raw to Top-cut	Top-cut Decl	%Diff Top-cut to Top-cut Decl	Domain			
Code	Lith	Min	Number	Min	Max	Mean	CV	Value	Num cut	Max	Mean	CV	Mean	CV	Mean	CV	Mean	CV
1	Pyrite	HG Co	16,657	1.00	5,590.0	170.84	0.91	1500.0	15	1500.0	169.68	0.80	-0.7%	-12.1%	152.91	0.79	-9.9%	-1.3%
2	Pyrite	LG Co	3,471	0.50	1,020.0	44.82	1.16	500.0	6	500.0	44.39	1.04	-1.0%	-10.3%	47.01	1.08	5.9%	3.8%
3	No pyrite	HG Co	31,585	1.00	3,430.0	113.86	0.91	1500.0	13	1500.0	113.66	0.88	-0.2%	-3.3%	107.77	0.90	-5.2%	2.3%
4	No pyrite	LG Co	68,579	0.50	1,780.0	23.65	1.21	500.0	12	500.0	23.59	1.15	-0.3%	-5.0%	22.25	1.16	-5.7%	0.9%

Table 14.32 Calcium statistics

Domain				Raw					Top-cut			%Diff Raw to Top-cut	Top-cut Decl	%Diff Top-cut to Top-cut Decl	Domain			
Code	Lith	Min	Number	Min	Max	Mean	CV	Value	Num cut	Max	Mean	CV	Mean	CV	Mean	CV	Mean	CV
5	All	HG Ca	47,950	0.02	20.30	1.46	0.89	13.00	3	13.00	1.46	0.88	0.0%	-1.1%	1.57	0.88	7.5%	0.0%
9	All	LG Ca	72,342	0.01	19.05	0.44	1.87	6.00	315	6.00	0.43	1.74	-2.3%	-7.0%	0.68	1.64	58.1%	-5.7%

Table 14.33 Iron statistics

Domain				Raw					Top-cut			%Diff Raw to Top-cut	Top-cut Decl	%Diff Top-cut to Top-cut Decl	Domain			
Code	Lith	Min	Number	Min	Max	Mean	CV	Value	Num cut	Max	Mean	CV	Mean	CV	Mean	CV	Mean	CV
1500000	F3B(1,2) Stg2	None	8,750	0.56	42.50	5.26	0.78	50.00	-	42.50	5.26	0.78	0.0%	0.0%	5.64	0.84	7.2%	7.7%
1500001	F3B(1,2) Stg2	Pyr	1,035	1.44	29.70	4.73	0.46	50.00	-	29.70	4.73	0.46	0.0%	0.0%	4.99	0.50	5.5%	8.7%
1500010	F3B(1,2) Stg2	S	10,043	0.31	39.40	3.65	0.70	50.00	-	39.40	3.65	0.70	0.0%	0.0%	3.63	0.78	-0.5%	11.4%
1500011	F3B(1,2) Stg2	Pyr S	9,064	0.03	35.10	4.03	0.47	50.00	-	35.10	4.03	0.47	0.0%	0.0%	4.25	0.61	5.5%	29.8%
5000000	RRLT LG Cu	None	32,755	0.25	50.10	4.83	0.74	50.00	1	50.00	4.83	0.74	0.0%	0.0%	4.97	0.77	2.9%	4.1%
5000001	RRLT LG Cu	Pyr	859	1.61	33.20	5.67	0.58	50.00	-	33.20	5.67	0.58	0.0%	0.0%	6.09	0.65	7.4%	12.1%
5000010	RRLT LG Cu	S	1,812	0.37	44.60	4.69	0.90	50.00	-	44.60	4.69	0.90	0.0%	0.0%	5.11	0.95	9.0%	5.6%
5000011	RRLT LG Cu	Pyr S	1,182	0.51	32.50	5.81	0.69	50.00	-	32.50	5.81	0.69	0.0%	0.0%	5.80	0.77	-0.2%	11.6%
9900000	Background	None	39,217	0.11	50.00	3.23	0.78	50.00	1	50.00	3.23	0.78	0.0%	0.0%	3.50	0.84	8.4%	7.7%

Domain				Raw					Top-cut			%Diff Raw to Top-cut	Top-cut Decl	%Diff Top-cut to Top-cut Decl	Domain			
Code	Lith	Min	Number	Min	Max	Mean	CV	Value	Num cut	Max	Mean	CV	Mean	CV	Mean	CV	Mean	CV
9900001	Background	Pyr	2,400	0.01	17.65	3.45	0.36	50.00	-	17.65	3.45	0.36	0.0%	0.0%	3.53	0.39	2.3%	8.3%
9900010	Background	S	7,588	0.25	50.10	2.56	0.88	50.00	-	50.00	2.56	0.88	0.0%	0.0%	2.66	1.26	3.9%	43.2%
9900011	Background	Pyr S	5,588	0.35	35.70	3.64	0.55	50.00	-	35.70	3.64	0.55	0.0%	0.0%	4.13	0.67	13.5%	21.8%

Table 14.34 Sulphur statistics

Domain				Raw					Top-cut			%Diff Raw to Top-cut	Top-cut Decl	%Diff Top-cut to Top-cut Decl	Domain			
Code	Lith	Min	Number	Min	Max	Mean	CV	Value	Num cut	Max	Mean	CV	Mean	CV	Mean	CV	Mean	CV
1500000	F3B(1,2) Stg2	None	8,750	0.01	10.10	0.90	0.90	10.00	4	10.00	0.90	0.90	0.0%	0.0%	0.88	0.93	-2.2%	3.3%
1500001	F3B(1,2) Stg2	Pyr	1,035	0.01	10.00	2.47	0.48	10.00	-	10.00	2.47	0.48	0.0%	0.0%	2.53	0.49	2.4%	2.1%
1500010	F3B(1,2) Stg2	S	10,043	0.01	10.10	1.53	0.62	10.00	1	10.00	1.53	0.62	0.0%	0.0%	1.51	0.67	-1.3%	8.1%
1500011	F3B(1,2) Stg2	Pyr S	9,064	0.01	10.10	2.75	0.52	10.00	5	10.00	2.75	0.52	0.0%	0.0%	2.84	0.54	3.3%	3.8%
5000000	RRLT LG Cu	None	32,755	0.01	10.10	0.23	1.99	5.00	25	5.00	0.23	1.90	0.0%	-4.5%	0.24	1.91	4.3%	0.5%
5000001	RRLT LG Cu	Pyr	859	0.01	10.10	2.26	0.63	10.00	2	10.00	2.26	0.63	0.0%	0.0%	2.26	0.69	0.0%	9.5%
5000010	RRLT LG Cu	S	1,812	0.01	10.10	0.80	1.25	5.00	13	5.00	0.79	1.19	-1.3%	-4.8%	0.93	1.21	17.7%	1.7%
5000011	RRLT LG Cu	Pyr S	1,182	0.01	10.10	2.39	0.69	10.00	5	10.00	2.38	0.68	-0.4%	-1.4%	2.55	0.69	7.1%	1.5%
9900000	Background	None	39,217	0.01	10.00	0.20	2.16	5.00	12	5.00	0.19	2.13	-5.0%	-1.4%	0.17	2.22	-10.5%	4.2%

Domain				Raw					Top-cut			%Diff Raw to Top-cut	Top-cut Decl	%Diff Top-cut to Top-cut Decl	Domain			
Code	Lith	Min	Number	Min	Max	Mean	CV	Value	Num cut	Max	Mean	CV	Mean	CV	Mean	CV	Mean	CV
9900001	Background	Pyr	2,400	0.01	8.98	2.25	0.41	10.00	-	8.98	2.25	0.41	0.0%	0.0%	2.29	0.40	1.8%	-2.4%
9900010	Background	S	7,588	0.01	9.50	0.65	1.24	5.00	10	5.00	0.65	1.22	0.0%	-1.6%	0.62	1.26	-4.6%	3.3%
9900011	Background	Pyr S	5,588	0.01	10.10	2.65	0.52	10.00	2	10.00	2.65	0.52	0.0%	0.0%	2.72	0.55	2.6%	5.8%

Table 14.35 Potassium statistics

Domain				Raw					Top-cut			%Diff Raw to Top-cut	Top-cut Decl	%Diff Top-cut to Top-cut Decl	Domain			
Code	Lith	Min	Number	Min	Max	Mean	CV	Value	Num cut	Max	Mean	CV	Mean	CV	Mean	CV	Mean	CV
111	F3B(1,2) LG Cu	HG Mo	1,595	0.50	2680.0	125.21	1.64	2700.0	-	2680.0	125.21	1.64	0.0%	0.0%	125.10	1.64	-0.1%	0.0%
112	F3B(1,2) HG Cu	HG Mo	910	0.50	8450.0	269.19	2.13	7000.0	1	7000.0	267.60	2.07	-0.6%	-2.8%	297.38	2.09	11.1%	1.0%
119	F3B(1,2) VLG Cu	HG Mo	1,962	0.50	4330.0	103.19	2.02	2000.0	5	2000.0	100.78	1.73	-2.3%	-14.4%	96.43	1.71	-4.3%	-1.2%
121	Stg2 LG Cu	HG Mo	8,784	0.50	6190.0	136.10	1.64	4000.0	2	4000.0	135.85	1.60	-0.2%	-2.4%	149.27	1.56	9.9%	-2.5%
122	Stg2 HG Cu	HG Mo	7,748	0.50	10000.0	213.16	1.49	5000.0	5	5000.0	211.93	1.37	-0.6%	-8.1%	219.86	1.31	3.7%	-4.4%
129	Stg2 VLG Cu	HG Mo	4,813	0.50	3850.0	120.98	1.58	2000.0	6	2000.0	119.81	1.46	-1.0%	-7.6%	119.05	1.44	-0.6%	-1.4%
131	Bckg LG Cu	HG Mo	2,999	0.50	2190.0	105.75	1.30	2700.0	-	2190.0	105.75	1.30	0.0%	0.0%	99.82	1.20	-5.6%	-7.7%
132	Bckg HG Cu	HG Mo	390	3.00	2120.0	124.76	1.29	1000.0	1	1000.0	121.89	1.09	-2.3%	-15.5%	129.43	1.07	6.2%	-1.8%
139	Bckg VLG Cu	HG Mo	2,907	0.50	1700.0	93.81	1.13	1000.0	4	1000.0	93.17	1.05	-0.7%	-7.1%	90.38	1.04	-3.0%	-1.0%
151	RRLT LG Cu	HG Mo	1,466	0.50	4360.0	94.32	1.79	1000.0	6	1000.0	91.29	1.34	-3.2%	-25.1%	87.74	1.36	-3.9%	1.5%
152	RRLT HG Cu	HG Mo	191	1.00	1070.0	112.72	1.38	600.0	5	600.0	106.70	1.20	-5.3%	-13.0%	111.56	1.19	4.6%	-0.8%
159	RRLT VLG Cu	HG Mo	1,406	0.50	2120.0	72.71	1.66	700.0	7	700.0	69.99	1.35	-3.7%	-18.7%	71.90	1.34	2.7%	-0.7%
911	F3B(1,2) LG Cu	LG Mo	217	0.50	982.0	56.18	2.22	350.0	5	350.0	47.02	1.49	-16.3%	-32.9%	48.28	1.54	2.7%	3.4%
912	F3B(1,2) HG Cu	LG Mo	30	1.00	557.0	111.73	1.29	400.0	2	400.0	104.43	1.20	-6.5%	-7.0%	78.76	1.38	-24.6%	15.0%

Domain				Raw					Top-cut			%Diff Raw to Top-cut	Top-cut Decl	%Diff Top-cut to Top-cut Decl	Domain			
Code	Lith	Min	Number	Min	Max	Mean	CV	Value	Num cut	Max	Mean	CV	Mean	CV	Mean	CV	Mean	CV
919	F3B(1,2) VLG Cu	LG Mo	520	0.50	1960.0	42.24	2.80	400.0	5	400.0	36.62	1.58	-13.3%	-43.6%	36.43	1.67	-0.5%	5.7%
921	Stg2 LG Cu	LG Mo	1,039	0.50	863.0	45.12	1.30	350.0	6	350.0	44.26	1.15	-1.9%	-11.5%	44.23	1.16	-0.1%	0.9%
922	Stg2 HG Cu	LG Mo	344	1.00	725.0	65.50	1.27	400.0	5	400.0	64.12	1.17	-2.1%	-7.9%	59.02	1.21	-8.0%	3.4%
929	Stg2 VLG Cu	LG Mo	930	0.50	409.0	35.43	1.29	450.0	-	409.0	35.43	1.29	0.0%	0.0%	34.32	1.38	-3.1%	7.0%
931	Bckg LG Cu	LG Mo	8,865	0.50	672.0	21.83	1.42	600.0	2	600.0	21.82	1.41	0.0%	-0.7%	19.98	1.60	-8.4%	13.5%
932	Bckg HG Cu	LG Mo	768	0.50	2960.0	39.79	2.97	400.0	3	400.0	36.18	1.46	-9.1%	-50.8%	32.65	1.63	-9.8%	11.6%
939	Bckg VLG Cu	LG Mo	38,864	0.39	2695.7	10.45	2.38	350.0	18	350.0	10.24	1.54	-2.0%	-35.3%	8.43	4.30	-17.7%	179.2%
951	RRLT LG Cu	LG Mo	8,252	0.50	1160.0	19.55	2.22	1000.0	1	1000.0	19.53	2.20	-0.1%	-0.9%	17.71	2.45	-9.3%	11.4%

Table 14.36 Aluminium statistics

Domain				Raw					Top-cut			%Diff Raw to Top-cut	Top-cut Decl	%Diff Top-cut to Top-cut Decl	Domain			
Code	Lith	Min	Number	Min	Max	Mean	CV	Value	Num cut	Max	Mean	CV	Mean	CV	Mean	CV	Mean	CV
111	F3B(1,2) LG Cu	HG Mo	909	0.58	10.65	7.19	0.17	12.00	-	10.65	7.19	0.17	0.0%	0.0%	7.16	0.17	-0.4%	0.0%
112	F3B(1,2) HG Cu	HG Mo	560	0.25	12.10	6.74	0.22	12.00	1	12.00	6.74	0.22	0.0%	0.0%	6.66	0.22	-1.2%	0.0%
119	F3B(1,2) VLG Cu	HG Mo	998	0.09	11.60	7.34	0.24	12.00	-	11.60	7.34	0.24	0.0%	0.0%	7.11	0.28	-3.1%	16.7%

Domain				Raw					Top-cut			%Diff Raw to Top-cut	Top-cut Decl	%Diff Top-cut to Top-cut Decl	Domain			
Code	Lith	Min	Number	Min	Max	Mean	CV	Value	Num cut	Max	Mean	CV	Mean	CV	Mean	CV	Mean	CV
121	Stg2 LG Cu	HG Mo	133	0.60	19.41	7.54	0.28	12.00	2	12.00	7.45	0.24	-1.2%	-14.3%	7.24	0.25	-2.8%	4.2%
122	Stg2 HG Cu	HG Mo	165	0.80	14.10	6.90	0.24	12.00	1	12.00	6.89	0.24	-0.1%	0.0%	6.77	0.23	-1.7%	-4.2%
129	Stg2 VLG Cu	HG Mo	151	1.17	11.80	7.42	0.25	12.00	-	11.80	7.42	0.25	0.0%	0.0%	7.22	0.26	-2.7%	4.0%
131	Bckg LG Cu	HG Mo	953	2.73	13.25	7.38	0.15	12.00	1	12.00	7.38	0.15	0.0%	0.0%	7.05	0.20	-4.5%	33.3%
132	Bckg HG Cu	HG Mo	91	2.29	10.25	7.19	0.16	12.00	-	10.25	7.19	0.16	0.0%	0.0%	6.93	0.19	-3.6%	18.8%
139	Bckg VLG Cu	HG Mo	3,058	0.01	12.90	7.35	0.23	12.00	14	12.00	7.35	0.23	0.0%	0.0%	7.13	0.23	-3.0%	0.0%
151	RRLT LG Cu	HG Mo	1,418	0.55	10.17	7.28	0.15	12.00	-	10.17	7.28	0.15	0.0%	0.0%	7.14	0.16	-1.9%	6.7%
152	RRLT HG Cu	HG Mo	3,029	0.15	10.95	7.49	0.13	12.00	-	10.95	7.49	0.13	0.0%	0.0%	7.37	0.13	-1.6%	0.0%
159	RRLT VLG Cu	HG Mo	9,548	0.30	12.55	6.94	0.15	12.00	2	12.00	6.94	0.15	0.0%	0.0%	6.91	0.15	-0.4%	0.0%
911	F3B(1,2) LG Cu	LG Mo	7,758	0.55	12.65	6.77	0.15	12.00	1	12.00	6.77	0.15	0.0%	0.0%	6.76	0.15	-0.1%	0.0%
912	F3B(1,2) HG Cu	LG Mo	5,318	0.15	13.70	7.20	0.19	12.00	1	12.00	7.20	0.19	0.0%	0.0%	7.14	0.20	-0.8%	5.3%
919	F3B(1,2) VLG Cu	LG Mo	8,490	0.08	12.00	7.00	0.13	12.00	-	12.00	7.00	0.13	0.0%	0.0%	6.94	0.13	-0.9%	0.0%
921	Stg2 LG Cu	LG Mo	918	1.61	12.80	6.86	0.13	12.00	1	12.00	6.86	0.13	0.0%	0.0%	6.79	0.13	-1.0%	0.0%
922	Stg2 HG Cu	LG Mo	18,940	0.30	16.30	7.23	0.14	12.00	10	12.00	7.23	0.14	0.0%	0.0%	7.22	0.13	-0.1%	-7.1%
929	Stg2 VLG Cu	LG Mo	6,488	0.20	11.05	6.90	0.13	12.00	-	11.05	6.90	0.13	0.0%	0.0%	6.83	0.14	-1.0%	7.7%
931	Bckg LG Cu	LG Mo	11,517	0.66	12.05	7.11	0.11	12.00	1	12.00	7.11	0.11	0.0%	0.0%	7.08	0.11	-0.4%	0.0%

Domain				Raw					Top-cut			%Diff Raw to Top-cut	Top-cut Decl	%Diff Top-cut to Top-cut Decl	Domain			
Code	Lith	Min	Number	Min	Max	Mean	CV	Value	Num cut	Max	Mean	CV	Mean	CV	Mean	CV	Mean	CV
932	Bckg HG Cu	LG Mo	903	0.16	12.10	7.44	0.19	12.00	1	12.00	7.44	0.19	0.0%	0.0%	7.22	0.23	-3.0%	21.1%
939	Bckg VLG Cu	LG Mo	380	0.35	12.75	6.82	0.25	12.00	2	12.00	6.82	0.24	0.0%	-4.0%	6.69	0.24	-1.9%	0.0%
951	RRLT LG Cu	LG Mo	1,484	0.11	13.45	7.51	0.28	12.00	17	12.00	7.50	0.28	-0.1%	0.0%	7.22	0.32	-3.7%	14.3%

14.1.13.1 Correlation

Correlations between all elements within the copper mineralised domains were calculated to assess the relationships between the elements. The correlation coefficient is a measure of the linear relationship between variables and varies between +1 and -1, with a positive correlation coefficient indicating a positive relationship and a negative correlation coefficient indicating a negative relationship. A correlation coefficient of close to zero indicates there is no linear relationship between the variables. Those elements which display strong correlations either positive or negative, should have similar spatial continuity, with variogram models showing similar ranges. Additionally, the correlations between elements should be preserved as much as possible in the block grade estimates.

The correlation coefficients for the four highest grade Cu domains presented in Table 14.37 for Facies 3B (1,2) low grade Cu, Table 14.38 for Facies 3B (1,2) high grade Cu, Table 14.39 for Stage 2 low grade Cu and Table 14.40 for Stage 2 high grade Cu.

The only elements which show strong correlations are Cu with Au and Co with S.

Table 14.37 Correlation matrix – Mid Area – F3B (1,2) LG Cu – 50011

	CU	AU	MO	AL	CA	CO	FE	K	S
CU	1	0.66	0.17	-0.11	0.01	0.11	0.09	0.10	0.15
AU	0.66	1	0.12	-0.01	0.05	0.07	0.04	0.00	0.15
MO	0.17	0.12	1	-0.07	0.02	0.05	-0.07	0.05	0.03
AL	-0.11	-0.01	-0.07	1	0.07	0.05	-0.21	0.28	0.01
CA	0.01	0.05	0.02	0.07	1	-0.21	0.27	-0.22	-0.14
CO	0.11	0.07	0.05	0.05	-0.21	1	0.07	0.11	0.68
FE	0.09	0.04	-0.07	-0.21	0.27	0.07	1	-0.14	0.08
K	0.10	0.00	0.05	0.28	-0.22	0.11	-0.14	1	0.05
S	0.15	0.15	0.03	0.01	-0.14	0.68	0.08	0.05	1

Table 14.38 Correlation matrix – Mid Area – F3B(1,2) HG Cu- 50012

	CU	AU	MO	AL	CA	CO	FE	K	S
CU	1	0.68	0.09	-0.16	-0.05	0.19	0.02	0.01	0.31
AU	0.68	1	0.09	-0.06	-0.04	0.12	0.02	0.05	0.23
MO	0.09	0.09	1	-0.05	0.11	-0.01	0.06	-0.06	0.08
AL	-0.16	-0.06	-0.05	1	0.05	-0.01	-0.17	0.39	-0.05
CA	-0.05	-0.04	0.11	0.05	1	-0.11	0.30	-0.04	0.06
CO	0.19	0.12	-0.01	-0.01	-0.11	1	0.16	0.06	0.60
FE	0.02	0.02	0.06	-0.17	0.30	0.16	1	-0.10	0.16
K	0.01	0.05	-0.06	0.39	-0.04	0.06	-0.10	1	0.06
S	0.31	0.23	0.08	-0.05	0.06	0.60	0.16	0.06	1

Table 14.39 Correlation matrix – Mid Area – Stage 2 LG Cu – 50021

	CU	AU	MO	AL	CA	CO	FE	K	S
CU	1	0.68	0.09	-0.16	-0.05	0.19	0.02	0.01	0.31
AU	0.68	1	0.09	-0.06	-0.04	0.12	0.02	0.05	0.23
MO	0.09	0.09	1	-0.05	0.11	-0.01	0.06	-0.06	0.08
AL	-0.16	-0.06	-0.05	1	0.05	-0.01	-0.17	0.39	-0.05
CA	-0.05	-0.04	0.11	0.05	1	-0.11	0.30	-0.04	0.06
CO	0.19	0.12	-0.01	-0.01	-0.11	1	0.16	0.06	0.60
FE	0.02	0.02	0.06	-0.17	0.30	0.16	1	-0.10	0.16
K	0.01	0.05	-0.06	0.39	-0.04	0.06	-0.10	1	0.06
S	0.31	0.23	0.08	-0.05	0.06	0.60	0.16	0.06	1

Table 14.40 Correlation matrix – Mid Area – Stage 2 HG Cu – 50022

	CU	AU	MO	AL	CA	CO	FE	K	S
CU	1	0.74	0.20	-0.10	-0.04	0.27	0.07	-0.08	0.41
AU	0.74	1	0.16	-0.07	-0.03	0.22	0.07	-0.06	0.36
MO	0.20	0.16	1	-0.07	0.04	0.08	-0.01	-0.05	0.12
AL	-0.10	-0.07	-0.07	1	-0.07	0.06	-0.28	0.34	-0.01
CA	-0.04	-0.03	0.04	-0.07	1	-0.08	0.28	-0.19	-0.01
CO	0.27	0.22	0.08	0.06	-0.08	1	0.08	-0.15	0.51
FE	0.07	0.07	-0.01	-0.28	0.28	0.08	1	-0.23	0.24
K	-0.08	-0.06	-0.05	0.34	-0.19	-0.15	-0.23	1	-0.07
S	0.41	0.36	0.12	-0.01	-0.01	0.51	0.24	-0.07	1

14.1.14 Variography

Mineralisation continuity was examined via variography. Variography examines the spatial relationship between composites and seeks to identify the directions of mineralisation continuity and to quantify the ranges of grade continuity. Variography was also used to determine the random variability or 'nugget effect' of the deposit. The results provide the basis for determining appropriate kriging parameters for resource estimation.

Snowden Supervisor Version 8.14.3.0 software was used to generate and model the variograms. The correlation coefficients were used to guide the variogram modelling, with moderate to high correlations between elements indicating that similar ranges of continuity should be observed for those elements.

In some cases, domains with similar characteristics were combined for continuity analysis to provide the most robust data for analysis.

A normal score transformation was applied to each of the variables prior to experimental variogram calculation. The normal score variogram model's variance was back-transformed to traditional space after modelling to adjust the variance using hermite polynomials in the Supervisor software. All models used spherical structures.

Due to the reduced amount and more widely spaced data the variogram models for the north area are not as robust as the mid and south areas. In this case there has been only one variogram model created for each element which has generally been interpreted from the higher-grade domains for the elements.

The variogram model parameters used for resource estimation, back-transformed, are shown in Table 14.41 for the mid area, Table 14.42 for the south area and Table 14.43 for the north area.

The normal score variogram model for mineralised Cu is illustrated in Figure 14.20.

Table 14.41 Grade variogram models – Mid Area

VREF	Variable	Rotation (Datamine ZXZ)			Nugget C ₀	Structure 1		Structure 2		Structure 3	
						C ₁	R ₁	C ₁	R ₁	C ₁	R ₁
1	Cu	120	90	0	0.172	0.490	20	0.160	50	0.178	180
							10		45		120
							10		45		45
2	Au	120	90	0	0.262	0.500	20	0.116	50	0.122	180
							10		55		140
							10		45		55
3	Mo high Mo low Cu	120	90	0	0.324	0.450	20	0.145	6	0.081	300
							15		120		160
							10		15		75
4	Mo high Mo high Cu	120	90	0	0.273	0.498	20	0.124	100	0.105	650
							20		40		200
							10		60		60
5	Mo low Mo high Cu	120	90	0	0.322	0.405	40	0.157	120	0.116	1100
							40		120		160
							40		60		400
6	Mo low Mo low Cu	120	90	0	0.155	0.440	30	0.193	40	0.212	640
							30		180		300
							10		40		250
7	Co High in pyr	60	90	0	0.205	0.499	30	0.113	40	0.183	550
							20		50		230
							10		90		90
8	Co High not in pyr	60	90	0	0.158	0.202	40	0.280	45	0.360	460
							20		180		200
							10		60		75
9	Co Low in pyr	60	90	0	0.204	0.610	20	0.095	60	0.091	240
							20		60		170
							10		30		50
10	Co Low not in pyr	60	90	0	0.104	0.375	30	0.251	100	0.270	380
							30		85		540
							30		70		200
11	Ca	110	60	0	0.074	0.521	25	0.167	60	0.238	470
							20		100		470
							15		150		150
12	Fe FB3Stg2	120	90	0	0.041	0.642	35	0.159	80	0.158	320
							10		25		180
							15		45		140
13	Fe RLLT	120	90	0	0.038	0.446	85	0.282	140	0.234	900
							40		230		500

VREF	Variable	Rotation (Datamine ZXZ)			Nugget	Structure 1		Structure 2		Structure 3	
					C ₀	C ₁	R ₁	C ₁	R ₁	C ₁	R ₁
							15		60		290
14	Fe Bcgk	120	90	0	0.040	0.554	40	0.174	170	0.232	850
							30		250		300
							20		90		170
15	S FB3Stg2	120	90	0	0.098	0.416	30	0.168	120	0.318	1000
							15		90		230
							15		110		230
16	S RLLT	120	90	0	0.030	0.278	35	0.239	120	0.453	1200
							20		60		120
							20		100		650
17	S Bcgk	120	90	0	0.030	0.393	35	0.312	190	0.265	600
							30		100		350
							30		200		300
18	Cu Ox	120	170	0	0.093	0.628	20	0.192	60	0.087	260
							20		60		260
							10		40		40
19	Al LG KAL	110	110	0	0.120	0.459	15	0.175	50	0.243	100
							15		60		60
							8		25		40
20	Al HG KAL	110	110	0	0.121	0.453	20	0.192	30	0.234	80
							20		60		140
							10		15		80
21	Al VLG KAL	90	110	0	0.075	0.532	20	0.243	50	0.150	55
							20		70		100
							10		20		20
22	K LG KAL	110	90	0	0.102	0.432	20	0.298	50	0.168	170
							15		40		160
							15		20		60
23	K HG KAL	110	90	0	0.102	0.490	20	0.239	45	0.169	200
							15		60		205
							10		40		75
24	K VLG KAL	110	90	0	0.031	0.575	25	0.227	120	0.167	600
							20		280		280
							20		100		100

Table 14.42 Grade variogram models – South Area

VREF	Variable	Rotation (Datamine ZXZ)			Nugget C ₀	Structure 1		Structure 2		Structure 3	
						C ₁	R ₁	C ₁	R ₁	C ₁	R ₁
30	Cu	125	135	0	0.170	0.50	25	0.140	100	0.170	300
							25		40		180
							10		15		70
31	Au	125	135	0	0.180	0.530	25	0.140	100	0.150	200
							25		40		150
							15		25		100
32	Mo high Mo low Cu	125	135	0	0.360	0.460	50	0.080	115	0.100	150
							20		40		90
							10		15		60
33	Mo high Mo high Cu	125	135	0	0.270	0.450	50	0.110	115	0.170	150
							20		40		90
							10		15		60
34	Mo low Mo high Cu	125	135	0	0.330	0.450	30	0.130	100	0.090	650
							20		80		350
							15		30		30
35	Mo low Mo low Cu	125	135	0	0.150	0.630	40	0.120	250	0.100	970
							20		120		350
							15		45		50
36	Co High in pyr	100	80	0	0.190	0.530	35	0.120	80	0.160	500
							20		125		255
							15		65		120
37	Co High not in pyr	100	80	0	0.210	0.520	35	0.150	130	0.120	210
							15		100		125
							10		55		55
38	Co Low in pyr	100	80	0	0.240	0.450	35	0.210	80	0.100	130
							20		75		120
							10		35		40
39	Co Low not in pyr	100	90	0	0.070	0.510	35	0.240	85	0.180	215
							20		85		375
							10		35		220
40	Ca	125	90	0	0.070	0.400	25	0.210	100	0.320	350
							20		40		220
							20		80		180
41	Fe FB3Stg2	125	110	0	0.190	0.250	25	0.340	100	0.220	400
							25		100		200
							25		100		100
42	Fe RLLT	125	90	0	0.070	0.370	25	0.360	110	0.200	310
							15		50		200

VREF	Variable	Rotation (Datamine ZXZ)			Nugget	Structure 1		Structure 2		Structure 3	
					C ₀	C ₁	R ₁	C ₁	R ₁	C ₁	R ₁
							15		50		275
43	Fe Bcgk	125	90	0	0.060	0.390	30	0.300	140	0.250	500
							30		140		350
							30		120		120
44	S FB3Stg2	100	110	0	0.130	0.480	70	0.180	120	0.210	750
							50		120		150
							40		120		150
45	S RLLT	125	90	0	0.030	0.390	35	0.270	650	0.310	750
							50		100		150
							35		300		700
46	S Bcgk	125	90	0	0.030	0.410	90	0.260	430	0.300	750
							50		100		150
							35		300		650
47	Cu Ox	110	110	0	0.120	0.490	60	0.240	90	0.150	100
							40		80		100
							20		60		70
48	Al LG KAL	110	110	0	0.120	0.450	30	0.200	55	0.230	180
							40		70		110
							20		40		90
49	Al HG KAL	90	110	0	0.100	0.510	20	0.240	60	0.150	120
							20		50		55
							20		50		60
50	Al VLG KAL	110	110	0	0.100	0.430	30	0.300	80	0.170	275
							40		80		160
							10		25		50
51	K LG KAL	110	110	0	0.100	0.430	30	0.210	100	0.260	275
							40		80		250
							20		30		80
52	K HG KAL	110	110	0	0.030	0.530	30	0.160	120	0.280	500
							20		60		320
							20		80		200
53	K VLG KAL	125	135	0	0.170	0.520	25	0.140	100	0.170	300
							25		40		180
							10		15		70

Table 14.43 Grade variogram models – North Area

VREF	Variable	Rotation (Datamine ZXZ)			Nugget C ₀	Structure 1		Structure 2		Structure 3	
						C ₁	R ₁	C ₁	R ₁	C ₁	R ₁
60	Cu	100	25	0	0.405	0.369	35	0.126	110	0.100	120
							25		50		80
							5		12		17
61	Au	100	25	0	0.408	0.379	35	0.123	110	0.090	120
							25		50		80
							5		12		17
62	Fe	100	25	0	0.078	0.413	50	0.229	330	0.280	450
							50		50		280
							10		20		30
63	S	100	25	0	0.063	0.317	70	0.249	350	0.371	1000
							50		200		250
							10		65		65
64	Mo	100	25	0	0.300	0.420	90	0.190	130	0.090	330
							50		50		80
							4		13		13
65	Co	30	25	0	0.275	0.474	40	0.166	100	0.085	130
							40		50		60
							4		13		130
66	Ca	120	150	0	0.070	0.473	40	0.243	85	0.214	330
							80		90		330
							15		70		150
67	Al	100	25	0	0.130	0.270	35	0.280	60	0.320	180
							25		50		80
							10		35		45
68	K	100	25	0	0.090	0.280	35	0.290	100	0.340	200
							25		40		140
							5		15		30

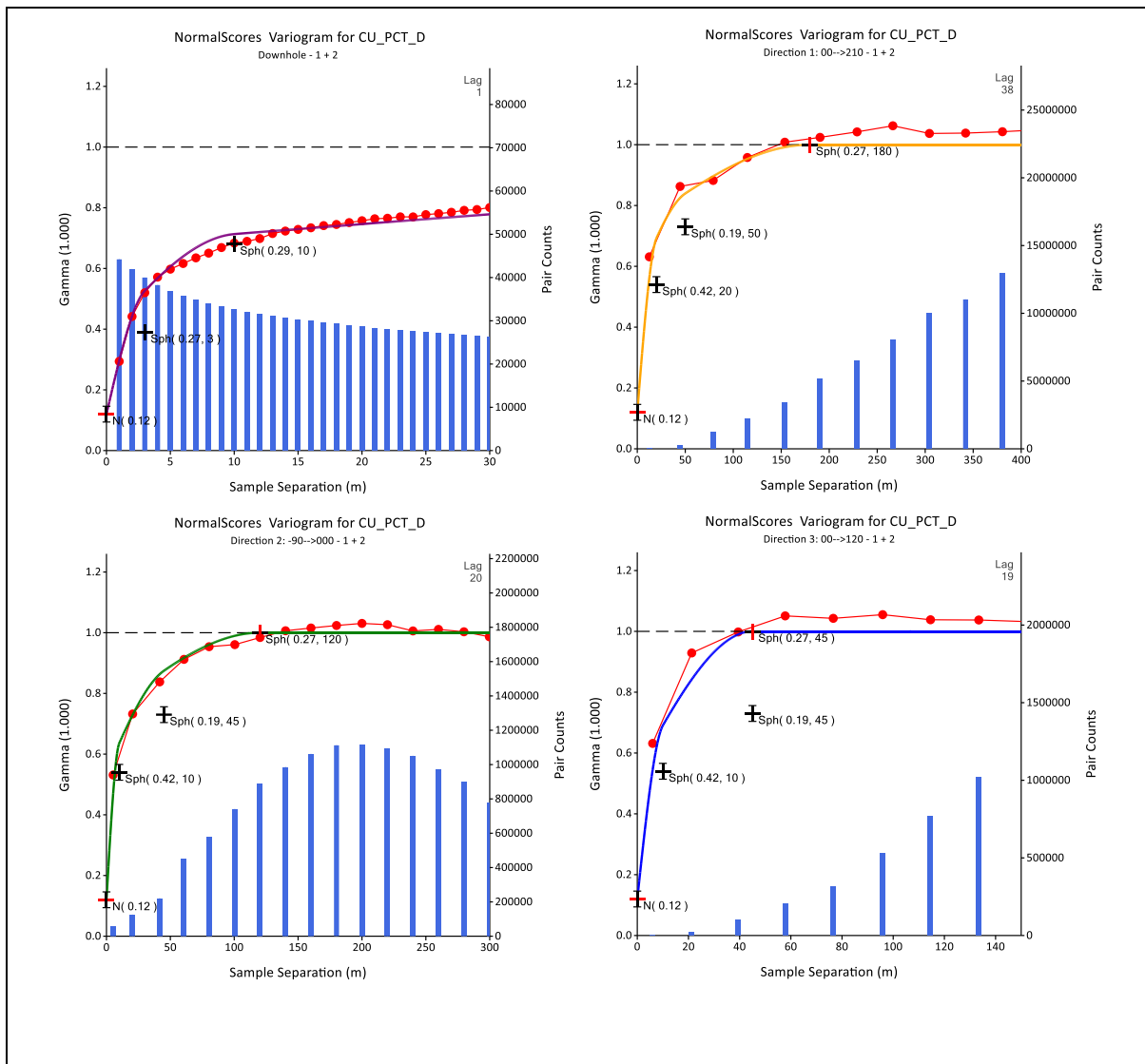


Figure 14.20 Normal score variogram model for mid area Cu high grade and low grade combined

14.1.15 Estimation

A suite of elements: copper (Cu), gold (Au), molybdenum (Mo), cobalt (Co), calcium (Ca), iron (Fe), sulphur (S,) potassium (K) and aluminium (Al) were estimated using ordinary kriging in Datamine software. Kriging accounts for the spatial distribution and grade continuity of the input data. Kriging is also able to account for the clustering of samples caused by variation in drilling density throughout the deposit.

Mineralisation was estimated using hard boundaries according to the domain conditions for each element. The boundaries between oxidation states were soft.

There was a hard boundary between domains cut by the Serrano fault and the Rancho fault but soft boundaries between other fault blocks in the north area.

The composite data was top-cut prior to estimation as discussed in the statistics section of this report.

For the estimation composites were selected from within a search ellipse of radius 100m in the principal direction along strike, 100m in the down dip direction and 50m across the plane of mineralisation. The search strategy for grade estimation mostly used the established dynamic anisotropy (DA) to locally tune the search orientations with the exception of Co and Cu oxide where a static search orientation was used derived from the continuity analysis.

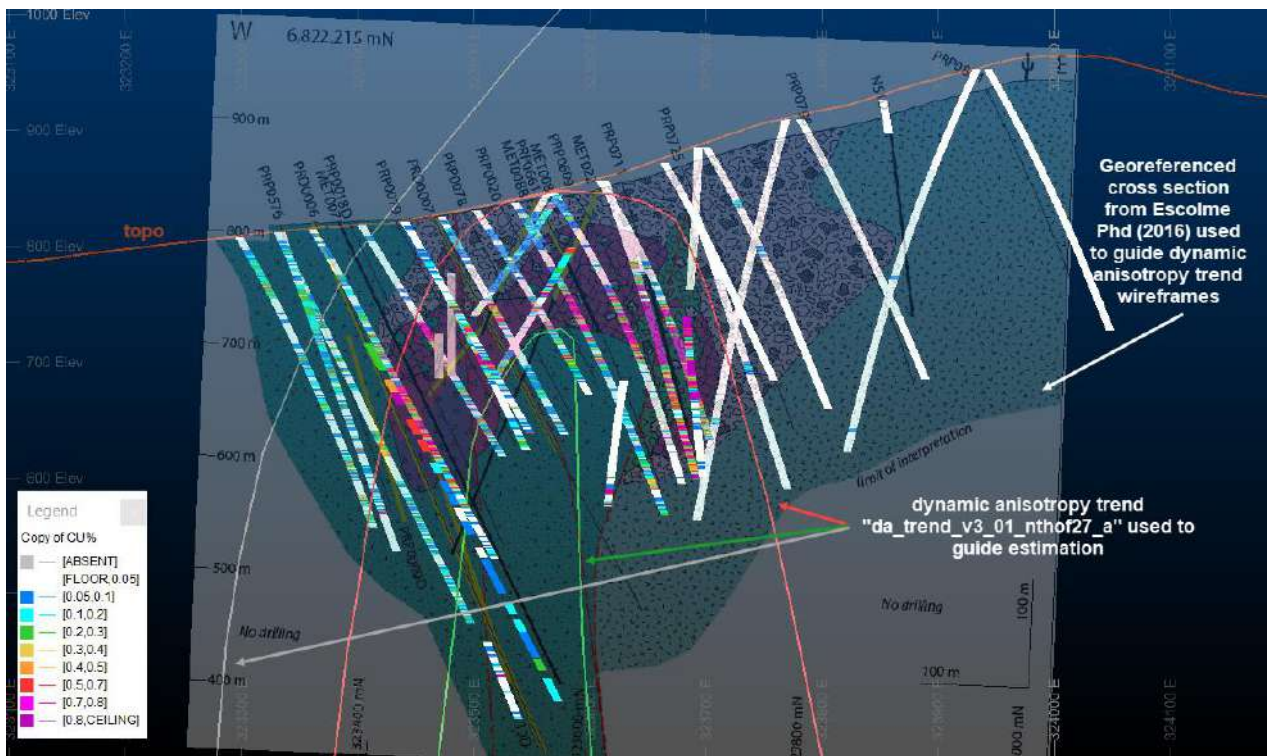
Interpretation of DA surfaces was based on graphic core logging, core photo library, drillhole data base, detailed hand specimen and thin section observations and WLSQ-QXRD data. These observations, in conjunction with iterative indicator estimation test work, resulted in the final manually created fault specific dynamic anisotropy trend wireframes, which were used for the final categorical indicator estimation and some of the grade estimations. An example of dynamic anisotropy is included in Figure 14.21.

The search strategy for each area and variable estimated is contained in Table 14.44 with the combination of search and variogram parameters listed in Table 14.45 for mid area, Table 14.46 for south area and Table 14.47 for north area.

No octant search was used.

Table 14.44 Search strategy for grade estimation

Area	Type	SREF	Orientation			Search			2 nd search factor	Number of Composites				
			Rot1	Rot2	Rot3	D1	D2	D3		First Search		Second Search		Max Per Drillhole
										Min	Max	Min	Max	
Mid	Generic	1	Dynamic			100	100	50	3	6	12	6	12	7
	Co	7	60	90	0	100	100	50	3	6	12	6	12	7
	Cu Ox	18	120	170	0	100	100	50	3	6	12	6	12	7
South	Generic	29	Dynamic			100	100	50	3	6	12	6	12	7
	Co	30	100	80	0	100	100	50	2	6	12	6	12	7
North	Generic	60	Dynamic			100	100	50	3	6	12	6	12	7



- | | | | |
|--|---|--|--|
| | Facies 3B-2 tourmaline - pyrite - chalcopyrite cemented breccia | | Drill hole with ICP-MS geochemistry ± QXRD |
| | Facies 3B-1 tourmaline - magnetite - pyrite - chalcopyrite cemented breccia | | Drill hole graphic logged from core |
| | Stage 2 matrix supported breccia | | Drill hole logged from core photography |
| | Stage 1 quartz - pyrite cemented breccia | | Fault (inferred) |
| | Rhyolite lapilli tuff | | Clast supported breccias |
| | Rhyodacite lapilli tuff | | Cement supported breccias |

Figure 14.21 Cross section at 6822215mN displaying a georeferenced interpreted distribution of breccia facies from Escolme (2016).

Table 14.45 Combination of variogram and search for grade estimation mid area

Cu Estimation			Fe Estimation			S Estimation		
CUDOM_EST1SOFT	SREF	VREF	FESDOM_EST1	SREF	VREF	FESDOM_EST1	SREF	VREF
50011	1	1	1550000	1	12	1550000	1	15
50012	1	1	1550001	1	12	1550001	1	15
50019	1	1	1550010	1	12	1550010	1	15
50021	1	1	1550011	1	12	1550011	1	15
50022	1	1	5050000	1	13	5050000	18	18
50029	1	1	5050001	1	13	5050001	1	16
50031	1	1	5050010	1	13	5050010	18	18
50032	1	1	5050011	1	13	5050011	1	16
50039	1	1	9950000	1	14	9950000	1	17
50051	1	1	9950001	1	14	9950001	1	17
50052	1	1	9950010	1	14	9950010	1	17
50059	1	1	9950011	1	14	9950011	1	17
50061	18	18	K Estimation			Al Estimation		
50062	18	18	KALDOM_EST1	SREF	VREF	KALDOM_EST1	SREF	VREF
50069	18	18	50111	1	22	50111	1	19
Co Estimation			50111	1	50112	1	22	50112
CODOM_EST1	SREF	VREF	50119	1	22	50119	1	19
50001	7	1	50121	1	22	50121	1	19
50002	7	2	50122	1	22	50122	1	19
50003	7	3	50129	1	22	50129	1	19
50004	7	4	50131	1	22	50131	1	19
Mo Estimation			50131	1	50132	1	22	50132
MODOM_EST1	SREF	VREF	50139	1	22	50139	1	19
50111	1	5	50151	1	22	50151	1	19
50112	1	5	50159	1	22	50159	1	19
50119	1	5	50221	1	23	50221	1	20

50121	1	5	50222	1	23	50222	1	20
50122	1	5	50229	1	23	50229	1	20
50129	1	5	50231	1	23	50231	1	20
50131	1	6	50232	1	23	50232	1	20
50132	1	6	50239	1	23	50239	1	20
50139	1	6	50251	1	23	50251	1	20
50151	1	6	50259	1	23	50259	1	20
50152	1	6	50911	1	24	50911	1	21
50159	1	6	50912	1	24	50912	1	21
50911	1	7	50919	1	24	50919	1	21
50912	1	7	50921	1	24	50921	1	21
50919	1	7	50922	1	24	50922	1	21
50921	1	7	50929	1	24	50929	1	21
50922	1	7	50931	1	24	50931	1	21
50929	1	7	50932	1	24	50932	1	21
50931	1	9	50939	1	24	50939	1	21
50932	1	9	50951	1	24	50951	1	21
50939	1	9	50952	1	24	50952	1	21
50951	1	8	50959	1	24	50959	1	21
50952	1	8						
50959	1	8						
Ca Estimation								
CADOM_EST1	SREF	VREF						
50005	1	5						
50009	1	9						

Table 14.46 Combination of variogram and search for grade estimation south area

Cu Estimation			Fe Estimation			S Estimation		
CUDOM_EST1SOFT	SREF	VREF	FESDOM_EST1	SREF	VREF	FESDOM_EST1	SREF	VREF
40011	29	29	1540000	29	41	1540000	29	44
40012	29	29	1540001	29	41	1540001	29	44
40019	29	29	1540010	29	41	1540010	29	44
40021	29	29	1540011	29	41	1540011	29	44
40022	29	29	5040000	29	42	5040000	29	45
40029	29	29	5040001	29	42	5040001	29	45
40031	29	29	5040010	29	42	5040010	29	45
40032	29	29	5040011	29	42	5040011	29	45
40039	29	29	9940000	29	43	9940000	29	46
40051	29	29	9940001	29	43	9940001	29	46
40052	29	29	9940010	29	43	9940010	29	46
40059	29	29	9940011	29	43	9940011	29	46
40061	23	23	K Estimation			Al Estimation		
40069	23	23	KALDOM_EST1	SREF	VREF	KALDOM_EST1	SREF	VREF
			40111	29	50	40111	29	47
Co Estimation			40111	1	40	40111	51	40112
CODOM_EST1	SREF	VREF	40119	29	52	40119	29	49
40001	30	36	40121	29	50	40121	29	47
40002	30	37	40131	29	50	40131	29	47
40003	30	38	40132	29	51	40132	29	48
40004	30	39	40139	29	52	40139	29	49
Mo Estimation			40151	29	50	40151	29	47
MODOM_EST1	SREF	VREF	40159	29	52	40159	29	49
40111	29	32	40221	29	50	40221	29	47
40112	29	32	40222	29	51	40222	29	48
40119	29	33	40229	29	52	40229	29	49

40121	29	32	40231	29	50	40231	29	47
40122	29	32	40232	29	51	40232	29	48
40129	29	33	40239	29	52	40239	29	49
40131	29	32	40251	29	50	40251	29	47
40132	29	32	40259	29	52	40259	29	49
40139	29	33	40911	29	50	40911	29	47
40151	29	32	40912	29	51	40912	29	48
40152	29	32	40919	29	52	40919	29	49
40159	29	33	40921	29	50	40921	29	47
40911	29	34	40922	29	51	40922	29	48
40919	29	35	40929	29	52	40929	29	49
40921	29	34	40931	29	50	40931	29	47
40922	29	34	40932	29	51	40932	29	48
40929	29	35	40939	29	52	40939	29	49
40931	29	34	40951	29	50	40951	29	47
40932	29	34	40952	29	51	40952	29	48
40939	29	35	40959	29	52	40959	29	49
40951	29	34	40111	29	50	40111	29	47
40952	29	34	40112	29	51	40112	29	48
40959	29	35						
Ca Estimation								
CADOM_EST1	SREF	VREF						
40005	1	5						
40009	1	9						

Table 14.47 Combination of variogram and search for grade estimation south area

Cu Estimation			Fe Estimation			S Estimation		
CUDOM_EST1SOFT	SREF	VREF	FESDOM_EST1	SREF	VREF	FESDOM_EST1	SREF	VREF
All	60	60	All	60	62	All	60	63
Co Estimation			K Estimation			Al Estimation		
CODOM_EST1	SREF	VREF	KALDOM_EST1	SREF	VREF	KALDOM_EST1	SREF	VREF
All	60	65	All	60	68	All	60	67
Mo Estimation			Ca Estimation					
MODOM_EST1	SREF	VREF	CADOM_EST1	SREF	VREF			
All	60	64	All	60	66			

14.1.16 Model Validation

The estimates were validated using a three-stage comparison between top-cut composites and the estimated variables. The first stage involves calculating the global statistics of the composites compared to the tonnage weighted averages of estimated variables. The second stage involves comparing statistics in slices along the mineralisation and the third involves a detailed visual comparison by section to ensure the estimated variables honour the input composite data.

14.1.16.1 Composites versus Estimates

The global comparisons were completed using the hard boundary domain coding. The global comparison for the copper domains is presented in Table 14.48. In general, the comparisons are excellent for the primary variables. Comparisons are poor for the extremely low-grade variables and low-grade domains where small differences in grade will result in large percentage differences. Comparisons are also poorer for those variables where the grade ranges vary over the mineralisation and the data distributions are mixed.

The validation by northing, in section 14.1.16.2 Trend Plots, which is a more local comparison, illustrates these effects.

Table 14.48 Global comparison of Cu composites and estimates

CUDOM	Composites		Model	% Difference		% Est	Model	% Difference	
	Top-cut	Top-cut Declustered	1 st pass	Top-cut	Top-cut Declustered	1 st pass	All	Top-cut	Top-cut Declustered
50022	0.65	0.62	0.61	-5.7%	-1.1%	73%	0.61	-5.6%	-1.0%
50012	0.57	0.55	0.58	2.0%	5.7%	82%	0.58	2.0%	5.7%
50032	0.63	0.62	0.75	19.3%	21.2%	48%	0.61	-3.8%	-2.3%
50052	0.53	0.51	0.54	2.6%	6.6%	84%	0.51	-3.5%	0.3%
50062	0.68	0.65	0.59	-12.9%	-8.9%	95%	0.59	-13.3%	-9.2%
50021	0.17	0.17	0.17	-1.0%	-1.0%	63%	0.17	-1.8%	-1.8%
50011	0.16	0.16	0.16	-2.4%	-2.4%	67%	0.16	-0.2%	-0.2%
50031	0.12	0.12	0.12	-1.2%	-1.2%	59%	0.11	-5.7%	-5.7%
50051	0.12	0.12	0.12	2.3%	2.3%	29%	0.12	3.4%	3.4%
50061	0.12	0.12	0.13	9.2%	9.2%	74%	0.13	10.3%	10.3%
50029	0.03	0.04	0.04	26.8%	-4.9%	67%	0.04	31.7%	-1.2%
50019	0.03	0.03	0.03	1.3%	1.3%	72%	0.04	17.5%	17.5%
50039	0.02	0.02	0.02	-11.7%	-11.7%	95%	0.02	17.4%	17.4%
50059	0.02	0.02	0.02	16.4%	16.4%	93%	0.02	14.6%	14.6%

14.1.16.2 Trend Plots

The average block values were compared to the average input composites over northing slices. These slices represent equal intervals through the model and input data, with 80 m slices used. An example for the copper estimation domain 50022 is presented in Figure 14.22.

The grade trends input data in the model slices are comparable to grade trends of the block estimates. The estimated grades are, as expected, smoother than the composites though the variation in grades can be clearly seen.

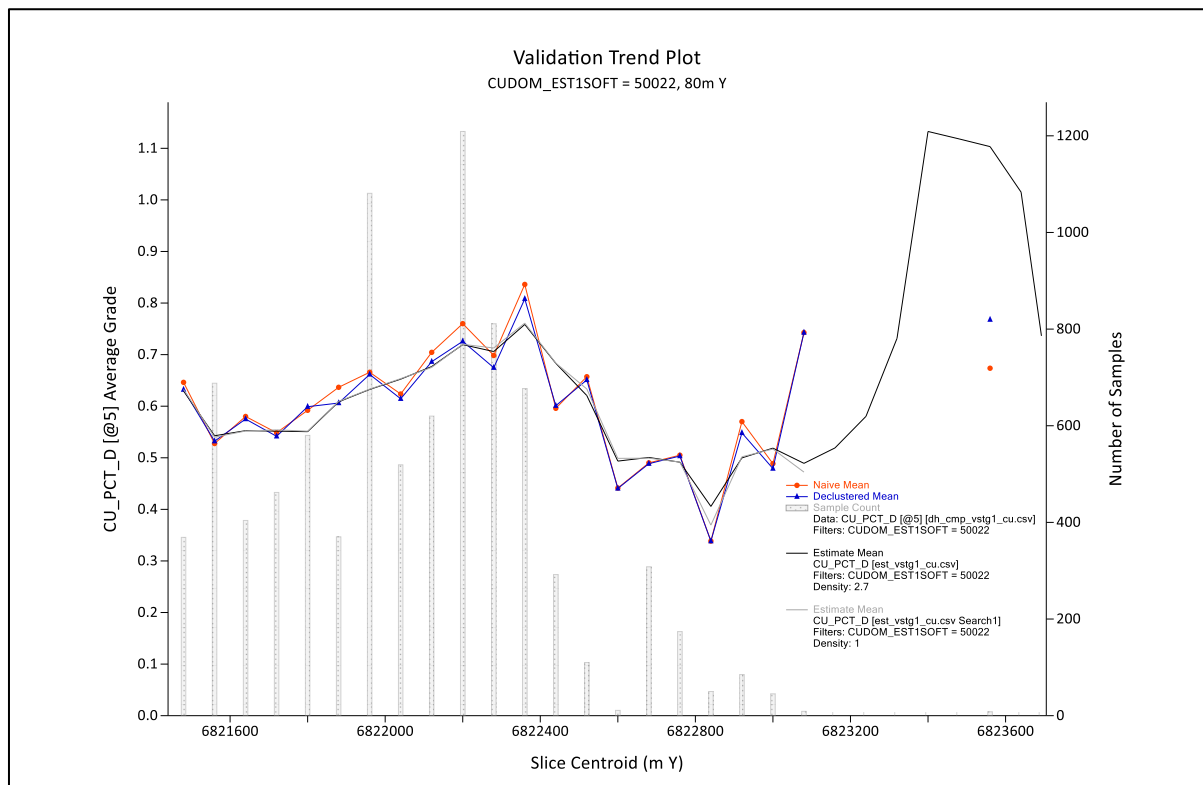


Figure 14.22 Northing trend validation for Cu in domain 50022

14.1.16.3 Visual Validation

The block model grades were compared with the input data visually on-screen. Overall the comparisons are good, with the block grades following the trends in the input data as illustrated for copper in Figure 14.23 and Figure 14.24.

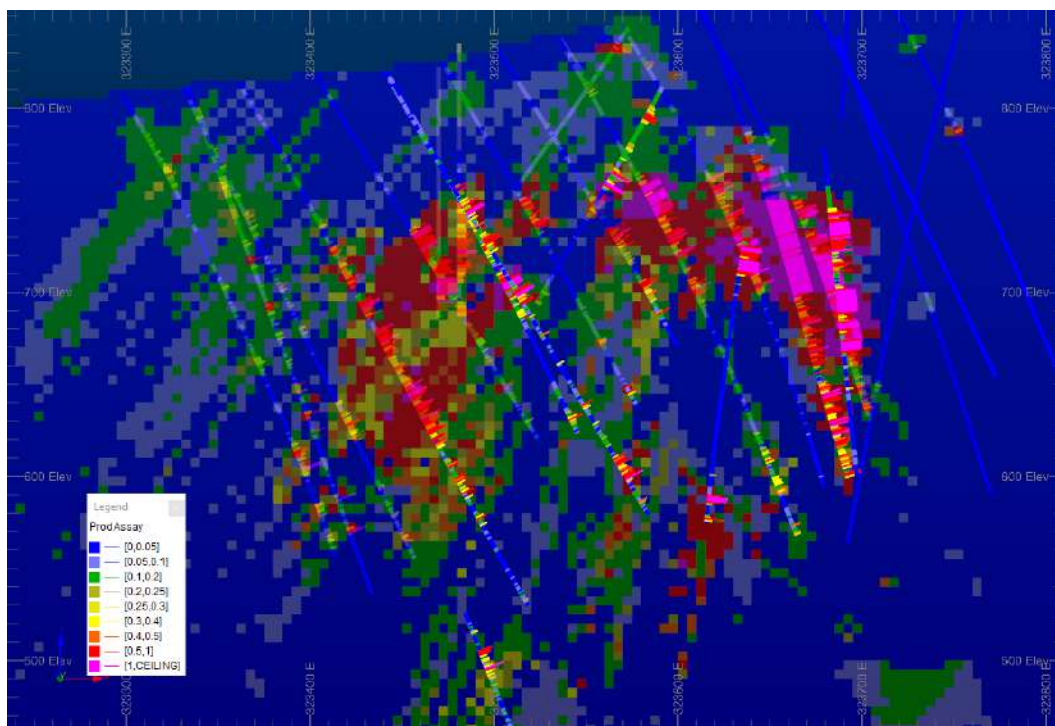


Figure 14.23 Visual validation of Cu for EW section 6822215 mN

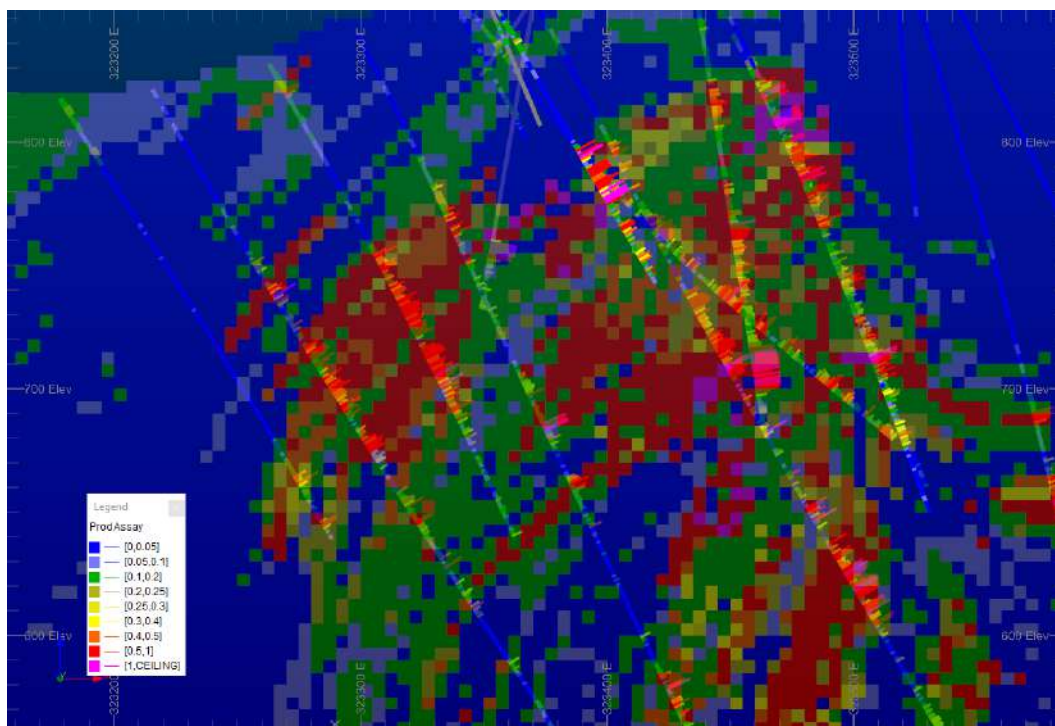


Figure 14.24 Visual validation of Cu for section 6821915 mN

14.1.17 Resource Classification

The Productora Mineral Resource estimate has been classified considering the guidelines provided in NI 43-101.

A 'Mineral Resource' is a concentration or occurrence of solid material of economic interest in or on the Earth's crust in such form, grade (or quality), and quantity that there are reasonable prospects for eventual economic extraction.

The location, quantity, grade (or quality), continuity and other geological characteristics of a Mineral Resource are known, estimated, or interpreted from specific geological evidence and knowledge, including sampling.

A range of criteria was considered in determining the Resource classification, including:

- Drill data density
- Sample/assay confidence
- Geological confidence in the interpretations and, similarly, geological continuity
- Grade continuity of the mineralisation
- Estimation method and resulting estimation output variables
- Estimation performance through validation, and
- Prospect for eventual economic extraction.

Wireframes were constructed to flag the blocks as Indicated or Inferred:

- 2022_prod_indicated_main
- 2022_prod_indicated_Sth_mantos
- 2022_prod_nth_indicated
- 2022_Inferred

Indicated classification was applied based using three different wireframes (south Mantos, main or north) due to the orientations of mineralisation.

No Measured classification was applied.

The reported grades and metal contents are presented without metallurgical factors or assumptions and should be considered 'total' metal endowment.

14.1.18 Alice

The Alice Mineral Resource has not been updated but is included in the Productora Mineral Resource Reporting for this documentation.

Commentary below refers to the most recent Mineral Resource for Alice, completed in September 2015.

14.1.18.1 Database Validation

The Alice database was validated through several checks. Validation steps included, but were not limited to the following:

- Drill collars – a comparison of planned and actual survey pick up coordinates is completed to check for any discrepancies or potential mislabelling of holes or survey errors.
- Drill collars are checked by 3D visual validation of location against expected centre of drill pads (as corresponded with the digital terrain model).
- A drill program “tracker” spreadsheet was filled out by field geologists during the drilling program. This tracker stores details such as hole identification, date drilled, geologist responsible for logging, sample dispatch date etc. The tracker data was cross-referenced with the final database export.
- Downhole surveys were cross-referenced against planned survey orientation, and drill traces were checked visually in 3D for obvious errors.
- Mineralisation intensity logs were completed for each drillhole, and this was compared by field geologist with the returned assay results from the laboratory. This mineralisation intensity log also serves as a tool for calibration of geologist’s mineralisation logging, and as a check for any obvious deviations between mineralisation intensity and assays returned.
- A 3D visualisation of assays is completed to check for any possible downhole sample smearing/contamination.
- Data entry objects are reviewed and validated through data import validation rules when imported into the AcQuire database. This ensured that there were no overlapping intervals, no blanks (data gaps), and that geological coding (and similar logging field) are valid.
- Routine batch QA/QC analysis such as results for certified standards, blanks and field duplicates are checked before loading to the AcQuire database.
- AcQuire database exported csv files are loaded into Surpac database and secondary validation was steps was performed by Surpac Software on import (i.e., checks for overlapping intervals, survey depths greater than hole depths etc.).

The above validation and audit steps have ensured that the database contains minimal errors, and thus the database is considered suitable for this resource estimate.

In addition to the above routine steps, a detailed internal review of data management was undertaken in 2014 which involved several randomly choses holes, and a full comparison between of lab certificates, data transfer and steps, and a check against final results as stored in the database. This review deemed the data and processes were satisfactory.

14.1.18.2 Alice Domaining

Field observations and geological logging suggested that there were several alteration and mineralogical domains to be assessed. Exploratory data analysis of the Alice drilling data was undertaken in a variety of software packages such as SURPAC, loGAS and Snowden Supervisor.

The initial data flagging confirmed the western boundary of Alice mineralisation as the Alice Fault. The hanging wall material is from the primary felsic volcanic succession which has undergone advanced argillic alteration. This alteration was flagged in loGAS (using a Feldspar Na-K GER diagram as shown in Figure 14.25) as intense or moderate and defined a coherent non-mineralised and hard boundary domain.

Secondary analysis involved flagging variations in albite alteration intensity (highest, high, moderate, and minor). These added definition of alteration-diluted low and waste zones within the Alice porphyry.

Mineralised oxide samples were flagged by sulphide species charts in loGAS (using an S vs. Cu atomic weight ratio diagram). Using the same method, the remaining mineralised samples were differentiated into two groups: chalcopyrite-, and pyrite-dominant groups. These groups were then analysed to confirm spatial continuity, and statistical representation of the copper populations (Figure 14.26 and Figure 14.27). The chalcopyrite domain corresponds to (approximately) a 0.2% Cu cut-off and the pyrite domain to (approximately) a 400ppm Cu cut-off. Wireframing was undertaken using both the grade values and copper species-flagged samples. The surface channel sampling undertaken by HCH geologists along the Docherty Road surface exposure (Figure 14.28) was also used to aid interpretation (but not used for estimation).

These domains were considered appropriate for both copper and gold.

The molybdenum presents a different domain control (compared to copper and gold) but within the broader copper anomaly. Field and drilling observations indicated that the molybdenum was more limited to specific vein arrays rather than being pervasive in the porphyry groundmass. This observation was also supported by spatial validation. A specific domain boundary was created to differential between the “high” and “low” molybdenum zones (Figure 14.29).

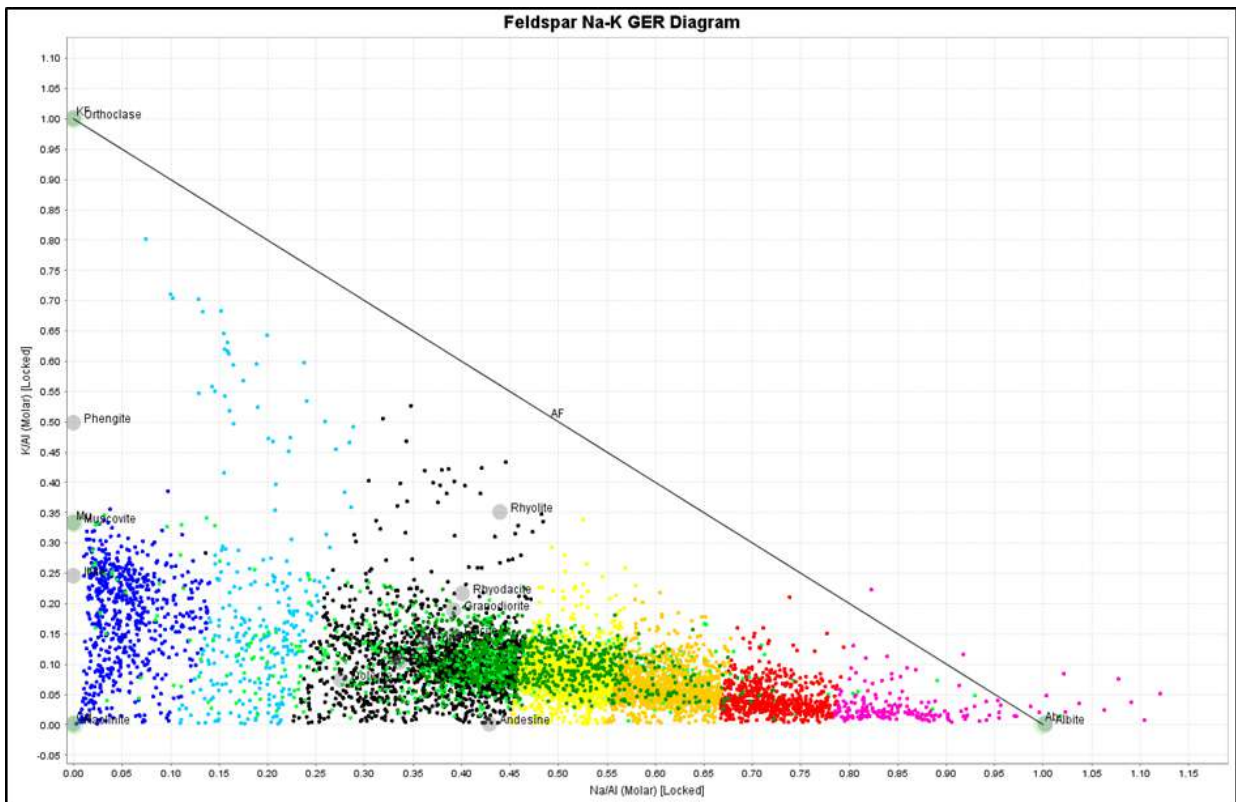


Figure 14.25 Graphical results of alteration mineral sample flagging at Alice

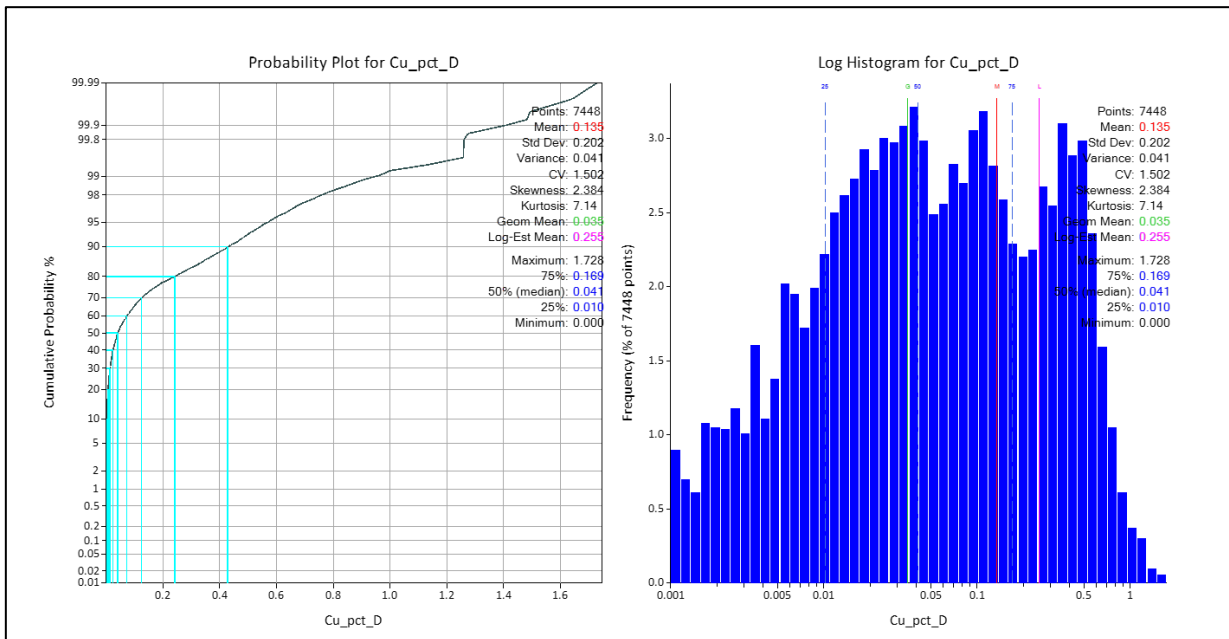


Figure 14.26 Statistical review of copper assay results from Alice drilling. Note: Population breaks

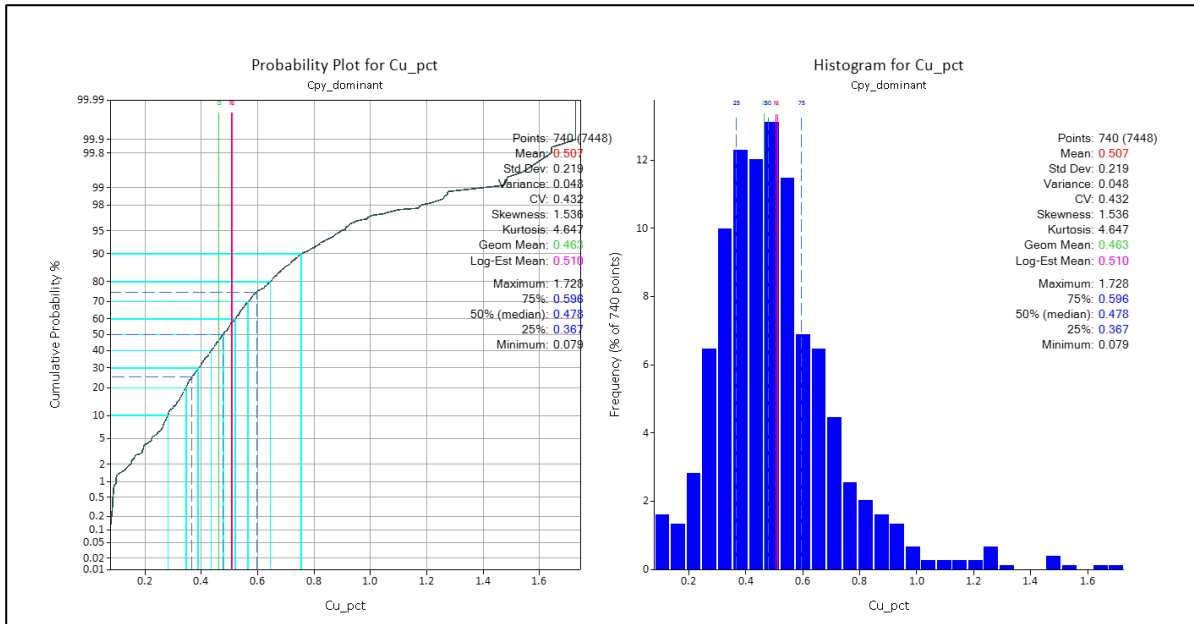


Figure 14.27 Statistical review of the "chalcopyrite dominant" flagged samples

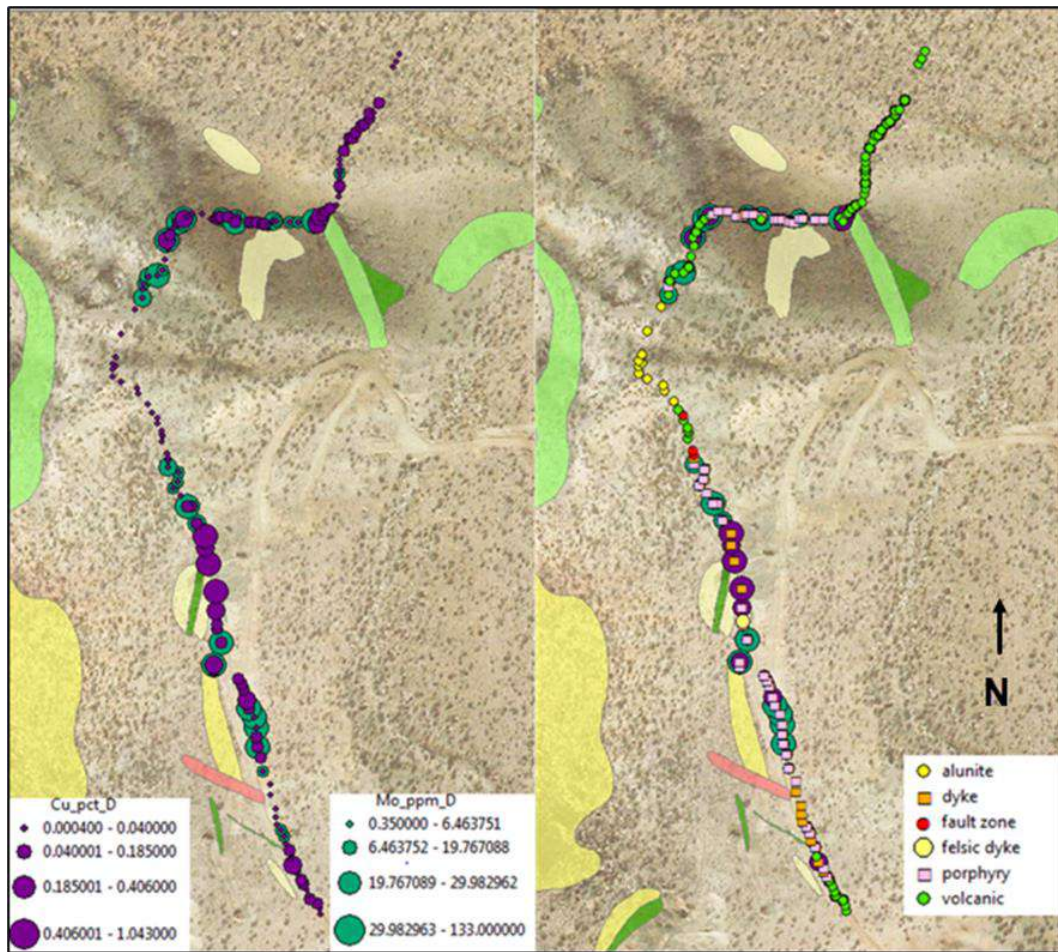


Figure 14.28 Lithology and select assays shown from the channel sampling along Docherty Road. (HCH, 2016)

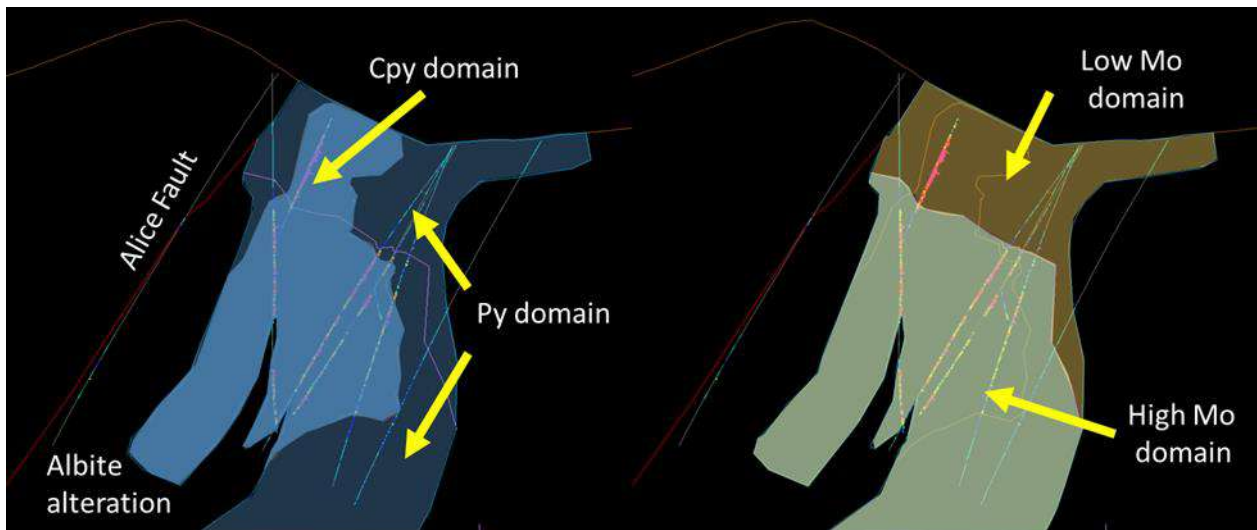


Figure 14.29 Section example of mineralisation domain creation, looking north (HCH, 2016)

14.1.18.3 Alice Weathering Domain Modelling

The weathering at Alice was notable in the overall absence of transitional zones. This was validated in drilling and reviewing copper species mineralogy as determined by copper: sulphur ratios and in IoGAS.

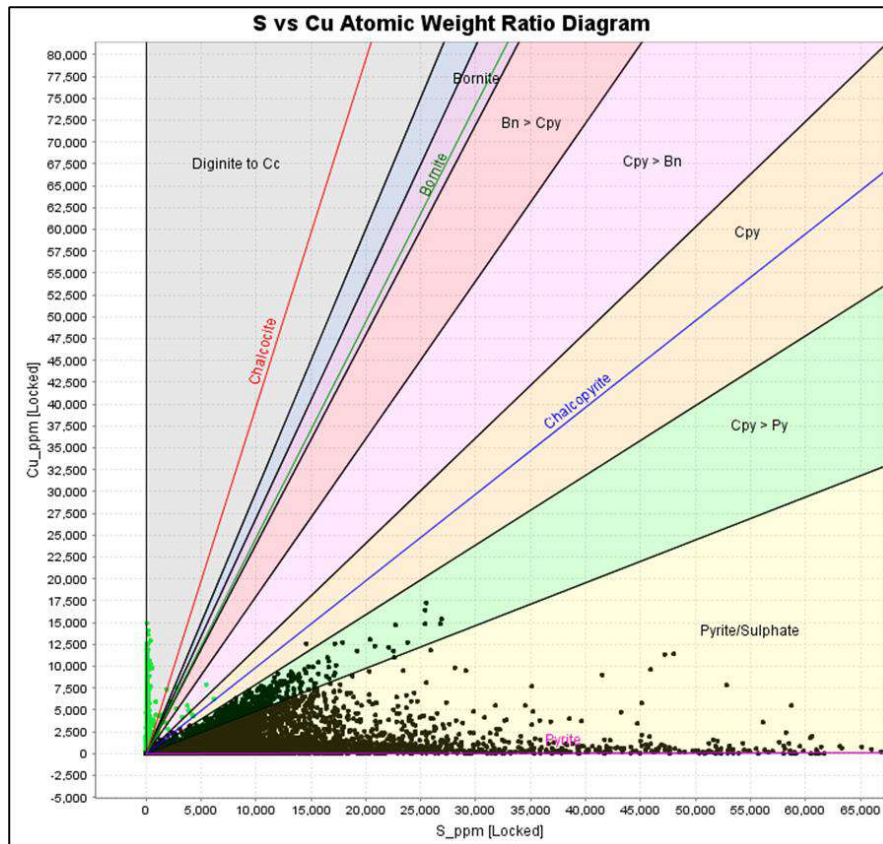


Figure 14.30 Example of copper oxide mineral flagging of Alice drilling

14.1.18.4 Alice Mineralized Material Domains

A list of the mineralized material domains and surfaces and their corresponding codes used to flag the Alice block model is provided in Table 14.49.

Table 14.49 List of mineralisation wireframes used for the Alice deposit model.

Function	Wireframe name (.dtm & .str)	Comment
Mineralisation	min_cpy_dom	Extent of high grade Cu+Au mineralisation (chalcopyrite dominant)
	min_py_dom	Extent of low grade Cu+Au mineralisation (pyrite dominant)
	min_mo_dom	Extent of high grade Mo mineralisation
Alteration	alt_albite	Extent of albite alteration
Weathering	weath_zn_boco_alice	Base of complete oxidation
Faults	fault_alice	Alice hangingwall fault

14.1.18.5 Alice Data Flagging and Compositing

93% of the drill sampling at Alice was on 1m lengths (Figure 14.31). The length, and sample collection methods of the 1m samples are considered acceptable for estimation for mineralised domains.

The overwhelming majority of 4m (composited) sample lengths occurred outside of the key economic mineralised domains.

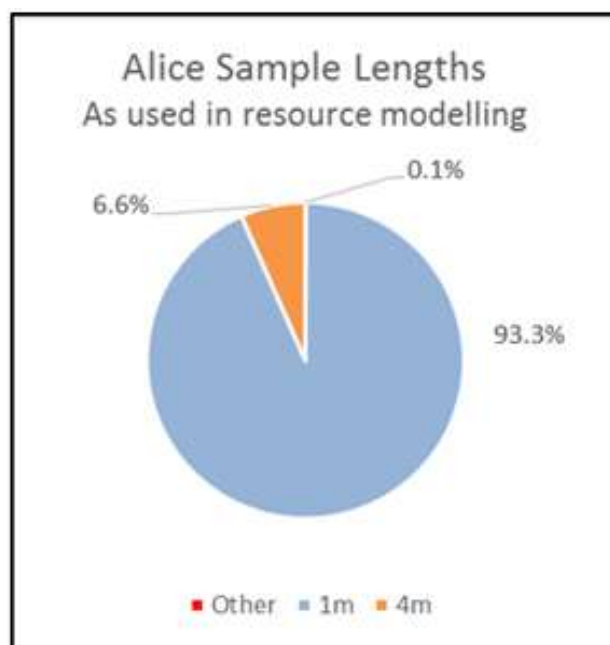


Figure 14.31 Alice sample lengths

The decision to composite data to 2m was based on a review of sample intervals, the wider deficiency of short-range mineral and structural control, and review of the relative homogeneity (compared to the Productora deposit).

Comparison of raw (un-composited) sample grades vs. composited sample grades was undertaken to confirm the validity of the compositing (Table 14.50).

Table 14.50 Validation of compositing samples to 2m for Alice

Validation of compositing - comparison between samples and 2m composites - Alice													
Cu Domain (LODE)	Variable	WEATH	Original Sample					2m Composites					% Change in Mean
			Count	Max	Mean	Std. Dev	CV	Count	Max	Mean	Std. Dev	CV	
2010	Cu (%)	0	335	1.493	0.47	0.28	0.60	169	1.376	0.47	0.27	0.58	0.00
		2	1729	1.728	0.39	0.22	0.57	887	1.402	0.38	0.20	0.53	0.01
	Au (g/t)	0	311	0.33	0.06	0.06	0.90	159	0.3	0.06	0.05	0.87	0.00
		2	1648	0.546	0.04	0.03	0.77	861	0.289	0.04	0.03	0.69	0.03
1010	Cu (%)	0	349	0.542	0.08	0.07	0.81	404	0.344	0.07	0.05	0.73	0.18
		2	1483	0.602	0.09	0.06	0.68	898	0.477	0.09	0.06	0.62	0.05
	Au (g/t)	0	103	0.138	0.02	0.02	0.99	85	0.13	0.02	0.02	0.88	0.05
		2	627	2.54	0.03	0.13	5.21	427	2.24	0.02	0.11	4.92	0.12
Mo Domain (GEO_DOM_MO)													
50	Mo (ppm)	-	2929	1480	45	74	1.65	1580	743	44	59.00	1.35	0.02
999		-	967	140	15	14	0.90	778	83	14	11.00	0.80	0.07

14.1.18.6 Alice Statistical Analysis

The copper, gold and molybdenum populations are positively skewed. Hot Chili Limited undertook statistical analysis to consider outlier top-cuts that could negatively impact estimation. Due to the homogenous mineralisation combined with the use of 2m composites, only limited top-cutting was utilised. Information on top-cuts is provided in Table 14.51.

Table 14.51 Application and validation of top-cuts on 2m composites at Alice

Validation of top cuts - comparison between 2m uncut, and cut composites													
Cu Domain (LODE)	Variable	WEATH	2m uncut composites				Upper cut vale	2m cut composites				% Change in Mean	
			Count	Max	Mean	Std. Dev		Count Cut	Cut Value	Max	Mean		Std. Dev
2010	Cu (%)	0	169	1.38	0.47	0.27	-	-	1.38	0.47	0.27	0.0%	
		2	887	1.40	0.38	0.20	-	-	1.40	0.38	0.20	0.0%	
	Au (g/t)	0	159	0.30	0.06	0.05	-	-	0.30	0.06	0.05	0.0%	
		2	861	0.29	0.04	0.03	-	-	0.29	0.04	0.03	0.0%	
1010	Cu (%)	0	404	0.34	0.07	0.05	-	-	0.34	0.07	0.05	0.0%	
		2	898	0.48	0.09	0.06	-	-	0.48	0.09	0.06	0.0%	
	Au (g/t)	0	85	0.13	0.02	0.02	-	-	0.13	0.02	0.02	0.0%	
		2	427	2.24	0.02	0.11	0.10	4	0.1	0.10	0.01	54.5%	
Mo Domain (GEO_DOM_MO)													
50	Au (g/t)	-	1580	743	44.00	59.00	-	-	743	44	59.00	0.0%	
999	Mo (ppm)	-	778	83	14	11.00	-	-	83	14	11.00	0.0%	

14.1.18.7 Alice Variography

The correlogram was selected as the best spatial measure to deal with the heteroscedastic characteristics of the data (clustering of data and zonal anisotropy in grades).

Modelled variograms were generated for each mineralisation domains within each orientation domain and for each element.

A summary of the variograms and subsequent search ellipses, is provided in Table 14.52.

Table 14.52 List of applied variograms and search ellipse directions

Alice Domain Variography and Ellipse orientations																		
Element	Weathering	Cu/Au domain (LODE)	Mo domain (GED_DOM_MO)	Major Axis		Semi-major Axis		Minor Axis		Relative Nugget (C0%)	Sill 1 (C1%)	Range Structure 1 (m)			Range Structure 2 (m)			
				Dip (°)	Azimuth (°)	Dip (°)	Azimuth (°)	Dip (°)	Azimuth (°)			Major Axis	Semi-major Axis	Minor Axis	Sill 2 (C2%)	Major Axis	Semi-major Axis	Minor Axis
Cu	Oxide	1010		0	10	60	280	30	100	0.05	0.5	10	10	5	0.45	100	100	30
		2010		0	10	60	280	30	100									
	Fresh	1010		0	10	60	280	30	100	0.3	0.2	10	10	10	0.5	65	65	40
		2010		0	20	60	280	30	100	0.6	0.6	15	15	15	0.2	110	110	55
Au	Oxide	1010		0	10	60	280	30	100	0.2	0.5	10	10	5	0.3	100	100	20
		2010		0	10	60	280	30	100									
	Fresh	1010		0	10	60	280	30	100	0.6	0.1	5	5	5	0.3	50	50	25
		2010		0	10	60	280	30	100	0.4	0.45	15	15	15	0.15	80	80	40
Mo			50	0	10	60	100	30	280	0.55	0.25	30	30	10	0.2	60	60	40
		999		0	10	60	100	30	280									

14.1.18.8 Alice Block Modelling

The block model was created using Surpac software, from the defined mineralisation, weathering, and orientation domains as well as mining and tenement wireframes.

The block model extents, parent cell, and subsequent sub-cell sizes, was established from an assessment of the geomorphology and distribution of copper and gold, as well as drill density and pattern. The model extents, cell sizes and variables used in the model are supplied in Table 14.53.

Table 14.53 Variables in the Alice Resource model

Block model variable summary				
Productora and Alice** models				
Type	Y	X	Z	
Minimum Coordinates	6819200	321000	200	
Maximum Coordinates	6827520	325352	1352	
User Block Size	20	8	6	
Min. Block Size	10	2	3	
Rotation	0	0	0	
Total Blocks	6277507			
Storage Efficiency %	96.38			
Attribute Name	Type	Decimals	background	Description
au_gt	Real	3	-99	gold g/t
class	Integer	-	-99	classification (0=waste,1=unclass min,2=inf,3=ind,4=meas)
cu_pct	Real	3	-99	copper %
den	Real	2	-99	insitu density
dist_au	Float	2	-99	average distance to sample - gold
dist_cu	Float	2	-99	average distance to sample - copper
dist_mo	Float	3	-99	average distance to sample - molybdenum
geo_dom**	Integer	-	-99	geological domain code
geo_dom_mo*	Integer	-	-99	flag for high/low Mo domains in Cu lodes
insitu	Integer	-	-99	insitu or mined (0=insitu,10=ROM,20=dump,30=mined void)
ke_au	Float	2	-99	kriging efficiency - gold
ke_cu	Float	2	-99	kriging efficiency - copper
ke_mo	Float	3	-99	kriging efficiency - molybdenum
lode	Integer	-	-99	lode code (1xxx=0.1%Cu,2xxx=0.2%,3xxx=0.3%Cu)
min_dom	Integer	-	-99	mineralisation domain flag(1=0.1%Cu,2=0.5%Cu,3=0.3%Cu)
mo_ppm	Real	-	-99	molybdenum ppm
nsam_au	Integer	-	-99	number of samples - gold
nsam_cu	Integer	-	-99	number of samples - copper
nsam_mo	Integer	-	-99	number of samples - moly
pass_au**	Integer	-	-99	estimation pass - gold
pass_cu**	Integer	-	-99	estimation pass - copper
slope_au	Float	2	-99	slope of regression - gold
slope_cu	Float	2	-99	slope of regression - copper
slope_mo	Float	3	-99	slope of regression - molybdenum
tene	Real	-	-99	tenement (1=SMEAL,2=CMP,3=CCHEN,4=excision,7=unknown)
topo	Integer	-	-99	topography (1=below topo,-99=above topo)
weath	Integer	-	-99	weathering (0=oxide,1=trans,2=fresh)
* The Productora model does not contain this variable				
**Not all variables were utilised in the Alice modelling				

14.1.18.9 Alice Grade Estimation

Estimation of the main grade variables (copper, gold, molybdenum) was undertaken using ordinary block kriging as the interpolation method.

Estimation at Alice only required a single pass.

14.1.18.10 Alice Estimation Parameters

Search parameters can be read in Table 14.54, and are as follows:

- The estimation took place as a single pass, and had a minimum sample count of between 6 and 8 composites (2m) required for block estimation
- The limits placed on the maximum number of composites per hole (8) was determined from an assessment of the drill spacing, and an iterative estimation validation
- The search ellipse was chosen to ensure that estimation was undertaken in a single pass.

Table 14.54 Estimation sample selection and search distances – Alice

Alice Sample Section												
Estimating variables	Pass	method	Cu/Au domain (LODE)	Mo domain (GEO_DOM_MO)	min sample	max samples	max samples per hole	ellipse			ellipse ratio	
								major	semi-major	minor	maj/semi	maj/min
Cu, Au	1	OK	1010		8	12	8	250	250	62.5	1.0	4.0
	1	OK	2010		6	12	8	250	250	62.5	1.0	4.0
Mo	1	OK		all	8	12	8	250	250	62.5	1.0	4.0

14.1.18.11 Alice Block Model Validation

During resource modelling, test modelling is undertaken on sample selection, orientation, and search criteria to ensure validity and model appropriateness and robustness.

Additional validation steps included, but were not limited to, visual validation of estimated blocks, on section and plan view, against drillhole assay grades. Swath plots were created for cross-checks.

Overall, the estimation was considered acceptable and honoured the composite data.

14.1.18.12 Alice Block Model Resource Classification

The block estimation parameters were scrutinised and used for as first-pass guide to classification based on the estimation pass, average distance to sample and theoretical slope of regression.

After this review, a set of criteria and several subjective “limiting wireframes” (Table 14.55) were developed to set the final Resource classification on blocks to ensure a realistic and continuous mineable volume for Resource classification.

Table 14.55 List of wireframes used in classification for Alice

Name	Function
limit_indicated.dtm	Used to flag maximum extent of Indicated Resource
limit_inferred.dtm	Used to flag maximum extent of Inferred Resource

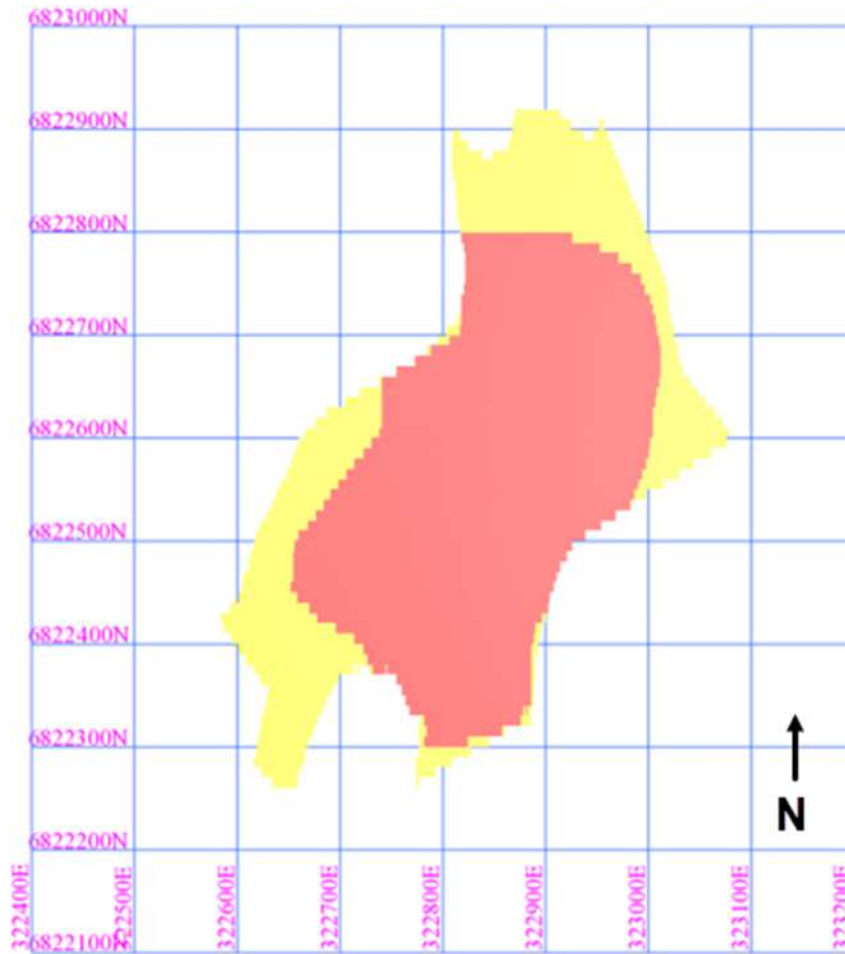


Figure 14.32 Plan view of Classified Resource in the Alice deposit (Indicated Resources shown in red, Inferred in yellow)

14.1.19 Reasonable Prospects for Eventual Economic Extraction (RPEEE)

The mining technique to be utilised at the Productora and Alice deposits is assumed to be a bulk tonnage conventional open pit mining.

Initial work done on the deposit as part of the 2016 Pre-feasibility study (PFS) was not considered as cost assumptions are not aligned with current conditions. As a result, no mining constraint has been applied for reporting on Productora or Alice.

An updated RPEEE will be completed as part of a combined Costa Fuego PFS.

14.1.20 Previous Mineral Resource Estimates

Hot Chili Limited reported the Productora Mineral Resource previously with an effective date of 29 October 2021 in connection with its long form prospectus dated December 20, 2021, as shown in Table 14.56.

Table 14.56 Productora Mineral Resource Summary (using +0.25% CuEq cut-off grade), 29 October 2021.

Productora Resource		Grade				Contained Metal			
Classification	Tonnes (millions)	CuEq	Cu %	Au g/t	Mo ppm	Copper Eq	Copper	Gold	Molybdenum
(+0.25% CuEq*)	(Mt)	(%)	(%)	(g/t)	(ppm)	(tonnes)	(tonnes)	(ounces)	(tonnes)
Measured	0	0	0	0	0	0	0	0	0
Indicated	208	0.54	0.46	0.10	140.0	1,122,000	960,000	643,000	29,200
Total	208	0.54	0.46	0.10	140.0	1,122,000	960,000	643,000	29,200
Inferred	67	0.44	0.38	0.08	109	295,000	255,000	167,000	7,200

Reported at or above 0.25% CuEq*. Figures in Table 14.56 are rounded, reported to appropriate significant figures, and reported in accordance with the CIM standards. Metal rounded to nearest thousand, or if less, to the nearest hundred. ** Copper Equivalent (CuEq) reported for the resource were calculated using the following formula: $CuEq\% = ((Cu\% \times Cu\ price\ 1\ \% \ per\ tonne \times Cu_recovery) + (Mo\ ppm \times Mo\ price\ per\ g/t \times Mo_recovery) + (Au\ ppm \times Au\ price\ per\ g/t \times Au_recovery) + (Ag\ ppm \times Ag\ price\ per\ g/t \times Ag_recovery)) / (Cu\ price\ 1\ \% \ per\ tonne)$. The Metal Prices applied in the calculation were: Cu=3.00 USD/lb, Au=1,550 USD/oz, Mo=12 USD/lb, and Ag=18 USD/oz. For Productora (Inferred + Indicated), the average Metallurgical Recoveries were Cu=83%, Au=43% and Mo=42%.

14.2 Cortadera

14.2.1 Introduction

Following the release of the maiden Mineral Resource Estimate (MRE) for Cortadera in September 2020, HCH undertook a Resource drill-out program focussed on extending and infilling previously reported Indicated and Inferred mineralisation. Drilling was successful in improving geological understanding and growing the Indicated resource.

Drilling completed by HCH between September 2020 and December 2021 comprises 105 Reverse Circulation (RC) holes, 38 RC-Diamond Drill (RCDD) holes, 4 RCDD hole extensions and 1 Diamond (DD) hole for a total of 21,262m of RC, 33,301m RCDD and 1,474m DD, for a total of 50,987m.

Drill spacing is nominally 80m across strike by 80m along strike. The current drilling density provides sufficient information to support a robust geological and mineralisation interpretation as the basis for Indicated and Inferred Classified Mineral Resources for the majority of the deposit.

The updated Cortadera Mineral Resource Estimate used a total drill inventory of 228 holes for a cumulative 96,847.7m (37,725.5 of RC and 59,142.2 m of DD), with drill data collected during the period from November 2011 to December 2021, using industry standard techniques for drilling and sampling collection.

Samples have been analysed by certified laboratories in Santiago, Chile and Lima, Peru by standard analytical techniques including:

- Copper, silver, and molybdenum were analysed by 4-acid digestion (Hydrochloric-Nitric-Perchloric-Hydrofluoric) followed by evaluation using Inductively Coupled Plasma - Optical Emission Spectrometry (ICP-OES) or Atomic Absorption Spectrometry (AAS)
- Copper results > 10,000 ppm were analysed by “ore grade” method Cu-AA62 (upper limit 40% Cu)
- Samples within the oxide and transitional weathering domains (as determined by geologists’ logging) were analysed for “soluble copper” (upper limit 10% Cu) to detect the leachability of copper oxide minerals within these domains
- Gold was analysed by 30 or 50 gram lead-collection Fire Assay, followed by ICP-OES or AAS.

Cortadera is likely to be processed under the same processing regime as the Productora deposit (which has had considerable metallurgical test work and a Prefeasibility study (PFS) completed), and as such it was considered appropriate to consider the elements of copper, gold, molybdenum, and silver as economically material for resource classification and reporting.

The verification of input data included the use of company QA/QC blanks and reference material, field and laboratory duplicates, umpire laboratory checks and independent sample and assay verification. The Qualified Person has assessed the drillhole database validation work and QAQC undertaken by HCH and was satisfied the input data could be relied upon for the estimation of Indicated and Inferred Classified Mineral Resources (Figure 14.33).

The Mineral Resource Estimation process included:

- Construction of mineralised domains based on geological understanding of the mineralised system, drilling results, drill spacing and orientation, mineralisation continuity and the potential mining methodologies
- Statistical analysis of drilling results within the mineralisation domains
- Compositing of the drilling results
- Variographic analysis within the mineralisation domains
- Estimation of a grade model via categorical indicator or ordinary block kriging, with boundary conditions selected to reflect geological understanding
- Assignment of model density using fresh density data (or a factor of the fresh density for weathered blocks)
- Validation of the estimated grades using visual and statistical analysis, swath and QQ plots and analysis of output estimation variables such as Kriging Efficiency and Slope of Regression.

A range of criteria were considered in determining the Resource Classification, including:

- Continuity of grade and geology between drillholes
- Drillhole spacing
- Proposed high-tonnage mining method.

3-dimensional (3D) surfaces have been created to define the limits of Indicated and Inferred material. Where significant extrapolation occurred, the mineralisation was categorised as Unclassified.

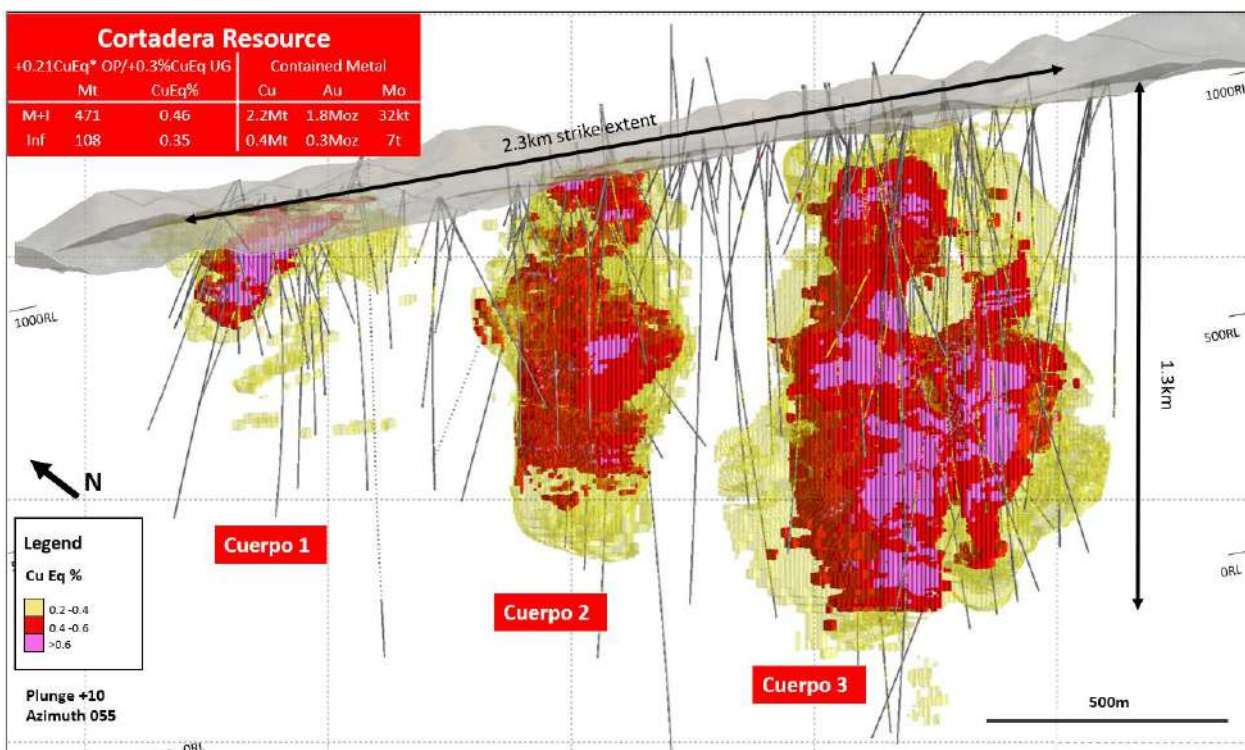


Figure 14.33 Oblique view looking northeast displaying Indicated and Inferred resource blocks +0.2% CuEq, coloured by CuEq% grade. (HCH, 2022)

14.2.2 Summary of Data Used in Estimate

All drilling data is stored in the HCH exploration acquire™ drillhole database. The system is backed up daily to a server based in Perth. Eight data tables were exported from the acquire™ drillhole database to create the estimation database.

Data table records consist of:

- Collar – ‘Collars.csv’
- Survey – ‘Survey.csv’
- Assays – ‘Assaypref.csv’
- Copper soluble assays – ‘cu_Sol.csv’
- Lithology – ‘Lithology.csv’
- Weathering – ‘Weathering.csv’
- Alteration – ‘Alteration.csv’
- Mineralisation – ‘Mineralisation.csv’

The drillhole database used for the MRE has been validated by several methods including checking of QA/QC data, extreme outlier values, zero values, negative values, possible miscoded

data based on geological domaining and assay values, sample overlaps, and inconsistencies in length of drillhole surveyed, length of drillhole logged and sampled, and sample size at laboratory.

14.2.3 Data Manipulation

Adjustments made to the data tables post-export from the acQuire™ database are listed below:

- Duplicate intervals have been deleted from the Lithology table (Table 14.57).
- 35 intervals were present where the soluble copper assay contained a higher value than the primary copper assay. 34 of these intervals are due to rounding errors during reporting (four decimal places used for primary copper vs. three decimal places for soluble copper). The remaining interval (CRP0025 from 12 m downhole) returned a soluble copper assay significantly higher than the primary copper assay (0.045% vs. 0.0137% respectively). In all cases, the soluble copper assay has been set as equal to the primary copper assay. Adjustments are shown in Table 14.58.
- Rules have been applied to Assay table entries where the value is below zero. These entries consist of cases where the returned assay is below the lower detection limit for the element. In all cases, the assay has been set to half the detection limit of the element (Table 14.59).

Table 14.57 Drillhole data edits to lithology table

Hole ID	From	To	Action/Reason
CRP0015	0	50	Delete data <i>Duplicate Lithologies present in table</i>
CRP0015	50	84	
CRP0015	84	86	
CRP0015	86	128	
CRP0015	128	136	
CRP0015	136	155	
CRP0015	155	238	
CRP0015	238	348	

Table 14.58 Drillhole data edits to Copper Soluble Assay table

Hole ID	Depth	Cu_AA_pct	Cu_pct_D	Action/Reason
CRP0025	12	0.045	0.0137	
CRP0042D	16	0.001	0.0005	
CRP0042D	20	0.001	0.0002	
CRP0042D	44	0.001	0.0005	
CRP0042D	52	0.001	0.0006	
CRP0043	0	0.001	0.0009	
CRP0043	12	0.001	0.0005	
CRP0043	16	0.001	0.0004	
CRP0043	20	0.001	0.0003	
CRP0043	24	0.001	0.0001	
CRP0043	26	0.001	0.0002	
CRP0043	28	0.001	0.0003	
CRP0043	32	0.001	0.0004	
CRP0043	36	0.001	0.0001	
CRP0043	40	0.001	0.0008	
CRP0047D	4	0.001	0.0005	Cu_AA_pct = Cu_pct_D
CRP0047D	74	0.001	0.0004	Cu_pct_D (copper assay) less than Cu_AA_pct (soluble copper assay)
CRP0050	26	0.001	0.0006	
CRP0052D	8	0.001	0.0001	
CRP0056	38	0.001	0.0008	
CRP0056	450	0.001	0.0003	
CRP0056	454	0.001	0.0004	
CRP0056	458	0.001	0.0003	
CRP0056	462	0.001	0.0003	
CRP0056	466	0.001	0.0007	
CRP0056	470	0.001	0.0005	
CRP0059	30	0.001	0.0008	
CRP0060	4	0.001	0.0009	
CRP0081	24	0.001	-0.001	
CRP0093	50	0.043	0.0164	
CRP0110	4	0.001	0.0007	
CRP0110	8	0.001	0.0004	
CRP0124D	4	0.001	0.0004	
CRP0167D	24	0.001	0.0004	
CRP0167D	42	0.001	0.0008	

Table 14.59 Rules applied to Assay table

Element (Assay Field)	Original Grade	Adjusted Grade	Reason
CU%	-0.001	0.00005	Assay results returned below detection set to nominal half detection limit
CU%	-0.0002	0.00005	
CU%	-0.0001	0.00005	
AU	-0.1	0.00025	
AU	-0.005	0.00025	
AU	-0.001	0.00025	
AU	-0.0005	0.00025	
MO	-10	0.1	
MO	-2	0.1	
MO	-1	0.1	
CO	-1	0.1	
S%	-0.01	0.005	

14.2.4 Geological and Mineralisation Interpretation

14.2.4.1 Geological Model

The geological model is based on surface mapping, drillhole logging, assay data and field data.

The Cortadera deposit is characterised by early- (10-series) and intra-mineralisation (20-series), porphyritic tonalitic to quartz dioritic intrusions and adjacent volcano-sedimentary wall-rocks that have been recrystallised to hornfels and skarn. The hydrothermal alteration consists of moderate- to strong-phyllitic (+ chloritic) alteration, characterised by quartz / silica, sericite and lesser amounts of chlorite.

Figure 14.34 and Figure 14.35 show long section and cross section views of the lithology model used to define the mineral resource. Figure 14.36 contains a plan view showing the lithological units that host much of the mineralisation at Cortadera.

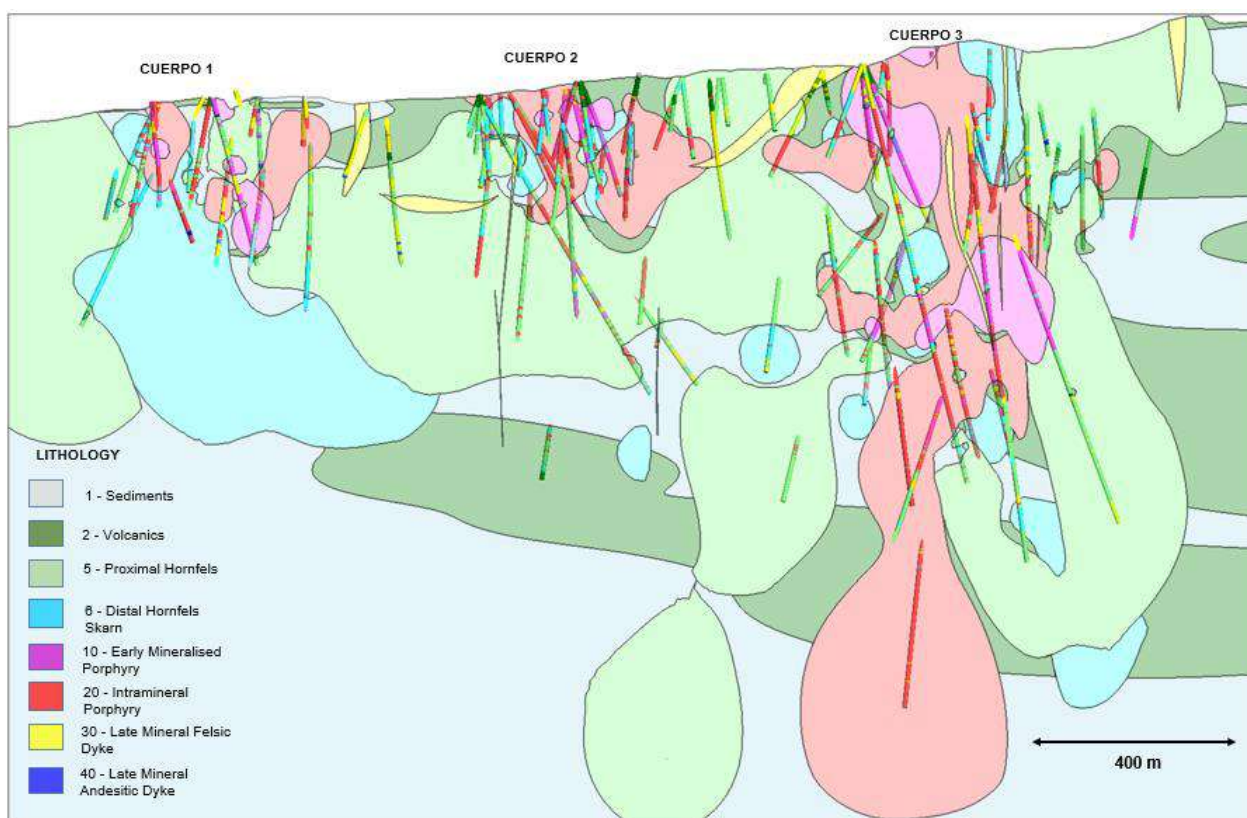


Figure 14.34 Long section looking NE showing lithological domains comprising Cuerpo 1, 2 and 3. (HCH, 2022)

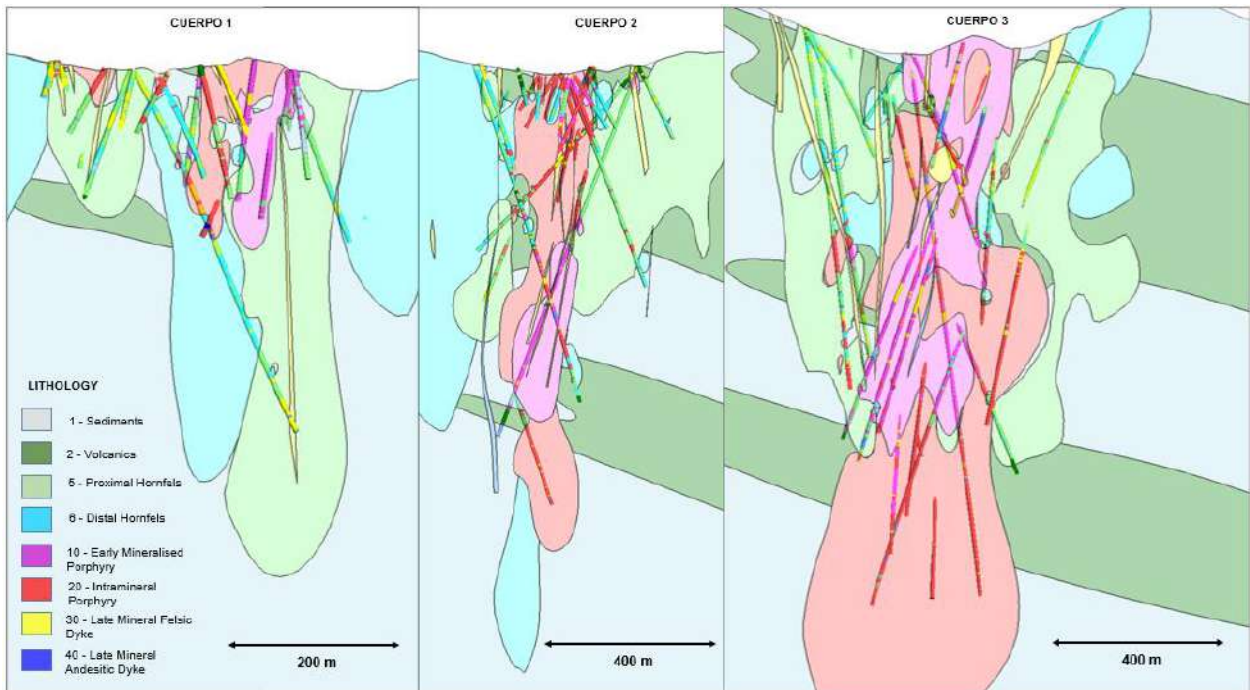


Figure 14.35 Cross sections looking NW showing lithological domains comprising Cuerpo 1, 2 and 3. (HCH, 2022)

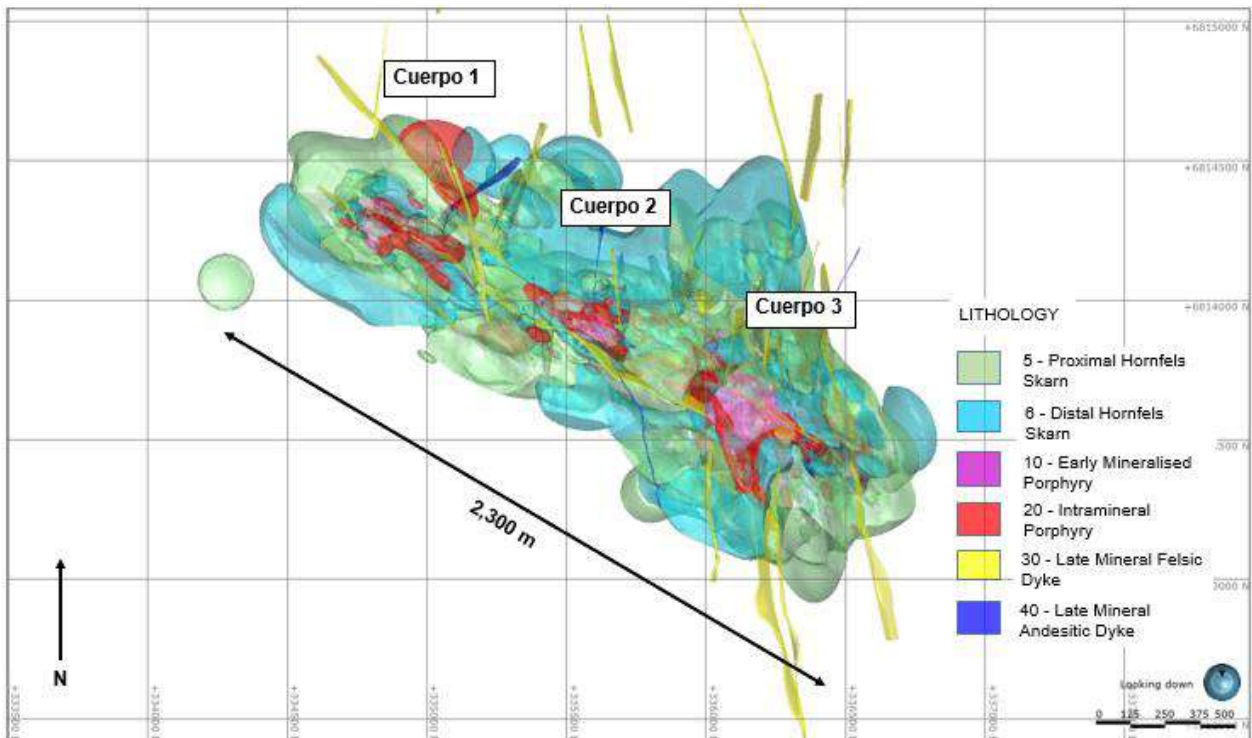


Figure 14.36 Combined geological model of Cortadera in plan-view illustrating the key lithological units (excluding host rocks). (HCH, 2022)

Lithological domains are built using the intrusion tool in Leapfrog Geo. This tool is well suited for modelling domains which have an 'inside' and an 'outside' and is thus well suited for modelling porphyry bodies (as well as the mineralised zones contained within). In areas of sparser data

density, edits may be required to constrain the model. These edits are made using polylines and points which force the interpretation to conform with the broader geological model.

The Felsic and Andesitic dykes (30- and 40-series) are more discrete geological units, with clear hanging wall and footwall contacts, and have been modelled with the vein system tool using a combination of drillhole and surface mapping data.

To build the vein models, an interval selection table is created so intervals can be assigned to a specific dyke (using nomenclature i.e., 30_01 and 40_01, etc). Polylines based upon surface mapping were digitised on topography. Additional polylines have been used to guide the interpretation, especially in areas where drillholes are oriented sub-parallel to the dyke.

The orientations of the overall dyke package were best supported by surface mapping, with only a few structural measurements from diamond core at Cortadera. The orientation is currently interpreted as predominantly N-S striking with near-vertical dip (although there is some NW-SE oriented 30- and 40-series dykes).

Figure 14.37 shows a plan view of the dyke model used to inform the mineral resource estimate, relative to 10- and 20-series porphyry models.

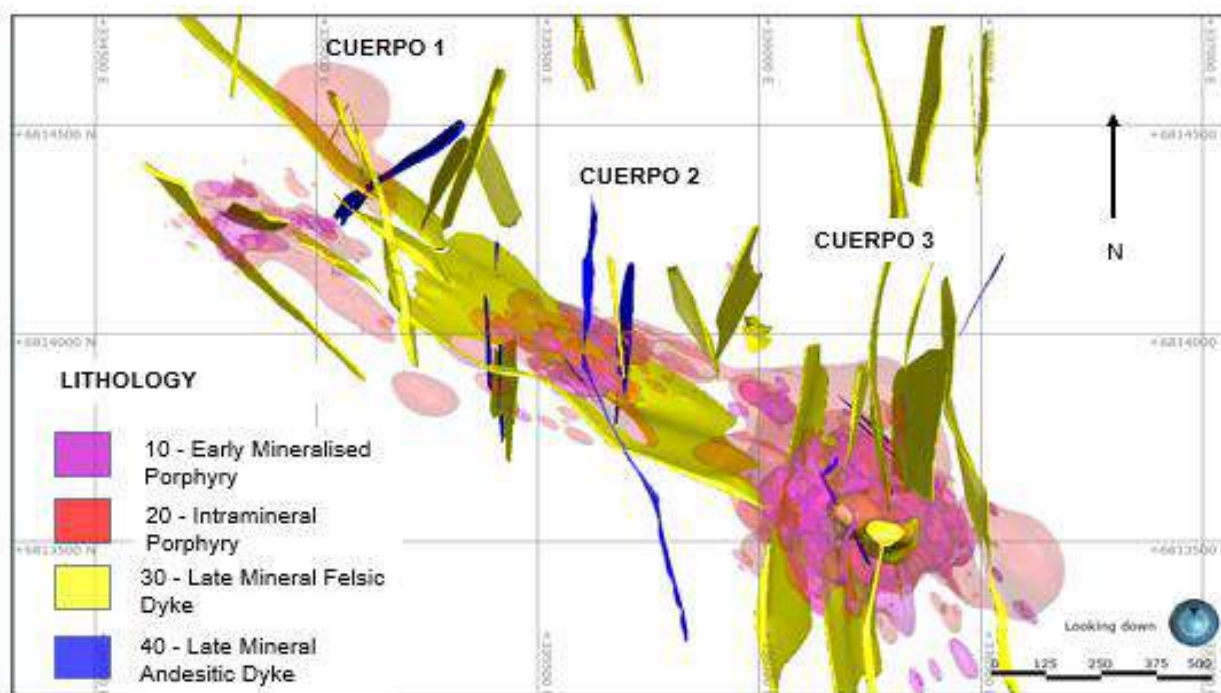


Figure 14.37 Plan view showing the Cortadera dyke model used for March 2022 Mineral Resource Estimate (HCH, 2022).

The importance of the dyke systems to the mineral resource estimate is acknowledged, especially as they comprise barren volumes which need to be ‘depleted’ from the block model. Due care has been taken to model dykes as accurately as possible without unreasonably impacting on the volume of the higher-grade 10- and 20-series porphyry bodies.

Dyke intervals with no clear continuity were not modelled. Reasons for intervals where logging suggests the presence of 30- or 40-series dyke not being included in a modelled dyke are:

- Insufficient supporting data to determine orientation of dyke: in areas of sparse data density and in the absence of structural measurements, it is not possible to interpret a dyke
- Dyke interval too narrow to be considered meaningful: in a bulk porphyry-style deposit, dykes less than 1 m true width are not considered material to the mineral resource
- Conflict between twinned drillholes: where twinned drillholes have inconsistent geological logging, no dyke has been interpreted
- No surface mapping available to support orientation of dyke (unless well supported by multiple drill intersections)
- Drilling subparallel to interpreted dyke: the optimal drill orientation to target the mineralised porphyry is steep, which results in many drillholes 'skimming' down the dykes as they drill sub-parallel. This makes it very difficult to sensibly interpret dyke geometry and where this cannot be rectified using polylines, no dyke is interpreted.

The potential volume of barren 30- and 40-series dyke which has not been included is not considered material to the mineral resource.

Dyke validation within Leapfrog Geo involved merging data (copper assay data, lithology, and total quartz-vein abundance), applying a query filter filtering and cross-checking against the drillhole logs. This aimed to reduce, as far as practicable, any intervals within the dyke volume which were not logged as dyke (i.e., were logged as 10- or 20-series porphyry) and that graded greater than 0.4 Cu% (first pass) and greater than 0.1 Cu% (second pass).

In some instances, validation checks resulted in intervals logged as 30- or 40-series dyke being re-logged. These intervals were corrected in the acquire database and the datasets re-exported.

Examples of query filters used for dyke validation are given in Table 14.60.

Table 14.60 Examples of Query Filters used to assist in dyke modelling at El Fuego

To identify intervals modelled as dyke but not logged as dyke	GM_Cortadera IN ('30 Dyke system' , '40_Dyke system') AND Geology_Model NOT IN ('30' , '40')
To identify intervals with Cu_pct > 0.4, logged as 10 or 20, modelled within 30/40 dyke	Cu_pct_D >= 0.4 AND GM_Cortadera IN ('30 Dyke system' , '40_Dyke system') AND Geology_Model IN ('10' , '20')
To identify intervals with Cu_pct > 0.1, logged as 10 or 20, modelled within 30/40 dyke	Cu_pct_D >= 0.1 AND GM_Cortadera IN ('30 Dyke system' , '40_Dyke system') AND Geology_Model IN ('10' , '20')
To identify intervals logged as 30 or 40 series dykes but not modelled as dyke	Geology_Model IN ('30' , '40') AND GM_Cortadera NOT IN ('30 Dyke system' , '40_Dyke system')

14.2.5 Mineralisation Model

Mineralisation at Cortadera is concentrated on three multi-phase tonalitic intrusions (Cuerpo 1, 2 and 3), as defined in the geological model.

Continuity of grade and geology is controlled by the emplacement of the mineralised intrusions into the gently south-easterly dipping host stratigraphic units. While these intrusions have a reasonably consistent pipe-like geometry, grade distribution is complex and extends into the host stratigraphic units. Statistical analysis suggests that the copper grade decreases outwards from

the porphyry core and that gradational boundary conditions exist between different rock units. While the distribution of rock types has guided mineralised zone interpretations, it has not been used to constrain the mineralised domains.

Mineralisation domains were constructed in Leapfrog Geo independently for each estimated element using cut-off grades guided by breaks in each elements grade distribution, shown in Table 14.61 below.

Mineralisation domains for gold, silver and molybdenum were created using grade interpolants on validated drillholes composited to 10m.

Copper mineralisation domains are created using a set of geological conditions (as described below) on validated drillholes composited to 10m intervals.

- Chalcopyrite (cpy) (as logged by site Geologists) above a set cut-off.
- Calculated mineralogy (ICP-MS) for chalcopyrite above a set cut-off.
- Copper assays (Cu%).
- Logged quartz-rich A- and B-type vein abundance above a set cut-off

Table 14.61 Grade cut-offs used for mineralised domain interpretations

Cuerpo	Element	HG Domain cut-off	MG Domain cut-off	LG Domain cut-off
1	Cu	1.0% cpy	-	0.1% CuEq
	Au	0.07 ppm Au	-	
	Ag	0.6 ppm Ag	-	
	Mo	70 ppm Mo	50 ppm Mo	
2	Cu	1.0 % cpy	-	
	Au	0.07 ppm Au	-	
	Ag	1.0 ppm Ag	0.6 ppm Ag	
	Mo	70 ppm Mo	50 ppm Mo	
3	Cu	1.2% cpy	-	
	Au	0.10 ppm Au	-	
	Ag	1.0 ppm Ag	0.6 ppm Ag	
	Mo	200 ppm Mo	150 ppm Mo	

All mineralisation domains are built using the intrusion tool within Leapfrog Geo. Surfaces were manually edited where appropriate to provide the best-fit for the composited assay data.

Additional points and/or strings may be used to guide the interpretation in areas of lower data density or complex geology.

While mineralisation domains do not always directly correlate with geological domains, each mineralisation domain is reconciled against the geological interpretation to ensure all observations (i.e., geological logging, surface mapping and knowledge of regional and local structural trends) are given proper consideration.

The presence of a calcium-rich alteration front is considered to exert a significant geological

control on mineralisation and appears to correlate well with zones of higher A- and B-type quartz vein abundances and copper grades that extend outward from the mineralised porphyry intrusions. This geometrical relationship is consistent with the addition of potassium and sodium to the porphyry core (along with copper, gold, molybdenum, silver, and other metals), where calcium has been depleted. The calcium has been remobilised and driven outwards along permeable pathways that developed in zones of higher fracture- and vein-abundance and within adjacent competent hornfels and permissive stratigraphic units.

The geometry of the mineralised domains for copper, gold, and silver estimates account for this, with mineralisation volumes manipulated to extend along the gently south-easterly dipping front that broadly conforms to the orientation and dip-direction of the host stratigraphic units.

Figure 14.38 below shows an example at Cuerpo 3 (section along 6,813,650mN), where the final copper HG estimation domain has been expanded from the original interpolant based on the shallow-dipping calcium-rich alteration front, logged A- + B-veining greater than 2%, and copper assays suggesting grade continuity in this orientation.

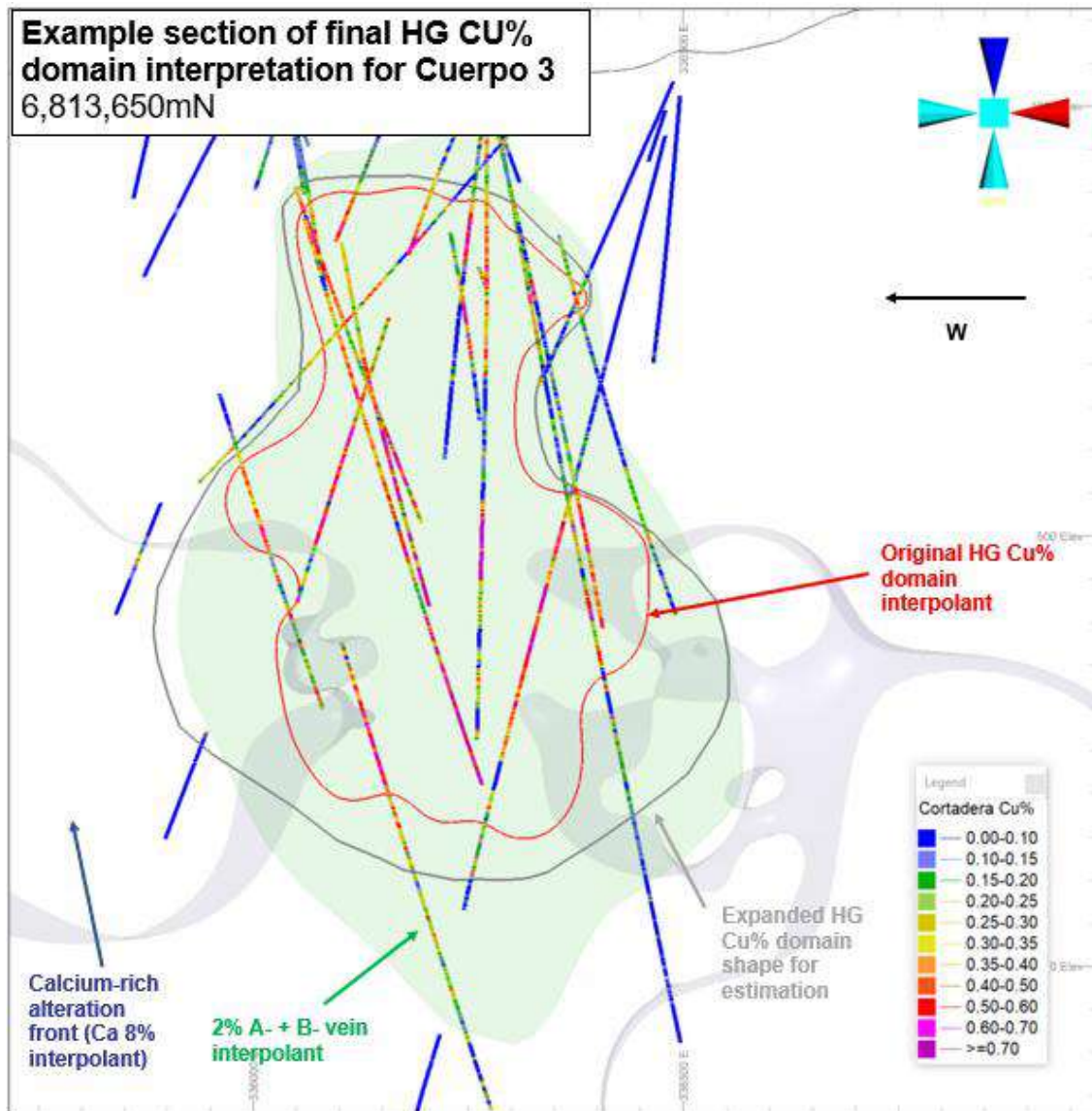


Figure 14.38 Cross section showing the final Cu% estimation domain (grey) for Cuerpo 3 compared to the original 1.2% cpy interpolant (red). Calcium-rich alteration front (blue) and 2% A- + B- vein interpolant (green) shown for reference.

Final estimation domains for copper, gold and silver have been adjusted based on the criteria above, with the wireframes created manually in Datamine along east-west trending sections at 50m spacing.

Figure 14.39 shows the final copper HG estimation domain volumes compared to the original interpolants.

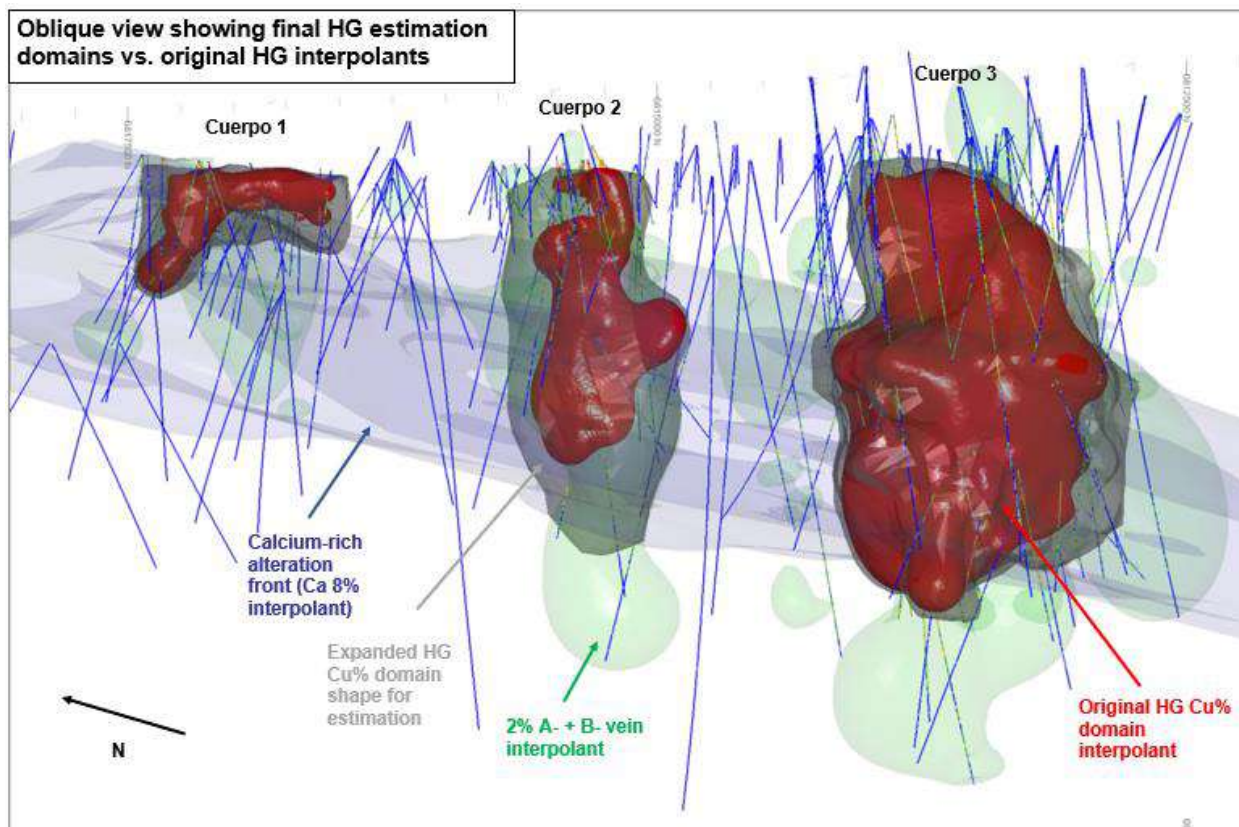


Figure 14.39 Final Cu% estimation domains (grey) compared to the original cpy interpolants (red). Calcium-rich alteration front (blue) and 2% A- + B- vein interpolants (green) shown for reference.

A strong correlation exists between gold and copper grades (statistical correlation $R=-0.7$). Gold interpolants have been validated against the copper interpolants to ensure that this correlation is preserved (Figure 14.40). This is especially important as there are fewer gold samples available (historic Minera Fuego holes did not assay for gold) so the interpolation can be controlled using interpretation points and strings derived from the copper interpolant.

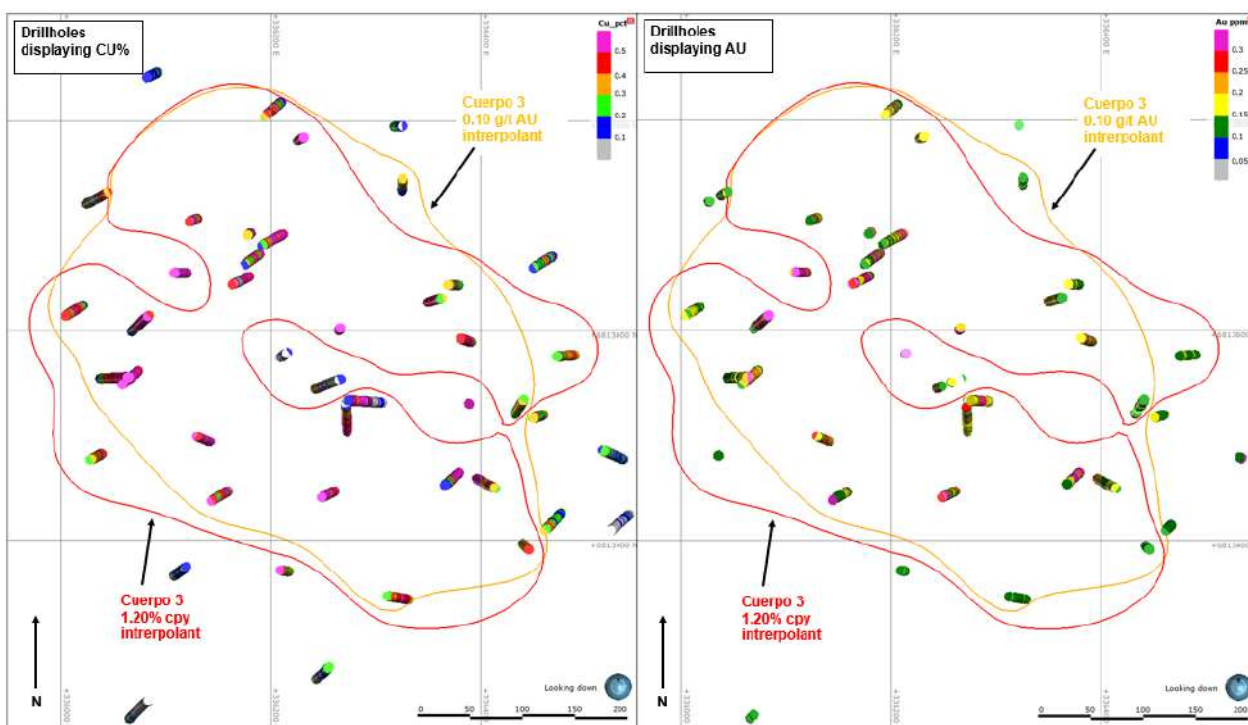


Figure 14.40 Comparison between Cu% and Au interpolants at 500 mRL. Drillholes displaying Cu% grades on left image and Au grades on right image.

The Ann-Mason Porphyry deposit at Yerington has been used as a guide of the interpretation of molybdenum and silver interpolants for estimation (Figure 14.41).

Copper and Gold form the 'core' of the mineralised system, with accumulations of molybdenum and silver forming 'lungs' around the fringes. Therefore, copper and gold interpolants can be used as a guide when creating the molybdenum and silver interpolants for estimation.

Figure 14.42 shows the molybdenum interpolant (150 ppm) with a 1.65% cpy interpolant (note the 1.65% cpy interpolant only included for reference, it was not used for the copper estimate). Molybdenum can be observed to form a halo to the known copper mineralisation ('lungs').

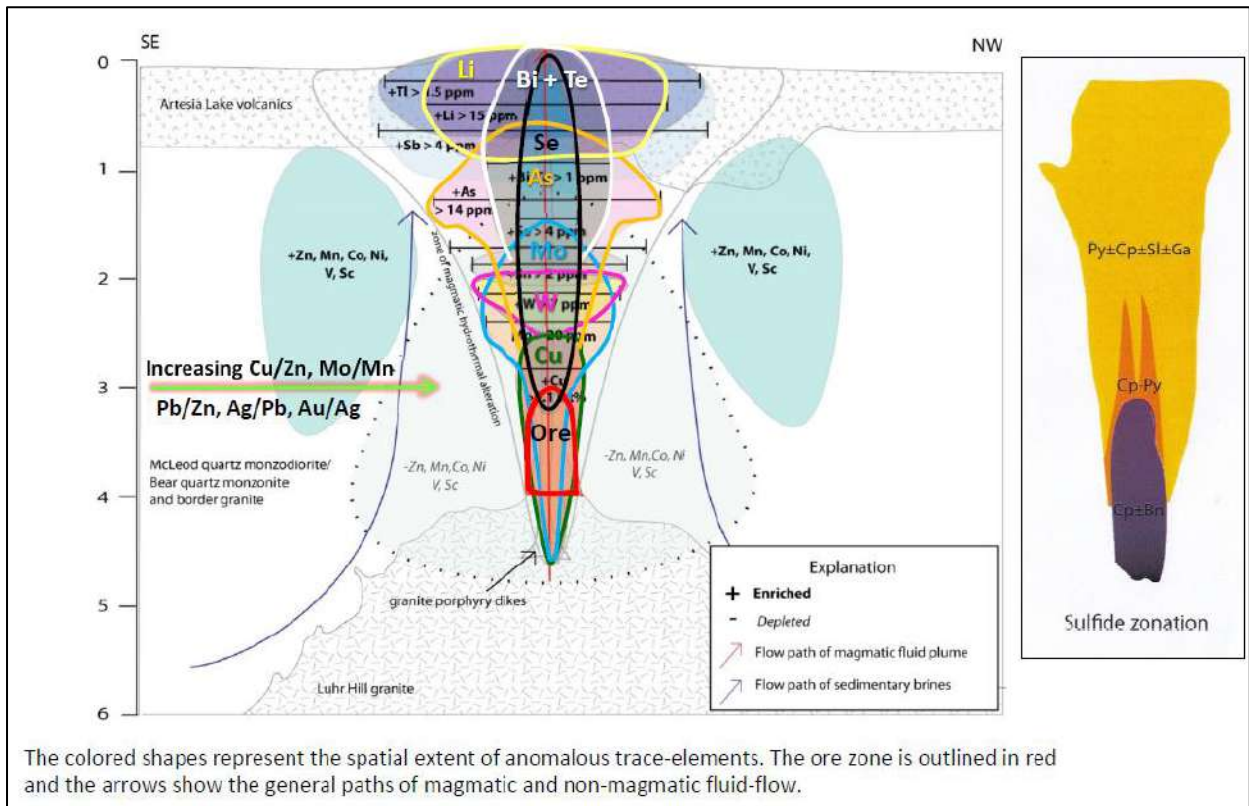


Figure 14.41 A cross section through the Ann-Mason Porphyry deposit at Yerington, showing the trace element distribution (Cohen, 2011 and Halley et al., 2015).

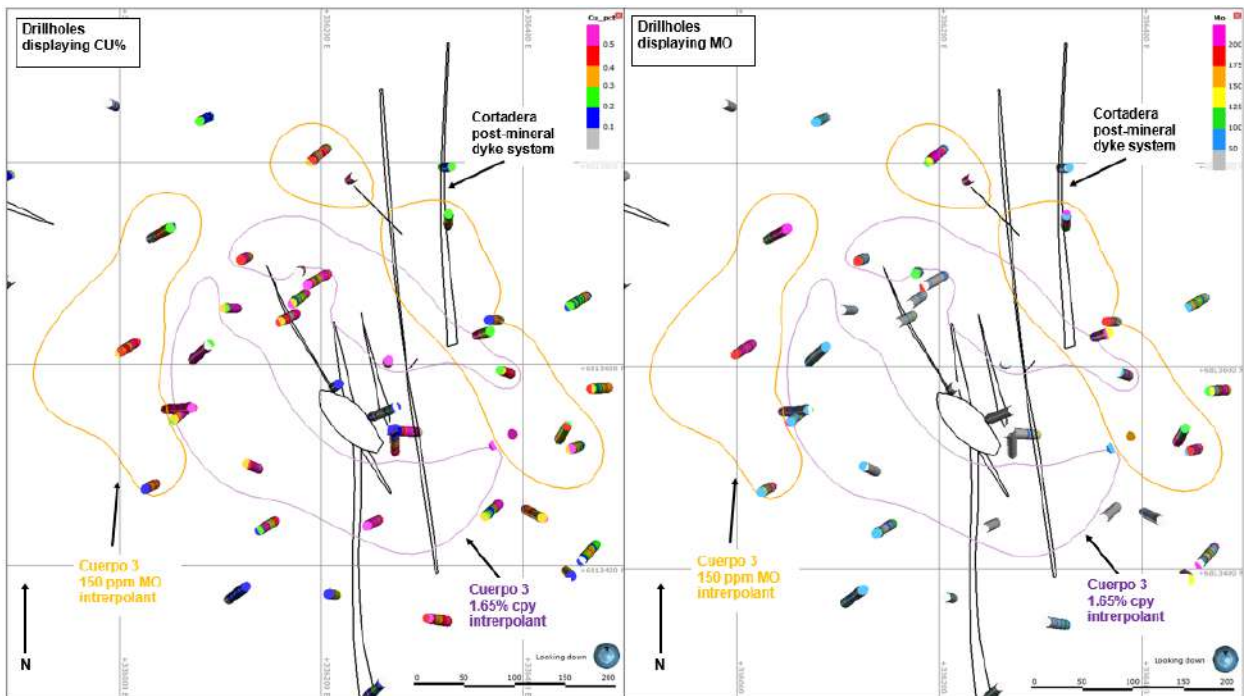


Figure 14.42 Plan section comparison between Cu% and Mo interpolants at 500 mRL. Drillholes displaying Cu% grades on left image and Mo grades on right image.

A 0.1% copper equivalent (CuEq) interpolant defines the outer extent of the mineralisation. The CuEq equation considers assayed copper, gold, silver, and molybdenum and provides volume constraint for the low-grade estimate for copper and gold.

The 0.1% CuEq shape has been validated against the 1% A- and B- type quartz vein interpolant, with strong correlation shown in most areas (Figure 14.43). Areas where the CuEq shape deviates from the 1% A- and B- vein interpolant include the saddles between the mineralised porphyries and the area to the north of Cuerpo 1 porphyry. In all cases, this can be explained by an increase in ancillary element grades silver or molybdenum).

The CuEq% formula used is from the Productora mineral resource, which differs slightly from the formula used for the Cortadera mineral resource. The difference is not considered material.

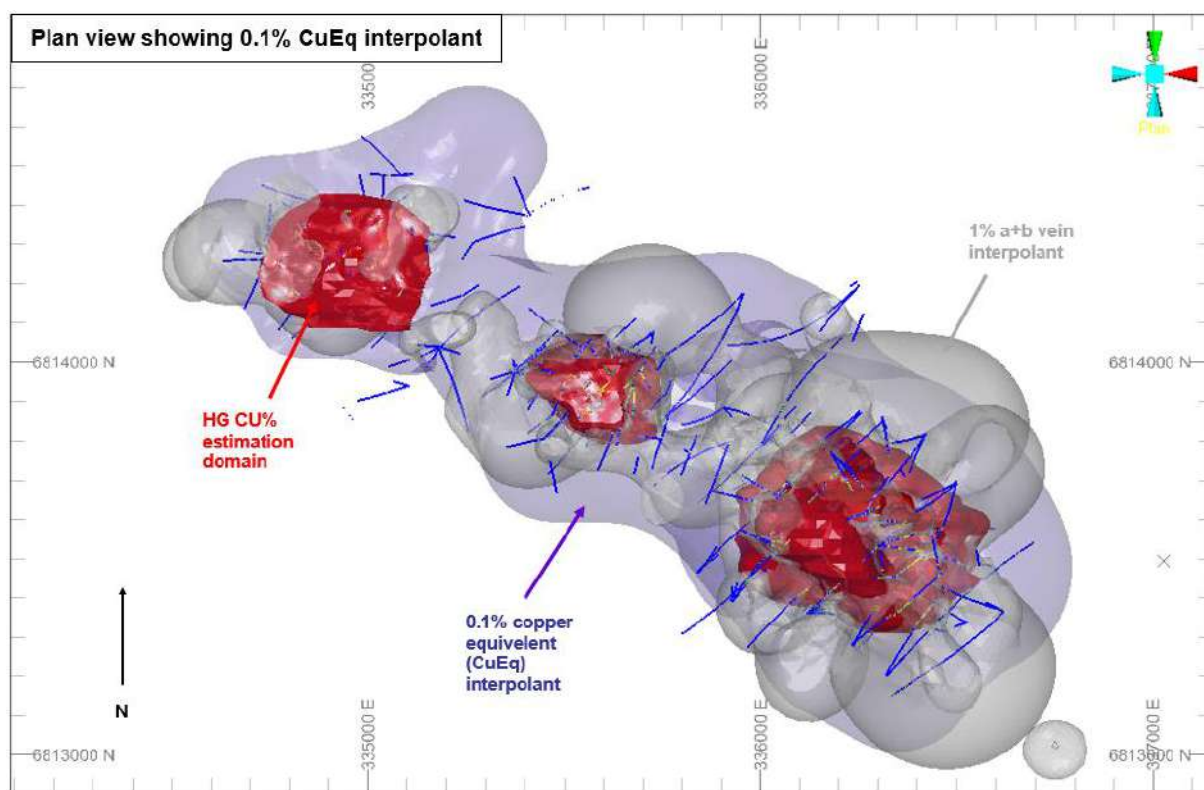


Figure 14.43 Plan view showing the 0.1% CuEq interpolant (blue) with 1% A- + B-vein interpolant (grey) and HG Cu% estimation domains (red) for reference

Work has commenced on a structural model for Cortadera and will attempt to link fault zones and structural domains mapped at surface with similar features encountered during drilling. The structural model will refer to rock-quality designation (RQD) and fracture frequency (FF) data, enabling comparison between this data and structural data collected during drillhole logging and mapping studies.

14.2.6 Weathering Domains

The modelling of weathering domains is based on:

- Copper species flagging using copper to sulphur ratio
- Total contained Sulphide (S^{2-}) percent
- Regolith logging from diamond core and reverse circulation (RC) chips (validated by viewing photographs, where possible).

Where a qualitative method has been used for interpretation of the weathering domains (i.e., Cu%:S% or total contained, validation has been completed using the regolith logging from diamond core and RC chips.

When no qualitative information was available, regolith logging from diamond core and RC chips was used to interpret the weathering domains which has been checked by viewing core and RC chip photographs.

Validation of the surfaces and refinement of the weathering model included resolving conflicting logging in twinned drillholes and reassigning anomalous intervals to help build geologically coherent weathering model surfaces.

Figure 14.44 and Figure 14.45 show two examples of the weathering model in cross-section, with surfaces created using the S^{2-} % and validated using the regolith logging and RC chip and core photographs.

Note that in the section shown in Figure 14.45, the weathering profile is much deeper around the edges of the porphyry intrusion. This may also be related to faulting, with the rock in these areas generally highly fractured. This observation has been validated by viewing core and RC chip photographs and is supported by both the total contained S^{2-} % and the Cu%:S% ratio.

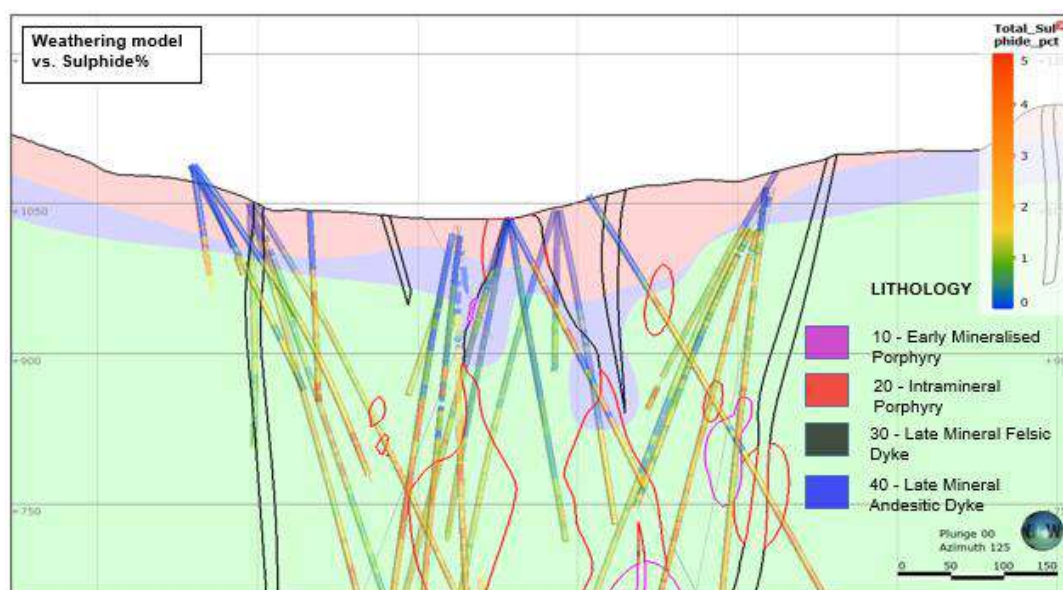


Figure 14.44 Cross section (looking SE) showing final weathering model (fresh is green, transitional is blue, oxide is red) compared to drillholes displaying sulphide percentage and the location of intrusive porphyries.

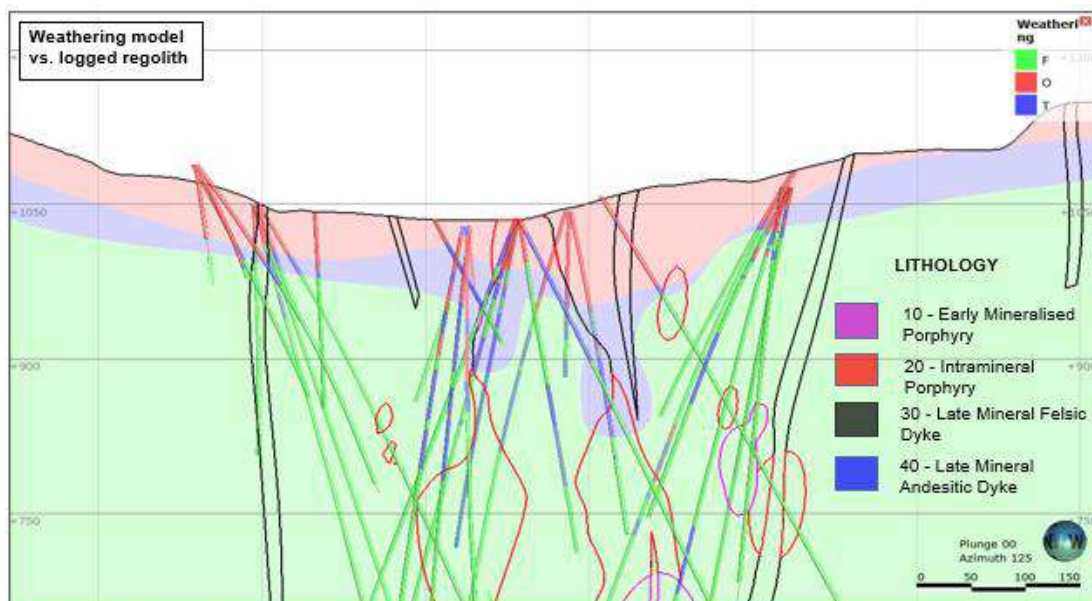


Figure 14.45 Cross section (looking SE) showing final weathering model compared to logged regolith (fresh is green, transitional is blue, oxide is red).

14.2.7 Data Flagging and Compositing

Geology, mineralisation, and weathering wireframes were supplied by Hot Chili Limited to Haren Consulting in Datamine .pt/.tr format. These wireframes were used to flag the drillhole data and block model. Additional wireframes were used to flag each CUERPO area. Wireframes used to create the volume model listed in Table 14.62.

Table 14.62 List of final wireframes used for estimation coding

Wireframe	Field	Code	Description	Type
cuerpo1_extent	CUERPO	1	Cuerpo 1 model area	Solid
cuerpo2_extent	CUERPO	2	Cuerpo 2 model area	Solid
cuerpo3_extent	CUERPO	3	Cuerpo 3 model area	Solid
06_20220213	LTCODE	6	Distal Skarn lithology coding	Solid
05_20220213	LTCODE	5	Proximal Skarn lithology coding	Solid
02_20220213	LTCODE	2	Volcanic and Sediment host coding	Solid
20_20220213	LTCODE	20	Intramineral porphyry coding	Solid
10_20220213	LTCODE	10	Early mineralised porphyry coding	Solid
30_stock_20220213	LTCODE	32	Late mineral felsic dyke stock coding	Solid
30_dyke_eye_20220211	LTCODE	31	Late mineral felsic dyke eye coding	Solid
30_dyke_system_20220211	LTCODE	30	Late mineral felsic dyke system coding	Solid
40_dyke_system_20220211	LTCODE	40	Late mineral andesitic dyke system coding	Solid

Wireframe	Field	Code	Description	Type
topo_2020	TOPO	10000	Topographic surface coding	Surface
transitional_20220214	WTCODE	2	Transitional weathering coding	Solid
fresh_20220214	WTCODE	3	Fresh rock weathering coding	Solid

The coding of the drillholes by the geology into the field LTCODE was adjusted in some cases where spatial and grade inconsistencies were noted.

14.2.8 Mining and Tenement Flagging In The Model

Cortadera tenements are flagged into the 'TENEMENT' field in the final estimate using binary code (0= inside of HCH tenement boundary and 1 = outside of tenement boundary).

As shown below (Figure 14.46) a small section of Cuerpo 1 lies outside the HCH tenement boundary. This material has been excluded from the reported mineral resource.

There are no material workings at Cortadera (surface or underground). No depletion has been applied to the reported mineral resource.

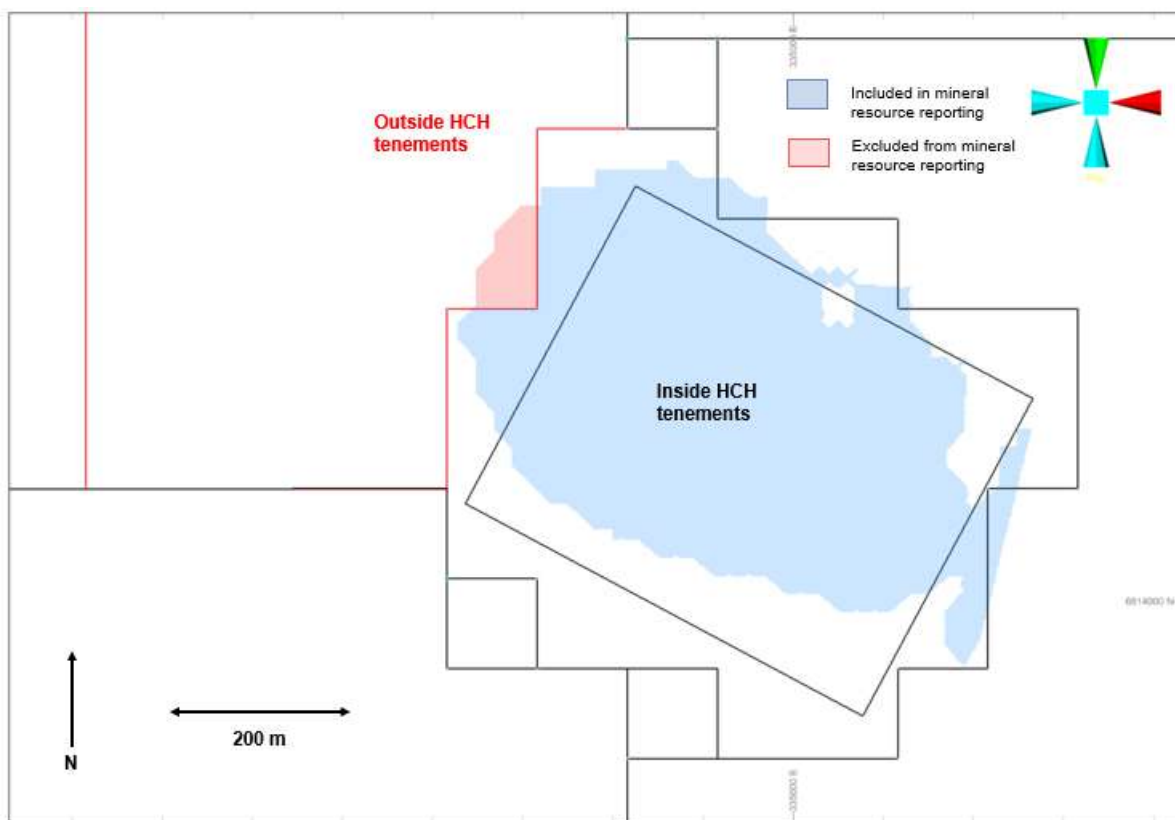


Figure 14.46 Plan view of the area of Cuerpo 1 which lies outside the current HCH tenement boundary.

14.2.9 Compositing

Compositing is the process of equalising the length of samples used for statistical and geostatistical analysis. This is required to ensure that samples of equal support are considered. Most estimation algorithms do not consider the sample size i.e., there is no difference between a 10m sample and a 1m sample.

Sample data for the Cortadera model has been composited to 2m. This length has been used to limit the impact of splitting individual samples into two or more composites (where individual samples are split into two or more composites). A histogram with statistics is presented in Figure 14.47 for sample length. Larger composite intervals would not allow the variability of mineralisation to be investigated and result in the grade estimation being overly smooth.

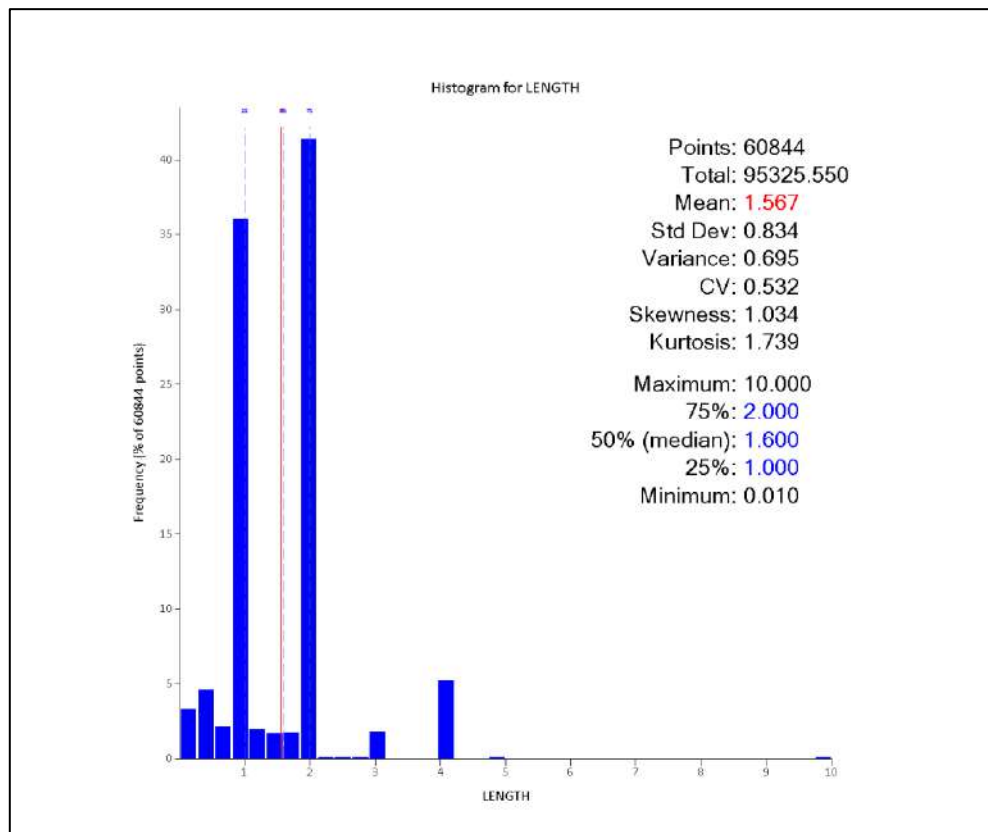


Figure 14.47 Histogram of Cortadera sample lengths

The compositing was run within a field which was a combination of the weathering, lithology, and grade envelope fields (WTCODE, LTCODE and GTCODE) to ensure that no composite intervals crossed any lithological and/or grade boundaries. To allow for uneven sample lengths within each of the domains, the Datamine composite process (COMP DH) was run using the variable sample length method (@MODE=1) and a minimum composite length of one metre. This adjusts the sample intervals where required to ensure all samples were included in the composite file (i.e., no residuals) while keeping the sample interval as close to the desired sample interval as possible. Figure 14.48 shows the final composite lengths used in the estimate.

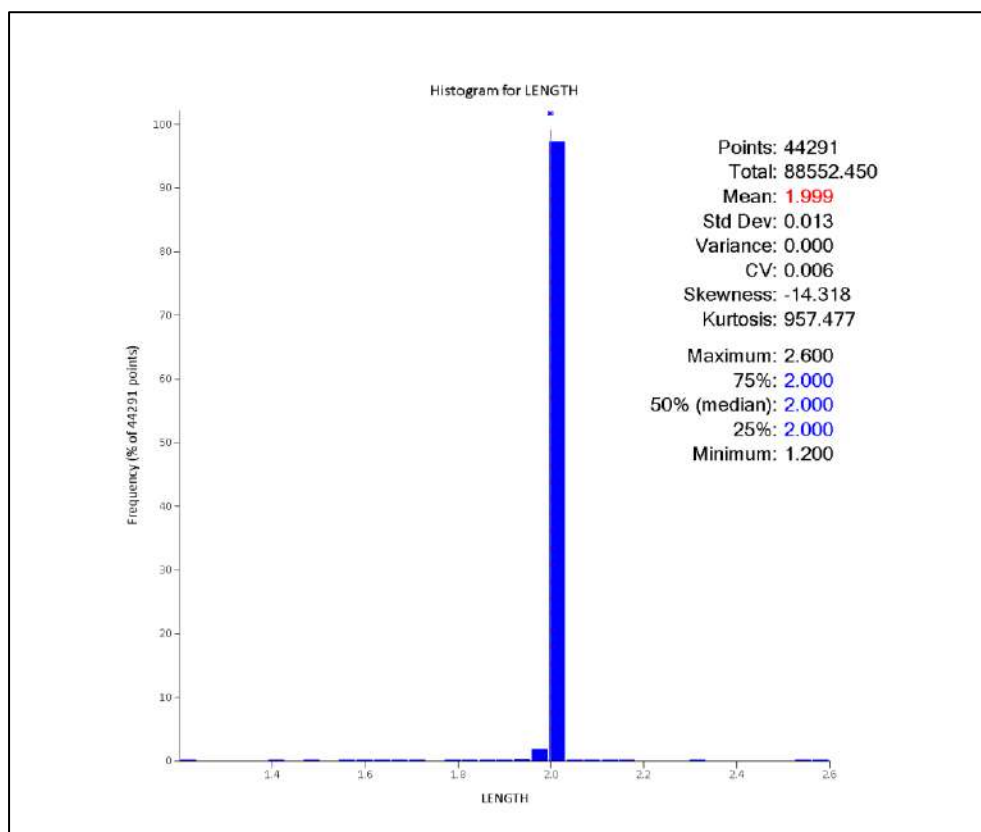


Figure 14.48 Histogram of Cortadera composite lengths

14.2.10 Statistical Analysis

The statistical, spatial, and geological characteristics of the data were examined within each estimation domain.

The 0.1% CuEq domain which comprises the low-grade boundary was initially analysed individually for each Cuerpo, but the output statistics suggested no hard boundary existed. For this reason, the low-grade domain has been analysed as a single domain straddling all three Cuerpos.

The effect of weathering was examined, with statistical analysis indicating a soft grade boundary between both weathering horizons. This, combined with the small number of samples in the oxide and transitional zones, meant that combining the weathering horizons for estimation was the most suitable methodology.

For the Cortadera mineral resource, a total of 49 domains have been estimated. Descriptions for each domain are shown in Table 14.63.

For the Limonite, Cu% and Au estimates, further domaining is applied through use of the categorical indicator kriging estimation methodology (CIK).

Table 14.63 Grade estimation domains

CUERPO/(DOMAIN)/ELEMENT	CONSTRAINING WIREFRAME (.PT/.TR)
Cuerpo 1/HG/CU%	c1_mgexp_cu_20220215
Cuerpo 1/LG/CU%	c123_lg_cu_20220215_cueq
Cuerpo 1/Waste/CU%	cuerpo1_extent
Cuerpo 2/HG/CU%	c2_mgexp_cu_20220212
Cuerpo 2/LG/CU%	c123_lg_cu_20220215_cueq
Cuerpo 2/Waste/CU%	cuerpo2_extent
Cuerpo 3/HG/CU%	c3_mgexp_cu_20220210
Cuerpo 3/LG/CU%	c123_lg_cu_20220215_cueq
Cuerpo 3/Waste/CU%	cuerpo3_extent
Cuerpo 1/HG/AU	c1_mgexp_au_20220215
Cuerpo 1/LG/AU	c123_lg_cu_20220215_cueq
Cuerpo 1/Waste/AU	cuerpo1_extent
Cuerpo 2/HG/AU	c2_mgexp_au_20220212
Cuerpo 2/LG/AU	c123_lg_cu_20220215_cueq
Cuerpo 2/Waste/AU	cuerpo2_extent
Cuerpo 3/HG/AU	c3_mgexp_au_20220211
Cuerpo 3/LG/AU	c123_lg_cu_20220215_cueq
Cuerpo 3/Waste/AU	cuerpo3_extent
Cuerpo 1/LIM	C1_Limonites_20220204
Cuerpo 2/LIM	C2_Limonites_20220203
Cuerpo 3/LIM	C3_Limonites_20220203
Cuerpo 1/MG/AG	C1_MG_Ag_20220204
Cuerpo 1/MG_EXP/AG	c1_mgexp_ag_20220215
Cuerpo 1/LG/AG	c123_lg_cu_20220215_cueq
Cuerpo 1/Waste/AG	cuerpo1_extent_ag
Cuerpo 2/HG/AG	c2_hg_ag_20220216
Cuerpo 2/HG_EXP/AG	c2_hgexp_ag_20220212
Cuerpo 2/MG/AG	C2_MG_Ag_20220204
Cuerpo 2/MG_EXP/AG	c2_mgexp_ag_20220212
Cuerpo 2/LG/AG	c123_lg_cu_20220215_cueq
Cuerpo 2/Waste/AG	cuerpo2_extent_ag
Cuerpo 3/HG/AG	C3_HG_Ag_20220204
Cuerpo 3/HG_EXP/AG	c3_hgexp_ag_20220211
Cuerpo 3/MG/AG	C3_MG_Ag_20220204
Cuerpo 3/MG_EXP/AG	c3_mgexp_ag_20220211
Cuerpo 3/LG/AG	c123_lg_cu_20220215_cueq
Cuerpo 3/Waste/AG	cuerpo3_extent_ag
Cuerpo 1/HG/MO	C1_HG_Mo_20220204
Cuerpo 1/MG/MO	C1_MG_Mo_20220204

CUERPO/(DOMAIN)/ELEMENT	CONSTRAINING WIREFRAME (.PT/TR)
Cuerpo 1/LG/MO	c123_lg_cu_20220215_cueq
Cuerpo 1/Waste/MO	cuerpo1_extent
Cuerpo 2/HG/MO	C2_HG_Mo_20220204
Cuerpo 2/MG/MO	C2_MG_Mo_20220204
Cuerpo 2/LG/MO	c123_lg_cu_20220215_cueq
Cuerpo 2/Waste/MO	cuerpo2_extent
Cuerpo 3/HG/MO	C3_HG_Mo_20220202
Cuerpo 3/MG/MO	C3_MG_Mo_20220202
Cuerpo 3/LG/MO	c123_lg_cu_20220215_cueq
Cuerpo 3/Waste/MO	cuerpo3_extent

Figure 14.49 below shows the domaining applied for the estimation of Cu% in Cuerpo 3.

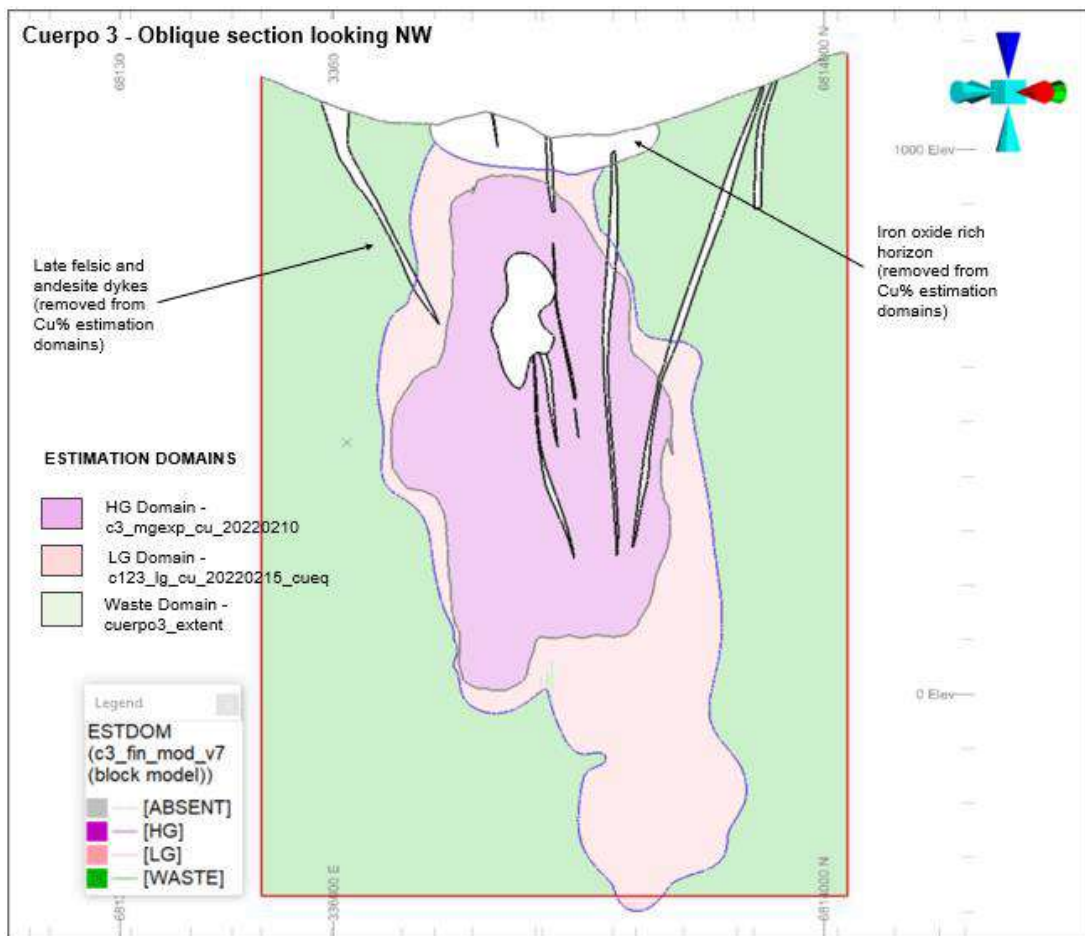


Figure 14.49 Oblique cross section of Cuerpo 3 showing Cu% estimation domains used for mineral resource

14.2.11 Top Cuts

Top cuts were applied to the composited sample data to reduce the impact of outlier values on the mean grade and coefficient of variation (CV). Using outliers in an estimate can result in material overestimation of grade and metal.

Top cuts were selected based on statistical analysis of the data (log histograms, log probability plots, and grade disintegration) and are summarised in Table 14.64.

No top-cuts were required for the copper and gold domains due to the absence of outliers

Table 14.64 Cortadera mineralised domains top-cut analysis

Element	Cuerpo	Domain	Sub-domain	Raw				Top cut				
				Number	Max	Mean	CV	Value	# Cut	Mean	CV	
CU%	Cuerpo 1	HG	HG_CIK	355	2.381	0.564	0.567	-	0	0.564	0.567	
			LG_CIK	1,364	0.978	0.169	0.534	-	0	0.169	0.534	
		LG	-	1,647	0.859	0.139	0.578	-	0	0.139	0.578	
		Waste	-	4,491	0.609	0.041	0.842	-	0	0.046	0.842	
	Cuerpo 2	HG	HG_CIK	2,261	3.875	0.332	0.914	-	0	0.332	0.914	
			LG_CIK	608	0.407	0.115	0.470	-	0	0.115	0.470	
		LG	-	1,647	0.859	0.139	0.578	-	0	0.139	0.578	
		Waste	-	4,491	0.608	0.046	0.766	-	0	0.046	0.766	
	Cuerpo 3	HG	HG_CIK	2,710	1.989	0.619	0.344	-	0	0.619	0.344	
			MG_CIK	5,089	1.076	0.301	0.382	-	0	0.301	0.382	
			LG_CIK	1,055	0.351	0.109	0.351	-	0	0.109	0.351	
		LG	HG_CIK	4,945	1.410	0.183	0.475	-	0	0.183	0.475	
			LG_CIK	741	0.354	0.072	0.646	-	0	0.072	0.646	
		Waste	-	10,711	1.251	0.044	1.191	-	0	0.044	0.891	
	AU	Cuerpo 1	HG	-	1,204	0.644	0.061	0.932	-	0	0.061	0.932
LG			-	1,680	0.257	0.026	0.930	-	0	0.026	0.930	
Waste			-	3,074	0.418	0.009	0.861	-	0	0.009	0.861	
Cuerpo 2		HG	HG_CIK	1,456	2.100	0.183	0.892	-	0	0.183	0.892	
			LG_CIK	2,059	0.400	0.053	0.655	-	0	0.053	0.655	
		LG	-	1,206	0.711	0.030	1.073	-	0	0.030	1.073	
		Waste	-	4,237	0.823	0.045	0.931	-	0	0.045	0.931	
Cuerpo 3		HG	HG_CIK	2,002	0.866	0.242	0.422	-	0	0.242	0.422	
			MG_CIK	4,834	0.583	0.124	0.522	-	0	0.124	0.522	
			LG_CIK	1,132	0.426	0.046	0.743	-	0	0.046	0.743	
		LG	HG_CIK	4,358	0.258	0.031	0.593	-	0	0.031	0.593	
			LG_CIK	702	0.152	0.011	0.788	-	0	0.011	0.788	
		Waste	-	8,422	0.288	0.004	1.001	-	0	0.004	1.001	
LIM		Cuerpo 1	LIM	HG_CIK	86	0.451	0.114	0.557	-	0	0.114	0.557
				LG_CIK	287	0.275	0.052	0.671	-	0	0.052	0.671
	Cuerpo 2	LIM	HG_CIK	227	0.850	0.206	0.597	-	0	0.206	0.597	

Element	Cuerpo	Domain	Sub-domain	Raw				Top cut			
				Number	Max	Mean	CV	Value	# Cut	Mean	CV
				LG_CIK	363	0.264	0.057	0.841	-	0	0.057
Cuerpo 3	LIM	HG_CIK	391	0.944	0.068	1.120	-	0	0.068	1.120	
		MG_CIK	407	9.430	0.063	7.476	0.25	4	0.037	0.971	
		LG_CIK	41	0.036	0.003	1.179	-	0	0.003	1.179	
		MG	-	917	10.30	0.879	0.920	5	3	0.871	0.854
Cuerpo 1	LIM	MG_EXP	-	2,553	10.30	0.546	1.058	3	4	0.537	0.939
		LG	-	3,223	4.80	0.362	0.804	2	9	0.358	0.702
		Waste	-	1,280	2.72	0.298	0.786	1	11	0.286	0.567
		HG	-	465	9.00	1.241	0.907	-	0	1.241	0.907
Cuerpo 2	LIM	HG_EXP	-	802	9.00	1.008	0.939	-	0	1.008	0.939
		MG	-	1,347	14.90	0.719	0.868	9	1	0.714	0.755
		MG_EXP	-	3,092	14.90	0.494	0.945	2	2	0.482	0.685
		LG	-	4,716	14.25	0.340	0.874	3	3	0.337	0.647
		Waste	-	1,476	4.34	0.272	0.843	4	4	0.272	0.829
		HG	-	2,594	100.0	1.277	1.654	10	2	1.235	0.558
Cuerpo 3	LIM	HG_EXP	-	4,651	100.0	1.015	1.603	10	2	0.992	0.648
		MG	-	5,225	8.00	0.713	0.629	5	2	0.712	0.618
		MG_EXP	-	7,300	8.00	0.537	1.561	5	2	0.527	0.741
		LG	-	13,283	59.60	0.346	1.789	3	3	0.339	0.699
		Waste	-	4,106	4.30	0.276	0.613	2	3	0.274	0.519
		HG	-	261	358.0	91.14	0.558	220	5	89.53	0.501
Cuerpo 1	LIM	MG	-	713	719.0	60.71	0.717	200	5	59.40	0.551
		LG	-	3,437	2,100	21.48	2.053	150	1	20.52	1.137
		Waste	-	1,785	90.00	8.494	1.324	50	0	8.238	0.903
		HG	-	197	581.0	121.4	0.781	-	0	121.4	0.781
Cuerpo 2	LIM	MG	-	332	308.0	61.95	0.653	200	3	61.22	0.606
		LG	-	7,320	1110	16.02	1.683	100	6	15.16	1.183
		Waste	-	1,080	171.0	7.241	1.649	100	3	7.150	1.535
		HG	-	587	2,890	355.6	0.912	1700	6	350.2	0.840
Cuerpo 3	LIM	MG	-	942	1,130	171.7	0.763	850	4	170.9	0.737
		LG	-	19,058	2,570	41.36	1.667	200	8	38.21	1.168
		Waste	-	4,089	307.5	4.821	1.861	110	4	4.746	1.547
		HG	-	587	2,890	355.6	0.912	1700	6	350.2	0.840

14.2.12 Variography

Top-cut composites have been reviewed for variographic analysis (variography). Variography examines the spatial relationship between composites and seeks to identify the directions of mineralisation continuity and to quantify the ranges that continuity.

Variography was also used to determine the random variability or 'nugget effect' of the deposit. The results ensure appropriate kriging parameters are selected for grade estimation.

Snowden Supervisor software was used to generate and model the variograms. Variograms were calculated in isolation for each element but then reviewed against elements with high correlation factors (i.e., Cu% and Au) to ensure logical relationships between those elements.

For elements estimated using a conventional approach (Ordinary Kriging), a single set of variograms have been constructed for each domain. A normal scores transformation was applied to the element data prior to the construction of the experimental variogram. Final variograms are then back-transformed to traditional space adjusting for variance.

For elements estimated using a probabilistic approach (Categorical Indicator Kriging), an additional set of variograms are created on the binary coded data.

Binary coding is dependent on the sample satisfying some criterion (or in some cases, a set of criteria). As the data is transformed using the binary coding approach, no additional transformation is required. Following the selection of probability thresholds, variography using the conventional approach described above is completed.

Knowledge of the underlying geological conditions was always considered when constructing variograms. Variogram orientations were overlain onto each lode during the validation step to ensure trends are coherent and agree with the broader geological model.

The variogram model parameters used for grade estimation are shown below (Table 14.65 to Table 14.68).

Table 14.65 Variogram models for Limonites

Cuerpo	Field	Sub-domain	Direction		Nugget	Structure 1		Structure 2		Structure 3	
					C ₀	C ₁	R ₁	C ₁	R ₁	C ₁	R ₁
Cuerpo 1	IND	-	1	00°-->220°	0.32	0.11	100	0.10	160	0.47	190
			2	00°-->130°			100		160		170
			3	90°-->000°			10		15		20
	AU	HG_CIK	1	00°-->150°	0.24	0.20	190	0.28	230	0.28	370
			2	00°-->060°			130		170		240
			3	90°-->000°			5		15		30
		LG_CIK	1	00°-->150°	0.24	0.20	190	0.28	230	0.28	370
			2	00°-->060°			130		170		240
			3	90°-->000°			5		15		30
	CU%	HG_CIK	1	00°-->310°	0.10	0.26	55	0.24	100	0.40	160
			2	00°-->220°			45		80		130
			3	90°-->000°			40		70		100
		LG_CIK	1	00°-->310°	0.10	0.26	55	0.24	100	0.40	160
			2	00°-->220°			45		80		130
			3	90°-->000°			40		70		100
	AG	-	1	00°-->260°	0.35	0.14	140	0.28	250	0.23	400
			2	00°-->170°			60		135		190
			3	90°-->000°			10		12		30
	MO	-	1	00°-->300°	0.24	0.21	30	0.26	70	0.30	180
			2	00°-->210°			30		70		180
			3	90°-->000°			30		70		180
Cuerpo 2	IND	-	1	00°-->100°	0.18	0.29	50	0.27	120	0.26	170
			2	-10°-->010°			30		80		130
			3	80°-->000°			15		32		50
	AU	HG_CIK	1	00°-->300°	0.16	0.32	30	0.21	60	0.31	160
			2	00°-->210°			25		50		90
			3	90°-->000°			15		30		50
		LG_CIK	1	00°-->100°	0.03	0.26	70	0.30	160	0.41	190
			2	00°-->010°			50		80		110
			3	90°-->000°			40		60		80
	CU%	HG_CIK	1	00°-->320°	0.37	0.33	35	0.14	60	0.16	100
			2	10°-->230°			35		60		100
			3	80°-->050°			30		40		65
		LG_CIK	1	00°-->310°	0.08	0.28	150	0.31	210	0.33	290
			2	00°-->220°			35		80		170
			3	90°-->000°			30		50		110
Cuerpo 2	AG	-	1	06°-->300°	0.27	0.29	30	0.23	80	0.21	180
			2	08°-->210°			30		80		180

Cuerpo	Field	Sub-domain	Direction		Nugget	Structure 1		Structure 2		Structure 3		
					C ₀	C ₁	R ₁	C ₁	R ₁	C ₁	R ₁	
			3	80°-->350°			30		40		70	
	MO	-	1	00°-->245°	0.26	0.21	40	0.28	88	0.31	225	
			2	00°-->155°			20		50		126	
			3	90°-->000°			15		30		70	
Cuerpo 3	IND/ INDH	-	1	00°-->090°	0.16	0.30	110	0.14	140	0.40	165	
				2			00°-->000°		20		40	110
				3			90°-->000°		20		40	50
	AU	HG_CIK	1	00°-->110°	0.35	0.22	50	0.18	130	0.25	250	
				2			00°-->020°		25		50	100
				3			90°-->000°		10		15	40
			MG_CIK	1	00°-->280°	0.23	0.16	60	0.31	150	0.30	260
				2	00°-->190°			60		130		250
				3	90°-->000°			5		10		15
			LG_CIK	1	00°-->280°	0.23	0.16	60	0.31	150	0.30	260
				2	00°-->190°			60		130		250
				3	90°-->000°			5		10		15
	CU%	HG_CIK	1	00°-->090°	0.23	0.18	50	0.26	140	0.33	300	
				2			00°-->000°		50		140	280
				3			90°-->000°		10		40	90
			MG_CIK	1	00°-->270°	0.19	0.42	30	0.21	125	0.18	370
				2	00°-->000°			15		40		100
				3	-80°-->230°			4		15		20
			LG_CIK	1	00°-->270°	0.10	0.26	55	0.24	100	0.40	160
				2	00°-->000°			45		80		130
				3	-80°-->230°			40		70		100
	AG		1	00°-->310°	0.35	0.20	50	0.13	214	0.32	360	
				2			00°-->220°		50		120	215
				3			90°-->000°		45		72	80
	MO		1	00°-->320°	0.28	0.39	36	0.15	140	0.18	234	
				2			00°-->230°		25		130	155
				3			90°-->000°		25		35	50

Table 14.66 Variogram models for Cu%

Cuerpo	Field/ Domain	Sub-domain	Direction		Nugget	Structure 1		Structure 2		Structure 3	
					C ₀	C ₁	R ₁	C ₁	R ₁	C ₁	R ₁
Cuerpo 1	IND	-	1	49°-->129°	0.24	0.38	48	0.14	77	0.24	205
			2	-26°-->186°			45		77		140
			3	-30°-->080°			45		60		70
	CU%/ HG	HG_CIK	1	-62°-->097°	0.29	0.24	11	0.19	32	0.28	70
			2	19°-->147°			11		32		70
			3	-20°-->230°			11		32		70
		LG_CIK	1	-62°-->097°	0.29	0.24	11	0.19	32	0.28	70
			2	19°-->147°			11		32		70
			3	-20°-->230°			11		32		70
	CU%/ LG	-	1	00°-->240°	0.19	0.11	60	0.27	150	0.43	250
			2	-30°-->330°			40		100		220
			3	-60°-->150°			40		70		80
	CU%/ WASTE	-	1	00°-->300°	0.20	0.80	200	-	-	-	-
			2	00°-->210°			100		-		-
			3	90°-->000°			100		-		-
Cuerpo 2	IND	-	1	-34°-->123°	0.33	0.21	60	0.17	145	0.29	220
			2	54°-->144°			60		110		160
			3	-10°-->220°			60		110		160
	CU%/ HG	HG_CIK	1	49°-->351°	0.36	0.43	28	0.14	74	0.07	100
			2	-26°-->294°			28		60		91
			3	30°-->220°			21		44		75
		LG_CIK	1	49°-->351°	0.36	0.43	28	0.14	74	0.07	100
			2	-26°-->294°			28		60		91
			3	30°-->220°			21		44		75
	CU%/ LG	-	1	-50°-->310°	0.25	0.28	35	0.17	109	0.31	226
			2	40°-->310°			35		72		141
			3	00°-->040°			23		57		81
	CU%/ WASTE	-	1	24°-->333°	0.12	0.24	64	0.38	232	0.26	450
			2	-29°-->258°			64		173		375
			3	50°-->210°			64		173		320
Cuerpo 3	IND/ HG	-	1	50°-->210°	0.2	0.15	80	0.29	205	0.36	245
			2	00°-->300°			55		150		205
			3	-40°-->210°			55		115		165
	INGH/ HG	-	1	50°-->300°	0.36	0.16	50	0.27	110	0.21	200
			2	00°-->030°			50		59		165
			3	-40°-->300°			30		55		125
CU%/ HG	HG_CIK	1	90°-->000°	0.33	0.17	5	0.33	25	0.17	70	
		2	00°-->130°			5		25		70	

Cuerpo	Field/ Domain	Sub-domain	Direction		Nugget	Structure 1		Structure 2		Structure 3		
					C ₀	C ₁	R ₁	C ₁	R ₁	C ₁	R ₁	
			3	90°-->040°			5		25		50	
		MG_CIK	1	90°-->000°	0.36	0.24	5	0.09	15	0.31	100	
			2	00°-->270°			5		15		100	
			3	-80°-->180°			5		15		60	
		LG_CIK	1	90°-->000°	0.20	0.33	7	0.22	15	0.26	80	
			2	00°-->180°			7		15		80	
			3	00°-->090°			7		15		60	
	IND/ LG	-	1	00°-->000°	0.20	0.80	200	-	-	-	-	
				2			00°-->270°		200		-	-
				3			90°-->000°		200		-	-
	CU%/ LG	HG_CIK	1	-70°-->030°	0.24	0.38	33	0.19	120	0.19	256	
				2			00°-->120°		33		120	256
				3			-20°-->210°		33		120	220
			LG_CIK	1	-70°-->030°	0.24	0.38	33	0.19	120	0.19	256
				2	00°-->120°			33		120		256
				3	-20°-->210°			33		120		220
	CU%/ WASTE	-	1	00°-->315°	0.07	0.30	40	0.27	195	0.36	460	
				2			00°-->225°		30		87	255
				3			90°-->000°		21		75	255

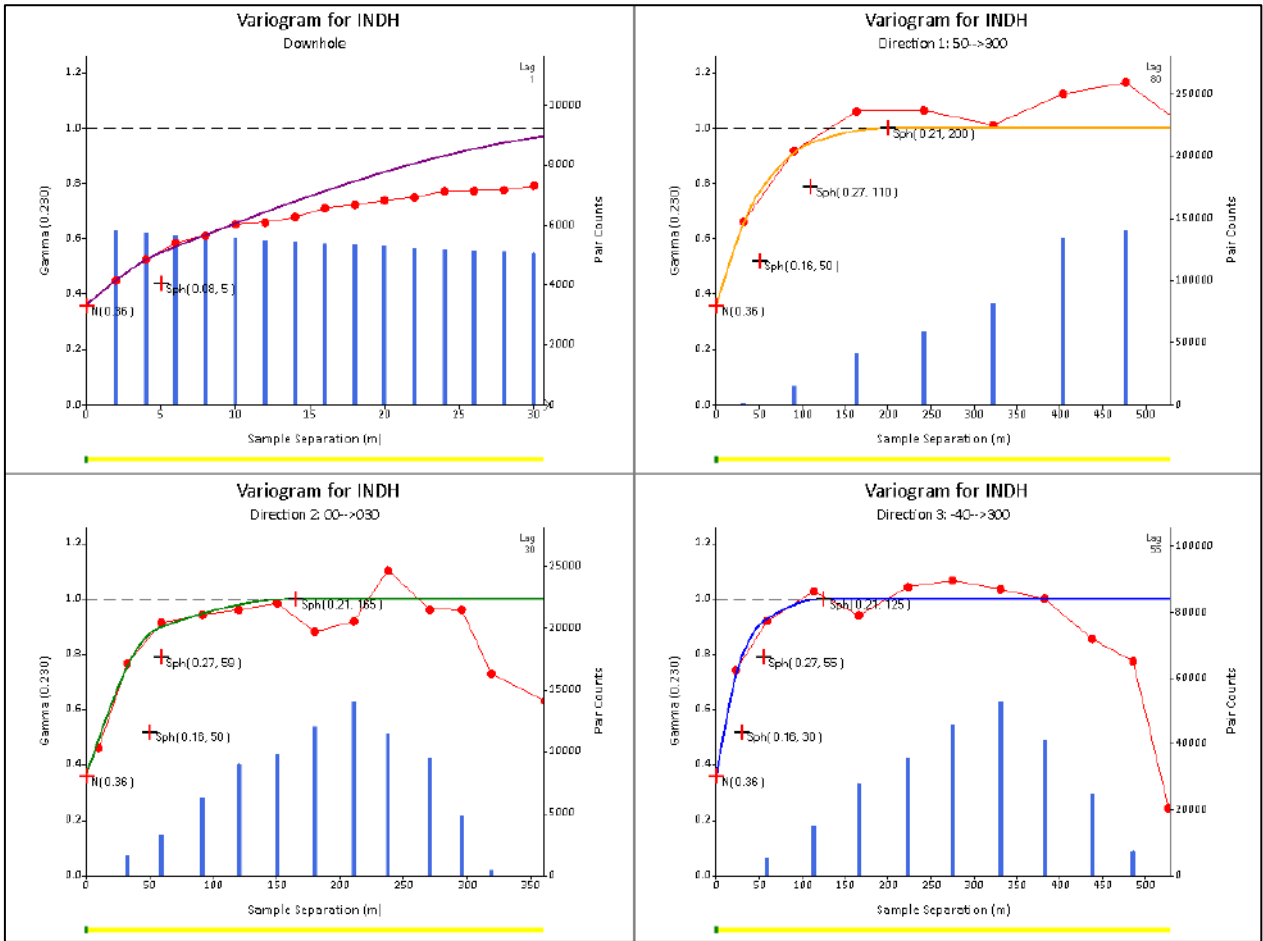


Figure 14.50 Variogram for IND field – Cuerpo 3

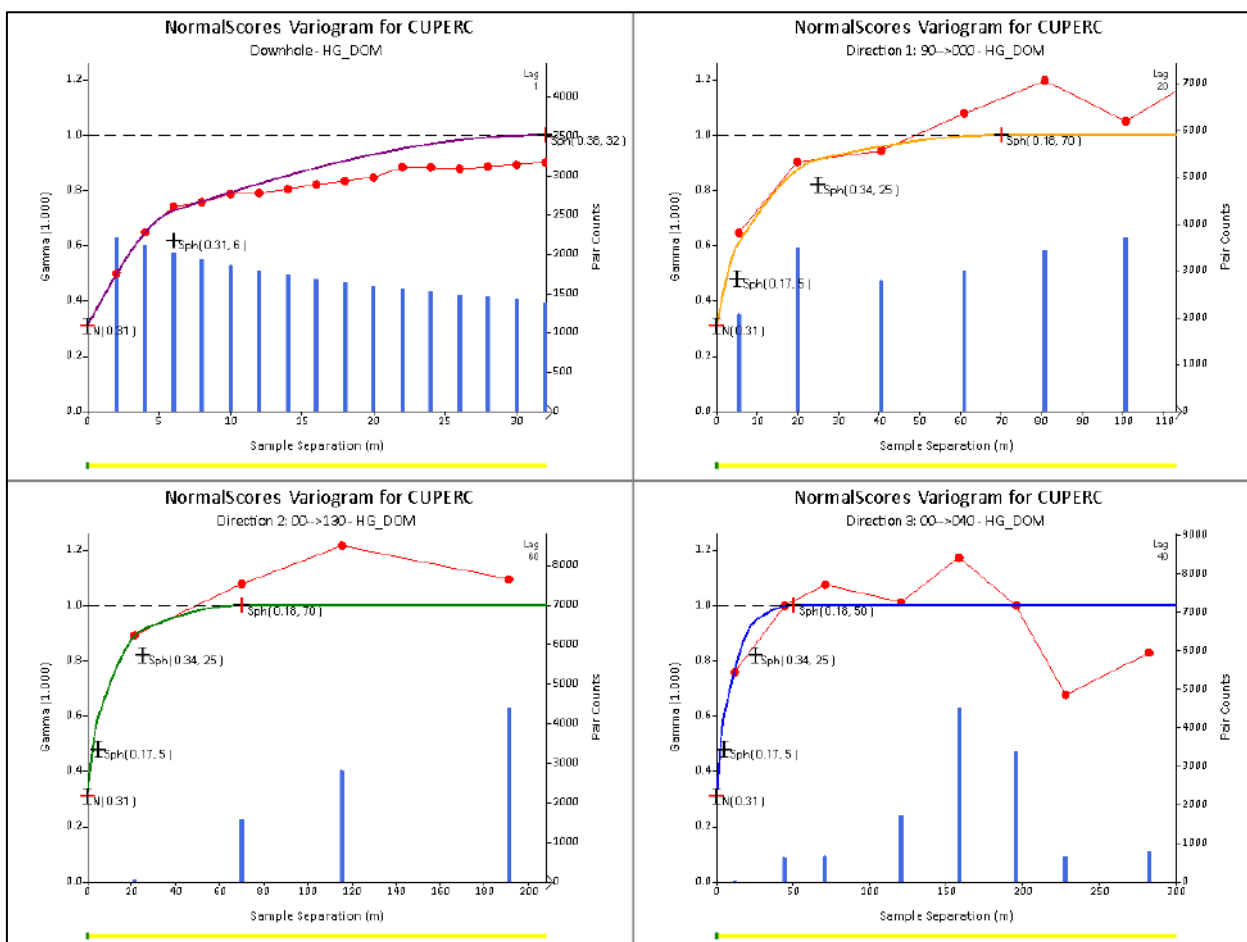


Figure 14.51 Normal Scores Variogram for Cu% HG_CIK domain – Cuerpo 3

Table 14.67 Variogram models for Ag

Cuerpo	Field/ Domain	Direction		Nugget	Structure 1		Structure 2		Structure 3	
				C ₀	C ₁	R ₁	C ₁	R ₁	C ₁	R ₁
Cuerpo 1	AG/ HG,HG_EXP, MG,MG_EXP	1	-90°-->000°	0.32	0.34	20	0.23	90	0.11	130
		2	00°-->065°			20		90		130
		3	00°-->155°			20		30		120
Cuerpo 2	AG/ HG,HG_EXP, MG,MG_EXP	1	-90°-->000°	0.36	0.27	40	0.16	140	0.21	280
		2	00°-->320°			25		100		160
		3	00°-->050°			20		30		50
Cuerpo 3	AG/ MG,MG_EXP	1	-90°-->000°	0.26	0.39	30	0.13	110	0.22	260
		2	00°-->320°			20		50		120
		3	00°-->050°			20		40		100
	AG/ LG,WASTE	1	-90°-->000°	0.36	0.43	50	0.10	130	0.11	390
		2	00°-->320°			50		130		200
		3	00°-->050°			20		30		90

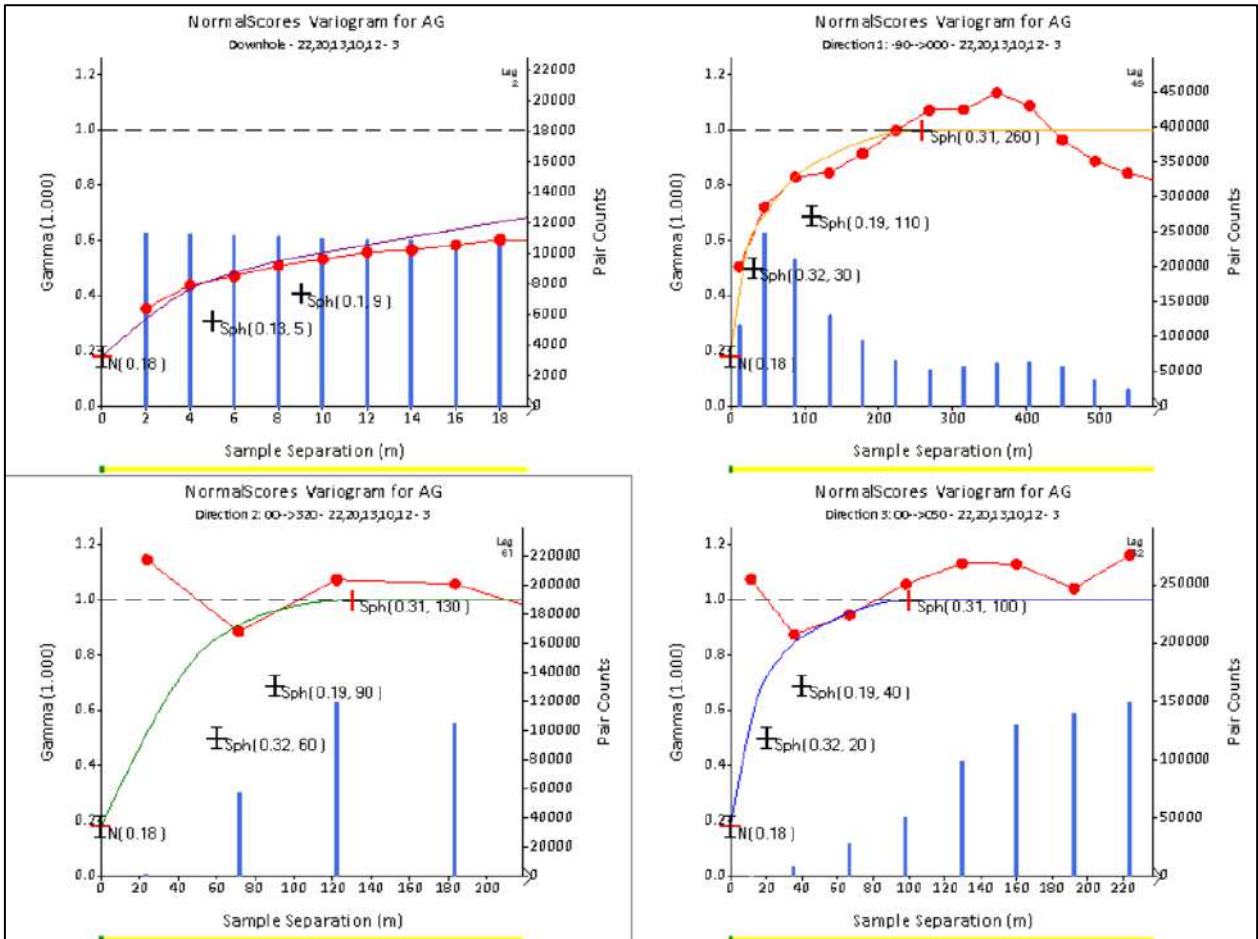


Figure 14.52 Normal Scores Variogram for AG – Cuerpo 3

Table 14.68 Variogram models for MO

Cuerpo	Field/ Domain	Direction		Nugget	Structure 1		Structure 2		Structure 3	
				C ₀	C ₁	R ₁	C ₁	R ₁	C ₁	R ₁
Cuerpo 1	MO/ HG, MG	1	-90-->000	0.32	0.25	10	0.22	15	0.21	35
		2	00-->305			10		15		35
		3	00-->035			10		15		35
	MO/ LG	1	-90-->000	0.37	0.36	80	0.15	250	0.13	290
		2	00-->305			90		150		250
		3	00-->035			40		130		140
	MO/ WASTE	1	00-->340	0.18	0.33	30	0.23	70	0.26	300
		2	00-->070			70		180		300
		3	-90-->000			70		100		140
Cuerpo 2	MO/ HG, MG	1	-90-->000	0.52	0.28	20	0.05	30	0.16	130
		2	00-->320			20		50		100
		3	00-->050			20		50		100
	MO/ LG	1	-90-->000	0.28	0.30	80	0.22	250	0.21	290
		2	00-->320			90		150		250
		3	00-->050			40		130		140
	MO/ WASTE	1	-90-->000	0.19	0.33	30	0.23	70	0.26	300
		2	00-->320			70		180		300
		3	00-->050			70		100		140
Cuerpo 3	MO/ HG, MG	1	00-->295	0.44	0.23	20	0.13	90	0.21	140
		2	00-->025			20		90		110
		3	-90-->000			20		70		80
	MO/ LG	1	-90-->000	0.18	0.44	55	0.19	290	0.20	820
		2	00-->320			90		480		560
		3	00-->050			80		220		320
	MO/ WASTE	1	-90-->000	0.13	0.19	40	0.36	470	0.32	570
		2	00-->320			40		470		570
		3	00-->050			40		160		570

14.2.13 Block Modelling

Two different parent block sizes have been used for the grade estimates to account for different data densities present in separate areas of the deposit.

- 20mE by 20mN by 20mRL
- 10mE by 10mN by 10mRL

Sub-blocking to a minimum of 2m was completed to honour the volume and geometry of the wireframes.

Kriging neighbourhood analysis ensures the suitability of parent block sizes selected.

Indicator estimates (on Cu%, Au and the iron oxide horizons) have used a parent block of 5mE x 5mN x 5mRL to ensure sufficient granularity in the estimate. Sub-celling is down to 1m in all directions.

Block model parameters are shown in Table 14.69. The block model was flagged by the wireframes as shown in Table 14.70 and Table 14.71. Final model fields are listed in Table 14.72.

Table 14.69 Block model dimensions

Dimension	Minimum	Maximum	Extent	Size	Number	Sub-cell
Easting (mE)	334100	337100	3000	10	300	2
Northing (mN)	6812700	6814780	2080	10	208	2
Elevation (mRL)	-400	1280	1680	10	168	2

Dimension	Minimum	Maximum	Extent	Size	Number	Sub-cell
Easting (mE)	334100	337100	3000	20	150	2
Northing (mN)	6812700	6814780	2080	20	104	2
Elevation (mRL)	-400	1280	1680	20	84	2

Table 14.70 Cortadera volume model coding

Field	Description	Code
CUERPO	Cuerpo	1 = Cuerpo 1
		2 = Cuerpo 2
		3 = Cuerpo 3
LTCODE	Geology	1 = Sediments
		2 = Volcanics
		5 = Hornfels Proximal
		6 = Hornfels Distal
		10 = Early Mineralised Porphyry
		20 = Intramineral Porphyry
		30 = Late Mineral Felsic Dyke
		31 = Late Mineral Felsic Dyke Eye
		32 = Late Mineral Felsic Dyke stockwork
WTCODE	Oxidation state	1 = Oxide
		2 = Transitional
		3 = Fresh
TOPO	Topographic Surface	10000 = above topographic surface
RESCAT	Classification	1 = Measured
		2 = Indicated
		3 = Inferred
		4 = Unclassified

Table 14.71 Cortadera Mineralisation model coding

Field	Description	Code
CUEQAREA	Extent of Mineralisation	1 = Inside mineralised extent
DOM_AG1	Silver Mineralisation Domains	10000 = HG Domain 20000 = MG Domain
DOM_AU1	Gold Mineralisation Domains	100 = HG Domain 200 = MG Domain
DOM_CU1	Copper Mineralisation Domains	10 = HG Domain 20 = MG Domain 30 = LG Domain
DOM_MO1	Molybdenum Mineralisation Domains	1000 = HG Domain 2000 = MG Domain
DOM_LI1	Limonite Mineralisation Domains	10000 = Limonite Domain

Table 14.72 Cortadera Final Block Model Coding

Field	Description
IJK	Unique Block Identifier
XC	X coordinate for block centroid
YC	Y coordinate for block centroid
ZC	Z coordinate for block centroid
XINC	Block size in X direction
YINC	Block size in Y direction
ZINC	Block size in Z direction
XMORIG	X coordinate origin for block model
YMORIG	Y coordinate origin for block model
ZMORIG	Z coordinate origin for block model
NX	Number of blocks in X direction
NY	Number of blocks in Y direction
NZ	Number of blocks in Z direction
RESCAT	Numeric code for resource classification
WTCODE	Numeric code for weathering domain
DENSITY	Assigned density
AG	Estimated Ag g/t
MO	Estimated Mo ppm
AU	Estimated Au g/t
CU%	Estimated Cu %
CUEQ%_RES	Calculated CuEq %

14.2.14 Grade Estimation

14.2.14.1 Overview

Extensive estimation test work has been completed for the Cortadera mineral resource, the primary goal of which was to ascertain which estimation technique best reflected the understanding of the mineralisation at Cortadera.

14.2.14.2 Copper (Cu%) estimate

Initial work for Cu% estimation focussed on constraint via constructed domains that each constituted a single grade population suitable for estimation (high-grade (HG), medium-grade (MG) and low-grade (LG) sub-domains for Cuerpo 3 and MG sub-domains and LG sub-domains for Cuerpo 1 and 2).

Additional work was completed to create extended domain wireframes which considered other geological factors. This included the presence of a calcium-rich alteration front is considered to exert a significant geological control on mineralisation and appears to correlate well with zones of higher A- and B-type quartz vein abundances and copper grades that extend outward from the mineralised porphyry intrusions (as described in 14.2.5)

Statistical analysis completed on these domains suggest step-changes in grade, supporting the use of these domain boundaries (Figure 14.53).

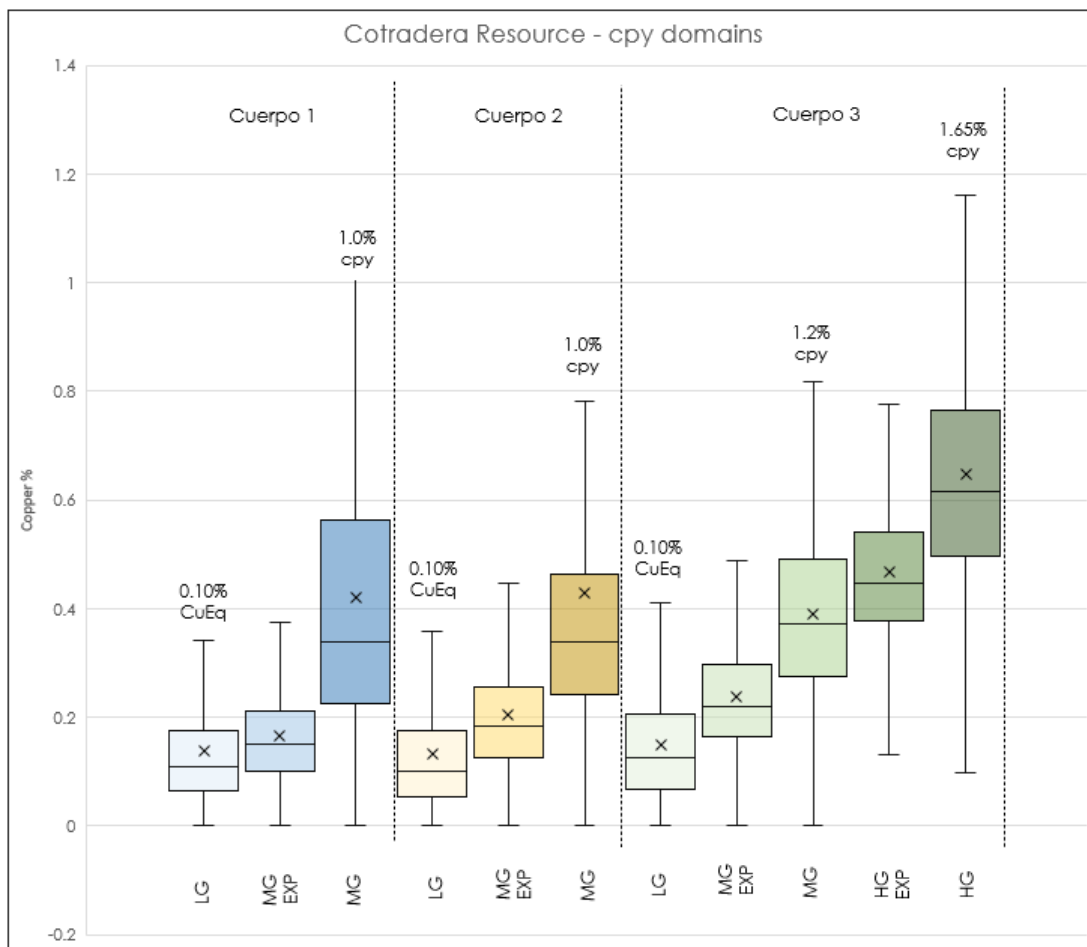


Figure 14.53 Box-whisker plots showing Cu% grade distributions for each initial estimation domain

Many different estimation iterations have been tested in an attempt to produce an estimate that reconciles with the geological understanding of the system. Despite multiple methods tested to relax the boundary conditions between domains, it was not possible to produce an estimate that reflected the gradational decrease in grade outward from the core of the porphyry system. The subsequent estimations either over- or under-called the estimated blocks when compared to drillhole assays.

Conversely, running an estimate with soft boundaries across the grade sub-domains resulted in an overly smoothed model which did not adequately represent the high-grades or low-grades in the data set.

The response to this was to use a categorical indicator kriged (CIK) estimate for selected domains. Indicator kriging is used to estimate the probability of a variable to exceeding a threshold value at a single point. Sub-domains are then defined through selection of the probability threshold. CIK requires a considerable volume of data to be used with confidence, and the doubling of drilling at Cortadera since the maiden MRE in 2020 enabled this technique to be applied.

Constraint was still applied, using the extended domain wireframes as described above to constitute the HG domain. These volumes were considered appropriate for estimation as they comprised low-variance grade populations, while also accounting for the other geological considerations (as described above).

The 0.1% CuEq interpolant defines the LG domain, and a waste estimate has been completed out to the extents of the model.

Grade cut-offs were selected for the probability model by analysing the log-probability plots for each domain and ascertaining breaks in the distribution. Two cut-offs have been used in Cuerpo 3, as three distinct grade populations exist. One cut-off has been used for Cuerpo 1 and Cuerpo 2. An example of a log-probability plot is shown in Figure 14.54. Grade cut-offs used to define the CIK model are listed in Table 14.73 below.

Note that a conventional ordinary kriging approach has been used for the Cuerpo 1 and Cuerpo 2 LG and WASTE domains, and the Cuerpo 3 WASTE domain.

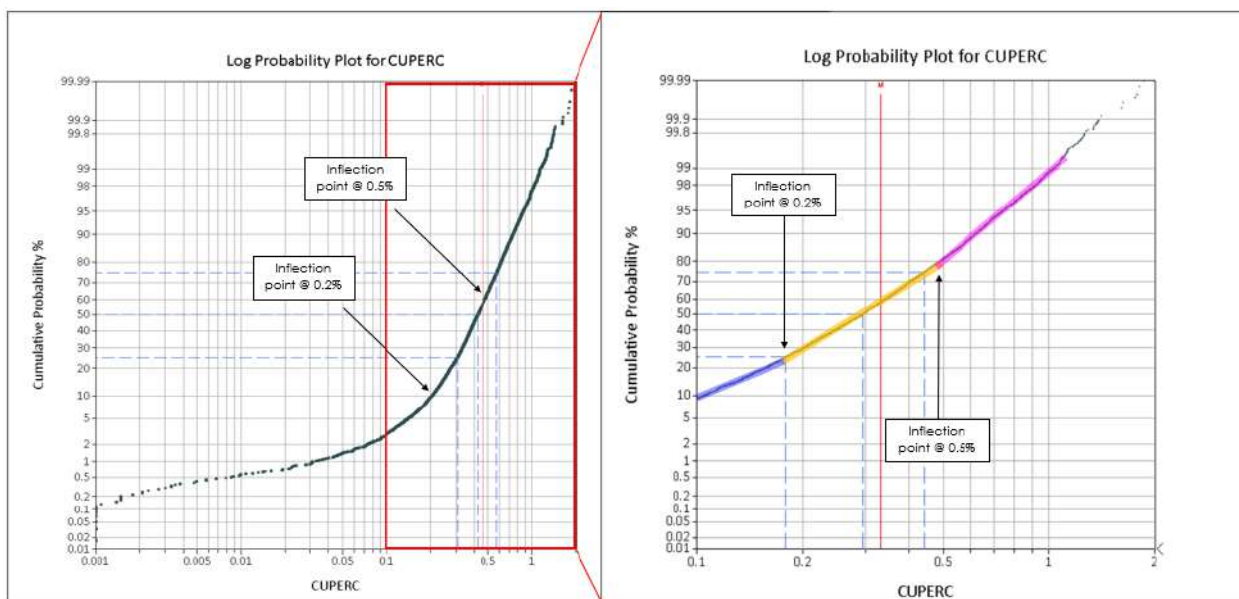


Figure 14.54 Log-probability plot for Cuerpo 3 Cu%, showing interpreted 'breaks' in the grade population to be used as cut-offs for the binary indicator coding.

Table 14.73 Cu% estimate cut-off grades used for probability estimate

Cuerpo	Domain (Estimate Type)	Cut-off Grade(s)
Cuerpo 1	HG (2 bin CIK)	0.10%
	LG (OK)	-
	WASTE (OK)	-
Cuerpo 2	HG (2 bin CIK)	0.17%
	LG (OK)	-
	WASTE (OK)	-
Cuerpo 3	HG (3 bin CIK)	0.20%/0.50%
	LG (2 bin CIK)	0.10%
	WASTE (OK)	-

Variography and kriging neighbourhood analysis (KNA) is completed on the binary coded fields (IND and INDH) to define the kriging neighbourhoods. Variograms are tabulated in 14.2.12.

Figure 14.55 below shows the output estimate completed using the binary BIND and BINDH values for the HG domain at Cuerpo 3, with the originally interpreted grade interpolants overlain for reference.

Output estimates are carefully reviewed to determine the appropriate threshold for CIK sub-domaining. Multiple iterations are completed at different probability thresholds to ensure misallocation of samples across domains is limited (for instance a LG sample (BIND=0) being included in the HG CIK sub-domain).

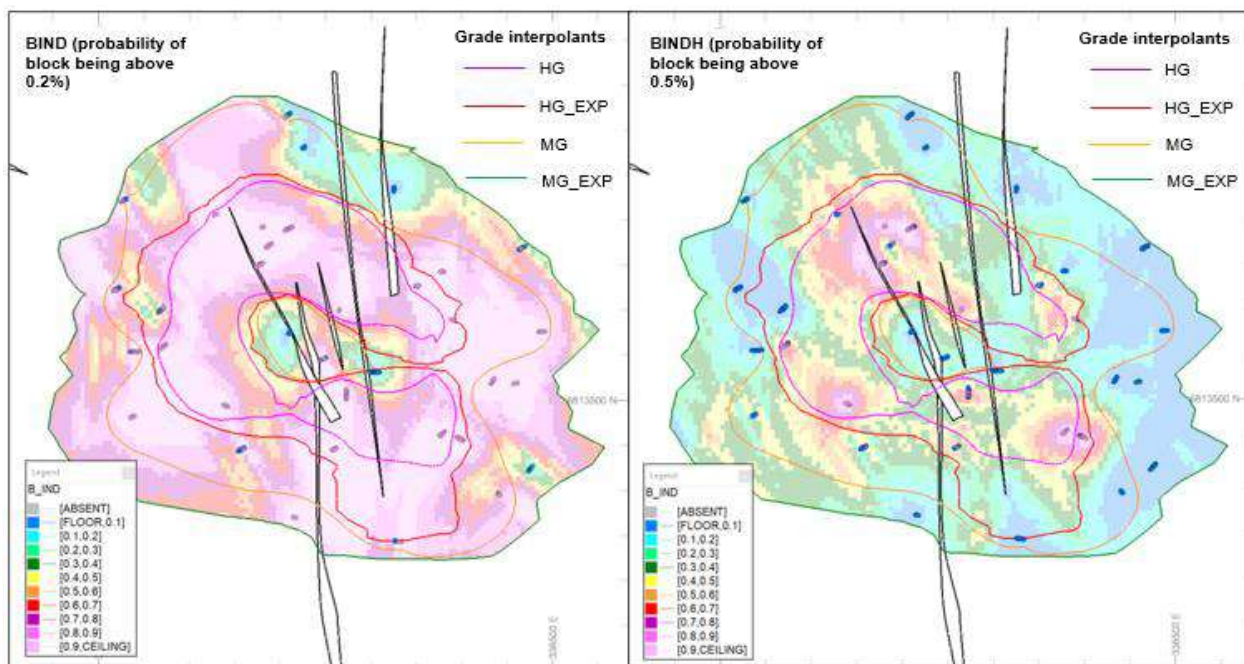


Figure 14.55 Indicator estimate on binary fields BIND and BINDH showing the probability of a block being above 0.2% (left) and 0.5% (right). Plan view section at 500 mRL.

Two different probability threshold iterations are shown below in Figure 14.56.

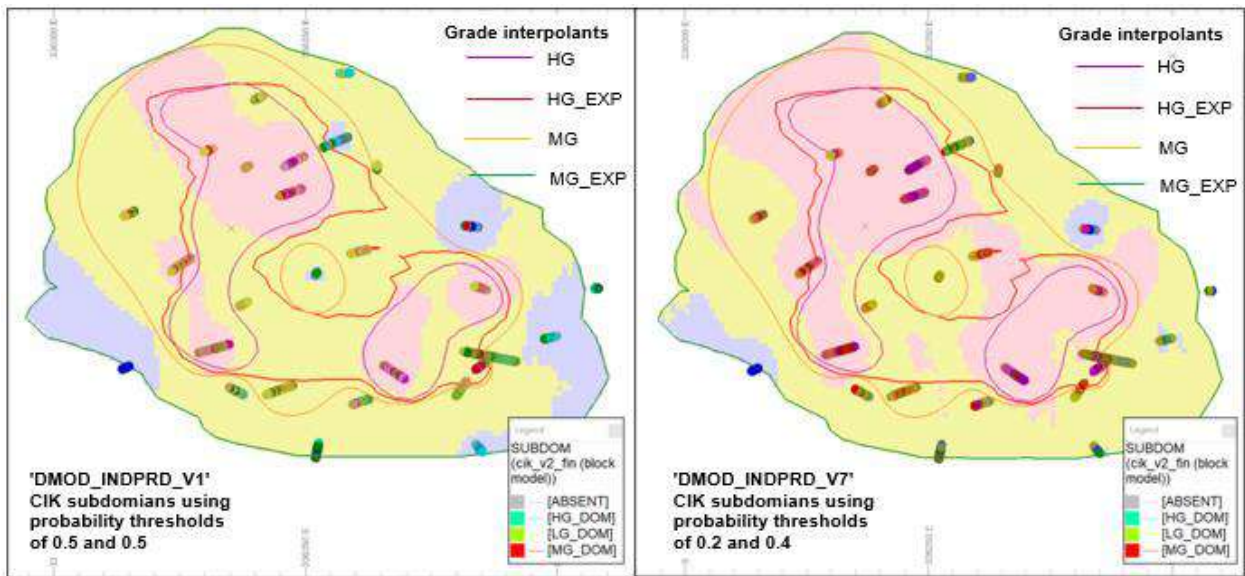


Figure 14.56 Iterative CIK sub-domain selection, showing two different probability threshold selections (from v1 (left) and v7 (right) estimates). Plan view section at 300 mRL.

Final probability thresholds selected for the CU% CIK estimates are shown in Table 14.74 and an example of the distribution of the binary coded composites within each of the resultant CIK sub-domains is shown in Figure 14.57, along with a log-probability plot showing the different grade distributions within each sub-domain. Ideally, the misallocation of composites between sub-domains (i.e., samples below the grade-cut off used to inform a higher-grade domain and vice versa) is kept below 10%.

Table 14.74 Cu% probability threshold selection

Cuerpo	Domain	Probability Threshold selected
Cuerpo 1	HG (2 bin CIK)	0.4
Cuerpo 2	HG (2 bin CIK)	0.4
Cuerpo 3	HG (3 bin CIK)	0.2/0.4
	LG (2 bin CIK)	0.5

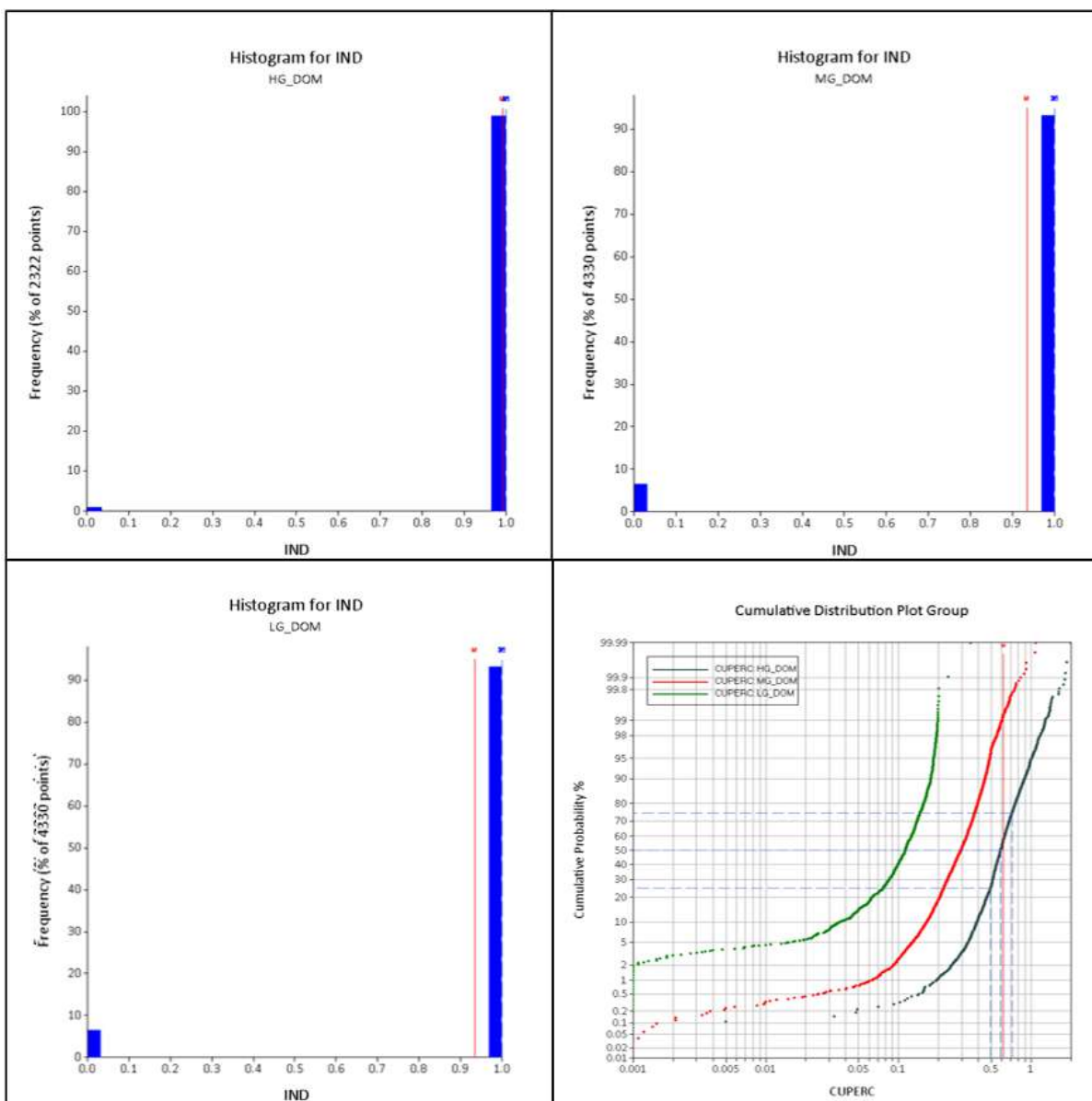


Figure 14.57 Distribution of binary coded samples within each of the CIK sub-domains and log-probability plot showing grade distributions within each sub-domain.

Following the selection of the probability thresholds, top-cuts were reviewed for each estimation data set and applied if appropriate. Due to the application of a coherent geological interpretation,

and sub-domaining via the CIK approach, no top-cuts were necessary for the Cu% estimates in any sub-domain. Coefficient of variance (CoV) for each sub-domain was less than 1.0, and there is low risk of outliers influencing the estimate due to the sub-domaining approach used providing strict constraint.

Variography has been attempted independently for each CIK sub-domain. In some cases, it was not possible to construct coherent variograms for a sub-domain due to low sample pair counts. In these cases, the variogram for an adjacent sub-domain was used (for instance, a HG_CIK sub-domain may share the variogram from the MG_CIK sub-domain).

Care has been taken to ensure reasonable correlation between sub-domains (orientations, nugget effect and variogram ranges). For instance, it would not be considered reasonable for this style of deposit to have variogram orientations for adjacent sub-domains at right angles to one another.

One-way soft boundaries have been used between CIK sub-domains (from HG_CIK to MG_CIK and MG_CIK to LG_CIK in cases where three bin CIK is used and HG_CIK to LG_CIK in cases where two bin CIK is used).

This approach is based on the observation that the mineralised system comprises a high-grade 'core' with gradational copper grade decreasing outwards to the edge of the porphyry intrusion and into wall rock. Rigorous test work has shown that the CIK approach with one-way soft boundaries is the optimal way to estimate the observed grade trends. This is also supported geostatistically by boundary analysis completed between the CIK sub-domains (Figure 14.58).

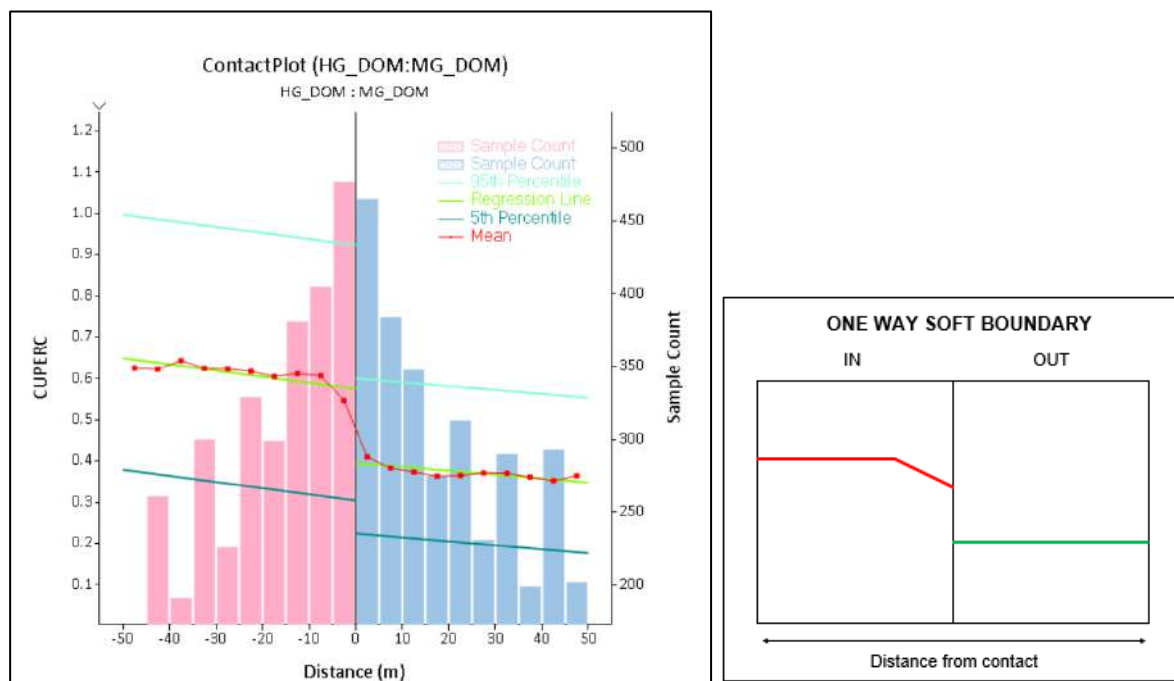


Figure 14.58 Boundary analysis (completed using Snowden Supervisor) comparing HG and MG Cu% CIK sub-domains for Cuerdo 3 justifying the use of a one-way soft boundary. Schematic shown to the right shows the typical trend displayed by one-way soft boundaries.

One-way soft boundaries are controlled using the Datamine MAXKEY approach. Correct application of the soft boundary is checked for all sub-domains using the SAMPOUT file created

during the estimation process, with outputs the samples used to estimate each block, as well as the kriging weight applied.

Table 14.75 details the soft boundaries used for each estimate, including minimum and maximum sample counts for the estimate.

Table 14.75 Soft boundary usage for Cu% estimates

Cuerpo	Domain	Sub-domain	MAXKEY FIELD	MAXKEY value	Minimum sample count	Maximum sample count
Cuerpo 1	HG	HG_CIK	BHID	7	10	20
		LG_CIK	LGDOMSFT	7	10	20
	LG	-	HGDOMSFT	5	10	20
	WASTE	-	LGDOMSFT	7	10	20
Cuerpo 2	HG	HG_CIK	BHID	7	10	20
		LG_CIK	LGDOMSFT	7	10	20
	LG	-	HGDOMSFT	5	10	20
	WASTE	-	LGDOMSFT	5	8	18
Cuerpo 3	HG	HG_CIK	BHID	5	6	12
		MG_CIK	MGDOMSFT	5	10	20
		LG_CIK	LGDOMSFT	5	10	20
	LG	HG_CIK	HGDOMSFT	4	6	12
		LG_CIK	LGDOMSFT	4	10	20
	WASTE	-	LGDOMSFT	4	10	20

Kriging neighbourhood analysis has been completed for each domain (or sub-domain in the case of the CIK estimates) and used as a guide for the selection of sample counts, search distances, discretisation points and block size.

Table 14.76 outlines the search parameters used for all Cu% estimates. Search orientations were defined by the variogram, and three search passes were used to ensure all blocks were estimated. For all estimates, the third pass had the minimum sample count set to 1. This is considered when applying the resource classification, with all blocks estimated on pass 3 set to unclassified.

Estimation was into parent blocks and no octant search has been used.

Table 14.76 Cu% search parameters

Cuerpo	Domain	Sub-domain	Minimum/ Maximum sample count	Search pass volume factors (Pass2/ Pass3)	Major/Semi- Major/Minor search rotations (Dir1/Dir2/Dir3)	Major/Semi- Major/Minor search distances (Dir1/Dir2/Dir3)
Cuerpo 1	HG	HG_CIK	10/20	1.5/10	-130/110/-110	70/70/70
		LG_CIK	10/20	1.5/10	-130/110/-110	70/70/70
	LG	-	10/20	1.5/10	050/150/150	165/145/50
	WASTE	-	10/20	1.5/10	0/0/-150	200/100/100
Cuerpo 2	HG	HG_CIK	10/20	1.5/10	-140/060/060	70/60/50
		LG_CIK	10/20	1.5/10	-140/060/060	70/60/50
	LG	-	10/20	1.5/10	-140/040/050	150/100/50
	WASTE	-	8/18	1.5/10	-150/040/040	300/250/210
Cuerpo 3	HG	HG_CIK	6/12	1.5/10	090/090/090	150/150/150
		MG_CIK	10/20	1.5/10	090/090/090	150/150/150
		LG_CIK	10/20	1.5/10	090/090/090	150/150/150
	LG	HG_CIK	10/20	1.5/10	090/090/090	150/150/150
		LG_CIK	10/20	1.5/10	090/090/090	150/150/150
	WASTE	-	10/20	1.5/10	050/090/050	300/170/170

Test iterations (variably comparing estimation methodology, block size, boundary conditions, and probability thresholds (for CIK)), were compared against one another, with the estimate best reflecting the input data and the geological understanding of the mineralised system selected.

Detail on model validation is included in section 14.2.16.

14.2.14.3 Gold (Au) estimate

Given the strong statistical correlation between Au and Cu ($R \approx 0.7$) (Figure 14.59), Cu% CIK sub-domains and boundary conditions have been used for the gold estimate for both the Cuerpo 3 HG and LG domain, and the Cuerpo 2 HG domain.

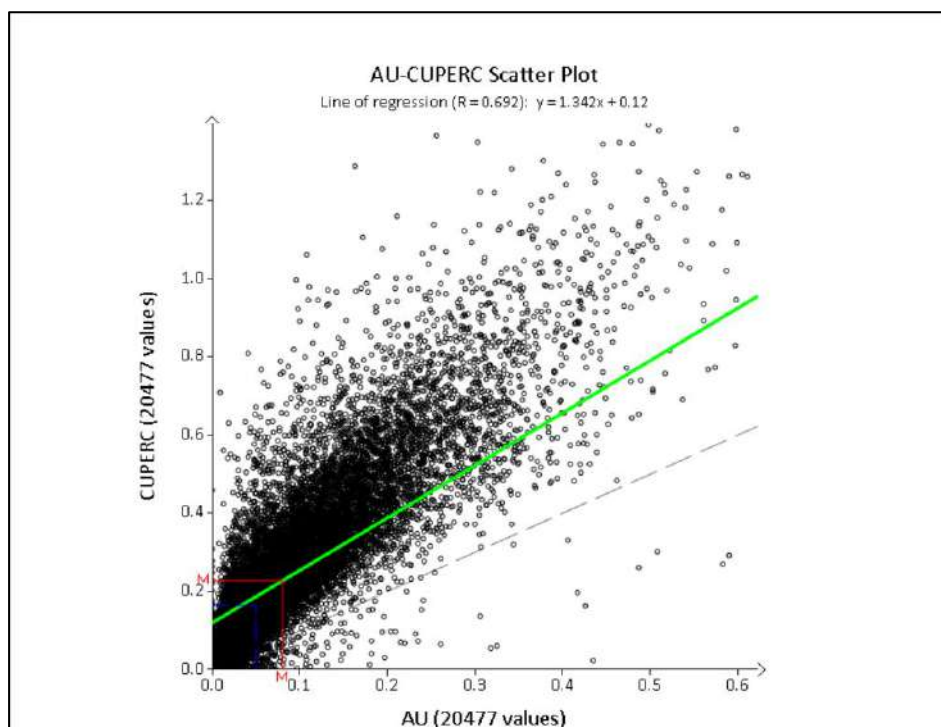


Figure 14.59 Scatter plot between Cu% (y-axis) and AU (x-axis) showing strong correlation between two elements.

All other domains are estimated independently for gold, using Ordinary Kriging as described in Table 14.77.

Table 14.77 Au estimation methodologies used by domain

Cuerpo	Domain (Estimate Type)
Cuerpo 1	HG (OK)
	LG (OK)
	WASTE (OK)
Cuerpo 2	HG (2 bin CIK using CU% sub-domains)
	LG (OK)
	WASTE (OK)
Cuerpo 3	HG (3 bin CIK using CU% sub-domains)
	LG (2 bin CIK using CU% sub-domains)
	WASTE (OK)

Following the selection of data within the various domains and sub-domains, top-cuts were reviewed and applied if appropriate. Due to the application of a coherent geological interpretation, and sub-domaining via the CIK approach, no top-cuts were necessary for the Au estimates in any sub-domain. Coefficient of variance (CoV) for each sub-domain was less than 1.0, and there is low risk of outliers influencing the estimate due to the sub-domaining approach used providing strict constraint (Figure 14.60).

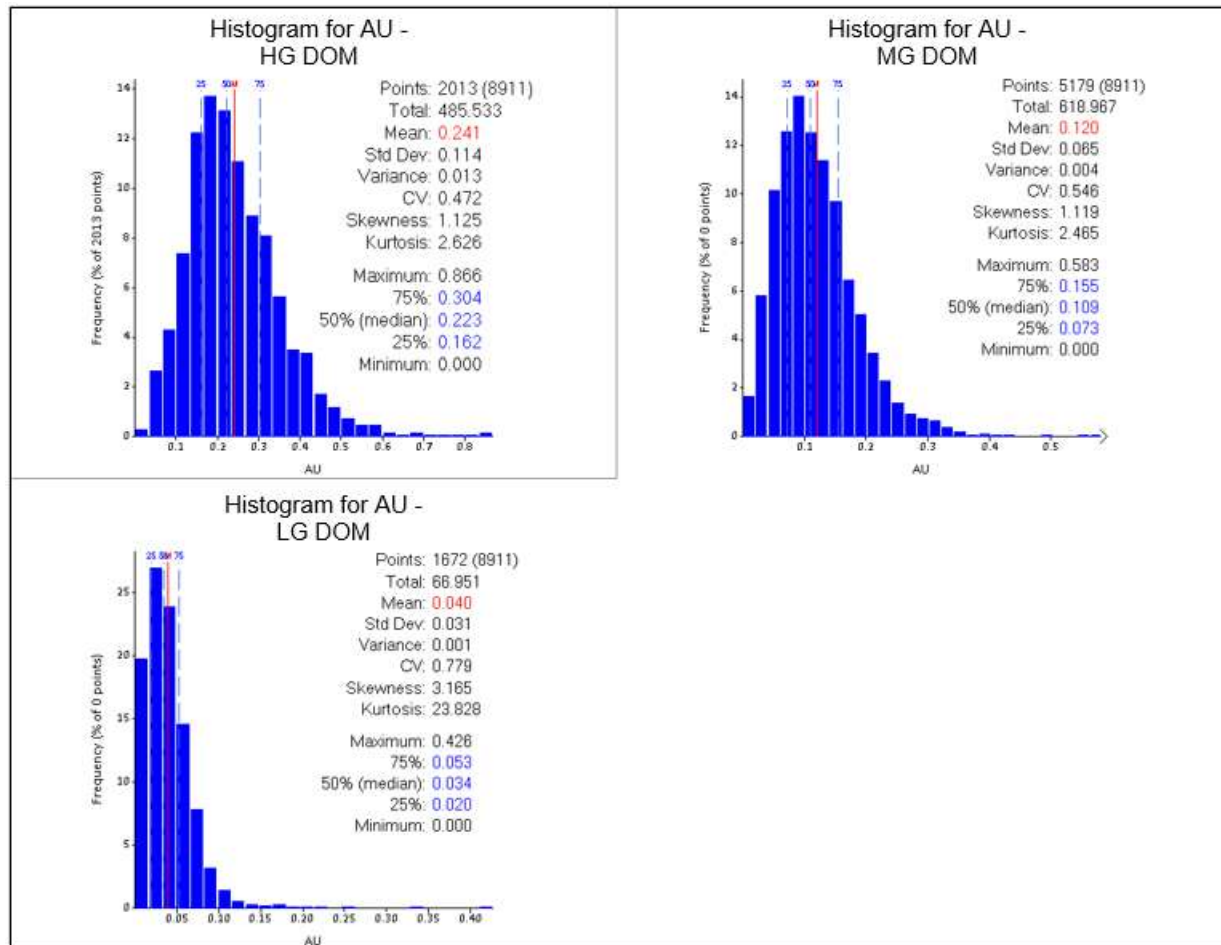


Figure 14.60 Composites selected in CIK sub-domains for Cuerpo 3 HG Au estimate

For domains which use the Cu% CIK sub-domains, Cu% variography and kriging neighbourhoods have also been used. All other domains had variography completed independently although, as with the Cu% domains, in some cases, it was not possible to construct coherent variograms due to low sample pair counts.

One-way soft boundaries have been used between CIK sub-domains (from HG_CIK to MG_CIK and MG_CIK to LG_CIK in cases where three bin CIK is used and HG_CIK to LG_CIK in cases where two bin CIK is used). Rationale for this approach is the same as used for the Cu% estimate (14.2.14.2) and justified by geological understanding of the mineralised system and boundary analysis completed between CIK sub-domains (Figure 14.61).

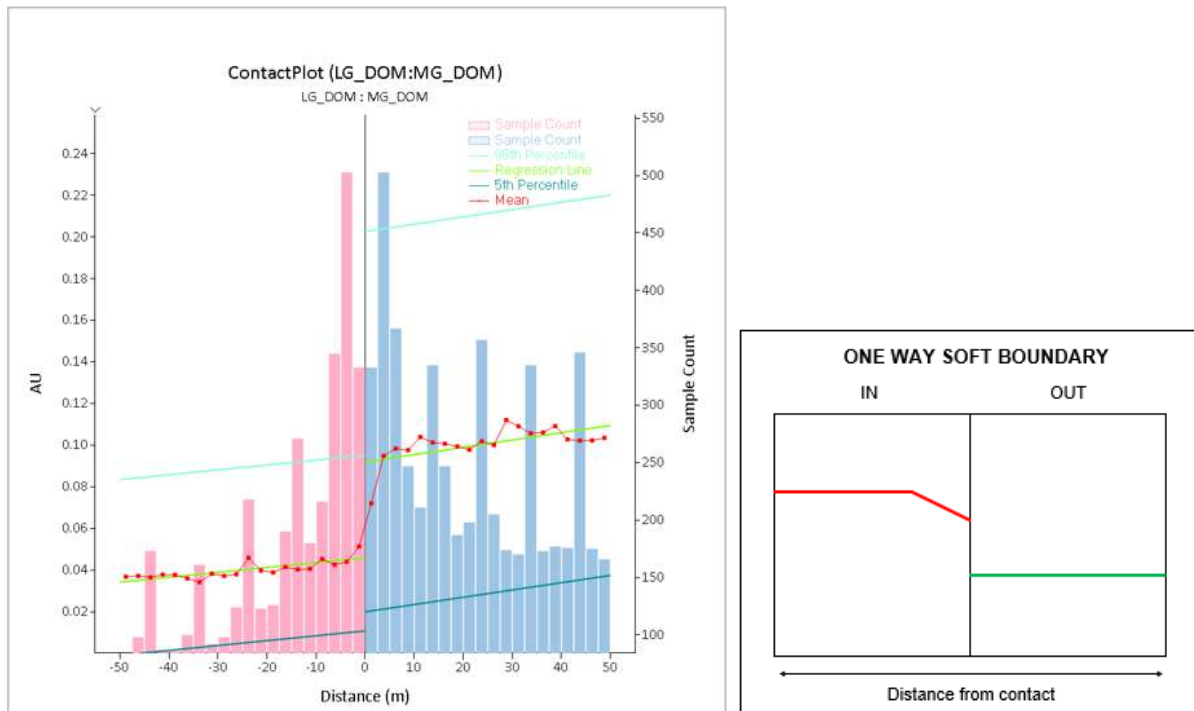


Figure 14.61 Boundary analysis (completed using Snowden Supervisor) comparing MG and LG CIK Au sub-domains for Cuerpo 3 justifying the use of a one-way soft boundary. Schematic shown to the right shows the typical trend displayed by one-way soft boundaries (HCH, 2022).

The one-way soft boundaries are controlled using the Datamine MAXKEY approach. Correct application of the soft boundary is checked for all sub-domains using the SAMPOUT file created during the estimation process, with outputs the samples used to estimate each block, as well as the kriging weight applied.

Table 14.78 details the soft boundaries used for each estimate, including minimum and maximum sample counts.

Table 14.78 Soft boundary usage for Au estimates

Cuerpo	Domain	Sub-domain	MAXKEY FIELD	MAXKEY value	Minimum sample count	Maximum sample count
Cuerpo 1	HG	-	BHID	5	10	20
	LG	-	HGDOMSFT	5	10	20
	WASTE	-	LGDOMSFT	5	10	20
Cuerpo 2	HG	HG_CIK	BHID	7	10	20
		LG_CIK	LGDOMSFT	7	10	20
	LG	-	HGDOMSFT	5	10	20
	WASTE	-	LGDOMSFT	4	8	18
Cuerpo 3	HG	HG_CIK	BHID	5	6	12
		MG_CIK	MGDOMSFT	5	10	20
		LG_CIK	LGDOMSFT	5	10	20
	LG	HG_CIK	HGDOMSFT	4	6	12
		LG_CIK	LGDOMSFT	4	10	20
	WASTE	-	LGDOMSFT	4	10	20

Kriging neighbourhood analysis has been completed for each domain (or sub-domain in the case of the CIK estimates) and used as a guide for the selection of sample counts, search distances, discretisation points and block size.

Table 14.79 outlines the search parameters used for all Au estimates. Search orientations were defined by the variogram, and three search passes were used to ensure all blocks were estimated. For all estimates, the third pass had the minimum sample count set to 1. This is considered when applying the resource classification, with all blocks estimated on pass 3 set to unclassified.

Estimation was into parent blocks and no octant search has been used.

Table 14.79 Au search parameters

Cuerpo	Domain	Sub-domain	Minimum/ Maximum sample count	Search pass volume factors (Pass2/ Pass3)	Major/Semi- Major/Minor search rotations (Dir1/Dir2/Dir3)	Major/Semi- Major/Minor search distances (Dir1/Dir2/Dir3)
Cuerpo 1	HG	-	10/20	1.5/10	-140/090/000	80/40/25
	LG	-	10/20	1.5/10	040/150/180	125/125/110
	WASTE	-	10/20	1.5/10	040/130/180	230/150/130
Cuerpo 2	HG	HG_CIK	10/20	1.5/10	-140/060/060	70/60/50
		LG_CIK	10/20	1.5/10	-140/060/060	70/60/50
	LG	-	10/20	1.5/10	170/100/000	100/60/60
	WASTE	-	8/18	1.5/10	-130/090/000	200/100/100
Cuerpo 3	HG	HG_CIK	6/12	1.5/10	090/090/090	150/150/150
		MG_CIK	10/20	1.5/10	090/090/090	150/150/150
		LG_CIK	10/20	1.5/10	090/090/090	150/150/150
	LG	HG_CIK	10/20	1.5/10	090/090/090	150/150/150
		LG_CIK	10/20	1.5/10	090/090/090	150/150/150
	WASTE	-	12/24	1.5/10	050/130/180	200/10/100

Output iterations were compared against one another, with the estimate which best reflected the input data and the geological understanding of the mineralised system chosen.

Further detail around model validation is included in section 14.2.16.

14.2.14.4 Silver (Ag) estimate

Ag estimates were completed using a conventional ordinary kriging (OK) approach into grade domains as defined in Table 14.63. As with the Cu% and Au estimates, additional domains have been created based on the presence of a calcium-rich alteration front, as described in 14.2.14.2.

The Cuerpo 2 and Cuerpo 3 HG_EXP (an additional domain based on the HG Ag interpolant) has been split into two, with an additional lithological constraint applied. A higher-grade population is hosted within the early mineralisation porphyry (10-series) lithological domain, with this domain given the code HG_EXP1. Samples that sit within the HG_EXP domain but are not 10-series hosted are given the code HG_EXP2.

Two LG domains have been used, one informed by the volume inside the 0.05% Cu interpolant, and one informed by the volume inside the 0.1% CuEq interpolant.

The WASTE domain covers all blocks out to the model extents.

Estimated Ag domains are listed in Table 14.77. These are estimated independently by Cuerpo.

Table 14.80 Ag estimation methodologies used by domain

Cuerpo	Domain (Estimate Type)
Cuerpo 1	MG (OK)
	MG_EXP (OK)
	LG1 (OK)
	LG2 (OK)
	WASTE (OK)
Cuerpo 2	HG (OK)
	HG_EXP1 (OK)
	HG_EXP2 (OK)
	MG (OK)
	MG_EXP (OK)
	LG1 (OK)
	LG2 (OK)
WASTE (OK)	
Cuerpo 3	HG (OK)
	HG_EXP1 (OK)
	HG_EXP2 (OK)
	MG (OK)
	MG_EXP (OK)
	LG1 (OK)
	LG2 (OK)
WASTE (OK)	

Table 14.81 details the soft boundaries used for each estimate, including minimum and maximum sample counts.

Table 14.81 Soft boundary usage for Ag estimates

Cuerpo	Domain	One-way Soft Boundary Domain(s)	MAXKEY FIELD	MAXKEY value	Minimum sample count	Maximum sample count
Cuerpo 1	MG	-	BHID	7	10	16
	MG_EXP	MG	SOFT22	7	10	16
	LG1	MG_EXP	SOFT30	7	10	16
	LG2	MG_EXP	SOFT30	7	10	16
	WASTE	-	BHID	7	10	16
Cuerpo 2	HG	-	BHID	7	10	16
	HG_EXP1	HG	BHID	7	10	16
	HG_EXP2	-	BHID	7	10	16
	MG	HG_EXP1, HG_EXP2	SOFT22	7	10	16
	MG_EXP	MG	SOFT30	7	10	16
	LG1	-	BHID	7	10	16
	LG2	-	BHID	7	10	16

	WASTE	-	BHID	7	10	16
Cuerpo 3	HG	-	BHID	7	10	16
	HG_EXP1	-	BHID	7	10	16
	HG_EXP2	-	BHID	7	10	16
	MG	HG_EXP1, HG_EXP2	SOFT22	7	10	16
	MG_EXP	MG	SOFT30	7	10	16
	LG1	-	BHID	7	10	16
	LG2	-	BHID	7	10	16
	WASTE	-	BHID	7	10	16

Kriging neighbourhood analysis has been completed for each domain and used as a guide for the selection of sample counts, search distances, discretization points and block size.

Table 14.82 outlines the search parameters used for all Ag estimates. Search orientations were defined by the variogram.

Only two search passes were run for the Ag estimates, with all blocks successfully filled on either the first or second pass.

Estimation was into parent blocks and no octant search has been used.

Table 14.82 Ag search parameters

Cuerpo	Domain	Minimum/ Maximum sample count	Search pass volume factors (Pass2)	Major/Semi- Major/Minor search rotations (Dir1/Dir2/Dir3)	Major/Semi- Major/Minor search distances (Dir1/Dir2/Dir3)
Cuerpo 1	MG	10/16	3	155/090/-090	150/150/100
	MG_EXP	10/16	3	155/090/-090	150/150/100
	LG	10/16	3	155/090/-090	150/150/100
	WASTE	10/16	3	155/090/-090	150/150/100
Cuerpo 2	HG	10/16	3	050/090/-090	150/150/100
	HG_EXP1	10/16	3	050/090/-090	150/150/100
	HG_EXP2	10/16	3	050/090/-090	150/150/100
	MG	10/16	3	050/090/-090	150/150/100
	MG_EXP	10/16	3	050/090/-090	150/150/100
	LG	10/16	3	050/090/-090	150/150/100
	WASTE	10/16	3	050/090/-090	150/150/100
Cuerpo 3	HG	10/16	3	050/090/-090	150/150/100
	MG_EXP	10/16	3	050/090/-090	150/150/100
	HG_EXP1	10/16	3	050/090/-090	150/150/100
	HG_EXP2	10/16	3	050/090/-090	150/150/100
	MG	10/16	3	050/090/-090	150/150/100
	MG_EXP	10/16	3	050/090/-090	150/150/100
	LG	10/16	3	050/090/-090	150/150/100

Output models are compared to the input data, with the estimate validated to ensure fair reflection of the mineralised system.

Figure 14.62 shows a type-section of the Ag estimate for each Cuerpo. Further detail around model validation is included in section 14.2.16.

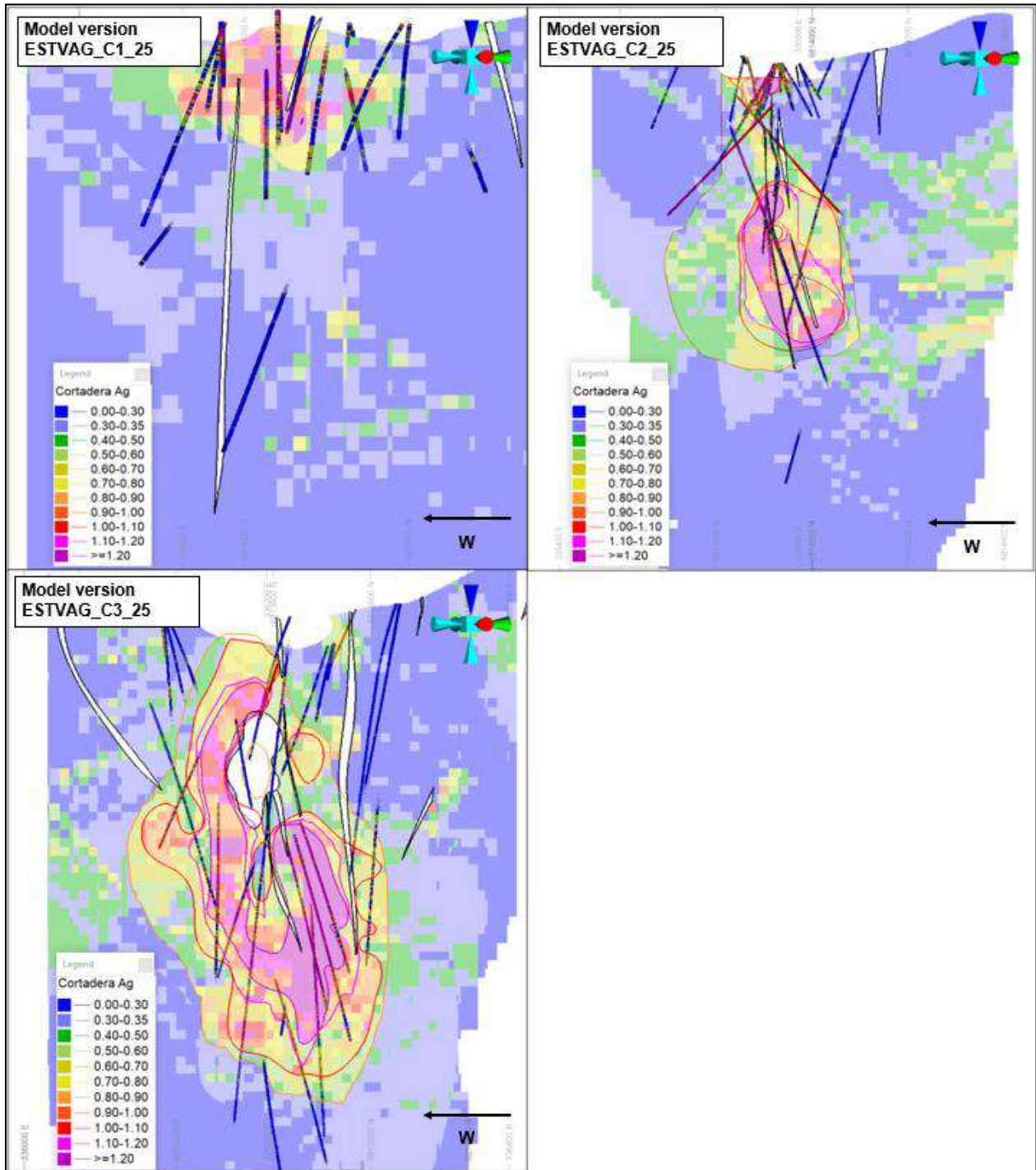


Figure 14.62 Various cross-section views showing Ag estimates for each Cuerpo. (Cuerpo 1 – top left, Cuerpo 2 – top right, Cuerpo 3 – bottom left)

14.2.14.5 Molybdenum (Mo) estimate

Mo estimates were completed using a conventional ordinary kriging (OK) approach into grade domains as defined in Table 14.63.

Estimated Mo domains are listed in Table 14.83. These are estimated independently by Cuerpo. As with the Ag estimate, two LG domains have been used, one informed by the volume inside the 0.05% Cu interpolant, and one informed by the volume inside the 0.1% CuEq interpolant. The WASTE domain covers all additional blocks out to the model extents.

Table 14.83 Mo estimation methodologies used by domain

Cuerpo	Domain (Estimate Type)
Cuerpo 1	HG (OK)
	MG (OK)
	LG1 (OK)
	LG2 (OK)
	WASTE (OK)
Cuerpo 2	HG (OK)
	MG (OK)
	LG1 (OK)
	LG2 (OK)
	WASTE (OK)
Cuerpo 3	HG (OK)
	MG (OK)
	LG1 (OK)
	LG2 (OK)
	WASTE (OK)

Soft domains were used between LG and WASTE domains, as defined in Table 14.84.

Table 14.84 Soft boundary usage for Mo estimates

Cuerpo	Domain	One-way Soft Boundary Domain(s)	MAXKEY FIELD	MAXKEY value	Minimum sample count	Maximum sample count
Cuerpo 1	HG	-	BHID	7	10	16
	MG	-	BHID	7	10	16
	LG1	LG2, WASTE	MAXKEY3A	7	10	16
	LG2	LG1, WASTE	MAXKEY5A	7	10	16
	WASTE	LG1, LG2	MAXKEY9A	7	10	16
Cuerpo 2	HG	-	BHID	7	10	16
	MG	-	BHID	7	10	16
	LG1	LG2, WASTE	MAXKEY3A	7	10	16
	LG2	LG1, WASTE	MAXKEY5A	7	10	16
	WASTE	LG1, LG2	MAXKEY9A	7	10	16
Cuerpo 3	HG	-	BHID	7	10	16
	MG	-	BHID	7	10	16
	LG1	LG2, WASTE	MAXKEY3A	7	10	16
	LG2	LG1, WASTE	MAXKEY5A	7	10	16
	WASTE	LG1, LG2	MAXKEY9A	7	10	16

Kriging neighbourhood analysis has been completed for each domain and used as a guide for the selection of sample counts, search distances, discretization points and block size.

Table 14.85 outlines the search parameters used for all Mo estimates. Search orientations were defined by the variogram.

Only two search passes were run for the Mo estimates, with all blocks successfully filled on either the first or second pass.

Estimation was into parent blocks and no octant search has been used.

Table 14.85 Mo search parameters

Cuerpo	Domain	Minimum/ Maximum sample count	Search pass volume factors (Pass2)	Major/Semi- Major/Minor search rotations (Dir1/Dir2/Dir3)	Major/Semi- Major/Minor search distances (Dir1/Dir2/Dir3)
Cuerpo 1	HG	10/16	3	035/090/-090	150/150/150
	MG	10/16	3	035/090/-090	150/150/150
	LG1	10/16	3	035/090/-090	150/150/150
	LG2	10/16	3	050/090/-090	150/150/150
	WASTE	10/16	3	050/090/-090	150/150/150
Cuerpo 2	HG	10/16	3	050/090/-090	150/150/150
	MG	10/16	3	050/090/-090	150/150/150
	LG1	10/16	3	050/090/-090	150/150/150
	LG2	10/16	3	050/090/-090	150/150/150
	WASTE	10/16	3	050/090/-090	150/150/150
Cuerpo 3	HG	10/16	3	050/090/-090	150/150/150
	MG	10/16	3	050/090/-090	150/150/150
	LG1	10/16	3	050/090/-090	150/150/150
	LG2	10/16	3	050/090/-090	150/150/150
	WASTE	10/16	3	050/090/-090	150/150/150

Output models are compared to the input data, with the estimate validated to ensure fair reflection of the mineralised system.

Figure 14.63 shows a type-section of the Mo estimate for each Cuerpo. Further detail around model validation is included in section 14.2.16.

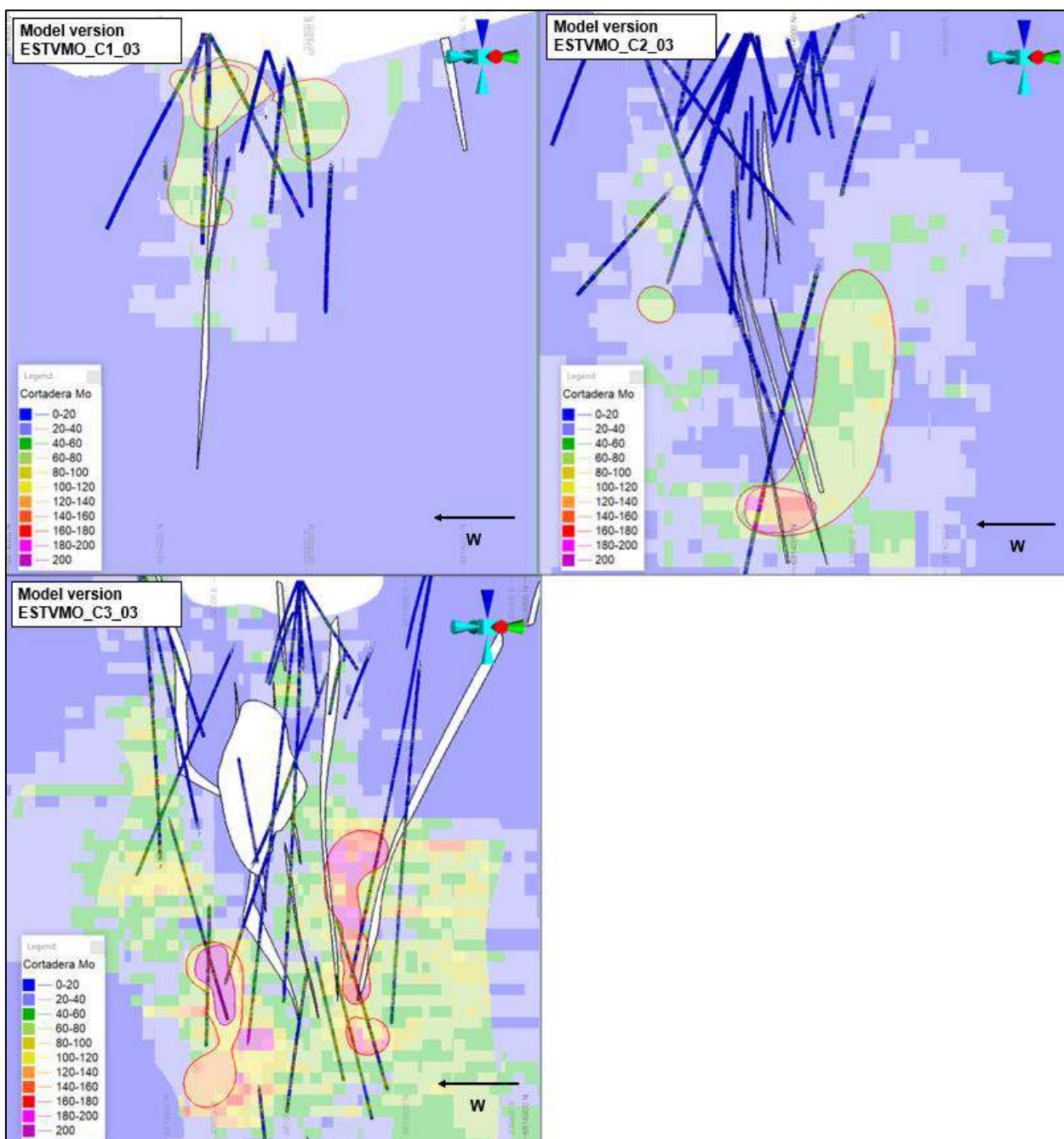


Figure 14.63 Various cross-section views showing Mo estimates for each Cuerpo. (Cuerpo 1 – top left, Cuerpo 2 – top right, Cuerpo 3 – bottom left)

14.2.14.6 Estimation inside of Iron Oxide horizons

Limonite-rich iron oxide horizons are found above each of the Cuerpos at Cortadera, into which Cu%, Au, Ag and Mo are estimated.

As the iron oxides are separated by significant distance, each one is estimated independently. A hard boundary has been used between the iron oxide horizon and the fresh-rock underneath as they comprise separate grade populations.

The interpretation comprises a geological domain (including volume where lower grades exist, to ensure geometric continuity) (Figure 14.64). As a result of this, mixed grade populations for some elements in the iron oxide horizon (Figure 14.65).

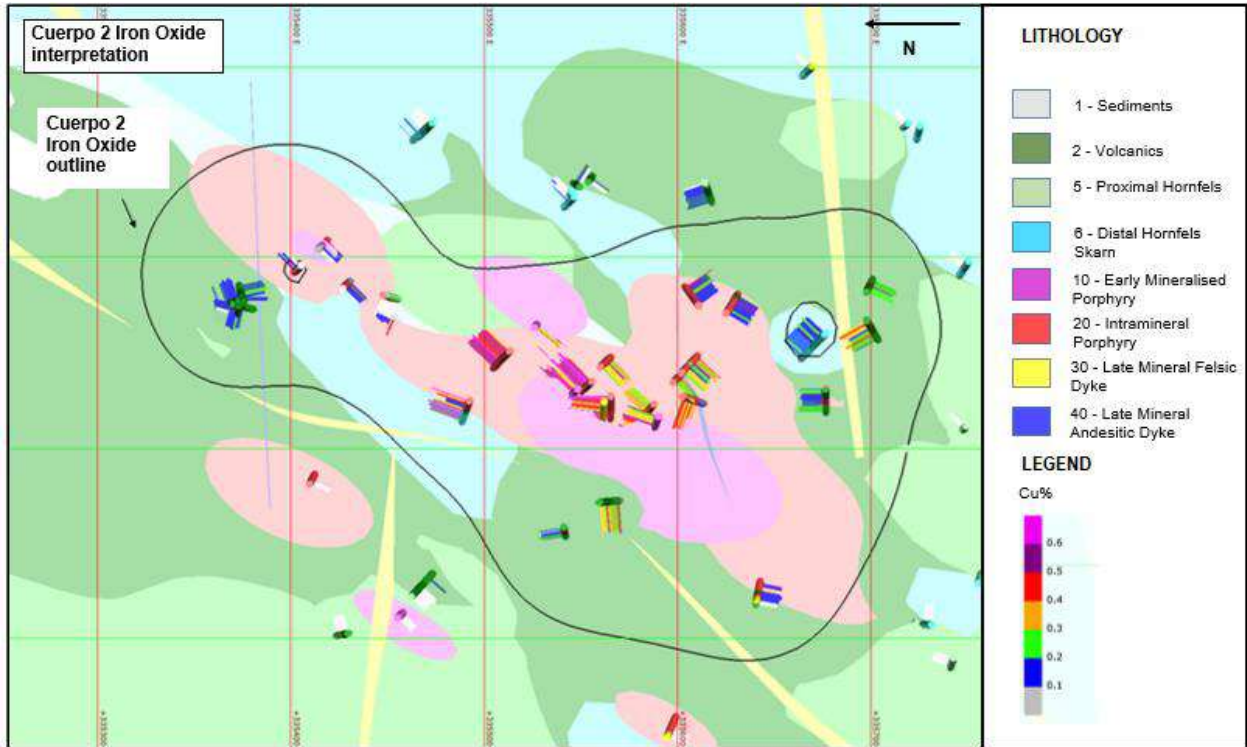


Figure 14.64 Plan view of the Cuerpo 2 iron oxide horizon interpretation, showing geology model compared to drillhole Cu% grades.

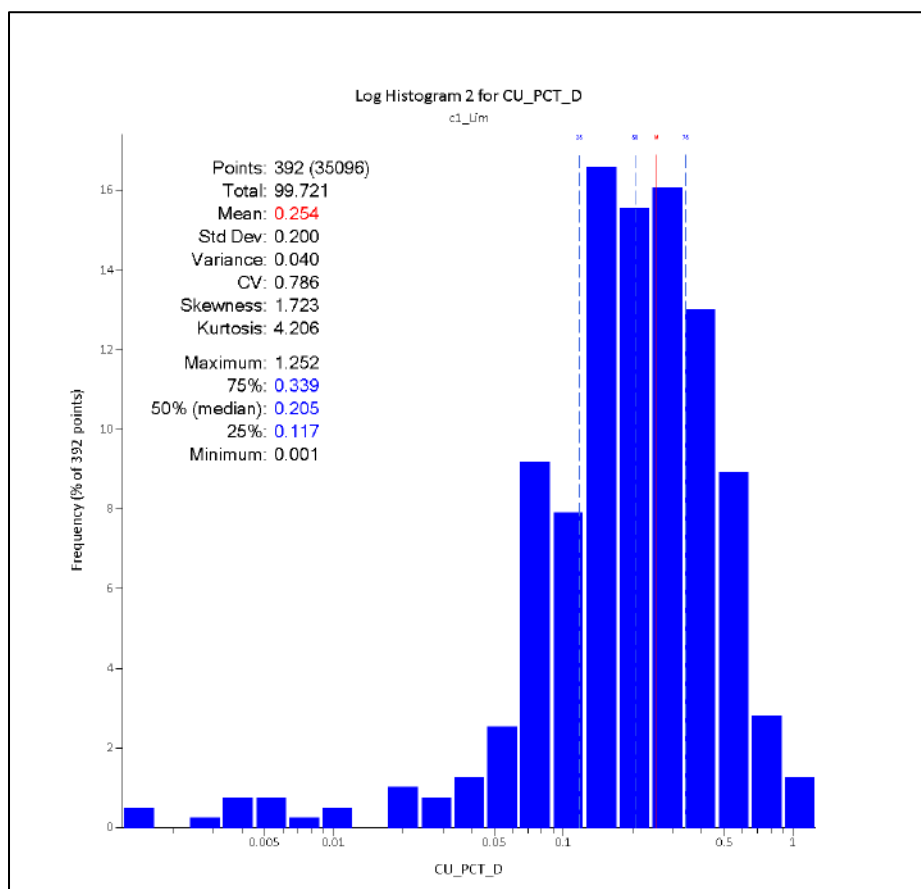


Figure 14.65 Example of mixed grade distribution in Cuerpo 1 iron oxide horizon

For elements with mixed populations, it has been determined that a conventional linear estimation methodology would not effectively preserve the distribution of the input data (with the output estimate likely 'smoothing' out the data set towards a single mean grade).

14.2.14.6.1 Cu% and Au estimates

The CIK approach (as described in section 14.2.14.2) has been used to estimate Cu% and Au within the iron oxide horizons, with both grade and logged lithology considered when applying the binary coding to the data set.

Grade cut-offs were selected for the probability model by analysing the log-probability plots and ascertaining breaks in the distribution. Two cut-offs have been used in Cuerpo 3, as three distinct grade populations exist. One cut-off has been used for Cuerpo 1 and Cuerpo 2. An example of a log-probability plot is shown in Figure 14.65.

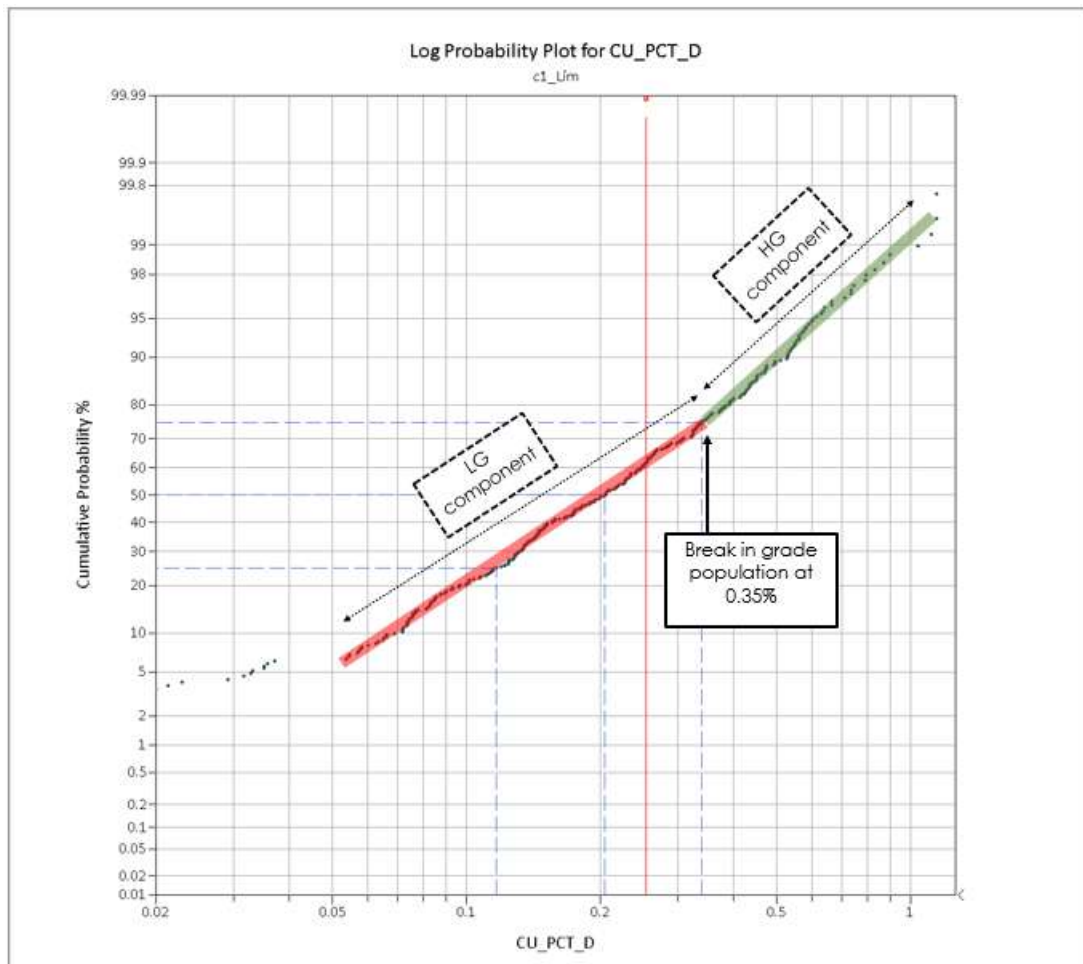


Figure 14.66 Log-probability plot for Cuerpo 2 Cu%, showing interpreted 'break' in the grade population to be used as cut-offs for the binary indicator coding.

Within the iron oxide horizons, it is observed that the highest grades are associated with the 10- and 20-series porphyry intrusions (early and intra-min porphyries) (Table 14.86). This justifies using lithology as a condition for assigning the binary coding for indicator estimation, with all samples hosted within the 10- or 20-series porphyry intrusions included in the upper bin (IND = 1).

Table 14.86 Comparison between lithology and Cu% grade for Cuerpo 2 iron oxide horizon

Cu_pct							
RockModel	WF	Number samples	Mean	Median	St Dev	CoV	Comments
Sediments	01_sediments_20220213	20	0.111	0.015	0.15	1.36	
Volcanics	02_20220213	198	0.190	0.170	0.10	0.50	
Hornfels proximal	05_20220213	12	0.081	0.059	0.06	0.72	Low number of samples
Hornfels distal	06_20220213	12	0.346	0.238	0.20	0.58	Low number of samples - high grades likely porphyry (20 series)
Early porphyry	10_20220213	65	0.370	0.385	0.18	0.49	
Intramin porphyry	20_20220213	279	0.309	0.291	0.23	0.73	

Grade cut-offs and lithology conditions used to define the CIK model are listed in Table 14.87 below.

Table 14.87 Iron Oxide estimate types and cut-off grades/conditions used

Cuerpo	Element	Estimate Type	Cut-off Grade(s)	Other Condition(s)
Cuerpo 1	CU%	2 bin CIK	0.35% CU	OR LTCODE=10
	AU	2 bin CIK	0.35% CU	OR LTCODE=10
Cuerpo 2	CU%	2 bin CIK	0.30% CU	OR LTCODE = 10 OR LTCODE = 20
	AU	2 bin CIK	0.30% CU	OR LTCODE = 10 OR LTCODE = 20
Cuerpo 3	CU%	3 bin CIK	0.02% CU / 0.09% CU	-
	AU	3 bin CIK	0.02% CU / 0.09% CU	-

Variography and kriging neighbourhood analysis (KNA) is completed on the binary coded fields (IND and INDH) to define the kriging neighbourhoods. Variograms are tabulated in 14.2.12.

Figure 14.67 below shows the output estimate completed using the binary BIND values for the iron oxide horizon at Cuerpo 1, with the modelled porphyry units overlain for reference.

Output estimates are reviewed to determine the appropriate threshold for CIK sub-domaining. Multiple iterations are completed at different probability thresholds to ensure misallocation of samples across domains (for instance a LG sample (BIND=0) being included in the HG CIK sub-domain) is limited.

Probability threshold selection and subsequent sub-domaining are shown below for the iron oxide horizon above Cuerpo 2 in Figure 14.68.

Final probability thresholds selected for the Cu% CIK estimates are shown in Table 14.88.

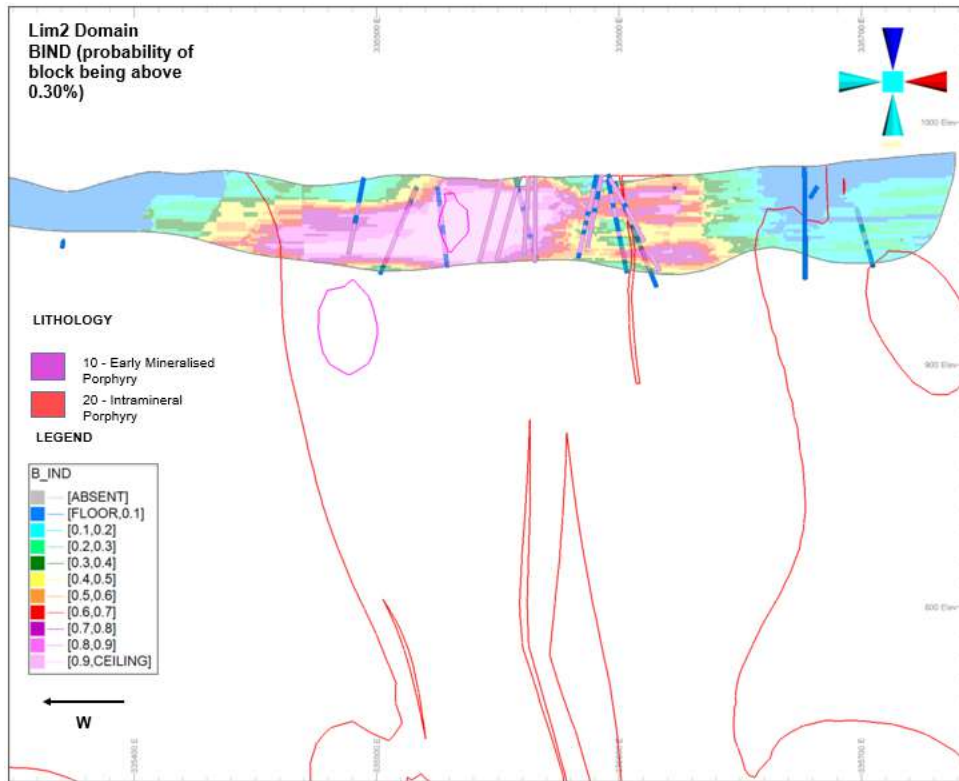


Figure 14.67 Cross-section showing indicator estimate on binary field BIND showing the probability of a block being above 0.30%. Long-section view at 6,813,935 mN.

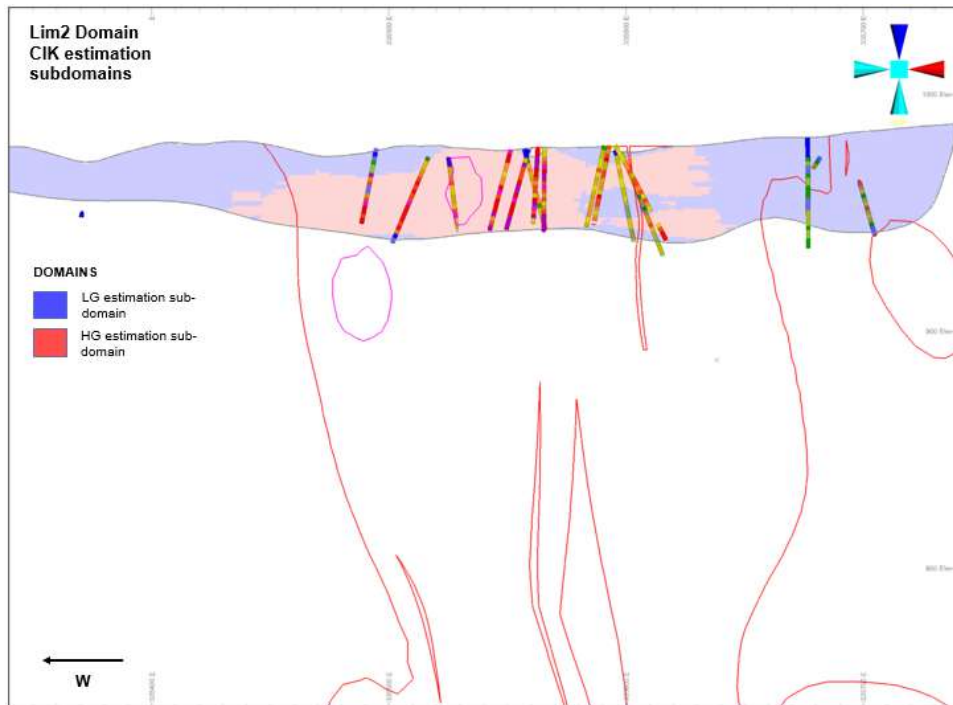


Figure 14.68 CIK sub-domain selection for iron oxide horizon above Cuerpo 2. Long-section view at 6,813,935 mN.

Table 14.88 Cu%/Au probability threshold selection

Cuerpo	Estimate Type	Probability Threshold selected
Cuerpo 1	2 bin CIK	0.5
Cuerpo 2	2 bin CIK	0.5
Cuerpo 3	3 bin CIK	0.8/0.5

Hard boundaries are used between CIK sub-domains, with no geological evidence that sample sharing would be appropriate for the iron oxide horizons.

Downhole declustering has been tested for the Cu% and Au estimates within the iron oxide horizons, using the MAXKEY function in Datamine. This is particularly important for these lodes given the flat geometry of the lodes; including too many composites from a single hole could result in grade smear in the vertical orientation. Estimate iterations with a maximum of 4 and 7 samples per BHID have been tested, with 7 samples per BHID giving the optimum result.

Kriging neighbourhood analysis has been completed for each sub-domain and used as a guide for the selection of sample counts, search distances, discretization points and block size. Table 14.89 outlines the search parameters used for all Cu% and Au estimates.

In all cases, search orientations were defined by the variogram, and three search passes were used to ensure all blocks were estimated. For all estimates, the third pass had the minimum sample count set to 1. This is considered when applying the resource classification, with all blocks estimated on pass 3 set to unclassified.

Table 14.89 Cu%/Au search parameters

Cuerpo	Element	Sub-domain	Minimum/ Maximum sample count	Search pass volume factors (Pass2/ Pass3)	Major/Semi- Major/Minor search rotations (Dir1/Dir2/Dir3)	Major/Semi- Major/Minor search distances (Dir1/Dir2/Dir3)
Cuerpo 1	AU	HG_CIK	6/16	1.5/10	000/000/020	245/160/20
		LG_CIK	6/16	1.5/10	000/000/020	245/160/20
	CU%	HG_CIK	6/16	1.5/10	000/000/-140	105/85/65
		LG_CIK	6/16	1.5/10	000/000/-140	105/85/65
Cuerpo 2	AU	HG_CIK	6/16	1.5/10	000/000/010	125/75/55
		LG_CIK	6/16	1.5/10	000/000/-150	105/60/35
	CU%	HG_CIK	6/16	1.5/10	000/000/-140	190/110/75
		LG_CIK	6/16	1.5/10	050/010/180	130/130/90
Cuerpo 3	AU	HG_CIK	6/16	1.5/10	000/000/-170	170/165/20
		MG_CIK	6/16	1.5/10	000/000/-170	170/165/20
		LG_CIK	6/16	1.5/10	000/000/60	165/65/25
	CU%	HG_CIK	6/16	1.5/10	-130/170/050	245/65/20
		MG_CIK	6/16	1.5/10	-130/170/050	245/65/20
		LG_CIK	6/16	1.5/10	000/000/000	200/185/60

Output iterations were compared, with the estimate which best reflected the input data and the geological understanding of the mineralised system chosen. Figure 14.69 and Figure 14.70 show type-sections of the Cu% and Au estimates, respectively. Further detail around model validation is included in section 14.2.16.

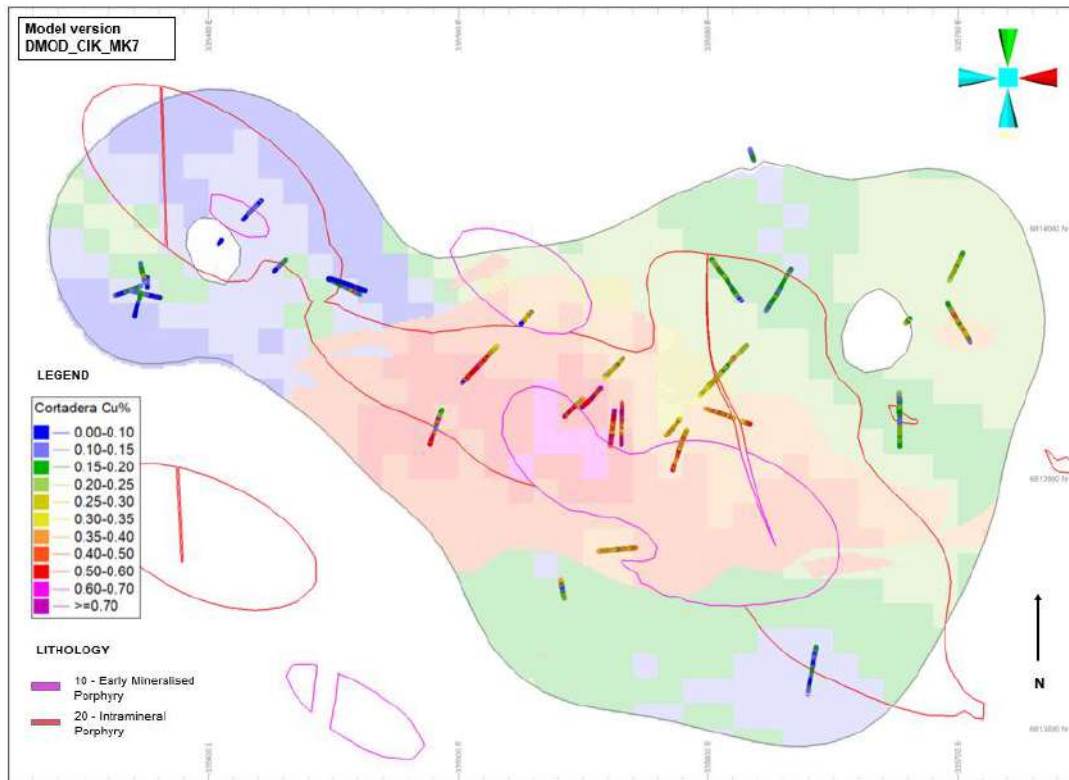


Figure 14.69 Plan-view section at 950 mRL showing Cuerpo 2 Cu% estimate within iron oxide horizon compared to the 10 and 20 series porphyries

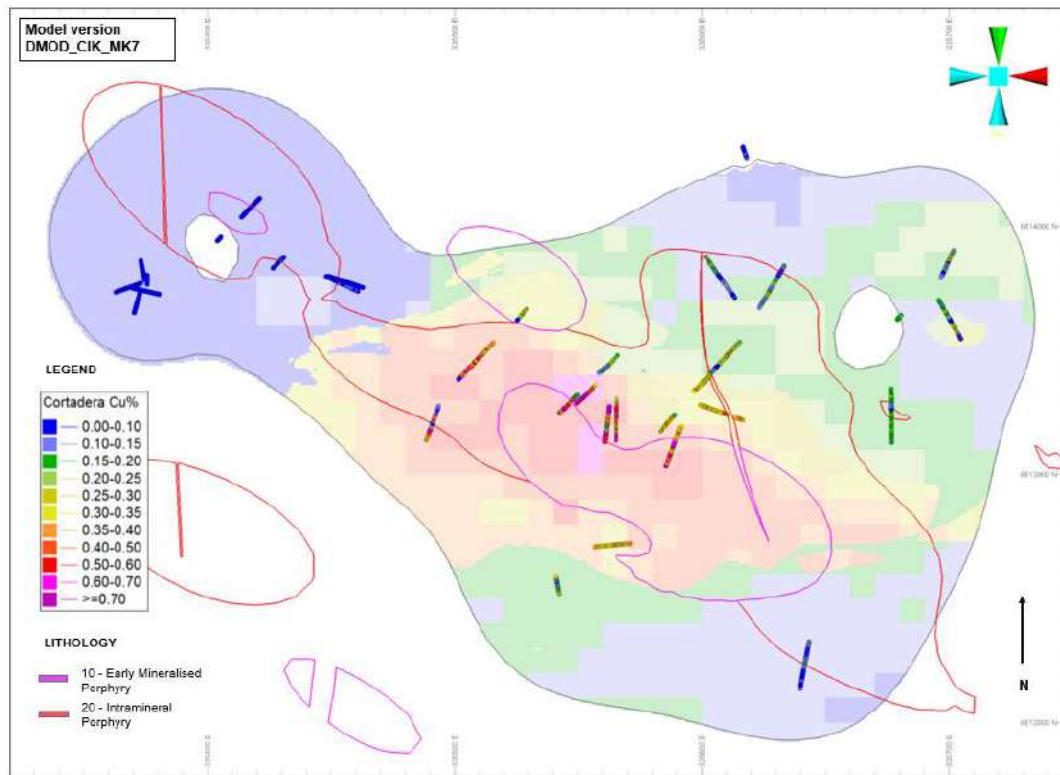


Figure 14.70 Plan-view section at 950 mRL showing Cuerpo 2 Au estimate within iron oxide horizon compared to the 10 and 20 series porphyries

14.2.14.6.2 Ag and Mo estimates

Ag and Mo estimates were completed inside of the iron oxide horizons using a conventional ordinary kriging (OK) approach.

No additional domaining (except the splitting of the iron oxide horizons by Cuerpo) has been completed for the Ag and Mo estimates, with each Cuerpo displaying a near log-normal population, with low data variance (Figure 14.71).

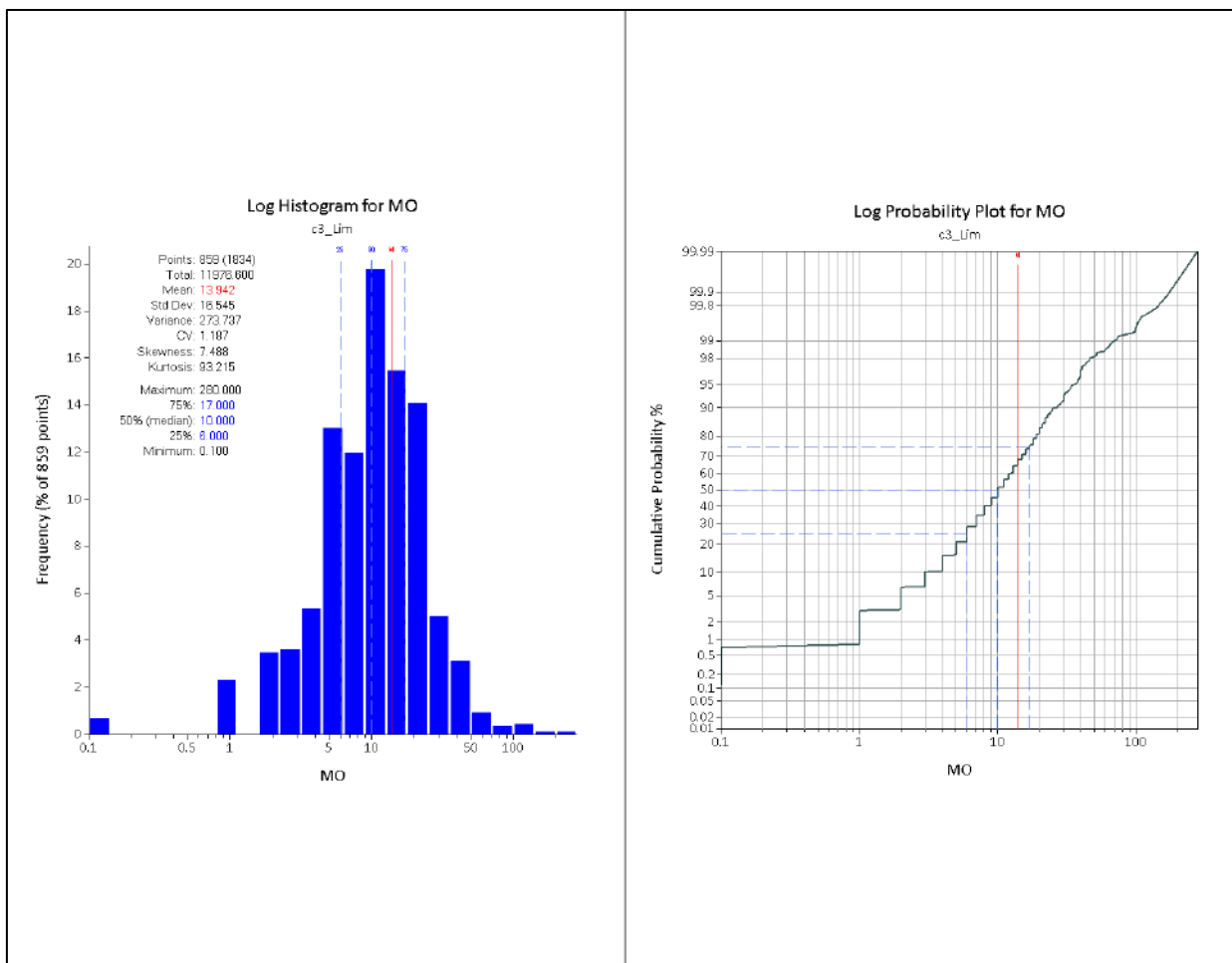


Figure 14.71 Log-histogram (left) and log-probability plot (right) showing near log-normal distribution of Mo grades for Cuerpo 3 within iron oxide horizon.

As with the Cu% and Au estimates, downhole declustering has been tested, using the MAXKEY function in Datamine. Estimate iterations with a maximum of 4 and 7 samples per BHID have been tested, with 7 samples per BHID giving the optimum result.

Kriging neighbourhood analysis has been completed for each domain and used as a guide for the selection of sample counts, search distances, discretization points and block size. Table 14.90 outlines the search parameters used for all Ag and Mo estimates. In all cases, search orientations were defined by the variogram.

Table 14.90 Ag/Mo search parameters

Cuerpo	Element	Minimum/ Maximum sample count	Search pass volume factors (Pass2/ Pass3)	Major/Semi- Major/Minor search rotations (Dir1/Dir2/Dir3)	Major/Semi- Major/Minor search distances (Dir1/Dir2/Dir3)
Cuerpo 1	AG	6/16	1.5/10	000/000/170	265/125/20
	MO	6/16	1.5/10	000/000/-150	120/120/50
Cuerpo 2	AG	6/16	1.5/10	-010/010/-140	120/120/45
	MO	6/16	1.5/10	000/000/155	110/80/35
Cuerpo 3	AG	6/16	1.5/10	000/000/-140	240/140/55
	MO	6/16	1.5/10	000/000/-130	155/100/35

Output models are compared to the input data, with the estimate validated to ensure fair reflection of the mineralised system. Figure 14.72 and Figure 14.73 show type-sections of the Mo and Ag estimates, respectively.

Further detail around model validation is included in 14.2.16.

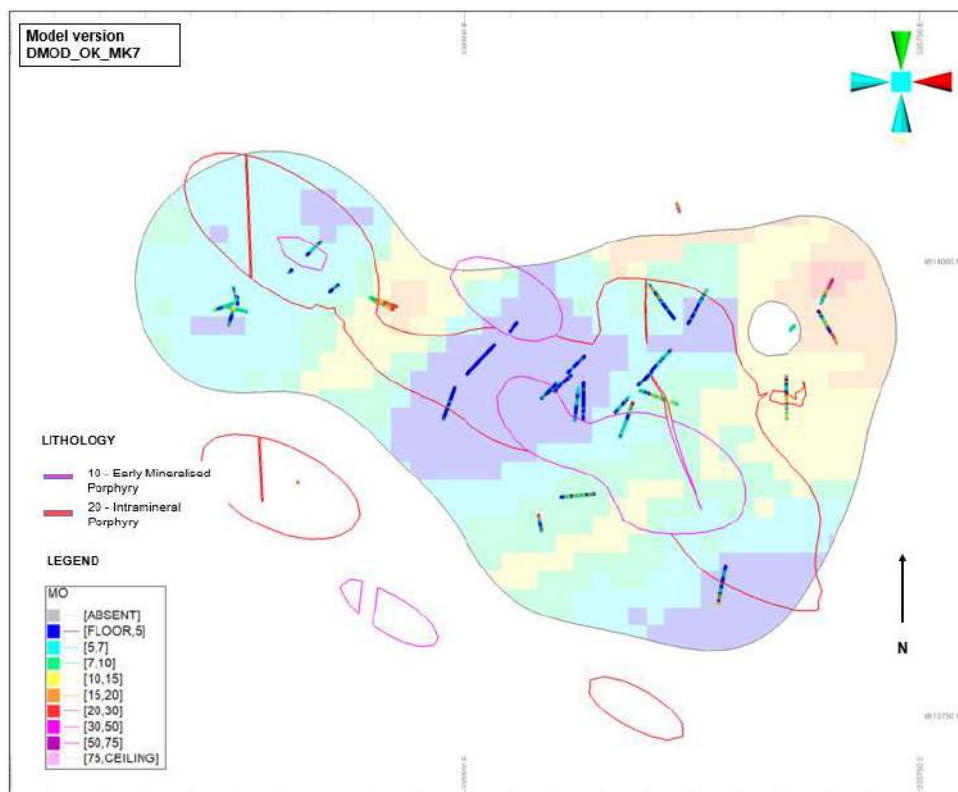


Figure 14.72 Plan-view section at 950 mRL showing Cuerpo 2 Mo estimate within iron oxide horizon compared to the 10 and 20 series porphyries

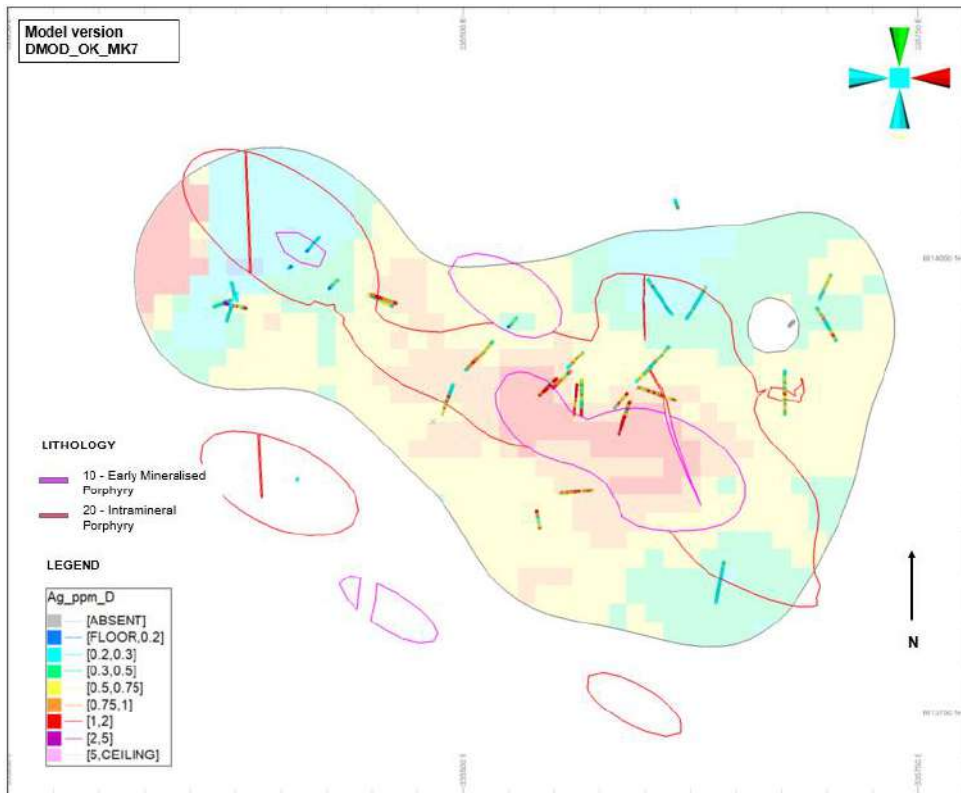


Figure 14.73 Plan-view section at 950 mRL showing Cuerpo 2 Ag estimate within iron oxide horizon

14.2.15 Bulk Density

1,218 bulk density samples were analysed and average density values for each LTCODE was determined for the fresh material. The mean fresh density was discounted by 10% for transitional and 20% for oxide (owing to the lack of density data for the oxide and transitional material).

These densities were then applied to the block model based on the coded LTCODE (lithology code) and WTCODE (weathering code) in the final block model.

Densities as coded are tabulated in Table 14.91.

Table 14.91 Bulk density value assignment

LTCODE	WTCODE	DENSITY ASSIGNED
1 = Sediments	1000 (Oxide)	2.29
2 = Volcanics		2.24
5 = Hornfels Proximal		2.29
6 = Hornfels Distal		2.26
10 = Early Mineralised Porphyry		2.16
20 = Intramineral Porphyry		2.17
30 = Late Mineral Felsic Dyke		2.21
31 = Late Mineral Dyke Eye		2.21
32 = Late Mineral Dyke stockwork		2.21
40 = Post Mineral Andesitic Dyke		2.10
1 = Sediments	2000 (Trans)	2.57
2 = Volcanics		2.52
5 = Hornfels Proximal		2.57
6 = Hornfels Distal		2.54
10 = Early Mineralised Porphyry		2.43
20 = Intramineral Porphyry		2.44
30 = Late Mineral Felsic Dyke		2.48
31 = Late Mineral Dyke Eye		2.48
32 = Late Mineral Dyke stockwork		2.48
40 = Post Mineral Andesitic Dyke		2.37
1 = Sediments	3000 (Fresh)	2.86
2 = Volcanics		2.80
5 = Hornfels Proximal		2.86
6 = Hornfels Distal		2.82
10 = Early Mineralised Porphyry		2.70
20 = Intramineral Porphyry		2.71
30 = Late Mineral Felsic Dyke		2.76
31 = Late Mineral Dyke Eye		2.76
32 = Late Mineral Dyke stockwork		2.76
40 = Post Mineral Andesitic Dyke		2.63

Figure 14.74 shows the densities as coded in the final block model.

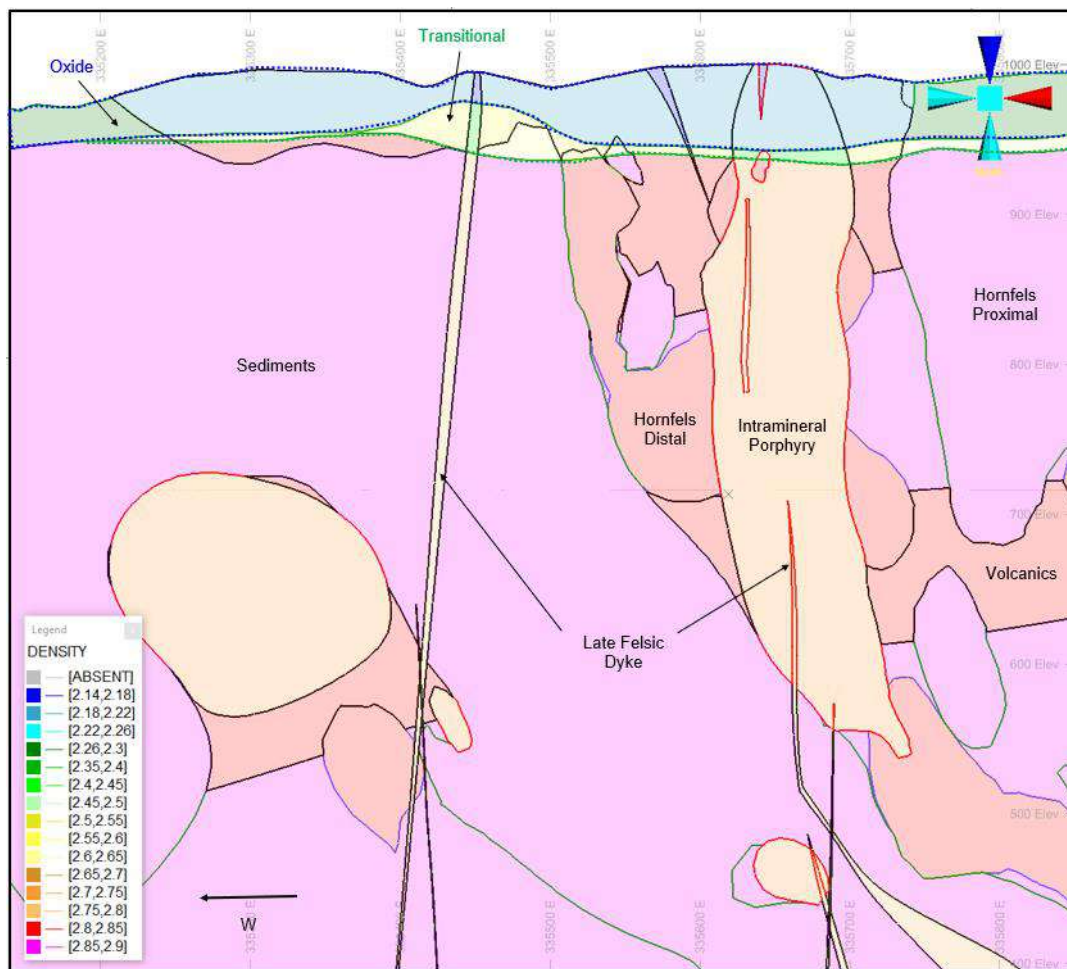


Figure 14.74 Cross section (at 6,813,840 mN) looking north through Cuerpo 2 showing the bulk density assignment to the block model.

14.2.16 Estimate Validation

Estimates for all elements were validated using a three-stage comparison between top-cut composites and the estimated variables.

The first stage involves calculating the global statistics of the composites compared to the tonnage weighted averages of estimated variables. The second stage involves comparing statistics in elevation slices along the mineralisation and the third involves a detailed visual comparison by section to ensure the estimated variables honour the input composite data.

CIK sub-domains were validated independently (by sub-domain) and as a combined estimate and dataset (sub-domains combined).

The use of one-way soft boundaries between estimation domains makes the comparison of block grades and composites problematic. To compare output blocks with the informing data set, a validation wireframe is created, offset by a distance (based on the search distance and MAXKEY

value used, but between 20 and 50 metres for all domains). This wireframe is then used to select the dataset used for the comparative validation.

An example below shows the validation of the Cu% LG domain for Cuerpo 3. The wireframe is offset by a distance of 20m, to include data from the HG domain used to inform the LG estimate across the one-way soft boundary (Figure 14.75).

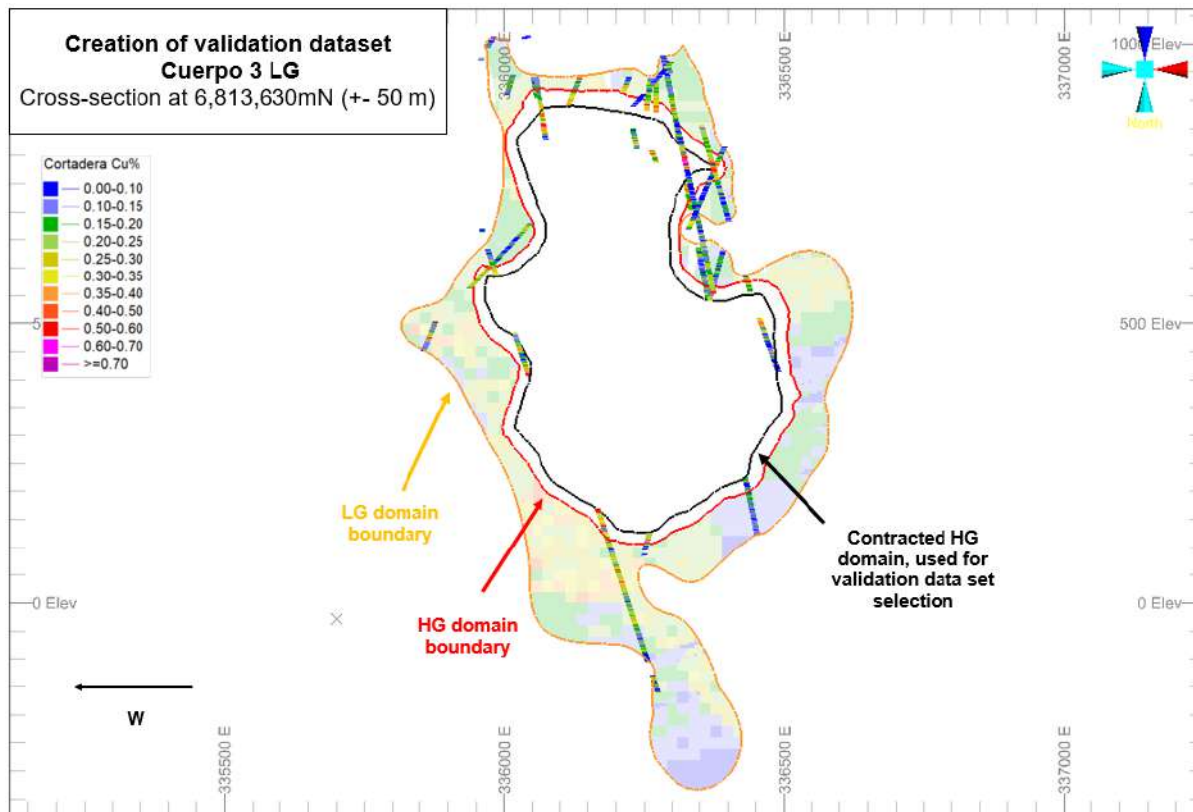


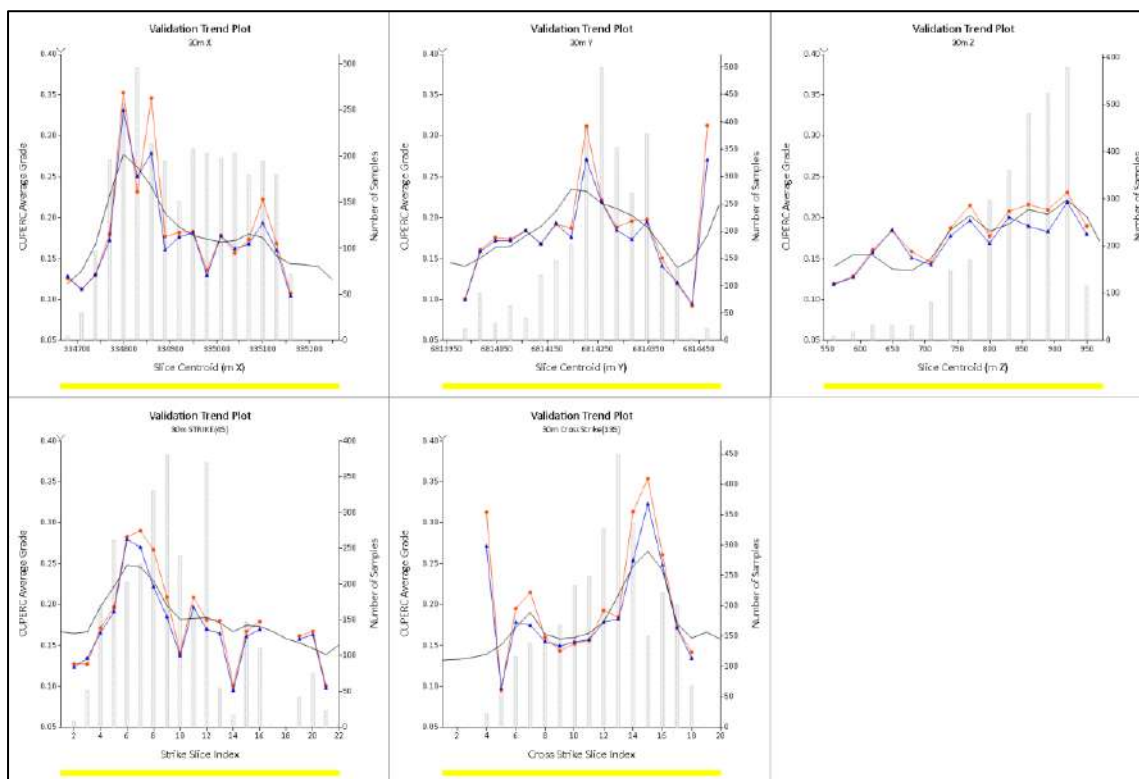
Figure 14.75 Creation of validation data set for Cuerpo 3 Cu% LG domain

The comparison of average grade of the composites to the block grade estimate (excluding blocks estimated on third pass) for a selection of elements is contained in Table 14.92.

Table 14.92 Estimation validation – comparison of top-cut, declustered composites to output block model

Cuerpo	Element	Domain(s)	Composites – top-cut and declustered	Model (excluding third pass blocks)	% Difference
Cuerpo 1	CU%	HG	0.248	0.268	+8%
		LG	0.143	0.129	-7%
		WASTE	0.068	0.072	+5%
	AU	HG	0.234	0.244	+4%
		LG	0.103	0.997	-4%
		WASTE	0.039	0.037	-5%
Cuerpo 2	CU%	HG	0.282	0.299	+6%
		LG	0.183	0.191	+4%
		WASTE	0.062	0.056	-10%
	AU	HG	0.124	0.121	-2%
		LG	0.053	0.055	+4%
		WASTE	0.024	0.024	+0%
Cuerpo 3	CU%	HG	0.374	0.403	+8%
		LG	0.237	0.236	-0%
		WASTE	0.078	0.073	-7%
	AU	HG	0.061	0.063	+3%
		LG	0.026	0.031	+19%
		WASTE	0.009	0.007	-22%

Trend analysis was completed within each domain in all three dimensions (X-axis, Y-axis, and Z-axis). An example is shown in Figure 14.76 which shows the HG Cuerpo 1 Cu% estimate.



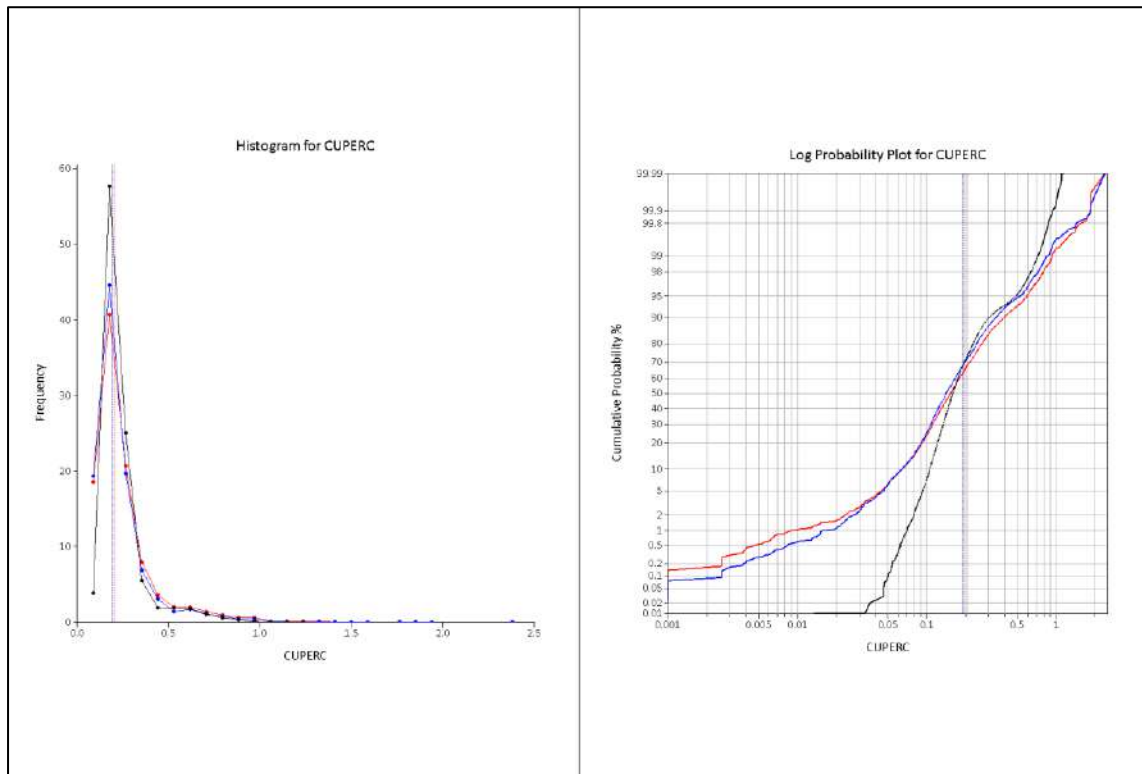


Figure 14.76 Validation trend plot – Cu% – Cuerpo 1 - HG domain. Red = composite grades, blue = declustered composite grades, black = estimated block grades.

Visual validation was completed in various orientations of drillhole grades and model grades, Figure 14.77.

The validations show a reasonable reflection of the input composite grades in the output model although comparisons are poor for the extremely low-grade variables and low-grade domains where small differences in grade will result in large percentage differences. Comparisons are also poorer for those variables where the grade ranges vary over the mineralisation and the data distributions are mixed.

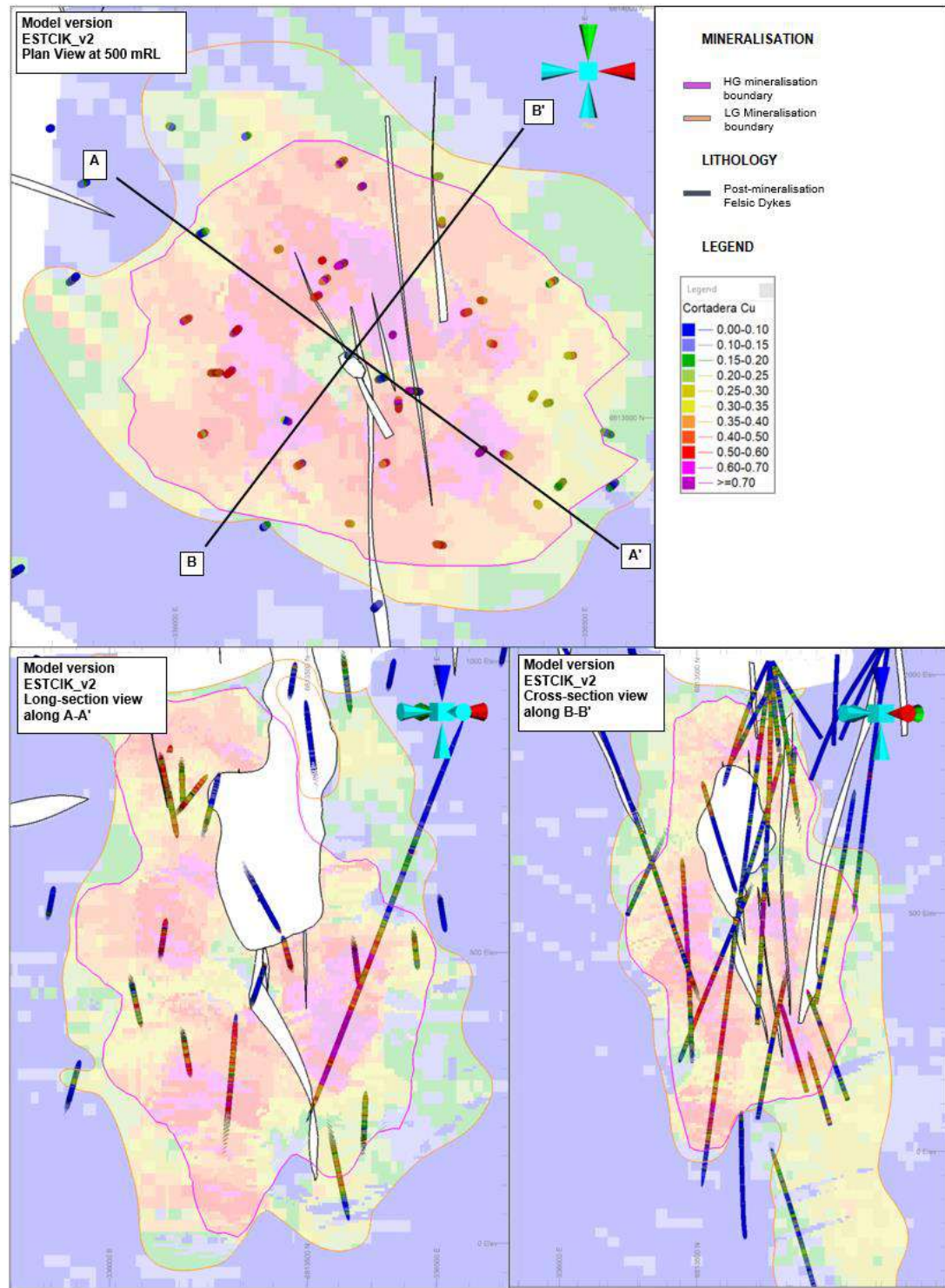


Figure 14.77 Visual validation of drillholes versus modelled Cu% grade. Plan view (top) showing location of sections A-A' and B-B'; cross sections shown on bottom.

14.2.17 Resource Classification

The Cortadera Mineral Resource estimate has been classified considering the guidelines provided in NI 43-101.

A 'Mineral Resource' is a concentration or occurrence of solid material of economic interest in or on the Earth's crust in such form, grade (or quality), and quantity that there are reasonable prospects for eventual economic extraction.

The location, quantity, grade (or quality), continuity and other geological characteristics of a Mineral Resource are known, estimated, or interpreted from specific geological evidence and knowledge, including sampling.

Mineral Resources are sub-divided, in order of increasing geological confidence, into Inferred, Indicated and Measured categories (Figure 14.78).

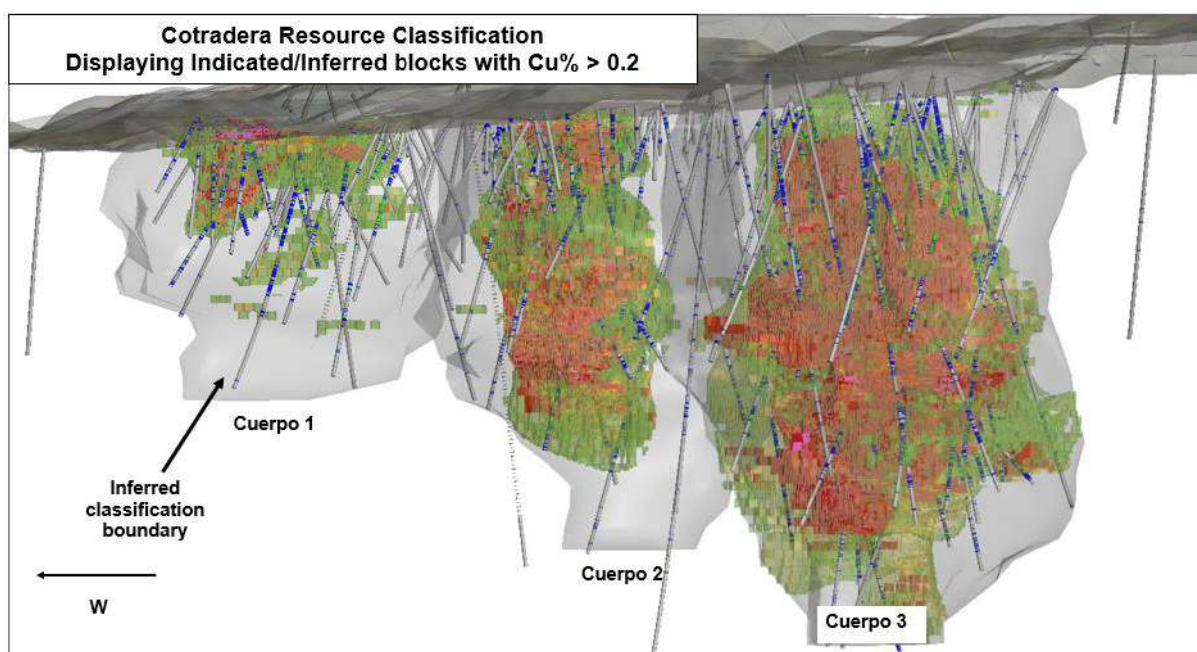


Figure 14.78 Long-section view looking north showing Indicated and Inferred blocks where $Cu\% \geq 0.2$

Classification wireframes were constructed to define the limits of Indicated and Inferred material. No Measured resource has been defined in this update.

These took account of geological and grade continuity between drillholes, number of samples informing the estimate, quality of the estimate (slope of regression, kriging efficiency and search pass block is filled on) and confidence in the estimate (with a conservative approach taken where the use of soft-domain boundary conditions were coupled with sparse data density). The Competent Person has assessed the drillhole database validation work and QA/QC undertaken by HCH and was satisfied that the input data could be relied upon for the estimation of Indicated and Inferred Mineral Resources.

The Mineral Resources have been classified based on confidence in geological and grade continuity and considering data quality (including sampling methods), data density and confidence in the block grade estimation.

Wireframes were constructed in Datamine to control the extents of classification, with the following file names:

- Cuerpo 1 Inferred – 202202_rescat_3_inf_c1_1
- Cuerpo 2 Inferred – 202202_rescat_3_inf_c2_1
- Cuerpo 3 Inferred – 202202_rescat_3_inf_c3_3
- Cuerpo 1 Indicated – 202202_rescat_2_ind_c1_1
- Cuerpo 2 Indicated – 202202_rescat_2_ind_c2_1
- Cuerpo 3 Indicated – 202202_rescat_2_ind_c3_2

14.2.18 Reasonable Prospects for Eventual Economic Extraction

The metal prices used for reporting has incorporated third-party advice and considers trailing three-monthly averages spot prices, consensus forecasts from analysts and prices used in resource reports published on the Toronto Stock Exchange in the previous year.

The cost basis for cut-off grade analysis has utilised the costs from the 2016 study at Productora (nominally inflated and adjusted to current values) and a benchmarking study into block-cave mining.

The key revenue and cost inputs, plus other relevant controls, are provided in Table 14.93 and Table 14.94. Payable metals (other than copper) use the same prices as the Mineral Resource Estimate.

Table 14.93 Key revenue and cost parameters for estimating the breakeven grade for Reasonable Prospects of Eventual Economic Extraction by Block Cave Mining

Value	Units	Description
4.3	USD/lb	Copper Price – 30% above the long-term copper price assumption
86	USD/%Cu	Gross Copper Revenue
83	%	Processing Recovery of Copper
0.36	USD/lb	Copper Selling Cost
96	%	Copper Payability
87	%	Copper Net Smelter Return (net of payability and selling costs)
75	USD/%Cu	Net Copper Revenue
5	%	Royalty (lowest rate assuming <35% profit margin)

Table 14.94 The calculation of the breakeven caving grade to define Reasonable Prospects of Eventual Economic Extraction

CuEq %	USD/t	Description
0.16	8	Mining Cost
	7.6	Processing Cost incl. additional crushing underground
	15.6	Required Mining & Processing Revenue Grade (USD/t)
0.16	18.8	(Apply Average Fresh ore Flotation Recovery) – 83%
	19.6	(Apply Net Smelter Payability) – 96%
	0.15	5% Royalty (assume 15% margin above \$19.1)
	19.75	Breakeven Cave Grade
0.21	USD/t	Description

Using the breakeven cut-off grade of 0.21% CuEq, as an input cut-off grade to simulate a block cave/massive underground economic mining shape, the resource model was then processed by mining software generally used to develop future potential economic underground shapes (Mineable Shape Optimizer/MSO) which applied a minimum-dimension, mining shape. The minimum-dimension geometry applied was a cave draw shape typically 80m wide x 80m long x 80m high (although sub-shapes were allowed within the MSO software as it might be included in a draw point if included in the typical footprint of the cave shape). This geometry was considered a reasonable size to initiate a cave albeit assuming pre-stress and a hydraulic radius of +20m.

The resulting cave shapes produced by the MSO software are shown in Figure 14.79 and serve to identify material that has reasonable prospects of eventual economic extraction (RPEEE) by exploring a typical block cave mining strategy. The geotechnical work for a potential block cave propagation at Cortadera is subject to further study and these are based on preliminary concept geotechnical parameters.

Pictured in Figure 14.79 are (above) the opaque mining shapes in green, compared to a transparent blue, 0.1% CuEq mineralisation surface. Pictured below (bottom) are the same green mining shapes made transparent to display the purple, HG copper domains used to constrain estimation.

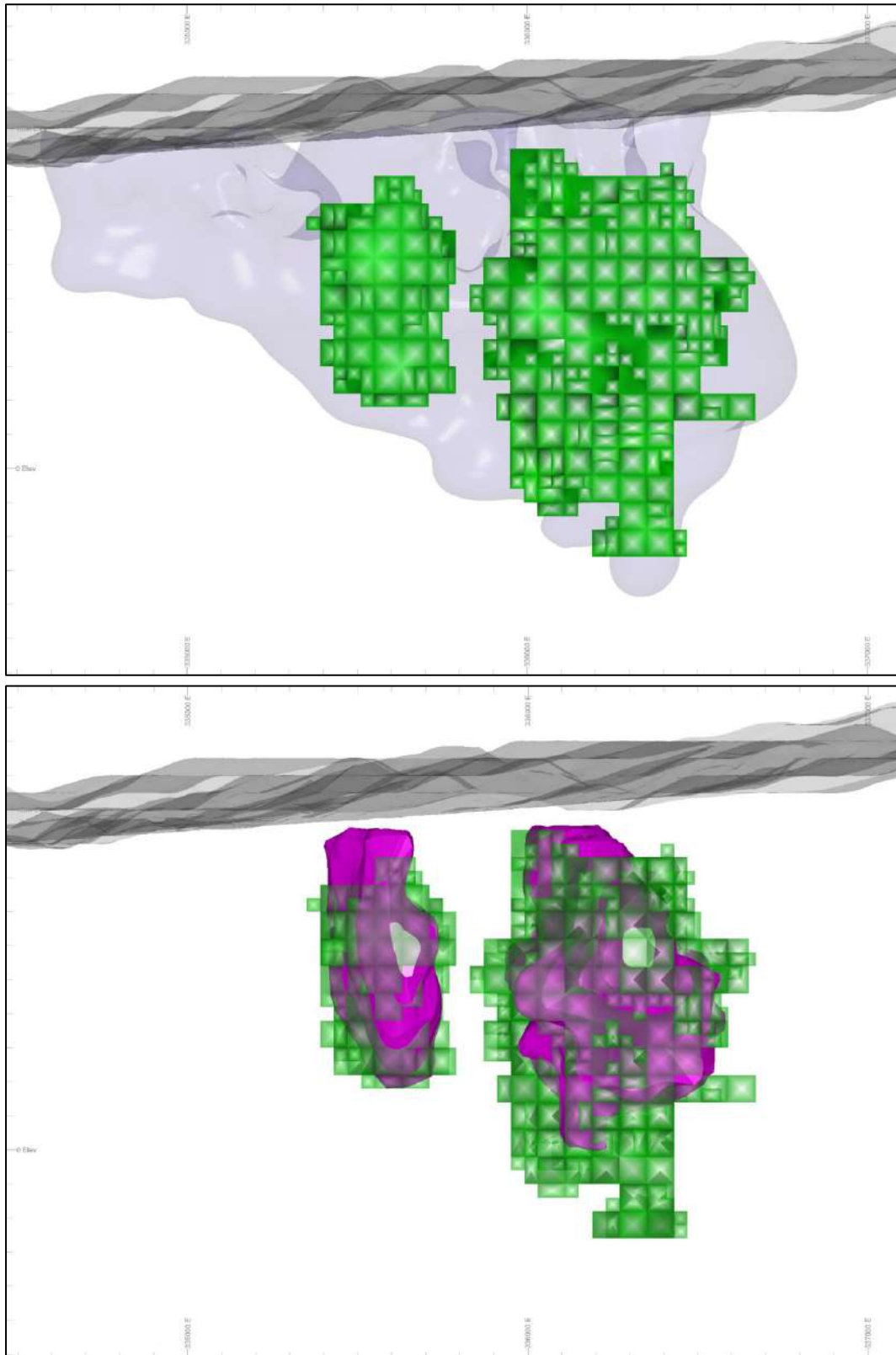


Figure 14.79 Long-section looking north showing mining shapes used to define Reasonable Prospects of Eventual Economic Extraction by Block Cave Mining. (HCH, 2022)

Since mineralisation extends from the surface, an open pit shell was also generated using the industry-standard Lerchs-Grossman algorithm and the parameters listed in Table 14.95. Selling costs incorporate transport and handling costs, as well as any treatment and refining costs. Payable terms assume that the copper concentrate is sold into the Asian smelter market, for which these terms are standard.

Table 14.95 Key open pit optimisation parameters applied to generate a pit shell defining Reasonable Prospects of Eventual Economic Extraction

<u>Lowest Grade that Pays for Itself for Bulk, Open Pit Mining</u>		
Value	Units	Description
4.3	USD/lb	Optimistic Copper Price (30% above assumed price)
1.8	USD/t	Open Pit Mining Cost (incremental cost of 0.025/10m bench)
7.23	USD/t	Sulphide Processing Cost
7.15	USD/t	Oxide Processing Cost
35° to 45°	Degrees	Overall Pit Slope Angles (35° in oxide, 40° in transition and 45° in fresh rock)
0.52	USD/lb	Sulphide Copper Selling Cost
0.24	USD/lb	Oxide Copper Selling Cost
5	USD/oz	Gold Selling Cost
2.27	USD/lb	Molybdenum Selling Cost
83 to 70	%	Sulphide Copper Recovery (Fresh to Transitional) - variable
50 to 56	%	Sulphide Gold Recovery (Fresh to Transitional)- variable
83 to 46	%	Sulphide Molybdenum Recovery (Fresh to Transitional) - variable
37 to 30	%	Sulphide Silver Recovery (Fresh to Transitional) - variable
50	%	Oxide Copper Recovery - variable
96	%	Sulphide Copper Payability
90	%	Sulphide Gold and Silver Payability
98	%	Sulphide Molybdenum Payability
100	%	Oxide Copper Payability

The resulting pit shells identifying the economic limit of mining are shown in Figure 14.80. Pictured are (above) are the opaque RPEEE pit shape in red, compared to a transparent blue, 0.1% CuEq mineralisation surface. Pictured below (bottom) is the same red pit shape made transparent to display the purple, HG copper domains used to constrain estimation.

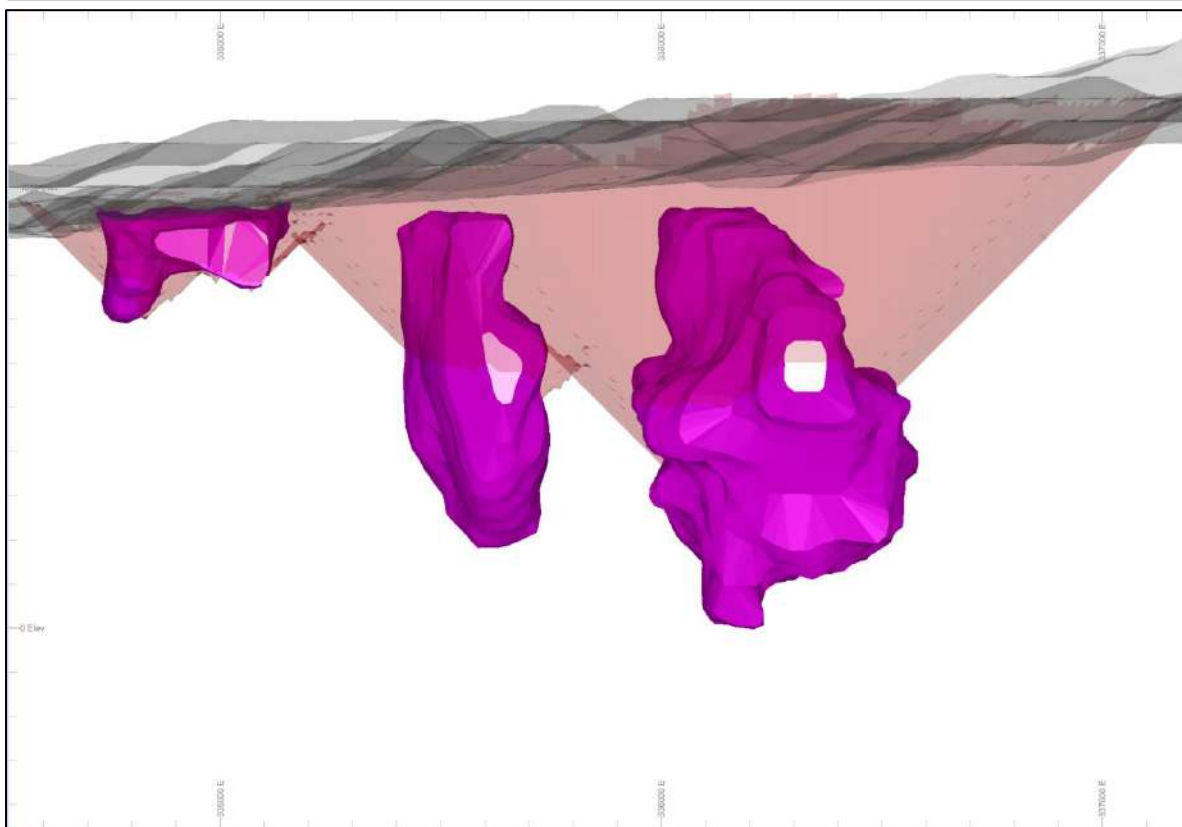
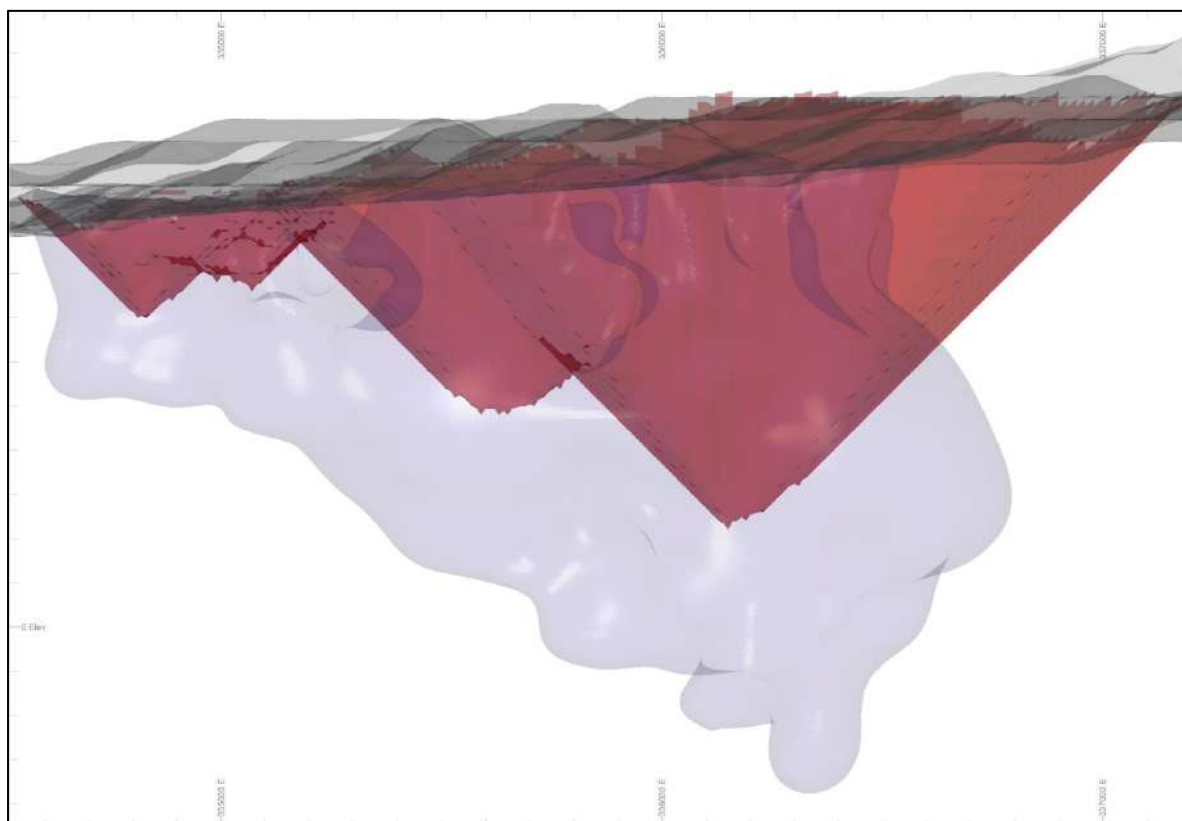


Figure 14.80 Long-section view looking north showing pit shell surfaces used to define Reasonable Prospects of Eventual Economic Extraction by Open Pit Mining. (HCH, 2022)

The controlling surfaces for RPEEE are combined in Figure 14.81 and Figure 14.82 to show the significant overlap in the near surface mineralisation. Material that sits above the RPEEE pit shells is assumed as being extracted using open pit methodologies and has therefore been reported at a CuEq% cut-off grade aligned with open pit mining.

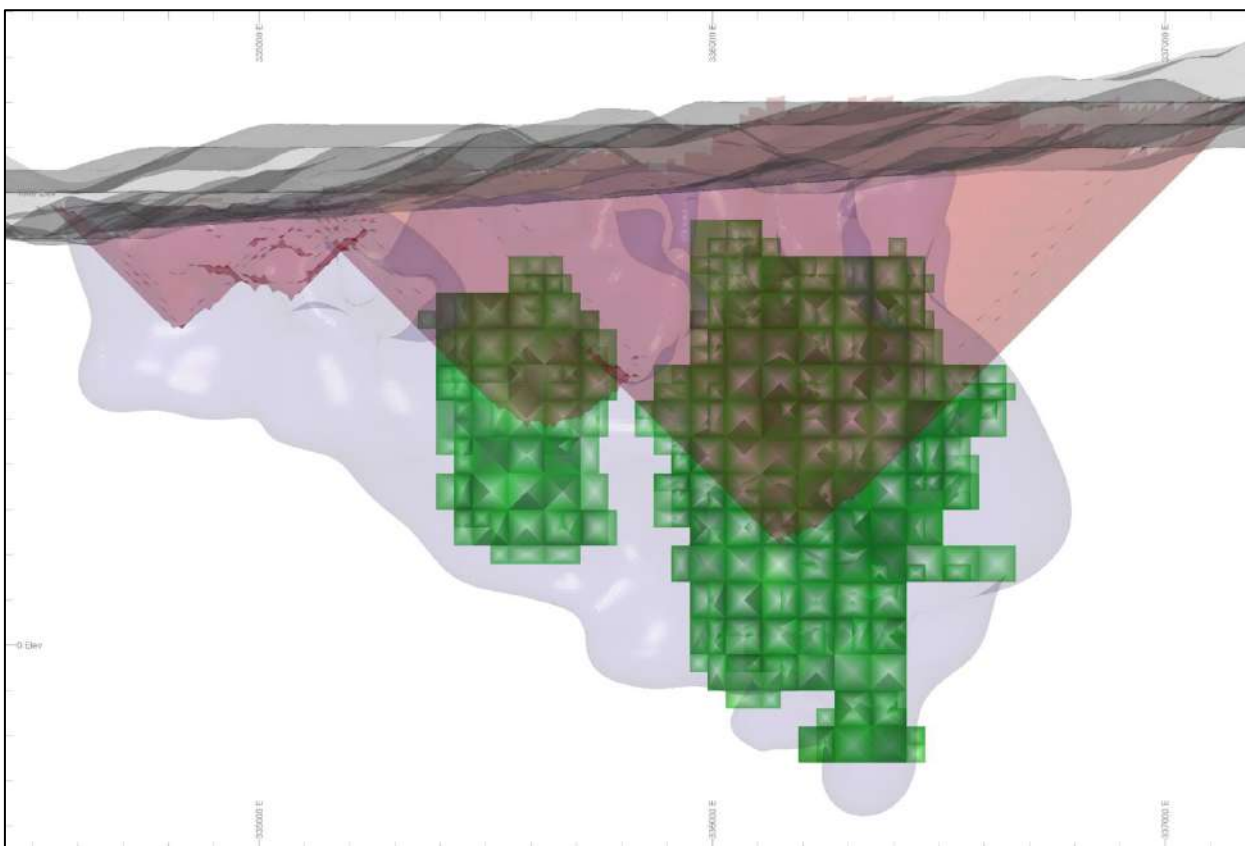


Figure 14.81 Long-section view looking north showing pit shell surfaces and block cave mining shapes used to define Reasonable Prospects of Eventual Economic Extraction by Open Pit Mining. (HCH, 2022)

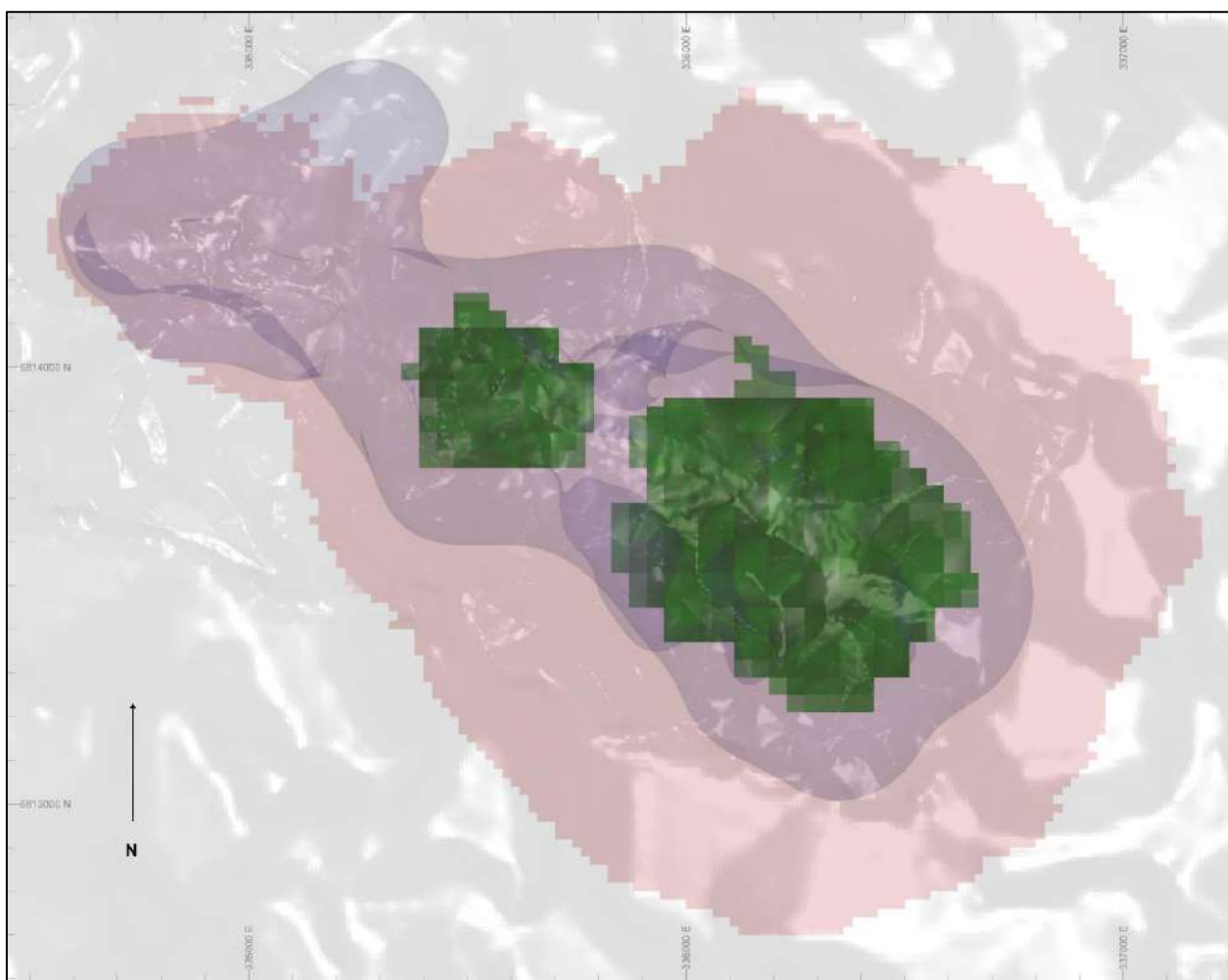


Figure 14.82 Plan view showing pit shell surfaces and block cave mining shapes used to define Reasonable Prospects of Eventual Economic Extraction by Open Pit Mining. (HCH, 2022)

14.3 San Antonio

14.3.1 Introduction

Following execution of the San Antonio option agreement in 2017, HCH undertook a Resource drill-out focussed on extending and infilling previously defined mineralisation. Drilling was successful in improving geological understanding and growing the deposit size. Several iterations of the geological model and mineral estimates were conducted by HCH and external consultants, with HCH delivering the maiden mineral resource estimate in 2022. This followed the completion of a critical drone survey project to better understand the location and extent of the current underground workings.

Drilling completed by HCH in 2018 comprises 41 RC holes for a total of 4,922m. Additional sample data incorporated into the estimate includes drilling completed prior to HCH securing the project, and a suite of underground face, channel and sludge samples taken under the direction of HCH.

Drill spacing is nominally 80 m across strike by 120 m along strike. The current drilling density provides sufficient information to support a robust geological and mineralisation interpretation as the basis for an Inferred Classified Mineral Resources for the drill-defined deposit.

HCH drill data collected uses industry standard techniques for drilling and sampling collection. Samples have been analysed by certified laboratories in Chile and Lima, Peru by standard analytical techniques including:

- Copper, silver, and molybdenum were analysed by 4-acid digestion (Hydrochloric-Nitric-Perchloric-Hydrofluoric) followed by evaluation using Inductively Coupled Plasma - Optical Emission Spectrometry (ICP-OES) or Atomic Absorption Spectrometry (AAS)
- Copper results > 10,000 ppm were analysed by “ore grade” method Cu-AA62 (upper limit 40% Cu)
- Gold was analysed by 30 or 50 gram lead-collection Fire Assay, followed by ICP-OES or AAS.

San Antonio is likely to be processed under the same processing regime as the Productora deposit (which has had considerable metallurgical test work and a PFS completed), and as such it was considered appropriate to consider the elements of copper, gold, molybdenum and silver as economically material for resource classification and reporting.

The verification of input data included the use of company QA/QC blanks and reference material, field and laboratory duplicates, umpire laboratory checks and independent sample and assay verification. The Qualified Person has assessed the drillhole database validation work and QAQC undertaken by HCH and was satisfied the input data could be relied upon for the estimation of Inferred Classified Mineral Resources (Figure 14.83).

The Mineral Resource Estimation process included:

- Statistical analysis of the composites, within appropriate mineralisation domains
- Compositing of the drilling results to 1 m lengths
- Top-cut analysis within mineralisation domains as appropriate
- Volume modelling within mineralisation domains, taking into consideration drill spacing, mineralisation continuity and potential mining methods
- Estimation of a grade model via ordinary block kriging and inverse distance methodologies within resultant estimation domains, using hard boundaries to reflect current geological understanding
- Assignment of density using a default value derived from consideration of nearby Cortadera density data and in consideration for similar Copper deposits
- Validation of the estimated grades using visual and statistical analysis, swath and QQ plots.

A range of criteria were considered in determining the Resource Classification, including:

- Geological and grade continuity between drillholes
- Drillhole spacing
- Proposed mining method
- Degree of confidence in mined excavations and depletion model
- 3-dimensional (3D) surfaces to define the limits of Inferred and unclassified material.

Where significant extrapolation occurred, the mineralisation was categorised as Unclassified. The lack of density measurements and uncertainty around the extent of current underground workings were also factors in limiting the classification as Inferred.

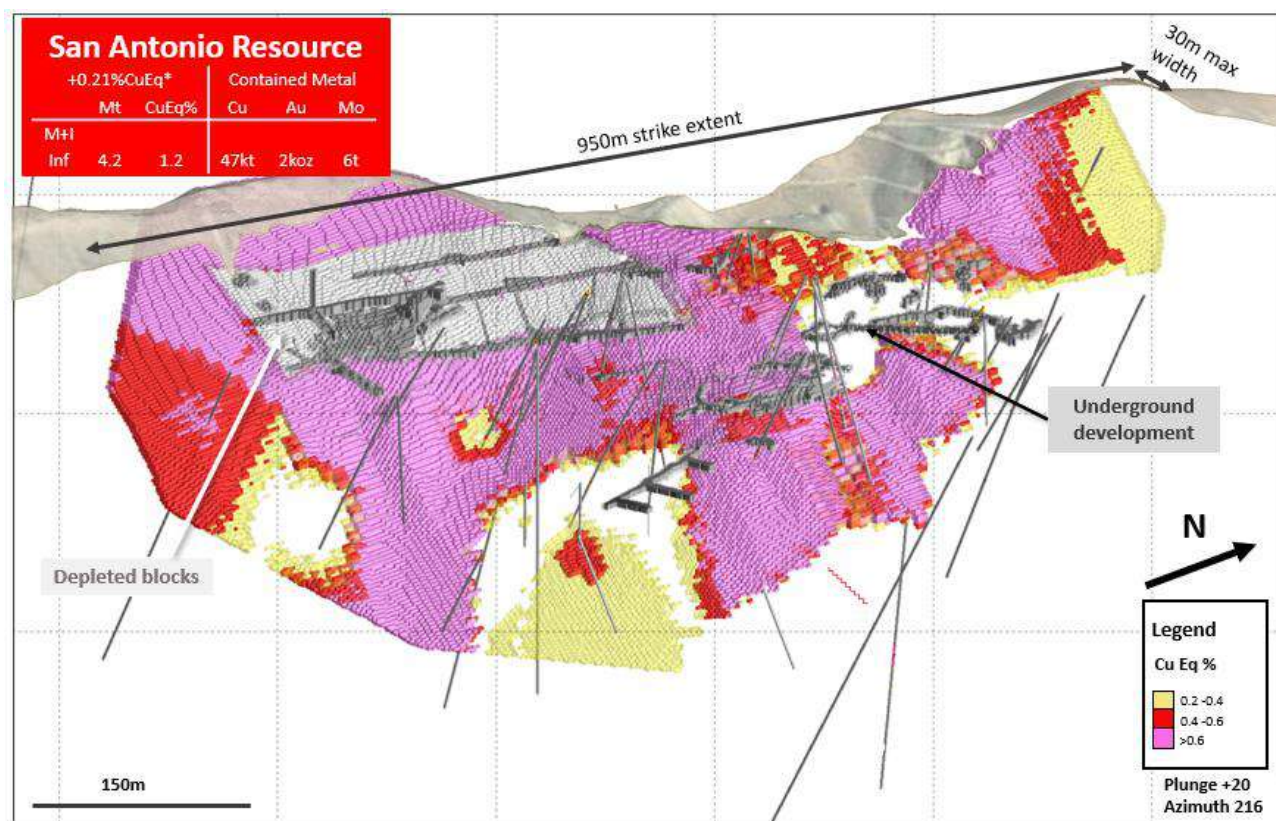


Figure 14.83 Oblique view looking northwest displaying Inferred resource blocks +0.2% CuEq, coloured by copper equivalent grade. (HCH, 2022)

14.3.2 Summary of Data Used in Estimate

A Studio RM database file was exported from the Acquire database for use in estimation. Survey was checked for severe variations down hole. Where no survey record occurred at 0 m depth the first record was used.

Negative values were set to detection limit for the estimated elements silver, gold, copper, and molybdenum.

The database composition is described in Table 14.96.

Table 14.96 Number of Drillhole Samples used in estimation

Hole Type	# of Hole_ID	# of Sample_ID	# of Cu_pct Assays	# of Au_ppm Assays	# of Ag_ppm Assays	# of Mo_ppm Assays	# of Co_ppm Assays
(Surface) Drillhole	52	4332	4311	2163	2073	2073	2073
Underground Drillhole (UGD)	54	656	307	0	0	0	0
Channel	85	0	0	0	0	0	0
Totals	191	4988	4618	2163	2073	2073	2073

14.3.3 Interpretation and Modelling

14.3.3.1 Geology Domains

A 3D modelling project was initiated for San Antonio using the Studio RM package which comprised a combined mineralisation and lithology model. An existing (and still considered relevant) structural model was referred to during this interpretation. Pre-existing work considered during the updated modelling project included:

- Internal geology and structural models by HCH Geologists
- Externally commissioned geology models by Entech and AMC
- Surface mapping reports by HCH and external consultants Geoscience Now and Model Earth
- Drone surveys of the current UG and surface mine workings, to inform the mineralized material position.

Base data for these models included surface mapping, underground mapping, underground workings, drillhole logging and assay data, as well as topographic data.

Much of the San Antonio deposit is characterised by mineralisation within a microdiorite. Lesser mineralisation is also noted in adjacent felsic intrusives. Surface mapping suggests that mineralisation is controlled by narrow (<1-2m width) fault zones that strike NE to N and are typically steeply dipping wither NW, SE to E, or W (Figure 14.84 and Figure 14.85). Parallel lodes were also mapped at surface and modelled at depth.

Changes in the San Antonio lode interpretation for the 2022 mineral resource are shown in Figure 14.86. Note that previous interpretations were used to inform internal estimates, and no Mineral Resource has been reported externally for San Antonio.

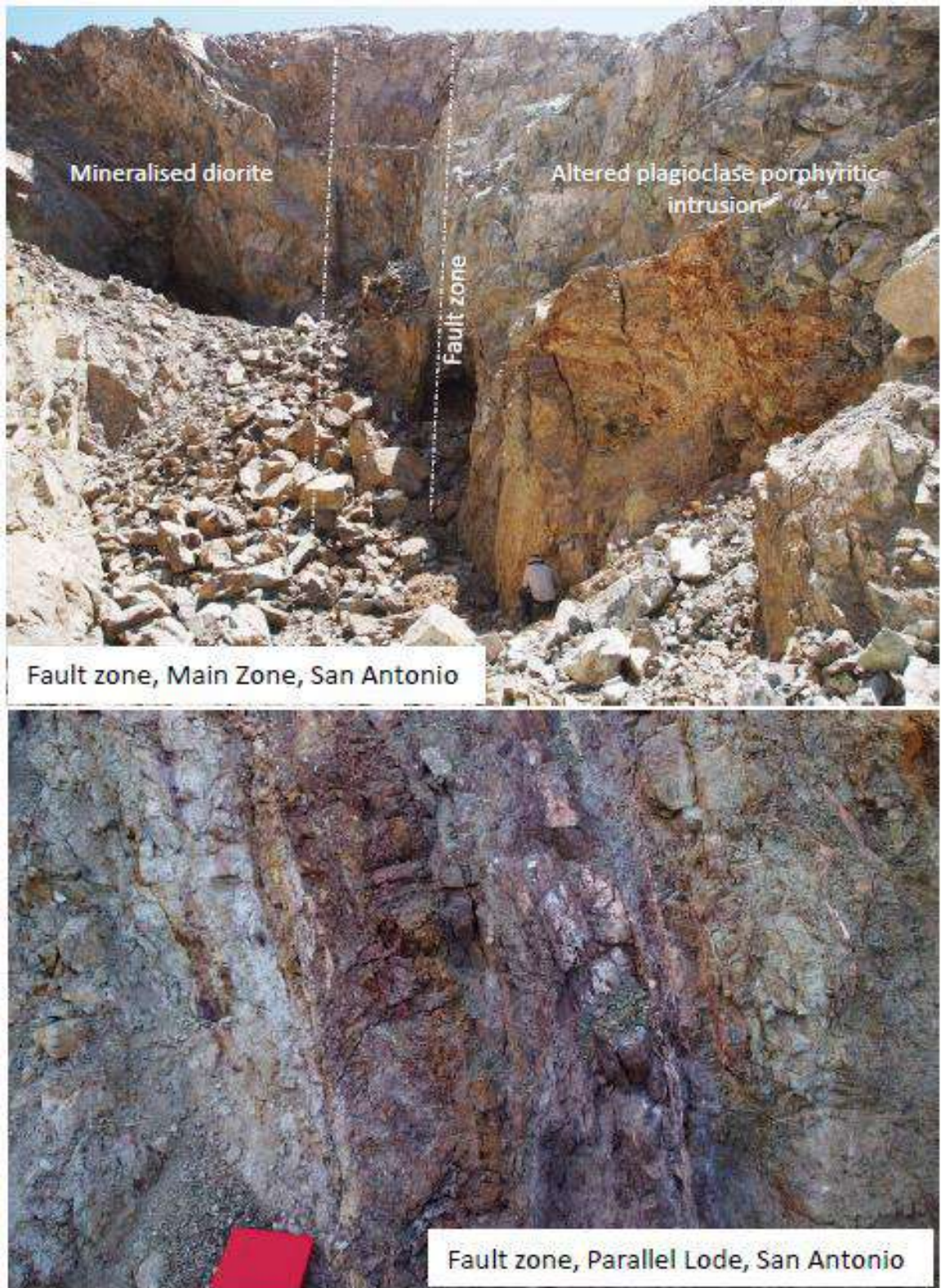


Figure 14.84 Surface Expressions of Main and Parallel lodes at San Antonio

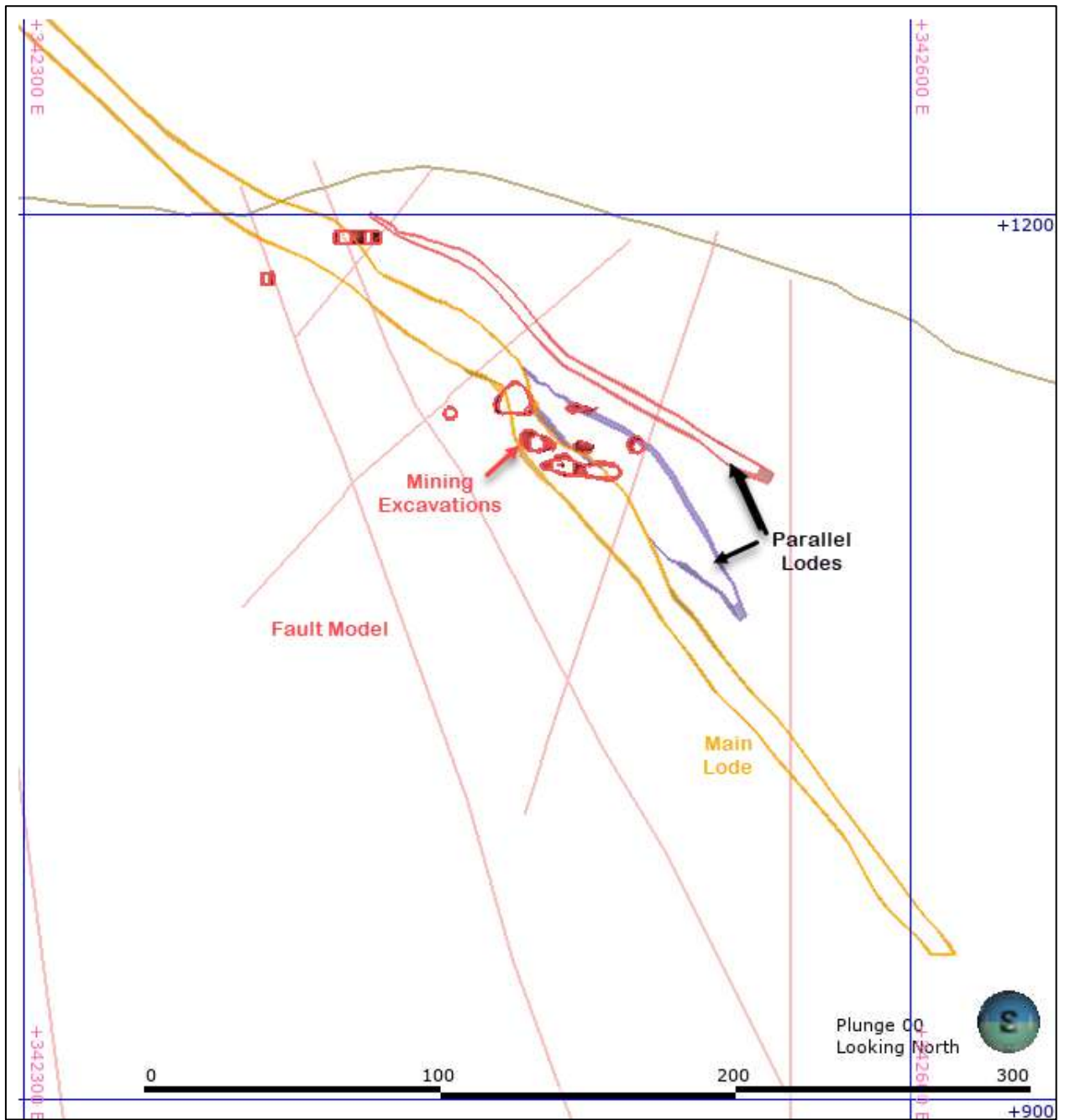


Figure 14.85 Typical cross section of the San Antonio lodes (looking north at 6,818,965mN).

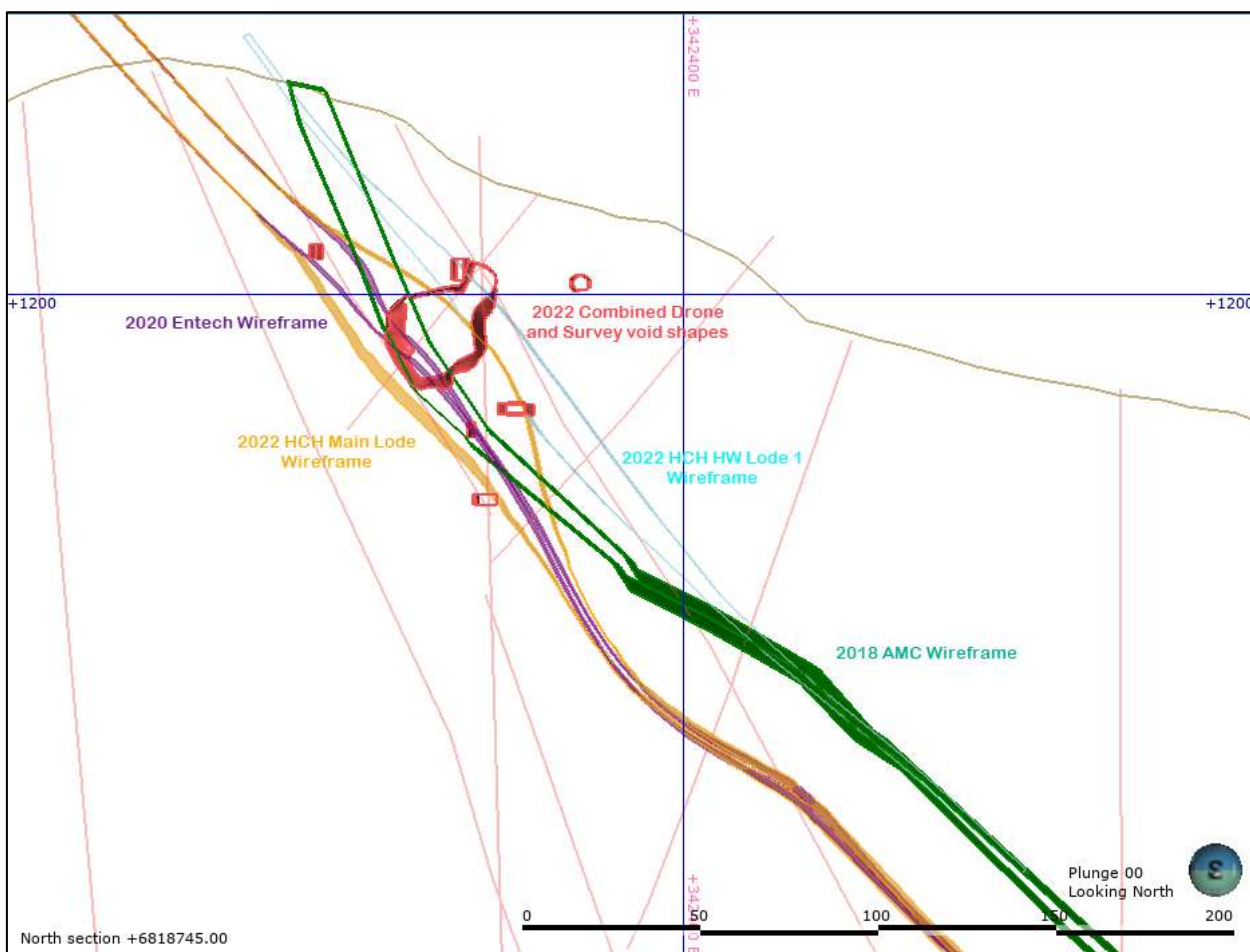


Figure 14.86 Cross Section on San Antonio showing chronology of different interpretations.

The method used to build the combined domains for lithologies, as well as for mineralised zones, was a manual interpretation and digitisation on 20m E-W sections within Studio RM. This method is well suited for the stage of resource definition, where data varies from dense coverage (within the mined areas) to sparse on the peripheries.

This approach also allows for appropriate consideration of inconsistent logging codes and assay data availability within different generations of data, oblique or off section drillholes, and non-geological data such as the drone survey of mined voids.

The interpretation followed a best fit approach to the following criteria, allowing for professional assessment in the cases of missing or conflicting data:

- The host lithology is a diorite unit (HCH lithology code IVO).
 - Mineralisation is permitted to extend into felsic units, as noted in surface mapping, however this was restricted to the main lode.
- A mineralisation cut-off of 0.1% Cu.
 - Mineralisation naturally occurs with well-defined hanging wall and footwall contacts, generally with increased shear.

- Shears, faults, and intervals of no recovery can be used to approximate the mineralized material where no sample exists (and continuity is likely based on knowledge of the mineralised system).
- Mined voids spatially approximate the mineralized material, given consideration for access and infrastructure drives.
- Faults appear to coincide with orientation changes and thickening of the mineralisation lode.

14.3.3.2 Mineralisation Domains

No separate mineralisation domains have been created in addition to the geology domains.

14.3.3.3 Weathering Domains

No overlaying weathering horizon has been interpreted and it is assumed that the deposit is fresh from surface. This is supported by the available drill data.

14.3.4 Data Flagging and Compositing

Interpretation wireframes defining the mineralised envelopes were used to flag both the drillhole data and block model. Wireframes were constructed to limit the model and topography and void model wireframes were also used to flag the block model.

Table 14.97 List of final wireframes used for estimation coding

Wireframe	Field	Code	Description	Type
Main_Lode_15022022	DOMAIN	MAIN	Main Lode	Solid
HW_Lode_1_18022022	DOMAIN	HW1	Parallel Lode	Solid
HW_Lode_2_18022022	DOMAIN	HW2	Parallel Lode	Solid
HW_Lode_3_18022022	DOMAIN	HW3	Parallel Lode	Solid
HW_Lode_4_18022022	DOMAIN	HW4	Parallel Lode	Solid
topo	DOMAIN	AIR	Natural topography	Surface (above)

14.3.5 Mining and Tenement Flagging In The Model

San Antonio tenements have not been flagged in the Resource model. The San Antonio model is situated inside a single tenement.

A drone survey using a mobile laser scanner was completed in August 2021 by Aerodyne Chile. In total, 23 scans were completed of the underground environment as well as eight scans covering the outdoor terrain. The purpose of the survey was to confirm location and extent of the current San Antonio underground workings (including development headings and stoped voids).

While the drone survey was successful in validating the spatial interpretation of mineralised wireframes, it was unable to access all areas of the mine due to poor ground conditions (falls of

ground). As a result of this, assumptions have been made with regards to the depletion of the San Antonio resource.

The San Antonio resource uses all information available to assign depletion, including the drone survey, historic mining pickups and maps and local knowledge. Despite this, there is still uncertainty around the depleted volume at San Antonio. This uncertainty is a major contributor to the decision to only apply Inferred classification to the resource.

Depletion as coded is shown in Figure 14.87 and Figure 14.88. Note that the 'cookie cutter' string in long-section used to deplete the upper levels at San Antonio only depletes the Main lode. There is no evidence that development and stoping have been completed on the parallel lodes.



Figure 14.87 Long section looking east showing mined voids as informed by historic pickups and drone survey (HCH, 2022)

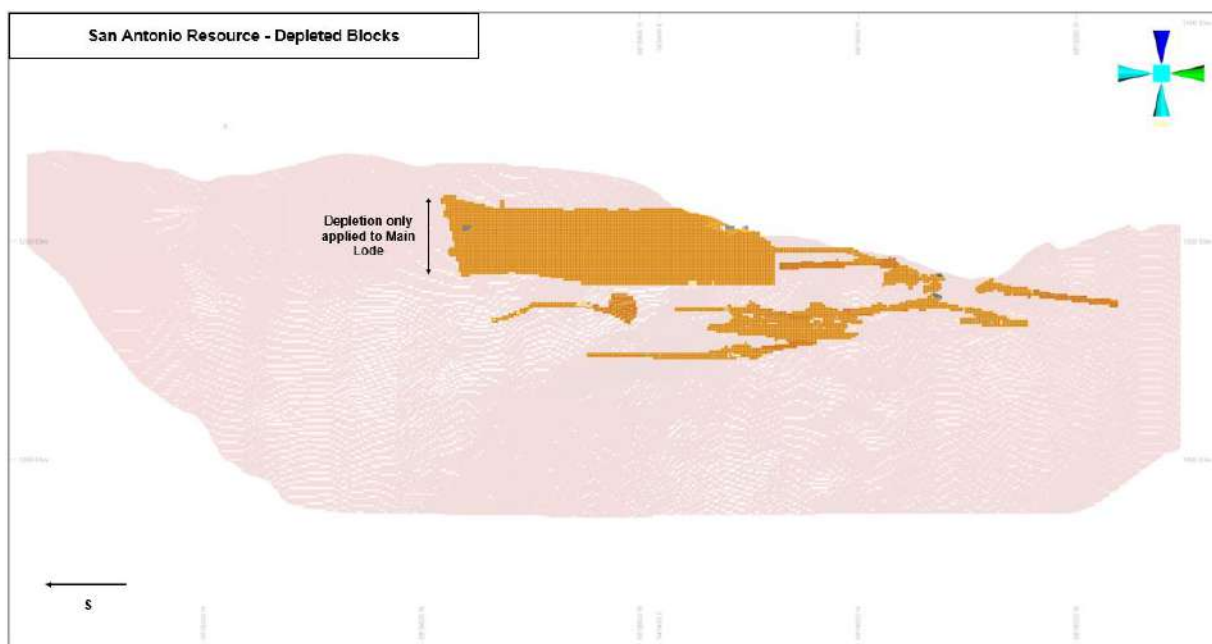


Figure 14.88 Long section looking east showing San Antonio depleted blocks (HCH, 2022)

14.3.6 Compositing

The samples were composited to one metre lengths. One metre composites were chosen as the dominant drill sample length is one meter, and in reflection of the style of mineralisation. A histogram with statistics is presented in Figure 14.47 for sample length. Larger composite intervals would not allow the variability of mineralisation to be investigated and result in the grade estimation being very smooth.

Compositing is the process of equalising the length of samples used for statistical and geostatistical analysis. This is required to ensure that samples of equal support are considered, and it is essential from a statistical viewpoint. Most estimation algorithms do not take into account the sample size, e.g., there is no difference between a 10 m sample and a 1 m sample. A one metre composite length was chosen as this represented the dominant sample length. A histogram with sample length statistics (pre-compositing) is presented in Figure 14.89.

Datamine software (process COMPDH) was used to extract variable length 1 m down-hole composites. This adjusts the sample intervals where required to ensure all samples were included in the composite file (i.e., no residuals) while keeping the sample interval as close to the desired sample interval as possible.

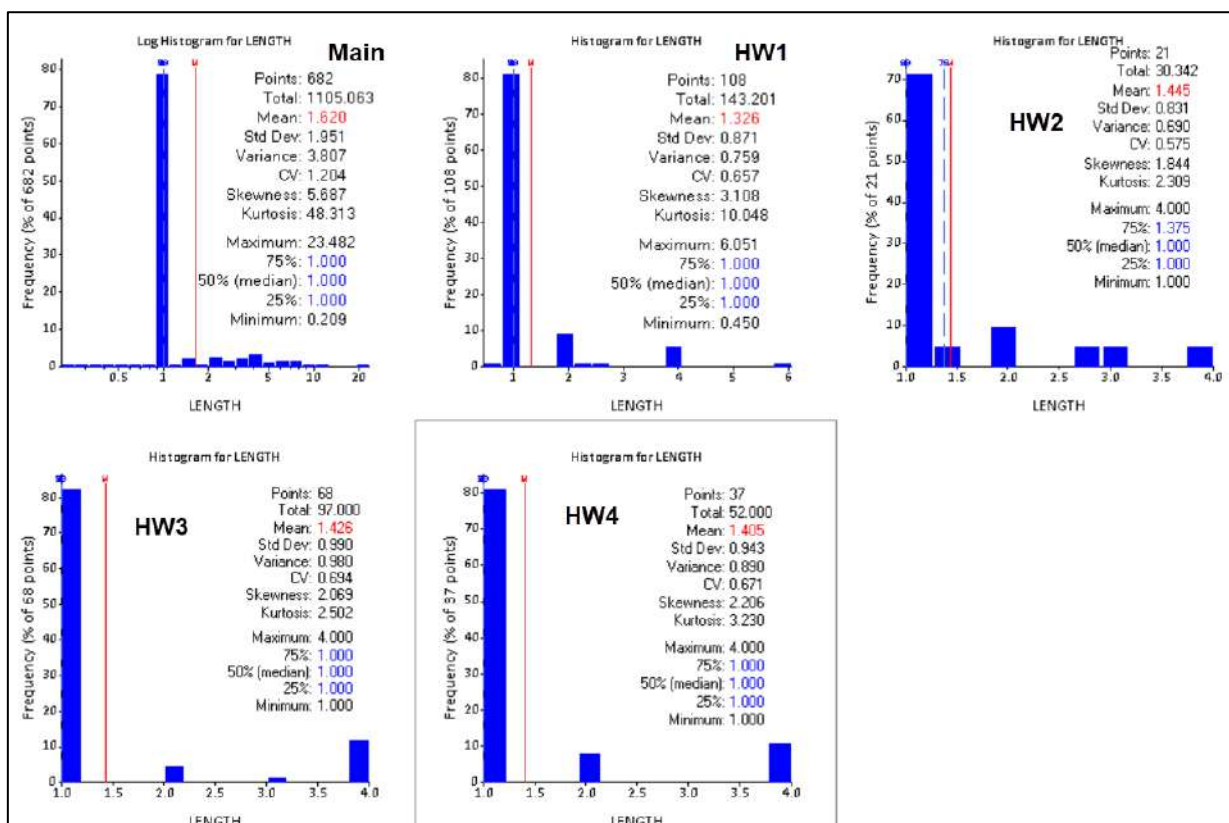


Figure 14.89 Histograms of San Antonio sample lengths by lode

14.3.7 Statistical Analysis

Statistical analysis of copper, gold, and silver were undertaken using Snowden Supervisor Version 8.14.3.0 software and TIBCO Spotfire for data visualisation (Figure 14.90).

The analysis was completed to understand the global representative distribution of each element and account for any bias introduced by clustering of data or by extreme outliers.

Analysis of the ratio of Copper to Sulphide across domains indicates that there may be non-sulphide copper species such as limonites which are not yet interpreted and estimated (Figure 14.91).

Future work at San Antonio will provide constraint to non-sulphide species samples and review the impact on domains

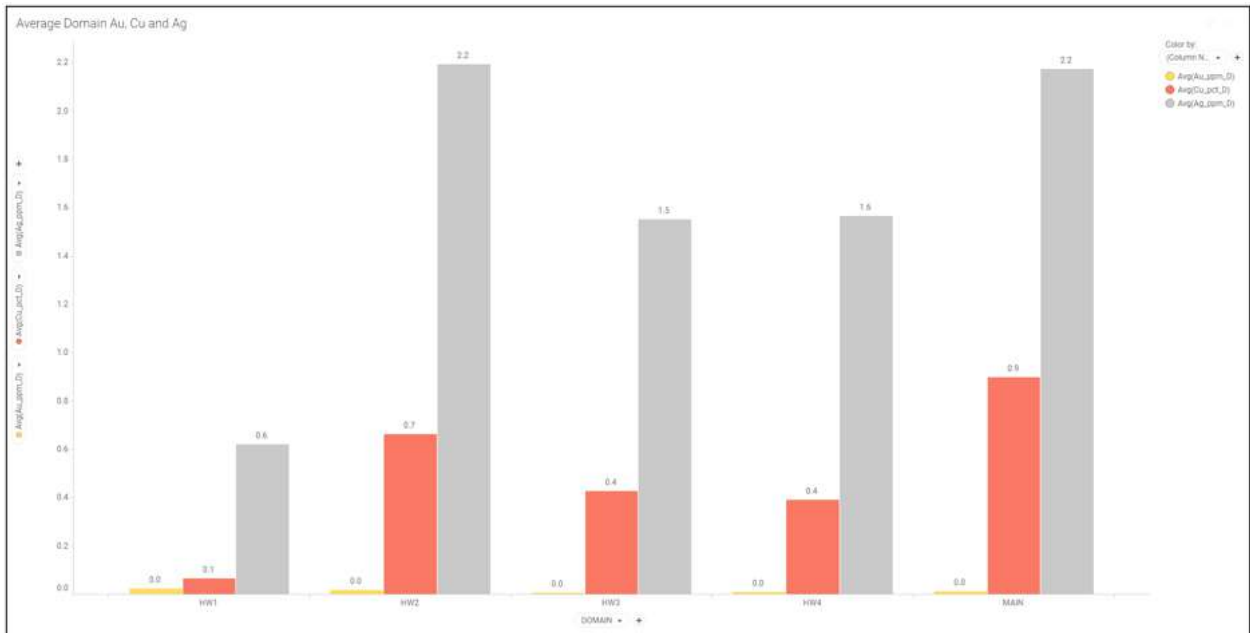


Figure 14.90 Domain Analysis by lode for Au, Ag and Cu% elements

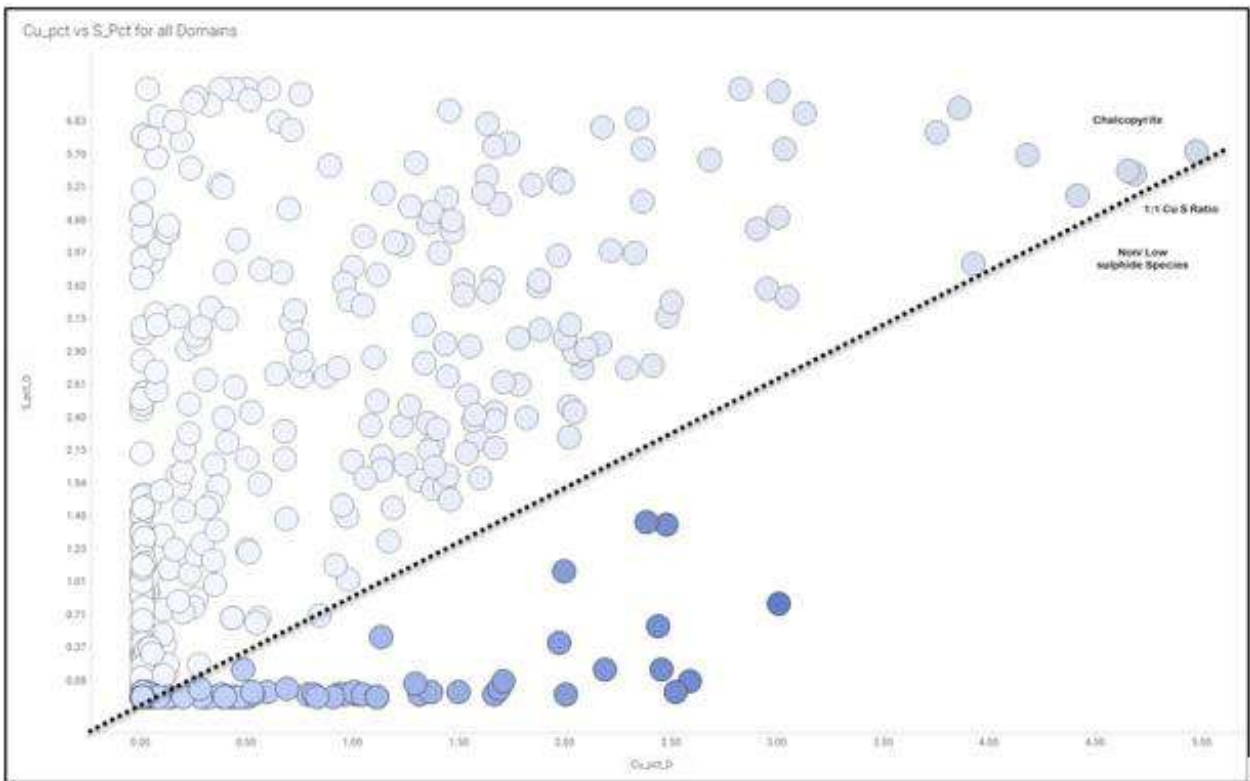


Figure 14.91 Cu/S scatter plot showing presence of non-chalcopyrite species

14.3.8 Top Cuts

Top-cutting is the process where the values greater than the top-cut value are reduced to the top-cut value. When computing statistics, we assume that there is only one population and that all

samples belong to that population. Outliers or extreme values are often observed. Their impact can be a serious overestimation of the average grade and metal and their variability. The mean, variance, variogram and block model estimates are also affected by extreme values. The selection of an appropriate top cut involves some subjectivity but takes into account the characteristics of the population distribution.

Each element in each domain were examined using log histograms, log probability plots, grade disintegration and the general statistics of each lode. The top-cuts have been chosen to reduce the potential smearing of extremely high grades. Top-cuts are summarised in Table 14.98.

Table 14.98 San Antonio mineralised domains top-cut analysis

Element	Domain	Raw				Top cut			
		Number	Max	Mean	CV	Value	# Cut	Mean	CV
Cu%	Main	516	8.55	1.38	0.91	6	1	1.38	0.90
	HW1	81	2.80	0.33	2.02	2	3	0.30	1.90
	HW2	28	3.00	0.62	1.43	-	-	0.62	1.43
	HW3	97	2.34	0.43	1.44	-	-	0.43	1.44
	HW4	52	4.60	0.44	2.01	3	2	0.38	1.80
AU	Main	265	0.17	0.01	1.86	0.1	2	0.01	1.47
	HW1	59	0.85	0.04	3.46	0.3	2	0.03	2.36
	HW2	26	0.10	0.02	1.35	-	-	0.02	1.35
	HW3	97	0.03	0.01	1.18	-	-	0.01	1.18
	HW4	52	0.05	0.01	1.17	-	-	0.01	1.17
AG	Main	260	82.5	2.41	2.24	20	1	2.17	1.09
	HW1	53	2.00	0.62	0.55	-	-	0.62	0.55
	HW2	26	6.90	2.19	1.15	-	-	2.19	1.15
	HW3	97	8.60	1.55	1.18	-	-	1.55	1.18
	HW4	37	14.2	1.84	1.65	8	3	1.56	1.32
MO	Main	260	8.00	1.74	0.72	-	-	1.74	0.72
	HW1	53	54.0	2.72	2.68	2	5	1.51	0.49
	HW2	26	2.00	1.63	0.30	-	-	1.63	0.30
	HW3	97	2.00	0.97	0.24	-	-	0.97	0.24
	HW4	52	6.00	2.12	0.70	-	-	2.12	0.70

14.3.9 Block modelling

An unrotated block model was constructed with a parent block size of 5mE by 10mN by 5mRL.

Parent block estimation was used with the blocks sub-celled down to 1m (in mE and mRL) or 2m (in mN) to sufficiently honour the volume and geometry of the wireframes.

Block model parameters are shown in Table 14.99. The block model was flagged by the wireframes as shown in Table 14.100.

Final model fields are listed in Table 14.101.

Table 14.99 Block model dimensions

Dimension	Minimum	Maximum	Extent	Size	Number	Sub-cell (m)
Easting (mE)	342000	342700	700	5	140	1
Northing (mN)	6818180	6819349	1170	10	117	2
Elevation (mRL)	920	1350	430	5	86	1

Table 14.100 San Antonio volume model coding

Field	Description	Code
DOMAIN	Estimation Domain	WASTE = Unmineralised
		AIR = Above Topography
		MAIN = Main Lode
		HW1 = Parallel Lode 1
		HW2 = Parallel Lode 2
		HW3 = Parallel Lode 3
		HW4 = Parallel Lode 4
WTCODE	Oxidation state	1000 = Oxide (Not Used)
		2000 = Transitional (Not Used)
		3000 = Fresh
INSITU	Depletion State	0= Insitu
		1= Depleted
RESCAT	Classification	1 = Measured (Not Used)
		2 = Indicated (Not Used)
		3 = Inferred
		4 = Unclassified

Table 14.101 Block Model fields

Field	Description
DOMAIN	Text code for domain
WTCODE	Numeric code for weathering domain
DENSITY	Assigned density
INSITU	Depletion status of blocks
CU	Estimated Cu %
AU	Estimated Au g/t
AG	Estimated Ag g/t
MO	Estimated Mo ppm
CO	Estimated Co ppm
RESCAT	Numeric code for resource classification
CUEQ_RES	Calculated copper equivalent
XC	Real world X centroid
YC	Real world Y centroid
ZC	Real world Z centroid

14.3.10 Grade Estimation

14.3.10.1 Introduction

Grade estimation has been completed using typical narrow-vein style estimation strategies. For all lodes, inverse distance (ID) (with powers of 2 and 3) and conventional ordinary kriging (OK)

methodologies were tested to ascertain the estimation technique which best reflects the understanding of the mineralisation at San Antonio.

The biggest factor for San Antonio is modelling short-range variability as the dense spaced channel data suggests metal grades (particularly Cu%) can be highly variable over a short distance.

14.3.10.2 Estimation Methodology

14.3.10.2.1 Main Lode

Inverse distance (ID^2 and ID^3) and OK estimation approaches were tested for the Main lode at San Antonio, for copper, gold, silver, and molybdenum.

Variography was attempted for all elements, although only the copper variogram was suitable for use (Figure 14.92). All estimated elements use the copper variogram for the OK estimate.

Kriging neighbourhood analysis has been completed for each domain and used as a guide for the selection of sample counts, search distances, discretization points and block size (Figure 14.93).

Search parameters are tabulated in Table 14.102.

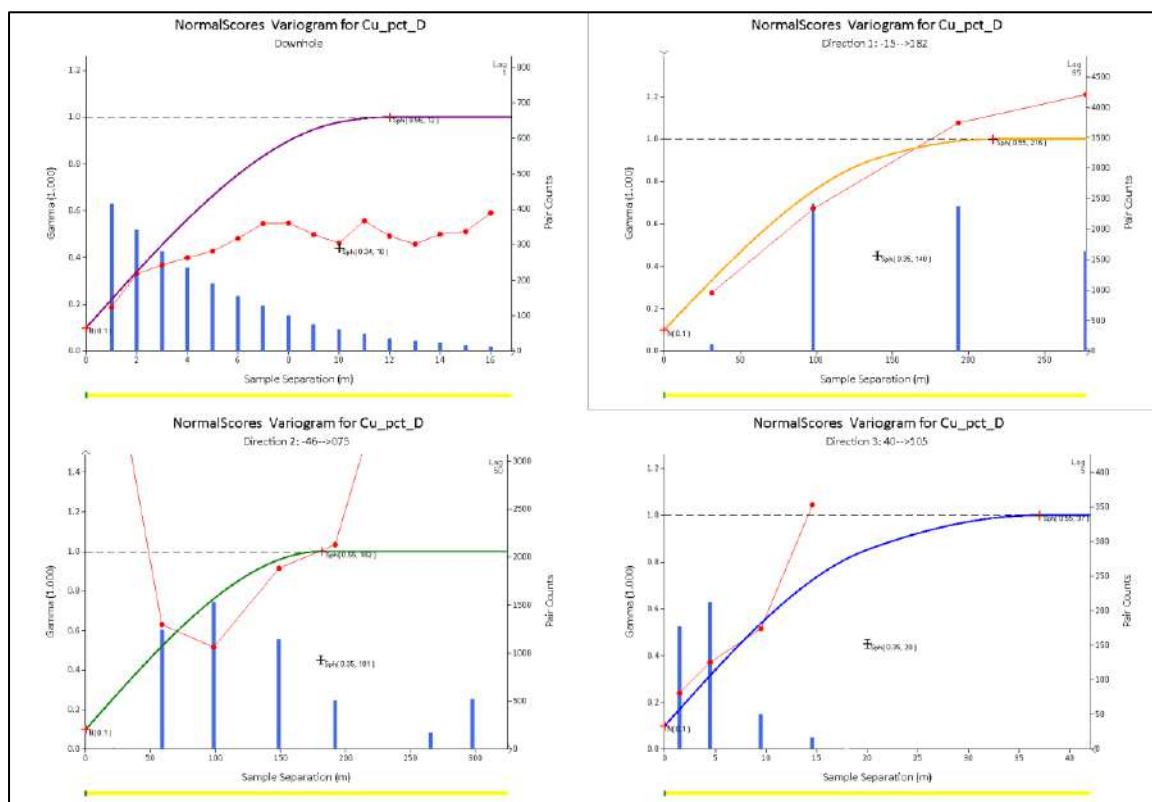


Figure 14.92 Variograms for Main lode Cu% variable

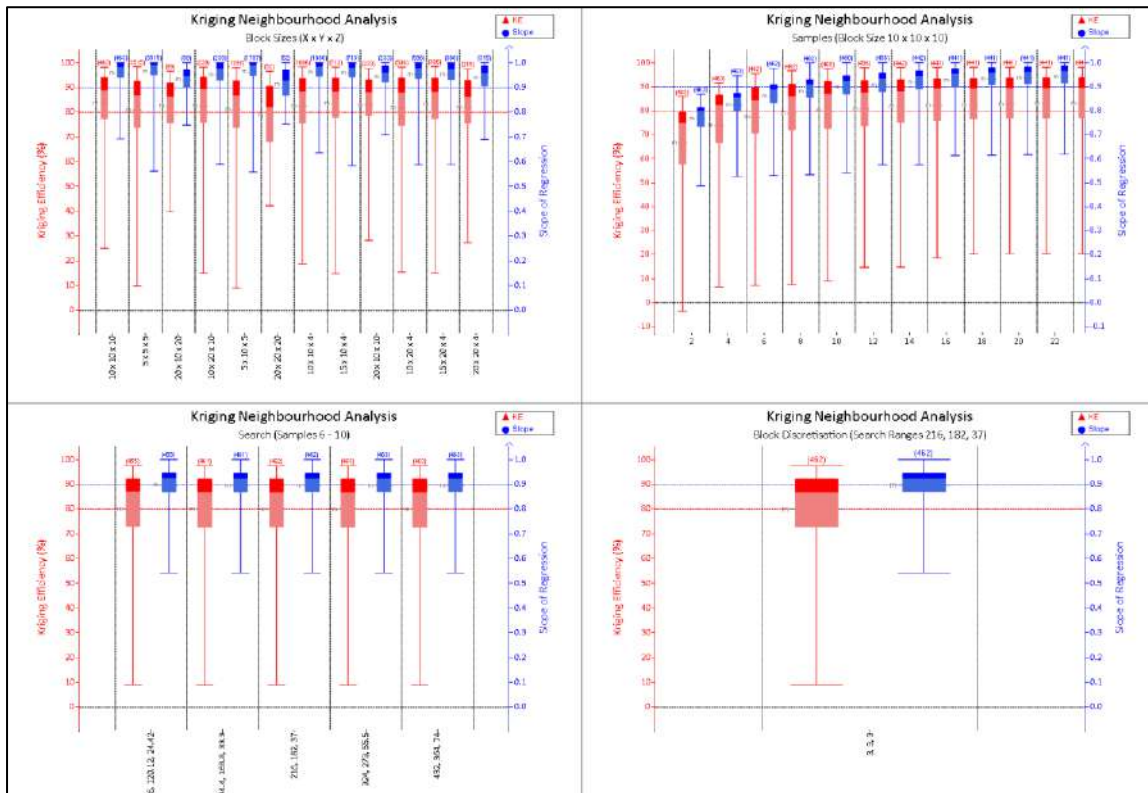


Figure 14.93 KNA for Main lode Cu% variable

Table 14.102 Estimation parameters

Parameter	1 st Search Pass	2 nd Search Pass	3 rd Search Pass
Direction 1 Search	140 m	280 m	560 m
Direction 2 Search	120 m	240 m	480 m
Direction 3 Search	30 m	60 m	120 m
Minimum Composites	5	5	6
Maximum Composites	8	10	12
Octant Strategy	No	No	No
Parent Estimation	Yes	Yes	Yes
Max composites per drillhole	unlimited	unlimited	unlimited

Output models are compared to the input data for all elements estimated. For the Main lode at San Antonio, it has been determined that the ID³ estimate provides the best representation of the input data variability and is used for all elements (Figure 14.94).

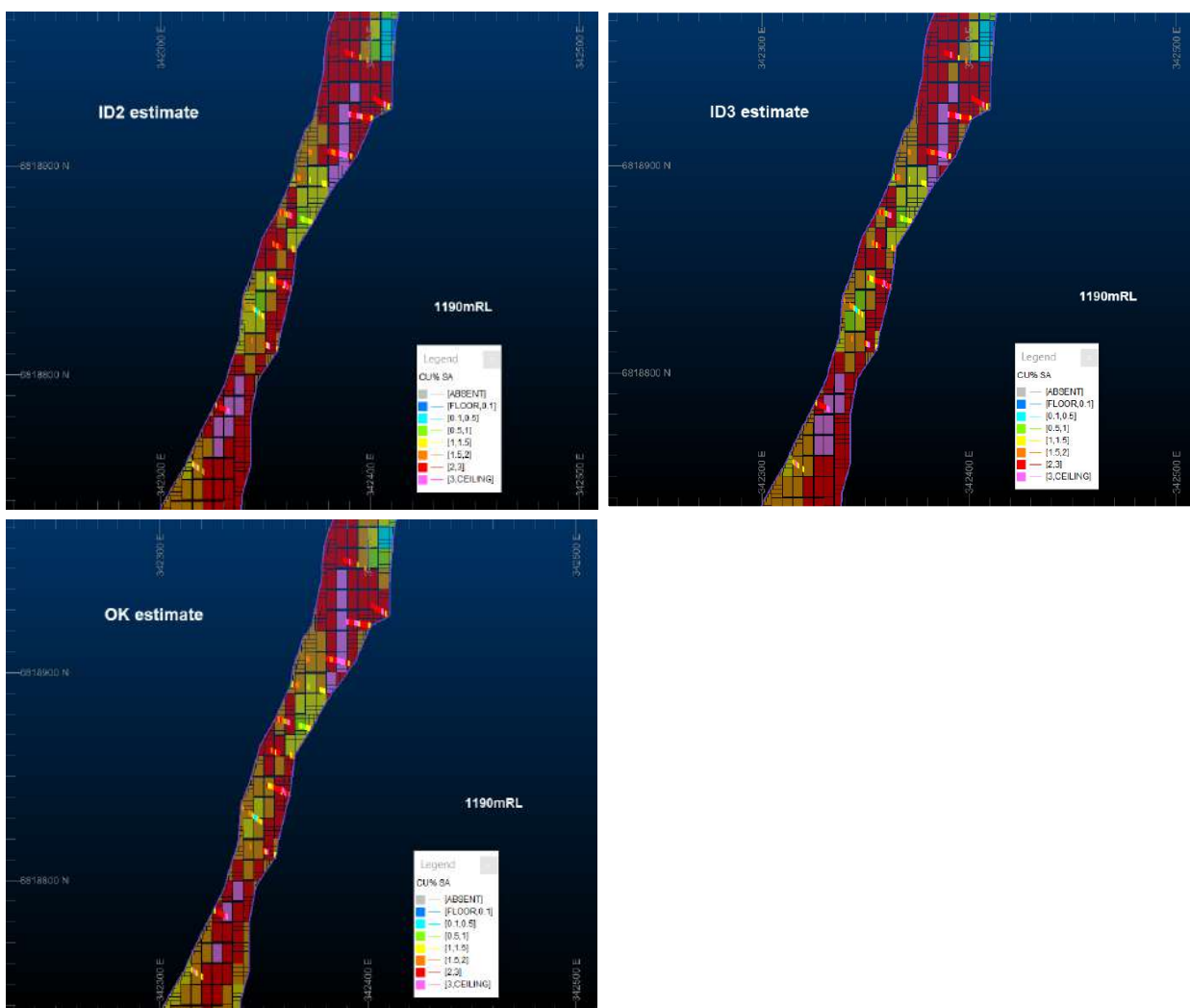


Figure 14.94 Comparison of different estimation methodologies for the San Antonio Main lode Cu% estimate (plan view section at 1,190 mRL)

14.3.10.2.2 Hanging Wall Lodes

ID³ and OK estimation approaches were tested for the HW lodes at San Antonio, for copper, gold, silver, and molybdenum.

Variography was not attempted due to low sample counts in the HW lodes. The OK estimate utilised the copper variogram from the Main lode.

Kriging neighbourhood analysis was also taken from the copper Main lode.

Output models are compared to the input data for all elements estimated (Figure 14.95). For all HW lodes at San Antonio, the OK estimate provides the best representation of the input data.

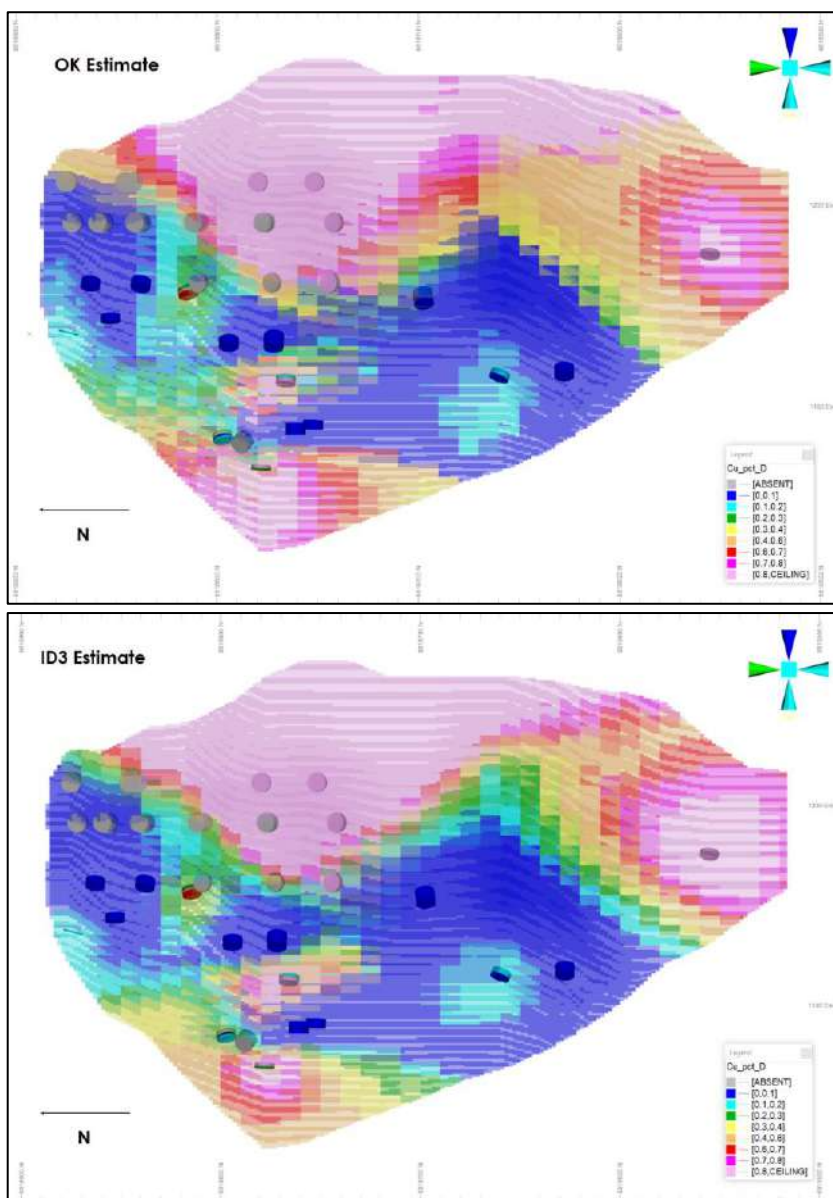


Figure 14.95 Comparison of OK and ID³ methodologies for the San Antonio HW1 lode Cu% estimate (long section view looking east)

14.3.11 Bulk Density

107 bulk density samples were analysed and an average density value of 3 t/m³ assigned to all blocks in the San Antonio estimate (Table 14.103). No differentiation was made by lithology as:

- Most of the contained metal within the San Antonio estimate is IDO (dolerite) hosted
- Limited measurements exist for samples outside of the IDO unit

Table 14.103 Bulk Density Values by Lithology

LITHOLOGY	NUMBER OF ANALYSES	AVERAGE DENSITY
FPF (Felsic Porphyry)	10	2.95
SAQ (Quartz Arenite)	7	2.80
IDO (Dolerite)	89	3.01

An upcoming metallurgical drilling campaign will provide additional density data, with plans also in place to take bulk sample from the current underground operations for bulk density testwork.

14.3.12 Estimate Validation

The estimates were validated using a three-stage comparison between top-cut composites and the estimated variables. The first stage involves calculating the global statistics of the composites compared to the tonnage weighted averages of estimated variables. The second stage involves comparing statistics in elevation slices along the mineralisation and the third involves a detailed visual comparison by section to ensure the estimated variables honour the input composite data.

The comparison of average grade of the composites with the first search pass estimation is contained in Table 14.104 for copper.

Trend analysis was completed for each domain using elevation. An example is shown in Figure 14.96 which presents the main domain.

Visual validation was completed in various orientations of drillhole grades and model grades, Figure 14.97 and Figure 14.98.

Excluding the HW2 lode, validations show an excellent reflection of the input composite grades in the output model. The somewhat poor global validation in HW2 is a reflection of the variability in grade across the domain, where the trend plot and visual validation show a good reflection of the input composite grades in the output model.

Table 14.104 Estimation global validation – Cu%

Domain	Composites – top-cut, declustered	Model – 1 st estimation pass	% Difference of 1 st pass
Main	1.33	1.30	-2.2%
HW1	0.43	0.46	7.8%
HW2	0.53	0.87	66.1%
HW3	0.38	0.39	3.1%
HW4	0.38	0.39	4.5%

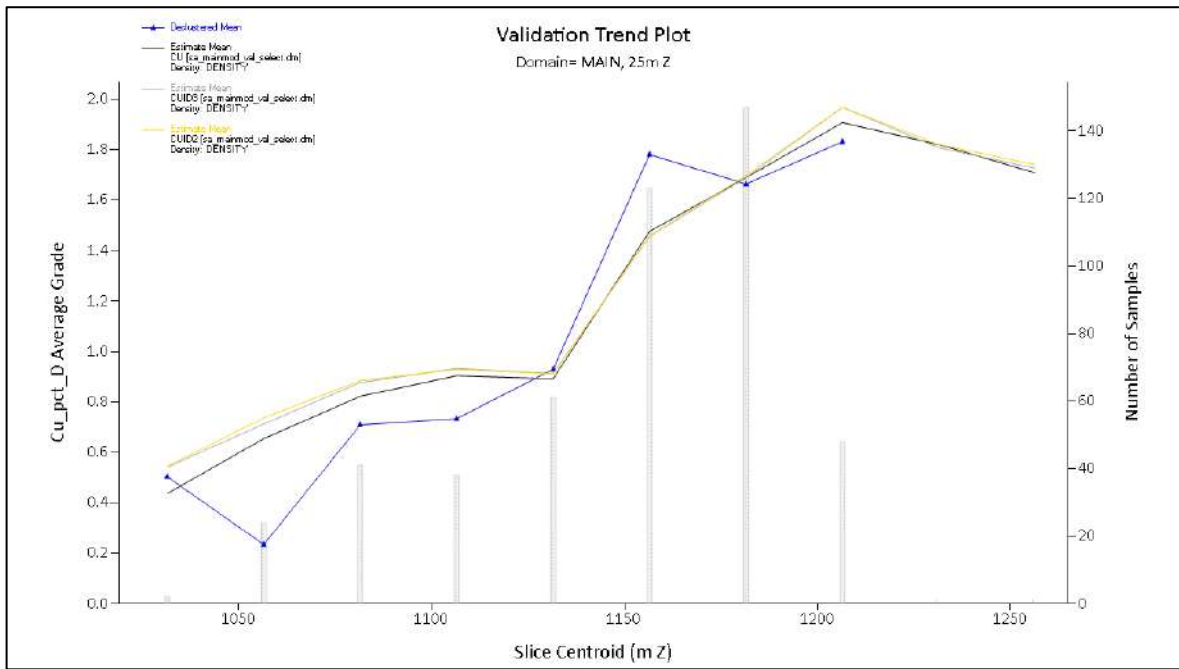


Figure 14.96 Validation trend plot – Cu% – Main Lode search pass 1

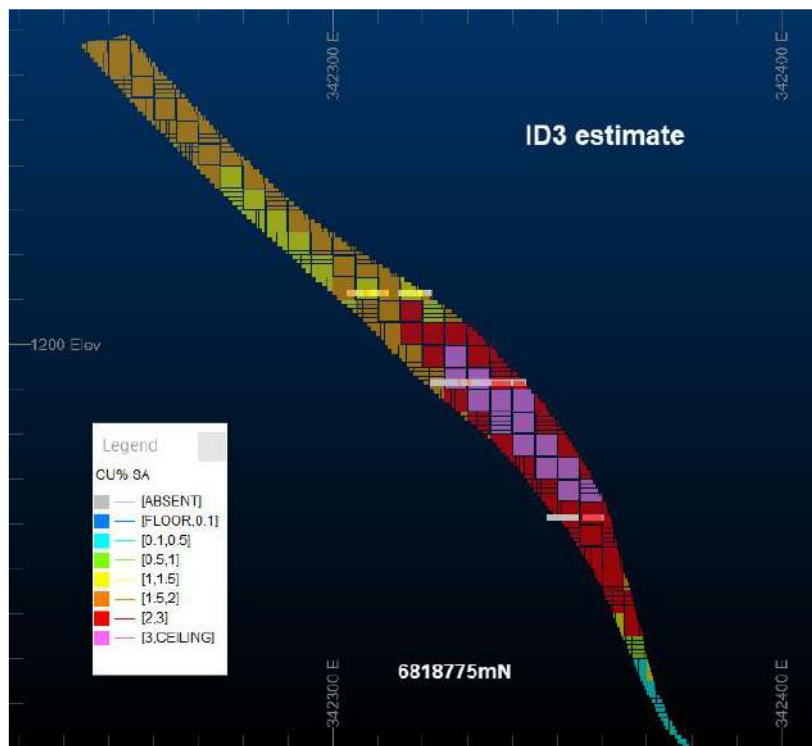


Figure 14.97 Visual validation of drillholes versus model Cu% grade – Main Lode, Cross Section 6818775mN

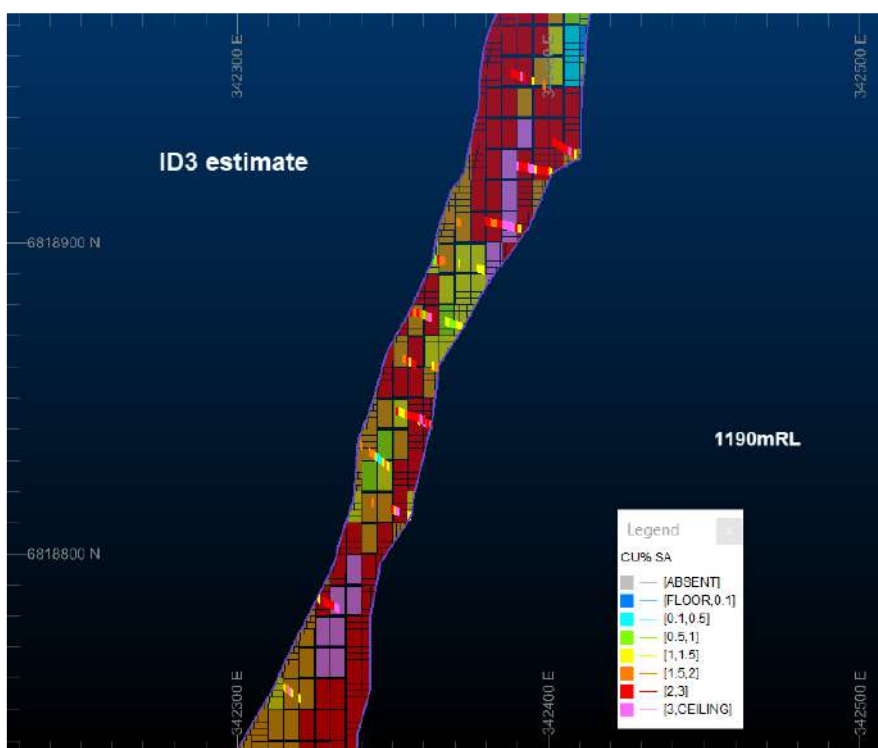


Figure 14.98 Plan view on 1190mRL showing Main domain and Cu% in the drillholes and mineralised block model.

14.3.13 Resource Classification

The San Antonio Mineral Resource estimate has been classified considering the guidelines provided in NI 43-101.

A 'Mineral Resource' is a concentration or occurrence of solid material of economic interest in or on the Earth's crust in such form, grade (or quality), and quantity that there are reasonable prospects for eventual economic extraction. The location, quantity, grade (or quality), continuity and other geological characteristics of a Mineral Resource are known, estimated or interpreted from specific geological evidence and knowledge, including sampling. Mineral Resources are sub-divided, in order of increasing geological confidence, into Inferred, Indicated and Measured categories (Figure 14.78 and Figure 14.100).

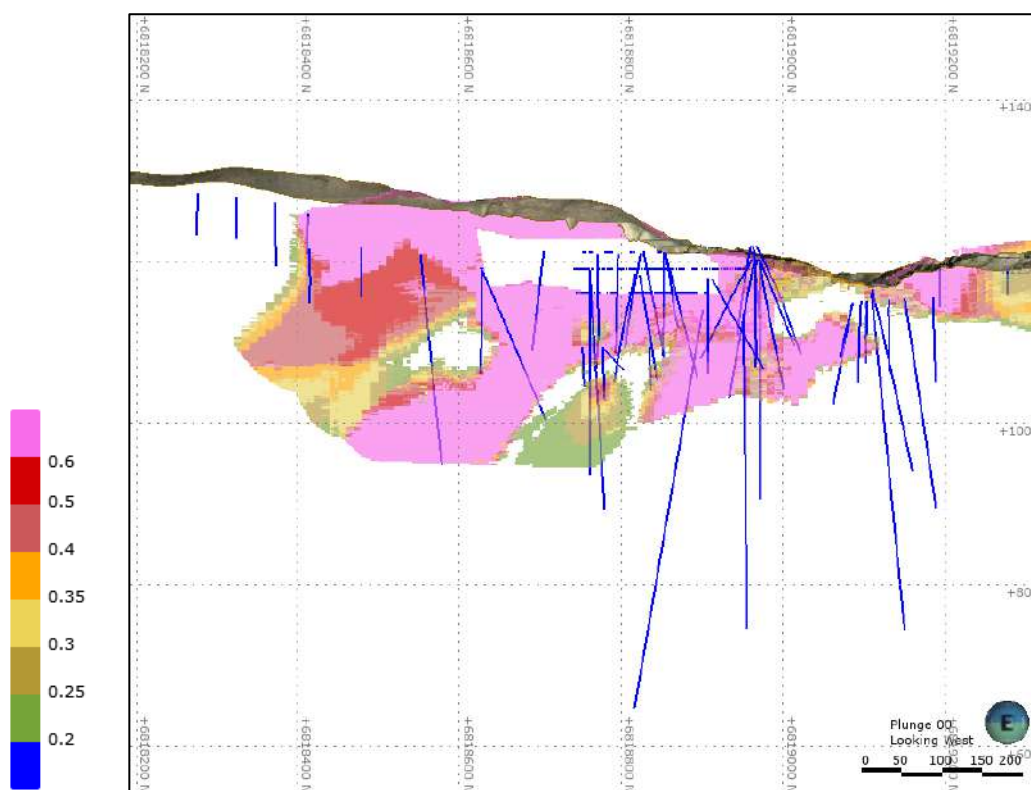


Figure 14.99 Oblique view looking west Blocks CuEq% \geq 0.2 , and insitu =0. Inferred only.

The classification applied to the San Antonio Mineral Resource estimate is based on an assessment of several factors including:

- Nature of data and data quality including QAQC.
- Data spacing.
- Confidence in the geological interpretation and mineralisation interpretation.
- Demonstrated continuity of geology and mineralisation.
- Reliability of estimated variables.
- Prospects of eventual economic extraction.

The data quality underpinning the estimate is considered to be appropriate for the maximum Inferred classification. Data derived from recent (2018) drilling by HCH is considered to be of an excellent nature and represents 49.5% of the total length of drillhole data.

A string was constructed to control the extents of classification, with the file inf.str used to constrain inferred resources. Blocks outside of this zone were classified as Unclassified. The boundary was determined based on the drillhole spacing and complexity of mineralisation.

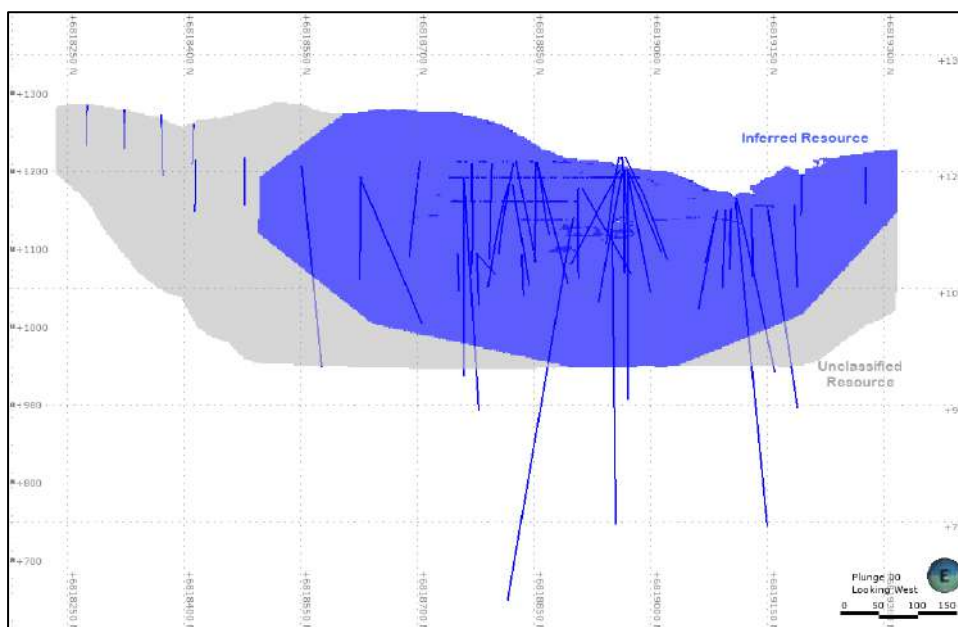


Figure 14.100 Longsection looking West, showing Inferred and Unclassified block extents across San Antonio

14.4 Calculation of Copper Equivalent

Copper Equivalent (CuEq) reported for the resource were calculated using the following formula:

$$CuEq\% = ((Cu\% \times Cu \text{ price } 1\% \text{ per tonne} \times Cu_recovery) + (Mo \text{ ppm} \times Mo \text{ price per g/t} \times Mo_recovery) + (Au \text{ ppm} \times Au \text{ price per g/t} \times Au_recovery) + (Ag \text{ ppm} \times Ag \text{ price per g/t} \times Ag_recovery)) / (Cu \text{ price } 1\% \text{ per tonne}).$$

The Metal Prices applied in the calculation were:

$$Cu=3.00 \text{ USD/lb}, Au=1,700 \text{ USD/oz}, Mo=14 \text{ USD/lb}, Ag=20 \text{ USD/oz}$$

For Cortadera, the average Metallurgical Recoveries were:

$$Cu=83\%, Au=56\%, Mo=82\%, Ag=37\%$$

For Productora, the average Metallurgical Recoveries were:

$$Cu=83\%, Au=43\%, Mo=42\%$$

14.5 Costa Fuego Resource Reporting

The Cortadera, San Antonio and Productora Mineral Resource Estimates have been combined to create the Costa Fuego Mineral Resource Estimate. This represents an update to the Cortadera and Productora Resource Estimates, and maiden Estimate for San Antonio. The final reported tonnes and grade by classification can be found in Table 14.105 to Table 14.108 (Costa Fuego combined and broken down by Resource area). Grade Tonnage curves for both the Open Pit and Underground Resource can be found in Figure 14.101.

The information in this report that relates to Mineral Resources for Cortadera, Productora and San Antonio which constitute the combined Costa Fuego Project is based on information compiled by Ms. Elizabeth Haren, a Qualified Person who is a Member and Chartered

Professional of The Australasian Institute of Mining and Metallurgy and a Member of the Australian Institute of Geoscientists.

Table 14.105 Costa Fuego Project Mineral Resource Summary – reported by classification (31st March 2022)

Costa Fuego OP Resource		Grade					Contained Metal				
Classification (+0.21% CuEq*)	Tonnes (Mt)	CuEq (%)	Cu (%)	Au (g/t)	Ag (g/t)	Mo (ppm)	Copper Eq (tonnes)	Copper (tonnes)	Gold (ounces)	Silver (ounces)	Molybdenum (tonnes)
Indicated	576	0.46	0.37	0.10	0.37	91	2,658,000	2,145,000	1,929,000	6,808,000	52,200
M+I Total	576	0.46	0.37	0.10	0.37	91	2,658,000	2,145,000	1,929,000	6,808,000	52,200
Inferred	147	0.35	0.30	0.05	0.23	68	520,000	436,000	220,000	1,062,000	10,000

Costa Fuego UG Resource		Grade					Contained Metal				
Classification (+0.30% CuEq*)	Tonnes (Mt)	CuEq (%)	Cu (%)	Au (g/t)	Ag (g/t)	Mo (ppm)	Copper Eq (tonnes)	Copper (tonnes)	Gold (ounces)	Silver (ounces)	Molybdenum (tonnes)
Indicated	148	0.51	0.39	0.12	0.78	102	750,000	578,000	559,000	3,702,000	15,000
M+I Total	148	0.51	0.39	0.12	0.78	102	750,000	578,000	559,000	3,702,000	15,000
Inferred	56	0.38	0.30	0.08	0.54	61	211,000	170,000	139,000	971,000	3,400

Costa Fuego Total Resource		Grade					Contained Metal				
Classification	Tonnes (Mt)	CuEq (%)	Cu (%)	Au (g/t)	Ag (g/t)	Mo (ppm)	Copper Eq (tonnes)	Copper (tonnes)	Gold (ounces)	Silver (ounces)	Molybdenum (tonnes)
Indicated	725	0.47	0.38	0.11	0.45	93	3,408,000	2,755,000	2,564,000	10,489,000	67,400
M+I Total	725	0.47	0.38	0.11	0.45	93	3,408,000	2,755,000	2,564,000	10,489,000	67,400
Inferred	202	0.36	0.30	0.06	0.31	66	731,000	605,000	359,000	2,032,000	13,400

Reported on a 100% Basis - combining Mineral Resource estimates for the Cortadera, Productora and San Antonio deposits. Figures are rounded, reported to appropriate significant figures, and reported in accordance with CIM and NI 43-101. Metal rounded to nearest thousand, or if less, to the nearest hundred. Total Resource reported at +0.21% CuEq for open pit and +0.30% CuEq for underground.

Table 14.106 Cortadera Mineral Resource Summary – reported by classification (31st March 2022)

Cortadera OP Resource		Grade					Contained Metal				
Classification	Tonnes	CuEq	Cu	Au	Ag	Mo	Copper Eq	Copper	Gold	Silver	Molybdenum
(+0.21% CuEq*)	(Mt)	(%)	(%)	(g/t)	(g/t)	(ppm)	(tonnes)	(tonnes)	(ounces)	(ounces)	(tonnes)
Indicated	323	0.44	0.34	0.12	0.66	53	1,411,000	1,102,000	1,284,000	6,808,000	17,100
M+I Total	323	0.44	0.34	0.12	0.66	53	1,411,000	1,102,000	1,284,000	6,808,000	17,100
Inferred	53	0.32	0.25	0.08	0.46	62	168,000	132,000	135,000	778,000	3,300

Cortadera UG Resource		Grade					Contained Metal				
Classification	Tonnes	CuEq	Cu	Au	Ag	Mo	Copper Eq	Copper	Gold	Silver	Molybdenum
(+0.30% CuEq*)	(Mt)	(%)	(%)	(g/t)	(g/t)	(ppm)	(tonnes)	(tonnes)	(ounces)	(ounces)	(tonnes)
Indicated	148	0.51	0.39	0.12	0.78	102	750,000	578,000	559,000	3,702,000	15,000
M+I Total	148	0.51	0.39	0.12	0.78	102	750,000	578,000	559,000	3,702,000	15,000
Inferred	56	0.38	0.30	0.08	0.54	61	211,000	170,000	139,000	971,000	3,400

Cortadera Total Resource		Grade					Contained Metal				
Classification	Tonnes	CuEq	Cu	Au	Ag	Mo	Copper Eq	Copper	Gold	Silver	Molybdenum
(+0.21% CuEq*)	(Mt)	(%)	(%)	(g/t)	(g/t)	(ppm)	(tonnes)	(tonnes)	(ounces)	(ounces)	(tonnes)
Indicated	471	0.46	0.36	0.12	0.69	68	2,161,000	1,680,000	1,843,000	10,509,000	32,200
M+I Total	471	0.46	0.36	0.12	0.69	68	2,161,000	1,680,000	1,843,000	10,509,000	32,200
Inferred	108	0.35	0.28	0.08	0.50	62	379,000	301,000	274,000	1,749,000	6,700

Reported on a 100% Basis. Figures are rounded, reported to appropriate significant figures, and reported in accordance with CIM and NI 43-101. Metal rounded to nearest thousand, or if less, to the nearest hundred. Total Resource reported at +0.21% CuEq for open pit and +0.30% CuEq for underground

Table 14.107 Productora Mineral Resource Summary – reported by classification (31st March 2022)

Productora Total Resource		Grade					Contained Metal				
Classification	Tonnes	CuEq	Cu	Au	Ag	Mo	Copper Eq	Copper	Gold	Silver	Molybdenum
(+0.21% CuEq*)	(Mt)	(%)	(%)	(g/t)	(g/t)	(ppm)	(tonnes)	(tonnes)	(ounces)	(ounces)	(tonnes)
Indicated	253	0.49	0.41	0.08		139	1,247,000	1,043,000	646,000		35,100
M+I Total	253	0.49	0.41	0.08		139	1,247,000	1,043,000	646,000		35,100
Inferred	90	0.34	0.29	0.03		75	305,000	259,000	91,000		6,800

Reported on a 100% Basis. Figures are rounded, reported to appropriate significant figures, and reported in accordance with CIM and NI 43-101. Metal rounded to nearest thousand, or if less, to the nearest hundred. Total Resource reported at +0.21% CuEq for open pit.

Table 14.108 San Antonio Mineral Resource Summary – reported by classification (31st March 2022)

San Antonio Total Resource		Grade					Contained Metal				
Classification	Tonnes	CuEq	Cu	Au	Ag	Mo	Copper Eq	Copper	Gold	Silver	Molybdenum
(+0.21% CuEq*)	(Mt)	(%)	(%)	(g/t)	(g/t)	(ppm)	(tonnes)	(tonnes)	(ounces)	(ounces)	(tonnes)
Inferred	4.2	1.2	1.1	0.01	2.1	1.5	48,100	47,400	2,000	287,400	6

Reported on a 100% Basis. Figures are rounded, reported to appropriate significant figures, and reported in accordance with CIM and NI 43-101. Metal rounded to nearest thousand, or if less, to the nearest hundred. Total Resource reported at +0.21% CuEq for open pit

Table 14.109 Costa Fuego Grade Tonnage CuEq cut-offs by classification (Open pit – top and Underground – bottom)

CuEq Cut-off	Costa Fuego Open Pit Indicated						CuEq Cut-off	Costa Fuego Open Pit Inferred					
	MT	CuEq%	Cu%	Au	Ag	Mo		MT	CuEq%	Cu%	Au	Ag	Mo
0.70	76	0.89	0.73	0.19	0.46	160	0.70	6	1.22	1.12	0.10	1.25	93
0.65	98	0.84	0.69	0.18	0.46	153	0.65	7	1.11	1.01	0.10	1.04	102
0.60	123	0.80	0.65	0.17	0.45	148	0.60	9	1.00	0.89	0.10	0.84	118
0.55	156	0.75	0.61	0.16	0.45	140	0.55	13	0.89	0.78	0.10	0.68	124
0.50	201	0.70	0.57	0.16	0.46	129	0.50	17	0.79	0.68	0.10	0.57	120
0.45	253	0.65	0.53	0.15	0.46	118	0.45	24	0.70	0.60	0.09	0.48	113
0.40	305	0.62	0.50	0.14	0.44	111	0.40	32	0.63	0.54	0.08	0.41	106
0.35	355	0.58	0.47	0.13	0.43	105	0.35	45	0.56	0.47	0.07	0.35	97
0.30	412	0.55	0.44	0.12	0.41	101	0.30	68	0.48	0.40	0.06	0.31	87
0.28	440	0.53	0.43	0.12	0.40	98	0.28	81	0.45	0.38	0.06	0.30	83
0.25	488	0.50	0.41	0.11	0.39	95	0.25	103	0.41	0.34	0.05	0.27	77
0.23	529	0.48	0.39	0.11	0.38	93	0.23	122	0.38	0.32	0.05	0.25	73
0.21	576	0.46	0.37	0.10	0.37	91	0.21	147	0.35	0.30	0.05	0.23	68
0.15	747	0.40	0.32	0.09	0.32	82	0.15	277	0.27	0.23	0.04	0.16	56

CuEq Cut-off	Costa Fuego Underground Indicated						CuEq Cut-off	Costa Fuego Underground Inferred					
	MT	CuEq%	Cu%	Au	Ag	Mo		MT	CuEq%	Cu%	Au	Ag	Mo
0.70	18	0.81	0.62	0.20	1.16	167	0.70	1	0.76	0.59	0.17	0.86	163
0.65	25	0.78	0.59	0.18	1.10	167	0.65	1	0.72	0.57	0.15	0.82	141
0.60	33	0.74	0.56	0.17	1.04	164	0.60	1	0.69	0.55	0.14	0.81	125
0.55	46	0.69	0.53	0.16	0.98	156	0.55	2	0.64	0.52	0.13	0.74	103
0.50	64	0.64	0.49	0.15	0.93	141	0.50	5	0.58	0.48	0.12	0.68	83
0.45	85	0.60	0.46	0.14	0.88	128	0.45	8	0.53	0.44	0.11	0.65	72
0.40	106	0.57	0.44	0.13	0.84	118	0.40	15	0.48	0.39	0.10	0.63	68
0.35	127	0.54	0.41	0.12	0.81	109	0.35	30	0.43	0.34	0.09	0.58	67
0.30	148	0.51	0.39	0.12	0.78	102	0.30	56	0.38	0.30	0.08	0.54	61
0.28	159	0.49	0.38	0.11	0.76	99	0.28	70	0.36	0.29	0.07	0.54	60
0.25	171	0.47	0.37	0.11	0.75	96	0.25	90	0.34	0.27	0.07	0.53	57
0.23	181	0.46	0.36	0.11	0.74	94	0.23	106	0.32	0.26	0.07	0.53	56
0.21	190	0.45	0.35	0.10	0.73	92	0.21	123	0.31	0.25	0.07	0.52	55
0.15	212	0.42	0.32	0.10	0.71	88	0.15	156	0.28	0.22	0.06	0.51	53

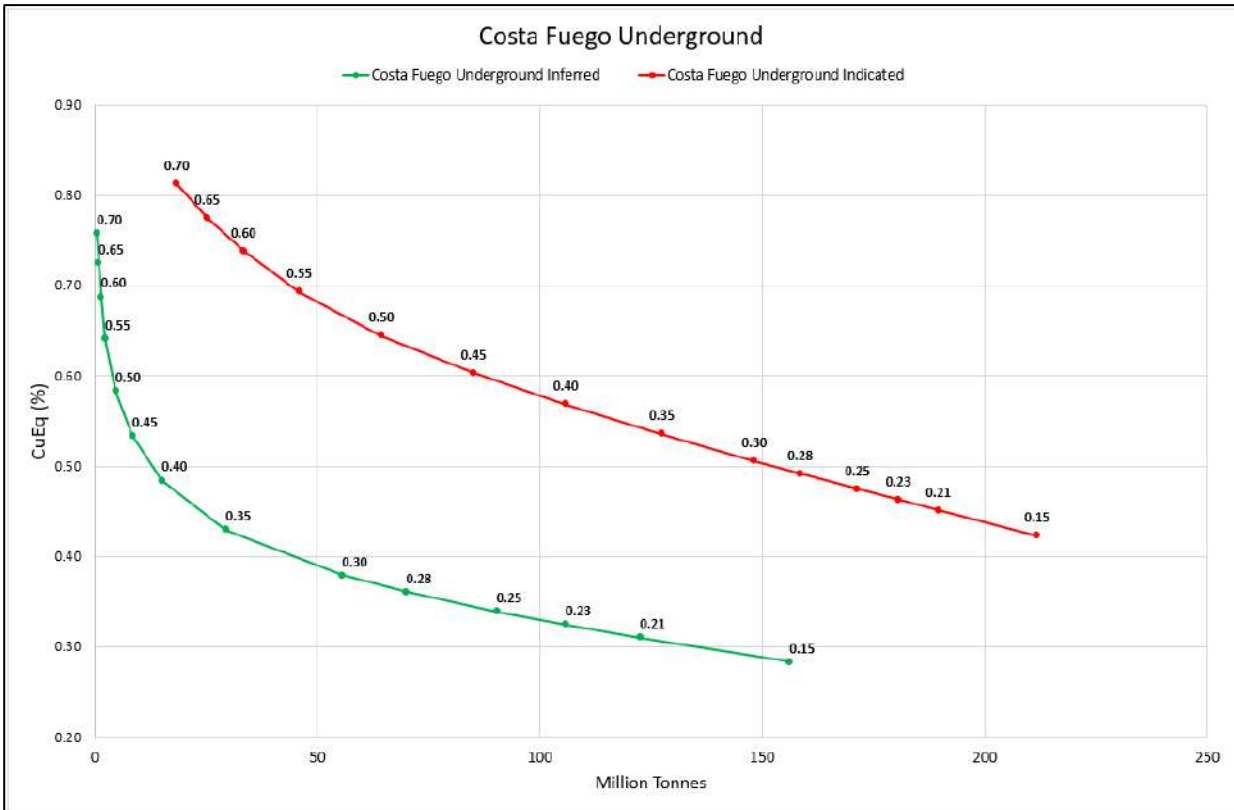
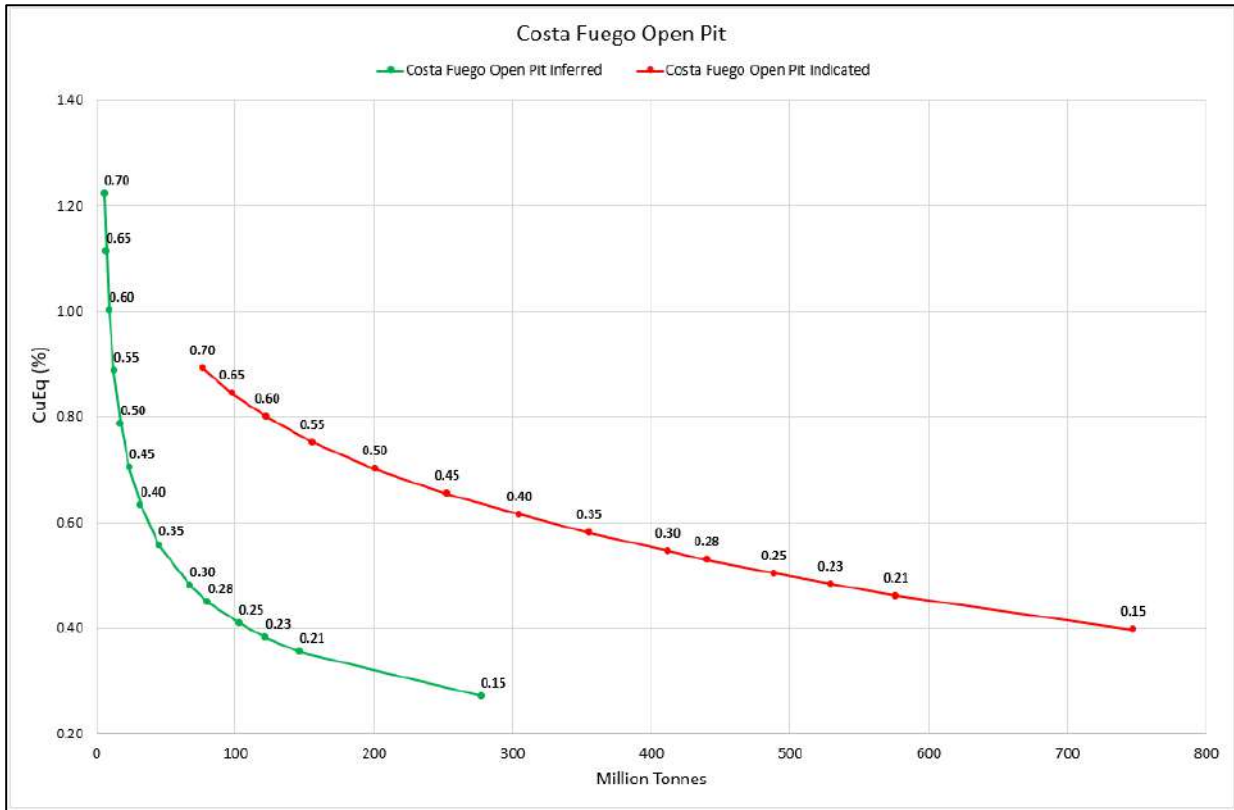


Figure 14.101 Costa Fuego grade-tonnage curves – (Open pit – above and Underground – below)

14.6 Relevant Factors Affecting Resource Estimates

There is currently no known mining, metallurgical, infrastructure, environmental, permitting, legal, title, taxation, socio-economic, marketing, political or other relevant factors which could affect the Mineral Resource estimate

15 MINERAL RESERVE ESTIMATES

As no current feasibility or pre-feasibility studies have been completed to the standard of NI 43-101 at this time, no Mineral Reserves have been estimated for the Costa Fuego Project.

16 MINING METHODS

As no current feasibility or pre-feasibility studies have been completed to the standard of NI 43-101 at this time, no Mineral Reserves have been estimated for the Costa Fuego Project.

17 RECOVERY METHODS

As no current feasibility or pre-feasibility studies have been completed to the standard of NI 43-101 at this time, no Mineral Reserves have been estimated for the Costa Fuego Project.

18 PROJECT INFRASTRUCTURE

As no current feasibility or pre-feasibility studies have been completed to the standard of NI 43-101 at this time, no Mineral Reserves have been estimated for the Costa Fuego Project.

19 MARKET STUDIES AND CONTRACTS

As no current feasibility or pre-feasibility studies have been completed to the standard of NI 43-101 at this time, no Mineral Reserves have been estimated for the Costa Fuego Project.

20 ENVIRONMENTAL STUDIES, PERMITTING AND SOCIAL OR COMMUNITY IMPACT

20.1 Summary

The Environmental Impact Assessment (EIA) of the Project will be submitted for approval using the Environmental Impact Assessment System (EIA System) that is currently being applied in Chile.

The environmental baselines describe the condition of relevant environmental components that may be affected by the Project. Baselines for the Project included the following activities:

- Multiple baseline campaigns covering the Project area and all associated infrastructure areas. For seasonal baselines like flora and fauna, four campaigns have been organised to cover passive and active season's changes.
- The list of non-seasonal baselines comprises 19 components such as archaeology, landscape, palaeontology, human environment, geomorphology, natural risks, etc.
- Main findings in the Project area refer to flora and fauna species under conservation status, archaeology findings with high value and the presence of some families living at the Project.

HCH interacts with many regional and local stakeholders who have an interest in the Project. The stakeholder engagement plan will be divided in two sections to cover firstly the consultation of key stakeholders and secondly, the community development issues. Key stakeholders have been identified in the three concerned districts: Vallenar, Freirina and Huasco. The outcomes of this exercise will be used as the basis to create a stakeholder engagement plan.

The process to assess the environmental impacts of the Project utilised a methodology comprising three stages:

1. Identification of impacts in relation to the activities and Project works
2. Impacts evaluation
3. Impacts ranking.

The outcome of the assessment process identified four significant impacts that require special attention for the baseline campaigns and subsequent studies;

- Alteration and/or loss of terrestrial flora and vegetation
- Alteration and/or loss of habitat for fauna
- Significant changes in the livelihood of human groups
- Alteration of archaeological sites with high value.

20.2 Permit Requirements, Status of Permit Applications and Bond Requirements

20.2.1 Legislation

Since 1997, Chile has adopted an institutional system to prevent environmental degradation caused by projects development. The Environmental Impact Assessment System (EIA System) ensures that investment projects – public and private – introduce the environmental aspect in their design, construction, operation and closure stages to comply with the environmental requirements applicable to them. The EIA System requires the participation of key government agencies to enforce the application of the Environmental Law (Law 19.300 modified by Law 20.417), and sets the framework to obtain specific permits as well as to comply with relevant regulations.

The Environmental Assessment Authority (*SEA – Servicio de Evaluación Ambiental*) is the organisation coordinating the process to provide environmental authorisation to the projects under assessment. The Environmental Assessment Authority requests the views and opinions of specialised government agencies so that the Environmental Commission grants or refuses an Environmental License (*RCA – Resolución de Calificación Ambiental*) and the conditions associated with it.

The Environmental Enforcement Authority (*SMA – Superintendencia de Medio Ambiente*) and the Environmental Courts are in charge of supervising the Project's environmental compliance and resolving environmental claims and allegations, respectively.

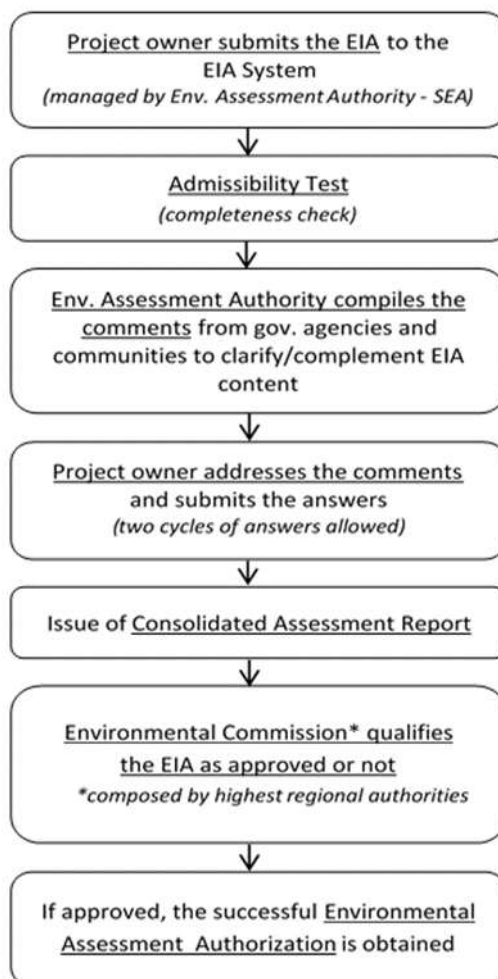


Figure 20.1 Environmental Assessment Process

20.3 EIA Content

Currently, the Project has an EIA study being developed; some figures related with the EIA are outlined below.

- USD \$1.5M spent so far
- Around 11,000 ha covered with baselines studies during four campaigns
- More than eight volumes of information generated
- More than 50 specialists involved.

The EIA breakdown of the Project will cover the following items, in accordance with the Environmental Impact Assessment System Standard (EIAS Standard) requirements:

- Executive summary
- Project description
- Determination and justification of the area of influence and baselines
- Prediction and assessment of the environmental impact of the project

-
- Description of the effects that give rise to an EIA
 - Plan for mitigation, compensation and repair measures
 - Plan contingencies for prevention and emergency management
 - Plan of environmental monitoring
 - Plan for compliance of applicable environmental law and environmental permits
 - Identification of regional and local policies, plans and programs applicable to the project
 - Voluntary commitments
 - Summary sheets
 - Stakeholders engagement actions
 - Negotiation with stakeholders.

20.4 Environmental Protection Act Approvals

The EIAS Standard sets out all the requirements and conditions needed to obtain an RCA¹ and the other permits delivered by specific government agencies; those permits cover a wide range of issues, such as tailing storage facility (TSF) construction and operation, wastewater treatment, land use change, closure plans, etc.

The Project will be assessed within the EIA System through a full EIA, since the nature of the project is listed – under EIAS Standard article 3.i.1 – as one of those that have to be evaluated due to its environmental impacts:

Article 3.i.1: Mining development projects whose activities and works aim to the extraction and exploitation of one or more deposits above 5,000 tonnes/month of extraction capacity.

20.5 Main Environmental Considerations

The Project RCA will include:

- The technical considerations on which such license has been based
- Considerations based on the community comments
- The environmental assessment results
- All standards and requirements the project must follow during its implementation period, including all the specific permits given by the government agencies
- Mitigation, compensation and repair measures to address environmental impacts
- Measurements, analysis and other data that Project owners must provide for checking compliance against the standards, conditions and measures above mentioned.

20.6 Social and Community Related Requirements

HCH interacts with many regional and local stakeholders who have an interest in the Project. HCH has planned diverse actions to engage early with them to find opportunities for creating dialogue and building trust.

20.6.1 Stakeholder Engagement Plan

This overall plan is divided in two sections, firstly the consultation to key stakeholders over the Project, and secondly the community development issues. The first one is the so-called Stakeholder Consultation Plan while the second one is the Community Development Plan. Figure 20.2 shows how the objectives of these plans give shape to the overall Stakeholder Engagement Plan.

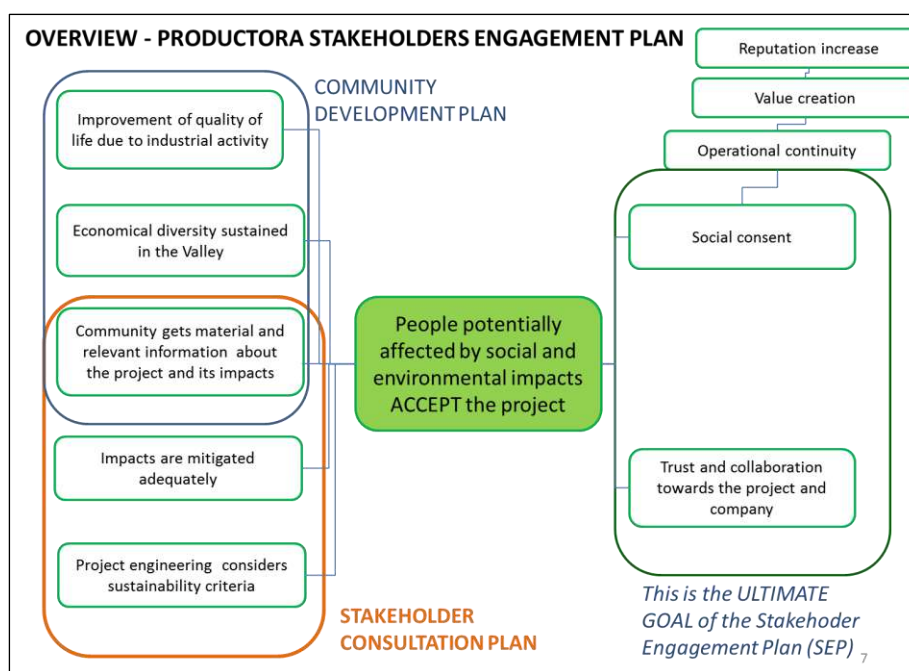


Figure 20.2 Stakeholder Engagement Plan

The most important aspect of engagement at this stage of the Project is to make sure that the EIA considers the opinion of key stakeholders through a robust consultation process. Any issue that is not directly related with the impacts of the EIA will be addressed later once the baselines, the impact assessment and the mitigation measures have been discussed with key stakeholders. HCH has already designed the Stakeholder Consultation Plan and will address the Community Development Plan later, which is a logical way forward. One aspect that is fundamental to organise the engagement activities is to decide on which stakeholders to talk with.

20.7 Closure and Rehabilitation

In Chile, all mining projects exploiting an ore body with an extraction capacity above 10,000 t/month are required to present an official closure plan that has to be approved by the Mining

Authority. No mining operations can start without an approved plan; the mining exploitation method has to be approved before obtaining the closure plan approval. Infrastructure affected by a closure plan needs to be developed at least at scoping engineering level.

A closure plan is a document specifying the technical measures and activities that the project must implement from the start of the mining operations. This addresses the measures taken to prevent, minimise or control the risks and effects, that may affect the people and the environment, by ensuring the physical and chemical stability of the project infrastructure after closure.

Main content of a closure plan is listed below:

1. Executive summary
2. Background information of the site
3. Risks Assessment Methodology used for the closure of site infrastructure
4. Environment description
5. Life of mine
6. Mine infrastructure description: closure analysis and commitments
7. Closure measures valuation
8. Post-closure program
9. Post-closure information (monitoring, measures valuation, etc.)
10. Financial guarantees
11. Strategic information
12. Communication program

21 CAPITAL AND OPERATING COSTS

As no current feasibility or pre-feasibility studies have been completed to the standard of NI 43-101 at this time, no Mineral Reserves have been estimated for the Costa Fuego Project.

22 ECONOMIC ANALYSIS

As no current feasibility or pre-feasibility studies have been completed to the standard of NI 43-101 at this time, no Mineral Reserves have been estimated for the Costa Fuego Project.

23 ADJACENT PROPERTIES

HCH knows of no immediately adjacent properties which might materially affect the interpretation or evaluation of the mineralization or exploration targets of the Costa Fuego Project.

24 OTHER RELEVANT DATA AND INFORMATION

To the authors' best knowledge, there is no other relevant data and information.

The authors know of no other relevant technical or other data or information that might materially impact the interpretations and conclusions presented herein, nor of any additional information necessary to make the report more understandable or not misleading.

25 INTERPRETATION AND CONCLUSIONS

25.1 Geology and Resources

25.1.1 Productora and Alice

An updated Mineral Resource Estimate (MRE) has been reported for the Productora and Alice deposits.

The Productora Cu-Au-Mo deposit is an enigmatic breccia complex that presents characteristics consistent with both the porphyry and IOCG models (Escolme, 2016).

The Alice Cu-Mo porphyry deposit is situated 400 m to the west of Productora. The Alice porphyry is spatially associated with the Silica Ridge lithocap, which is characterised by massive quartz-altered rock above domains of alunite, pyrophyllite and dickite (Escolme, 2016).

The Productora and Alice deposits are defined by approximately 1.04 million tonnes (Mt) of copper within 253 Mt of Indicated Resource at an average grade of 0.49% copper equivalent (CuEq*) above a cut-off grade of 0.21% CuEq.

** Copper Equivalent (CuEq) reported for the resource were calculated using the following formula: $CuEq\% = ((Cu\% \times Cu\ price\ 1\% \text{ per tonne} \times Cu_recovery) + (Mo\ ppm \times Mo\ price\ per\ g/t \times Mo_recovery) + (Au\ ppm \times Au\ price\ per\ g/t \times Au_recovery) + (Ag\ ppm \times Ag\ price\ per\ g/t \times Ag_recovery)) / (Cu\ price\ 1\% \text{ per tonne})$. The Metal Prices applied in the calculation were: Cu=3.00 USD/lb, Au=1,550 USD/oz, Mo=12 USD/lb, and Ag=18 USD/oz. For Productora (Inferred + Indicated), the average Metallurgical Recoveries were Cu=83%, Au=43% and Mo=42%.*

25.1.2 Cortadera

Following the release of the maiden MRE for Cortadera in September 2020, HCH undertook a Resource drill-out program focussed on extending and infilling previously reported Indicated and Inferred mineralisation. Drilling was successful in improving geological understanding and growing the Indicated resource.

The Cortadera deposit is characterised by early- and intra-mineralisation, porphyritic tonalitic to quartz dioritic intrusions and adjacent volcano-sedimentary wall-rocks that have been recrystallised to hornfels and skarn. The hydrothermal alteration consists of moderate- to strong-phyllic (+ chloritic) alteration, characterised by quartz / silica, sericite and lesser amounts of chlorite.

Drill spacing is nominally 80 m across strike by 80 m along strike. The current drilling density provides sufficient information to support a robust geological and mineralisation interpretation as the basis for Indicated and Inferred Classified Mineral Resources for the majority of the deposit.

The Cortadera Mineral Resource comprises an Indicated Resource of 471Mt at 0.46% CuEq*. This includes a higher-grade component (+0.6% CuEq) of 87Mt at 0.75% CuEq.

The Cortadera Mineral Resource is broken down into surface (open-pit) and underground (block cave) components based on Reasonable Prospects for Eventual Economic Extraction (RPEEE) shapes completed for both the open-pit and block cave.

A cut-off grade of 0.21% CuEq has been used for the Open Pit Resource, while 0.30% CuEq is used for the Underground Resource.

**Copper Equivalent (CuEq) reported for the Resource were calculated using the following formula: $CuEq\% = ((Cu\% \times Cu\ price\ 1\% \text{ per tonne} \times Cu_recovery) + (Mo\ ppm \times Mo\ price\ per\ g/t \times Mo_recovery) + (Au\ ppm \times Au\ price\ per\ g/t \times Au_recovery) + (Ag\ ppm \times Ag\ price\ per\ g/t \times Ag_recovery)) / (Cu\ price\ 1\% \text{ per tonne})$. The Metal Prices applied in the calculation were: Cu=3.00 USD/lb, Au=1,550 USD/oz, Mo=12 USD/lb, and Ag=18 USD/oz. For Cortadera (Inferred + Indicated), the average Metallurgical Recoveries were Cu=83%, Au=56%, Mo=82%, and Ag=37%.*

25.1.3 San Antonio

Following execution of the San Antonio option agreement in 2017, HCH undertook a Resource drill-out focussed on extending and infilling previously defined mineralisation. Drilling was successful in improving geological understanding and growing the deposit size.

Much of the San Antonio deposit is characterised by mineralisation within a microdiorite. Lesser mineralisation is also noted in adjacent felsic intrusives. Surface mapping suggests that mineralisation is controlled by narrow (<1-2m width) fault zones that strike NE to N and are typically steeply dipping wither NW, SE to E, or W. Parallel lodes were also mapped at surface and modelled at depth.

Drill spacing is nominally 80 m across strike by 120 m along strike. The current drilling density provides sufficient information to support a robust geological and mineralisation interpretation as the basis for an Inferred Classified Mineral Resources for the drill-defined deposit.

No Indicated Mineral Resource is reported for San Antonio.

25.2 Relevant Risks and Opportunities

HCH does not consider there to be significant risks or uncertainties present which would affect the Mineral Resource Estimation results. HCH has conducted exploration and resource development work in the region and on the Project for over 10 years.

The approach taken by the QPs to complete these Mineral Resource Estimates incorporated detailed data validation and analysis, and several tens of iterations were completed before the final estimation was finalized.

Additional data including metallurgical testwork, bulk density analysis and expanded geological information is required to increase the confidence in the Mineral Resource Estimate to a higher proportion of Indicated, as well as Measured Classification.

The maiden Cortadera Mineral Resource Estimate has been reported using realistic economic constraints to produce a CuEQ calculation, as well as an estimate of the Reasonable Prospect for Eventual Economic Extraction for both surface (open-pit) and underground (block cave) operations.

The Productora Mineral Resource Estimate has been reported using realistic economic constraints to produce a CuEQ calculation.

No Indicated Mineral Resource is reported for San Antonio.

26 RECOMMENDATIONS

The following items outline this report's risks and recommendations.

26.1 Prefeasibility Study

Based on the results of the 2022 Costa Fuego MRE, it is recommended that the Costa Fuego Project be advanced to the Pre-feasibility stage. Following positive results to the outcome of this work, a Feasibility study would then be recommended.

26.2 Costa Fuego Environmental Works

Ongoing environmental works at Costa Fuego will include drill permitting with associated palaeontology and archaeology surveys and coincident fauna and flora relocation during track and drill pad construction.

26.3 Regional Targeting

Drilling to test regional targets within the range of the Costa Fuego development will determine if these targets can be incorporated into the Project. This includes both drilling (Reverse Circulation and Diamond Drilling) and assaying as required.

26.4 Mineral Resource Development Drilling and Estimation

Resource development drilling at Cortadera paused in December 2021 for the Costa Fuego Mineral Resource. The result has provided a number of prospective targets around the Cortadera mineralised porphyry system which have the potential to grow both the underground and open pit mineral resource.

The Productora Resource and mineralisation is currently open at depth in several places as well as laterally. Additional drilling may add additional mineralisation volume and has the potential to upgrade resource classification of currently Inferred resource.

Additional exploration drilling around the Alice area is still very prospective and should be considered. An updated Alice resource estimate should incorporate learnings from the recently completed Cortadera resource as both are centred on porphyry intrusions.

The San Antonio deposit requires the drilling of twinned diamond holes to validate the location of the mineralisation and improve confidence in a data set derived mostly of pre-HCH data.

26.5 Cortadera Geotechnical and Metallurgical Drilling and Development Studies

A specific metallurgical and geotechnical drilling program of approximately 2,600m is required for a better definition of geotechnical domains and the drill core will also supply further variability and composite samples to the metallurgical test work program. This metallurgy program is predominantly assessing comminution, flotation, filtration and thickening at Cortadera. A smaller program at Productora will add to the substantial work already completed for this resource.

The development studies for Costa Fuego are ongoing, having commenced in June 2021. A mining study will be required, comprising the entire open cut mining studies involving pit optimisation, mine designs, mining schedule/sequence, waste dump designs, mine fleet analysis and operating cost and capital cost estimates

The mining study will cover open pit and underground mining, geotechnical and groundwater and surface water studies.

Geotechnical drilling will allow better definition of geotechnical domains and additional engineering will be undertaken to prepare detailed pit slope stability analysis for the first mining phase and the final pit as a minimum. It will also include detailed stability analysis for waste dumps.

Groundwater and surface water studies shall include hydrogeological assessment and complementary field works to improve the information quality for a robust PFS.

26.6 Summary

The estimated work programme budget for the 12 months beginning January 2022 within the Project area is summarised below (Table 26.1).

Table 26.1 Future Work Programme

Work Programme	Cost (USD)
Environmental Costs – Costa Fuego	340,000
Cortadera Resource Development Drilling	600,000
Regional Targets Drilling and Assaying	6,675,000
Cortadera Geotechnical and Metallurgical Drilling and Assaying	1,850,000
Development Studies – Mining, Metallurgy, Geotechnical and Environmental	3,590,000
Total	13,055,000

The Qualified Persons (QPs) have reviewed the proposed program of work and budget and finds them to be reasonable and justified considering the observations made in this report. The recommended work program and proposed expenditures are appropriate and well thought out. The proposed budget reasonably reflects the type and scope of the contemplated activities.

The QPs recommend that HCH conduct the planned activities subject to availability of funding and any other matters which may cause the objectives to be altered in the normal course of business activities.

27 REFERENCES

- Alegria A., Harvey T.V., Hawkins M.A., Rehnfeldt J. & Wall V.J. 1995. The Joanna Project, Region III, Chile. Report to Minera Mt Isa, Chile., 40p (unpublished).
- Alegria A. 2011. Resultados programa exploracion geoquimica BLEG franja Vallenar Cachiyuyo. SEGEA LTDA (Servicios Geológicos y Ambientales), 19p (unpublished).
- Armstrong R. 2020. SHRIMP U-Pb geochronology of samples from the Cortadera project, Chile. GIG Consultancy Pty Ltd, 20p (unpublished).
- Battig E. 2011. 2D MIMDAS MT/IP/RES Survey Project Johana, III Region of Atacama, Chile Logistics Report, GRS Chile, 30p (unpublished).
- Barton, M.D., and Johnson, D.A., 1996, Evaporitic-source model for igneous-related Fe oxide-(REE-Cu-Au-U) mineralization: *Geology*, v. 24, p. 259–262.
- Beeson, J., Noble, M., Outhwaite, M., McCormack, B., and Halley, S. 2012. “Geology of the Productora Project, Republic of Chile; Confidential Report to Hot Chili Limited, July 2012”. Jigsaw Geoscience Pty Ltd & Mineral Mapping Pty Ltd. Internal Company report.
- Brionnes E. 2013. Información generada en el Proyecto Johana. Minera Fuego Limitada internal report, 27p (unpublished).
- Cohen, J.F., 2011, Mineralogy and geochemistry of alteration at the Ann-Mason copper deposit, Nevada: Comparison of large-scale ore exploration techniques to mineral chemistry: M.Sc. thesis, Corvallis, Oregon, Oregon State University, 112 p. plus appendices
- Dietrich A. 2012. Reconocimiento y mapeo geológico, Proyecto Johana, Región III Atacama, Chile. Consulting Exploration Geologist Report to Minera Fuego Limitada, 63p (unpublished).
- Escolme, A. J. 2016. “Geology, geochemistry and geometallurgy of the Productora Cu-Au-Mo deposit, Chile”. Doctorate of Philosophy, University of Tasmania
- Fox, K.A., 2000, Fe-Oxide (Cu-U-Au-REE) Mineralisation and Alteration at the Productora Prospect, Colorado School of Mines, 114 p.
- Garwin S. 2019. The geological characteristics, geochemical signature and geophysical expression of porphyry copper-(gold) deposits in the circum-Pacific region. AEGC2019 Data to Discovery. Perth.
- Garwin S. 2020a. Cortadera 4D Model: Integration and analysis of geoscientific data with the aim of target definition and resource expansion. HCH internal report, 32p (unpublished).
- Garwin S. 2020b. Cortadera Alteration Modified. PowerPoint presentation to Hot Chili Limited, 2p (unpublished).

Gustafson, L. B. and Hunt, J. P., 1975, The Porphyry Copper Deposit at El Salvador, Chile, Society of Economic Geologists, Inc, v. 70, p 857-912.

Halley, S., Dilles, J.H, and Tosdal, R.M., 2015, Footprints: Hydrothermal alteration and geochemical dispersion around porphyry copper deposits, Society of Economic Geologists Newsletter v. 100, p 1, 12-17.

HCH5Productora-Delivers-PFS-Resource-Reserve-Upgrade02032016-1,ASX Announcement, 2nd March 2016, 78 pages (<https://www.hotchili.net.au/wp-content/uploads/2020/05/HCH5Productora-Delivers-PFS-Resource-Reserve-Upgrade02032016-1.pdf>)

Hitzman, M.W., Oreskes, N., and Einaudi, M.T., 1992, Geological characteristics and tectonic setting of proterozoic iron oxide (Cu-U-Au-REE) deposits: Precambrian Research, v. 58, p. 241–287.

Jordan J. 2009. Report on Ground Magnetic Surveys conducted at the Johanna Project Region III, Chile on behalf of Minera Fuego Limitada. Argali Geofisica E.I.R.L, 30p (unpublished).

Kirchner, I. 2014. “Productora Project Site Visit, Chile. Memorandum of Findings”. Internal company report.

Law S. & Garwin S. 2020. Seequent Cortadera 3D Model. Report to Hot Chili Limited, 14p (unpublished).

Leighton, M., Gillman, A., Beeson, J., and Milne, A. 2011. “Productora Resource Report. Productora 1/16”. Internal company report.

Llaumett, C., Olcay, L., Marín, C., Marquardt, J.C., and Reyes, R., 1975, El yacimiento cobre porfídico “Andacollo”, Provincia de Coquimbo, Chile: Revista Geologica de Chile v. 2, p. 56–66.

Muhling J. 2020. Petrographic examination of six samples from the Cortadera Cu-Au prospect. Report to Hot Chili Limited, 27p (unpublished).

Maksaev, V., Townley, B., Palacios, C., and Camus, F., 2007, Metallic ore deposits, in Moreno, T., and Gibbons, W., eds., The Geology of Chile:, The Geological Society, London, p. 179–199.

Maksaev, V., and Zentilli, M., 2002, Chilean strata-bound Cu-(Au) deposits: An overview, in Porter, T.M., ed., Hydrothermal iron oxide copper-gold and related deposits; a global perspective, 2: Adelaide, PGC Publishing, p. 22.

Marschik, R., and Fontbote, L. 2001. “The Candelaria-Punta del Cobre Iron Oxide Cu-Au (-Zn-Ag) Deposits, Chile”. Economic Geology, vol. 96, 2001, pp. 1799-1826

Macdonald, J.L. 2014. “Productora Resource Revision 2 Report”. Internal company report.

- Macdonald, J.L. 2015. "Productora Project Resource 2015 Report". Internal company report.
- Muller, F., Leighton, M., Beeson, J., and Voortman, A. 2013. "Productora Resource Upgrade 1 Resource Report". Internal Company Report.
- Pollard, P.J., 2001, Sodic(-calcic) alteration in Fe-oxide-Cu-Au districts: an origin via unmixing of magmatic H₂O-CO₂-NaCl ± CaCl₂-KCl fluids: *Mineralium Deposita*, v. 36, p. 93–100.
- Productora Pre- Feasibility Report, 22 February 2016, Mintrex Pty Ltd, Report Nr 1426-RPT-001 Sections 0 to 16. Internal Company Report.
- Ruiz, C., Aguirre, L., Corvalan, J., Klohn, C., Klohn, E., and Levi, B., 1965, *Geología y Yacimientos Metalíferos de Chile*: Instituto de Investigaciones Geológicas de Chile: Santiago, v. 1.
- Sillitoe, R.H., 1992, Gold and copper metallogeny of the Central Andes; past, present, and future exploration objectives: *Economic Geology*, v. 87, p. 2205–2206.
- Sillitoe, R.H., 2003, Iron oxide-copper-gold deposits: An Andean view: *Mineralium Deposita*, v. 38, p. 787–812.
- Sillitoe, R.H., and Perelló, J., 2005, Andean copper province: Tectonomagmatic settings, deposit types, metallogeny, exploration, and discovery: *Economic Geology 100th Anniversary Volume*, p. 845– 890.
- Szakács A. & Pop N. 2001. Informe: Reconocimiento y evaluación geológica de preliminar de las concesiones: Las Canas 1 al 15, Las Canas 16, Cortadera Uno, Cortadera 1 al 40, Cortadera 41, Cortadera 42 y Falla Maipo 2, 3, 4 y 5, Comuna Vallenar Provincia de Huasco, Tercera Region de Atacama. Sociedad Contractual Mineral Carola, 69p (unpublished).
- Tapia M. 2019. Geological Report: Cortadera Surface Mapping. Report to Hot Chili Limited, 8p (unpublished).
- Tobey E. 2011a. Activity Report for Minera Fuego, March - April, 2011. Bushwalker Exploration, 13p (unpublished).
- Tobey E. 2011b. Activity Report for Minera Fuego, November - December, 2011. Bushwalker Exploration, 14p (unpublished).
- Tobey E. 2012a. Activity Report for Minera Fuego, January, 2012. Bushwalker Exploration, 13p (unpublished).
- Tobey E. 2012b. Activity Report for Minera Fuego, February - March, 2012. Bushwalker Exploration, 18p (unpublished).
- Tobey E. 2012c. Activity Report for Minera Fuego, July, 2012. Bushwalker Exploration, 7p (unpublished).

Tobey E. 2013a. Activity Report for Minera Fuego, January, 2013. Bushwalker Exploration, 15p (unpublished).

Tobey E. 2013b. Activity Report for Minera Fuego, April, 2013. Bushwalker Exploration, 2p (unpublished).

Voortman, A.W. 2012. "Productora Site Visit Report. Internal memorandum to Hot Chili Limited, December 2012". Coffey Mining Ltd. Internal company report.

Certificate of Qualifications

I, Anton von Wielligh, Principal Mining Engineer, and Director of ABGM PTY LTD (ABGM), Australia do hereby certify that:

- 1 I am currently employed as an Independent Consultant of ABGM PTY LTD, with an office in 66 Orsino blvd, North Coogee, Western Australia 6163.
- 2 This certificate applies to the technical report titled "NI 43-101 Resource Report Costa Fuego Copper Project, Located in Atacama Chile", with an effective date of 14th March 2022, (the "Technical Report") prepared for Hot Chili Limited ("the Issuer");
- 3 I am a graduate from the University of Pretoria with a bachelor's degree in mining engineering and completed my Honors degree in Mining Engineering at the University of Pretoria. I have 21 years of post-graduate mining industry experience and 25 years of mining industry experience in total. I am a Fellow Grade Member of the Australian Institute of Mining and Metallurgy (FAUSIMM No: 325251)

My professional experience includes +21 years working on projects, studies and includes practical mining experience with open pit operations and underground mines including Copper, Gold, Platinum, Iron Ore, and other commodities with similar styles of mineralisation's to that of all the Costa Fuego deposits modelled. I have been a Qualified Person (Mining) for several large Copper Open pit and Underground projects and operations during my career.

I have read the definition of "qualified person" set out in National Instrument 43-101 (NI 43-101) and certify that by reason of my education, affiliation with a professional association (as defined in NI 43-101) and past relevant work experience, I fulfill the requirements to be a "qualified person" for the purposes of NI 43-101;

- 4 I have not yet inspected the Productora Project site but intend to do so in the next few months. Other Qualified Persons visited the site locations on behalf of the project team. Travel challenges related to Covid-19 have impacted earlier site visits planned.
- 5 I am responsible for Sections 4-6, 13, 15-24 and 27 of the Technical Report;
- 6 I am independent of Hot Chili Limited and the Costa Fuego property applying all of the tests in Section 1.5 of the NI 43-101;
- 7 I have had limited technical involent prior to 2021. The only involvement I had was in assisting with technical reviews during 2016, specifically on the Productora deposit's 2016 Pre-Feasibility Study. I have no vested interest in any of the project areas or deposits of Costa Fuego and am contracted as an independent consultant.
- 8 I have read NI 43-101, and the Technical Report has been prepared in compliance with NI 43-101 and Form 43-101F1; and
- 9 As of the effective date of the Technical Report and the date of this certificate, to the best of my knowledge, information and belief, this Technical Report contains all scientific and technical information that is required to be disclosed to make the Technical Report not misleading.

Effective Date: 31st March 2022

Signing Date: 13th May 2022



Anton von Wielligh - FAUSIMM

Principal Mining Engineer and Director ABGM PTY LTD

I, Elizabeth Haren, Director of Haren Consulting, of the Greater Perth Area, Australia, do hereby certify that:

- 1 I am currently employed as the Director of Haren Consulting, with an office at PO Box 1159 Scarborough, Western Australia, 6922;
- 2 This certificate applies to the technical report titled "NI 43-101 Resource Report Costa Fuego Copper Project, Located in Atacama Chile", with an effective date of 14th March 2022, (the "Technical Report") prepared for Hot Chili Limited ("the Issuer");
- 3 I am a graduate from the University of Newcastle with a Bachelor of Science – Geology Geography. I have continually practiced my profession since 1996 as a geologist.

I have worked in the mining industry for 25 years with experience in underground geology, open pit geology and geostatistics. I also have experience providing specialist mineral resource geology services for the mining industry, including mineral resource estimation and reporting, reconciliation analysis for strategic evaluation, conditional simulation for risk analysis, and quality and control analysis.

I am a member and Chartered Professional (Geology) of the Australasian Institute of Mining and Metallurgy (208050) and a Member of the Australian Institute of Geoscientist (6646).

I have read the definition of "qualified person" set out in National Instrument 43-101 (NI 43-101) and certify that by reason of my education, affiliation with a professional association (as defined in NI 43-101) and past relevant work experience, I fulfill the requirements to be a "qualified person" for the purposes of NI 43-101;

- 4 I have not visited the Productora Project or Cortadera Project site;
- 5 I am responsible for Sections 1-3, 7-12, 14, 25 and 26 of the Technical Report;
- 6 I am independent of Hot Chili Limited and the Costa Fuego property applying all of the tests in Section 1.5 of the NI 43-101;
- 7 I have had prior involvement with the subject property. In 2020 and 2021, I was co-author of private reports and technical memos for the property that is the subject of the Technical Report;
- 8 I have read NI 43-101, and the Technical Report has been prepared in compliance with NI 43-101 and Form 43-101F1; and
- 9 As of the effective date of the Technical Report and the date of this certificate, to the best of my knowledge, information and belief, this Technical Report contains all scientific and technical information that is required to be disclosed to make the Technical Report not misleading.

Effective Date: 31st March 2022

Signing Date: 13th May 2022



Elizabeth Haren, MAusIMM (CP), MAIG
Director of Haren Consulting

Rev No	Date	Revision	By	Reviewed	Approved